

ICES Marine Science Symposia

Actes du Symposium

ISSN 0906-060X

Volume 219 September 2003

Hydrobiological Variability in the ICES Area, 1990–1999

A Symposium held in Edinburgh, 8–10 August 2001

International Council for the Exploration of the Sea

Conseil International pour l'Exploration de la Mer

ISSN 0906–060X

ICES Marine Science Symposia

Actes du Symposium

Volume 219 September 2003

Hydrobiological Variability in the ICES Area, 1990–1999

A Symposium held in Edinburgh,
8–10 August 2001

Celebrating the scientific contributions of John Lazier, Svend-Aage Malmberg, David Ellett, Johan Blindheim, and Leo Otto

Edited by William Turrell, Alicia Lavín, Kenneth F. Drinkwater, Michael St John, and Jennifer Watson

International Council for the Exploration of the Sea
Conseil International pour l'Exploration de la Mer

ICES MSS 219
ISSN 0906-060X
September 2003

Hydrobiological Variability in the ICES Area, 1990–1999

Contents

R. R. Dickson, J. Meincke, and W. R. Turrell	Introduction	1
	List of referees	13
	A. Papers Presented at the Symposium	14
	I. GENERAL OCEAN CLIMATE	
R. R. Dickson and J. Meincke	The North Atlantic Oscillation and the ocean's response in the 1990s	15
P. D. Jones	The decade of the 1990s over the Atlantic in comparison with longer instrumental and palaeoclimatic records	25
	II. REGIONAL OCEAN CLIMATE	
I. Yashayaev, J. R. N. Lazier, and R. A. Clarke	Temperature and salinity in the central Labrador Sea during the 1990s and in the context of the longer-term change	32
K. F. Drinkwater, B. Petrie, and P. C. Smith	Climate variability on the Scotian Shelf during the 1990s	40
S.-A. Malmberg and H. Valdimarsson	Hydrographic conditions in Icelandic waters, 1990–1999	50
B. Planque, P. Beillois, A. M. Jégou, P. Lazure, P. Petitgas, and I. Puillat	Large-scale hydroclimatic variability in the Bay of Biscay: the 1990s in the context of interdecadal changes	61
J. M. Cabanas, A. Lavín, M. J. García, C. Gonzalez-Pola, and E. Tel Pérez	Oceanographic variability in the northern shelf of the Iberian Peninsula, 1990–1999	71
H. M. van Aken	Decadal changes of the hydrography between Ireland and Cape Farewell	80
G. Ottersen, H. Loeng, B. Ådlandsvik, and R. Ingvaldsen	Temperature variability in the Northeast Atlantic	86
N. P. Holliday	Extremes of temperature and salinity during the 1990s in the northern Rockall Trough: results from the "Ellett line"	95
B. Hansen, W. R. Turrell, and S. Østerhus	Indications and consequences of weakened Iceland–Scotland overflow	102
W. R. Turrell, B. Hansen, S. Hughes, and S. Østerhus	Hydrographic variability during the decade of the 1990s in the Northeast Atlantic and southern Norwegian Sea	111
C. Schrum, F. Siegismund, and M. A. St. John	Decadal variations in the stratification and circulation patterns of the North Sea. Are the 1990s unusual?	121
W. Matthäus and G. Nausch	Hydrographic-hydrochemical variability in the Baltic Sea during the 1990s in relation to changes during the 20th century	132
K. A. Mork and J. Blindheim	Heat loss of the Norwegian Atlantic Current toward the Arctic	144
R. Sætre, J. Aure, and D. S. Danielssen	Long-term hydrographic variability patterns off the Norwegian coast and in the Skagerrak	150
R. Ingvaldsen, H. Loeng, G. Ottersen, and B. Ådlandsvik	Climate variability in the Barents Sea during the 20th century with a focus on the 1990s	160

III. PLANKTON COMMUNITIES

E. B. Colbourne and J. T. Anderson — Biological response in a changing ocean environment in Newfoundland waters during the latter decades of the 1990s — 169

E. Gaard — Plankton variability on the Faroe Shelf during the 1990s — 182

M. A. St. John, P. Budgell, M. H. Nielsen, and A. Lucas — Resolving variations in the timing and intensity of the spring bloom in the central North Sea during the 1990s: a comparison of remote sensing and 2-D modelling approaches — 190

N. Ladwig, K.-J. Hesse, F. Colijn, and U. Tillmann — Has the eutrophic state of German Wadden Sea waters changed over the past 10 years due to nutrient reduction? — 199

W. Fennel and T. Neumann — Variability of copepods as seen in a coupled physical-biological model of the Baltic Sea — 208

C. Möllmann, F. W. Köster, G. Kornilovs, and L. Sidrevics — Interannual variability in population dynamics of calanoid copepods in the Central Baltic Sea — 220

IV. FISH POPULATIONS

E. Buch, M. H. Nielsen, and S. A. Pedersen — On the coupling between climate, hydrography, and recruitment variability of fishery resources off West Greenland — 231

O. Le Pape, Y. Désaunay, and D. Guérault — Relationship between fluvial discharge and sole (*Solea solea* L.) recruitment in the Bay of Biscay (France) — 241

F. Sánchez and A. Serrano — Variability of groundfish communities of the Cantabrian Sea during the 1990s — 249

K. Brander, G. Blom, M. F. Borges, K. Erzini, G. Henderson, B. R. MacKenzie, H. Mendes, J. Ribeiro, A. M. P. Santos, and R. Toresen — Changes in fish distribution in the eastern North Atlantic: Are we seeing a coherent response to changing temperature? — 261

M. Dickey-Collas, M. J. Armstrong, R. A. Officer, P. J. Wright, J. Brown, M. R. Dunn, and E. F. Young — Growth and expansion of haddock (*Melanogrammus aeglefinus* L.) stocks to the west of the British Isles in the 1990s — 271

V. K. Ozhigin, S. S. Drobysheva, N. G. Ushakov, N. A. Yaragina, O. V. Titov, and A. L. Karsakov — Interannual variability in the physical environment: zooplankton, capelin (*Mallotus villosus*), and Northeast Arctic cod (*Gadus morhua*) in the Barents Sea — 283

F. W. Köster, C. Möllmann, S. Neuenfeldt, M. Vinther, M. A. St. John, J. Tomkiewicz, R. Voss, H.-H. Hinrichsen, B. MacKenzie, G. Kraus, and D. Schnack — Fish stock development in the Central Baltic Sea (1974–1999) in relation to variability in the environment — 294

B. Posters Presented at the Symposium — **307**

I. GENERAL OCEAN CLIMATE

W. R. Turrell and N. P. Holliday — The ICES Annual Ocean Climate Status Summary: 2000/2001 — 309

A. S. Krovnin and G. P. Moury — Climatic variations in the North Atlantic and the North Pacific in the 1990s: a comparative study — 311

A. S. Krovnin and G. P. Moury — The 1990s in the context of climatic changes in the North Atlantic region during the past 40 years — 315

II. REGIONAL OCEAN CLIMATE

B. Rudels, P. Eriksson, E. Buch, G. Budéus, E. Fahrbach, S.-A. Malmberg, J. Meincke, and P. Mälkki — Temporal switching between sources of the Denmark Strait overflow water — 319

S. Jónsson and J. Briem — Flow of Atlantic Water west of Iceland and onto the north Icelandic Shelf — 326

J. Ólafsson — Winter mixed layer nutrients in the Irminger and Iceland Seas, 1990–2000 — 329

I. Puillat, P. Lazure, A. M. Jégou, B. Planque, and L. Lampert	Mesoscale, interannual, and seasonal hydrological variability over the French continental shelf of the Bay of Biscay during the 1990s	333
J. Gil and R. Sánchez	Aspects concerning the occurrence of summer upwelling along the southern Bay of Biscay during 1993–2000	337
V. Valencia, Á. Borja, A. Fontán, F. F. Pérez, and A. F. Ríos	Temperature and salinity fluctuations along the Basque Coast (southeastern Bay of Biscay), from 1986 to 2000, related to climatic factors	340
C. G.-Pola and A. Lavín	Seasonal cycle and interannual variability of the heat content on a hydrographic section off Santander (southern Bay of Biscay), 1991–2000	343
J. Meincke, M. Bersch, K.-P. Koltermann, and A. Sy	Changes in subarctic and subtropical water masses in the upper layer of the northern North Atlantic during the 1990s	346
M. Stein	XBT-Transects along 60°N, Greenland–Scotland, 1989–1999	349
G. Alcock, B. Moate, and L. Rickards	Climate of UK waters at the millennium: status and trends	352
A. E. Lucas and W. P. Budgell	Frontal climatology based on advanced very high resolution radiometer sea surface temperatures in the eastern North Sea	356
H. M. van Aken	One-hundred-and-forty years of daily observations in a tidal inlet (Marsdiep)	359
L. S. Andersson and K. M. Borenäs	Long-term variations of the hydrography around Sweden	362
K. K. Kahma, H. Boman, M. M. Johansson, and J. Launiainen	The North Atlantic Oscillation and sea level variations in the Baltic Sea	365
P. K. Jakobsen, M. H. Nielsen, D. Quadfasel, and T. Schmith	Variability of the surface circulation of the Nordic Seas during the 1990s	367
J. E. Ø. Nilsen	Variability at Ocean Weather Station M in the Norwegian Sea	371
J. Karstensen, P. Schlosser, J. Blindheim, J. Bullister, and D. Wallace	Formation of intermediate water in the Greenland Sea during the 1990s	375
E. Fahrbach, G. Rohardt, U. Schauer, J. Meincke, S. Østerhus, and J. Verduin	Direct measurements of heat and mass transports through Fram Strait	378

III. PLANKTON COMMUNITIES

N. González, A. Bode, M. Varela, and R. Carballo	Interannual variability in hydrobiological variables in the coast of A Coruña (NW Spain) from 1991 to 1999	382
M. H. Nielsen and M. St. John	Inter- and intra-annual variations in the stratification, timing, and intensity of phytoplankton blooms in the Central North Sea in the 1990s	384
O. Lindahl, A. Belgrano, and B. A. Malmgren	Increased phytoplankton production in the Gullmar Fjord, Sweden, 1985–1999	387
S. Skreslet and A. Borja	Interannual correlation between hemispheric climate and northern Norwegian wintering stocks of two *Calanus* spp.	390
H. Wehde	Influence of mixed-layer depth variations on primary production	393

IV. FISH POPULATIONS

M. A. Sundermeyer, B. J. Rothschild, and A. R. Robinson	Environmental indicators and the predictability of commercial fish stocks	396
R. Sánchez, F. Sánchez, J. Landa and Á. Fernández	Influence of oceanographic parameters on recruitment of megrim (*Lepidorhombus whiffiagonis*) and four-spot megrim (*L. boscii*) on the Northern Spanish continental shelf (ICES Division VIIIc)	400
A. Lavín, X. Moreno-Ventas, P. Abaunza, and J. M. Cabanas	Environmental variability in the Atlantic and Iberian waters and its influence on horse mackerel recruitment	403
F. Velasco, I. Olaso, and F. Sánchez	Annual variations in the prey of demersal fish in the Cantabrian Sea and their implications for food web dynamics	408
J.-C. Poulard, F. Blanchard, J. Boucher, and S. Souissi	Variability in the demersal fish assemblages of the Bay of Biscay during the 1990s	411

R. Sánchez, F. Sánchez, and J. Gil	The optimal environmental window that controls hake (*Merluccius merluccius*) recruitment in the Cantabrian Sea	415
P. Steingrund, L. H. Ofstad, and D. H. Olsen	Effect of recruitment, individual weights, fishing effort, and fluctuating longline catchability on the catch of Faroe Plateau cod (*Gadus morhua* L.) in the period 1989–1999	418
S. L. Hughes, W. R. Turrell, and A. Newton	Hydrobiological variability on the northwest European continental shelf during the 1990s and its relation to changes in fish stocks	421
S. H. Kabuta and E. M. Hartgers	Development of ecological indicators for the Dutch section of the North Sea	426
L. Urho, J. Kjellman, and T. Pelkonen	Eutrophication and herring reproduction success in the northern Baltic Sea	430
T. Raid, A. Järvik, O. Kaljuste, A. Lankov, and T. Drevs	Principal developments in the structure and dynamics of main fish stocks in the northeastern Baltic in the 1990s within the context of environmental changes	433
A. O. Laine and S. Unverzagt	Baltic Sea benthos in the 1990s: a comparison of the distribution of oxygen deficiency and macrozoobenthos communities	437
A. Järvik and T. Raid	Impact of the environmental changes in the northeastern Baltic on the Estonian fishery in the 1990s	440
E. Sentyabov, V. Borovkov, N. Plekhanova, and A. Krysov	Hydrographic conditions in the Norwegian Sea in the 1990s and their influence on plankton status and Atlanto-Scandian herring migrations	443
E. L. Orlova, V. D. Boitsov, M. Y. Antsiferov, V. N. Nesterova, and N. G. Ushakov	Status of food zooplankton in the feeding period of capelin from the central latitudinal zone of the Barents Sea in cold and warm years	447
A. V. Dolkov	Feeding and food consumption of the most abundant fishes of the Barents Sea in the 1990s	450

International Council for the Exploration of the Sea
Conseil International pour l'Exploration de la Mer

ICES Marine Science Symposia, 219: 1–12. 2003

Hydrobiological Variability in the ICES Area, 1990–1999

Introduction

Robert R. Dickson and Jens Meincke
Co-Conveners

William Turrell
Chair, Editorial Panel

This volume records the proceedings of the second in a series of Decadal Symposia, in this case focusing on the decade of the 1990s and set up by ICES to meet a quite specific purpose. As in the first volume (Dickson *et al.*, 1992), it is worth recalling why the series was begun, since this explains the aims and content of the Symposium.

In October 1987, during the 75th Statutory Meeting in Santander, the Council endorsed the conclusion of its Consultative Committee that annual publication of the *Annales Biologiques* series was no longer feasible within the available budget, and Volume 41 for the year 1984 became the last in that distinguished series. From the expressions of regret recorded by many Standing Committees at its discontinuation (*Procès-Verbal*, 1987), it was plain that the *Annales* had been providing a valuable compilation of data and information not readily available elsewhere. Hence, as there remained a scientific justification, ICES aimed to meet the same scientific purpose via a different and more affordable route.

On the advice of a small working party, consisting of the Chairs of the (then) Hydrography, Marine Environmental Quality, and Biological Oceanography Committees, together with the ICES Hydrographer and ICES Environment Officer, the Consultative Committee recommended that the essential purpose of *Annales Biologiques* might be met by promoting symposia on "Overviews of the Decade", in which, following the approach of NAFO, the relevant climatic, oceanographic, and biological material might be pulled together and compared. This recommendation was accepted by the Council, and at the 76th Statutory Meeting in Bergen it was given substance when it was decided that the first such symposium should be held in Mariehamn in the Baltic during June 1991 (C. Res. 1988/2.2).

While the above describes the bare facts of the decision, it fails to describe the continuity of purpose which has maintained the issue of long-term change in the forefront of ICES activities throughout its century-long existence.

As early as 1890, Otto Pettersson and Gustav Ekman had begun the process of applied hydrographic monitoring in the Baltic and North Seas, and it was the utility of Pettersson's scheme that was a key factor in prompting the founding of ICES in 1902. Though these early initiatives were invaluable in establishing a basis for the long-term detection of "change", something more was required for this to develop into the wealth of decade-to-century time-series that today form so much of the focus, interest, and expertise of ICES. That extra stimulus was provided by the large-scale, long-period shifts in ocean climate that have successively worked their way through ICES waters during much of the present century: the "Warming in the North", the "Russell Cycle", the "Great Salinity Anomaly", and the varied effects of the North Atlantic Oscillation (NAO).

The stimulus of extreme climatic events has certainly continued in the decade under review. During the early 1990s, the NAO evolved to positive values unprecedented in the instrumental record. In fact, in his invited Keynote Address, Dr Phil Jones of the Climate Research Unit, University of East Anglia, suggests that the recent amplification of the NAO from the 1960s to the 1990s may be unique even in proxy records of 600 years' duration (Jones, 2003). The latter part of the decade was hardly less spectacular; following a rapid drop to extreme low-index values in the winter of 1996 (again, one of the largest year-on-year changes of record), the two main pressure-anomaly cells of the NAO pattern showed a marked tendency to shift eastwards during the last winters of the decade.

As the principal recurrent mode of atmospheric forcing in the Atlantic Sector, such extreme patterns of NAO behaviour were associated with changes of large amplitude throughout the ocean-atmosphere system of the Atlantic. As varied examples of that response, we note that in the early 1990s the storm index for the southern Norwegian Sea rose to a 100-year maximum, an extreme freshening visited

the two dense overflows, the transport of the eastern overflow slackened by 20%, convection in the Labrador Sea reached unprecedented depths, contributing to a full-depth change in the NW Atlantic that is thought to be the largest of the modern oceanographic record, the main Atlantic gyre circulation spun up to a century-long maximum, as did the transport of Atlantic Water passing through the Faroe—Shetland Channel, and the warmth recorded off northern Norway rose to a 40-year peak. These and other remarkable changes in the physical environment will be documented in the papers that follow, together with evidence of the ecosystem response.

Had the climate of the 1990s been rather less anomalous, there would still have been point to this decadal review. Only by achieving continuity of observation are we able to recognize what is extreme from what is normal and identify the subtle shifts in the marine climate that may have important effects on the ecosystem. Yet it is a sobering fact, captured by Duarte *et al.* (1992), that although there has been an exponential increase in the initiation of new time-series monitoring programmes in European marine stations in recent decades, there has also been an exponential increase in their termination, so that "long-term monitoring programmes are, paradoxically, among the shortest projects in marine sciences: many are initiated, but few survive a decade". Put differently, policy-makers are rather easily startled into initiating actions, but the time scales of policy, funding, and even of scientific "fashion" are not normally imbued with much stamina.

"Consequently", as Duarte *et al.*, point out, "the continuation of long-term monitoring programmes is often heavily dependent on the personal effort and dedication of individual scientists", and nowhere is the truth of that statement better recognized than in the Standing Committees of ICES, where individuals and groups of individuals have long taken the responsibility for piecing together the evidence for change in their regional marine environments and for attributing these changes as to cause.

The early history and purpose of these efforts were beautifully captured by Johan Hjort, the ICES President at the time, in his Preface to the first volume of the *Annales Biologiques* series, when he explained the watershed in scientific thought and the progression in our thinking which had necessitated the new publication. There were three main links to that new chain of thought: first, "the hypothesis, which at the beginning seemed so daring . . . that the statistics of the catches of the fishermen or research vessels may be considered as representative of the existing stock"; second, the idea that "samples collected from a series of years disclosed the important fact of fluctuations in the stock from the one year to the other"; and finally "from the closer understanding of these changes arose the conviction that such changes were governed by the influence of the environment which might be investigated not only for a rational understanding of the contemporary situation but also for prognoses as to events in future" (Hjort, 1943).

Though the idea of a permanent International Commission to make and administer such prognoses was proposed at the Berlin Meeting of the International Council, such a degree of official international cooperation proved impossible in the climate of May 1939. At the level of the individual scientist, however, there was no such problem, and the Consultative Committee under Chair E. S. Russell, Vice Chairs A. Hagmeier and E. Le Danois, and its Sub-Committee on "Hydrographical and Biological Investigations" chaired by Martin Knudsen, went right ahead with a plan to collect the biological and environmental data that such an International Commission would one day require when hostilities ceased.

Annales Biologiques was the expression of that plan, and with an energetic Jens Smed returning from his Master's degree in physics in 1939 to play his key dual role in developing the Service Hydrographique as an effective regional data centre, and in piecing together the accumulated data into reliable long time-series, the plan was rapidly equipped with the necessary physical infrastructure to match the data products of the Fish Committees.

These actions, however necessary and effective, still do not add up to the long time-series of multidisciplinary data against which the slow shifts of environmental change can be recognized and explained. To achieve that required simple continuity of enthusiasm and effort while the time-series and data sets lengthened. As we noted in the first of these symposium proceedings, if we sometimes appear to be unduly preoccupied with the personalities and history of this subject within ICES, it is a preoccupation that is readily explained as one practical way of acknowledging and encouraging these efforts.

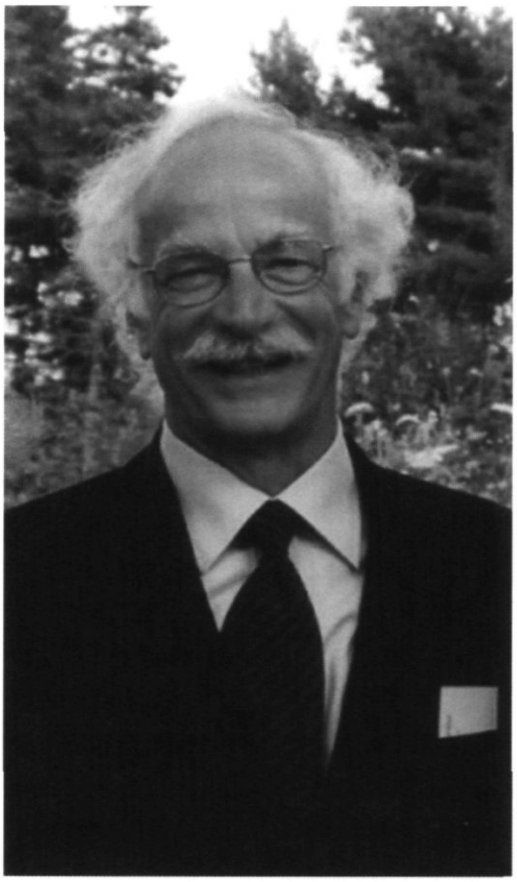
Hence, a further purpose of the Decadal Symposium series was to acknowledge the actions of the individuals who had taken part in lengthening and broadening our description of the marine environment throughout recent decades, still fired with the idea that motivated the *Annales* in the first place; namely that changes in the ecosystem and the physical environment are linked in some understandable way.

In many ways their task was the hardest of all, as the certainty with which Hjort and his contemporaries viewed the connection between the great fisheries and their physical environment sometimes proved difficult to pin down, as the time scale of

Government policies and the stamina of their funding both shortened, and even to some extent as the fashions of science switched away from the long haul of monitoring and description to the short-term intensive study of process.

As in Mariehamn, the five individuals whose efforts are especially acknowledged in this proceedings volume were leaders and long-time contributors to the study of environmental variation and effects on biota over many decades within ICES. On this occasion the scientists honoured at the Symposium were John Lazier (BIO, Dartmouth, NS, Canada), Svend-Aage Malmberg (MRI, Reykjavík, Iceland), David Ellett (DML, Oban, Scotland, UK), Johan Blindheim (IMR, Bergen, Norway) and Leo Otto (NIOZ, The Netherlands). Though ill-health prevented David Ellett from attending, Stig Fonselius and Odd Sælen, whose contributions were celebrated at the original Mariehamn Symposium in 1991, were able to participate once again on this occasion. We are profoundly sorry to note Stig Fonselius' death in January 2003. It is perhaps one of the best design features of the "Decadal Symposium" idea that it will provide a recurring opportunity to acknowledge and encourage the efforts by others into the future.

For the present, these individuals will forgive us if, with five long careers to consider, we are forced to describe them in only a few inadequate sentences.



John Lazier

John Robert Nicholas Lazier (born 1 November 1936) entered oceanography via a BA in physics at the University of Toronto, then an MSc in oceanography at the University of British Columbia in 1963, ultimately completing a PhD at Southampton University under Henry Charnock in 1977. So far as oceanography is concerned, the gap between the MSc and PhD is highly significant, since it was during this period that he completed his first pioneering studies of the oceanography of the NW Atlantic.

Already since June 1960 a scientist at BIO, the young John Lazier was able to seize on a lull in ship schedules to undertake two long campaigns of hydrography, first to the Davis Strait in 1965 aboard CCGS "Labrador", then to the Labrador Sea in late winter 1966 aboard CSS "Hudson". The impetus for the latter came from conversations with Val Worthington of Woods Hole, who, along with John Swallow, had recently surveyed the northern North Atlantic as part of the IGY surveys on the "Erika Dan". They had not found indications of convection capable of renewing the intermediate Labrador Sea Water, and Val had encouraged John Lazier to try again with a denser survey. The result was the first, and to date the only, fully three-dimensional survey of the physics, oxygen, and nutrients of the Labrador Sea. It could probably not be afforded today.

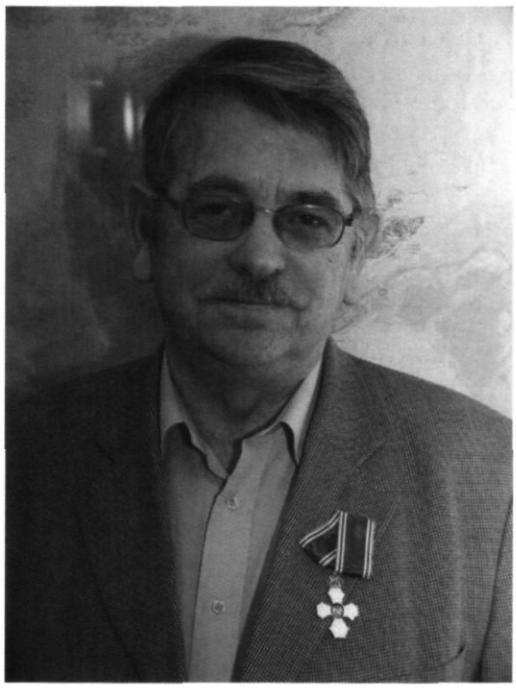
Of course, as we now know, the NAO in winter 1966 was in the middle of its most strongly negative state in the instrumented record, with exceptionally gentle conditions in the Labrador Sea and no deep convection to be found, no matter how closely spaced the stations. But as a result, this survey gave us the vital benchmark for what Peter Rhines has called the "Crouching Tiger stage" of the NW Atlantic circulation. It came none too soon. From the explosive resumption of convection in winter 1972 to the NAO-positive extreme of the early 1990s, the continuation of hydrographic time-series from the Labrador Sea by John Lazier, Allyn Clarke, and others has described a remarkable intensification and deepening of convection, reaching to 2300 m by 1993.

The radical nature of the change is evident from John's own 1995 assessment. From 1966 to 1992, the overall cooling of the water column of the

Labrador Sea has been equivalent to a loss of 8 W m^{-2} continuously for 26 years, the overall freshening was equivalent to mixing in an extra 6 m of freshwater at the sea surface, and as a result the steric height in the central Labrador Sea was typically 6–9 cm lower than in the late 1960s. These full-depth changes are arguably the largest ever observed in the modern instrumental oceanographic record. Maintenance of the WOCE AR7W Section into the late 1990s identified a new period of restratification in which convection was confined to 1000–1500 m and the deeper convected water drained away from the region.

There have been other accomplishments. Ninety days with Val Worthington in the Denmark Strait in 1967 failing to measure its outflow, failed also to dampen John's enthusiasm for direct current measurements in difficult environments. By maintaining current meters on the Labrador Shelf and slope during the late 1970s and throughout the 1980s, in spite of losses to corrosion, icebergs, and trawlers, he measured the 30 Sv return flow of the subpolar gyre which had been predicted but not observed, as well as the annual cycle in strength of the Labrador Current.

In 1994 John changed state at BIO from Scientist to Scientist Emeritus, though with such discoveries, and prompted throughout his career by such delightful and stimulating mentors as the late Val Worthington, John Swallow, Henry Charnock, and George Needler, it is unsurprising that John has found retirement unappealing. A glimpse at his current and recent fieldwork plans on the BIO Website will explain just how unretired he is, to our great benefit!



Svend-Aage Malmberg

Perhaps more than any other, **Svend-Aage Malmberg** (born 8 February 1935) has epitomized the collaborative international spirit of ICES in observing and then piecing together the evidence for the dramatic hydrographic changes that have passed through ICES waters over the past several decades. Though born and schooled in Reykjavík, his initial oceanographic training, qualifications, and employment were obtained at the University of Kiel (1955–1962) and, although employed at the Marine Research Institute in Reykjavík from 1963 to 2001, he has taken care to refresh and renew his international links from time to time through study periods at the Universities and/or Marine Research Institutes of Gothenberg, Bergen, Copenhagen, and Washington. Over this entire period, he also served as Icelandic representative on the Hydrography Committee of ICES and its Working Groups.

As a research scientist, Head of the Hydrography Division (1976–1985), and Head of the Physical Oceanographic Group within the Ecology Division at MRI (to 2000), Svend-Aage had responsibility for providing an annual description of the hydrographic status of Icelandic waters as necessary input to the successful management of Iceland's marine fisheries and ecosystem. While the requirement itself may have been routine its delivery was not, since it relied on the annual working of a radiating network of standard hydrographic sections around Iceland each season for decades in some of the most daunting weather on Earth. Straddling the Ocean Polar Front and crossed by the cold dense overflows that ventilate the deep ocean, these Icelandic waters have also formed a key component of a succession of physical oceanographic campaigns that have explored the local, regional, and global importance of Atlantic ocean-climate variability; the ICES Overflow '73 project, the Iceland Sea Project (1974/1975), the ICES Deep Water Project of 1980/1981, the ICES NANSEN Project of 1986–1990, the Greenland Sea Project of 1987–1991, the World Ocean Circulation Experiment of 1992–1998, and the EC VEINS project of 1997–2000. As his long series of publications will show, Svend-Aage and his Group contributed significantly to all of these.

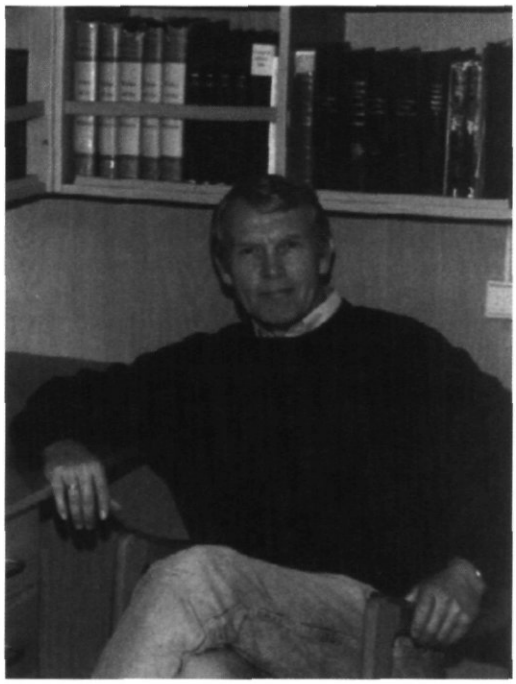
Rather than deal inadequately with a longer list, the description of a single key paper will serve to underline both the remarkable nature and long ramifications of the changes Svend-Aage describes and the importance of his contribution. His 1969 Jokull paper "Hydrographic changes in the waters between Iceland and Jan Mayen in the last decade" provided just such a benchmark in our understanding. During the NAO minimum of the 1960s, a record northerly airflow swept the Norwegian-Greenland Sea, bringing an increasing proportion of Polar Water south to the seas north of Iceland in a swollen East Greenland Current. The East Icelandic Current, which had been

an ice-free Arctic current in 1948–1963, became a Polar Current in 1965–1971 as Malmberg described, transporting drift ice and preserving it.

Aided by active ice formation in these Polar conditions, sea ice extended to the north and east coasts of Iceland, and the 14-year propagation of the "Great Salinity Anomaly" through the Northern Gyre (foreshadowed, then co-authored by Malmberg in 1988) was one dramatic result. Jakobsson has concluded that "the 'Great Salinity Anomaly' has probably generated more variability in fisheries during the last quarter of a Century than any other hydrographic event in recent years"; during its passage, Cushing found a significant reduction in recruitment in 11 out of 15 deepwater fish stocks examined. Its harsh conditions not only closed down the larval drift that had supplied and supported a major cod fishery at West Greenland in the middle decades of the century but also set in train an ecological upheaval in Icelandic waters that changed the species composition of the zooplankton community north of Iceland from boreal to Arctic in character and brought about a progressive dislocation in the traditional migration pattern of the Norwegian spring-spawning herring in the Nordic Seas that has taken 35 years to unfold, as Vilhjalmsson showed in 1997.

It will be a source of satisfaction to Svend-Aage in his retirement that the remarkable physical changes he discovered and described should have had as fundamental an importance to the functioning of the ecosystem in Icelandic waters as it has to our understanding of change in ocean climate at all scales out to those of "global change".

NOTE: The President of Iceland recently conferred the title of "Riddari" on Svend-Aage Malmberg in recognition of his work for his country and for its environment. In the photograph he is seen wearing the medal that was presented to him on that occasion. We extend to him our heartiest congratulations on this well-deserved honour.



Johan Blindheim

When **Johan Blindheim** (born 25 January 1933) joined the Section of Physical and Chemical Oceanography of the Institute of Marine Research (IMR), Bergen, in 1961, he already had experience both as a sailor and fisherman. In parallel with studies in physical oceanography at the University of Bergen, he became responsible for hydrographic fieldwork in Greenland waters as part of the international NORTH WESTLANT surveys. His demand for accurate and precise observations and his interest and knowledge in electronic data-logging and data-processing made him a key person at the IMR from the 1960s to 1970s, the beginning of the "digital age" in marine science.

Johan's responsibilities included calibration and maintenance of oceanographic instruments, planning design and maintenance of the data-logging systems (oceanographic, acoustic, biological) aboard the then new "G. O. Sars" (1970), and he served as the leader of the group that developed and maintained the computer and data-logging systems at the Institute as a whole. Although he must at times have been bored by explaining to his less well-informed colleagues how computer systems worked, he always brought back Arctic char as large and tasty gifts to co-workers when returning from his East Greenland cruises, gifts that were delivered along with stories about the unbelievable amounts and size of fish in the East Greenland rivers and the vast amounts of midges which made fishing a real challenge.

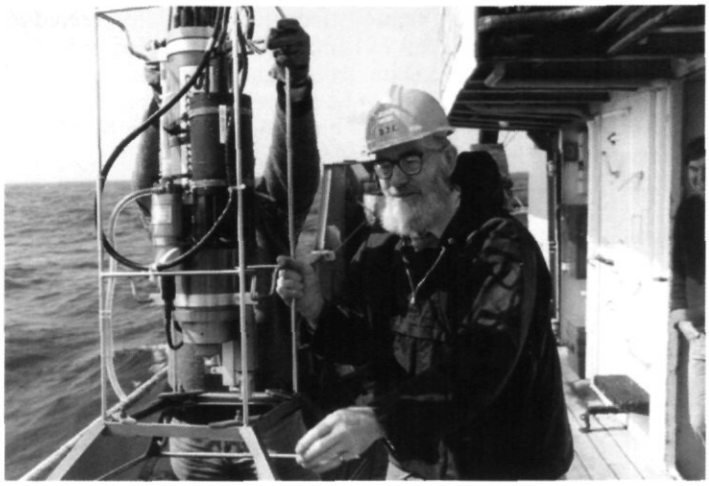
Besides his extensive work in preparing modern and adequate computer facilities for co-workers, Johan managed to conduct his own research. His comprehensive and detailed descriptions of the variability of the hydrography, in particular the Atlantic influence in northern waters from Labrador to the Barents Sea, have been benchmark studies. For a long period he also was his institute's "counterpart" to Jens Smed and responsible for the quality control of data delivered to the Service Hydrographique. During the 1970s he was heavily involved in work for FAO and in 1974/1975 he served as project manager for the Pelagic Fishery Project in Cochin, India.

After returning home, he was given overall responsibility for oceanographic investigations in the Norwegian and Greenland Seas. He strongly advocated the value of the IMR's standard hydrographic sections in the routine monitoring of ocean climate variability on occasions when these were threatened. He was an active participant in the planning group of the IMR research vessel "Johan Hjort" delivered in 1990, where he had the main responsibility for specifying its oceanographic equipment. His colleagues experienced and appreciated his scientific knowledge when he acted as head of the oceanographic division for six years, since in this position he always kept science before bureaucracy.

Johan has also been heavily involved in the administration of marine science at national and international levels, for example in his role as Chair of the ICES Hydrography Committee, as member of the ICES Working Group on Oceanic Hydrography,

where he strongly advocated the necessity of regularity and accuracy in ocean measurements, and as Chair of the ICES Working Group on Marine Data Management.

This continuous involvement in time-series of hydrographic observations, notably in the Nordic Seas, has clearly shaped the topics of his research in the period approaching his retirement (2001) and beyond. With several high-level articles, he has documented and interpreted the decadal scale water-mass changes which are of utmost importance for the highly productive ecosystem of the northern seas and are pivotal to understanding the controls that the processes in the Nordic Seas exert on the North Atlantic climate system. Friends and colleagues from the community very much hope that they can continue to draw on Johan's expertise for many more years to come.



David Ellett

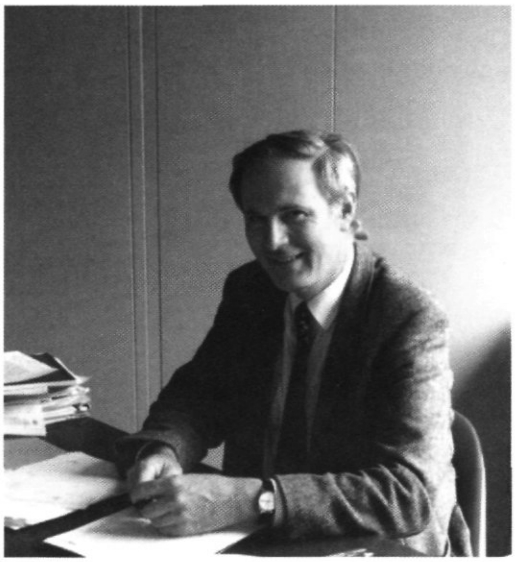
David James Ellett (born 22 July 1934) began his career in ocean science by transfer from the Met Office to the Lowestoft Laboratory in January 1954 as assistant to Lt Cdr J. R. Lumby and Arthur Lee. Over the next decade he learned Atlantic hydrography by participation in wide-ranging cruises to the Barents Sea, North Sea, Irish Sea, and Atlantic, including, notably, the ICES Faroe—Iceland Overflow Experiment of 1958. With long spells on both Irish and UK Weather Ships, this period also saw the beginnings of his life-long involvement with Ocean Weather Ships and their data.

The themes of David's career can be traced from the research interests of his two mentors. Arthur Lee had begun his own career in 1948 with the amazing events of the "Warming in the North" when such a protracted wave of warmth passed though the Atlantic subpolar gyre as to influence the global mean temperature curve. Jack Lumby and Haakon Mosby of Norway had been fastest to react when in 1946 the International Civil Aviation Organization set up a committee to see how the North Atlantic Ocean Weather Stations could be used for oceanographic investigations; the former set up hydrographic sampling en route and on station at OWS "India", "Juliett", and "Kilo", the latter at OWS "Mike" and "Alpha". Couple these influences to the shift in UK fisheries hydrography from distant to home waters in the 1960s and early 1970s and you have the essential "building blocks" of David's career in ocean variability west of Britain.

The Rockall Trough was to be David's main working area and interest to the end of his career, bringing a succession of new insights to what had so long been a data desert; the so-called "shadow of Europe". His collaboration with the Dunstaffnage Laboratory began when he sailed with SMBA aboard RRV "Challenger" for the second ICES Overflow Survey in 1973. This led to his secondment in 1975 and ultimately to his transfer to Oban. Until his official retirement in 1994, he thoroughly explored these waters, deploying the first long-term current-meter moorings in the Trough from 1975, planning then participating in the JASIN Air–Sea Interaction Experiment in 1978, recovering the first unequivocal evidence of a Slope Current west of Scotland in 1979, and making the first direct measurements of overflow crossing the Wyville-Thomson Ridge in 1987/1988.

Many campaigns, but one suspects that David would have derived greatest satisfaction from being designated (1992–1995) a Data Quality Evaluator for WOCE, from the adoption by the community of the term the "Ellett Line" for his repeat hydro-section across the Rockall Trough, and from the use of its time-series to record the arrival-time of particular vintages of Labrador Sea Water, thus establishing for the first time their trans-Ocean spreading rates. As he happily admitted, he was first and foremost a "watermass man". In 1997 he shared the Oceanography Prize of the Society for Underwater Technology with John Gould for his work.

Though unable to join us in Edinburgh through ill health, David will have known better than most of the high esteem in which he was held by the marine science community. Sadly he passed away on 5 October 2001.



Leo Otto

Dr Leonard Otto (born 24 September 1929) received his academic education in physics at the Delft Technical University, from which he graduated in 1955. While on military service with the Royal Dutch Navy he worked on infrared detection systems. In 1957 he entered the Oceanography Department at the Royal Netherlands Meteorological Institute and participated in campaigns on board the submarine HMS "Walrus" in the Caribbean and the Eastern Pacific, carrying out gravity measurements with the famous Vening Meinesz pendulum instrument. These were part of the Dutch Gravity Expeditions of 1948–1958 with their final publication by the National Geodetic Commission in 1960.

Back to the surface, Leo was engaged in the estuarine and North Sea hydrography at KNMI with special interest in optical tracers. Among the many results were the analysis and descriptions of the long-term oceanographic observations at the Netherlands lightvessels in the North Sea for the period 1910–1939 (published 1964) and also his doctoral thesis on the oceanography of the Ria de Arosa, northwest Spain (1975).

This work led into Leo's active interest in the ICES Hydrography Committee and in North Sea projects like JONSDAP (Joint North Sea Data Acquisition Programme). He was in charge of the ICES Study Group on Flushing Times of the North Sea, which provided the physical base for the then much debated issues of dumping industrial wastes in the North Sea. He played an important role in raising political awareness for the need to continue the oceanographic observations at the North Atlantic Ocean Weather Stations when the aviation agencies stopped their support, and he managed to maintain a Dutch contribution to OWS "Mike" for the years beyond.

In his period as Chair of the Hydrography Committee from 1980 to 1982, Leo succeeded in providing effective support for the Service Hydrographique. The annual meetings when he held the chair were at a high scientific and social level.

In 1980 Leo took office with the Netherlands Institute of Sea Research in Texel and became active in the organization of the Dutch observational programmes in North Atlantic hydrography. It was in particular with the World Ocean Circulation Experiment in its initial phase that he fruitfully merged national and ICES interests for this core activity in contemporary oceanography.

Leo retired from his official duties in 1994. He is now following his interest in the history of oceanography as exemplified by his co-authoring a contribution on the Dutch involvement in fisheries research prior to and within early ICES. His friends and colleagues in the ICES community wish him all the best and will keep looking out for his further contributions to our field.

Continued overleaf

Despite the inadequacy of these few remarks to describe such very different people, it is hoped at least that a common thread shows through: namely, that each has been concerned with maintaining the time-series, which are the only means we have of determining if change has taken place in our environment, of assessing its cause, and of identifying its effects on the ecosystem. In other words, the goals that Hjort's ICES had in setting up *Annales Biologiques* in the first place.

The ICES Symposium on Hydrobiological Variability in the ICES Area, 1990–1999, was held at the Royal College of Physicians in Edinburgh, 8–10 August 2001. Scientifically, the "2nd Decadal Symposium" was highly successful, attracting 155 participants and a full programme of 42 selected talks and 55 posters over three days to describe the variability of the plankton, fish, ocean, and atmosphere of the ICES Area during the 1990s. Following a selection and review process conducted by an Editorial Panel, the great majority of the contributions to the meeting were revised for publication in the current volume under the guidance of the Chair of the Panel, William Turrell, and the editors: Alicia Lavin, Kenneth F. Drinkwater, Michael St John, and Jennifer Watson. It is now for the ICES Council to decide whether the provision of a "state description" of the ICES Area at decadal intervals as represented by these proceedings will continue to meet their purpose and budget as a replacement for the *Annales Biologiques.*

The present volume has been organized as follows; the oral presentations are represented by full papers, followed by extended abstracts describing the poster presentations. Manuscripts in each of these two sections are organized first by subject (General Ocean Climate, Regional Ocean Climate, Plankton Communities, Fish Populations), then by geographical region. The convention currently in use by the ICES Annual Ocean Climate Summary has been used, whereby the regional descriptions are presented roughly following the path of the sub-polar gyre in the North Atlantic, commencing west of Greenland.

Robert R. Dickson: CEFAS, Lowestoft Laboratory, Lowestoft, Suffolk NR33 0HT, England, UK. Jens Meincke: Institut für Meereskunde der Universität Hamburg, D-22529 Hamburg, Germany. William Turrell: FRS Marine Laboratory, PO Box 101, Victoria Road, Aberdeen AB11 9DB, Scotland, UK.

References

Dickson, R. R., Mälkki, P., Radach, G., Sætre, R., and Sissenwine, M. P. 1992. Hydrobiological Variability in the ICES Area, 1980–1989. Proceedings of an ICES Symposium held in Mariehamn, 5–7 June 1991. ICES Marine Science Symposia, 195. 514 pp.

Hjort, J. 1943. Annales Biologiques, 1: 5–9. Copenhagen.

Jones, P. D. 2003. The decade of the 1990s over the Atlantic in comparison with longer instrumental and palaeoclimatic records. ICES Marine Science Symposia, 219: 25–31. (This volume).

ICES Marine Science Symposia, 219: 13. 2003

List of referees

The following scientists kindly contributed their expertise as referees for the articles submitted to this volume on "Hydrobiological Variability in the ICES Area, 1990–1999".

Aken, H. van
Blanchard, F.
Brander, K.
Buch, E.
Colbourne, E.
Colijn, F.
Dickey-Collas, M.
Dickson, R. R.
Dooley, H. D.
Fennel, W.
Gaard, E.
Hansen, B.
Harris, R.
Holliday, P. N.
Jones, P.
Lazier, J. R.
Loeng, H.
Malmberg, S.-A.
Meincke, J.
Melle, W.
Möllmann, C.
Ozhigin, V.
Planque, B.
Pollard, R. T.
Porteiro, C.
Schrum, C.
Skreslet, S.
Stein, M.
Valdés, L.
White, M.

A. Papers Presented at the Symposium

ICES Marine Science Symposia, 219: 15–24. 2003

The North Atlantic Oscillation and the ocean's response in the 1990s

Robert R. Dickson and Jens Meincke

Dickson, B., and Meincke, J. 2003. The North Atlantic Oscillation and the ocean's response in the 1990s. – ICES Marine Science Symposia, 219: 15–24.

The North Atlantic Oscillation (NAO) is the dominant recurrent mode of atmospheric behaviour in the North Atlantic sector, dictating much of the climate variability from the eastern seaboard of the United States to Siberia and from the Arctic to the subtropical Atlantic, especially during boreal winter. During the 1990s, the behaviour of the NAO became extreme in two main ways, both of which had deep-reaching effects on Atlantic hydrography and on the marine ecosystem. First, in the early 1990s (1989–1995 approximately), the NAO Index evolved to its most extreme positive state in a 175-year instrumental record, following a long if irregular amplification over the previous three decades. Then, after a brief return to extreme NAO-negative values in 1996, the NAO dipole pattern in sea-level pressure (slp) showed some tendency to shift eastward as the Index recovered to more positive values. Through the associated variability in the intensity of open-ocean deep convection, in the production-rates and characteristics of the main convectively formed mode waters, in the freshwater accession to the Nordic Seas and in the hydrography of the dense northern overflows, these extreme trends in NAO behaviour have been associated with radical effects throughout the water column of the North Atlantic. The evidence for this is described.

Keywords: climate change, hydrographic change, North Atlantic Oscillation, ocean circulation, overflow.

R. R. Dickson: Centre for Environment, Fisheries and Aquaculture Science, Lowestoft NR33 OHT, Suffolk, UK [e-mail: r.r.dickson@cefas.co.uk]. J. Meincke: Institut für Meereskunde, Universität Hamburg, Troplowitzstrasse 7, D-22529, Hamburg, Germany [e-mail: meincke@meer.ijm.uni-hamburg.de].

Introduction

The NAO in the 1990s

The period under review is a most unusual one in the climatic history of the North Atlantic, one in which the NAO Index evolved to extreme positive values unprecedented in the instrumental record (Figure 1, updated from Hurrell, 1995a). The NAO is not of course the only source of variability in Atlantic climate; it accounts for about one-third of the variance in Atlantic sea-level pressure (slp) during December to March. And the NAO pressure pattern does not simply change sign as it switches from one extreme state to the other; the chaotic nature of the atmospheric circulation means that at most times there are significant local departures from the idealized NAO pattern. However, the importance of the recent unprecedented long-term shift in the NAO lies in the wide range of variables attributed to it which have the potential to cause change in the marine environment. These include variations in wind speed, latent and sensible heat flux (Cayan, 1992a,b,c), evaporation/precipitation (Cayan and Reverdin, 1994; Hurrell, 1995a), the distribution, prevalence, and intensity of Atlantic storms (Rogers, 1990, 1994, 1997; Hurrell, 1995b; Alexandersson *et al.*, 1998), hence effects on the wave climate (Bacon and Carter, 1993; Kushnir *et al.*, 1997; Carter 1999), sea surface temperature (Cayan, 1992c, Hansen and Bezdek, 1996), the strength of the Labrador Current (Myers *et al.*, 1989), the characteristics and distribution of water masses (Lazier, 1995; McCartney *et al.*, 1997; Joyce and Robbins, 1996; Houghton, 1996; Molinari *et al.*, 1997; Sy *et al.*, 1997; Joyce *et al.*, 1999; Curry *et al.*, 1998; Curry and McCartney, 2001), the extent of the marginal ice zone (Fang and Wallace, 1994; Mysak *et al.*, 1996; Deser *et al.*, 2000), Davis Strait ice volume (Deser and Blackmon, 1993), the iceberg

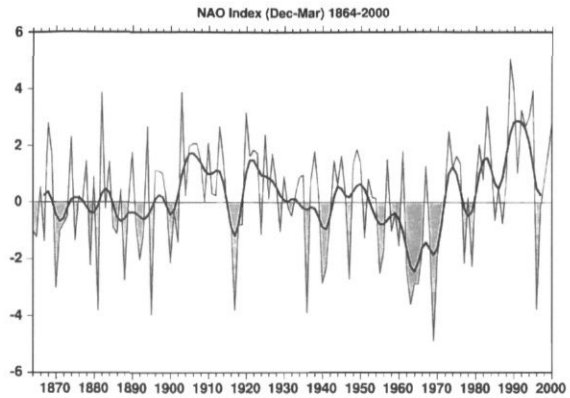


Figure 1. Winter (December–March) index of the NAO based on the difference of normalized sea level pressure (slp) between Lisbon, Portugal, and Stykkisholmur/Reykjavik, Iceland from 1864 through 2000. The indicated year corresponds to January (e.g. 1950 is December 1949 to March 1950). The average winter slp data at each station were normalized by division of each seasonal pressure by the long-term mean (1864–1983) standard deviation. The heavy solid line represents the index smoothed to remove fluctuations with periods less than 4 years.

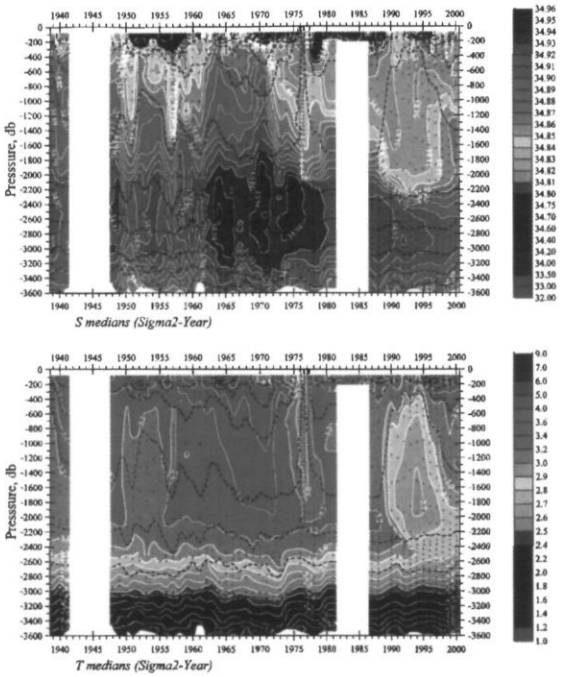


Figure 2. Changes in the salinity (upper panel) and potential temperature (θ; lower panel) of the water column in the Central Labrador Sea over the complete period of the hydrographic record since 1938. The data set was selected to lie within the 3300 m isobath of the Labrador Sea, and the plots represent the median values of vertical property profiles, binned according to σ_2 density intervals. Kindly provided by Igor Yashayaev, Bedford Institute of Oceanography, Dartmouth, N.S., Canada, pers. comm.

flux past Newfoundland (Drinkwater, in Rhines, 1994), and the intensity of deep convection at the main Atlantic sites (Greenland Sea, Labrador Sea, and Sargasso; Dickson *et al.*, 1996; Talley, 1996; Dickson, 1997; Joyce *et al.*, 2000).

It is beyond the scope of this work to document all of these changes as they occurred during the 1990s. In the sections which follow, we focus on a subjective selection of four chains of response which best illustrate the full-ocean and full-depth nature of these events.

1. Spin-up of the North Atlantic gyre circulation

In our first example, we highlight the radical interannual and interdecadal changes in the production of the convectively formed mode waters of the West Atlantic (Labrador Sea Water (LSW) and '18-Degree Water') which Dickson *et al.* (1996) suggest to be part of a coordinated pan-Atlantic pattern of convective activity, driven by the changing NAO. Following the trend in the NAO Index, convective activity at all three main sites has evolved over decades between opposite extrema. From the NAO minimum of the 1960s, when the ventilation of the Greenland Sea and Sargasso was at a maximum and that of the Labrador Sea was tightly capped, convective activity evolved towards the opposite extreme state in the early 1990s, in which convection in the Greenland Sea and Sargasso was suppressed but vertical exchange in the Labrador Sea was reaching deeper than previously observed.

The mechanism is thought to involve the sort of change in the distribution of Atlantic winter storm activity that has long been associated with opposite extreme states of the NAO (Rogers, 1990), and which latterly brought an intense storminess and a record northwesterly windstress to the Labrador Sea during winters of the early 1990s. The result was intensifying and deepening ventilation of the Labrador Sea, with a progressive cooling and freshening of LSW into the 1990s (Figure 2, from Igor Yashayaev, pers. comm.), and ultimately, during the deepest-reaching convection since 1992, to an increase in LSW density as convection began to excavate the cold but saline sublayer of North Atlantic Deep Water (Dickson *et al.*, 1996). Thus in the early 1990s LSW was fresher, colder, and denser than at any other time in the history of deep measurements in the Labrador Sea. From 1966 to 1992, in what we believe to be the largest change in the modern instrumental oceanographic record, the overall freshening of the water column of the Labrador Sea was equivalent to mixing-in an extra

6 m of freshwater at the sea surface (7 m if we extend the period to 1994), and its cooling has been equivalent to a loss of 8 W m^{-2} continuously for 26 years (Lazier, 1995). (Beneath the convective layer, the freshening by ≈ 0.01 per decade over the past three to four decades, apparently still continuing (Figure 2), reflects the recent large-scale freshening of the upper Nordic Seas transferred via the dense northern overflows through Denmark Strait and the Faroe Bank Channel; see below. As the net result of both these changes, the steric height in the central Labrador Sea in the mid-1990s was typically 6–9 cm lower than in the late 1960s).

These changes in the mode water of the Labrador Sea have a value in identifying the rates and pathways by which LSW spreads across the basin (e.g. Sy *et al.*, 1997]. However, their major importance is likely to lie in their influence on the Atlantic gyre circulation itself. As Curry and McCartney (2001) point out, the main North Atlantic Current is driven by the gradient of potential energy anomaly (PE') across the mutual boundary between the subtropical and subpolar gyres. Since PE' reflects the vertical density structure and heat content of the upper ocean to well below the wind-driven layer, it follows that coordinated changes of opposite sign in the production and characteristics of the mode waters in each gyre will have the potential to drive deep-seated changes in the PE' gradient and hence in the strength of the Atlantic gyre circulation. And if these changes in the density and heat content of mode waters are attributable to the NAO, then the amplification of the NAO to extreme values over the past three or four decades is likely to have been followed by a corresponding multi-decadal spin-up of the Atlantic gyre circulation.

From the observed PE' differences between the centres of the two gyres, Curry and McCartney calculate that the long-term increase in the NAO Index to the mid-1990s was accompanied by a 30% increase in the 0–2000 dbar east-going baroclinic mass transport along the gyre:gyre boundary, from 50 Mts^{-1} (= Sv = $10^6 m^3 s^{-1}$) in 1970 to 65 Mts^{-1} in the mid-1990s. Both subpolar and subtropical gyres contributed equally to the changes in their transport index (shown schematically in Figure 3). Thus, in response to the NAO, the North Atlantic gyre circulation during the period under review is likely to have been at its strongest for more than a century.

2. Altered patterns of exchange with the Nordic Seas during the 1990s

Though their wider influence is certainly regulated by the gaps and passageways that form their connections to neighbouring seas, the Nordic Seas are potentially important as a source of change for both the climatically sensitive Arctic Ocean and for the northern overflows which form the deep south-going limb of the meridional overturning circulation (MOC). It is worth recording, then, that over much of the water column the hydrographic character of these seas during the 1990s was beyond the range of our past experience; and that in one way or another these extreme anomalies appear to have arisen through a changing balance, sense, or pattern of "exchange". We note four changes in particular.

The 1990s were remarkable both for our increased ability to measure or estimate the Atlantic inflow to Nordic Seas and for the evidence of change that these studies revealed. Modern estimates based on direct measurements (e.g. Hansen and Osterhus, 2000; Orvik *et al.*, 2001) describe two main branches of inflow to the Norwegian Sea carrying a total mean transport of order 7 Sv (a third inflow of order 1 Sv passes north to the west of Iceland). The eastern branch appears as a narrow, topographically trapped current carrying order 4 Sv northward

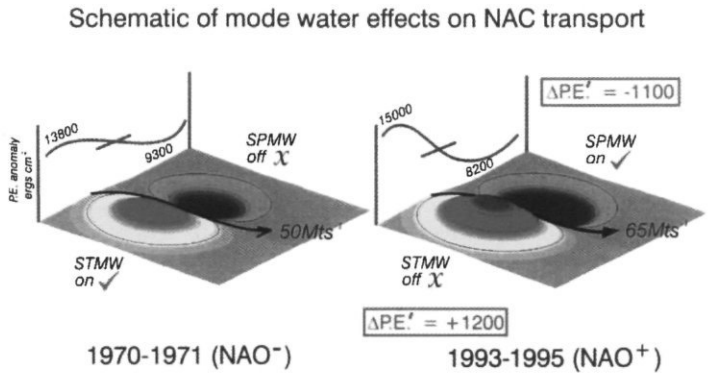


Figure 3. Schematic of mode water effects on the North Atlantic gyre circulation during opposite extreme states of the NAO. Based on the analysis by Curry and McCartney (2001)

against the upper continental slope. The offshore branch takes the form of an unstable frontal jet about 400 m deep and is less well measured in consequence, carrying an estimated transport of order 3 Sv into the central Norwegian Sea.

These two inflow streams thus carry only a small fraction of the Atlantic Water transport brought east by the North Atlantic Current and the variations in inflow, at least for the main branch passing through the Faroe–Shetland Channel, are ascribed to changes in the local windfield rather than to the large-scale changes in the Atlantic gyre circulation, just described (section 2.3). As the dominant mode of slp variability in the Atlantic sector, the NAO can be expected to be implicated in these changes, and in fact specific associations with NAO variability have been described for the inflow and subsequent northward transport of Atlantic Water through the eastern Norwegian Sea.

First, using a box inverse method, Dye (1999) uses the century-long hydrography from the Faroe–Shetland and Nolso–Flugga standard sections to identify long-term changes in the upper layer transport through the Channel, continuously since 1946, discontinuously before that. Perhaps because the box inverse method does not, in this case, give complete access to the barotropic component, the transports calculated are no more than half of the order 4 Sv that we believe passes north along the Scottish Continental Slope. However, this analysis does demonstrate a clear association between inflow and the NAO, with the upper-layer transport increasing steadily by a little more than 1 Sv after the mid-1960s, in parallel with the NAO Index; the Faroe–Shetland through-flow (or at least this component of it) was at a century-long maximum in the early 1990s. The hydrographic analysis of data from the Svinoy Section by Mork and Blindheim (2000) would appear to support this conclusion. They find that the NAO Index is closely associated with the temperature, salinity, and transport variations on this Section, which intercepts the inflow some 350 km further north at 62°–64°40′N. They suggest that since 1978 (thus covering much of the recent long-period change in the NAO Index) the transport through the whole section has increased by 1.1 Sv, mostly in the eastern branch. The current may also have narrowed. Using the 35 isohaline as a proxy for its westward extent, Blindheim *et al.* (2000) show that the width of the Norwegian Atlantic Current (NwAC) at 65° 45′N has been closely (inversely) correlated with the winter NAO Index since 1963 ($r = 0.86$ for a 2-year delay). Since NAO-positive conditions are associated with a greatly strengthened southerly airflow west of Norway (see Dickson *et al.*, 2000, their Figure 2e), these changes in the transport and width of the NwAC are both perhaps in the expected sense.

Upper-ocean temperatures in the Nordic Seas have also reflected the recent extreme amplification of the NAO. During winters of positive NAO index, the northeastward extension of Atlantic winter storm activity to the Nordic Seas together with the outflow of cold and dry air from the Canadian Arctic results in broadscale cooling across Atlantic mid-latitudes from the Davis Strait and West Greenland Banks across the Labrador and Irminger Seas to Iceland, Faroes, and much of the Nordic Seas. By contrast, as already mentioned, the warm, moist southerly airflow that is directed along the eastern boundary of the North Atlantic under these NAO-positive conditions is held responsible for driving a warmer (Dickson *et al.*, 2000), stronger (Dye, 1999; Mork and Blindheim, 2000; Orvik *et al.*, 2001), and probably narrower (Blindheim *et al.*, 2000) flow of Atlantic Water northwards to the Barents Sea and Arctic Ocean (Quadfasel, *et al.* 1991; Tereschenko, 1996; Grotefendt *et al.*, 1998), resulting in very warm SSTs west of Norway along the domain of the Norwegian Atlantic Current despite a parallel increase in windspeeds there. The rising trend and interannual variability in the NAO Index since the 1960s is for this reason reflected in a similar rising trend in upper-ocean temperatures in the eastern Fram Strait over the past few decades (Figure 4A, B, updated from Dickson *et al.*, 2000) and it will be suggested below that we can trace the propagation of this characteristic temperature pattern around the boundary of the Nordic Seas to the Denmark Strait and from there into the abyssal layers of the Labrador Sea.

A third notable change in these waters during the period under review is a large-scale, large amplitude freshening that has taken place in the upper 1–1.5 km of the Nordic Seas over the past three or four decades. Once again the cause is largely attributed to the amplifying NAO, but with a variety of area-specific mechanisms: (a) The direct export of sea ice from the Arctic Ocean is one such cause (Vinje *et al.*, 1998; Kwok and Rothrock, 1999). A combination of current measurements, upward-looking sonar, and satellite imagery reveals that the annual efflux of ice through the western Fram Strait increased with the NAO to a record volume flux of 4687 km^3 $year^{-1}$ in 1994–1995. Although the relationship is not robust in the longer term, each 1-sigma increase in the NAO Index since 1976 has been associated with an approximately 200 km^3 increase in the annual efflux of ice to the Greenland Sea (Dickson *et al.*, 2000). (b) Throughout the marginal ice zone of the Nordic Seas, a steady decrease in the local late-winter production of sea ice has accompanied the increasing trend in the NAO over the past 40 years (Deser *et al.*, 2000). (c) The extension of storm activity to the Nordic Seas under extreme NAO-positive conditions is calculated to increase precipitation along the Norwegian Atlantic Current by approximately 15 cm per winter compared with the

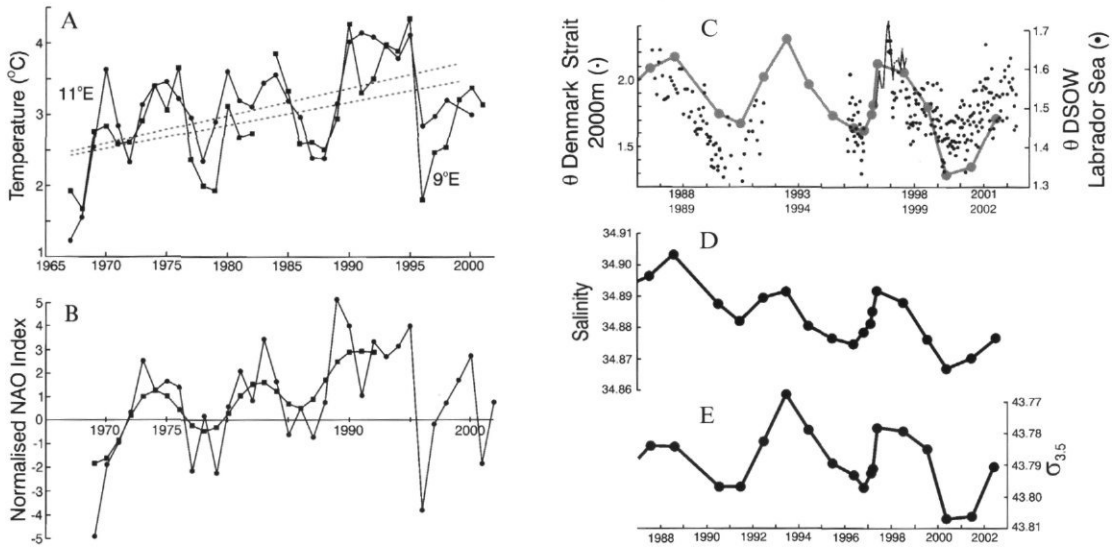


Figure 4. Transfer of a climatic signal from the upper high-latitude ocean to the deep Atlantic. The mean temperatures in the eastern Fram Strait reflect the increased southerly airflow west of Norway associated with NAO-positive conditions. Shown are (A) the 50–500 m mean temperatures (°C) in August–September at 9°E and 11°E on the Sorkapp Section, 76°20'N, 1967–2002, compared with (B) the normalized winter NAO Index (updated from Dickson *et al.*, 1999, 2000). In turn, the temperature of the Denmark Strait overflow 2500 km further south appears to be the lagged reflection of Fram Strait temperatures 3 years earlier. Shown are (C) the 30-day mean temperatures at 2000 m in the overflow core off Angmagssalik SE Greenland (dots). And the temperatures of the descending plume off SE Greenland affect the hydrographic character of the abyssal Labrador Sea a further 1 year later. Shown as circles in (C), (D), (E) are the potential temperature, salinity, and density of the DSOW-derived bottom layer of the Labrador Sea, with time-scales shifted by 1 year.

equivalent NAO-negative conditions (Dickson *et al.*, 2000). Other factors and mechanisms have undoubtedly contributed to the long and gradual but dramatic freshening of the European subarctic seas in recent decades, most of them associated in some way with the amplifying NAO. Blindheim *et al.* (2000) describe a range of factors internal to the Nordic Seas, including an increased freshwater supply from the East Icelandic Current and the narrowing of the salty Norwegian Atlantic Current towards the Norwegian Coast. Thus, while it may not yet be possible to partition the recent freshening of the Nordic Seas into its individual contributory components, it will become clear below that the change is sufficiently widespread and has occurred over a sufficiently deep layer to affect the hydrographic character of both dense overflows crossing the Greenland–Scotland Ridge.

As with the Labrador Sea, a radical interdecadal change in the depth and intensity of open-ocean convection was a fourth major change to affect the Nordic Seas, part of the same coordinated pan-Atlantic pattern of convective activity driven by the changing NAO that we described earlier (Dickson *et al.*, 1996; Verduin and Quadfasel, 1999). From the NAO minimum of the 1960s, the intensity of deep convection in the Greenland Sea became progressively more suppressed as the NAO Index amplified to extreme positive values in the early-to-mid-1990s. At the same time, a steady deepening of intermediate and deep isopycnals in the Greenland Sea from the early 1980s (Boenisch *et al.*, 1997) provides evidence of a collapse of the "domed" density structure in the Greenland Sea as a reduced windstress curl (Jonsson, 1991) supported a less intense cyclonic basin circulation there (Meincke *et al.*, 1992; Rudels and Quadfasel, 1991). Perhaps in compensation there is evidence of an increased influx of deep waters from the Arctic Ocean into the Greenland Sea basin at intermediate depths (Meincke and Rudels, 1995; Meincke *et al.*, 1997).

3. Changes in overflow hydrography: the propagation of the climate signal to the deep Atlantic

The overflow and descent of cold dense water from the sills of the Denmark Strait and Faroe–Shetland Channel is the principal means by which the deep ocean is ventilated and so these overflows are key elements of the global thermohaline circulation (THC). In the period under review, we have evidence that hydrographic variability induced by climate forcing at the surface of the high latitude

ocean is being passed on via both intermediate-depth overflows to affect the hydrographic character of the deep and abyssal ocean south of the Greenland–Scotland Ridge. Two such climate "signals" are apparent.

The transfer of near-surface temperature variability from the upper waters of the eastern Fram Strait to the abyssal Labrador Sea: 30-day means of temperature from the core of the Denmark Strait overflow at ~2000 m off Southeast Greenland have provided evidence of a well-defined multiannual-to-decadal variability (dots, Figure 4C). Following Dickson *et al.* (1999), this pattern of change in overflow temperature appears to correspond to the temperature variability of the upper 500 m of the eastern Fram Strait, some 2500 km upstream and 3 years earlier (Figure 4A). In other words, we believe we see evidence – admittedly from short and gappy records – that the hydrographic character of the overflow waters descending from the Denmark Strait sill (DSOW) may be the lagged reflection of high-latitude climate-forcing of the surface ocean in Fram Strait. Tracking these changes further downstream, we also appear to find a clear correspondence between the temperature at 2000 m in the Denmark Strait Overflow core off Angmagssalik, Southeast Greenland and the temperature, salinity, and density of the abyssal layer of the Labrador Sea a further 1 year later (circles, Figure 4C–E), perhaps an early demonstration of a direct climatic effect on the abyssal limb of the Atlantic Thermohaline Circulation.

Transfer of the multi-decadal freshening signal of the Nordic Seas via both overflows to the deep and abyssal layers of the North Atlantic: Below the convectively formed mode water layer of the Labrador Sea in depths of 2300–3500 m, repeat hydrography has indicated a steady freshening over the past three to four decades. At these depths, beyond the reach of deep convection, such a change cannot be due to local climate forcing. Instead, it appears to reflect the large-scale freshening of the upper 1–1.5 km of the Nordic Seas, already described, transferred to the deep Atlantic via both dense overflows.

Hydrographic sections monitoring the outflow of Norwegian Sea Deep Water and Arctic Intermediate Water (NSDW and NSAIW) through the Faroe–Shetland Channel confirm that salinities have decreased almost linearly by ~0.01 per decade since the mid-1970s (Turrell *et al.*, 1999); and by constructing salinity time-series at intervals along the spreading pathways of both overflows from their sills to the Labrador Sea, Dickson *et al.* (2002) confirm that the entire system of overflow and entrainment that ventilates the deep Atlantic has rapidly freshened over the past four decades. Both dense overflows, therefore, appear to have tapped and delivered to the headwaters of the THC the freshening signal of the upper Nordic Seas. (For changes in overflow transport, see section 5 below.)

4. Eastward shift of the NAO dipole pattern during the late 1990s

Following its long period of amplification, the winter NAO index suddenly underwent a sharp decrease to a short-lived minimum in the winter of 1995–1996 (Figure 1) with radical and recognizable changes in Atlantic sea level, in the poleward transport of heat by ocean currents, in the pattern of the Atlantic gyre circulation, in the storm climate and precipitation regime over northwest Europe, in the efflux of ice from the Arctic, and on cod recruitment. Since that temporary minimum, as the NAO Index recovered towards more positive values, we have noted a new type of NAO behaviour. Comparing the Atlantic sea level pressure anomaly pattern for the early 1990s with those for winters 1999 and 2000, we find that the NAO pattern in these recent winters was displaced slightly towards the east or northeast.

This subtle change had little effect on the subtropical gyre of the Atlantic or along its eastern boundary to the Barents Sea, where there was evidence of the widespread warming we would normally associate with the positive NAO. However, in the northwest Atlantic, this slight eastward retraction of the "normal" NAO pattern made an important difference to the marine climate of the Labrador Sea and West Greenland Banks. Instead of a chill and strong northwesterly airflow promoting cooling there as it did in the early 1990s with intense and deep-reaching convection (to > 2300 m) in the Labrador Sea, we now find that any northwesterly airflow is mainly confined to the east of Greenland so that the Labrador Sea is instead occupied by light or southerly anomaly winds.

Thus reports from the West Greenland Banks in these winters were of continued warmth rather than cooling, and convection in the Labrador Sea remained weak and shallow. The latter change was particularly dramatic. The intense and deep-reaching convection that we have come to associate with NAO-positive conditions not only produces a deep homogeneous LSW water mass, but drives a strong cyclonic circulation in the Labrador Sea. With that stimulus removed, the centre of the Labrador Sea was occupied in these two anomalous winters by a stack of different water masses, reflecting not only the past products of a weakening convection, but the lateral intrusion of other water masses from a variety of sources around the boundary.

This observation (that NAO-positive conditions can locally drive quite different ocean responses depending on the detailed configuration of the associated slp pattern) offers a timely reminder of the limitations of using a simple 2-point pressure difference as our index of NAO behaviour. It may offer a convenient shorthand indication of atmospheric behaviour and ocean response but it may not capture important detail. It remains to be seen whether this eastward shift in the NAO dipole is just further evidence of the chaotic nature of the atmospheric circulation (NAO noise) or part of a more concerted trend in NAO behaviour. Hilmer and Jung (2000) suggest that the centres of maximum interannual variability in slp associated with the NAO have been located further to the east since the late 1970s, and some climate simulations (Ulbrich and Christoph, 2000) suggest that one accompaniment of CO_2 warming will be an eastward or northeastward shift in the locus of the two cells that form the NAO dipole. So it is possible (but not yet "likely") that the more easterly distribution we have experienced in winters 1999 and 2000 may be part of that shift.

5. Issues of NAO forcing in the Atlantic sector: detection, prediction, and change

Of the 13 recurrent atmospheric circulation modes world-wide considered by Barnston and Livesey (1987), the NAO is among the most robust. During the decade under review, the winter NAO attained its most extreme and persistent positive state in the instrumental record and, unsurprisingly, the ocean-atmosphere system reflects this. Century-long extrema were experienced in parameters as diverse as storminess over the Norwegian Sea, the strength of the Atlantic gyre circulation, the depth and intensity of Labrador Sea convection, and the hydrographic character of the northern overflows. All of these changes (and others) are in some way attributable to NAO forcing. And these four cases are enough to explain why the signature of NAO forcing is identifiable from the ocean surface to abyssal depths.

Three main scientific issues remain: (1) detecting the NAO response in our sparse observing system of standard stations and sections, (2) assessing the causes, effects, and predictability of change in the NAO itself, and (3) determining the mutual involvement of the Atlantic's ocean and atmosphere in global change. These issues are not mutually exclusive.

Even with what might be termed 'standard' NAO behaviour, the ocean or ecosystem response is likely to exhibit different degrees of delay, from the local and immediate to the multi-year delays imposed by advection. Very recent model experiments (Eden and Willebrand, 2001) alert us to the probable co-existence of a fast (intra-seasonal) barotropic response and a delayed (time scale 6–8 year) baroclinic response to the same NAO-positive forcing. The difficulties of detecting and tracing the ocean's response in our available record are compounded by the fact that NAO behaviour may not be standard. The slight eastward shift of the NAO dipole pattern in certain winters of the late 1990s (section 5 above) was enough to reverse the cooling and freshening tendency of the Northwest Atlantic mode water in the early 1990s (one of the largest changes in oceanography) and warm the West Greenland Banks, despite a positive NAO Index. Yet some such eastward shift is an anticipated part of NAO behaviour in some simulations (Ulbrich and Christoph, 1999).

'Detection' would thus seem to presuppose some knowledge of how the NAO might vary. In the instrumental record in fact there is little evidence for the NAO to vary on any preferred time scale. Large changes can occur from one winter to the next, and there is also a considerable amount of variability within a given winter season (Nakamura, 1996). This is consistent with the notion that much of the atmospheric circulation variability in the form of the NAO arises from processes internal to the atmosphere, in which various scales of motion interact with one another to produce random (and thus unpredictable) variations (Wallace and Lau, 1985; Lau and Nath, 1991; Ting and Lau, 1993; Hurrell, 1995b).

There are, nonetheless, periods when anomalous NAO-like circulation patterns persist over many consecutive winters, as with the persistent NAO-positive conditions of most of the 1990s. In fact, as already described, the magnitude of the recent upward trend is unprecedented in the observational record (Hurrell, 1995a; Thompson *et al.*, 2000) and, based on reconstructions using palaeoclimate and model data, perhaps over the past several centuries as well (Osborn *et al.*, 1999; Stockton and Glueck, 1999). The question therefore arises as to whether such unusual behaviour is explicable – even predictable. But whether such low frequency (interdecadal) NAO variability arises from interactions of the North Atlantic atmosphere with other, more slowly varying, components of the climate system such as the ocean (McCartney *et al.*, 1997; Rodwell *et al.*, 1999; Mehta *et al.*, 2000; Hoerling *et al.*, 2001), whether the recent upward trend reflects a human influence on climate (Corti *et al.*, 1999; Osborn *et al.*, 1999; Shindell *et al.*, 1999; Ulbrich and Christoph, 1999; Fyfe *et al.*, 1999; Gillett *et al.*, 2000 and in press; Monahan *et al.*, 2000), or whether the longer time scale variations in the relatively short instrumental record simply reflect finite sampling of a purely random process (Wunsch, 1999), is a topic which remains, for the present, unresolved.

The onset of global change adds an additional unknown to NAO variability. The analysis of temperature change by latitude and time (Delworth and Knutson, 2000) appears to show clearly enough that the recent observed warming is global and thus quite distinct from the earlier episode of high latitude warming in our sector during the middle decades of this century. The third IPCC Report concludes more categorically than before that "there is new and stronger evidence that most of the warming observed over the last 50 years is attributable to human activities" (Anon., 2001). And coupled climate models seem to be reaching some kind of consensus that a slowdown of North Atlantic Deep Water (NADW) production will be one outcome. However, the issue of whether such effects are yet evident in our ocean time-series remains open. For the first time, Hansen *et al.* (2001) have been able to couple a moderately long, modern set of direct flow measurements to a half-century of frequent hydrography at OWS M to provide evidence of a 20% decrease in the coldest and densest part ($t < 0.3°C$, $\sigma t > 28.0$) of the overflow from the Faroe Bank Channel since 1950, but the necessary companion data sets on Denmark Strait outflow or on Atlantic inflow to the Nordic Seas are not yet adequate to confirm the point. Overflow hydrography has detected a multi-decadal freshening of both overflows that can be followed into the deep and abyssal layers downstream (Dickson *et al.*, 2002), but we are only just beginning to detect the subtle effects of this change on deep and abyssal density.

Conclusion

In a decade of stark climatic signals, these unresolved issues leave only one conclusion. Our past hydrographic record has provided clear enough evidence of the socio-economic impacts of ocean climate changes in our sector, and our present records are already hinting that certain important global change processes may be controlled or modulated by the oceanic exchanges that connect the Arctic Ocean to the open Atlantic via Nordic Seas. Our observational series must be maintained to keep pace with such changes, and broadened in key locations until present uncertainties are resolved.

References

Alexandersson, H., Schmith, T., Iden, K., and Tuomenvirta, H. 1998. Long-term variations of the storm climate over NW Europe. The Global Ocean Atmosphere System, 6: 97–120.

Anon., 2001. Summary for policymakers. A report of Working Group 1 of the Intergovernmental Panel on Climate Change.

Bacon, S., and Carter, D. J. T. 1993. A connection between mean wave height and atmospheric pressure gradient in the North Atlantic. International Journal of Climatology, 13: 423–436.

Barnston, A. G., and Livesey, R. E. 1987. Classification, seasonality, and persistence of low-frequency atmospheric circulation patterns. Monthly Weather Review, 115: 1083–1126.

Blindheim, J., Borovkov, V., Hansen, B., Malmberg, S. A., Turrell, W. R., and Osterhus, S. 2000. Upper layer cooling and freshening in the Norwegian Sea in relation to atmospheric forcing. Deep-Sea Research I, 47: 655–680.

Boenisch, G., Blindheim, J., Bullister, J. L., Schlosser, P., and Wallace, D. W. R. 1997. Long-term trends of temperature, salinity, density and transient tracers in the central Greenland Sea. Journal of Geophysical Research, 102: 18,553–18,571.

Carter, D. J. T. 1999. Variability and trends in the wave climate of the North Atlantic: a review. *In* Proceedings of the 9th ISOPE Conference, Brest, 30 May to 4 June 1999, Vol. III, pp. 12–18.

Cayan, D. R. 1992a. Latent and sensible heat flux anomalies over the Northern Oceans: the connection to monthly atmospheric circulation. Journal of Climate, 5: 354–369.

Cayan, D. R. 1992b. Variability of latent and sensible heat fluxes estimated using bulk formulae. Atmosphere Ocean, 30: 1–42.

Cayan, D. R. 1992c. Latent and sensible heat flux anomalies over the northern oceans: driving the sea surface temperature. Journal of Physical Oceanography, 22: 859–881.

Cayan, D. R., and Reverdin, G. 1994. Monthly precipitation and evaporation variability estimated over the North Atlantic and North Pacific. *In* Atlantic Climate Change Program. Proceedings of PI's Meeting, Princeton, 9–11 May, pp. 28–32.

Corti, S., Molteni, F., and Palmer, T. N. 1999. Signature of recent climate change in frequencies of natural atmospheric circulation regimes. Nature, 398: 799–802.

Curry, R. G., McCartney, M. S., and Joyce, T. M. 1998. Oceanic transport of subpolar climate signals to mid-depth subtropical waters. Nature, 391: 575–577.

Curry R., and McCartney, M. S. 2001. Ocean gyre circulation changes associated with the North Atlantic Oscillation. Journal of Physical Oceanography. (In press.)

Delworth, T. L., and Knutson, T. R. 2000. Simulation of early 20th century global warming. Science, 287: 2246–2250.

Deser, C., and Blackmon, M. L. 1993. Surface climate variations over the North Atlantic Ocean during winter: 1900–1989. Journal of Climate, 6: 1743–1753.

Deser, C., Walsh, J. E., and Timlin, M. S. 2000. Arctic sea ice variability in the context of recent wintertime atmospheric circulation trends. Journal of Climate, 13: 617–633.

Dickson, R. R. 1997. From the Labrador Sea to global change. Nature, 386: 649–650.

Dickson, R. R., Lazier, J., Meincke, J., Rhines, P., and Swift, J. 1996. Long-term co-ordinated changes in the convective activity of the North Atlantic. Progresss in Oceanography, 38: 241–295.

Dickson, R. R., Meincke, J., Turrell, W. R., Dye, S. R., Yashayaev, I., and Holfort, J. 2002. Rapid freshening of the deep North Atlantic Ocean over the past four decades. Nature, 416: 832–837.

Dickson, B., Meincke, J., Vassie, I., Jungclaus, J., and Osterhus, S. 1999. Possible predictability in overflow from the Denmark Strait. Nature, 397: 243–246.

Dickson, R. R., Osborn, T. J., Hurrell, J. W., Meincke, J., Blindheim, J., Adlandsvik, B., Vigne, T., Alekseev, G., and Maslowski, W. 2000. The Arctic Ocean response to the North Atlantic Oscillation. Journal of Climate, 13: 2671–2696.

Dye, S. 1999. A century of variability of flow through the Faroe–Shetland Channel. Ph.D. thesis. University of East Anglia. 189 pp.

Eden, C., and Willebrand, J. 2001. Mechanism of interannual to decadal variability of the North Atlantic Circulation. Journal of Climate, 14: 2266–2280.

Fang, Z., and Wallace, J. M. 1994. Arctic sea-ice variability on a time-scale of weeks and its relation to atmospheric forcing. Journal of Climate, 7: 1897–1914.

Fyfe, J. C., Boer, G. J., and Flato, G. M. 1999. The Arctic and Antarctic oscillations and their projected changes under global warming. Geophysical Research Letters, 26: 1601–1604.

Gillett, N. P., Allen, M. R., McDonald, R. E., Senior, C. A., Shindell, D. T., and Schmidt, G. A. (in press). How linear is the Arctic Oscillation response to greenhouse gases? Journal of Geophysical Research.

Gillett, N. P., Hegerl, G. C., Allen, M. R., and Stott, P. A. 2000. Implications of changes in the Northern Hemisphere circulation for the detection of anthropogenic climate change. Geophysical Research Letters, 27: 993–996.

Grotefendt, K., Logemann, K., Quadfasel, D., and Ronski, S. 1998. Is the Arctic Ocean warming? Journal of Geophysical Research, 103: 27,679–27,687.

Hansen, D. V., and Bezdek, H. F. 1996. On the nature of decadal anomalies in North Atlantic sea surface temperature. Journal of Geophysical Research, 101: 8749–8758.

Hansen, B., and Osterhus, S. 2000. North Atlantic-Nordic Seas exchanges. Progress in Oceanography, 45: 109–208.

Hansen, B., Turrell, W. R., and Osterhus, S. 2001. Decreasing overflow from the Nordic seas into the Atlantic Ocean through the Faroe–Shetland Channel since 1950. Nature, 411: 927–930.

Hilmer, M., and Jung, T. 2000. Evidence for a recent change in the link between the North Atlantic Oscillation and Arctic sea ice export. Geophysical Research Letters, 27: 989–992.

Hoerling, M. P., Hurrell, J. W., and Xu, T. 2001. Tropical origins for recent North Atlantic climate change. Science.

Houghton, R. W. 1996. Subsurface quasi-decadal fluctuations in the North Atlantic. Journal of Climate, 9: 1363–1373.

Hurrell, J. W. 1995a. Decadal trends in the North Atlantic Oscillation regional temperatures and precipitation. Science, 269: 676–679.

Hurrell, J. W. 1995b. Transient eddy forcing of the rotational flow during northern winter. Journal of Atmospheric Science, 52; 2286–2301.

Jónsson, S. 1991. Seasonal and interannual variability of wind stress curl over the Nordic Seas. Journal of Geophysical Research, 96: C2, 2649–2659.

Joyce, T. M., Deser, C., and Spall, M. A. 2000. On the relation between decadal variability of subtropical mode water and the North Atlantic Oscillation. Journal of Climate, 13: 2550–2569.

Joyce, T. M., and Robbins, P. 1996. The long-term hydrographic record at Bermuda. Journal of Climate, 9: 3121–3131.

Joyce, T. M., Pickart, R. S., and Millard, R. C. 1999. Long-term hydrographic changes at 52 and 66°W in the North Atlantic Subtropical Gyre and Caribbean. Deep-Sea Research II, 46: 245–278.

Kushnir, Y., Cardone, V. J., Greenwood, J. G., and Cane, M. 1997. On the recent increase in North Atlantic wave heights. Journal of Climate, 10: 2107–2113.

Kwok, R., and Rothrock, D. A. 1999. Variability of Fram Strait ice flux and the North Atlantic Oscillation. Journal of Geophysical Research – Oceans, 104: 5177–5189.

Lau, N. C., and Nath, M. J. 1991. Variability of the baroclinic and barotropic transient eddy forcing associated with monthly changes in the midlatitude storm tracks. Journal of Atmospheric Science, 48: 2589–2613.

Lazier, J. R. N. 1995. The salinity decrease in the Labrador Sea over the past thirty years. *In* Natural Climate Variability on Decade-to-Century Time Scales, pp. 295–304. Ed. by D. G. Martinson, K. Bryan, M. Ghil, M. M. Hall, T. M. Karl, E. S. Sarachik, S. Sorooshian, and L. D. Talley. National Academy Press, Washington, D.C. 644 pp.

McCartney, M. S., Curry, R. G., and Bezdek, H. F. 1997. The interdecadal warming and cooling of Labrador Sea Water. ACCP Notes, IV (1): 1–11.

Mehta, V. M., Suarez, M. J., Manganello, J. V., and Delworth, T. L. 2000. Oceanic influence on the North Atlantic Oscillation and associated Northern Hemisphere climate variations: 1959–1993. Geophysical Research Letters, 27: 121–124.

Meincke, J., Jonsson, S., and Swift, J. H. 1992. Variability of convective conditions in the Greenland Sea. ICES Marine Science Symposium, 195: 32–39.

Meincke, J., and Rudels, B. 1995. Greenland Sea Deep Water: a balance between convection and advection. Nordic Seas Symposium., Hamburg, March 1995. Extended Abstract Volume, University of Hamburg, 143–148.

Meincke, J., Rudels, B., and Friedrich, H. J. 1997. The Arctic Ocean–Nordic Seas thermohaline system. ICES Journal of Marine Science, 54: 283–299.

Molinari, R. L., Mayer, D., Festa, J., and Bezdek, H. 1997. Multi-year variability in the near-surface temperature structure of the midlatitude western North Atlantic Ocean. Journal of Geophysical Research, 101: 1183–1197.

Monahan, A. H., Fyfe, J. C., and Flato, G. M. 2000. A regime view of Northern Hemisphere atmospheric variability and change under global warming. Geophysical Research Letters, 27: 1139–1142.

Mork, K. A., and Blindheim, J. 2000. Variations in the Atlantic inflow to the Nordic Seas, 1955–1996. Deep-Sea Research I, 47: 1035–1057.

Myers, R. A., Helbig, J., and Holland, D. 1989. Seasonal and interannual variability of the Labrador Current and West Greenland Current. ICES CM 1989/C: 16. 18 pp. (mimeo).

Mysak, L. A., Ingram, R. G., Wang, J., and van der Baaren, A. 1996. The anomalous sea-ice extent in Hudson Bay, Baffin Bay and the Labrador Sea during three simultaneous NAO and ENSO episodes, Atmosphere – Ocean, 34: 313–343.

Nakamura, H. 1996. Year-to-year and interdecadal variability in the activity of intraseasonal fluctuations in the Northern Hemisphere wintertime circulation. Theoretical and Applied Climatology, 55: 19–32.

Orvik, K. A., Skagseth, O., and Mork, M. 2001. Atlantic inflow to the Nordic Seas: current structure and volume fluxes from moored current meters, VM–ADCP and SeaSoar–CTD observations, 1995–1999. Deep-Sea Research I, 48: 937–957.

Osborn, T. J., Briffa, K. R., Tett, S. F. B., Jones, P. D., and Trigo, R. M. 1999. Evaluation of the North Atlantic oscillation as simulated by a climate model. Climate Dynamics, 15: 685–702.

Quadfasel, D., Sy, A., Wells, D., and Tunik, A. 1991. Warming in the Arctic. Nature, 350: 385.

Rhines, P. 1994. Climate change in the Labrador Sea, its convection and circulation. *In* Atlantic Climate Change Program: Proceedings of the PI's Meeting, pp. 85–96. Princeton, 9–11 May.

Rodwell, M. J., Rowell, D. P., and Folland, C. K. 1999. Oceanic forcing of the wintertime North Atlantic oscillation and European climate. Nature, 398: 320–323.

Rogers, J. C. 1990. Patterns of low-frequency monthly sea level pressure variability (1899–1986) and associated wave cyclone frequencies. Journal of Climate, 3: 1364–1379.

Rogers, J. C. 1994. Atlantic storm track variability and the North Atlantic Oscillation. *In* Atlantic Climate Change Program: Proceedings of the PI's Meeting, pp. 20–24. Princeton, 9–11 May.

Rogers, J. C. 1997. North Atlantic storm track variability and its association to the North Atlantic Oscillation and climate variability of Northern Europe. Journal of Climate, 10: 1635–1647.

Rudels, B., and Quadfasel, D. 1991. Convection and deep water formation in the Arctic Ocean–Greenland Sea system. Journal of Marine Systems, 2: 435–450.

Shindell, D. T., Miller, R. L., Schmidt, G., and Pandolfo, L. 1999. Simulation of recent northern winter climate trends by greenhouse-gas forcing. Nature, 399: 452–455.

Stockton, C. W., and Glueck, M. F. 1999. Long-term variability of the North Atlantic oscillation (NAO). *In* Proceedings of the American Meteorological Society Tenth Symposium, Global Change Studies, 11–15 January, Dallas, TX, pp. 290–293.

Sy, A., Rhein, M., Lazier, J. R. N., Koltermann, K. P., Meincke, J., Putzka, A., and Bersch, M. 1997. Surprisingly rapid spreading of newly formed intermediate waters across the North Atlantic Ocean. Nature, 386: 675–679.

Talley, L. D. 1996. North Atlantic circulation and variability, reviewed for the CNLS Conference, Los Alamos, May 1995. Physica D 98, 625–646.

Tereshchenko, V. V. 1996. Seasonal and year-to-year variations of temperature and salinity along the Kola meridian transect. ICES CM 1996/C: 11. 24 pp. (mimeo).

Ting, M., and Lau, N. C. 1993. A diagnostic and modeling study of the monthly mean wintertime anomalies appearing in an 100-year GCM experiment. Journal of Atmospheric Science, 50: 2845–2867.

Thompson, D. W. J., Wallace, J. M., and Hegerl, G. C. 2000. Annular modes in the extratropical circulation Part II: Trends. Journal of Climate, 13: 1018–1036.

Turrell, W. R., Slesser, G., Adams, R. D., Payne, R., and Gillibrand, P. A. 1999. Decadal variability in the composition of Faroe–Shetland Channel bottom water. Deep-Sea Research I, 46: 1–25.

Ulbrich, U., and Christoph, M. 1999. A shift of the NAO and increasing storm track activity over Europe due to anthropogenic greenhouse gas forcing. Climate Dynamics, 15: 551–559.

Verduin, J., and Quadfasel, D. 1999. Long-term temperature and salinity trends in the central Greenland Sea. *In* European Sub-Polar Ocean Programme II. Ed. by E. Jansen. Final Scientific Report.

Vinje, T., Nordlund, N., and Kvambekk, A. 1998. Monitoring ice thickness in Fram Strait. Journal of Geophysical Research, 103: 10437–10449.

Wallace, J. M., and Lau, N. C. 1985. On the role of barotropic energy conversions in the general circulation. Advances in Geophysics, 28A: 33–74.

Wunsch, C. 1999. The interpretation of short climate records, with comments on the North Atlantic and Southern Oscillations. Bulletin of the American Meteorological Society, 80: 257–270.

ICES Marine Science Symposia, 219: 25–31. 2003

The decade of the 1990s over the Atlantic in comparison with longer instrumental and palaeoclimatic records

P. D. Jones

Jones, P. D. 2003. The decade of the 1990s over the Atlantic in comparison with longer instrumental and palaeoclimatic records. – ICES Marine Science Symposia, 219: 25–31.

The North Atlantic Oscillation (NAO) is the principal mode of variability in surface pressure over the North Atlantic/European sector of the Northern Hemisphere (NH). The mode is particularly dominant during the winter season, explaining part of the surface temperature and precipitation variability over the region. Recent winter values of the NAO during the late 1980s and 1990s have been strongly positive, giving Northern Europe a succession of mild winters. Long instrumental records and palaeoclimatic reconstructions of the NAO indicate several earlier periods of comparable values over the past 500 years. The rise in NAO values from the 1960s to the 1990s, however, does appear unique in the long records. Although the NAO is capable of explaining some of the variability of surface temperature change during the 1990s in the winter season, it cannot explain the warming of the other seasons as the NAO influence is weak and the NAO has been less anomalous in these seasons.

Keywords: Atlantic, climate change, North Atlantic Oscillation, pressure, temperature.

P. D. Jones: Climatic Research Unit, School of Environmental Sciences, University of East Anglia, Norwich NR4 7TJ, UK [tel: +44 1603 592090; fax: +44 1603 507784; e-mail: p.jones@uea.ac.uk]. Correspondence to P. D. Jones.

Introduction

The strong anti-phase relationship between monthly pressure series from Iceland and the Azores was first referred to by Walker (1924) as the North Atlantic Oscillation (NAO). The traditional index has been calculated from the difference between normalized monthly pressures at Ponta Delgada (Azores) and Stykkisholmur (Iceland). These locations were chosen originally as they were the sites with the longest readily available series of pressure observations from the two centres-of-action that represent the phenomenon.

The NAO value is a measure of the westerly wind strength over the North Atlantic and the western half of Europe. Winter values have the strongest influence on surface climate features in the region. Positive values of the NAO, implying stronger westerlies, bring milder weather to Europe, north of about 40°N and vice versa (see Hurrell, 1995 and Osborn *et al.*, 1999). South of 40°N, the relationship is the inverse, particularly over the southern Balkans, Turkey and parts of the Middle East and over southern Spain and northwestern Africa. The NAO also influences the climate over eastern North America, with positive values associated with warmer winters over the southeastern United States and cooler winters over eastern Canada and western Greenland. The four main centres of influence have been extensively studied since Hurrell (1995) and referred to as a quadropole pattern by Slonosky and Yiou (2001). Positive NAO values are also associated with higher amounts of precipitation in Europe north of 45°N and reduced precipitation to the south (Hurrell, 1995).

In this article, several measures of the NAO are compared over as long periods as possible, including two palaeoclimatic reconstructions. Recent changes of the NAO have been unusual, and the anomalous nature of the 1990s with respect to the longer records is discussed. The strength of the relationships between the NAO and surface climate variability of the North Atlantic/European region is then assessed.

Longer records of the NAO

Figure 1 shows several winter (December to February) NAO indicators back to the beginning of instrumental and documentary historical records.

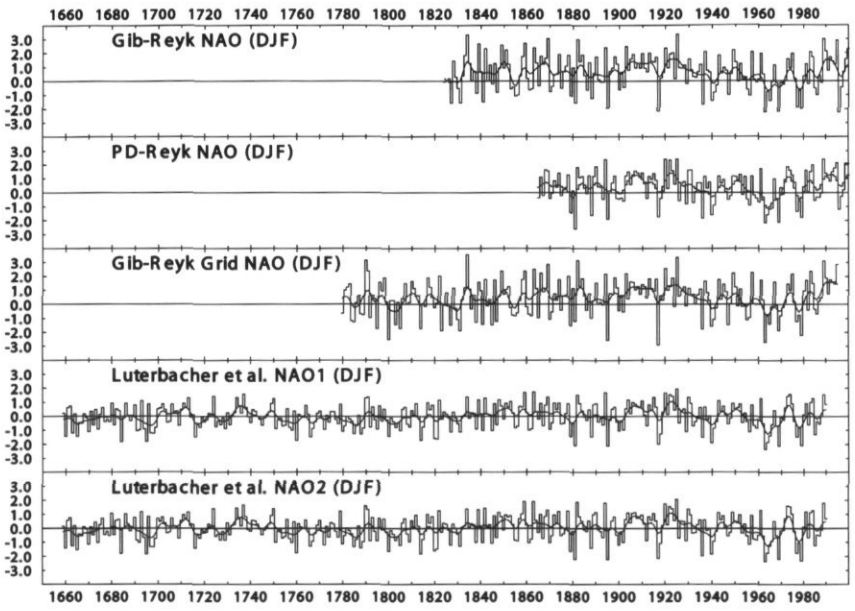


Figure 1. Winter (December to February) times-series of the NAO from long instrumental records (back to 1865, 1821, and 1780) and from documentary-based reconstructions (back to 1659).

The traditional measure uses the Ponta Delgada site in the Azores as the southern node where records began in 1865. For the northern node, Reykjavik has records back to 1821, 25 years earlier than Stykkisholmur (Jones *et al.*, 1997). Hurrell (1995) showed that using a Southwest European location as the southern node, instrumental indices could be extended back further during the winter season. The earliest location in this region is Gibraltar, with records back to 1821 (Jones *et al.*, 1997). Further extension of the NAO to 1780 is possible using the gridded surface pressure reconstructions from Jones *et al.* (1999), which use a network of varying numbers of surface pressure data (including Gibraltar and Reykjavik after 1820).

The final two curves in Figure 1 are two reconstructions of the NAO developed by Luterbacher *et al.* (1999, 2002) using regression analysis. Full details of the methods are given in the two articles. They make use of long pressure series but include additional information from many, even longer, series of monthly temperature averages and precipitation totals and documentary sources. These latter series incorporate information from documentary archives such as diaries, river and Baltic Sea freeze dates and reports of droughts in southern Europe. Rodrigo *et al.* (2001) have recently illustrated the potential for reconstructing the NAO from one such drought series for Andalusia in southern Spain since 1500.

Figure 2 compares the Luterbacher *et al.* (2002) reconstruction with another recent reconstruction by Cook *et al.* (2002). In Figure 2 the winter season is December to March, that used by Cook *et al.* (2002). To enable comparison, the Luterbacher *et al.* (2002) series, which is available monthly, is based on the 4-month average, so is marginally different from that shown in Figure 1. The Cook *et al.* (2002) reconstruction has been developed from natural archives of the past, incorporating several hundred tree-ring chronologies constructed from trees growing in Europe, north Africa, and eastern North America and a few Greenland ice cores. As both reconstructions involve many non-pressure variables (temperature, precipitation, and documentary series in the case of Luterbacher *et al.* (2002) and tree rings and ice cores in the case of Cook *et al.* (2002)), they will also incorporate changes in the influence of the NAO on these indicators as well as changes in the NAO itself (Jones *et al.*, 2001).

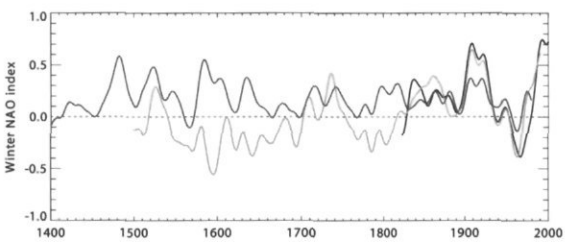


Figure 2. Comparison of two long 'winter' (December to March) reconstructions of the NAO [documentary and instrumental based from Luterbacher *et al.* (2002) (light grey) and from tree rings and ice cores from Cook *et al.* (2002) (dark grey)]. Both series and the observational NAO (black and based on Gibraltar and Reykjavik) have been smoothed with a 30-year Gaussian filter.

All the winter NAO series indicate relatively unusual conditions during the 1990s, but recent values for individual winters have not been entirely without precedent. Similarly, strongly positive values for individual winters occurred during the early decades of the 20th century and for several earlier periods of one or two decades in earlier centuries. Although recent values have not been entirely unique compared to earlier decades (except on the 30-year time scale of the filtered series), the rise in values over the 30-year period from 1965 to 1995 does stand out.

Relationships with surface variables

Figure 3 shows correlation coefficients between the NAO (the series developed from Ponta Delgada and Reykjavik) and surface temperatures and precipitation totals. The correlations have been calculated for the four climatological seasons, based on data for the 1951–2000 period. Figure 3A shows correlations with temperature and Figure 3B with precipitation. The strongest correlations are as expected in the winter season, but weaker and still significant

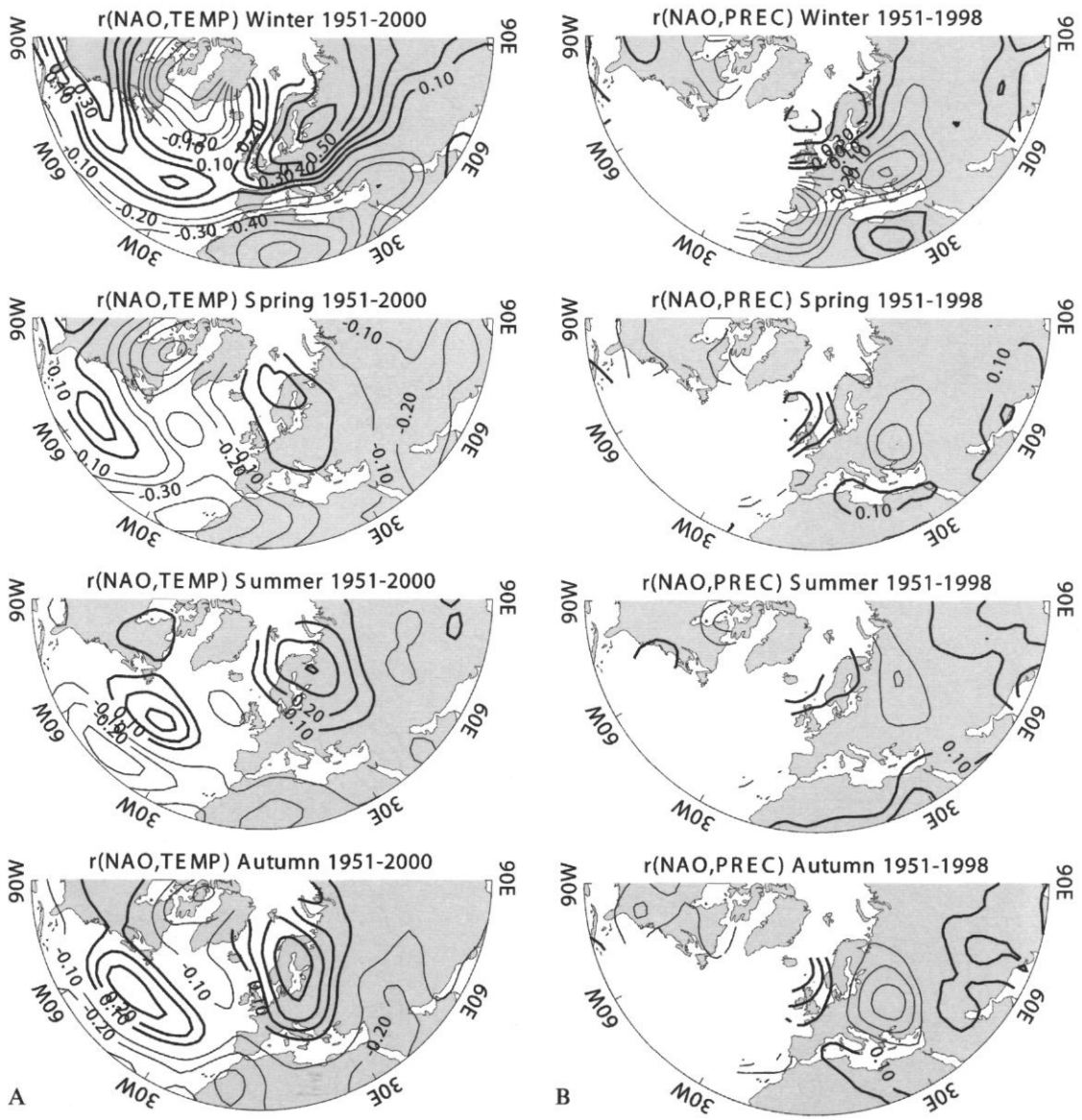


Figure 3. Seasonal correlation maps between surface climate features over the 1951–2000 period and the NAO defined by Ponta Delgada and Reykjavik: (A) temperature and (B) precipitation. In this and subsequent Figures, standard climatological seasons are used. Winter is December to February, Spring is March to May, etc.

correlations are sometimes evident in some areas in the other seasons. Correlations are weakest during the summer season.

Reid *et al.* (2001) and Jones *et al.* (2002) show similar analyses for different periods, illustrating that the strengths of relationships do vary with time. The stronger relationships (those in the key regions of the quadropole pattern), however, tend to maintain similar values through time, but the weaker relationships can be dependent on the time period used in their development. Jones *et al.* (2002) show, in particular, that precipitation/NAO relationships are much more variable with time, reflecting the greater spatial variability of precipitation processes and the greater difficulty of ensuring long homogeneous precipitation series.

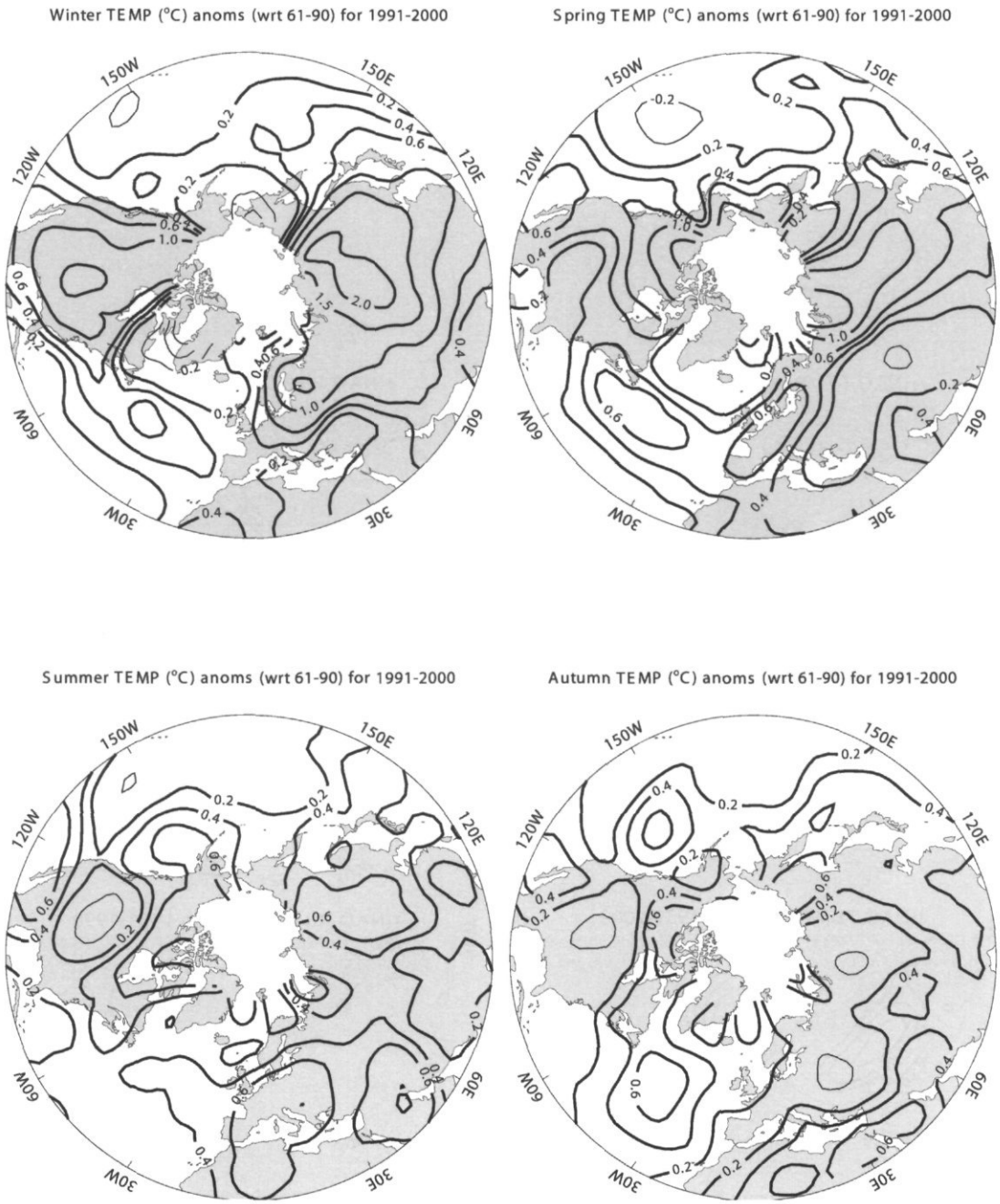


Figure 4. Seasonal surface temperature anomalies for 1991–2000 period (with respect to the 1961–1990 base period).

The 1990s in comparison to earlier decades

Figure 4 shows seasonal temperature anomalies for the 1991–2000 period, with respect to the 1961–1990 period, for the whole NH north of 20°N. For all seasons, most of the analysed area indicates warmer conditions than during the 1961–1990 period. Figure 5 shows similar maps for seasonal pressures, again expressed as anomalies from the 1961–1990. As average pressure across this region would be expected to be conserved, the maps reveal regions during 1991–2000, which experienced higher and lower pressures compared to 1961–1990. The most striking season is winter, where lower pressures

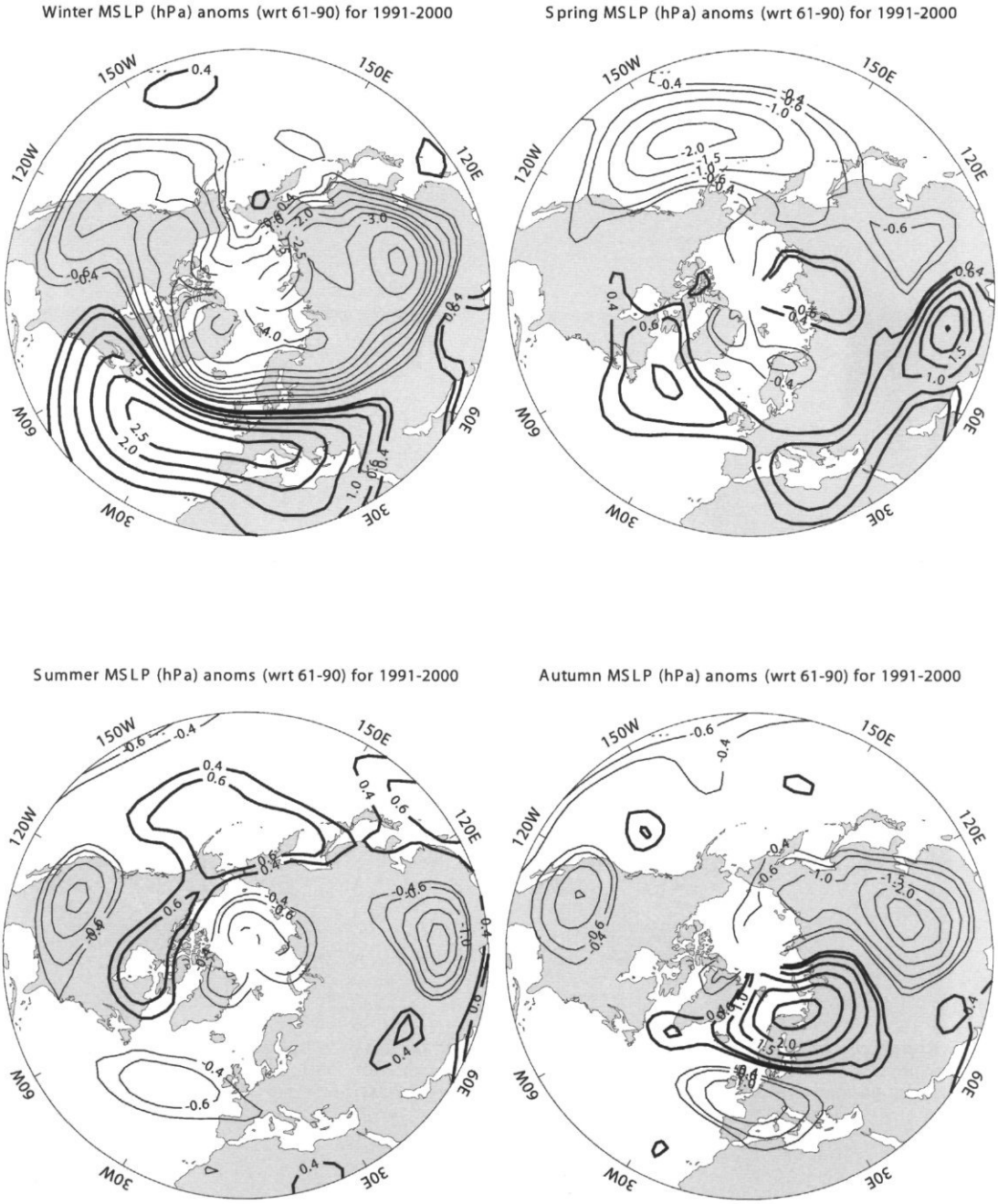


Figure 5. Seasonal surface pressure anomalies for the 1991–2000 period (with respect to the 1961–1990 base period).

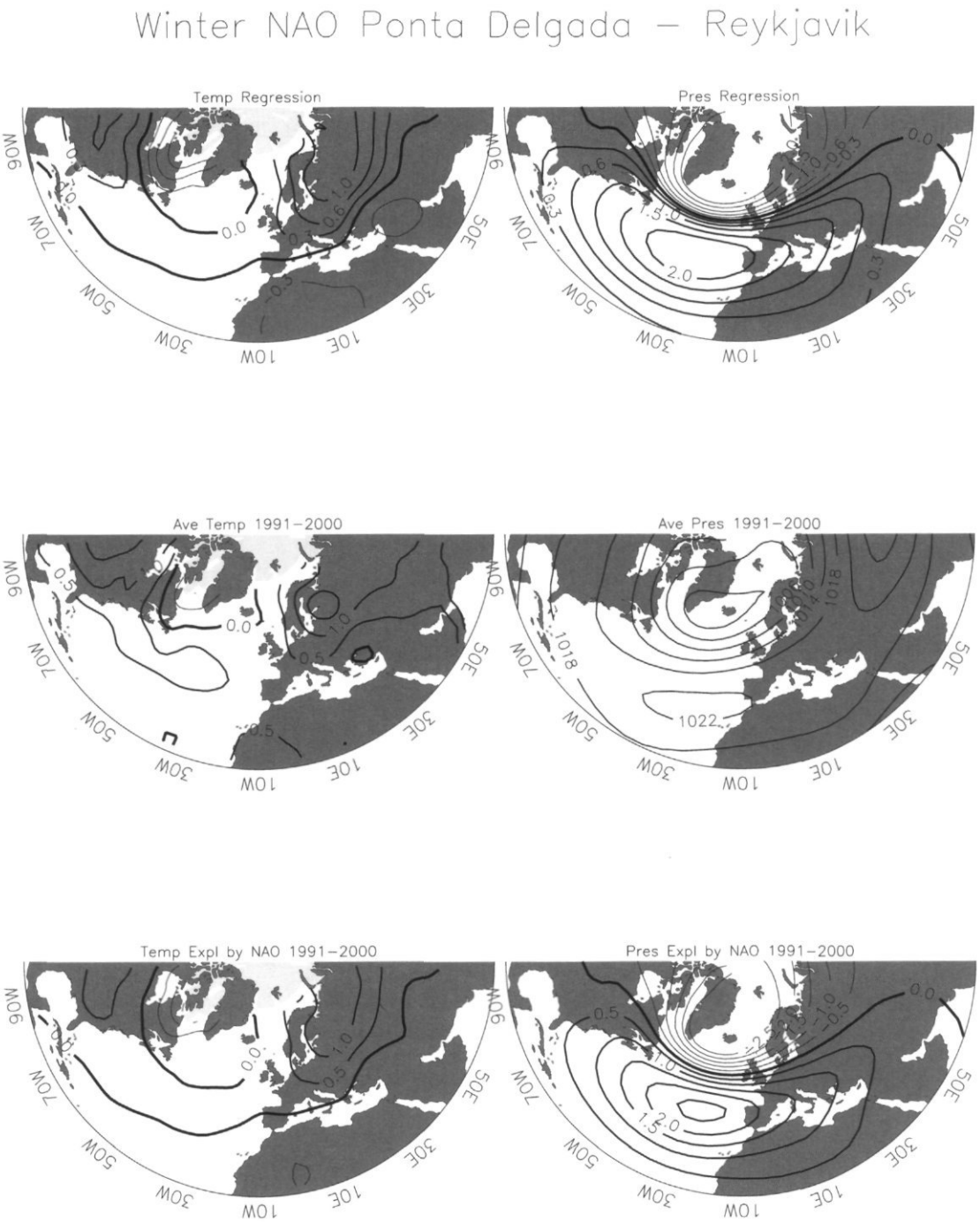


Figure 6. Regression coefficients (based on the winter season during the 1951–1990 period) between the NAO and surface temperature/pressure fields (top pair); temperature and pressure anomalies for 1991–2000 (middle pair) and the amount of temperature and pressure change explained by the regression during 1991–2000 (lower pair).

during 1991–2000 were evident over the Arctic region, northern Asia, and all of western North America. Pressures were higher over the southern North Atlantic and much of southern Eurasia.

Finally, Figure 6 illustrates for the winter season how much of the mean change of temperature and pressure during 1991–2000 can be explained by the NAO. Regression relationships for winter were derived between the Ponta Delgada–Reykjavik NAO and the temperature and pressure fields for the 1951–1990 period and then used to estimate the expected change in temperature and pressure for the 1991–2000 period. The NAO explains a significant fraction of the change, particularly over the expected areas of Europe, North Africa, and eastern North America. Similar analyses for the other three seasons (not shown) indicate that few of the changes can be explained by NAO variability, principally because the NAO has been less anomalous in these seasons and its influence is considerably weaker.

Conclusions

Recent individual winter NAO values during the 1990s have not been anomalous compared to longer records, although they appear unprecedented at the 30-year time scale. The rapid shift from negative values in the 1960s to the strongly positive values in the 1990s appears to have been unique. In the winter season the NAO explains a significant fraction of the change in climate over the greater North Atlantic region during the 1990s. The weaker influence of the NAO in the other seasons and its less anomalous behaviour mean that hardly any changes that have occurred in the 1990s can be significantly explained by the NAO.

Acknowledgements

I thank Tim Osborn for help with the figures. This work has been supported by the US Department of Energy under Grant No. DE-FG02-98ER62601.

References

Cook, E. R., D'Arrigo, R. D., and Mann, M. E. 2002. A well-verified, multi-proxy reconstruction of the winter North Atlantic Oscillation index since A.D. 1400. Journal of Climate. (In press.)

Hurrell, J. W. 1995. Decadal trends in the North Atlantic Oscillation: regional temperatures and precipitation. Science, 269: 676–679.

Jones, P. D., Jónsson, T., and Wheeler, D. 1997. Extensions to the North Atlantic Oscillation using early instrumental pressure observations from Gibraltar and southwest Iceland. International Journal of Climatology, 17: 1433–1450.

Jones, P. D., and 21 others. 1999. Monthly mean pressure reconstructions for Europe for the 1780–1995 period. International Journal of Climatology, 19: 347–364.

Jones, P. D., Osborn, T. J., and Briffa, K. R. 2001. The evolution of climate over the last millennium. Science, 292: 662–667.

Jones, P. D., Osborn, T. J., and Briffa, K. R. 2002. Pressurebased measures of the NAO: a comparison and an assessment of changes in the strength of the NAO and in its influence on surface climate parameters. *In* The North Atlantic Oscillation. Ed. by J. W. Hurrell, Y. Kushnir, G. Ottersen, and M. Visbeck. American Geophysical Union. (In press.)

Luterbacher, J., Schmutz, C., Gyalistras, D., Xoplaki, E., and Wanner, H. 1999. Reconstruction of monthly NAO and EU indices back to AD 1675. Geophysical Research Letters, 26: 2745–2748.

Luterbacher, J., Xoplaki, E., Dietrich, D., Jones, P. D., Davies, T. D., Portis, D., Gonzalez-Rouco, J. F., von Storch, H., Gyaliastras, D., Casty, C., and Wanner, H. 2002. Extending NAO indices back to 1500. Atmospheric Science Letters, doi:10.1006/asle.2001.0044.

Osborn, T. J., Briffa, K. R., Tett, S. F. B., Jones, P. D., and Trigo, R. M. 1999. Evaluation of the North Atlantic Oscillation as simulated by a coupled climate model. Climate Dynamics, 15: 685–702.

Reid, P. A., Jones, P. D., Brown, O., Goodess, C. M., and Davies, T. D. 2001. Assessments of the reliability of the NCEP circulation data and relationships with surface climate by direct comparisons with station-based temperature, precipitation and mean sea level pressure. Climate Research, 17: 247–261.

Rodrigo, F. S., Pozo-Vázquez, D., Esteban-Parra, M. J., and Castro-Díez, Y. 2001. A reconstruction of the winter North Atlantic Oscillation index back to A.D. 1501 using documentary data in southern Spain. Journal of Geophysical Research, 106: 14,805–14,818.

Slonosky, V. C., and Yiou, P. 2001. Secular changes in the North Atlantic Oscillation and its influence on 20th century warming. Geophysical Research Letters, 28: 807–810.

Walker, G. T. 1924. Correlations in seasonal variations of weather IX. Memoirs of the Indian Meteorological Department, 24: 275–332.

ICES Marine Science Symposia, 219: 32–39. 2003

Temperature and salinity in the central Labrador Sea during the 1990s and in the context of the longer-term change

Igor Yashayaev, John R. N. Lazier, and R. Allyn Clarke

Yashayaev, I., Lazier, J. R. N., and Clarke, R. A. 2003. Temperature and salinity in the central Labrador Sea during the 1990s and in the context of the longer-term change. – ICES Marine Science Symposia, 219: 32–39.

In the early years of the 1990s, in the Labrador Sea winters were exceptionally severe, while in the later years winters were relatively mild. High heat losses during the severe winters produced mixed layers increasing in depth to a maximum of 2300 m. This pool of convectively mixed water, Labrador Sea Water (LSW), is a well-recognized intermediate water mass in the North Atlantic Ocean. In the latter half of the decade, mixed layer depths, at less than 1500 m, were too shallow to maintain the recently created LSW. It slowly drained away from the Labrador Sea to other regions of the North Atlantic Ocean. This loss was balanced by a flow of warmer more saline water from the boundary currents. Changes in temperature and salinity associated with the build-up and decline of LSW over the decade are presented. Property variations in the Northeast Atlantic Deep Water and Denmark Strait Overflow Water lying below the LSW are also discussed.

Keywords: climate change, convection, Labrador Sea, North Atlantic Ocean, stratification, vertical mixing.

I. Yashayaev, J. R. N. Lazier, and R. A. Clarke: Bedford Institute of Oceanography, 1 Challenger Drive, PO Box 1006, Dartmouth, Nova Scotia, B2Y-4A2, Canada [tel: +1 902 426 9963; fax: +1 902 426 7827, e-mail: yashayaevi@mar.dfo-mpo.gc.ca; lazierj@mar.dfo-mpo.gc.ca; clarkea@mar.dfo-mpo.gc.ca]. Correspondence to I. Yashayaev.

Introduction

During winter, cold air from northeastern Canada flows over the Labrador Sea creating a convectively mixed surface layer that can reach deeper than 2000 m in the centre of the sea during exceptionally cold years. When the convection is greater than ≈ 1500 m the mixed water is recognized as a unique water mass known most commonly as Labrador Sea Water (LSW). Production of LSW varies greatly from year to year in step with the severity of the winter weather in the area (Curry *et al.*, 1998).

The formation of LSW provides an important pathway for atmospheric gases such as oxygen, carbon dioxide, and the chlorofluorocarbons (CFCs) to pass from the surface mixed layer to intermediate depths. As the convected water, LSW, flows to other regions of the ocean (Sy *et al.*, 1997), it distributes these dissolved gases to a large area of the ocean, thereby ventilating the deeper layers. Because of the importance of this process and because of the large variability in the production rate of LSW, the Bedford Institute of Oceanography has occupied a line of CTD stations across the Labrador Sea in the early summers of each year since 1990 (Figure 1). In addition multi-line surveys were conducted in the autumn of 1996 and the spring of 1997. Between 1990 and 1997 the work was a contribution to the World Ocean Circulation Experiment (WOCE) and since 1997 to the Climate Variability Program (CLIVAR).

The purpose of this article is to present a general description of the temperature and salinity variations which occurred during the years 1990–2001 within the three principal water masses found in the central Labrador Sea – the LSW, the Northeast Atlantic Deep Water (NEADW), and the Denmark Strait Overflow Water (DSOW) – and compare the recent state of these water masses with the history of more than five decades. We first describe the data in section 2, then in section 3 focus on each water mass in turn. This is followed in section 4 by a discussion of the results in section 3 with reference to the longer-term record and a summary in section 5.

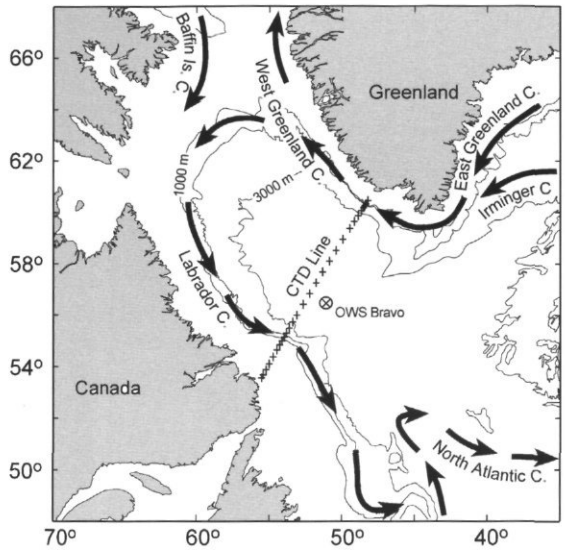


Figure 1. Map of the Labrador Sea showing the major currents in the region. The CTD line occupied each summer between 1990 and 2001 is indicated by the line of station positions indicated by crosses. OWS "Bravo" was an Ocean Weather Ship which regularly collected oceanographic data between 1964 and 1973.

Data

The data collected between 1990 and 2001 are presented in three diagrams. Salinity sections (Figure 2) show the distribution across the sea at the beginning and end of the observing period and in 1993. The 1993 salinity section represents the distribution following the series of most severe winters when the LSW appeared most extensive and most homogeneous. Figure 3 presents distributions of potential temperature (hereafter temperature), salinity, and potential density anomaly relative to 2000 db (σ_2) in the central region of the Labrador Sea in time–depth coordinates. The time-series of the vertical distributions were composed from the medians of temperature (T) and salinity (S) measurements in σ_2 bins for each year. The size of σ_2 bins was varied with depth to maintain even vertical separation between the centres of the bins and to provide sufficient data coverage. The σ_2 bin size was in the range between 0.02 and 0.005. The T–S diagrams in Figure 4 cover two time intervals associated with the build-up and decline of LSW. The data set for the analyses presented in Figures 3–6 was restricted to the central region of the sea (with water depth greater than 3300 m).

The 1993 salinity section in Figure 2 shows the distribution along the line following a winter of deep convection. The large mass of nearly homogeneous water between 500 and 2300 m between 360 and 800 km is the pool of LSW transformed through the deep convection during the previous winter.

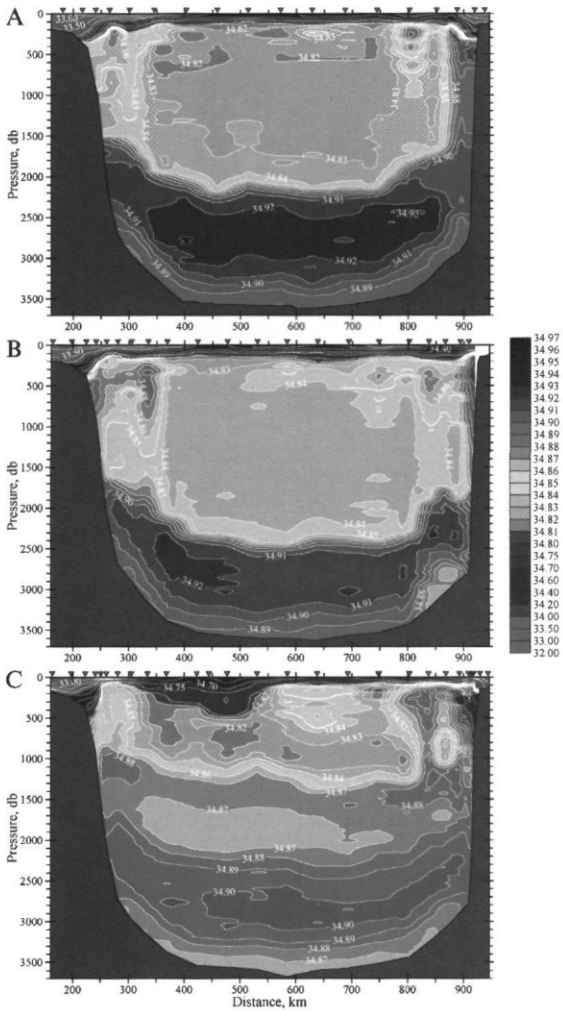


Figure 2. Salinity sections along the Labrador Sea CTD line (Figure 1) in the early summer of 1990 (A), 1993 (B), and 2001 (C). The distance scale is from the Labrador coast. Station positions are indicated by inverted triangles at the surface.

Above 500 m the water is more stratified than the layer between 500 and 2300 m. These observations were obtained in July about 3 months after deep convection ceased at the end of the cooling season, which was about 1 April. Since that time the surface layer has been flooded with freshwater derived from melting ice and river run-off. Solar heating has added to the stratification. In addition, the layer below this low salinity surface layer, to about 500 m, has been invaded by higher salinity water from the right, that is, the northeast. This more saline water is known as the Irminger Water (IW), because it is transported into the Labrador Sea from the Irminger Sea in the East and West Greenland Currents, which lie over the continental shelf and slope (Figure 1). On the left or southwest end of the section there is again a salinity maximum at about

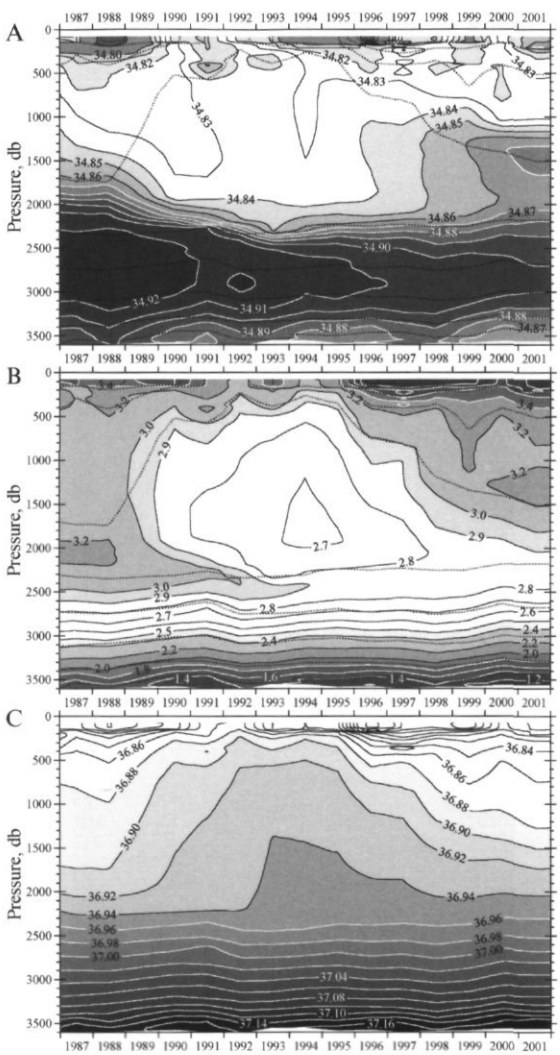


Figure 3. Time-series of the vertical distributions of salinity (A), temperature (B), and σ_2 (C) between 1987 and 2001. The black dashed lines in (A) and (B) indicate σ_2 contours.

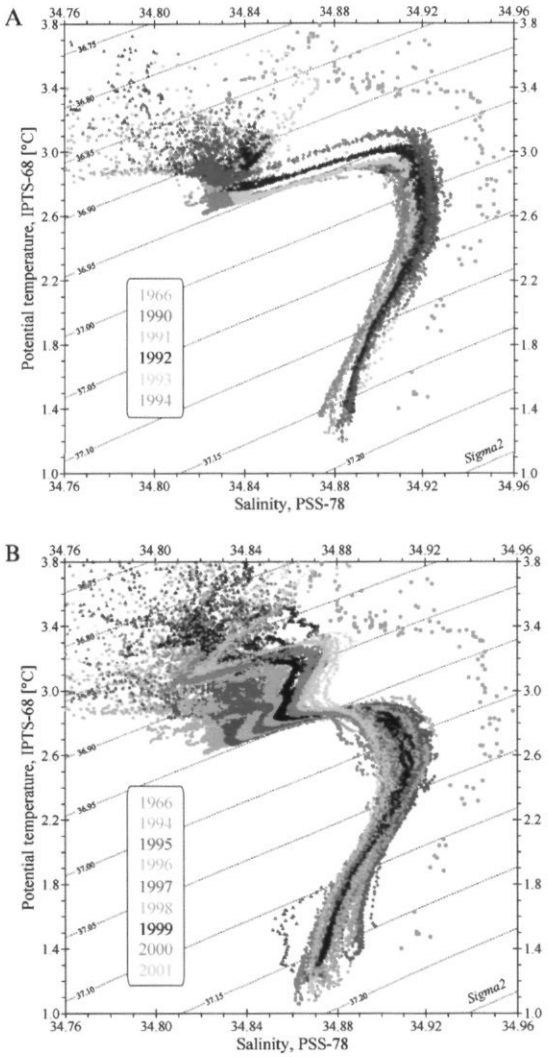


Figure 4. Temperature vs. salinity curves representing the average conditions in the centre of the Labrador Sea during the early summers of 1990–1994 (A) and 1994–2001 (B). We also show the *Hudson* 1966 data to indicate the longer-term freshening in the intermediate and deep layers.

300 m over the Labrador continental slope which also tends to invade the central region. This is again Irminger Water, which has been transported around the Labrador Sea in the West Greenland and Labrador Currents.

Beneath the LSW, between 2300 and 3300 m, lies a water mass identified by the salinity maximum at about 2800 m. This is the NEADW. It originates in the eastern basin of the North Atlantic from the overflow crossing the Iceland–Scotland Ridge (Turrell *et al.*, 1999). The Iceland–Scotland Overflow vigorously mixes with upper warm and saline water and LSW in the Iceland Basin and flows into the western basin through gaps in the Mid-Atlantic Ridge. NEADW found in the Labrador Sea is about 3°C warmer than the cold and dense overflow entering the Iceland Basin. However, we expect that the changes in the properties and transport of the overflow contribute to the long-term variability of NEADW in the Labrador Sea.

At the bottom of the section is the DSOW, with a slightly lower salinity than in the NEADW. DSOW is the densest water in the northern North Atlantic. It originates in the seas north of Iceland and comes to the Labrador Sea after flowing over the sill in Denmark Strait between Greenland and Iceland.

The last water mass of note in the section is the low salinity water over the Labrador continental shelf, which flows south out of Baffin Bay in the Baffin Island Current and the Labrador Current. A

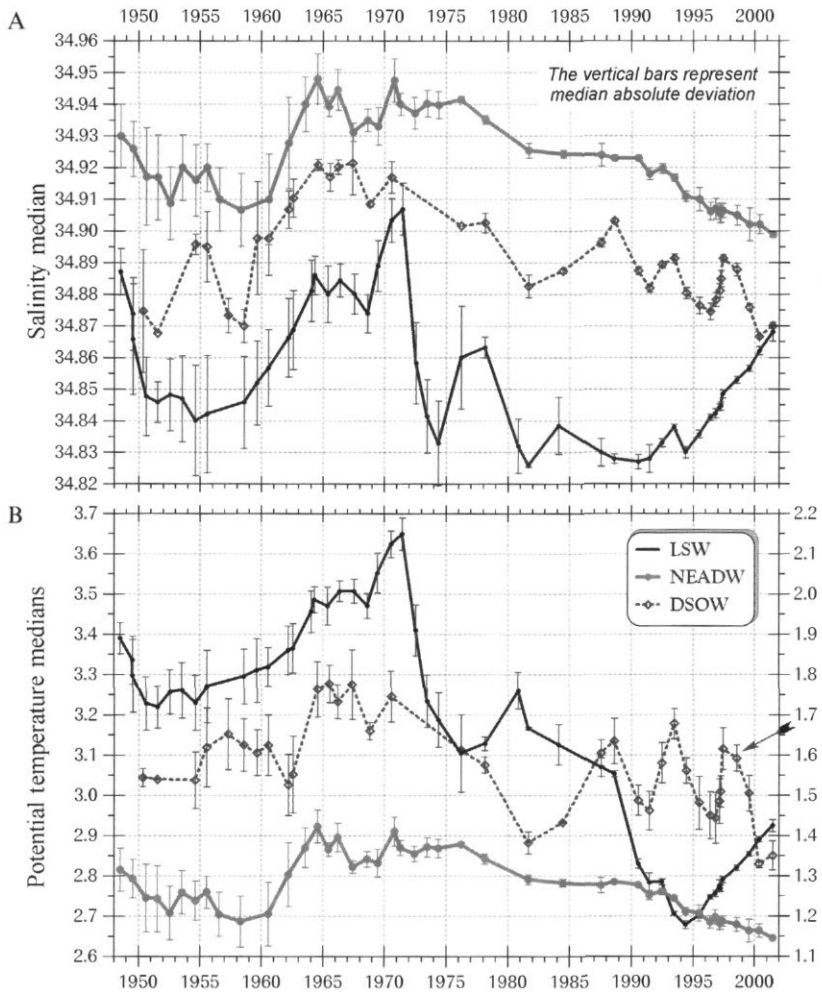


Figure 5. Salinity and temperature at the core of the Labrador Sea Water (LSW), Northeast Atlantic Deep Water (NEADW), and the Denmark Strait Overflow Water (DSOW) between 1948 and 2001. Note that the temperature scale for the DSOW is on the right.

similar band of low salinity water of Arctic origin lies over the Greenland continental shelf but it was covered by heavy ice in July 1993 and not sampled when the rest of these data were collected. However, it is visible in the other two sections. The rapid transition between the low salinity waters over the shelves and the higher salinity waters of the sea's interior mark the baroclinic currents lying over the upper part of the continental slopes, the Labrador, and West Greenland Currents.

Water masses in the 1990s

Labrador Sea Water

We divide the discussion of LSW into two parts. The first covers the period from the late 1980s to 1994 when a series of severe winters caused convection to proceed to greater depths until a maximum of 2300 m was reached in 1993 and 1994. The second period, following 1994, is characterized by normal to mild winters and convection limited to 1500 m. During this period the LSW below the mixed layer was isolated from the vertical mixing in the upper layer and changed its properties more by isopycnal mixing than via vertical mixing.

The 1990 and 1993 salinity sections in Figure 2 show LSW as the large mass of homogeneous water to >2000 m created in the central part of the sea via deep convection during the years of severe winters. Temperature in this water mass (Figures 3B, 5) decreased between 1987 and 1994 from greater than 3°C to less than 2.7°C. At the same time in the intermediate depths (400–2000 m), salinity tended to decrease between 1987 and 1990 but to increase

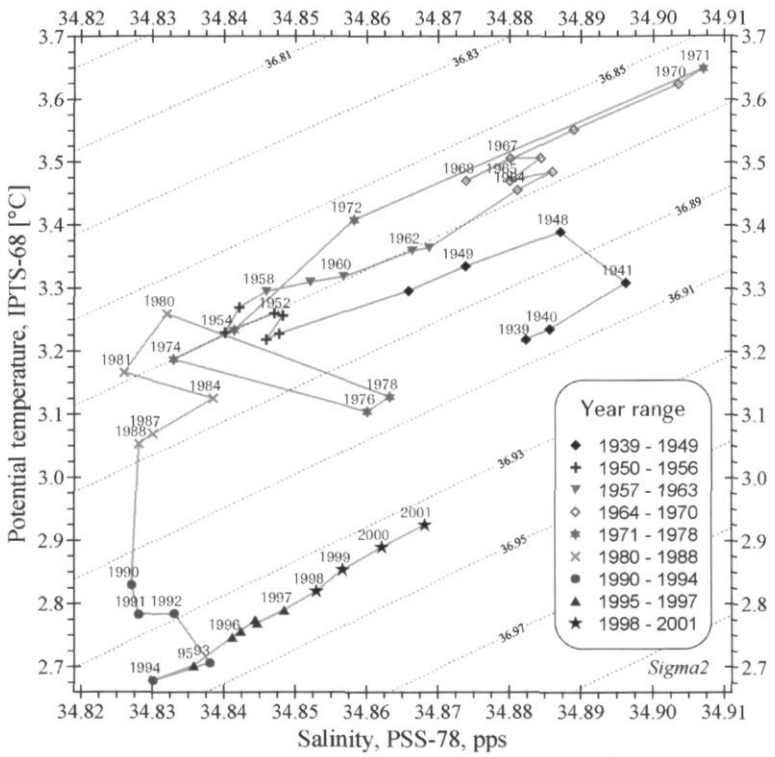


Figure 6. Temperature vs. salinity at the core of the Labrador Sea Water between 1939 and 2001.

from 1991 to 1993 (Figure 3A). In 1990 the average temperature and salinity of the LSW were roughly 2.85°C and 34.828. In 1993 the salinity had increased by 0.01 to 34.838, while the temperature decreased by 0.15°C to 2.7°C. The decrease in temperature was due to winter heat loss to the atmosphere. These changes in temperature and salinity of the LSW resulted in a significant increase in density of this water mass. This is well illustrated in Figure 3C, which shows the general increase in density over the 400 to 2200 m interval between 1987 and 1993 due to heat loss during the severe winters.

We believe that the noted decrease in LSW salinity to 1990 is due to the annual accumulation of freshwater in the upper layer being mixed down to intermediate depths through the development of a deep winter mixed layer. During 1991 to 1993, intense winter convection began eroding the salty NEADW into the expanding LSW layer with increasing salinity. This process will be discussed in more detail in the study of convection and re-stratification in the Labrador Sea that is submitted for publication. The salinity increase from 1990 to 1993 is best illustrated in the T–S diagram in Figure 4A. (The LSW appears there as a narrow temperature and salinity minimum closest to $\sigma_2 = 36.95$ kg m^{-3}.)

In the spring of 1994 the depth of the mixed layer was not noticeably deeper than in the spring of 1993, but the whole layer was colder in 1994 than in 1993. However, unlike that in the previous 3 years, the average salinity in the deep mixed layer decreased from 1993 to 1994 by 0.008 (Figures 5, 6). This 1-year freshening of the LSW is in concurrence with the fact that there was no further deepening of the deep winter mixed layer in 1994, and the water was ventilated to the same depth as in 1993 renewing the LSW of the previous winter. Whatever amount of the underlying NEADW with higher salinity was incorporated into the mixed layer in 1994, it was insufficient (ultimately zero) to compensate for the decrease in the mixed layer salinity derived from the mixing down of the low saline water which was accumulated in the upper layer between the winters. The discussed decrease in LSW salinity also implies that the amount of warm and salty IW involved in the convective mixing in the winter of 1994 was also small to compensate for the freshening in the mixed layer.

In the second half of the decade, when the winters were less severe, the deeper portion of the LSW created during the years of intense cooling is no longer renewed during the winter. Its volume in the central part of the Labrador Sea declines as it drains away to other regions of the ocean. This decline is especially clear in the time-series of temperature and σ_2 in Figure 3B, C. If the limits of LSW are taken as

$36.92 < \sigma_2 < 36.95$ kg m^{-3} its thickness declines from 1900 m to 300 m. This small remnant, even after 7 years' isolation, can still be identified in the T–S curves (Figure 4B) by the characteristic LSW salinity minimum at a $\sigma_2 = 34.94$ kg m^{-3}. Between 1994 and 2001 the water at this salinity minimum became warmer and more saline by 0.23°C and 0.039. This increase in temperature and salinity of the deep LSW was due, we assume, to isopycnal mixing, because LSW on isopycnal surfaces exhibits a T–S minimum in the centre of the Labrador Sea. As the volume of LSW decreases (Figure 3C) the volume of water at lower densities increases. The volume of water between 36.84 kg m^{-3} and 36.90 kg m^{-3}, for instance, increased between 1995 and 2001 by about 700 m. We postulate that this increase in volume is derived from water flowing into the central region of the Labrador Sea from the boundary currents. That this incoming water tends to be the warmer more saline IW accounts for the increases in temperature and salinity in the latter half of the decade above the LSW.

The salinity section for 2001 in Figure 2C illustrates the situation at the end of the decade. The remnant of the LSW created by intense convection during the first half of the decade lies within the 34.87 contour between 1500 and 2000 m. Above this is a slight maximum separating it from the upper layer characterized by lower salinity water. This salinity maximum at 34.875 is a prominent feature of the T–S curves (Figure 4B) at $\sigma_2 = 36.89$ kg m^{-3} in the years 1997–2001 and can be associated with replacement of the cold and fresh LSW produced between 1993 and 1994 in subsequent years with warmer and more saline water. Vertical and temporal continuity of the year-to-year changes of LSW properties (between 1300 and 2000 m in Figure 3A, B) implies that starting from 1994 the processes of LSW mixing, draining, and replacement with modified warmer and more saline water are steady in time and monotonic with depth.

Above this salinity maximum lies the upper layer influenced by winter convection. In Figure 2C it appears from the concentration of low salinity water on the south side of the central portion of the section (300–500 km) that convection in the previous winter was confined to this region rather than spread evenly across the whole section. On the northern half of the central area (550–700 km) salinity maxima are evident in the upper 700 m at 600 km. We feel this probably indicates a lack of convection in this region below 200 m during the previous winter. The effect of these salinity maxima are evident in the T–S curve for 2001 in Figure 4B. Here the salinity minimum (34.82) at $\sigma_2 = 36.865$ kg m^{-3} is capped by the higher salinity water. This layering, which also occurred in 2000, creates a curve similar to that associated with the LSW at $\sigma_2 = 36.94$ kg m^{-3}. For this reason the shallower minimum is sometimes referred to as upper LSW.

Northeast Atlantic Deep Water

NEADW lies beneath the LSW and is characterized by a salinity maximum at 3000 m. In the T–S curves (Figure 4A, B), this characteristic salinity maximum is clearly visible in the σ_2 range 36.95–37.05 kg m^{-3}. Because it lies beneath the layer of deep convection it was not greatly altered during the years of intense convection at the beginning of the decade. Although, as mentioned above, the deep convection layer did penetrate a few hundred metres into this deeper water mass during the winters of 1990–1993. The higher salinity, lower dissolved oxygen and chlorofluoromethanes of the deeper layer were incorporated into the mixing layer with measurable effects as noted above for salinity. Matching decreases in the dissolved oxygen and CFC concentrations were observed but are not discussed here. In spite of the influence from the convecting layer, temperature and salinity of the NEADW appear to decline uniformly throughout the decade. The declines in both temperature and salinity of this water mass are well seen in the T–S diagrams in Figure 4A, B ($36.97 < \sigma_2 < 37.05$). The decrease in salinity is especially clear in Figure 3A, which shows the salinity at 2800 m decreasing from above 34.92 in 1987 to near 34.90 in 2001. The temperature decrease over the record is also evident in Figure 3B by the slight rise in the isotherms over the record. We estimate the decreases of temperature and salinity at the core of this water mass to be 0.15°C from 2.8°C to 2.65°C and 0.021 from 34.923 to 34.902, respectively. These declines appear to be associated with the general freshening of the subpolar gyre, since the Great Salinity Anomaly (Dickson *et al.*, 1988) in the late 1960s. As the NEADW becomes colder and fresher and the remnant LSW becomes warmer and more saline the difference between the two water masses in both variables decreases. The change is very obvious in the T–S curves in Figure 4B, in which the salinity difference between the LSW minimum and the NEADW maximum has been reduced from about 0.085 to 0.037. Another feature of these changes in the water mass properties is the disappearance of the temperature maximum between the LSW and the NEADW. This maximum appeared at 1900–2400 m in the mid-1980s as LSW became colder than the underlying NEADW and narrowed as convection developed to 2300 m. The deep temperature maximum is illustrated in Figure 3B by the 2.9°C and 3.0°C isotherms at 2400 m, especially in 1990 to 1993. As the contrast between these water masses declines, this maximum fades away.

Denmark Strait Overflow Water

DSOW lies at the bottom of the water column, beneath the NEADW at $\sigma_2 > 37.10$ kg m^{-3}. Since the density of the bottom water fluctuates from year to year (the lowest in the last 12 years was observed in 1993, the highest in 2000 and 2001), we define the core of DSOW in the Labrador Sea as a 200 m bottom layer in the central region of the sea. As can be seen in the T–S diagram in Figure 4B it is colder and fresher than NEADW and like the other water masses its properties vary from year to year. Over the 1990s temperature and salinity at $\sigma_2 =$ 37.15 kg m^{-3} varied between 1.34°C and 1.50°C and 34.866 and 34.890, respectively. However, these variations were not monotonic, as in the NEADW. In Figure 3A, B the water is cooler and fresher in 1990–1991, 1995–1996, and 1999–1901 and warmer and more saline in 1992–1993 and 1997–1998. The coldest and freshest DSOW over the past 4 decades was observed in 2000. The time signal seen in DSOW (Figure 5) is coherent across the Labrador Sea, indicating that three quasi-pentadal cycles in DSOW between 1986 and 2001 can be linked with the variability at its source and the subsequent transformation of this water mass before it fills the abyss of the Labrador Sea. The rapid interannual changes of temperature and salinity are seen at the Denmark Strait sill. Downstream, in the Irminger Basin, the overflow undergoes substantial mixing which, we believe, alters the DSOW along its path. The DSOW properties between the Denmark Strait sill and the Labrador Sea respond to the changes in properties, volumes, and contributions of the entrained waters. One of the key factors here is the production of LSW, which has a great impact on the stratification and coupled dynamics of the intermediate and deep layers of the whole subpolar gyre.

Variations over the longer term

One aim of the ICES Decadal Symposium was to compare the water mass changes observed in the 1990s with those observed over the longer term. We present the longer-term variability in the central region of the Labrador Sea in Figures 5 and 6. Figure 5 shows temperature and salinity at the cores of the LSW, NEADW, and DSOW between 1948 and 2001. The time-series of the LSW properties are also presented in the T–S diagram in Figure 6.

Over the past 53 years the properties of LSW have varied over an exceptionally large range. Temperature was as low as 2.7°C and as high as 3.65°C, while salinity ranged between 34.825 and 34.907. Over the years there has been one major maximum, i.e. in 1970–1972. At the same time the LSW temperature was the highest in the record. The minima in the early 1950s, mid-1970s, and early 1990s do not always appear at the same time for both variables. This is best observed in the early 1990s, where the salinity reaches a minimum in 1990 while the temperature minimum is in 1994. In the discussion above we saw that a series of severe winters in the late 1980s and early 1990s caused winter mixed layers of increasing depth. The resulting heat loss is reflected in the decrease in temperature of the water mass. On the T–S curve in Figure 6 this decrease in temperature is accompanied, between 1988 and 1993, by an increase in σ_2 of 0.05 kg m^{-3}. Salinity rises through the years of intense convection as the mixed layer penetrates and incorporates the saltier NEADW water beneath. Following the period of intense convection, the LSW is getting warmer and more saline as it mixes isopycnally with the warmer and saltier waters that surround it. The fact that the salinity minimum in 1974 also precedes the temperature minimum in 1976 suggests a series of events similar to that observed in the 1990s.

The maxima of temperature and salinity in 1971 and the years leading up to it are better known than most of the other years because data were obtained through these years at OWS Bravo (Figure 1). It was during this period that winters in the Labrador Sea were exceptionally mild with shallow mixed layers and that the Great Salinity Anomaly (Dickson *et al.*, 1988) lowered the salinity of the upper layer. The LSW lying at intermediate depths and isolated from the mixed layer became warmer and more saline as it mixed with surrounding waters – as happened in the late 1990s. This situation ended with severe winters in 1972 and 1973, which produced mixed layers deeper than 1500 m (Lazier, 1980) leading to the creation of a new version of LSW which was colder and less saline. Between 1971 and 1974 the salinity, as shown in Figures 5 and 6, dropped from 34.91 to 34.83 and the temperature from 3.65°C to 3.18°C. Following 1974 the salinity and σ_2 increased as the temperature decreased during continued convection. Then following 1976 the LSW, both temperature and salinity, increased as horizontal mixing replaced vertical mixing as the dominant forcing agent.

Temperature and salinity in the NEADW also varied significantly over the longer term; however, not as much as the LSW. As noted above, temperature and salinity steadily declined in the NEADW during the 1990s. These decreases are evident in Figure 5 by a decrease in salinity from 34.923 in 1990 to 34.9 in 2001 and a decrease in temperature from 2.78°C in 1990 to 2.65°C in 2001. Following these curves back in time shows that the cooling and freshening of this water mass has been continuous since the late 1960s. The biggest change, however, occurred in the early 1960s when the salinity increased from 34.91 to 34.94 and the temperature rose from 2.7°C to 2.9°C.

Properties in the DSOW appear to vary on a shorter time scale than those in the other water masses. The oscillations during the 1990s, mentioned above,

are clear in Figure 5. Both temperature and salinity were high in 1988, 1993, and 1987 and low in 1992, 1996, and 2000 with amplitudes of 0.15°C and 0.1 for both temperature and salinity, respectively. As in the NEADW, a general cooling and freshening can be traced since the 1960s with preceding abrupt increase in both properties in the early 1960s when salinity increased from 34.87 to 34.92 and temperature increased from 1.55°C to 1.75°C.

Summary

Observations obtained across the Labrador Sea during the 1990s show the water column experienced exceptionally high cooling during the early part of the decade followed in the latter half of the decade by winters with normal to less than normal cooling. The colder winters led to deep convective mixing and the creation of a new version of LSW to 2300 m. During the milder years, most of this LSW was mixed into the boundary currents and drained away from the region while the remaining portion became warmer and saltier as the waters higher in temperature and salinity bordering the sea were mixed toward the centre. The loss of the LSW led to a re-stratification of the upper waters across the sea. This was marked by significant increases in both temperature and salinity as well as a decrease in density. Also noted were a steady cooling and freshening of the NEADW over the past four decades and 5-year oscillations in the DSOW properties.

Examination of the 53-year record of the water mass properties showed that the pattern of temperature and salinity variations noted in the LSW during the 1980s and 1990s was similar to that observed in the 1960s and 1970s. Similar time-series in the NEADW and DSOW showed rapid increases in temperature and salinity in the early 1960s with slow freshening and cooling into the 1990s except for marked oscillations in the DSOW over the past 15 years.

References

Curry, R. G., McCartney, M. S., and Joyce, T. M. 1998. Oceanic transport of subpolar climate signals to mid-depth subtropical waters. Nature, 391: 575–577.

Dickson, R. R., Meincke, J., Malmberg, S.-A., and Lee, A. J. 1988. The "Great Salinity Anomaly" in the Northern North Atlantic 1968–1982. Progress in Oceanography, 20: 103–151.

Lazier, J. R. N. 1980. Oceanographic Conditions at Ocean Weather Ship Bravo, 1964–1974. Atmosphere-Ocean, 18: 227–238.

Sy, A., Rhein, M., Lazier, J. R., Koltermann, P., Meincke, J., Putzka, P., and Bersch, M. 1997. Surprisingly rapid spreading of newly formed intermediate waters across the North Atlantic Ocean. Nature, 386: 675–679.

Turrell, W. R., Slesser, G., Adams, R. D., Payne, R. and Gillibrand, P. A. 1999. Decadal variability in the composition of Faroe–Shetland Channel bottom water. Deep-Sea Research I, 46: 1–25.

ICES Marine Science Symposia, 219: 40–49. 2003

Climate variability on the Scotian Shelf during the 1990s

K. F. Drinkwater, B. Petrie, and P. C. Smith

Drinkwater, K. F., Petrie, B., and Smith, P. C. 2003. Climate variability on the Scotian Shelf during the 1990s. – ICES Marine Science Symposia, 219: 40–49.

The temperature and salinity conditions of the waters on the Scotian Shelf during the 1990s are described. Three major features are highlighted. First is the presence of cold subsurface waters throughout much of the 1990s in the northeast and nearshore regions of the Shelf. The principal cause of these cold conditions, initially established in the mid-1980s, is thought to be along-shelf advection from the Gulf of St Lawrence and off southern Newfoundland with the possibility of some contribution from local *in situ* cooling. The second major feature was caused by the arrival in 1997–1998 of cold Labrador Slope water along the shelf break, which subsequently flooded the lower layers of the central and southwestern regions of the Scotian Shelf. While this event produced the coldest near-bottom conditions in these Shelf regions since the 1960s it was of short duration, lasting only for approximately one year. Finally, the changes in the near-surface waters of the Scotian Shelf are described. Of particular relevance were the extremely warm surface temperatures in the late 1990s and the strong vertical stratification throughout the decade. The latter was a result of record low salinities in the near-surface waters that appear to be advected onto the Shelf from off the Grand Banks. The impact of these changes in ocean climate on some of the Shelf fish stocks is briefly discussed.

Keywords: advection, cooling, impacts, Labrador Slope Water, stratification.

Ken Drinkwater, Brian Petrie, and Peter Smith: Department of Fisheries and Oceans, Ocean Science Division, Bedford Institute of Oceanography, Dartmouth, Nova Scotia, Canada B2Y 4A2 [tel: +1 902 426 2650; fax: +1 902 426 6927; e-mail: drinkwaterk@mar.dfo-mpo.gc.ca, petrieb@mar.dfo-mpo.gc.ca; smithpc@mar.dfo-mpo.gc.ca]. Correspondence to K. Drinkwater.

Introduction

The Scotian Shelf is located in the Northwest Atlantic off Nova Scotia, Canada (Figure 1). It consists of a series of outer shallow banks and inner basins separated by gullies and channels. The mean depth is approximately 116 m, with a maximum depth in Emerald Basin of around 270 m. The mean surface circulation is dominated by southwestward flow, much of which originates from the Gulf of St. Lawrence (Hachey *et al.*, 1954; Loder *et al.*, 1998). Anticyclonic circulation tends to occur over the banks and cyclonic circulation around the basins (Sheng and Thompson, 1996; Han *et al.*, 1997). The northeastern region of the Shelf is the southernmost limit of winter sea ice in the Atlantic Ocean. In the southwest, high tidal currents associated with the Gulf of Maine–Bay of Fundy tidal system result in strong bottom-generated mixing and tidally modulated mean flows (Tee *et al.*, 1988).

In this article we highlight the three most significant hydrographic changes in the waters on the Scotian Shelf during the 1990s. These include: (1) the presence throughout the decade of colder-than-usual waters in the northeast and nearshore regions of the Atlantic coast, (2) the arrival of cold Labrador Slope Water at the shelf edge in 1997–1998 and its subsequent movement onto the Shelf, and (3) the variability in the surface water properties included increased vertical stratification throughout the decade. Before discussing these three features we provide some background information on the hydrographic properties and their seasonal and interannual variability in order to place the changes observed in the 1990s into perspective.

Temperature and salinity of the Scotian Shelf waters vary spatially due to complex bottom topography, advection from upstream sources such as the Gulf of St Lawrence and the Grand Bank of Newfoundland, melting of sea ice in spring, local ocean-atmosphere fluxes and exchange with the adjacent offshore slope waters. The seasonal temperature range at the surface in northeastern and central shelf regions is upwards of 16°C, one of the highest in the Atlantic Ocean (Weare, 1977;

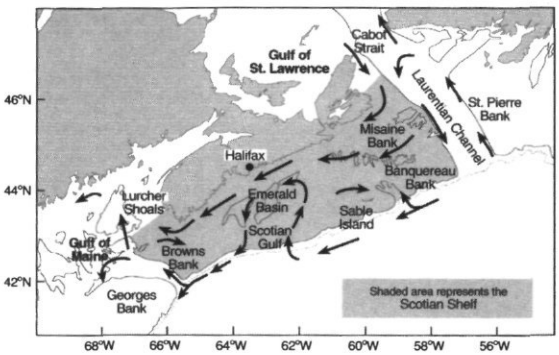


Figure 1. Scotian Shelf showing near-surface circulation and topographic features mentioned in the text. The solid line indicates the 200-m isobath and the dashed line 1000 m.

Yashayaev and Zveryaev, 2001). The range decreases almost exponentially with depth with near negligible changes at depths greater than ~150 m. Towards the southwest, the annual temperature range is more uniform with depth due to increased vertical mixing by the tidal currents. This results in a smaller temperature range at the surface and larger at depth, relative to elsewhere on the Shelf.

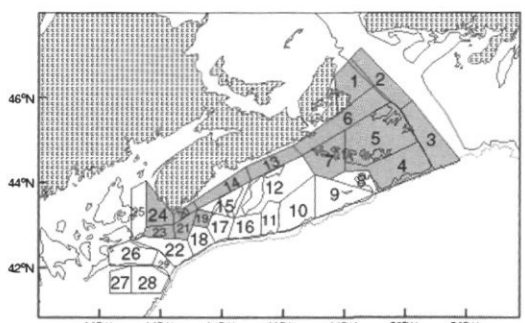
In the winter, the water column in the deep regions of the Scotian Shelf consists of two layers. The upper layer, which extents to 100 m and deeper, is mixed by the winter winds and contains cold, low salinity water. The bottom layer is relatively warm and salty, originating from the offshore "slope waters", and enters the Shelf through deep channels and gullies. In summer, the remnant winter-cooled waters are sandwiched between the solar-heated warm upper layer (30–40 m deep) and the warmer bottom waters. The former, referred to as the cold intermediate layer (CIL), occupies depths from approximately 40 to 150 m. Spatial variation in this vertical structure occurs over the shelf, however. The warm offshore waters cannot penetrate far onto the northeastern Scotian Shelf due to topographic restrictions; therefore the CIL (temperatures <5°C) generally extends to the bottom throughout the year in this area. In areas of strong tidal currents, such as off southwest Nova Scotia, the waters even in summer are relatively well-mixed and no CIL is present.

Horizontally over the Shelf, temperatures and salinities generally increase from northeast to southwest due to the decreasing influence of the Gulf of St Lawrence waters and from inshore to offshore due to mixing with the warmer, more saline offshore waters. For example, in the summer the 50-m temperatures typically range from 0°C to 3°C over the eastern Scotian Shelf, 3°C to 8°C over much of the central shelf and 6°C to 9°C over the western Scotian Shelf, eastern Gulf of Maine, and Bay of Fundy. The near-bottom temperatures display similar ranges to those at 50 m, except over the central shelf where the range increases to 4°C to >10°C, the slightly higher range being caused by the intrusion of the offshore slope waters. The one exception to the general trend in horizontal distributions is the surface temperature in summer, which decreases from northeast to southwest, due to the very warm (typically >16°C) surface outflow from the Gulf of St Lawrence.

Year-to-year, water temperatures on the Scotian Shelf and in the Gulf of Maine are among the most variable in the North Atlantic Ocean (Weare, 1977). Petrie and Drinkwater (1993), in an examination of hydrographic variability, found similar long-period temperature trends over much of the Scotian Shelf. Temperatures were near or above average in the 1950s, declined to below average in the 1960s, rose rapidly in the late 1960s and from the 1970s to 1990 generally were warmer-than-average. Periods of warm temperatures were generally associated with high salinities and cool temperatures with lower salinities.

Data and methods

Much of the temperature, salinity, and density data in this study were derived from an historical hydrographic database held at the Bedford Institute of Oceanography (Petrie *et al.*, 1996). Monthly and annual means of temperature, salinity, and density (sigma-t) and their anomalies were calculated by spatially averaging within areas selected on the basis of topography or oceanography (Figure 2). These



1. Sydney Bight; 11. Emerald Bank; ***21. Roseway Basin***;
2. N. Laurentian Channel; 12. Emerald Basin; 22. Browns Bank;
3. S. Laurentian Channel; ***13. Eastern Shore***; ***23. Roseway Channel***;
4. Banquereau; ***14. South Shore***; ***24. Lurcher Shoals***;
5. Misaine Bank; 15. Lahave Basin; 25. E. Gulf of Maine;
6. Canso; 16. Saddle; 26. Georges Basin;
7. Middle Bank; 17. Lahave Bank; 27. Georges Shoal;
8. The Gully; 18. Baccaro Bank; 28. E. Georges Bank;
9. Sable Island; ***19. Roseway Bank***; 29. N.E. Channel;
10. Western Bank; ***20. Shelburne***;

Figure 2. Areas on the Scotian Shelf in which the monthly and annual mean temperatures were estimated. Shading (and bold italic notation) denotes areas that experienced the cold conditions during the mid- to late-1980s and through most of the 1990s.

areas are those used by Petrie *et al.* (1996). The data were averaged within the areas by month for each year, regardless of the number of stations per month. These monthly means were averaged for the years 1961–1990 to obtain monthly normals. The normals were then subtracted from the monthly means to obtain monthly anomalies, although we note that there are not data in all months. The available monthly anomalies within a calendar year were then averaged to obtain an annual anomaly. High month-to-month variability is evident, which might reflect real temporal changes but also might be due to bias. This can arise due to either poor temporal coverage (e.g. a single measurement in a month) or poor spatial coverage (e.g. a single location within an area that contains horizontal temperature gradients). While individual values for a month or even a year may not represent true average conditions, the longer-term trends are considered real based on observed similarities between areas.

An index of vertical stratification was formed from the density (sigma-t) difference between the closest depths to 0 and 50 m and normalized to a density difference over 50 m. Monthly mean density profiles were estimated by averaging the available normalized density differences within each area in Figure 2 for each calendar year for which there were data. The long-term monthly mean density gradients for the years 1961–1990 were estimated and these then subtracted from the monthly values to obtain monthly anomalies. Annual anomalies were estimated by averaging all available monthly anomalies within a calendar year.

Annual anomalies of sea surface temperature, salinity, and density stratification over the entire Scotian Shelf were derived by averaging the annual anomalies for areas 4–23 in Figure 2.

Persistent presence of cold subsurface waters

One of the primary features of the water properties on the Scotian Shelf in the 1990s was the persistence of very cold conditions in the subsurface waters (deeper than 30–50 m) in the northeast. This is reflected in the 100-m temperature anomalies from Misaine Bank (Figure 3A). The cold waters first appeared in the mid- to late-1980s, reached a minimum temperature in the early 1990s, and gradually warmed to above normal temperatures by the end of the decade. The period of decreasing temperatures coincided with an expansion of the area of the bottom covered by waters with temperatures $< 2°C$ (Figure 4). Throughout the 1990s, the subsurface temperatures in this region generally remained colder-than-normal. These cold temperatures were typically accompanied by lower-than-normal salinities.

These conditions were not limited to the northeastern Shelf, but also appeared along the Atlantic coast of Nova Scotia through to Lurcher Shoals (Figure 3B). The latter are believed to be due to advection and are consistent with direct current observations and numerical models of the circulation that show water from the northeast Shelf tends to be squeezed inshore as it flows southwestward along the Atlantic coast of Nova Scotia (Han *et al.*, 1997) and eventually into the Gulf of Maine (Smith, 1983; Smith *et al.*, 2001). The presence of the cold anomalies in the surface waters at Halifax (Figure 3B) is due in part to the consistent upwelling in summer along the coast (Petrie *et al.*, 1987) and deep mixing in the winter. Both of these processes would act to bring the cold subsurface waters into the surface mixed layer. The cold anomalies during the late 1980s and into the 1990s were traced "downstream" past Lurcher Shoals through to the Maine coast but disappeared further south in the Gulf of Maine. On the Scotian Shelf, these colder waters were not observed in the outer half of the Shelf from Sable Island to Browns Bank. This is consistent with the central shelf region being dominated more by offshore waters. In the upper layers, part of the current along the shelf break flows onto the shelf at the southern end of Western Bank and contributes to the cyclonic flow around Emerald Basin (Figure 1; see also Sheng and Thompson, 1996; Han *et al.*, 1997) and, in the deep waters, the offshore slope waters penetrate onto the Shelf through the Scotian Gulf (Petrie and Drinkwater, 1993).

The cause of the cold water on the northeastern Scotian Shelf during the late 1980s and through most of the 1990s could be due to advection from more northern areas or *in situ* cooling or a combination of both processes. Advection is supported on the strength of the residual circulation patterns (Sheng and Thompson, 1996; Han *et al.*, 1997) and the similarity of the temperature changes in the upstream regions. Temperature trends in the Gulf of St. Lawrence (Gilbert and Pettigrew 1997) and off southern Newfoundland (Colbourne, 1999) mirror those on the northeastern Scotian Shelf including a shift from relatively high temperatures in the early to mid-1980s to low temperatures in the late 1980s and into the 1990s (Figure 3C). The amplitude of the temperature anomalies was similar in all three regions. The waters on the Scotian Shelf appear to warm up earlier and more quickly than in the more northerly regions, perhaps suggesting that the along-shelf advection might have gradually diminished in strength through the late-1990s.

The other possible cause was *in situ* cooling. To explore this possibility, we examined the monthly and annual mean heat fluxes estimated from the COADS (Comprehensive Ocean and Atmospheric

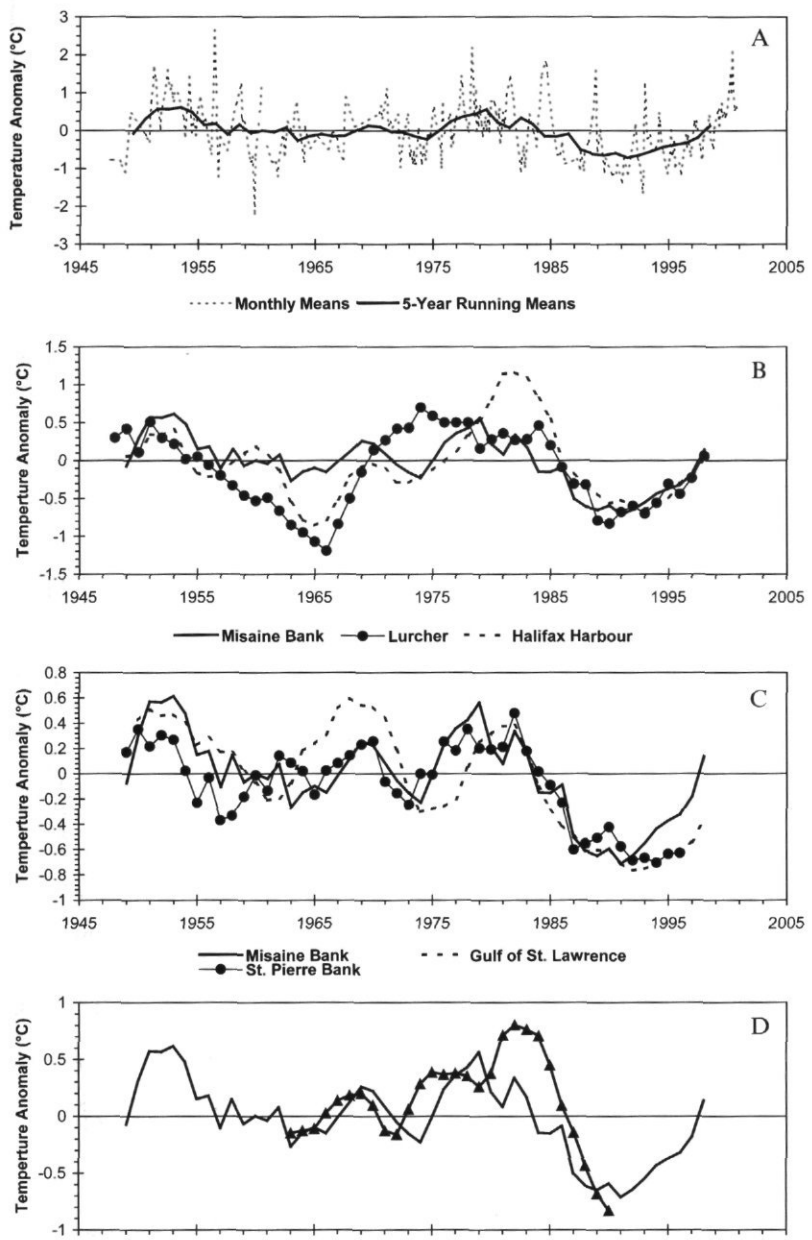


Figure 3. The 5-year-running means of the annual temperature anomalies at 100 m on Misaine Bank together with: (A) the monthly means of Misaine Bank temperature anomalies, (B) the 5-year running means of temperature anomalies at 75 m on Lurcher Shoals off southwest Nova Scotia and at 0 m in Halifax Harbour, (C) the 5-year running means of temperature anomalies at 75 m on St Pierre Bank off southern Newfoundland and of the CIL core temperature in the Gulf of St Lawrence, and (D) the 5-year running means at estimated temperature anomalies based on an annual heat flux model for the northeastern Scotian Shelf.

Data Sets) between 1960 and 1993 for the 2° × 2° latitude–longitude area centred over the northeastern Scotian Shelf. These show negative heat flux anomalies from 1986 through to the end of the available record, suggestive of colder-than-normal temperatures. Assuming that these annual heat flux anomalies are distributed over the top 200 m and do not accumulate (i.e. the water leaves the area within a year), the temperature change can be estimated from

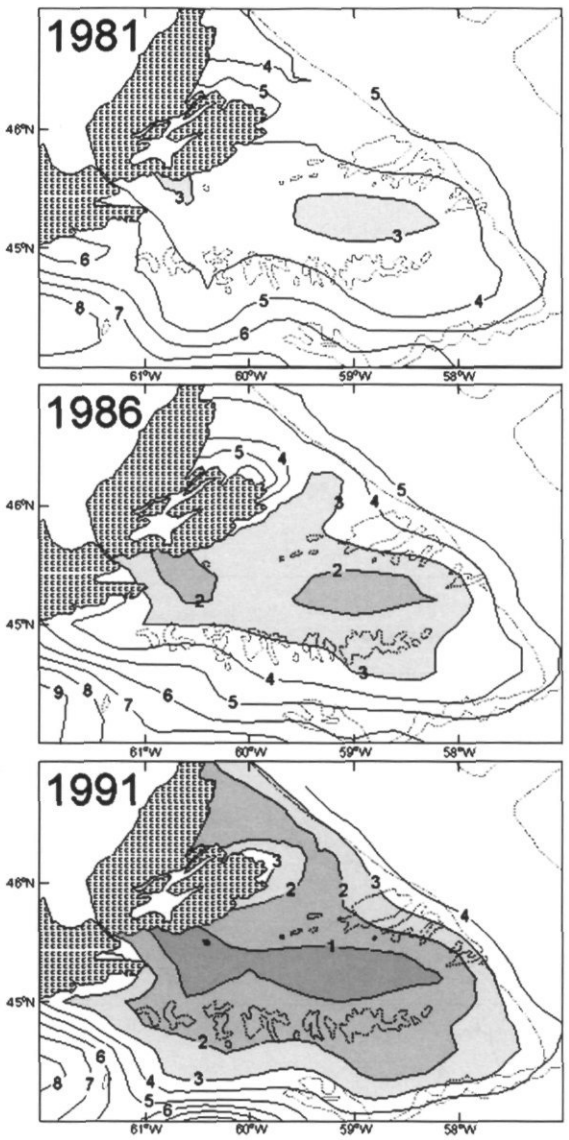


Figure 4. The near-bottom temperatures during July in 1981, 1986, and 1991. The 200-m contour on the shelf and the 1000 m off the shelf are denoted by dashed lines. Temperatures <3°C are shaded.

$$\Delta T = \frac{Q\Delta t}{\rho C_p z}$$

where ΔT is the temperature change produced by a heat flux anomaly Q during the time Δt over a water column of depth z. ρ is the density of the water and C_p is its heat capacity. Δt was taken to be 1 year, ρ was assumed to be 1025 kg m^{-3} and C_p to be 4200 joules kg^{-1}. The estimated temperature changes due to annual heat flux anomalies show a similar pattern to that of the observed temperature anomalies at Misaine Bank (Figure 3D). This simple heat flux model accounts for just under 50% of the variance in the observed anomalies in the overlapping years. However, there are several reasons for questioning this result. First, the heat flux model estimates lag the observed temperature anomalies by around 2 years. Second, the assumptions upon which the model estimates were made, such as constant mixing to 200 m and treating each year independently, are incorrect. Third, the temperature changes were accompanied by observed salinity fluctuations, which suggests changes in the component water masses, not just the heat content. Finally, temperatures in the upper 50 m show a different trend to that of the subsurface waters. If the heat fluxes were dominating the temperature changes one would expect that the temperature trends in the surface and subsurface layers would be similar. Based on all the available information, we conclude that the primary source of the cold, fresh conditions in the subsurface waters on the northeastern Scotian Shelf was most likely advection from the Gulf of St Lawrence and/or the southern Newfoundland Shelf, but that local *in situ* atmospheric cooling may have contributed to the persistent cold waters on the northeastern Scotian Shelf.

Slope water intrusion 1997–1998

Arguably, the most dramatic ocean climate event during the 1990s was the penetration of cold Labrador Slope Water from offshore onto the central and southwestern Scotian Shelf during 1998. Slope waters occupy the region between the continental shelf and the Gulf Stream from the Tail of the Grand Bank to Cape Hatteras. They are a combination of colder, fresher deep Labrador Current Water and warmer, saltier North Atlantic Central Water. Gatien (1976) identified two types of slope waters, Labrador Slope Water with temperatures generally 4°C to 8°C and salinities 34.3 to 35 and Warm Slope Water with temperatures typically 8°C to 12°C and salinities 34.7 to 35.5. The slope water properties at a particular location depend upon whether the North Atlantic Central or Labrador Current water mass component is dominant. The temperature and salinity characteristics of the Slope Water adjacent to the Scotian Shelf vary depending upon the volume flow of the deep (100–300 m) Labrador Current around the Tail of the Grand Bank (Petrie and Drinkwater, 1993). In years of high baroclinic transport, such as occurred in the 1960s, Labrador Slope Water was found along the shelf edge as far south as the Middle Atlantic Bight (Gatien, 1976). In years of low transport, such as in the 1950s and again in the 1970s through to the 1990s, the Labrador Slope Water seldom penetrates much farther south than the Laurentian Channel. During these times, Warm

Slope Water dominates the shelf edge off the Scotian Shelf. The slope waters are important to the Shelf since they penetrate onto the Shelf through gullies and channels to occupy the deep basins and the deep layers of the central and southwestern areas of the Scotian Shelf. The exchange between the offshore and shelf waters is forced by a combination of horizontal density gradients, warm-core Gulf Stream rings, and meteorological events. During the 1990s, at least until 1997, temperatures along the shelf break and in the deep basins of the Scotian Shelf and the Gulf of Maine remained relatively warm, indicative of Warm Slope Water. Indeed, the warmest extended period in the last 50 years within these deep basins was during the mid-1990s (Figure 5A).

In the autumn of 1997, the Labrador Slope water moved southward along the edge of the Scotian Shelf reaching the Gulf of Maine in January of 1998 and off the Middle Atlantic Bight by the spring of 1998 (Figure 6). Drinkwater *et al.* (2002) provided details of the timing of this water mass as it flowed south, as well as its subsequent movement onto the Scotian Shelf and into the Gulf of Maine. Although the Labrador Slope Water was first detected in the offshore waters adjacent to the central Scotian Shelf in October, it did not begin to penetrate into the deep reaches of Emerald Basin until December 1997. By February 1998 the lower layers of Emerald Basin were completely flushed. Temperatures dropped by over 4°C (Figure 5B) and salinities by approximately 1 during this event. By July 1998, waters with Labrador Slope Water characteristics covered most of the ocean bottom on the southwestern Shelf and temperatures were the lowest recorded in over 30 years. These waters were not restricted to the Scotian Shelf but also penetrated into the Gulf of Maine (Drinkwater *et al.*, 2002). The Labrador Slope Water along the edge of the Scotian Shelf began to retract during the summer of 1998 and late that year was confined to the Laurentian Channel area and north, having been replaced by the Warm Slope Water all along the Scotian Shelf. The Labrador Slope Water on the shelf also gradually disappeared through 1998 (Figure 5B).

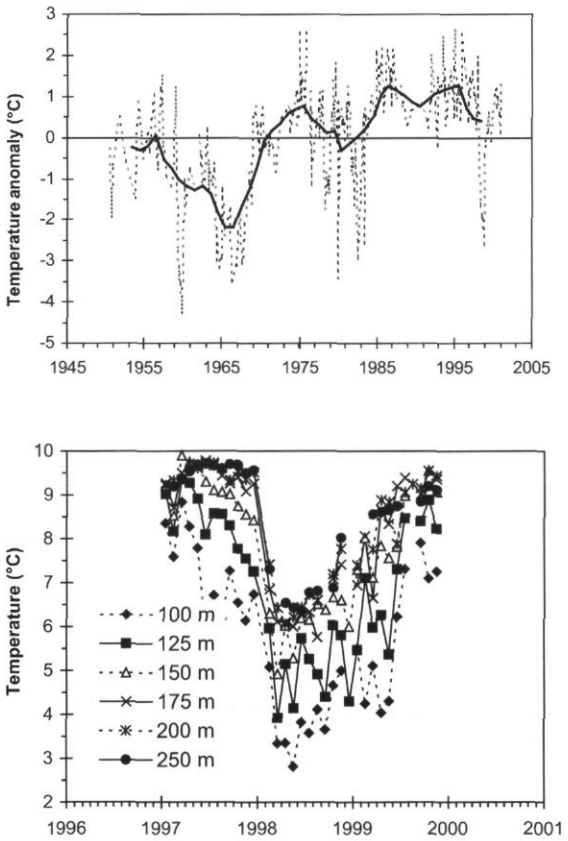


Figure 5. Monthly (dashed line) and 5-year running means (solid line) of the temperature anomalies near-bottom (250 m) in Emerald Basin (top panel). The monthly temperatures from 100 to 250 m in Emerald Basin during 1997–1999 (lower panel).

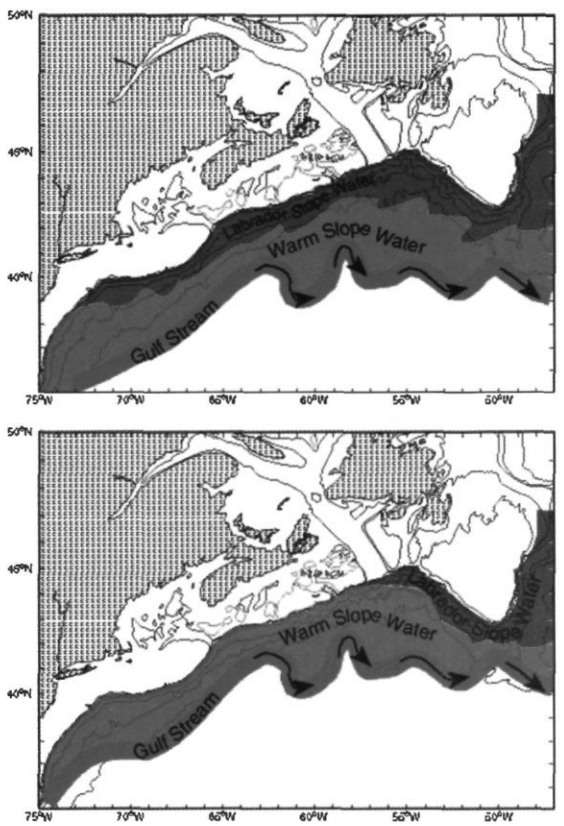


Figure 6. A schematic diagram of the distribution of the offshore Labrador Slope Water at approximately 200 m during the maximum southward extension in 1998 (top panel) and its more typical distribution during the past 30 years (bottom panel).

The southward extension of the Labrador Slope Water is believed to be due to an increased volume transport of the deep Labrador Current (Petrie and Drinkwater, 1993). This in turn is related to the strength of the large-scale atmospheric circulation patterns over the North Atlantic as reflected in the intensity of the Icelandic Low (Worthington, 1964) or its related North Atlantic Oscillation (NAO) index (Marsh *et al.*, 1999; Drinkwater *et al.*, 2002). Increased transport coincides with a weakened Icelandic Low (low NAO index). In 1996, the NAO index experienced the largest decline in its 100-year record as the Icelandic Low and the Azores High both weakened substantially. There was also increased geostrophic transport on the Newfoundland Shelf during several years of the mid-1990s (Colbourne, 2000). Drinkwater *et al.* (2002) suggest that this decline in the NAO and the increased geostrophic transport in the Labrador Current eventually led to the southward movement of the Labrador Slope Water through to the Middle Atlantic Bight in 1997–1998. However, the time delay between the NAO decline and the arrival of the Labrador Slope Water off the Gulf of Maine and Middle Atlantic Bight was of the order of 20 months, whereas during the 1958 event Worthington (1964) found a delay of only 8 months. The cause of the longer delay in 1997–1998 is unclear, although only 10 months after the low wintertime NAO index of 1996 cold water was observed upstream off St Pierre Bank at 50 m in January 1997 and 2–3 months later at 150 m (unpublished current meter data, P. C. Smith). The 5–7 month delay from St Pierre Bank to Banquereau Bank is unexplained.

Variability in the near-surface layer

During the 1950s to the 1990s, the temperature trends throughout the water column on the Scotian Shelf were generally similar and dominated by the warm 1950s, the cold 1960s, and the above normal temperatures in the 1970s and 1980s (Petrie and Drinkwater, 1993). In the 1990s, there were greater differences between the near-surface trends in the hydrographic properties and those elsewhere in the water column. There were three significant features of the surface layers in the 1990s.

The first relates to the surface layer temperatures. Following a decrease through the 1980s, temperature anomalies averaged over the Scotian Shelf were below normal in the early-1990s, rose slightly in the mid-1990s, then fell again before rising rapidly to near maximum values (approximately 1.3°C) over the 50-year record in the last years of the decade (Figure 7A). The ocean temperatures mirror air temperatures in the region with approximately 50%

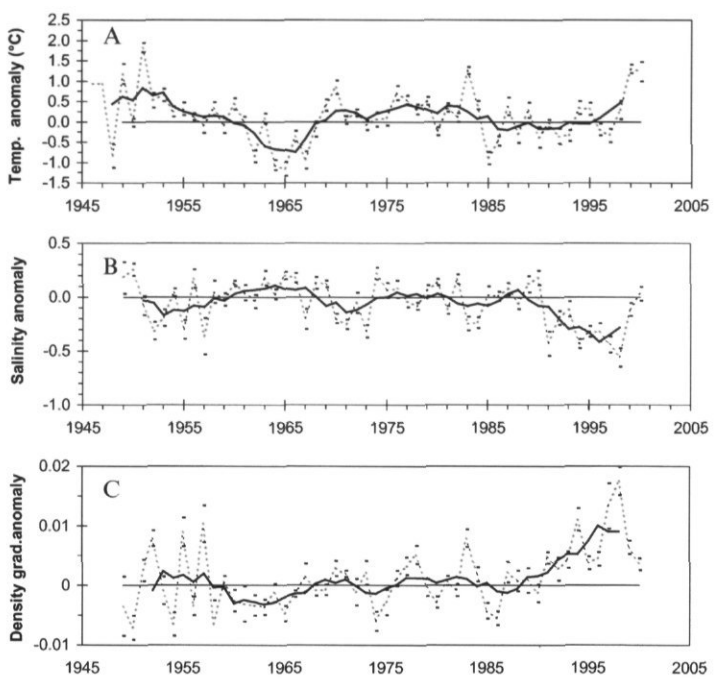


Figure 7. The estimated annual (dashed line) and 5-year running averages (solid line) of the anomalies (relative to their 1971–2000 means) of (A) surface temperature, (B) surface salinity, and (C) 0–50 m density gradient. All plots represent averages over the Scotian Shelf (areas 4–23 in Figure 2). The horizontal tick marks on the annual values denote the error of the mean.

of the variance in sea surface temperatures accounted for by air temperatures. Consistent with this, the high sea surface temperatures in the late 1990s coincided with high air temperatures. Indeed, historic highs of the annual air temperature in over 100 years of records were set in 1999 throughout the region from southern Labrador to the Gulf of Maine, including over the Scotian Shelf (Drinkwater *et al.*, 2000).

The second significant change was in the near-surface salinity anomalies averaged over the Shelf. They showed a general decline through most of the 1990s reaching a minimum in 1998 (Figure 7B). This minimum (approximately 0.5 fresher-than-normal) represented the lowest salinity recorded on the Scotian Shelf in the over 50-year time series. In 1999, salinities increased rapidly and returned to near normal values by 2000. Similar lower-than-normal salinities in the 1990s were observed in the eastern Gulf of Maine (areas 24–28; Figure 2), consistent with the findings of Smith *et al.* (2001). The primary source of the low surface salinities on the Scotian Shelf has generally been considered to be the outflow from the Gulf of St Lawrence through Cabot Strait (McLellan, 1954; Sutcliffe *et al.*, 1976). The Gulf of St Lawrence salinities in turn reflect the run-off from the St Lawrence River system (Lauzier, 1957). The freshwater discharge from the St Lawrence during the 1990s was higher than the long-term (1961–1990) mean but decreased relative to the 1970s and 1980s, and thus it cannot explain the low salinities on the Scotian Shelf. Sea ice was above normal on the Scotian Shelf in the early 1990s, but since 1995 has been at or near the lowest on record (Drinkwater *et al.*, 2000). Smith *et al.* (2001) suggested that the salinity variability on the inner Shelf for the years 1994 to 1996 was due to advection of anomalies from upstream off Newfoundland. We examined the sea-surface salinity changes at Station 27, the long-term monitoring site off St John's, Newfoundland, in the inner branch of the Labrador Current. It shows below normal salinities through most of the 1990s (consistent with the results of Colbourne, 2001) and reasonable correspondence with salinity fluctuations on the Scotian Shelf throughout the last half of the 1900s (Figure 8). Approximately 42% of the variance in the annual salinity over the Scotian Shelf can be accounted for by changes in the upstream salinities off Newfoundland. Thus, the most likely source of the Scotian Shelf low salinity surface water in the 1990s is from off the Newfoundland Shelf.

The third significant feature of the near-surface layer in the 1990s was a change in stratification. Monthly and annual means of the stratification index show high variability but the 5-year running means show distinctive trends. The dominant feature over the Scotian Shelf is higher stratification during the 1990s (Figure 7C). The stratification

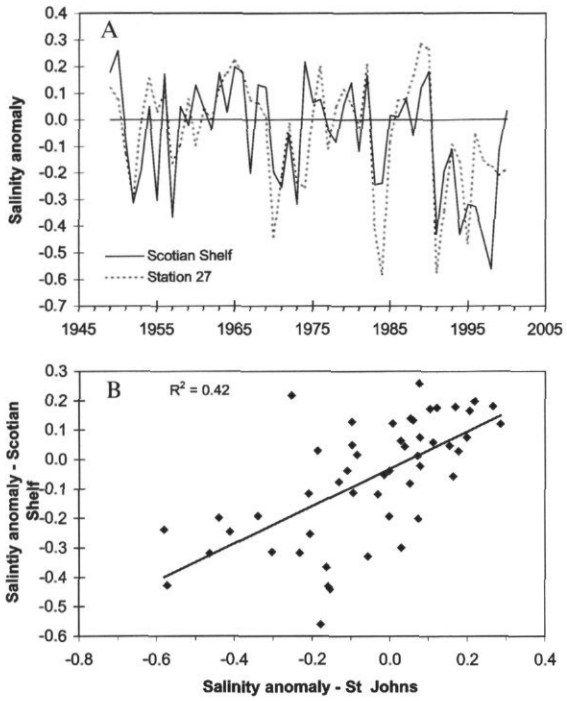


Figure 8. The annual sea-surface salinity anomalies averaged over the Scotian Shelf (areas 4–23 in Figure 2) and at Station 27 off St John's, Newfoundland, plotted as (A) time series and (B) an XY plot. The linear regression line is also plotted in (B) along with the R^2 value.

index began to increase steadily after 1990, reaching a peak around 1997–1998 and declining slightly after that. The late-1990 anomalies are, or are near to, the highest values in the approximate 50-year record. The principal cause of this increased stratification was the decrease in surface salinities (Figure 7B). The increased stratification was observed in all regions of the Scotian Shelf but did not extend into the Gulf of Maine region. This lack of signal might be due to the more intense tidal mixing in the Gulf of Maine.

Biological consequences

All three of the major ocean climate features that occurred in the 1990s on the Scotian Shelf and that were discussed above had measurable influences on the local biology. The presence of the cold water on the northeastern Scotian Shelf in the late 1980s and 1990s is believed to have led to an expansion of the distribution of cold-water species such as capelin (*Mallotus villosus*), Greenland halibut (*Reinhardtius hippoglossoides*), shrimp (*Pandalus borealis*), and snow crab (*Chionoecetes opilio*) (Frank *et al.*, 1996; Tremblay, 1997; Drinkwater, 1999; Zwanenburg

et al., 2002), and contributed to lower growth rates of Atlantic haddock (*Melanogrammus aeglefinus*) (Drinkwater *et al.*, 2000) and most demersals (Zwanenburg *et al.*, 2002). It also coincided with low abundance of Atlantic cod (*Gadus morhua*), but it is not clear to what extent the decline in cod in the northeastern Scotian Shelf was due to over-fishing or other possible factors (Zwanenburg *et al.*, 2002).

Although relatively short-lived, the penetration of the cold Labrador Slope Water onto the shelf in 1998 is known to have affected the catchability of certain fisheries on the Scotian Shelf and on Georges Bank (Drinkwater *et al.*, 2002). They noted, for example, that catches of porbeagle shark (*Lamna nasus*) and silver hake (*Merluccius bilinearis*) declined dramatically in the Emerald Basin in early 1998, shortly after the cold Labrador Slope Water replaced the Warm Slope Water. Also, fishermen on Georges Bank noted declines in their catches of lobster (*Homarus americanus*) that they attributed to the presence of cold water. Cold water has been shown to limit the activity of the lobsters and hence their likelihood of encountering a lobster trap (McLeese and Wilder, 1958).

Stratification of the upper water column is an important characteristic that influences both physical and biological processes. Stratification can affect the extent of vertical mixing, the vertical structure of the wind forcing, the timing of the spring bloom, vertical nutrient fluxes, and plankton speciation to mention just a few. Under increased stratification, there is a tendency for more primary production to be recycled within the upper mixed layer and hence less available for the deeper, lower layers. This general tendency led Frank *et al.* (1990) to speculate that increased stratification should lead to a higher percentage of pelagic fish relative to demersal species. Indeed, during the 1990s, the ratio of pelagic to demersal fish biomass did increase and by the mid-1990s the ratio was the highest in over 25 years (Zwanenburg, *et al.*, 2002; Frank and Drinkwater, 2002).

Conclusions

We have described three important ocean climate changes that occurred on the Scotian Shelf during the1990s, mainly associated with advective processes. These have included record setting or near record-setting conditions over the past 30 to 50 years. The first was an extended period of cold temperatures in the northeast region of the Shelf and along the Atlantic coast of Nova Scotia. This is believed to be due to along-shelf advection of cold waters from the Gulf of St Lawrence and southern Newfoundland, with the possibility of some contribution by local *in situ* atmospheric cooling. The second event, in 1998, occurred in the deep, near-bottom waters in Emerald Basin and the southwestern shelf. These waters, which originate offshore and then penetrate onto the Shelf, cooled dramatically due to the unusual appearance of cold, low saline Labrador Slope Water along the shelf edge, which replaced the high saline, Warm Slope Water. Finally, long-term records for warm temperatures, low salinities, and high stratification were set in the near-surface waters during the late 1990s. While the high sea surface temperatures most likely resulted from local atmospheric heat exchanges, the primary mechanism of the salinity changes and subsequent stratification appears to be through advection from off Newfoundland.

It is worth noting that at the beginning of the decade it appeared that the horizontal and vertical differences in the hydrographic trends over the Scotian Shelf were relatively small (Petrie and Drinkwater, 1993). This had suggested that a single station or area could be used as an index to capture much of the long-term hydrographic variability occurring over the Shelf. The past decade has seen much larger spatial variability in the anomalies of the hydrographic properties than in the past, both vertically and horizontally, and indicates that several hydrographic indices will be required in order to capture the long-term trends over the Scotian Shelf.

References

Colbourne, E. 1999. Oceanographic conditions in NAFO Subdivisions 3Pn and 3Ps during 1997 and 1998 with comparison to the long-term (1961–1990) average. Canadian Department of Fisheries and Oceans, Canadian Stock Assessment Secretariat, Research Document, 9/39. 19 pp.

Colbourne, E. 2000. Interannual variations in the stratification and transport of the Labrador Current on the Newfoundland Shelf. ICES CM 2000/L: 02. 20 pp.

Drinkwater, K. F. 1999. Changes in ocean climate and its general effect on fisheries: examples from the North-west Atlantic. *In* The Ocean Life of Atlantic Salmon – Environmental and Biological Factors Influencing Survival, pp. 116–136. Ed. by D. Mills. Fishing News Books, Oxford.

Drinkwater, K. F., Colbourne, E., and Gilbert, D. 2000. Overview of environmental conditions in the Northwest Atlantic in 1999. NAFO SCR Doc. 00/21. 98 pp.

Drinkwater, K. F., Mountain, D. B., and Herman, A. 2002. The southward excursion of Labrador Slope Water off eastern North America during 1997–1998 and its effect on the adjacent shelves. Journal of Geophysical Research (submitted).

Frank, K. T., Carscadden, J. E., and Simon, J. E. 1996. Recent excursions of capelin (*Mallotus villosus*) to the Scotian Shelf and Flemish Cap during anomalous hydrographic conditions. Canadian Journal of Fisheries and Aquatic Sciences, 53: 1473–1486.

Frank, K. T., and Drinkwater, K. F. 2002. Links between the recent increase in pelagic fishes and environmental changes on the Scotian Shelf. ICES CM 2002/O18.

Frank, K. T., Perry, R. I., and Drinkwater, K. F. 1990. Predicted response of northwest Atlantic invertebrate and fish stocks to CO_2-induced climate change. Transactions of the American Fisheries Society, 119: 353–365.

Gatien, M. G. 1976. A study in the Slope Water region south of Halifax. Journal of the Fisheries Research Board of Canada, 33: 2213–2217.

Gilbert, D., and Pettigrew, B. 1997. A study of the interannual variability of the CIL core temperature in the Gulf of St. Lawrence. Canadian Journal of Fisheries and Aquatic Sciences, 54 (Suppl 1): 57–67.

Hachey, H., Hermann, H., and Baily, W. 1954. Waters of the ICNAF convention area. ICNAF Annual Proceedings 1953–54, 4: 67–102.

Han, G., Hannah, C. G., Loder, J. W., and Smith, P. C. 1997. Seasonal variation of the three-dimensional mean circulation over the Scotian Shelf. Journal of Geophysical Research, 102: 1011–1025.

Lauzier, L. 1957. The St. Lawrence spring run-off and summer salinities in the Magdalen Shallows. Bulletin of the Fisheries Research Board of Canada, 111: 193–194.

Loder, J. W., Petrie, B., and Gawarkiewicz, G. 1998. The coastal ocean off northeastern North America: a large-scale view. The Sea, 11: 105–133.

Marsh, R., Petrie, B., Weidman, C. R., Dickson, R. R., Loder, J. W., Hannah, C. G., Frank, K., and Drinkwater, K. 1999. The Middle Atlantic Bight tilefish fill of 1882. Fisheries Oceanography, 8: 39–49.

McLellan, H. J. 1954. Temperature-salinity relations and mixing on the Scotian Shelf. Journal of the Fisheries Research Board of Canada, 11, 419–430.

McLeese, D. W., and Wilder, D. G. 1958. The activity and catchability of lobster (*Homarus americanus*) in relation to temperature. Journal of the Fisheries Research Board of Canada, 15: 1345–1354.

Petrie, B., and Drinkwater, K. 1993. Temperature and salinity variability on the Scotian Shelf and in the Gulf of Maine 1945–1990. Journal of Geophysical Research, 98: 20,079–20,089.

Petrie, B., Drinkwater, K., Gregory, D., Pettipas, R., and Sandström, A. 1996. Temperature and salinity atlas for the Scotian Shelf and the Gulf of Maine. Canadian Technical Report of Hydrography and Ocean Sciences, 171. 398 pp.

Petrie, B., Topliss, B. J., and Wright, D. G. 1987. Coastal Opwelling and eddy development off Nova Scotia. Journal of Geophysical Research, 92: 12,979–12,991.

Sheng, J., and Thompson, K. R. 1996. A robust method for diagnosing regional shelf circulation from scattered density profiles. Journal of Geophysical Research, 101: 25,647–25,659.

Smith, P. C. 1983. The mean and seasonal circulation off southwest Nova Scotia. Journal of Physical Oceanography, 13: 1034–1054.

Smith, P. C., Houghton, R. W., Fairbanks, R. G., and Mountain, D. G. 2001. Deep-Sea Research II, 48: 37–70.

Sutcliffe, W. H. Jr., Loucks, R. H., and Drinkwater, K. F. 1976. Coastal circulation and physical oceanography of the Scotian Shelf and the Gulf of Maine. Journal of the Fisheries Research Board of Canada, 33: 98–115.

Tee, K.-T., Smith, P. C., and Lefaivre, D. 1988. Estimation and verification of tidally induced residual currents. Journal of Physical Oceanography, 18: 1415–1434.

Tremblay, M. J. 1997. Snow crab (*Chionoecetes opilio*) distribution limits and abundance trends on the Scotian Shelf. Journal of Northwest Atlantic Fishery Science, 21: 7–22.

Weare, B. C. 1977. Empirical orthogonal function analysis of Atlantic Ocean surface temperatures. Quarterly Journal of the Royal Meteorological Society, 103: 467–478.

Worthington, L. V. 1964. Anomalous conditions in the Slope Water area in 1959. Journal of the Fisheries Research Board of Canada, 21: 327–333.

Yashayaev, I. M., and Zveryaev, I. I. 2001. Climate of the seasonal cycle in the North Pacific and North Atlantic Oceans. International Journal of Climatology, 21: 401–417.

Zwanenburg, K. C. T., Bowen, D., Bundy, A., Drinkwater, K., Frank, K., O'Boyle, R. N., Sameoto, D., and Sinclair, M. 2002. Decadal changes in the Scotian Shelf large marine ecosystem. *In* Changing States of the Large Marine Ecosystems of the North Atlantic and Global Environmental Trends, pp. 105–150. Ed. by K. Sherman and H. R. Skjoldal. Elsevier, Amsterdam, The Netherlands.

ICES Marine Science Symposia, 219: 50–60. 2003

Hydrographic conditions in Icelandic waters, 1990–1999

Svend-Aage Malmberg and Hedinn Valdimarsson

Malmberg, S-A., and Valdimarsson, H. 2003. Hydrographic conditions in Icelandic waters, 1990–1999. – ICES Marine Science Symposia 219: 50–60.

The main results of the hydrographic conditions in Icelandic waters in the 1990s reveal the same variability from year to year observed since the 1950s, including Atlantic, Polar, and Arctic periods in North Icelandic waters. Attention is paid to the hydrographic conditions in the warm water from the south (Irminger Current) which developed at the end of the 1990s into high saline conditions comparable with the period prior to the 1960s. This includes the northern component flowing into North Icelandic waters. The conditions in the East Icelandic Current also improved at the end of the 1990s with relatively high salinities. Thus the hydrobiological conditions in Icelandic waters were favourable at the end of the 1990s with regard to the various fish stocks.

Keywords: East-Icelandic Current, hydrographic conditions, Icelandic waters, Irminger Current, NAO.

S.-A. Malmberg and H. Valdimarsson: Marine Research Institute, Skúlagata 4, 121 Reykjvík, Iceland [tel: + 354 552 0240; fax: + 354 562 3790; e-mail: svam@hafro.is and hv@hafro.is].

Introduction

Icelandic waters are located at the boundary between warm Atlantic Water from the south and cold water from the north, i.e. the oceanic Polar Front in the northern North Atlantic and Nordic Seas (Figure 1). The warm Irminger Current flows northwards and splits into two branches west of Iceland. The western branch meets the cold East Greenland Current and flows southwards into the Irminger Sea. The eastern branch flows north and eastwards off Northwest Iceland into North Icelandic waters (The Iceland Sea) and disperses off the eastern coast of Iceland (Stefánsson, 1962). The cold low saline water masses are those of the East Greenland (Polar) Current, flowing southwards through the Denmark Strait, and the East Icelandic Current flowing southwards north and east of Iceland (Malmberg, 1984, 1985). This circulation is complicated by north–south fluctuations of the boundary zone from year to year, mainly expressed by the presence of Atlantic, Polar, or Arctic Water in North and East Icelandic waters. These shifts in the location of the oceanic Polar Front deeply affect the climate and ecology in Iceland as well as the surrounding waters.

Materials

Since 1970, hydrobiological investigations have been carried out in Icelandic waters on standard sections on a seasonal basis (Figure 1). Similar investigations were started on a more or less annual basis in the spring of 1948 in connection with herring surveys in North Icelandic waters (Stefánsson, 1962; Jakobsson, 1980; Stefánsson and Jakobsson, 1989; Jakobsson and Östvedt, 1999).

The current study mainly presents a follow-up, for the years 1990–1999/2000, of the hydrographic data series published previously in *Annales Biologiques* (e.g. Malmberg, 1980, 1983) and elsewhere by Malmberg (1984, 1985, 1986, 1988), Malmberg and Kristmannsson (1992), and Malmberg *et al.* (1996).

Water masses

The main water masses in Icelandic waters are given in Table 1. These water masses are of importance for the ecology of Icelandic waters. In addition, the deep and bottom water and fresh water flux of the Polar Currents play a very significant role in the

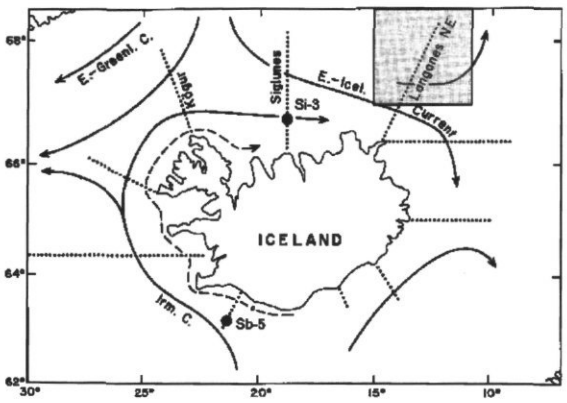


Figure 1. Main ocean currents and sections of hydrobiological standard sections in Icelandic waters. Selected areas and stations dealt with in the article are indicated.

Table 1.

Water mass	t	s	Water-mass origin/regime
Atlantic Water (AW)	3–8°	>34.9	North Atlantic and Irminger Current
Polar Water (PW)	<0°	<34.4	East Greenland Current
Arctic/Polar Water (ASW/PW)	<0–2°	34.3–34.9	East Icelandic Current
North Icelandic Winter Water (NIWW)	2–3°	34.8–34.9	North Icelandic Shelf
Bottom/Deep Water (DW)	<0°	3489–3492	Deeper layers north and east of Iceland
Arctic Intermediate Water (AIW)	0–2°	~34.95	Below the PW in the East Greenland Current
Coastal Water (CW)	Var.	<34.0	Shelves around Iceland diluted by run-off

water mass budget and climatic aspects of the northern North Atlantic and even globally (e.g. Swift, 1984; Hansen and Østerhus, 2000; Hansen *et al.*, 2001).

Results and discussion

East Icelandic Current

The water system in the Iceland and Norwegian Seas north and east of Iceland is mainly fed by the East Greenland Current and the Irminger Current, and known as the East Icelandic Current (Knudsen, 1899; Kiilerich, 1945; Stefánsson, 1962; and Swift and Aagaard, 1981). The East Icelandic Current, an ice-free so-called Arctic current in the period 1948–1963 (salinities above 34.7 and even 34.8 in spring) developed into a Polar Current from 1964–1971 (salinities below 34.7 and even 34.4), transporting and preserving drift-ice due to suppressed convective overturning in the upper layers (Malmberg, 1969, 1972; Dickson *et al.*, 1988). The "cold tongue" (< 0°C) of the current also advanced further south and east off Iceland into the Norwegian Sea than before (e.g. Vilhjalmsson, 1994; Blindheim *et al.*, 1999). These changes in the 1960s, along with a negative impact in North Icelandic waters on nutrient supply (Stefánsson and Olafsson, 1991), primary production (Thordardottir, 1977), and zooplankton concentrations (Astthorsson *et al.*, 1983; Astthorsson and Gislason, 1995), changed the feeding migration of the Atlanto-Scandian herring stock in the Iceland and Norwegian Seas (Malmberg, 1967; Jakobsson, 1980; Stefánsson and Jakobsson, 1989; Jakobsson and Östvedt, 1999). The herring disappeared from the traditional feeding grounds in North Icelandic waters and migrated into the Norwegian Sea along the eastern boundary of the "cold tongue" of the East Icelandic (Polar) Current. The Polar period in the East Icelandic Current in the 1960s occurred during the most negative NAO Index in the 20th century (Hurrell, 1995; Dickson *et al.*, 1996) and was the driving force for the "Great Salinity Anomaly" in the northern North Atlantic in the 1970s (Dickson *et al.*, 1988). More recently, Polar conditions ($S < 34.7$) were found in the East Icelandic Current in 1976–1979, 1982, 1988, and 1996–1998 (Figures 2A and 3B), but not so extreme as in the 1960s (Malmberg and Kristmannsson, 1992; Malmberg *et al.*, 1996; Malmberg *et al.*, 2001), and Arctic conditions ($S > 34.7$) during other years.

These results can be used to estimate variations in the volume transport and the fresh water flux in the East Icelandic Current from year to year. The current velocities are presumably relatively weak (Poulain *et al.*, 1996), except over the continental slope northeast of Iceland, where velocities in the order of 10 cm s^{-1} were obtained in the near-surface layer by direct current measurements and geostrophy in 1997–1998 (Valdimarsson and Jonsson, 2000). However, in 1995–1996, satellite-tracked drifters drogued at 15 m gave three times as high mean velocities (Valdimarsson and Malmberg, 1999). The width of the main branch of the current above the slope can be taken as 50 km and the depth of the current used for proxy volume estimates as 100 m. This results in an overall estimated transport of the East Icelandic Current above 100 m of 0.5×10^6 m^3 s^{-1} (0.5 Sv). For freshwater estimates, a reference salinity of 34.85 was used, which is based on repeated hydrographic observations (Malmberg and Kristmannsson, 1992). Thus, according to these estimates, during the ice-free Arctic period in the 1950s and early 1960s the freshwater thickness was

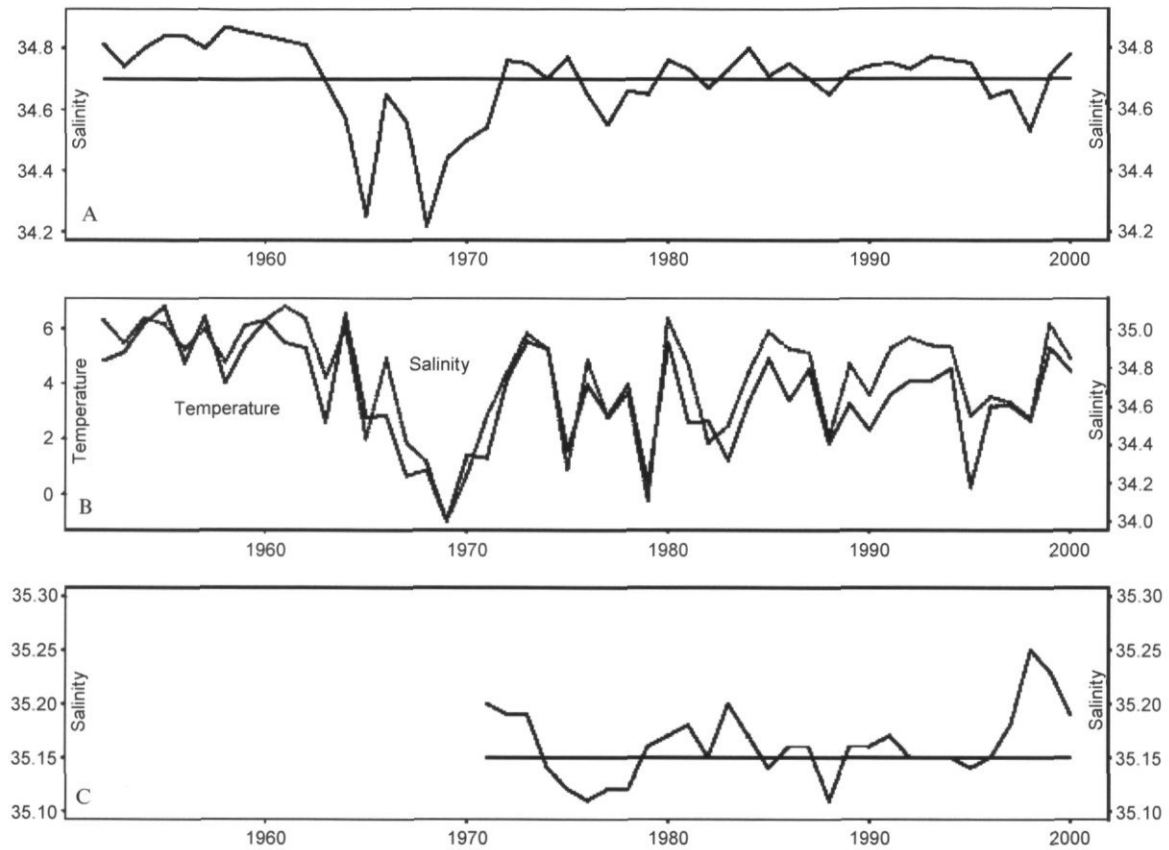


Figure 2. A. Means of salinity in spring at 25-m depth in a selected area in the East Icelandic Current northeast of Iceland 1952–2000. B. Temperatures and salinity in spring at 50-m depth on a hydrographic station in North Icelandic waters; Si-3; 1952–2000. C. Salinity in spring at 100-m depth in the Irminger Current south of Iceland; Sb-5; 1971–2000. For locations see Figure 1.

approximately 0.2 m, but 1.0–1.5 m during the Polar drift-ice period in the late 1960s, which is in good agreement with earlier results (Jonsson, 1992). These thicknesses result in different freshwater fluxes of $10^3\ m^3\ s^{-1}$ and at least $5 \times 10^3\ m^3\ s^{-1}$, i.e. 0.001 Sv during Arctic years and 0.005 Sv or more during the Polar years in the late 1960s (Figure 4). Much less variation has occurred since then, with generally less fresh water flux than in the late 1960s ($2 \times 10^3 - 4 \times 10^3\ m^3\ s^{-1}$ or 0.002–0.004 Sv).

North Icelandic waters

A selected hydrographic station on the shelf in North Icelandic waters (Si-3; 50 m; Figure 1) has been used to show seasonal and annual variability in the area since 1952 up to and including the past decade (Figures 2B and 5). The changes in the latter half of the 1960s (prior to the "Great Salinity Anomaly" (GSA) in the 1970s (Dickson *et al.*, 1988)) are notable. At this time of the extreme Polar Water period in the East Icelandic Current, the hydrographic conditions in North Icelandic waters changed from being Atlantic ($t > 4°C$; $S > 35.0$) to Polar conditions ($t \sim 0°C$; S as low as 34.0; Figure 2B) after decades of Atlantic conditions ever since the 1920s (Stefánsson 1962, 1969). After the Polar period, or so-called ice-years, in the late 1960s, the conditions shifted between Atlantic (1972–1974, 1980, 1984–1987, 1991–1994, and 1999–2000) and Polar conditions (1975–1979, 1988, 1996–1998). Furthermore, a third occurrence of so-called Arctic conditions (1981–1983, 1989–1990, and extremely so in 1995) was observed. These Arctic conditions in North Icelandic waters included moderate cold temperatures of 0–3°C and rather homogeneous salinities of around 34.8 throughout the water column into the near-surface layers. Thus the conditions revealed a relatively weak stratification in North Icelandic waters in 1981–1983 and 1989–1990 (downstream conditions of the GSAs in the 1970s and 1980s) (Dickson *et al.*, 1988; Belkin *et al.*, 1998). The relatively unstratified water was observed along with poor living conditions (Malmberg, 1986; Malmberg and Blindheim, 1994). In general, the inflow of Atlantic Water into the spawning and

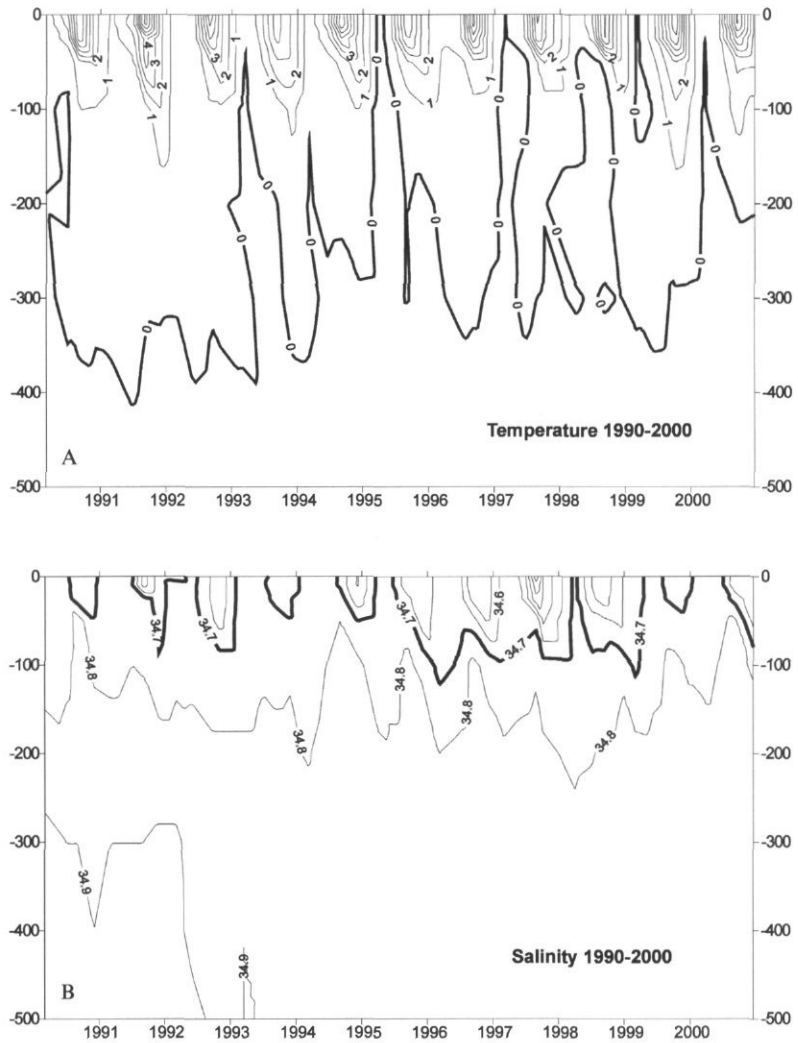


Figure 3. Temperature and salinity isopleths of monthly means for all data available in a selected area in the East Icelandic Current northeast of Iceland shown in Figure 1 during the period 1991–2000. Contours every 1°C and 0.1S.

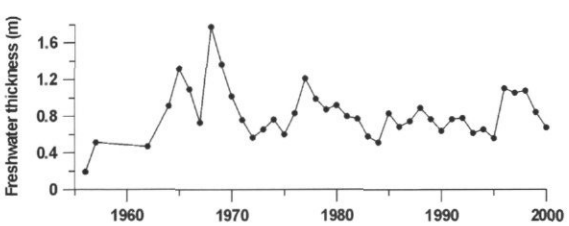


Figure 4. The freshwater thickness at a selected station of the Langanes NE section. (Station 4; Figure 1) above 150 m, relative to a salinity of 34.93, in spring 1956–2000 (Jonsson in Malmberg *et al.*, 2001).

feeding rounds in North Icelandic waters favours the recruitment and growth of commercial fish stocks such as cod (e.g. Vilhjalmsson, 1997; Astthorsson and Vilhjalmsson, 2001). Furthermore, the Icelandic capelin stock was at its lowest during the Arctic years in North Icelandic waters, presumably depending on zooplankton conditions, and growth of cod was also at its lowest, since it depends on the capelin as a food supply. Until the 1990s, the salinity of the Atlantic Water flowing into North Icelandic waters never reached the high values obtained prior to the mid-1960s ($S > 35.0$; Figure 7). This low salinity period ($S < 35.0$) may even reveal a general tendency, since the 1960s, to Arctic conditions. In 1999/2000, however, an increase in salinity towards former values was observed. The seasonal and annual variations in North Icelandic waters during the period 1974–2000 are further well established in Figure 8 with the highest temperatures

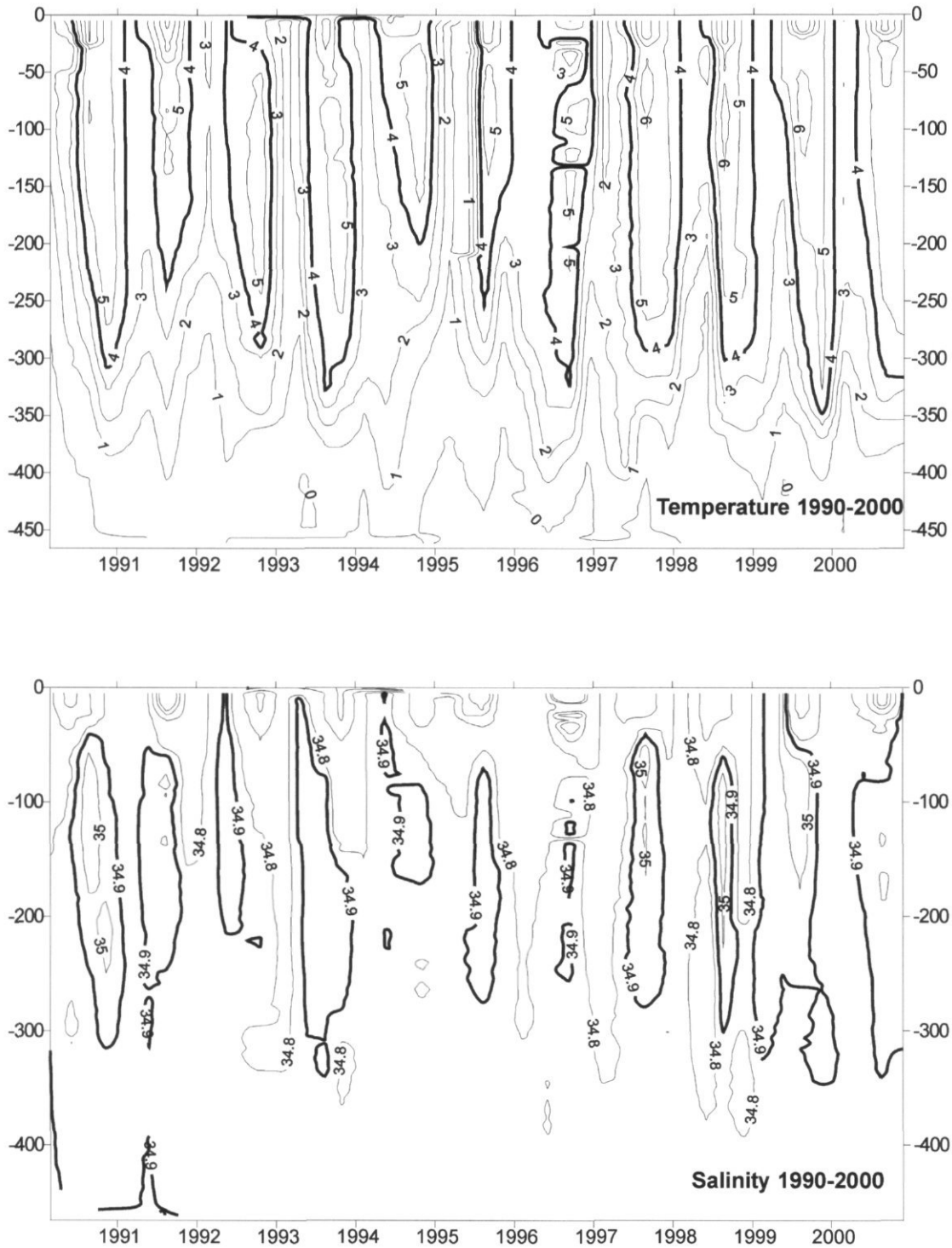


Figure 5. Temperature and salinity isopleths at station Si-3 in the Siglunes section, 1990–2000. For location, see Figure 1. Temperature contours every 1°C; salinity contours 34.0, 34.2, 34.5, 34.8, 34.9, 35.0.

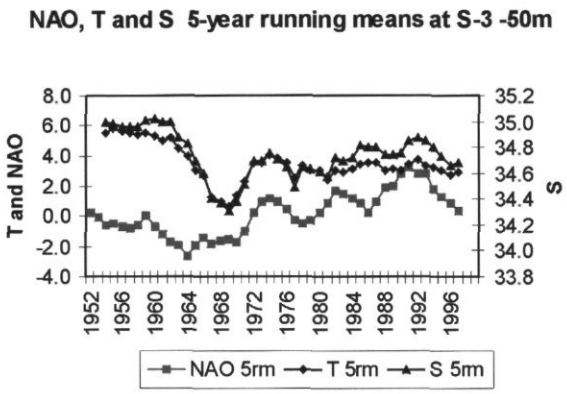


Figure 6. Five-year running means of the winter NAO Index and temperature and salinity in spring at 50-m depth at station Si-3 in the Siglunes section, 1950/1952–1999. For location, see Figure 1 (Malmberg and Desert, 1999).

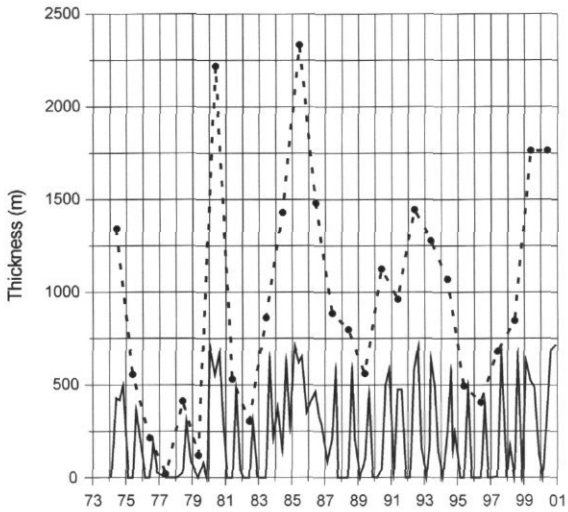


Figure 8. Atlantic layer thickness (t > 3°C; S > 34.9) at Stations 2, 3, and 4 in the Siglunes section, 1974–2000, seasonally and accumulated annually (Mortensen in Malmberg *et al.*, 2001).

and salinities during the years and periods 1972–1974, 1980, 1984–1986, 1991–1994, and 1999–2000. Sometimes these outstanding conditions are just seen during single years, as in 1980, and at other times they may last for a few years, as in the 1980s and early 1990s. This is important and renders forecasting difficult.

South Icelandic waters

The Selvogsbanki section crosses the South Icelandic shelf on the main spawning grounds of cod in Icelandic waters (Figure 1). The section includes the coastal water with its dilution of run-off as well as the Atlantic Water of the Irminger Current. The local variations in the coastal water are important for the spawning of cod (Jonsson, 1982; Olafsson, 1984; Thordardottir, 1988). The slight variations observed in the Atlantic Water are connected with large-scale features in the open ocean (Neumann, 1940; Smed, 1975; Rodewald, 1967, 1972; Dickson *et al.*, 1988; Belkin *et al.*, 1998). Thus the low

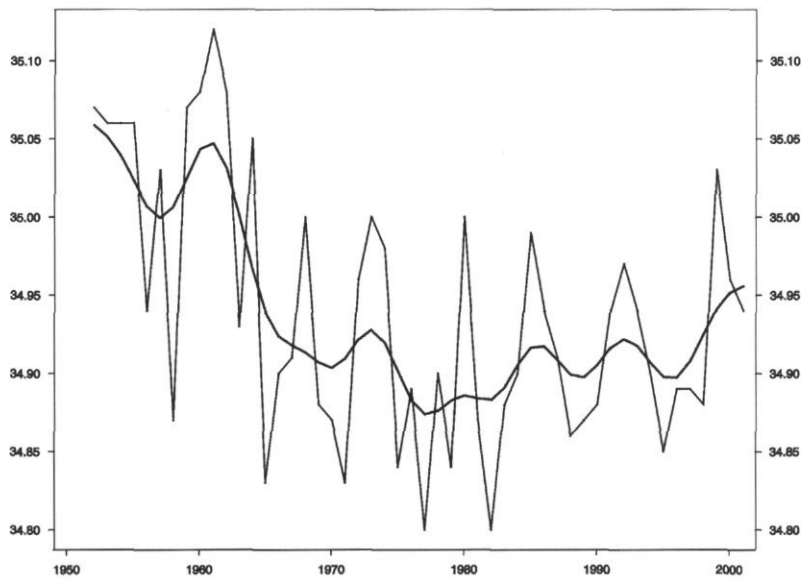


Figure 7. Maximum salinity in spring 1952–2000 in the upper 300 m at station Si-3 in the Siglunes section together with a 5-year smoothed running mean (Gaussian filter). For location, see Figure 1.

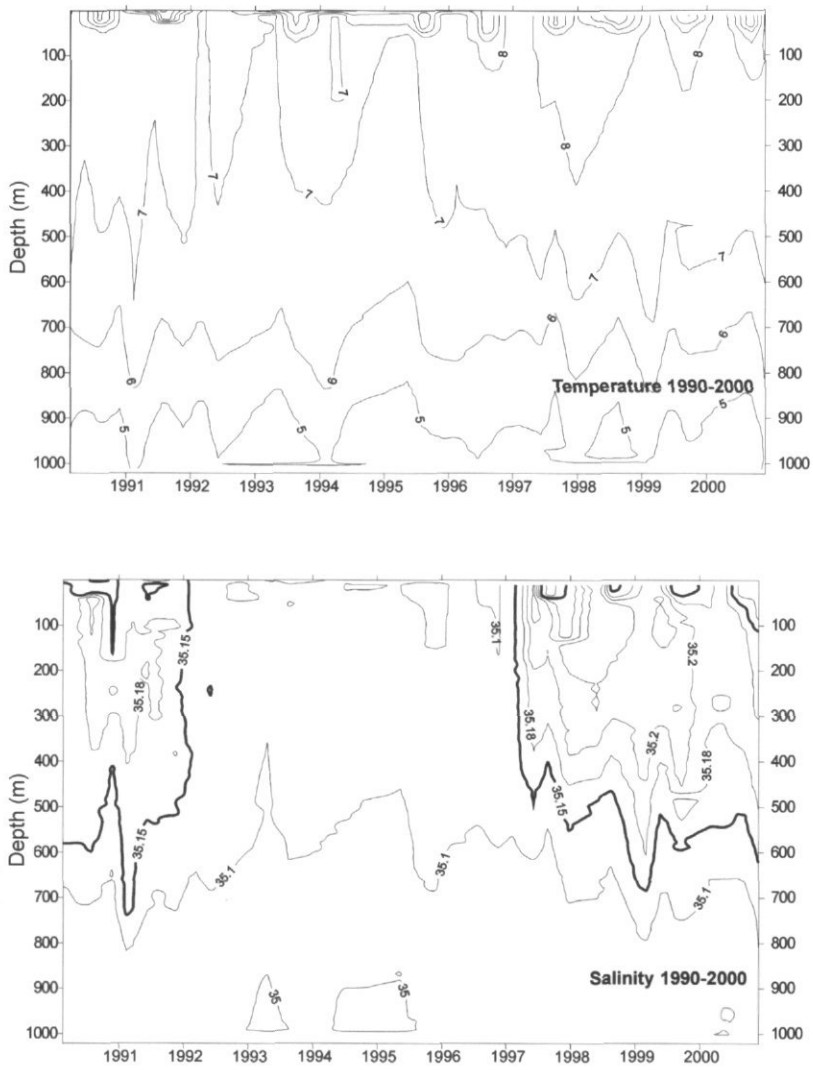


Figure 9. Temperature and salinity isopleths at station Sb-5 in the Selvogsbanki Section, 1990–2000. For location, see Figure 1. Temperature contours every 1°C; salinity contours 35.1, 35.15, 35.18, 35.20, 35.22.

salinity periods ($S < 35.15$) revealed at Sb-5 on the Selvogsbanki Section in the 1970s and 1980s (Figure 2C) were connected to the two GSAs. Furthermore, the relatively low salinity values found at Station Sb-5 during the years 1992–1996 (Figures 2C and 9), as well as those observed farther to the west in the Irminger Sea (Mortensen and Valdimarsson, 1999, 2000), may coincide with variations of hydrographic conditions in even the Labrador Sea (Reverdin *et al.*, 1999; Bersch *et al.*, 1999). This reflects the complex conditions in Icelandic waters and nearby waters, being located at the boundaries of northern, southern, and western ocean-atmospheric regimes. Looking further into the regime of the warm Irminger Current in the 1990s in South and West Icelandic waters, a distinct increase in salinity since 1997 is striking (Figures 2C and 8). These findings are similar to those found further downstream (West Greenland) and upstream in the North Atlantic Current System (ICES, 2001). Also North Icelandic waters benefited from this in 1999–2000, as already stated (Figures 2B, 5, and 7).

The NAO Index and hydrographic variability

The variable forcing of atmospheric conditions on the westerlies has an impact on oceanic circulation through different exchanges between atmosphere and ocean. Positive North Atlantic Oscillations

indices (NAO; Hurrell, 1995) are thus generally followed by relatively strong warm humid westerlies in the eastern North Atlantic, but by cold and dry winds in the western North Atlantic. On the other hand, negative NAO indices are followed by cold and dry northerly winds in the eastern part and warm and southerly winds in the western part of the North Atlantic (McCartney, 1996).

In the 1960s, during the period of the most extreme negative NAO indices in the 20th century (Figure 6), much attention was paid to atmospheric conditions and their reflection in hydrographic conditions. This was expressed, for example, by the so-called ice-years in North Icelandic waters in 1965–1971 or the Polar years in the East Icelandic Current. Positive versus negative conditions in the atmosphere were reported (Rodewald, 1967; Bjerknes, 1972; Dickson and Lee, 1972; Cushing, 1978) across the North Atlantic from the Labrador to the Barents Seas (Sundby, 1995).

Investigating hydrographic conditions in Icelandic waters, located between the western and eastern areas of the North Atlantic and also nearby the Polar and Arctic Fronts, more complex and sensitive conditions must be expected regarding variability both in the sea and the air. The question that arises is: Is there a significant relationship between the NAO and conditions in Icelandic waters, particularly in areas along the variable Arctic and Polar Fronts in North Icelandic waters? As before, the hydrographic conditions in spring on the Siglunes section (see Figures 1 and 2B) are used as an indicator for North Icelandic waters. According to Olafsson (1999), no relationship is found between the NAO and hydrographic conditions in North Icelandic waters. This is true for single years and means of temperature and salinity from 0–200 m at 5 stations on the Siglunes section. Both low saline near-surface water from the north and higher saline Atlantic Water from the south are included in these means. Also, it should be noted that both for temperature and salinity the spring observations from 50 m at Si-3 on the Siglunes section (Figure 2B) show a positive correlation ($r^2 = 0.90$) to those presented by Olafsson (1999) from 5 stations (Malmberg and Desert, 1999). The data from 50 m at Si-3 are also occasionally influenced by near-surface fluctuations of low saline water from the north, including advection and melting of ice. As seen from 5 years running means of the winter NAO and temperature and salinity at 50 m at station Si-3 m, there may be some coherence between the NAO and hydrography in North Icelandic waters in the 1970s and 1990s, but not in the 1980s (Figure 6). The maximum salinity in spring in the upper 0–300 m at station Si-3 (Figure 7) may correspond more closely to the NAO Index, as it reveals the variations in the Atlantic influx into North Icelandic waters from the south. The maxima and minima still coincide more or less in the 1960s, 1970s, and 1990s, but not in the 1980s. The discrepancy in the 1980s may be due to the effects of the GSAs during these years, as suggested by Curry and McCartney (1996). Certainly, an absolute linearity between the data series is not present, as the NAO Index generally increases during the period 1965 to 2000, whereas the maximum salinity decreases slightly. Indeed, when dealing with the NAO Index in waters like the Icelandic ones, one must bear in mind that the tracks of the Iceland Low expressed in the NAO Index are variable in time. Sometimes they run west of Iceland, other times south and east of Iceland.

Thus, when looking further into the relationship between 5-year running means of the winter NAO and the salinity maximum in the upper 300 m at Si-3 (Figure 10), three groups appear: one for the years prior to the ice-years in the 1960s; one for the ice-years 1965–1971; and finally one for the years after the ice-years or 1972–1996. This may reflect different tracks of the Iceland Low during the three different time periods. All three periods may indicate a slight positive relationship between the 5-year running means of the NAO winter index and maximum salinity in the upper 300 m at station Si-3. Figure 10 also reveals the high salinities found prior to the ice-years, but lower ones both during the ice-years and combined with extreme positive NAO indices since the ice-years. These three periods or phases of the hydrographic and atmospheric conditions may reflect the observed climatological periods referred to above, i.e. warm Atlantic, cold Polar and moderate Arctic conditions, related to different amplitudes of the NAO and the tracks of the Iceland Low. Generally, the flow of the westerlies over the northern North Atlantic changed in the 1960s after decades of being relatively northward bounded and zonal (Rossby waves of "small" amplitudes) to a shifting more meridional flow with different phases (Rossby waves of "large amplitudes" and shifting phases; Cushing, 1978). This is also well demonstrated in the winter NAO Index of the second half of the 20th century (Hurrell, 1995; Figure 6). Thus the three periods once more express the different conditions found in North Icelandic waters.

Conclusion

This article deals with long-term hydrographic variability in both North and South Icelandic waters. In North Icelandic waters, three phases of hydrographic conditions have been observed – Atlantic, Polar, and Arctic. In the 1990s, all these phases were observed. Polar conditions were observed in 1996–1998, although they were not as extreme as during the so-called ice-years in North Icelandic waters in

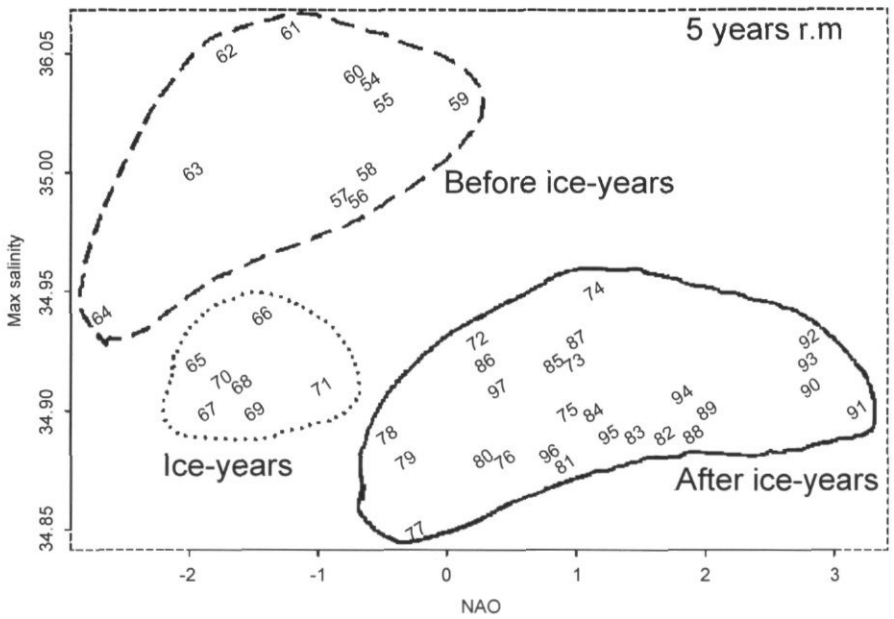


Figure 10. Relationship between 5-year running mean of maximum salinity in spring in the 0–300 m layer at station Si-3 on the Siglunes section (see Figure 7) and the 5-year running mean of the winter NAO Index (Figure 6) during the period 1950–1998.

the 1960s (Figure 2). The Arctic phase was observed in 1989–1990 and in 1995. The former two years were assumed to have been connected to the 1980s GSA (Belkin *et al.*, 1998) as the 1981–1983 Arctic phase was connected to the 1970s GSA (Dickson *et al.*, 1988). The extreme Arctic phase in 1995 has not yet been connected to any large-scale conditions in the North Atlantic and Nordic Seas, but the "low" salinity years in South Icelandic waters in 1992–1996 (Figures 2C and 8) were similar to reported variations of the Atlantic Water component in the Irminger and even Labrador Seas (Mortensen and Valdimarsson, 1999; Reverdin *et al.*, 1999; Bersch *et al.*, 1999). A striking change in salinity of the Atlantic Water influx into Icelandic waters occurred with a distinct increase at the end of the 1990s (Figures 2, 5, 9).

When considering the winter NAO Index in relation to hydrographic conditions in North Icelandic waters (Figures 6, 10) three periods also occur, one prior to the ice-years, a second one during the ice-years, and a third one after the ice-years. This occurs despite a more or less continuous increase in the NAO Index from the extreme low values in the 1960s to extreme high values in the 1990s. These three periods may reveal changes in the tracks of the air pressure fields, the track of the Iceland Low being more easterly after the ice-years than before.

Since the 1950s, three different hydrometeorological conditions or phases have occurred in the area around Iceland and in adjacent seas. These variable conditions also affected, directly or indirectly, the living marine resources in the area, as well as in wider areas throughout the North Atlantic and the Nordic Seas (e.g. Jakobsson, 1992; Malmberg and Blindheim, 1994; Vilhjalmsson, 1997).

Finally, as has been observed, the hydrographic conditions in Icelandic waters have reverted, towards the very end of the 20th century, to the "warm and saline" conditions similar to those found during the 1920s to the 1960s. The question arises, are we back to the "good old days" prior to the cold ice-years in the 1960s as regards hydrographic conditions in the northern North Atlantic and Nordic Seas with all their positive impact on climate and living marine conditions? This question is still unanswered at the start of the 21st century.

Acknowledgements

We thank our co-workers at the Marine Research Institute in Reykjávik for their valuable partnership in collecting and preparing the data described in this article. We also thank colleagues in the Working Group of Oceanic Hydrography (WGOH of ICES) for their cooperation through the years as well as the anonymous referees for their valuable suggestions. Lastly, we forward our sincere thanks to Dr. Olafur S. Astthorsson for reading and correcting the English text and making many valuable suggestions.

References

Astthorsson, O. S., Hallgrimsson, I., and Jonsson, G. 1983. Variations in zooplankton densities in Icelandic waters in spring during the years 1961–1982. Rit Fiskideildar, 7: 73–113.

Astthorsson, O. S., and Gislason, A. 1995. Long-term changes in zooplankton biomass in Icelandic waters in spring. ICES Journal of Marine Science, 52: 657–668.

Astthorsson, O. S., and Vilhjalmsson, H. 2002. Iceland Shelf LME: Decadal assessment and resource sustainability. Changing states of large marine ecosystems of the North Atlantic. Ed. by K. Sherman and H. R. Skjoldal. Blackwell Science, Oxford. (In press.)

Belkin, I. M., Levitus, S., Antonov, J., and Malmberg, S. A. 1998. The "Great Salinity Anomalies" in the North Atlantic. Progress in Oceanography, 41: 1–68.

Bersch, M., Meincke, J., and Sy, A. 1999. Innterannual thermohaline changes in the northern North Atlantic 1991–1996. Deep-Sea Research, 46: 55–75.

Bjerknes, J. 1972. Global ocean–atmosphere interaction. Rapports et Procès-Verbaux des Réunions du Conseil International pour l'Exploration de la Mer, 185: 170–178.

Blindheim, J., Borokov, V., Hansen, B., Malmberg, S. A., Turrell, W. R., and Østerhus, S. 1999. Upper layer cooling and freshening in the Norwegian Sea in relation to Atmospheric Forcing. Deep-Sea Research, 47: 655–680.

Curry, R. G., and McCartney, M. S. 1996. Labrador Sea Water Carries Northern Climate Signal South. Oceanus, 39: 24–28.

Cushing, D. H. 1978. Biological effects of climatic change. Rapports et Procès-Verbaux des Réunions du Conseil International pour l'Exploration de la Mer, 15: 107–116.

Dickson, R., Lazier, J., Meincke, J., and Rhines, P. 1996. Long-term coordinated changes in the convective activity of the North Atlantic. NATO ASI Series, 44: 211–261. Decadal Climate Variability. Dynamics and Predictability. Ed. by L. T. Anderson and J. Willebrand. Springer-Verlag, Berlin.

Dickson, R. R., and Lee, A. 1972. Recent hydrometeorological trends in the North-Atlantic fishing grounds. Fish Industry Review, 2: 2.

Dickson, R. R., Meincke, J., Malmberg, S. A., and Lee, A. 1988. The "Great Salinity Anomaly" in the northern North Atlantic 1968–1982. Progress in Oceanography, 20: 103–151.

Hansen, B., and Østerhus, S. 2000. North Atlantic–Nordic Seas Exchanges. Progress in Oceanography, 45: 109–208.

Hansen, B., Turrell, W. R., and Østerhus, S. 2001. Decreasing overflow from the Nordic Seas into the Atlantic Ocean through the Faroe Bank Channel since 1950. Nature, 411, 6840: 927–930.

Hurrell, J. W. 1995. Decadal trends in the North Atlantic Oscillation. Regional temperature and precipitation. Science, 296: 676–679.

ICES. 2001. The annual ICES Ocean Climate Status Summary, 2000/2001. ICES WGOH. Ed. by B. Turrell and P. Holliday.

Jakobsson, J. 1980. The North Icelandic herring fishery and environmental conditions. Rapports et Procès-Verbaux des Réunions du Conseil International pour l'Exploration de la Mer, 177: 460–465.

Jakobsson, J. 1992. Recent variability in the fisheries of the North Atlantic. ICES Marine Science Symposia, 195: 291–315.

Jakobsson, J., and Østvedt, O. J. 1999. A review of joint investigations on the distribution of herring in the Norwegian and Iceland Seas 1950–1970. Rit Fiskideildar, 16: 209–238.

Jonsson, E. 1982. A survey of spawning and recruitment of Icelandic Cod. Rit Fiskideildar, 6: 1–45.

Jonsson, S. 1992. Cyclonic gyres in the North Atlantic. ICES Marine Science Symposia, 198: 287–291.

Kiilerich, A. 1945. On the hydrography of the Greenland Sea. Meddelelser Grønland, 144. 63 pp.

Knudsen, M. 1899. Hydrography. The Danish Ingolf Expedition, 1: 23–161.

Malmberg, S. A. 1967. Breytingar á ástandi sjávar milli Íslands og Jan Mayen (Changes in hydrographic conditions between Iceland and Jan Mayen). Ægir, 60: 219–222.

Malmberg, S. A. 1969. Hydrographic conditions in the Waters between Iceland and Jan Mayen in the last Decade. Jökull, 19: 30–43.

Malmberg, S. A. 1972. Annual and seasonal variations in the East Icelandic Current between Iceland and Jan Mayen. Sea Ice Proceedings. International Conference, Reykjavik. Ed. by T. Karlsson. National Research Council, 4: 42–54.

Malmberg, S. A. 1980. Hydrographic conditions in Icelandic waters in May/June 1978. Annals of Biology, Copenhagen, 36: 55–62.

Malmberg, S. A. 1983. Hydrographic conditions in Icelandic Waters in May/June 1979 and 1980. Annals of Biology, Copenhagen, 37: 47–56.

Malmberg, S. A. 1984. Hydrographic conditions in the East Icelandic Current and sea ice in North Icelandic Waters, 1970–1980. Rapports et Procès-Verbaux des Réunions du Conseil International pour l'Exploration de la Mer, 185: 170–178.

Malmberg, S. A. 1985. The water masses between Iceland and Greenland. Rit Fiskideildar, 9: 127–140.

Malmberg, S. A. 1986. The ecological impact of the East Greenland current in North Icelandic waters. NATO ASI, Series G, 7: 389–404. The Role of Fresh Water in Coastal Marine Ecosystems. Ed. by S. Skreslet. Springer-Verlag, Berlin, Heidelberg.

Malmberg, S. A. 1988. Ecological impact of hydrographic conditions in Icelandic waters. International Symposium Long-Term Changes Mar. Fish. Pop. Vigo 1986: 96–123. Ed. by T. Wyatt and M. G. Larraneta.

Malmberg, S. A., and Blindheim, J. 1994. Climate, cod and capelin in northern waters. ICES Marine Science Symposia, 1998: 297–310.

Malmberg, S. A., and Desert, J. 1999. Hydrographic conditions in North Icelandic waters and annual air temperature in Iceland. ICES CM 1999/L: 14. 21pp.

Malmberg, S. A., and Kristmannsson, S. S. 1992. Hydrographic conditions in Icelandic waters, 1980–1989. ICES Marine Science Symposia, 105: 76–92.

Malmberg, S. A., Mortensen, J., and Jonsson, S. 2001. Ocean fluxes in Icelandic waters, 2001. ICES CM 2001/W: 08.

Malmberg, S. A., Valdimarsson, H., and Mortensen, J. 1996. Long time-series in Icelandic waters in relation to physical variability in the northern North Atlantic. NAFO SCR Doc. 24: 69–80.

McCartney, M. S. 1996. North Atlantic Oscillation. Oceanus, 39: 13.

Mortensen, J., and Valdimarsson, H. 1999. Thermohaline changes in the Irminger Sea. ICES CM 1999/L: 11. 11 pp.

Mortensen, J., and Valdimarsson, H. 2000. Annual variations in the Irminger Sea. Environmental conditions in Icelandic Waters 1999. Hafrannsóknarstofnun. Fjölrit, 77: 23–24.

Neumann G. 1940. Die ozeanographischen Verhältnisse an der Meeresoberfläche im Golfstromsektor nördlich und nordwestlich der Azoren. Wiss. Ergebn. d. int. Golfstromuntersuchungen 1938. Hamburg.

Olafsson, J. 1984. Recruitment of Icelandic haddock and cod in relation to variability in the physical environment. ICES CM 1985/G: 59.

Olafsson, J. 1999. Connection between oceanic conditions off N-Iceland, Lake Mývatn temperature, regional wind direction variability and the North Atlantic Oscillation. Rit Fiskideildar, 16: 41–57.

Poulain, P. M., Warnas, A. W., and Niiler, P. P. 1996. Near surface circulation of the Nordic Seas as measured by Lagrangian drifters. Journal of Geophysical Research, 101: 18237–18258.

Reverdin, G. N., Verbrugge, H., and Valdimarsson, H. 1999. Upper Ocean variability between Iceland and Newfoundland. Journal of Geophysical Research, 104 (C12): 29599–29611.

Rodewald, M. 1967. Recent variations of North Atlantic sea surface temperature and the "type tendencies" of the atmospheric circulation. ICNAF Redbook 1967, Part IV: 6–23.

Rodewald, M. 1972. Long-term variations of the sea temperature in the areas of the nine North Atlantic ocean weather stations during the period 1951–1968. Rapports et Procès-Verbaux des Réunions du Conseil International pour l'Exploration de la Mer, 162: 139–158.

Smed, J. 1975. Monthly anomalies of the sea surface temperature in the areas of the northern North Atlantic in 1972. Annals of Biology, Copenhagen, 30: 15–17.

Stefánsson, U. 1962. North Icelandic waters. Rit Fiskideildar, 3. 269 pp.

Stefánsson, U. 1969. Temperature variations in the North Icelandic coastal area during recent decades. Jökull, 19:18–28.

Stefánsson, U., and Jakobsson, J. 1989. Oceanographical variations in the Iceland Sea and their impact on biological conditions. A brief review. Proc. Conf. Com. Arc. Int. May 1985: 427–455.

Stefánsson, U., and Olafsson, J. 1991. Nutrients and fertility of Icelandic waters. Rit Fiskideildar, 7: 1–56.

Sundby, S. 1995. Havklimasvigninger i Nord-Atlanteren. Miljörapport 1995. Fisken og havet, 2: 75–80.

Swift, J. H. 1984. A recent Q–S shift in the deep water of the North Atlantic. *In* Climate Proc. and Climate Sensitivity, pp. 34–47. Ed. by J. E. Hanson and T. Takahashi. Geophys. Monogr. 29, Maurice Ewing. Vol. 5, 47AGU, Washington DC.

Swift, J. H., and Aagaard, K. 1981. Seasonal transitions and water mass transformations in the Iceland and Greenland Seas. Deep-Sea Research, 20A: 1107–1129.

Thordardottir, Th. 1977. Primary production in North Icelandic Waters in relation to recent climatic changes. *In* Polar Oceans, pp. 655–665. Ed. by M. J. Dunbar. Proc. Oc. Congress Montreal 1974.

Thordardottir, Th. 1988. Timing and duration of spring blooming south and southwest of Iceland. NATO ASI, Series G: 389–404. The role of fresh water in coastal marine ecosystems. Ed. by S. Skreslet S. Springer-Verlag, Berlin, Heidelberg.

Valdimarsson, H., and Jonsson, S. 2000. Measuring Arctic fresh water flux in Icelandic waters. Strawman 3. Science Plan for Arctic–Subarctic Flux Array (ASOF). Ed. by R. R. Dickson.

Valdimarsson, H., and Malmberg, S. A. 1999. Near-surface circulations in Icelandic waters derived from satellite tracked drifters. Rit Fiskideildar, 16: 23–39.

Vilhjalmsson, H. 1994. The Icelandic capelin stock. Capelin *Mallotus villosus* (Muller) in the Iceland–Greenland–Jan Mayen area. Rit Fiskideildar, 13. 281 pp.

Vilhjalmsson, H. 1997. Climatic variations and some examples of their effects on the marine ecology in Icelandic and Greenland waters, in particular during the present century. Rit Fiskideildar, 15: 1–29.

ICES Marine Science Symposia, 219: 61–70. 2003

Large-scale hydroclimatic variability in the Bay of Biscay: the 1990s in the context of interdecadal changes

Benjamin Planque, Pierre Beillois, Anne-Marie Jégou, Pascal Lazure, Pierre Petitgas, and Ingrid Puillat

Planque, B., Beillois, P., Jégou, A.-M., Lazure, P., Petitgas, P., and Puillat, I. 2003. Large-scale hydroclimatic variability in the Bay of Biscay: the 1990s in the context of interdecadal changes. – ICES Marine Science Symposia, 219: 61–70.

On its western side, the Bay of Biscay is located at the limit between the North Atlantic sub-polar and subtropical gyres, while the eastern and southern sides are bounded by land with a large continental shelf to the east and a narrow one to the south. The sharp continental slope results in a separation between hydrological processes taking place on and off the shelf. On the shelf, mesoscale hydrodynamic features, such as coastal upwellings, river plumes, and freshwater lenses, mostly depend upon regional climate forcing rather than upon the general oceanic circulation. Here, we review how three key regional climate and hydrological forcing factors (sea surface temperature, windspeed and river run-off) have varied during the past decade in comparison with multi-decadal historical records. The 1990s were characterized by warmer temperature and windier conditions than during the previous century, while the river run-off is slightly lower than average and highly variable. The Bay of Biscay lies between two regions where the responses to the North Atlantic Oscillation are opposite, and, as a result, it is expected that the NAO would only account for a very small fraction of the variability observed in temperature, windspeed, and river run-off in this region. Our results confirm this hypothesis.

Keywords: Bay of Biscay, long-term changes, North Atlantic Oscillation, river discharge, temperature, wind.

B. Planque, P. Beillois, and P. Petitgas: IFREMER. Laboratoire Ecologie halieutique, rue de l'Ile d'Yeu. B.P. 21105. 44311 Nantes Cedex 3. France [tel: +33 240 374117; fax: +33 240 374075; e-mail: Benjamin.Planque@ifremer.fr]. A.-M. Jégou, P. Lazure and I. Puillat: IFREMER. DEL/AO. BP 70. 29280 Plouzané. France.

Introduction

The Bay of Biscay encompasses a region bounded by the Spanish coast to the south at approximately 44°N and the French coast to the east at approximately 2°W, and is open to the North Atlantic Ocean on its western and northern sides. The continental shelf is narrow along the Spanish coast and its extent increases from south to north along the French coast.

Hydrological features in the Bay of Biscay are therefore under the influence of (1) oceanic processes taking place in the North Atlantic and (2) coastal processes associated with the French and Spanish coasts. The shelf break, with a depth reaching more than 4000 m on the oceanic side and less than 200 m on continental shelf, is the natural separation between oceanic and coastally driven hydrodynamic features.

Coastal currents on the shelf are mainly influenced by the coastal topography, river discharges, wind regime, and tides. River discharge generates vertical and horizontal density gradients. This results in density circulation, which under the action of the Coriolis force is oriented northward. By contrast, dominant winds over the Bay of Biscay are westerlies and result in wind-driven coastal currents being oriented principally to the south (Pingree and Le Cann, 1989). The spatial extent and latitudinal position of river plumes results from the interaction of river flow and wind regimes. Offshore parts of river plumes can sometimes become detached and isolated from the main plume structure to become independent mesoscale low salinity lenses (see Puillat *et al.*, submitted). In the southern part of the Bay of Biscay, particular wind regimes can lead to the onset of coastal upwelling. This is the case for northerly winds (upwelling on French coast) or

easterly winds (upwelling on Spanish coast). In the northern part of the Bay of Biscay, contrasting conditions of heat exchanges between atmosphere and ocean, wind/tide mixing and surface haline stratification result in the isolation of a deep "cold pool" (Vincent and Kurc, 1969; Vincent, 1973; Puillat *et al.*, submitted). During autumn, a hydrological structure termed a "warm water tongue" can develop in the central part on the continental shelf (Le Cann, 1982; Koutsikopoulos and Le Cann, 1996); the origin of this structure is still unclear. Finally, geographical differences in tidal mixing result in the formation of tidal fronts in the northern part of the bay (Sournia *et al.*, 1990).

In summary, there is a great diversity in the nature of hydrodynamic features in the Bay of Biscay. While the deep regions of the bay may be affected principally by general oceanic circulation, the shelf is characterized by the dominance of mesoscale structures which are strongly influenced by regional or local hydroclimatic conditions. It is therefore expected that variability in the dynamics of mesoscale hydrographic structures on the French continental shelf may result mainly from the variability in climatic factors, such as wind, temperature regime, and river discharge.

On a larger scale, it has been demonstrated that the North Atlantic Oscillation (NAO), the dominant mode of atmospheric interannual variability in the North Atlantic sector, can be related to interannual variability in wind, precipitation, and SST fields over the eastern North Atlantic (Hurrell, 1995). The NAO may therefore be a potential proxy for climatic conditions around the Bay of Biscay (as is often the case for other European regions). However, the way in which the NAO effects translate into local climate conditions is region-dependent, e.g. wind and precipitation responses to the NAO being opposite in Scandinavian and North African regions (Xie and Arkin, 1996; Reid and Planque, 1999; Pérez *et al.*, 2000). The Bay of Biscay lies between these two extremes and the influence of the NAO on this region has received little attention until now.

Here, we review how three climatic parameters that are crucial to the dynamics of mesoscale hydrological features on the Bay of Biscay shelf (i.e. temperature, wind, and river discharge) have varied during the 1990s, in comparison with previous decades. We also investigate the relationships between these factors and larger climatic fluctuations expressed in the North Atlantic Oscillation (NAO).

Data sources

Wind and air temperature

Data on wind and air temperature (AT) have been recorded by Météo-France at a number of meteorological stations (semaphores) along the French Atlantic coast. Here, we selected data from eight semaphores, namely Ouessant, Pointe du Raz, Penmarch, Pointe du Talut, Saint Sauveur, Chassiron, Cap Ferret, and Biarritz (Figure 1). At each location, wind (speed, direction) and air temperature are recorded at 3-h intervals. The period of available records extends from 1948 to now, although for some semaphores the digitized record starts at a later date (between 1949 and 1958). Mean monthly wind data from the Comprehensive Ocean Atmosphere Data Set (COADS, Woodruff *et al.*, 1993) were also used. COADS data are constituted by monthly averages of climate records over a grid constituted by cells of 2°long × 2°lat over the world's oceans. Here, we selected data from a limited number of COADS grid cells, as indicated in Figure 1. The technique used for aggregating wind data in the COADS data set results in less robust estimates of true wind than those derived from the meteorological stations. This is mainly because the number of samples collected, or their spatial location within a given grid cell, may vary from month to month. However, the period covered by COADS is much longer, as it extends from 1844 to 2000 (over the grid shown in Figure 1), therefore allowing for comparison of recent wind records with historical ones over the past 150 years.

Sea surface temperatures

A first data set, consisting of SST values averaged over 10-day periods and presented on a regular spatial grid was provided by Météo-France. The gridded data (0.5°long × 0.5°lat [9.0°W–1.5°W, 44.0°N–48.5°N], Figure 1) result from an interpolation procedure performed on SST measurements from selected vessels, meteorological buoys, and, more recently, satellite. Details on the interpolation procedure can be found in Koutsikopoulos *et al.* (1998), Ratier (1986), and Taillefer (1990). The Météo-France data are available from 1971 to 2001. As for wind, COADS SST estimates may be less robust than those from the Météo-France data set, but the period covered by COADS is much longer and therefore allows for the study of long-term variability in temperature.

River flows

We selected river outflow measurements from three rivers: the Loire, the Gironde, and the Adour (Figure 1). River flows are derived from the water vertical heights measured at specific locations. The empirical relationship between water height and flow varies through time and is difficult to estimate

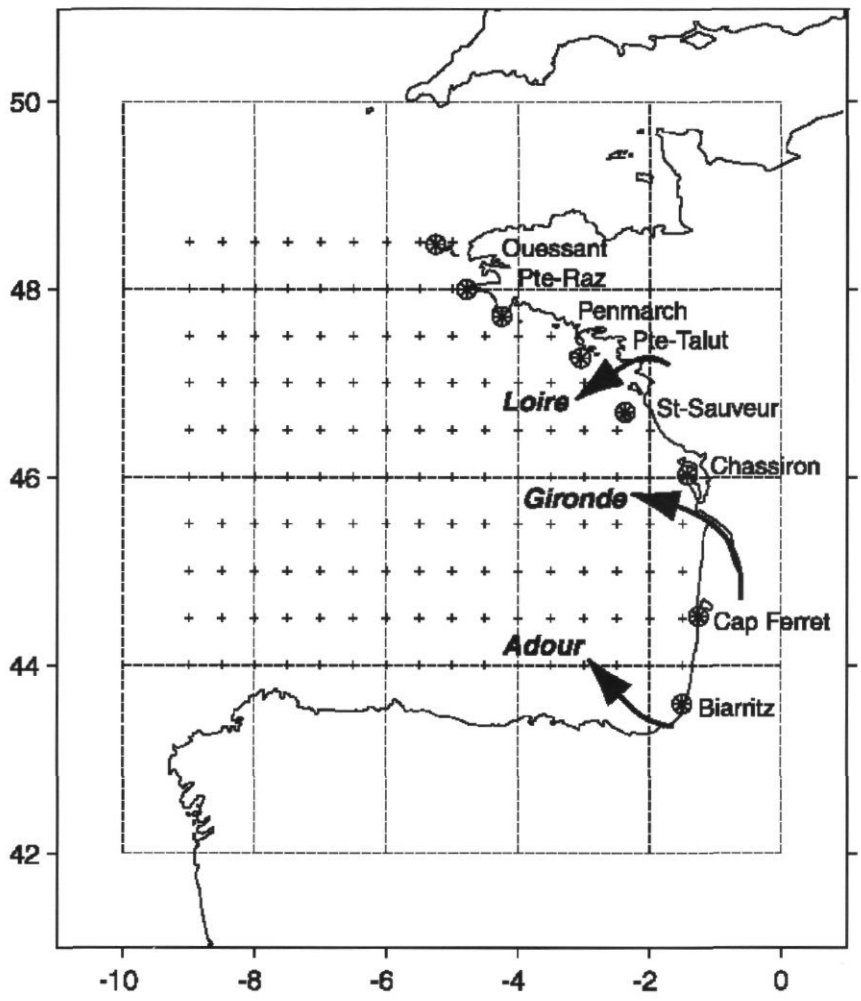


Figure 1. Location of the four data sets used. Sea surface temperature and scalar wind from COADS were extracted from the 20 rectangular boxes delimited by dashed lines. SSTs from Météo-France were interpolated over the grid, which is shown as crosses. Meteorological stations where coastal wind and air temperature are recorded are named and highlighted by crossed-circles. The three rivers are named and their flow materialized by large arrows.

for extreme low or high levels owing to the limited number of calibration measurements available for these extreme levels. Here, we have not accounted for the uncertainties in flow estimations when comparing flows through time for the three rivers. Daily river flow data are available for the period 1843–2000 for the Loire, 1978–2000 for the Gironde, and 1984–1999 for the Adour.

NAO index

The North Atlantic Oscillation (NAO) index is defined as the difference between the normalized winter (December to March) sea-level pressures measured at Stykkisholmur (Iceland) to represent the Iceland Low and at Lisbon (Portugal) to approximate the Azores High pressure cell. Values of this index are available from a number of sources. Here, we have used the data provided by the National Center for Atmospheric Research in Boulder for the period 1864–2000 (http://www.cgd.ucar.edu/cas/climind/nao_winter.html).

Data transformation and analysis

Since different data sets have distinct temporal resolutions, we have standardized the series by calculating monthly averages prior to analyses (except for the winter NAO). Temperature, river discharge, and winds vary seasonally, and we have often

used anomalies rather than parameter values to correct for seasonal effects. Monthly anomalies are obtained by subtracting the long-term mean value for the same month of the year from the raw data.

Wind data can be used in several ways. Here, we have concentrated on scalar windspeed only. In the case of river discharge, we have log-transformed the anomalies when necessary to correct for the very skewed statistical distribution of discharge values. We applied no transformation to the NAO data.

Correlation analysis has been used to investigate the relationships between series of distinct parameters or between spatially distinct series of the same parameter. We have accounted for the presence of autocorrelation in the series by either correcting the number of "true independent observation" (i.e. degrees of freedom), or by first-ifferencing the time-series prior to testing for correlation, using the methods of Pyper and Peterman (1998), Thompson and Page (1989), and Chatfield (1996) outlined in Fox *et al.* (2000).

Table 1. Correlations between series of annual averages of monthly temperature anomalies for the period 1971–1998. AT: air temperature measured at Chassiron, SST (Météo-France): sea surface temperature extracted from the Météo-France gridded data set, SST (COADS): sea surface temperature extracted from the COADS data set. R: Pearson correlation coefficient, n: number of observations, n*: number of observations corrected for serial autocorrelation, p: associated probability.

	AT (Chassiron)	SST (Météo-France)
SST (Météo-France)	R = 0.70 (n=28, n*=10, p<0.01)	–
SST (COADS)	R = 0.79 (n=28, n*=13, p<0.01)	R = 0.97 (n=28, n*=18, p<0.01)

Results

Temperature

Monthly anomalies (against the period of reference 1971–1990) were calculated for air temperature at Chassiron, SST from Météo-France, and SST from COADS. The patterns of interannual variability in temperature anomalies between the three data sets are very close, and in all cases the correlation between series is significant ($p < 0.01$, Table 1). This reflects the consistency of COADS and Météo-France data sets and the correspondence between local air temperature records (like those measured at Chassiron) and larger scale SST variations.

Over the past century, COADS records show an increase in the mean annual SST of 1.03°C (Figure 2). The analysis of monthly increase from COADS data indicates that this warming exists for every month (Table 2), but it is more pronounced during the winter season (December through to March) with 1.21°C/100 years. The Météo-France data set allows for geographical comparison of the rates of temperature change during the recent decades (1970s to 1990s). It is clear from Figure 3 that recent warming has taken place over the whole

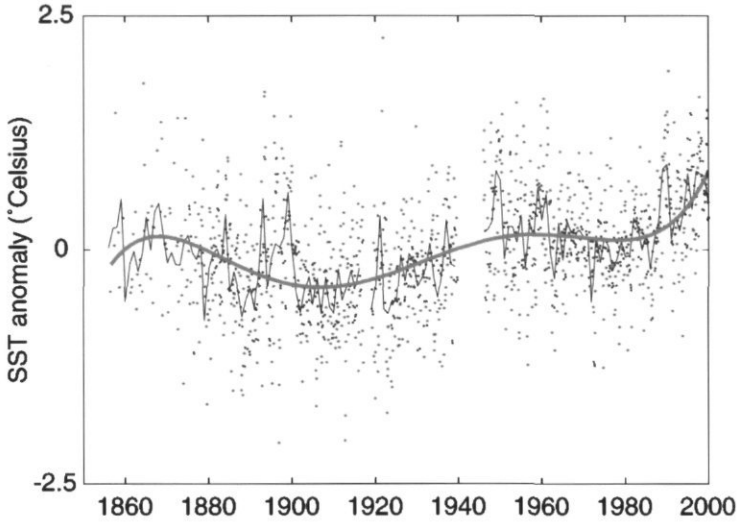


Figure 2. Sea surface temperature anomalies in the Bay of Biscay derived from the COADS data set. Dots indicate monthly anomalies; the thin line shows the annual anomalies and the heavy line the long-term trend estimated by polynomial regression (order 5).

Table 2. Average monthly differences in SST between 1991–2000 and 1901–1990 from COADS. **Significant at the 1% level, *significant at the 5% level, ns: not significant.

Month	DeltaT (°C)	p
Jan	0.62 (**)	≪0.01
Feb	0.78 (**)	≪0.01
Mar	0.73 (**)	≪0.01
Apr	0.55 (**)	0.001
May	0.59 (**)	0.002
Jun	0.14 (ns)	0.278
Jul	0.31 (ns)	0.130
Aug	0.79 (**)	0.003
Sep	0.47 (ns)	0.052
Oct	0.36 (ns)	0.067
Nov	0.60 (**)	0.004
Dec	0.60 (**)	0.002

of the Bay of Biscay, but that the rate of temperature increase is greatest in the southeastern part of the bay, where it reaches values up to 0.6°C per decade.

Winds

The analysis of COADS scalar wind data since the mid-19th century over the Bay of Biscay shows a clear u-shaped trend (Figure 4). From the 1850s to the 1920s, the general trend has been for a decrease in wind intensity, whilst an upward trend is observed for the period 1920s–2000. On average, the windspeed over the Bay of Biscay during the years 1991–2000 is greater, by 1 ms^{-1}, than the average over the previous decades of the century ($p \ll 0.01$). The increase in windspeed expressed in the COADS data is seen for all seasons (Table 3), but is most significant outside the winter period.

Along the French coast the trends in windspeed revealed by data from meteorological stations vary with geographical locations. On average, annual mean windspeed has decreased in the southern part of the Bay, while it has increased in the northern part (Figure 5). Nevertheless, these trends are small in comparison with the degree of interannual variability at each station.

River flows

The comparison of monthly flow anomalies between the Loire, Gironde, and Adour rivers reveals a very strong synchrony between all three rivers (Table 4) and the two types of test conducted for the detection of synchrony (adjusted number of independent observations and first-order differencing) are highly significant. We have therefore considered the Loire series, which goes back to the mid-19th century, as an acceptable proxy for river run-off along the whole French Atlantic coast.

A plot of interannual changes in the Loire run-off (Figure 6) shows a strong degree of interannual variability, with some extreme low and high values. During the 1990s, the Loire discharge has been average to low in comparison with the past 150 years. A large degree of interannual variability in flow has been observed during the 1990s, but extreme values (high or low) have not gone beyond the range of previously observed minimum or maximum flows.

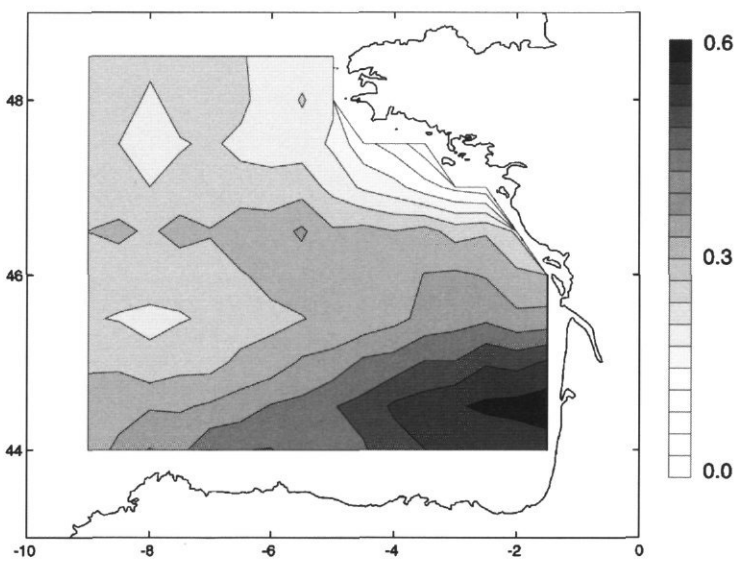


Figure 3. Rate of sea surface temperature increase (°C/decade) during the period 1971–1998, based on Météo-France data. The rates are estimated by linear regression.

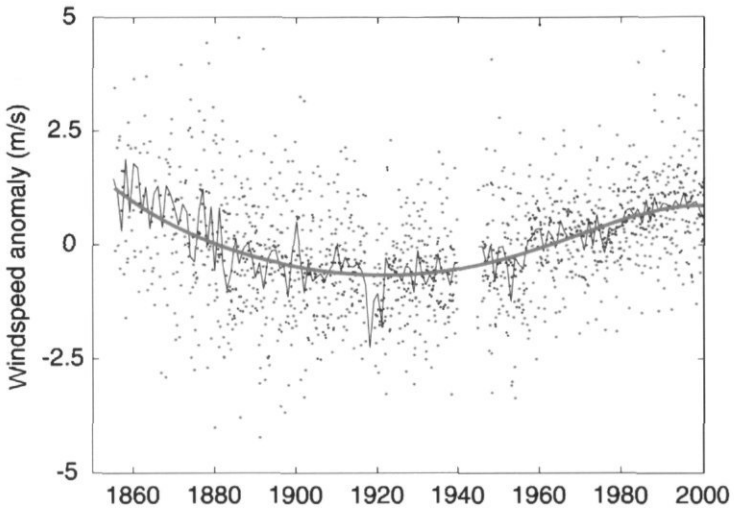


Figure 4. Scalar wind anomalies in the Bay of Biscay, derived from the COADS dataset. Dots indicate monthly anomalies, thin line shows the annual anomalies and heavy line the long-term trend estimated by polynomial regression (order 5).

Table 3. Average monthly differences in scalar wind between 1991–2000 and 1901–1990, from COADS. **Significant at the 1% level, *significant at the 5% level, ns: not significant.

Month	DeltaW ($m.s^{-1}$)	p
Jan	1.36 (ns)	0.058
Feb	0.42 (ns)	0.281
Mar	0.27 (ns)	0.302
Apr	1.33 (**)	0.001
May	1.40 (**)	$\ll$0.01
Jun	1.73 (**)	$\ll$0.01
Jul	1.19 (**)	0.002
Aug	0.91 (**)	0.002
Sep	1.67 (**)	$\ll$0.01
Oct	2.00 (**)	$\ll$0.01
Nov	1.65 (**)	0.002
Dec	1.05 (*)	0.044

NAO and other parameters

During the past 150 years, the relationship between the winter NAO index and the winter SST, wind and Loire run-off appear to be weak. The three plots on Figure 7 reveal scattered data, and the fractions of variance explained by the NAO for SST, scalar wind, and river run-off, respectively, amounts to 8%, <1%, and 6%. Although we have restricted our analysis to the use of simple linear regressions, it is clear from the scatter of the data that other models would only have provided little improvement, if any, in the amount of variance explained. Despite these weak relationships, the correlations between NAO, SST, and river run-off are significant, after

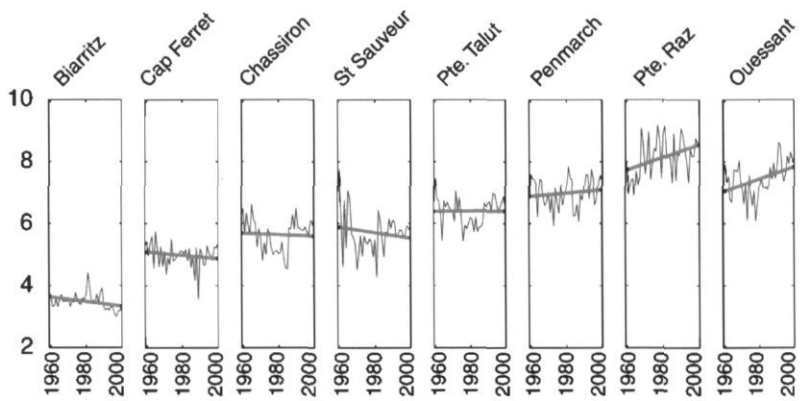


Figure 5. Time-series of annual mean anomalies in wind speed ($m.s^{-1}$) from eight meteorological stations along the French coast (see Figure 1 for geographical locations of the stations). Heavy lines show long-term trends estimated by linear regression.

Table 4. Correlations between monthly anomalies in flow from the Loire, Gironde, and Adour rivers. R: Pearson correlation coefficient, n: number of observations, n*: number of observations corrected for serial autocorrelation. Results in italics show correlation analysis on first-order differenced series.

	Gironde	Adour
Loire	R=0.80, n=276, n*=156, p≪0.01 *R=0.75, n=275, p≪0.01*	R=0.70, n=192, n*=117, p≪0.01 *R=0.56, n=191, p≪0.01*
Gironde	–	R=0.88, n=192, n*=123, p≪0.01 R=0.79, n=191, p≪0.01

correction for autocorrelation (NAO/SST: n = 135, n-corrected = 112, p = 0.003, NAO/run-off: n = 137, n-corrected = 133, p = 0.008). There is no apparent relationship between NAO and windspeed (r = –0.02, n = 137, n-corrected = 121 and p = 0.39).

There are two main reasons why these relationships can be significant but weak over the past 1.5 centuries. The first is that the true underlying relationships are weak. The second possible reason is that the relationships may be time-dependent, i.e. that periods when a relationship exists alternate with periods with reversed or absence of relationship, resulting in an apparent absence of relationship. To investigate the possible time dependence of

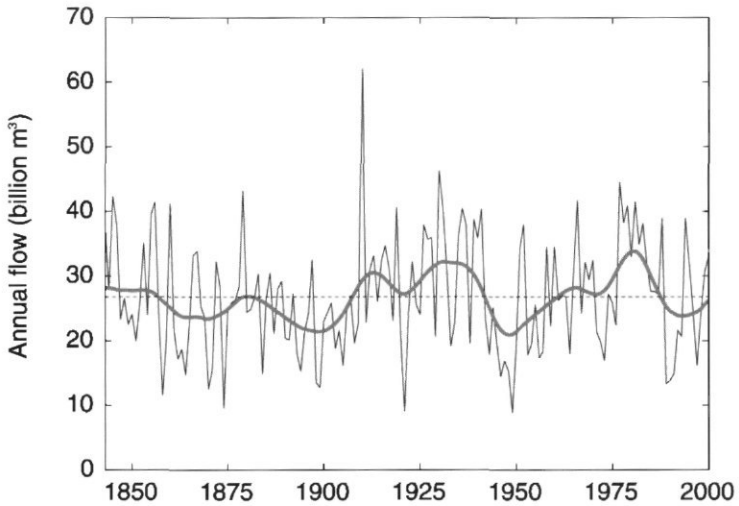


Figure 6. Annual discharge from the Loire river (thin line) and fitted long-term trend estimated by eigen vector filtering (heavy line). Dashed line indicates mean annual flow over the entire period of records.

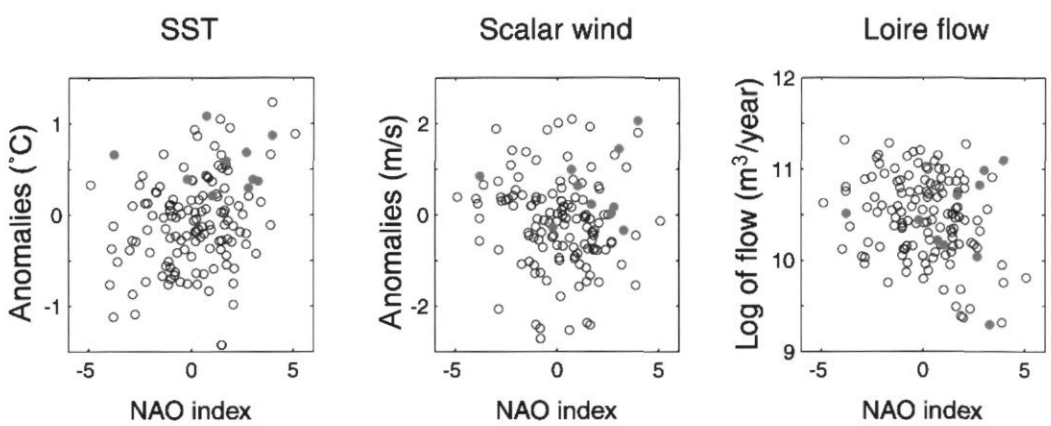


Figure 7. Sea surface temperature anomalies (left), scalar wind anomalies (middle), and log-transformed run-off of the Loire river (right) plotted against the NAO winter index. Each parameter has been averaged for the period Dec-Mar to match the period over which the NAO index is calculated. Closed circles indicates years 1991–2000.

the NAO effects, we have calculated decadal correlations between NAO, SST, windspeed, and river run-off (Figure 8). For all the decades studied before the 1990s, the correlation between the NAO and SST is positive. This suggests that the relationship between NAO and SST is weak, but is robust through time. In this context, the 1990s are distinct from the previous decades, with a slightly negative (and not significant) correlation. Decadal relationships between NAO and windspeed have been both positive and negative in the past, and the relationship presents an apparent persistence of several decades, with the correlation gradually changing from positive to negative values and vice versa. During the 1990s, the correlation is close to zero. In the case of river run-off, both positive and negative correlations with the NAO have been observed, but decades with negative relationships are the most frequent. As for SST and windspeed, the correlation coefficient is close to zero during the 1990s.

Discussion

The comparison of recent hydroclimatic records with historical ones is strongly dependent upon the comparability of data collected over a long period of time. During the past 1.5 centuries, changes in sampling intensity or design and modifications of the instrumentation used to record hydroclimatic parameters have occurred, and the results presented here are conditional on the consistency of historical data sets. In the case of temperature, the correspondence between the results obtained with three independent data sets suggests that the changes observed in recent decades (since the 1950s) reflect the true variability in the temperature in the Bay of Biscay. The true correspondence between COADS monthly averages and historical 3-h records from coastal meteorological stations is difficult to establish because of the large differences in sampling frequency and geographical variability. This is particularly so for the wind data. Indeed, wind records vary greatly over small spatial and temporal scales, so that 3-h records from meteorological stations cannot readily be compared to monthly averages calculated over large oceanic areas. In the case of river run-off, measures of flow are derived from measures of river height at particular points using empirical correspondences between river height and river flow. Changes in the locations of river height measurement, and natural and human induced variations in the shape of river bottoms, have led to changes in these empirical relationships and potential biases in the flow estimates. The very strong correspondence in flow anomalies between the three rivers studied suggests that, despite these changes, the historical records for recent decades reflect the true variability in river discharge along the western coast of France. For the longer term, the comparability of data collected more than a century ago with contemporary data is difficult to assess and long-term trends in river discharge are therefore uncertain.

Since 1989, the Bay of Biscay is on average warmer than usual at all seasons and all locations. The warming, however, is greater in the southeastern part of the bay and during the winter season. This is consistent with the observations by Koutsikopoulos *et al.* (1998) of the warming in the southeastern Bay of Biscay during the period 1972–1993, and confirms the warming trend for the whole of the 1990s. The latitudinal gradient in SST is reinforced by the geographical differences in warming trends, with rapid warming of warmer water in the South and slower warming of colder water in the North.

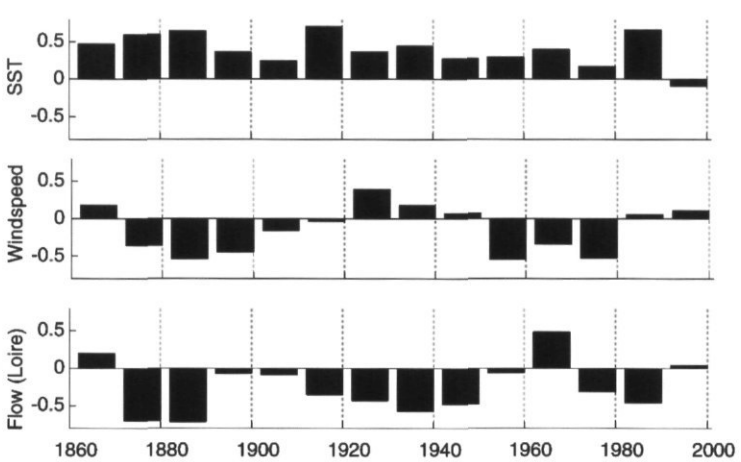


Figure 8. Decadal correlations between the NAO index and SST anomalies (top), scalar wind anomalies (middle), and log-transformed run-off of the Loire river (bottom).

Assuming that the series of windspeeds derived from COADS is consistent through time, the records suggest that average windspeed in the Bay of Biscay has increased during the 20th century to reach maximum values in the 1990s – it being most evident outside the winter season. These maximum windspeed values are similar to those recorded in the mid-19th century. Coastal records from meteorological stations provide some indications about the geographical variability of the trend in wind, with increasing windspeed in the northern part of the bay (consistent with the results of Pirazzoli, 2000) and decreasing speed in the south. As for temperature, the latitudinal gradient in windspeed is reinforced with strong winds getting stronger in the North and weak winds getting weaker in the South.

The warming that has taken place during winter in the southern part of the bay occurs in parallel with a decrease in windspeed in the same area and for the same months (as recorded at Biarritz meteorological station), which suggests that a decrease in wind mixing may be partly responsible for the warming in this region. In such a case, the warming would not necessarily reflect an increase in the heat content of the southern Bay of Biscay, but the presence of a stronger and/or shallower thermocline which would distribute most of the heat content in the upper part of the water column. In addition, the more rapid warming in the southern part of the Bay of Biscay in comparison with the north, may reflect the differences in tidal mixing intensity between the two areas (Pingree *et al.*, 1982; Le Cann, 1990). Indeed, lesser mixing in the south can result in more rapid increase in SST than in the north. Alternatively, changes in SST observed in the southeastern Bay of Biscay may result from a true change in heat content driven by advective transport of warmer water. Variations in the flow of warm East North Atlantic Central Water (ENACW, Pingree, 1994) towards the southeastern Bay of Biscay could drive such changes in water temperature. This possibility is supported by the observations carried out during the 1990s along a hydrographic section off Santander which suggest increase in the eastward flow of ENACW (Gonzàlez-Pola and Lavín, submitted, this issue).

Previous studies conducted on mesoscale hydrological structures in the Bay of Biscay have revealed that there is great spatial and temporal hydrological variability on this scale (e.g. see Dickson and Hughes, 1981; Pingree and Le Cann, 1992; Koutsikopoulos and Le Cann, 1996; Froidefond *et al.*, 1998; Lazure and Jégou, 1998). Here, we have not directly studied the mesoscale structures, but instead some of the hydroclimatic factors that influence the development and dynamics of these structures. Results from Puillat *et al.* (submitted) show that variability in climatic patterns can be transferred to mesoscale hydrodynamic structures. It is therefore expected that the strong degree of interannual variability in the forcing factors observed in our results (Figures 2, 4, and 6) has had a major influence upon the development of the mesoscale hydrodynamics in the Bay of Biscay during the past century.

The link between temperature, wind, river run-off, and general climatic conditions, if there are any, is not expressed in the NAO signal (Figures 7, 8). The relationships are weak and changeable through time, except for SST. The 1990s are characterized by particularly weak relationships and in any case the NAO index accounts for only 8%, <1%, and 6% of the interannual variability in winter SST, wind, and river run-off. The NAO is a large-scale oscillation that affects temperature, wind, and precipitation fields over the North Atlantic, but these effects are region-dependent. For example, Hurrell, (1995) showed that precipitation was positively correlated to the NAO in the northern part of Europe while negatively related in southern Europe. A similar result is presented in an analysis of global precipitation fields by Xie and Arkin (1996). Similarly, positive phases of the NAO have been associated with warmer conditions in Northern Europe but cooler ones in the subpolar gyre region, and with greater windspeed in the northeastern part of the North Atlantic but lower windspeeds in most of the subtropical North Atlantic (Reid and Planque, 1999). The Bay of Biscay has a particular geographical status with regard to the NAO effects, as it lies close to the line of no correlation with the NAO for precipitation, temperature, and wind. This geographical status explains the very poor or lack of response of these three parameters to the NAO, and strongly suggests that direct physical or biological responses to the NAO are not to be expected in the Bay of Biscay.

Despite this lack of apparent effect of the NAO, it is likely that the development of distinct mesoscale physical structures in the Bay of Biscay is associated with particular large-scale climatic situations. Techniques for relating large-scale climatic situations or weather regimes to smaller-scale weather patterns exist in terrestrial meteorology (see, e.g., von Stroch *et al.*, 1993; Plaut and Simonnet, 2001; Simonnet and Plaut, 2001). Such downscaling methods have not yet been used to relate weather regimes to mesoscale hydrography. It is expected that they should prove useful in the case of the Bay of Biscay.

In conclusion, the 1990s have been exceptional with regard to SST and wind, but river discharge has varied within its natural range. The way in which the variability in these factors has been reflected in the onset and dynamics of mesoscale hydrological structures needs further investigation. Variations in these parameters cannot be directly related to the NAO. The role of the general and slope circulation

on the hydrology of the French continental shelf, or of atmospheric circulation patterns not reflected in the NAO signal, is likely to be of greater importance than the NAO itself.

Acknowledgements

We thank the National Center for Atmospheric Research (NCAR), Météo-France, Diren-Centre, Diren-Midi-Pyrénées, and Port Autonome de Bordeaux for providing easy access to their data.

References

Chatfield, C. 1996. The Analysis of Time Series: an Introduction, 3rd edn. Chapman and Hall, London. 283 pp.

Dickson, R. R., and Hughes, D. G. 1981. Satellite evidence of mesoscale eddy activity over the Biscay abyssal plain. Oceanologica Acta, 4: 43–46.

Fox, C. J., Planque, B., and Darby, C. D. 2000. Synchrony in the recruitment time-series of plaice (*Pleuronectes platessa* L.) around the United Kingdom and the influence of sea temperature. Journal of Sea Research, 44: 159–168.

Froidefond, J. M., Jégou, A. M., Hermida, J., Lazure, P., and Castaing, P. 1998. Variability of the Gironde turbid plume by remote sensing. Effects of climatic factors. Oceanologica Acta, 21: 191–207.

Gonzàlez-Pola, C., and Lavín, A. (submitted). Seasonal and interannual variability on a hydrographic section off Santander (Southern Bay of Biscay) 1991–2000. ICES Decadal Symposium.

Hurrell, J. W. 1995. Decadal trends in the North Atlantic Oscillation: regional temperatures and precipitations. Science, 269: 676–679.

Koutsikopoulos, C., Beillois, P., Leroy, C., and Taillefer, F. 1998. Temporal trends and spatial structures of the sea surface temperature in the Bay of Biscay. Oceanologica Acta, 21: 335–344.

Koutsikopoulos, C., and Le Cann, B. 1996. Physical processes and hydrological structures related to the Bay of Biscay anchovy. Scientia Marina, 60 (Suppl 2): 9–19.

Lazure, P., and Jégou, A.-M. 1998. 3D modelling of seasonal evolution of Loire and Gironde plumes on Biscay Bay continental shelf. Oceanologica Acta, 21: 165–177.

Le Cann, B. 1982. Evolution annuelle de la structure hydrologique du plateau continental au sud de la Bretagne: modélisation numérique. Thèse de 3ème cycle, Université de Bretagne Occidentale.

Le Cann, B. 1990. Barotropic tidal dynamics of the Bay of Biscay shelf: observations, numerical modelling and physical interpretation. Continental Shelf Research, 10: 723–758.

Pérez, F. F., Pollard, R. T., Read, J. F., Valencia, V., Cabanas, J. M., and Ríos, A. F. 2000. Climatological coupling of the thermohaline decadal changes in the central water of the eastern North Atlantic. Scientia Marina, 64: 347–353.

Pingree, R. D. 1994. Winter warming in the southern Bay of Biscay and lagrangian eddy kinematics from a deep-drogued argos buoy. Journal of the Marine Biological Association of the United Kingdom, 74: 107–128.

Pingree, R. D., and Le Cann, B. 1989. Celtic and Armorican slope and shelf residual currents. Progress in Oceanography, 23: 303–338.

Pingree, R. D., and Le Cann, B. 1992. Three anticyclonic Slope Water Oceanic eDDIES (SWODDIES) in the southern Bay of Biscay in 1990. Deep-Sea Research 1, 39: 1147–1175.

Pingree, R. D., Mardell, G. T., Holligan, P. M., Griffiths, D. K., and Smithers, J. 1982. Celtic Sea and Armorican current structure and the vertical distributions of temperature and chlorophyll. Continental Shelf Research, 1: 99–116.

Pirazzoli, P. A. 2000. Surges, atmospheric pressure and wind change and flooding probability on the Atlantic coast of France. Oceanologica Acta, 23: 643–661.

Plaut, G., and Simonnet, E. 2001. Large-scale circulation classification, weather regimes, and local climate over France, the Alps and Western Europe. Climate Research, 17: 303–324.

Puillat, I., Lazure, P., Jégou, A.-M., and Planque, B. (submitted). Mesoscale, interannual, and seasonal hydrological variability over the French continental shelf of the Bay of Biscay during the 1990s. ICES Decadal Symposium.

Pyper, B. J., and Peterman, R. M. 1998. Comparison of methods to account for autocorrelation in correlation analyses of fish data. Canadian Journal of Fisheries and Aquatic Sciences, 55: 2127–2140.

Ratier, A. 1986. Température de la mer et analyse objective. Metéorologie Maritime, 130: 13–17.

Reid, P. C., and Planque, B. 1999. Long-term planktonic variations and the climate of the North Atlantic. *In* Atlantic Salmon Trust Workshop. Problems Facing Salmon in the Sea, pp. 153–169. Ed. by D. Mills. Blackwell Science, Oxford.

Simonnet, E., and Plaut, G. 2001. Space-time analysis of geopotential height and SLP, interseasonal oscillations, weather regimes, and local climates over the North Atlantic and Europe. Climate Research, 17: 325–342.

Sournia, A., Brylinski, J.-M., Dallot, S., Le Corre, P., Leveau, M., Prieur, L., and Forget, C. 1990. Fronts hydrologiques au large des côtes Françaises: les sites-ateliers du programme Frontal. Oceanologica Acta, 13: 413–438.

Taillefer, F. 1990. Le point sur les modèles d'analyse en exploitation à la météorologie Nationale. Metéorologie Maritime, 146: 7–11.

Thompson, K. R., and Page, F. H. 1989. Detecting synchrony of recruitment using short, autocorrelated time series. Canadian Journal of Fisheries and Aquatic Sciences, 46: 1831–1838.

Vincent, A. 1973. Les variations de la situation thermique dans le Golfe de Gascogne en 1969 et 1979. Revue des Travaux de l'Institut des Pêches Maritimes, 37: 5–18.

Vincent, A., and Kurc, G. 1969. Hydrologie, variations saisonnières de la situation thermique du Golfe de Gascogne en 1967. Revue des Travaux de l'Institut des Pêches Maritimes, 33: 79–96.

von Stroch, H., Zorita, E., and Cubasch, U. 1993. Downscaling of global climate change estimates to regional scales: an application to Iberian rainfall in wintertime. Journal of Climate, 6: 1161–1171.

Woodruff, S. D., Lubker, S. J., Wolter, K., Worley, S. J., and Elms, J. D. 1993. Comprehensive Ocean-Atmosphere Data Set (COADS) Release 1a: 1980–1992. Earth System Monitor – NOAA, 4.

Xie, P., and Arkin, P. A. 1996. Analyses of global monthly precipitation using gauge observations, satellite estimates and numerical model predictions. Journal of Climate, 9: 840–858.

ICES Marine Science Symposia, 219: 71–79. 2003

Oceanographic variability in the northern shelf of the Iberian Peninsula, 1990–1999

J. M. Cabanas, A. Lavín, M. J. García, C. Gonzalez-Pola, and E. Tel Pérez

Cabanas, J. M., Lavín, A., García, M. J., Gonzalez-Pola, C., and Tel Pérez, E. 2003. Oceanographic variability in the northern shelf of the Iberian Peninsula, 1990–1999. – ICES Marine Science Symposia, 219: 71–79.

Atmospheric and oceanographic variability off the northern Iberian Peninsula in the 1990s is described from climatological databases and Spanish hydrographic surveys. The wind regime during the decade can be divided into two principal periods. In the first, northerly (upwelling favourable) winds are prominent, while in the second, southwesterly winds dominate, resulting in diminished upwelling, an increase in sea surface temperatures and the occurrence of the winter poleward current. In the subsurface waters during summer, a warming trend through the 1990s of between 0.02 and 0.05°C year^{-1} is found, with the maximum amplitude between 150 and 200 m. The warmest year was 1998. Salinity also varied during the decade, with higher salinities generally reflecting an increase in the poleward current and low salinities indicating advection from the inner Bay of Biscay. In 1995/1996 and 1997/1998, a strong winter surface Poleward Current carrying warm, salty water was present along the Portuguese coast and reached the southern Bay of Biscay. It contributed significantly to the heat content in the upper 500 m of the water column. The intensification of the Poleward Current is associated with increased onshore Ekman transport during autumn in western Galicia. Sea level variability also reflects wind changes with stronger southwesterly winds resulting in higher levels. Mean sea level increased from 1993 to 1997, giving a somewhat greater increasing trend for the last decade compared to the long-term over the past 55 years.

Keywords: decadal variability, hydrography, Iberian waters, sea level.

J. M. Cabanas: Instituto Español de Oceanografía. Apdo. 1552, ES-36280 Vigo, Spain. E-mail: jmanuel.cabanas@vi.ieo.es; A. Lavín: Instituto Español de Oceanografía. Apdo. 240, ES-39080 Santander, Spain; M. J. García and E. Tel Pérez: Instituto Español de Oceanografía. Corazón de María 8, ES-28002 Madrid, Spain; C. Gonzalez-Pola: Instituto Español de Oceanografía. C.O. Gijon. Apdo. ES-33212 Gijón, Spain. Correspondence to J. M. Cabanas.

Introduction

Atlantic waters near the Iberian Peninsula are situated between the southern branch of the North Atlantic Current to the north and the Azores Current to the south. Most of the water over the continental shelf corresponds to Eastern North Atlantic Central Water (ENACW) with, respectively, subtropical and subpolar branch characteristics, south and north of Cape Finisterre, where the two branches converge (Fraga *et al.*, 1982; Fraga, 1990). Dynamically, it is a region of relatively weak currents, seasonal upwelling, and fronts off the northwest corner of the Peninsula (Fiuza *et al.*, 1998; Cabanas, 2000).

The oceanic climate over the northern Iberian Shelf has two principal seasons. In summer, northerly winds cause the surface currents to be equatorward and there is associated upwelling on the west coast of the Iberian Peninsula (Cabanas, 2000). In addition, fronts develop off the northwest corner of the Iberian Peninsula and eddies form in the Cantabrian Sea. The upwelling is the most important physical characteristic for biological production over the shelf (Fiuza, 1984; Blanton *et al.*, 1987; Blanton and Tenore, 1998). In winter, a surface Poleward Current appears (Frouin *et al.*, 1990) that transports relatively warm and salty waters from off the Azores to the Iberian margin.

Mean sea levels also show marked seasonality, with low levels in spring and summer (lowest during the upwelling season) and higher in autumn and winter. The sea level responses to changes in atmospheric pressure vary spatially, being higher at Santander and Coruña than at Vigo. At the latter site, other meteorological factors such as local winds play a relatively more important role in determining sea level variability (Lavin and García, 1992; García *et al.*, 2000)

Year-to-year changes in meteorological forcing over northern Iberia reflect large-scale atmospheric variability as captured by climatological indexes such as the North Atlantic Oscillation (NAO; Hurrell, 1995). When the NAO index is in its positive phase, the mid-latitude westerly winds increase in strength over the North Atlantic and shift northward. This results in the Iberian Peninsula becoming relatively isolated from this wind regime (and their associated lows) and the weather is generally dry. In the negative phase of the NAO, the westerlies diminish in intensity and shift southward towards the Iberian Peninsula. This produces wet years and increases the run-off from rivers in northern Spain and southern France (Perez *et al.*, 2000). These atmospheric changes induce significant interannual and decadal variability in the properties of the waters off Iberia. The objective of this article is to characterize the atmospheric and oceanographic variability of the 1990s off the northern Iberian Peninsula and to compare it with previous decades.

Data and methods

To examine the hydroclimatic variability off the Iberian Peninsula (Figure 1) we used time-series of: the North Atlantic Oscillation (NAO; 1970–1997) from Hurrell (1995); the position of the Gulf Stream (GULF; 1976–1997) from Taylor (1996); winds at 43°N 11°W (1970–1999), from which indices related to the intensity of the seasonal upwelling (I_w index; Bakun, 1973, Lavín *et al.*, 1991, 2000) and the alongshore wind-induced currents (as monitored by the zonal Ekman transport in October–December period, ETOD index, Cabanas, 2000) were derived; temperatures along the Santander and Vigo standard sections (see Figure 1) during 1990–2000; and the COADS 2° × 2° database for wind, air, and sea surface temperature at 42°N 10°W (1970–1997).

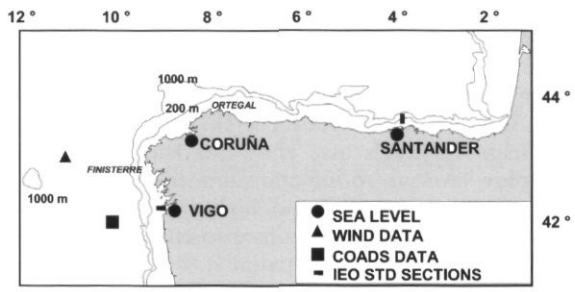


Figure 1. Study area showing the location of the tide gauges, wind site, the location of the COADS data grid point, and the standard hydrographic (STD) sections. Isobaths of 200 m and 1000 m are also shown.

Temperature and salinity time-series were separated into a mean, a linear trend, and a seasonal cycle using a least squares technique. The seasonal cycle is approximated by a combination of the annual and semi-annual harmonics (Yashayaev, 2000). To estimate confidence intervals ($p = 0.05$), we used the inverse of the statistical F cumulative distribution function (see Gonzalez-Pola and Lavín, 2003).

Data from tide gauges at Santander, Coruña, and Vigo (1945–1999) were used to study trends in sea level. An analysis of relative monthly mean sea level was performed with the same model used for temperature and salinity. To remove the effects of the Post-Glacial Rebound (PGR), the correction given by Peltier's (2000) geodynamic model was used. Principal components analysis (PCA) was applied to the monthly mean sea levels to examine the "zonal trend". Time-series with at least 25 consecutive years were used in order to search for sea level trends.

Standard correlation analysis was used to determine possible relationships between variables such as the NAO index with sea level elevations. Levels of $p = 0.05$ or less were considered significant.

Results

Ekman transport

A notable shift in the winds occurred during the last two decades, resulting in a reduction in the spring–summer upwelling off the Iberian Peninsula. The annual mean of the summer (April–September) upwelling index, I_w, decreased from approximately 400 $m^3\ s^{-1}\ km^{-1}$ in the 1970s to around 200 $m^3\ s^{-1}\ km^{-1}$ through the 1980s and 1990s (Figure 2A). Periods of especially weak upwelling were observed in the early 1980s and also in the late 1990s. There were also seasonal changes between the 1970s and 1980s with the reduction in upwelling being larger in spring (50%) than in summer (25%). At the same time there was also a shift in the period of the most intense southwesterly winds, from winter to autumn. Within the decade of the 1990s, upwelling intensity was relatively steady until 1997, when it decreased. In 2000, the lowest I_w value in the 31-year record and the only negative value of the index was observed.

Winter temperatures along the northern Spanish slope can be used to examine the interannual variability of the Poleward Current (Pingree, 1994). Warm temperatures from the Vigo hydrographic sections in the winters of 1983/1984 and 1989/1990 suggest a strong Poleward Current in those years. Another strong event in the winter of 1995/1996 was cited by Diaz del Rio *et al.* (1996) and 1997/1998 was

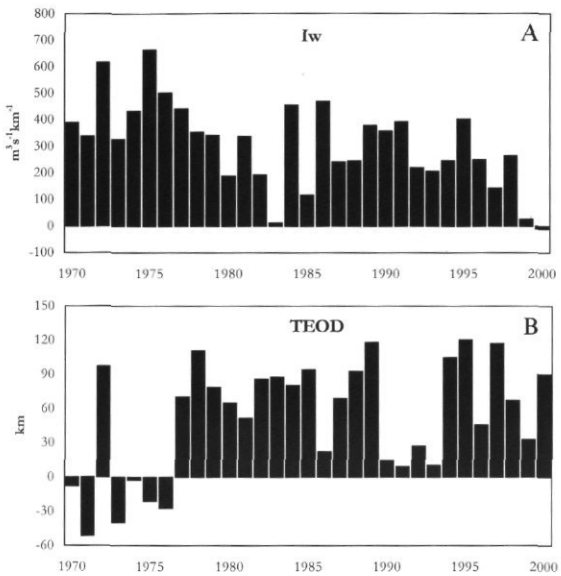


Figure 2. (A) Upwelling index (Iw) and (B) the strength of winter Poleward Current (ETOD) at 43°N 11°W, derived from the seasonal zonal Ekman transports (Bakun, 1973): April–September for Iw and October--December for ETOD.

the warmest winter throughout the North Atlantic (Levitus, *et al.*, 2000). All these years had above average values of autumn (October–December) Ekman transport, i.e. ETOD (Figure 2B). This is consistent with a strong positive correlation between sea surface temperatures (SSTs) and ETOD derived from COADS data from the grid site 42°N, 10°W. The highest correlation was $r = 0.81$ ($p < 0.05$) using December SSTs, with still significant but lower amplitude correlations using SSTs from November ($r = 0.68$) or January ($r = 0.67$). The strength of the correlations diminish eastward, for example, in the central Cantabrian Sea (44°N 7°W) the maximum $r = 0.35$ ($p < 0.05$) (using December SSTs), and is even lower in the eastern Cantabrian Sea (44°N 4°W), with a maximum $r = 0.33$ (using January SSTs). All the values were corrected for autocorrelation. The progress of the warm Poleward Current into the Bay of Biscay can be traced from time-series of satellite pictures for well-defined events, such as those of December 1989 and 1997.

Sea surface temperature

From the COADS SSTs at 42°N 10°W, values from 1980 to 1997 were averaged for autumn/winter (October–March) under predominantly southwesterly winds and spring/summer (April–September) with generally northerly winds. SST anomalies from these long-term means for each year are presented in Figure 3. Autumn/winter conditions were cooler

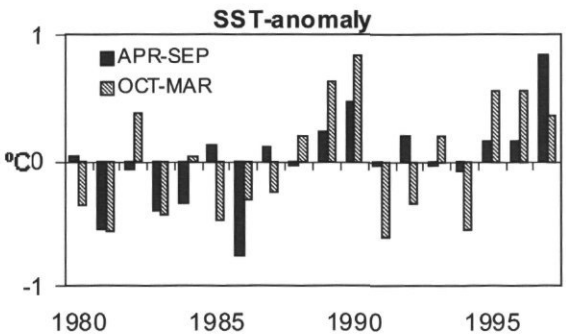


Figure 3. Sea surface temperature anomalies of April–September (black) and October–March relative to the long-term mean for the period 1980–1997 at 42°N, 10°W. Data are from the COADS database.

than the mean through most of the 1980s and into the early 1990s with warmer conditions in 1982, 1988–1990, and again from 1995 to 1997. The highest available SST anomaly, nearly 1°C, was observed in 1990. Note that several years of positive anomalies were earlier identified as years with increased transport of the winter Poleward Current. Although no COADS SST data were available for 1998, other information indicates that it too was an extremely warm year. In spring/summer, SSTs in the1990s are clearly higher than in the1980s. Upwelling is the principal mechanism reducing the SSTs in this season. Average upwelling (Figure 2A) and reduced winter transport in the Poleward Current produced the relatively low temperatures at the beginning of the 1990s, while weaker upwelling in the second part of the decade led to a notable increase in SST, reaching an anomaly of nearly 1°C in 1997.

Subsurface hydrographic conditions

Upper water conditions were examined using data from a shelf-break station on the Santander section in the southern Bay of Biscay and from the shelf off Ria de Vigo for the Atlantic coast. In the southern Bay of Biscay, the properties of the upper layer are closely related to the local atmospheric heating, as well as being influenced by wind-driven circulation, summer upwelling, and autumn mixing. They are also affected by advection of saltier and warm waters in winter originating from the south and west and less saline water from the eastern part of the Bay of Biscay in summer.

Monthly mean temperatures near surface (10 m) at the shelf break along the Santander section during the 1990s indicate a typical summer (August) maximum and a late winter (February–March)

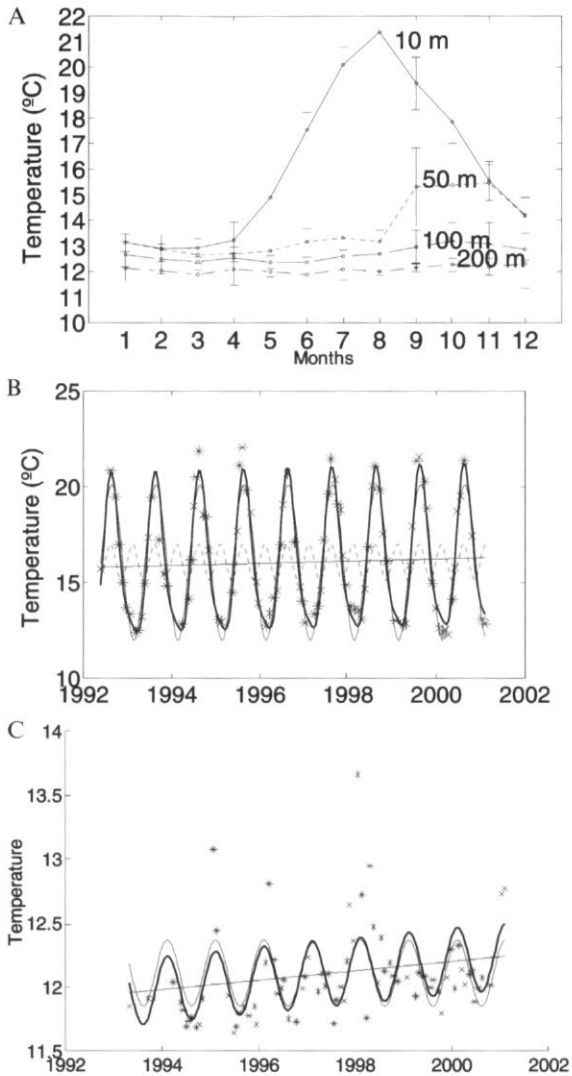


Figure 4. A. Monthly mean temperatures at 10, 50, 100, and 200 m over the self-break (Station 6) along the Santander standard section. Vertical lines represent ± 1 standard deviation. B. Observed temperatures at 10 m (asterisks) as well as the linear trend, the annual (fine line) and semi-annual (dashed line) components without the linear trend and the signal reconstruction that includes both the linear trend and the annual and semi-annual components (bold line). C. Same as the 10 m plot but at 200 m and minus the semi-annual component.

minimum (Figure 4A). Deeper in the water column the maximum occurs later in the year and with a reduced amplitude. A reasonable fit to the annual temperature cycle at 10 m (Figure 4B) requires both the annual and the semi-annual harmonic terms, whereas at 200 m only the annual component is needed (Figure 4C). Indeed, below 100 m, only the annual cycle is significant at 95% confidence limits. The annual amplitude decreases with depth (from 4°C at 10 m, to 0.5°C at 100 m, and 0.1°C at 400 m). The phase of the annual harmonic also changes with depth.

For temperatures at 200 m, there is an indication of a linear warming trend during the 1990s (Figure 4C), although it is not statistically significant. Temperature trends in winter (January, February, and March) and summer (July, August, and September) are quite different, however. In winter there is no trend, but in summer (Figure 5) there is a significant trend of $0.054° \pm 0.042°C\ year^{-1}$. In 1998, the 200-m temperatures during both summer and winter were the highest in the decade (Figure 4C).

Salinity has also shown large variability during the 1990s, from high in the early years to low in the middle of the decade, rising towards the end of the 1990s and finally declining again. This is clearly shown at 50 m (Figure 6) and is a pattern repeated throughout the entire upper layer. The increases in salinity are coherent with the years of strong forcing

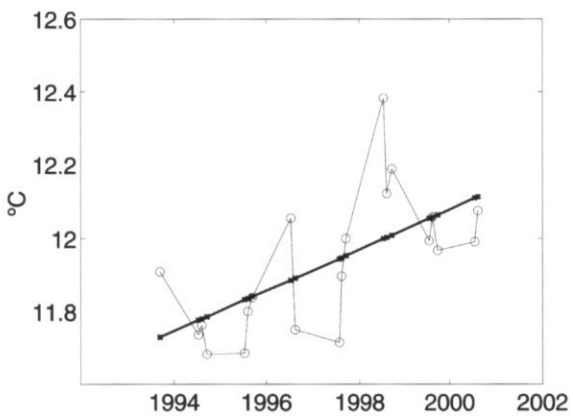


Figure 5. Monthly temperatures at 200 m during summer at Santander Station 6 and the linear fit.

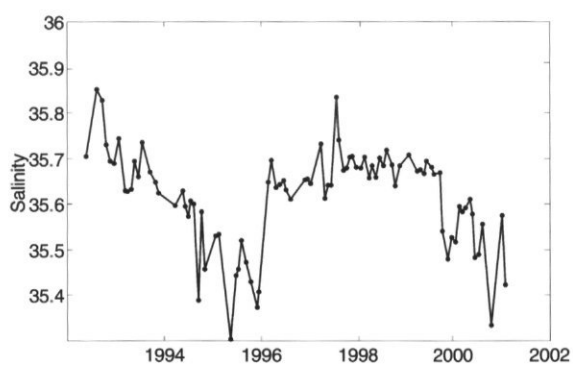


Figure 6. Monthly salinities at 50 m at Santander Station 6.

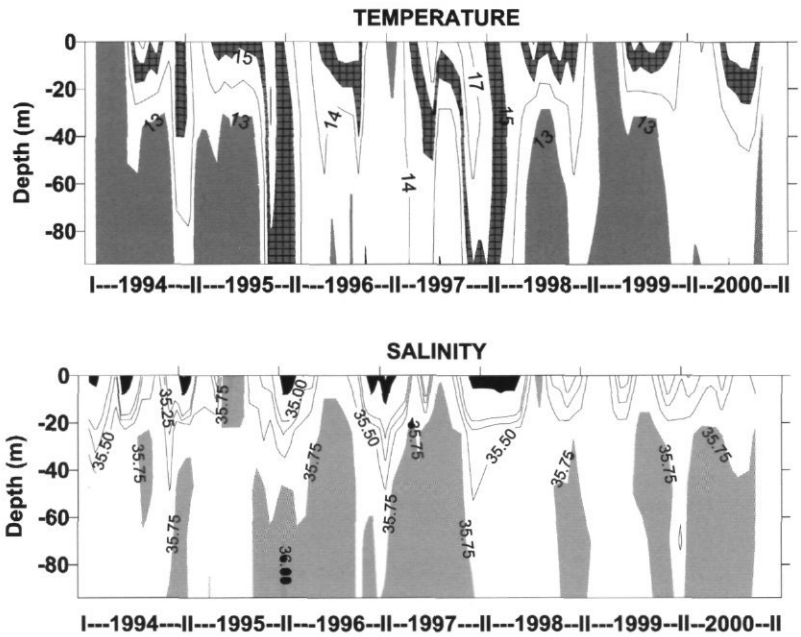


Figure 7. Time-series of temperature and salinity at a shelf site offshore of Vigo. Temperatures below 13°C and salinities up to 35.75 (corresponding to upwelled waters) are shaded. Also $15° < T < 16°C$ are partly shaded to show years when the winter poleward current was detected.

from southwesterly winds (ETOD) or a winter Poleward Current event. For example, the strong inflow in 1995/1996 marks a salty period in the southern Bay of Biscay and the 1997/1998 inflow slightly accentuates the salinity. During 1999/2000 and 2000/2001, the reduction in salinity appears to be through advection of fresher water from the east.

At the coastal station (94 m depth) close to Ria of Vigo, temperatures from 1994 to 2000 (Figure 7) show a seasonal cycle in temperature in the upper layers and thermal stratification between May and October, interrupted by summer upwelling events. Salinity contours show high values during the winters of 1996, 1997, and 2000, due to the increased presence of the Poleward Current, with occasionally high values during the spring–summer period due to seasonal upwelling events. The highest salinities in the spring–summer period were in 1997 and 2000. The autumn of 1997 and winter of 1998 were the warmest periods observed due to the intensified Poleward Current. Salinity was high from the middle of 1997. By the summer 1998, the main part of the water column had cooled, presumably due to strong upwelling. The Poleward Current was weak during autumn 1998 and through 1999 but intensified in autumn 2000 but did not reach the Cantabrian Sea. Indeed, in some winters, the Poleward Current reaches the Cantabrian Sea and the French shelf break, while in others it only reaches the Western Iberian area. Nutrient levels generally reflect upwelling intensity and the presence of the winter Poleward Current. Nitrates range from 0 μmol/l in warm surface waters to 10 μmol/l in upwelled waters.

On the Vigo Shelf, summer upwelling and the winter Poleward Current prevent a significant annual cycle. Trend analysis by seasons indicated that only summer temperatures at 20 m show a warming trend ($0.20° \pm 0.18°C$ between 1994 and 2000), which is significant at the 85% level.

Heat content

To examine the heat content, the water column was divided into two layers: 0–100 m (Figure 8A) and 100–500 m (Figure 8B). The upper layer shows a seasonal temperature pattern similar to that at 10 m, while the deeper layer shows a peak in late autumn or early winter. The heat content in the deep layer is high in 1996 and highest in 1998, years of strong autumn onshore Ekman transport. The year 1998 marks the historical maximum and is coherent with the maximum temperatures found by Levitus *et al.* (2000) for the Atlantic and Indian Oceans. After 1998, the heat content in the deep layer shows a slight reduction and remains relatively stable. The heat content patterns are different for each layer (Figure 8C; Gonzalez-Pola and Lavín, this volume). The trough to peak range in heat content for

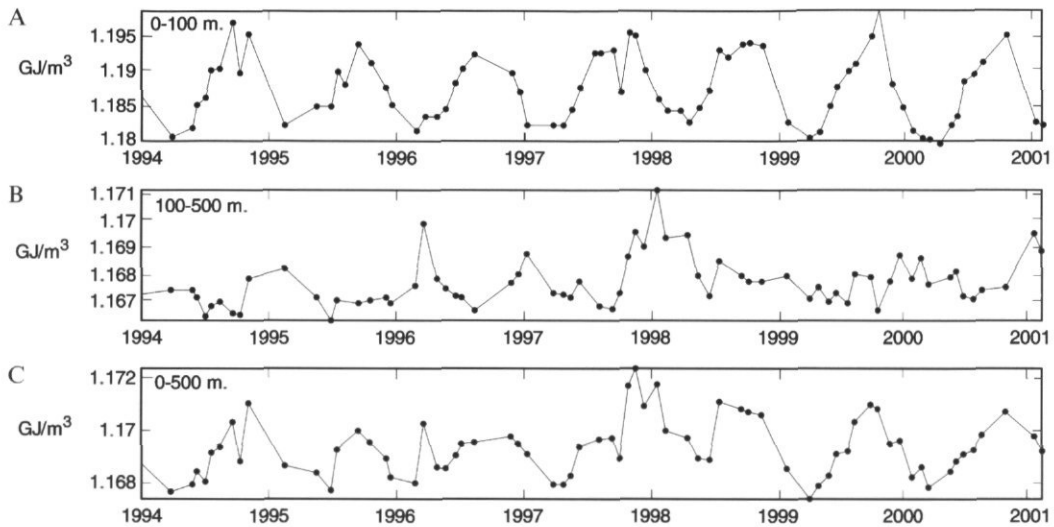


Figure 8. Monthly values of the integrated heat content between (A) 0–100 m from 1992 to 2001 and (B) 100–500 m, and (C) 0–500 m from 1994 to 2001.

Table 1. A. Annual and semi-annual amplitudes and composite range of sea level. B. Results of trend analysis using filtered annual and semi-annual components and Peltier's (2000) correction.

A	Annual	Semiannual	Annual+semiannual	
	Amplitude (mm)	Amplitude (mm)	Range (mm)	Max
Vigo	43	12	94	Oct
Coruña	41	10	87	Nov
Santander	42	8	84	Nov

B	Begin	End	n	Mean (cm)	Trend (mm/y)	Peltier (mm/y)	t+Peltier (mm/y)
Vigo	Jan-43	dic-99	676	252.21	2.66	0.22	2.88
	Jan-80	dic-89	119	254.09	5.41	0.22	5.63
	Jan-90	dic-99	119	257.93	15.54	0.22	15.76
Coruña	Jan-44	dic-99	660	263.69	1.34	0.13	1.47
	Jan-80	dic-89	119	265.14	4.43	0.13	4.56
	Jan-90	dic-99	111	266.99	10.60	0.13	10.73
Santander	Jan-44	dic-99	651	278.63	1.75	0.27	2.02
	Jan-80	dic-89	113	282.14	3.71	0.27	3.98
	Jan-90	dic-99	109	281.66	9.86	0.27	10.13
Zonal*	Jan-44	dic-99	672	—	2.08	0.20	2.28

*The KMO (Kaiser-Meyer-Olkin sampling fitness measure) value is 0.743, the first component (regional trend) extracted from PCA accounts for 83.6% of the total sea level variance.

the 0–500 m layer (Figure 8C) corresponds to a temperature increase of around 0.02°C.

Mean sea level

The amplitude of the semi-annual and annual tidal signals and their composite range determined from the monthly mean sea levels are presented in Table 1A. The significant correlation coefficients with the monthly NAO index at each station ($r = -0.41$ in Vigo, –0.42 in Coruña, and –0.31 in Santander, at $p < 0.01$), indicate the atmospheric influence in sea level (see also Figure 10). Values were corrected for autocorrelation. To remove the meteorological signal a moving average filter was used.

Because of decadal variability, it is important to have an extended time-series of sea level to observe the long-term trend. In our case we have a 55-year record. The long-term trends vary from 2.02 mm

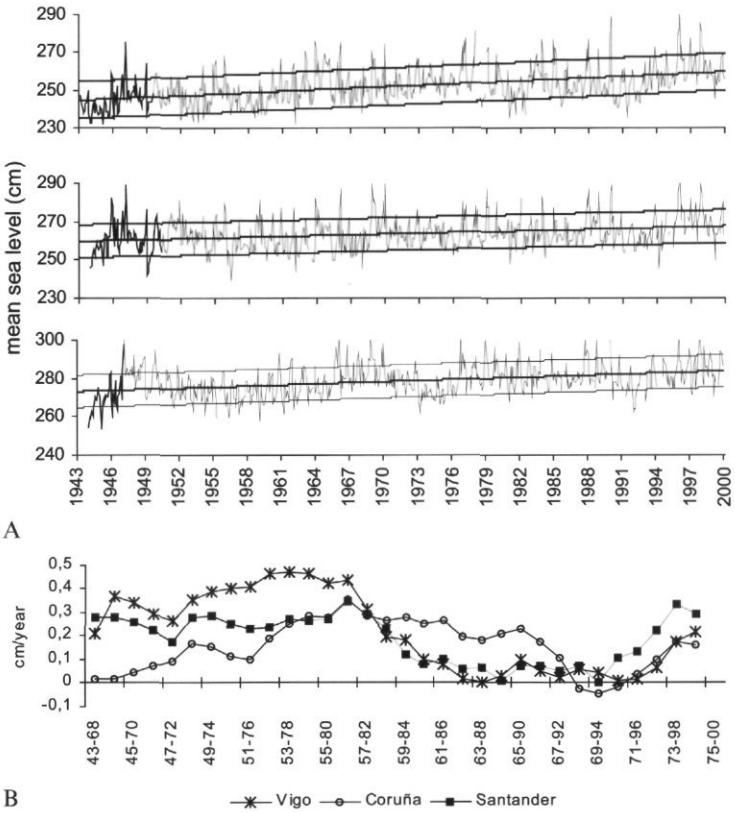


Figure 9. A. Monthly means and linear trends in sea level at Vigo, Coruna, and Santander. B. The sequence of 25-year trends at the three sea level sites.

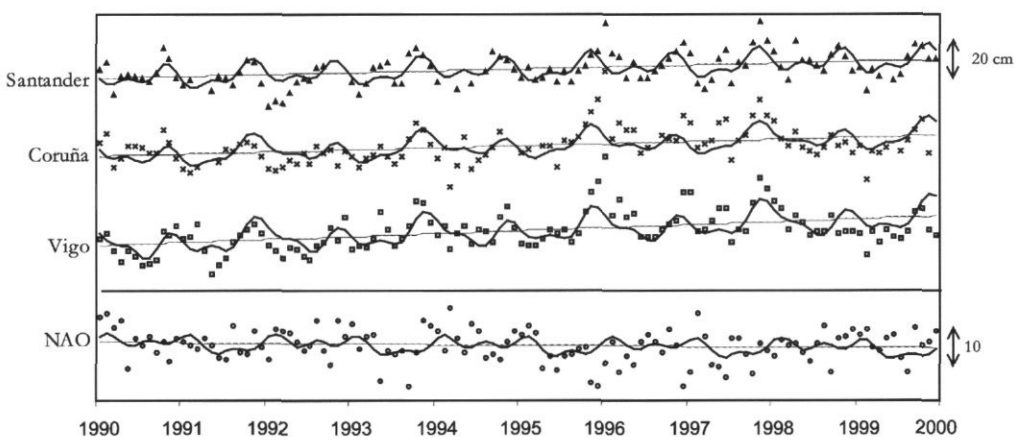


Figure 10. Monthly means of sea level and the NAO index during the 1990s.

year^{-1} in Santander, 1.45 mm year^{-1} in Coruña, and 2.88 mm year^{-1} in Vigo (Figure 9A), which are significantly above the estimates of the increase due to post-glacial rebound (Table 1). The result of a Principal Component Analysis (PCA) provides a "zonal trend" of 2.28 mm year^{-1}. The amplitude of the rise in sea level is not constant, however. Plotting the trends over 25-year periods, the amplitude of the rise declined from 1957–1982 to 1962–1987, remained low and then increased once more after the period 1969 to 1994. Note that sea level trends estimated over a decade, e.g. the 1980s or 1990s, are usually much greater than for the whole period (Table 1B) but generally are not statistically reliable.

During the 1990s, sea level was low during the early years, a period corresponding to a dry, northerly influenced cold period. In the second half of the decade, sea level was higher, corresponding to a time of more humid and warmer period.

Conclusions

There have been significant changes in the meteorological patterns over the northern Iberian Peninsula during the 1990s relative to previous years, in particular an increase in the strength of the southwesterly winds. This resulted in a stronger inflow of waters of subtropical origin in the northern Iberian Shelf, bringing with it waters with higher temperatures and salinities than usual. This contributed to a measurable warming trend during the 1990s, although it was not found to be statistically significant. Within the decade, there were several years with well above average temperatures, corresponding to increased southwesterly winds and a winter Poleward Current. 1998 was the warmest year on record.

Salinity also underwent strong variability during the decade; the maximum was reached in 1992, declined in the mid-1990s, rose again and declined rapidly towards the end of the decade. The high salinities generally corresponded to periods of westerly winds. The reduced salinity at the end of the decade occurred during a period of increased northerly winds and eastward ocean currents.

The mean sea level shows a general increase during the 1990s and is negatively correlated with the NAO Index. High sea levels tend to occur during southwesterly winds and intense poleward flows with lower levels during northerly winds and reduced poleward or equatorward flow. Thus high sea levels coincide with high temperatures. In the winter and summer of 1998, sea level and temperature increased greatly in the southern Bay of Biscay, reaching their highest values in the decade.

In summary, southwesterly winds produce onshore Ekman flow and a strong winter Poleward Current off the northern Iberian Peninsula, warmer temperatures, higher salinities, and higher sea levels. The opposite occurs under northerly winds. Relative to preceding decades, the winds over the Iberian Shelf in the 1990s were more southwesterly. This reduced the amount of upwelling and increased the strength of the Poleward Current.

Acknowledgements

We thank COADS for the meteorological and oceanographic data, IEO for the time-series of sea level and hydrographic data, J. Hurrell and B. Dickson for the NAO index, A. Taylor for the Gulf index, and M. Vargas for his help with the statistics. We also thank the editor and reviewers for their valuable help.

References

Bakun, A. 1973. Coastal upwelling indices, west coast of North America, 1946–1971. NOAA Technical Report National Marine Fisheries Service SSRF-671, US Department of Commerce. 103 pp.

Blanton, J. O., and Tenore, K. R. 1998. Interannual variability of upwelling strength and mussel production in the Iberian Peninsula. ICES CM/R: 4. 8 pp.

Blanton, J. O., Tenore, K. R., Castillejo, F., Atkinson, L. P., Schwing, F. B., and Lavín, A. 1987. The relationship of upwelling to mussel production in the rias of western coast of Spain. Journal of Marine Research, 45: 497–511.

Cabanas, J. M. 2000. Variabilidad temporal de las caracteristicas oceanográficas en la plataforma continental Gallega. Algunas consecuencias biológicas. Tesis Doctoral. Universidade de Vigo, Spain. 155 pp. (In Spanish.)

Díaz del Río, G., Lavín, A., Alonso, J., Cabanas, J. M., and Moreno-Ventas, X. 1996. Hydrographic variability in Bay of Biscay shelf and slope waters in spring 1994, 1995 and 1996 and relation to biological drifting material. ICES CM 1996/S: 18. 8 pp.

Fiuza, A. 1984. Hidrologia e dinámica das augas costeiras de Portugal. Tesis Doctoral. Universidade de Lisboa, Portugal. 294 pp. (In Portugese.)

Fiuza, A., Hamann, M., Ambar, I., Diaz del Rio, G., Gonzalez, N., and Cabanas, J. M. 1998. Water masses and their circulation in the Western Iberian coastal ocean during May 1993. Deep-Sea Research I, 45: 1127–1160.

Fraga, F. 1990. Circulación de las masas de agua en el golfo de Vizcaya. Oceanografía del golfo de Vizcaya. Ed. by J. Urrutia and A. Rallo. San Sebastian. (In Spanish.)

Fraga, F., Mouriño, C., and Manriquez, M. 1982. Las masas de agua en la costa de Galicia: Junio-Octubre. Resultados Expediciones. Cientificas B/O Cornide de Saavedra, 10: 51–77.

Frouin, R., Fiuza, A., Ambar, I., and Boyd, T. 1990. Observations of a poleward surface current off the coast of Portugal and Spain during winter. Journal of Geophysical Research, 95: 679–691.

García, M. J., Pérez, B., Fraile, M. A., and Millán, J. G. 2000. Sea level variability along the Spanish coast. 1990–1999. The Tenth General Assembly of the WEGENER Project (WEGENER 2000). Extended Abstracts Book. Boletin Roa, 3/2000. 5 pp.

Gonzalez-Pola, C., and Lavín, A. 2003. Seasonal cycle and interannual variability on a hydrographic section off Santander (Southern Bay of Biscay). 1991–2000. ICES Marine Science Symposia, 219: 343–345.

Hurrell, J. W. 1995. Decadal trends in the North Atlantic Oscillation: regional temperatures and precipitation. Science, 269: 676–679.

Lavín, A., Diaz del Rio, G., Cabanas, J. M., and Casas, G. 1991. Afloramiento en el Noroeste de la Peninsula Iberica. Indices de afloramiento para el punto 43° N 11° W. Periodo 1966–1989. Informes Técnicos del Instituto Español de Oceanografía, 91: 1–40. (In Spanish.)

Lavín, A., Diaz del Rio, G., Cabanas, J. M., and Casas, G. 2000. Afloramiento en el Noroeste de la Peninsula Iberica. Indices de afloramiento para el punto 43° N 11° W. Periodo 1990–1999. Datos y Resumenes del Instituto Español de Oceanografía, 15: 1–25. (In Spanish.)

Lavin, A. and García, M. J. 1992. Mean sea level along the North Atlantic coast 1980–1989. ICES Marine Science Symposia, 195: 187–192.

Levitus, S., Antonov, J. I., Boyer, T. P., and Stephens, C. 2000. Warming of the world ocean. Science, 287: 2225–2229.

Peltier, W. R. 2000. ICE (VM2) Glacial Isostatic Adjustment Correction on Sea Level Rise, History and Consequences. Academic Press, New York. 228 pp.

Perez, F. F., Pollard, R. T, Read, J. F., Valencia, V., Cabanas, J. M., and Rios, A. F. 2000. Climatological coupling of the thermohaline decadal changes in the Central Water of the Eastern North Atlantic. Scientia Marina, 64: 347–353.

Pingree, R. D. 1994. Winter warming in the Southern Bay of Biscay and Lagrangian eddy kinematic from a deep-drogued Argos buoy. Journal of Marine Biological Association of the United Kingdom, 74: 106–128.

Pingree, R. D., and Le Cann, B. 1990. Structure, strength, and seasonality of the slope current in the Bay of Biscay region. Journal of Marine Biological Association of the United Kingdom, 70: 857–885.

Taylor, A. H. 1996. North–south shifts of the Gulf Stream: ocean–atmosphere interactions in the North Atlantic. International Journal of Climatology, 16: 559–583.

Yashayaev, I. M. 2000. 12-year hydrographic survey of the Newfoundland basin: seasonal cycle and interannual variability of water masses. ICES CM 2000/L: 17. 17 pp.

ICES Marine Science Symposia, 219: 80–85. 2003

Decadal changes of the hydrography between Ireland and Cape Farewell

Hendrik M. van Aken

van Aken, H. M. 2003. Decadal changes of the hydrography between Ireland and Cape Farewell. – ICES Marine Science Symposia, 219: 80–85.

In April 1991 and October 2000 surveys were carried out along a section from the Irish Shelf to southern Greenland. Between 200 and 1500 m the temperatures increased. In the Rockall Channel and the Iceland Basin the increase, in the order of 0.5°C, is connected with a salinity increase, while only minor differences in the θ-S diagram can be observed. In the Rockall Channel the permanent thermocline has deepened. In the Iceland Basin the Subarctic Front (also known as Subpolar Front) has shifted westwards over a distance of 200 to 250 km. In the Irminger Sea the temperature in the upper 1500 m has increased by a few tenths °C with minor salinity changes. This is probably a recovery from the low temperatures in 1991. At intermediate levels, a decrease in salinity and temperature is observed along the whole section, reflecting the eastward spreading of the cold vintage of Labrador Sea Water produced around 1990. The Iceland–Scotland Overflow Water along both the eastern and the western slopes of the Reykjanes Ridge has slightly increased in temperature, while the salinity has hardly changed. The Denmark Strait Overflow Water shows a decrease in temperature of over 0.2°C, with a minor decrease in salinity.

Keywords: decadal variability, hydrography, North Atlantic.

H. M. van Aken: Royal Netherlands Institute for Sea Research, PO Box 59, 1790AB, Den Burg/Texel, The Netherlands [tel: +31 222 369416; fax: +31 222 319674; e-mail: aken@nioz.nl]

Introduction

Within the framework of the Dutch contribution to CLIVAR, the Royal Netherlands Institute of Sea Research at Texel regularly surveys the former WHP A1E/AR7E section in the North Atlantic between the Irish continental shelf and the Greenland Shelf at 60°N. The purpose of these surveys is to monitor climate-related changes in the hydrography and circulation of the Subarctic gyre in the North Atlantic Ocean. These surveys take place every 2 years, coincident with surveys of the former A2 line by BSH, Hamburg (K. P. Koltermann, pers. comm.).

From 26 September to 19 October 2000, RV "Pelagia" carried out the first CLIVAR survey of the AR7E line (the dots in Figure 1). This line was also surveyed in April 1991 by RV "Tyro" and in August of the same year by RV "Charles Darwin" for the WOCE Hydrographic Program. The western part of the section, west of 31°W, was also surveyed by RV "Tyro" in 1990, by RV "Meteor" in 1991, 1994, 1997, and 1999, and by RV "Valdivia" in 1992, 1995, 1996, and 1999. The eastern part of those surveys followed a more southerly course (the crosses in Figure 1), skimming the southern slopes of the Rockall–Hatton Plateau instead of crossing this plateau and the main currents at more or less right angles.

Bersch *et al.* (1999) have described interannual changes in the hydrography along the southern leg of the AR7E section from 1991 to 1996. Bersch (2002) interprets the observed interannual changes in the upper layers in terms of the varying North Atlantic Oscillation (NAO). The repeat of the more zonal Tyro 1991 section by RV "Pelagia" 9 years later allows an indication of decadal change in the hydrography of the North Atlantic further to the northeast. Moreover, the extension of the time-series of coinciding sections in the Irminger Sea to 2000 allows an update on interannual variability for this ocean region.

The 2000 section

The sections of potential temperature, salinity, and potential vorticity from the 2000 survey (Figure 2)

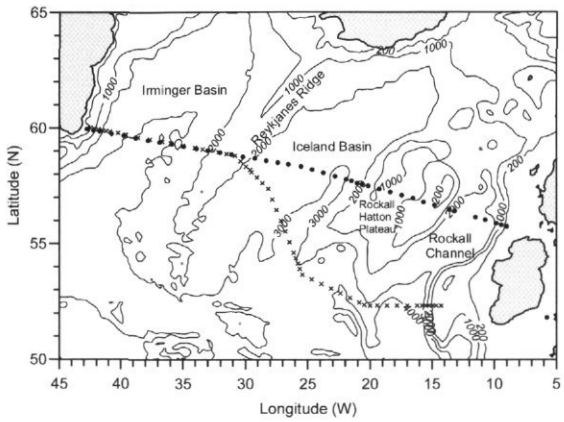


Figure 1. The North Atlantic Ocean with the hydrographic stations along the AR7E section occupied by RV "Pelagia" in October 2000 (black dots). This line of stations was also surveyed by RV "Tyro" and by RV "C. Darwin", both in 1991. The crosses are the hydrographic stations of the Meteor survey of the AR7E section in 1991. This southern course of the section is typical for the surveys of RV "Tyro" in 1990, RV "Meteor" in 1991, 1994, and 1997 and of RV "Valdivia" in 1992, 1995, 1996, and 1999.

show qualitatively the well-known features in the Rockall Channel and the Iceland Basin (van Aken and Becker, 1996). Here the large-scale potential vorticity λ is defined as $\lambda = fN^2/g$, where f and N are the Coriolis and the Brunt-Väisälä frequencies, and g is the gravitational acceleration. The relatively warm and saline water of the North Atlantic Current ($S > 35.0$) occupies the upper layers of the water column in these basins. The Subarctic Front forms the northwestern boundary of this Atlantic Water and coincides approximately with the 35.0 isohaline at about 33°W. In the Atlantic Water the subsurface minimum of λ between ~300 and 500 dbar indicates the presence of Subarctic Mode Water (SAMW, also known as Subpolar Mode Water), formed by convective mixing in the previous winter (McCartney and Talley, 1982). Between 1500 and 2000 dbar, salinity minima are found, indicative of the presence of Labrador Sea Water (LSW). These salinity minima coincide with minima in potential vorticity, reflecting the convective origin of LSW (Talley and McCartney, 1982). Over the slope of the Reykjanes Ridge in the Iceland Basin relatively saline water with a potential temperature below 3°C is found in the lowest 500 dbar, representing the Iceland–Scotland Overflow Water (ISOW; van Aken and Becker, 1996).

Similarly to the 1991 survey, a minimum in potential vorticity is encountered directly above the crest of the Reykjanes Ridge. This is the lowest potential vorticity of the whole section. An explanation for this feature is not yet known. It may be that enhanced diapycnal mixing over the rough topography of the Icelandic and Reykjanes slopes is the cause of the nearly homogenous water over the ridge.

In the Irminger Basin, the vertical temperature gradient is quite small over a very large part of the water column, between the seasonal pycnocline at about 300 dbar and the cold Denmark Strait Overflow water (DSOW) over the Greenland slope (Figure 2A). The nearly homogenous temperature distribution, however, is not indicative of the presence of a single, convectively formed water type like LSW. The distributions of salinity and potential vorticity (Figure 2B, C) show a figure-of-eight-like form, reflecting the presence of two different convectively formed water types with low salinity, centred at about 680 and 1750 dbar, respectively. This form was quite common in the 1950s and early 1960s (Sv.-A. Malmberg, pers. comm.), but has not been observed in more recent surveys. Surrounding the upper low salinity core, higher salinities are observed over the western slope of the Reykjanes Ridge as well as over the Greenland slope, reflecting the cyclonic transport of saline Atlantic Water from the Irminger Current around the Irminger Basin. Over the continental shelf and shelf break off Greenland the cold low salinity East Greenland current is observed. In the deepest few hundred metres over the bottom of the Greenland slope and central Irminger Basin the cold ($1 < \theta < 2$°C) and relatively fresh DSOW ($S \approx 34.87$) is encountered. Directly above the DSOW core, the salinity maximum of the core of ISOW in the Irminger Basin is encountered. The salinity of this ISOW core is about 0.05 below the salinity of the ISOW in the Iceland Basin.

Differences between 1991 and 2000

The changes in potential temperature and salinity from 1991 to 2000 have been derived (Figure 3). The upper 200 dbar are not included in this analysis because of the relatively strong seasonal signal in that surface layer. The large decrease in θ and S near 30°W is caused by the presence of a warm core eddy in 1991, which was absent in 2000, and will be omitted from the following discussion.

Along the whole section, a temperature increase is observed in the upper layers, extending to a pressure of about 1500 dbar. Extremes in the temperature increase are found in the permanent thermocline of the Rockall Channel ($\Delta\theta > 2$°C) and in the upper 1000 dbar of the central Iceland Basin ($\Delta\theta > 1$°C). In the Irminger Basin the temperature increase also includes the subsurface salinity minimum near 680 dbar. At the levels of the salinity minimum in the Rockall Channel and Iceland Basin, connected

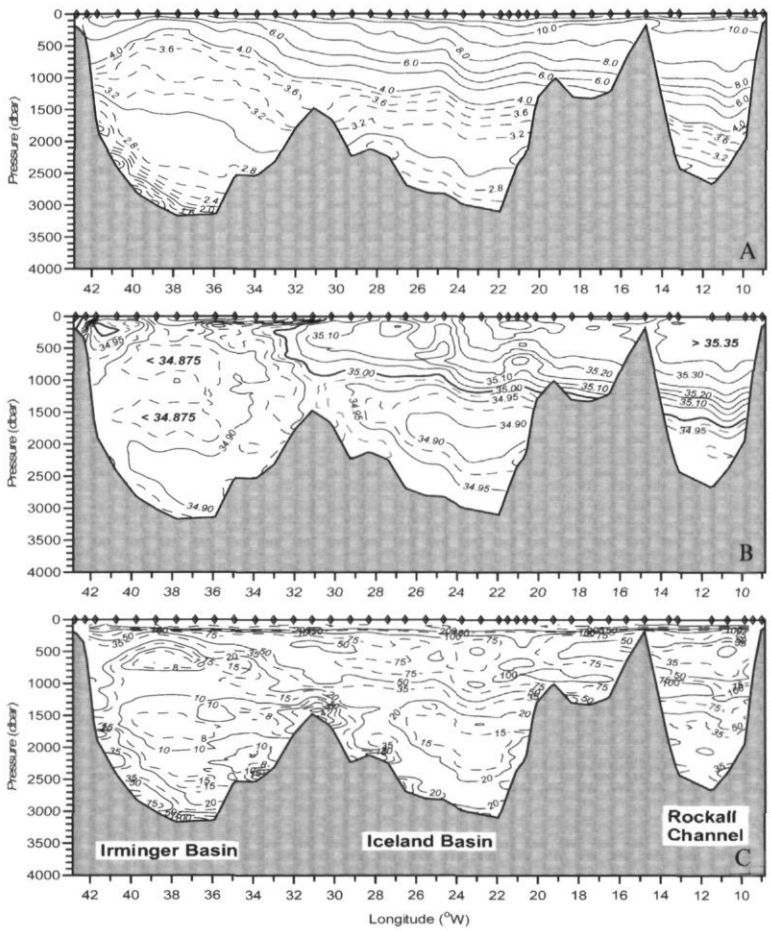


Figure 2. Distributions of (A) potential temperature [°C], (B) salinity [pss-78], and (C) potential vorticity [10^{-12} m^{-1} s^{-1}] along the AR7E section as observed during the survey by RV "Pelagia" in October 2000. The potential vorticity λ is defined as $\lambda = fN^2/g$, where f and N are the Coriolis and the Brunt-Väisälä frequencies, and g is the gravitational acceleration.

with the LSW core, a temperature decrease of about 0.2°C is observed. A similar temperature decrease is also observed in the salinity minimum at 1750 dbar in the Irminger Basin. The temperature changes in the ISOW cores in the Iceland Basin as well as in the Irminger Basin barely exceed 0.1°C, whereas the DSOW core has cooled by about 0.2°C.

The salinity in the upper 400 dbar over the Rockall Channel and Rockall–Hatton Plateau decreased slightly from 1991 to 2000. Below this layer, and also in the near-surface layers of the Iceland Basin, a relatively strong salinity increase was observed ($\Delta S > 0.1$) extending downwards to about 500 dbar. In the underlying LSW cores the salinity decreased from 1991 to 2000. In the Irminger Basin the salinity change in the upper 1500 dbar was variable, but overall it increased. In the salinity minimum at 1650 dbar in the Irminger Basin, as well as in the underlying ISOW and DSOW cores, a salinity decrease of 0.02 to 0.06 was observed. The salinity decrease of the ISOW core in the Iceland Basin was very small ($\Delta S < 0.02$).

Details of the observed change

The Rockall Channel

The mean profiles of salinity and potential temperature from the Rockall Channel as well as the θ-S diagram for both years are given in Figure 4. The temperature profiles show that the effects of the seasonal stratification are limited to the upper 250 dbar. The potential temperature of the SAMW (at the potential vorticity minimum or pycnostad above the permanent thermocline) differs by less than 0.2°C between the 2 years. In 2000 the permanent thermocline was found to be about 300 dbar deeper than in 1991. The salinity profiles show a

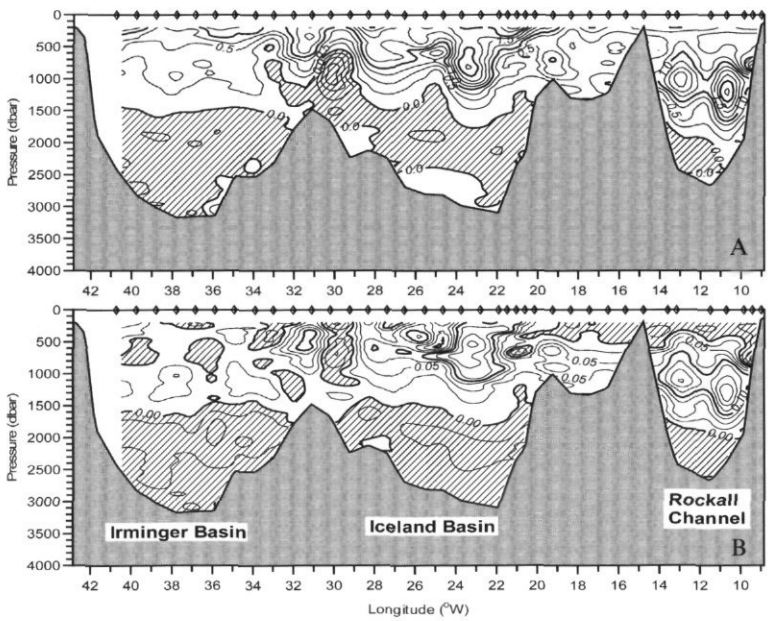


Figure 3. Distribution of the change of potential temperature (A) and salinity (B) along the AR7E section between 1991 and 2000. The upper 200 dbar are omitted from the analysis to avoid seasonal influences. In 1991 no data were collected over the upper continental slope near Greenland.

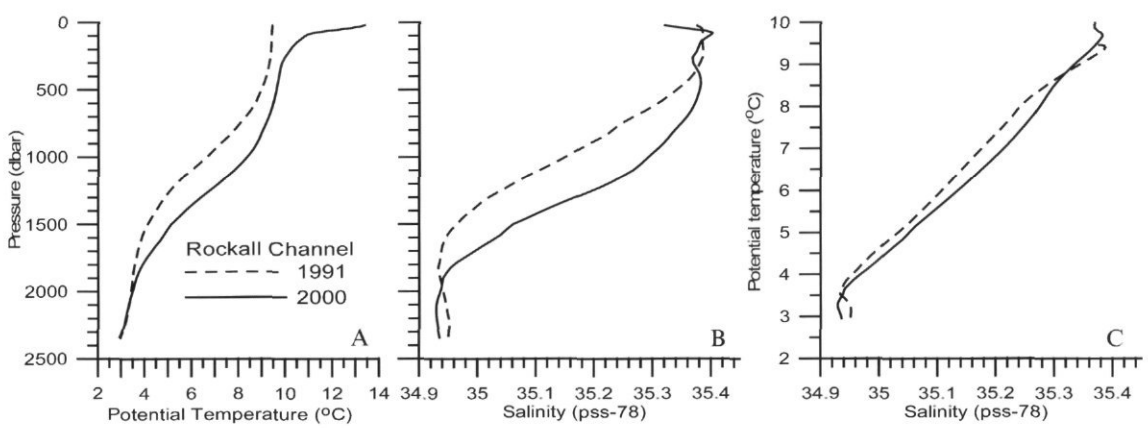


Figure 4. Mean hydrographic properties from the Rockall Channel (11°30′ to 13°30′W) for 1991 (thick grey line) and 2000 (thin black line): (A) potential temperature profiles, (B) salinity profiles, (C) θ-S diagram.

coincident downward shift, as does the salinity minimum, connected with the LSW core. This downward shift caused the strong increase in temperature and salinity centred around 1100 dbar, as well as the decrease of salinity at the level of the LSW core. The θ-S diagram shows that at similar temperatures the permanent thermocline was slightly more saline in 2000 than in 1991 ($\Delta S \approx 0.03$). Potential temperature as well as salinity in the LSW core decreased from 1991 to 2000, while the potential density increased.

The Iceland Basin

In Figure 5 the mean hydrographic properties of the deep Iceland Basin (21°45′ to 23°45′W) are shown. In the entire upper 600 dbar the potential temperature was higher in 2000 than in 1991. The SAMW in 2000 was about 1.3°C warmer than in 1991. The permanent thermocline was located deeper in 2000 than in 1991, while the LSW core had also moved downwards over about 400 dbar. The increase in the SAMW temperature and the lowering of the

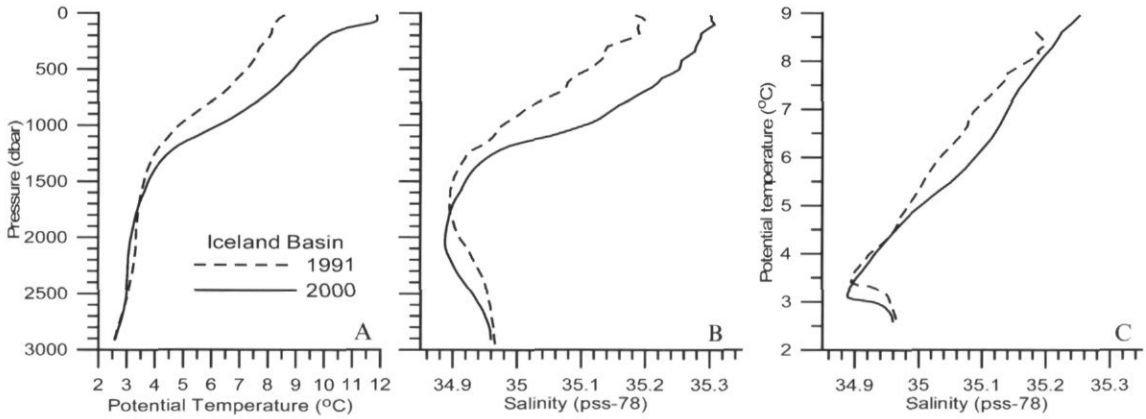


Figure 5. Mean hydrographic properties from the Iceland Basin (21°45′ to 23°45′W) for 1991 (dashed) and 2000 (full line): (A) potential temperature profiles, (B) salinity profiles, (C) θ-S diagram.

thermocline was probably connected with a westward shift of the North Atlantic Current in the Iceland Basin and of the Subarctic Front (Bersch, 2002). The water mass properties of the permanent thermocline also changed over that period, resulting in higher salinities at similar isotherms (Figure 5C). At the potential temperature of the main thermocline (5°C to 7°C) this difference is about 0.05. Therefore about half of the observed salinity increase in the main thermocline was due to the vertical shift of the thermocline, the other half to the change in water mass properties. Both temperature and salinity of the LSW core in the Iceland Basin were lowest in 2000, concurrent with an increase in potential density.

The Irminger Basin

Bersch *et al.* (1999) have described the change in the deep water mass properties from 1991 to 1996 relative to the potential density with a reference pressure of 1500 dbar, $\gamma_{1.5}$. They ascribe the observed change of LSW properties to the inflow of a new vintage of LSW produced by deep convection in the Labrador Sea.

When plotting the contours of potential temperature, salinity, and potential vorticity in time-potential density space until 2000 (Figure 6), the change of the LSW core in the Irminger Sea clearly can be followed further. Potential temperature, salinity, and potential vorticity decreased from 1991 to 1996, while the potential density anomaly of the core increased from $\gamma_{1.5} \approx 34.66$ to 34.69. From 1996 to 2000 the potential density of this LSW core remained approximately constant, while potential temperature, salinity, and potential vorticity on the LSW core steadily increased. Also in the overlying thermocline potential temperature and salinity decreased until 1996, while between 1997 and 1999 salinity increased in the upper part of the water column. Bersch (2002) ascribed this to a westward shift of the Subarctic Front in the Iceland Basin, which brought high salinity water across the Reykjanes Ridge into the Irminger Current. This change was probably triggered by deviation of the wind forcing, related to the low NAO index in 1996 and 1997 with weak westerlies and weak cooling. In 1999 a shallower potential vorticity minimum had developed at a potential density level of $\gamma_{1.5} = 34.585$ kg/m^3 ($p \approx 500$ dbar). In 2000 this pycnostad had moved to a density level of $\gamma_{1.5} = 34.600$ kg/m^3 at a pressure of 660 dbar, coinciding with a new subsurface salinity minimum.

Summary

By comparing hydrographic data from the North Atlantic from 1991 and 2000 we have established evidence for decadal change of the hydrographic structure. Observed changes in the Rockall Channel and the Iceland Basin appear to reflect advective redistribution of existing water masses under the influence of a changing atmospheric forcing (Bersch, 2002). This redistribution is reflected in the deepening of the permanent thermocline and the westward shift of the Subarctic Front. However, observed changes in the temperature–salinity structure of the thermocline in the Iceland Basin and the development of new minima of potential vorticity in the Irminger Basin probably show the influence of altered (local?) air–sea fluxes of heat and freshwater. The observed changes in the hydrographic properties of the cores of LSW, ISOW, and DSOW are indicative of changes in the source regions of these

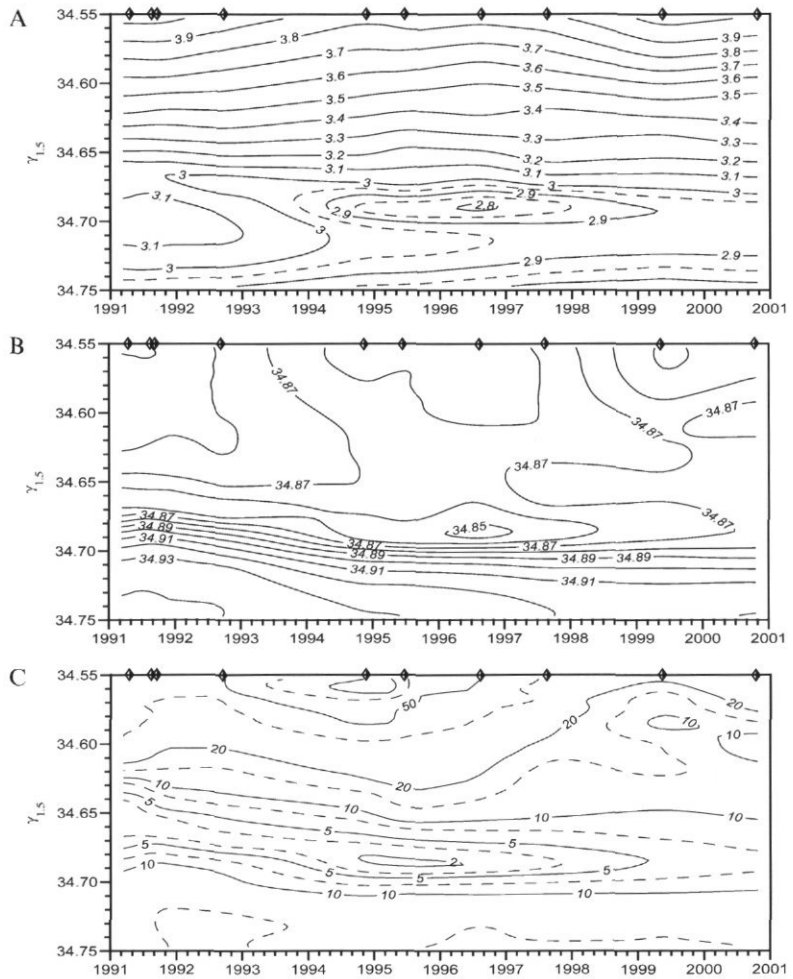


Figure 6. The temporal development of potential temperature (A), salinity (B), and potential vorticity (C) in time-potential density space, derived from the mean hydrographic profiles from the central Irminger Basin (35° to 39°W). The potential density anomaly $\gamma_{1.5}$ relative to 1500 dbar has been used as the vertical coordinate. The symbols at the top indicate the time of the individual surveys.

water types. Using the availability of a series of observations in the Irminger Sea, the development of the water mass structure in this basin could be followed in most years.

Acknowledgements

The research reported here forms the NIOZ contribution to Clivarnet, the Dutch implementation of the CLIVAR programme. Manfred Bersch and Alexander Sy are acknowledged for making available the German data from the Irminger Sea. This is NIOZ-publication 3613.

References

Bersch, M. 2002. NAO-induced changes of the upper-layer circulation in the northern North Atlantic Ocean (submitted).

Bersch, M., Meincke, J., and Sy, A. 1999. Interannual thermohaline changes in the northern North Atlantic 1991–1996. Deep-Sea Research II, 46: 55–75.

McCartney, M. S., and Talley, L. D. 1982. The Subpolar Mode Water of the North Atlantic Ocean. Journal of Physical Oceanography, 12: 1169–1188.

Talley, L. D., and McCartney, M. S. 1982. Distribution and circulation of Labrador Sea Water. Journal of Physical Oceanography, 12: 1189–1205.

van Aken, H. M., and Becker, G. 1996. Hydrography and through-flow in the north-eastern North Atlantic Ocean: the NANSEN project. Progress in Oceanography, 38: 297–346.

ICES Marine Science Symposia, 219: 86–94. 2003

Temperature variability in the Northeast Atlantic

Geir Ottersen, Harald Loeng, Bjørn Ådlandsvik, and Randi Ingvaldsen

Ottersen, G., Loeng, H., Ådlandsvik, B., and Ingvaldsen, R. 2003. Temperature variability in the northeast Atlantic. – ICES Marine Science Symposia, 219: 86–94.

Time-series of sea temperature from the North Atlantic are statistically analysed and compared. We focus on the Norwegian coast and the Barents Sea, with supporting data from the waters off eastern Canada and the Faeroes. The longest time-series are sea surface temperature (SST) observations from Norwegian lighthouses, starting in the mid-1860s. Correlations all along the Norwegian coast are unlagged, suggesting that large-scale atmospheric forcing is important. Antisynchrony between Northeast and Northwest Atlantic sea temperature fluctuations is indicated. The North Atlantic Oscillation (NAO) is generally positively correlated to winter temperatures in Norwegian waters and negatively correlated to the temperature off Newfoundland. Correlations between the NAO and coastal SST on the west and south coasts of Norway are strong and persistent right back to the beginning of the observational record. However, Barents and Labrador Sea temperature seem to have been closely linked to the NAO only during the past 3–4 decades. Spectral analysis reveals that the four subsurface sea temperature series have oscillations from about 8 to about 14 years, the NAO has most variance at high frequencies (< 1 year), while the SST series lie between.

Keywords: North Atlantic Oscillation, sea temperature, spectral analysis, time-series.

G. Ottersen: Institute of Marine Research, PO Box 1870 Nordnes, NO-5024 Bergen, Norway. Present address: Division of Zoology, Department of Biology, University of Oslo, PO Box 1050, Blindern, NO-0316 Oslo, Norway [tel: +47 22 857288; fax: +47 22 854605; e-mail: geir.ottersen@bio.uio.no]; H. Loeng, B. Ådlandsvik, and R. Ingvaldsen: Institute of Marine Research, PO Box 1870 Nordnes, NO-5024 Bergen, Norway. Correspondence to G. Ottersen at University of Oslo address.

Introduction

Early work by Helland-Hansen and Nansen (1909) described temperature variability in ocean climate as being advective phenomena and suggested a time-lag of 2–3 years between the Rockall Channel and the western Barents Sea. On the other hand, Deser and Blackmon (1993) and Battisti *et al.* (1995) argued that much of the decadal variability in the North Atlantic wintertime sea surface temperature (SST) can be explained as a local oceanic response to atmospheric variability. Ådlandsvik and Loeng (1991) demonstrated that the inflow of Atlantic Water to the Barents Sea is determined, to a large degree, by local atmospheric forcing. They further argued for the importance of wind-driven inflow of Atlantic water masses for temperature conditions in the Barents Sea, an opinion later supported by, among others, Ottersen and Stenseth (2001).

Interactions between the atmosphere, ocean, and cryosphere create feedbacks across a range of time scales. Although not truly periodic, these feedbacks lead to quasi-cyclic behaviour in recorded climate variables. Mann and Park (1994) presented an overview of quasi-periodic behaviour in global temperature and reviewed the candidate mechanisms causing this variability. Besides episodic volcanic activity, the likely causes of organized large-scale variability on interannual time scales are the quasi-biennial oscillation (QBO), El Niño-Southern Oscillation (ENSO), and more regional atmospheric circulation patterns such as the North Atlantic Oscillation (NAO).

The NAO is an alternation in the pressure difference between the subtropic atmospheric high-pressure zone centred over the Azores and the atmospheric low-pressure zone over Iceland. It is the dominant mode of atmospheric behaviour in the North Atlantic sector throughout the year, but it is most pronounced during winter and accounts for more than one-third of the total variance in sea-level pressure. A number of earlier authors have related NAO variability to a wide range of climatic factors (e.g. Hurrell, 1995; Dickson, 1997; Hurrel and van

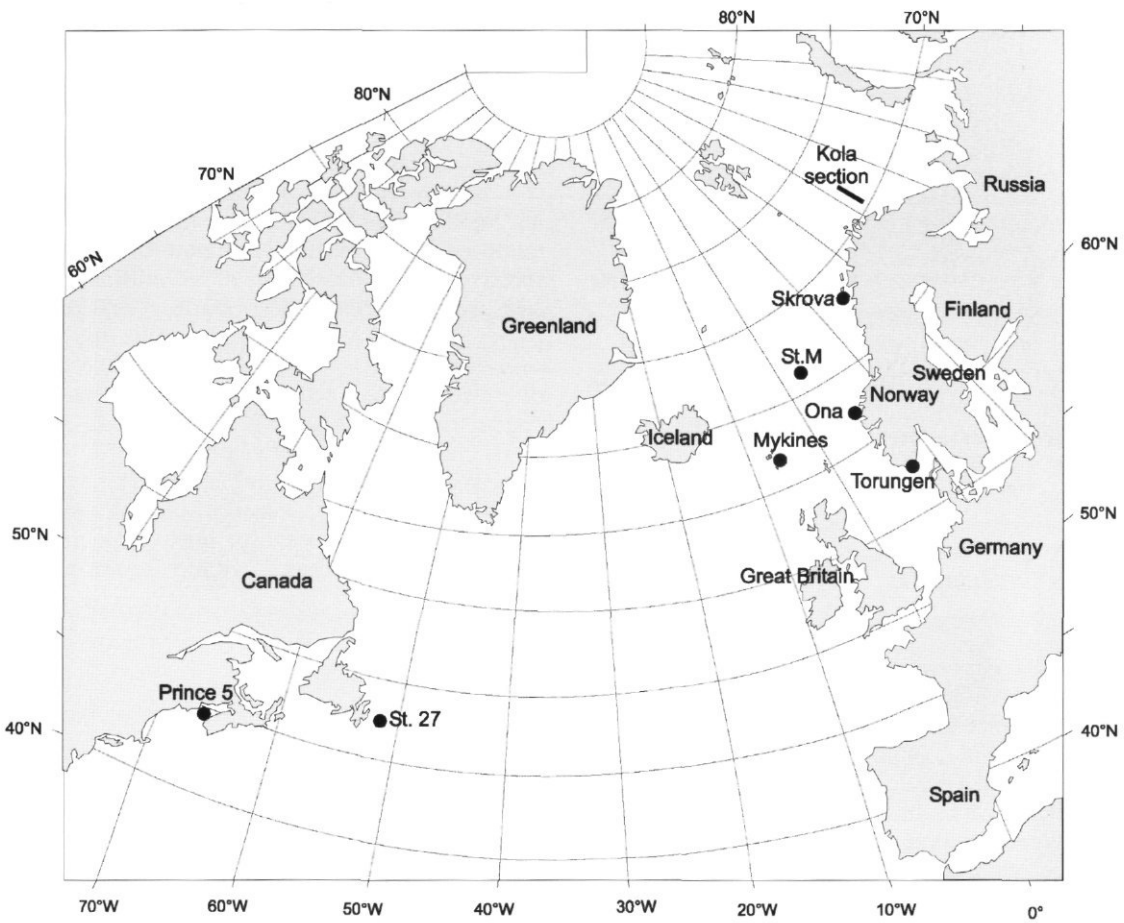


Figure 1. The northern North Atlantic with locations of stations and sections indicated.

Loon, 1997; Curry *et al.*, 1998). The relationship between the state of the NAO and climatic patterns is particularly strong in Northern Europe and surrounding waters (Ottersen *et al.*, 2001).

For the Mariehavn symposium in 1991, Loeng *et al.* (1992) wrote an article on climatic variability in the Norwegian and Barents seas. They gave a descriptive account of the developments in the region during the 1980s in addition to analyses of several hydrographic and meteorological time-series in search of cyclic variations. Ten years later, for the Edinburgh symposium, we find it timely to continue this work. While spatial and temporal variability in the Barents Sea during the 1990s is thoroughly analysed in a companion article (Ingvaldsen *et al.*, 2003; pp. 160–168 in this volume), we take a broader view. Our main area of interest is the Barents Sea and Norwegian coast, but we include data from the Canadian east coast and the Faroes. Long time-series, some dating back to the 1860s, are analysed by means of cross-correlations and spectral analysis. By studying potential cyclic patterns and synchronous or lagged relations we wish to gain new insight regarding the nature of sea temperature fluctuations in the Northeast Atlantic, and possible links to variability in the Northwest Atlantic and large-scale climate forcing as represented by the NAO.

Material and methods

A number of sea temperature series were made available to us thanks to helpful colleagues. All series used, with location, time span covered, and depth at which our analyses were done, are listed in Table 1.

NAO indices, slightly modified from the winter (Dec–Mar) index of Hurrell (1995), for 1864–2001 Were obtained from the World Wide Web page of Jim Hurrell of NCAR's Climate and Global Dynamics Division (http://www.cgd.ucar.edu/~jhurrell/nao.html). Hurrell's indices are based on the difference of normalized sea level pressures (SLP)

Table 1. Temperature time-series used.

Name	Location	Depth	Period
Kola Section	70°30′N to 72°30′N along 33°30′E	0–200 m	1921–2000
Skrova	68°07′N 14°32′E	1 m	1936–2000
Station M	66°0′N 2°0′E	50 m	1949–1999
Ona	62°52′N 6°33′E	SST	1868–1999
Torungen	58°20′N 8°53′E	SST	1867–1999
Mykines	62°05′N 7°50′W	SST	1914–1969
Prince 5	44°54′N 66°48′W	SST	1924–2000
Station 27	47°33′N 52°35′W	50 m	1947–2000

between Lisbon, Portugal, and Stykkisholmur, Iceland from 1864 through 1995. He normalized the SLP anomalies at each station by division of each seasonal pressure by the long-term (1864–1995) standard deviation. Monthly NAO values dating back to 1821, used in the spectral analyses, are from Jones *et al.* (1997) based on the SLP difference between Gibraltar and Stykkisholmur. They were downloaded from the Tiempo web page http://www.cru.uea.ac.uk/ftpdata/nao.dat

Standard Pearson product–moment correlations are applied with various time-lags. However, the true significance level (p-value) of a test may deviate from the intended nominal level if the series are autocorrelated. Therefore, in calculating significance levels for correlations, the effective number of independent observations, adjusted for order 1 and 2 autocorrelations (N_e), was estimated using the formula of Quenouille (1952): $N_e = N/(1 + 2r_{a1}r_{b1} + 2r_{a2}r_{b2})$, where N is the number of data points common to the two series a and b, r_{a1} and r_{b1} are the lag-one autocorrelations, r_{a2} and r_{b2} the lag-two autocorrelations.

Monthly anomalies were calculated by subtracting the 1948–1999 monthly mean from each value for this specific month. We restricted the data applied in time and to series with (more or less) complete monthly coverage throughout, to allow for all anomalies to be based on the same period and thus be more directly comparable. Winter mean temperatures were calculated as unweighted arithmetic means of the January to April values based on all available data for each individual time-series. Only years with data from all 4 months were included to avoid bias.

Spectral analysis was applied to monthly time-series. Before the actual analysis, the seasonal cycle was removed by subtracting the mean annual cycle. In the resulting anomaly series eventual missing values were filled by linear interpolation. Thereafter linear regression was used to remove the linear trend.

As a guard towards spurious features in the spectral analysis, the analyses were performed using two different methods. The first method, a smoothed periodogram, is carried out by computing the autocorrelation function and making a Fourier transformation smoothed by the Parzen window. This is a conventional method, described for instance in Chatfield (1989). In our case, the width of the window is taken as 400 months. The second method is maximum entropy spectral analysis as described in Press *et al.* (1989). In our case the order (or number of poles) used is 90. In both cases, the power spectrum was evaluated at 3600 equidistant frequencies, giving periods from 2 months to 600 years. All power spectra are normalized so that the integral over the frequency domain is 1000, allowing for direct comparison between series of different units. A spectral peak is a local maximum. In addition to its height or value, the percentage of variance described by the peak is tabulated. This is defined here by the integral between the adjacent local minima. Note that a sharp, high, peak may thus contain less energy than a broader, lower, peak.

Results

Time-series of 5-year running means of winter mean sea temperature from 5 selected northern North Atlantic locations and the NAO show that although variability at high frequencies obviously has been removed by the smoothing, considerable variation remains (Figure 2). The most striking feature is the high temperatures observed in the early 1990s all along the Norwegian coast from Torungen, in the southeast, to the Barents Sea. The 1930s and 1950s were also pronounced warm periods in Norwegian waters, in the Barents Sea even warmer than in the 1990s (as more closely examined in Ingvaldsen *et al.*, 2002). Temperatures were particularly low in Norwegian waters during the late 1970s and early 1980s; similarly cold conditions had not been seen since the late 19th century. Since the late 1960s, the three Northeast Atlantic series show similar main oscillations.

Cross-correlations were calculated between monthly anomalies from the most complete time-series along the Norwegian coast at all lags from 0 to ±12 months. In each case the direct, unlagged correlations were highest. However, none of them were particularly high, the highest being between Ona and Torungen ($r = 0.42$).

Cross-correlations at all lags from −5 to +5 years were also calculated between winter mean temperatures for some of the longer time-series (Table 2). The correlations between the Norwegian stations were much higher here than between the monthly anomalies; again there is a particular clear unlagged connection between Ona and Torungen. SST at the

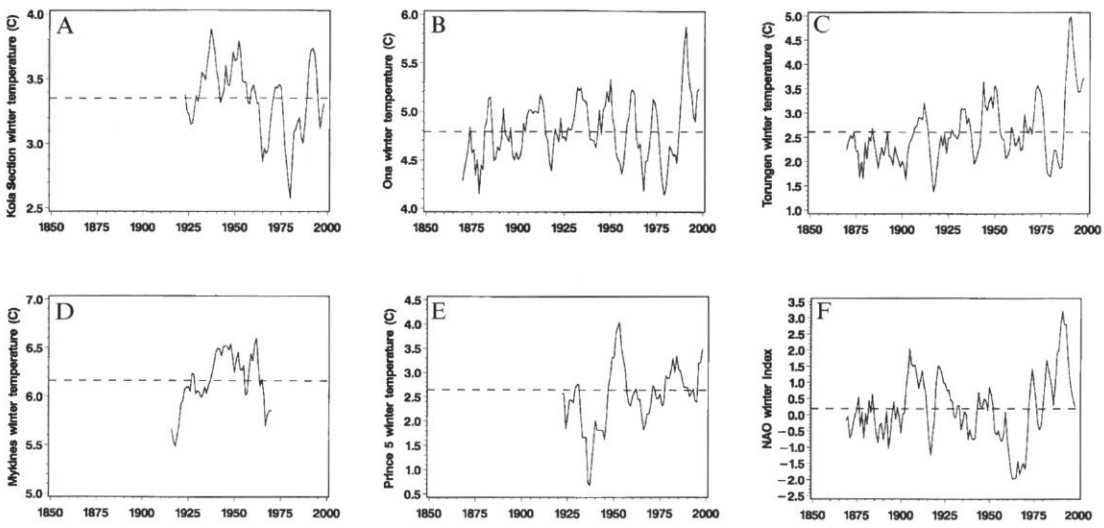


Figure 2. Five-year running means of winter (Jan–Apr) sea temperature at selected locations in the northern North Atlantic and the NAO winter (Dec–Mar) index. A. Kola meridian hydrographical section 0–200 m depth average. B. Meteorological station Ona SST. C. Meteorological station Torungen SST. D. Meteorological station Mykines SST. E. Hydrographical station Prince 5 temperature at 0 m. F. NAO winter index slightly modified from Hurrell (1995). The horizontal broken lines indicate the means for the full observation period.

Table 2. Maximum correlations within lags ±5 among time-series of winter (Jan–Apr) mean temperatures based on all available data and with the NAO winter index. Only years with data for all 4 months used. Statistical significance levels (p-values) are adjusted for autocorrelation; lag indicates lag of maximum correlation; lag +2 means, e.g., that the station named above follows the station named to the left by 2 years. n indicates the number of years common to both series and is thus used for calculating the correlation.

R	Ona	Torungen	Mykines	Station 27	Prince 5	NAO
Kola	r = 0.48	r = 0.45	r = 0.42	r = –0.43	r = 0.14	r = 0.29
p-value	< 0.001	< 0.001	< 0.01	< 0.01	> 0.10	< 0.05
lag	0	0	–1	+2	0	0
n	75	77	47	32	53	80
Ona		r = 0.80	r = 0.36	r = –0.49	r = –0.31	r = 0.59
p-value		< 0.001	< 0.01	< 0.01	< 0.05	< 0.001
lag		0	0	0	+4	0
n		125	51	29	51	127
Torungen			r = 0.33	r = –0.44	r = 0.21	r = 0.72
p-value			< 0.05	< 0.05	> 0.10	< 0.001
lag			0	0	+2	0
n			51	30	51	130
Mykines				r = –0.50	r = –0.20	r = –0.24
p-value				< 0.10	> 0.10	< 0.10
lag				0	–3	+2
n				10	26	53
Station 27					r = 0.35	r = –0.60
p-value					> 0.10	< 0.10
lag					+2	0
n					24	32
Prince 5						r = 0.28
p-value						< 0.10
lag						–5
n						53

Faroese station at Mykines is also positively correlated with the Norwegian stations. The highest correlations between Prince 5, close to the border to the US, and the Northeast Atlantic stations are fairly low, varying from –0.31 to +0.20 and with a confusing lag structure. On the other hand, temperature at 50 m at Station 27, off Newfoundland, is clearly negatively correlated with all the European stations. While the highest correlations are unlagged with the 3 SST stations, temperature at Station 27 seems to lag that at Kola by 2 years.

Relations between the NAO winter index and winter (Jan–Apr) means for six time-series are shown in Figure 3. The high correlations between the NAO and SST at Torungen and Ona reflected similarity not only in long-term trends, but also when the linear trend had been removed. The connection between the NAO and sea temperature at 50 m at Station 27 is clearly negative, while the connection to surface temperature at both Prince 5 and at Mykines is weak.

By splitting the time-series into two shorter periods we were able to detect possible temporal changes in the NAO–sea temperature correlation. The high positive correlation between the NAO and Torungen and Ona was consistent through time, as was the negative correlation between the NAO and Station 27. On the other hand, Barents Sea temperature seems to be more closely linked to the NAO since the early 1970s (1921–1971: $r = 0.25$ ($p < 0.10$); 1972–2000: $r = 0.58$ ($p < 0.005$).

Spectral analysis by the periodogram and maximum entropy methods give similar results. Complex patterns in the frequency domain are revealed, with some time-series having a great deal of energy in the short periodic (< 1 year) area, while others have their main peaks at decadal and longer scales (Table 3).

The sea temperature series from Station M, Skrova, Kola, and Station 27 all have a peak in the decadal region, varying from about 8 to about 14 years. The Kola Section series displays several of the most dominant peaks, with regard to both height and percentage of variance explained. The 12–13 years peak at Station M is also distinct.

The SST time-series from Ona and Torungen have much energy in the high frequency domain and little in the area from about 2.5 to 6 years. However, Ona has a peak at around 8 years, which Torungen does not, and flattens out more towards the long periods, while the variance in Torungen increases slowly. Mykines and Prince 5 SST have peaks at 2–4 and 7–9 years, but most of the variance is in the 20–30 year area. The NAO is very close to being white noise, but a peak at around 8 years shows in the MESA analysis.

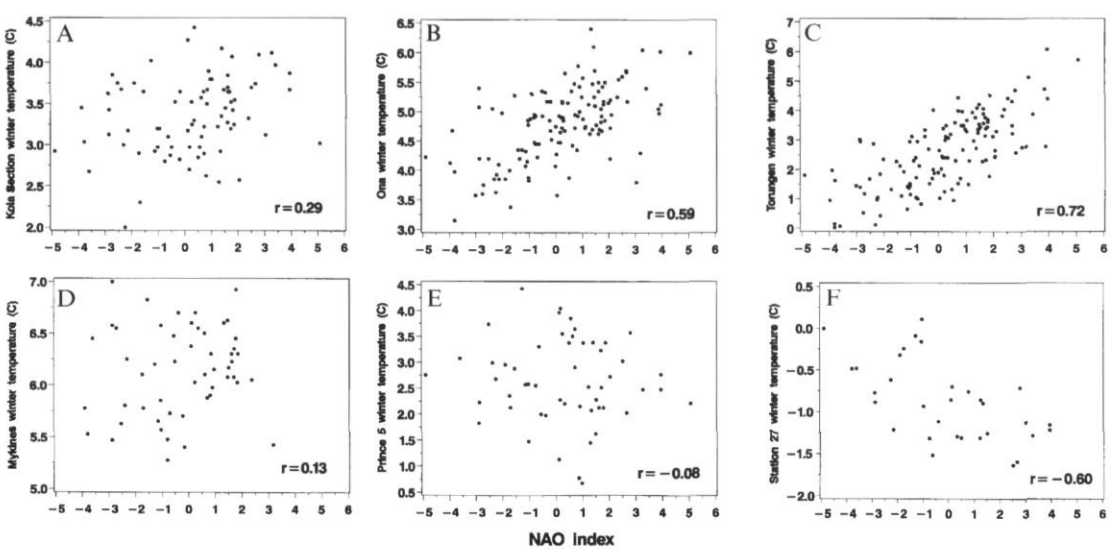


Figure 3. The NAO winter (Dec–Mar) index plotted against winter (Jan–Apr) sea temperature at selected locations in the northern North Atlantic (n=number of non-missing values). A. Kola meridian hydrographical section 0–200 m depth average, 1921–2000, n = 80. B. Meteorological station Ona SST, 1869–1999, n = 127. C. Meteorological station Torungen SST, 1868–1999, n = 130. D. Meteorological station Mykines SST, 1914–1968, n = 53. E. Hydrographical station Prince 5 SST, 1924–2000, n = 53. F. Hydrographical station Station 27 at 50 m, 1948–1999, n = 32. The correlations between the NAO and the Norwegian stations Kola, Ona, and Torungen are statistically significant at the 5% level.

Table 3. Results of the spectral analysis. For each station the results of the periodogram method are given in the first three columns, the results of the maximum entropy method in the last three. The information given for each method is the period (in years), height of the power peak multiplied by 1000 (normalized power spectrum density), and percentage of the total variance explained by this peak (where a peak is defined to be between two surrounding local minima). Objective criteria are used to select the peaks included. Separately for each method the five highest peaks in the spectre are always included, as are additional peaks explaining more than 5% of the variability. The table is sorted by the height of the peaks for each station and method.

	Periodogram			MESA		
Series	Period	Power	% Variance	Period	Power	% Variance
Kola						
	8.3	5.7	19.6	10.0	6.2	51.1
	16.2	5.5	24.9	2.6	4.4	15.3
	2.6	3.7	12.5	4.3	2.5	14.3
	5.1	3.0	9.6	1.8	0.7	3.7
	4.1	2.5	7.4	1.2	0.5	3.0
	3.2	1.9	5.6			
Skrova						
	9.2	2.5	13.4	9.2	3.0	14.2
	85.7	2.0	4.9	600.0	2.0	5.2
	1.3	1.5	7.6	1.4	1.8	8.1
	1.8	1.2	5.4	1.8	1.4	6.2
	2.7	1.1	3.4	3.6	1.1	6.4
Station M						
	13.0	5.1	27.6	11.8	5.4	40.4
	31.6	3.8	8.4	1.8	1.4	7.1
	1.9	1.3	3.9	1.0	0.8	5.1
	1.0	0.8	2.6	1.1	0.6	3.1
	1.7	0.8	3.0	0.6	0.5	4.3
Ona						
	1.0	1.7	8.1	1.0	1.5	10.8
	7.9	1.4	5.6	1.7	1.4	13.8
	2.3	1.4	4.3	2.2	1.3	8.1
	46.2	1.2	3.5	10.9	1.2	13.0
	12.2	1.2	3.0	1.2	0.8	5.7
	1.6	1.1	5.0	3.4	0.8	5.6
				0.9	0.6	5.0
Torungen						
	1.3	2.1	11.9	1.3	2.0	14.9
	1.0	1.8	8.4	1.0	1.6	18.0
	66.7	1.5	7.5	54.5	1.5	9.0
	1.1	1.4	5.4	1.6	1.2	9.0
	1.6	1.4	5.5	2.1	1.1	11.1
				5.7	0.8	5.5
				0.8	0.8	6.5
Mykines						
	46.2	4.6	12.5	600.0	4.6	30.6
	15.4	3.9	11.3	2.5	2.0	10.8
	7.1	1.9	6.3	3.7	1.5	9.8
	2.5	1.9	7.0	1.4	1.4	7.1
	3.3	1.6	6.0	1.8	1.1	6.1
	4.3	1.6	5.2			
	1.4	1.6	5.2			
Prince 5						
	27.3	5.3	17.4	20.7	4.9	19.4
	1.0	1.8	8.9	1.0	2.1	9.3
	3.7	1.5	5.8	2.1	1.4	6.1
	2.1	1.4	5.3	1.3	1.3	4.7
	8.7	1.1	2.9	3.4	1.2	6.3
Station 27						
	14.3	1.9	9.1	11.5	2.0	12.0
	3.2	1.4	6.0	2.3	1.4	7.8
	2.5	1.4	8.6	0.8	1.2	6.1
	0.8	1.3	5.2	0.6	1.2	5.4
	1.1	1.0	3.3	1.3	1.1	5.5
	1.0	0.9	6.1	3.1	1.1	8.5
				0.9	1.0	5.3
NAO monthly index						
	0.7	0.6	2.1	0.2	0.6	3.2
	0.2	0.6	2.8	1.2	0.6	3.5
	1.2	0.5	2.5	0.8	0.5	5.7
	0.4	0.5	2.4	0.4	0.5	3.2
	0.5	0.5	2.4	0.5	0.5	5.0
				7.8	0.5	5.3

Discussion

Our results show that the correlations between sea temperatures from Norwegian stations are highest when unlagged, both for monthly anomalies and winter means. We take the more or less synchronous fluctuations observed in upper layer sea temperatures all along the Norwegian coast as suggestive evidence for sea temperature in the region being mainly driven by atmospheric forcing rather than by advection in the ocean.

Recent work by Ottersen and Stenseth (2001) and Dippner and Ottersen (2001) shows statistical links between the NAO and Barents Sea temperatures during the past three to four decades, with higher temperatures connected to positive NAO phases. They took this as an indication of sea temperatures in the region being controlled by large-scale atmospheric patterns.

However, this close connection does not seem to be valid for the preceding part of the 20th century. Our statistical results indicate that Barents Sea temperatures have only been closely linked to the NAO since the early 1970s. This supports the results of Dickson *et al.* (2000), who calculated 30-year moving correlations between the winter NAO and annual Kola Section 0–200 m temperature means. They concluded that the markedly stronger relationship detected during recent decades, and also during the early years of the last century, corresponded roughly to periods of strong positive phase of the NAO, when the storm track penetrates the Barents Sea, as also indicated by Ingvaldsen *et al.* (2002). Related to this is the more easterly position of the NAO pressure centres during the period 1978–1997 as compared to 1958–1977 shown by Hilmer and Jung (2000), which we believe may play an important role.

A negative correlation between Station 27 and the Northeast Atlantic time-series is evident (Table 2). Positive temperature anomalies in the Barents Sea seem to be followed by lower than average temperatures off Newfoundland 2 years later. This supports earlier findings of inverse fluctuation in Barents and Labrador Sea temperatures (Izhevskii, 1964; Sundby, 1998).

The NAO index is negatively correlated to sea temperature at Station 27 (Table 2; Figure 3). A strongly positive NAO has earlier been shown to lead to low air temperatures and strong wind, which again leads to larger ice cover resulting in an extended volume of cold intermediate water on the Labrador Shelf and ultimately low surface and bottom temperature (Mann and Drinkwater, 1994). As opposed to the Barents Sea, there is no statistical indication of this relation weakening during the recent decades with an extended positive NAO phase and easterly shifted Icelandic Low.

Further south along each coastline the NAO–temperature relation evolves differently. The correlations between the NAO and coastal winter SST on the west and south coasts of Norway are strong and persistent right back to the beginning of the observational record in the 1860s (Table 2; Figure 3). Although such strong relations have not been demonstrated previously, Ottersen *et al.* (2001) showed that this area has the most pronounced regional correlation with the NAO both for winter SST and scalar wind. This is also on roughly the same latitude as the Labrador Sea, where the NAO correlation is at its highest on the American side. Further south on the western side of the Atlantic, the link between the NAO and sea temperature is weak or non-existent (Figure 3).

While our coastal SST series only display a minor part of their variability in the decadal region, the subsurface sea temperature series (Kola, Skrova, Station M, and Station 27) all have oscillations from about 8 to about 14 years (Table 3). The latter also compares well with the results of Deser and Blackmon (1993) and Sutton and Allen (1997) for the open North Atlantic, while Moron *et al.* (1998) found SST oscillations at both 7–8 and 13–15 years. A particularly large part of the variance was found in the decadal range at the Kola Section and Station M. This is not only one single peak; the two series have spectra with highest variance at long periods. One can relate this to these locations being more oceanic in nature, while Skrova and Station 27, being closer to the coast, are more strongly influenced by processes at shorter time scales, typically related to wind conditions. It should also be noted that the Skrova time-series at only 1-m depth must be taken as more or less recording SST.

The atmospheric NAO series has most variance at high frequency, while the SST series tend to lie between the NAO and the redder spectra of the subsurface series (among the SST series, Mykines and Prince 5 stand out with red spectra). This can be explained by the atmosphere having high variability at the synoptic weather scale, with the ocean acting as a low-pass filter on the atmospheric input, giving a shift towards longer periods when passing from SST to the ocean interior.

Although there exist large-scale physical phenomena with similar cyclic patterns to those observed in our time-series, the linking mechanisms are far from straightforward, even for the most well-documented periodic components. In the decadal region, the influence of the variability in solar irradiance throughout the 11-year sunspot cycles on temperature is described by numerous earlier authors, several dealing with marine time-series (e.g. Izhevskii, 1964). We found power spectrum peaks in the vicinity of 11 years in several of our subsurface series (Kola Section, Station M, Station 27), but we

have no way of deciding whether this is linked to the solar cycle or not.

Of the tidal components acting on the interannual and interdecadal time scale, the nodal tide with a period of 18.61 years is generally considered to be the most important. The significance of this is that when the declination of the moon's orbit to the equator is at its maximum, the tidal forces at high latitudes are greatest. Using a general system theoretical approach, Yndestad (1999) linked the temperature fluctuations in the Barents Sea to this earth nutation period. Our results lend little support to this; we found no peaks in any of our series between 16.2 and 27.3 years. However, it should be noted that recent peaks in these forces have occurred in 1913, 1931, 1950, 1969, and 1988, coinciding with the beginning of a warm period in the Barents Sea (Ottersen *et al.*, 2000). The 2.6-year quasi-biennial oscillation, described by Burroughs (1992) to exist in a number of time-series worldwide, is seen in the Kola and Mykines series.

The spectral peak at around 8 years found in the subsurface temperature series also shows up in the MESA analysis of the NAO. This is the peak with the second most variance in the NAO time-series according to this method. Rogers (1984) and Hurrell and van Loon (1997) have earlier reported similar oscillations. However, it must be stressed that this peak only contains 5.3% of the total variance; most of the rest is concentrated at much higher frequencies. Furthermore, the NAO series is non-stationary, when calculating the spectre for only the last 100 years (from 1902), peaks were found at around 5 and 10 years. Hurrell and van Loon (1997) point to the NAO power spectrum becoming redder with time.

To conclude, with this article we present statistical backing for upper layer sea temperatures all along the Norwegian coast and the Barents Sea having a simultaneous response to North Atlantic scale atmospheric forcing. However, while the effect of the NAO on sea temperatures along the southern and western coast of Norway is persistent back to the 1860s, a clear NAO–Barents Sea relation is only evident from around 1970 onwards. By means of spectral analysis we furthermore document that the subsurface sea temperature series studied have pronounced decadal oscillations, notably the Kola Section and Station M, both situated in Atlantic water masses.

Acknowledgements

This work was partly financed by the Research Council of Norway's Strategical Institute Programme "Variation in space and time of cod and other gadoids: the effects of climate and density dependence on population dynamics" and the national NOClim" programme. We are also grateful to the Norwegian Meteorological Institute for temperature data from meteorological stations Ona and Torungen, Geophysical Institute, University of Bergen for data from Station M, PINRO (Murmansk, Russia) for Kola Section data, Ken Drinkwater and Eugene olbourne for data from the Canadian stations Prince 5 and Station 27, Bogi Hansen for the Mykines station data, and Jim Hurrell for the NAO index. We acknowledge Karen Gjertsen, IMR, for preparing the map of Figure 1. The work was done within the framework of the international GLOBEC (Global ocean ecosystem dynamics) programme.

References

Ådlandsvik, B., and Loeng, H. 1991. A study of the climate system in the Barents Sea. Polar Research, 10: 45–49.

Battisti, D. S., Bhatt, U. S., and Alexander, M. A. 1995. A modelling study of the interannual variability in the wintertime North Atlantic Ocean. Journal of Climate 8: 3067–3083.

Burroughs, W. J. 1992. Weather cycles real or imaginary. Cambridge University Press, London. 207 pp.

Chatfield, C. 1989. The Analysis of Time Series. Chapman and Hall, London. 241 pp.

Curry, R. G., McCartney, M. S., and Joyce, T. M. 1998. Oceanic transport of subpolar climate signals to mid-depth subtropical waters. Nature, 391: 571–575.

Deser, C., and Blackmon, M. L. 1993. Surface climate variations over the north Atlantic Ocean during winter: 1900–1989. Journal of Climate, 6: 1743–1753.

Dickson, R. R. 1997. From the Labrador Sea to global change. Nature, 386: 649–650.

Dickson, R. R., Osborn, T. J., Hurrell, J. W. *et al.* 2000. The Arctic Ocean response to the North Atlantic Oscillation. Journal of Climate, 13: 2671–2696.

Dippner, J., and Ottersen, G. 2001. Cod and climate variability in the Barents Sea. Climate Research, 17: 73–82.

Helland-Hansen, B., and Nansen, F. 1909. The Norwegian Sea. Fiskeridirektoratets Skrifter Serie Havundersøkelser, 2: 1–360.

Hilmer, M., and Jung, T. 2000. Evidence for a recent change in the link between the North Atlantic Oscillation and Arctic sea ice export. Geophysical Research Letters, 27: 989–992.

Hurrell, J. W. 1995. Decadal trends in the North Atlantic Oscillation: regional temperatures and precipitation. Science, 169: 676–679.

Hurrell, J. W., and van Loon, H. 1997. Decadal variations in climate associated with the North Atlantic Oscillation, Climate Change, 36: 301–326.

Ingvaldsen, R., Loeng, H., Ottersen, G., and Ådlandsvik, B. 2003. Climate variability in the Barents Sea during the 20th century with focus on the 1990s. ICES Marine Science Symposium, 219: 160–168. (This volume.)

Izhevskii, G. K. 1964. Forecasting of oceanological conditions and the reproduction of commercial fish. Moskva. Pishcepromizdat, Moscow. 95 pp.

Jones, P. D., Jonsson, T., and Wheeler, D. 1997. Extension to the North Atlantic Oscillation using early instrumental pressure observations from Gibraltar and South-west England. International Journal of Climatology, 17: 1433–1450.

Loeng, H., Blindheim, J., Ådlandsvik, B., and Ottersen, G. 1992. Climate variability in Norwegian and Barents Seas. ICES Marine Science Symposia, 195: 52–61.

Mann, K. H., and Drinkwater, K. F. 1994. Environmental influences on fish and shellfish production in the Northwest Atlantic. Environmental Review, 2: 16–32.

Mann, M. E., and Park, J. 1994. Global-scale modes of surface temperature variability on interannual to century timescales. Journal of Geophysical Research, 99: 25,819–25,833.

Moron, V., Vautard, R., and Ghil, M. 1998. Trends, inderdecadal and interannual oscillations in global sea-surface temperatures. Climate Dynamics, 14: 545–569.

Ottersen, G., and Stenseth, N. C. 2001. Atlantic climate governs oceanographic and ecological variability in the Barents Sea. Limnology and Oceanography, 46: 1774–1780.

Ottersen, G., Ådlandsvik, B., and Loeng, H. 2000. Predicting the temperature of the Barents Sea. Fisheries Oceanography, 9: 121–135.

Ottersen, G., Planque, B., Belgrano, A., Post, E., Reid, P. C., and Stenseth, N. C. 2001. Ecological effects of the North Atlantic Oscillation. Oecologia, 128: 1–14.

Press, W. H., Flannery, B. P., Teukolsy, S. A., and Vetterling, W. T. 1989. Numerical Recipes (FORTRAN Version). Cambridge University Press, London. 701 pp.

Quenouille, M. H. 1952. Associated measurements. Butterworths, London. 241 pp.

Rogers, J. C. 1984. The association between the North Atlantic Oscillation and the Southern Oscillation in the northern hemisphere. Monthly Weather Revue, 112: 1999–2015.

Sundby, S. 1998. The North Atlantic Oscillation, the temperature seesaw and the effects of cod recruitment in the North Atlantic. *In* Report of the ICES/GLOBEC Workshop on Prediction and Decadal-Scale Ocean Climate Fluctuations of the North Atlantic, Denmark, 8–10 September 1997. 52 pp.

Sutton, R. T., and Allen, M. R. 1997. Decadal variability in North Atlantic sea-surface temperature and climate. Nature, 388: 563–567.

Yndestad, H. 1999. Earth nutation influence on the temperature regime of the Barents Sea. ICES Journal of Marine Science, 56: 381–387.

ICES Marine Science Symposia, 219: 95–101. 2003

Extremes of temperature and salinity during the 1990s in the northern Rockall Trough: results from the "Ellett line"

N. P. Holliday

Holliday, N. P. 2003. Extremes of temperature and salinity during the 1990s in the northern Rockall Trough: results from the "Ellett line". – ICES Marine Science Symposia, 219: 95–101.

A time-series of deep hydrographic measurements in the northern Rockall Trough is analysed to determine the nature and origin of interannual to decadal variability of water mass properties. The repeat section (Barra Head to Rockall Island) was started in 1975 by David Ellett of Dunstaffnage Marine Laboratory and has been occupied between one and six times per year since then. Both the surface and deep water masses have shown extremes in their properties during the past decade compared to the previous 15 years. The 1990s began with relatively low temperature and salinity in the surface water mass (Eastern North Atlantic central Water, ENAW), but since 1995 there has been a dramatic increase, culminating in the highest salinity in 1998 and highest temperature in early 2000. In contrast, the deep Labrador Sea Water (LSW) is fresher and cooler in the late 1990s than at any time in the series. The ENAW is subject to local modification by exchange of heat and freshwater with the atmosphere, but the variability is mainly determined by mixing with other water masses at the southern entrance to the Rockall Trough. The LSW is a re-circulating reservoir periodically flushed by newer water from the southwest.

Keywords: atmospheric fluxes, circulation, interannual variability, mixing, North Atlantic, Rockall Trough.

N. P. Holliday: Southampton Oceanography Centre, European Way, Southampton, SO14 3ZH, UK [tel: +44 23 8059 6206; fax: +44 23 8059 6204; e-mail: nph@soc.soton.ac.uk].

Introduction

The Rockall Trough lies to the west of Scotland and provides a route for warm Atlantic Water to flow northwards into the Nordic Seas. It has a deep opening to the south (4000 m), but through-flow is restricted to the top 1200 m by gaps in the shallow topography to the north, and flow into the Nordic Seas is restricted to the upper 500–600 m by the Iceland to Scotland ridge. The Trough is bounded to the east by the northwest European continental shelf, and to the west by the Rockall Plateau (Figure 1). The upper ocean consists of warm saline Eastern North Atlantic central Water (ENAW), which has a net northward drift; the majority of the transport is in the shallow poleward shelf edge current, but there is also a smaller northward current in the western Trough (Ellett *et al.*, 1986, Holliday *et al.*, 2000). Approximately one-third of the volume flux of Atlantic Water that reaches the Nordic Seas has come via the Rockall Trough, with the majority passing though the Iceland Basin (Hansen and Østerhus, 2000). Below 1200 m the Trough is filled with a reservoir of fresher Labrador Sea Water (LSW), which enters from the south but cannot flow northwards because of the shallowing topography. The Rockall Trough does not contain a significant quantity of overflow water; rather the vast majority of the returning cold dense overflow from the Nordic Seas flows though the Iceland Basin (Hansen and Østerhus, 2000).

The time-series, started in 1975, has not been sampled consistently, but, with the exception of 1986, has been occupied at least once per year. There were 4–6 sections per year in the late 1970s and 1–4 sections per year through the 1980s and early 1990s, but sampling has dwindled to 1–2 sections per year since 1996. The section is currently occupied through a UK cooperative programme between Southampton Oceanography Centre, Dunstaffnage Marine Laboratory, and FRS Marine Laboratory (Aberdeen).

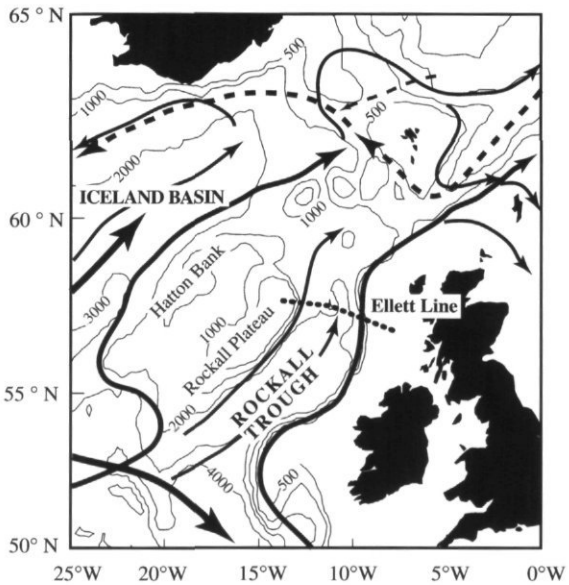


Figure 1. The location and schematic circulation in the region of the Rockall Trough and the Ellett line. Upper ocean currents indicated by the solid black arrows, mid-depth circulation by grey arrows, and bottom flow by dashed arrows; Ellett line indicated by dotted black line.

Temperature and salinity anomalies of the upper ocean

The mean properties of the upper 800 dbar can be used to illustrate the variability as sampled by the section. The sampling of the Ellett line is irregular through the seasons, so in order to highlight the interannual variability the climatological seasonal means (1975–2000) are removed from each occupation. The calculation of seasonal means does not unduly alias the interannual variability, despite the low number of winter occupations, since the seasonal cycle (particularly in salinity) is smaller than the interannual (Holliday *et al.*, 2000; Holliday, 2002a). However, it does reduce the noise in the time-series, thus helping to highlight long-term variability. The potential temperature and salinity anomalies are shown in Figure 2, with a 3-point running mean applied to further reduce the impact of sampling noise. The ranges of the properties over the time series are ± 0.5°C and ± 0.05 in salinity, with maxima of both temperature and salinity in the late 1990s. The maximum temperature anomaly of the time-series occurred in February 2000, when the absolute mean temperature was unchanged from the previous autumn, despite deep winter mixing providing evidence of the usual winter heat loss to the atmosphere. The salinity maximum of the time-series also occurred at the end of the 1990s (May 1998). In contrast, the early part of the 1990s was

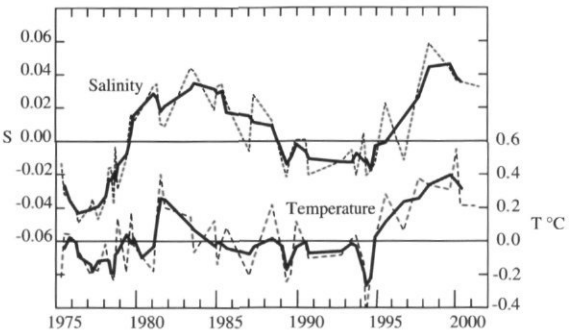


Figure 2. Potential temperature (lower curve) and salinity (upper curve) anomalies for the upper ocean of the Rockall Trough (0–800 dbar). Dashed lines are anomalies from seasonal means; solid line is 3-point running mean.

characterized by relatively low salinity and low temperatures, the latter reaching a time-series low in May 1994, though salinity remained higher than the depressed values caused by the passage of the Great Salinity Anomaly in the late 1970s (Dickson *et al.*, 1988). The result was that the 1990s, as a whole, was a period of maximum change in the properties of the upper ocean.

The hydrographic time-series dates back to 1975, but sea surface observations were made in this region from 1948 onwards (Ellett and Jones, 1994), providing a longer term context for the results presented here. Figure 3 shows the Ellett and Jones (1994) time-series and the surface values from the Ellett line time-series. Both are annual means of anomalies from a monthly climatology derived from the long surface time-series. The Ellett line time-series is biased by the low temporal resolution, especially in the 1990s when the scatter of points increases. However, the period of overlap shows that the decadal scale pattern is reasonably consistent between the two time-series. The figures show that while the 1990s were characterized by increasing temperature and salinity, the decade is not perhaps as unusual as indicated by the shorter time-series; the highest temperatures reached in the 1990s were similar to the peak reached in 1960 following a decade of increasing values.

Variability of the deep water

The LSW fills the Rockall Trough below the permanent thermocline, and the variability of properties is best highlighted by extracting the potential temperature and salinity at the core of the water mass as indicated by the zone of minimum stratification (as represented by the potential vorticity minimum, Holliday *et al.*, 2000). Figure 4 shows the properties at the core of the LSW, highlighting the overall

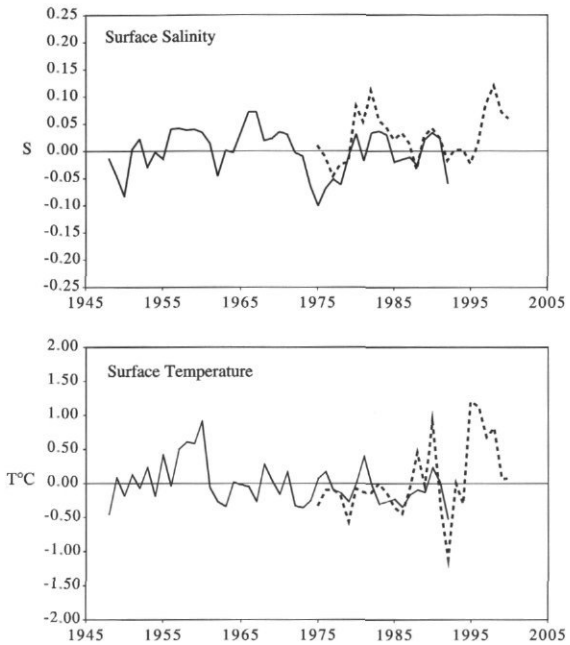


Figure 3. Sea surface temperature and salinity anomalies in the Rockall Trough (black line) as shown by a 12-month running mean of monthly surface anomalies (1948–1992 climatological monthly mean subtracted; data source was Ellett and Jones (1994)). Subsurface anomalies from Figure 2 are shown by the grey line.

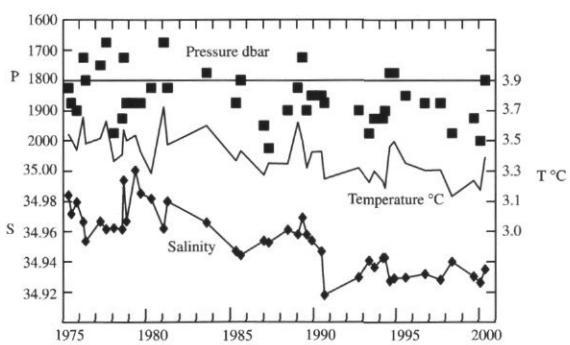


Figure 4. Potential temperature (solid line), salinity (line and diamonds), and pressure (squares) of the core of the Labrador Sea Water in the Rockall Trough.

decrease in values since 1975, which occurs as two periods of rapid freshening in 1981–1985 and 1989–1990. This pattern of variability has been interpreted by Holliday *et al.* (2000) as periods of re-circulation of LSW in isolation from the cooler fresher LSW to the south and west, with periodic major incursions of external LSW. The continued decrease in temperature and salinity probably reflects the decadal scale cooling and freshening of the LSW at source (Dickson *et al.*, 1996; Sy *et al.*, 1997). After a major incursion of external LSW into the Rockall Trough in 1990, there has been little change in the properties of the deep water in the 1990s.

Mechanisms causing the upper ocean variability

Two possible origins of the upper ocean variability were discussed in Holliday *et al.* (2000): the basin-scale atmospheric conditions as measured by the NAO index and the variation in the source region of the main water mass, the ENAW. The NAO winter index shows no statistically significant correlation with the time-series of subsurface temperature and salinity. Maps of correlation of the NAO index with surface temperature (e.g. Rodwell *et al.*, 1999) show that the Rockall Trough lies in a region of low to zero correlation, between the high positive correlation to the south and east and high negative correlation to the west. Therefore the conditions in the Rockall Trough do not appear to be directly related to atmospheric conditions, as indicated by the NAO index. The time-series of ENAW in the Bay of Biscay (Perez *et al.*, 1995) shows no statistically significant positive correlation with the Rockall subsurface time-series, suggesting that the patterns observed are not merely the advection of anomalies generated further south (Holliday *et al.*, 2000).

Two further hypotheses are discussed here: firstly, that the variations observed on the Ellett line are caused by local atmospheric interaction, and secondly that they are caused by varying amounts of contrasting water masses entering the basin (Holliday, 2002a, b). The first hypothesis, that of local modification of the properties by air–sea exchange, can be tested by examining a time-series of heat and freshwater fluxes in the region and comparing them with change in oceanic heat and freshwater content anomalies. The second can be tested by examining sporadic hydrographic data to the south of the Rockall Trough to investigate possible changes in water mass distribution.

The SOC Flux Climatology (Josey *et al.*, 1998) provides a time-series of carefully quality controlled ship-based measurements of heat and freshwater fluxes. A time-series of precipitation based on satellite observations (CPC Merged Analysis of Precipitation, CMAP, Xie and Arkin, 1997) avoids ship-based sampling errors and was used in conjunction with the SOC Climatology to test the robustness of the results. The region over which the fluxes were averaged spans most of the Rockall Trough (55–57°N, 10–15°W and 50–55°N, 12–17°W), covering the maximum area a body of water may have travelled over the period of one year. The net heat flux is the sum of sensible, latent, longwave, and shortwave fluxes, the net freshwater flux the sum of

evaporation (negative) and precipitation (positive), and for the whole region the annual net fluxes were calculated. In this analysis, the 12-month period ran from April to March to cover the annual cycle from the start of spring to the end of winter (Holliday (2002a) describes the methodology and error analysis in detail). The net heat flux time-series was adjusted to zero mean using the sample mean (–44 W m^{-2}) and the anomalies plotted in Figure 5A. The net freshwater flux was calculated using precipitation from both SOC Climatology and the CMAP data (evaporation was calculated from the SOC Climatology) and there was little difference in the final result (Figure 5B). The error bars in both figures are standard error, and the absolute bias of the means remains unknown.

The heat content anomaly and freshwater content anomalies of the upper ocean (0–900 m) were calculated referenced to 0°C and to 36.00 salinity for each section. Heat content anomaly $H = \int \rho C_p T dz$ where

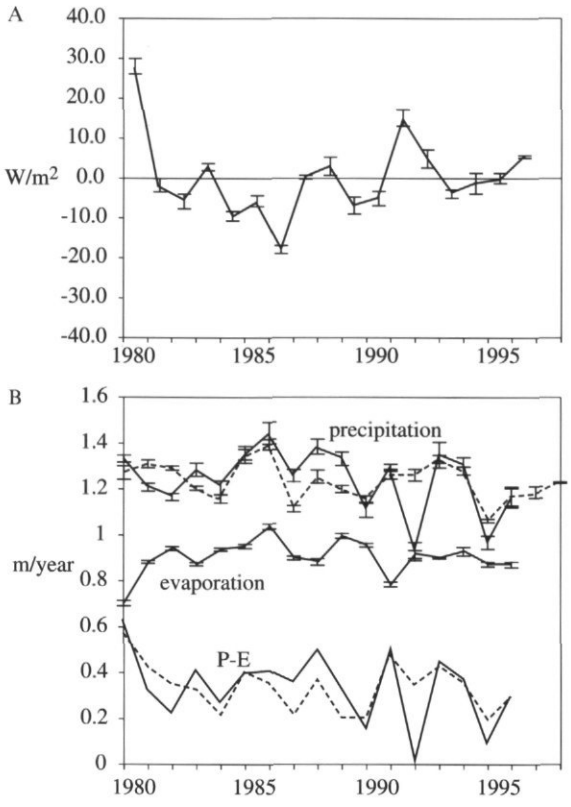


Figure 5. Atmospheric flux variations in the Rockall Trough region: (A) annual net heat flux anomalies (1980–1996 mean = –44 W m^{-2}); (B) annual precipitation (P), evaporation (E), and net freshwater flux (P–E). For P and P–E dashed lines are SOC Climatology; solid lines are CPC Merged Analysis of Precipitation (CMAP, Xie and Arkin, 1997). In all figures, error bars are standard error and absolute bias is unknown.

ρ is density, C_p is specific heat capacity of seawater, T is temperature and z is depth (m). Freshwater content anomaly $F = \int \{(\frac{S_{ref}}{S(z)}) - 1\} dz$, where S_{ref} is the reference salinity (here 36.00) and S is the salinity at depth z (m). Seasonal cycles of heat and freshwater content anomalies were modelled by fitting a sinusoidal curve to all observations in the time-series, and the modelled monthly values removed from each occupation to leave a time-series of anomalies (again more details can be found in Holliday (2002a)). The oceanic heat and freshwater content anomalies are shown in Figure 6, plotted alongside the atmospheric flux anomalies. The atmospheric heat flux variations are half the amplitude of the changes in heat content anomaly, and the cycles appear to act in opposition to each other. The atmospheric freshwater fluxes are an order of magnitude smaller than the oceanic freshwater content anomalies. We conclude that there is no evidence that the variations in the heat and freshwater content anomalies can be explained by the variations in the local atmospheric fluxes.

The second hypothesis is that the variations in the Rockall Trough are the result of varying amounts of different water masses entering the basin. The upper ocean water masses that lie to the south of the

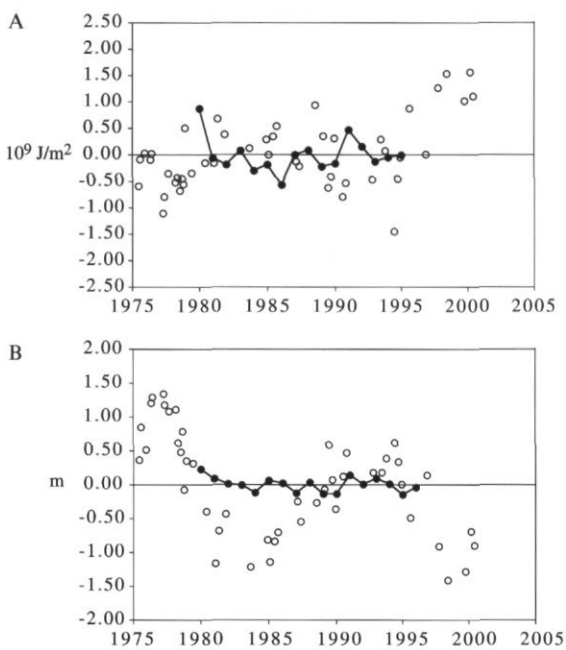


Figure 6. Oceanic heat and freshwater content anomalies (0–900 m, open circles) compared to variations in annual heat and freshwater exchange with the atmosphere (solid line and dots): (A) heat content anomalies and (B) freshwater content anomalies.

Rockall Trough are the "eastern" water masses, the warm saline ENAW and the Mediterranean Outflow Water (MEDW), and the relatively cooler and fresher "western" water of the North Atlantic Current (NAC) (a form of Western North Atlantic Water, WNAW), and the SubArctic Intermediate Water (SAIW). Most of the upper ocean water flowing into the Rockall Trough is ENAW, with small input of NAC water (Ellett *et al.,* 1986). The intermediate depth SAIW and MEDW are mixed together in a region of intense mixing at the entrance to the basin, leaving the water within the Rockall Trough relatively homogeneous with a tight T–S relationship (Read and Ellett, 1991). Below, I discuss whether the eastward extent of western water masses influences the properties in the northern Rockall Trough.

Two recent surveys of the Rockall Trough and region to the south were analysed to test the hypothesis, and evidence was found to support it. The surveys were at periods of contrasting properties at the Ellett line; in October 1996 the ENAW at the Ellett line was relatively cool and fresh, whereas in May 1998 it was the most saline of the time-series and very warm. To the south of the Rockall Trough, the NAC water was observed east of 17°W in October 1996, whereas in May 1998 no NAC waters were found east of 20°W. The interesting difference between these meridians is their relative location to the Rockall Trough; 20°W is the longitude of the southern tip of the Rockall Plateau (50–55°N) at water depth of 1000 m (17°W at 500 m), so water moving northwards west of 17–20°W will be forced to flow westwards around the topography. East of 17–20°W, northward flowing water can move freely into the Rockall Trough. Therefore if the NAC waters reach east of 20°W they could enter the basin and cool and freshen the ENAW (as may have occurred in October 1996), but if they stay to the west the ENAW will remain relatively warm and salty (as may have occurred in May 1998). The temperature–salinity relationship of the water column at the Ellett line and south of the basin during the contrasting 1996 and 1998 periods is shown in Figure 7. Profiles B and C are both from the same location on the Ellett line, but in different years (B in 1996, C in 1998). Note that both converge to the LSW salinity minimum below 1200 dbar. Profile A is an example of station west of the NAC, with WNAW at the surface, SAIW at intermediate levels and LSW below. Profile D is a typical eastern margin station with ENAW overlaying

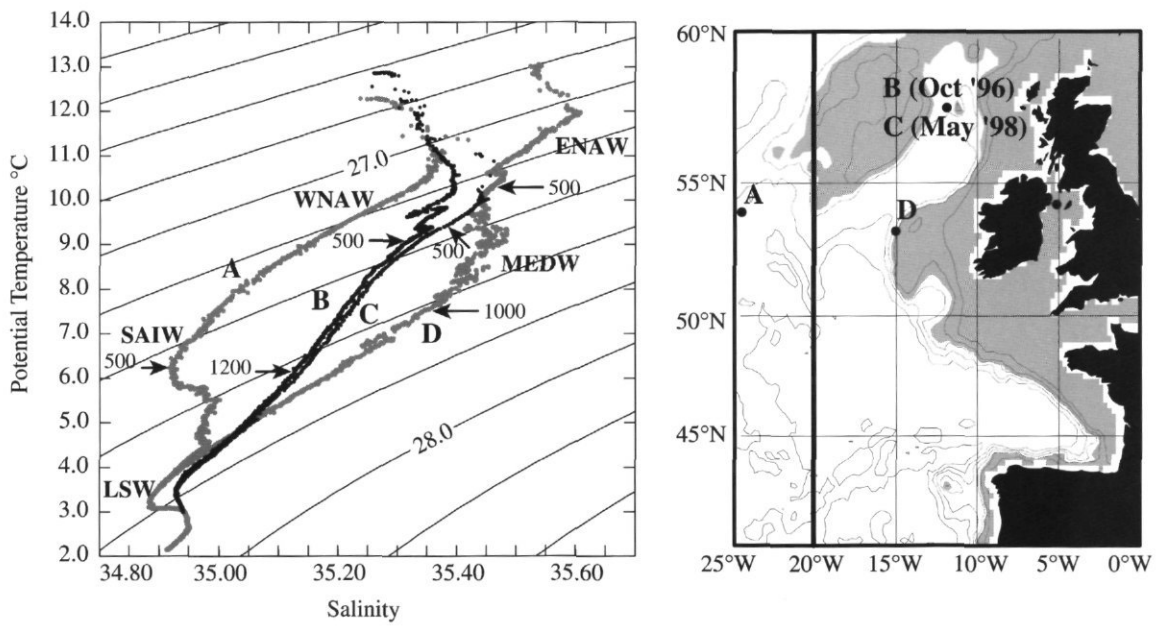


Figure 7. Potential temperature vs. salinity for stations around the Rockall Trough (with potential density contours). Locations of profiles A, B, C, and D are shown on the map on the right. Profiles A and D illustrate the water masses that can flow into the basin (CTD stations from October 1996); Profile A is an example of the cool fresh Western North Atlantic Water (WNAW) and SubArctic Intermediate Water (SAIW), and Profile D is an example of the warm saline Eastern North Atlantic central Water (ENAW) and Mediterranean outflow Water (MEDW). Profiles B and C are both in the same location on the Ellett line but at different times; B in October 1996, C in May 1998. Selected pressure levels are indicated by the arrows and numbers (500, 1000, and 1200 dbar).

MEDW. Both profiles A and D converge to identical LSW properties at 3.5–4.5°C, though that range of θ–S is deeper in the eastern profile. There is indeed evidence that in 1996 the Ellett line upper ocean (profile B) is influenced by NAC water, whereas in 1998 the Ellett line curve mixes to and overlays the "pure" ENAW curve from south of the basin (profile C). The shift to more saline conditions in 1998 can be seen down to 1200 dbar, through the permanent thermocline zone in which the MEDW and SAIW mix in the entrance to the Rockall Trough according to Read and Ellett (1991). This suggests that the impact of the varying NAC contribution to the basin is in both the upper WNAW and the intermediate SAIW, and explains the observation that the variability persists beyond the depth of the central waters, and deeper than winter mixing (Holliday *et al.*, 2000).

The literature provides further historical evidence to support the hypothesis that the regional extent of the contributing water masses does vary, and appears to co-vary with the properties in the northern Rockall Trough. Read and Ellett (1991) show WNAW and SAIW reaching all the way to the eastern margin of the North Atlantic in 1989, a period when the Ellett line water was cool and fresh (actually the start of the cool fresh period that extended to 1996). Read (2001) shows that in 1991 WNAW of the NAC was seen east of 17°W at 52°N. Similarly, Ellett *et al.* (1986) described data from Ocean Weather Station J that showed WNAW and SAIW east of 20°W in 1974 and 1977; the latter year also being the time of the cold fresh Great Salinity Anomaly (GSA) in this region. Other examples show NAC water remaining west of 20°W at times when the Rockall Trough was relatively warm and saline. The Harvey (1982) description of ENAW was based on data from 1957 and 1958; he noted at the time that WNAW and SAIW were only found west of 20°W; Ellett and Jones (1994, data reproduced in Figure 3 here) showed the water in the Rockall Trough to be unusually warm and saline in the late 1950s. In 1966 the Rockall Trough was cool but with high salinity and Wade *et al.* (1997) note from OWS J data that in 1966 WNAW and SAIW are only found west of 20°W.

Finally, the hypothesis does not exclude the influence of changing properties of the source waters. Property variations in both ENAW and WNAW can influence the Rockall Trough temperature and salinity even though they cannot alone explain the variability at the Ellett line. In 1966 the cool but saline Rockall Trough water probably reflected cooler than usual ENAW to the south. During the GSA period the Rockall Trough salinity was especially low, not just because it contained a greater amount of WNAW and SAIW than average, but also because those water masses were unusually fresh.

Conclusions

The time-series of hydrographic data in the northern Rockall Trough (the Ellett line) provides unique insight into the variability of Atlantic Water flowing into the Nordic Seas. Over the period of the full depth time-series (1975–2001), the upper ocean temperature range was ±0.5°C and the salinity range was ±0.05, with maxima of both occurring during the late 1990s. The decade of the 1990s was characterized by a period of significant change in upper ocean properties, from cool and fresh in the early years to warm and saline at the end of the decade. The rate of change was similar to that observed in sea surface temperature and salinity in the 1950s, though the maximum surface anomalies of 1960 were higher than the current subsurface anomalies.

The time-series of upper ocean temperature and salinity in the Rockall Trough does not correlate with basin-scale atmospheric conditions as represented by the NAO index. The variability observed cannot be explained simply as advected anomalies formed in the source region of the major water mass, the central North Atlantic Water (ENAW). Evidence was found that variations in local net atmospheric heat and freshwater fluxes are too small to account for the observed variations in heat and freshwater content. Instead, it has been shown that the variations in properties are caused by varying inputs of the water masses to the south. Most of the upper and intermediate water flowing into the Rockall Trough comes from the Eastern Atlantic, the ENAW, and Mediterranean outflow Water (MEDW). When North Atlantic Current water masses (Western North Atlantic Water (WNAW) and SubArctic Intermediate Water (SAIW)) spread east of 17–20°W south of the Rockall Trough (50–55°N) they flow into the basin and cool and freshen the upper water column to 1200 dbar.

The deep water of the Rockall Trough is a relatively saline and warm form of Labrador Sea Water (LSW) partially isolated by topography from the same water type to the south of the basin. In 1990 the LSW freshened and cooled suddenly owing to an influx of external (newer) LSW. For the rest of the decade the LSW properties remained unchanged as the isolated reservoir re-circulated around the basin with little input from the south.

Acknowledgements

This article is dedicated to the memory of David Ellett, who was the originator and champion of the hydrographic time-series in the Rockall Trough, and who compiled the surface time-series. Without his foresight, energy, and dedication to time-series work, this analysis would not have been possible. I

thank Harry Bryden and Raymond Pollard for their advice during the writing of the PhD thesis from which these results were drawn.

References

Dickson, R., Lazier, J., Meincke, J., Rhines, P., and Swift, J. 1996. Long-term co-ordinated changes in the convective activity of the North Atlantic. Progress in Oceanography, 38: 241–295.

Dickson, R. R., Meincke, J., Malmberg, S.-A., and Lee, A. J. 1988. The "Great Salinity Anomaly" in the Northern North Atlantic 1968–82. Progress in Oceanography, 20: 103–151.

Ellett, D. J., Edwards, A., and Bowers, R. 1986. The hydrography of the Rockall Channel: an overview. Proceedings of the Royal Society of Edinburgh, 88 (B): 61–81.

Ellett, D. J., and Jones S. R. 1994. Surface temperature and salinity time-series from the Rockall Channel. MAFF Directorate of Fisheries Research, Lowestoft. 24 pp.

Hansen, B., and Østerhus, S. 2000. North Atlantic: Nordic Seas Exchanges. Progress in Oceanography, 45: 109–208.

Harvey, J. 1982. Theta-S relationships and water masses in the eastern North Atlantic. Deep-Sea Research, 29 (8A): 1021–1033.

Holliday, N. P. 2002a. Interannual variability of the circulation and ventilation of the North Atlantic subpolar gyre. PhD thesis, University of Liverpool. 236 pp.

Holliday, N. P. 2002b. Air–sea interaction and circulation changes in the northeast Atlantic. Submitted to Journal of Geophysical Research.

Holliday, N. P., Pollard, R. T., Read, J. F., and Leach, H. 2000. Water mass properties and fluxes in the Rockall Trough: 1975 to 1998. Deep-Sea Research I, 47 (7): 1303–1332.

Josey, S. A., Kent, E. C., and Taylor, P. K. 1998. The Southampton Oceanography Centre (SOC) Ocean-Atmosphere Heat, Momentum and Freshwater Flux Atlas. Southampton Oceanography Centre. 30 pp.

Perez, F. F., Rios, A. F., King, B. A., and Pollard, R. T. 1995. Decadal changes of the Theta-S relationship of the Eastern North Atlantic Central Water. Deep-Sea Research I, 42 (11/12): 1849–1864.

Read, J. F. 2001. CONVEX-91: water masses and circulation of the Northeast Atlantic subpolar gyre. Progress in Oceanography, 48: 461–510.

Read, J. F., and Ellett, D. J. 1991. Subarctic Intermediate Water in the eastern north Atlantic. ICES C42.

Rodwell, M. J., Rowell, D. P. and Folland, C. K. 1999. Oceanic forcing of the wintertime North Atlantic Oscillation and European climate. Nature, 398: 320–323.

Sy, A., Rhein, M., Lazier, J. R. N., Koltermann, K. P., Meincke, J., Putzka, A., and Bersch, M. 1997. Surprisingly rapid spreading of newly formed intermediate waters across the North Atlantic Ocean. Nature, 386: 675–679.

Wade, I. P., Ellett, D. J., and Heywood, K. J. 1997. The influence of intermediate waters on the stability of the eastern North Atlantic. Deep-Sea Research I, 44 (8): 1405–1426.

Xie, P., and Arkin, P. A. 1997. Global precipitation: a 17-year monthly analysis based on gauge observations, satellite estimates and numerical model outputs. Bulletin of the American Meteorological Society, 78: 2539–2558.

ICES Marine Science Symposia, 219: 102–110. 2003

Indications and consequences of weakened Iceland–Scotland overflow

Bogi Hansen, William R. Turrell, and Svein Østerhus

Hansen, B., Turrell, W. R., and Østerhus, S. 2003. Indications and consequences of weakened Iceland–Scotland overflow. – ICES Marine Science Symposia, 219: 102–110.

The overflow of cold water from the Arctic Mediterranean (Arctic Ocean and Nordic Seas) across the Greenland–Scotland Ridge into the Atlantic is a key process in the formation of North Atlantic Deep Water (NADW) and a driving mechanism for the Atlantic inflow to the Nordic Seas. About half the overflow flux passes east of Iceland, carried by three separate branches. Previous investigations have shown that the branch that flows through the Faroe Bank Channel decreased in flux from 1950 to 2000. We argue that the same conclusion can be drawn for the cold component of the overflow across the southern part of the Iceland–Faroe Ridge and for the cold component of the overflow across the Wyville–Thomson Ridge. If not compensated by unobserved increases in other sources, the results imply a reduced production of NADW and reduced inflow of Atlantic Water to the Nordic Seas. We briefly discuss the potential biological consequences of the changing transport of organisms by overflow currents, changing bottom temperature regimes in areas affected by overflow water, and changing Atlantic inflow.

Keywords: Atlantic inflow, climate change, Nordic Seas, overflow, thermohaline circulation.

Bogi Hansen: Faroese Fisheries Laboratory, PO Box 3051, FO-110 Torshavn, Faroe Islands [tel: +298 315092; fax: +298 318264; e-mail: bogihan@frs.fo]. William R. Turrell: FRS Marine Laboratory, PO Box 101, Aberdeen AB11 9DB, Scotland. Svein Østerhus: Bjerknes Centre for Climate Research and Geophysical Institute, NO-5024 Bergen, Norway. Correspondence to Bogi Hansen.

Introduction

The Greenland–Scotland Ridge separates the Arctic Mediterranean (Arctic Ocean and Nordic Seas) from the Atlantic Ocean. Across several of its deeper areas there is, however, an overflow of cold, dense, water from the north into the Atlantic (Figure 1) that is a key process in the formation of North Atlantic Deep Water (NADW) (Dickson and Brown, 1994). The overflow can be divided into two parts of similar magnitudes in terms of flux (Hansen and Østerhus, 2000). One of these is the overflow through the Denmark Strait west of Iceland (the DSB. Hansen et al. overflow), the other is the Iceland–Scotland overflow, which is carried by three branches (Figure 1), across the Iceland–Faroe Ridge (the IFR overflow), through the Faroe Bank Channel (the FBC overflow), and across the Wyville–Thomson Ridge (the WTR overflow).

The most important branch of the Iceland–Scotland overflow is the deep flow through the Faroe Bank Channel. By itself, this branch is estimated to carry more than half of the Iceland–Scotland overflow flux and about one-third of the total overflow flux (Hansen and Østerhus, 2000). Owing to the large sill-depth of the channel, this branch also carries the coldest and most dense overflow water. Using a combination of modern current measurements and historic hydrographic observations, we have previously shown that the FBC overflow has decreased in flux since at least 1950 (Hansen *et al.*, 2001).

This conclusion was based on observations of the interface between the dense overflow water and the lighter water above in the southern Norwegian Sea. As shown in Figure 2, the deep parts of this region are fairly homogeneous in density and the top of this homogeneous layer can be defined by the $\gamma_0 = 28.0$ kg m^{-3} density level. (Here and elsewhere in the article, the density anomaly γ is calculated from the 1980 equation of state, EOS-80.) This level we term the "interface" and observations from Ocean Weather Station M (OWS-M) show that it deepened

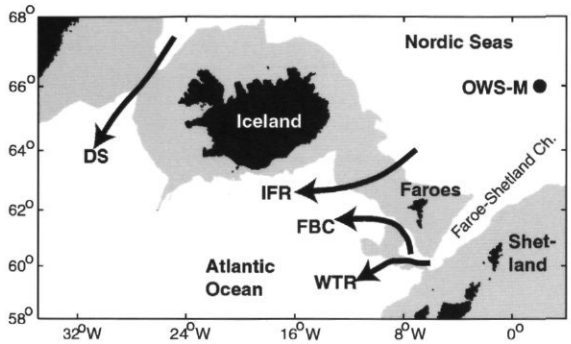


Figure 1. The Greenland–Scotland Ridge. Areas shallower than 700 m are shaded. The four overflow branches are indicated by arrows and the position of Ocean Weather Station M (OWS-M) is also indicated.

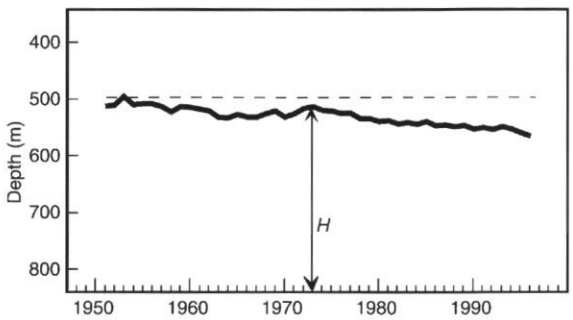


Figure 3. Five-year running mean of the depth of the interface defined as the $\gamma_\theta = 28.0$ kg m^{-3} density level at OWS-M. H indicates the height of the interface above the sill level (at a depth of 840 m) of the Faroe Bank Channel. The deepening trend is significantly different from zero ($p < 0.001$). (Adapted from Hansen *et al.*, 2001.)

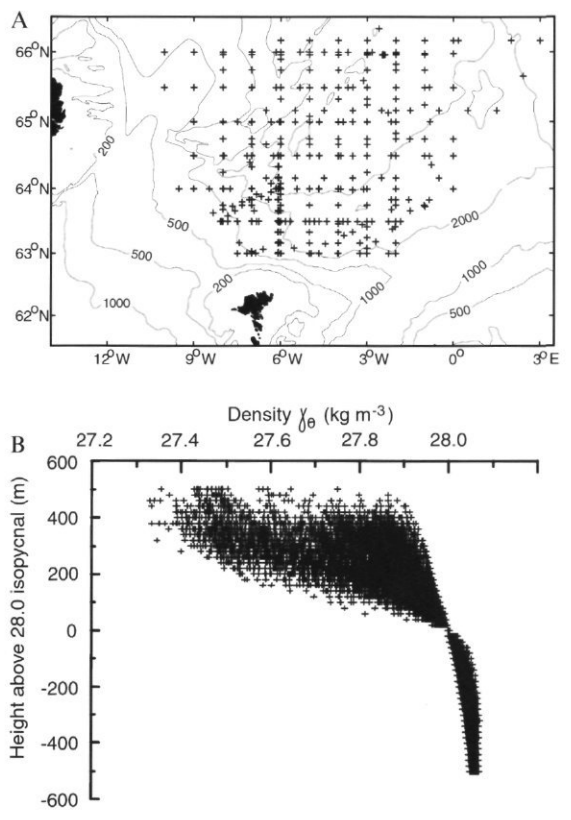


Figure 2. A. Map of CTD stations occupied by RV "Magnus Heinason" in the southern Norwegian Sea with bottom depths greater than 750 m in the period 1976–1999. B. Density (γ_θ) profiles measured at the stations shown in A. To illustrate that the 28.0 kg m^{-3} isopycnal marks the upper limit of the deep, near-homogeneous layer, each density profile has been moved vertically so that the γ_θ = 28.0 kg m^{-3} density is at level zero.

in that region from 1950 to 2000 (Figure 3). In the Northeast Atlantic at the exit of the Faroe Bank Channel, similar density changes are not seen and a deepening interface in the Norwegian Sea therefore implies a reduced along-flow baroclinic pressure gradient (Hansen *et al.*, 2001). This pressure gradient is generally smaller than the cross-flow pressure gradient and the Coriolis force that largely balances it. A force that is perpendicular to the velocity cannot, however, do any work on the flow and these two cross-flow forces do not therefore contribute to accelerating the flow up to the large speeds observed in the Faroe Bank Channel. Neither can they counteract the frictional forces that retard the flow. In this sense they do not contribute to driving the flow. Rather, the FBC overflow is maintained by the along-flow baroclinic pressure gradient, and a decrease in this gradient therefore implies a weakened FBC overflow (Hansen *et al.*, 2001).

It is therefore natural to ask whether the same conclusion can be drawn for the IFR overflow and the WTR overflow. This question is the main motivation for this article. A priori, the answer might seem obvious, since a deepening of the interface due east of these ridges should lead to reduced overflow at all points along the ridges of the appropriate depth. The answer is not that obvious, however. The close link between the interface depth at OWS-M and FBC overflow follows from the observation that the interface at the entrance to the combined Faroe–Shetland and Faroe Bank channels is at the same depth as at OWS-M (Hansen *et al.*, 2001). Apparently, the internal circulation of the Norwegian Basin at these depths does not have an appreciable component that crosses a line between OWS-M and the channel entrance, probably because the Faroe Bank Channel drains the waters at these depths across the basin. In contrast, both

the Iceland–Faroe Ridge and the Wyville–Thomson Ridge have strong flows parallel to the ridge close to sill level and these flows can be expected to distort the isopycnal surfaces.

Following this introduction, we first discuss the properties of the overflow water masses and briefly review the results for the FBC overflow. We then discuss in some detail the IFR overflow and the WTR overflow and end by discussing potential consequences of the overflow changes. In the first instance, changing overflows may lead to other changes in the physical circulation system, but effects on the biological conditions are also to be expected.

Water mass characteristics of the Iceland–Scotland overflow

The overflow between Iceland and Scotland is generally considered to be composed of three water masses of different origin and characteristics (Figure 4): Norwegian Sea Deep Water (NSDW), Norwegian Sea Arctic Intermediate Water (NSAIW), and Modified East Icelandic Water (MEIW). The production and characteristics of these water masses were reviewed by Hansen and Østerhus (2000). The relative contribution of the three water masses to the overflow is not the same in all regions. According to Read and Pollard (1992), MEIW is produced in the Iceland–Faroe Front and its contribution is probably largest for the IFR overflow. The other two water masses are generally found together in the southern Norwegian Sea, but with NSAIW on top of NSDW. Thus, only the Faroe Bank Channel is sufficiently deep to allow appreciable amounts of NSDW to overflow, but even there the ratio of NSDW to NSAIW appears to have been declining during the last decades of the 20th century (Turrell *et al.*, 1999; Hansen and Kristiansen, 1999).

Unfortunately, the temperature and salinity values used to discriminate between different water masses are not determined accurately. Also, the overflow water mixes with ambient waters on its way towards the ridge and some of this mixture accompanies the overflow into the Atlantic. Traditionally, only that fraction of the mixture that is sufficiently dense to contribute to NADW production (e.g. $\gamma_\theta > 27.8$ kg m^{-3}; Saunders, 1994; Dickson and Brown, 1994) has been included in the overflow. In our discussion, we focus on the undiluted overflow water masses of Figure 4.

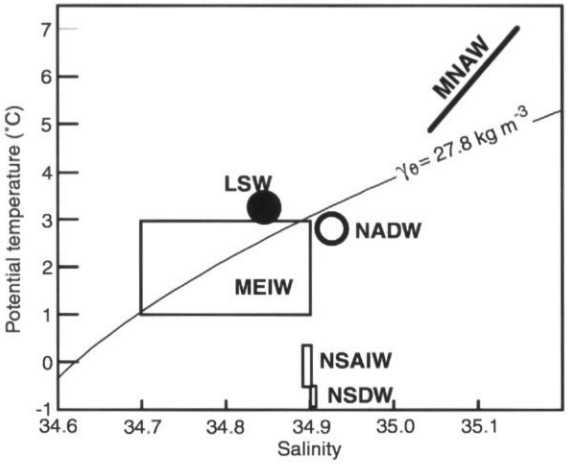


Figure 4. Rectangles indicate temperature and salinity characteristics of the three overflow water masses: Norwegian Sea Deep Water (NSDW), Norwegian Sea Arctic Intermediate Water (NSAIW), and Modified East Icelandic Water (MEIW). The filled circle and the thick line indicate water masses that are entrained into the overflow after it has crossed the ridge: Modified North Atlantic Water (MNAW) and Labrador Sea Water (LSW). The open circle indicates the end product: North Atlantic Deep Water (NADW).

The FBC overflow

The Faroe Bank Channel is by far the deepest passage across the Greenland–Scotland Ridge (Figure 1) and all modern observations show the deeper parts of this channel to be dominated by cold overflow water on its way into the Atlantic (Østerhus *et al.*, 1999). Measurements using moored Acoustic Doppler Current Profilers (ADCPs) have shown a statistically significant ($p < 0.001$) reduction in the flux of overflow < 0.3°C (NSAIW+NSDW) in the period 1995–2000 and the reduction has been linked to the deepening interface at OWS-M (Figure 5).

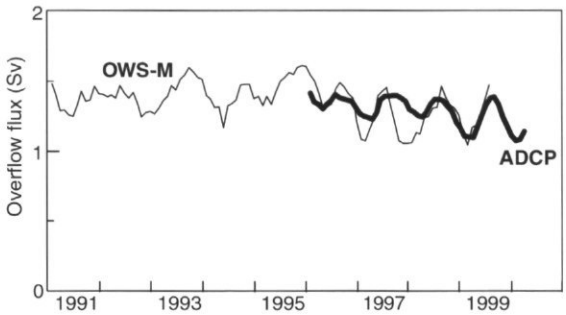


Figure 5. Five-month running mean of the flux of water colder than 0.3°C ($\gamma_\theta > 28.0$ kg m^{-3}) through the Faroe Bank Channel as measured by moored ADCPs (thick curve) and calculated from the interface depth at OWS-M (thin curve) by assuming proportionality and an 8-month delay (Hansen *et al.*, 2001).

Using this link, the steady deepening of the interface at OWS-M through the latter half of the 20th century (Figure 3) implies a flux reduction of the overflow. Its magnitude depends on the model used, but Hansen *et al.* (2001) concluded that the reduction from 1950 to 2000 was at least 20%. The flux reduction comes in addition to the decrease in the average density implied by the shift in composition with reduced NSDW influence compared to NSAIW (Turrell *et al.*, 1999; Hansen and Kristiansen, 1999). Both the observations at OWS-M and the ADCP measurements in the Faroe Bank Channel indicate an accelerated decrease in the period 1995–2000, with an annual flux decrease of 2–4% (Figure 5).

The IFR overflow

The topography of the Iceland–Faroe Ridge (Figure 6) is fairly regular with a depth that varies between 300 and 480 m along the crest. The shallowest areas are in the northernmost half, but the ridge is crossed by a number of passages that seem to be the main conduits for overflow (Hermann, 1967). The deepest passage (480 m) is close to the Faroe Slope, but a channel close to the Icelandic Slope is also fairly deep (420 m).

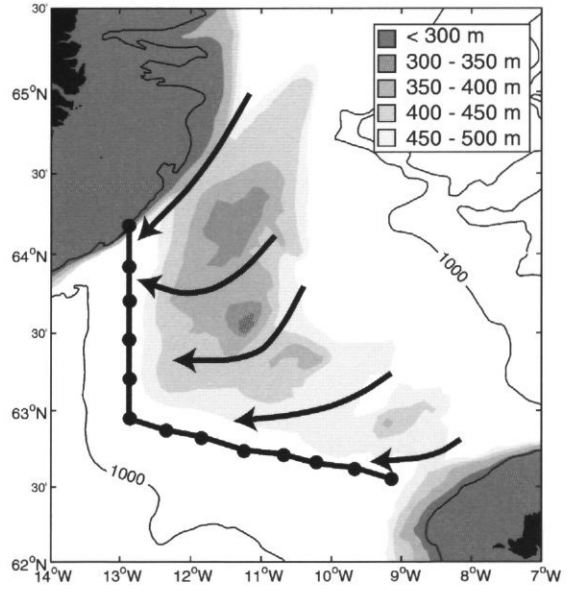


Figure 6. The topography of the Iceland–Faroe Ridge. Arrows indicate the main overflow paths (Hermann, 1967; Hansen and Østerhus, 2000). Black circles connected by thick line indicate location of a German standard section shown in Figure 7.

In the period 1959–1971, German research vessels occupied a standard section (Figure 6) west of the ridge on 14 cruises. From these, Meincke (1972) constructed an average water mass distribution on the section (Figure 7) which shows that the two different overflow water masses have different spatial distributions. The MEIW occurs higher up in the water column and mainly close to Iceland compared to the NSAIW that is only found close to the bottom, but both over the northern and southern regions.

This difference in distribution is reasonable when taking into account that the two water masses probably cross the ridge by different processes. As described by Read and Pollard (1992), the MEIW is produced in the frontal zone of the Iceland–Faroe Front by mixing and sinking, and on hydrographic sections crossing the ridge this water is often seen as a salinity minimum in the middle of the front (e.g. Meincke, 1978). Since the front tends to touch bottom on the ridge, close to the crest, frontal instabilities and movement will be important for MEIW overflow.

To produce an overflow of NSAIW, on the other hand, the interface between this water and the waters above needs to be raised above the sill level east of the ridge. The movement of the interface may be linked to frontal variations, but we have no basis for assuming that the two different overflow components over the Iceland–Faroe Ridge will vary according to a consistent relationship. Thus, we draw no conclusions on the temporal trends of MEIW overflow, but we explore the question whether the observed interface deepening at OWS-M (Figure 3)

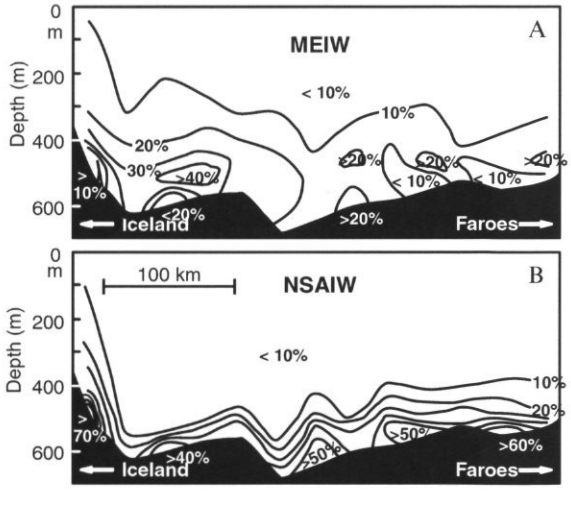


Figure 7. Average percentage content of MEIW (A) and NSAIW (B) on a section due west of the crest of the Iceland–Faroe Ridge (Figure 6) based on Meincke (1972).

is likely to have affected the overflow of NSAIW across the Iceland–Faroe Ridge.

To answer this question, we need to know whether the deepening of the interface at OWS-M has also occurred in the region due east of the Iceland–Faroe Ridge. The horizontal depth variation of the interface is shown in Figure 8. It is based on CTD stations that have not been systematically sampled in space or time and the small-scale details may be fictitious. The overall slope of the interface from the Iceland–Faroe Ridge to OWS-M, however, is too large and based on too many observations (887 CTD stations plus the OWS-M observations) to be accidental. If we follow a transect from OWS-M to the area east of the southern part of the Iceland–Faroe Ridge (A on Figure 8), the isopycnal is seen to become about 100 m shallower.

To evaluate whether the interface has deepened due east of the Iceland–Faroe Ridge, we therefore have to consider whether a possible change in the slope of the interface could offset the deepening at OWS-M. We therefore ask the cause of the slope and the answer clearly lies in the thermal-wind equation, which implies that there must be a vertical shear in the horizontal current at the depth of the interface. The sign of the shear implies that the southward velocity component increases with depth. This can occur either if the flow is north-going and weakening with depth, or south-going and strengthening with depth. In the western side of the basin, close to the ridge, the second case definitely applies as shown by long-term current measurements at site A (Figure 8). Farther to the east, we do not have long-term current measurements, but the result from a short-term mooring at OWS-M supports the same interpretation (Figure 8).

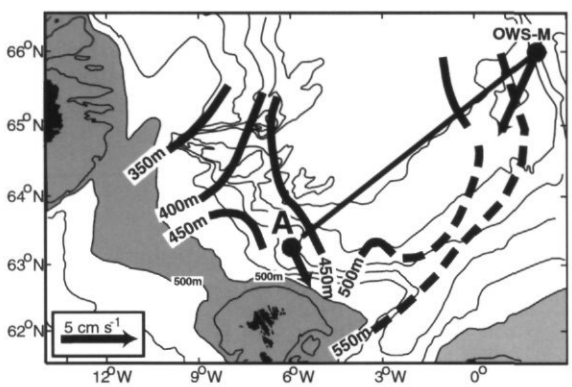


Figure 8. Depth of the $\gamma_\theta = 28.0$ kg m^{-3} isopycnal between the Iceland–Faroe Ridge and OWS-M. In the open waters, the depth is based on the CTD stations in Figure 2A. The two broken lines are based on the observation that, in the period 1994–1999, this isopycnal was at similar depths, slightly more than 550 m, at OWS-M and at the entrance to the Faroe–Shetland Channel (Hansen *et al.*, 2001). Shadings indicate areas shallower than 500 m. The arrow at A indicates the average residual flow at about 450 m based on current (ADCP) measurements lasting more than 4 years (Hansen *et al.*, 1999; Larsen *et al.*, 2000). The arrow at OWS-M indicates the residual flow from a mooring at 550 m depth lasting for 44 days (S. Østerhus, unpubl. data). The velocity scale for the arrows is indicated in the lower left corner.

This general southward flow at these depths in the Norwegian Basin is, no doubt, the water that feeds the FBC overflow. The interface is close to the top of this layer and the vertical velocity shear, as well as the slope of the interface in Figure 8, is therefore most likely caused by that flow. If this interpretation is correct, then it is the flow field driven by the FBC overflow that is the main reason for the slope of the interface. The observed deepening of the interface at OWS-M since 1950 (Figure 3) implies a weakened FBC overflow, which again implies a reduced slope. Thus the interface has probably deepened even more in the area due east of the southern part of the Iceland–Faroe Ridge than at OWS-M in the period 1950–2000. Since the interface is close to the sill depth of the southern part of the Iceland–Faroe Ridge, we conclude that the overflow across this part of the ridge has most likely been reduced.

For the northern part of the Iceland–Faroe Ridge, this line of evidence may not necessarily apply. From the rather coarse data set of Figure 2A, the $\gamma_\theta = 28.0$ kg m^{-3} isopycnal seems to be lifted an additional hundred metres in this region and the isopycnals seem to run perpendicular to the ridge. This behaviour appears to be associated with an overflow over the ridge mainly through the channel close to the Icelandic slope. This flow is seen as a very pure (> 70%) core of NSAIW in Figure 7B and probably derives more or less directly from the Iceland Sea.

The link between interface depth at OWS-M and overflow is thus not so evident for the northern part of the ridge. On the available evidence, we can only conclude that the overflow of NSAIW water across the southern part of the Iceland–Faroe Ridge most likely has decreased in the period 1950–2000.

The WTR overflow

The Wyville–Thomson Ridge connecting the Faroe Bank to the European continental shelf has a sill depth of slightly more than 600 m (Figure 9). This is not much deeper than the $\gamma_\theta = 28.0$ kg m^{-3} isopycnal at OWS-M by the end of the 20th century (Figure 3), but, as for the Iceland–Faroe Ridge, there is the question how the circulation affects the interface height. As noted previously (Figure 8), the interface seems to keep a constant depth from

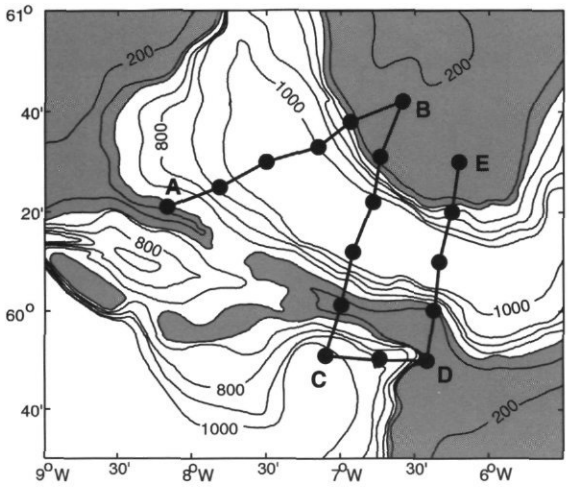


Figure 9. Topography of the Wyville–Thomson Ridge shown with isobaths at depths 200, 500, 600, 700, 800, 900, and 1000 m. Areas shallower than 600 m are shaded. Circles connected by line show a CTD section occupied by RV "Magnus Heinason" in May 1997, May 1998, and May 1999.

OWS-M to the entrance of the Faroe–Shetland Channel, but within the channel system there are strong currents that could well be expected to tilt isopycnals appreciably.

To study this, we have analysed the density field along the section shown in Figure 9. This section was occupied three times in 1997–1999 and Figure 10 shows the average density on the section. For intermediate densities ($27.5\ \text{kg m}^{-3} < \gamma_\theta < 27.9\ \text{kg m}^{-3}$), the isopycnals slope downwards from the Faroe Plateau towards the Wyville–Thomson Ridge. The thermal wind equation implies that this is equivalent to a vertical velocity shear on the order of $10^{-3}\ \text{s}^{-1}$. Water of these densities is found

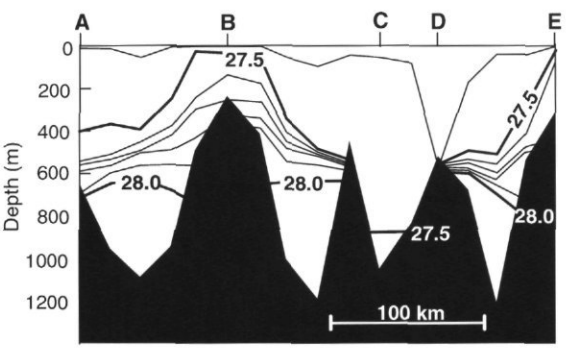


Figure 10. Density (γ_θ) on the section shown in Figure 9 calculated as the average for three cruises. Letters refer to locations shown in Figure 9. Lightly shaded areas have $\gamma_\theta > 28.0\ \text{kg m}^{-3}$.

in the transition layer between the overflow and the Atlantic waters above, where the along-channel velocity increases strongly with depth.

For the pure overflow water ($\gamma_\theta > 28.0\ \text{kg m}^{-3}$), however, Figure 10 does not indicate a consistent isopycnal slope northeast of the ridge, which implies a small vertical gradient of velocity. We therefore argue that changes in the depth of this isopycnal at OWS-M probably give rise to similar changes northeast of the Wyville–Thomson Ridge. From Figure 10, the depth of the $\gamma_\theta = 28.0\ \text{kg m}^{-3}$ isopycnal northeast of the ridge is close to the sill depth. The data are not sufficiently representative to be able to calculate the height of this isopycnal above sill level with any great accuracy, but it seems likely that a 50 m descent of the isopycnal must have affected this height in a relative sense; perhaps even changed its average sign. We therefore conclude that the flux of pure ($\gamma_\theta > 28.0\ \text{kg m}^{-3}$) overflow across the Wyville–Thomson Ridge most likely decreased from 1950 to 2000.

For less dense overflow water ($27.8\ \text{kg m}^{-3} < \gamma_\theta < 28.0\ \text{kg m}^{-3}$), the conclusion is not as straightforward. A decreasing overflow through the Faroe Bank Channel would tend to decrease the velocity gradient and hence also the isopycnal slope. Thus the effect of a deepening interface at OWS-M could be partly offset by relaxation of the slope close to the ridge. Whatever the conclusion, the estimated flux of WTR overflow was so small towards the end of the 20th century (Saunders, 1990; Ellett, 1998) that it had little effect on the total Iceland–Scotland overflow.

Physical effects of reduced overflow

Above, we have argued that there was a flux decrease from 1950 to 2000 of the Iceland–Scotland overflow. We have focused on the dense component ($\gamma_\theta > 28.0\ \text{kg m}^{-3}$), but the isopycnals of lighter overflow water ($27.8\ \text{kg m}^{-3} < \gamma_\theta < 28.0\ \text{kg m}^{-3}$) also deepened at OWS-M in the same period and there is therefore no reason to believe that the flux of this component should have increased to compensate. The most immediate consequence of this is a decrease in the Iceland–Scotland contribution to the production of North Atlantic Deep Water (NADW) with implications for the global thermohaline circulation. The effect of an overflow change on NADW production, however, is highly dependent upon the characteristics of the overflow and on mixing processes. After crossing the ridge, much of the overflow experiences intensive mixing and entrains appreciable amounts of ambient water. This increases the volume flux but reduces the density of the mixture (Figure 11).

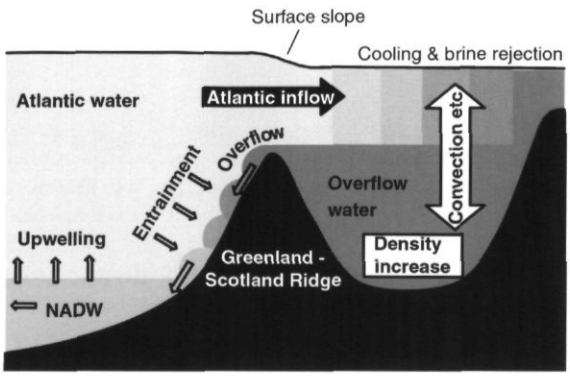


Figure 11. Schematic illustration of the effect of Arctic Mediterranean thermohaline circulation and overflow on NADW production and Atlantic inflow to the Nordic Seas. Cooling and brine rejection induce convection and other vertical exchange of water in various areas of the Arctic Mediterranean. The vertical exchange may involve both sinking and rising of water parcels, but has the net effect of increasing the density at deep and intermediate layers. This process maintains the density difference between the Nordic Seas and the Atlantic at and above sill level and the density difference gives rise to the horizontal pressure gradient that drives the overflows. Entrainment of ambient water decreases the density and increases the flux of overflow water. The export of water from the Arctic Mediterranean in the overflows will tend to lower the sea level northeast of the ridge and create a barotropic pressure gradient that drives an inflow to the Arctic Mediterranean from the Atlantic.

Much of the entrainment occurs shortly after passing the ridge and will involve mainly Atlantic Water (MNAW), but at a later stage Labrador Sea Water (LSW) is also entrained. Clearly, NSDW can entrain more ambient water than NSAIW and still be sufficiently dense to contribute to NADW, while the lightest components of MEIW are already too light even before entrainment (Figure 4). Using hydrochemical observations and CFC tracers, Fogelqvist *et al.* (2002) found the mixture of Iceland–Scotland overflow and entrained water to contain 43% of NSDW+NSAIW and 11% of MEIW when it had arrived in the Irminger Basin. Thus, a given flux reduction of NSDW and NSAIW overflow can be expected to lead to a reduced contribution to NADW by slightly more than twice the magnitude.

There remains the question of what effect an overflow reduction would have on the meridional overturning circulation (MOC). Munk and Wunsch (1998) stated that "the strength of the MOC and associated heat flux may well be primarily determined not by the high-latitude buoyancy forcing, but by the power available to return the fluid to the surface layers". For our system, this statement reflects the undeniable fact that without global mixing the deep regions of the world's oceans would be filled up with cold water and the density difference driving the overflow across the ridge would disappear. However, that would require from several centuries to thousands of years (Munk and Wunsch, 1998). On time scales of decades to one or a few centuries, on the other hand, changes in global ocean mixing should not affect the processes illustrated in Figure 11 significantly and, on these time scales, reduced overflow should lead to reduced meridional overturning.

In addition to the effects on global circulation, there is the possibility of an effect on the Atlantic inflow to the Nordic Seas. The link between overflow and Atlantic inflow is illustrated schematically in Figure 11. Other forces (e.g. windstress) may contribute to driving the Atlantic inflow, but flux estimates (Hansen and Østerhus, 2000) indicate that 75% of the total Atlantic inflow returns to the Atlantic as overflow rather than surface outflow. This implies that the thermohaline forcing of Figure 11 accounts for most of the Atlantic inflow and, hence, that an overflow reduction can be expected to lead to a reduction in Atlantic inflow of similar magnitude. It is important to note, however, that it is the total overflow flux that enters into the balance.

The effect of a reduced Iceland–Scotland overflow on Atlantic inflow therefore depends on the Denmark Strait overflow. Unfortunately, measurements of Denmark Strait overflow are either based on the geostrophic method which is questionable in slope regions (Bacon, 1998), or are of too short duration to indicate long-term trends. Thus, we cannot exclude the possibility of an increased Denmark Strait overflow that compensates for our observed Iceland–Scotland overflow decrease, but we find no evidence for it. Barring this possibility, we can conclude that the Atlantic inflow to the Nordic Seas most likely decreased in the period 1950–2000.

The Atlantic inflow is an important source of heat to the atmosphere over the Nordic Seas, but the oceanic heat flux carried by the Atlantic inflow involves water temperature as well as volume flux. From long-term monitoring, the temperature of the Atlantic Water close to the continental shelf has increased slightly, while the component further offshore does not show clear long-term trends (Turrell *et al.*, 2003). Overall, temperature changes are not enough to compensate the flux reduction and the reduced volume flux of Atlantic inflow should therefore imply a reduced oceanic heat flux. This implies that the overflow reduction may have had a cooling effect on the atmosphere and, indeed, there is some evidence of this. Thus the air temperature in the Faroe Islands, which is in the middle of the Atlantic inflow, did not experience the general warming observed in the last decades of the 20th century as observed at most other locations (Cappelen and Laursen, 1998).

Biological effects of reduced overflow

As discussed above, the geographical extent and magnitude of the overflow decrease is not well known throughout the Iceland–Scotland region. Most conclusions on biological effects must therefore also be qualitative and their extent speculative. We shall not attempt to make a complete list of biological effects, but rather briefly mention three mechanisms: transport of organisms by overflow currents, changing bottom temperature regimes in areas affected by overflow water, and effects of changing Atlantic inflow.

Changing transport of organisms by changing overflow has already been suggested by Heath *et al.* (1999) to be responsible for the decreasing import of the copepod *Calanus finmarchicus* to the North Sea. These scientists focused on the changing ratio between deep (NSDW) and intermediate water (NSAIW) in the overflow, but our results of a decreasing overflow flux can only strengthen their conclusion. Similar effects can be expected for other areas that receive overwintered copepods through advection by the overflow. The Faroe Shelf, in particular, seems to be sensitive, since imported *Calanus* from the FBC overflow has been suggested to regulate the primary production on the inner Faroe Shelf through grazing (Gaard *et al.*, 1998). Furthermore, productivity changes are seen to penetrate through the whole ecosystem (Gaard *et al.*, 2002).

Changing bottom temperature regimes are another potential effect of changing overflow. The most sensitive areas are probably the western flanks of the Iceland–Faroe Ridge and the Wyville–Thomson Ridge. During an overflow event, bottom temperatures in the areas affected may presumably decrease by more than 5°C in a matter of hours. With the decreased overflow, some areas on these two ridges will probably have experienced a reduced frequency of overflow events and the benthos especially will experience a more stable temperature regime.

Lastly, but perhaps of greatest overall significance, the Atlantic inflow to the Nordic Seas is one of the most important factors determining the living conditions there. The waters north of Iceland and in the Norwegian Sea are especially sensitive to the Atlantic inflow. Potential changes in the inflow must be expected to lead to changes in flow patterns, temperature, and salinity and hence also stability in these areas that presently maintain rich ecosystems including commercially valuable species such as herring and blue whiting. Predicting the potential biological effects of a changing physical environment is no easy task, but if the Atlantic inflow should be significantly reduced, the effects on marine ecosystems will, no doubt, be huge.

References

Bacon, S. 1998. Decadal variability in the outflow from the Nordic Seas to the deep Atlantic Ocean. Nature, 394: 871–874.

Cappelen, J., and Laursen, E. V. 1998. The climate of the Faroe Islands. Danish Meteorological Institute Technical Report, 98–14. 62 pp.

Dickson, R. R., and Brown, J. 1994. The production of North Atlantic Deep Water, sources, rates, and pathways. Journal of Geophysical Research, 99: 12,319–12,341.

Ellett, D. J. 1998. Norwegian Sea Deep Water overflow across the Wyville–Thomson Ridge during 1987–1988. ICES Cooperative Research Report, No. 225: 195–205.

Fogelqvist, E., Blindheim, J., Tanhua, T., Østerhus, S., Buch, E., and Rey, F. 2002. Greenland–Scotland overflow studied by multivariate analysis of hydro-chemical data, temporal variations of properties in overlying water masses and associated age determinations by CFC tracers. Deep-Sea Research. (In press.)

Gaard, E., Hansen, B., and Heinesen, S. P. 1998. Phytoplankton variability on the Faroe Shelf. ICES Journal of Marine Science, 55: 688–696.

Gaard, E., Hansen, B., Olsen, B., and Reinert, J. 2002. Ecological features and recent trends in the physical environment, plankton, fish stocks and seabirds in the Faroe shelf ecosystem. *In* Large Marine Ecosystems of the North Atlantic. Changing States and Sustainability, pp. 245–265. Ed. by K. Sherman and H. R. Skjoldal. Elsevier Amsterdam. 449 pp.

Hansen, B., and Kristiansen, R. 1999. Variations of the Faroe Bank Channel overflow. Rit Fiskideildar, 16: 13–22.

Hansen, B., Larsen, K. M. H., and Kristiansen, R. 1999. ADCP deployments in Faroese waters 1997–1999. Faroese Fisheries Laboratory Technical Report, No. 99–07, Tórshavn. 113 pp.

Hansen, B., Turrell, W. R., and Østerhus, S. 2001. Decreasing overflow from the Nordic seas into the Atlantic Ocean through the Faroe Bank channel since 1950. Nature, 411: 927–930.

Hansen, B., and Østerhus, S. 2000. North Atlantic – Nordic Seas Exchanges. Progress in Oceanography, 45: 109–208.

Heath, M. R., Backhaus, J. O., Richardson, K., McKenzie, E., Slagstad, D., Beare, D., Dunn, J., Fraser, J. G., Gallego, A., Hainbucher, D., Hay, S., Jónasdóttir, S., Madden, H., Mardaljevic, J., and Schacht, A. 1999. Climate fluctuations and the spring invasion of the North Sea by *Calanus finmarchicus*. Fisheries Oceanography, 8 (Suppl 1): 163–176.

Hermann, F. 1967. The T–S diagram analysis of the water masses over the Iceland–Faroe Ridge and in the Faroe Bank Channel (Overflow '60). Rapports et Procès-Verbaux des Réunions du Conseil International pour l'Exploration de la Mer, 157: 139–149.

Larsen, K. M. H., Hansen, B., and Kristiansen, R. 2000. Nordic WOCE ADCP deployments in Faroese waters 1999–2000. Faroese Fisheries Laboratory Technical Report, No. 00–01, Tórshavn. 54 pp.

Meincke, J. 1972. The hydrographic section along the Iceland–Faroe Ridge carried out by RV "Anton Dohrn" in 1959–1971. Berichte der Deutschen Wissenschaftlichen Kommission für Meeresforschung, 22: 372–384.

Meincke, J. 1978. On the distribution of low salinity intermediate waters around the Faroes. Deutsche Hydrographische Zeitschrift, 31: 50–64.

Munk, W., and Wunsch, C. 1998. Abyssal recipes II: energetics of tidal and wind mixing. Deep-Sea Research I, 45: 1977–2010.

Østerhus, S., Hansen, B., Kristiansen, R., and Lundberg, P. 1999. The overflow through the Faroe Bank Channel. The International WOCE Newsletter, 35: 35–37.

Read, J. F., and Pollard, R. T. 1992. Water masses in the region of the Iceland–Faeroes Front. Journal of Physical Oceanography, 22: 1365–1378.

Saunders, P. M. 1990. Cold outflow from the Faroe Bank Channel. Journal of Physical Oceanography, 20: 28–43.

Saunders, P. M. 1994. The flux of overflow water through the Charlie-Gibbs Fracture Zone. Journal of Geophysical Research, 99 (C6): 12343–12355.

Turrell, W. R., Slesser, G., Adams, R. D., Payne, R., and Gillibrand, P. A. 1999. Decadal variability in the composition of Faroe Shetland Channel bottom water. Deep-Sea Research I, 46: 1–25.

Turrell, W. R., Hansen, B., Østerhus, S., and Hughes, S. 2003. Hydrographic variability during the decade of the 1990s in the northeast Atlantic and southern Norwegian Sea. ICES Marine Science Symposia, 219: 111–120. (This volume.)

ICES Marine Science Symposia, 219: 111–120. 2003

Hydrographic variability during the decade of the 1990s in the Northeast Atlantic and southern Norwegian Sea

William R. Turrell, Bogi Hansen, Sarah Hughes, and Svein Østerhus

Turrell, W. R., Hansen, B., Hughes, S., and Østerhus, S. 2003. Hydrographic variability during the decade of the 1990s in the Northeast Atlantic and southern Norwegian Sea. – ICES Marine Science Symposia, 219: 111–120.

Throughout the decade of the 1990s, hydrographic conditions in the Northeast Atlantic have been monitored along standard sections in the Faroe Shetland Channel and at Ocean Weather Station Mike in the southern Norwegian Sea. Transport monitoring has also taken place since 1994 in the Faroe Shetland Channel; series of five semi-permanent acoustic Doppler current profiler (ADCP) moorings have been used. The combination of repeat hydrographic sections and ADCP measurements has provided a new description of the annual mean and seasonal variation of temperature, salinity, and along-channel velocity within the Faroe Shetland Channel. These, combined in a simple transport model, have permitted annual mean and seasonal cycles of mass, heat, and salt flux in the poleward flowing Atlantic Water to be estimated for the period 1994–2000. The historical hydrographic data have then been used to set 1994–2000 into the context of decadal variability since 1960. Using recent estimates of Iceland–Scotland overflow variability, it is suggested that the net heat flux towards the Arctic has remained constant during the 1990s, as the observed warming in the inflowing surface waters has been offset by reduced transport. However, salt flux may have reduced, contributing to the freshening tendency in many areas of the Arctic Mediterranean.

Keywords: Atlantic Water, Faroe Shetland Channel, long-term change, Norwegian Sea, seasonal cycle, transports.

W. R. Turrell and S. Hughes: FRS Marine Laboratory, PO Box 101, Aberdeen AB11 9DB, Scotland [tel: +44 1224 876544; fax: +44 1224 295511; e-mail: turrellb@marlab.ac.uk]. B. Hansen: Faroese Fisheries Laboratory, Faroe Islands. S. Østerhus: Geophysical Institute, University of Bergen. Correspondence to W. R. Turrell.

Introduction

New, intensive, and coordinated monitoring of exchange across portions of the Greenland Scotland Ridge took place during the decade of the 1990s, which, for the first time, utilized sustained direct measurements of transports in conjunction with frequent hydrographic surveys. This article examines aspects of water mass characteristics during that period, and some properties of the Atlantic water flux towards the Norwegian Sea through the Faroe Shetland Channel.

Historical perspective

Regular surveys of the Faroe Shetland Channel commenced at the beginning of the 20th century as part of the international cooperative research which ultimately led to the formation of the International Council for the Exploration of the Sea (Helland-Hansen and Nansen, 1909). From the start, the intention was to monitor not only water mass characteristics but also transport, as it was already known that the region was a key gateway between the Atlantic and the Arctic, and that the northward flows through the region were responsible for significant fluxes of heat, salt, and nutrients; all essential for the region's climate and health of the ocean. The surface poleward flowing oceanic waters inundate adjacent shelf seas (the North Sea, Barents Sea, and the Norwegian Shelf) within which commercially important fisheries occur, and so monitoring oceanic transports was considered essential for studies in support of fisheries management within these adjacent regions.

During the first decade of surveys, transport pathways were inferred by detailed water mass analysis and geostrophic calculations (Helland-Hansen and Nansen, 1909). Indeed, it was while Helland-Hansen was working with the Fisheries Laboratory in Aberdeen in 1903, during early cooperative work between oceanographers from Scotland and Norway, that he was developing the use of Bjerknes's dynamical theory (Helland-Hansen, 1903). Over the following 40 years the geostrophic method continued to provide estimates of transport through the Channel (e.g. Tait, 1957). However, when reliable mechanical current meters were developed in the 1960s (one of the most common styles being developed for studies in this region by NATO and Aanderaa), it was shown that the geostrophic method was often in error owing to strong barotropic flows above the slope areas (Dooley and Meincke, 1981; Hansen and Østerhus, 2000).

Conventional moorings with mechanical current meters were used successfully to reveal many aspects of the circulation of the region (e.g. Steele, 1967; Hansen *et al.*, 1986; Sherwin, 1991). However, instrumented moorings could not be used to provide long-term estimates of transport owing to their damage or loss due to the increasingly intensive fishing throughout the area, which now occurs down to 1000 m. One notable exception to the lack of long-term transport estimates was the year-long measurement of transport in the Scottish slope current by Gould *et al.* (1985). It was only until remote measuring, using near-bed-mounted acoustic profiling current meters, became possible at the start of the 1990s that long-term direct measurements of transports became reliable and a practical monitoring tool.

The Nordic WOCE Program

The Nordic WOCE (World Ocean Circulation Experiment) project exploited the potential of the acoustic Doppler current profiler (ADCP). The project commenced in 1994 and consisted of intensive CTD surveys and semi-permanent ADCP deployments along a network of sections radiating out from Faroe, and at other points along the Greenland Scotland Ridge (Hansen *et al.*, 1999). The monitoring which Nordic WOCE initiated has since been maintained during the EU funded VEINS and MAIA projects, and will form components of the ASOF programme.

Using data from this programme, we first examine the water mass properties within the Faroe Shetland Channel during the 1990s. This analysis provides details of the mean, seasonal, and interannual variability of the properties of the poleward flowing surface Atlantic Water. These are then combined with mean and seasonal variations of transport, from direct measurements using ADCPs, to provide an indication of the seasonality of Atlantic Water flux through the Channel, and of the mean heat and salt transport during the 1990s. Using long-term data from the Faroe Shetland Channel, and from Ocean Weather Station "Mike" (OWSM), the 1990s are placed into a longer-term context. Finally, some aspects of the interannual variability of water mass transport, heat, and salt flux during the decade are discussed.

Background and methods

Figure 1 shows the location of the Nordic WOCE standard sections north (FN), east (FE), and south (FS) of the Faroes, along with suspected transport pathways of poleward flowing surface waters. In summary, Modified North Atlantic Water (MNAW), originating from the North Atlantic Current, crosses the Iceland–Scotland Ridge between Iceland and Faroe, and flows through the FN section as the Faroe Current before entering the Norwegian Sea basin close to the location of OWSM. Some water from the Faroe Current turns south at the eastern edge of the Faroese plateau to enter the Faroe Shetland Channel. However, most of the water from this source, which crosses the FS section, recirculates and again flows polewards at the offshore edge of the Shetland Current (Hansen and Østerhus, 2000). North Atlantic Water (NAW) flows above the slope of the northwest European continental shelf, entering the Norwegian Sea through the FS section in the Shetland Current and continuing northwards along the Norwegian Coast as the Norwegian Atlantic Current (Hansen and Østerhus, 2000).

A total of 34 CTD surveys were performed along the FS section during the period 1994–2000 by the Faroes Fishery Laboratory and the Marine Laboratory Aberdeen (Figure 2). Following initial data quality control and calibration, data have been averaged into 5-m-depth bins at each standard station. A first-order estimate of the seasonal cycles of temperature and salinity of the form

$$A = A_0 + H_0.\cos(\omega t + \phi) \qquad (1)$$

was then obtained at each depth and at each station using a least squares fitting procedure.

The FS section was also instrumented with five ADCP moorings (Figure 1 inset). In total, 6616 days of current profile measurements were recorded between 1994 and 2000 (Figure 2). Data gaps at sites D and E (Figure 1) were partly filled using ADCP data made available by the North West Approaches Group (NWAG); a consortium of oil companies working in the area. The additional data were

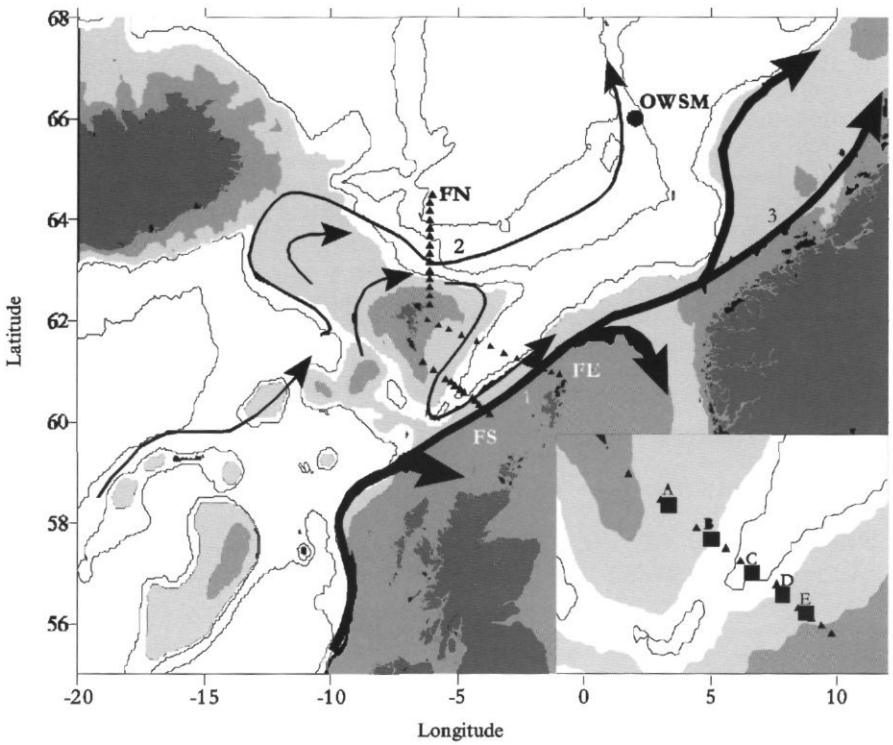


Figure 1. Map showing the location of the CTD sections (FN, FE, and FS) surveyed intensively during the 1990s by the Faroese and Scottish Fishery Laboratories, as well as Ocean Weather Station "Mike" (OWSM) run by the University of Bergen. Dark shading = depths less than 200 m; light shading = depths less than 750 m. White contour 500 m, all others at 1000-m intervals, from 1000 m. Thin black arrows = transport path of Modified North Atlantic Water (MNAW). Thick black arrows = transport path of North Atlantic Water (NAW) (after Hansen and Østerhus (2000)). The FS line with the positions of the five semi-permanent ADCP moorings (filled squares A–E) is shown inset. Numbers indicate named currents in text: 1 = Shetland Current, 2 = Faroe Current, 3 = Norwegian Atlantic Current.

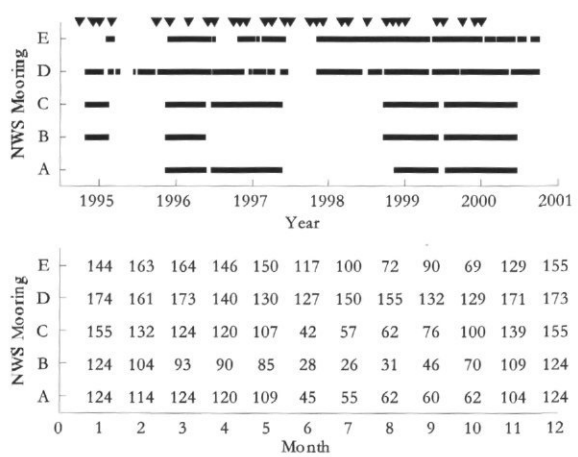


Figure 2. Data inventory for the period 1994–2000. Upper panel shows the availability of valid data from the five ADCP moorings (Figure 1) as solid lines, and the timing of surveys across the FS CTD section as filled triangles. The lower panel shows the number of valid data days per month at each of the five ADCP moorings. (Note duplicate surveys performed in November 1995, June 1996, and September 1999).

obtained from downward looking instruments attached to offshore platforms, as well as conventionally moored instruments deployed over short periods (Turrell *et al.*, 1999a). The daily mean, along-channel current velocity (towards 038°) was computed within 25-m bins, and a seasonal cycle fitted using the same procedure as that applied for temperature and salinity. Transports were computed by interpolation of the along-channel velocities onto a regular grid across the FS section, with 25-m-deep boxes centred on each standard CTD station. Seasonal variations of the flux of mass, heat, and salt were then computed using combinations of daily temperature, salinity, and current velocity, recreated for each model box using the fitted seasonal cycle parameters.

Monthly averaged observations of temperature and salinity from OWSM, derived from weekly bottle casts, were treated in the same way as a station on the FS section, and the same seasonal model applied to compute mean, seasonal, and residual temperature and salinity anomalies. In order to examine long-term hydrographic variability in the

Faroe Shetland Channel, indices of temperature and salinity variability were also calculated using data from both the FS and FE standard sections (Figure 1). The two stations on the Scottish side of both sections were used together in order to lengthen the period over which valid data were available. Data were interpolated onto standard depths, and sinusoidal seasonal models fitted at each depth in order to remove the annual cycle of temperature and salinity. The temperature and salinity of the salinity maximum observed in any one survey were then selected as the index values for NAW (Turrell *et al.*, 1999b). A similar process was carried out for the two most northern stations on each line, on the Faroese side of the Channel, in order to provide similar de-seasoned indices of MNAW temperature and salinity variability.

Results

Seasonal model sections

Figure 3 (upper panels) shows the sections of mean temperature, salinity, and current velocity derived from fitting the seasonal model to data collected along the FS section. Maximum poleward velocities (> 26 cm s^{-1}) were found in the slope current above the 500-m contour. The base of the poleward flow in the slo pe current intersected the shelf edge at 575 m, with flow towards the southwest below this depth, and at all depths offshore from Station 7. Temperature and salinity maxima lay above the 180-m contour inshore from the core of maximum poleward current.

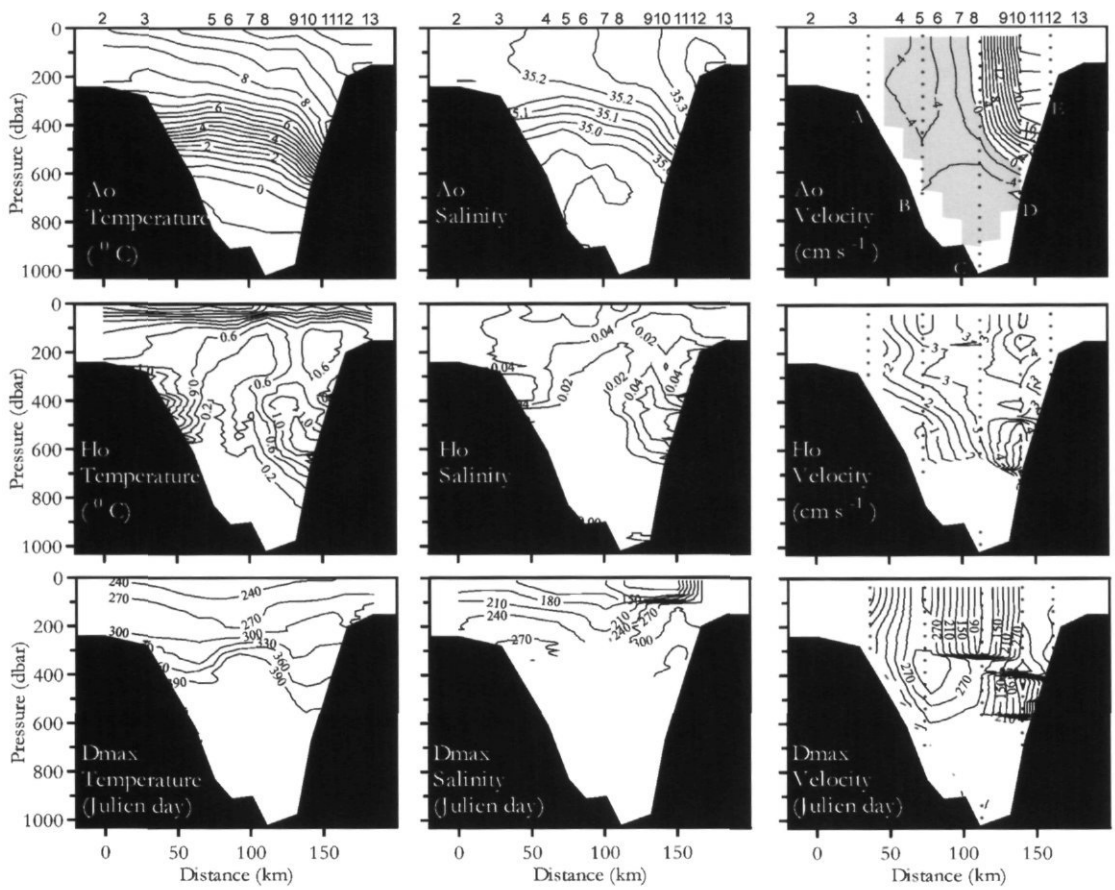


Figure 3. Upper panels = annual mean (A_0) potential temperature, salinity, and along-channel current velocity across the FS section, orientated with Faroe to the left, Scotland to the right (see Figure 1). The upper axis indicates location of the standard CTD stations (Stations 2–13). Also indicated in the velocity figures are the locations of valid data from the near-bottom ADCPs (A to E) deployed across the section in the period 1994–1999. Shading in the mean velocity figure indicates flow towards the southwest through the section. Centre panels = amplitude (H_0) of seasonal cycles. Lower panels = phase (D_{max}) of seasonal cycles presented as: Temperature and Salinity = Julien day of maximum, Velocity = Julien day of maximum northeast-going flow for bins with positive A_0 (see upper panel), and of maximum southwest-going flow for bins with negative A_0.

Amplitudes of the seasonal temperature cycle (Figure 3, centre panels) increased in the vertical uniformly across the Channel, from approximately 0.6°C at 100-m depth to 2°C at the surface. Two subsurface maxima of the amplitude of the seasonal temperature cycle lay at approximately 400 m on the Faroe side of the Channel, and at 600 m on the Scottish side, below the slope current. Both may have been associated with seasonality of the depth of the permanent thermocline. The subsurface seasonal cycle amplitude maximum on the Scottish side was repeated in the salinity and along-channel current fields. Salinity amplitudes typically varied between 0.02 and 0.04. The amplitude of the seasonal cycle of along-channel velocities was typically 0.02 to 0.03 m s^{-1}, increasing to 0.05 m s^{-1}, in the core of the slope current and at the intersection of the permanent thermocline with the shelf.

The phases of the seasonal cycles of temperature (Figure 3, lower panels) reveal that maximum temperatures in the surface waters occurred at approximately the same time across the channel, during late August and early September, with a delay to late September to early October in the core of the slope current. The time of maximum temperature propagated down through the water column, with a 2-month delay at a depth of 200 m. Surface waters exhibited maximum salinities in about June on the Faroe side of the Channel, while towards the slope current surface water salinity reached a maximum as early as April, possibly due to the reduction in salinity in surface waters caused by the offshore extension of low salinity shelf water during the summer. Salinities in the core of the slope current, however, exhibited maximum values in early October, irrespective of depth. This coincides with the maximum poleward velocity in the slope current. The maximum poleward flow at moorings D and E in the slope current, and the maximum southwestward flow at mooring B occurred at the same time, in October.

θS Curves and Water Mass Transformation Processes

The mean profiles from the FS section of temperature and salinity, from values of A_0 (see Equation (1)), are shown in Figure 4 as potential temperature–salinity (θS) curves, along with all individual θS curves observed across the section during the period 1994–1999. The mean θS properties of the surface waters can be seen to lie on the high salinity extreme of Eastern North Atlantic Water (ENAW). Only one station (Station 12, Figure 3) had mean properties which lay within the range of NAW as defined by Hansen and Østerhus (2000). Below the surface waters, the mean profiles showed an inflection

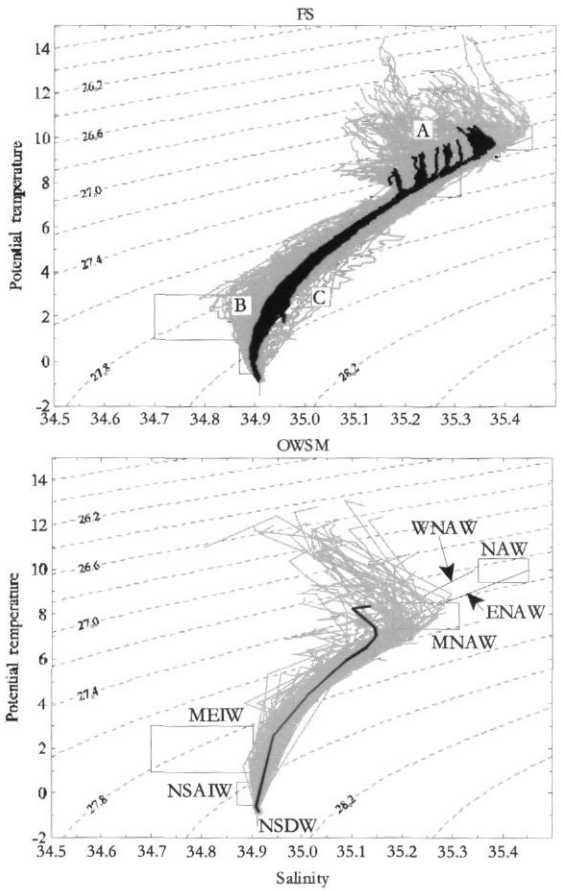


Figure 4. Potential temperature–salinity θS diagram for the (upper panel) FS section and (lower panel) Ocean Weather Station "Mike" (Figure 1). All θS curves for the period 1994–2000 are plotted in light grey. The heavy black lines indicate the mean θS profiles derived using the seasonal cycle fitted at each of the standard stations across the section. Also indicated are water mass characteristics from Hansen and Østerhus (2000). These are shown as boxes indicating the typical ranges for this region of North Atlantic Water (NAW), Modified North Atlantic Water (MNAW), Modified East Icelandic Water (MEIW), and Norwegian Sea Arctic Intermediate Water (NSAIW). The constant salinity Norwegian Sea Deep Water (NSDW) is also indicated, as are the θS boundaries of Eastern North Atlantic Water (ENAW) and Western North Atlantic Water (WNAW) shown by inflected single lines. The regions A, B, and C in the upper panel indicate regions of the θS curve where different water mass modification processes are active (see text).

corresponding to the depths influenced by Modified East Icelandic Water (MEIW), below which a salinity minimum was evident corresponding to depths receiving Norwegian Sea Arctic Intermediate Water (NSAIW). Below the NSAIW salinity increased, indicating the presence of Norwegian Sea Deep Water (NSDW).

Three distinct mechanisms for water mass transformation influencing the inflowing Atlantic Water at the FS section may be seen in Figure 4. Seasonal heating in the surface waters accounts for zone A. Analysis of individual temperature and salinity sections reveals that salinity is often reduced in the surface waters above the seasonal thermocline by the westward extension of low salinity shelf water above the saline slope current core. Hence, the warmest waters are not the most saline in the summer months. At intermediate depths the intrusion of new forms of MEIW accounts for zone B, with occasional intrusions of extremely fresh versions of this water mass. Mixing then between the MEIW and the surface Atlantic waters results in the slope of the θS curves. Direct mixing between NSDW and surface waters accounts for zone C. This generally occurs on the Scottish side of the Channel, below the slope current where the intermediate water masses MEIW and NSAIW are "pinched" out and direct contact occurs between the coldest and warmest waters in the Channel. Direct mixing between the two water masses may be the result of Ekman transport near the bed, mixing by the internal tide in the region or vertical exchange associated with mesoscale eddies.

These transformation processes have all varied through the decade of the 1990s, and have played a role in modifying the inflowing surface Atlantic waters (I-AW) entering the Norwegian Sea. Historically, the data from the FS section have been used to determine the long-term variability of the properties of I-AW, and the method most often used has been to record the temperature and salinity of the most saline water located in a survey (i.e. the apex of a θS curve). Some studies imply that this method provides a measure of the "true" temperature and salinity of Atlantic Water at some point downstream of the FS section, before any mixing with surrounding water masses has occurred. In the past, high salinity maxima have been taken as indicative of strong transport within the slope current under the implicit assumption that more rapid transport results in less reduction in salinity of the I-AW due to mixing processes. Finally, three point mixing models have been used, assuming some constancy of the three end members (NAW, MEIW, and NSAIW) to define percentage water mass distributions in the FS section. All of these concepts may be of doubtful use when computing long-term heat and salt transport across the Greenland Scotland Ridge through the FS section, and require further examination outside the scope of the present article.

Atlantic Water reaching OWSM (Figure 4) also predominantly had θS properties lying towards the higher salinity ENAW characteristic line, for $\theta > 6°C$, although water mass transformation processes had reduced the maximum salinity values observed in the surface waters compared to those observed in the Faroe Shetland Channel.

Mean transports

Table 1 presents the results of the transport calculations, using the mean sections of temperature, salinity, and along-channel velocity (Figure 3). The transports have been calculated for the surface Atlantic Water only, defined as $\theta > 6°C$. The mean net mass, heat, and salt fluxes were 3.2 Sv, 123 TW, and 115 kT s^{-1}, respectively. These values approximate to previous estimates using Nordic WOCE data (Turrell *et al.*, 1999a; Hansen *et al.*, 2000). Differences compared to the earlier estimates are accounted for by the inclusion of more data, specifically at mooring B, which had poor coverage prior to 1999, and by restricting the calculations to the Atlantic Water. There was insufficient coverage of the water column, particularly at the deeper moorings, to calculate total transports.

Seasonal variability of transports

Figure 5 shows the seasonal variation of mass, heat, and salt flux in the surface Atlantic waters. These differ from those presented by Hansen *et al.* (2000) owing to the reasons given in the previous section. While the inflow of Atlantic Water into the Norwegian Sea through the FS section on the Scottish side varied between 4.9 Sv and 3.7 Sv, the outflow towards the southwest through the section co-varied between 1.4 Sv and 0.7 Sv, resulting in the net flux through the section having a small seasonal amplitude of approximately 0.2 Sv. The corresponding amplitudes of net heat and salt flux through the section were ~20 TW and ~8 kTs^{-1}, respectively. The

Table 1. Mean transports of mass (Q), heat (H), and salt (S) through the FS section (Figure 1) in Atlantic Water ($\theta > 6°C$) for the period 1994–1999, calculated using the model described by Turrell *et al.* (1999a) and the mean values of temperature, salinity, and along-channel velocity seen in Figure 3. Positive values are directed towards the northeast. Terms in first column are: Total NE refers to transport through the section towards the northeast into the Norwegian Sea; Total SW refers to transport out from the Norwegian Sea, towards the southwest; Net refers to net transport through the FS section. Effective temperature (Tf) and salinity (Sf) calculated from overall mass, heat, and salt fluxes.

	Q(Sv)	H(TW)	S(k tonnes s^{-1})	Tf(°C)	Sf
Total NE	4.3	159	155	9.1	35.30
Total SW	−1.0	−33	−37	7.8	35.20
Net	3.2	127	118	9.5	35.33

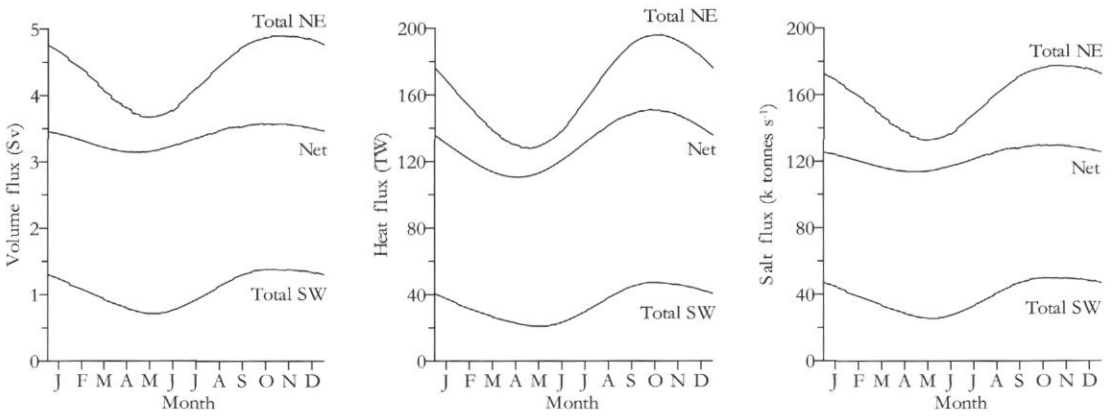


Figure 5. The calculated seasonal cycles of mass, heat, and salt flux within the surface Atlantic waters ($\theta > 6°C$). Terms in figures are: Total NE = refers to transport through the section, into the Norwegian Sea, towards the northeast. Total SW = refers to transport out from the Norwegian Sea, towards the southwest. Net = refers to the net transport through the FS section.

seasonal cycle of net mass transport seen in Figure 5 differs significantly from that of Gould *et al.* (1985). This difference has been examined extensively, and is due to two factors. Gould *et al.* (1985) did not distinguish between water masses. Hence much of their transport was of recirculated intermediate and deep waters as well as inflowing Atlantic Water. Secondly, the Gould *et al.* (1985) section only extended out from the Scottish continental shelf to the 1000-m isobath, hence did not sample the recirculating Atlantic waters on the Faroese side of the Channel.

Decadal variability of water mass properties

Figure 6 shows the residual temperature and salinity indices for the two principal Atlantic water masses observed in the Faroe Shetland Channel (NAW and MNAW) for the period 1900–2000, and of Atlantic Water at OWSM for the period 1948–2000. The temperature index derived for NAW exhibited quite large variability during the period 1900–1940, with frequent cold periods. From 1940 to 1965, temperatures were more stable, and generally warmer than average. The period 1965–1975 was persistently cold, followed by an overall warming trend for the remainder of the record, with decadal scale variability similar to that of the North Atlantic Oscillation (NAO) over the same period (Hurrell, 1995). Prior to 1965, there did not seem to be any relationship with the NAO. Salinity showed a similar development to that of temperature, with generally negative salinity index values during the 1900–1940 period, positive values during the middle period of the century, ending in the freshening event of the mid-1970s. Salinity variability during the final 30 years again followed similar trends to that of the NAO over the same period, imposed upon a general increase in salinity.

The temperature index for MNAW showed a similar development over the century as for NAW, but with a significant warm episode between 1955 and 1965, and a less marked warming trend during the last decades of the century. This was repeated at OWSM. Salinity index values within the MNAW varied similarly as those within NAW, but with greater amplitude. For example, the mid-1970s freshening event was more marked in MNAW compared to NAW, and in fact greater in amplitude at OWSM than within the MNAW. The general trend towards the end of the century of rising salinity in NAW was not so marked in the MNAW, and at OWSM there was an overall freshening in the last few decades.

Table 2 presents the trends over the whole records (1900–2000 for MNAW and NAW, 1948–2000 for OWSM). The NAW index exhibited a general warming trend over the century of 0.03°C decade^{-1}, compared to a more rapid warming of 0.36°C decade^{-1} during the 1990s. The salinity index showed no significant trend over the century as a whole, but an increase of 0.06 during the last decade. Both MNAW and OWSM had an overall cooling over the entire length of their records. However, MNAW exhibited a warming of similar magnitude as observed within NAW during the 1990s, whereas OWSM had a warming trend about one-third of that of NAW or MNAW. Both MNAW and OWSM exhibited freshening during the 1990s.

Discussion

The decade of the 1990s has been perhaps the most intensively monitored period, in terms of the surface

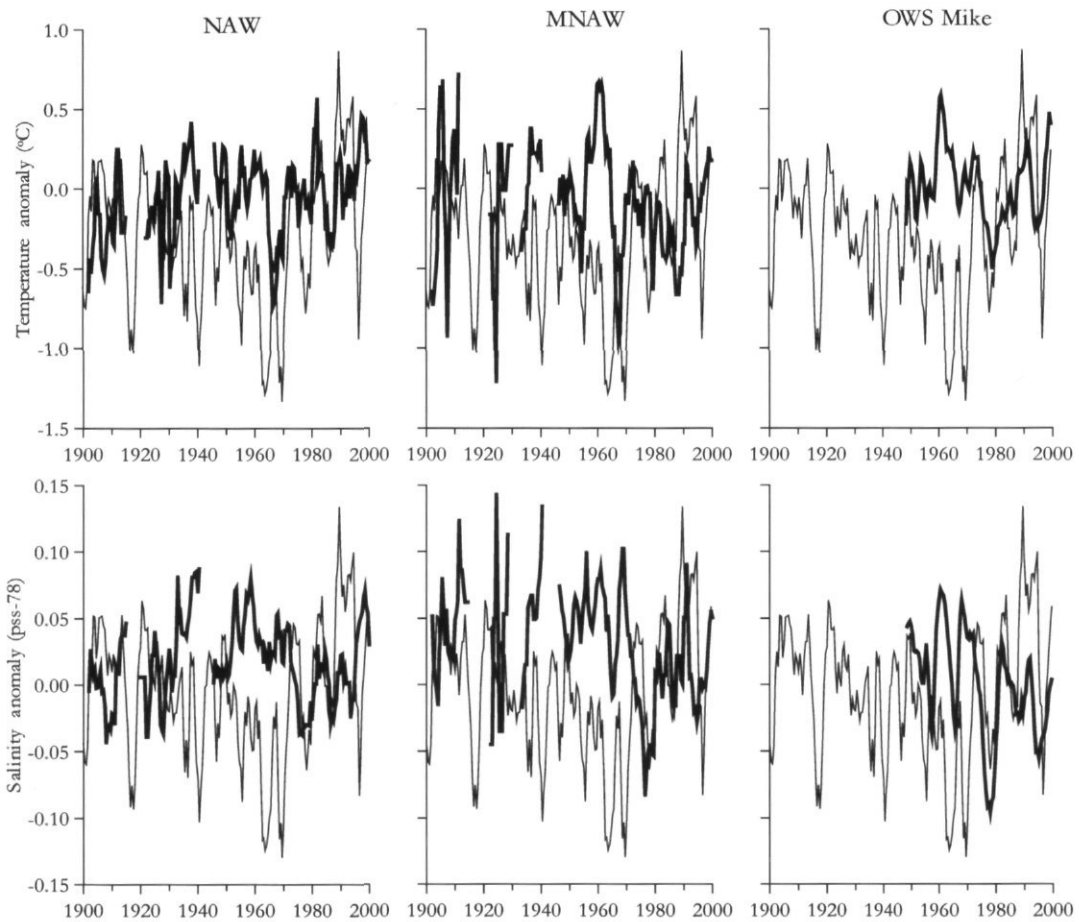


Figure 6. Index values of temperature and salinity variability within North Atlantic Water (NAW) and Modified North Atlantic Water (MNAW) in the Faroe Shetland Channel, and surface Atlantic water at Ocean Weather Station "Mike" (OWSM) (heavy lines). NAW index = the temperature and salinity anomaly (seasonal cycle removed) at the standard depth which exhibits the maximum salinity within an individual survey of the two most southeasterly stations, on both the FS and FE standard sections, on the Scottish side of the Channel. The criteria were designed to produce the characteristics of the NAW lying within the slope current at the Scottish shelf edge, typified by a salinity maximum on a θS diagram. MNAW index = the temperature and salinity anomaly (seasonal cycle removed) at the standard depth which exhibits the maximum salinity within an individual survey of the first two stations, on both the FS and FE standard sections, on the Faroese side of the Channel. OWSM index = temperature and salinity anomaly (seasonal cycle removed) averaged over the upper 100 m. Light line = NAO index following Hurrell (1995). All time-series have been filtered using a 2-year running average.

Table 2. Rates of change of temperature (°C decade^{-1}) and salinity (decade^{-1}) over the whole record length (1900–2000 for North Atlantic Water (NAW) and Modified North Atlantic Water (MNAW), 1948–2000 for Ocean Weather Station "Mike" (OWSM) indicated by italics), and over the decade of the 1990s.

	1900–2000 *(1948–2000)*		1990–2000	
	dT/dt °C decade^{-1}	dS/dt decade^{-1}	dT/dt °C decade^{-1}	dS/dt decade^{-1}
NAW	0.03	<0.01	0.36	0.06
MNAW	–0.04	–0.01	0.34	–0.01
OWS Mike	*–0.02*	*–0.01*	0.11	–0.02

Atlantic Water entering the Arctic mediterranean across the Greenland Scotland Ridge, since instrumental records began. The results have provided the best estimates yet of mean and seasonal water mass characteristics and along-channel velocities, giving a fairly complete picture of the slope current, and the recirculating surface waters within the Faroe Shetland Channel. The combination of regular CTD surveys, permitting the correct resolution of the seasonal cycle of temperature and salinity, with semi-permanent ADCP moorings has allowed mean and seasonal transports of mass, heat, and salt to be calculated. The longer-term hydrographic observations, a century long in the Faroe Shetland

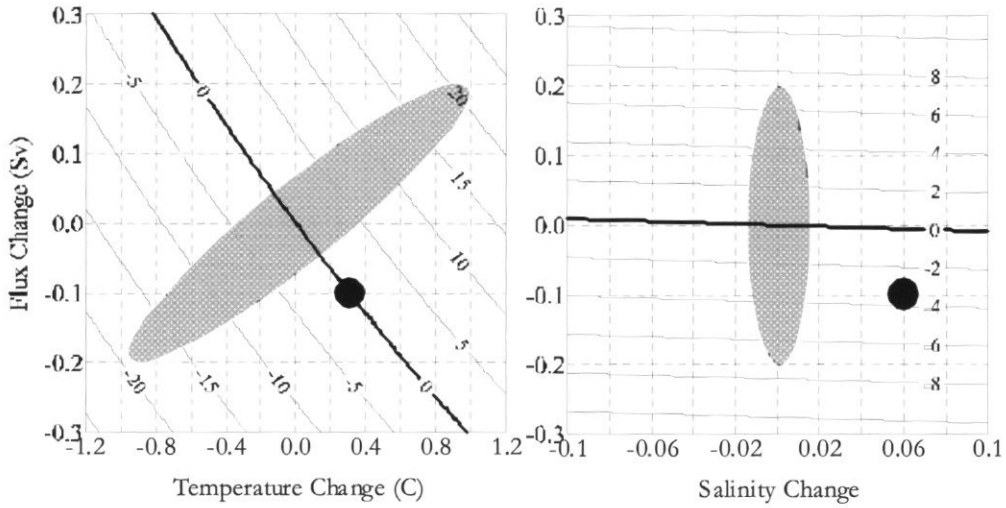


Figure 7. The relationships between the variability of temperature (T), salinity (S), and transport (Q), and the resulting changes in heat flux (Q_h, where $Q_h = \rho.C_T.T.Q$; ρ is ambient density; and C_T specific heat constant) and salt flux (Q_s, where $Q_s = \rho.S.Q$). The ranges used for temperature and salinity variability, as well as for transport change, are within the range of observed seasonal and decadal change. Horizontal axes are temperature change (°C) and salinity change. Vertical axis is mass transport change (Sv). Contoured values are: left = heat flux change (TW), right = salt flux change (kTs^{-1}). The shaded ellipses indicate the typical seasonal variability of heat and salt flux in the 1990s, the black circles show one possible decadal change scenario under present warming (0.36°C decade^{-1}) and salinity increase (0.06 decade^{-1}) conditions (Table 2), assuming a decrease of transport of 0.1 Sv decade^{-1}.

Channel, and half a century long at OWSM, has permitted the decade of the 1990s to be placed in a centennial scale context.

Two aims remain unaddressed when considering transports of mass, heat, and salt through the Faroe Shetland Channel: to examine and quantify short-term (days–weeks) transport variability and to estimate decadal scale transport variability. The former is frustrated by the lack of high frequency hydrographic observations, while the latter suffers from the absence of long-term velocity measurements.

Estimates of decadal scale variability of mass, heat, and salt transport into the Norwegian Sea are important requirements of climate studies. From consideration of the heat and salt flux equations, it is evident that, over the observed range of seasonal and decadal salinity variation in the Faroe Shetland Channel, salt flux through the Channel is almost independent of salinity change and varies directly with mass transport (Figure 7), while the observed seasonal and decadal temperature changes in the Channel are great enough to influence heat transport.

We presently do not have long enough records to be able directly to estimate the transport variation over a 10-year period. However, based on existing information we may arrive at a hypothetical scenario for the decade of the 1990s. In one recent study (Hansen *et al.*, 2001) a 20% decline in outflow was reported through the Faroe Bank Channel since 1950, corresponding to a decline of 0.5 Sv, or approximately 0.1 Sv decade^{-1}. It could be assumed that the inflow of Atlantic Water towards the Arctic decreased at a similar rate. Under a climate change scenario of warming and salinity increase in Atlantic Water as at present (i.e. 0.36°C decade^{-1} and 0.06 decade^{-1}), but a reduction of inflow of 0.1 Sv decade^{-1}, heat flux towards the Arctic remains unchanged, while salt flux reduces by 4 kT s^{-1} decade^{-1} (or by 3% decade^{-1}).

We do not yet know how inflow is changing decadally, and how the Faroe Shetland Channel inflow relates to the inflow north of the Faroes, in the Faroes Current, but certainly salt flux must be considered as well as heat flux if we are to determine the influence these changes may have on the thermohaline circulation. The present observation of freshening throughout the Nordic Seas may be partly related to a decline in salt flux across the Greenland Scotland Ridge. These ideas are forming part of an ongoing study.

References

Dooley, H. D., and Meincke, J. 1981. Circulation and water masses in the Faroese Channels during Overflow '73. Deutsche Hydrographische Zeitschrift, 34: 41–54.

Gould, W. J., Loynes, J., and Backhaus, J. 1985. Seasonality in slope current transports NW of Shetland. ICES CM 1985/C: 7.

Hansen, B., Jonsson, S., Turrell, W. R., and Østerhus, S. 2000. Seasonal variations in the Atlantic water inflow to the Nordic Seas. ICES CM 2000/L: 03.

Hansen, B., Larsen, K. M. H., Østerhus, S., Turrell, W. R., and Jonsson, S. 1999. The Atlantic Water inflow to the Nordic Seas. International WOCE Newsletter, 35: 33–35.

Hansen, B., Malmberg, S. A., Salen, O. H., and Østerhus, S. 1986. Measurement of flow north of the Faroe Islands June 1986. ICES CM 1986/C: 12.

Hansen, B., and Østerhus, S. 2000. North Atlantic–Nordic Seas Exchanges. Progress in Oceanography, 45: 109–208.

Hansen, B., Turrell, W. R., and Østerhus, S. 2001. Decreasing overflow from the Nordic seas into the Atlantic Ocean through the Faroe Bank Channel since 1950. Nature, 411: 927–930.

Helland-Hansen, B. 1903. Faeroe–Shetland Channel and the northern part of the North Sea in the year 1902. Northern Area First Report 1902–1903, North Sea Fisheries Investigation Committee, Fishery Board for Scotland.

Helland-Hansen, B., and Nansen, F. 1909. The Norwegian Sea. Fiskeridirektoratets Skrifter Serie Havundersøkelser, 2: 1–390.

Hurrell, J. W. 1995. Decadal trends in the North Atlantic Oscillation: regional temperatures and precipitation. Science, 269: 676–679.

Sherwin, T. J. 1991. Evidence of a deep internal tide in the Faroe–Shetland Channel. *In* Tidal Hydrodynamics, pp. 469–488. Ed. by B. B. Parker. John Wiley, Chichester.

Steele, J. H. 1967. Current measurements on the Iceland –Faroe Ridge. Deep-Sea Research, 14: 469–473.

Tait, J. B. 1957. Hydrography of the Faroe–Shetland Channel 1927–1952. Marine Research Scotland, 2: 309.

Turrell, W. R., Hansen, B., Østerhus, S., Hughes, S., Ewart, K., and Hamilton, J. 1999. Direct observations of inflow to the Nordic Seas through the Faroe Shetland Channel 1994–1998. ICES CM 1999/L: 01.

Turrell, W. R., Slesser, G., Adams, R. D., Payne, R., and Gillibrand, P. A. 1999b. Decadal variability in the composition of Faroe Shetland Channel Bottom Water. Deep-Sea Research, 46: 1–25.

ICES Marine Science Symposia, 219: 121–131. 2003

Decadal variations in the stratification and circulation patterns of the North Sea. Are the 1990s unusual?

Corinna Schrum, Frank Siegismund, and Michael St. John

Schrum, C., Siegismund, F., and St. John, M. 2003. Decadal variations in the stratification and circulation patterns of the North Sea. Are the 1990s unusual? – ICES Marine Science Symposia, 219: 121–131.

The variability of transport processes and stratification in the North Sea is investigated using the results of a 40-year simulation with the 3-D hydrodynamic model HAMSOM (HAMburg Shelf Ocean Model). The results show that there is considerable variability of physical processes potentially impacting on ecosystem dynamics. Stratification and transport processes are characterized by year-to-year variability. However, resolution of decadal variability is possible. Long periods with similar stratification as well as transport conditions have been resolved and the 1990s have been identified as having been an outstanding period with respect to two key biologically relevant physical parameters both potentially impacting on the ecosystem dynamics; the exchange flow into the North Sea and Skagerrak in February/March and the timing of the onset of stratification in spring. There is pronounced interannual variability and a comparison of variability in different seasons indicates that the between-season correlations are small for water transports as well as for stratification conditions.

Keywords: circulation, decadal variability, North Sea, stratification.

Corinna Schrum [e-mail: schrum@dkrz.de] and Frank Siegismund: Zentrum für Meeres- und Klimaforschung der Universität Hamburg, Institut für Meereskunde, Troplowitzstr. 7, D-22529 Hamburg, Germany. Correspondence to C. Schrum.
Mike St. John: Zentrum für Meeres- und Klimaforschung der Universität Hamburg, Institut für Hydrobiologie und Fischereiwissenschaft, Olbersweg 24, D-22767 Hamburg, Germany.

Introduction

The influence of environmental conditions on the marine ecosystem has been the subject of discussion over the past 5–10 years. International research programmes such as GLOBEC have been established to investigate the linkage between environmental conditions and ecosystem dynamics. Furthermore, national and international projects (LIFECO, GLOBEC related projects) and international workshops (e.g. ICES Backward-Facing Workshops) have been initiated in order to improve the understanding of environmental variability and its impact on higher trophic levels in the marine ecosystem. The first natural step towards a comprehensive understanding of ecosystem variability is the investigation of the effects of climate variability on the physical environment, i.e. on the physical features that control the ecosystem dynamics.

Recently, many attempts have been made to investigate the climatically induced long-term variability in the North Sea. A couple of investigations have been based on the analysis of observational data focused, in particular, on quasi-synoptic surface data (e.g. Becker and Pauly, 1996; Dippner, 1997) and on long-term hydrographic time-series (e.g. within the NOWESP project; Sündermann *et al.*, 1996). Although valuable understanding was achieved, e.g. on the connection between winter North Atlantic Oscillation (NAO) and sea surface temperature (SST) in the North Sea, observational data are sketchy in time and space and thus investigation of variability based on field data is strongly limited. In particular, field-based studies on the variability of subsurface conditions such as water column stability and intensity and duration of thermal stratification, key to resolving the timing of the spring bloom as well as transport of nutrients into the euphotic zone, are rare. Furthermore, studies examining intra-annual and interannual variations in transport, impacting on the invasion of *Calanus finmarchicus* into the North Sea as well as on the

transport of fish eggs and larvae from spawning to nursery areas, are limited. Both of these transport processes have been proposed to impact on North Sea fish stocks (e.g. Heath and Gallego, 1998; Heath *et al.*, 1999; ICES, 2001).

Realistic hindcast simulations provided by complex numerical models are valuable tools to fill this gap and to provide more information on the variability in the physical marine environment. Deterministic numerical models can be used to interpolate dynamically in space and time, depending on the prescribed boundary forcing and initial conditions. This has been done in the past in the North Sea by several authors (e.g. Kauker, 1999; Langenberg *et al.*, 1999; Pohlmann, 1996; Smith *et al.*, 1996). These models have been integrated for different periods, and describe the hydrodynamic state of the North Sea on different levels of spatial and temporal resolution.

A similar model, the HAMburg Shelf Ocean Model (HAMSOM), has been utilized to examine the dynamics of the coupled system of North Sea and Baltic Sea (Schrum, 1997a) to provide a more realistic description of the exchange flow between both seas. In particular, it has been used to study two different periods, namely 1979–1993 and 1958–1997. In the following, results of the latter longer run will be used to investigate the decadal and interannual variability of stratification and circulation in the North Sea in order to relate the 1990s to trends over previous decades. As the variability of stratification and circulation in the North Sea is closely connected with the atmospheric variability, in particular the windfield variability, the discussion of oceanic conditions (model results) will not be separated from the discussion of forcing wind conditions.

Model configuration

The model is based on the HAMSOM, which has been described in detail by Schrum and Backhaus (1999). The model region, the North Sea from 49° to 59°N and the Baltic Sea, is resolved with a horizontal resolution of 10 km ($\Delta\varphi = 6'$ and $\Delta\lambda = 10'$) and by a maximum of 20 vertical levels. The vertical resolution is 5 m from surface to 40 m, 8 m from 40 to 88 m with subsequent depth layers at 100, 125, 150, 200, 400, and 630 m.

To investigate the impact of climatic induced variability, the model employs forcing from consistent atmospheric gridded data sets. Typically these atmospheric data sets are provided by weather services, using an analysis model to interpolate the sketchy meteorological observations in time and space. Since the analysis and forecast models have been changed many times from the beginning of the operational analysis, the resulting long-term data sets are highly heterogeneous and thus not suitable for describing climate variability of the atmosphere. This was the motivation to set up independent re-analysis projects by the European Center of Medium-Range Weather Forecast (ECMWF) and by the NCEP/NCAR to provide consistent global 3-D atmospheric data sets. The re-analysis has been carried out with a 'frozen' version of the data assimilation system for the respective hindcast periods ECWMF: 1979–1993 (ERA-15); NCEP: 1958–1997 (NCEP-40)). The main features of the assimilation schemes can be characterized as follows: The horizontal resolution corresponds to the spectral wave number T106 (ECMWF, about 1.1°) and T62 (NCEP, about 2°); the time stepping of the models output corresponds to 6 h, i.e. 4 times daily. More details about the re-analysis project of the ECMWF have been given by Gibson *et al.* (1996), while for the NCEP/NCAR re-analysis project a detailed description is presented in Kalnay *et al.* (1996).

The HAMSOM has been integrated for both re-analysis periods. The initial conditions for the respective runs are provided by the climatology for temperature and salinity as presented by Janssen *et al.* (1999), with additional corrections in the initial state for 1958 and 1979 (based on the ICES database that was also used for the climatology). At the open boundaries, sea surface elevation was taken from a coarser shelf sea model (for details, see Schrum *et al.*, 2000). Boundary conditions for temperature and salinity were prescribed based on climatological temperature and salinity data from Janssen *et al.* (1999), with an additional annual correction calculated from the ICES database. More information regarding the incorporation of freshwater run-off boundary forcing and validation of the model sensitivity is given by Schrum *et al.* (2000).

Detailed analysis of the skill of the model using ECMWF atmospheric forcing data are presented by Schrum *et al.* (2000) and Janssen *et al.* (2001). In these studies it was shown by comparisons to tide gauges, *in situ* and satellite data that sea surface elevation, sea surface temperature, salinity and sea ice were described with considerable accuracy. Correlations of observed and modelled sea surface elevation, which is a measure for the quality of modelled volume transports, are in the order of 0.9 for different tide gauges in the Baltic and along the continental coast of the North Sea. Correlations along the British coast are slightly lower (about 0.8). It should be recognized that a detailed validation has not yet been carried out using the NCEP-40 generated estimates. However, the overlapping period of both runs will be used to compare the estimates of both model realizations and thereby compare the behaviour of the latter model configuration with respect to the description of variability.

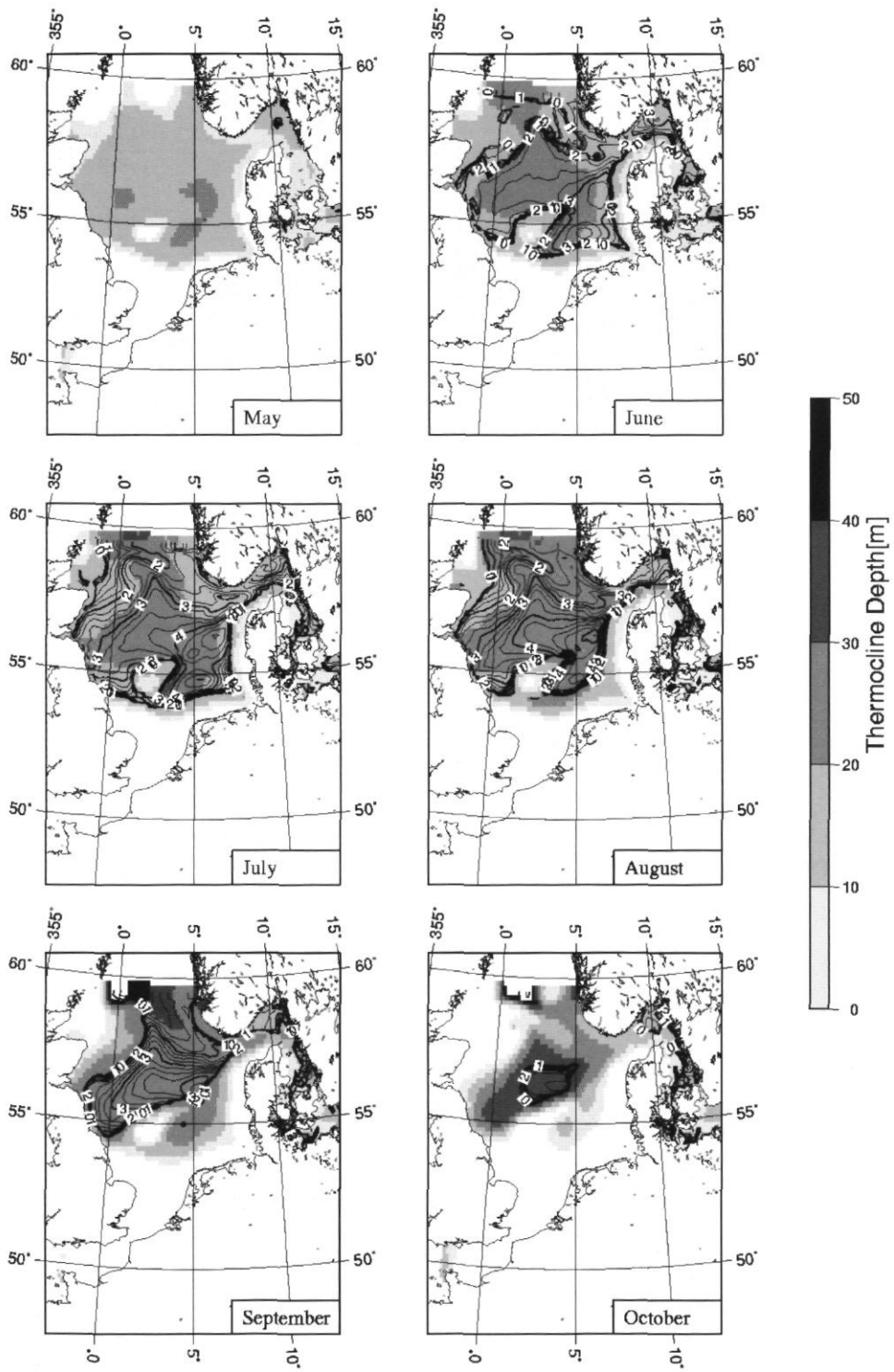


Figure 1. Calculated monthly mean stratification pattern for the period 1958–1997. The contour lines give the maximum temperature difference across the modelled thermocline. Contour levels are 0.25°C. The shading indicates the depth level (m) of the maximum gradient.

Stratification

Methods and general remarks

The monthly mean stratification pattern calculated by the model in response to the NCEP-40 forcing is presented in Figure 1 in terms of temperature difference across the thermocline. Here, the thermocline is assumed to be located at the depth of the strongest temperature difference between the vertical levels. Furthermore, we assume that the critical level for defining stratified conditions is a temperature difference of at least 0.5°C between the levels. Information on the depth of the thermocline is provided by contouring. Additional information about the depth of the thermocline is given by the shaded area. However, it should be noted that these estimates are strongly limited by the coarse vertical resolution of the model, as the estimates are based on a 5-m integrated value in the surface layers.

It is possible that the stratified area identified by the pattern of temperature difference is larger than the shaded area estimated from mean thermocline depth. This could be explained as follows: the temperature difference is to be interpreted as a monthly mean difference, unstratified situations included as zero temperature difference. It is thus possible that, after averaging, the monthly mean temperature difference at a respective grid point is less than the critical temperature difference of about 0.5°C. Hence, the respective grid point appears as unstratified in the contouring of Figure 1. The mean thermocline depth is estimated slightly differently, i.e. only the stratified conditions are taken into account. It is therefore possible that an estimate of the thermocline depth is based on only a few (or possibly only one) stratified days. This implies that the mismatch between the two respective patterns is also a measure of variability in the respective averaging period.

Seasonal cycles and extreme situations

Comparison of the modelled stratification pattern to estimates based on climatological data analysis (Janssen *et al.*, 1999) shows that seasonal extension and intensity of stratification are similar for model results and observations. The onset of stratification occurs in May with thermocline depths between 10 and 20 m. Strongest mismatches between the pattern of thermocline intensity and thermocline depth are found at the beginning and end of the stratified period, i.e. in May and October. The onset and breakdown of stratification are subject to strong interannual variability. Thus, the resulting climatological mean temperature difference in May and October is below 0.5°C for almost the whole area, indicating climatologically unstratified conditions. However, occasionally stratification has developed in May, as shown in the monthly mean pattern for May 1993 (Figure 2), and can persist in a diagonal band across the northern North Sea until October.

The maximum temperature gradient increases continuously during the summer, reaching its maximum values in August. Local maxima up to 5°C can be found in the eastern North Sea, off the Jutland coast. Significant deepening of the thermocline occurs from July onwards caused by increasing windspeed (not shown here) and decreasing heating from short wave radiation, resulting in increasing vertical mixing due to wind induced turbulence and thermal convection. This process is connected with a decrease in the stratified area.

Variability of stratified conditions can be also be detected from the monthly mean model data. In the summer months, variability occurs roughly in a band of 100 km extension (June, July), which expands until the breakdown of stratification, starting in the region of the shallower southeastern North Sea in August. The variability here is strongly

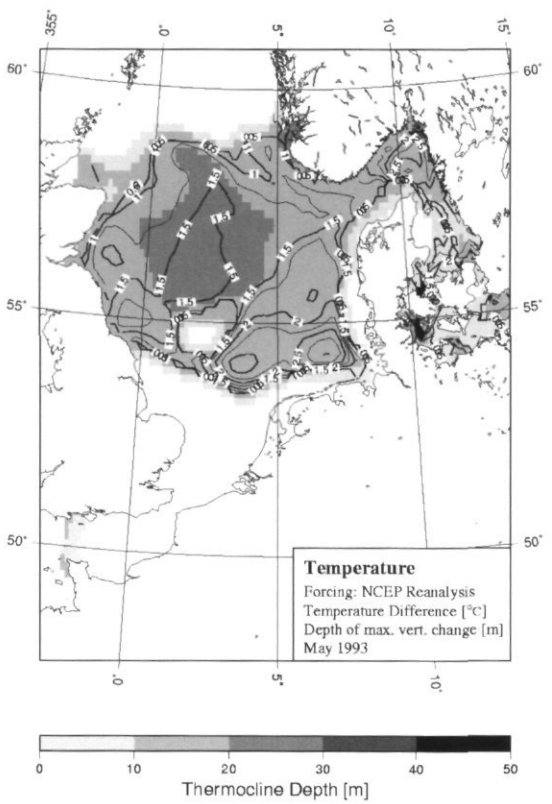


Figure 2. Calculated stratification for May 1993, an extremely stratified situation. Contour lines give the maximum temperature difference across the modelled thermocline; the shading indicates the depth level (m) of the maximum gradient. Contour levels are 0.25°C.

connected to windspeed and wind direction changes, with tidal and wind-induced turbulent mixing limiting stratification. Along the continental coast, offshore wind-induced transport of less saline surface water has a stabilizing effect on the water column and allows the development of thermal stratification even very near the coast, where tidal mixing is high. The near surface advection of less saline coastal waters offshore, connected to more easterly and northerly wind forcing, is responsible for a stabilization of the water column and counteracts the strong tidal and wind induced stirring. This was earlier investigated for the region of the German Bight by Schrum, 1997b and it was found that a necessary pre-condition for near-coastal stratification was the wind-induced haline stratification.

To answer the question whether the variability results in coherent patterns of monthly distribution, i.e. to estimate whether the variability occurs on interannual rather than on intra-monthly time scales, two extreme conditions are presented in Figure 3: The August 1997 situation shows high temperature differences between layers of up to 6.5°C and an extended near coastal stratification towards the Danish and German coasts. A contrasting situation was seen in August 1985, when stratification was at a minimum. The maximum temperature difference across the thermocline was 1.5°C less than maximum values reached in August 1997. In August 1985 the near coastal region is unstratified, with stratification found only west of 7°E. The pattern was coherent for the whole month, with the variability below the monthly time scale being small, as indicated by a good correspondence of the shaded region (estimated only for the stratified cases) and the contoured area (averaged over all cases).

In Figure 4, the respective wind density distributions are presented for the region of the eastern North Sea (2.5°E–10°E). The wind density is calculated from the 6-hourly values of the NCEP re-analysis by division of the wind rose into 36 classes, i.e. 10° steps were chosen. The angle of 0° corresponds to wind blowing from the East. Within the respective classes k, the wind speeds v^i_j (i and j indicate the position of the respective event in time and space) were summed and normalized by the total number of events. The normalized wind density function for a respective class k is defined as:

$$w_k = \sum_{c(i,j)=k} v^i_j \frac{\text{number of classes}}{\text{total number of events}}$$

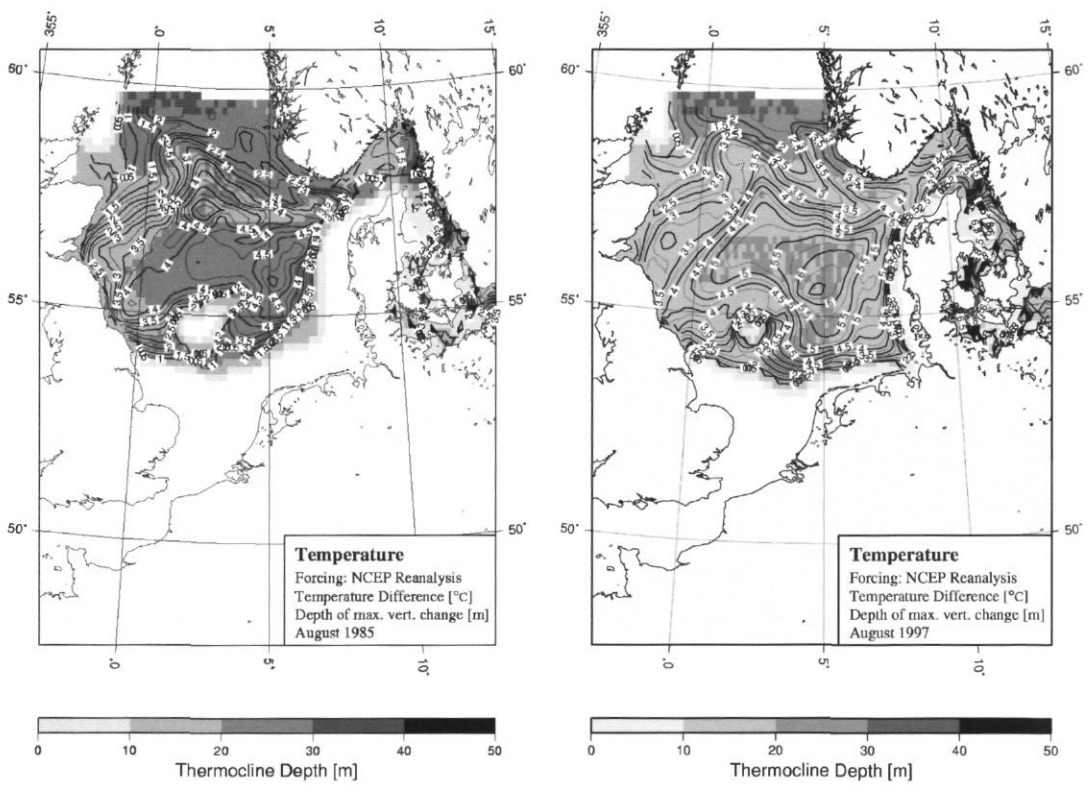


Figure 3. Calculated stratification for two extreme situations in August: extended stratification in August 1997 (right) and less extended stratification in August 1985 (left). Contour lines give the maximum temperature difference across the modelled thermocline; the shading indicates the depth level (m) of the maximum gradient. Contour levels are 0.25°C.

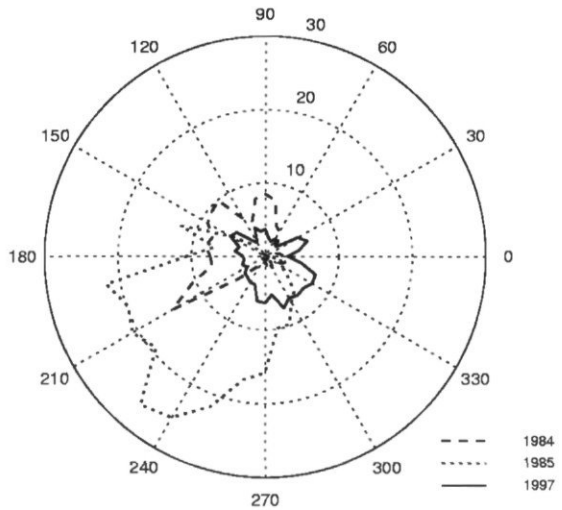


Figure 4. Normalized wind density distribution for August 1984 (stable stratification occurred), August 1985 and August 1997. The wind density function for class k is defined as

$$w_k = \sum_{c(i,j)=k} v_j^i \frac{\text{number of classes}}{\text{total number of events}}$$

According to the definition of the wind density function, high values indicate high frequency of winds blowing from a respective direction or result from high windspeeds. Increasing total area of the wind density function (over all classes) indicates an overall increase in windspeed. Further details about the calculation of the wind density function are given by Siegismund and Schrum (2001). Comparing the forcing wind field for the two years 1985 and 1997, and for 1984, which is also an example of an intensively stratified situation, the reason for the different stratification pattern is understandable: For the extreme stratified situations, the August wind distribution show only weak winds. Prevailing wind directions are east (1997) and northwest (1984), favouring stratification by offshore advection of fresher coastal waters. Contrasting wind forcing can be found for August 1985. Here, the prevailing wind direction was southwest, resulting in near-coastal northward advection of the coastal waters and no haline stratification. The larger area covered by the wind density pattern in August 1985 indicates higher windspeeds compared to 1984 and 1997, which results in increasing wind mixing and thus faster stratification breakdown.

Interannual and decadal variability

Investigation of interannual and decadal stratification variability was focused on the southeastern North Sea in a coastal band from 3°E to the continental coast for latitudes between 52.5°N and 56.5°N, an area found to be representative of the changes in the whole North Sea system and, furthermore, a key habitat for juvenile cod (e.g. St. John and Lund, 1996). Stratified grid points were identified by the critical temperature difference of 0.5°C, to be reached in monthly mean values. The onset of stratification differs strongly from year to year, as can be seen in Figure 5, where the stratified area in terms of stratified grid points (each corresponding to an approximate area of about 100 km^2) are shown. A 5-year running mean shows that more stratified periods and periods with less stratification (caused by frequent unstratified years) can be distinguished on longer time scales. It is obvious from Figure 5 that a long period with less unstratified conditions in May exists from 1967 to 1985. Contrastingly, from the mid-1980s to the end of the investigation period, the North Sea tends to be stratified again earlier in the year, with only 2 exceptions in 1992 and 1997. Most of the years with highest extent of stratification can be found within this latter period, at the end of the 1980s and the 1990s from 1986–1991 and 1993–1996.

A similar outstanding period can be found by analysing the distribution of stratification in August. The modelled extent of stratification is significantly higher during August from 1963 to 1984. This is followed by a period with low stratification from 1985–1994 with increasing stratification for the last years of the investigation period.

The year-to-year variability late in the year is less compared to the decadal trends for this period. The higher frequency variability, which is dominant at the beginning of the stratified period, is damped during the summer. The respective curves for June and July are given in Figure 5. In principle, they confirm this with higher frequency variability (i.e. the year-to-year variability) stronger earlier in the year. The variability in July is similar to that in August, whereby stratification in June is only weakly correlated to pattern earlier and later in the year. This is the case for the year-to-year variability as well as for the filtered time-series. The only coherent signal in June, July, and August is found for the year 1962 when stratification shows a significant minimum after relatively strong stratification in May 1962.

Circulation

General circulation

The typical circulation pattern in the North Sea shows a prevailing cyclonic circulation with inflow

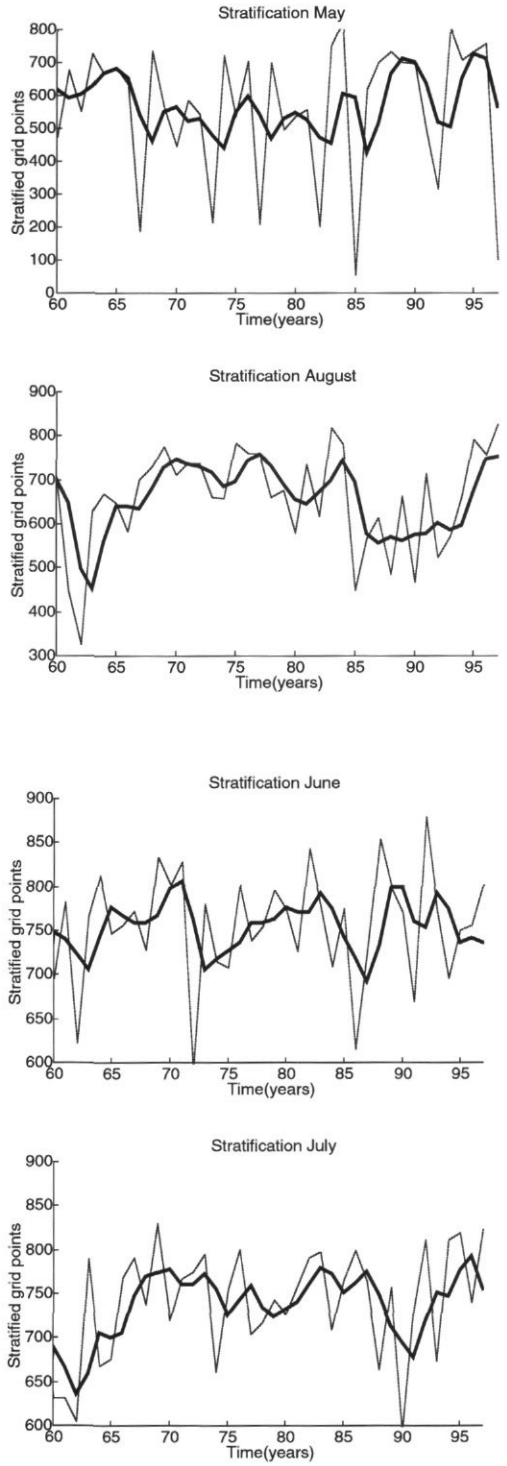


Figure 5. Interannual variability of the stratified area in a band from 3°E–10°E and 52.5°N–56.5°N. The stratified area is given in units of grid points, each approximately corresponding to an area of 100 km^2, annual values (thin line, dashed) and 5-year moving average (thick line). May (upper left) and August (lower left), June (upper right), and July (lower right).

of salty Atlantic Water along the western and central part of the northern boundary (about 1 Sv in annual mean) and outflow of less saline water from the Norwegian Coastal Current (about 1.13 Sv), as presented earlier by a large number of authors (e.g., see the review article by Rodhe, 1998). From the Baltic Sea, typically a net outflow of freshwater occurs, which is potentially compensated on shorter time scales by a wind-induced inflow into the Baltic Sea. The annual mean net exchange between the North Sea and the Skagerrak shows a complicated flow regime with near-surface inflow in the northern Skagerrak and near-surface outflow in the southern part (inflow and outflows are named from the view to the North Sea). Vertically integrated, this picture changes into a net outflow in the northern Skagerrak and a net inflow in the southern part. This typical circulation pattern is reproduced by the model, with results in close correspondence to earlier work (e.g. Rodhe, 1998; Lenhart and Pohlmann, 1997) as the earlier analysis of Schrum *et al.* (2000) has already indicated.

Transport variability

The volume transports across the boundaries show significant variability on all time scales. It should be noted, however, that below the daily time scale, tidal advection plays the most important role in the variability of the water transports. On longer time scales, the net tidal transports across the open boundaries are negligible, relative to the wind-induced variability; the most important forcing parameter influencing circulation variability. In order to identify seasonal variability we distinguished four different situations: The winter situation with wind forcing mainly dominated by southwesterly winds (Oct–Jan), the late winter (Feb–Mar), characterized by winds from westerly-southerly to easterly directions, April–May with wind forcing from all directions, and finally the summer period (Jun–Sep), which is characterized by less intense wind forcing, mainly from westerly directions. This classification was chosen based on windfield analysis of the monthly mean windfields from the NCEP-40 data set. The criteria for the classification of the seasons were the similarity of the monthly mean windfields.

Significant transport anomalies occur for all investigated seasons on all inflow and outflow sections of the North Sea. First we examined the section Orkney to Norwegian Trench (from 3°W–3°E, 59°20, 5′N), where the main inflow into the North Sea takes place. Figure 6 shows the monthly mean inflow anomalies (positive anomalies indicate higher inflows) during the four periods of interest. The fifth curve in black-dashed is given for validation purposes and

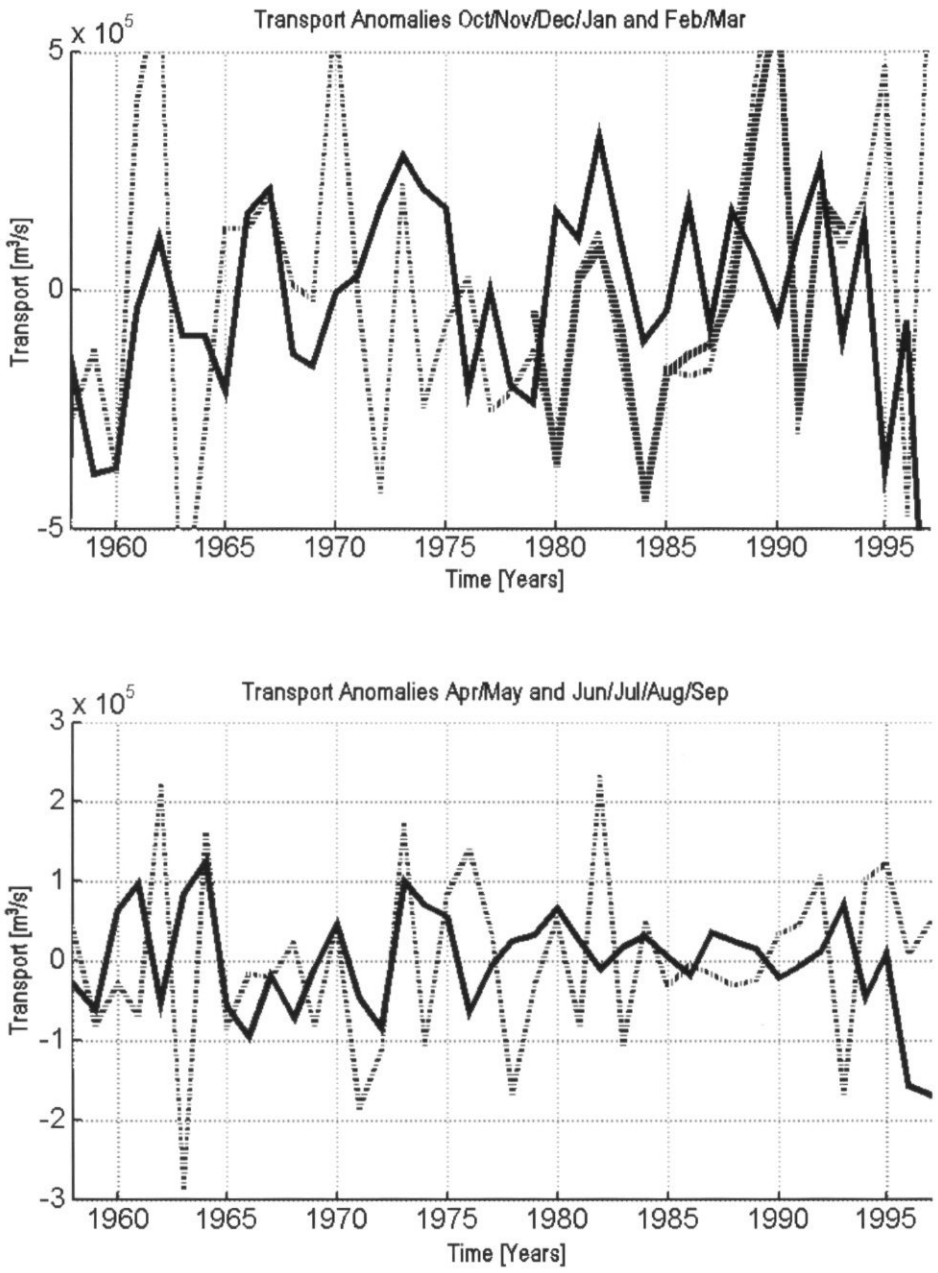


Figure 6. Transport anomalies of North Sea inflows for four respective seasons. The seasons are chosen to be Oct/Nov/Dec/Jan (I, upper solid), Feb/Mar (II, upper dashed-dotted and dashed from ERA-15 forcing), Apr/May (III lower dashed-dotted) and Jun/Jul/Aug/Sep (IV lower solid).

shows the anomalies calculated from the 15-year ECMWF forced run. The two runs came up with almost identical variability and hence support the utility of the NCEP-40 outputs.

The strongest variability on a monthly time scale was found for the North Sea/Skagerrak exchange. Here, the variability at the northern open boundary ranged from 10% to 50% of the annual inflow, depending on the season. Comparing the correlations between the anomalies in different seasons, it is clear that transport anomalies are uncorrelated between the different periods, with a maximum correlation of 0.4 found for period II (Feb/Mar) and III (Apr/May). It cannot therefore be expected that the index of the North Atlantic Oscillation (NAOI; for further details, see Hurrell, 1995), normally calculated from

the winter period December to March, is a measure for transport anomalies in periods other than the winter season. Within the present contribution it is not possible to discuss all details of transport anomalies. Hence, for a first step, only winter (Oct–Mar) and summer anomalies (Apr–Sep) of the inflow are discussed (Figure 7). Two conspicuous features can be identified for the different periods: the winter period shows significant high positive inflows for the last decade compared to the previous decade and could be interpreted as a positive trend, regarding only the past 20 years. However, when examined over the entire time period, resolution of a trend is not possible. The summer period shows a different behaviour: a clear positive trend can be identified for the last three decades. The first decade behaves differently, showing the highest as well as lowest summer inflow anomalies.

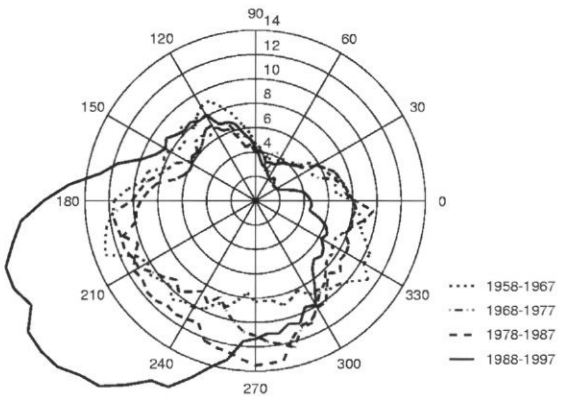


Figure 8. Normalized wind density distribution in Feb/Mar for the four respective decades 1958–1967, 1968–1977, 1978–1987, and 1988–1997. Different to the definition of the wind density function used in Figure 4 the number of classes used here is 72.

Variability of late winter conditions

The second focus of the present study is the period February to March. In an earlier wind analysis (Siegismund and Schrum, 2001) it was shown that the 1990s were an outstanding period of wind forcing in the late winter with mean monthly windspeeds increasing in Feb–Mar over the last decade (1988–1997) and the prevailing wind direction changing to a more south–westerly orientation (Figure 8). This has serious implications for the water transports: the exchange across the northern boundary (inflow and outflow, i.e. the cyclonic circulation) is intensified in the period 1988–1997 (Figure 6, also identified in the half year winter mean in Figure 7). Transport anomalies for the 2-month mean of about 0.5 Sv were calculated by the model. These transport changes were found to be in correspondence with the timing and magnitude observed in earlier studies (Iversen *et al.*, 1998; ICES, 2001). These increased inflows in the last decade occurred after a long period with significantly lower inflows from 1974 to 1987.

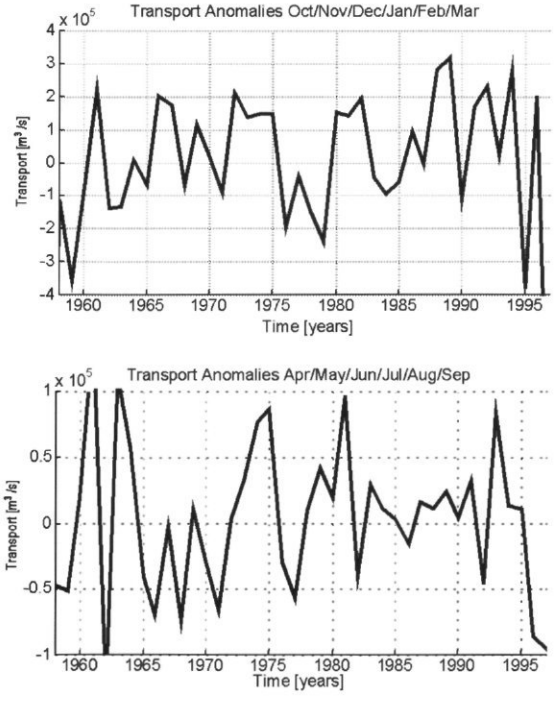


Figure 7. Transport anomalies of North Sea inflows for October to March (upper) and April to September (lower). The transports are given in $m^3 s^{-1}$.

The influence on the exchange flow in the Skagerrak region, which shows high variability, in Feb/Mar is even more pronounced (Figure 9). The wind-forcing fluctuations result in pronounced anomalies in the flow field from 1988 to 1997 (two exceptions being in 1991 and 1996) an exceptional period within the investigated 40-year period. The surface exchange was enhanced, with more surface inflow into the North Sea in the southern part of the Skagerrak (positive anomalies) and more surface outflow in the northern part of the Skagerrak (negative anomalies) with a reduction in deep water exchange. The calculated anomalies are exceptionally high for the near surface inflow (upper 30 m, increasing inflow, negative anomaly) in the southern part of the Skagerrak and for the deep water inflow in the northern part (decreasing inflow, negative anomaly). The calculated transport anomalies are in the order of 0.5 Sv, which is about twice that of anomalies found during the previous 30 years.

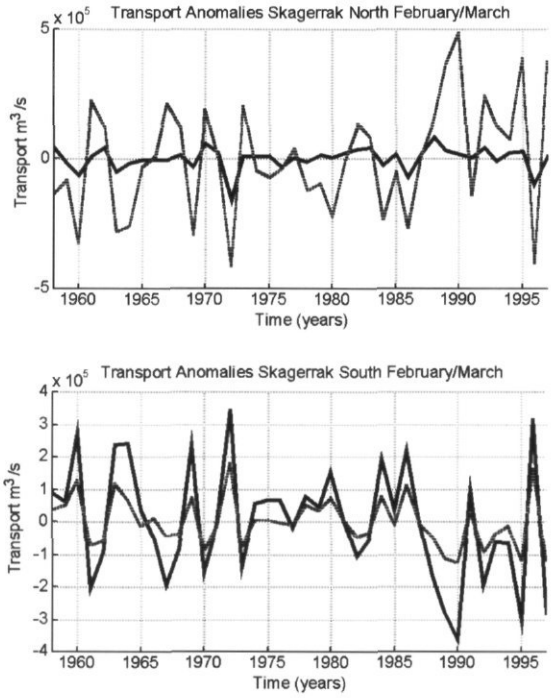


Figure 9. Transport anomalies for the Skagerrak exchange flow in Feb/Mar. Upper: Northern Skagerrak surface inflow (solid) and lower layer outflow (dashed). Lower: Southern Skagerrak surface outflow (solid) and lower layer inflow (dashed). The transports are given in $m^3 s^{-1}$.

Discussion and biological implications

Investigations of the variability of water transports and stratification showed that there is considerable variability in the North Sea hydrodynamic environment. Although the variability is mainly dominated by the year-to-year variability, decadal variability can be identified as well. Longer periods with frequent occurrence of similar conditions were identified for stratification as well as for transport processes.

Yes, regarding the period February and March, the 1990s were unusual with respect to water transports! The anomalous wind forcing found in the 1990s for this period resulted in transport anomalies across the northern boundary and in exceptionally anomalous exchange circulation in the Skagerrak. This potentially impacts on the degree of transport of newly emerged *Calanus finmarchicus* into the Northern North Sea (Heath *et al.*, 1999). A key species whose abundance is linked to variations in recruitment success of North Sea fish stocks (Rothschild, 1998). Furthermore, variations in transport have also been identified as a key issue in the survival success of key fish stocks, impacting on the transport of early life stages of these stocks to optimal larval and juvenile habitats (e.g. ICES, 2001; Heath and Gallego, 1998; Voss *et al.*, 1999).

Similarly, stratification of the North Sea in the 1990s can also be classified as unusual; the years of the most extended stratification in May can be found in the 1990s, with the flux of limiting nutrients into the euphotic zone reduced due to a reduction in turbulent mixing – a situation that reduces the total potential production of the ecosystem by limiting production of lower trophic levels (e.g. Sharples and Tett, 1994; Nielsen and St. John, 2002). Variations in stratification intensity and its effects on lower trophic level production and phasing (Kiørboe, 1991) is the basis of the so-called 'bottom-up' control of higher trophic level production.

In summary, we have identified how the 1990s have varied with respect to two key biologically relevant physical parameters, stratification and transport, both potentially impacting on the ecosystem dynamics. Future research within the European Union-funded LIFECO programme will address the mechanisms by which these parameters impact on the population dynamics of key species in the North Sea.

Acknowledgements

We are grateful to Dorothee von Berg for the preparation of figures and for help in analysing the data. The study was partly financed by the Zentrum für Meeres- und Klimaforschung der Universität Hamburg, the Deutschen Forschungsgemeinschaft SFB512 and the European Union in the frame of the LIFECO project (Q5CA-2000-30183).

References

Becker, G., and Pauly, 1996. Sea surface temperature changes in the North Sea and their causes. ICES Journal of Marine Science, 53: 887–898.

Dippner, J. 1997. SST anomalies in the North Sea in relation to the North Atlantic Oscillation and the influence on the theoretical spawning time of fish. Deutsche Hydrographische Zeitschrift, 49: 267–275.

Gibson, R., Kallberg, P., and Uppala, S. 1996. The ECMWF Re-Analysis (ERA) project. ECMWF Newsletter, 73: 7–17.

Heath, M. R., Backhaus, J. O., Richardson, K., Mckenzie, E., Slagstad, D., Beare, D., *et al.* 1999. Climate fluctuations and the spring invasion of the North Sea by *Calanus finmarchicus*. Fisheries Oceanography, 8: 163–176.

Heath, M. R., and Gallego, A. 1998. Bio-physical modelling of the early life stages of haddock, *Melanogrammus aeglefinus*, in the North Sea. Fisheries Oceanography, 7: 110–125.

Hurrell, J. W. 1995. Decadal trends in the North Atlantic Oscillation: regional temperatures and precipitation. Science, 269: 676–679.

ICES. 2001. Report of the Workshop on Gadoid Stocks in the North Sea During the 1960s and 1970s – Aberdeen 11–13 March 1999. Ed. by K. Brander and M. Heath. ICES Cooperative Research Report, No. 244. 55 pp.

Iversen, A. S., Skogen, M., and Svendsen, E. 1998. Influx of Atlantic water and feeding migration of horse mackerel. ICES CM 1998/R: 18.

Janssen, F., Schrum, C., and Backhaus, J. 1999. A climatological data set of temperature and salinity for the Baltic Sea and the North Sea. Deutsche Hydrographische Zeitschrift, Suppl 9. 245 pp.

Janssen, F., Schrum, C., Hübner, U., and Backhaus, J. 2001. Validation of a decadal simulation with a regional model for North Sea and Baltic Sea. Climate Research, 18: 55–62.

Kalnay, E., Kanamitsu, M., Kistler, R., Collins, W., Deaven, D., Gandin, L., *et al.* 1996. The NCEP/NCAR 40-Year Reanalysis Project. Bulletin of the American Meteorological Society.

Kauker, F. 1999. Regionalization of climate model results for the North Sea. PhD thesis, University of Hamburg. 109 pp.

Kiørboe, T. 1991. Pelagic fisheries and spatio-temporal variability in zooplankton productivity. Proceedings of the Fourth International Conference on Copepoda. Bulletin of the Plankton Society of Japan, Special Volume, pp. 229–249.

Langenberg, H., Pfitzenmayer, A., von Storch, H., and Sündermann, J. 1999. Storm-related sea-level variations along the North Sea coast: natural variability and anthropogenic change. Continental Shelf Research, 19: 821–842.

Lenhart, H.-J., and Pohlmann, T. 1997. The ICES-boxes approach in relation to results of a North Sea Circulation model. Tellus, 49A: 139–160.

Nielsen, M. H., and St. John, M. 2003. Inter and intra annual variations in the stratification and the timing and intensity of phytoplankton blooms in the Central North Sea in the 1990s. ICES Marine Science Symposia, 219: 384–386. (This volume.)

Pohlmann, T. 1996. Predicting the thermocline in a circulation model of the North Sea. Part I: Model description, calibration and verification. Continental Shelf Research, 16: 131–146.

Rodhe, J. 1998. The Baltic and North Seas: a process-oriented review of the physical oceanography. The Sea, 11: 699–732.

Rothschild, B. J. 1998. Year class strengths of zooplankton in the North Sea and their relation to cod and herring abundance. Journal of Plankton Research, 20: 1721–1741.

Schrum, C. 1997a. A coupled ice-ocean model for the North Sea and the Baltic Sea. *In* Sensitivity of North Sea, Baltic Sea and Black Sea to Anthropogenic and Climatic Changes, pp. 311–325. Ed. by Alexander Mikaelyan. NATO ASI Series. Kluwer Academic Publishers, Amsterdam.

Schrum, C. 1997b. Thermohaline stratification and instabilities at tidal mixing fronts. Results of an eddy resolving model for the German Bight. Continental Shelf Research, 17: 689–716.

Schrum, C., and Backhaus, J. O. 1999. Sensitivity of atmosphere–ocean heat exchange and heat content in North Sea and Baltic Sea. A comparative assessment. Tellus, 51 A: 526–549.

Schrum, C., Janssen, F., and Hübner, U. 2000. Recent climate modelling for North Sea and Baltic Sea. Part A: Model description and validation. Berichte des Zentrums für Meeres- und Klimaforschung. Universität Hamburg. 37. 59 pp.

Sharples, J., and Tett, P. 1994. Modelling the effect of physical variability on the midwater chlorophyll maximum. Journal of Marine Research, 52: 219–238.

Siegismund, F., and Schrum, C. 2001. Decadal variability in the wind field over the North Sea. Climate Research, 18: 39–45.

Smith, J. A., Damm, P., Skogen, M. D., Flather, R. A., and Pätsch, J. 1996. An investigation into the variability of circulation and transport on the North-West European shelf using three hydrodynamic models. Deutsche Hydrographische Zeitung, 48: 325–348.

St. John, M. A., and Lund, T. 1996. Lipid biomarkers: linking the utilization of frontal plankton biomass to enhanced condition of juvenile North Sea cod. :Marine Ecology Progress Series, 131: 75–85.

Sündermann, J., Becker, G., Damm, P., Van den Eynde, D., Laane, R., van Leussen, W., *et al.* 1996. Decadal variability on the North-West European Shelf. Deutsche Hydrographische Zeitung, 48: 365–400.

Voss, R., Hinrichsen, H.-H., and St. John, M. 1999. Variations in the drift of larval cod (*Gadus morhua* L.) in the Baltic Sea: combining field observations and modelling. Fisheries – Oceanography, 8: 199–211.

ICES Marine Science Symposia, 219: 132–143. 2003

Hydrographic–hydrochemical variability in the Baltic Sea during the 1990s in relation to changes during the 20th century

Wolfgang Matthäus and Günther Nausch

Matthäus, W., and Nausch, G. 2003. Hydrographic–hydrochemical variability in the Baltic Sea during the 1990s in relation to changes during the 20th century. – ICES Marine Science Symposia, 219: 132–143.

The hydrographic–hydrochemical variability in the Baltic Sea during the 1990s was characterized by the general tendency of decreasing frequency and intensity of major inflows observed since the mid-1970s. At the end of the 1990s, the area of the central Baltic deep water which was affected by oxygen deficiency and anoxic conditions was the largest it had been for 15 years. The most important hydrographic events were the effects of the very strong inflow in January 1993 and the weak inflows in 1993/1994 and 1997/1998 on the central Baltic deep water. Weak inflows in 1993/1994 led to deepwater temperatures of around 4°C, i.e. among the lowest values observed in the last century. Effects of a weak inflow of very warm, saline, and oxygen-rich water in autumn 1997 resulted in temperatures up to 7°C, i.e. among the highest values ever observed. Five of the summers were the warmest of the 20th century and caused sea surface temperature anomalies up to 5–6 K in the open Baltic Sea. The decrease in surface salinity observed since the mid-1970s continued during the 1990s. The concentrations of inorganic nutrients in the surface layer are still high compared with background levels of the 1950s. A distinct decrease in phosphate concentrations has been identified, whereas there has been no observed decrease in nitrate concentrations. Nitrogen levels remain high.

Keywords: Baltic Sea, climate change, deep water, inflows, stagnation, variability.

W. Matthäus and G. Nausch: Baltic Sea Research Institute Warnemünde, Seestrasse 15, D-18119 Warnemünde, Germany [e-mail: Ro:wolfgang.matthaeus@io-warnemuende.de; guenther.nausch@io-warnemünde.de]

Introduction

The Baltic region, located in temperate latitudes of the Northern Hemisphere, consists of the sea area itself (Figure 1) and its drainage area, which is four times larger. The Baltic Sea is almost entirely landlocked. Like other landlocked seas in humid climatic regions, the Baltic Sea has a positive water balance. A narrow, shallow transition area consisting of the Kattegat and Belt Sea greatly restricts the water exchange with the North Sea, giving the water in the Baltic Sea a residence time of about 25–35 years. Because of this long residence time and the specific ecological conditions, the Baltic is extremely sensitive to any changes in its environment.

The environmental conditions of the surface and deep water depend strongly on the meteorological forcing over the Baltic, the hydrological processes in its drainage area, and the hydrographic processes in the sea, as well as the interaction between them. These processes govern the water exchange with the North Sea and between the sub-basins, as well as transport and mixing of water within the various sub-regions of the Baltic.

The water body of the central Baltic is permanently stratified, consisting of an upper layer of brackish water with salinities of about 6–8 and a more saline deep water layer of about 10–14. A strong permanent pycnocline at depths between 60 and 80 m prevents vertical circulation and, consequently, ventilation down to the bottom all the year round. During spring, a thermocline develops at 25–30 m depth and restricts additionally vertical exchange within the upper layer until late autumn. The horizontal deep water circulation is restricted by a series of sub-basins separated by submarine sills.

Effects on abiotic environmental conditions in the central Baltic deep water are mainly caused by variations in water exchange. The deep water is influenced by inflows of saline water from the Kattegat and North Sea. The very frequent but weak inflows (10–20 km^3) have little impact on the deep and bottom waters because their water will be

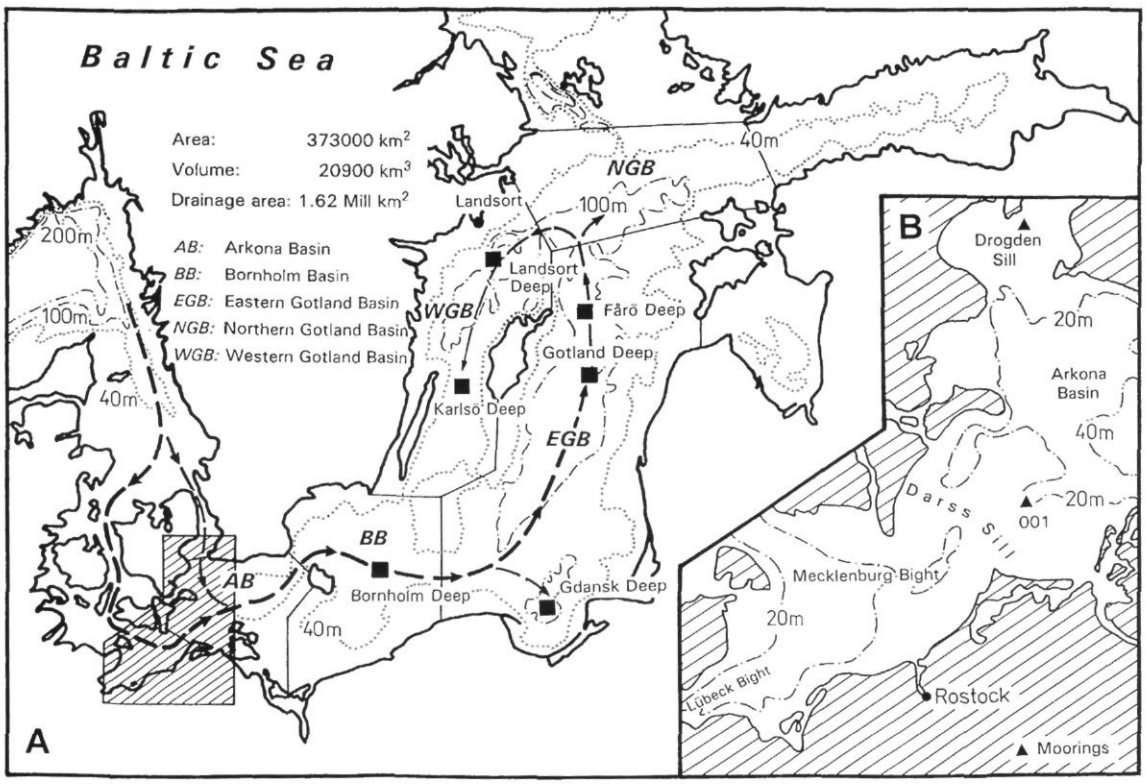


Figure 1. Sub-regions of the central Baltic Sea, their representative stations (squares) and the main transport route of inflowing water during salt water inflows (arrows). Figures correspond to the Baltic Sea inside the entrance sills.

interleaved in or flow just beneath the permanent halocline. Episodic inflows of larger volumes (100–250 km³) of highly saline (17–25) and oxygenated water – termed major Baltic inflows (MBIs) – represent the only mechanism by which the central Baltic deep water is renewed to a significant degree. A total of 111 MBIs has been identified between 1880 and 2001. The water entering the sea during MBIs is dense enough to replace the deep and bottom waters. The criteria used to identify MBIs have been published by Matthäus and Franck (1992) and Fischer and Matthäus (1996). The relative intensity of MBIs between 1880 and 2001 was re-estimated after a method given by Fischer and Matthäus (1996).

Because such inflows are restricted by narrow channels (Little Belt, Great Belt, Sound) and shallow sills (Darss Sill: 0.8 km² cross section, 18 m sill depth; Drogden Sill: 0.1 km² cross section, 7 m sill depth; location cf. Figure 1B), the deep water in the central basins tends to stagnate for periods of several years. The consequences are depletion of nitrate, increasing phosphate and ammonium concentrations, decreasing salinity and oxygen content, sometimes culminating in the formation of considerable hydrogen sulphide concentrations in the deep basins.

During the late 19th and the first three quarters of the 20th century, MBIs were recorded more or less regularly (Figure 2). Since the mid-1970s, their frequency and intensity have decreased (Schinke and Matthäus, 1998). The abiotic environmental conditions changed dramatically during this period, which culminated in the two most significant stagnation periods, from 1977–1992 and from 1995 onward, ever observed in the Baltic Sea (cf. Figures 3, 4).

The general meteorological conditions during the 1990s were characterized by a series of mild winters, several unusually warm summers and above normal precipitation. The winter run-off (September–March) was unusually high since the late 1970s (cf. Figure 2). Details are published in Bergström and Matthäus (1996), Bergström *et al.* (2001), and Matthäus *et al.* (2002).

The general hydrographic conditions were characterized by both mainly positive anomalies in sea surface temperatures (SSTs) in winter due to the mild winters and positive anomalies in SST (cf. also Siegel *et al.*, 1999) in the upper layer during summer (cf. e.g. Matthäus *et al.*, 1998) due to the unusually warm summers. The latter caused temperatures between 20°C and 23°C in the upper 15 m layer of the open Baltic Sea. Positive anomalies of 5–6 K

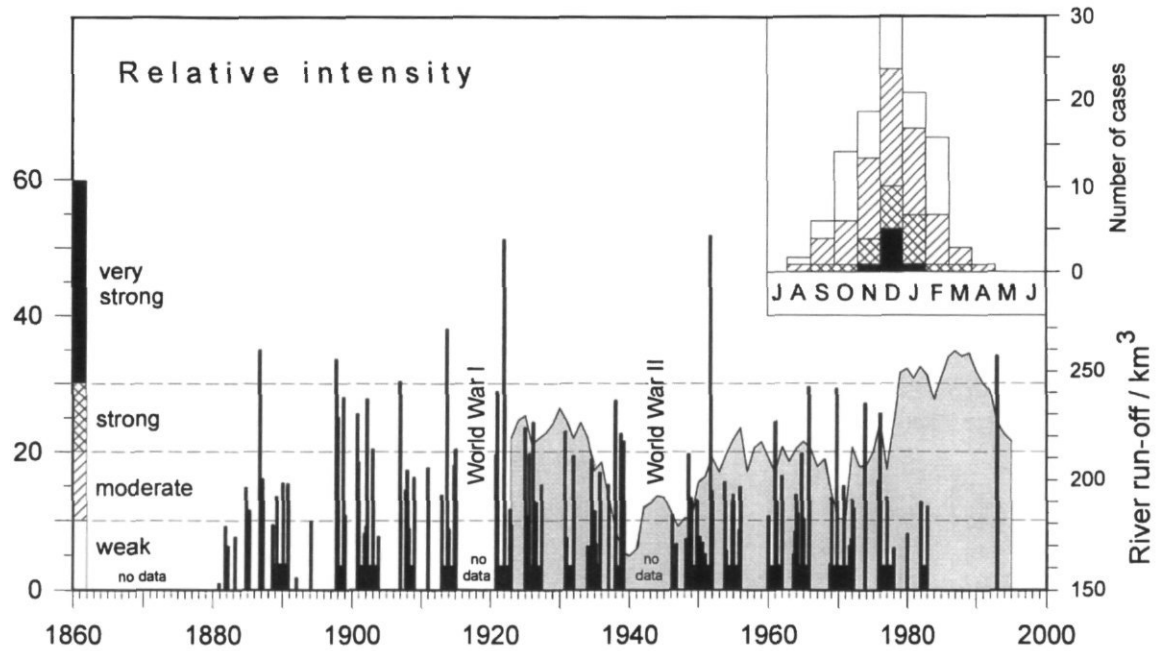


Figure 2. Major Baltic inflows (MBIs) between 1880 and 2001 and their seasonal distribution (upper right) shown in terms of their relative intensity (Matthäus and Franck, 1992; Fischer and Matthäus, 1996; supplemented and updated) and 5-year running means of river run-off to the Baltic Sea (inside the entrance sills) averaged from September to March (shaded). Black boxes on the time axis: MBIs arranged in clusters.

were recorded in the central Baltic in the unusually warm summers of 1994 and 1997 (Nehring *et al.*, 1995a; Matthäus *et al.*, 1998). Since the late 1970s, a decrease in surface salinity has been observed (cf. also Samuelsson, 1996).

During the first half of the 1990s, the conditions in the central Baltic deep water were dominated by the late phase of the long stagnation period 1977–1992 (Matthäus, 1990; Nehring and Matthäus, 1991, 1991/92; Nehring *et al.*, 1993), by the effects of the very strong inflow of saline and oxygen-rich water in January 1993 (Håkansson *et al.*, 1993; Jakobsen, 1995; Matthäus and Lass, 1995) and the subsequent weak inflow events in 1993/1994 (Nehring *et al.*, 1995a). The second half was characterized by the early phase of a new stagnation with a large extension of areas of oxygen depletion and anoxic conditions. A weak inflow in early autumn 1997 caused extraordinary high temperatures in the deep water (Matthäus *et al.*, 1999).

This article is focused on the hydrographic–hydrochemical conditions of the Baltic Sea during the 1990s in relation to changes during the 20th century. The main basis for hydrographic and nutrient data is the ICES and HELCOM database and the data collected under the German National Monitoring Programme 1969–2000. Numerous tables on annual means of hydrographic data and nutrient concentrations during the 1990s are given in Matthäus *et al.* (2001).

Conditions during the 1990s

Stagnation in the central Baltic deep water

Stagnation is a natural process in the deep water of nearly completely landlocked sea areas like the Baltic Sea. Stagnation periods are characterized by the depletion of nitrate, increasing phosphate and ammonium concentrations and decreasing salinity and oxygen depletion due to remineralization of organic material that has settled from the surface layers. This can completely consume the dissolved oxygen, thereby creating anoxic conditions and leading to the formation of considerable concentrations of hydrogen sulphide.

Role of the Bornholm Basin

Realizing the topography of the Baltic Sea along the main transport route of the inflowing saline water (cf. Figure 1A), the thermohaline conditions in the first Baltic deep basin downstream from the entrance sills, the Bornholm Basin, are of considerable importance for the evolution of stagnation in the central Baltic deep water. In general, there is a frequent inflow of lower amounts of highly saline water which penetrates across the sills into the Arkona Basin during each baroclinic or weak

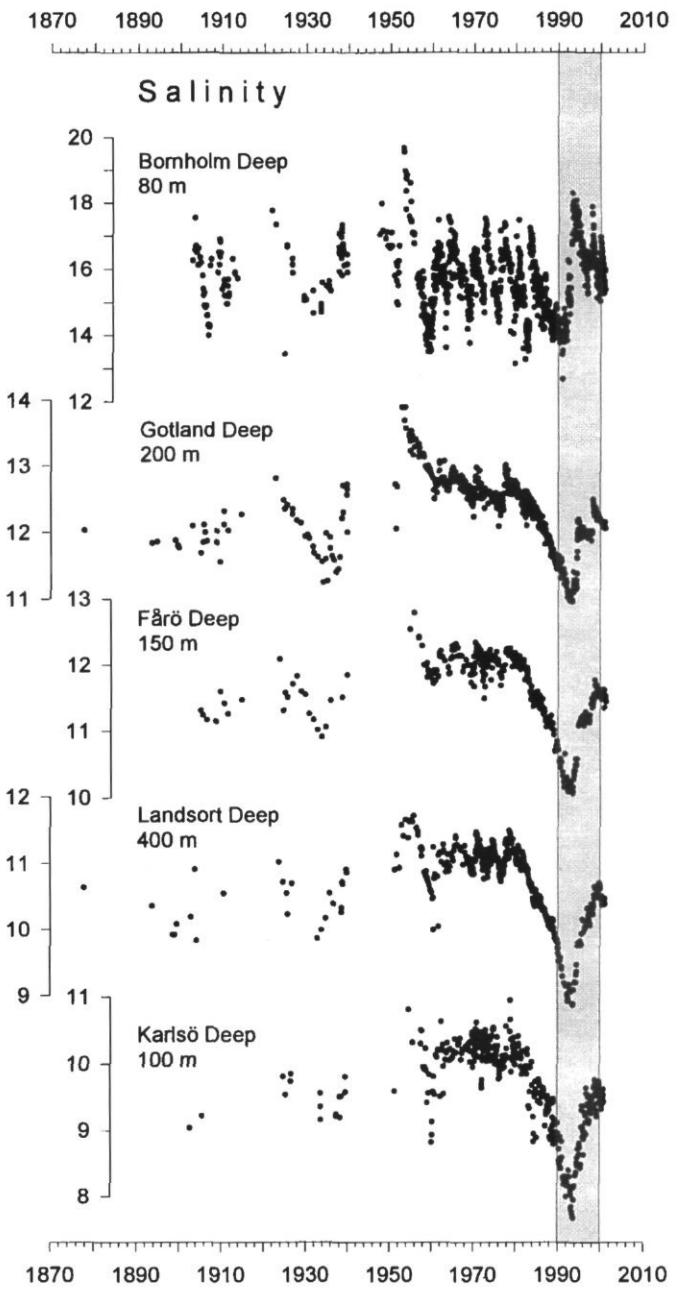


Figure 3. Long-term variations of salinity in the central Baltic deep water during the past century.

barotropic inflow event. This water is trapped in the Bornholm Basin, renewing the ambient deep water to a certain extent and causing an annual variation in the deep water.

The filling stage of the Bornholm Basin with saline water, below the permanent halocline, is a measure of the estimation of the impact of weak inflows on the central Baltic deep water. During periods of low inflow activity, salinity and thus density of the Bornholm Basin deep water decreases (Figure 3). Depending on the inflowing volume of saline water, weak inflows and even MBIs only fill up this basin and the saline water generally does not pass the Stolpe Sill downstream through the Stolpe Channel into the central Baltic.

When the buffering capacity of the Bornholm Basin is exhausted, weak inflows of saline and oxygen-rich water crossing the entrance sills into the

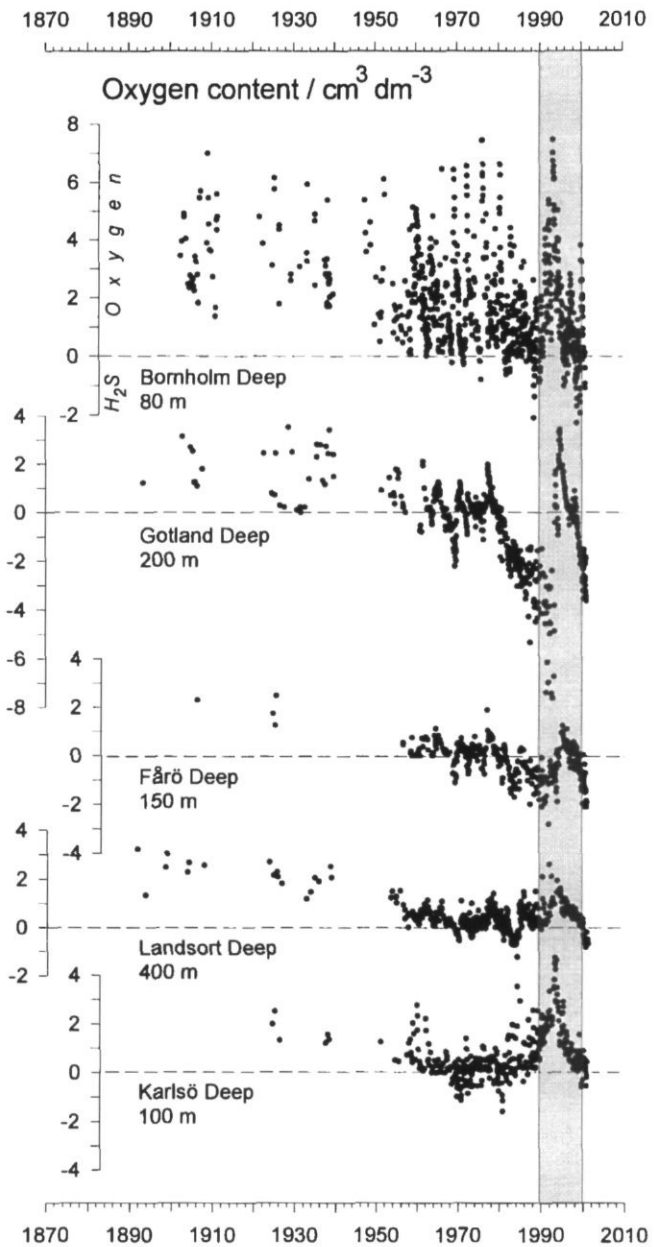


Figure 4. Long-term variation of oxygen and hydrogen sulphide concentrations in the central Baltic deep water during the past century (hydrogen sulphide converted into negative oxygen equivalents).

Baltic can pass that basin in depths of 50–60 m, propagate downstream relatively quickly and cause significant effects in the central Baltic deep water.

Stagnation period during the 1990s

The inflow into the Bornholm Basin strengthened during the early 1990s and both salinity and oxygen concentration increased in the deep water of that basin (cf. Bornholm Deep in Figures 3 and 4). In the central Baltic deep water, however, salinity continued decreasing. The stagnation period with high hydrogen sulphide concentrations in the deep water continued in the eastern Gotland Basin (Gotland and Farö Deeps), while the oxygen concentrations of the western Gotland Basin deep water (Landsort and Karslö Deeps) increased until 1993.

The MBI in January 1993 filled up the Bornholm Basin with highly saline and oxygen-rich water (Figures 3, 4); the impact on the central Baltic deep water remained small (Nehring *et al.*, 1994). In May 1994, the deep water of the whole Baltic Sea was free of hydrogen sulphide. In the 200 m level of the Gotland Deep, temperature decreased by 1.1 K and salinity increased by 1 (Figure 3). The oxygen concentration of 3–3.8 $cm^3\ dm^{-3}$ measured between 170 m depth and bottom were the highest since the 1930s (Figure 4 and Matthäus, 1990).

The absence of MBIs since then has resulted in a new stagnation period in central Baltic deep water. After the renewal, oxygen depletion started and anoxic conditions developed (cf. Figure 4). In the deep water of the western Gotland Basin, continuous oxygen depletion started in 1993 (cf. Landsort and Karlsö Deeps in Figure 4). The decrease in oxygen concentration, which is characteristic of this basin for the early phase of stagnation periods (Matthäus, 1995), led in 1999 to the lowest oxygen content since the mid-1980s and the formation of hydrogen sulphide in the near-bottom layers (Figure 4).

The weak inflow events in December 1993 and March 1994 transported cold, saline, and oxygen-rich water into the central deep basins. The temperatures below 100 m depth in the Gotland Deep decreased from >5°C at the beginning of the year to 4–4.5°C in May 1994. Temperatures of 4°C are among the lowest values observed in the deep water of the Gotland and Fårö Deeps during the present century (cf. Matthäus *et al.*, 1999).

The exceptionally high SSTs in summer 1997 led to an unusual increase in deep water temperatures in late autumn due to an inflow in September and early October. This inflow of warm (7–8°C), saline (14–15), and oxygen-rich deep water (2 $cm^3\ dm^{-3}$) reached the Gotland Deep in spring 1998. As a result, temperature and salinity increased to >7°C and 12.7, respectively, in the near-bottom water. The inflow process into the central Baltic was settled in May 1998 (cf. Hagen and Feistel, 2001).

In 1999/2000, the areas of both oxygen deficiency and anoxic conditions in the central Baltic deep water reached their largest extent since 1993.

Nutrient situation in the deep water during the 1990s

The nutrient situation in the deep basins is mainly characterized by the alternation between MBIs and stagnation periods. In the presence of oxygen, phosphate is partly bound in the sediment and onto sedimented particles as iron-III-hydroxophosphate complexes, resulting in phosphate concentrations of only 1–2 μmol dm^{-3} (compare Figures 4 and 5). If the redox status changes, this complex is reduced by hydrogen sulphide. Phosphate and iron-II-ions are liberated.

Inorganic nitrogen compounds are also strongly influenced by the presence or absence of oxygen and hydrogen sulphide, respectively. Under aerobic conditions, inorganic nitrogen compounds are present nearly exclusively in the oxidized form as nitrate. Under anoxic conditions, the available nitrate is denitrified to dinitrogen gas. On the other hand, ammonium, which is liberated due to the mineralization processes, cannot be oxidized. As a result, ammonium is enriched and nitrate vanishes.

The water renewal during the first half of the 1990s and the subsequent development of a new stagnation period can be recognized most distinctly by the variations of nutrient concentrations in the eastern Gotland Basin (cf. e.g. Gotland and Farö Deeps in Figure 5). At the end of the 16-year stagnation period in 1992 hydrogen sulphide concentrations up to –8 $cm^3\ O_2\ dm^{-3}$, in the near-bottom layer up to –10 $cm^3\ O_2\ dm^{-3}$, were measured with a high degree of variability (Figure 4). The nutrient situation is characterized by the absence of nitrate and nitrite and a considerable enrichment of ammonium up to 40 μmol dm^{-3} (Nehring *et al.* 1995b).

In 1993, the nutrient distribution reacted distinctly to the changes in the redox regime in the eastern Gotland Basin (for phosphate, cf. Figure 5) despite the impact of the January event remaining small in the central Baltic. Ammonium decreased strongly and was not detectable in June and August 1993. Nitrate concentrations increased and the amount of phosphate was reduced (Nausch and Nehring, 1994). But the layer below 200 m depth became anoxic again in November 1993. Only the weak inflows at the end of 1993/beginning of 1994 resulted in a longer improvement in the aerobic situation in the Gotland Deep (Figure 4) due to their fast penetration into the eastern Gotland Basin. As a result, lowest annual means in phosphate (Figure 5) and ammonium concentrations but highest nitrate concentrations were observed in 1995 before the new stagnation had started. From mid-1998 onwards, when permanent anoxic conditions prevailed, nitrate was not detectable and phosphate and ammonium concentrations were increasing. However, the concentrations had not yet achieved the high values measured at the end of the stagnation period 1977–1992 (Figure 5). The development in the Faroe Deep can be compared with the conditions in the Gotland Deep, but the processes are delayed and reduced in their intensity due to the submarine sill between the two basins.

In the western Gotland Basin, nitrate concentrations in the 1990s were stable over a longer period with around 10 μmol dm^{-3}. At the end of 1998, however, oxygen conditions had depleted so much that denitrification could take place (Goering, 1968)

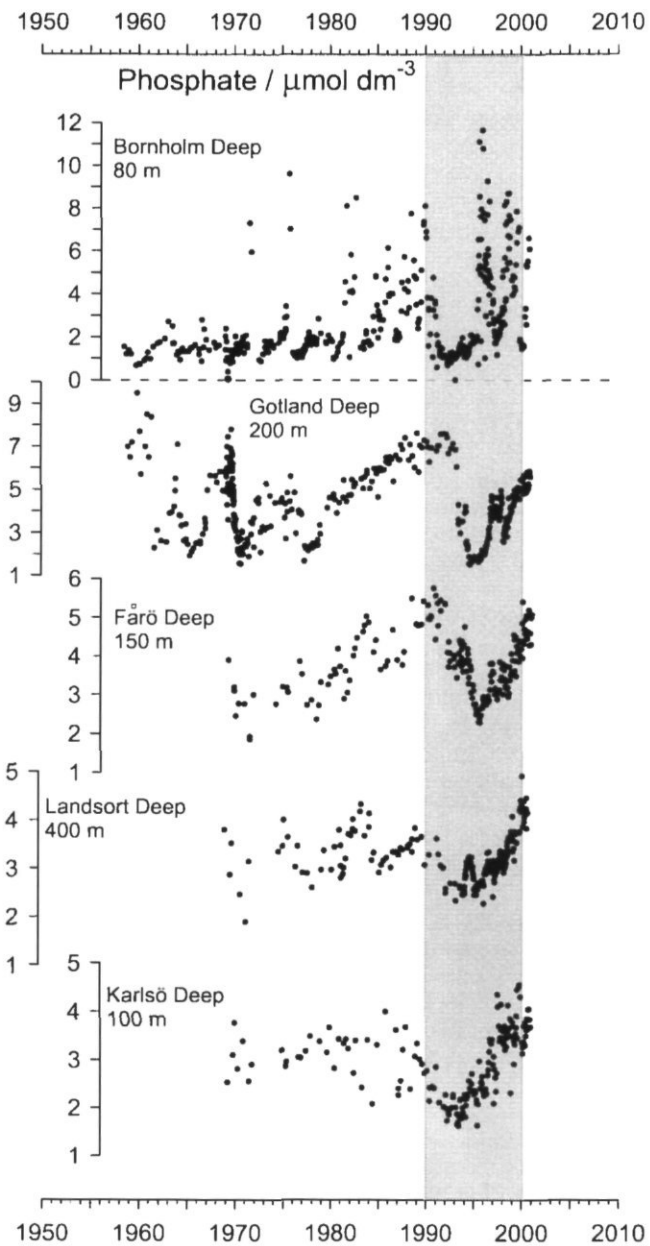


Figure 5. Long-term variation of phosphate concentrations in the central Baltic deep water during the second half of the past century.

resulting in a decrease in nitrate which is clearly marked in 1999. In 1999, the highest ammonium concentrations were measured (Matthäus *et al.*, 2001). The increase in phosphate concentrations, especially in the Landsort Deep, is lower compared to the eastern Gotland Basin (Figure 5), probably because of the different structure of the sea floor. This development in nutrient balance seems to be characteristic for the early stage of stagnation.

State of eutrophication during the 1990s

The increasing supply of inorganic nutrients due to human impacts in the drainage area and the subsequently increasing primary production are known as eutrophication. Therefore nutrients have been used to describe the state of eutrophication. Phosphate and nitrate are the final products of biochemical

mineralization of organic matter under aerobic conditions. They are therefore the most important nutrients in trend analysis.

In the whole Baltic Sea, the nutrient concentrations are characterized by a pronounced seasonality with high concentrations in winter and often a decrease near to the detection limit during the period of high biological activity beginning in spring and ending in late autumn (Nausch and Nehring, 1996). For nutrient trend studies only the mixed surface layer in winter can be used when the biological productivity is low and nutrient concentrations are high (Nehring and Matthäus, 1991; Nausch and Nehring, 1996). The duration of this "winter plateau" differs in the Baltic Sea regions and is best developed in the eastern and western Gotland Basins (Matthäus *et al.*, 1998). In general, trend analysis should identify long-term developments in relation to changes in load. In the past decade, they have to answer the question whether reduction measures, initiated within the Joint Comprehensive Environmental Action Plan (Helcom, 1993) and by the decrease in fertilizer application in the drainage area (Nehring *et al.*, 1995b), result in decreased phosphate and nitrate concentrations in the mixed winter surface layer.

This can be shown more clearly by comparing the periods 1989/1993 and 1994/1998 (Figure 6). Comparing the second with the first half of the 1990s, a distinct decrease in phosphate winter concentrations was identified, mainly in the nearshore areas of the western Baltic (Lübeck, Mecklenburg and Pomeranian Bights), but also in the central Baltic Sea (Figure 6A). Measures undertaken to reduce phosphate input from point sources in the drainage area seem to be effective. A clear relation can be drawn to the riverine discharge. Thus, the phosphate concentrations in the Oder river decrease from 1986 to 1999 (Helcom, 2002). Recent measurements, however, show that a new equilibrium is already established, and therefore a further decrease in phosphate concentrations cannot be expected. But this reduction is not evident in all regions. For example, phosphate concentrations have increased in the inner Gulf of Gdańsk, thereby influencing the whole bight. The reasons can be assumed to be less effective reduction of phosphate discharge from point sources and the specific character of the Vistula river drainage area dominated by diffuse nutrient inputs (Helcom, 2002).

Nitrate concentrations do not show any significant decrease between both periods in most of the investigated regions. Moreover, the concentrations in the Pomeranian Bight and in the Gdańsk Bight are higher (Figure 6B). Several reasons can be mentioned for the failing reduction. In the central Baltic Sea, the atmospheric input still plays an important role despite first signs of positive developments for this route (Helcom, 1997). Also the yearly input of nitrogen through nitrogen-fixing cyanobacteria in summer must be taken into consideration (Wasmund *et al.*, 2001). The most important reason, however, is that nitrate originates mainly from diffuse sources in the drainage area.

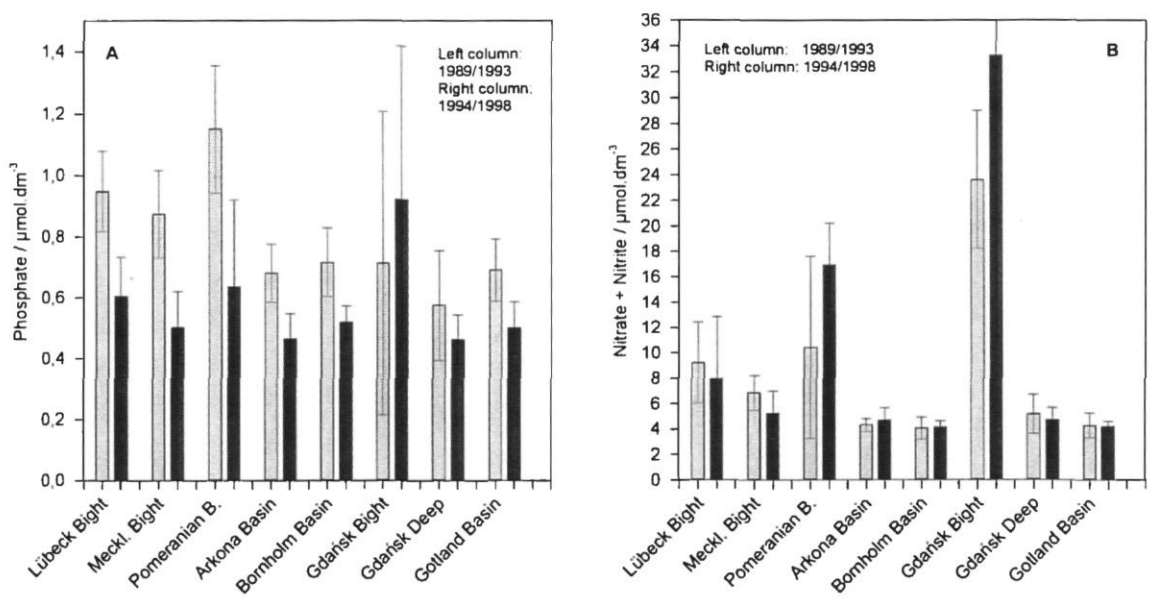


Figure 6. Changes in phosphate (A) and nitrate+nitrite concentrations (B) in the winter surface layer (February; 0–10 m depth) of the western and central Baltic Sea during the periods 1989–1993 (left column) and 1994–1998 (right column).

Thus the input into the coastal areas is closely related to the freshwater run-off (Pastuszak *et al.*, 1996; Nausch *et al.*, 1999). Therefore reduction measures are much more complicated to convert and need longer time perspectives.

Climate change and Baltic deep water

Backhaus (1996) investigated the climate sensitivity of the Baltic Sea based on regional model results. According to him the Baltic seems to be much more susceptible to climate change than the North Sea because of a strong feedback between sea surface and air temperatures with the haline stratification.

Air–sea interactions are a main source of the observed variability in seas in time scales ranging from years to centuries. On decadal time scales, variations in atmospheric circulation over the northern Atlantic Ocean and Europe govern fluctuations in the water exchange between the North Sea and the Baltic and are mainly reflected in marine climatic changes in the central Baltic deep water (e.g. Hupfer, 1975; Makkonen *et al.*, 1984; Matthäus, 1984; Launiainen and Vihma, 1990; Matthäus, 1995).

The schematic diagram in Figure 7 illustrates the pathway of the influence of the atmospheric circulation on the central Baltic deep water. The variability in atmospheric circulation governs the water exchange of the Baltic with the ocean, especially the occurrence or absence of major inflows (Matthäus and Schinke, 1994; Gustafsson, 2000). MBIs have an essential impact on the oceanographic conditions in the deep water (temperature, salinity, oxygen, inorganic nutrients). There are indications that MBIs may also affect the transformation of contaminants (PAHs) and the modification of their distribution in the deep water (cf. Witt and Matthäus, 2001). There seems to be an impact of run-off variation on the occurrence of MBIs. Drastic changes in environmental conditions in the deep water can be explained by increased zonal circulation linked with more intensive precipitation in the Baltic region and increased river run-off into the Baltic (Matthäus and Schinke, 1999; Hänninen *et al.*, 2000; Zorita and Laine, 2000). Launiainen and Vihma (1990) demonstrated a correlation between river run-off and Baltic deep water salinity (cf. also Samuelsson, 1996). There is also a connection between aerobic/anoxic conditions and the concentration of inorganic nutrients (Nehring, 1987, 1989).

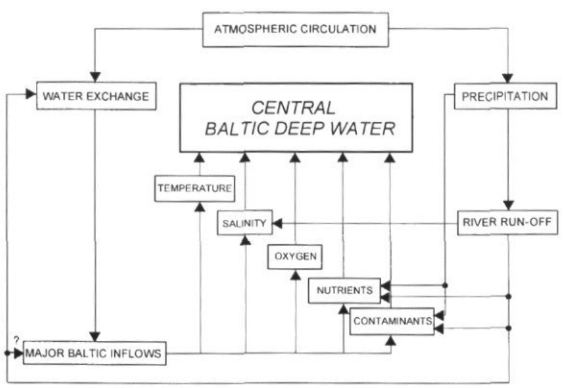


Figure 7. Schematic diagram of the influence of variability in atmospheric circulation on the central Baltic deep water.

Changed conditions in the central Baltic deep water could be an indicator of climate change. Climate model simulations predict a climate change due to the increasing concentrations of greenhouse gases and sulphate aerosols in the atmosphere. World-wide human activities may already have affected the global climate (Storch and Hasselmann 1995; Santer *et al.*, 1996; Hasselmann, 1997) and caused changes in the atmospheric circulation affecting the water exchange between the North Sea and the Baltic. The sensitivity of MBIs to variations in climatic factors has been modelled by Gustafsson (2000) and Gustafsson and Andersson (2001).

An attempt to analyse potential impacts of future climate change on the run-off from the drainage area to the Baltic Sea indicated that global warming may lead to a changed annual cycle and less pronounced spring run-off as winters become less stable (Graham *et al.*, 2001). Run-off seems generally to increase from the northernmost parts of the drainage area and decrease to the central Baltic.

In order to estimate the impact of climate change on the central Baltic deep water the effects of human activities on the deep water must be identified. Man-made impacts affect the concentration of both inorganic nutrients (cf. e.g. Elmgren 1989; Jansson and Dahlberg, 1999; Nausch *et al.*, 1999; Wulff *et al.*, 2001) and contaminants (cf. e.g. Helcom, 1991, 1997, 1998; Bernes, 1999; Skei *et al.*, 2000; Elmgren and Larsson, 2001; Wulff *et al.*, 2001) in the surface layer via land-based (point and diffuse sources) and airborne inputs (precipitation). Increases in nutrient levels lead to higher organic productivity in the euphotic layer (Cederwall and Elmgren, 1990; Wulff *et al.*, 1990). This causes an increase in dead organic material partly loaded with contaminants which, settling to the bottom, have an impact on both oxygen regime and concentrations of contaminants in the deep water. Both the lack of MBIs and man-made impacts are responsible for oxygen depletion and increase in hydrogen sulphide concentrations. However, it is not possible presently to state how much of this variability is due to which cause. Moreover, there are indications that the man-made

redistribution of the water run-off through river regulation measures may have an impact on the water exchange (Carlsson and Sanner, 1994) and may also affect the frequency and intensity of MBIs (Matthäus and Schinke, 1999; Rödel, 2001).

Nevertheless, the variation in water exchange between the North Sea and the Baltic during the 1990s, which is clearly reflected at least in the hydrographic conditions of the central Baltic deep water, seems to remain within the range of natural fluctuation (cf. Figure 3). Alternations between oxidizing and reducing marine environments in the Baltic deep water have also occurred in the past centuries (cf. Ignatius *et al.*, 1971; Neumann *et al.*, 1997).

Conclusions

During the 1990s, a distinct decrease in phosphate winter concentrations but no significant change in the nitrate concentrations of the mixed winter surface layer was observed. The general tendency of decreasing frequency and intensity of MBIs continued, interrupted only by the very strong single MBI in January 1993.

Investigating the long stagnation periods in the Baltic deep water, there are similarities between the current stagnation period and the stagnation in 1977–1992. The maximum extent of oxygen deficiency and anoxic conditions occurred during both periods about 5–7 years after a strong MBI, i.e. 1982/1983 during the previous stagnation and 1999/2000 during the present stagnation period. After 1982/1983, an increase in oxygen concentration started in the western Gotland Basin deep water (cf. Landsort and Karlsö Deeps in Figure 4) and is assumed to be caused by both increased vertical exchange due to decreasing stability of the water column and the effects of weak inflows. The water of such inflows propagates along the main transport route (cf. Figure 1A) and can relatively quickly pass the eastern Gotland Basin at intermediate levels below the halocline. Because of the density it can penetrate up to the near-bottom layers of the western Gotland Basin.

The area of central Baltic deep water affected by oxygen deficiency and anoxic conditions at the turn of the century was the largest for 15 years. In general, the anoxic layer seems to be thickest when the area affected by oxygen deficiency and anoxic conditions is largest. This was also observed during the stagnation period of 1977–1992. As the stagnation continues the redoxcline moves to greater depths because of weak inflows in intermediate layers below the permanent halocline, and the hydrogen sulphide concentrations increase in the deep water. In general, an intensive phosphate accumulation occurs at the beginning of stagnation periods. Thereafter, the concentrations increase only slowly and fluctuate around an average (cf. Figure 5). The phosphate reserves seemed to be exhausted and the further increase in hydrogen sulphide concentrations did not result in a further liberation of phosphate.

If the decrease in frequency and intensity of MBIs and, thus, the present stagnation in the central Baltic continue, a decrease in the extent of areas affected by oxygen deficiency and anoxic conditions in the deep basins and a further increase in hydrogen sulphide concentration in the deep water of the eastern Gotland Basin will occur. However, an increase in oxygen concentration can be expected in the deep water of the western Gotland Basin starting within the next few years.

Acknowledgements

We are grateful to all colleagues of the Baltic Sea Research Institute Warnemünde and the masters and crews of RV "A. v. Humboldt" and RV "Professor Albrecht Penck", who supported or took part in the monitoring activities during the past three decades. We thank the Oceanographical Laboratory of the Swedish Meteorological and Hydrological Institute (SMHI) in Göteborg and the Maritime Branch of the Institute of Meteorology and Water Management (IMGW) in Gdynia for providing oceanographic data. River run-off data were made available by courtesy of Bengt Carlsson, SMHI Norrköping.

References

Backhaus, J. O. 1996. Climate-sensitivity of European marginal seas, derived from the interpretation of modelling studies. Journal of Marine Systems, 7: 361–382.

Bergström, S., and Matthäus, W. 1996. Meteorology, hydrology and hydrography. In: Third Periodic Assessment of the State of the Marine Environment of the Baltic Sea, 1989–1993; Background Document, pp. 9–18. Baltic Sea Environment Proceedings, 64B.

Bergström, S., Alexandersson, H., Carlsson, B., Josefsson, W., Karlsson, K.-G., and Westring, G. 2001. Climate and hydrology of the Baltic Sea. In: Ecological Studies, 148: A Systems Analysis of the Baltic Sea, pp. 75–112. Ed. by F. Wulff, L. Rahm, and P. Larsson. Springer-Verlag, Berlin, Heidelberg. 455 pp.

Bernes, C. 1999. Persistent organic pollutants: a Swedish view of an international problem. Monitor, 16, Swedish Environmental Protection Agency, Stockholm. 152 pp.

Carlsson, B., and Sanner, H. 1994. Influence of river regulation on runoff to the Gulf of Bothnia. SMHI Reports Hydrology, 9: 1–30.

Cederwall, H., and Elmgren, R. 1990. Biological effects of eutrophication in the Baltic Sea, particularly the coastal zone. Ambio, 19: 109–112.

Elmgren, R. 1989. Man's impact on the ecosystem of the Baltic Sea: energy flows today and at the turn of the century. Ambio, 18: 326–332.

Elmgren, R., and Larsson, U. 2001. Eutrophication in the Baltic Sea area. In: Dahlem Workshop Report, 85: Science and integrated coastal management, pp. 15–35. Ed. by B. v. Bodungen and R. K. Turner. Dahlem University Press, Berlin. 378 pp.

Fischer, H., and Matthäus, W. 1996: The importance of the Drogden Sill in the Sound for major Baltic inflows. Journal of Marine Systems, 9: 137–157.

Goering, J. J. 1968. Denitrification in the oxygen minimum zone of the eastern tropical North Pacific. Deep Sea Research, 15: 157–164.

Graham, L. P., Rummukainen, M., Gardelin, M., and Bergström, S. 2001. Modelling climate change impacts on water resources in the Swedish regional climate modelling programme. In: Detecting and Modelling Regional Climate Change and Associated Impacts, pp. 567–580. Ed. by M. Brunet and D. López. Springer-Verlag, Heidelberg.

Gustafsson, B. G. 2000. Time-dependent modeling of the Baltic entrance area. 2. Water and salt exchange of the Baltic Sea. Estuaries, 23: 253–266.

Gustafsson, B. G., and Andersson, H. C. 2001. Modeling the exchange of the Baltic Sea from the meridional atmospheric pressure difference across the North Sea. Journal of Geophysical Research, 106(C9): 19,731–19,744.

Hänninen, J., Vuorinen, I., and Hjelt, P. 2000. Climatic factors in the Atlantic control the oceanographic and ecological changes in the Baltic Sea. Limnology and Oceanography, 45: 703–710.

Hagen, E., and Feistel, R. 2001. Spreading of Baltic deep water: a case study for the winter 1997–1998. Meereswissenschaftliche Berichte/Marine Science Reports, Warnemünde, 45: 99–133.

Håkansson, B., Broman, B., and Dahlin, H. 1993. The flow of water and salt in the Sound during the Baltic major inflow event in January 1993. ICES CM 1993/C: 57. 26 pp.

Hasselmann, K. 1997. Are we seeing global warming? Science, 276: 914–915.

Helcom, 1991. Airborne pollution load to the Baltic Sea 1986–1990. Baltic Sea Environment Proceedings, 39. 162 pp.

Helcom, 1993. The Baltic Sea joint comprehensive environmental action plan. Baltic Sea Environment Proceedings, 48. 58 pp.

Helcom, 1997. Airborne pollution load to the Baltic Sea 1991–1995. Baltic Sea Environment Proceedings, 69. 57 pp.

Helcom, 1998. The third Baltic Sea pollution load compilation (PLC-3). Baltic Sea Environment Proceedings, 70. 133 pp.

Helcom, 2002: Fourth periodic assessment of the state of the environment of the Baltic marine area, 1994–1998; Background document. Baltic Sea Environment Proceedings, 82B. (In press.)

Hupfer, P. 1975. Marine climatic fluctuations in the Baltic Sea area since 1900. Zeitschrift für Meteorologie, 25: 85–93.

Ignatius, H., Niemistö, L., and Voipio, A. 1971. Variations of redox conditions in the recent sediments of the Gotland Deep. Eripainos Geologilehdestä, 27: 43–46.

Jakobsen, F. 1995. The major inflow to the Baltic Sea during January 1993. Journal of Marine Systems, 6: 227–240.

Jansson, B.-O., and Dahlberg, C. 1999. The environmental status of the Baltic Sea in the 1940s, today, and in the future. Ambio, 28: 312–319.

Launiainen, J., and Vihma, T. 1990. Meteorological, ice and water exchange conditions. In: Second periodic assessment of the state of the marine environment of the Baltic Sea, 1984–1998; Background document. Baltic Sea Environment Proceedings, 35B: 22–33.

Makkonen, L., Launiainen, J., Kahma, K., and Alenius, P. 1984. Long-term variations in some physical parameters of the Baltic Sea. In: Climate Changes on a Yearly to Millennial Basis, pp. 391–399. Ed. by N. A. Mörner and W. Karlen.

Matthäus, W. 1984. Climatic and seasonal variability of oceanological parameters in the Baltic Sea. Beiträge zur Meereskunde Berlin, 51: 29–49.

Matthäus, W., 1990. Langzeittrends und Veränderungen ozeanologischer Parameter während der gegenwärtigen Stagnationsperiode im Tiefenwasser der zentralen Ostsee. Fischerei-Forschung, Rostock, 28: 25–34.

Matthäus, W. 1995: Natural variability and human impacts reflected in long-term changes in the Baltic deep water conditions: a brief review. Deutsche Hydrographische Zeitschrift, 47: 47–65.

Matthäus, W., and Franck, H. 1992. Characteristics of major Baltic inflows: a statistical analysis. Continental Shelf Research, 12: 1375–1400.

Matthäus, W., and Lass, H. U. 1995. The recent salt inflow into the Baltic Sea. Journal of Physical Oceanography, 25: 280–286.

Matthäus, W., and Schinke, H. 1994. Mean atmospheric circulation patterns associated with major Baltic inflows. Deutsche Hydrographische Zeitschrift, 46: 321–339.

Matthäus, W., and Schinke, H. 1999. The influence of river runoff on the deep water conditions of the Baltic Sea. Hydrobiologia, 393: 1–10.

Matthäus, W., Nausch, G., Lass, H. U., Nagel, K., and Siegel, H. 1998. The Baltic Sea in 1997: impacts of the extremely warm summer and of the exceptional Oder flood. Deutsche Hydrographische Zeitschrift, 50: 47–69.

Matthäus, W., Nausch, G., Lass, H. U., Nagel, K., and Siegel, H. 1999. The Baltic Sea in 1998: characteristic features of the current stagnation period, nutrient conditions in the surface layer and exceptionally high deep water temperatures. Deutsche Hydrographische Zeitschrift, 51: 67–84.

Matthäus, W., Nausch, G., Lass, H. U., Nagel, K., and Siegel, H. 2001. The Baltic Sea in 1999: stabilization of nutrient concentrations in the surface water and increasing extent of oxygen deficiency in the central Baltic deep water. Meereswissenschaftliche Berichte/Marine Science Reports, Warnemünde, 45: 3–25.

Matthäus, W., Bergström, S., Carlsson, B., Graham, L. P., and Andersson, L. 2002. General meteorology, hydrology and hydrography. In: Fourth Periodic Assessment of the State of the Environment of the Baltic Marine Area, 1994–1998; Background document. Baltic Sea Environment Proceedings, 82B. (In press.)

Nausch, G., and Nehring, D. 1994: Nutrient dynamics in the Gotland Deep: reactions to the major salt water inflow in 1993. Proceedings of the 19th Conference of Baltic Oceanographers, 29 August to 1 September 1994, Sopot, 2: 551–559.

Nausch, G., and Nehring, D. 1996. Baltic proper, hydrochemistry. In: Third Periodic Assessment of the State of the Marine Environment of the Baltic Sea, 1989–1993; Background Document. Baltic Sea Environment Proceedings, 64B: 80–85.

Nausch, G., Nehring, D., and Ærtebjerg, G. 1999. Anthropogenic nutrient load of the Baltic Sea. Limnologica, 29, 233–241.

Nehring, D. 1987. Temporal variations of phosphate and inorganic nitrogen compounds in central Baltic deep waters. Limnology and Oceanography, 32: 494–499.

Nehring, D. 1989. Phosphate and nitrate trends and the ratio oxygen consumption to phosphate accumulation in central Baltic deep waters with alternating oxic and anoxic conditions. Beiträge zur Meereskunde Berlin, 59: 47–58.

Nehring, D., and Matthäus, W. 1991. Current trends in hydrographic and chemical parameters and eutrophication

in the Baltic Sea. Internationale Revue der gesamten Hydrobiologie, 76: 297–316.

Nehring, D., and Matthäus, W. 1991/92. Die hydrographisch-chemischen Bedingungen in der westlichen und zentralen Ostsee im Jahre 1991. Deutsche Hydrographische Zeitschrift, 44: 217–238.

Nehring, D., Matthäus, W., and Lass, H. U. 1993. Die hydrographisch-chemischen Bedingungen in der westlichen und zentralen Ostsee im Jahre 1992. Deutsche Hydrographische Zeitschrift, 45: 281–312.

Nehring, D., Matthäus, W., Lass, H.-U., and Nausch, G. 1994. Die hydrographisch-chemischen Bedingungen in der westlichen und zentralen Ostsee im Jahre 1993. Deutsche Hydrographische Zeitschrift, 46: 151–162.

Nehring, D., Matthäus, W., Lass, H.-U., Nausch, G., and Nagel, K. 1995a. The Baltic Sea 1994: consequences of the hot summer and inflow events. Deutsche Hydrographische Zeitschrift, 47: 131–144.

Nehring, D., Matthäus, W., Lass, H.-U., Nausch, G., and Nagel, K. 1995b. The Baltic Sea in 1995: beginning of a new stagnation period in its central Baltic deep waters and decreasing nutrient load in its surface layer. Deutsche Hydrographische Zeitschrift, 47: 319–327.

Neumann, T., Christiansen, C., Clasen, S., Emeis, K.-C., and Kunzendorf, H. 1997. Geochemical records of salt-water inflows into the deep basins of the Baltic Sea. Continental Shelf Research, 7: 95–115.

Pastuszak, M., Nagel, K., and Nausch, G. 1996. Variability in nutrient distribution in the Pomeranian Bight in September 1993. Oceanologia, 38: 195–225.

Rödel, R. 2001. Die Auswirkungen des historischen Talsperrenbaus auf die Zuflußverhältnisse der Ostsee. Ernst-Moritz-Arndt-Univ. Greifswald, Greifswalder Geographische Arbeiten, 18. 118 pp.

Samuelsson, M. 1996. Interannual salinity variations in the Baltic Sea during the period 1954–1990. Continental Shelf Research, 16: 1463–1477.

Santer, B. D., Wigley, T. M. L., Barnett, T. P., and Anyamba, E. 1996. Detection of climate change and attribution of causes. In: Climate Change 1995: The Science of Climate Change. Contr. of Working Group I to the Second Assessment Report of the Intergovernmental Panel of Climate Change, pp. 407–444. Ed. by J. T. Houghton, L. G. Meira Filho, B. A. Callander, N. Harris, N., A. Kattenberg, and K. Maskell. Cambridge University Press, Cambridge.

Schinke, H., and Matthäus, W. 1998: On the causes of major Baltic inflows: an analysis of long time series. Continental Shelf Research, 18: 67–97.

Siegel, H., Gerth, M., Tiesel, R., and Tschersich, G. 1999. Seasonal and interannual variations in satellite derived sea surface temperature of the Baltic Sea in the 1990s. Deutsche Hydrographische Zeitschrift, 51: 407–422.

Skei, J., Larsson, P., Rosenberg, R., Jonsson, P., Olsson, M., and Broman, D. 2000. Eutrophication and contaminants in aquatic ecosystems. Ambio, 29: 184–194.

Storch, H. v., and Hasselmann, K. 1995. Climate variability and change. Max-Planck-Institut für Meteorologie, Hamburg, Report, 152. 26 pp.

Wasmund, N., Voss, M., and Lochte, K. 2001. Evidence of nitrogen fixation by non-heterocystous cyanobacteria in the Baltic Sea and re-calculation of budget of nitrogen fixation. Marine Ecolology Progress Series, 214: 1–14.

Witt, G., and Matthäus, W. 2001. The impact of salt water inflows on the distribution of polycyclic aromatic hydrocarbons in the deep water of the Baltic Sea. Marine Chemistry, 74: 279–301.

Wulff, F., Rahm, L., and Larsson, P. (Eds.) 2001. A systems analysis of the Baltic Sea. Ecological Studies, 148. Springer-Verlag, Berlin, Heidelberg. 455 pp.

Wulff, F., Stigebrandt, A., and Rahm, L. 1990. Nutrient dynamics of the Baltic Sea. Ambio, 19: 126–133.

Zorita, E., and Laine, A. 2000. Dependence of salinity and oxygen concentrations in the Baltic Sea on the large-scale atmospheric circulation. Climate Research, 14: 25–42.

ICES Marine Science Symposia, 219: 144–149. 2003

Heat loss of the Norwegian Atlantic Current toward the Arctic

Kjell Arne Mork and Johan Blindheim

Mork, K. A., and Blindheim, J. 2003. Heat loss of the Norwegian Atlantic Current toward the Arctic. – ICES Marine Science Symposia 219: 144–149.

Hydrographic data from three standard sections (Svinøy, Gimsøy, and Sørkapp) in the Norwegian Sea are used along with a simple analytical model to investigate the heat loss of the Norwegian Atlantic Current toward the Arctic. The sections include data from 1978 to 2000. Only in the northern part of the Norwegian Sea is there a significant negative trend in salinity. The area occupied by Atlantic Water in the Svinøy Section decreased over a similar period, but showed a similarly rising temperature trend. Summer heat contents in the Svinøy and Gimsøy sections, however, show no prominent trend from 1979 to 2000. Results from the analytical model show that the lateral mixing process and the ocean-atmosphere heat flux in the Norwegian Atlantic Current are of the same order. The model also indicates a propagation speed of 3.2 cm s^{-1} from the Svinøy to the Gimsøy Section.

Keywords: heat loss, mixing, Norwegian Atlantic Current, Norwegian Sea, time-series.

Kjell Arne Mork and Johan Blindheim: Institute of Marine Research, PO Box 1870 Nordnes, NO-5817 Bergen, Norway [tel: +47 5523 8454; fax: +47 5523 8584; e-mail: Kjell.Arne.Mork@imr.no]. Correspondence to K. A. Mork.

Introduction

The main features of the circulation system in the Nordic Seas (Greenland, Iceland, and Norwegian Seas) were well described almost 100 years ago (Helland-Hansen and Nansen, 1909). The overall cyclonic circulation is characterized by a northward flow of warm water on the eastern side and a cold current flowing southward on the western side. The zone between the warm and the cold water masses in the Nordic Seas is referred to as the Arctic Front. The Atlantic inflow to the Norwegian Sea forms the most northern limb of the North Atlantic Current system and carries relatively warm and saline water from the North Atlantic to high latitudes. An update of the knowledge on these inflows was recently presented by Hansen and Østerhus (2000). Atlantic Water enters the Norwegian Sea through the Faroe–Shetland Channel, and Modified Atlantic Water enters between the Faroes and Iceland, flowing eastward along the Iceland–Faroe Front into the Norwegian Sea. A smaller branch, the North Icelandic Irminger Current, enters the Nordic Seas on the western side of Iceland (e.g. Stefansson, 1962; Kristmannsson, 1998). The Norwegian Atlantic Current (NwAC) splits into two main branches at about 71°N. One branch flows into the Barents Sea while the other one (West Spitsbergen Current) flows northward toward the Arctic Ocean (e.g. Swift *et al.*, 1997; Dickson *et al.*, 2000). The temperature and salinity conditions in these currents are monitored in three standard sections, as shown in Figure 1, and reported on annually as for example in Mork (2001) and on a decadal basis as in Loeng *et al.* (1992) and in the present report. These currents carry a large amount of heat and are important for the regional climate. They keep the entire Norwegian Sea and large areas of the Barents Sea ice free and open for biological production. The condition of the fish stocks in this region is normally best during high temperatures (e.g. Cushing, 1982; Holst, 1996).

Based on current measurements and hydrography, Orvik *et al.* (2001) estimated the annual Atlantic inflow to the Norwegian Sea to be 7.6 Sv. By studying other works along with new ADCP measurements of bottom currents Hansen and Østerhus (2000) estimated that about 9 Sv leave the Nordic Seas, which is compensated by an inflow of nearly 1 Sv through the Bering Strait (Roach *et al.*, 1995) and an 8 Sv inflow of Atlantic Water. With climatological data from COADS and ECMWF Simonsen and Haugan (1996) calculated the net heat loss in the Nordic Seas and Arctic Ocean to be

about 300 TW, which must be balanced by the Atlantic inflow through the Greenland–Scotland passage. In contrast, Blindheim (1993) estimated the annual heat inflow by dynamic calculation from hydrography data to be only 120 TW.

The properties of the north-going NwAC change due to heat loss to the atmosphere and by mixing with other water masses that are relatively colder and fresher. One goal of this work is to find the relative importance of the mixing process and the ocean–atmosphere heat loss of the NwAC.

Data

Positions of the sections from which data are obtained are shown in Figure 1. The sections that have been repeated regularly across the Atlantic inflow are: the Svinøy Section between 62°22′N, 05°12′E and 64°44′N on the prime meridian, the Gimsøy Section between 68°24′N, 14°04′E and 70°24′N, 08°12′E off the Lofoten Islands since 1978, while the zonal Sørkapp Section off the southern tip of West Spitsbergen, has been worked mainly along 76°20′N across the West Spitsbergen Current since 1965. The time-series from these sections are from July/August and also from March/April when used in the analytical model.

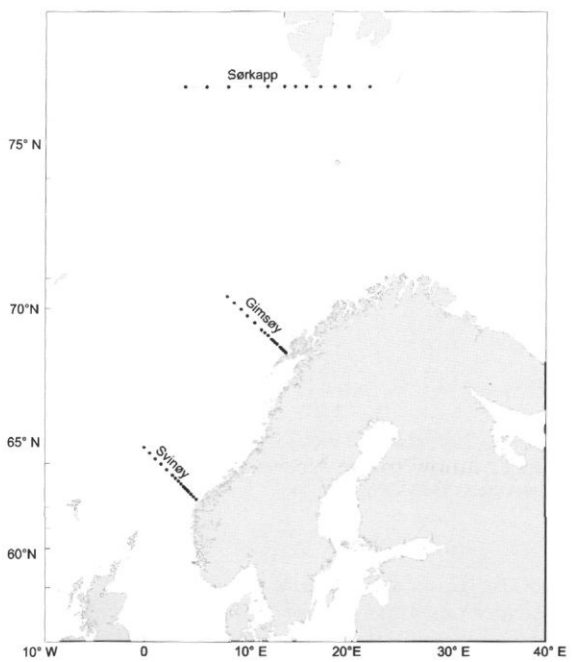


Figure 1. Locations of the Svinøy, Gimsøy, and Sørkapp sections.

Results and discussion

Figure 2 shows variations in temperature and salinity since 1978 in the three sections: Svinøy, Gimsøy, and Sørkapp. The values are averages between 50 m and 200 m in the core of Atlantic Water near the shelf edge. The data from the years 1978–1980 are ignored in calculating the trends because of the influence of the Great Salinity Anomaly (GSA, Dickson *et al.*, 1988). Trends with relatively high confidence levels are only seen in the Sørkapp Section, where a positive temperature trend is seen but with a confidence level of only 77%. It also has a negative trend in salinity with a confidence level as high as 98%.

In this work we have defined Atlantic Water as water masses with salinities greater than 35. Figure 3 shows the relative area for different water masses in "per thousand" from the total area of the Svinøy section. Areas of water masses are calculated in intervals of 0.025 and 0.25°C for salinity and temperature, respectively. Only summer data down to 1000 m depth from 1978 to 1999 are used. The figure shows that the salinity limit of 35 lies in a region with small values. Our choice of definition of Atlantic Water therefore seems acceptable, since small changes in salinity of the inflowing Atlantic Water will only change the integrated area with salinity above 35 to a small extent. Figure 4 shows that the area in the Svinøy Section occupied by Atlantic Water has decreased, and is also associated with a similar positive temperature trend. The confidence levels are 87% and 94%, respectively. A decreasing area is mainly a result of a narrowing NwAC generated by wind-forcing (Blindheim *et al.*, 2000; Mork and Blindheim, 2000). One result of a narrowing current will be that less Atlantic Water is exposed to the atmosphere; heat export to the atmosphere should be reduced correspondingly, so that more heat is conserved in the Atlantic Water as it flows northward. Blindheim *et al.* (2000) suggested that the negative trend in salinity is a result of increased mixing with Arctic water masses that are relatively colder and fresher. The temperature increase seen in the northern part of the Norwegian Sea might have been larger without this mixing.

We calculated the time-series of heat content anomaly, accumulated for temperatures above 0°C, and salt content in the Svinøy and Gimsøy sections to check their variability. The heat and salt contents were calculated for waters with salinity greater than 35. It must be mentioned that the westward spreading of Atlantic Water in the Gimsøy Section often reaches further westward than the section itself. This introduces some uncertainties in the heat content values for the Gimsøy Section. The time-series are shown in Figure 5. Comparing between the time-series for heat and salt contents in the Gimsøy

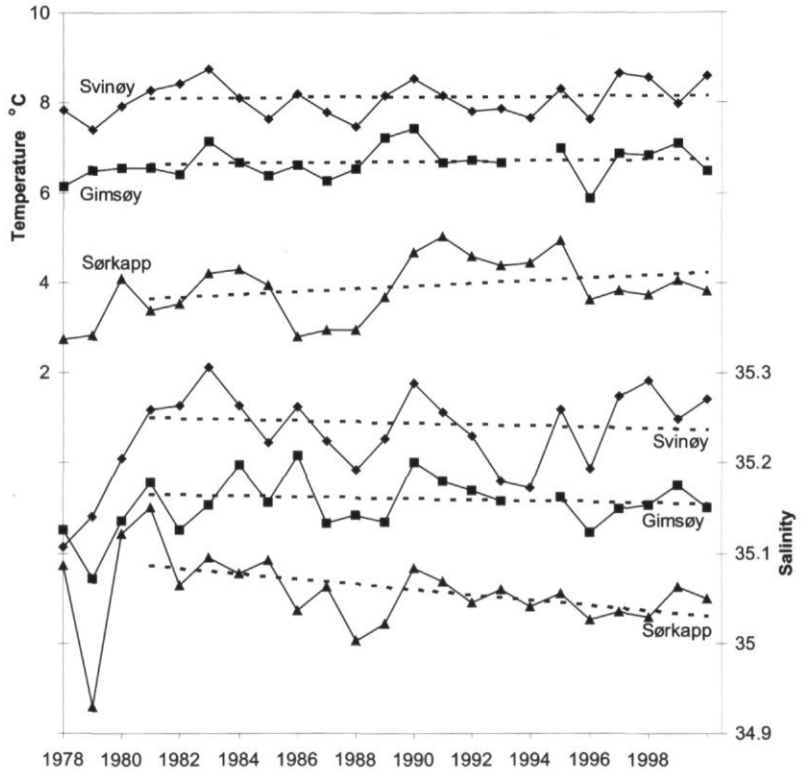


Figure 2. Temperature and salinity in the core of Atlantic Water in the Svinøy, Gimsøy, and Sørkapp sections, averaged between 50 and 200 m depth.

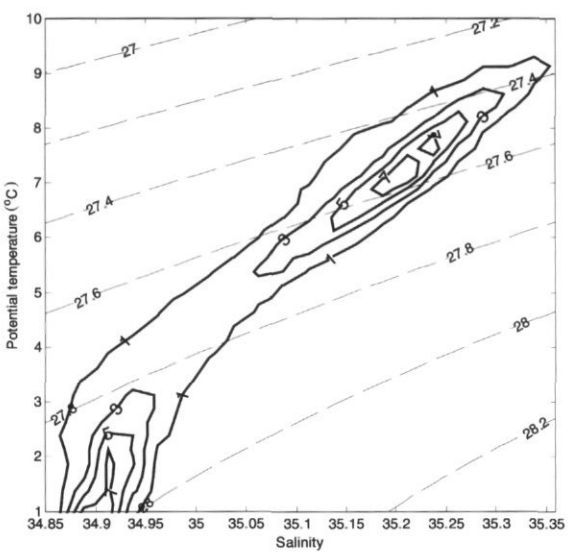


Figure 3. Relative areas of different water masses from the total area of the Svinøy Section. Values are in per thousands. The areas are calculated by integrating the found areas of salinities and temperature within intervals of 0.025 and 0.25°C, respectively. The figure represents the summer condition from 1978 to 1999 and only data down to 1000 m depth are used. Only values for temperatures above 1°C are shown.

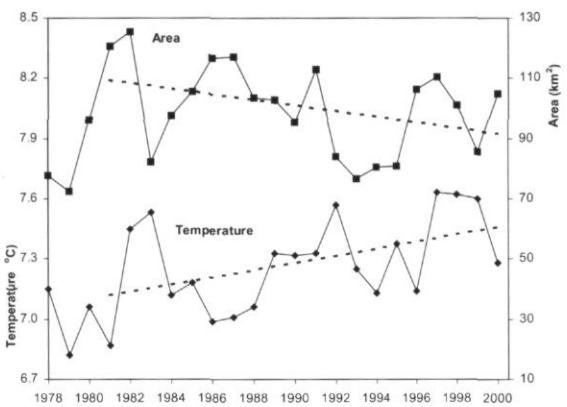


Figure 4. Time-series of area (in km²) and averaged temperature of Atlantic Water in the Svinøy Section, observed during July/August 1978–2000.

Section shows very similar variability. This should indicate that the mixing process is clearly more important than the ocean–atmosphere loss. However, there are also years with differences, e.g. 1996 and 2000, and these differences might be a result of increased or reduced heat loss to the atmosphere.

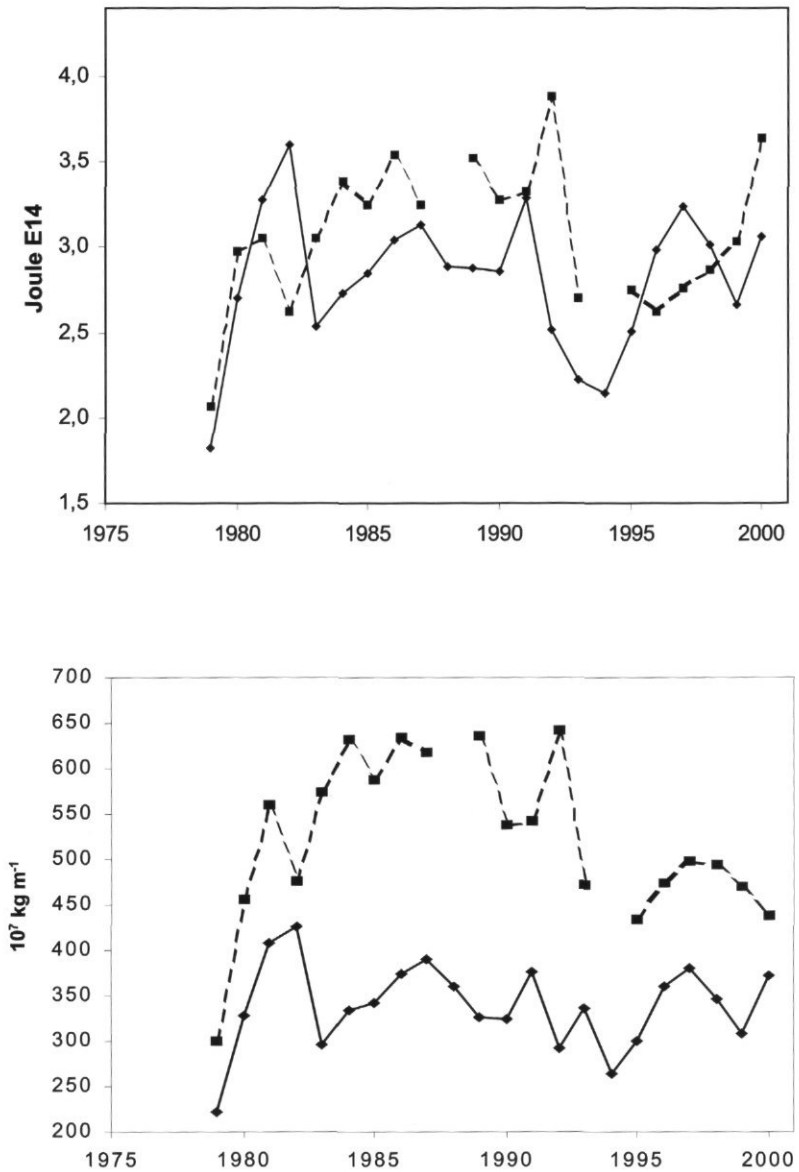


Figure 5. Heat content anomaly (top) and salt content (bottom) of Atlantic Water in the Svinøy (solid line) and Gimsøy (broken line) sections, 1979–2000.

A simple analytical model

A simple stationary model is introduced to further investigate the lateral mixing contra the ocean–atmosphere heat flux. For salinity, we assume a balance between north–south advection (between Svinøy and Gimsøy) and east–west mixing, while for temperature a heat loss term is included. The equations are therefore:

$$vS_y = AS_{xx} \quad (1)$$

$$vT_y = AT_{xx} + Q\,, \quad (2)$$

where v is the northward velocity, S is the salinity, T is the temperature, A is the horizontal diffusion coefficient, and Q is the vertical heat flux. The subscripts (y and xx) indicate partial derivative in a northward direction and double partial derivative in an eastward direction, respectively. For simplicity, we assume that v, S, and T are depth independent in the upper Atlantic layer. Vertical integration over the Atlantic layer, from the depth ($z = -h$) where

salinity equals 35 (the lower bound of the Atlantic layer) to the surface yields

$$v\frac{\partial}{\partial y}\left(\int_{-h}^{0} S dz\right) - vS_{-h}hy = A\int_{-h}^{0} S_{xx}dz \qquad (3)$$

$$v\frac{\partial}{\partial y}\left(\int_{-h}^{0} T dz\right) - vT_{-h}hy = A\int_{-h}^{0} T_{xx}dz + \int_{-h}^{0} Q dz. \qquad (4)$$

S_{-h} and T_{-h} are salinity and temperature, respectively, at the base of the Atlantic layer ($z = -h$) and are set constant in the north–south direction. By introducing an anomaly ($P' = P - P_{-h}$) where P is S or T and using $(P_{-h})_y = 0$, the equations can be written as:

$$(hS')_y = \frac{A}{v}\int_{-h}^{0} S_{xx}dz \qquad (5)$$

$$(hT')_y = \frac{A}{v}\int_{-h}^{0} T_{xx}dz + \frac{1}{v}\int_{-h}^{0} Q dz. \qquad (6)$$

Eliminating A/v and integrating from y = 0 to y = L gives

$$\Delta(hT') = R\Delta(hS') + \frac{L}{v}\int_{-h}^{0} Q dz \qquad (7)$$

where

$$R = \frac{\int_{-h}^{0} T_{xx}dz}{\int_{-h}^{0} S_{xx}dz} \qquad (8)$$

which we have assumed to be independent of y. Δ is the North–South difference operator and L is the distance between the Svinøy and Gimsøy sections.

It is now possible to compare the relations between the processes. The term on the left-hand side in Equation (7) is the north–south advection, the first term on the right side represents the diffusion, while the last term is the heat loss from the ocean to the atmosphere. The time, L/v, in Equation (7) is the time for an anomaly to move from the Svinøy Section to the Gimsøy Section. A large time span results in a large heat loss from the ocean to the atmosphere, because the water is exposed to the atmosphere for longer.

Using averaged hydrography data from 1978 to 2000 in the Svinøy and Gimsøy sections we can calculate the advection and diffusion terms from Equation (7). Figure 6 shows the averaged R in the Svinøy section for Mar/Apr and Jul/Aug. From the shelf edge and offshore R is about 10°C for both Mar/Apr and Jul/Aug. We have therefore used a constant R = 10°C. In calculating hS' and hT' in the

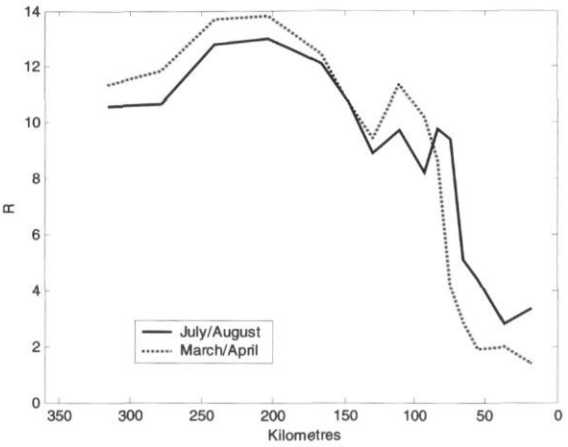


Figure 6. Averaged R ($\int T_{xx}dz$ / $\int S_{xx}dz$) in the Svinøy Section calculated for Mar/Apr and Jul/Aug, 1978–2000. Right-hand side is at the Norwegian coast.

Svinøy and Gimsøy sections we have used hydrographic data in the region with largest values of temperature and salinity, which is in the core of the Alantic layer. That region is roughly located over the 600 m isobath. Table 1 gives the averaged values used in the model.

The vertical heat flux Q is $(KT_z)_z$, where K is the ve'rtical diffusion coefficient and the subscript z indicates partial derivative in the vertical direction. The vertical integration of Q yields $H_f/(\rho_0 c_p)$ at the sea surface neglecting the vertical diffusion at $z = -h$. H_f (in W/m^2) is the heat flux from the ocean to the atmosphere, ρ_0 is a reference density and c_p is the heat capacity of seawater. For simplicity we have used $H_f = -37$ W m^{-2}, which we calculated as the annual mean heat flux in the eastern Norwegian Sea from the NOAA-CIRES data set. The distance L between the Svinøy and Gimsøy sections is about 10^6 m. Using the values in Table 1 we have calculated the time (L/v) to 12 months and the speed v to 3.2 cm s^{-1}. The speed is close to the speed of 2.5 cm s^{-1} that Dickson and Blindheim (1984) found by tracing a salinity anomaly from the Faroe–Shetland Channel to Spitsbergen during the late 1970s. The model also shows that mixing and heat loss processes are of similar orders (see Table 1).

Table 1. Values used in the analytical model and the results.

	Svinøy				Gimsøy		Advection	Mixing	Heat loss
	S_{-h}	T_{-h}	hT'	hS'	hT'	ST'	Δ(hT')	RΔ(hS')	L/v $\int$Qdz
Mar/Apr	35	4.0	1700	94	1190	72	−490	−220	−270
Jul/Aug	35	3.7	1790	101	1200	70	−590	−310	−280

Conclusion

Only the time-series of summer temperatures in the Atlantic core for the northern section shows a significant increasing linear trend and a decreasing salinity trend. The area in the Svinøy section occupied by Atlantic Water has decreased with a similar positive temperature trend during the same period. Results from the analytical model suggest that lateral mixing and ocean–atmosphere heat flux processes are of similar orders. The model also suggests that the time for an anomaly to move from the Svinøy Section to the Gimsøy Section is about 1 year, corresponding to a propagation speed of 3.2 cm s^{-1}.

Acknowledgements

This work received financial support from the NOCLim project at the Research Council of Norway and from the EU-project MAIA. Heat flux data are provided from the NOAA-CIRES Climate Diagnostics Center, Boulder, Colorado, USA, from their Web site at http://www.cdc.noaa.gov/. Thanks to Karen Gjertsen and Jan Erik Stiansen for help with figures and heat flux data, respectively.

References

Blindheim, J. 1993. Seasonal variations in the Atlantic inflow to the Nordic Seas. ICES CM 1993/C: 39.

Blindheim, J., Borovkov, V., Hansen, B., Malmberg, S. Aa., Turrell, W. R., and Østerhus, S. 2000. Upper layer cooling and freshening in the Norwegian Sea in relation to atmospheric forcing. Deep-Sea Research, 47: 655–680.

Cushing, D. H. 1982. Climate and Fisheries. Academic Press, London. 373 pp.

Dickson, R. R., and Blindheim, J. 1984. On the abnormal hydrographic conditions in the European Arctic during the 1970s. Rapports et Procès-Verbaux des Réunion du Conseil International pour l'Exploration de la Mer, 185: 201–213.

Dickson, R. R., Meincke, J., Malmberg, S.-Aa., and Lee, A. J. 1988. The "Great Salinity Anomaly" in the Northern North Atlantic 1968–1982. Progress in Oceanography; 20: 103–151.

Dickson, R. R., Osborn, T. J., Hurrell, J. W., Meincke, J., Blindheim, J., Adlandsvik, B., Vinje, T., Alekseev, G., and Maslowski, W. 2000. The Arctic Ocean response to the North Atlantic Oscillation. Journal of Climate, 13: 2671–2696.

Hansen, B., and Østerhus, S., 2000. North Atlantic–Nordic Seas exchanges. Progress in Oceangraphy, 45: 109–208.

Helland-Hansen, B., and Nansen, F. 1909. The Norwegian Sea. Its physical oceanography based upon the Norwegian researches 1900–1904. Report on Norwegian Fishery and Marine Investigations, vol. 2. 390 pp.

Holst, J. C. 1996. Long term trends in the growth and recruitment pattern of the Norwegian Spring spawning herring (*Clupea harengus Linnaeus* 1758). Thesis. University of Bergen. 131 pp.

Kristmannsson, S. S. 1998. Flow of Atlantic Water into the northern Icelandic shelf area, 1985–1989. ICES Cooperative Research Report, No. 225: 124–135.

Loeng, H., Blindheim, J., Ådlandsvik, B., and Ottersen, G. 1992. Climatic variability in the Norwegian and Barents Seas. ICES Marine Science Symposia, 195: 52–61.

Mork, K. A. 2001. The ecosystem in the Norwegian Sea, ocean climate (in Norwegian). *In* Havets miljø 2001, Fisken og havet, 2: 23–28. Ed. by J. H. Fossså.

Mork, K. A., and Blindheim, J. 2000. Variations in the Atlantic inflow to the Nordic Seas, 1955–1996. Deep-Sea Research, 47: 1035–1057.

Orvik, K. A., Skagseth, Ø., and Mork, M. 2001. Atlantic inflow to the Nordic Seas: current structure and volume fluxes from moored current meters, VM-ADCP and SeaSoar-CTD observations, 1995–1999. Deep-Sea Research I, 48: 937–957.

Roach, A. T., Aagaard, K., Pease, C. H., Salo, S. A., Weingartner, T., Pavlov, V., and Kulakov, M. 1995. Direct measurements of transport and water properties through the Bering Strait. Journal of Geophysical Research, 100: 18,443–18,457.

Simonsen, K., and Haugan, P. M. 1996. Heat budgets of the Arctic Mediterranean and sea surface heat flux parameterisations for the Nordic Seas. Journal of Geophysical Research, 101: 6553–6576.

Stefansson, U. 1962. North Icelandic waters. Rit Fiskideildar, 3. 269 pp.

Swift, J. H., Jones, E. P., Aagaard, K., Carmack, E. C., Hingston, M., Macdonald, R. W., McLaughlin, F. A., and Perkin, R. G. 1997. Waters of the Makarov and Canada basins. Deep-Sea Research II, 44: 1503–1529.

ICES Marine Science Symposia, 219: 150–159. 2003

Long-term hydrographic variability patterns off the Norwegian coast and in the Skagerrak

R. Sætre, J. Aure, and D. S. Danielssen

Sætre, R., Aure, J., and Danielssen, D. S. 2003. Long-term hydrographic variability patterns off the Norwegian coast and in the Skagerrak. – ICES Marine Science Symposia, 219: 150–159.

The Norwegian Coastal Oceanographic Observing System consists of observations of temperature and salinity in the surface layer, carried out at fixed positions from coastal liners, and measurements in the whole water column, carried out by local observers. The observations date back to 1935. Additionally, long-term data from the Institute of Marine Research station in Flødevigen on the Skagerrak coast and some selected data from the Torungen–Hirtshals hydrographic section are included. These data have been used to elucidate the long-term hydrographic variability along the Norwegian coast. Four relatively warm winter periods could be identified in the surface layer, culminating around 1950, 1960, 1975, and in 1990–1992. The long-term temperature and salinity trend 1950–1989 is negative along the whole coast. The 1990s, however, are characterized by having the highest mean decadal temperature for the whole period of observations along the southern coast. The importance of the 1990s in the surface layer is gradually reduced northwards. Along the northernmost coast, other decades, such as the 1950s or the 1960s, show higher decadal mean temperature. Also for the salinity the 1990s show high values along the southern coast, while other high salinity decades dominate further north. The high temperatures and salinities along the southern coast in the 1990s are caused by an increase in the Atlantic inflow in the late 1980s and early 1990s combined with the atmospheric conditions associated with periods of a high level of the North Atlantic Oscillations.

Keywords: long-term hydrographic variability, Norwegian coast, Skagerrak.

R. Saetre and J. Aure: Institute of Marine Research, PO Box 1870, NO-5817 Bergen, Norway. D. S. Danielssen: Institute of Marine Research, Flødevigen Marine Research Station, NO-4817 His, Norway.

Introduction

Norwegian Coastal Water (NCW) originates primarily from the freshwater outflow from the Baltic and the freshwater run-off from Norway. This water mixes with North Sea Water (NSW) and Atlantic Water (AW) to form the Norwegian Coastal Current, which flows northwards along the coast of Norway as a wedge-shaped low-salinity current bordered by the Norwegian North Atlantic Current off the central and northern parts of Norway (Figure 1). A description of the characteristic feature of this current system was given by Sætre and Ljøen (1972) and in Sætre and Mork (1981). The current system and water masses in the Skagerrak area have been described by Gustavsson and Stigebrandt (1996) and by Danielssen *et al.* (1997).

The Norwegian shelf is the spawning and hatching area for several commercially important fish species. Early in the previous century it was acknowledged that fluctuations in the hydrographic conditions along the coast might influence the recruitment, growth, and distribution of fish stocks. This was used as an argument for establishing the Norwegian Coastal Oceanographic Observing System (NCOOS) consisting both of observations from the surface layer by ships of opportunity and of fixed hydrographic station carried out by local observers. The observing system was established in the mid-1930s and is still operational. It represents some of the longest continuous oceanographic time-series in the world. Data from this observing system have been used in a large number of reports and publications for various purposes, including highlighting long-term variations (e.g. Ljøen and Sætre, 1978; Blindheim *et al.*, 1981; Danielssen *et al.*, 1996).

The aim of this contribution is to elucidate the long-term hydrographic variability patterns along the Norwegian coast and identify possible regional

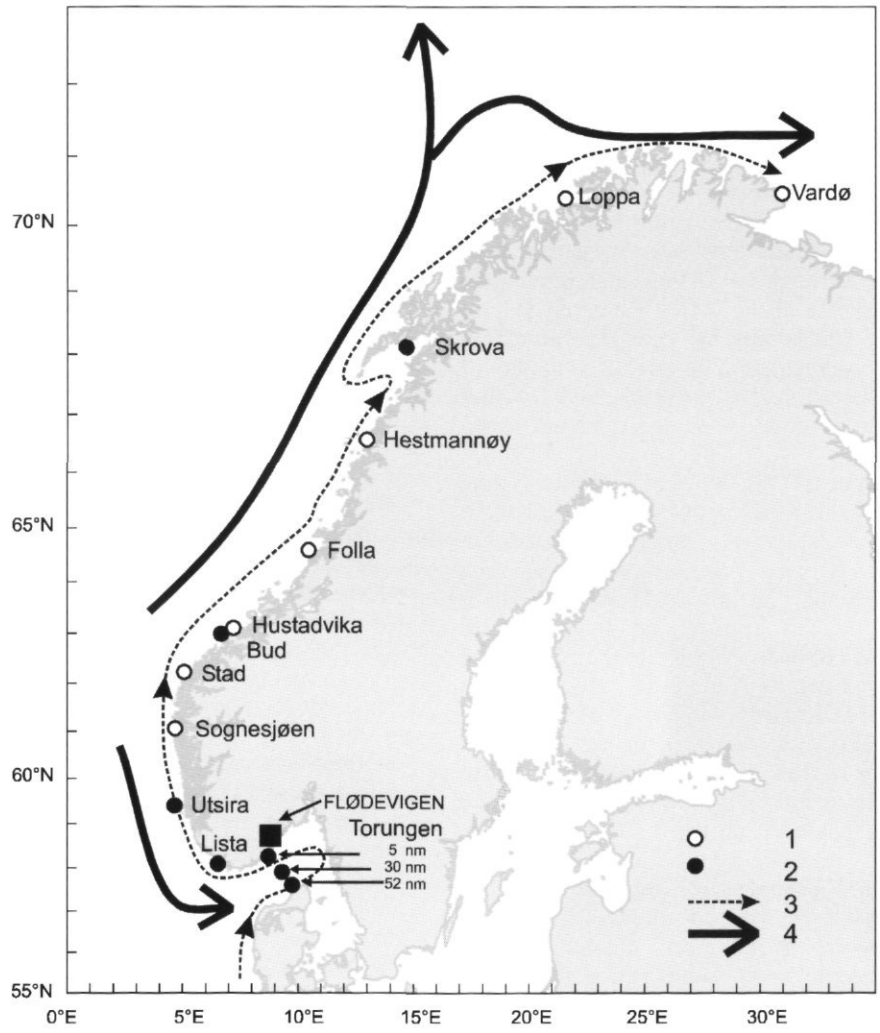


Figure 1. Selected stations for the present study along with the persistent currents. (1) Surface layer observations from coastal liners. (2) Fixed hydrographic stations. (3) Norwegian Coastal Current. (4) Norwegian North Atlantic Current.

differences with special emphasis on the situation in the 1990s. It is mainly confined to the winter situation, as this season is believed better to reflect the long-term climatic signals.

Material and methods

During the period 1935 to 1947 Jens Eggvin at the Institute of Marine Research (IMR) established a number of fixed hydrographic stations in Norwegian coastal waters (Eggvin, 1938, 1948). He also initiated a surface layer observation programme from ships of opportunity. Since 1951, the IMR has operated a standard hydrographic section across the central part of the Skagerrak between Torungen on the Norwegian side to Hirtshals on the Danish side. Since 1961 the section has on average been worked out 8–12 times a year. Some data from this section are presented as seasonal means as a basis for assessing possible biological effects of the variability in the physical environment. From this section three different positions are selected: one at 10 m depth, 5 nmi off Torungen in the Norwegian coastal current (Torungen 5 nmi), one at 300 m depth, 30 nmi from Torungen in the Atlantic water masses in the central Skagerrak (Torungen 30 nm), and one at 10 m depth, 52 nmi from Torungen near the Danish coast in the North Sea water masses (Torungen 52 nmi).

Figure 1 shows the location of the stations selected for the present study. For the ship of opportunity programme, regular coastal liners measure the temperature at predetermined locations at the intake of cooling water to the engine. Simultaneously, a water

sample is taken for analysis of the salinity. The depth of observations is approximately 4 m. The frequency of observations is usually 8–10 times per month.

At the fixed hydrographic stations the vertical temperature and salinity profiles are measured 2–4 times per month by local observers. Aure and Østensen (1993) present both mean values and long-term variations from the fixed stations. Since 1919 temperature and salinity have been measured daily in the pipeline through which seawater is pumped from various depths at the IMR's Research Station in Flødevigen. The salinity has been determined by means of an aerometer (pycnometer). The quality of the salinity observations is uncertain and for that reason only the temperature observations have been used.

The NORWegian ECOlogical Model system (NORWECOM) is a 3-D coupled physical, chemical, biological model system (Skogen *et al.*, 1995). In the present study, only results from the physical module are presented. The physical forcing variables are 6-hourly hindcast atmospheric pressure fields provided by the Hindcast Archive of the Norwegian Meteorological Institute (Eide *et al.*, 1985, Reistad and Iden, 1995), 6-hourly windstress derived from the pressure fields and freshwater run-off. The mean oceanic winter inflow (Jan–Mar) to the North Sea across the whole Orkney–Shetland–Norway section was calculated from the daily mean current component.

The long-term temperature and salinity trends along the coast have been normalized by taking the ratio between the long-term change and the standard deviation for the same period. Similarly, the deviation in the mean value between two mean periods has been normalized by using the ratio between the temperature or salinity deviation for the two periods and the standard deviation for the first period. The terms "warm winter" or "cold winter" mean that the temperature is above or below the long-term mean ±1 standard deviation.

Results and discussion

Surface layer

Figure 2 shows the mean temperature and salinity for the first quarter of the year (Jan–Mar) for selected stations along the whole Norwegian coast, along with the modelled winter inflow to the North Sea during Jan–Mar. The curves have been smoothed by 5-year running means. During the period 1940–2000 four relatively warm winter periods could be identified, culminating around 1950, 1960, 1975, and in 1990–1992. Up to the end of the 1980s there was a negative temperature trend along the whole coast (Table 1). The highest normalized temperature trend for the period 1950–1989 was −0.9 and −1.2 for Lista in the extreme south and Vardø in the extreme north, respectively.

The last period of warm winters started in 1987 and culminated at the beginning of the 1990s (Figure 2). During this period the highest winter temperatures since 1936 were observed along the southern and central parts of the Norwegian coast. Daily observations from the Torungen lighthouse back to 1867 strongly indicate that the winter of 1990 in southern Norway was the warmest in the last 130 years (Anon., 1993). Further north the temperature increase in the 1990s was significantly less, and at the stations of Folda, Loppa, and Vardø the 1960s show higher values. Comparing the mean decadal temperature for the 1990s with the mean for the period 1940–1989 the normalized deviation is reduced from 1.28 at Flødevigen to 0.17 at Vardø (Table 2, Figure 4A). The numbers of warm winters in the 1990s reduce from 8 along the Skagerrak coast to 1 at Loppa. Consequently, the effect of the warm 1990s was gradually reduced from south to north.

In the surface layer there is also a significant negative trend in winter salinity along the whole coast up to the end of the 1980s with the strongest salinity reduction at the end of this period (Figure 2, Table 1). The normalized salinity trend (the salinity trend/standard deviation) up to 1989 was highest along the southern and central coasts (Table 1) with a maximum at Stad of about −1.8. From the end of the 1980s there was again an increase in the salinity of the surface layer (Figure 2). Just as for the temperature, the salinity increase in the 1990s was markedly higher along the southern coast. However, the negative long-term trend before 1990 resulted in the salinity of the surface layer along most of the coast in the 1990s remaining below the long-term mean for the period 1940–1989. Only in the extreme south were the salinities in the 1990s above the 1940–1989 mean value (Table 2, Figure 4B).

Along most of the southern coast there appears to have been a shift in the temperature regime around 1988, and after that the temperatures reached above normal. This feature is especially pronounced at 19-m depth at Flødevigen (Figure 2). If we compare the seasonal mean temperature for the period 1940–1987 with the period 1988–2000 we can see that during winter and spring there has been a jump of more than 1°C. At the surface layer of the Torungen–Hirtshals section, the station on the Norwegian side (Torungen 5 nmi, Figure 1) during the same periods shows a difference of 1° to 1.7°C in winter and spring or 0.5–0.7 standard deviations, respectively (Table 4,

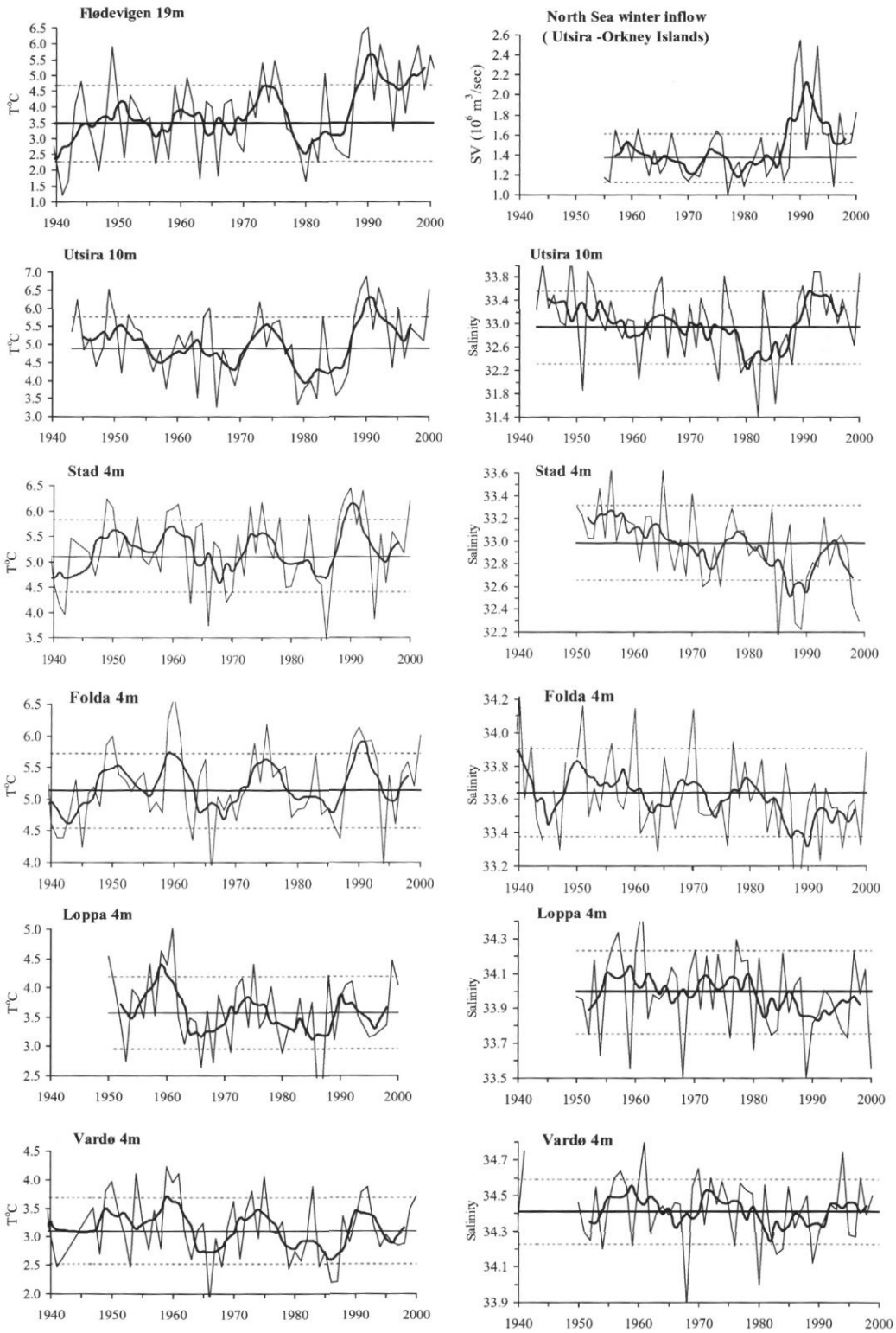


Figure 2. Mean temperature and salinity in the surface layer for the first quarter of the year (Jan–Mar) along the coast from north (upper) to south (lower) and the modelled winter inflow to the North Sea (upper right). Five-year running means are indicated.

Table 1. Temperature and salinity trends (T, S trend), standard deviation (stdev), and normalized trend (trend/stdev) at the surface layer stations and in 150-m depth at the fixed hydrographic stations during winter (Jan–Mar) from 1950 to 1989.

Station	T trend	T stdev	T trend/ T stdev	S trend	S stdev	S trend/ stdev
Surface layer						
Vardø	–0.68	0.58	–1.17	–0.11	0.18	–0.61
Loppa	–0.68	0.61	–1.11	–0.10	0.23	–0.43
Skrova	–0.48	0.61	–0.79	–0.14	0.38	–0.37
Folla	–0.32	0.59	–0.54	–0.28	0.26	–1.08
Stad	–0.40	0.71	–0.56	–0.60	0.33	–1.82
Utsira	–0.36	0.87	–0.41	–0.60	0.63	–0.95
Lista	–1.08	1.23	–0.88	–1.48	1.14	–1.30
150 depth						
Skrova	–0.16	0.55	–0.29	–0.12	0.20	–0.60
Sognesjøen	–0.22	0.29	–0.77	–0.07	0.07	–1.03
Utsira	–0.21	0.41	–0.52	–0.16	0.11	–1.45
Lista	–0.48	0.47	–1.02	–0.12	0.12	–1.02

Figure 6). There has also been an increase in salinity, except for the summer (Figure 6).

Approximately the same feature is seen in the surface layer on the Danish side (Torungen 52 nmi) of the section (Table 4, Figure 6), where the North Sea water masses enter the area. There has been a pronounced increase in temperature, especially in winter and spring, but not very much during the rest of the year. Here, the spring was also the period with the largest increase, 1.44°C, which is about 0.72 of the standard deviation for the period 1962–1987. There has also been an increase in salinity in all seasons except the summer. The largest increase has been in the autumn, with 0.61 of the standard deviation of the period 1962–1987 (Table 4, Figure 6).

The deeper layer (150–200 m)

There has also been a negative temperature trend in the deeper layer of the coastal water from about 1945 to the beginning of the 1980s (Figure 3). The normalized temperature trend 1950–1989 was highest at the southern stations (Figure 3, Table 1), with values between –0.3 and –1.0 standard deviation. As in the surface layer, there was also a significant temperature increase after 1987. The winter temperature at Utsira, Sognesjøen, and Skrova was the highest observed since 1936. The normalized temperature deviation in the 1990s compared to the period 1940–1989 was highest at the stations with highest salinity, i.e. those most influenced by the Atlantic Water, such as Torungen 30 nmi, Utsira, and Sognesjøen (Figures 3, 4C, Table 2). The Torungen 5 nmi, Lista, and Skrova stations are more influenced by the coastal water with lower salinity (Table 2).

In the deeper layer there is, in general, also a decrease in salinity from around 1950 to the early 1980s (Figure 3, Table 1). At the Lista, Utsira, and Sognesjøen stations, the reduction was highest during the period 1970 to the early 1980s, while further north at Skrova there was a gradual decrease from the mid-1960s to the beginning of the 1990s. At the stations in southern Norway the normalized salinity trend during the period 1950–1989 was between –1 and –1.4 standard deviations (Table 1). The increase in salinity from the mid-1980s and in the 1990s was highest at the stations with the highest salinity, i.e. those mostly influenced by Atlantic Water, such as in the open Skagerrak (Torungen 30 nmi) and at Utsira (Figure 4D, Table 2). The relatively cold and low salinity period at the end of the 1970s to early 1980s, which is most pronounced at Sognesjøen (Figure 3), appears to be associated

Table 2. Mean temperature and salinity (Tm, Sm) during the period from 1940(50) to 1989, mean deviation from this mean in the 1990s (Dev_{90s}), and normalized deviation ($Dev_{90s}/stdev_{40-89}$) for the surface stations and in 150 m depth at the fixed hydrographic stations during winter (Jan–Mar).

Stations (surface layer)	Tm_{40-89}	$DevT_{90s}$	$Dev\ T_{90s}/Tstdev_{40-89}$	Sm_{50-89}	$Dev\ S_{90s}$	$DevS_{90s}/Sstdev_{50-89}$
Vardø	3.10	0.10	0.17	34.41	–0.01	–0.06
Loppa	3.58	0.12	0.20	34.00	–0.10	–0.42
Skrova	3.46	0.24	0.39	33.15	–0.25	–0.66
Folla	5.14	0.29	0.49	33.64	–0.10	–0.38
Stad	5.10	0.40	0.57	32.98	–0.18	–0.55
Utsira	4.89	0.79	0.91	32.95	0.45	0.71
Lista	3.98	1.01	0.84	31.97	0.69	0.61
Flødevigen	3.50	1.53	1.28	30.37	1.34	0.55
Stations (150 m depth)	Tm_{50-89}	$DevT_{90}$	$DevT_{90s}/Tstdev_{50-89}$	Sm_{50-89}	$Dev\ S_{90s}$	$Dev\ S_{90s}/Sstdev_{50-89}$
Skrova	6.74	0.28	0.51	34.56	–0.12	–0.60
Sognesjøen	7.72	0.28	0.97	34.93	0.00	0.00
Utsira	7.38	0.35	0.85	34.92	0.06	0.55
Lista	6.87	0.07	0.15	34.81	–0.07	–0.59
Torungen 5 nmi	6.60	0.20	0.33	34.86	–0.07	–0.41
Torungen 30 nmi	6.89	0.51	0.78	35.09	0.05	0.42

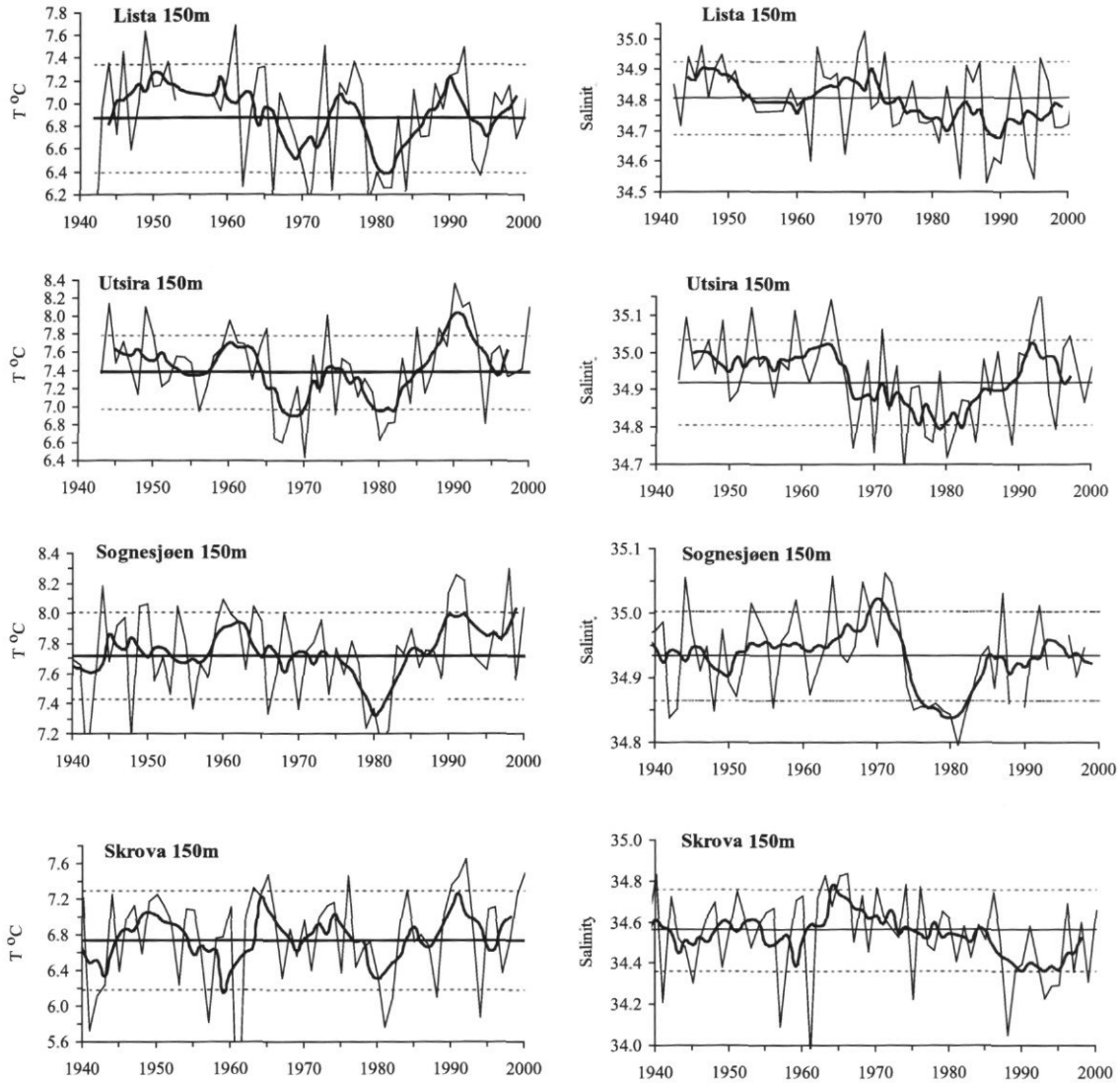


Figure 3. Mean temperature and salinity at 150-m depth for the first quarter of the year at the fixed hydrographic stations along the coast. Five-year running means are indicated.

with the "Great Salinity Anomaly" of the North Atlantic (Dickson *et al.*, 1988).

At 300-m depth in the central Skagerrak the normalized seasonal temperature deviation from the period 1962–1987 to the period 1988–2000 is 1.1 to 1.7 standard deviations, while that of salinity is 0.5 to 0.9 (Table 4, Figure 6). There was also an increase in the salinity in all seasons, between 0.5 and 0.9 of the standard deviation of the period 1962–1987 (Table 4, Figure 6). There is a very good correlation between the temperature and the salinity in the Atlantic water masses of the central Skagerrak, which is in accordance with the increased inflow of Atlantic Water to the North Sea during the past decade (Figure 2).

Discussion

The variable inflow of oceanic water to the Norwegian and North Seas will influence the hydrographic conditions along the Norwegian coast and in the Skagerrak. The modelled winter inflow to the North Sea during January–March from 1955 to 2000 appears in Figure 2. As the large-scale wind pattern is the main driving force, the fluctuation in this inflow will most likely also reflect the variability in the inflow to the Norwegian Sea. As seen, there was a significant increase in the inflow in the late 1980s and 1990s. During the period 1988–2000 there were 6 winters with extremely high inflow (> long-term mean +1 standard deviation). The mean

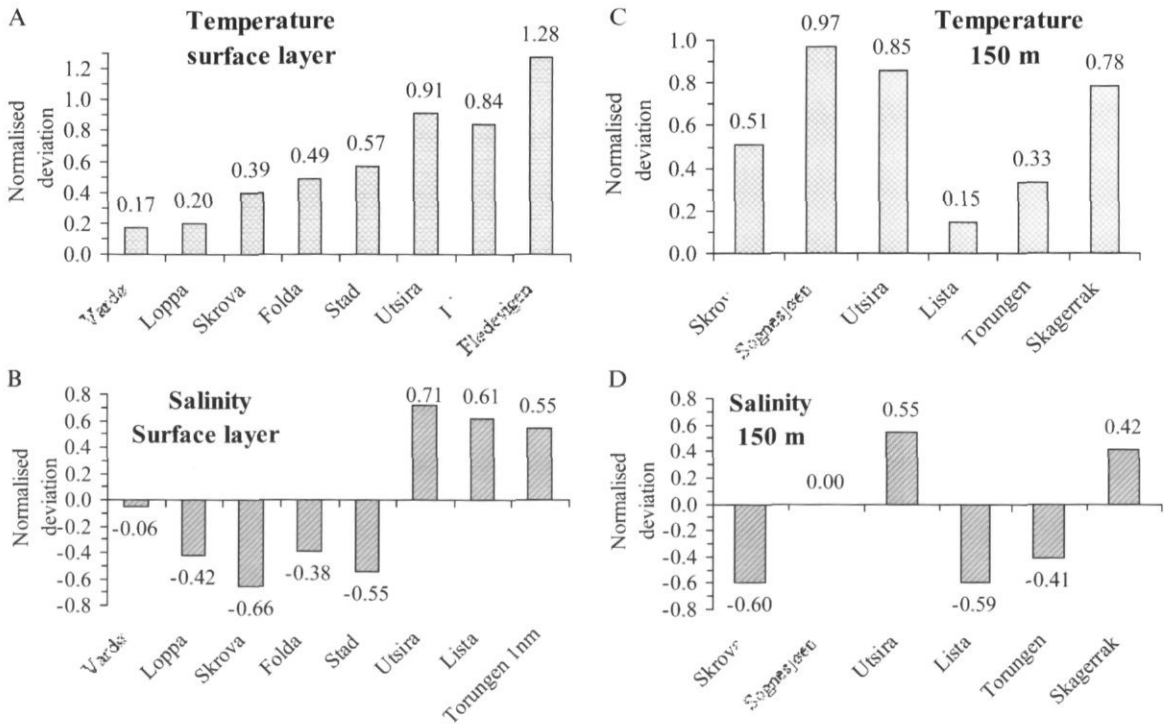


Figure 4. The normalized temperature and salinity deviation (temperature difference-salinity difference/standard deviation) between the decadal mean during the 1990s and the period 1940–1989 (temperature) and 1950–1989 (salinity).

inflow in the 1990s was 1.75 Sv or 1.6 standard deviations above the long-term mean for 1955–1989. This inflow was highly correlated with the North Atlantic Oscillation (NAO) winter index (Hurrell, 1995) with r^2 approaching 0.5. A high NAO index is associated with mild winters and an increase in the westerly winds and the winter precipitation over Scandinavia.

The wedge-shaped Norwegian Coastal Current is deep and narrow during winter and wide and shallow during summer. The driving mechanism for this seasonal lateral oscillation of the current is most likely an effect of the monsoon-like wind pattern along the Norwegian coast (Sætre *et al.*, 1988). High NAO levels mean increased southwesterly winds, and this will deepen the Norwegian Coastal Current off most of the coast and could result in colder and less saline coastal water. Consequently, a high NAO winter index is not necessarily synonymous with higher temperature and salinity in coastal waters.

The increased temperatures and salinities during winter in Norwegian coastal water in the 1990s are clearly related to a significant increase of the inflow of relatively warm and saline Atlantic Water during the same period and especially in the deeper layers which are more directly influenced by the Atlantic Water. Figure 5 shows the relationship between the winter inflow to the North Sea and the temperature in the upper layer for the period 1989–2000. Off the

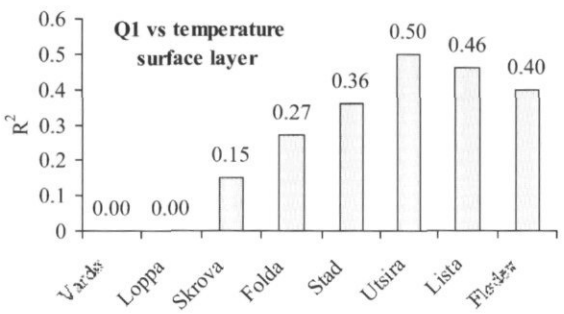


Figure 5. The correlation coefficient (r^2) between the winter inflow to the North Sea (Jan–Mar) and the temperature in the upper layer for the period 1989–2000.

southern coast the correlation is reasonably good (Table 3), but is markedly reduced further north. The variability pattern in the Atlantic inflow to the Norwegian Sea will most likely be similar to that of the North Sea. The Stad station is believed to reflect the fluctuations in this northern branch of the Atlantic inflow towards the Norwegian coast. The correlation between the winter temperatures at Stad versus those of the other coastal stations (Table 3) indicates low Atlantic influence off the coast of northern Norway.

Table 3. The correlation coefficient (r^2) between the winter inflow of Atlantic Water to the North Sea (Q_1) and surface layer temperature in Jan–Mar at the coastal stations and between winter temperature at the station Stad versus the other coastal stations during the period 1989–2000.

Station	r^2 (Q1)	r^2 (Stad)
Vardø	0	0.28
Loppa	0	0.10
Skrova	0.15	0.14
Folda	0.27	0.90
Stad	0.36	*
Utsira	0.50	0.70
Lista	0.46	0.68
Flødevigen	0.40	0.75

Table 4. Mean seasonal temperature and salinity in the periods 1962–1987 and 1988–2000, the difference in means between the two periods, the standard deviation for the period 1962–1987 and the normalized deviation (Diff/stdev) between the two periods at the stations Torungen 30 nmi (300 m), Torungen 5 nmi (10 m) and Torungen 52 nmi (10 m) (Torungen–Hirtshals section).

	$S_{62\text{-}87}$	$S_{88\text{-}00}$	Diff S	stdev $S_{62\text{-}87}$	Diff S/stdev
30 nmi 300 m S-Season					
Winter	35.12	35.15	0.03	0.07	0.47
Spring	35.08	35.14	0.06	0.07	0.86
Summer	35.11	35.17	0.06	0.07	0.82
Autumn	35.13	35.18	0.05	0.06	0.87
30 nmi 300 m T-Season					
Winter	6.27	6.91	0.63	0.56	1.1
Spring	5.72	6.61	0.88	0.62	1.4
Summer	5.68	6.57	0.89	0.51	1.7
Autumn	6.02	6.78	0.76	0.5	1.5
5 nmi 10 m S-Season					
Winter	31.15	32.13	0.97	2.08	0.47
Spring	29.08	29.74	0.65	2.87	0.23
Summer	30.01	30.35	0.34	1.67	0.20
Autumn	31.33	30.97	–0.36	2.02	–0.18
5 nmi 10 m T-Season					
Winter	4.63	5.68	1.06	2.27	0.46
Spring	4.36	6.09	1.72	2.63	0.65
Summer	14.34	14.32	–0.02	2.63	–0.01
Autumn	12.14	13.06	0.92	2.30	0.40
52 nmi 10 m S-Season					
Winter	33.78	34.14	0.36	0.95	0.38
Spring	33.40	33.67	0.28	1.31	0.21
Summer	32.39	32.25	–0.14	1.14	–0.12
Autumn	32.94	33.48	0.55	0.90	0.61
52 nmi 10 m T-Season					
Winter	5.69	6.51	0.82	1.68	0.49
Spring	5.14	6.58	1.44	1.99	0.72
Summer	13.89	14.29	0.40	2.50	0.16
Autumn	12.40	12.54	0.14	2.34	0.06

This, combined with the reduced normalized temperature and salinity deviation from south to north during the 1990s (Table 2, Figure 4A, B), indicates that the increased inflow of Atlantic Water in the 1990s mostly influenced the hydrographic conditions in the upper layer along the southern and central Norwegian coasts. There is a rather strong positive correlation between the temperature and salinity variations (r^2 around 0.5) along the southern coast, while further north the two parameters appear to be uncorrelated. This supports the above statement.

The long-term decreasing salinity trend in the surface layer along the Norwegian coast is probably mainly caused by the increased precipitation and thereby the substantial increase in freshwater run-off. Førland *et al.* (2000) demonstrated that the winter precipitation in western Norway is more than 25% higher during 1980–1999 than for the normal period 1961–1990. It is likely that this precipitation pattern reflects that of northwestern Europe, so in the 1990s the Norwegian Coastal Current has been supplied with more freshwater from the Baltic and from the North Sea. One of the effects of the regulation of the freshwater run-off due to construction of hydroelectric power plants is increased winter discharge and this may also be an important explanatory factor. Asvall (1976) shows that in the southeastern region of Norway the mean natural winter freshwater discharge during the period 1969–1973 increased by up to 170% due to flow regulation.

Along the southern and central Norwegian coasts the winters of the 1990s are characterized by the highest decadal mean temperatures both in the surface and in deeper layers for the whole period of observations. In the upper layer this tendency is most pronounced in the southern parts. Along the northern coast, however, other decades, such as the 1950s and the 1970s, show higher decadal mean temperatures.

Along the northern Norwegian coast bordering the Barents Sea, variability patterns seem to follow that observed in the open Barents Sea (Ingvaldsen *et al.*, 2003), where the 1950s were notably colder than the 1990s. Although the NAO has a significant effect on the climatic variability of the area, local wind and atmospheric pressure forces seem to be major factors determining the degree of Atlantic inflow to, as well as the circulation and water mass distribution within, the Barents Sea (Ingvaldsen *et al.*, 2003).

The observations of long-term temperature and salinity variability in Norwegian Coastal waters suggest that the fluctuations may be due either to direct changes in the heat transfer of the region or be advective in nature (Blindheim *et al.*, 1981). However, this is most likely not a case of "either/or". The two types of climatic signals probably interact in a rather complicated way.

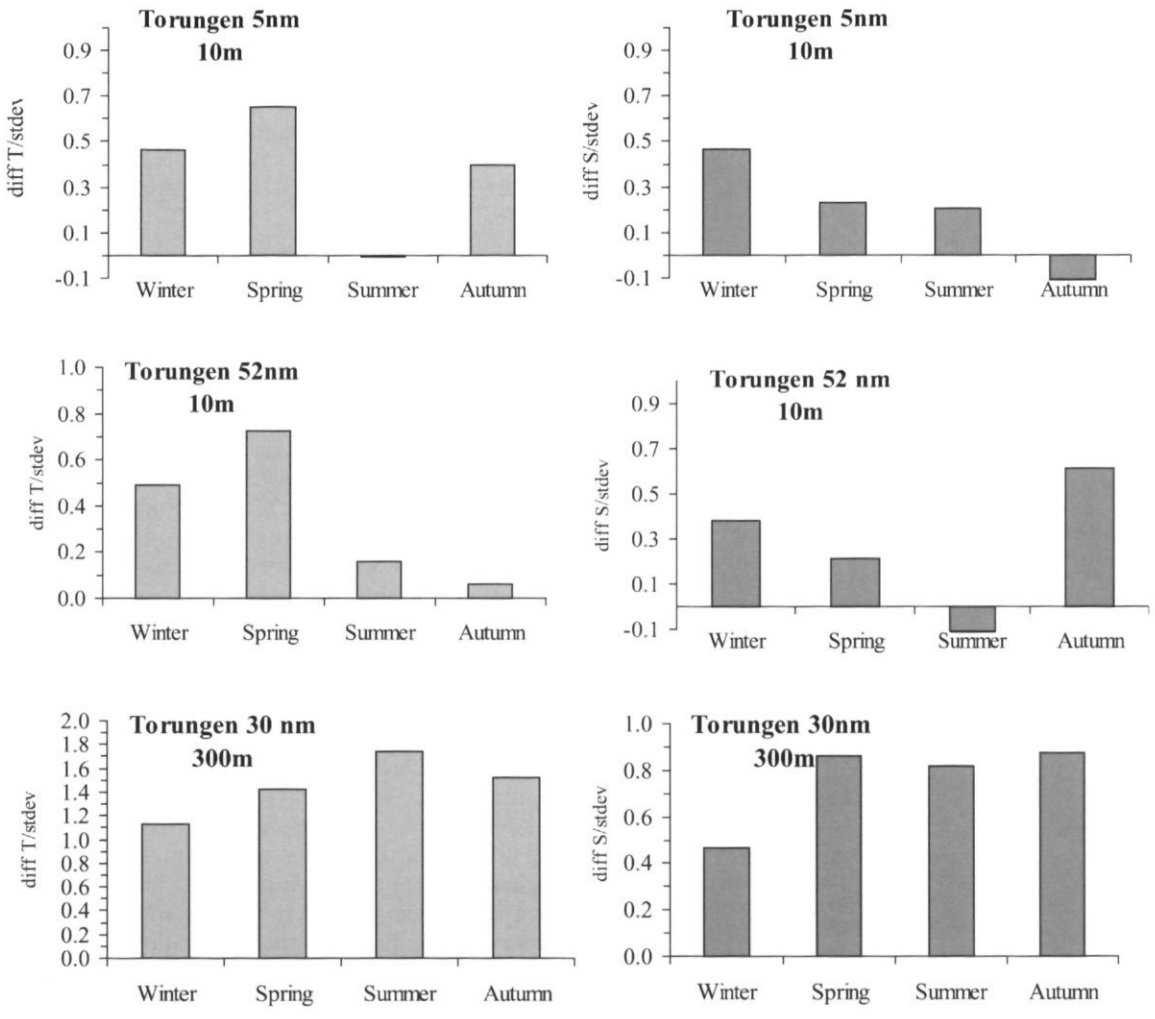


Figure 6. The normalized seasonal deviation (deviation/standard deviation) in temperature and salinity between the periods 1962–1987 and 1988-2000 for 3 stations on the Torungen-Hirtshals section.

References

Anon. 1993. North Sea subregion 8. Assessment report 1993. North Sea Task Force. State Pollution Control Authority (SFT) Oslo, Norway. 77 pp.

Asvall, R. P. 1976. Effects of regulations on fresh water runoff. *In* Fresh Water on the Sea, pp. 15–20. Ed. by S. Skreslett, R. Leinebø, J. B. L. Matthews, and E. Sakshaug. Association of Norwegian Oceanographers, Oslo.

Aure, J., and Østensen, Ø. 1993. Hydrographic normals and long-term variations in Norwegian coastal waters. Fisken og Havet, 6. 75 pp.

Blindheim, J., Loeng, H., and Sætre, R. 1981. Long-term temperature trends in Norwegian Coastal waters. CM 1981/C: 19. 13 pp.

Danielssen, D. S., Svendsen, E., and Ostowski, M. 1996. Long-term hydrographic variations in the Skagerrak based on the section Torungen–Hirtshals. ICES Journal of Marine Science, 53: 917–925.

Danielssen, D. S., Edler, S., Fonselius, L., Hernroth, L., Ostrowski, M., Svendsen, E., Talpsepp, L. 1997. Oceanographic variability in the Skagerrak and Northern Kattegat, May–June, 1990. ICES Journal of Marine Science, 54: 753–773.

Dickson, R. R., Meincke, J., Malmberg, S. Aa., and Lee, A. 1988. The "Great Salinity Anomaly" in the Northern North Atlantic 1968–1982. Progressive Oceanography, 20: 103–151.

Eggvin, J. 1938. The bottom temperatures. Fiskeridirektorats Skrifter Serie Havundersøkelser, 5(6): 50–68.

Eggvin, J. 1948. De oseanografiske forhold på norskekysten i de senere år og deres forhold til fiskeriene. Naturen, 72: 267–276. (In Norwegian.)

Eide, L. I., Reistad, M., and Guddal, J. 1985. Database av beregnede vind og bølgeparametre for Nordsjøen, Norskehavet og Barentshavet hver sjette time for årene 1955 til 1981. DNMI Report, Norwegian Meteorological Office, Oslo/Bergen, Norway. 38 pp. (In Norwegian.)

Fromentin, J. M., and Planque, B. 1996. Calanus and environment in the eastern North Atantic. II. Influence of the

North Atlantic Oscillation on *C. finmarchicus* and *C. helgolandicus*. Marine Ecology Progress Series, 134: 111–118.

Førland, E., Roald, L. A., Tveito, O. E., and Hanssen-Bauer, I. 2000. Past and future variations in climate and runoff in Norway. Klima, Report no. 19. 77 pp.

Gustavsson, B., and Stigebrandt, A. 1996. Dynamics of the freshwater-influenced layers in the Skagerrak. Journal of Sea Research, 35: 39–53.

Hurrell, J. W. 1995. Decadal trends in the North Atlantic Oscillation: regional temperatures and precipitation. Science, 269: 676–679.

Ingvaldsen, R., Loeng, H., Ådlandsvik, B., and Ottersen, G. 2003. The Barents Sea climate during the 1990s. ICES Marine Science Symposia, 219: 160–168. (This volume.)

Ljøen, R., and Sætre, R. 1978. Long-term hydrographic variations off southern Norway. Rapports et Procès-Verbaux des Réunions du Conseil International pour l'Exploration de la Mer, 172: 345–349.

Reistad, M., and Iden, K. A. 1995. Updating, correcting and evaluation of a Hindcast Data Base of air pressure, winds and waves for the North Sea, Norwegian Sea and Barents Sea. Technical Report No. 9. Norwegian Meteorological Institute.

Sætre, R., and Ljøen, R. 1972. The Norwegian Coastal Current. Proceedings from the First International Conference on Port and Ocean Engineering under Arctic Conditions, vol. 1: 514–535.

Sætre, R., and Mork, M. (Eds.). 1981. The Norwegian Coastal Current. Proceedings from the Norwegian Coastal Current Symposium. Geilo, 9–12 September 1980. Vols. I and II. University of Bergen.

Sætre, R., Aure, J., and Ljøen, R. 1988. Wind effects on the lateral extension of the Norwegian Coastal Water. Continental Shelf Research, 8: 229–253.

Skogen, M., Berntsen, J., Svendsen, E., Aksnes, D., and Ulvestad K. 1995. Modelling the primary production in the North Sea using a coupled three-dimensional physical chemical biological ocean model. Estuarine and Coastal Shelf Science, 41: 545–565.

ICES Marine Science Symposia, 219: 160–168. 2003

Climate variability in the Barents Sea during the 20th century with a focus on the 1990s

Randi Ingvaldsen, Harald Loeng, Geir Ottersen, and Bjørn Ådlandsvik

Ingvaldsen, R., Loeng, H., Ottersen, G., and Ådlandsvik, B. 2003. Climate variability in the Barents Sea during the 20th century with a focus on the 1990s. – ICES Marine Science Symposia, 219: 160–168.

Time-series of temperature in three sections representative of Atlantic Water in the Barents Sea reveal that the climate in the region has both long-term and short-term quasi-regular periods. Compared with other decades during the 20th century, the 1990s were colder than both the 1930s and 1950s. The 1990s started out warm, with a short, relatively cold, period in 1996–1998. During the final years of the decade there was a gradual build-up towards higher temperatures, with very high anomalies during late autumn and early winter. Through regional and local effects, the North Atlantic Oscillation (NAO) has a significant influence on the Barents Sea on decadal time scales and during extreme NAO events. Still, local atmospheric forcing not captured by the NAO index seems to dominate the distribution of the water masses within the area. The local pressure field appears to change the relative strength of the two branches going respectively northeast and east, thereby having a significant effect on the local climate. The local pressure distribution not captured by the NAO index also has some influence on the total inflow to the Barents Sea.

Keywords: Barents Sea, climate variability, decadal, North Atlantic Oscillation, 1990s.

R. Ingvaldsen, H. Loeng, G. Ottersen, and B. Ådlandsvik: Institute of Marine Research, PO Box 1870 Nordnes, NO-5817 Bergen, Norway [tel: +47 55 238 596; fax: +47 55 238 584; e-mail: firstname.surname@imr.no]. Correspondence to R. Ingvaldsen.

Introduction

The first broad analysis of the hydrography, currents, and climate variability in the Barents Sea was carried out by Helland-Hansen and Nansen (1909), who suggested that the climate variations in this region were probably of an advective nature. However, not all changes in the Barents Sea are traceable upstream, and advection in the ocean does not explain a major part of the variability in the temperature conditions (Ottersen *et al.*, 2000). Ådlandsvik and Loeng (1991) demonstrated that the inflow of Atlantic Water (AW) to the Barents Sea is determined, to a large degree, by local atmospheric forcing. Their conceptual feedback model stated that cyclonic airflow in the Barents Sea would increase the Atlantic inflow and thereby increase the temperature. The higher temperatures would then maintain a low air pressure. The Barents Sea temperature conditions are further influenced by local winter cooling and ice processes. Formation of water of high density during winter, followed by draining from the sea in bottom currents, may be an important temperature-regulatory factor (Midttun, 1985). The activity in building up dense bottom water may vary from one year to the next, followed by variations in the outflow with corresponding changes in the inflow. In recent years, a relation between the Barents Sea climate and the North Atlantic Oscillation (NAO) has been proposed by Grotefendt *et al.* (1998), Dickson *et al.* (2000), Ottersen and Stenseth (2001), and Ottersen *et al.* (2003).

The Barents Sea is a pathway for AW to the Arctic Ocean, and the transformation of AW when it passes through the Barents Sea is important for the ventilation of the Arctic Ocean (e.g. Aagaard and Woodgate, 2001). Observations have shown that the Barents Sea provides intermediate water reaching to a depth of 1200 m in the Arctic Ocean (Rudels *et al.*, 1994; Schauer *et al.*, 1997). Barents Sea climate is therefore also important for large-scale climate developments linked to the Arctic Ocean.

The present study deals with climatic variability in the Barents Sea, emphasizing the Atlantic domain

in the 1990s. Temperature data from three hydrographic sections and a geographically distributed data set were analysed. The relationship between temperature variability in the different sections and horizontal distribution of temperature was investigated. Finally, causes for the observed climatic variability are suggested.

Material and methods

Location of the stations and sections from which data were obtained are shown in Figure 1. This includes time-series of temperature in the section Fugløya-Bear Island (FB) at the western entrance of the Barents Sea and the section Vardø-N along 31°13′E. The time-series go back to 1953 in the Vardø-N Section, while in the FB Section the regular observations started in 1964. In the beginning, regular observations were taken only once a year, in late August or early September. Since 1977, regular observations have been carried out more frequently: six times a year at the FB Section and four times a year at the Vardø-N Section. The data presented here are average temperatures for 50–200 m in the part of the section where the main Atlantic inflow takes place as identified by salinity (Blindheim and Loeng, 1981). For the FB Section this means between 71°30′N and 73°30′N and for the Vardø-N Section the area between 72°15′N and 74°15′N was used. Data from the Russian records on the Kola Section along 33°30′E are also included. Data from 1921 to the present day are presented as monthly mean values calculated for the depth interval between 0 and 200 m in the area between 70°30′N and 72°30′N. Historical data were taken from Bochkov (1982) and Tereshchenko (1996), while data from recent years were provided by PINRO, Murmansk.

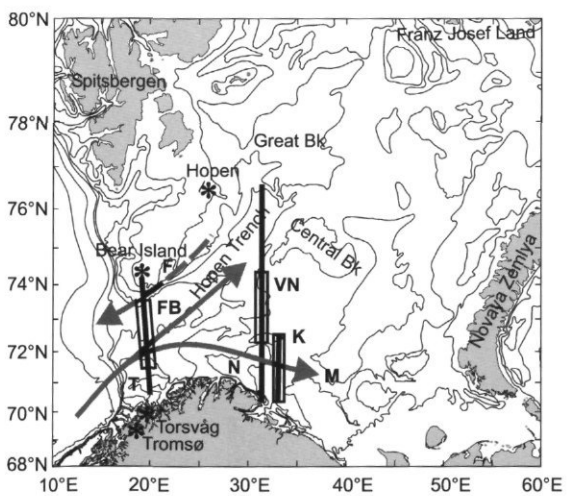


Figure 1. The Barents Sea. The solid and dashed arrows indicate flow of Atlantic Water (AW) and Arctic Water, respectively. The sections Fugløya-Bear Island (FB), Vardø-N (VN), and Kola (K) are shown, and the area where average temperatures were calculated is indicated. The locations of the meteorological stations are symbolized by an asterisk. Letters symbolize Tromsø Bank (T), the Nordkapp Bank (N), Finger Canyon (F), and the Murmansk Current (M).

The meteorological data were supplied by the Norwegian Meteorological Institute. The surface air temperatures are from their stations at Torsvåg, Tromsø, Bear Island, and Hopen (Figure 1), while the winter mean sea level pressures (SLP) are from their hindcast archive (Eide *et al.*, 1985).

Horizontal fields of temperature from 1970 to 2000 were constructed based on data sampled during international fish surveys carried out every year. Data from the area south of 75°N were sampled by 2 Norwegian and 2 USSR research vessels between 20 August and 10 September each year. Data from the area north of 75°N were sampled by 2–3 Norwegian and USSR vessels in the period 10 September to 10 October. Gaps in the vertical were filled by simple linear interpolation separately for each station. For each separate vertical level a 2D algorithm (Taylor, 1976), combining Laplace and cubic spline interpolation, was applied. The grid distance was 20×20 km. No extrapolation was performed nor smoothing, except for the implicit effect of the interpolation.

The long-term means for the sections were calculated for the period 1961–1990, following the international meteorological mean period, and all anomalies were calculated based on this mean period. For the horizontal temperature fields the long-term mean was prepared for the shorter period 1970–2000 due to the availability of data.

Results

The Barents Sea climate alternates between warm and cold periods, which have both long-term and short-term quasi-regular fluctuations (Figure 2). The temperature fluctuation is similar in all the sections. During the 1950s and 1960s the variability was high and fluctuations with periods of about 3–5 years were predominant. Prior to and after these decades, longer periods were more pronounced. Comparisons of the August temperature anomalies decade by decade reveal the same for the oceanographic sections and meteorological stations: the 1990s were warm, but the 1930s and 1950s were even warmer (Figure 3).

In order to investigate how representative the sections are for the rest of the Barents Sea, the time-series of temperature in each point in the horizontal

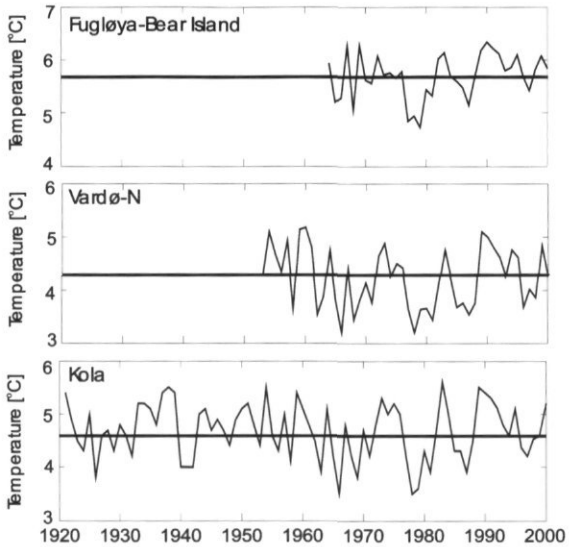


Figure 2. Time-series of mean August temperature for the hydrographic sections.

field were correlated with mean temperature of the section time-series averaged over the same months (Figure 4). In general, all sections show relatively high correlation, with values of 0.6 or higher throughout the Atlantic domain. An exception is in a narrow north–south band near 22°E, where the maps indicate two patches of poor correlation (Figure 4). The northern patch seems to be located in the area of Finger Canyon, where the local topography modifies the circulation and the frontal position (Parsons *et al.*, 1996). The southern patch is confined to the 400 m deep trough between Tromsø Bank and Nordkapp Bank (Figure 1) where there is a more or less permanent eddy (Loeng *et al.*, 1989). All maps also indicate that the temperature in the northern and northeastern Barents Sea, which is occupied by Arctic water masses, is more or less uncorrelated with the standard section temperatures, at least when considering unlagged correlations. Also in the bank areas the sections fail to relect the temperature conditions. This is not surprising, as local forcing is dominant in these areas. The Central Bank is covered by a large-scale eddy with long residence time that prevents AW entering (Quadfasel *et al.*, 1992).

A closer examination of the 1990s reveals that this decade started out warm, followed by a period with temperatures slightly below the long-term mean in 1996–1998 (Figure 5). During the last 2 years of the decade the temperature increased to above the long-term mean, with especially high anomalies during winter in 1999 and 2000. In fact, during the winter of 1999 the anomaly in the FB Section was 1°C above the long-term mean (Figure 5). During the 1990s the total temperature variability spanned a range of 1.5°C.

Temperature anomalies at 100 m show that the 1990s started out warm in the Atlantic and in most of the Arctic domain (Figure 6). Thereafter there was a gradual temperature decrease in the western and increase in the eastern parts in 1991 and 1992. The year 1993 was significantly colder than the previous years, followed by a short warming period

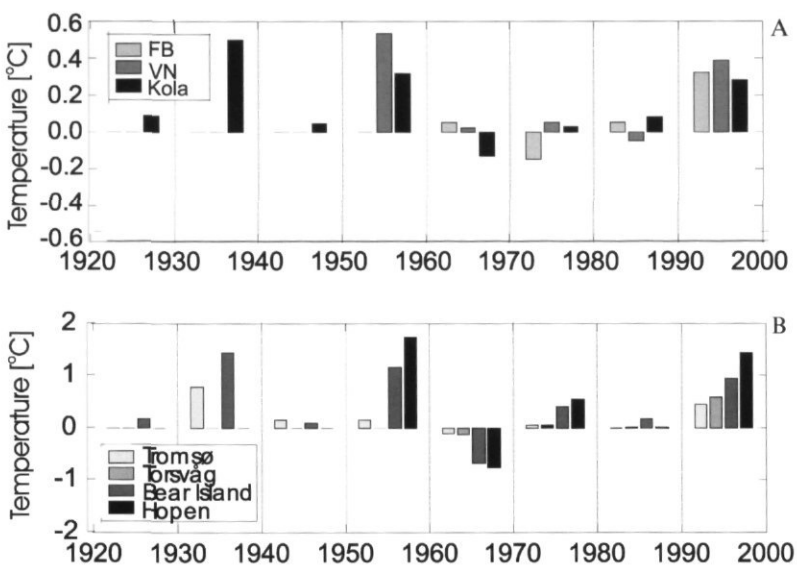


Figure 3. Decadal temperature anomalies for (A) the hydrographic sections and (B) the air temperatures at the meteorological stations.

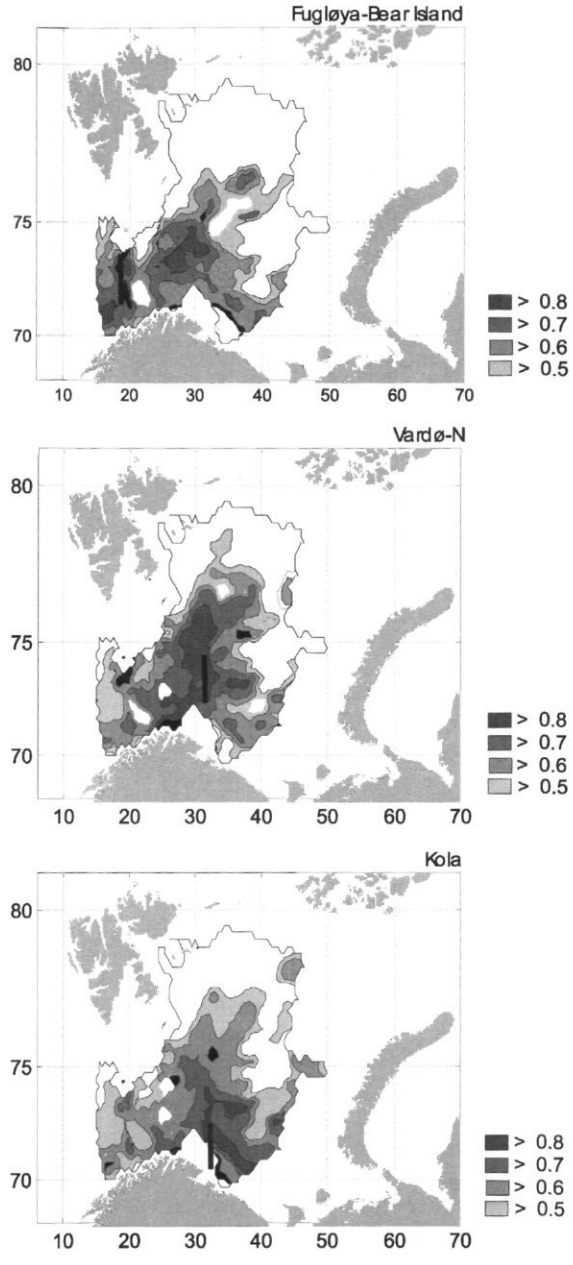


Figure 4. Maps of correlation coefficients between the temperature in 100 m and the time-series from the sections (A) FB, (B) Vardø-N, and (C) Kola. Only coefficients above 0.5 are drawn. The data were from the period 1970–2000, and sampled in August–October. The portion of the sections where mean values have been constructed is shown.

towards 1995. The temperature drop in 1996 was sudden and simultaneous in most of the Barents Sea (Figures 5, 6). A recovery towards higher temperatures was evident in the western parts in 1998, apparently progressing eastwards towards the central parts of the Barents Sea in 1999.

Discussion

The correlation maps between the sections and horizontal fields of temperature (Figure 4) demonstrated that all three sections are fairly representative of the Atlantic domain in the Barents Sea. However, because or their more northerly position and thereby distance from the Norwegian Coast, the mean values from FB and Vardø-N are most representative for the northern branch of inflow to the Barents Sea, i.e. for the AW going north into Hopen Trench (Figure 4). The Kola Section on the other hand is located in the Murmansk Current, and is more representative for the portion of AW continuing east towards Novaya Zemlya.

Decadal variability and effect of the NAO in the Barents Sea

In the 1990s the temperatures in the Barents Sea were well above the long-term mean (Figure 3). However, both the 1930s and the 1950s were warmer, indicating that the warming of the last decade may very well be related to natural variability rather than anthropogenic effects. However, since the 1960s there has been a general increase in both oceanic and atmospheric temperatures in the Barents Sea (Figure 3). During this period the NAO winter index (Hurrell, 1995) changed from its most negative phase in the 1960s to its most positive phase in the late 1980s/early 1990s. The Nordic Seas/Arctic response of this shift is well documented (e.g. Dickson *et al.*, 2000), although not fully understood. The shift has been accomplished by, among several other changes, (1) a significant increase in winter cyclone activity for the region north of 60°N as a whole, with locally significant increases over the central Arctic Ocean, the Barents Sea, and the Kara Sea (Serreze *et al.*, 1997; Rogers, 1997), (2) a decrease in late winter ice-extent in the Arctic and eastern Nordic Seas (Johannessen *et al.*, 1999; Vinje, 2001), (3) an increase in the annual volume flux of ice from the Fram Strait (Dickson *et al.*, 2000; Vinje, 2001), (4) an increase in the amount of Atlantic inflow to the Arctic Ocean (Grotefendt *et al.*, 1998; Dickson *et al.*, 2000).

A positive NAO index will result in at least three (obviously connected) oceanic responses in the Barents Sea, reinforcing each other and causing both higher volume flux and higher temperature of the inflowing water. The first response is connected with the direct effect of the increasingly anomalous southerly winds during high NAO (see Figure 7 A). Secondly, the increase in winter storms penetrating the Barents Sea during positive NAO (Serreze *et al.*, 1997; Rogers, 1997) will, according to the conceptual feedback model of Ådlandsvik and Loeng (1991), give higher Atlantic inflow to the Barents

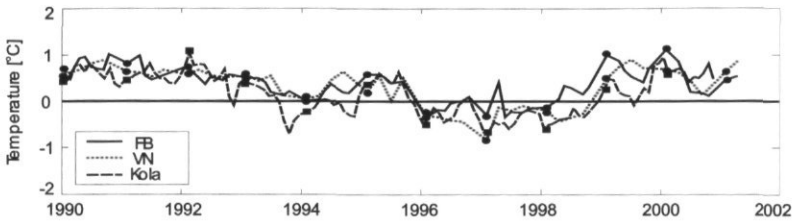


Figure 5. Time-series of temperature anomaly in the 1990s for the hydrographic sections. The January values are labelled.

Sea. The third aspect is connected to the branching of the Norwegian Atlantic Current (NAC) before entering the Barents Sea. Blindheim *et al.* (2000) found that a high NAO index corresponds to a narrowing of the NAC towards the Norwegian Coast. The narrowing will result in a reduction in heat loss, i.e. higher temperatures in the inflowing water also in the Barents Sea (Furevik, 2001). In addition, we might speculate that a narrower current forced towards the Norwegian Coast may result in that larger portion going into the Barents Sea, although this has not been documented.

For a negative NAO winter index, there may on the other hand be opposing forces. Associated with a negative NAO winter index is a secondary low-pressure centre over the Barents Sea (e.g. Figure 5 in Serreze *et al.*, 1997; Figure 2 in Dickson *et al.*, 2000). While the weaker winds associated with a low NAO will decrease the inflow, there is the possibility of the weak low enhancing it if located over the Barents Sea, thereby reducing the effect of the low NAO. This could be one of the reasons why the correlation between NAO and Barents Sea temperature are best during positive NAO phases, as observed by Dickson *et al.* (2000) and Ottersen *et al.* (2003).

Variability within the 1990s

The high NAO in the late 1980s/early 1990s resulted in high temperatures in the entire Barents Sea. The temperature decreased throughout the Barents Sea in 1993 (Figure 5). In the Norwegian Sea, too, the temperatures decreased after the first few years of the 1990s (e.g. Figure 5 in Blindheim *et al.* (2000) and the cold anomaly in southwestern parts in 1992 in Figure 6), indicating that the water masses entering the Barents Sea in 1993 were colder than the long-term mean. In the Atlantic domain the cooling was most pronounced along the Norwegian–Russian coast and in the eastern parts (Figures 5, 6). This cooling was more likely an effect of the local atmospheric fields than the NAO, as the NAO index was only slightly lower this year compared to 1992 and 1994 (e.g. ICES, 2000). To seek explanations for the observed variations, the mean SLPs for the previous winter were examined. The motivation for this was based on the following: during winter the vertical stratification in the Atlantic domain is weak because of vertical convection, and the water column may be homogeneous down to 2–300 m. Although local cooling and freezing are important in the northern and eastern parts, winter temperatures in the areas occupied by Atlantic water masses vary in parallel with the variations in the inflowing AW even at the surface (Midttun, 1990). The stratification of the upper layers starts in April–May and during the summer the warming of the water column reaches down to 50–60 m due to turbulent mixing. The AW is therefore effectively isolated from the surface during summer, and the local conditions that determine the surface temperatures (Midttun, 1990) have little influence on the AW. This, in combination with a higher inflow in winter than summer, is probably the reason why the temperature level for the rest of the year has been found to be "set" by the hydrographic winter, only adjustments to this level taking place later (Ottersen *et al.*, 2000). Izhevskii (1964) found the temperature level for the coming year to be "set" as early as in December. The winter mean SLP shown in Figure 7B reveals that the major difference between 1990 and 1993 was the presence of an elliptical low-pressure centre over the Barents Sea and northeastern Norwegian Sea. The east–west extent of the low might have steered a larger portion of the inflowing waters into the Murmansk Current. This can explain the tongue of cold waters extending from the Norwegian Sea into the Barents Sea along the Norwegian–Russian coast (Figure 6). The cyclonic centre probably also resulted in more northeasterly winds and lower air temperatures northwest of Novaya Zemlya. This would in turn enhance heat loss to the atmosphere and increase the ice production. In northern parts the ice could drift into the AW, causing a further cooling due to melting. The temperature decrease in eastern and northern parts was therefore probably related to local cooling rather than changing in relative strength between the two main branches.

In 1995 there were extremely high summer temperature anomalies in the eastern and northern parts of the Barents Sea (Figure 6). The hydrographic sections show that there was a rapid temperature

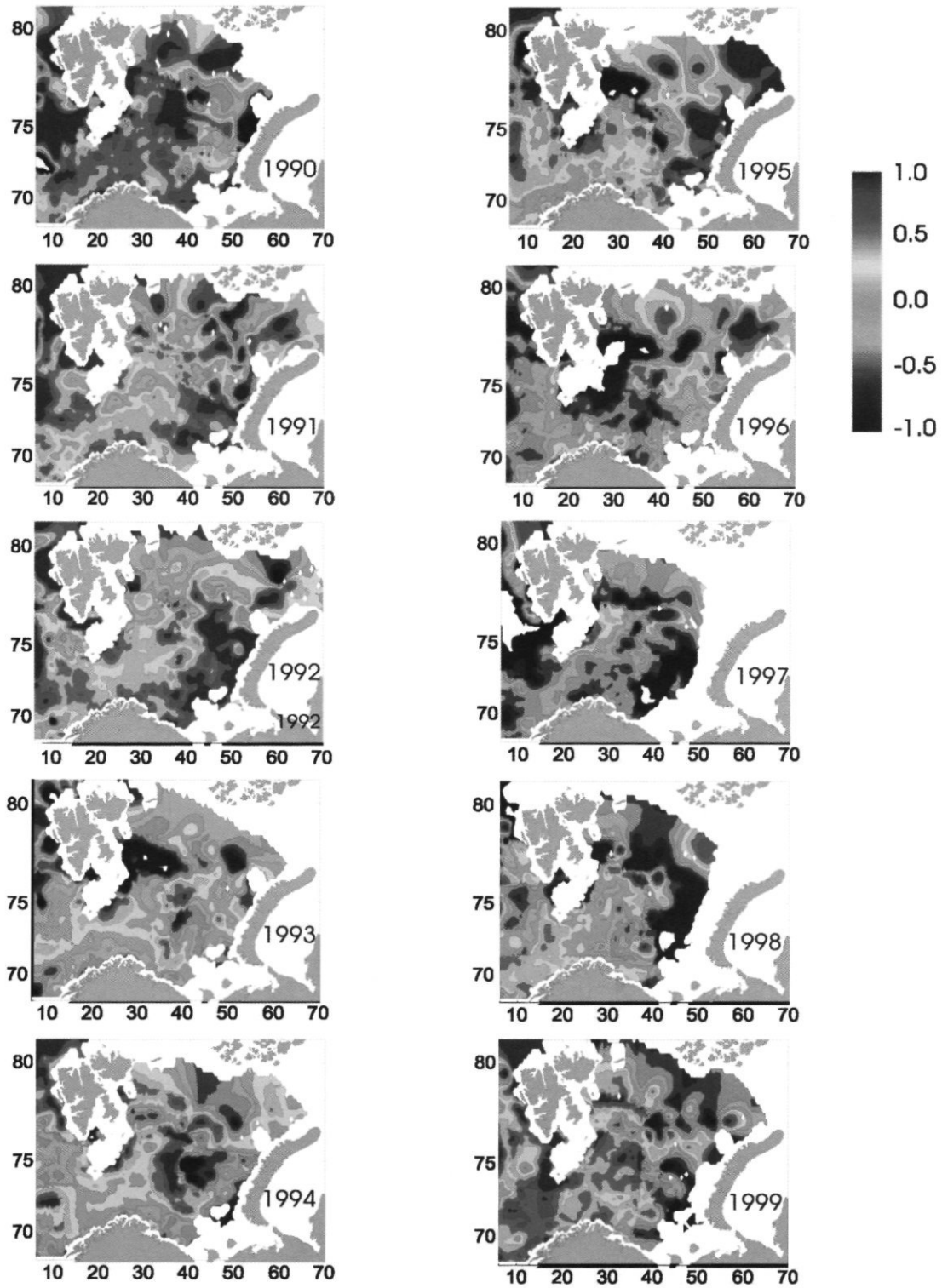


Figure 6. Horizontal fields of August–October mean temperature anomalies at 100 m depth in the 1990s.

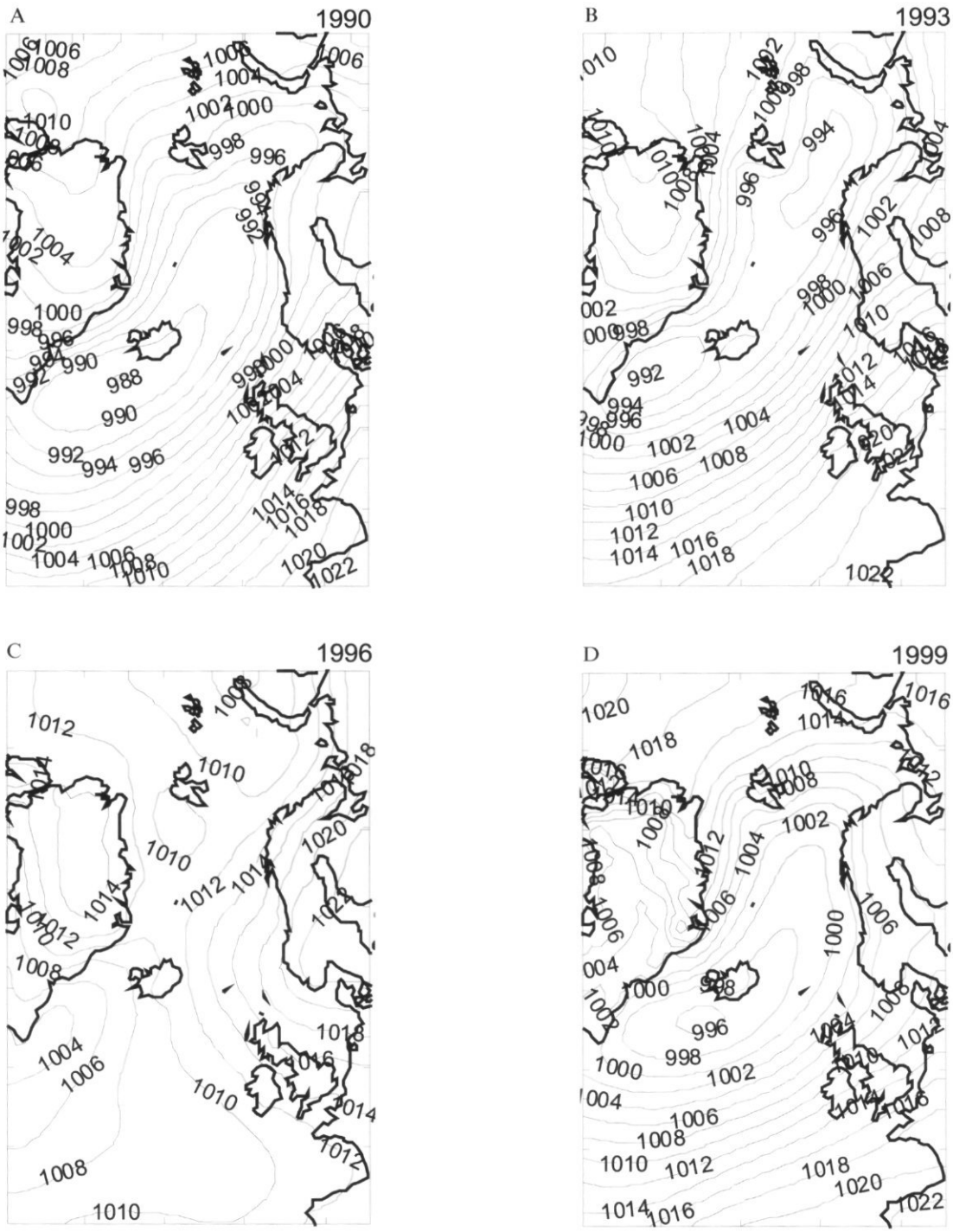


Figure 7. Mean SLP for December–March. (A) Typical situation with high NAO winter index 1990, (B) 1993, (C) 1996, and (D) 1999. Year is decided by the time of the January.

increase in the southern Barents Sea in late 1994 and early 1995 (Figure 5 and Anon., 2001). Advection of this relatively warm water to the eastern Barents Sea may explain some of the positive temperature anomaly. According to Vinje (2001), there was also a minimum extent of winter sea ice this year, and the Kara Sea was partly ice-free for the first time since 1864. He ascribed the minimum to the concerted action from atmospheric and oceanic reducing effects, i.e. reduced northerly winds and higher heat content in the ocean.

The dramatic drop in the NAO winter index in 1996 (e.g. ICES, 2000) resulted in a strong decrease in ocean temperatures in the entire Barents Sea, except in some areas in the northern and eastern parts (Figure 6). The drop was simultaneous in the whole southern area (Figure 5). The mean SLP for this year (Figure 7C) reveals that the secondary low-pressure centre usually found in the Barents Sea during low NAO index, was located east in the Fram Strait. The necessary conditions for a counteracting effect on a low NAO as suggested earlier were not therefore present in 1996.

During the last 3 years of the 1990s there was a gradual build-up towards higher temperatures (Figures 5, 6). By the end of the decade the western parts were even warmer than at the beginning of the decade (Figure 5), while east of 40°E temperatures were still well below average (Figure 6). The clear shift in the temperature anomalies in 1999 from warm to cold along 40°E indicates that the warming in the branch going north into the Hopen Trench was much higher than the warming in the Murmansk Current (Figure 6). The winter mean SLP for the preceding winter (i.e. 1999) shows much stronger pressure gradients compared to the high index year of 1990 (Figure 7A, D). The difference in SLP between the eastern and western parts of the Barents Sea was 14 hPa in 1999 compared to 10 hPa in 1990. Consequently, there might have been an atmospheric blocking causing the inflowing water to go northwards into the Hopen Trench rather than eastwards enhancing the Murmansk Current. The temperature anomalies for the sections (Figure 5) reveal that very high temperatures were observed in FB in January 1999. By March the same year the high anomalies were observed in Vardø-N, but they never reached Kola. The atmospheric blocking probably decreased the oceanic winter inflow and pushed the incoming warmer water northwards, thereby confining it to a smaller area. It is also possible that the change in wind pattern caused a change in ice distribution which may have contributed to the lack of heating in the eastern parts, but this is probably less likely as the pressure field should not give less cooling in the western parts nor more cooling in the east. The warming in the late 1990s can therefore be attributed to a different distribution of AW within the Barents Sea, as well as higher temperatures of the inflowing water due to the recovery of the winter NAO.

The high temperature anomalies observed during the early winters of 1999 and 2000 are worth noting (Figure 5). These are ascribed to mild autumns and late onset of winter cooling, as there were relatively high air temperatures during the late autumn/early winter months in these 2 years. High sea temperature anomalies during late autumn and early winter were also observed along the Norwegian coast in the same period (Anon., 2001), indicating a regional phenomenon which we at this point cannot link to any specific forcing.

Summary and conclusions

The investigation may be summarized as follows:

1) The 1990s was the warmest decade since the 1950s. As both the 1930s and the 1950s were warmer than the last decade, the warming of the 1990s may very well be related to natural variability rather than anthropogenic effects.
2) The 1990s started out warm both in the Atlantic and most of the Arctic domain. The low NAO winter index in 1996 resulted in a sudden and simultaneous drop in temperature in the entire Barents Sea, except in small areas in the northern parts. During the final years of the decade the temperatures gradually increased in the western parts, but were still well below average east of 40°E.
3) The temperature variability in the three standard sections Fugløya-Bear Island, Vardø-N, and Kola in the southern parts of the Barents Sea all give a fairly good representation of the climate fluctuations in the Atlantic domain.
4) During positive NAO winter index the joint action of (at least) three oceanic responses may give an increase in the Barents Sea temperatures. These responses are: (i) more southerly winds enhancing the inflow, (ii) more winter storms penetrating the Barents Sea, (iii) the narrowing of the NAC (Blindheim *et al.*, 2000) and the associated lower heat loss to the atmosphere, giving higher temperatures in the inflowing AW.
5) Through regional and local effects the NAO has a significant influence on the Barents Sea on decadal time scales, and during extreme NAO events. Still, local atmospheric forcing not captured by the NAO index seems to be dominating for the distribution of the water masses within the area. The local pressure field appears to change the relative strength of the two branches going northeast and east, respectively, thereby having a significant effect on the local climate. The local pressure distribution not captured by the NAO index also has some influence on the total inflow to the Barents Sea.

Acknowledgements

We are grateful to PINRO for providing hydrographic data from the Kola Section and the Norwegian Meteorological Institute for the SLP and air temperature data. We thank reviewers and colleagues for valuable comments and Karen Gjertsen for help with some of the figures. This work received financial support from the Research Council of Norway through the projects "Variation in space and time of cod and other gadoids: the effect of climate and density dependence and population dynamics" and "NOCLIM".

References

Aagaard, K., and Woodgate, R. A. 2001. Some thoughts on the freezing and melting of sea ice and their effects on the ocean. Ocean Modeling, 3: 127–135.

Ådlandsvik, B., and Loeng, H. 1991. A study of the climatic system in the Barents Sea by a wind–driven model. Polar Research, 10: 45–49.

Anon. 2001. Havets miljø 2001. Fisken og havet, særnr. 2-2001. 118 pp. (In Norwegian, English summary.)

Blindheim, J., Borovkov, V., Hansen, B., Malmberg, S.-Aa., Turrell, W. R., and Østerhus, S. 2000. Upper layer cooling and freshening in the Norwegian Sea in relation to atmospheric forcing. Deep-Sea Research I, 47: 655–680.

Blindheim, J., and Loeng, H. 1981. On the variability of Atlantic influence in the Norwegian and Barents Seas. Fiskeridirektoratets Skrifter Serie Havundersøkelser, 17: 161–189.

Bochkov, Y. A. 1982. Water temperature in the 0–200 m layer in the Kola-Meridian in the Barents Sea, 1900–1981. Sb. Nauchn. Trud. PINRO, 46: 113–122. (In Russian.)

Dickson, R. R., Osborn, T. J., Hurrell, J. W., Meincke, J., Blindheim, J., Ådlandsvik, B., Vinje, T., Alekseev, G., and Maslowski, W. 2000. The Arctic Ocean response to the North Atlantic Oscillation. Journal of Climate, 13: 2671–2696.

Eide, L., Reigstad, M., and Guddal, J. 1985. Database av beregnede vind og bølgeparametere for Nordsjøen, Norskehavet og Barentshavet hver 6. time for årene 1955–1981. Norwegian Meteorological Institute, Oslo/Bergen. 38 pp.

Furevik, T. 2001. Annual and interannual variability of the Atlantic Water temperatures in the Norwegian and the Barents Seas: 1980–1996. Deep-Sea Research I 48: 383–404.

Grotefendt, K., Logemann, K., Quadfasel, D., and Ronski, S. 1998. Is the Arctic Ocean warming? Journal of Geophysical Research, 103: 27,679–27,687.

Helland-Hansen, B., and Nansen, F. 1909. The Norwegian Sea. Fiskeridirektoratets Skrifter Serie Havundersøkelser, 2(2): 1–360.

Hurrell, J. W. 1995. Decadal trends in the North Atlantic Oscillation: regional temperatures and precipitation. Science, 269: 676–679.

ICES. 2000. The Annual ICES Ocean Climate Status Summary 1999/2000. <http://www.ices.dk/status/clim9900/>

Izhevskii, G. K. 1964. Forecasting of Oceanological Conditions and the Reproduction of Commercial Fish. Moscow: [Transl. 1966: Israel Progr. Sci. Transl., Jerusalem]. 99 pp.

Johannessen, O. M., Shalina, E. V., and Miles, M. W. 1999. Satellite evidence for an Arctic sea ice cover in transformation. Science, 286: 1937–1939.

Loeng, H., Sundby, S., and Østensen, Ø. 1989. Drifting buoys in the Barents Sea. ICES, CM 1989/C19: 10 pp.

Midttun, L. 1985. Formation of dense bottom water in the Barents Sea. Deep-Sea Research, 32: 1233–1241.

Midttun, L. 1990. Surface temperatures of the Barents Sea. Polar Research, 8: 11–16.

Ottersen, G., and Stenseth, N. C. 2001. Atlantic climate governs oceanographic and ecological variability in the Barents Sea. Limnology and Oceanography, 46: 1774–1780.

Ottersen, G., Ådlandsvik, B., and Loeng, H. 2000. Predicting the temperature of the Barents Sea. Fisheries Oceanography, 9: 121–135.

Ottersen, G., Ådlandsvik, B., Loeng, H., and Ingvaldsen, R. 2003. Temperature variability in the northeast Atlantic. ICES Marine Science Symposia, 219: 86–94. (This issue.)

Parsons, A. R., Bourke, R. H., Muench, R. D., Chiu, C.-S., Lynch, J. F., Miller, J. H., Plueddemann, A. J., and Pawlowicz, R. 1996. The Barents Sea Polar Front in summer. Journal of Geophysical Research, 101(C6): 14,201–14,221.

Quadfasel, D., Rudels, B., and Selchow, S. 1992. The Central Bank vortex in the Barents Sea: water mass transformation and circulation. ICES Marine Science Symposia, 195: 40–51.

Rogers, J. C. 1997. North Atlantic storm track variability and its association to the North Atlantic Oscillation and Climate Variability of Northern Europe. Journal of Climate, 10: 1635–1647.

Rudels, B., Jones, E. P., Anderson, L. G., and Kattner, G. 1994. On the intermediate depth waters of the Arctic Ocean. *In* The Polar Oceans and Their Role in Shaping the Global Environment, Geophysical Monograph Series, 85, pp. 33–46. Ed. by O. M. Johannessen, R. D. Muench, and J. E. Overland, AGU, Washington, D.C.

Schauer, U., Muench, R. D., Rudels, B., and Timokhov, L. 1997. The impact of Eastern Arctic Shelf Waters on the Nansen Basin intermediate layers. Journal of Geophysical Research, 102: 3371–3382.

Serreze, M., Carse, F., and Barry, R. G. 1997. Icelandic Low Cyclone Activity: Climatological Features, Linkages with the NAO, and Relationships with Recent Changes in the Northern Hemisphere Circulation. Journal of Climate, 10: 453–464.

Taylor, J. 1976. CONMAP: A computer program for contouring oceanographic data. Marine Environmental Data Service, Canada.

Tereshchenko, V. V. 1996. Seasonal and year-to-year variations of temperature and salinity along the Kola meridian transect. ICES CM 1996/C11: 24 pp.

Vinje, T. 2001. Anomalies and trends of sea-ice extent and the atmospheric circulation in the Nordic Seas during the period 1864–1998. Journal of Climate, 14: 255–267.

ICES Marine Science Symposia, 219: 169–181. 2003.

Biological response in a changing ocean environment in Newfoundland waters during the latter decades of the 1900s

Eugene B. Colbourne and John T. Anderson

Colbourne, E. B., and Anderson, J. T. 2003. Biological response in a changing ocean environment in Newfoundland waters during the latter decades of the 1900s. – ICES Marine Science Symposia, 219: 169–181.

Ocean temperatures on the Newfoundland Shelf during the past several decades have experienced near-decadal oscillations superimposed on a general downward trend. In particular, the decade of the 1990s has experienced some of the most significant variations since measurements began during the mid-1940s. Ocean temperatures, for example, have ranged from record low values during 1991 to record highs during 1999 in many areas, particularly on the Grand Bank of Newfoundland. Coincident with the trends in ocean climate many commercial fish species have shown changes in abundance, particularly during the decade of the 1990s. Recruitment in Newfoundland cod stocks, for example, has declined almost steadily since the 1960s, reaching historical low values by the early 1990s. During the cold early 1990s, with fishing moratoria in place, recruitment continued to decline. However, by 1995, ocean temperatures began to warm and the pelagic ecosystem responded, with the biomass of invertebrate zooplankton increasing by a factor of 2 from the early to late 1990s. This was followed by a sharp increase in the nekton biomass during the late 1990s, although this increase lagged that observed in the zooplankton. We conclude that the observed decline in cod recruitment since the late 1960s was due to a declining spawning-stock biomass caused in part by a deteriorating ocean environment. Furthermore, the subsequent increase in the abundance of pelagic organisms observed during the latter half of the 1990s is consistent with the expected biological response to changes in the physical ocean environment.

Keywords: Atlantic cod, ocean environment, pelagic ecosystem, recruitment, survival, temperature.

E. B. Colbourne and J. T. Anderson: Northwest Atlantic Fisheries Centre, PO Box 5667, St John's, Newfoundland, Canada A1C 5X1 [e-mail: Colbourn@dfo-mpo.gc.ca; andersonjt@dfo-mpo.gc.ca]. Correspondence to E. B. Colbourne.

Introduction

The latter half of the 20th century has been a time period of considerable variability in the marine ecosystem of the Newfoundland Shelf. In the years prior to the early 1970s the ocean environment was dominated by a general warming phase that reached its maximum by the mid-1960s. Beginning in the early 1970s, climate conditions in the Northwest Atlantic experienced near-decadal oscillations, with a general downward trend in ocean temperatures. In particular, the decade of the 1990s has experienced some of the most dramatic variations since measurements began during the mid-1940s. During the same time period many commercial fish species also showed dramatic changes in abundance and distribution, particularly during the decade of the 1990s. For example, populations of Atlantic cod (*Gadus morhua*) off Newfoundland decreased from all time highs in the 1960s to commercial collapse by the early 1990s.

Many studies have suggested that variations in the physical ocean environment influence growth, recruitment, and distribution of many marine organisms in Newfoundland waters (deYoung and Rose, 1993; Myers *et al.*, 1993; Rose *et al.*, 1994, 1995; Taggart *et al.*, 1994; Narayanan *et al.*, 1994; Colbourne *et al.*, 1997; Carscadden *et al.*, 2001). More recently, Parsons and Lear (2001) provided an overview of recent climate variability in the North Atlantic and its impact on the productivity of the marine ecosystem. However, overall, physical and biological interactions in the marine environment are usually non-linear and operate through complex mechanisms throughout the ecosystem over a broad range of time scales. These interactions are

further complicated by fishing mortality. Therefore, correlations between individual environmental indices with measures of fish production often break down as different physical factors begin to influence various levels of the ecosystem and life stages of marine organisms (Mann and Drinkwater, 1994). However, long-term trends which coincide in the physical and biological environment may reflect significant change related to production in marine ecosystems and may provide some insight into physical–biological processes.

Following the collapse of cod stocks off Newfoundland (NAFO 2J + 3KL) and on the Grand Banks (NAFO 3NO; Figure 1), fishing moratoria were put in place in 1992 and 1994, respectively. Fishing moratoria provide a unique opportunity to observe and study the response of marine ecosystems to variations in the physical environment in the absence of significant fishing mortality. In this article we first review the long-term trends in both the physical environment and cod abundance and survival during the 1960s to 1980s, noting that during this period it is difficult to disassociate environmental influences from the effects of fishing mortality. We then focus in more detail on the decade of the 1990s, examining variation in pelagic fish production in Newfoundland waters in relation to a warming physical environment.

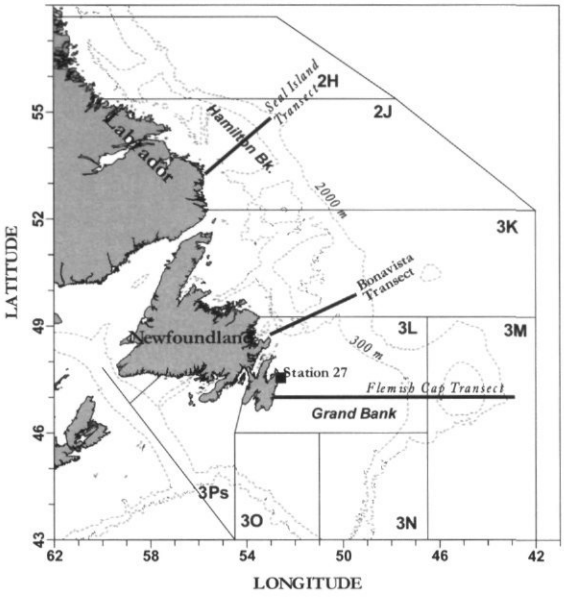


Figure 1. Regional map showing the positions of standard monitoring transects, Stn 27 and the statistical fish management areas established by the Northwest Atlantic Fisheries Organization (NAFO).

Data

The data utilized in this aticle were derived from three main sources: (1) spring and autumn bottom trawl surveys by the Canadian Department of Fisheries and Oceans, (2) annual oceanographic monitoring surveys along standard sections, and (3) large-scale surveys of the pelagic environment on the Newfoundland Shelf. Canada has been conducting stratified random ground fish trawl surveys on the Newfoundland Shelf in NAFO Divisions 2J3KLNO since the early 1970s (Doubleday, 1981; Bishop, 1994). The random stratified fish samples obtained from these surveys form a basis on which to determine recruitment and population abundance for demersal fish stock assessments. Oceanographic data were collected during these surveys at all fishing locations.

Oceanographic measurements along standard sections on the Newfoundland and Labrador Shelves were initiated by the International Ice Patrol of the US Coast Guard soon after the Titanic disaster in 1912 to monitor variations in the Labrador Current. Since the 1940s, oceanographic data have been collected on research surveys along standardized sections (Figure 1) under the auspices of the International Commission for Northwest Atlantic Fisheries (ICNAF) by several countries and currently for the Northwest Atlantic Fisheries Organization (NAFO). Additionally, as part of an expanded Canadian Atlantic zonal oceanographic monitoring programme some of these transects are now sampled on a seasonal basis (Therriault *et al.*, 1998).

In recent years, 1994–1999, a comprehensive large-scale survey of the marine pelagic environment on the Newfoundland and Labrador Shelf has been conducted (Anderson and Dalley, 1997; Dalley and Anderson, 1997, 1998; Dalley *et al.*, 1999, 2000). These surveys, initiated after the collapse of the cod stocks of Newfoundland, were designed to monitor the expected recovery of Atlantic cod by providing a measure of pre-recruit pelagic (0-group) cod as well as providing a full multispecies measure of plankton and nekton for the study area. The surveys were carried out during late summer of each year and also provided a comprehensive temperature and salinity survey of the shelf waters.

Traditionally, two stocks of Atlantic cod have been managed off the east coasts of Newfoundland and Labrador. The northern cod stock (NAFO 2J + 3KL) was the largest cod stock in the Northwest Atlantic, ranging from southern Labrador to the northern Grand Bank. It was recognized that the northern cod stock was in fact a stock complex made up of a number of population components. However, it was managed and assessed as a single

population using traditional analytical techniques. The southern Grand Bank cod stock (NAFO 3NO) is confined to the ice-free relatively warm waters of the southern Grand Banks. We considered these two cod stocks in relation to environmental variability because of the long time series of population estimates based on Virtual Population Analysis (VPA) and the different ecosystems that they occupy.

Recruitment (R) was defined as the abundance of cod at 3 years of age and spawning-stock biomass (SSB) was based on the total biomass of mature fish. Data for recruitment and SSB were obtained from the most relevant assessment documents (Bishop *et al.*, 1993; Stansbury *et al.*, 1999). An index of cod pre-recruit survival was estimated as the abundance of cod at age 3 divided by the SSB that produced each year class (R/SSB).

We recognize the retrospective problems associated with the VPA methodology, where the most recent year-class abundances are overestimated (Mohn, 1999). However, given the extreme declines in abundance of each stock in recent years, such estimation errors are relatively small in our analysis. For the northern cod stock, the VPA models have not produced reliable estimates since 1993. Therefore we have only presented data up to the 1990 year class. A research vessel trawl survey estimate is available for the offshore area since 1981, and it indicates that recruitment has remained at historically low levels since 1990 and population biomass has remained at extremely low levels since 1993 (Lilly *et al.*, 1999).

Collectively, these surveys provided a comprehensive oceanographic data set for the Newfoundland Shelf region with good temporal and spatial coverage for most of the decades since the 1950s. Oceanographic data from other available sources archived at the Marine Environmental Data Service (MEDS) in Ottawa were also used to define long-term means. In this article we present environmental time series as differences from their long-term averages (anomalies) referenced to a standardized base period from 1961–1990 (normal) in accordance with the convention of the World Meteorological Organization. In addition, we present correlations between environmental indices and with indices of fish survival and recruitment (all of which show significant autocorrelation) only to highlight the associations between long-term trends in fish production and the environment.

Long-term trends

The strength of the cyclonic atmospheric circulation over the North Atlantic during the winter months largely determines ocean climate variations through its influence on ice extent and duration, ocean temperatures, and shelf stratification (Colbourne *et al.*, 1994; Drinkwater, 1996). A convenient meteorological index representing the strength of this circulation has been termed the North Atlantic Oscillation (NAO) index and is defined as the difference in the winter sea level air pressure between the quasi-stationary winter high and low pressure cells over the Azores and Iceland, respectively (Rogers, 1984). When the NAO index is strongly negative, warm saline ocean conditions generally prevail in the Northwest Atlantic and colder fresher conditions predominate in the Northeast Atlantic; and, conversely, when the NAO index is high positive. Spatial variations in the positions and extent of the pressure cells sometimes result in significant interannual variations in the strength of the winter wind patterns in any one location. Overall, the NAO index accounts for only one-third of the total variance in the winter pressure anomaly field, but represents the most dominant signal of environmental variability for the North Atlantic (Dickson and Meincke, 1999).

The NAO index is generally characterized by large amplitude fluctuations with periods ranging from annual to approximately 20-year cycles. Superimposed on these oscillations was a long-term decline in the index from the early 1950s to the late 1960s, a period of generally warm saline ocean conditions on the Newfoundland Shelf. This was also a time period of increased landings of Atlantic cod resulting from an expansion of the fishing industry (Figure 2A). Since the early 1970s, the NAO shifted towards more positive values and began to oscillate at quasi-decadal time scales superimposed on a generally increasing trend. As a result, the ocean environment in the Northwest Atlantic experienced more frequent periods of cold-fresh conditions following the 1960s. Landings of northern cod peaked in 1968, shortly after the NAO minimum, and subsequently declined to a minimum in 1977, increased during the 1980s and then collapsed to near zero by the middle 1990s (Figure 2A). The declines in the 1970s and 1990s have been attributed to high fishing mortality, first by foreign fishing prior to the extension of jurisdiction in 1977, and secondly to foreign and domestic fishing in the 1980s and 1990s (Hutchings and Myers, 1994; Myers *et al.*, 1996; Bundy, 2001). However, we note that the decline in cod landings also coincided with a changing ocean environment during this 20+ year period.

The responses of the ocean on the Newfoundland Shelf to variations in the NAO are clearly evident by comparing long-term trends (Figures 2, 3). The combined effects of variations in air-sea heat fluxes, storm forced mixing and intense winter convection

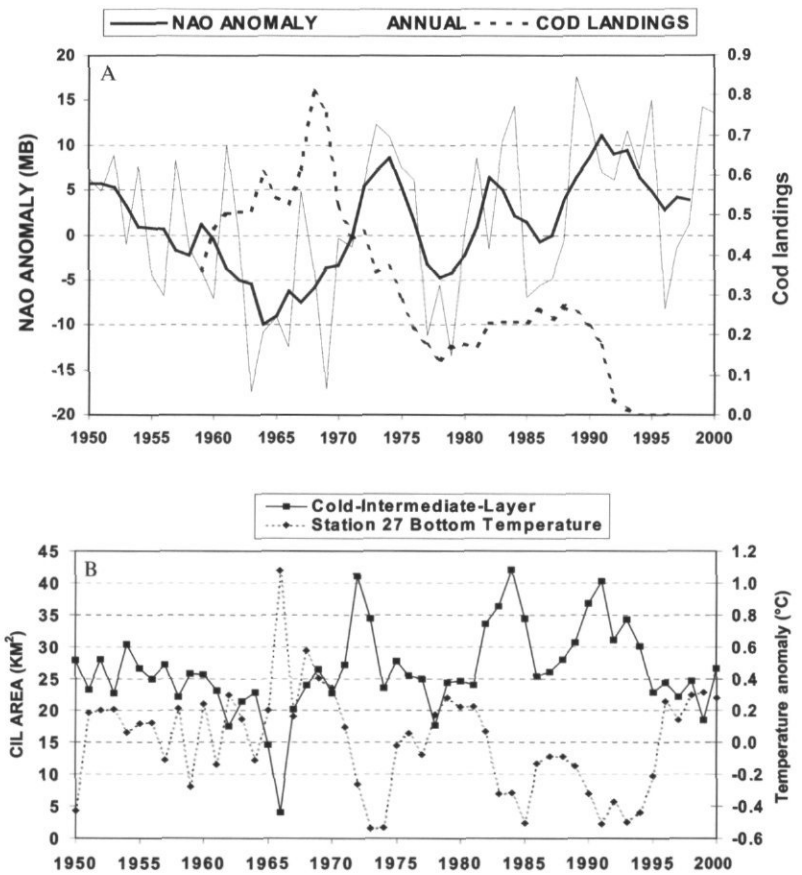


Figure 2. (A) North Atlantic Oscillation (NAO) index and historical cod landings (millions of tonnes) from the northern cod stock (2J3KL) and (B) average annual values of the cold intermediate layer (CIL) areas defined by water $\leq 0°C$ along the Seal Island, Bonavista and Flemish Cap transects (Figure 1) and bottom temperature anomalies on the inner Newfoundland Shelf at Stn 27.

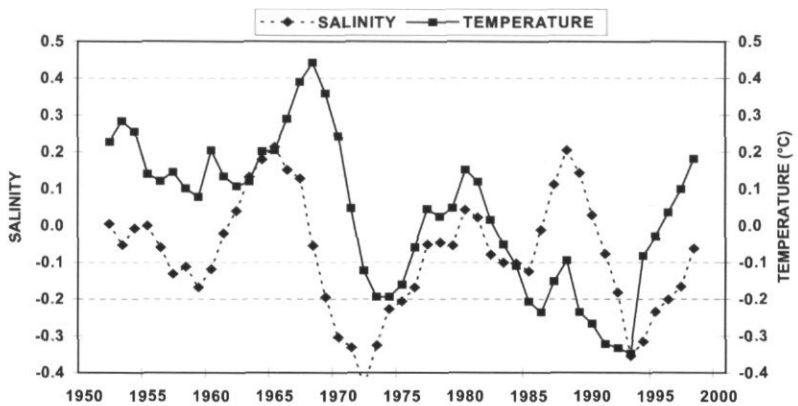


Figure 3. Five-year running means of the depth (0–176 m) averaged annual temperature and the depth (0–50 m) averaged summer salinity anomalies on the inner Newfoundland Shelf at Stn 27.

on the shelf, coupled with summer stratification are the primary mechanisms responsible for the formation of cold intermediate waters on the Newfoundland Shelf (Petrie *et al.*, 1988). The cold intermediate layer (CIL), defined as water with temperatures $\leq 0°C$ overlying the continental shelf during the summer months is a robust index of ocean climate conditions resulting from these physical processes. In summer, CIL water remains relatively isolated between the seasonally heated upper layer and the deeper shelf-slope water, but undergoes a gradual decay during autumn due to intense vertical mixing. As a result, the area of summer CIL waters reflects environmental forcing that spans all four seasons. The annual CIL index is therefore strongly associated with the long-term trends in the large-scale winter atmospheric circulation (NAO) ($r = 0.6$), air temperatures ($r = 0.61$), and winter and spring sea-ice cover on the Newfoundland Shelf. During the mid-1960s, when the NAO reached the lowest value of the 20th century, the volume of the CIL on the Newfoundland Shelf reached the lowest value ever observed in the time series (Figure 2B). During the early part of the 1990s the NAO increased to well above normal, and the volume of CIL water on the shelf reached near record high values. However, these cold conditions were immediately followed by a warming trend beginning in 1992, and by 1996 ocean temperatures had warmed to above normal values, which continued into 1999 when the area of CIL on the Shelf reached near record low values (Colbourne, 2001).

Ocean temperature and salinity have been measured routinely since 1946 at a standard hydrographic monitoring station (Stn 27, Figure 1) located in the inshore branch of the Labrador Current on the Newfoundland Continental Shelf (Colbourne and Fitzpatrick, 1994). This inshore site is representative of ocean conditions over the Newfoundland Shelf down to a water depth of 176 m (Petrie *et al.*, 1991). Bottom temperatures at this site reached a maximum during the mid-1960s then decreased to a record low during the early 1970s before increasing to above normal values from 1975 to 1982. After 1982 they remained below normal until 1996, the longest time period of below normal temperatures in the 50-year record (Figure 2B). The depth averaged temperature and salinity at Stn 27 have varied from periods of warm-salty conditions prior to the 1970s to cold-fresh conditions during the early 1970s and early 1980s. Conditions during the mid-to-late 1980s were generally cold and salty and during the first half of the 1990s they were generally cold and fresher than normal (Figure 3). Superimposed on these near-decadal oscillations was a downward trend in ocean temperatures from the record high in the late 1960s to the record low in the early 1990s. From the 1950s to the mid-1990s temperature and salinity varied in phase, although the phase difference changed over time. The phase of the salinity cycle preceded that of the temperature cycle by approximately 5 years in the late 1960s and decreased to 1 to 2 years from the late 1970s to early 1990s. During the 1990s, while both cycles were more or less in phase, the amplitudes were quite different. During 1985, both temperature and salinity began to increase; however, the temperature never recovered to above normal values until the latter half of the 1990s. Salinity increased to above normal values during 1988 but then fell to below normal values during the early 1990s, which continued into the mid-1990s (Figure 3). The trends in temperature and salinity were strongly associated with the trend in the NAO for the period 1952–1998 with correlation coefficients of –0.42 and –0.30, respectively.

Recruitment for the northern (2J + 3KL) and Grand Bank (3NO) cod stocks experienced long-term declines during the 1970s until the middle to late 1980s from the highs of the early to mid-1960s (Figure 4A). Superimposed on the long-term declines were short-term variations, which were significantly autocorrelated up to 5-year time periods. By the mid-1980s recruitment in the northern cod stock was in a steep decline and by 1990 recruitment similarly declined in the Grand Banks cod stock. Throughout the 1990s recruitment has remained at historically low levels. The SSB of both cod stocks also experienced long-term declines since the 1960s and 1970s reaching record low levels by the early 1990s (Anderson and Colbourne, 2000). Survival, expressed as the number of recruits produced by the spawning population (biomass), has declined in both cod stocks to historically low values in the 1990s (Figure 4B). Survival of the Grand Banks cod peaked in the 1960s and was high again in the late 1970s before declining to low values from the mid-1980s to the present. Survival of the northern cod peaked in the late 1970s, coincident with the Grand Banks cod, before declining to very low survival rates by the late 1980s. Survival estimates are correlated with the trend in both temperature and salinity at Stn 27 and the NAO index at lags of 0 and 1 year for 3NO stock ($r = 0.4$) and 1 and 2 years for the northern cod stock, indicating a possible environmental effect on the survival of pre-recruit fish.

In both the northern and Grand Bank cod stocks recruitment was associated with the long-term trends in the NAO, with low recruitment generally associated with a cold environment (high positive NAO anomaly) (Figure 5). It also appears that the Grand Bank cod stock responded over the full range of NAO variability, while the northern cod stock may be more tolerant to short-term changes in the ocean environment, showing less response until the

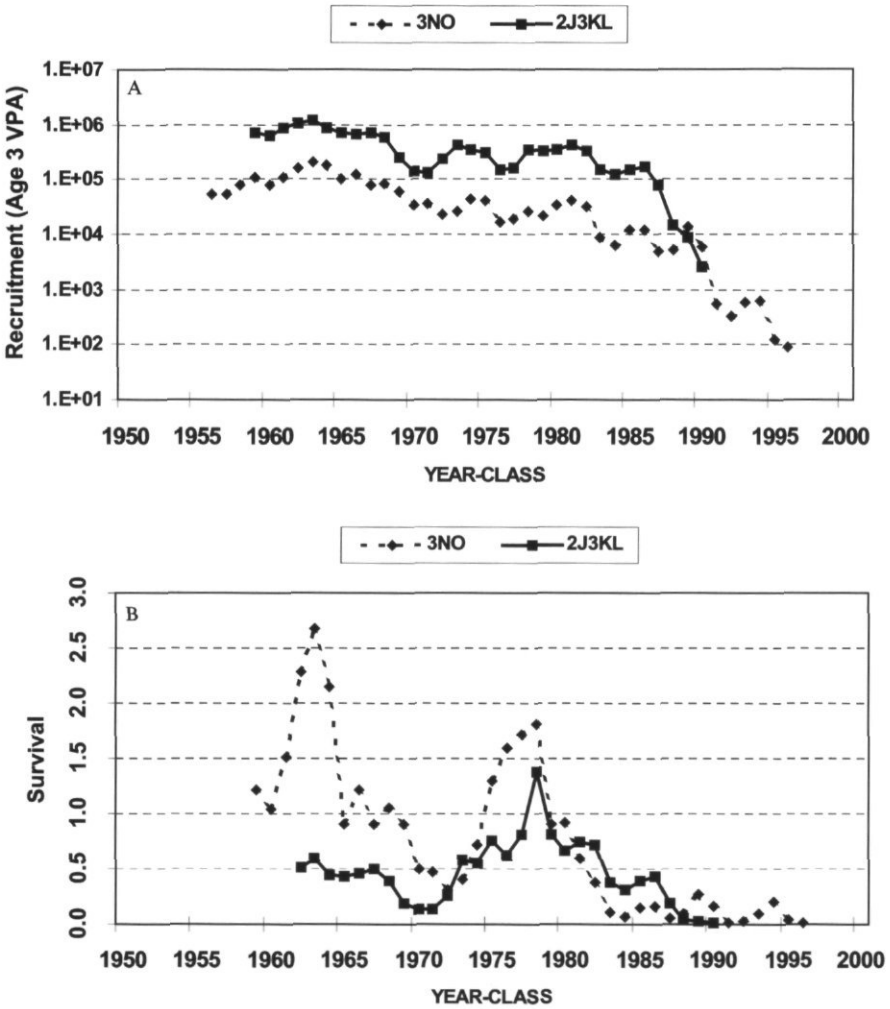


Figure 4. (A) Recruitment in Grand Bank (3NO) cod and the northern cod (2J3KL) estimated from Sequential Population Analysis. Recruitment is defined as abundance estimated at age 3 years and (B) the year-class survival indices estimated as the number of recruits produced by the spawning biomass for northern (2J3KL) cod and Grand Bank (3NO) cod.

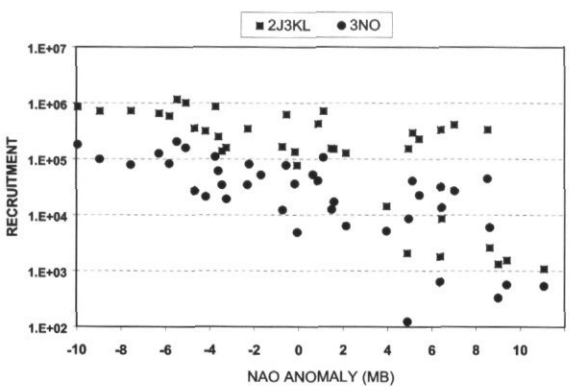


Figure 5. Recruitment defined as abundance estimated at age 3 years in northern (2J3KL) and Grand Bank (3NO) cod plotted against the 5-year averaged NAO values.

NAO reached its most positive values. Noting that ocean climate variability forced by atmospheric circulation (NAO) has the greatest influence on the upper layers of the ocean, effecting sea-ice dynamics, shelf stratification, and water temperatures, a plausible explanation may be related to differences in the habitat of the two stocks. The Grand Banks, being much shallower than regions to the north and occurring within the CIL, generally experiences more extreme ocean climate variations at shorter time scales than the deeper waters of the northeast shelf regions. However, it is not possible to partition environmental influences from the confounding effects of fishing mortality, predator–prey interactions and other factors during the time period preceding the fishing moratoria of the 1990s.

The 1990s

Physical environment

During the first half of the 1990s the NAO index was well above its long-term mean, reaching the third highest value of this century by 1995. During the winter of 1996 it underwent a sharp reversal, decreasing to the lowest value since 1979 (Figures 2A, 6) and one of the 10th most negative values this century. By the winter of 1997 and 1998 it increased from the low of 1996 to near normal values; however, by 1999 and 2000 the NAO anomaly increased again to well above normal. Thus the NAO anomaly during 1999 and 2000 was similar to that observed during the first half of the 1990s. However, during the past 2 years the colder-than-normal winter conditions usually associated with a high NAO index did not extend into the Northwest Atlantic. This exceptional response appeared to result from an eastward displacement of the negative pressure anomalies towards the east over the Barents Sea region. Thus, while that region experienced widespread warming, the Northwest Atlantic was under the influence of a milder southerly wind field (ICES, 2001). These variations in the NAO index during the decade of the 1990s fit the pattern of quasi-decadal variability that has persisted since the 1960s (Figure 2A).

In response to the oscillations in the NAO, the ocean environment on the eastern Canadian Continental Shelf during the decade of the 1990s experienced some of the most dramatic variations

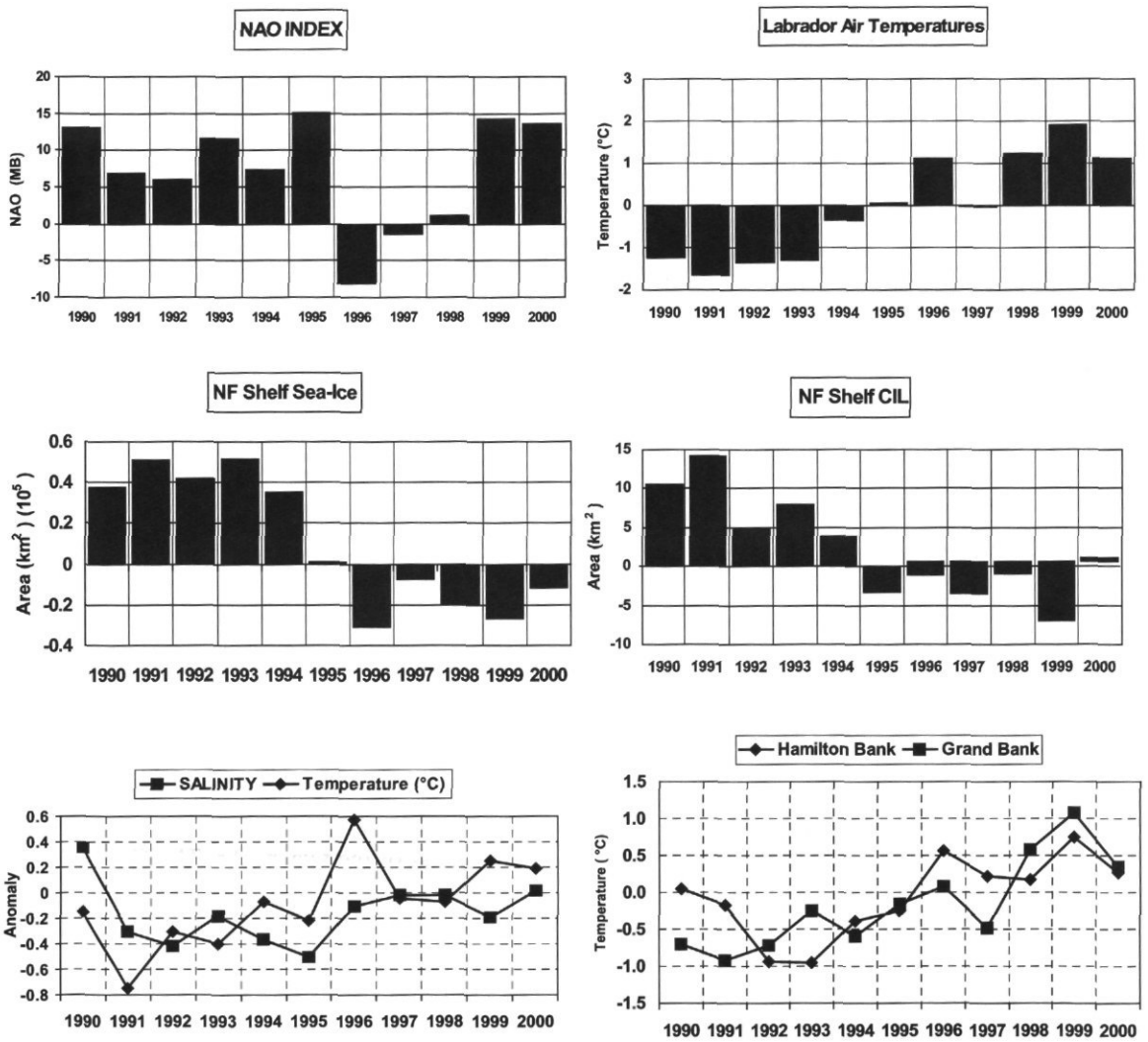


Figure 6. Annual anomalies in the NAO, Labrador air temperatures, Newfoundland Shelf sea-ice extent (adopted from Drinkwater *et al.*, 2000) and CIL area, Stn 27 depth averaged temperature and salinity and the Grand Bank and Hamilton Bank spatially averaged bottom temperature anomalies during the decade of the 1990s.

since measurements began during the mid-1940s (Figure 6). Annual air temperatures increased to above normal values in 1996 which increased to record highs in 1999 setting a 126-year record over Newfoundland and a 65-year record over Labrador (Drinkwater *et al.*, 2000). Sea ice extent on the Newfoundland Shelf decreased rapidly from the heavy ice years of 1990–1994 to the lightest ice-year since 1969 by 1996 (Figure 6). These changes resulted in a significant reduction in the area of CIL waters on the Newfoundland Shelf from the third highest ever-recorded in 1991 to the third lowest in 1999, a 22-year record. Off eastern Newfoundland, the depth-averaged ocean temperature at Stn 27 (Figure 1) ranged from a record low during 1991 to the highest value in 32 years by 1996 (Figure 6). The annual upper layer summer salinity at Stn 27 also increased from fresher than normal during 1991–1995 to near-normal values from 1996–2000. On the Grand Bank of Newfoundland and on the Hamilton Bank of southern Labrador the spatially averaged bottom temperature also ranged from record low values in 1990 and 1991 to near record highs by 1999 (Figure 6). The profound changes in the ocean climate in the Northwest Atlantic during the mid-1990s followed the sharp reversal in the NAO during the winter of 1995–1996. Furthermore, the subsequent displacement of the normal atmospheric pressure patterns during 1999–2000 resulted in a continuation of the climate regime typical of negative NAO conditions to the end of the decade.

The thermal habitat of many demersal fish species on the eastern Canadian Shelf, particularly on the Grand Banks of Newfoundland, also shifted from one extreme to the other during the past decade. During the cold years of the early 1990s most of the Grand Bank (except the deeper slope regions) and the southernmost areas were covered by <0°C water, with a large area of the northern half of the banks covered with < 1°C water in the autumn. Over the southern areas bottom temperatures ranged from 0°C to above 3.5°C on the southwestern slopes of the bank (Colbourne, 2001). During these years temperatures for the most part were below normal over the entire region, with anomalies reaching at least 0.5°C below normal, but also as low as 2°C below normal in some regions (Figure 7). By the late 1990s the area of <0°C water began to retract and was restricted to a small area near the coast. Temperatures ranged from <0°C off southern Newfoundland to 8°C on the southeast shoal of the Grand Bank (Colbourne, 2001). As a result, above normal conditions persisted over the entire Grand Bank with temperatures up to 1°C above average in northern areas and up to 4°C above normal on the southern Grand Banks (Figure 7).

The shift in the thermal habitat from the Arctic-like conditions of the early 1990s to the more temperate conditions of the late 1990s is clearly evident in Figure 8. The percentage area of the Grand Bank

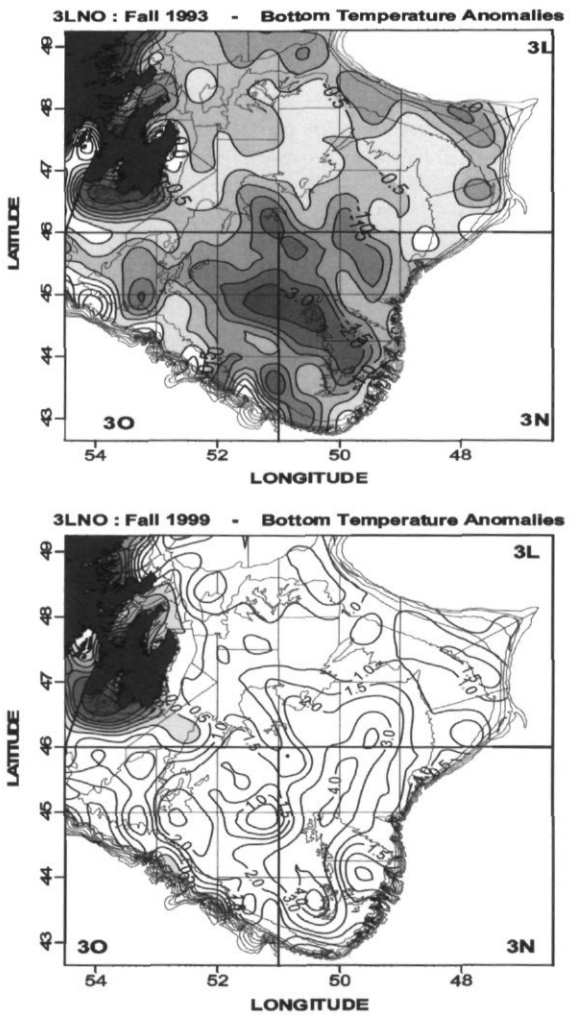


Figure 7. Contour maps of bottom temperature anomalies (in °C) during the fall of 1993 and 1999 for the Grand Bank region. The anomalies are referenced to all available data collected in the area from 1961–1990. Shaded values are negative.

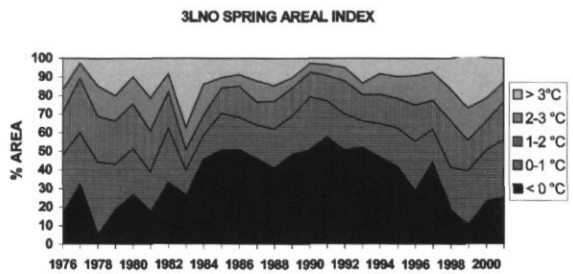


Figure 8. Time series of the percentage area of the bottom in NAFO Divisions 3LNO covered by water with temperatures ≤0°C, 0–1°C, 1–2°C, 2–3°C, and ≥3°C during spring.

covered by <0°C water decreased significantly from near 60% in 1991 to about 10% by 1999. This decrease in the area of the seabed habitat covered by very cold water follows a time period from the early 1980s up to the early 1990s when the thermal habitat on the Grand Bank was in a cooling phase (Figure 8). A corresponding increase in the areal extent of water °C occurred during the late 1990s increasing to near 60% by 1999, similar to values prior to the mid-1980s. During 2000 the area of subzero °C water remained below the values of the early 1990s but increased over 1999 values to near 20%. The 1998 and 1999 values represent the largest area of relatively warm water on the Grand Bank since 1983.

Changes in the stratification at Stn 27 (defined as dρ/dz over the top 50 m of the water column) during the 1990s indicate that the winter stratification was above normal from 1990 to 1995, while spring values were below normal from 1990 to 1992, but then increased to above normal values from 1993 to 1998 (Figure 9). We emphasize, however, that these calculations are based on a limited data set, particularly during the winter months, at a single point on the inner Newfoundland Shelf. Nevertheless, they show relatively large changes in the stability of the water column during the past decade.

Biological environment

During the early 1990s, with fishing moratoria in place, the recruitment and biomass of cod stocks of Newfoundland continued to decline to their lowest level ever-observed (Figure 4A). However, by 1995, as ocean temperatures began to warm the pelagic ecosystem responded, with the biomass of invertebrate zooplankton and nekton increasing sharply during the late 1990s. This response was monitored by large-scale surveys of the pelagic environment (described above) conducted off Newfoundland and Labrador during the years 1994 to 1999. The surveys sampled a wide spectrum of sizes of marine organisms from macrozooplankton to over 70 species of the nekton community ranging in size from 0-group Atlantic cod to 3-year-old capelin.

In 1994, the estimated biomass of invertebrate zooplankton, primarily copepods, was at a relatively low level. However, in subsequent years the biomass increased linearly, reaching a peak in 1997 after which it declined moderately in 1998 and 1999 but still remaining relatively high (Figure 10A). In contrast, the total nekton biomass remained relatively low from 1994 until 1997 before increasing by a factor 2–3 times in 1998 followed by a further increase in 1999. Increases occurred in all components of the nekton biomass, including euphausiids, amphipods, jellyfish, juvenile squid, and pelagic 0-group fish. The increase in nekton biomass occurred first in the south over the Grand Banks in 1998 and then extended to the north in 1999 as ocean temperatures continued to increase and warmer water spread further northward. The lag between the increase in nekton, compared to the zooplankton, is notable (Figure 10A), suggesting that feeding conditions for high production in the nekton were insufficient prior to 1997 in spite the warming ocean environment.

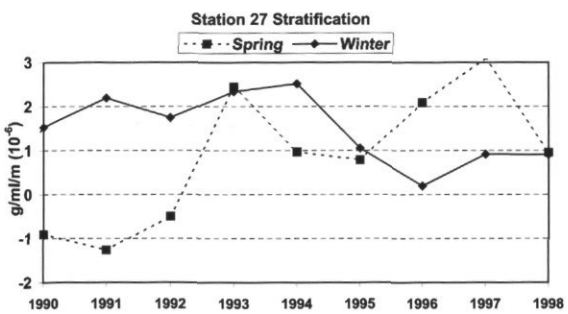


Figure 9. Stn 27 stratification index, define as dρ/dz over the top 50 m of the water column for the winter (Jan–Mar) and spring (Apr–Jun) during the decade of the 1990s.

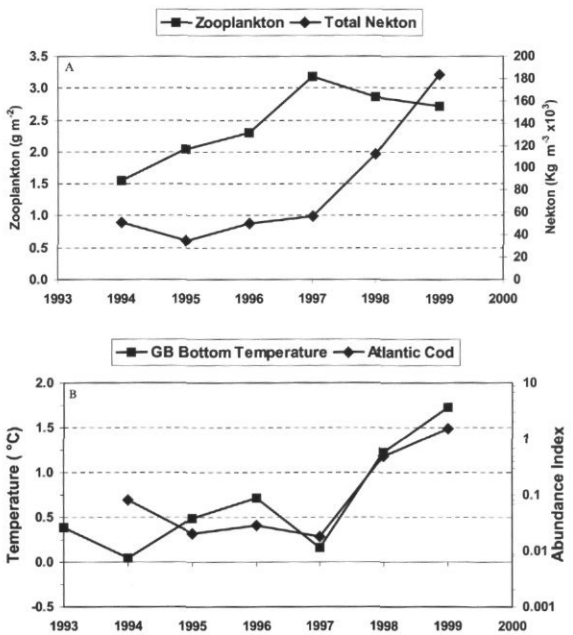


Figure 10. (A) Recent trends in biomass of invertebrate zooplankton and nekton in the pelagic ecosystem of the shelf waters of Newfoundland and Labrador during late summer from 1994–1999 and (B) the relative abundance of Atlantic cod and the spatially averaged spring bottom temperature (in °C) for Divisions 3LNO.

The abundance of individual species of 0-group pelagic fish remained low from 1994 to 1997. However, beginning in 1998 a dramatic increase in abundance occurred for several species on the Grand Banks including Atlantic cod, sandlance (*Ammodytes* sp.), redfish (*Sebastes* sp.) and American plaice (*Hippoglossoides platessoides*). Atlantic cod remained at relatively low levels of abundance on the Grand Banks until 1997, after which it increased by at least two orders of magnitude in 1998 and 1999 (Figure 10B). During this time period the spatially averaged bottom temperature on the Grand Banks during the spring increased from near 0°C in 1994 to over 1°C in 1998 and to over 1.5°C by the spring of 1999 (Figure 10B). The large increase in pelagic fish abundance, which first appeared over the Grand Banks in 1998, was detected further northward along the northeast coast of Newfoundland in 1999 as warm ocean conditions progressed northward. In contrast, the abundance of 0-group Arctic cod (*Boreogadus saida*) decreased from 1994 to 1999, consistent with the observed contraction of Arctic species and the expansion of the boreal and temperate species during the latter half of the 1990s (Anderson *et al.*, 1999; Dalley *et al.*, 2000).

Other biological indicators show similar results. For example, data from the annual multispecies bottom trawl surveys of the 2J3KLNO region while showing only a slight increase in the biomass of cod from 1995 to 1997 showed a 70% increase from 1998 to 1999 during the fall survey (DFO, 2000). The biomass in 1999, however, was still only a fraction of the biomass prior to the 1990s. The relative year-class strength, derived from a number of independent surveys conducted by the Department of Fisheries and Oceans, including the pelagic 0-group surveys and the stratified-random bottom trawl surveys showed that the 1998 and 1999 year classes of cod to be the strongest since 1992. Additionally, since the spring of 1998 there has been a significant increase in the number of cod caught per tow of fish at age 3 years and less in survey sets on the Grand Banks (Colbourne and Murphy, 2000). These were mainly confined to water temperatures above 2°C and it is stressed that these catch rates were still an order of magnitude lower than pre-1990s rates. Finally, the recently observed expansion in the spatial distribution and increase in abundance of yellowtail flounder (*Limanda ferruginea*) on the Grand Banks coincided with the improved thermal environment during the latter half of the 1990s (Walsh *et al.*, 2000; Colbourne and Bowering, 2001). These observations may have been due to a temperature dependent increase in catchability, or the increase in water temperature may have made the Grand Banks a more suitable environment for improved survival and growth rates of these fish species.

Discussion and summary

The shelf waters off Newfoundland and Labrador are a habitat to many overlapping Subarctic, boreal, and temperate marine species. Therefore variations in the thermal habitat are probably one of the most important physical variables influencing biological production in this region. Ocean climate in the Northwest Atlantic, particularly on the Newfoundland Continental Shelf (NAFO 2J3KLNO), during the recent past has experienced sharp annual fluctuations, quasi-decadal oscillations, and longer-term trends over several decades. In particular, the decade of the 1990s has experienced some of the most dramatic variations since measurements began during the mid-1940s. Coincident with these climate variations many commercial fish species have shown dramatic changes in abundance and distribution, particularly during the decade of the 1990s. Prior to the 1990s, it has been impossible to disassociate environmental effects from fishing mortality. However, the low survival, which occurred in both the northern and Grand Bank cod stocks through the 1980s into the 1990s, suggests a link between a cooling environment and survival. During the 1990s, with fishing moratoria in place, the production of juvenile cod remained low until 1998. Together, these observations support the conclusion that poor environmental conditions were responsible, in part, for the declines of cod in the 1980s as well as the delayed recovery of these populations in the 1990s.

By the mid to late 1990s, ocean temperatures began to warm and the pelagic ecosystem responded, with the biomass of invertebrate zooplankton increasing by a factor of 2 from the relatively low levels of the early 1990s. This was followed by a significant increase in the nekton biomass during the late 1990s, although this increase lagged that observed in the zooplankton by at least 2 years (Figure 10A). The reason for this lag is unknown at present. The low zooplankton biomass observed during the early 1990s most likely negatively impacted fish growth and survival. The increase in the abundance of pelagic 0-group fish did not occur until zooplankton biomass increased to high levels beginning in 1997, even though water temperatures were at and above normal before that time. This suggests that conditions for feeding and growth of young fish were insufficient prior to 1998.

While ocean temperatures no doubt play a critical role in defining fish habitat and determining survival of eggs and larvae, the success of fish production or recruitment most likely depends on many other complex non-linear physical and biological processes. Changes in shelf stratification arising from variations in salinity, for example, likely play an important part in lower trophic level production. For maximum primary production to occur, several

requirements are necessary, including sufficient vertical mixing of nutrients through the water column prior to the onset of stratification. The timing of these events is a critical factor and one that is greatly influenced by broad-scale physical forcing. Variations in the timing of peak primary production in relation to fish larvae production has been hypothesized to be an underlying mechanism by which climate variations influence recruitment in fish stocks, the so-called "match-mismatch" hypothesis (Cushing, 1975). Some of the possible physical mechanisms that may influence ecosystem productivity in this respect have been reviewed by Mann and Drinkwater (1994).

The dynamics causing variations in the timing and magnitude of shelf stratification is complex, involving ocean advection, water temperature (which is influenced by the large-scale NAO forcing), and salinity (determined to a great extent by sea-ice dynamics). These processes cause temporal and spatial variations in local anomalies and, as a result, temperature and salinity relationships are often out of phase (Figure 3). Within the recent prolonged period of below normal temperatures, seasonal salinities have varied from fresher to saltier than normal. As a result, the relatively strong winter stratification may have impeded the normal vertical flux of nutrients to the euphotic zone on the Newfoundland Shelf, while the above normal values during the spring from 1993 to 1998 may have provided more favourable conditions for increased primary production. A more detailed analysis of the timing of stratification in relation to the annual plankton bloom from more recent data is in progress. Nevertheless, it appears that the early 1990s was a period of low zooplankton production, and while an increase in biomass did occur during 1995 to 1997 it is possible that the timing of peak production did not coincide with the early larval stages of many species of fish until at least 1998. There are insufficient data, however, throughout the 1990s to fully test this hypothesis. Therefore the mechanisms effecting primary production, nutrient supply, and fish recruitment remain for the most part speculative, but should become clearer as more data become available.

In summary, during the last several decades of the 20th century environmental conditions on the Newfoundland Shelf continued to change, showing extreme variability and often exhibiting different responses during different time periods. For example, temperature and salinity anomalies often show differences in phase and amplitude due to the combined influences of advection and the temporal and spatial variability in sea-ice formation and melting. The NAO index, which is correlated with ocean conditions, has also experienced spatial variability in the most recent years and a subsequent breakdown in the expected ocean response in the Northwest Atlantic. Superimposed on the non-linear dynamics of the physical environment are the dynamics of the fish stocks, which have been subjected to enormous levels of fishing mortality during different periods. More observations over longer time periods may begin to resolve the interplay of environmental effects and fishing, on fish population dynamics and production. Alternatively, unravelling the perplexity between natural and anthropogenic factors will more likely proceed with better measures of the ecosystem and stock production. Among these, measuring fish population production earlier in the life history, for example, is an essential step in this direction. In addition, new initiatives presently carried out under an Atlantic Zonal Monitoring Program (AZMP) (Therriault *et al.*, 1998) are designed to monitor interannual variations in plankton production. Data from these efforts should provide information on the timing of peak production and physical processes that can be compared to year-class success rates of fish.

In conclusion, the decline in fish production, cod in particular, observed since the 1960s and 1970s in Newfoundland waters was due to a declining SSB, most likely caused by excessive fishing that occurred within a deteriorating ocean environment. The continued decrease during most of the 1990s with fishing moratoria in place indicates an unfavourable ocean environment for survival or production of young fish resulting in low SSB. It is noted, however, that other biological factors may be affecting the recovery of many fish stocks, such as depensation in the presence of continued mortality both natural and through limited fisheries (Shelton and Healey, 1999; Anderson and Rose, 2001). Finally, the subsequent increase in the productivity of the pelagic ecosystem observed during the late 1990s is consistent with the expected biological response to a warming ocean environment. However, the extent to which these early signs of increased production translate into significant year classes of cod, for example, remains to be seen.

Acknowledgements

We thank the technical staff of the Northwest Atlantic Fisheries Center for data collection and processing during many oceanographic and fisheries research surveys on the Newfoundland Shelf. We also thank the many scientists at the Department of Fisheries and Oceans for collecting and providing much of the data contained in this analysis and to the Marine Environmental Data Service (MEDS) in Ottawa for providing most of the historical data. We thank Dr Brian Dempson and two anonymous reviewers for many valuable comments and suggestions.

References

Anderson, J. T., and Colbourne, E. B. 2000. Recruitment, pre-recruit survival and mortality in three Newfoundland cod stocks: northern (2J3KL), southern Grand Banks (3NO) and St. Pierre Bank (3Ps). Department of Fisheries and Oceans Canadian Science Advisory Secretariat Research Document No. 00/116. 26 pp.

Anderson, J. T., Dalley, E. L., and Colbourne, E. B. 1999. Recent trends in the dominant pelagic fish species and environment in the Northwest Atlantic, NAFO 2J3KLNO. Department of Fisheries and Oceans Canadian Science Advisory Secretariat Research Document No. 99/114. 15 pp.

Anderson, J. T., and Dalley, E. L. 1997. Nekton of the coastal and shelf waters of Newfoundland. Department of Fisheries and Oceans Canadian Science Advisory Secretariat Research Document No. 97/124. 30 pp.

Anderson, J. T., and Rose, G. A. 2001. Offshore spawning and year-class strength of northern cod (2J3KL) during the fishing moratorium, 1994–1996. Canadian Journal of Fish and Aquatic Science, 58: 1386–1394.

Bishop, C. A. 1994. Revisions and additions to the stratification scheme used during research vessel surveys in NAFO Subareas 2 and 3. NAFO SCR Doc. 94/43 (Ser. no. N2413). 23 pp.

Bishop, C. A., Murphy, E. F., Davis, M. B., Baird, J. W., and Rose, G. A. 1993. An assessment of the cod stock in NAFO Divisions 2J+3KL. NAFO SCR Doc. 93/86 (Ser. no. N2271). 51 pp.

Bundy, A. 2001. Fishing on ecosystems: the interplay of fishing and predation in Newfoundland–Labrador. Canadian Journal of Fish and Aquatic Science, 58: 1153–1167.

Carscadden, J. E., Frank, K. T., and Leggett, W. C. 2001. Ecosystem changes and the effects on capelin (*mallotus villosus*), a major forage species. Canadian Journal of Fish and Aquatic Science, 58: 73–85.

Colbourne, E. B. 2001. Physical oceanographic conditions on the Newfoundland and Labrador Shelves during 2000. Department of Fisheries and Oceans Canadian Science Advisory Secretariat Research Document No. 01/18b. 58 pp.

Colbourne, E. B., and Bowering, W. R. 2001. Recent trends in bottom temperatures and distribution and abundance of Yellowtail Flounder (*Limanda ferruginea*) in NAFO Divisions 3LNO during the spring and fall. NAFO SCR Doc. no. 01/32 (Ser. no. N4409). 17 pp.

Colbourne, E., deYoung, B., and Rose, G. A. 1997. Environmental analysis of Atlantic cod (*Gadus morhua*) migration in relation to the seasonal variations on the Northeast Newfoundland Shelf. Canadian Journal of Fish and Aquatic Science, 54 (Suppl 1): 149–157.

Colbourne, E. B., and Fitzpatrick, C. 1994. Temperature, salinity and density at Station 27 from 1978 to 1993. Canadian Technical Report of Hydrography and Ocean Science, 159. 117 pp.

Colbourne E. B., and Murphy, E. F. 2000. Recent trends in bottom temperatures and distribution and abundance of Atlantic cod (*Gadus morhua*) in NAFO Divisions 3LNO during spring and fall. NAFO SCR Doc. 00/20 (Ser. no. N4249). 30 pp.

Colbourne, E. B., Narayanan, S., and Prinsenberg, S. 1994. Climatic change and environmental conditions in the Northwest Atlantic during the period 1970–1993. ICES Marine Science Symposia, 198: 311–322.

Cushing, D. H. 1975. Marine Ecology and Fisheries. Cambridge University Press, Cambridge. 278 pp.

Dalley, E. L., and Anderson, J. T. 1997. Plankton and nekton of the northeast Newfoundland Shelf and Grand Bank in 1996 compared to 1994 and 1995. Department of Fisheries and Oceans Canadian Science Advisory Secretariat Research Document No. 97/120. 17 pp.

Dalley, E. L., and Anderson, J. T. 1998. Plankton and nekton of the northeast Newfoundland Shelf and Grand Bank in 1997. Department of Fisheries and Oceans Canadian Science Advisory Secretariat Research Document No. 98/121. 29 pp.

Dalley, E. L., Anderson, J. T., and Davis, D.J. 1999. Plankton and nekton of the northeast Newfoundland Shelf and Grand Bank in 1998. Department of Fisheries and Oceans Canadian Science Advisory Secretariat Research Document No. 99/142. 37 pp.

Dalley, E. L., Anderson, J. T., and Davis, D.J. 2000. Short term fluctuations in the Pelagic Ecosystem of the Northwest Atlantic. Department of Fisheries and Oceans Canadian Science Advisory Secretariat Research Document No. 00/101. 36 pp.

deYoung, B., and Rose, G.A. 1993. On recruitment and distribution of Atlantic cod (*Gadus morhua*) off Newfoundland. Canadian Journal of Fish and Aquatic Science, 50: 2729–2741.

DFO. 2000. Northern (2J3KL) cod. Department of Fisheries and Oceans Science Stock Status Report A2–01.

Dickson, R. R., and Meincke, J. 1999. Atlantic hydrography in 1998–99: continued recovery from extreme forcing? Report of the Working Group on Oceanic Hydrography (WGOH). ICES CM 1999/C: 8, 24–35.

Doubleday, W. G. (Ed.) 1981. Manual on groundfish surveys in the Northwest Atlantic. NAFO SCR Doc. 81/2. 56 pp.

Drinkwater, K. F. 1996. Atmospheric and oceanic variability in the northwest Atlantic during the 1980s and early 1990s. Journal of Northwest Atlantic Fishery Science, 18: 77–97.

Drinkwater, K. F., Pettipas, R., and Petrie, L. 2000. Overview of meteorological and sea ice conditions off eastern Canada during 1999. Department of Fisheries and Oceans Canadian Science Advisory Secretariat Research Document No. 00/59. 28 pp.

Hutchings, J. A., and Myers, R. A. 1994. What can be learned from the collapse of a renewable resource? Atlantic cod, *Gadus morhua*, of Newfoundland and Labrador. Canadian Journal of Fish and Aquatic Science, 51: 2216–2146.

ICES. 2001. The annual ICES ocean climate status summary for 2000. ICES. 18 pp.

Lilly, G. R., Shelton, P. A., Brattey, J., Cadigan, N. G., Murphy, E. F., and Stansbury, D. E. 1999. An assessment of the cod stock in NAFO Divisions 2J+3KL. Department of Fisheries and Oceans Canadian Science Advisory Secretariat Research Document No. 99/42. 165 pp.

Mann, K. H., and Drinkwater, K. F. 1994. Environmental influence on fish and shellfish production in the Northwest Atlantic. Environment Review, 2: 16–32.

Mohn, R. 1999. The retrospective problem in sequential population analysis: an investigation using cod fishery and simulated data. ICES Journal of Marine Science, 56: 473–488.

Myers, R. A., Drinkwater, K. F., Barrowman, N. J., and Baird, J. W. 1993. Salinity and recruitment of Atlantic cod (*Gadus morhua*) in the Newfoundland region. Canadian Journal of Fish and Aquatic Science, 50: 1599–1609.

Myers, R. A., Hutchings, J. A., and Barrowman, N. J. 1996. Hypotheses for the decline of cod in the North Atlantic. Marine Ecology Progress Series, 138: 293–308.

Narayanan, S., Carscadden, J., Dempson, J. B., O'Connell, M. F., Prinsenberg, S., Reddin, D.G., and Shackell, N. 1994. Marine climate off Newfoundland and its influnece on Atlantic salmon (*Salmo salar*) and capelin (*Mallotus villosus*). *In* Climate Change and Northern Fish Populations. Ed. by R. J. Beamish. Canadian Special Publication Journal of Fish and Aquatic Science, 121: 461–474.

Parsons, L. S., and Lear, W. H. 2001. Climate variability and marine ecosystem impacts: a North Atlantic perspective. Progress in Oceanography, 49: 167–188.

Petrie, B., Akenhead, S., Lazier, J., and Loder, J. 1988. The cold intermediate layer on the Labrador and northeast Newfoundland Shelves, 1978–1986. Northwest Atlantic Fisheries Organization Scientific Council Studies, 12: 57–69.

Petrie, B., Loder, J., Akenhead, S., and Lazier, J. 1991. Temperature and salinity variability on the eastern Newfoundland Shelf: the annual harmonic. Atmosphere–Ocean, 29: 14–36.

Rogers, J. C. 1984. The association between the North Atlantic oscillation and the southern oscillation in the Northern Hemisphere. Monthly Weather Review, 112: 1999–2105.

Rose, G. A., Atkinson, B. A., Baird, J., Bishop, C. A., and Kulka, D. W. 1994. Atlantic cod distributional changes and thermal variations in Newfoundland waters, 1980–1992. ICES Marine Science Symposia, 198: 542–552.

Rose, G. A., deYoung, B., and Colbourne, E. 1995. Cod (*Gadus morhua*) migration speeds and transport relative to currents on the Northeast Newfoundland Shelf. ICES Journal of Marine Science, 52: 903–913.

Shelton, P. A., and Healey, B. P. 1999. Should depensation be dismissed as a possible explanation for the lack of recovery of the northern cod (*Gadus morhua*) stock? Canadian Journal of Fish and Aquatic Science, 56: 1521–1524.

Stansbury, D. E., Shelton, P.A., Murphy, E. F., and Brattey, J. 1999. An assessment of the cod stock in NAFO Divisions 3NO. NAFO SCR Doc. 99/62 (Ser. no. N4121). 43 pp.

Taggart, C., Anderson, J., Bishop, C., Colbourne, E., Hutchings, J., Lilly, G., Morgan, J., Murphy, E., Myers, R., Rose, G., and Shelton, P. 1994. Overview of cod stocks, biology, and environment on the Northwest Atlantic region of Newfoundland, with emphasis on northern cod. ICES Marine Science Symposia, 198: 140–157.

Therriault, J.-C., Petrie, B., Pepin, P., Gagnon, J., Gregory, D., Helbig, J., Herman, A., Lefaivre, D., Mitchell, M., Pelchat, B., Runge, J., and Sameoto, D. 1998. Proposal for a northwest Atlantic zonal monitoring program. Canadian Technical Report of Hydrography and Ocean Science, 194. 57 pp.

Walsh, S. J., Veitch, M. J., Morgan, M. J., Bowering, W. R., and Brodie, W. B. 2000. Distribution and abundance of yellowtail flounder (*Limanda ferruginea*) on the Grand Bank, NAFO Divisions 3LNO, as derived from annual Canadian bottom trawl surveys. NAFO SCR Doc. 00/35 (Ser. no. N4264). 54 pp.

ICES Marine Science Symposia, 219: 182–189. 2003

Plankton variability on the Faroe Shelf during the 1990s

Eilif Gaard

Gaard, E. 2003. Plankton variability on the Faroe Shelf during the 1990s. – ICES Marine Science Symposia, 219: 182–189.

A mixture of neritic copepod species, meroplanktonic larvae, and ichthyoplankton usually dominates the zooplankton on the Faroe Shelf during spring and summer. The ecosystem, however, is very much affected by the interannually variable influx of *Calanus finmarchicus*. During the 1990s, the plankton production, abundance, and species composition fluctuated greatly, the zooplankton biomass on the Shelf (which is mainly *C. finmarchicus* biomass) by a factor of 10. When the abundance of *C. finmarchicus* was high, the abundance of neritic zooplankton was generally low and *vice versa*. Interannually, there is a strong inverse relationship between zooplankton biomass on the Shelf and new primary production. During the 1990s, new primary production from spring to mid-summer fluctuated by a factor of about 5, inversely related to the zooplankton biomass. The good relationship between primary production and fish reproduction and growth and is most likely the result of variable production of zooplankton of a suitable size for fish larvae during spring.

Keywords: ecosystem, Faroe Shelf, ichthyoplankton, phytoplankton, solar radiation, zooplankton.

Eilif Gaard, Faroese Fisheries Laboratory, Box 3051, FO-110 Tórshavn, Faroe Islands [tel: +298 31 30 92, fax: +298 31 82 64, e-mail: eilifg@frs.fo]

Introduction

The tides on the Faroe Shelf are primarily semi-diurnal with peak currents of about 1 m sec^{-1} inside the 100 m bottom contour (Figure 1). The currents are even stronger in the shallow areas and, locally, can exceed 4–10 knots (Hansen, 1992; Simonsen, 1999). This leads to intense mixing, resulting in homogeneous water masses. The well-mixed shelf water is separated from the offshore stratified waters by a persistent tidal front located at about the 100–130 m contour (Gaard *et al.*, 1998). In addition, residual currents have a persistent anticyclonic circulation around the islands, with typical speeds of about 0.1–0.15 m s^{-1} (Hansen, 1992; Hansen and Larsen, 1999; Simonsen, 1999; Gaard and Hansen, 2000).

The extreme turbulence of the Faroe Shelf Water, and the separation of the Shelf Water from the offshore led to maintenance of a shelf planktonic community that is quite different from that offshore. Both the phytoplankton production and species composition in these two regions are quite different. Most years the phytoplankton spring bloom starts earlier on the Shelf than offshore (Gaard, 1996, 2000). Since the nutrient pool is limited, the primary production decreases nutrient concentrations during spring and summer (Gaard, 1996; Gaard *et al.*, 1998). In high nutrient concentrations, diatoms dominate in the Shelf Water; however, when the nutrient concentrations decrease much smaller flagellates tend to take over (Gaard *et al.*, 1998).

The zooplankton species composition, production, and abundance on the Shelf are also usually quite different from the offshore environment. The Shelf community is essentially a mixture of neritic copepod (mainly *Acartia* spp. and *Temora longicornis*) and meroplanktonic larvae (Gaard, 1999; Debes, 2000), and ichthyoplankton (Gaard and Steingrund, 2000; Gaard and Reinert, 2002) during spring and summer. The ecosystem is also affected by advection of zooplankton from the surrounding offshore environment, e.g. the copepod *Calanus finmarchicus* may be advected onto the Shelf in highly variable abundance (Gaard and Hansen, 2000). The abundance of *C. finmarchicus* is usually much lower on the Shelf than offshore.

The Faroe Shelf Water can be characterized as a relatively isolated, well-defined, small (approximately 8,000–10,000 km^2) and uniform ecosystem which is suitable for ecological studies.

The aim of this article is to demonstrate the interannual variability of phytoplankton, zooplankton, and ichthyoplankton during the period 1990–2000. Possible environmental causes and their effects on higher trophic levels in the Faroe Shelf ecosystem are discussed.

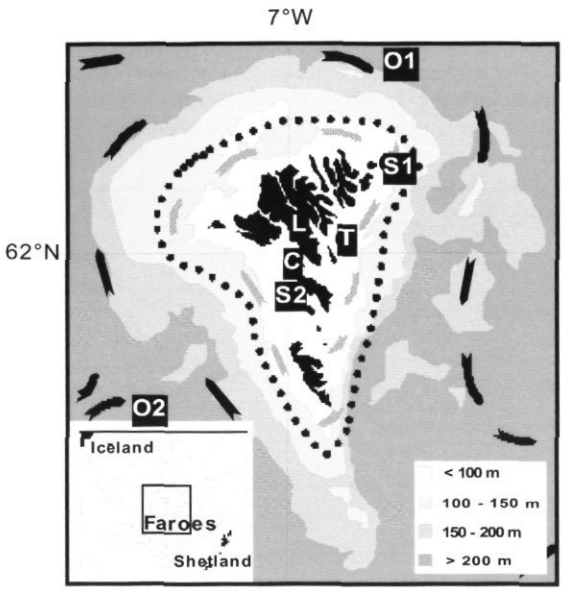


Figure 1. Bottom topography and main features of the flow field. The dotted line indicates a typical position of the tidal front that separates the Shelf Water from the open ocean. The black squares with letters refer to observational sites visited for monitoring of time-series investigations.

Materials and methods

Oceanic observations and measurements of hydrography, nutrients, and plankton were carried out in late June 1990–2000 at about 50 stations distributed around the Faroe Shelf and slope. In addition, time-series of salinity were collected at two shelf stations (S1 and S2) and at two offshore stations (O1 and O2) in May 1990–2000 (Figure 1).

At a coastal station (Station C in Figure 1), nutrients and chlorophyll *a* were collected twice a week at 18-m depth. Nutrient samples were collected from May 1995 and chlorophyll *a* samples during spring and summer from 1999. In addition, chlorophyll *a* was frequently collected at station T during 1997. Solar radiation in the 300–2500 nm spectral range was measured from 1990 to 1999 at station L with an automatic measuring weather station (Anderaa). Salinity was obtained by CTDs. An EG&G CTD was used until May 1995 and a Seabird Electronics SBE 911 plus CTD afterwards.

The nutrient samples from 1990 were stored in a refrigerator and analysed 7–11 days after sampling. In 1991–1994 they were frozen immediately after sampling and analysed ashore. Since 1995 the samples that were collected onboard the research vessel were analysed onboard, and the samples that were taken at the coastal station (C) were preserved with 12 drops of chloroform per 100 ml of sample. Nitrate + nitrite were measured with an autoanalyzer in accordance with the method of Grasshoff *et al.* (1983).

Chlorophyll *a* was measured following the method of the Baltic Marine Biologists (1979) and the Jeffrey and Humprey equation (1975).

Zooplankton was sampled by vertical hauls from 50-m depth to the surface. A Hensen net was used in 1989–1991 and a WP2 net in 1992–2000. Both nets had a mesh size of 200 μm and operated at a towing speed of 0.3–0.5 m sec^{-1}. The samples were preserved in 4% formaldehyde. Subsamples were identified and counted, and biomass obtained after drying at 60–65°C until they reached constant weight.

Results

The average solar radiation for March, April, May, and June 1990–1999 showed increasing values during the seasons (Figure 2). During spring, the interannual variability was generally smaller than differences between the months.

The salinity is always lower in the Faroe Shelf Water than in the surrounding ocean (Figure 3A). This salinity gradient is maintained by precipitation and run-off from the islands, retention of the water masses on the shelf and shallower bottom depths on the Shelf. The front between the oceanic and the Shelf Water can be identified based on the isohalines. The average salinity difference in the upper 50 m of the water column between the shelf stations (S1 and S2) and offshore stations (O1 and O2) in May 1990–2000 was 0.10. However, there was interannual variability in salinity with a difference of between 0.05 and 0.13. This variability is due to variable retention of the Shelf Water or variable precipitation.

The amounts of nutrients on the Shelf are limited to those available to the spring bloom plus the net

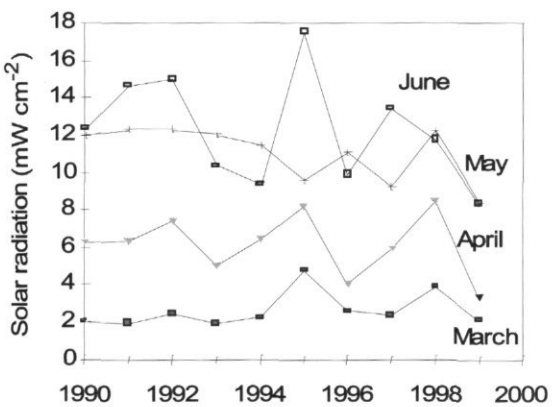


Figure 2. Mean solar radiation (300–2500 nm spectral range) at station L in March, April, May, and June 1990–1999.

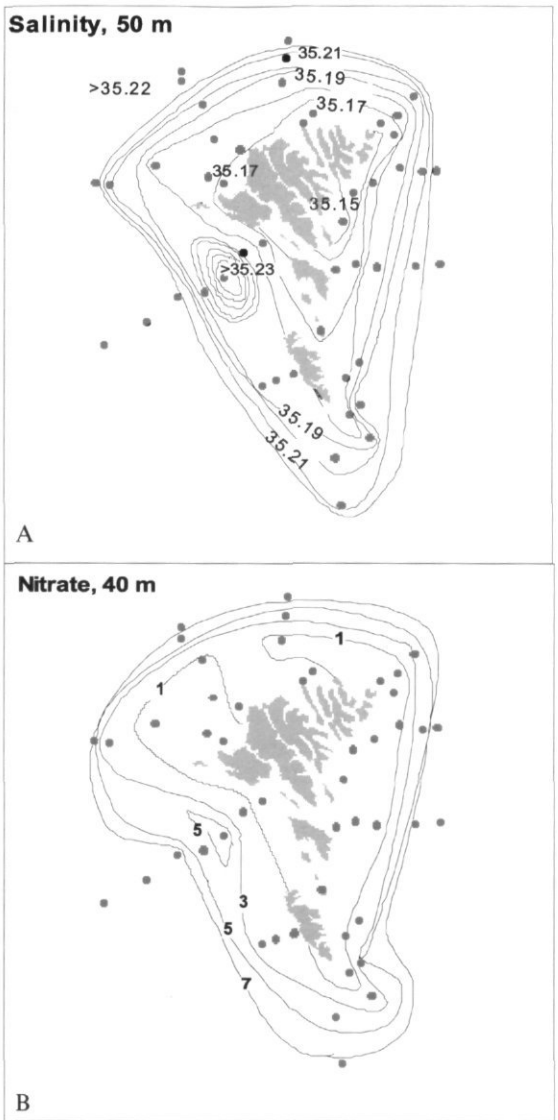


Figure 3. Salinity at 50 m depth (A) and nitrate (μM) at 40 m depth (B) around the Faroe Shelf, 23 June to 1 July 2000.

influx of nutrients from offshore during the productive season. During summer, the nutrient concentrations may decrease to very low levels in the Shelf Water (Figure 3B).

In most years, shelf nitrate concentrations begin to decrease in May – rapidly during the spring bloom and generally more than offshore. Nitrate concentrations reach a minimum in July and then slowly increase again. By November they again reach winter levels of around 12.0–12.5 μM (Figure 4). The timing of the spring bloom and decrease of the nitrate concentrations as well as the phytoplankton biomass can vary significantly between years. Generally the years with the earliest spring bloom had the lowest nitrate concentrations during summer, and *vice versa* (Figures 4 and 5).

There was high interannual variability in (decrease of) the nitrate concentrations on the Faroe Shelf during the 1990s (Figure 6). During the early

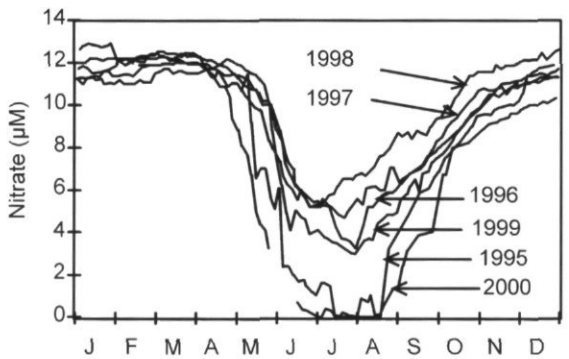


Figure 4. Nitrate concentrations at station C from May 1995 to December 2000.

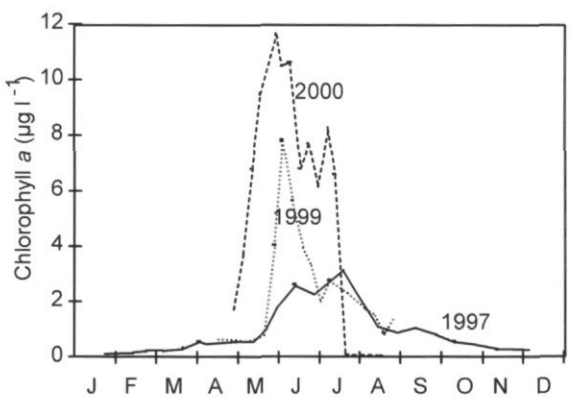


Figure 5. Chlorophyll *a* concentrations at station T during 1997 and station C from April to August 1999 and 2000.

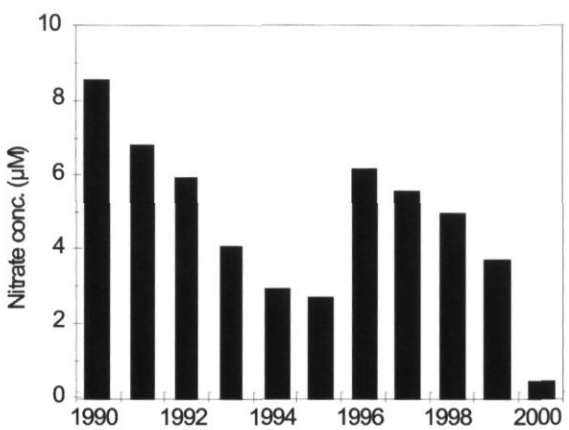


Figure 6. Mean nitrate concentrations on stations S1 and S2 in late June 1990–2000.

1990s, the nitrate concentrations remained high throughout the year. However, during the early-mid-1990s and again in 2000 the nitrate concentrations decreased greatly in the Shelf Water during summer.

Between 1989 and 2000, the interannual abundance of oceanic species (mainly *C. finmarchicus*) and neritic species (mainly the copepods *Acartia* spp. and *Temora longicornis* and barnacle larvae) on the Faroe Shelf fluctuated greatly (Figure 7). During the first few years of the period, the ecosystem was dominated by *C. finmarchicus*. The mid-summer abundance of *C. finmarchicus* fluctuated from about 400 copepods m^{-3} in 1989 to about 25 in 1994 and up again to about 150 copepods m^{-3} in the late 1990s. At the same time the neritic zooplankton fluctuated inversely, from about 120 in late June 1989 to 960 in 2000. Relatively, the system fluctuated from 80% of *C. finmarchicus* + *Oithona* and 20% neritic species in 1989 to 10% of *C. finmarchicus* + *Oithona* and 90% neritic species in 2000.

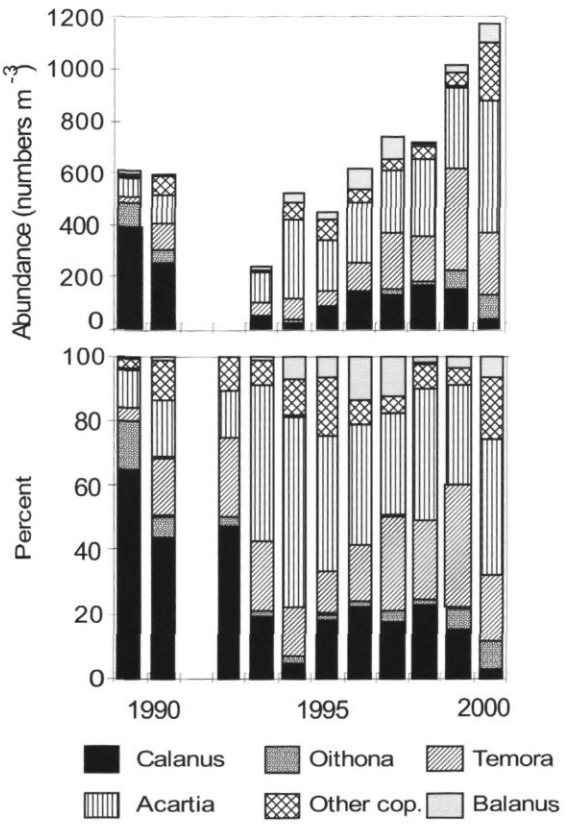


Figure 7. Mean absolute (upper) and relative (lower) abundance of the dominant copepod species and barnacle larvae in the upper 50 m of the water column at stations S1 and S2 in June 1989–2000.

Since *C. finmarchicus* is a much bigger copepod than the neritic species, it dominates the zooplankton biomass. Therefore the changes in abundance of *C. finmarchicus* on the Shelf during the 1990s dominated the zooplankton biomass, which, during this period, fluctuated by a factor of 10 on the Shelf while remaining relatively constant in the oceanic environment outside the tidal front (Figure 8).

Discussion

Phytoplankton variability

In most years, the primary production increases in May and decreases again in August or September. Phytoplankton production usually increases earlier in spring on the Shelf than offshore, and is believed to be the result of a shallower mixed layer on the Shelf compared to outside the tidal front during early spring (prior to establishment of a summer thermocline offshore). According to Sverdrup's (1953) theory, the spring bloom can only start when the depth of the upper mixed layer is less than the critical depth. Inside the tidal front on the Faroe Shelf, the mixed layer is the total water column (mean depth 70–80 m) and in spring the critical depth may exceed the bottom depth. The spring bloom may therefore start on the Shelf before the development of a summer thermocline makes this possible in the surrounding offshore area. The spring bloom usually starts in the central and northern shelf regions (Gaard, 1996, 2000) and then spreads over the entire Shelf.

Nitrate concentrations during spring and summer on the Faroe Shelf varied dramatically during the 1990s, because of variable new primary production (Dugdale and Goering, 1967), variable net influx

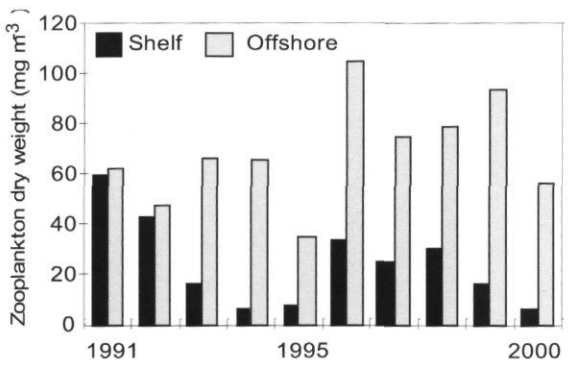


Figure 8. Mean zooplankton dry weight in the upper 50 m of the water column on the Faroe Shelf (inside the 100 m bottom contour) and offshore (outside the 150 m bottom contour) in June 1990–2000. The data derive from stations similar to those in Figure 3.

of nitrate from offshore or a combination of both. An approximation of relative nitrate assimilation (potential new primary production) during the high-productive period can be calculated as the sum of the nitrate decrease in the Shelf Water and net nitrate inflow. The latter can be expressed as the renewal rate of the Self Water multiplied by $[NO_3^-]_{offshore}$ minus $[NO_3^-]_{shelf}$ during the investigated period.

The amount of nitrate in shallow regions on the Faroe Shelf is limited and interannual variability in its decrease during spring and summer is fairly easily monitored. The flushing rate of the Shelf Water can be approximated from salinity on the Shelf and offshore water, precipitation, and depth of the Shelf Water column (Gaard and Hansen, 2000). Assuming a mean precipitation of 1000 mm $year^{-1}$, the average flushing time in spring during the 1990s is estimated to be about 2.5 months, but is variable. The flushing time is only an approximation, due to the averaging period used and the difficulty in obtaining representative precipitation measurements.

The above calculations can be used as a proxy for a relative potential new primary production (Figure 9). The index is based on calculation from spring to a fixed date (26 June) each year. Variable nitrate influx (owing to variable renewal rates of the Shelf Water) is markedly lower than the nitrate loss. This therefore suggests that the nutrient changes are due mainly to variable assimilation. Potential new primary production thus appears to have varied by a factor of about 5 during the 1990–2000 decade.

The primary production index only provides relative values, from spring to midsummer. Using a Redfield ratio of C:N = 106:16, and assuming that the mean bottom depth is 75 m, the index corresponds to a mean potential new primary production ranging from about 17 gC m^{-2} in 1990 to 95 gC m^{-2} in 2000. During the period from about 10 May to 26 June, the mean daily potential new production on the central Faroe Shelf varied between about 0.4 mgC m^{-2} day^{-1} (1990) and 2 gC m^{-2} day^{-1} (2000).

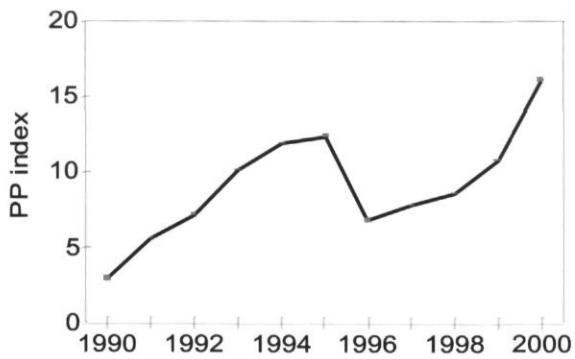


Figure 9. Calculated index of the potential new primary production on the Faroe Shelf.

The onset of primary production on the Shelf varied by more that a month during the years 1990–2000 (Gaard *et al.*, 1998; Figures 4 and 5). The timing of the spring bloom is thought to have important ecological consequences for copepod reproduction (e.g. Diel and Tande, 1992; Kiørboe *et al.*, 1990; Kiørboe and Nielsen, 1994; Hirche, 1996; Niehoff *et al.*, 1999; Niehoff and Hirche, 2000), and therefore also for feeding and survival of fish larvae (e.g Ellertsen *et al.*, 1980; Cushing, 1990; Leggett and DeBlois, 1994; Gaard and Steingrund, 2000).

The initiation and evolution of the spring bloom are determined by a combination of events that reflect a balance between the amount of solar radiation received by the phytoplankton population, the variability in concentrations of dissolved inorganic nutrients, and phytoplankton losses associated with respiration, grazing, and sedimentation (Smetacek and Passow, 1990; Platt *et al.*, 1991) and, in this case, possible flushing out of the area.

Unfortunately, no data-series are available for light penetration on the Faroe Shelf during spring. However, data-series from meteorological stations ashore (Figure 2) indicate that the variability in timing of the spring bloom onset and the calculated new primary production are not related to variability in intensity in solar radiation.

The depth (or stratification) of the upper, mixed layer is often an important factor in determining the photosynthetic rate, and hence the development of the spring bloom (e.g. Sakshaug and Slagstad 1991). However, on the Faroe Shelf, variability in physical forces (e.g. wind, tidal currents, and stratification) does not correlate with the variability of timing of the spring bloom development or the primary production (Gaard *et al.*, 1998). This is not surprising, since the strong tidal currents do not permit any marked stratification on the Shelf. Consequently the depth of the (productive) water column on the Faroe Shelf is fairly constant, and not influenced by forcing. Therefore effects from variable phytoplankton loss seem to be a more likely reason for the observed variability in phytoplankton growth. Losses may be due to flushing out of the ecosystem and grazing.

Although the flushing rates of seawater on the Faroe Shelf may vary, they seem to be too low to be the main factor affecting the observed variability in spring bloom development and primary production.

Sakshaug *et al.* (1991) showed in a mathematical model that variable loss rates of phytoplankton may affect the timing of spring bloom development, and Yin *et al.* (1997) reported an impact by the large oceanic copepod, *Neocalanus plumchrus*, during early spring from the Strait of Georgia, British Columbia. The presence of a high biomass of this copepod prior to the spring bloom may be able to

repress, and thus delay, spring bloom development in that area. Bathmann *et al.* (1990) also suggested that copepod grazing may influence spring bloom development in the Norwegian Sea. On the other hand, other researchers have stated the opposite and concluded that the grazer community cannot control or postpone a spring bloom (e.g. Smith *et al.*, 1985; Hirche *et al.*, 1991; Nielsen and Hansen, 1995).

There is a strong inverse relationship between the zooplankton biomass and the nitrate loss, i.e. new primary production (Figure 10). In years with low zooplankton biomass, the primary production developed early and levels were high, while in years with high zooplankton biomass, the spring bloom occurred later and the production was reduced. The variability in zooplankton biomass is dominated by *C. finmarchicus*. During early spring, substantial (but interannually highly variable) amounts of overwintered *C. finmarchicus* are advected onto the Shelf (Gaard and Hansen, 2000). A key question is whether grazing by *C. finmarchicus* could have delayed the spring bloom and decreased the total new primary production during spring and early summer. Unfortunately, simultaneous measurements of copepod ingestion rates and primary production *in situ* during pre-bloom and bloom periods are not available, and without such data a final conclusion is not possible. However, the inverse relationship between zooplankton biomass (largely *C. finmarchicus* biomass) and primary production supports this.

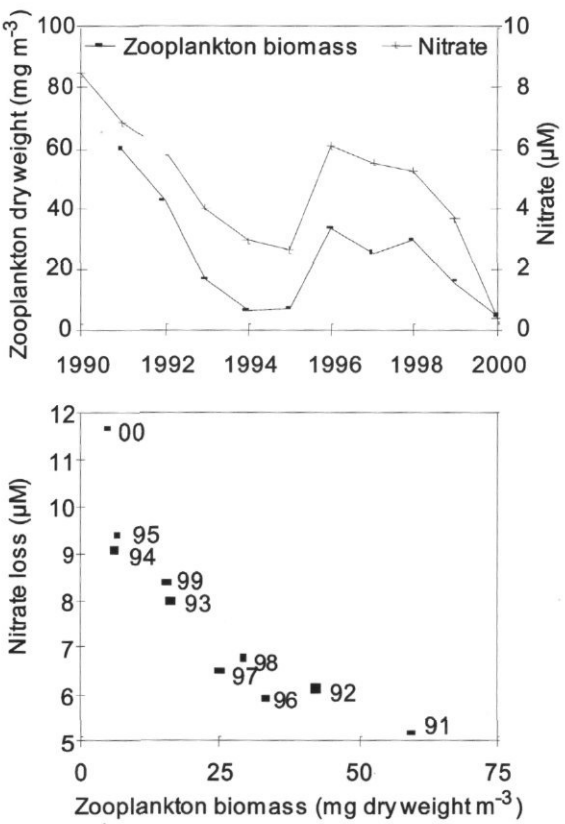


Figure 10. Variability in zooplankton biomass in late June and nitrate concentrations on 26 June (upper panel) and the relationship between zooplankton biomass and nitrate loss from winter levels to 26 June (lower panel) from 1990 to 2000.

Zooplankton variability

During the period 1989–2000, considerable variability was observed in zooplankton abundance and species composition. The ecosystem fluctuated interannually between high influence of the oceanic environment and neritic dominance with lower oceanic influence.

During 1989–1990, the ecosystem was dominated by *C. finmarchicus*, while neritic zooplankton species were of minor importance. Differences between the Shelf area and the surrounding offshore area were generally small. However, during the early 1990s the species composition on the Faroe Shelf changed and the area gradually became more and more neritic (Figure 7). *C. finmarchicus*, which was still the dominant copepod outside the tidal front (Gaard, 1999), gradually became less abundant inside the tidal front, while other copepod species, mainly *Acartia longiremis* and *Temora longicornis*, increased in numbers. *C. finmarchicus* was scarce on the shelf, especially during the period 1993–1995 and in 2000. Although predation on *C. finmarchicus* obviously must have affected its abundance in the ecosystem, variable advection of individuals from offshore is presumed to be a main reason for the changes in abundance. The main inflow area seems to be on the western shelf slope (Gaard and Hansen, 2000).

Egg production of copepods is highly affected by food availability (e.g. Kiørboe *et al.*, 1990; Kiørboe and Nielsen, 1994; Hirche 1996 and references therein; Niehoff *et al.*, 1999). This effect is also seen on the Faroe Shelf, where development of the copepods reflects the seasonal production of phytoplankton (Gaard, 1999, 2000). However, there is a considerable pre-bloom reproduction of overwintered *C. finmarchicus*, mainly on the western and northwestern shelf slope region that is advected from the offshore (Gaard, 2000; Gaard and Steingrund, 2000). Thus copepod reproduction and development seems to start with *C. finmarchicus* in early spring and then, as the phytoplankton biomass increases during spring, the neritic species increase their reproduction.

Effect on higher trophic levels

During the 1990s, fish reproduction, growth, and catches on the Faroe Shelf have undergone quite

extensive and dramatic changes. The annual landings of cod and haddock, which in the long term fluctuate between 20 000 and 40 000 and between 15 000 and 25 000 tonnes, respectively, decreased in the early 1990s to historically low levels of only ~6000 and ~4000 tonnes, respectively, in 1993. Landings of both species increased rapidly to maximum levels in 1996 and 1998, respectively, and then fell to average levels by the end of the 1990s (ICES, 2000). Although high fishing mortality undoubtedly influenced these trends, their main cause seems to have been variable recruitment and growth rates induced by environmental changes (Gaard *et al.*, 2002; Steingrund *et al.*, 2003). During the late 1980s and the beginning of the 1990s there was a general recruitment collapse of many fish species and their food in the ecosystem. At the same time as the recruitment was low, fish growth was low, and seabirds also declined (Gaard *et al.*, 2002). The production of their main food sources also seems to have been low. By the mid-1990s the recruitment and growth rates had increased again. Variability coincided well with variability in the calculated new primary production (Gaard *et al.*, 2002; Steingrund *et al.*, 2003), which, during the 1990s. was reflected in trophic levels throughout the ecosystem, including fish and seabirds. The entire ecosystem changed between low-production and high-production periods in all trophic levels.

The negative relationship between zooplankton biomass (largely *C. finmarchicus* variability) and fish recruitment and growth may seem contradictory. However, first-feeding fish larvae depend on high concentrations of small-sized zooplankton. Spawning of the main fish species on the Shelf (cod, haddock, sandeel, and Norway pout) takes place in early spring and the successful survival and feeding conditions of the larvae depend largely on high copepod reproduction in spring. During the first years of the period for which plankton data are available (mainly 1989–1991), production was at a very low level and zooplankton on the Shelf was mainly composed of oceanic plankton. The zooplankton was dominated by *C. finmarchicus* and its reproduction during early spring seems to have been low. Thus, although the zooplankton biomass on the shelf was quite high during that period, to a large extent it consisted of large-sized *C. finmarchicus* during spring. Such a food environment does not favour feeding conditions for small fish larvae. Gradually, however, during the early 1990s, primary production markedly improved at the same time as the ecosystem gradually became more and more dominated by small-sized neritic zooplankton. It is hypothesized that an increased production of small-sized zooplankton organisms (both *C. finmarchicus* and neritic species), mainly during spring, has caused a corresponding increase in food availability for fish larvae in general on the Faroe Shelf during the early 1990s and that this has been a major reason for the fish recruitment and growth recovery. Environmental conditions may not only affect survival of cod and haddock larvae, but also of their prey species (e.g. sandeel). A negative relationship between zooplankton abundance and cod and haddock recruitment has also been observed on the Scotian Shelf (Drinkwater *et al.*, 2000).

In summary, primary production has fluctuated very much during the 1990s, and the fluctuations are reflected through all trophic levels, including fish and seabird growth and reproduction. The production was negatively correlated with abundance of *C. finmarchicus* and it is hypothesized that a potential grazing effect may delay and reduce the phytoplankton production. During years with high advection of overwintered *C. finmarchicus* onto the Shelf the abundance of small-sized zooplankton was low. The general decrease in fish production during the period from the 1980s to the beginning of the 1990s may have been due to low abundance on the Shelf of suitable sized prey for fish larvae during spring.

Acknowledgements

I thank Dr. Bogi Hansen for processing the CTD data, Karina Nattestad for technical assistance, and two unknown reviewers for their helpful comments on the manuscript.

References

Baltic Marine Biologists. 1979. Recommendation on methods for marine biological studies in the Baltic Sea. Phytoplankton and Chlorophyll. The Baltic Marine Publication, 5: 1–38.

Bathmann, U. V., Noji, T. T., and Bodungen, B. v. 1990. Copepod grazing potential in late winter in the Norwegian Sea: a factor in the control of spring phytoplankton growth? Marine Ecology Progress Series, 60: 225–233.

Cushing, D. H. 1990. Plankton production and year-class strength in fish populations and update of the match/mismatch hypothesis. Advances in Marine Biology, 26: 249–293.

Debes, H. 2000. Plankton community structure and the relative importance of mesozooplankton and protozooplankton as grazers on the Faroe shelf. Cand. Scient. Thesis. University of Copenhagen. 28 pp.

Diel, S., and Tande, K. 1992. Does the spawning of *Calanus finmarchicus* follow a reproductible pattern? Marine Biology, 113: 21–31.

Drinkwater, K. F., Frank, K. T., and Petrie, B. 2000. The effects of *Calanus* on the recruitment, survival and condition of cod and haddock on the Scotian Shelf. ICES CM 2000/M: 7. 18 pp.

Dugdale, R. C., and Goering, J. J. 1967. Uptake of new and regenerated forms of nitrogen in primary productivity. Limnology and Oceanography, 12: 196–206.

Ellertsen, B., Solemdal, P., Strømme, P., Tilseth, S., Westergård, T., Moksness, E., and Øiestad, V. 1980. Some

biological aspects of cod larvae (*Gadus morhua* L.). Fiskeridirektoratets Skrifter Serie Havundersøkelser, 17: 29–47.

Gaard, E. 1996. Phytoplankton community structure on the Faroe shelf. Fróðskaparrit, 44: 95–106.

Gaard, E. 1999. The zooplankton community structure in relation to its biological and physical environment on the Faroe Shelf, 1989–1997. Journal of Plankton Research, 21: 1133–1152.

Gaard, E. 2000. Seasonal abundance and development of *Calanus finmarchicus* in relation to phytoplankton and hydrography on the Faroe Shelf. ICES Journal of Marine Science, 57: 1605–1611.

Gaard, E., and Hansen, B. 2000. Variations in the advection of *Calanus finmarchicus* onto the Faroe Shelf. ICES Journal of Marine Science, 57: 1612–1618.

Gaard, E., Hansen, B., and Heinesen, S. P. 1998. Phytoplankton variability on the Faroe Shelf. ICES Journal of Marine Science, 55: 688–696.

Gaard, E., Hansen, B., Olsen, B., and Reinert, J. 2002. Ecological features and recent trends in physical environment, plankton, fish stocks and sea birds in the Faroe Plateau ecosystem. *In* Large Marine Ecosystems of the North Atlantic. Changing Stages and Sustainability, pp. 245–265. Ed. by K. Sherman and H.-R. Skjoldal. 449 pp.

Gaard, E., and Reinert, J. 2002. Pelagic cod and haddock juveniles on the Faroe Plateau: distribution, diets and feeding habitats. Sarsia, 87. (In press.)

Gaard, E., and Steingrund, P. 2000. Reproduction of Faroe Plateau cod: spawning, egg advection and larval feeding. Fróðskaparrit, 48: 87–103.

Grasshoff, K., Erhardt, M., and Kremling, K. (Eds.) 1983. Methods for Seawater Analysis. Second revised and extended edition. Verlag Chemie. 419 pp.

Hansen, B. 1992. Residual and tidal currents on the Faroe Plateau. ICES CM 1992/C: 12. 18 pp.

Hansen B., and Larsen, K. M. 1999. Traditional current meter observations in Faroese offshore waters 1977–1994. Technical Report No. 99–01, Faroese Fisheries Laboratory. 193 pp.

Hirche, H.-J. 1996. The reproductive biology of the marine copepod *Calanus finmarchicus*: A review. Ophelia, 44: 111–128.

Hirche, H.-J., Baumann, M. E. M., Kattner, G., and Gradinger, R. 1991. Plankton distribution and the impact of copepod grazing on the primary production in Fram Strait, Greenland Sea. Journal of Marine Systems, 2: 477–494.

ICES. 2000. Report of the North-Western Working Group. ICES CM 2000/ACFM: 15. 328 pp

Jeffrey, S. W., and Humphrey, G. F. 1975. New spectrophotometric equations for determining chlorophyll a, b, c_1 and c_2 in higher plants and natural phytoplankton. Biochemie und Physiologie der Pflanzen, 167: 191–194.

Kiørboe, T., Kaas, H., Kruse, B., Møhlenberg, F., and Ærtebjerg, G. 1990. The structure of the pelagic food web in relation to water column structure in Skagerrak. Marine Ecology Progress Series, 59: 19–32.

Kiørboe, T., and Nielsen, T. G. 1994. Regulation of zooplankton biomass and production in a temperate coastal ecosystem. Copepods. Limnology and Oceanography, 39: 493–507.

Leggett, W. C., and DeBlois, D. 1994. Recruitment of marine fishes: is it regulated by starvation and predation in the egg and larval stages? Netherlands Journal of Sea Research, 32: 119–134.

Niehoff, B., Klenke, U., Hirche, H.-J., Irigoien, X., Head, R., and Harris, R. 1999. A high frequency time series at Weathership M, Norwegian Sea, during the 1997 spring bloom: the reproductive biology of *Calanus finmarchicus*. Marine Ecology Progress Series, 176: 81–92.

Niehoff, B., and Hirche, H.-J. 2000. The reproduction of *Calanus finmarchicus* in the Norwegian Sea in spring. Sarsia, 85: 15–22.

Nielsen, T. G., and Hansen, B. 1995. Plankton community structure and carbon cycling on the western coast of Greenland during and after the sedimentation of a diatom bloom. Marine Ecology Progress Series, 96: 115–131.

Platt, T., Bird, D. F., and Sathyendranath, S. 1991. Critical depth and marine primary production. Proceedings of the Royal Society London B., 246: 205–217.

Sakshaug, E., and Slagstad, D. 1991. Light and productivity of phytoplankton in polar marine ecosystems: a physiological view. Polar Research, 10: 69–85

Sakshaug, E., Slagstad, D., and Holm-Hansen, O. 1991. Factors controlling the development of phytoplankton blooms in the Antarctic Ocean: a mathematical model. Marine Chemistry, 35: 259–271.

Simonsen, K. 1999. Tides and tidal simulations in the area around the Faroe Islands. Technical Report, 116, Nansen Environmental and Remote Sensing Center. 104 pp.

Smetacek, V., and Passow, U. 1990. Spring bloom initiation and Sverdrup's critical-depth model. Limnology and Oceanography, 35: 228–234.

Smith, S. L., Smith, W. O., Codispoti, L. A., and Wilson, D. L. 1985. Biological observations in the marginal ice zone of the east Greenland Sea. Journal of Marine Research, 43: 693–717.

Steingrund, P., Ofstad, L. H., and Olsen, D. H. 2003. Effect of recruitment, individual weights, fishing pressue, and longline growth-dependent catchability on the catch of Faroe Plateau cod (*Gadus morhua* L.) in the period 1989–1999. ICES Journal of Marine Science Symposia, 219: 418–420. (This volume.)

Sverdrup, H. U. 1953. On conditions for the vernal blooming of phytoplankton. Journal du Conseil International pour l'Exploration de la Mer, 18: 287–295.

Yin, K., Harrison, P. J., Goldblatt, R. H., St. John, M. A., and Beamish, R. J. 1997. Factors controlling the timing of the spring bloom in the Strait of Georgia estuary, British Columbia, Canada. Canadian Journal of Fisheries and Aquatic Science, 54: 1985–1995.

ICES Marine Science Symposia, 219: 190–198. 2003

Resolving variations in the timing and intensity of the spring bloom in the central North Sea during the 1990s: a comparison of remote sensing and 2-D modelling approaches

Michael A. St. John, Paul Budgell, Morten H. Nielsen, and Anne Lucas

St. John, M. A., Budgell, P., Nielsen M. H., and Lucas A. 2003. Resolving variations in the timing and intensity of the spring bloom in the central North Sea during the 1990s: a comparison of remote sensing and 2-D modelling approaches. – ICES Marine Science Symposia, 219: 190–198.

Key to understanding the dynamics of the North Sea ecosystem is resolving the timing, intensity, and duration of spring and fall phytoplankton blooms. In order to do so, we apply a potential energy model of thermal stratification based on the energy equation (for turbulence) coupled to a biochemical model Sharples and Tett (1994). Using this approach we examine the timing and intensity of the spring and fall phytoplankton blooms for the years 1981, 1982, and 1986 as well as 1997 to 2000. These estimates are then compared with temporal estimates of and biomass from CZCS (1981, 1982, and 1986) and SeaWiFS (1997 to 2000). A relatively high degree of similarity was observed between the modelled and observed timing of the spring bloom, with the model prediction earlier by 6.1 days (s.d. ± 8.3). Predictions of the timing of the fall bloom from the model were also earlier than observed by 9.4 days (s.d. ± 15.4). Comparisons of biomass from the two techniques resulted in a ratio of 3.0 and 1.2 (Model vs. CZCS) and 6.4 and 2.7 (Model vs. SeaWiFS) for the spring and fall blooms, respectively. A number of inherent weaknesses are suggested for the lack in coherence between the two approaches. For the modelling approach, these include species-specific variations in nutrient uptake and growth rate, error in biomass estimates of phytoplankton seed populations, and lack of temperature effects on phytoplankton growth. Remotely sensed estimates suffer from a lack of depth penetration (thus missing subsurface biomass), cloud cover, and the patchy distribution of blooms. It is suggested that high resolution 3-D modelling may better address the dynamics of phytoplankton blooms in the North Sea, while 2-D models may be more appropriate for the development of indices for examining the effects of climate change due to their lack of dependence on boundary conditions.

Keywords: biophysical modelling, Coastal Zone Colour Scanner (CZCS), North Sea, phytoplankton blooms, Sea-viewing Wide Field-of-view Sensor (SeaWiFS).

M. St. John: Hamburg University, Center for Marine and Climate Research, Institute for Hydrobiology and Fisheries Research, Olberweg 24, D-22767 Hamburg, Germany [e-mail: michael.st.john@uni-hamburg.de; P. Budgell: Institute of Marine Research, Marine Environment Centre, Physical Oceanography Section Nordnesgate 50, PO Box 1870, Nordnes, NO-5817 Bergen, Norway; M. H. Nielsen: Danish Institute for Fisheries Research, Department of Marine Ecology, Kavalergaarden 6, DK-2920 Charlottenlund, Denmark; A. Lucas: University of Bergen, Institute for Geography, Breiviken 2, NO-5035 Bergen-Sandviken, Norway.

Introduction

The spring phytoplankton bloom in high latitude marine ecosystems fuels subsequent production at higher trophic levels and is presumed to be critical for the recruitment success of associated fish stocks. However, the transport of phytoplankton biomass to higher trophic levels can vary dramatically with the duration of the bloom (e.g. Kiørboe, 1991) and the dominant algal species (e.g. Thompson and Harrison, 1992; St. John *et al.*, 2001). For example, a period of rapid, prolonged high stratification initially exposes phytoplankton cells to an optimal light and nutrient environment resulting in the rapid production of biomass, the so-called spring bloom. This situation, due to subsequent nutrient depletion

caused by the bloom, is followed by a reduction of primary production and a shift in phytoplankton dominance from diatoms to a recycling community comprised of the microbial loop. In this scenario, diatom cells, dominant in the spring bloom, rapidly sediment out of the water column (e.g. Waite *et al.*, 1992) enhancing benthic production in shallow coastal seas (e.g. Josefson and Conley, 1997). However, this sedimentation removes nutrients and biomass from the water column, as herbivorous zooplankton are unable to utilize the production due to a mismatch in population growth rates (Kiørboe, 1991). In an alternative scenario, stratification develops more slowly with periods of ephemeral mixing, resulting in a slow build-up of phytoplankton biomass and a replenishment of nutrients from deep water. This system allows for a higher degree of coupling between the primary and secondary trophic levels, resulting in a more efficient transfer of biomass between levels. Furthermore, because of the replenishment of nutrients from the deep layers due to mixing, a higher level of production of primary producers occurs. Finally, as phytoplankton biomass is consumed and retained due to tighter coupling with higher trophic levels in the euphotic zone, an increased level of dissolved organic nutrients is made available to fuel the microbial loop.

Thus variations in water column stratification driven by climatic forcing provide a mechanism via the modification of the light and nutrient regimes to modify the potential production of not only phytoplankton cells but also higher trophic levels.

The simulation of thermal stratification, the dominant mode in the central North Sea (e.g. Schrum and Backhaus, 1999) using 2 and 3-D modelling approaches (e.g. Schrum *et al.*, 2002; Nielsen and St. John, 2001) is well established with simulations and field measurements in close agreement.

However, it is difficult to validate the development and timing of simulated spring and fall phytoplankton blooms due to the lack of observational data. Field programmes, in general, will not be active in the area of interest during the bloom events. One source of data that can provide coverage of the study area during spring and fall blooms for a number of years is remotely sensed ocean colour. The application of remote sensors such as the Coastal Zone Colour Scanner (CZCS) and the Sea-viewing Wide Field-of-view Sensor (SeaWiFS) allow the synoptic estimation of chlorophyll and phytoplankton production (e.g Kuring *et al.*, 1990), thus enabling the validation of phytoplankton bloom dynamics simulations. A time-series of chlorophyll estimates for the study area can be constructed from the CZCS for the interval November 1978 to June 1986 and from SeaWiFS from September 1997 until 2001. Unfortunately, estimates from CZCS and SeaWiFS could not be merged into a single time-series due to a difference in sensors with different wavelengths and spectral resolutions. While, as will be discussed, ocean colour-based chlorophyll estimates for the North Sea region can be subject to considerable error, insight into the timing, time evolution, and relative intensities of spring and fall blooms can be obtained from the time-series.

Hence, in light of the importance of variations in the dynamics of the phytoplankton blooms, and their variability in transfer efficiency to higher trophic levels for the North Sea ecosystem, the goal of this article is to validate simulation techniques. This will enable the development of time-series to address the implications of fluctuations in climatic forcing on ecosystem dynamics.

Materials and methods

Simulations

The coupled 2-D biophysical model is based on a model for thermal stratification presented by Nielsen and St. John (2001). This model is a potential energy model, based on the energy equation for turbulence (Bo Pedersen, 1986). The energy equation relates the temporal and spatial changes of turbulent kinetic energy (TKE), the production of TKE, and the dissipation of TKE to the change in potential energy as water masses of different densities are mixed in the field of gravity (Turner, 1973; Bo Pedersen, 1986). This approach treats transport across density gradients as entrainment, i.e. a turbulent exchange of eddies which leads to a net transport of, for example, volume, heat, salt, and nutrients. A constant ratio between the input of mixing energy and the gain in potential energy is assumed, known as the flux Richardson number:

$$Ri_f = \frac{E_{pot}}{P_{tke}}$$

In the case of input of heat, Q, to the sea surface the gain in potential energy, E_{pot}, can be calculated as

$$E_{pot} = \tfrac{1}{2} \cdot g \cdot y \cdot \frac{\alpha \cdot Q}{c_p}$$

where y is the upper layer depth and α is the coefficient of thermal expansion. c_p, the specific heat of seawater, can be assumed to be constant in the present case. In the case of entrainment from below, the change in potential can be found as

$$E_{pot} = \tfrac{1}{2} \cdot g \cdot y \cdot \Delta\rho \cdot V_E$$

in which Dr is the dimensionless density difference between the water masses, ρ is the density of seawater, and V_E is the entrainment velocity. The production of turbulent kinetic energy in shear flows is calculated as the vertically integrated product of the shear stress and the vertical velocity gradient. For

wind and tidally driven flows, respectively, P_{tke}, can be expressed as

$$P_{tke} = {}^{f_w}\!/_2 \cdot \rho \cdot (\rho_a/\rho)^{3/2} \cdot W^3, \text{ and}$$

$$P_{tke} = {}^{f_t}\!/_2 \cdot \rho \cdot u_t^3$$

In these equations, f/2, is the friction factor, ρ_a is the density of air, W is the windspeed, and u_t is the tidal velocity. The product of the flux Richardson number and the friction factor are as presented in Nielsen and St. John (2001):

$$Ri_f \cdot {}^{f_w}\!/_2 = 2.3 \cdot 10^{-5} \quad \text{for wind mixing and}$$

$$Ri_f \cdot {}^{f_t}\!/_2 = 1.5 \cdot 10^{-5} \quad \text{for tidal mixing.}$$

The heat input to the surface is calculated as (James, 1977; Simpson and Bowers, 1984)

$$Q = Q_s + k \cdot (T_d - T_s)$$

in which Q_s is incoming atmospheric radiation (taken as a sine function; Simpson and Bowers, 1981), T_d is the dew point temperature, and T_s is the sea surface temperature. k is a positive function of the windspeed and the sea surface temperature as utilized by Simpson and Bowers (1984). The boundary data for running the model are observations of meteorological parameters (windspeed and dew point temperature) obtained by the Norwegian Meteorological Institute at the Ekofisk oil platform located near the study area (Fig. 1A) with an example of the boundary given in Figure 1B.

The biochemical model is as presented by Sharples and Tett (1994) and is based on one nutrient, dissolved inorganic nitrogen (DIN), being the limiting nutrient in the North Sea, and one phytoplankton with the characteristics of diatoms. The equation for the phytoplankton biomass X reads

$$\frac{\partial X}{\partial t} = \mu X - gX$$

in which mX is the growth rate (maximum of 1.2 d^{-1}) and g is the grazing impact rate equal to 0.12 d^{-1}. The phytoplankton growth rate is determined by light or nutrient limitation; see Sharples and Tett (1994). The equations for algal nitrogen *N* and DIN are

$$\frac{\partial N}{\partial t} = uX - gN$$

$$\frac{\partial S}{\partial t} = -uX - egN$$

in which the uptake rate of DIN, *u*, is determined by Michaelis-Menten kinetics. e, the recycled portion of grazed nutrients, amounts to 0.5. Input of nutrient at the bottom boundary is assumed linearly proportional to the difference between DIN concentration at the bottom and maximum near bed concentration of DIN equal to 6.0 mmol m^{-3}. The biological model is driven by the availability of light and nutrient as calculated from the stratification model and is initialized each year in January/February using observations of temperature and nutrient obtained from the ICES Hydrographic Database. The choice of parameters for the biochemical model follows Sharples and Tett (1994), except for the maximum near bed concentration of DIN as available from ICES. The coupled stratification and biochemical model is run for the years 1981 to 1986 and 1997 to 2000 to cover periods with remote sensing data.

Remote sensing

Daily mean time-series for surface chlorophyll concentrations in the area 0–4°E and 56–57°N were constructed from CZCS and SeaWiFS archived data sets. The CZCS daily chlorophyll Level 3 product (Williams *et al.*, 1986 and http://daac.gsfc.nasa.gov/DATASET_DOCS/CZCS_L3_dataset.html), obtained from the NASA/Goddard Distributed Active Archive Center (DAAC) was used to construct a daily time-series for the interval November, 1981 to June, 1986. The Level 3 data are binned to a fixed, linear latitude (equal angle) grid with an approximate 18.5 km resolution at the equator. The daily, binned Level 3 chlorophyll values were averaged over the study area to produce a single time-series. Aarup *et al.* (1989, 1990) have demonstrated the utility of CZCS data for the North Sea region. However, it should be noted that in Case 2 waters (shelf seas and coastal waters) coloured dissolved organic materials (yellow substances) can seriously corrupt chlorophyll estimates. By selecting a study area in the central North Sea, we have attempted to minimize these errors by placing the region as far as possible from the high concentrations of yellow substances known to be found in zones of freshwater river influence (Højerslev *et al.*, 1996; Aarup *et al.*, 1996a, b). Estimates of chlorophyll in coastal waters will also have errors due to the presence of suspended particulate matter. Using a study area in the central North Sea is expected to minimize these errors as well. In general, the errors in chlorophyll estimation are approximately 35% in Case 1 (open ocean) waters and within a factor of 2 (200%) in Case 2 waters (Evans and Gordon, 1994).

SeaWiFS daily Level 3 chlorophyll a datasets (Acker *et al.*, 1998; http://daac.gsfc.nasa.gov/DATASET_DOCS/SeaWiFS_L3_Guide.html) were obtained through the SeaWiFS Project at the NASA/Goddard DAAC. The Level 3 daily data are binned to a 9×9 km resolution global grid. The

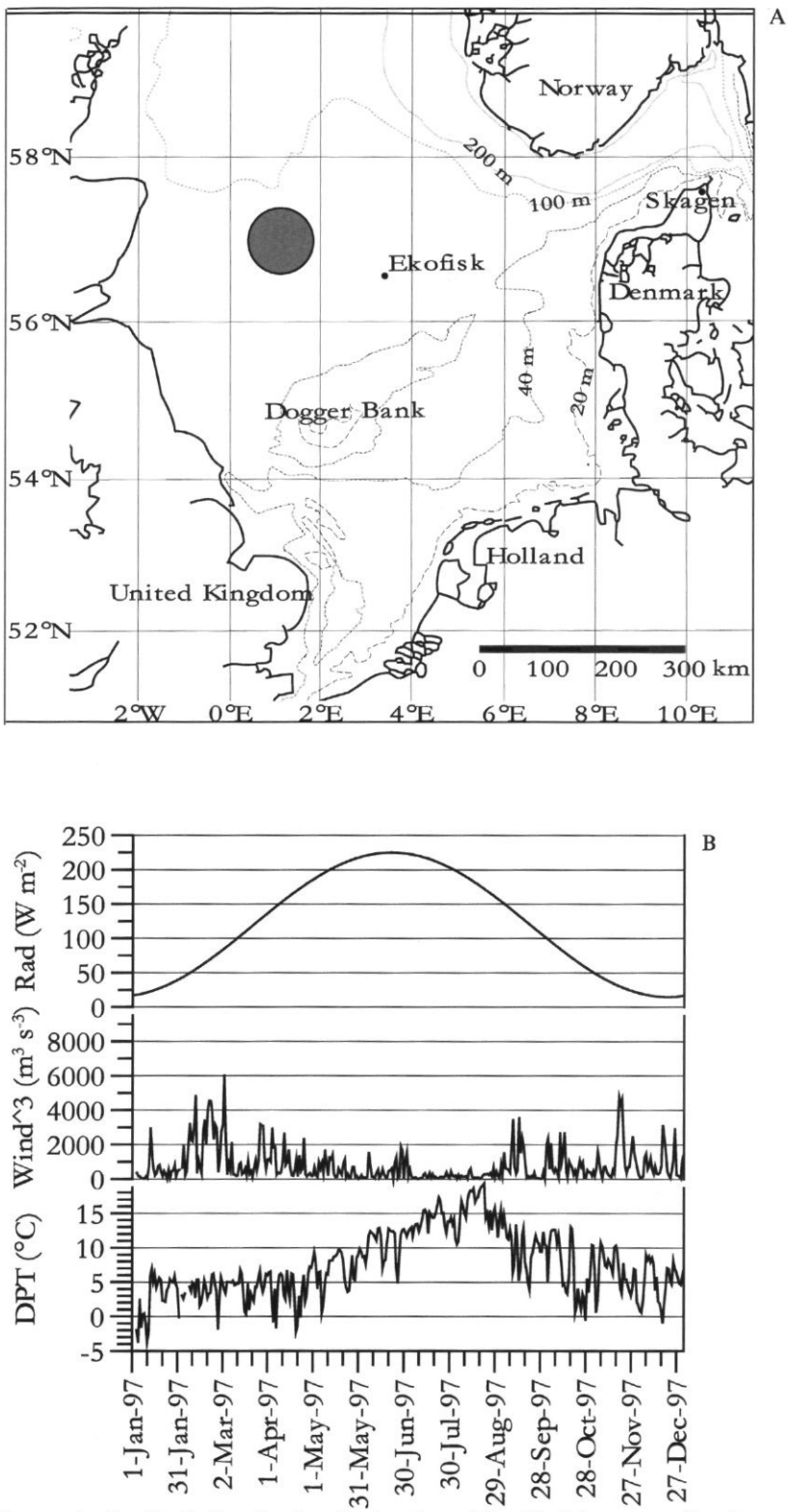


Figure 1. A. Study area in the North Sea showing the location of the Ekofisk source of environmental forcing data. B. An example of forcing data for the 2-D model from 1997. Top: radiation. Middle: windspeed cubed. Bottom: dew point temperature. All values are daily mean of hourly measurements.

values in the study area were averaged to produce a single, daily time-series from September, 1997 to June 2001. Chlorophyll estimates from SeaWiFS are subject to the same sorts of errors as described for CZCS, but the SeaWiFS errors should be lower due to a better signal to noise ratio, better atmospheric correction, high spectral resolution in the visible range (6 bands instead of 4) and narrower spectral band widths on SeaWiFS than CZCS.

As part of the Level 3 data sets for CZCS and SeaWiFS, binning statistics for the daily mean values are supplied. These statistics include the number of 4.5 km resolution Global Area Coverage (GAC) pixels that went into producing the means on each 18.5 km and 9 km cell for CZCS and SeaWiFS, respectively. Only days in which the total number of cloud-free sampled GAC pixels over the whole study area was at least 20 were included in the time-series.

In order to compare the timing of bloom events in the modelled and observed data, cross-correlations were computed between the two series. The usual methods of computing the cross-correlation versus time-lag could not be used because of gaps in the observed time-series. Instead, the modelled time-series was used as a reference series that was shifted by −30 to +30 day lags and cross-correlations were computed for each lag using only days for which observed values exist. The model lag relative to the observed series was taken to be that lag at which the cross-correlation between the two series was the maximum positive value. The spring and fall periods were analysed separately, since it was anticipated that the development of the blooms would differ between the two seasons.

Results

Examples of time-series obtained from the 2-D model simulations are presented in Fig. 2A (CZCS) and Fig. 2B and C (SeaWiFS). Both the model and remote sensing demonstrate the classic occurrence of the spring and fall blooms in the central North Sea. The model and remote sensed estimates of the timing of the spring bloom are similar, with the model predicting the timing of the blooms to be 6.1 (± 8.3) days earlier than observed (see Table 1). In general, mean estimates of chlorophyll *a* (minimum 20 pixels) from the CZCS and SeaWiFS series possess much lower amplitude peaks than the modelled series (Table 1). This is, in part, due to the patchiness of phytoplankton distributions in the study area. As can be seen from Figure 3 (spring bloom SeaWiFS, 1999) the horizontal structure of the bloom is fairly patchy. Pixels are either in a high-productivity patch with concentrations greater than 10 mg m^{-3}, or they are not in a bloom and possess values near zero. Hence, mean values are heavily

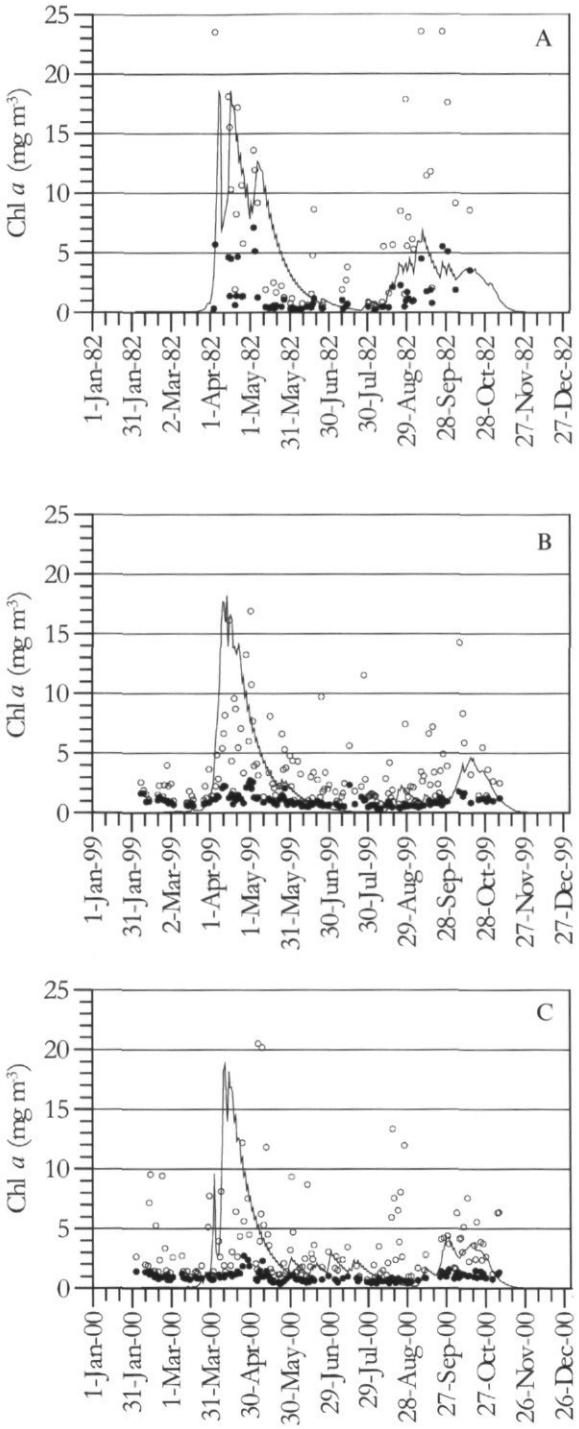


Figure 2. Modelled daily upper layer chlorophyll *a* concentration m^{-3} (line) versus daily mean composite chlorophyll *a* (filled circles) and the peak value found in the grid (empty circles) observed in the modelled area (A) modelled vs. CZCS estimates of chlorophyll *a* for 1982; (B) modelled vs. SeaWiFS estimates of chlorophyll *a* for 1999; (C) modelled vs. SeaWiFS estimates of chlorophyll *a* for 2000.

Table 1. Comparisons of modelled vs. remote-sensed estimates of timing (commencement and duration (DUR)) and intensity (Chl *a* mg m^{-3}) of the spring and fall blooms. Shaded values are comparisons of CZCS vs. modelled estimates, while non-shaded comparisons are those of obtained from comparison with SeaWiFS.

Year	DayModel Spring bloom	DayRS Spring bloom	Dur.Model Spring (days)	Dur.RS Spring (days)	Max. cross-corr. Spring	Model Lag (days) spring	Model peak	RS peak	Ratio
1981	14/4 (102)	19/4 (109)	61	26	0.670	−7	19.028	4.299	4.43
1982	15/4 (105)	2/5 (122)	85	49	0.683	+7	18.652	7.143	2.61
1986	29/4 (119)	14/5 (134)	79	28	0.431	−8	20.296	9.374	2.17
1998	17/4 (107)	3/5 (123)	82	34	0.722	−17	18.853	3.352	5.62
1999	13/4 (103)	30/4 (120)	88	81	0.628	−1	18.203	2.749	6.62
2000	10/4 (101)	24/4 (115)	66	40	0.594	−11	18.797	2.741	6.86

Year	DayModel Fall bloom	DayRS Fall bloom	Dur.Model Fall(days)	Dur.RS Fall(days)	Max. cross-corr.Fall	Model lag (days) Fall	Model peak	RS peak	Ratio
1982	9/9 (252)	24/9 (267)	76	72	0.801	−15	6.915	5.546	1.24
1997	19/9 (262)	8/10 (281)	70	—	0.636	+10	6.142	1.786	3.44
1998	29/8 (241)	27/10 (300)	44	14	0.376	−13	3.626	1.662	2.18
1999	16/10 (289)	7/10 (280)	55	18	0.482	−30	4.665	1.793	2.60
2000	28/9 (272)	28/9 (272)	68	60	0.723	+1	4.273	1.592	2.68

impacted by the patchiness of bloom. The importance of spring bloom patchiness is clearly demonstrated when examining the maximum values (open symbols Fig. 2A–C). In all years examined, the maximum values estimated by remote sensing and the model are in close agreement for the spring bloom, a feature not clearly seen in the mean values. Comparisons between modelled and remote sensed estimates of the timing and intensity of the fall bloom are in general not in as close agreement as those of the spring bloom. Here, the model was observed to predict the occurrence of the bloom 9.4 (±15.4) before observation in satellite images. Again fall blooms were patchy in distribution (e.g. Figure 4) with the mean abundance being lower than that predicted by the model in all but 1982, when estimates in biomass were relatively similar.

Discussion

Both the CZCS and SeaWiFS time-series used in this study suffer from under-sampling problems. It is well known (e.g. Fasham, 1978a, b; Platt, 1978; Denman and Gargett, 1995) that phytoplankton distributions are patchy during bloom events; taking a mean value for chlorophyll from satellite imagery during such periods is therefore problematic. The histogram of concentrations is bi-modal; the values are either near a maximum value of (~25 mg m^{-3}), if the samples are from patches that are biologically productive, or are near zero, if the samples are from locations that are not in a local bloom. This problem, compounded by the fact that the study area is fully or partially cloud-covered much of the time, is particularly severe during the fall bloom period. If the cloud-free pixels do not match any of the local, high-concentration patches, the bloom could be missed completely. It should also be noted that the remotely sensed chlorophyll values are near surface, integrated over depths of 1 to 5 m in the North Sea. These depths are significantly less than typical upper layer thicknesses (15–50 m) produced by the model during bloom events.

The 2-D modelling approach chosen here, because of its highly resolved vertical resolution, allows a realistic estimation of the vertical flux of nutrients. However, the model requires additional terms analogous to estimation of spatially variable turbulent fluxes if it is to produce a spatially averaged estimate of such a regime. This approach would give an estimation similar to that produced by a large number of local "patch" models. This approach is much more appropriate than the results from a single model producing values that are assumed to be representative of the whole region (as is done in this study). A preferable approach when existing boundary data are available is to conduct high-resolution three-dimensional ecosystem modelling of the region that would resolve the larger patches (those detectable from remote sensing) and perform time-space statistical analysis on the modelled and remotely-sensed fields.

The coupled 2-D phytoplankton production model employed in this study has previously been validated with regard to its ability to resolve the physical water column characteristics in the central North Sea (Nielsen and St. John, 2001). Coupling this with a well-accepted phytoplankton Nutrient-Phytoplankton model (Sharples and Tett, 1994) allows examination of the timing and intensity of, in particular, the spring bloom. The coupled model employed utilizes the physiological characteristics of diatom cells as the phytoplanker modelled, making it appropriate for characterizing the spring bloom dominated by this algal group. Later in the year,

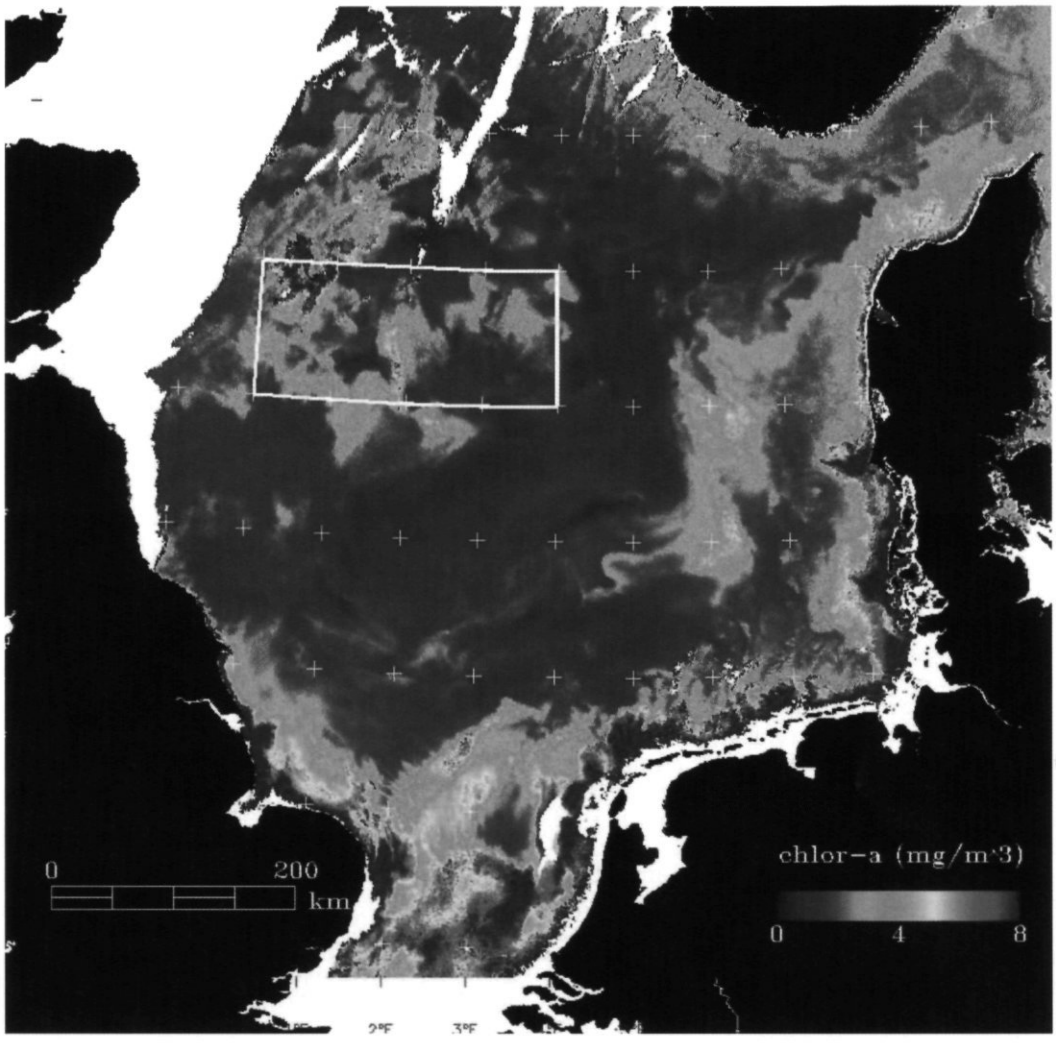


Figure 3. High resolution SeaWiFS chlorophyll *a* image showing typical spring bloom conditions and the modelled region (rectangle) from 27 April 1999 at 1214 UTC. Image provided by the SeaWiFS Project, NASA/Goddard Space Flight Center and ORBIMAGE.

other algal groups dominate production having different physiological and behavioural characteristics making validation via remote sensing difficult. For example, during the highly stratified summer period, a high degree of phytoplankton production, ca. 40% as a conservative estimate (Richardson *et al.*, 2000), occurs in an area invisible to remote sensors. It is thus likely that the remotely sensed chlorophyll values will underestimate the upper-layer mean values at this time.

In summary, the model validation performed here using for validation data CZCS and SeaWiFS imagery has verified the applicability of this coupled 2-D model for examining in particular the temporal dynamics and intensity of the spring phytoplankton bloom in the Central North Sea. Hence, our results justify the utilization of this modelling approach for the development of time-series of spring bloom dynamics. Future activities with this modelling tool will include comparison of simulated annual spring bloom dynamics with variations of higher trophic levels.

Acknowledgements

We thank our colleagues in LIFECO for valuable discussions – in particular Drs. Andy Visser and Corrina Schrum as well as the Norwegian Meteorological Institute for providing meteorological observations from the Ekofisk oil platform and ICES for providing oceanographic observations from its Hydrographic Database. SeaWiFS data were provided by the SeaWiFS Project, NASA/Goddard

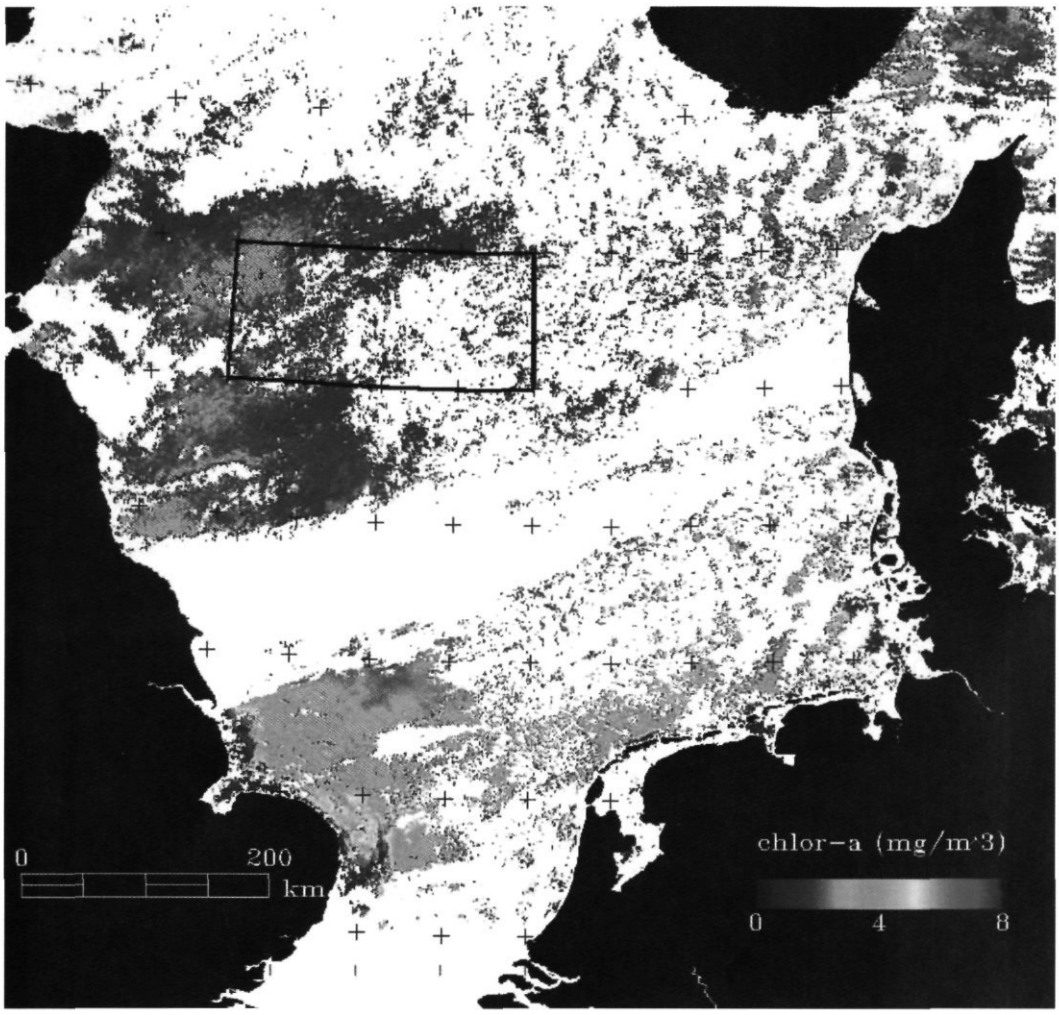


Figure 4. High resolution SeaWiFS chlorophyll *a* image showing typical fall bloom conditions and the modelled region (rectangle) from 11 October 1999 at 1225 UTC. Image provided by the SeaWiFS Project, NASA/Goddard Space Flight Center and ORBIMAGE.

Space Flight Center and ORBIMAGE and were accessed through the NASA/Goddard DAAC. CZCS data were supplied by the NASA/Goddard Space Flight Center DAAC. The study was carried out as a part of the EU-funded LIFECO Project.

References

Aarup, T., Groom, S., and Holligan, P. M. 1989. CZCS imagery of the North Sea. Remote Sensing of Atmospheres and Oceans, Advances in Space Research, 9: 443–451.

Aarup, T., Groom, S., and Holligan, P. M. 1990. The processing and interpretation of North Sea CZCS imagery. Netherlands Journal of Sea Research, 25: 3–9.

Aarup, T., Holt, N., and Højerslev, N. K. 1996a. Optical measurements in the North Sea–Baltic Sea transition zone. II. Water mass classification along the Jutland west coast from salinity and spectral irradiance measurements. Continental Shelf Research, 16: 1343–1353.

Aarup, T., Holt, N., and Højerslev, N. K. 1996b. Optical measurements in the North Sea–Baltic Sea transition zone. III. Statistical analysis of bio-optical data from the Eastern North Sea, the Skagerrak and the Kattegat. Continental Shelf Research, 16: 1355–1377.

Acker, J., Leptoukh, G., Shen, S., Wang, Y., Winterfield, D., and Simmon, R. 1998. Goddard DAAC data services for SeaWiFS ocean color data. In: Proceedings of the Fifth International Conference Remote Sensing for Marine and Coastal Environments, vol. 2, II: 325–332. ERIM International Inc., Ann Arbor, MI, USA.

Bo Pedersen, Fl. 1986. Environmental Hydraulics: Stratified Flows. Springer-Verlag, Berlin.

Denman, K. L., and Gargett, A. E. 1995. Biological and physical interactions in the upper ocean: the role of vertical and small-scale transport processes. Annual Review of Fluid Mechanics, 27: 225–255.

Evans, R. H., and Gordon, H. R. 1994. Coastal zone color scanner "system calibration": a retrospective examination. Journal of Geophysical Research, 99: 7293–7307.

Fasham, M. J. R. 1978a. The application of some stochastic processes to the study of phytoplankton patchiness. *In* Spatial Pattern in Plankton Communities, pp. 132–156. Ed. by J. H. Steele. Plenum Press, New York.

Fasham, M. J. R. 1978b. The statistical and mathematical analysis of plankton patchiness. Oceanography and Marine Biology, 16: 43–79.

Højerslev, N. K., Holt, N., and Aarup T. 1996. Optical measurements in the North Sea–Baltic Sea transition zone. I. On the origin of the deep water in the Kattegat. Continental Shelf Research, 16: 1329–1342.

James, I. D. 1977. A model of the annual cycle of temperature in a frontal region of the Celtic Sea. Estuarine and Coastal Marine Science, vol. 5, pp. 339–353.

Josefson, A. B., and Conley, D. J. 1997. Benthic response to a pelagic front. Marine Ecology Progress Series, 147: 49–62

Kiørboe, T. 1991. Pelagic fisheries and spatio-temporal variability in zooplankton productivity. Proceedings of the Fourth International Conference on Copepoda; Bulletin of the Plankton Society of Japan, special volume, pp. 229–249.

Kuring, N., Lewis, M. R., Platt, T., and O'Reilly, J. E. 1990. Satellite-derived estimates of primary production on the northwest Atlantic continental shelf. Continental Shelf Research, 10: 461–484.

Nielsen, M. H., and St. John, M. 2001. Modelling thermal stratification in the North Sea: application of a 2-D potential energy model. Estuarine, Coastal and Shelf Science. (In press).

Platt, T. 1978. Spectral analysis of spatial structure in phytoplankton populations. *In* Spatial Pattern in Plankton Communities, pp. 73–84. Ed. by J. H. Steele. Plenum Press, New York.

Richardson, K., Visser, A. W., and Bo Pedersen, F. 2000. Subsurface phytoplankton blooms fuel pelagic production in the North Sea. Journal of Plankton Research, 22: 1663–1671.

Schrum, C., and Backhaus, J. O. 1999. Sensitivity of atmosphere-ocean heat exchange and heat content in North Sea and Baltic Sea. A comparative assessment. Tellus, 51A, 526–549.

Sharples , J., and Tett, P. 1994. Modelling the effect of physical variability on the midwater chlorophyll maximum. Journal of Marine Research, 52: 219–238.

Simpson, J. H., and Bowers, D. 1981. Models of stratification and frontal movement in shelf seas. Deep-Sea Research, 28A: 7,727–7,738.

Simpson, J. H., and Bowers, D. 1984. The role of tidal stirring in controlling the seasonal heat cycle in shelf seas. Annales Geophysicae, 2: 411–416.

St. John, M. A., Clemmesen, C., Lund, T., and Köster, F. W. 2001. Diatom production in the marine environment: implications for larval fish growth and condition. ICES Journal of Marine Science, 58: 1106–1113.

Thompson, P. A., and Harrison, P. J. 1992. Effects of monospecific algal diets of varying biochemical composition on the growth and survival of Pacific oyster (*Crassostrea gigas*) larvae. Marine Biology, 113: 645–654.

Turner, J. S. 1973 Buoyancy Effects in Fluids. Cambridge University Press, London.

Waite, A., Bienfang, P. K., and Harrison, P. J. 1992. Spring bloom sedimentation in a subarctic ecosystem. I. Nutrient sensitivity. Marine Biology, 114: 119–129.

Williams, S. P., Szajna, E. F., and Hovis, W. A. 1986. Nimbus 7 Coastal Zone Color Scanner (CZCS) Level 1 Data Product Users' Guide, NASA TM 86203, Goddard Space Flight Center, Greenbelt, MD 20771. 53 pp.

ICES Marine Science Symposia, 219: 199–207. 2003

Has the eutrophic state of German Wadden Sea waters changed over the past 10 years due to nutrient reduction?

Norbert Ladwig, Karl-Jürgen Hesse, Franciscus Colijn, and Urban Tillmann

Ladwig, N., Hesse, K.-J., Colijn, F., and Tillmann, U. 2003. Has the eutrophic state of German Wadden Sea waters changed over the past 10 years due to nutrient reduction? – ICES Marine Science Symposia, 219: 199–207.

For a period of more than 10 years, two basic eutrophication indicators, dissolved inorganic macronutrients and chlorophyll *a*, have been measured along with physical parameters at a permanent coastal station in the northern German Wadden Sea near Büsum. despite distinctly reduced phosphorus inputs, the data have not revealed any long-term trend in nutrient winter concentrations or algal biomass compared to other available time-series in the area of investigation, i.e. River Elbe nutrient loads and nutrient concentrations in the German Bight near Helgoland. Instead, there are indices of slightly higher winter phosphate concentrations in recent years as well as a decrease in maximum annual N:P ratios due to elevated residual phosphate concentrations in spring. This is in contrast to the situation in the adjacent German Bight, where a declining trend in dissolved inorganic phosphate concentrations is observed. It is suggested that persistent high phosphate concentrations in the northern German Wadden Sea result from local sources of phosphate such as remobilization from the sediments, as well as remineralization of imported organic matter. The comparison with a comprehensive assessment of seasonal light and nutrient availability in the water column indicates that on an annual basis, phytoplankton biomass development in the northern German Wadden Sea is still insensitive to current nutrient reduction measures because of the predominant role of light limitation in this turbid environment.

Keywords: Elbe, eutrophication, German Bight, nutrients, phytoplankton, Wadden Sea.

N. Ladwig, K.-J. Hesse, and F. Colijn: Research and Technology Centre Westcoast, University of Kiel, Hafentörn, D-25761 Büsum, Germany [tel: +49 4834 604 202; fax: +49 4834 604 299; e-mail: office@ftz-west.uni-kiel.de]. U. Tillmann: Alfred Wegener Institute for Polar and Marine Research, Am Handelshafen 12, D-27570 Bremerhaven, Germany [tel. +49 471 4831 1470; e-mail: utillmann@awi-bremerhaven.de]. Correspondence to N. Ladwig.

Introduction

The northern German Wadden Sea forms a broad and shallow interface between the waters of the German Bight and its surrounding mainlands. The area is subjected to a direct nutrient enrichment deriving mainly from the River Elbe and, to a lesser extent, from the River Weser. Annual nutrient discharge of the Elbe is in the range 136 200 t N (total nitrogen) and 5200 t P (total phosphorus), whereas the Weser accounts for 64 600 t N and 2400 t P, respectively (average for 1994–1998) (Lenhart and Pätsch, 2001). In addition, the adjacent coastal waters of the German Bight receive a considerable amount of nitrogen and phosphorus from indirect inputs from more remote sites. For example, advective transport of continental coastal water imports nutrients from the River Rhine which may be transported into the Wadden Sea through tidal mixing. During the growth season a large fraction of nutrients enters the Wadden Sea in the form of organic particles. These inputs are difficult to quantify on an annual basis because of their inaccessibility during field assessments. Rough estimates of the particulate import based on seasonal field data and numerical simulations are in the range 240 g C m^{-2} yr^{-1} for the Western Dutch Wadden Sea (De Jonge and Postma, 1974) and 100 g C m^{-2} yr^{-1} in the North Frisian area (Dick *et al.*, 1999). In addition to these water-bound inputs, about 7600 t N is estimated to enter the Wadden Sea by direct atmospheric deposition (De Jong *et al.*, 1993).

Calculated on the basis of data from 1994, approximately 70% of the nitrogen and 55% of the phosphorus pool in the northern German Wadden Sea during winter result from anthropogenic sources (Hesse *et al.*, 1995). The high anthropogenic nutrient supply to the Wadden Sea is assumed to be responsible for direct and indirect eutrophication effects, such as the proliferation of benthic macroalgal mats (Siebert and Reise, 1997), increases in phytoplankton production (Cadée, 1986; Asmus *et al.*, 1998) and phytoplankton biomass (Schaub and Gieskes, 1991; Riegman, 1995; De Jonge *et al.*, 1996; Philippart *et al.*, 2000), and shifts in benthic communities (van Beusekom *et al.*, 2001). Because of nuisance effects of anthropogenic nutrient enrichment in the coastal zone, the continental countries bordering the North Sea agreed to reduce the anthropogenic nutrient loads in rivers by 50% in the period 1985–1995. The level was agreed upon at the "Second International North Sea Conference" in 1987. With respect to the Elbe, a 55% reduction of phosphorus loads has been achieved, but only about a 17% reduction in nitrogen loads in the period 1985–1996 (De Jong *et al.*, 1999).

Several long-term monitoring studies have been carried out in the River Elbe (e.g. Gaumert, 1991; ARGE Elbe, 2001), the East-Frisian Wadden Sea (e.g. Hanslik *et al.*, 1998; De Jong *et al.*, 1999; Rahmel *et al.*, 1999), and the open German Bight (e.g. Hagmeier, 1978; Radach and Berg, 1986; Weichart, 1986; Gillbricht, 1988, 1994; Radach and Bohle-Carbonell, 1990; Körner and Weichart, 1991; Hickel *et al.*, 1992, 1993, 1994; Hickel, 1998; Gaul, 2000). These studies give some insight into changes in the trophic state of the systems during recent decades. In order to investigate the long-term variability of plankton and nutrients in the more estuarine part of the northern German Wadden Sea, the Research and Technology Centre Westcoast (FTZ) of Kiel University started a monitoring programme in 1991. This initiative coincided with the period when intensive political programmes for nutrient reduction in the main freshwater sources of the area were implemented as a consequence of the massive *Chrysochromulina* bloom in summer 1988.

To evaluate the effects of nutrient reduction efforts in the northern German Wadden Sea, we examined the evolution of two basic eutrophication-related indicators, dissolved inorganic nutrients (nitrogen, phosphorus) and chlorophyll *a* (as a proxy for phytoplankton biomass) at the permanent station of Büsum Mole during the past decade (1991–2000). The dynamics of these indicators are then considered with respect to cause–effect relationships and interpreted taking into consideration some other information available for the area, especially information concerning the role of light limitation for phytoplankton growth and internal nutrient sources.

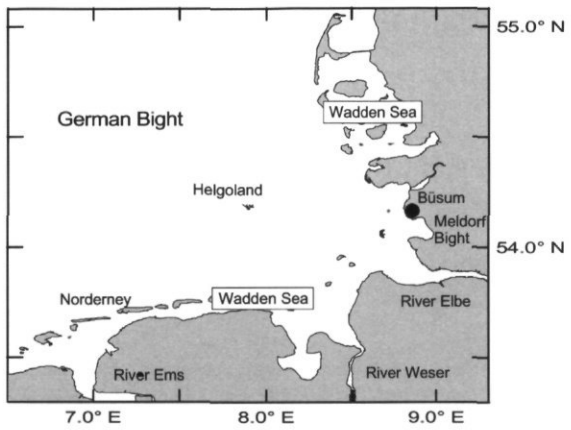


Figure 1. Map of the German Bight showing the area of investigation with the position of the permanent station Büsum Mole (large dot).

Material and methods

In the period 1991–2000, surface samples were taken weekly at the eastern mole of Büsum port (Figure 1) during the growth season (April–September) or fortnightly in winter (October–March). Sampling was implemented at high tide in order to reduce tidal influences. Water depth at this station is ca. 10 m at high tide. Subsamples for inorganic dissolved nutrient determination (DIN = nitrate + nitrite + ammonia, DIP = phosphate) were filtered through glass microfibre filters (GF/C, Whatman) and immediately analysed in accordance with Grasshoff *et al.* (1983). For chlorophyll *a* analysis, 200–2200 ml of the sample was filtered through Whatman GF/C filters, which were stored deep frozen (–20°C) before undergoing spectrophotometric analysis according to Lorenzen (1967). Records of temperature and salinity were made with a WTW probe (LF 191, Wissenschaftlich-Technische Werkstätten) calibrated for salinity. Vertical profiles revealed that the water column is permanently well mixed owing to high tidal current speeds of up to 1.5 m s^{-1} (K. Rickleffs, pers. comm.). It is therefore assumed that the samples are representative of the entire water column.

The spatial distribution of nutrients as well as primary production data were evaluated within the framework of two integrated projects, TRANSWATT (Transport, Transfer and Transformation of Biomass Elements in Wadden Sea Waters) and KUSTOS (Near Coastal Fluxes of Energy and Matter in the German Bight). For further information, see Sündermann *et al.* (1998).

Several additional time-series were made available from other institutions for this analysis. From the long-term monitoring station in the Elbe at Hamburg (Seemannshöft) we obtained observations of total

phosphorus and dissolved phosphate, total nitrogen and dissolved inorganic nitrogen compounds from 1985 until 2000 (ARGE Elbe, Arbeisgemeinschaft für die Reinhaltung der Elbe, Hamburg). Furthermore, the AWI/BAH (Alfred-egener-Institut für Polar- und Meeresforschung/Biologische Anstalt Helgoland, Bremerhaven) provided nutrient data from the permanent station at Helgoland Roads for the period 1962–1996. Data of winter nutrient trends in the open German Bight were provided by the BSH (Federal Maritime and Hydrographic Agency, Hamburg).

Results

1. Nutrient concentrations

A quasi-synoptic picture of inorganic nitrogen distribution in winter (February 1994) illustrates the influence of the Elbe discharge on the nutrient distribution in the inner German Bight and the German Wadden Sea (Figure 2). Steep gradients occurred, with maximum concentrations of more than 300 µM DIN in the River Elbe and more than 50µM DIN offshore.

River Elbe

The long-term development of concentrations of phosphorus and nitrogen compounds (total-P, DIP, total-N, DIN) at the Elbe monitoring station Seemannshöft (Hamburg) clearly reveals a decrease since intense point-source reduction measures were put in place at the end of the 1980s (Figure 3). Both total-P and DIP data show that levels have been successfully reduced by approximately 60–70%. A reduction of about 50% can be observed for nitrogen (ARGE Elbe, 2001).

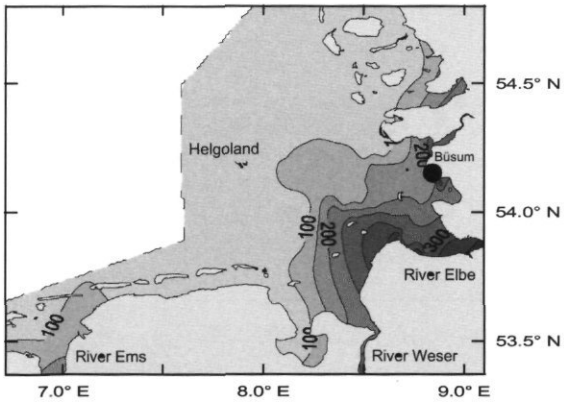


Figure 2. Surface winter concentrations of dissolved inorganic nitrogen (DIN) in the German Wadden Sea and the German Bight in 1994 (dashed line = seaward border of the area of investigation; data: TRANSWATT/KUSTOS).

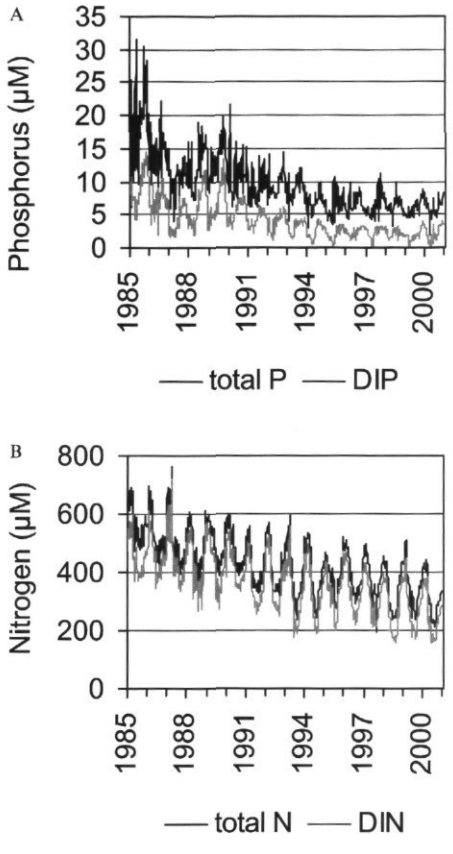


Figure 3A, B. Development of total phosphorus (total P), phosphate (DIP), and total nitrogen (total N), dissolved inorganic nitrogen (DIN) levels at the Elbe monitoring station Seemannshöft, Hamburg (data: ARGE Elbe).

German Bight

The salinity-normalized mean winter phosphate concentrations in the German Bight (Figure 4) decreased over the past decade to levels (< 0.6 µm P at 34 PSU) close to those observed by Kalle in 1935/36 (Kalle, 1937; Weichart, 1986; Körner and Weichart, 1991; Gaul, 2000). However, no similar decrease was observed for inorganic nitrogen. A comparison with historical reference values for nitrogen is hindered by the lack of reliable analytical methods in the 1930s as well as a lack of adequate monitoring activities before the 1970s.

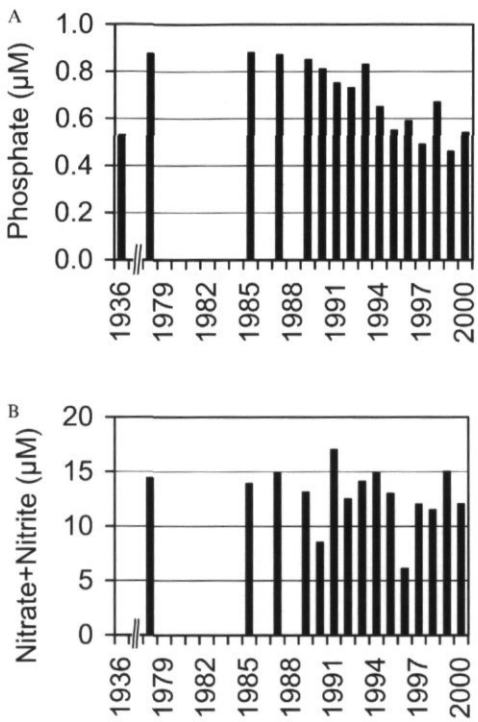


Figure 4A, B. Mean surface winter concentrations of dissolved inorganic phosphate and dissolved inorganic nitrogen compounds (sum of nitrate + nitrite) at salinity 34 in the German Bight (data: BSH).

Wadden Sea

The data set at the monitoring station of Büsum Mole does not allow for the establishment of a nutrient/salinity correlation for each of the different winter seasons, because sampling was restricted to a single point with a restricted sampling frequency.

However, in order to evaluate whether there is a similar trend in the northern Wadden Sea as that observed in the open German Bight and the Elbe water, the Wadden Sea data of winter nutrient concentrations (December–February) at Büsum Mole were split into two 5-year periods and plotted against salinity (Figure 5). Neither data set revealed any significant relationship between nutrient concentrations and salinity, and no temporal decline over a broad range of salinities was evident. Rather, the available winter phosphate concentrations had a significant tendency to be higher during the 1996–2001 period than the preceding 5-year period from 1991 to 1995 (t-test: $p = 0.008$). No statistically significant differences were found for DIN.

2. Nutrient ratios and chlorophyll *a* concentrations

In addition to absolute levels of nutrient concentrations, the molar N:P ratio can be used as an index for changed nutrient conditions. Chlorophyll *a*, as another basic eutrophication indicator, is analysed for the Büsum Mole time-series exclusively.

Wadden Sea

Annual cycles of the molar DIN:DIP ratio at Büsum Mole exhibit a clear seasonal pattern with pronounced maxima (> 200:1) in the aftermath of the phytoplankton spring bloom (March–May) and

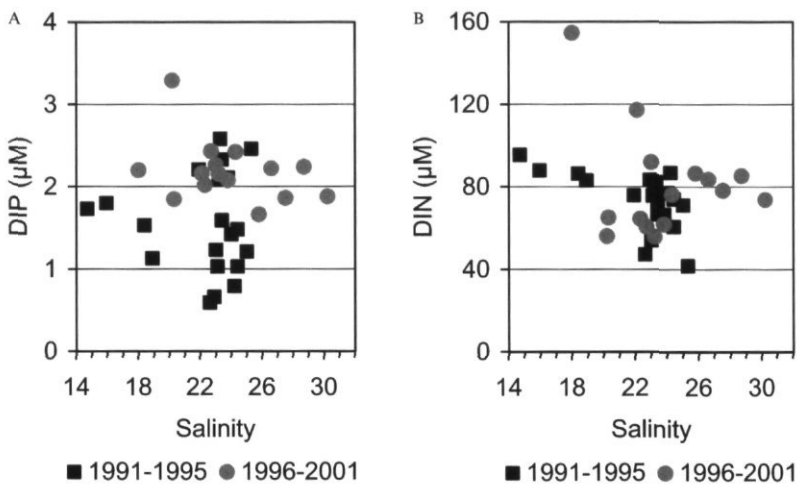


Figure 5 A, B. Winter concentrations of dissolved inorganic phosphorus and nitrogen at different salinities at the Büsum Mole station (northern German Wadden Sea).

minima (< 16:1) in summer (Figure 6A). During the annual cycle, phosphorus compounds are exhausted at first, followed by an annual minimum in nitrogen concentrations in summer which causes a reversal from high to low DIN:DIP ratios below 16:1. The temporal development at the permanent station of Büsum Mole reveals that there are recurrent low DIN:DIP maxima (< 100:1) in recent years (1998–2000).

The reason for the observed lower annual DIN:DIP maxima in the Wadden Sea near Büsum is an increase in the annual minima of phosphate concentrations during the last 3 years of the time-series (1998–2000), while the respective DIN concentrations remained more or less stable (Figure 7). These years were usually preceded by mild absolute winter temperatures.

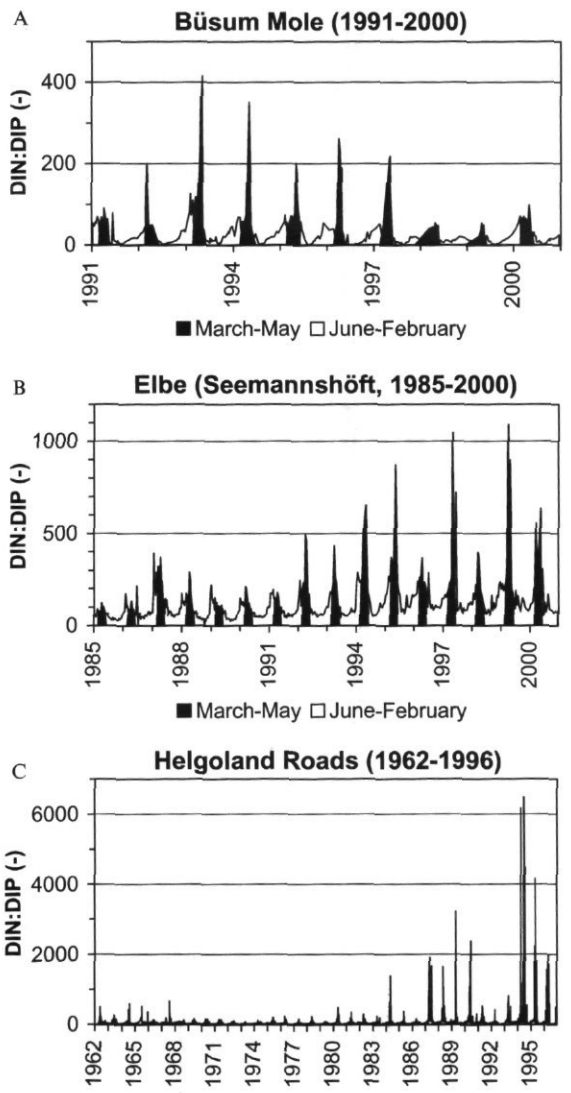


Figure 6A–C. Annual cycles of molar DIN:DIP ratios in the northern German Wadden Sea (Büsum Mole), River Elbe (Seemannshöft, Hamburg), and German Bight (Helgoland Roads). Periods of phytoplankton spring bloom (March–May) indicated in black in A and B; different scales and periods (data: ARGE Elbe, BAH/AWI).

River Elbe

In contrast to the Wadden Sea, the maximal ratios in the Elbe, which occur at the same time of year, show an inverse trend (Figure 6B). In the second half of the 1980s, annual DIN:DIP maxima in the Elbe were below 400:1. Since 1992 the DIN:DIP ratio has regularly exceeded 400:1, with a maximum in 1999 (> 1000:1). This development is assumed to be a result of the more pronounced phosphate reduction in the river compared to that of inorganic nitrogen.

German Bight

With respect to the long-term development of DIN:DIP ratios in the German Bight near Helgoland the annual maxima show a similar trend as in the River Elbe with extreme ratios of more than 6000:1 occurring in the past decade (e.g. 1994) (Figure 6C). These high values are caused by the pronounced phosphate exhaustion during the spring bloom and presumably also by the reduced phosphorus inputs from the Elbe.

2. Chlorophyll *a* concentration at Büsum Mole

A comparison with another indicator of eutrophication, chlorophyll *a*, revealed that no statistical relationship of chlorophyll *a* concentrations with

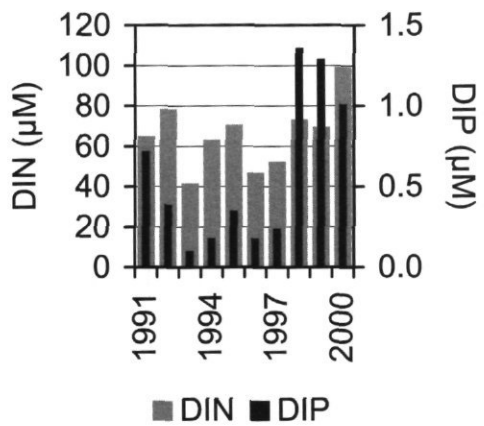


Figure 7. Concentrations of dissolved inorganic nitrogen and phosphorus at the Büsum Mole station during the annual N:P maximum after the phytoplankton spring bloom.

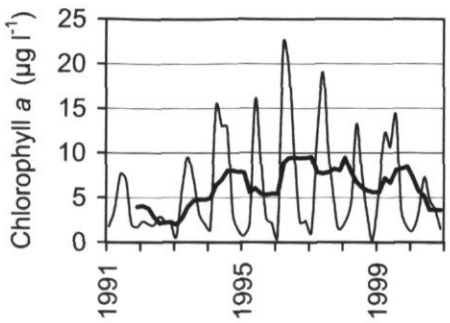


Figure 8. Bimonthly averaged chlorophyll *a* concentrations at Büsum Mole from 1991 to 2000 (bold line indicates a running mean of one year).

the nutrient conditions was found at the Wadden Sea station (Figure 8). There is a pronounced interannual variability both in the running means for each year and in the annual maxima of the bimonthly averaged chlorophyll *a* values lacking any significant trend. Despite the increase in residual phosphate concentrations after the spring bloom, a corresponding increase in chlorophyll *a* concentrations is lacking.

Discussion

The long-term observations made at the Büsum Mole station have not shown any decrease in winter nutrient concentrations over the past 10 years (1991–2000) (Figure 5), whereas the input from the River Elbe has been reduced considerably in the same period (Figure 3). This was unexpected for the area of investigation, which is clearly under the sphere of influence of the River Elbe and contrary to the trend observed in the East-Frisian Wadden Sea near Norderney, where a decrease in dissolved inorganic phosphorus and nitrogen concentrations was found (Rahmel *et al.*, 1999).This, together with the observation of elevated minimum (or residual) phosphate concentrations in the final 3 years of the decade (1998–2000), suggests an additional source for nutrients in the region (see section "Phosphorus release from the sediments" below), which counteracts the effects of successful reduction efforts in riverine nutrient inputs. Sedimentary release may be among the possible causes overriding the reduction in riverine phosphorus discharge.

Furthermore, phytoplankton development (measured as chlorophyll *a* concentration) does not exhibit any trend during the investigated period from 1991 to 2000 (Figure 8). The lack of a significant nutrient/phytoplankton relation in the Wadden Sea poses the question whether light limitation is more effective on phytoplankton primary production in the area of investigation than limitation by inorganic nutrients (see section "Light limitation of phytoplankton primary production" below).

1. Phosphorus release from the sediments

A common feature of the northern German Wadden Sea is an annual late summer maximum (August/September) of dissolved ortho-phosphate derived from P released from the sediments (e.g. Hesse *et al.*, 1992; Dick *et al.*, 1999) (Figure 9A). Contrary to this, the annual cycle of dissolved inorganic nitrogen (Figure 9B) rather follows the normal pattern for temperate zones with high winter concentrations and minima in summer. The excess phosphate remobilized from the Wadden Sea sediments stems from the decomposition of both autochthonous and allochthonous organic material (Postma, 1961; Hesse *et al.*, 1992; Dick *et al.*, 1999). Annual particulate organic matter imported from the adjacent German Bight into the northern Wadden Sea is estimated to be in the range 120 000 t POC yr^{-1} (Dick *et al.*, 1999). Part of the remineralized P is temporarily stored as insoluble iron-bound DIP in the sediments. Release is induced by a shift in the redox potential due to an increase in organic load and temperature during the growth season. The amount of excess DIP mixed out into the adjacent German Bight is in the range 1700 t DIP yr^{-1} (Dick *et al.*, 1999).

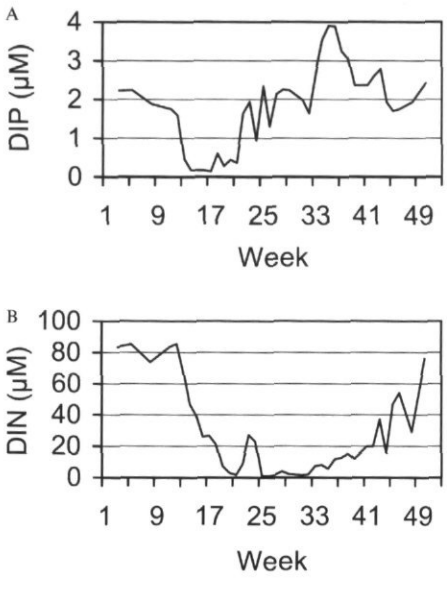


Figure 9A, B. Annual cycle (1996) of dissolved phosphate (DIP) and inorganic nitrogen (DIN) at the Büsum Mole station.

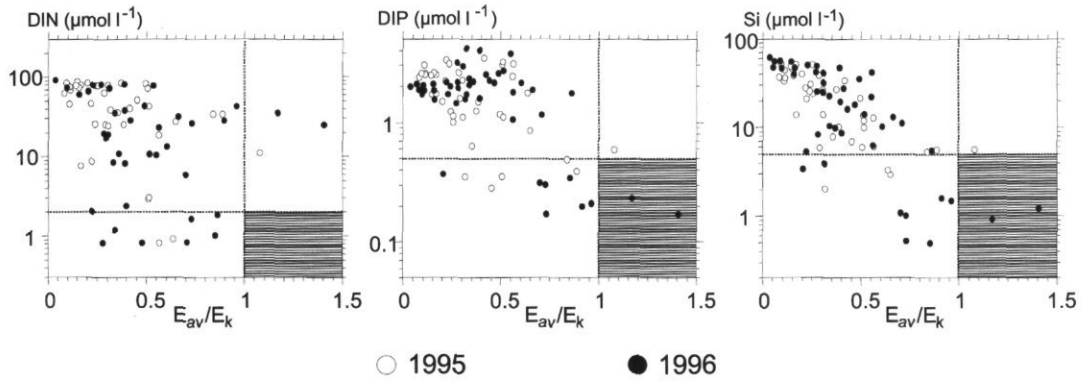


Figure 10. Ratio of the daily average light availability (E_{av}) and the measured light saturation onset parameter (E_k) with ambient nutrient conditions. The shaded area defines the region for which $E_{av}/E_k > 1$ (light saturation) and nutrient concentrations are below half-saturation constants for phytoplankton nutrient uptake as published in the literature (modified after Tillmann *et al.* (2000) with permission from the Journal of Plankton Research).

It is suggested that sedimentary phosphate remobilization may affect winter phosphate levels and also occurs in spring. Remineralization of the organic load in the Wadden Sea sediments may not be totally completed during winter. The amount of phosphate release from this process may be triggered by winter temperatures. In addition, the degree of sediment remobilization is related to stochastic wind-induced sedimentary shear stress during winter time. As already mentioned, the last 3 years were characterized by mild absolute winter temperatures which may have contributed to a higher phosphate remobilization from the sediment.

2. Light limitation of phytoplankton primary production

For two annual cycles (1995, 1996) the importance of light limitation versus inorganic nutrient control of phytoplankton growth in the Wadden Sea was assessed by Tillmann *et al.* (2000). In Figure 10, periods of ambient light limiting conditions in the mixed water column are compared with periods when nutrient concentrations dropped below published half-saturation constants for nutrient uptake. It turned out that light limitation prevailed at most sampling days and that nutrient limitation under light saturated conditions (shaded area in Figure 10) was likely to occur only for DIP and Si (silicate) on 2 days in April 1996 (Tillmann *et al.*, 2000). Comparable observations have been made by Cloern (1999) and Lohrenz *et al.* (1999) in several estuaries in the USA.

Conclusions

In contrast to the long-term decrease of inorganic nutrient inputs from the River Elbe and the decrease observed in the German Bight, a similar development could not be revealed for the northern German Wadden Sea near Büsum. As shown for winter nutrient concentrations, effects of reduction measures are not measurable at this site during the period 1991–2000. Phosphorus release from the sediments is assumed to counteract the reduction efforts in this part of the Wadden Sea. Mild winter temperatures in recent years may have caused the observed increase in phosphate concentrations in the period 1996–2001. Nutrients are still available in excess with respect to the requirements of phytoplankton growth in the area.

Phytoplankton development is rather controlled by limited light availability. Hence, the long-term development of phytoplankton biomass at Büsum Mole, as shown by means of the chlorophyll *a* concentration (Figure 8), does not show any change during the period 1991–2000. Similar observations have been made previously in the Dutch part of the western Wadden Sea (Marsdiep). Here, phytoplankton primary production remained high, although phosphate concentrations declined (Cadée and Hegeman, 1993).

It is concluded that efforts made towards nutrient reduction have not yet had a measurable impact on the trophic state in the primary steps of the food web in this part of the northern German Wadden Sea. However, nothing can be concluded with respect to changes in the absolute amounts of particulate organic matter entering the area from the adjacent German Bight, but it seems likely that these amounts are still high enough to exceed the sedimentary buffer capacity in the region.

Acknowledgements

Special thanks to Britta Egge, who prepared the Büsum Mole time-series data. We are indebted to

Michael Bergemann, Justus van Beusekom, Uwe Brockmann, Horst Gaul, and Wolfgang Hickel for providing valuable nutrient data sets. Thanks also to the anonymous referees for their comments on this article. Part of the study was supported by a grant from the German Ministry for Education and Research (grant no. 03F0130) and of the Federal Environmental Agency (grant no. 29825233).

References

Arbeitsgemeinschaft für die Reinhaltung der Elbe (ARGE Elbe). 2001. Wassergütedaten der Elbe. Zahlentafel 2000. Wassergütestelle Elbe, Hamburg. (In press.)

Asmus, R., Jensen, M. H., Murphy, D., and Doerffer, R. 1998. Primary production of microphytobenthos, phytoplankton and the annual yield of macrophytic biomass in the Sylt-Rømø Wadden Sea. *In* Ökosystem Wattenmeer, pp. 367–391. Ed. by C. Gätje and C. Reise. Springer-Verlag, Berlin.

Beusekom, J. E. E. van, Fock, H., De Jong, F., Diel-Christiansen, S., and Christiansen, B. 2001. Wadden Sea Specific Eutrophication Criteria. Common Wadden Sea Secretariat. Wilhelmshaven, Germany. 116 pp.

Cadée, G. C. 1986. Increased phytoplankton primary production in the Marsdiep area (western Dutch Wadden Sea). Netherlands Journal of Sea Research, 20: 285–290.

Cadée, G. C., and Hegeman, J. 1993. Persisting high levels of primary production at declining phosphate concentrations in the Dutch coastal area (Marsdiep). Netherlands Journal of Sea Research, 31: 147–152.

Cloern, J. E. 1999. The relative importance of light and nutrient limitation of phytoplankton growth: a simple index of coastal ecosystem sensitivity to nutrient enrichment. Aquatic Ecology, 33: 3–15.

De Jong, F., Bakker, J. F., Dankers, N., Dahl, K., Jäppelt, W., Madsen, P. B., and Koßmagk-Stephan, K. (Eds.). 1993. Quality Status Report of the North Sea, Subregion 10, The Wadden Sea. Wilhelmshaven: Common Wadden Sea Secretariat. 174 pp.

De Jong, F., Bakker, J. F., van Berkel, C. J. M., Dankers, N. M. J. A., Dahl, K., Gätje, C., Marencic, H., and Potel, P. (Eds.). 1999. Wadden Sea Quality Status Report. Wadden Sea Ecosystem No. 9. Common Wadden Sea Secretariat, Trilateral Monitoring Group. Wilhemlshaven, Germany. 259 pp.

De Jonge, V. N., and Postma, H. 1974. Phosphorus compounds in the Dutch Wadden Sea. Netherlands Journal of Sea Research, 8: 139–153.

De Jonge, V. N., Bakker, J. F., and van Stralen, M. 1996. Recent changes in the contributions of River Rhine and North Sea to the eutrophication of the western Dutch Wadden Sea. Netherlands Journal of Aquatic Ecology, 30: 27–39.

Dick, S., Brockmann, U. H., van Beusekom, J. E. E., Fabiszisky, B., George, M., Hentschke, U., Hesse, K.-J., Mayer, B., Nitz, T., Pohlmann, T., Poremba, K., Schaumann, K., Schönfeld, W., Starke, A., Tillmann, U., and Weide, G. 1999. Exchange of matter and energy between the Wadden Sea and the coastal waters of the German Bight: estimations based on numerical simulations and field measurements. Deutsche Hydrographische Zeitschrift, 51: 181–219.

Gaul, H. 2000. MURSYS – Nährstoffkonzentrationen in der küstennahen Zone und in der Deutschen Bucht (GAUSS-Fahrt Nr. 345 , Februar). http://www.bsh.de/Meeresumweltschutz/Mursys/Gaumert, T. 1991. Trend-Entwicklung der Nährstoffe im Elbwasser von 1980 bis 1989. Wassergütestelle Elbe/ARGE Elbe, Hamburg, 23 S.

Gillbricht, M. 1988. Phytoplankton and nutrients in the Helgoland region. Helgoländer Meeresuntersuchungen, 42: 435–467.

Gillbricht, M. 1994. Phytoplankton and the physical environment in the Helgoland region. Helgoländer Meeresuntersuchungen, 48: 431–443.

Grasshoff, K., Ehrhardt, M., and Kremling, K. (Eds.). 1983. Methods of Seawater Analysis. Verlag Chemie, Weinheim, New York. 317 pp.

Hagmeier, E. 1978. Variations in phytoplankton near Helgoland. Rapports et Procès-Verbaux des Réunions du Conseil International pour l'Exploration de la Mer, 172: 361–363.

Hanslik, M., Rahmel, J., Bätje, M., Knieriemen, S., Schneider, G., and Dick, S. 1998. Der Jahresgang blütenbildender und toxischer Algen an der niedersächsischen Küste seit 1982. Umweltbundesamt, Forschungsbericht 102 04 248, Berlin. 234 pp.

Hesse, K.-J., Hentschke, U., and Brockmann, U. 1992. A synoptic study of nutrient and phytoplankton characteristics in the German Wadden Sea with respect to coastal eutrophication. *In* Marine Eutrophication and Population Dynamics. 25th European Marine Biology Symposium, Ferrara, pp. 45–53. Ed. by G. Colombo *et al.* Olsen and Olsen, Fredensborg.

Hesse, K.-J., Tillmann, U., and Brockmann, U. 1995. Nutrient-phytoplankton relations in the German Wadden Sea. ICES CM/T, 8. 13 pp.Hickel, W. 1998. Temporal variability of micro- and nanoplankton in the German Bight. ICES Journal of Marine Science, 55: 600–609.

Hickel, W. 1998. Temporal variability of micro- and nanoplankton in the German Bight. ICES Journal of Marine Science, 55: 600–609.

Hickel, W., Berg, J., and Treutner, K. 1992. Variability in phytoplankton biomass in the German Bight near Helgoland, 1980–1990. Hydrobiological Variability in the ICES Area, 195: 249–259.

Hickel, W., Eickhoff, M., and Spindler, H. 1994. Changes in the German Bight pelagic environment during three decades. ICES CM 1994/E, 18. 8 pp.

Hickel, W., Mangelsdorf, P., and Berg, J. 1993. The human impact in the German Bight: eutrophication during three decades (1962–1991). Helgoländer Meeresuntersuchungen, 47: 243–263.

Kalle, K. 1937. Nährstoff-Untersuchungen als hydrographisches Hilfsmittel zur Unterscheidung von Wasserkörpern. Annalen der Hydrographie und Maritimen Meteorologie, 65: 1–18.

Körner, D., and Weichart, G. 1991. Nährstoffe in der Deutschen Bucht, Konzentrationsverteilung und Trends 1978–1990. Deutsche Hydrographische Zeitschrift. Ergänzungsheft Reihe A, 17. 41 pp.

Lenhart, H., and Pätsch, J. 2001. Daily nutrient loads of the European continental rivers for the years 1977–1998. Berichte aus dem Zentrum für Meeres- und Klimaforschung. Reihe B: Ozeanographie, 40. 146 pp.

Lohrenz, S. E., Fahnenstiel, G. L., Redalje, D. G., Lang, G. A., Dagg, M. J., Whitledge, T. E., and Dortch, Q. 1999. Nutrients, irradiance, and mixing as factors regulating primary production in coastal waters impacted by the Mississippi River plume. Continental Shelf Research, 19: 1113–1141.

Lorenzen, C. J. 1967. Determination of chlorophyll and pheopigments: spectrophotometric equations. Limnology and Oceanography, 12: 343–346.

Philippart, C. J. M., Cadée, G. C., van Raaphorst, W., and Riegman, R. 2000. Long-term phytoplankton–nutrient interactions in a shallow coastal sea: algal community structure, nutrient budgets, and denitrification potential. Limnology and Oceanography, 45: 131–144.

Postma, H. 1961. Transport and accumulation of suspended matter in the Dutch Wadden Sea. Netherlands Journal of Sea Research, 1: 148–190.

Radach, G., and Berg, J. 1986. Trends in den Konzentrationen der Nährstoffe und des Phytoplanktons in der Helgoländer Bucht (Helgoland Reede Daten). Berichte der Bioligischen Anstalt Helgoland, 2: 1–63.

Radach, G., and Bohle-Carbonell, M. 1990. Strukturuntersuchungen der meteorologischen, hydrographischen, Nährstoff- und Phytoplankton-Langzeitreihen in der Deutschen Bucht bei Helgoland. Berichte der Biologischen Anstalt Helgoland, 7: 1–425.

Rahmel, J., Bätje, M., Jakobs, R., and Michaelis, H. 1999. Nutrient trends in the East-Frisian Wadden Sea (Germany). Senckenbergiana maritima, 29 (Suppl): 119–123.

Riegman, R. 1995. Nutrient-related selection mechanisms in marine phytoplankton communities and the impact of eutrophication on the planktonic food web. Netherlands Journal of Sea Research, 32: 63–75.

Schaub, B. E. M., and Gieskes, W. W. C. 1991. Eutrophication of the North Sea: the relation between Rhine river discharge and chlorophyll *a* concentration in Dutch coastal waters. *In* Estuaries and Coasts: Spatial and Temporal Intercomparisons, pp. 85–90. Ed. by M. Elliot *et al.* Olsen and Olsen, Fredensborg.

Siebert, I., and Reise, K. 1997. Grünalgenausbreitung im Wattenmeer. Umweltbundesamt, Forschungsvorhaben 102 04 245, Berlin. 152 pp.

Sündermann, J., Hesse, K.-J., and Beddig, S. (Eds.). 1998. Abschlußbericht der BMBF-Verbundprojekte TRANSWATT und KUSTOS. Bd. 1, 2. 511 pp.

Tillmann, U., Hesse, K.-J., and Colijn, F. 2000. Planktonic primary production in the German Wadden Sea. Journal of Plankton Research, 22: 1253–1276.

Weichart, G. 1986. Nutrients in the German Bight, a trend analysis. Deutsche Hydrographische Zeitschrift, 39: 197–206.

ICES Marine Science Symposia, 219: 208–219. 2003

Variability of copepods as seen in a coupled physical–biological model of the Baltic Sea

Wolfgang Fennel and Thomas Neumann

Fennel, W., and Neumann, T. 2003. Variability of copepods as seen in a coupled physical–biological model of the Baltic Sea. – ICES Marine Science Symposia, 219: 208–219.

A key factor for the survival of fish larvae is the availability of prey (nauplii and copepodites) at the right time, place, and quality. This depends on several physical and biological processes and factors which can be studied theoretically by means of coupled physical–biological models with a stage-resolving zooplankton component. This study is based on an advanced ecosystem model of the Baltic Sea (ERGOM) with an increased resolution of the zooplankton stage variable. The model zooplankton consists of five stages: eggs, nauplii, two aggregated groups of copepodites, and adults. Food availability and temperature control the transfer processes, such as reproduction, hatching, and moulting. A simulation of the annual cycle is used to explore theoretically the temporal and spatial development of the various stages in relation to the physical forcing and the food web interactions. The dynamic equations for the "model copepod" were guided by *Pseudocalanus*; however, the model amounts to a stage-resolving description of aggregated zooplankton state variables. The effects and implications of increased process resolution are highlighted by comparisons of stage-resolving model runs and simulations with a single bulk-zooplankton variable.

Keywords: copepods, coupled biological–physical models, nauplii dynamics, stages.

W. Fennel and T. Neumann: Institut für Ostseeforschung Warnemünde an der Universität Rostock, Seestr. 15, D-18119 Rostock-Warnemünde, Germany [tel: +49 381 5197 110; fax: +49 381 5197 480; e-mail: wolfgang.fennel@io-warnemuende.de]. Correspondence to W. Fennel.

Introduction

Progress in theoretical understanding and quantitative description of marine ecosystems, and their responses to changes in physical forcing or nutrient input, can be achieved by coupling ocean circulation models and chemical–biological models. Model equations of General Ocean Circulation Models follow directly from fundamental principles, such as conservation of momentum, energy, and mass. Although the biological processes have to obey the basic physical laws, it is a theoretical challenge to find appropriate mathematical formulations which govern food web dynamics.

Many marine ecosystem models truncate the food chain at the level of zooplankton, either including grazing implicitly in phytoplankton mortality, e.g. Fransz and Verhagen (1985), Stigebrandt and Wulff (1987), and Humborg *et al.* (2000), or by a bulk-zooplankton state variable which provides grazing pressure on the phytoplankton, e.g. Wroblewski (1977), Aksnes and Lie (1990), Aksnes *et al.* (1995), Fasham *et al.* (1990), Broekhuizen *et al.* (1995), Fennel and Neumann (1996), and Neumann (2000). The feedback to the lower trophic levels is established directly by respiration and exudation rates or through the detritus pathway, where material is transferred to detritus by excretion and mortality, and recycled to the nutrient pool. These models have been applied in studying fluxes of matter among the state variables, in understanding and quantifying carbon fluxes in the ocean, in studying eutrophication in coastal seas, and in examining the mesoscale distribution of nutrients and plankton in response to the circulation patterns.

Model studies of fish recruitment require stage-resolving descriptions of zooplankton in order to address size-selective feeding of larvae, juvenile, and adult fish. They should involve growth, development, and reproduction of copepods, food web interactions, and physical control through advection and small-scale turbulence.

A model of zooplankton biomass including several species and stages was developed by Vinogradov *et al.* (1972). Stage-resolving population models

were used by Wroblewski (1982), Gupta *et al.* (1994), and Lynch *et al.* (1998). Individual-based modelling of population dynamics has been considered, for example by Batchelder and Miller (1989) and Miller and Tande (1993). Such an individual-based population model was linked to circulation by using archives of modelled advection (Miller *et al.*, 1998). These population models used experimental data of stage duration as prescribed parameters, which depend on temperature and are known as Belehradek formulas (e.g. Corkett and McLaren, 1978).

An integration of mean individual properties and population dynamics was proposed by Carlotti and Sciandra (1989), where the equations for the numbers of individuals have been linked to the evolution of the mean individual mass, $\overline{m}$, that in turn obeys an equation of the type

$$\frac{d}{dt}\overline{m}(t) = (g(t) - l(t))\overline{m}^{p} \qquad (1)$$

Here g and l prescribe growth and losses, and p is an allometric exponent, which generally is less than unity. The transfer and mortality rates needed in the population model are not prescribed by data, but controlled by the development of the "mean individual". Moulting occurs only if the critical moulting mass, X_i, is approached (see Carlotti and Sciandra (1989) and Carlotti and Nival (1992) for a detailed description). Attempts to couple this type of model to 1-D (one-dimensional) water column models including phytoplankton dynamics were presented by Carlotti and Radach (1996) in Eulerian fashion and by Carlotti and Wolff (1998) in a Lagrangian ensemble theory. Models incorporating phytoplankton production and population dynamics as described by a von Foerster equation (see Murray, 1993) for the population density in conjunction with growth of the mean individual mass, as in Equation (1), have been embedded in flow fields in Lagrangian fashion by Heath *et al.* (1997) and as a spatially distributed array of boxes in an Eulerian approach by Bryant *et al.* (1997). A variety of existing zooplankton models was recently reviewed by Carlotti *et al.* (2000).

In the present article we aim to integrate a stage-resolving zooplankton model (Fennel, 2001) into a 3-D Baltic Sea ecosystem model (Neumann, 2000). The model system consists of a circulation model and an embedded chemical-biological model which describes the dynamics of nutrients, phytoplankton, stage-resolved zooplankton, and detritus. The explicit description of the food web allows, in principle, simulation of the survival conditions of larvae, i.e. timing and location of nauplii abundance, and has the potential also to simulate, among other issues, the effects of food quality.

The model

This study is based on an advanced 3-D ecosystem model of the Baltic Sea, which is described in some detail in Neumann (2000) and Neumann *et al.* (2002). The biological component of the model consists of nine state variables. The phytoplankton functional groups are diatoms, flagellates, and cyanobacteria; the nutrients are ammonium, nitrate, and phosphate. Moreover, detritus and oxygen (hydrogen sulphate as negative oxygen) are included. The model zooplankton, which was originally introduced as a bulk biomass state variable, is described in the present study by a stage-resolving model (Fennel, 2001).

Stage-resolving model of copepod dynamics

We start with a brief outline of the copepod model of copepods. For integration of such a model into a General Circulation Model it is desirable to keep the number of state variables and hence the number of evolution equations small. The model copepod develops through five stages: eggs, nauplii, copepodites 1 and 2, and adults. The nauplii stages are merged into one state variable "model nauplii" and the copepodites stages are aggregated into the state variables "model copepodites 1 and 2", and partly into "model adults". The corresponding stage-dependent biomass variables per unit volume are Z_e, Z_n, Z_{c1}, Z_{c2}, and Z_a. The corresponding numbers of individuals per unit volume are N_e, N_n, N_{c1}, N_{c2}, and N_a.

We assume that the numbers of individuals per unit volume is high enough that the state variables behave like continuous functions and, hence, the dynamics can be expressed by differential equations.

Population density and state variables

The state variables Z_i and N_i ($i = e, n, c_1, c_2, a$), are related to the population density, $\sigma(m, t)$, of individuals of mass m. Thus $\sigma(m, t)dm$ is the number of individuals in the interval $(m, m + dm)$ at time t. The total zooplankton biomass and the total number of individuals are related to $\sigma(m, t)$ as:

$$Z_{tot} = \int_{m_e}^{x_a} \sigma(m) m dm \qquad \text{and} \qquad N_{tot} = \int_{m_e}^{x_a} \sigma(m) dm,$$

where m_e is the egg mass and X_a is the maximum mass of mature adults.

The dynamics of $\sigma(m)$, i.e. its changes over time, are controlled by losses due to mortality and gains through production of new eggs:

$$\frac{d}{dt}\sigma = -\mu\sigma + T_{ae}\sigma\delta(m - m_e) \qquad (2)$$

where T_{ae} is an egg rate, prescribing the transfer of mass from adults to eggs, and $\delta(m - m_e)$ is the Dirac delta-function. For stage, i, the individual mass (m) is confined to the interval $X_{i-1} \le m \le X_i$, where X_{i-1} and X_i are the moulting mass of the previous and the current stages, respectively. The biomass (Z_i) and number of individuals (N_i) are:

$$Z_i = \int_{X_{i-1}}^{X_i} \sigma(m)m\,dm \quad \text{and} \quad N_i = \int_{X_{i-1}}^{X_i} \sigma(m)\,dm \qquad (3)$$

Owing to the growth of the individuals the distribution density $\sigma(m, t)$ will propagate along the m-axis with the "propagation speed" ($\frac{d}{dt}m$), which is controlled by growth (grazing minus losses) according to

$$\frac{d}{dt}m_i(t) = (g_i(t) - l_i(t))m_i \qquad (4)$$

where m_i refers to the mass within a certain stage, i.e., $X_{i-1} \le m \le X_i$. Contrary to (1), we use stage-dependent rates for grazing, $g_i(t)$, and losses, $l_i(t)$, to avoid an allometric exponent different from unity.

For the population density (σ_i) of stage i, it follows similar to (2) that:

$$\frac{d}{dt}\sigma_i = -\mu_i\sigma_i + T_{(i-1),i}\delta(m - X_{i-1}) - T_{i,(i+1)}\delta(m - X_i) \qquad (5)$$

where $T_{(i-1),i}\delta(m - X_{i-1})$ and $T_{i,(i+1)}\delta(m - X_i)$ prescribe the rates at which individuals of stage $i-1$ are transferred to stage i, and individuals of stage i moult into stage $i+1$, respectively.

The dynamical equations for Z_i and N_i follow from (3), (4), and (5) as

$$\begin{aligned}\frac{d}{dt}Z_i &= \int_{X_{i-1}}^{X_i} \left(\frac{d\sigma_i}{dt}m + \frac{dm}{dt}\sigma_i\right)dm \\ &= (g_i - l_i - \mu_i)Z_i + T_{(i-1),i}X_{i-1} - T_{i,(i+1)}X_i \end{aligned} \qquad (6)$$

and

$$\frac{d}{dt}N_i = \int_{X_{i-1}}^{X_i} \frac{d\sigma_i}{dt}dm = -\mu_i N_i + T_{(i-1),i} - T_{i,(i+1)}. \qquad (7)$$

In order to prescribe the transfer among the stages, filter functions are introduced that decrease the growth and activate the transfer if a substantial part of the population in a certain stage has approached the moulting mass. This can be accomplished by comparing the mean individual mass $\overline{m} = Z_i/N_i$ with the maximum mass (X_i) represented by the moulting mass. We choose a Fermi function, which provides a representation of the step-function with a smooth transition,

$$f(\overline{m}_i, X_i) = \frac{1}{1 + \exp\left(\frac{\kappa}{X_i}(\overline{m}_i - X_i)\right)}. \qquad (8)$$

In a statistical sense, the function (8) provides the connection of the individual level to the bulk biomass of the stage. The function drops from unit to zero if the mean individual mass ($\overline{m} = Z_i/N_i$) of a stage approaches the moulting mass X_i. The grazing rate (g_i) will be multiplied by this function.

At the same time, a transfer rate to the next stage must be activated. Noting the property of the Fermi functions, $f(x, y) = 1 - f(y, x)$, the transfer rates ($T_{i,i+1}$) can be defined as:

$$T_{i,i+1} = g_i\, f(< m >_i, m_i), \qquad (9)$$

where g_i is the grazing rate and $f(< m >_i, \overline{m}_i)$ is a highpass filter function, which ensures that the transfer to the next stage does not start before the mean individual mass, $\overline{m}$, exceeds a value $< m >_i$. We chose $< m >_i$ to be smaller than the moulting mass of the corresponding stages. Moreover, because the transitions in real systems are not as sharp as indicated by the δ functions in (5), we modify the transfer terms in (6) as $T_{i,i+1}X_i \approx T_{i,i+1}Z_i$, where, because of the highpass filter property of $T_{i,i+1}$, these terms are activated only for values of Z_i close to X_i (see Fennel (2001) for more details).

Then the equations for the stage-dependent biomass can be written as

$$\begin{aligned}\frac{d}{dt}Z_e &= T_{ae}Z_a - T_{en}Z_e - \mu_e Z_e, \\ \frac{d}{dt}Z_n &= T_{en}Z_e + (g_n - l_n - \mu_n)Z_n - T_{nc_1}Z_n, \\ \frac{d}{dt}Z_{c_1} &= T_{nc_1}Z_n + (g_{c_1} - l_{c_1} - \mu_{c_1})Z_{c_1} - T_{c_1c_2}Z_{c_1}, \\ \frac{d}{dt}Z_{c_2} &= T_{c_1c_2}Z_{c_2} + (g_{c_2} - l_{c_2} - \mu_{c_2})Z_{c_2} - T_{c_2a}Z_{c_2}, \\ \frac{d}{dt}Z_a &= T_{c_2a}Z_{c_2} + (g_a - l_a - \mu_a)Z_a - T_{ae}Z_a. \end{aligned} \qquad (10)$$

The dynamics of the state variables are controlled by transfer rates ($T_{i,i+1}$), growth rates (g_i), loss rates (l_i), and mortality rates (μ_i), where $i = (e, n, c_1, c_2, a)$. The process rates are specified below. The corresponding equations for the number of individuals are,

$$\begin{aligned}\frac{d}{dt}N_e &= \tau_{ae} - \mu_e N_e - \tau_{en}, \\ \frac{d}{dt}N_n &= \tau_{en} - \mu_n N_n - \tau_{nc_1}, \\ \frac{d}{dt}N_{c_1} &= \tau_{nc_1} - \mu_{c_1} N_{c_1} - \tau_{c_1c_2}, \end{aligned} \qquad (11)$$

$$\frac{d}{dt}N_{c_2} = \tau_{c_1c_2} - \mu_{c_2}N_{c_2} - \tau_{c_2a},$$

$$\frac{d}{dt}N_a = \tau_{c_2a} - \mu_a N_a - \tau_{ae}.$$

The mortality rates (μ_i) are the same as in Equation (10). The transfer rates ($\tau_{i,i+1}$) are closely related to $T_{i,i+1}$, i.e. $\tau_{i,i+1} = T_{i,i+1}Z_i/X_i$.

Use of the filter functions (8) and (9) implies that both biomass variables and number of individuals are needed to compute the mean mass of the individuals for each stage. The interfaces for the integration of the two sets of biological equations, (10) and (11), into the circulation model are advection-diffusion equations, one for each state variable. An attractive feature of including the biomass state variables is the explicit conservation of mass in the model. Population models are not constrained in such an easy way because there is no law for the conservation of the number of individuals.

Process descriptions and parameter choices

In order to specify our model copepod, we follow Fennel (2001) and focus on *Pseudocalanus*, which is an important copepod in the Baltic. The mass parameters listed in Table 1 were derived from Baltic Sea data (Hernroth, 1985). However, coupled models require that other species, such as *Acartia*, with different life cycles be taken into account by means of aggregated, stage-resolving state variables. Since most of the process descriptions are outlined in Neumann (2000) and Fennel (2001), we confine the discussion to the extension developed in the present model.

The grazing rates, which describe the amount of ingested food per day in relation to the biomass, are formulated in terms of modified Ivlev expressions:

$$g_i(P) = \beta_i(1 - \exp(-I_i^2 P_{sum}))f(\overline{m}, X_i) \qquad (12)$$

Table 1. Mass parameters.

Egg mass	$m_e = 0.1$ µgC		
Stage	Moulting mass	Maturation mass	Mean mass
Nauplii	$X_n = 0.3$ µgC	–	$< m >_n = 0.22$ µg C
Copepodites 1	$X_{c1} = 0.8$ µgC	–	$< m >_{c1} = 0.6$ µg C
Copepodites 2	$X_{c2} = 2$ µgC	–	$< m >_{c2} = 1.6$ µg C
Adults	–	$X_a = 3$ µgC	$< m >_a = 2.6$ µg C

Table 2. Grazing rates (β_i) at different temperatures, Ivlev constants (I_i^2), and mortality rates (μ_i).

Stage	β_i (0°C) d^{-1}	β_i (10°C) d^{-1}	β_i (15°C) d^{-1}	$I_i^2 10^{-3}$ mmol $C^{-2}\,m^{-6}$	μ_i d^{-1}
Eggs	–	–	–	–	0.2
Nauplii	0.5	0.93	1.3	2.5	0.033
Copepodites1	0.35	0.66	0.9	4.7	0.05
Copepodites 2	0.25	0.47	0.64	7	0.05
Adults	0.12	0.22	0.31	10.1	0.025

where P_{sum} is the food concentration, i.e. $P_{sum} = P_d + P_f + P_c$, ($P_d$ diatoms, P_f flagellates, P_c cyanobacteria), the I_i's are stage-dependent Ivlev constants, and f is the Fermi function (8). The maximum grazing rate, β_i, depends on the temperature through an Eppley factor, $\beta_i = b_i \exp(aT)$, with $a = 0.063(°C)^{-1}$. The numerical values of the involved parameters are listed in Table 2. The decrease of β_i for the higher stages reflects that older stages with more body mass ingest a smaller amount of food, in relation to their body mass, than the younger stages. Moreover, we have included a lower preference of cyanobacteria (Müller-Navarra *et al.*, 2000) by a factor $(P_d + P_f + \frac{1}{2}P_c)/P_{sum}$, which for simplicity is not included in (12).

The ingested food is partly used for growth and partly for the metabolism of the animals. About 35% of the ingestion is lost as egestion, 10% as excretion, 10% by respiration, and 15% is needed for the moulting processes (see Corkett and McLaren, 1978). These losses are expressed by the rates $l_i = 0.7\ g_i\ (P,T)$ for $(i = n, c_1, c_2)$ and $l_a = 0.8\ g_a\ (P, T)$ for the adults $(i = a)$. Note that these rates depend on temperature and food through the grazing rates (g_i).

The transfer rates involve moulting, egg laying, and hatching. The rate of reproduction (T_{ae}), describes the egg production of the female adults after reaching the maturation mass. We assume that half of the adults are female and 30% of the ingested food is transferred into egg biomass.

$$T_{ae} = (\tfrac{1}{2})\ 0.3\ g_i\ .$$

Then the number of new eggs per day is given by $\tau_{ea} = T_{ae}\ Z_a/m_e$. This approach implies that the egg-rate depends on food availability and temperature through the grazing rates, but ignores the discontinuous release of clutches of eggs with time intervals of a couple of days; see, e.g., Hirche *et al.* (1997). The transfer from eggs to nauplii (hatching) is set by the embryonic duration at low temperatures, about 10 days (Corkett and McLaren, 1978). The effect of temperature is accounted for by an Eppley factor:

$$T_{en} = h\ \theta\ (T - T_0)\ \exp(a(T - T_0)),$$

with $h = 0.124\ d^{-1}$. The involved step-function, $\theta(x)$, ($\theta(x) = 1$ for $x > 0$ and $\theta(x) = 0$ for $x < 0$) implies that the model eggs hatch to model-nauplii only for temperatures exceeding the threshold, $T_0 = 2.5°C$.

The model food chain is truncated at the level of zooplankton and mortality involves both death rates and predation by planktivorous fish. The choice of mortality rate is difficult because the basic factors are poorly known. In the literature, stage-dependent mortalities with some seasonal variation are often used, e.g. Gupta *et al.* (1994). The typical orders of magnitude vary from $\mu \sim 0.01$ to $1\ d^{-1}$. In the present simulations we choose stage-dependent mortality rates. For simplicity, the mortality is held constant within each stage. The numerical values are listed in Table 2.

The performance of the model was illustrated in Fennel (2001). For example, a simulation of the development of a cohort of eggs in a rearing tank with constant food and temperature conditions can be achieved by integrating the equation sets (10) and (11). In a first phase, the egg-signal propagates through the following stages, while the total number of individuals decreases due to mortality. After a generation time of 30 days adults have developed and start to lay new eggs, and after 55 days the abundance of adults has increased significantly in response to the reproduction.

Experimental simulations

The zooplankton model outlined in the preceding section was integrated into the 3-D ecosystem model of the Baltic Sea (Neumann, 2000; Neumann *et al.* 2002) and run to simulate the production cycle over one year. We chose 1980 because of the availability of initial data as well as comprehensive sets of forcing data. The model was driven with meteorological data from the ERA 15 project (http://wms.ecmwf.int/research/era/Era-15.html), and with river run-off, nutrient loads and atmospheric nutrient deposition provided by the Baltic Environmental Database of the University of Stockholm (http://data.ecology.su.se/Models/bed.htm). The initial distributions of temperature and salinity fields were taken from a climatological data set (Janssen *et al.*, 1999). Initialization of the biogeochemical state variables was accomplished with the help of an existing initialization run (Neumann *et al.*, 2002).

Since there are no data available for a proper initialization of the copepod distribution, we chose an evenly distributed background population of overwintering copepods of 2400 ind m^{-3}. The seed population starts to lay eggs in response to the model-generated phytoplankton spring bloom. Although the model parameterization was guided by *Pseudocalanus* data compiled for the Baltic (Hernroth, 1985), we consider this as a "model copepod" which comprises several species implicitly. In particular, *Acartia* is included, although these are characterized by smaller mass (Hernroth, 1985) and their life cycle is characterized by overwintering of dormant eggs resting at the bottom in the shallower areas. It is assumed that the dormant eggs of *Acartia* commence hatching at the same time as *Pseudocalanus* starts to lay eggs. The model copepod develops both in colder and warmer areas, where the state variables refer to *Acartia* in the nearshore regions and to *Pseudocalanus* in the offshore areas and below the seasonal thermocline. Thus, the state variables may refer to different species at different locations.

In this article we explore the dynamics of the model zooplankton. For a discussion of the biogeochemical aspects of the model simulation, see Neumann (2000) and Neumann *et al.* (2002). The most effective way to present the results of the simulations is by animation, showing the development of the state variables in time and space. Computer animation files can be obtained on request. Here we show only a selection of snapshots. A map of the Baltic is shown in Figure 1, indicating two stations and sections referred to later.

The modelled phytoplankton spring bloom (not shown) commences in the southwestern Baltic by the end of March and propagates toward the central Baltic during April and May. The seed population of adult copepods starts to lay eggs in response to the spring bloom of phytoplankton. The response patterns emerge, with some delay due to the hatching process, in the model nauplii distribution (Figure 2). With further delay, the signals propagate through the copepodite stages until the abundance of the adults showed an increase 2 months after the spring bloom (Figure 3). In the summer, the

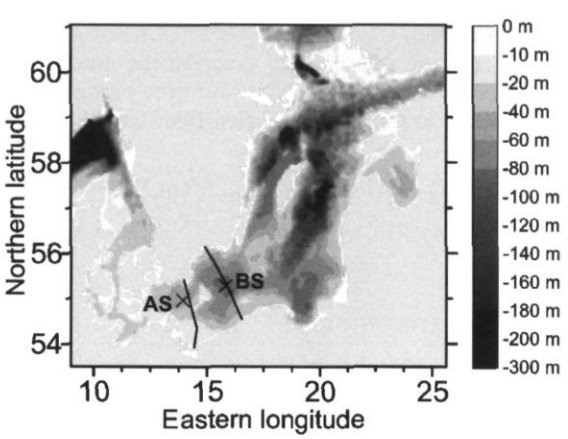


Figure 1. Map of the southwestern and central part of the Baltic Sea. The stations in the Arkona Sea (AS) and Bornholm Sea (BS) refer to the sampling locations of the Baltic Monitoring Programme and data from the indicated sections are used to compare with model results.

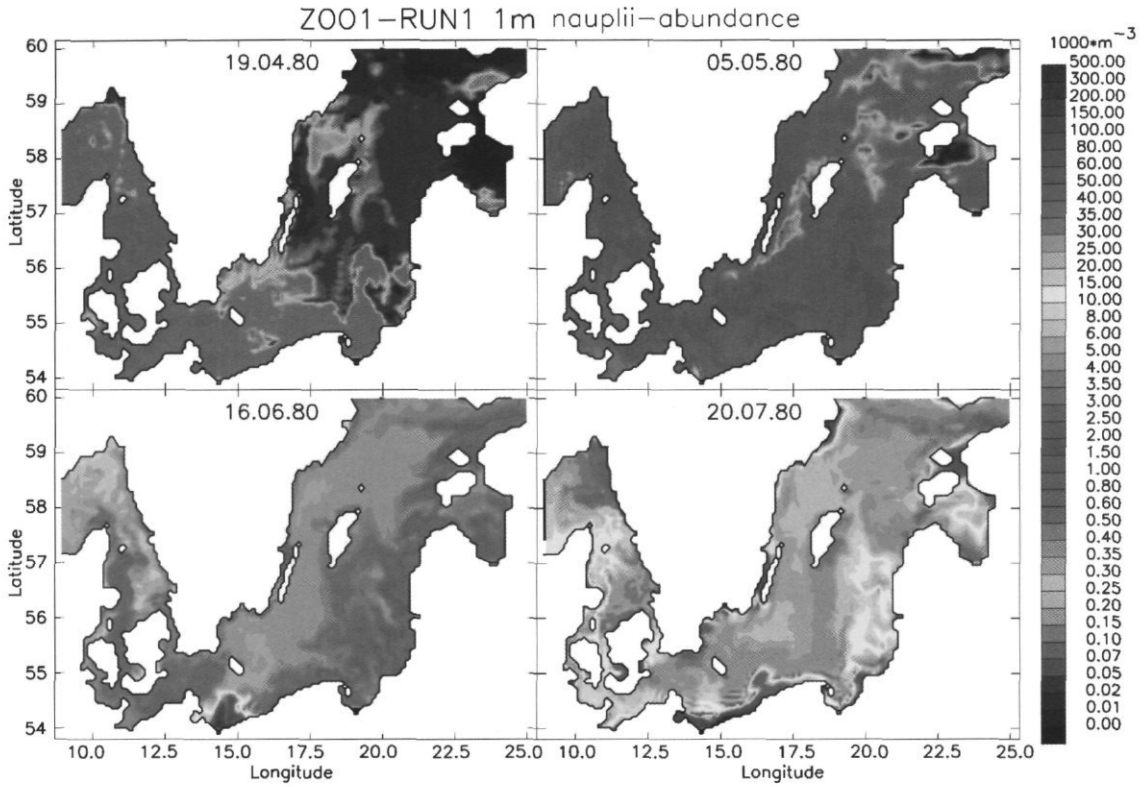


Figure 2. The development of model nauplii near the sea surface (uppermost layer, thickness 2 m).

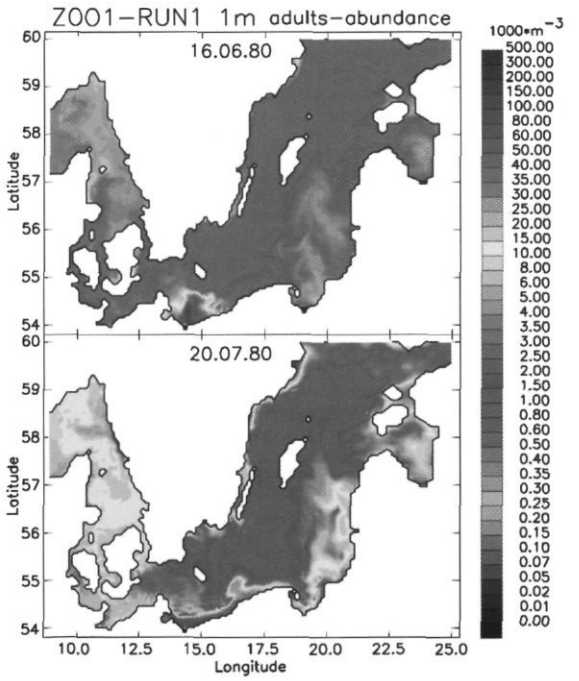


Figure 3. Development of model adults near the sea surface (uppermost layer, thickness 2 m).

abundance of all stages reaches the maximum level (Figure 4). The spatial distribution of the different stages shows similarities and differences which are due to the interplay of the mesoscale current patterns and the different temporal development of the stages.

The general development and distribution patterns are qualitatively as would be expected, but a quantitative comparison with observations is difficult due to limited observations. In order to provide a qualitative comparison, snapshots of the vertical distribution of model nauplii along sections in the Arkona Sea and the Bornholm Sea are examined (Figure 1). These sections include stations from the Baltic Monitoring Programme. An overview of the observed abundance of mesozooplankton from the monitoring programme for 1980 to 1990 has been published in the HELCOM Assessment (Helcom, 1996). The data refer to the vertically integrated bulk abundance of copepods, where stages were not resolved. The data have been compiled from three stations in the central Arkona Sea, with about 20 samples per season. These stations correspond to the central part of the model sections, as discussed below.

In the central Arkona Sea, the abundance of copepods in 1980 was 6000 ind m^{-3} for the period

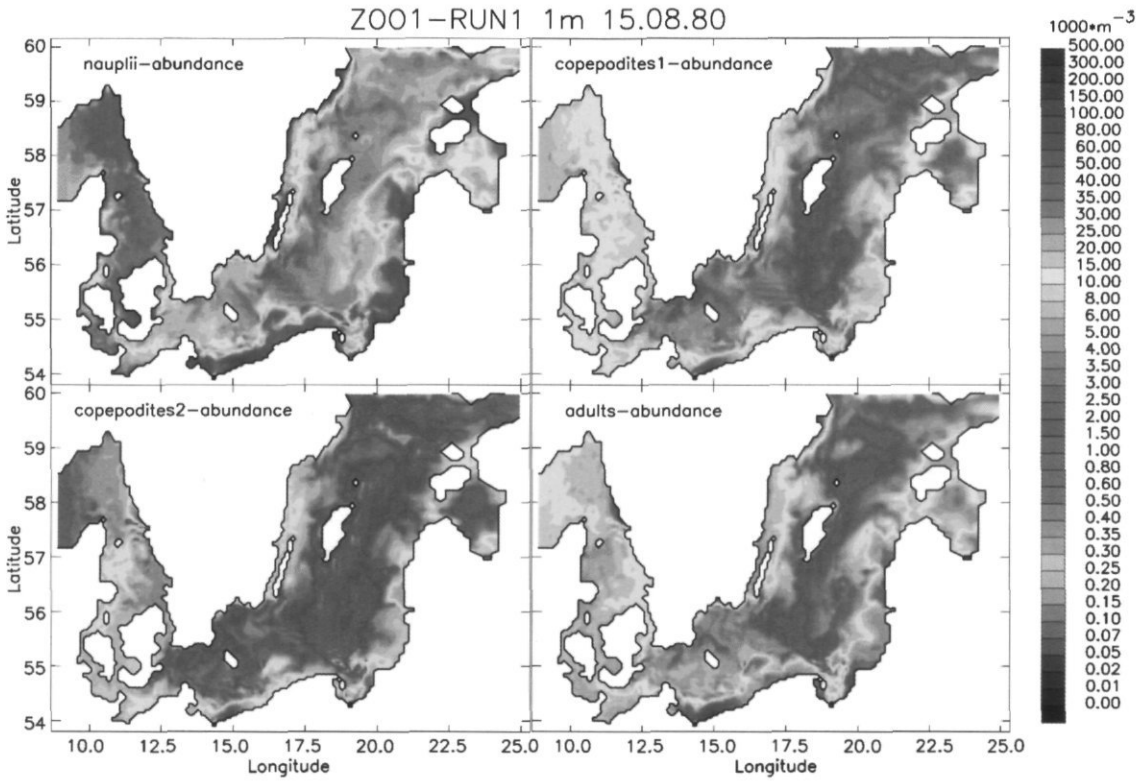


Figure 4. The summer peak of abundance of model nauplii, copepodites 1 and 2, and adults.

before the spring bloom (January to March), 15 000 ind m^{-3} for the period April and May, and 25 000 ind m^{-3} during the summer.

The simulated spring bloom maximum occurs in the central part of the Arkona Sea at the end of March. Thereafter, the concentration decreases to low summer levels. Elevated values are found in the area of the shallow bank (Oder Bank), which is influenced by the nutrient loads of the Oder river. The abundance of eggs (not shown) and nauplii (Fig. 5) responds with some delay to the chlorophyll signal (not shown).

The model-nauplii abundance, which is an important indicator for the potential survival of larvae, shows a slight increase, from 4000 to 10 000 ind m^{-3}, in the central part of the Arkona Sea and a substantial increase, from 4000 to 200 000 ind m^{-3}, in the shallow coastal area from spring to summer. This figure is qualitatively in accordance with observation in the shallow area in 1988 (Postel *et al.*, 1991). Below the surface layer the abundance is smaller and varies between 4000 and 6000 ind m^{-3} (Figure 5). Development of the model copepodite 1 follows that of the nauplii, with a delay of several weeks. The abundance of model adults increases slowly and reaches its maximum in August. The strongest signals are found in the area of the Oder Bank.

Next we examine the section through the Bornholm Sea (Figure 1). The available data from the Baltic Monitoring Programme are confined to one station in the central Bornholm Sea. Copepod abundance was compiled from 17 samples in winter, 43 samples in spring, and 63 samples in summer. For 1980, the data for the central Bornholm Sea indicate 2000 ind m^{-3} for the period before the spring bloom (January to March), 10 000 ind m^{-3} for the period April and May, and 8000 ind m^{-3} for the summer (Helcom, 1996). The observed abundance is generally higher in the Arkona Sea than in the Bornholm Sea.

In the central part of the Bornholm Sea, the model phytoplankton spring bloom (not shown) occurs in mid-April, i.e. later than in the Arkona Sea. The summer values are low and confined to the surface layer. The model eggs (not shown) and nauplii respond to the phytoplankton signal with a delay of a couple of weeks with a patchy distribution. Relative high levels appear near the eastern coast (Figure 6). The model nauplii abundance, which is an important food source for larvae, increases from spring to summer, from 4000 to 10 000 ind m^{-3} in the central part of the Bornholm Sea, while in the coastal region off Poland increased up to 40 000 ind m^{-3}. Below the surface layer, values

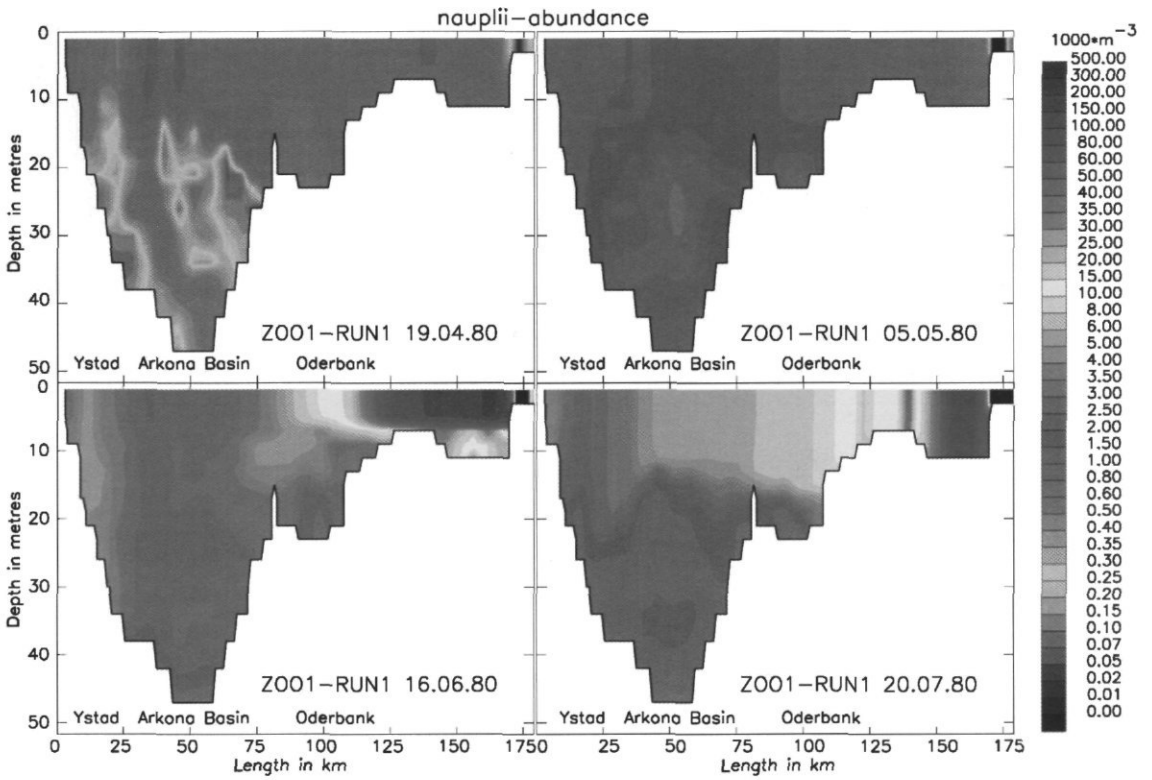


Figure 5. Development of the model nauplii along the Arkona Sea section (Figure 1).

are much smaller and exceed 2000 ind m^{-3} only in a few patches.

The response patterns of the model copepodite abundances show a similar offshore gradient. The model adults do not increase significantly before July and their maximum abundance is reached in August (not shown). The model generally reproduces the observed higher abundance in the Arkona Sea than in the Bornholm Sea.

The observational site corresponds to the central part of the model section. Contrary to observations, the model abundance of copepods is slightly higher in summer than in spring. However, this difference becomes negligible when we look at the total observed mesozooplankton, which also assumes maximum values in the summer. This implies that our model copepod ingest food, which in nature is taken by other species, in particular *Cladocera* and *Rotifera*.

In both basins, the vertical distribution patterns in the model show the strongest signals in the upper layer, while below the seasonal thermocline adults, as well as eggs and nauplii, are less abundant. This applies, in particular, to the Bornholm Sea during the summer. The reason is that the model phytoplankton in the summer season consists mainly of flagellates, with zero sinking speed, and blue greens, with a slight buoyancy, while the spring bloom is dominated by diatoms, which sink relatively quickly Neumann (2000). Thus, the summer chlorophyll concentrates mainly in the surface layer.

The vertical motion of the model copepods is passive, i.e. driven by currents and turbulent diffusion in a similar manner as in a bulk-zooplankton description. While a background stock of adults is maintained by setting the adult mortality to zero for low abundance there is still some egg laying and hatching to nauplii, whereas the model copepodites in the deeper layers are short of food and damped by mortality. This could be amended by allowing copepods some grazing on detritus, including vertical motion, i.e. dial migration, to draw from the food in the surface mixed layer.

It is interesting to compare the stage-resolving simulations (Figure 7) with the model containing one bulk-zooplankton variable (Figure 8). Compared to the bulk-zooplankton run, the stage-resolving case displays a lower grazing pressure during the spring bloom and a higher grazing pressure in the summer. While the bulk-zooplankton reacts immediately with an increase of biomass, the overwintering adults in the stage- resolving model first increase their body mass and start to lay eggs, then have to propagate through all stages until they

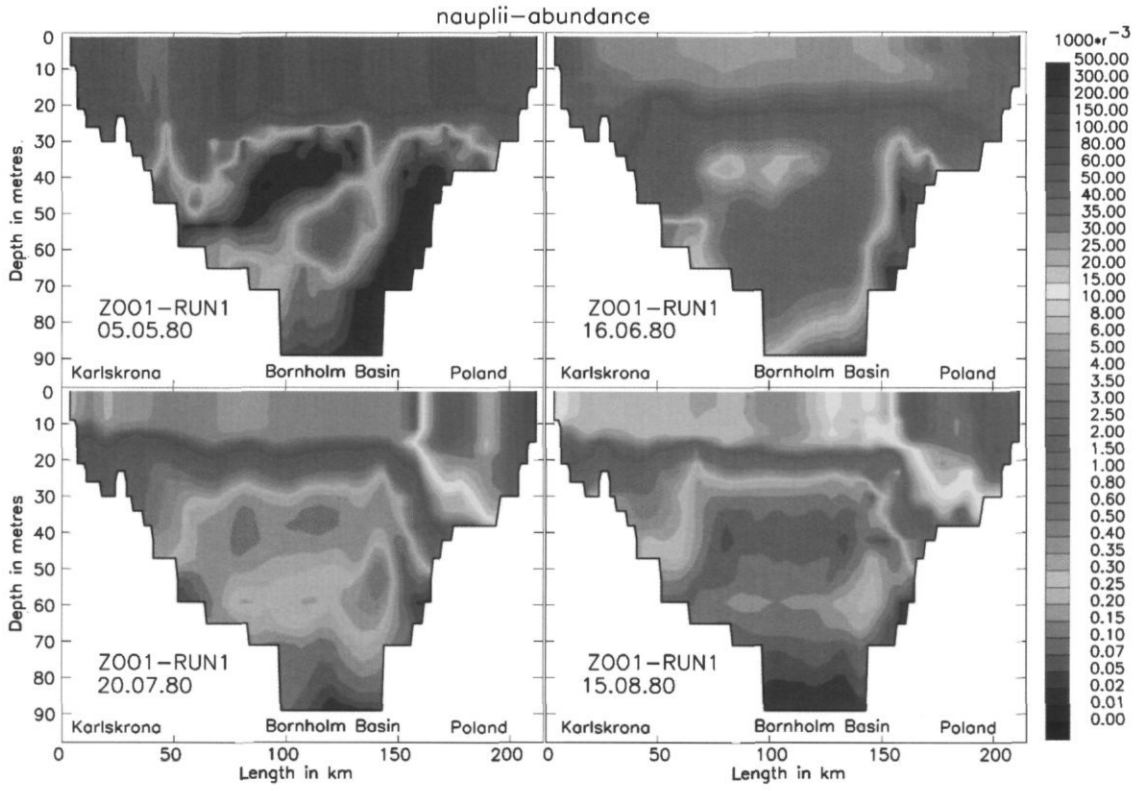


Figure 6. Development of the model nauplii along the Bornholm Sea section (Figure 1).

become adults, which then increases the reproduction. Thus a time interval of a full generation is needed before the zooplankton mass and the number of individuals increase through reproduction. The difference of both simulations is relatively small for the summer. The main deviations occur after the spring bloom.

Discussion and conclusions

The present study extends an advanced ecosystem model of the Baltic Sea in which the zooplankton biomass was considered as one aggregated bulk variable (Neumann, 2000; Neumann *et al.*, 2002) to a stage-resolving model of copepods (Fennel, 2001). The stage-resolving model combines elements of biomass models and stage-dependent population models and uses the concept of critical moulting mass (Carlotti and Sciandra, 1989). This approach allows a consistent formulation of the equations of the state variables, where abundance and biomass are based on a function of the population density, and obey von Foerster equations. In order to bridge the levels of individual and population dynamics, we introduced statistical aspects by means of the filter functions (Fermi function). An attractive property of the present model is its ability to conserve mass distributed within the food web explicitly. Such a conservation law cannot generally be applied to population models, because there is no law of conservation of the number of individuals. Only in special cases can it be assumed that for limited time periods the total number of individuals is constant, e.g. Wroblewski (1982).

An unavoidable disadvantage of the model is the need for two sets of state variables, biomass and the number of individuals, and hence the need for two equations at each stage. This is because of the connection of individual to population and bulk biomass levels in a statistical treatment.

Formulation of the dynamic signatures of the "model-copepod" was guided by properties of *Pseudocalanus* in the Baltic. However, in order to integrate the stage-resolving model into the coupled physical–biological model, it was assumed that the model copepod comprises other copepod species (aggregated state variables), although their parameters differ from those of *Pseudocalanus*. Species such as *Cladocera* and *Rotifera* were not explicitly taken into account in the present model approach.

Although not discussed in this article, we note that the model calculates, in a consistent way, the

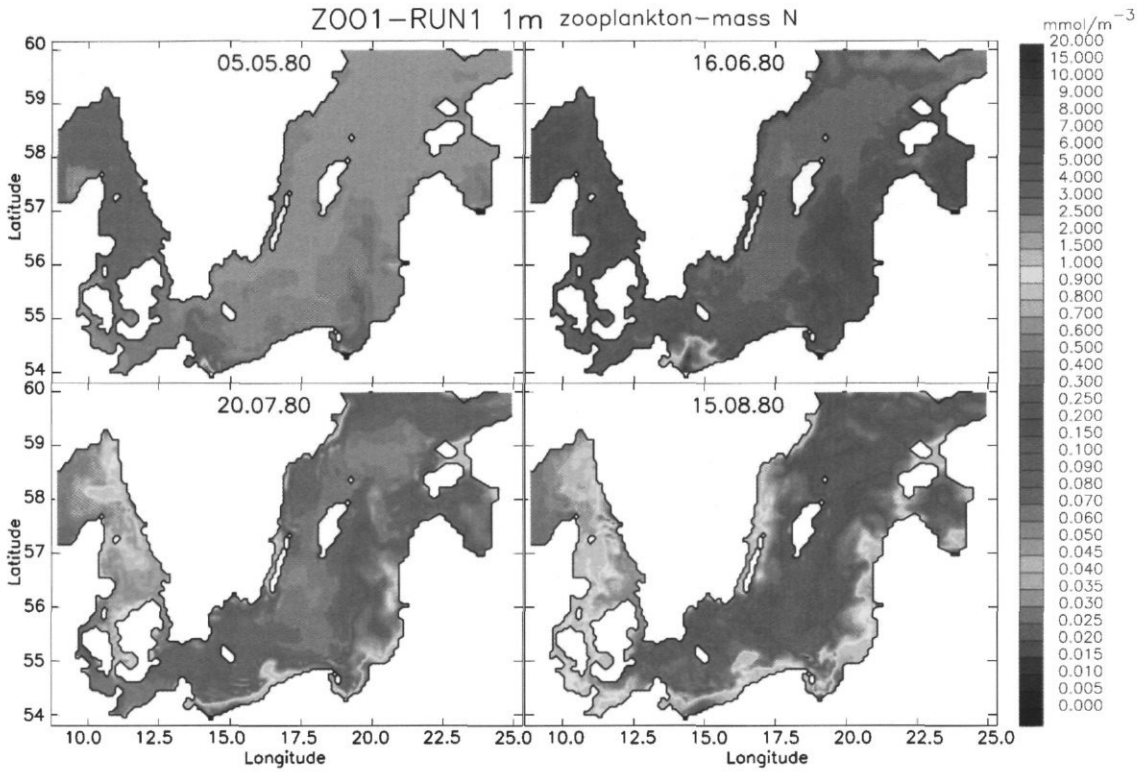


Figure 7. Development of the total zooplankton biomass near the sea surface (uppermost layer, thickness 2 m).

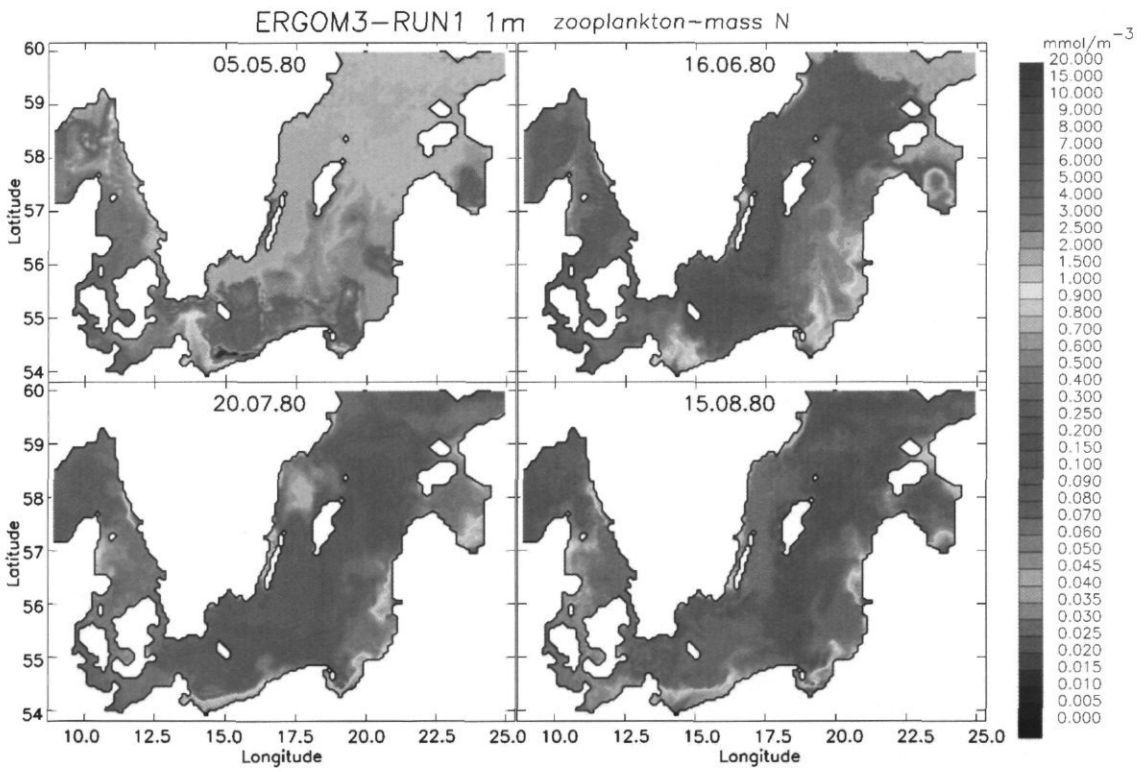


Figure 8. As Fig. 7, but for a model run with only one bulk zooplankton state variable.

food-web dynamics controlled by physics and the chemical–biological processes. It includes biogeochemistry and has the potential to simulate oxygen depletion in the bottom waters of the central Baltic Sea (Neumann, 2000; Neumann *et al.*, 2002).

The food web is truncated at the level of the zooplankton although the zooplankton mortality includes predation by planktivorous fish. Nevertheless, the model provides a basis from which to explore variations in the recruitment condition, by computing development of larvae food (distribution of nauplii) in time and space in response to climate changes or altered river loads. Inclusion of the lower trophic levels allows, for example, simulation of how signals propagate through the food web and study of the effects of food quality on reproduction.

Although the present model is complex, it still involves a substantial simplification of the real system. For example, the stage-resolving formulation used in the 3-D ecosystem model has elements of a bulk approach by its lumping together several species into the corresponding stages. The description of vertical migration of the higher stages must be improved and grazing on detritus as a low quality food resource can be included. The influence of salinity and oxygen on the physiological rates has not been considered.

This study also highlights the need for more observational data, both for model initialization and for comparison of model results with observations.

It is generally accepted that models should be as simple as is reasonable and only as complex as is necessary. This implies that the choice of model equations depends on the problem considered and involves the assumption that enhancing or reducing the complexity of a model system by parameterization is possible to a certain degree. The quality of parameterizations can only be judged by comparison with measurements and by exploring models of different complexity. The present study indicates, for example, that the spring bloom is more strongly controlled within models using bulk zooplankton parameterization and responds faster than in a stage-resolving model where the eggs have to propagate through the stages before a significant increase in the grazing pressure develops. This delay has a time-scale of a full generation at relatively low temperatures. Thus, the presented simulations provide arguments to improve parameterizations of bulk-zooplankton biomass models.

The present model study was a first attempt to include a stage-resolving zooplankton component within a full 3-D physical–chemical–biological model of the Baltic Sea. Although the simulation was made for the year 1980, the model provides the means for studying the zooplankton response to decadal hydrographical variability. However, this will be the subject of future work.

Acknowledgements

Supercomputing power was provided by the Computing Center of the University of Rostock and the John von Neumann Institute for Computing. We thank the modelling group of the Baltic Sea Research Institute for supporting the circulation model, Thomas Fennel for his help with the graphics, and two anonymous referees for constructive comments.

References

Aksnes, D. L., and Lie, U. 1990. A coupled physical,-biological pelagic model of a shallow sill fjord. Estuarine, Coastal and Shelf Science, 31: 459–486.

Aksnes, D. L., Ulvestad, K. B., Balino, B. M., Berntsen, J., Egge, J. K., and Svendsen, E. 1995. Ecological modeling in coastal waters: towards predictive physical–chemical–biological simulation models. Ophellia, 41: 5–36.

Batchelder, H. P., and Miller, C. B. 1989. Life history and population dynamics of *Metridia pacifica*: results from simulation modelling. Ecological Modelling, 48: 113–136.

Broekhuizen, N., Heath, M. R., Hay, S. L., and Gurney, W. S. C. 1995. Modelling the dynamics of the North Sea's mesozooplankton. Netherlands Journal of Sea Research, 33: 381–406.

Bryant, A. D., Heath, M. R., Gurney, W. S. C., Beare, D. J., and Robertson, W. 1997. The seasonal dynamics of *Calanus finmarchicus:* development of a three-dimensional structured population model and application to the northern North Sea. Netherlands Journal of Sea Research, 38: 361–379.

Carlotti, F., Giske, J., and Werner, F. 2000. Modeling zooplankton dynamics. *In* ICES Zooplankton Methodology Manual. Ed. by R. Harris, P. Lenz, H. R. Skjoldal, and M. Huntley. Academic Press, San Diego. 684 pp.

Carlotti, F., and Nival, P. 1992. Model of copepod growth and development: moulting and mortality in relation to physiological processes during an individual moult cycle. Marine Ecology Progress Series, 84: 219–233.

Carlotti, F., and Radach, G. 1996. Seasonal dynamics of phytoplankton and *Calanus finmarchicus* in the North Sea as revealed by a coupled one-dimensional model. Limnology and Oceanography, 41: 522–539.

Carlotti, F., and Sciandra, A. 1989. Population dynamics model of *Euterpina acutifrons* (copepoda: Harpacticoida) coupling individual growth and larval development. Marine Ecology Progress Series, 56: 225–242.

Carlotti, F., and Wolf, K. U. 1998. A Lagrangian ensemble model of *Calanus finmarchicus* coupled with a 1-D ecosystem model. Fisheries Oceanography, 7: 191–204.

Corkett, C. J., and McLaren, I. A. 1978. The Biology of *Pseudocalanus. In* Advances in Marine Biology. Ed. by F. S. Russel and M. Yonge. Academic Press, London. 562 pp.

Fasham, M. J. R., Ducklow, H. W., and McKelvie, S. M. 1990. A nitrogen-based model of plankton dynamics in the oceanic mixed layer. Journal of Marine Research, 48: 591–639.

Fennel, W. 2001. Modeling of copepods with links to circulation models. Journal of Plankton Research, 23: 1217–1232.

Fennel, W., and Neumann, T. 1996. The mesoscale variability of nutrients and plankton as seen in a coupled model. German Journal of Hydrography, 48: 49–71.

Fransz, H. G., and Verhagen, J. H. G. 1985. Modelling research on the production cycle of phytoplankton in the southern bight of the North Sea in relation to river-borne nutrient loads. Netherlands Journal of Sea Research, 19: 241–250.

Gupta, S., Lonsdale, D. J., and Wang, D. P. 1994. The recruitment pattern of an estuarine copepod: a biological–physical model. Journal of Marine Research, 52: 687–710.

Heath, M., Robertson, W., Mardaljeviz, J., and Gurney, W. S. G. 1997. Modelling population dynamics of *Calanus* in the Fair Isle off northern Scotland. Journal of Sea Research, 38: 381–412.

Helcom. 1996. Baltic Sea Environment Proceedings No. 64 B, Baltic Marine Environment Protection Commission, Third periodic assessment of the state of the marine environment of the Baltic Sea 1989–1993. 252 pp.

Hernroth, L. 1985. Recommendations on methods for marine biological studies in the Baltic Sea: mesozooplankton assessment, Baltic Marine Biologists WG 14, Publication No. 10. 32 pp.

Hirche, H. J., Meyer, U., and Niehoff, B. 1997. Egg production of *Calanus finmarchicus*: effect of temperature, food and seasons. Marine Biology, 127: 609–620.

Humborg, C., Fennel, K., Pastuszak, M., and Fennel, W. 2000. A box model approach for a long-term assessment of estuarine eutrophication, Szczecin Lagoon, southern Baltic. Journal of Marine Systems, 25: 387–403.

Janssen, F., Schrum, C., and Backhaus, J. 1999. A climatological data set of temperature and salinity for the North Sea and the Baltic Sea. German Journal of Hydrography, 9: 1–245.

Lynch, D. R., Gentleman, W. C., McGillycuddy, D. J., and Davis, C. S. 1998. Biological–physical simulations of *Calanus finmarchicus* population dynamics in the Gulf of Maine. Marine Ecology Progress Series,169: 189–210.

Miller, C. B., and Tande, K. S. 1993. Stage duration estimation for *Calanus* populations, a modelling study. Marine Ecology Progress Series, 102: 15–34.

Miller, C. B., Lynch, D. R., Carlotti, F. C., Gentleman, W., and Lewis, C. V. W. 1998. Coupling of an individual-based population model of *Calanus finmarchicus* to a circulation model of the Georges Bank region. Fisheries Oceanography, 7: 219–234.

Müller-Navarra, D. C., Brett, M. T., Liston, A. M., and Goldman, C. R. 2000. A highly unsaturated fatty acid carbon transfer between primary producers and consumers. Nature, 403: 74–76.

Murray, J. D. 1993. Mathematical Biology. Springer-Verlag, Berlin. 767 pp.

Neumann, T. 2000. Towards a 3d-ecosystem model of the Baltic Sea. Journal of Marine Systems, 25: 405–419.

Neumann, T., Fennel, W., and Kremp, C. 2002. Experimental simulations with an ecosystem model of the Baltic Sea: a nutrient load reduction experiment. Global Biogeochemical Cycle, 16. (In press.)

Postel, A., Postel, L., and Hantke, H. 1991. Untersuchungen zur raum-zeitlichen Verteilung der Heringslarvennahrung von April bis Juni 1988 im südlichen Greifswalder Bodden. Fischereiforschung Rostock, 29: 42–55.

Stigebrandt, A., and Wulff, F. 1987. A model for the dynamics of nutrients and oxygen in the Baltic proper. Journal of Marine Research, 45: 729–759.

Vinogradov, M. E., Menshutkin, V. V., and Shushkina, E. A. 1972. On the mathematical simulation of a pelagic ecosystem in tropical waters of the ocean. Marine Biology, 16: 261–268.

Wroblewski, J. 1977. A model of phytoplankton plume formation during variable Oregon upwelling. Journal of Marine Research, 35: 357–394.

Wroblewski, J. S. 1982. Interaction of currents and vertical migration in maintaining *Calanus marshallae* in the Oregon upwelling zone: a simulation. Deep-Sea Research, 29: 665–686.

ICES Marine Science Symposia, 219: 220–230. 2003

Interannual variability in population dynamics of calanoid copepods in the Central Baltic Sea

Christian Möllmann, Friedrich W. Köster, Georgs Kornilovs, and Ludvigs Sidrevics

Möllmann, C., Köster, F. W., Kornilovs, G., and Sidrevics, L. 2003. Interannual variability in population dynamics of calanoid copepods in the Central Baltic Sea. – ICES Marine Science Symposia, 219: 220–230.

Interannual dynamics (1959–1999) of calanoid copepods *Pseudocalanus elongatus*, *Temora longicornis* and *Acartia* spp. in the Central Baltic Sea are described for different life-stages. Using principal component (PCA) and correlation analysis the association of the stage-specific abundance to salinity and temperature was investigated. *P. elongatus* dynamics were related to high salinities in spring favouring maturation and reproduction. Additionally, low temperatures appear to be favourable for reproduction, whereas intermediate copepodite stages were positively correlated to temperature. *T. longicornis* and *Acartia* spp. life-stages were consistently associated with higher temperatures in spring. Furthermore, there are indications that *T. longicornis* maturation and reproductive success in summer is affected by salinity levels similarly to *P. elongatus*.

Keywords: *Acartia* spp., Central Baltic Sea, copepod life-stages, *Pseudocalanus elongatus*, salinity, stock dynamics, *Temora longicornis*, temperature.

C. Möllmann and F. W. Köster: Institute of Marine Sciences, Düsternbrooker Weg 20, D-24105 Kiel, Germany [tel: +49 431 600-4557; fax: +49 431 600-1515; e-mail: cmoellmann@ifm.uni-kiel.de; fkoester@ifm.uni-kiel.de]. *Present address: Danish Institute for Fisheries Research, Charlottenlund Slot, DK-2920 Charlottenlund, Denmark [tel: +45 3396 3350; fax: +45 3396 3333; e-mail: fwk@dfu.min.dk]. G. Kornilovs and L. Sidrevics: Latvian Fisheries Research Institute, Daugavgrivas Street 8, LV-1007 Riga, Latvia [tel: +371 7613775; fax: +371 7616946; e-mail: georgs_k@latfri.lv]. Correspondence to C. Möllmann.*

Introduction

Mesozooplankton species, especially calanoid copepods, play an important role in the Baltic Sea ecosystem. Changes in the species composition have been shown to influence the growth of their major predators, the clupeid fish herring (*Clupea harengus*) and sprat (*Sprattus sprattus*) (e.g. Flinkman *et al.*, 1998). Recent individual-based modelling approaches have demonstrated the dependence of larval survival and consequently recruitment of cod (*Gadus morhua*) on the dynamics of their main prey species (Hinrichsen *et al.*, 2002).

Long-term dynamics of copepod species have been investigated in different parts of the Baltic Sea, and their abundance and biomass were shown to depend to a large extent on hydrographic conditions (Ojaveer *et al.*, 1998; Viitasalo, 1992; Viitasalo *et al.*, 1995; Vuorinen and Ranta, 1987; Vuorinen *et al.*, 1998; Möllmann *et al.*, 2000) controlled by climatic factors (Dippner *et al.*, 2000, 2001; Hänninen *et al.*, 2000). In the Central Baltic basins especially, decreasing salinities since the late 1970s, caused by increased river run-off (Bergström and Carlsson, 1994) and lower frequency of pulses of saline water intrusions from the North Sea and Skagerrak (Matthäus and Franck, 1992; Matthäus and Schinke, 1994) caused a declining biomass of *Pseudocalanus elongatus*, the dominant copepod in the area (Dippner *et al.*, 2000; Möllmann *et al.*, 2000). Two other important species, *Temora longicornis* and *Acartia* spp., were found to depend mainly on the prevailing temperature conditions in spring; *Acartia* spp. in particular showed a general increase in biomass in the 1990s, concurrent with prevailing relatively high temperature (Möllmann *et al.*, 2000).

Former studies from the Central Baltic investigated trends in total standing stocks of copepod species, while no stage-specific dynamics were considered. The latter may result in the identification of a critical life-stage or population dynamic processes driving the dynamics. Here we explored the stage-specific long-term dynamics of *P. elongatus, T. longicornis*, and *Acartia* spp. in the combined area of the Gdańsk Deep and the central Gotland Basin (Figure 1) and their association with temperature

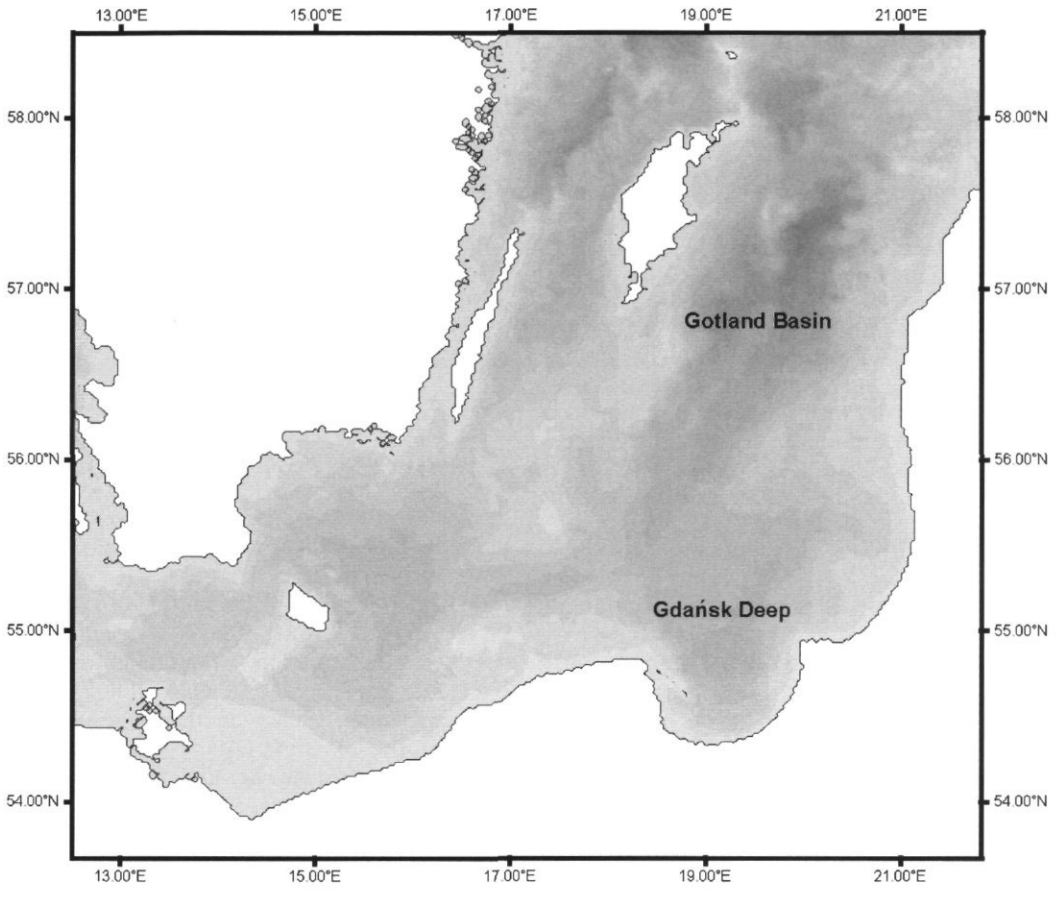


Figure 1. Map of the Central Baltic Sea with the area of investigation, i.e. the Gdańsk Deep and the Gotland Basin.

and salinity by using principal component (PCA) and correlation analysis.

Material and methods

Temperature and salinity

Temperature and salinity were measured by the Latvian Fisheries Research Institute (LATFRI) in Riga at 8 stations covering the Gdańsk Deep and the Central Gotland Basin. Measurements were performed during several cruises from 1961 to 1999 using a water sampler (Nansen type; 1l capacity) in 5 or 10-m steps. A Deep Sea Reversing Thermometer was used for temperature measurements, whereas salinity was measured either by the Knudsen Method (until 1992) or with an Inductivity Salinometer (since 1993).

Average values of temperature and salinity per season were calculated for the depth range 0–50 m, being the water layer mainly inhabited by *T. longicornis* and *Acartia* spp. (Sidrevics, 1979, 1984). As *P. elongatus*, especially the older stages, show a deeper distribution (Sidrevics, 1979 and 1984), the layer between 50 and 100 m was also considered for this species.

Copepod stage-specific abundance

Copepod abundance data were collected during seasonal surveys of LATFRI, i.e. mainly in February, May, August, and November (later called winter, spring, summer, and autumn, respectively) conducted from 1959 to 1999. Sampling was performed mostly in the daytime using a Jeddy Net (UNESCO Press, 1968) operating vertically with a mesh size of 160 µm and an opening diameter of 0.36 m. The gear is considered to quantitatively catch all copepodite stages as well as adult copepods, whereas nauplii may be underestimated (Anon., 1979).

Individual hauls were carried out in vertical steps, resulting in full coverage of the water column to a depth of 100 m at every station. For the present analysis, data from LATFRI stations in the Gdańsk Deep and the Central Gotland Basin were used. Each sample was divided into two subsamples. A mean value was calculated from both subsamples to derive the number per m^3. Nauplii (N), copepodites

I to V (CI–CV) as well as adult females (CVI-f) and males (CVI-m) of the species *P. elongatus, T. longicornis*, and *Acartia* spp. (including *A. bifilosa*, *A. longiremis*, and *A. tonsa*) were identified in the samples.

Numerical analyses

Data were log-transformed to stabilize the variance. Missing values in the original time-series were interpolated using a linear trend regression (Statsoft, 1996). Principal component analyses (PCA) for classification (Le Fevre-Lehoerff *et al.*, 1995) were conducted in order to investigate (i) differences in the time trends between the different copepod stages, and (ii) associations between specific stages and salinity and temperature. One PCA was performed for every season and species with eight biological descriptors (stages N, CI, CII, CIII, CIV, CV, CVI-f, CVI-m) as well as salinity and temperature as supplementary variables. Associations between the variables were displayed by correlations between the first two principal components.

Additionally, simple correlation analyses were performed for the main reproduction periods, i.e. spring for *P. elongatus* as well as spring and summer for *T. longicornis* and *Acartia* spp. To account for autocorrelation in the data, the degrees of freedom (d.f.) in the statistical tests were adjusted using the equation by Chelton (1984), modified by Pyper and Peterman (1998):

$$\frac{1}{N^*} = \frac{1}{N} + \frac{2}{N}\sum_j r_{XX}(j) r_{YY}(j) \qquad (1)$$

where N*, is the "effective number of degrees of freedom" for the time-series X and Y, N is the sample size, and rXX (j) and rYY (j) are the autocorrelation of X and Y at lag j. The latter were estimated using an estimator by Box and Jenkins (1976):

$$r_{XX}(j) = \frac{\sum_{t=1}^{N-j}(X_t - \overline{X})(X_{t+j} - \overline{X})}{\sum_{t=1}^{N}(X_t - X)^2} \qquad (2)$$

where $\overline{X}$ is the overall mean. We applied approximately N/5 lags in Equation (1), which ensures the robustness of the method (Pyper and Peterman, 1998).

Results

Temperature and salinity

Temperature in the upper 50 m showed a rather high interannual variability (Figure 2). Three marked peaks are visible in the winter and spring time-series: in the middle of the 1970s as well as in the early 1980s and 1990s. Fluctuations were less pronounced in the deeper water layer (50–100 m), but exhibited in general the same time-trend. Compared to the earlier decades, the 1990s appeared to be the warmest period.

The time-series on salinity are characterized by a fairly stable situation in the 1960s and 1970s. From the 1980s onwards salinity declined continuously in both depth layers. Whereas salinity increased again from the middle of the 1990s onwards in the lower depth layer, it declined further in the upper layer.

Pseudocalanus elongatus

The overwintering stock of *P. elongatus* is dominated by CIV and CV copepodites and additionally lower proportions of CIII and CVI (Figure 3). Peak reproduction takes place in spring, when mainly N and CI constituted the *P. elongatus* stock. In summer, these stages have developed further, resulting in a dominance of CII, CIII, and CIV. The overwintering stock builds up in autumn, comprising mainly CIII, CIV, and CV.

The time-series display a period of a high overwintering stock in the late 1970s to the middle of the 1980s. Before and after this period, abundance was low and decreased since the late 1980s. This development is also found in spring for CVI-f as well as for the dominating N and CI. The latter two stages, however, also showed a period of high abundance at the beginning of the time-series. All other copepodite stages experienced an undulating development during the observed period. In summer and autumn the dominating stages (CII–CV) again showed a peak abundance period in the 1970s and 1980s and a drastic decline during the 1990s.

PCAs revealed pronounced differences in the behaviour of the seasonally dominating stages in spring (Figure 6). A group comprising the adult (CVI) and the youngest stages (N, CI) is separated from the intermediate copepodites (CII–CV). Both groups also showed a different association to hydrography, with the first group being associated with salinity in both depth horizons and the second group being connected to temperature. Correlation analyses confirmed the pattern with significant positive associations between N and salinity as well as an indication of a relationship between CVI-f and salinity (Table 1A). In contrast, intermediate copepodite stages were significantly related to temperatures. A relatively high negative correlation between N and temperature, however, was not statistically significant.

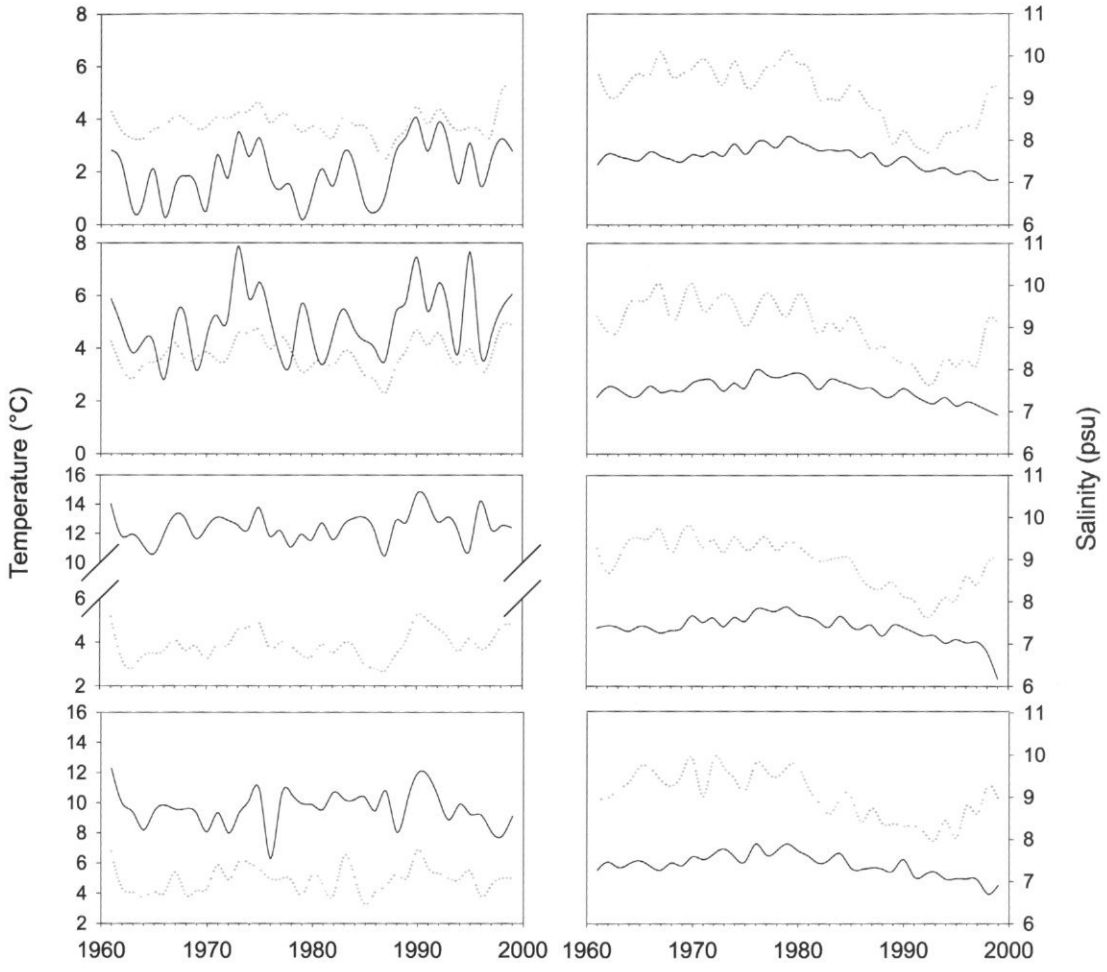


Figure 2. Seasonal time-series on temperature (left panels) and salinity (right panels); 1st row – winter, 2nd row – spring, 3rd row – summer, 4th row – autumn; solid line 0–50 m, dotted line 50–100 m.

Temora longicornis

T. longicornis hibernates mainly as CIV-CVI, although generally the overwintering stock is low compared to *P. elongatus* (Figure 4). Reproduction starts in spring and lasts throughout the year, as indicated by the continuous occurrence of N and the younger copepodite stages. Highest total abundance was found in summer, which coincides with the highest amount of CVI within the yearly cycle. In autumn, N and copepodites CI–CIV dominate with similar abundances.

The winter time-series showed increasing abundances of CIII–CV and CVI-f in the 1990s. Similarly in spring, exceptionally high standing stocks were observed for all stages from the late 1980s. Before the mid-1980s, spring abundances of all stages were low with an intermediate rise in the mid-1970s; however, only pronounced for N. Contrary to spring, the summer time-series is characterized by mainly low and decreasing abundances in the 1990s with the exception of CIII–CV, which were relatively abundant. Generally a high variability is encountered in the summer time-series with high values at the beginning for N and copepodites, but lower ones for CVI. A similar high variability is found in autumn with peaks in the middle of the 1970s for N and CI–III and in the early 1980s for CIV–CV. In the 1990s, the standing stock of N and CI was low and on average higher for CII-CIV.

PCAs revealed no clear associations between the stage-specific abundance of *T. longicornis* and the hydrographic variables in winter and autumn (Figure 6). On the contrary, in spring, all stages had high positive correlations with the first principal axis, as was observed for temperature. In summer, no association with temperature was obvious, while all stages showed negative correlations to the second principal axis, as was found for salinity. Correlation

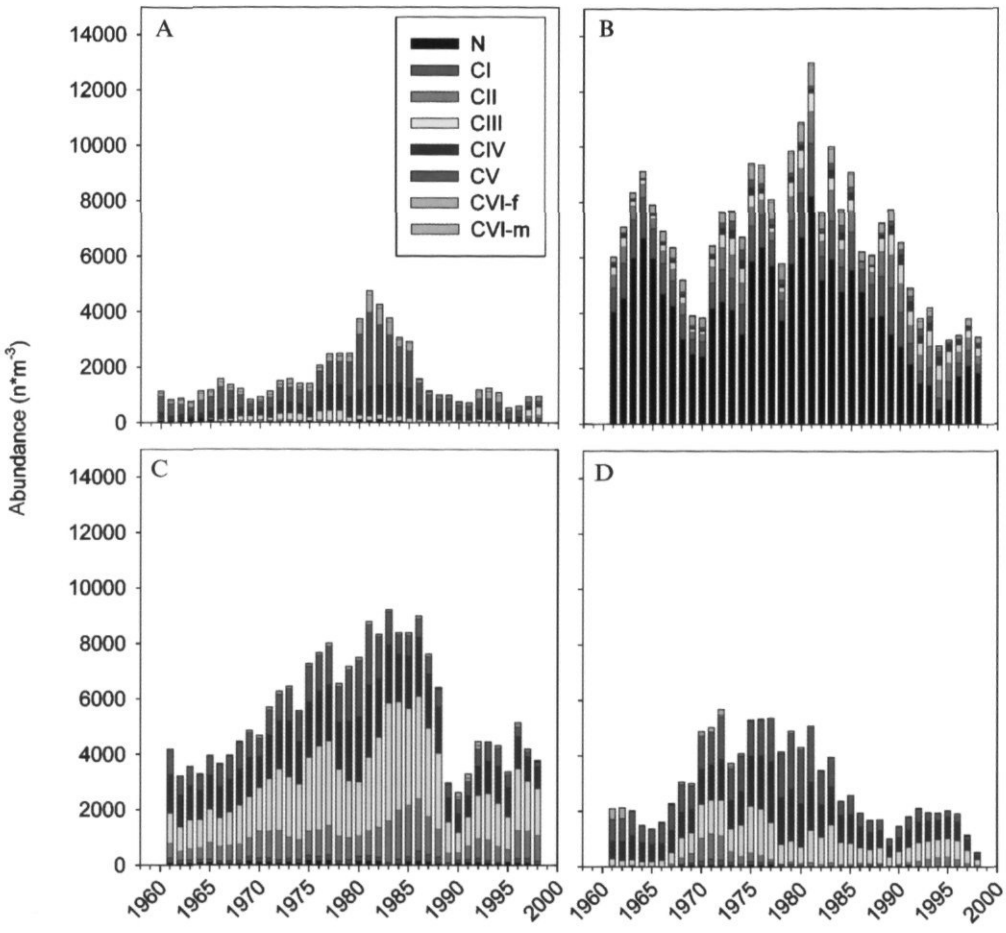


Figure 3. Seasonal time-series on stage-specific abundance of *Pseudocalanus elongatus*. Time-series are smoothed by a three-point running mean. (A) winter, (B) spring, (C) summer, (D) autumn.

analyses for the main reproductive periods confirmed a clear positive relationship between all stages and temperature in spring (Table 1B). The association to salinity is negative in spring, but significant only for CI and CII. In summer, correlations with salinity were positive but only significant for CI, CII, and CVI.

Acartia spp.

The seasonal dynamics of *Acartia* spp. are similar to those of *T. longicornis* (Figure 5). The overwintering stock is relatively small; reproduction starts in spring and lasts throughout the year. Peak abundance is in summer.

Increasing winter abundances of all stages were observed in the 1990s. Compared to *T. longicornis*, higher abundances of N and CVI-f of *Acartia* spp. were encountered showing a wave-like development. Also in spring the time-trend was comparable to that of *T. longicornis*, i.e. with a marked increase in abundance since the late 1980s for all stages. Contrary to *T. longicornis*, this stepwise increase in standing stock was also encountered in summer and autumn, although mainly for CII and older stages.

Similarly to *T. longicornis*, PCAs for *Acartia* spp. showed only a weak association between hydrographic variables and stage-specific abundance in winter and autumn, as well as in summer (Figure 6). In spring, all stages were associated with temperature, whereas there is a clear opposition to salinity. Correlation analyses confirmed a clear positive and highly significant relationship of all stages to temperature in spring (Table 1C). The association to salinity is negative in spring (significant only for CIII and CIV) and in summer (significant only for CIII–CV).

Table 1A. Correlation tests between *Pseudocalanus elongatus* stage-specific abundance and temperature and salinity time-series. N^{eff} = "effective" number of degrees of freedom, r = Pearson correlation coefficient, p = associated probability (α).

Stage	Salinity			Temperature		
	N^{eff}	r	p	N^{eff}	r	p
N	13	0.61	<0.001*	26	–0.25	0.119
CI	16	0.31	0.056	28	0.10	0.562
CII	16	–0.08	0.627	29	0.43	0.006*
CIII	27	–0.15	0.352	35	0.48	0.002**
CIV	19	–0.11	0.491	29	0.64	<0.001**
CV	19	–0.07	0.670	27	0.50	0.001**
CVI-f	15	–0.41	0.009	23	0.05	0.748
CVI-m	21	–0.10	0.563	32	-0.14	0.399

*Significant at 0.05 and ** at 0.01 level.

Table 1B. Correlation tests between *Temora longicornis* stage-specific abundance and temperature and salinity time-series. N^{eff} = "effective" number of degrees of freedom, r = Pearson correlation coefficient, p = associated probability (α).

Stage	Spring						Summer					
	Salinity			Temperature			Salinity			Temperature		
	N^{eff}	r	p	N^{eff}	r	p	N^{eff}	r	p	N^{eff}	r	p
N	17	–0.17	0.302	31	0.63	<0.001**	22	0.38	0.018	34	0.16	0.317
CI	20	–0.44	0.005*	32	0.66	<0.001**	26	0.43	0.006*	34	0.03	0.835
CII	19	–0.46	0.003*	32	0.73	<0.001**	28	0.45	0.004*	36	–0.21	0.196
CIII	14	–0.47	0.003	28	0.66	<0.001**	26	0.25	0.129	35	–0.20	0.218
CIV	23	–0.34	0.033	34	0.60	<0.001**	29	0.07	0.680	37	–0.17	0.289
CV	19	–0.15	0.367	31	0.56	<0.001**	23	0.15	0.362	35	0.05	0.770
CVI-f	19	–0.31	0.055	32	0.35	0.028**	23	0.39	0.015*	34	0.10	0.548
CVI-m	21	–0.01	0.948	32	0.32	0.045**	18	0.54	<0.001*	31	–0.04	0.800

*Significant at 0.05 and ** at 0.01 level.

Table 1C. Correlation tests between *Acartia* spp. stage-specific abundance and temperature and salinity time-series. N^{eff} = "effective" number of degrees of freedom, r = Pearson correlation coefficient, p = associated probability (α).

Stage	Spring						Summer					
	Salinity			Temperature			Salinity			Temperature		
	N^{eff}	r	p	N^{eff}	r	p	N^{eff}	r	p	N^{eff}	r	p
N	18	–0.04	0.797	29	0.48	0.002**	22	0.19	0.240	32	0.19	0.244
CI	15	–0.39	0.013	29	0.44	0.005*	24	–0.01	0.990	32	0.27	0.097
CII	11	–0.41	0.009	26	0.55	<0.001**	22	–0.37	0.021	33	–0.03	0.860
CIII	15	–0.50	0.001*	29	0.44	0.005*	21	–0.43	0.007*	31	–0.14	0.399
CIV	14	–0.58	<0.001*	28	0.55	<0.001**	13	–0.58	<0.001*	26	–0.11	0.524
CV	16	–0.37	0.020	30	0.46	0.003**	14	–0.51	0.001*	27	–0.03	0.863
CVI-f	11	–0.43	0.006	26	0.63	<0.001**	19	–0.17	0.303	30	0.10	0.539
CVI-m	18	–0.33	0.042	32	0.50	0.001**	25	–0.17	0.301	34	–0.06	0.703

*Significant at 0.05 and ** at 0.01 level.

Discussion

Temperature and salinity

Hydrographic conditions in the Central Baltic Sea are mainly controlled by climatic factors (Dippner *et al.*, 2000, 2001; Hänninen *et al.*, 2000). The North Atlantic Oscillation (NAO), the dominant signal of interannual variability in atmospheric circulation over Northern and Central Europe (e.g. Hurrell, 1995), has been clearly related to water temperature in the Central Baltic (Dippner *et al.*, 2000). Thus, the period of relatively high water temperatures in the 1990s was caused mainly by mild winters during the phase of high NAO in this period.

Similar to temperature, salinity in the Central Baltic is ultimately controlled by the large-scale

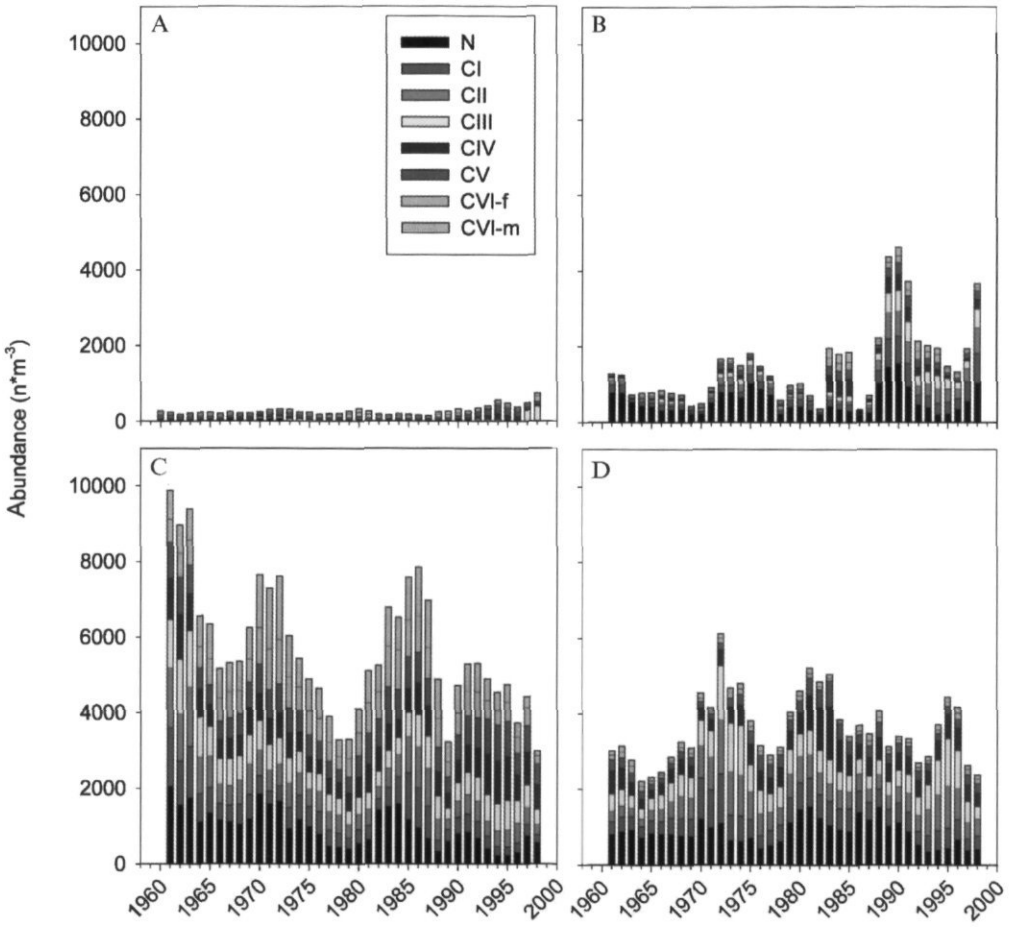


Figure 4. Seasonal time-series on stage-specific abundance of *Temora longicornis*. Time-series are smoothed by a three-point running mean. (A) winter, (B) spring, (C) summer, (D) autumn.

atmospheric circulation. A stronger meridional sea level pressure gradient over the North Atlantic since the 1980s resulted in an increase in rainfall and run-off, and consequently in reduced salinities at all depths (Zorita and Laine, 2000). Similarly, Hänninen *et al.* (2000) found a chain of events from NAO to freshwater run-off and deepwater salinity in the Gotland Basin. Salinity in and below the permanent halocline in the deep basins of the Central Baltic is mainly controlled by lateral advection of highly saline water from the North Sea (Matthäus and Franck, 1992; Matthäus and Schinke, 1994). The absence of these events between 1983 and 1993 was hypothesized to be due also to the changed atmospheric circulation along with intensified precipitation and run-off (Schinke and Matthäus, 1998; Hänninen *et al.*, 2000). The increase in salinity in the deep layer, observed in the presented time-series, was clearly a result of the last major inflow event in 1993.

Pseudocalanus elongatus

A clear stage-specific response of *P. elongatus* to the prevailing hydrographic conditions during the season of peak reproduction in spring is indicated. At this time of the year most of the CVI-f mature, and their number depends upon the size of the overwintering stock, which is dependent upon salinity. If salinity is low, fewer individuals reach the CV-stage in winter and are available for maturation in spring. Consequently, egg production and recruitment of N is low. A possible reason for this might be that low salinities cause osmotic stress and thus a higher energy requirement for this marine species. This may have resulted in retarded development and also lower egg production.

The development of the intermediate stages CII–CV in spring, and thus the development of older stages, is highly dependent on temperature; higher temperatures accelerate develoPment times.

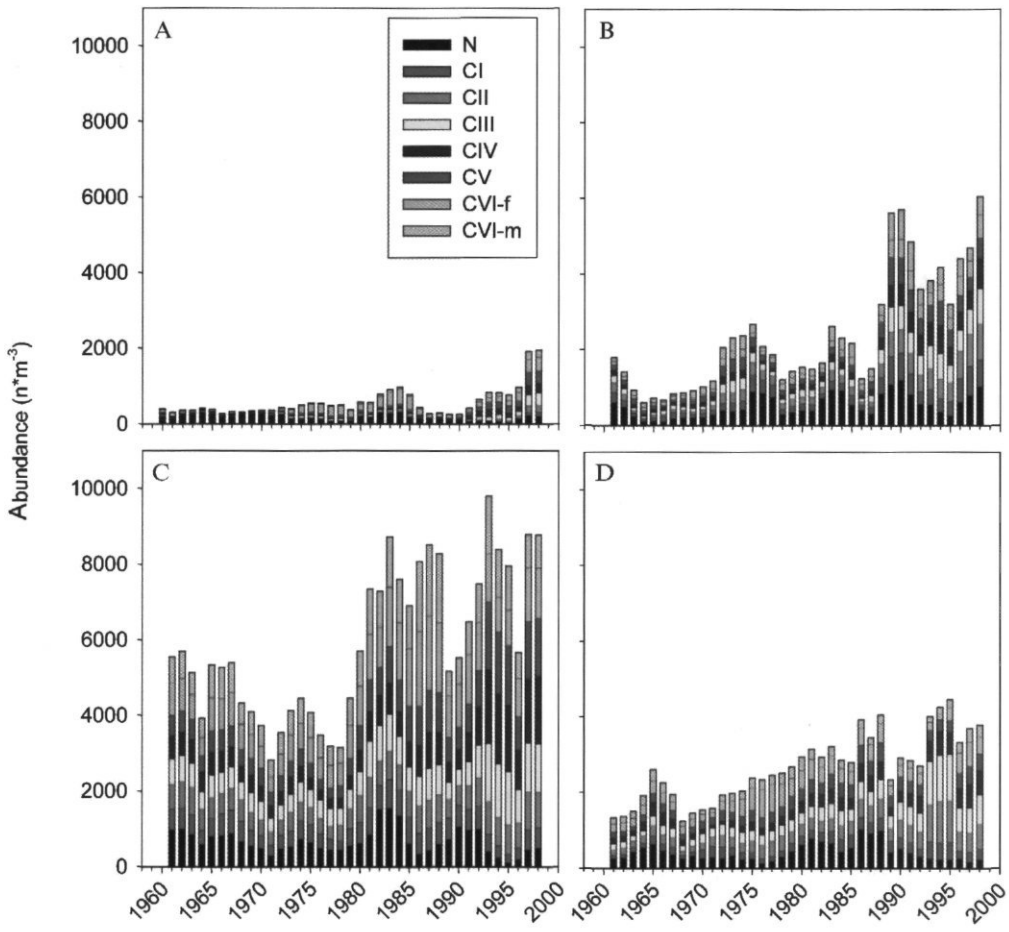


Figure 5. Seasonal time-series on stage-specific abundance of *Acartia* spp. Time-series are smoothed by a three-point running mean. (A) winter, (B) spring, (C) summer, (D) autumn.

However, as *P. elongatus* has only one generation in the Central Baltic (Line, 1979, 1984), the long-term dynamics of this species were triggered by the magnitude of the CVI-f stock formed in spring, which depends mainly on salinity. The peak recruitment period from the middle of the 1970s to the early 1980s is obviously caused by high CVI-f standing stocks during a period of high salinity. This peak in reproduction is carried through the rest of the year and determines the overwintering stock. With decreasing salinities in the last two decades the abundance of CVI-f decreased and so did N. Contradicting this, a period of high N abundance and relatively low CVI-f numbers was encountered during the 1960s. A possible explanation may be that low temperatures in this period favoured reproduction (Möllmann *et al.*, 2000). This is indicated by the negative correlation of N with temperature in spring, although it is not statistically significant.

Temora longicornis

In contrast to *P. elongatus*, all life-stages of *T. longicornis* showed a uniform association with higher temperatures in spring. For this copepod species, which has up to five generations per year (Line, 1979, 1984), the building up of the population in spring is obviously strongly dependent on the warming of upper water layers. Thus, the drastic increase in spring standing stocks during the 1990s appears to be coupled to the high water temperatures accelerating development times. The increase in winter standing stocks in the 1990s may be related to an earlier onset of the warming.

A further mechanism may be the activation of resting eggs due to the spring rise in temperature. *T. longicornis* is known to produce these dormant stages to overcome low winter temperatures (Madhupratab *et al.*, 1996). Although the eggs have until now only been found in the North Sea (Lindley,

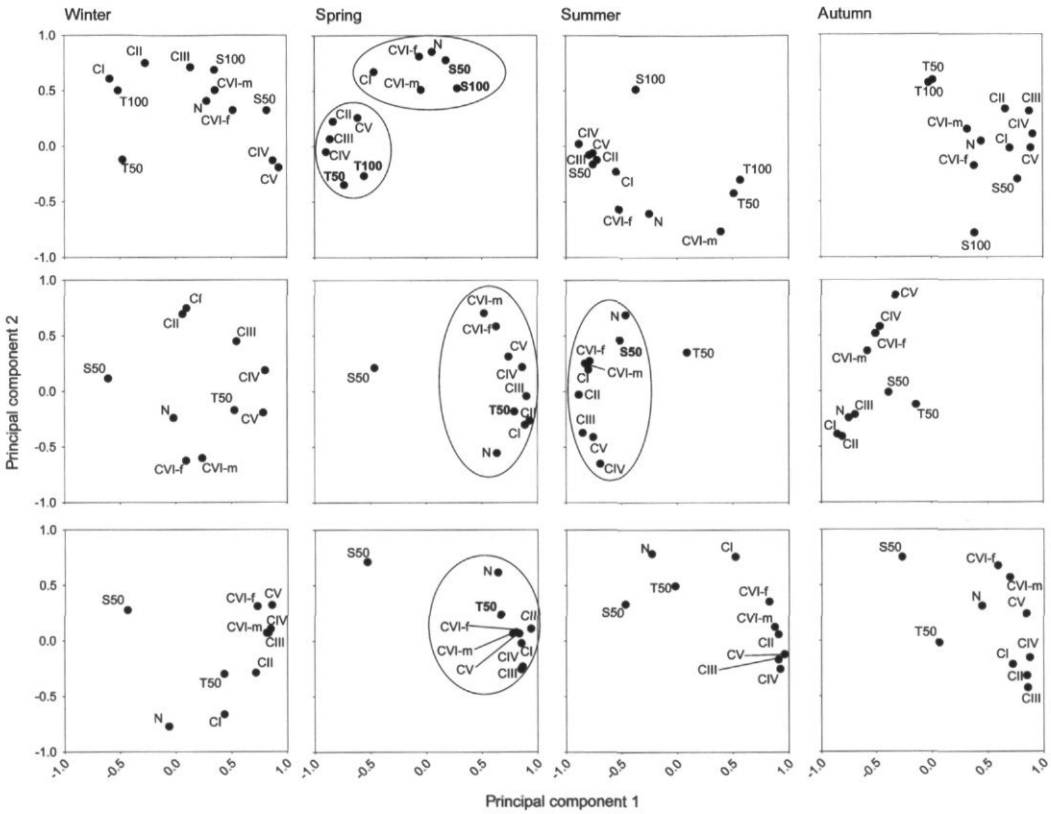


Figure 6. Results of principal component analyses (PCA): Correlation between the first 2 principal components per season and copepod species: 1st row – *Pseudocalanus elongatus*, 2nd row – *Temora longicornis*, 3rd row – *Acartia* spp.; T50 and S50 – average temperature and salinity in 0–50 m depth; T100 and S100 – average temperature and salinity in 50–100 m depth.

1986), it is very likely that they also occur in the Baltic (Madhupratab *et al.*, 1996).

The negative correlation of all stages with salinity in spring, although significant only for CI and CII, can be considered a result of the opposite development of temperature and salinity. To test this, additional multiple linear regression analyses were performed with temperature and salinity as independent variables, and the stage-specific abundance of *T. longicornis* as the dependent variable. Partial correlation coefficients for both independent variables were all highly significant for temperature ($p < 0.01$), whereas for salinity significant ($p < 0.05$) partial correlation coefficients were only found for CI, CII, and CIII. In all these cases coefficients for temperature were higher than for salinity, confirming temperature to be the most influential variable. We consider this finding reasonable, as *T. longicornis* is a species of marine origin not favouring explicitly low saline conditions (Raymont, 1983).

In summer the association to salinity was positive. Interestingly, significant correlations could be found only for CVI and the early stages CI and CII (with N being almost significant). Obviously maturation and consequently reproductive success of *T. longicornis* in summer, when temperature is generally sufficiently high, suffers similarly to *P. elongatus* from low salinities. The general decrease in summer abundance may thus be caused by the decreasing salinity.

Acartia spp.

The group of *Acartia* species has a similar life-cycle as *T. longicornis* with up to seven generations per year (Line, 1979, 1984) and PCAs as well as correlation analyses also revealed for *Acartia* spp. the significant association of all stages with temperature in spring. For *Acartia* spp., the beginning of population development is obviously also strongly dependent on spring warming, which explains the drastic increase in abundance during the warm 1990s. The activation of resting eggs, which is known to occur in the Baltic (Katajisto *et al.*, 1998; Madhupratab *et al.*, 1996; Viitasalo and Katajisto, 1994), may be especially important for this copepod.

Negative correlations with salinity were found again in spring and, in contrast to *T. longicornis*, in

summer. This suggests that reproduction of *Acartia* spp. in either season is favoured by lower salinities. To test whether the significant negative correlations with salinity are only due to the mainly opposite trend of the hydrographic variables, as found for *T. longicornis*, multiple linear regression analyses were conducted. As for *T. longicornis*, highly significant ($p < 0.01$) partial correlation coefficients in spring were found for temperature and all stages, whereas for salinity highly significant ($p < 0.01$) coefficients were derived only for CIII and CIV, and significant ($p < 0.05$) ones only for CII and CVI. In contrast, for summer, highly significant ($p < 0.01$) negative partial correlation coefficients were observed for CIII to CV and salinity, whereas coefficients for temperature were not significant. These results confirm that, in spring, temperature is the limiting factor, although lower salinities are favourable for *Acartia* spp.; this is especially true for summer.

The difference in summer response to salinity between *Acartia* spp. and *T. longicornis* is clearly visible in the time-series. A generally high abundance was found for *Acartia* spp. during the 1990s, whereas the standing stock of *T. longicornis* decreased.

Conclusions

Investigations of the long-term stage-specific dynamics of major Central Baltic copepod species provide new insights into the effects of hydrography. The study confirmed the impact of salinity during maturation and reproduction in spring on the stock development of *P. elongatus* (Möllmann *et al.*, 2000), but additionally a stage-specific response to temperature was detected. While lower temperatures are favourable for reproduction, the development of intermediate copepodite stages is accelerated by warmer conditions. The dynamics of *T. longicornis* and *Acartia* spp. are mainly related to temperature in spring as previously demonstrated (Dippner *et al.*, 2000; Möllmann *et al.*, 2000). Additionally, we show that in summer, when temperature is not critical, higher salinities favour the maturation and subsequent reproduction of *T. longicornis*, similar to *P. elongatus*.

In addition to hydrography, predation by planktivores (e.g. Rudstam *et al.*, 1994) may contribute to copepod dynamics. In particular, the drastically enlarged sprat stock (Köster *et al.*, 2001) may have the potential to control the stock of *P. elongatus* and *T. longicornis* (Möllmann and Köster, 1999, 2002). Also food availability can influence copepod dynamics, especially moulting and egg production (e.g. Berggreen *et al.*, 1988). In relation to this, competition between the copepod species may play a role. *Acartia* spp. may have taken advantage of the decreasing standing stock of *P. elongatus*, which may have contributed to the drastic increase in abundance. This issue needs further investigation, but unfortunately, to our knowledge, no reliable time-series on phytoplankton standing stocks are available for the area. Nevertheless, we believe that the main time-trends of the considered copepod species are explainable mainly by temperature and salinity changes.

Acknowledgements

We thank all persons from the Latvian Fisheries Research Institute in Riga involved in the setup of the databases forming the basis of the present analysis. Two referees considerably improved an earlier version of the manuscript. The study was carried out with financial support from the Commission of the European Union within the "Baltic Sea System Study" (BASYS; MAS3-CT96-0058) and the "Baltic STORE Project" (FAIR 98 3959). The article does not necessarily reflect the view of the Commission.

References

Anon. 1979. Recommendations on methods for marine biological studies in the Baltic Sea. In: Hernroth, L. (Ed.), Baltic Marine Biologists. 15 pp.

Berggreen, U., Hansen, B., and Kiørboe, T. 1988. Food size spectra ingestion and growth of the copepod *Acartia tonsa* during development: implications for determination of copepod production. Marine Biology, 99: 341–352.

Bergström, S., and Carlsson, B. 1994. River runoff to the Baltic Sea 1950–1990. Ambio, 23: 4–5.

Box, G. E. P., and Jenkins, G. W. 1976. Time Series Analysis: Forecasting and Control. Holden-Day, San Francisco, CA. xxi + 575 pp.

Chelton, D. B. 1984. Commentary: short-term climate variability in the Northeast Pacific Ocean: in the influence of ocean conditions on the production of salmonids in the North Pacific, pp. 87–99. Edited by W. Pearcy. Oregon State University Press, Corvallis, Oregon, USA.

Dippner, J. W., Hänninen, J., Kuosa, H., and Vuorinen, I. 2001. The influence of climate variability on zooplankton abundance in the northern Baltic Archipelago Sea (SW Finland). ICES Journal of Marine Science, 58: 569–578.

Dippner, J. W., Kornilovs, G., and Sidrevics, L. 2000. Long-term variability of mesozooplankton in the Central Baltic Sea. Journal of Marine Systems, 25: 23–32.

Flinkman, J., Aro, E., Vuorinen, I., and Viitasalo, M. 1998. Changes in northern Baltic zooplankton and herring nutrition from 1980s to 1990s. Top-down and bottom-up processes at work. Marine Ecology Progress Series, 165: 127–136.

Hänninen, J., Vuorinen, I., and Hjelt, P. 2000. Climatic factors in the Atlantic control the oceanographic and ecological changes in the Baltic Sea. Limnology and Oceanography, 45: 703–710.

Hinrichsen, H.-H., Möllmann, C., Voss, R., Köster, F. W., and Kornilovs, G. 2002. Bio-physical modelling of larval Baltic cod (*Gadus morhua*) growth and survival. Submitted to Canadian Journal of Fisheries and Aquatic Sciences.

Hurrell, J. W. 1995. Decadal trends in the North Atlantic Oscillation and regional temperature and precipitation. Science, 269: 676–679.

Katajisto, T., Viitasalo, M., and Koski, M. 1998. Seasonal occurrence and hatching of calanoid eggs in sediments of the northern Baltic Sea. Marine Ecology Progress Series, 163: 133–143.

Köster, F. W., Möllmann, C., Neuenfeldt, S., St. John, M. A., Plikshs, M., and Voss, R. 2001. Developing Baltic cod recruitment models. I: Resolving spatial and temporal dynamics of spawning stock and recruitment. Canadian Journal of Fisheries and Aquatic Sciences, 58: 1516–1533.

Le Fevre-Lehoerff, G., Ibanez, F., Poniz, P., and Fromentin, J. M. 1995. Hydroclimatic relationships with planktonic time series from 1975 to 1992 in the North Sea off Gravelines, France. Marine Ecology Progress Series, 129: 269–281.

Lindley, J. A. 1986. Dormant eggs of calanoid copepods in sea-bed sediments of the English Channel and southern North Sea. Journal of Plankton Research, 8: 399–400.

Line, R. J. 1979. Some observations on fecundity and development cycles of the main zooplankton species in the Baltic Sea and the Gulf of Riga. In: Fisheries investigations in the basin of the Baltic Sea. Riga, Zvaigzne, 14: 3–10. (In Russian.)

Line, R. J. 1984. On reproduction and mortality of zooplankton (Copepoda) in the south-eastern, eastern and north-eastern Baltic. In: Articles on Biological Productivity of the Baltic Sea. Moscow, 2: 265–274. (In Russian.)

Madhupratab, M., Nehring, S., and Lenz, J. 1996. Resting eggs of zooplankton (Copepoda and Cladocera) from the Kiel Bay and adjacent waters (southwestern Baltic). Marine Biology, 125: 77–87.

Matthäus, W., and Franck, H. 1992. Characteristics of major Baltic inflows: a statistical analysis. Continental Shelf Research, 12: 1375–1400.

Matthäus, W., and Schinke, H. 1994. Mean atmospheric circulation patterns associated with major Baltic inflows. Deutsche Hydrographische Zeitschrift, 46: 321–339.

Möllmann, C., and Köster, F.W. 1999. Food consumption by clupeids in the Central Baltic: evidence for top-down control? ICES Journal of Marine Science, 56 (Suppl): 100–113.

Möllmann, C., and Köster, F. W. 2002. Population dynamics of calanoid copepods and the implications of their predation by clupeid fish in the Central Baltic Sea. Journal of Plankton Research. (In press.)

Möllmann, C., Kornilovs, G., and Sidrevics, L. 2000. Long-term dynamics of main mesozooplankton species in the Central Baltic Sea. Journal of Plankton Research, 22: 2015–2038.

Ojaveer, E., Lumberg, A., and Ojaveer, H. 1998. Highlights of zooplankton dynamics in Estonian waters (Baltic Sea). ICES Journal of Marine Science, 55: 748–755.

Pyper, B. J., and Peterman, R. M. 1998. Comparison of methods to account for autocorrelation in correlation analyses of fish data. Canadian Journal of Fisheries and Aquatic Sciences, 55: 2127–2210.

Raymont, J. E. G. 1983. Plankton and Productivity in the Oceans, 2nd edn, vol. 2: Zooplankton. Pergamon Press. 824 pp.

Rudstam, L. G., Aneer, G., and Hildén, M. 1994. Top-down control in the pelagic Baltic ecosystem. Dana, 10: 105–129.

Schinke, H., and Matthäus, W. 1998. On the causes of major Baltic inflows and analysis of long time series. Continental Shelf Research, 18: 67–97.

Sidrevics, L. L. 1979. Some peculiarities of vertical distribution of zooplankton in the Central Baltic. In: Fisheries investigations in the basin of the Baltic sea. Riga, Zvaigzne, 14: 11–19. (In Russian.)

Sidrevics, L. L. 1984. The main peculiarities of zooplankton distribution in the South-eastern, Eastern and North-eastern Baltic. In: Articles on Biological Productivity of the Baltic Sea. Moscow, 2: 172–187. (In Russian.)

Statsoft. 1996. STATISTICA for Windows. StatSoft Inc., Tulsa, USA.

UNESCO Press. 1968. Zooplankton sampling. Monographs on Oceanographic Methodology, 2. 174 pp.

Viitasalo, M. 1992. Mesozooplankton in the Gulf of Finland and Northern Baltic proper: a review of monitoring data. Ophelia, 35: 147–168.

Viitasalo, M., and Katajisto, T. 1994. Mesozooplankton resting eggs in the Baltic Sea: identification and vertical distribution in laminated and mixed sediments. Marine Biology, 120: 455–465.

Viitasalo, M., Vuorinen, I., and Saesmaa, S. 1995. Mesozooplankton dynamics in the northern Baltic Sea: implications of variations in hydrography and climate. Journal of Plankton Research, 17: 1857–1878.

Vuorinen, I., and Ranta, E. 1987. Dynamics of marine mesozooplankton at Seili, Northern Baltic Sea, in 1967–1975. Ophelia, 21: 31–48.

Vuorinen, I., Hänninen, J., Viitasalo, M., Helminen, U., and Kuosa, H. 1998. Proportion of copepod biomass declines together with decreasing salinities in the Baltic Sea. ICES Journal of Marine Science, 55: 767–774.

Zorita, E., and Laine, A. 2000. Dependence of salinity and oxygen concentrations in the Baltic Sea on large-scale atmospheric circulation. Climate Research, 14: 25–41.

ICES Marine Science Symposia, 219: 231–240. 2003.

On the coupling between climate, hydrography, and recruitment variability of fishery resources off West Greenland

Erik Buch, Mads Hvid Nielsen, and Søren Anker Pedersen

Buch, E., Nielsen, M. H., and Pedersen, S. A. 2003. On the coupling between climate, hydrography, and recruitment variability of fishery resources off West Greenland. – ICES Marine Science Symposia, 219: 231–240.

In this article we review the past 50 years of climatic conditions off West Greenland, where there has been large variability in the atmospheric and oceanographic conditions as well as in fish stocks. A positive relationship is found between the hydrographic conditions expressed by the water temperature and the fish recruitment of cod and redfish, whereas the recruitment of shrimp and halibut seems to react positively to lower temperatures. Observed shifts in the hydrographic conditions during the second half of the 1990s indicate that a change in the fish stock environment may be expected in the coming years. Relationships between the past variations in fisheries resources, hydrographic conditions, and the large-scale climatic conditions expressed by the North Atlantic Oscillation (NAO) strongly support the incorporation of environmental variability in prediction models for fish stock recruitment and thereby in the assessment of fisheries resources.

Keywords: biomass, climate, cod, fishery, Greenland, salinity, shrimp, temperature, variability.

E. Buch and M. H. Nielsen: Danish Meteorological Institute, Lyngbyvej 100, DK-2100 Copenhagen, Denmark [tel: +45 39 157210; fax: +45 39 270684; e-mail: ebu@dmi.dk and mhn@dmi.dk]. S. A. Pedersen: Greenland Institute of Natural Resources, Kavalergaarden 6, DK-2920 Charlottenlund, Denmark [tel: +45 33963406; fax: +45 33963434; e-mail: sap@dfu.min.dk]. Correspondence to E. Buch.

Introduction

In the 20th century, Greenland experienced two great transitions, one from seal hunting to cod fishery, the other from cod to shrimp fishery, both affecting the human population centres of West Greenland and the economy (Hamilton *et al.*, 2000). The economic transitions reflected large-scale shifts in the underlying marine ecosystems, driven by interactions between climate and human resource use.

The marine shelf ecosystems off East and West Greenland are intermediate between the cold Polar water masses of the Arctic region and the temperate water masses of the Atlantic Ocean. They are important fishing grounds and are characterized by relatively few dominant species which interact strongly (Pedersen and Kanneworff, 1995; Rätz, 1999; Pedersen and Zeller, 2001). Ocean currents that transport water from the polar and temperate regions affect the marine productivity in the Greenland shelf areas, and changes in the North Atlantic circulation system therefore have major impacts on the distribution of species and fisheries yield (Pedersen and Smidt, 2000; Pedersen and Rice, 2001).

The climate around Greenland has undergone major changes during the 20th century. The period 1920–1970 was generally warm, while the subsequent 30 years were dominated by three extremely cold periods: around 1970, the early 1980s, and the early 1990s. These atmospheric changes are also reflected in the oceanographic conditions of Greenland waters (Buch, 2000a, b).

In assessments of fishery resources, information on how climate changes will affect the fish species composition and future fisheries in Greenland waters will be extremely valuable.

In this article we describe the recent development in the West Greenland fishery, climate, and hydrography using available time-series, indices of biological and climatic variability, and discuss possible relationships.

Biological variability

A rich Atlantic cod (*Gadus morhua*) fishery started off West Greenland in the 1920s after a general warming of the northern hemisphere (Dickson *et al.*, 1994; Buch *et al.*, 1994; Horsted, 2000). The West

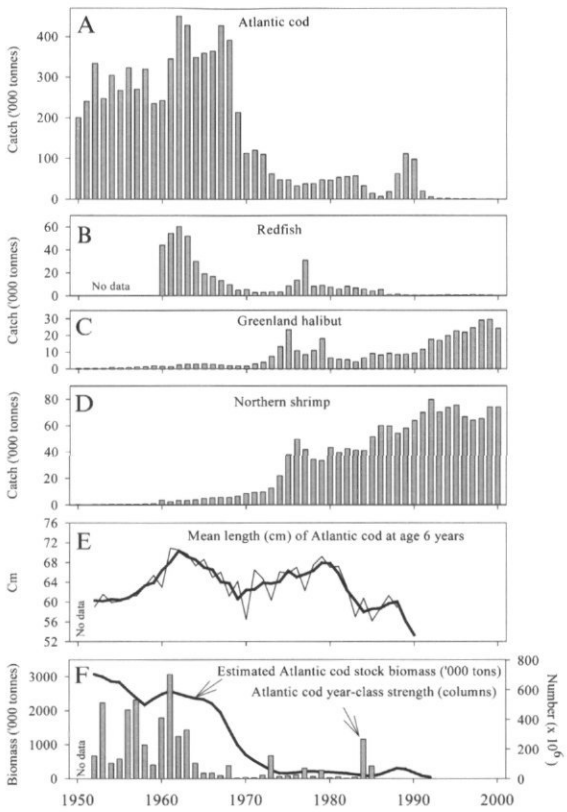


Figure 1. (A–D) Catches of the four major commercial fish species off West Greenland (NAFO Subarea 1, inshore and offshore combined) from Horsted (2000) and NAFO Scientific Council Meeting Reports and Documents for 2001 at www.nafo.ca. (E) The mean length of age 6 West Greenland cod from Riget and Engelstoft (1998) (where the heavy line is the 3-year running mean) and (F) their year-class strength from ICES (1996, 2000b).

Greenland cod fishery peaked in the 1960s at annual catches of between 400 000 and 500 000 t. During the late 1960s, the cod catches declined dramatically, as did the catches of other commercially important fish species – redfish (*Sebastes marinus* and *S. mentella*), Atlantic halibut (*Hippoglossus hippoglossus*), and wolffish (Atlantic wolfish (*Anarhichas lupus*) and spotted wolffish (*A. minor*)) – mainly taken as bycatch in the fishery for cod. After 1969, catches of cod and redfish fluctuated around a much lower mean than prior to the late 1960s (Figure 1).

With the exception of a temporary improvement of the cod abundance during 1988–1990, due to the strong 1984 year-class recruited from Iceland, data from the annual groundfish survey for cod on the West Greenland shelf (0–400 m depth) conducted by Germany since 1982 show a dramatic decline in overall biomass and size (mean individual weight) of fish (Rätz, 1999).

The decline in the amount caught is not the only supposed effect of climate change on the Greenland cod. The centre of the cod fishery moved south during the 1980s, and the sizes of fish at age also declined (Hovgård and Buch, 1990; Riget and Engelstoft, 1998; Horsted, 2000). At the same time, catches of two other commercially important species, northern shrimp (*Pandalus borealis*) and Greenland halibut (*Reinhardtius hippoglossoides*), increased (Figure 1). In recent years a new fishery for snow crab (*Chionoectes opilio*) shows a steep increasing trend from a few hundred tonnes in 1994 to close to 5000 t in 1999.

During the past two decades, northern shrimp has been by far the most important fishery resource in Greenland. The export of shrimp to Japan has provided a high-value economic alternative to cod, comprising 73% of Greenland's total exports in 1995. The shrimp stock off West Greenland is distributed from 60 to 73°N. There is no evidence of distinct subpopulations and the entire shrimp stock is assessed as a single population. Overall shrimp catches increased until 1992, varied at slightly lower levels from 1993 to 1998, and increased thereafter (see Figure 1).

From 1975 to 1984, the annual effort in the shrimp fishery showed a slightly increasing trend from about 75 000 to about 93 000 h. In the subsequent years a considerable enlargement of the offshore fleet took place and effort went up by a factor of almost 3, reaching 250 000 h in 1991–1992 (Figure 2). Thereafter effort decreased as a result of management measures and a general increased fishing efficiency of the participating vessels. The

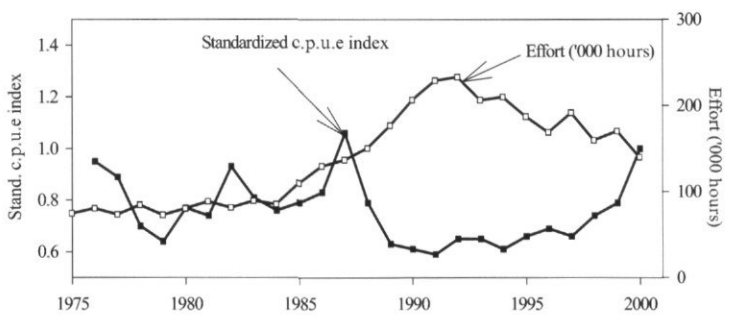


Figure 2. Effort and standardized c.p.u.e. index of the West Greenland shrimp fishery 1975–2000 from Siegstad (2000).

catch per unit effort (c.p.u.e.) time-series for the West Greenland shrimp fishery can be used as a stock biomass index (Figure 2). The marked spike in 1987 is likely to be the result of some very strong year classes produced in the early 1980s. From 1990 to 2000 the c.p.u.e. indices show an increasing trend indicating an increasing shrimp stock biomass.

The Greenland Fisheries Research Institute (GFRI) has conducted annual stratified-random shrimp trawl surveys since 1988 in the main West Greenland shrimp distribution area (Carlsson and Kanneworff, 2000). For the period 1988–1997, biomass indices of the fishable shrimp stock in the offshore areas were stable at a level of about 250 000 t (Figure 3A). From 1998 the biomass indices show a significant increase to a record high biomass estimate in the year 2000 of 350 000 t.

A change in geographical distribution of the commercial fishing effort has been observed since the late 1980s (Hvingel, 2000). Up through the 1990s

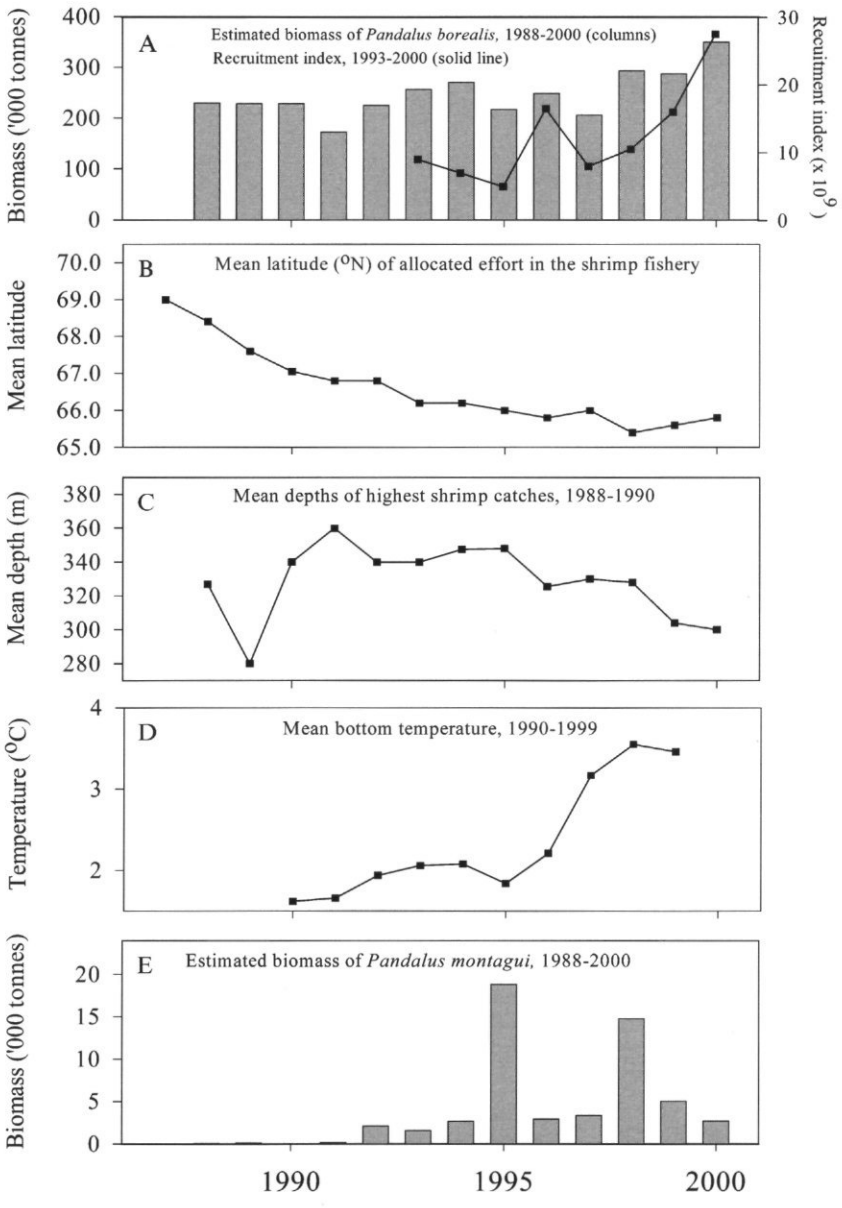


Figure 3. (A) Northern shrimp biomass indices from the annual shrimp survey and (B) the mean latitude of the effort in the commercial fishery from Siegstad (2000). (C) Mean depths of highest shrimp catches and (D) mean bottom temperature during the survey from Carlsson and Kanneworff (2000, 1999), respectively. (E) The annual biomass indices of *Pandalus montagui* during the survey from Kanneworff (2000).

the fishery has gradually moved southward, as indicated by the mean latitude of effort allocation (Figure 3B). At the same time the highest shrimp catches in the annual shrimp survey showed a trend of moving towards shallower depths (Figure 3C). The changes in shrimp catch distributions observed during the survey period, both geographical and over depth, may indicate stock migrations towards preferable habitat temperatures due to changes in the ocean climate in the same period. From 1995 to 1999 the average sea bottom temperature during shrimp surveys (July–August) show a clear increasing trend (Figure 3D). However, the increasing bottom temperature has not yet moved the mean latitude of the commercial fishery northward again (Figure 3B).

During the 1990s there was a slight increase in catches of striped pink shrimp (*Pandalus montagui*) in local commercial fishing areas and during the annual shrimp survey (Figure 3E). This shrimp species is well adapted to cold conditions and the increased catches may indicate a positive biological effect on this cold ocean climate species from the late 1980s to the mid-1990s. The peaks in abundance indices from the shrimp survey in 1995 and 1998 are unexplained (Kanneworff, 2000), but a lag between increased larval production and recruitment to the catchable stock should be expected.

From 1950 to 1984, GFRI collected annual zooplankton samples in June–July from West Greenland waters. The zooplankton displacement volume and most of the zooplankton taxa showed higher abundance indices in the generally warmer period 1950–1968 compared to the colder period 1969–1984 (Pedersen and Smidt, 2000). However, abundance indices of sandeel larvae were negatively correlated with sea temperature. Historic sandeel and shrimp larvae abundance indices (1950–1984, in Pedersen and Rice, 2001) updated with abundance indices from zooplankton samples collected in 1996, 1999, and 2000 showed similar trends and correlated positively ($r = 0.48$, $p < 0.05$, $n = 23$; Spearman rank correlation).

Climate variability

Oceanographic measurements have been made at least once a year by the GFRI, since its foundation in 1947, along the NAFO (earlier International Commission for North Atlantic Fisheries) standard sections off the west coast of Greenland. The Fylla Bank Section was for many years occupied several times per year. Additional observations were collected at trawl sites during fisheries surveys. The Danish Meteorological Institute (DMI) has carried out meteorological observations in Greenland since 1873 and has, for almost the same period, collected information on the distribution of sea ice in Greenland waters. The West Greenland area has experienced some fairly dramatic fluctuations in climate over the past 50 years, which have influenced the living conditions of all species on land as well as in the ocean. These fluctuations may therefore be regarded as one of the reasons for the observed variability in the various fish stocks described in the previous paragraph.

Several articles over the past decade have dealt with the importance of the North Atlantic Oscillation Index (NAO index) in forming the climate in the North Atlantic region (Dickson *et al.*, 1996, 2000; Blindheim *et al.*, 2000) and thereby also in the West Greenland area (Buch, 2000b). A simple NAO index was defined by Hurrell (1995) as the difference between the normalized mean winter (December–March) SLP anomalies at Lisbon, Portugal, and Stykkisholmur, Iceland. The SLP anomalies at each station were normalized by dividing each seasonal pressure by the long-term mean (1964–1995) standard deviation.

The variability in the NAO index since 1864 is shown in Figure 4, where the heavy solid line represents the low-pass filtered meridional pressure gradient. Positive values of the index indicate stronger than average westerlies over the mid-latitudes associated with low-pressure anomalies over the region of the Icelandic Low and anomalous high pressures across the subtropical Atlantic.

In addition to a large amount of interannual variability, there have been several periods when the NAO index persisted in one phase for many winters (Barnett, 1985; Hurrell and van Loon, 1997). Over the region of the Icelandic Low, the seasonal pressures were anomalously low during winters from the turn of the century until about 1930 (with the

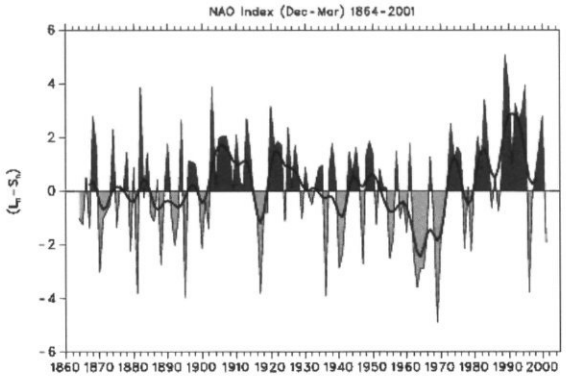


Figure 4. Time-series of the winter (December–March) index of the NAO (as defined in the text) from 1864–2001. The heavy solid line represents the meridional pressure gradient smoothed with low-pass filter to remove fluctuations with periods less than 4 years. (Updated from Hurrell and van Loon, 1997). (www.cru.uea.ac.uk/cru/data/nao.htm)

exception of the 1916–1919 winters), while pressures were higher than average at lower latitudes. Consequently, the wind over Europe had a strong westerly component and the moderating influence of the ocean contributed to higher than normal temperatures over much of Europe (Parker and Folland, 1988). From the early 1940s until the 1960s, the NAO index exhibited a downward trend into the extremely low NAO of the 1960s, and this period was marked by European wintertime temperatures that were frequently lower than normal (Moses *et al.*, 1987). A sharp reversal has occurred over the past 30 years and, since 1970, the NAO has remained in a highly positive phase, with SLP anomalies of more than 3 mb in magnitude over both the subpolar and the subtropical Atlantic (Figure 5). The 1983, 1989, 1990, 1994, and 1995 winters were marked by some of the highest positive values of the NAO index recorded since 1864 (Figure 4).

A detailed analysis suggests that the recent temperature anomalies of the North Atlantic and surrounding land masses have been strongly related to the persistent and exceptionally strong positive phase of the NAO index since the early 1980s (Hurrell and van Loon, 1997). This clearly illustrates a strong correlation between the strength of the westerlies across the North Atlantic, the NAO index, and the climate in Greenland and Europe. It also shows that the climate in Greenland and the climate in Europe are negatively correlated (Figure 5). West Greenland offshore air masses were significantly warmer in the 1960s than in the 1990s. A detailed analysis using wind observations (6-h intervals) from a number of observation sites in Greenland shows that changes in the wind pattern in the Greenland area are minor because of the large influence of the local orography.

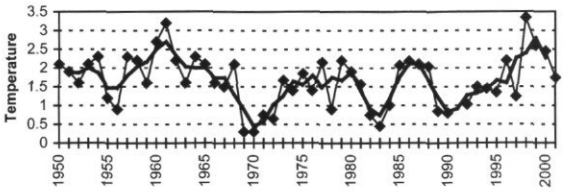


Figure 6. Mean sea temperatures of the upper 40 m on Fylla Bank Stn 2, medio June, 1950–2001. Dots = observations; heavy line = 3-year running mean.

The waters off West Greenland are dominated by the advection of water masses (Buch, 2000a, b):

- In the surface layer close to the coast, cold and low saline Polar Water originates from the East Greenland Current.
- Water below and to the west of the Polar Water derives from the North Atlantic Current.

The changes in the atmospheric conditions caused by the shift from low NAO to high NAO conditions have affected the ocean circulation and ocean conditions in the North Atlantic (Dickson *et al.*, 1996, 2000). These in turn have affected the oceanographic conditions off West Greenland. The most complete oceanographic time-series from West Greenland is the mid-June mean temperature on top of Fylla Bank (Fylla Bank Stn 2, 0–40 m; Figure 6), which the Greenland Fisheries Research Institute has carefully maintained.

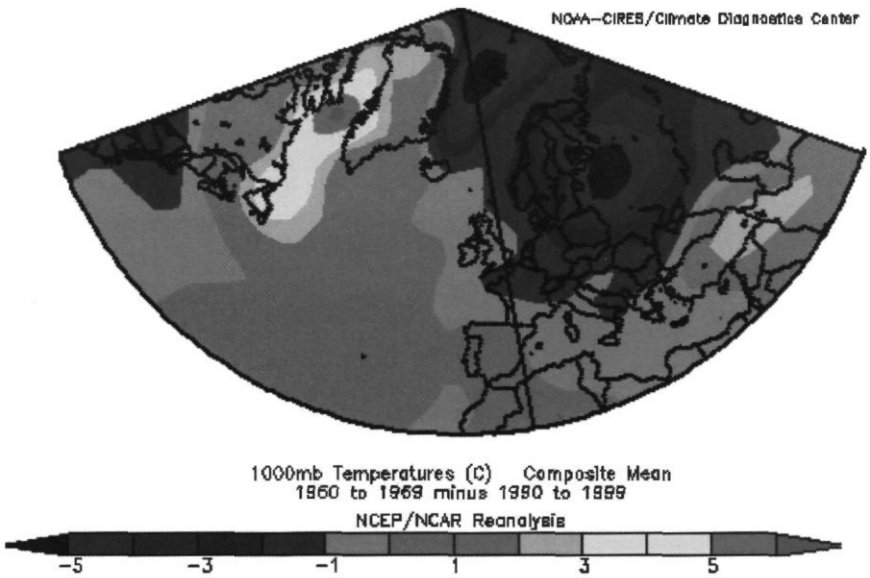


Figure 5. Difference in air temperatures at the 1000 mb level between 1960–1969 and 1990–1999, calculated using the NCEP/NCAR re-analysis database (www.cdc.noaa.gov).

The temperature can vary dramatically from one year to the next, often by more than 1°C, reflecting the variability of both the atmospheric forcing and the inflow of Polar Water. The curve showing the 3-year running mean values smoothes the variations and better reflects the large-scale climatic variability.

The 50-year temperature time-series reveals some very distinct climatic events:

- The 1950–1968 period generally showed high temperatures around 2°C above normal.
- The coldest period was experienced around 1970. The cold climate of this period was due to an anomalous high inflow of Polar Water, which was closely linked to the "Great Salinity Anomaly" (Dickson *et al.*, 1988; Belkin *et al.*, 1998). In the same period the NAO negative index changing to positive indices reflected in a shift from warm to cold atmospheric conditions.
- In the early 1980s and early 1990s two extremely cold periods were observed reflecting the cold atmospheric conditions associated with the high NAO indices during these years.
- A remarkably low temperature was observed in 1997, although the atmospheric conditions were quite warm. Along with low salinity measurements (Figure 7), this indicates a high inflow of Polar Water.
- During recent years, temperatures have been fairly high despite high NAO values. This was due to a displacement of the NAO pattern towards the east or northeast (ICES, 2000a).

Figure 7 shows the time-series of the mid-June salinity on top of Fylla Bank (actual observations as well as a 3-year running mean). The "Great Salinity Anomaly" around 1970 is clearly reflected in this data set, while the high NAO indices in the early 1980s and 1990s do not show up in any significant way in the surface salinities at Fylla Bank, which of course was not to be expected because these cold periods were due to atmospheric cooling.

Relatively low salinities were observed in 1996 and 1997, indicating that the inflow of Polar Water was above normal in these years.

At greater depth three water masses of Atlantic origin are found (Buch, 2000b):

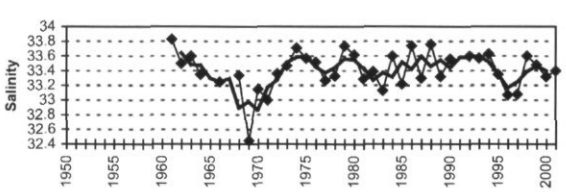


Figure 7. Mean salinity of the upper 40 m on Fylla Bank Stn 2, medio June 1961–2001. Dots = observations; heavy line = 3-year running mean.

- *Irminger Water* – temperature around 4.5°C and salinity above 34.95.
- *Irminger Mode Water* – Irminger Water mixed with surrounding water masses on its way to Southwest Greenland – temperature around 4°C and salinities between 34.85 and 34.95.
- *Northwest Atlantic Mode Water* – Temperature above 2°C and salinities between 34.5 and 34.85. In late autumn the temperatures rise to above 5°C.

Analysis of temperature and salinity data collected off West Greenland over the past six to seven decades are given in Figure 8 showing time-series of temperature, salinity, and density from stations just west of the shelf at the Cape Farewell and Fylla Bank sections, respectively. It is seen that the inflow of water of Atlantic origin has changed. Before the 1970s pure Irminger Water ($S > 34.95$) was present at the Cape Farewell Stn 3 in large quantities at depths greater than 100–400 m, although the inflow was gradually decreasing. It was also noticed that the heat inflow was markedly greater at that time with temperatures above 4.5°C in the entire upper 600 m water column; the upper 200 m had temperatures above 5.5°C. Since 1970, Irminger Water has only been observed in smaller quantities after 1995 and a similar statement can be given for temperatures above 5.5°C. In the intermediate period the dominant water mass was Irminger Mode Water. The increased activity in the circulation of Irminger Water has also been observed in the interior of the Irminger Sea after 1995 (Mortensen and Valdimarsson, 1999).

At the Fylla Bank Stn 4 we observed a similar trend in reduced inflow of salt and heat. The Irminger Mode Water was present in much higher quantities before the mid-1970s than after, and we notice that the three cold periods are clearly reflected in the temperatures of the upper 200 m. A weak freshening in the upper 150–200 m has additionally been observed since 1965, resulting in a less dense water mass within this layer. This freshening, however, is most dominant in the upper 50–100 m. A similar freshening during the same period has also been observed in the Irminger Water component north of Iceland (Malmberg, 1985), indicating a reduction in the strength of the Irminger Current after 1965 and/or a more dominant influence of Polar Water. From the mid-1960s to the early 1970s, the freshening was caused by an anomalous high inflow of Polar Water closely linked to the "Great Salinity Anomaly", whereas afterwards it is believed to have been caused by a high NAO anomaly reducing the strength of the Irminger Current both directly by the increased windstress forcing the North Atlantic Current towards east and indirectly by spinning up the Irminger gyre resulting in an increasing surface Ekman transport out from the centre.

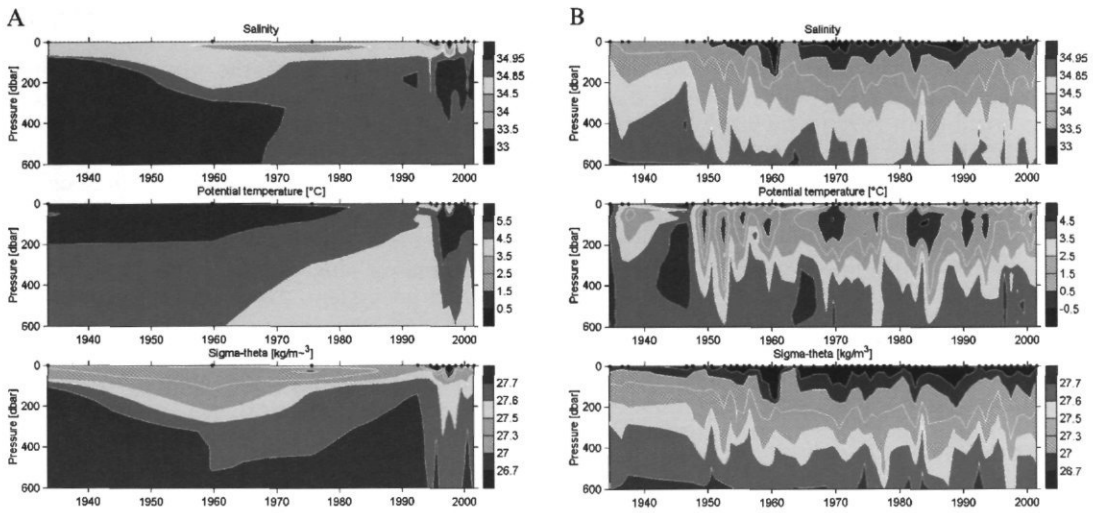


Figure 8. Time-series of summer (June to August) salinity, temperature, and density at (A) Cape Farewell Stn 3, (B) Fylla Bank Stn 4.

Discussion

The shift in community structure and landing composition of fish in Greenland during the second half of the 20th century coincides in time with the large climatic changes observed in the Greenland area. It is therefore believed that the observed changes in recruitment patterns are largely driven by changes in ocean climate. In terms of mechanisms linking oceanographic factors to recruitment of fish and shellfish in West Greenland, sea temperature, larval drift caused by surface currents, water-mass stability (oceanographic fronts) have been proposed (Pedersen and Rice, 2001). Variability in these factors is related in turn to the inflow of water from other parts of the North Atlantic, which in turn is highly related to NAO variations. The individual strengths of the East Greenland and Irminger Currents have a dominating effect on the physical environment of the shelf areas around southern Greenland.

The ocean transports of salt and heat towards West Greenland are believed to have decreased dramatically after 1970, as did the heat exchange with the atmosphere. This seems to have had a negative effect on the recruitment success of the West Greenland cod stock, and a number of other boreal fish stocks, and a positive effect on the production of northern shrimp and Greenland halibut.

The massive reduction (almost disappearance) in the West Greenland cod fishery is believed to have had two causes:

- *Reduction in the West Greenland spawning stock.* The number of cod recruits at age 3 years has been documented to be significantly correlated with the spawning-stock biomass and June water temperature on top of Fyllas Bank (Hansen and Buch, 1986; Hovgaard and Buch, 1990). Both factors positively affected the number of offspring and explained 51% of the observed variation in recruitment (Rätz *et al.*, 1999).
- *Reduced inflow of cod larvae from Icelandic spawning grounds.* The inflow of cod larvae occurred almost every year in the 1950s and early 1960s (Figure 2 in Hansen and Buch, 1986), but has since been absent except for the 1973 and 1984 year classes.

Changes in the thermal regime can have a considerable impact on the abundance of ground fishes and pandalid shrimps (Anderson, 2000; Koeller, 2000; Stein, 2000). In the summer of 1982, cod larvae were abundant in West Greenland, but the following extremely cold winter was assumed to have terminated this year class (Pedersen and Smidt, 2000).

Northern shrimp prefer relatively cold temperatures in the range 1–6°C, and their larvae are less vulnerable to low temperatures compared to cod (Shumway *et al.*, 1985), which may partly explain the positive reaction of the West Greenland shrimp stock to the changed climatic conditions. However, the shift in the underlying marine ecosystem at West Greenland may have been amplified by the declining cod stock due to a release in predation pressure on for example sandeel and northern shrimp (Koeller, 2000; Lilly *et al*, 2000). Additionally, bycatches of fish in the steadily growing fishery for northern shrimp during the last part of the 20th century may have played a role in reducing and keeping the mean trophic level low (Kingsley *et al.*, 1999; Pauly *et al.*, 2001).

The observed increase in shrimp biomass during recent years is related to an increase in individual

shrimp growth (decrease in mean length at sex change) and recruitment (Carlsson and Kanneworff, 1999; Siegstad, 2000). The shrimp recruitment indices (number of juvenile shrimp) show a steep increasing trend from 1997 to 2000, which is a good prospect for the shrimp fishery (Figure 3A). This positive development is believed to be related to the favourable temperature conditions observed off West Greenland during this period, when the increased inflow of Irminger Water (Figure 8) has carried warm water to the area.

The relatively cold period from the late 1980s to mid-1990s, when shrimp habitat temperatures decreased below the temperature preference (3–4°C), seems to have caused a southern migration of the shrimp stock and the fishery. The warming trend from 1995 to 2000 towards the preferred habitat temperatures seems to have favoured growth and recruitment for northern shrimp, whereby an extraordinary increase in the shrimp biomass has been observed in very recent years.

Pandalid shrimps have been demonstrated to be indicator species in the cold regime community structure of the Gulf of Alaska (GOA) ecosystem (Anderson, 2000). On the Labrador Shelf, extensive ice cover in cold years may contribute positively to the survival of larvae and juveniles in the same year and the effect can be detected in the c.p.u.e. several years later (the mean age of shrimp in the catch is about 6 years) (Parsons and Colbourne, 2000). A recent study by Ramseier *et al.* (2000) showed that the extent of localized sedimentation of particulate organic carbon (POC) can be derived from information about ice cover. POC probably plays an important role as a food supply for shrimp, and it is possible that the explanation of the functional relationship between ice cover and shrimp production is related more to nutrient supply than temperature-related phenomena. According to Parsons and Colbourne (2000) this would help explain the apparent inconsistencies between *in situ* observations, which suggest "cold conditions" are favourable for shrimp, and laboratory studies, which indicate that larval growth and survival are enhanced at higher temperatures.

Conclusions

From the description of the development in the West Greenland fishery and the climate variability in the area it can be concluded:

- The Greenland economy, formerly being highly dependent on a rich cod fishery, is today almost entirely dependent on the Greenland shrimp stock.
- Since 1970, the Greenland climate has been considerably colder than during the 1920–1970 period, which can be related to a shift in the NAO index from negative to positive values.
- The redistribution of the atmospheric pressure fields has altered the surface ocean currents of the North Atlantic in that the inflow of heat, salt, and cod larvae to the West Greenland area via the various current components of Atlantic origin has decreased considerably.
- There seems to be a good correlation between the climate changes and the observed shift in the marine ecosystem. However, this correlation is based mainly on the use of ocean temperatures as a proxy for climate change. Until now there has been little scientific investigation to understand the ecological, chemical, and physical processes behind changes in the marine ecosystem.
- The increase in the West Greenland shrimp stock biomass can probably not be attributed solely to climate changes. The almost complete disappearance of the cod stock has reduced the predator pressure and bycatches of the shrimp fishery contribute to keeping the predator pressure low.
- The close relationship between climate variability and the marine ecosystem off West Greenland strongly supports the incorporation of environmental variability into prediction models for fish stock recruitment and thereby in the assessment of fisheries resources. However, this will require increased research in process studies seeking to understand the processes linking fisheries recruitment to environmental factors. These efforts must be supplemented with the development of coupled ocean and ecological models to increase our knowledge of the interacting physical and biological processes. Models of ecosystem developments under changing climatic conditions should be considered in fishery assessments in the future, and they should lead to better planning for Greenland society.

Acknowledgements

During this work, S.A.P. was funded by the Danish National Research Council project no. 9803018, and M.H.N was part of "West-Nordic Ocean Climate Research Programme" funded by the Nordic Council of Ministers.

References

Anderson, P. J. 2000. Pandalid shrimp as indicators of ecosystem regime shift. Journal of Northwest Atlantic Fishery Science, 27: 1–10.

Barnett, T. P. 1985. Variations in near-global sea level pressure. Journal of Atmospheric Science, 42: 478–501.

Belkin, I. M., Levitus, S., Antonov, J., and Malmberg, S. A. 1998. "Great Salinity Anomalies" in the North Atlantic. Progress in Oceanography, 41: 1–68.

Blindheim, J., Borovkov, V., Hansen, B., Malmberg, S. Aa., Turrell, B., and Østerhus, S. 2000. Upper layer cooling and freshening in the Norwegian Sea in relation to atmospheric forcing. Deep-Sea Research I, 47: 655–680.

Buch, E. 2000a. A monograph on the physical oceanography of the Greenland waters. Danish Meteorological Institute, Scientific Report, 00-12. 405 pp. (Re-issued version of a Greenland Fisheries Research Institute report from 1990 with the same title.)

Buch, E. 2000b. Air-sea-ice conditions off southwest Greenland, 1981–97. Journal of Northwest Atlantic Fishery Science, 26: 1–14.

Buch, E., Horsted, S. Aa., and Hovgård, H. 1994. Fluctuations in the occurrence of cod in Greenland waters and their possible causes. ICES Marine Science Symposia, 198: 158–174.

Carlsson, D. M., and Kanneworff, P. 1999. Bottom temperatures and possible effect on growth and size at sex reversal of northern shrimp in West Greenland. NAFO SCR Doc. 110 (Ser. no. N4190). 6 pp.

Carlsson, D. M., and Kanneworff, P. 2000. Stratified-random trawl survey for northern shrimp (*Pandalus borealis*) in NAFO Subareas 0+1, in 2000. NAFO SCR Doc. 78 (Ser. no. N4335). 27 pp.

Dickson, R. R., Briffa, K. R., and Osborn, T. J. 1994. Cod and climate: the spatial and temporal context. ICES Marine Science Symposia, 198: 280–286.

Dickson, R. R., Lazier, J. R. N., Meincke, J., Rhines, P., and Swift, J. 1996. Long-term coordinated changes in the convective activity of the North Atlantic. Progress in Oceanography, 38: 241–295.

Dickson, R. R., Meincke, J., Malmberg, S. A., and Lee, A. J. 1988. The "Great Salinity Anomaly" in the northern North Atlantic 1968–1982. Progress in Oceanography, 20: 103–151.

Dickson, R. R., Osborn, T. J., Hurrell, J. W., Meincke, J., Blindheim, J., Adlandsvik, B., Vinje, T., Alekseev, G., and Maslowski, W. 2000. The Arctic Ocean Response to the North Atlantic Oscillation. Journal of Climate (August).

Hamilton, L., Lyster, P., and Otterstad, O. 2000. Social change, ecology and climate in 20th-century Greenland. Climatic Change, 47: 193–211.

Hansen, H., and Buch, E. 1986. Prediction of year-class strength of Atlantic cod (*Gadus morhua*) off West Greenland. NAFO Science Council Studies, 10: 7–11.

Horsted, S. A. 2000. A review of the cod fisheries at Greenland, 1910–1995. Journal of Northwest Atlantic Fishery Science, 28: 1–109.

Hovgård, H., and Buch, E. 1990. Fluctuation in the cod biomass of the West Greenland Ecosystem in relation to climate. *In* Large Marine Ecosystems: Patterns, Processes, and Yields, pp. 36–43. Ed. by K. Sherman, L. M. Alexander, and B. D. Gold. AAAS Press, Washington.

Hurrell, J. W. (1995). Decadal trends in the North Atlantic oscillation regional temperatures and precipitation. Science, 269: 676–679.

Hurrell, J. W., and van Loon, H. 1997. Decadal variations in climate associated with the North Atlantic oscillation. Climate Change, 36: 301–326.

Hvingel, C. 2000. The Greenlandic fishery for northern shrimp (*Pandalus borealis*) off West Greenland, 1970–2000. NAFO SCR Doc. 81 (Ser. no. N4338). 27 pp.

ICES. 1996. Report of the North-Western Working Group. ICES CM 1998/Assess: 15. 377 pp.

ICES. 2000a. Report of the North-Western Working Group. ICES CM 2000/Assess: 15. 328 pp.

ICES. 2000b. The 1999/2000 ICES Annual Ocean Climate Status Summary. Prepared by the Working Group on Oceanic Hydrography. Editor: Bill Turrell. (http://www.ices.dk/status/clim9900/)

Kanneworff, P. 2000. Occurrence of *Pandalus montagui* in trawl survey samples from NAFO Subarea 0+1. NAFO SCR Doc. 77 (Ser. no. N4334). 6 pp.

Kingsley, M. C. S., Kanneworff, P., and Carlsson, D. M. 1999. By-catches of fish in the West Greenland Shrimp Survey: an initial analysis. NAFO SCR Doc. 111 (Ser. no. N4191). 7 pp.

Koeller, P. A. 2000. Relative importance of abiotic and biotic factors to the management of the northern shrimp (*Pandalus borealis*) fishery on the Scotian Shelf. Journal of Northwest Atlantic Fishery Science, 27: 21–33.

Lilly, G. R., Parsons, D. G., and Kulka, D. W. 2000. Was the Increase in shrimp biomass on the Northeast Newfoundland Shelf a consequence of a release in predation pressure from cod? Journal of Northwest Atlantic Fishery Science, 27: 45–61.

Malmberg, S. A. 1985. The water masses between Iceland and Greenland. Rit Fiskideildar, 9, 127–140.

Mortensen, J., and Valdimarsson, H. 1999. Thermohaline changes in the Irminger Sea. ICES CM 1999/L: 16.

Moses, T., Kiladis, G. N., Diaz, H. F., and Barry, R. G. 1987. Characteristics and frequency reversals in mean sea level pressure in the North Atlantic sector and their relationships to long-term temperature trends. Journal of Climatology, 7: 13–30.

Parker, D. E., and Folland, C. K. 1988. The nature of climatic variability. Meteorological Magazine, 117: 201–210.

Parsons, D. G., and Colbourne, E. B. 2000. Forecasting fishery performance for northern shrimp (*Pandalus borealis*) on the Labrador Shelf (NAFO Divisions 2HJ). Journal of Northwest Atlantic Fishery Science, 27: 11–20.

Pauly, D., Palomares, M. L., Froese, R., *et al.* 2001. Fishing down Canadian aquatic food webs. Canadian Journal of Fisheries and Aquatic Sciences, 58: 51–62.

Pedersen, S. A., and Kanneworff, P. 1995. Fish on the West Greenland shrimp grounds, 1988–1992. ICES Journal of Marine Science 52: 165–182.

Pedersen, S. A., and Rice, J. 2001. Dynamics of fish larvae, zooplankton, and hydrographical characteristics in the West Greenland large marine ecosystem 1950–1984. *In* Changing States of the Large Marine Ecosystems of the North Atlantic. Ed. by K. S. Shermann, H.-R., and Skjoldal. Elsevier, Amsterdam.

Pedersen, S. A., and Smidt, E. L. B. 2000. Zooplankton distribution and abundance in West Greenland waters, 1950–1984. Journal of Northwest Atlantic Fishery Science, 26: 45–102.

Pedersen, S. A., and Zeller, D. 2001. A mass balance model for the West Greenland marine ecosystem. *In* Fisheries Impact on North Atlantic Ecosystems: Models and Analyses. Ed. by S. Guenette, V. Christensen, and D. Pauly. Fisheries Centre Research Reports 9(4). (In press.)

Ramseier, R. O., Garrity, C., Parsons, D. G., and Koeller, P. 2000. Influence of particle organic carbon sedimentation within the seasonal sea-ice regime on the catch distribution of northern shrimp (*Pandalus borealis*). Journal of Northwest Atlantic Fishery Science, 27: 35–44.

Rätz, H.-J. 1999. Structures and changes of the demersal fish assemblage off Greenland, 1982–96. NAFO Science Council Studies, 32: 1–15.

Rätz, H.-J., Stein, M., and Lloret, J. 1999. Variation in growth and recruitment of Atlantic cod (*Gadus morhua*) off Greenland during the second half of the twentieth century. Journal of Northwest Atlantic Fishery Science, 25: 161–170.

Riget, F., and Engelstoft, J. 1998. Size-at-age of cod (*Gadus morhua*) off West Greenland, 1952–92. NAFO Science Council Studies, 31: 1–12.

Shumway, S. E., Perkins, H. C., Shick, D. F., and Stickney, A. P. 1985. Synopsis of biological data on the pink shrimp, *Pandalus borealis* Krøyer, 1838. NOAA Technical Report NMFS 30 (FAO Fisheries Synopsis No. 144). 57 pp.

Siegstad, 2000. Preliminary assessment of shrimp (*Pandalus borealis*) in Davis Strait, 2000 (Subareas 0+1). NAFO SCR Doc. 84 (Ser. no. N4341). 22 pp.

Stein, M. 2000. Hydrographic and atmospheric conditions off East Greenland - their potential effect on the distribution of shrimp (*Pandalus borealis*). Journal of Northwest Atlantic Fishery Science, 27: 63–67.

ICES Marine Science Symposia, 219: 241–248. 2003

Relationship between fluvial discharge and sole (*Solea solea* L.) recruitment in the Bay of Biscay (France)

Olivier Le Pape, Yves Désaunay, and Daniel Guérault

Le Pape, O., Désaunay, Y., and Guérault, D. 2003. Relationship between fluvial discharge and sole (*Solea solea*, L.) recruitment in the Bay of Biscay (France). – ICES Marine Science Symposia 219: 241–248.

In this study we investigated whether the estuarine-opportunism of the Bay of Biscay sole affects its recruitment level. First, we estimated the abundance of juvenile sole on the basis of a survey of an estuarine nursery ground within the Bay of Biscay. A significant relationship between fluvial discharges in winter–spring and abundance of juveniles surviving into the second autumn of their existence indicated the sustaining effects of freshwater supply on the size of the nursery and its ability to support young sole. The second part of the work consists of a similar approach at the stock scale. The recruitment results from the respective contributions of different nurseries, and overall recruitment strength, tends to be smoothed relative to local variations. However, a correlation also exists between freshwater inputs in winter–spring and juvenile abundance in the scale of the French part of the Bay (ICES Division VIIIa/b). Sole recruitment in the Bay of Biscay appears to be driven by freshwater inputs. Hence, the variability of sole recruitment depends on fluvial discharge, but the lack of any trend in river run-off regimes in the Bay of Biscay prevents any forecast on the evolution of sole stocks with regard to climate changes.

Keywords: Bay of Biscay, fluvial discharge, nursery ground, recruitment, *Solea solea*.

O. Le Pape, Y. Désaunay, and D. Guérault: IFREMER, Laboratoire d'Ecologie Halieutique, rue de l'Ile d'Yeu, B.P. 21105, 44311 Nantes Cedex, France [tel: + 33 2 40 37 41 99; fax: + 33 2 40 37 40 75; e-mail: olepape@ifremer.fr]. Correspondence to O. Le Pape.

Introduction

Various marine fish species, and especially flatfish, widely distributed on the continental shelf are directly affected by freshwater inputs at a given stage of their life cycle (Miller *et al.*, 1984). As estuarine areas are more productive than other parts of the coast, they serve as nursery grounds and ensure continuity of the life cycle for a number of fish species (Lenanton and Potter, 1987; Thiel *et al.*, 1997), and especially for sole (Rijnsdorp *et al.*, 1992). Quantitative (nursery area) and qualitative factors (food supply, temperature, mortality due to predation, etc.) have a considerable influence on recruitment level (Gibson, 1994; Schmitt and Holbrook, 2000; van der Veer *et al.*, 2000). The relationship between recruitment level and the area of estuarine nursery grounds has been demonstrated for sole (*Solea solea* L.) in comparisons of different systems (Rijnsdorp *et al.*, 1992). In the present study we investigated whether interannual variations in fluvial discharge, and hence in the extent of river plumes, affects the recruitment level for this species.

The Bay of Biscay (Figure 1) is an arm of the North Atlantic indenting the west coast of France and the north coast of Spain (ICES Area VIIIa/c). Sole is the most frequent and most abundant (Koutsikopoulos *et al.*, 1995; Guérault *et al.*, 1996) of the large demersal species at least on the French part of the continental shelf. It is also the main species for fisheries in this part of the Bay (ICES Division VIIIa/b), with mean annual landings of 5000 t (ICES, 2001) for a value of 50×10^6 Euros per year. ICES Divisions VIIIa/b are regarded as a unit for stock management of the common sole (ICES, 2001). In the Bay of Biscay, sole spawn in the early part of the year, and newly metamorphosed individuals settle between April and June into estuarine areas which act as nursery grounds (Marchand, 1991; Amara *et al.*, 2000). The role of coastal and estuarine areas in recruitment processes for sole in the Bay of Biscay has been described (Dorel and Désaunay, 1991; Koutsikopoulos *et al.*, 1991), all

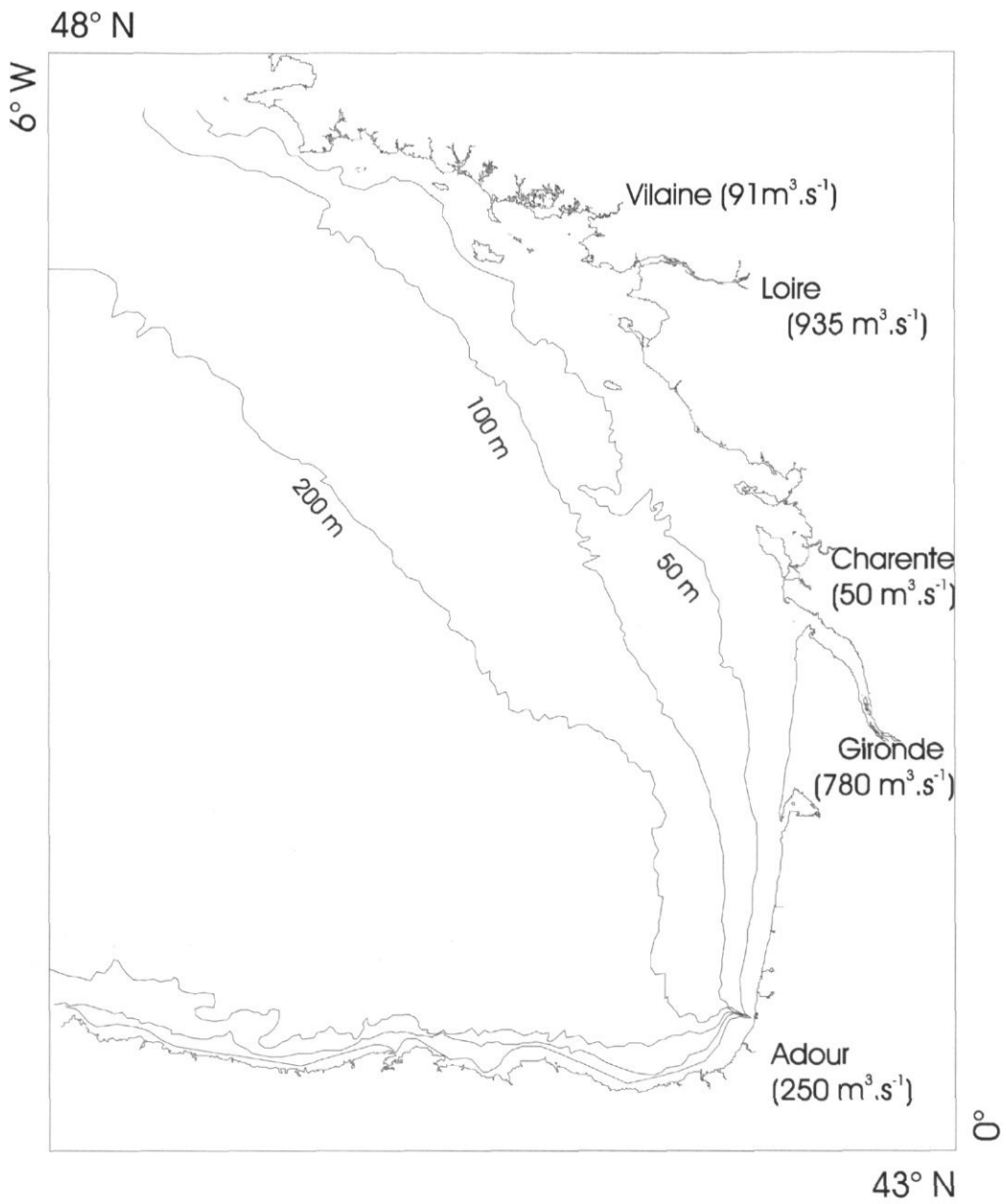


Figure 1. Map of the Bay of Biscay showing the main rivers with their average flow (Romana, 1998) and the 50, 100, and 200 m isobaths.

nursery grounds for sole in the Bay of Biscay being located in estuarine and peri-estuarine areas (Lagardère, 1982; Guérault *et al.*, 1996; Koutsikopoulos *et al.*, 1989a). Koutsikopoulos *et al.* (1989b) and Amara *et al.* (2000) showed that susceptibility to habitat (growth and mortality) is high for the youngest juvenile sole, then decreases with age in the Bay of Biscay.

We investigated whether the estuarine opportunism of the Bay of Biscay sole affects its recruitment level. The relationship between interannual variability of river flow and juvenile abundance was first studied in Vilaine Bay (Figure 2), a shallow coastal inlet of the northern Bay of Biscay identified by Koutsikopoulos *et al.* (1989a) as an important nursery ground for sole within the Bay of Biscay. A similar relationship was then examined between freshwater inputs and recruitment at the stock scale (ICES Area VIIIa/b). Finally, the results are discussed with respect to determining recruitment

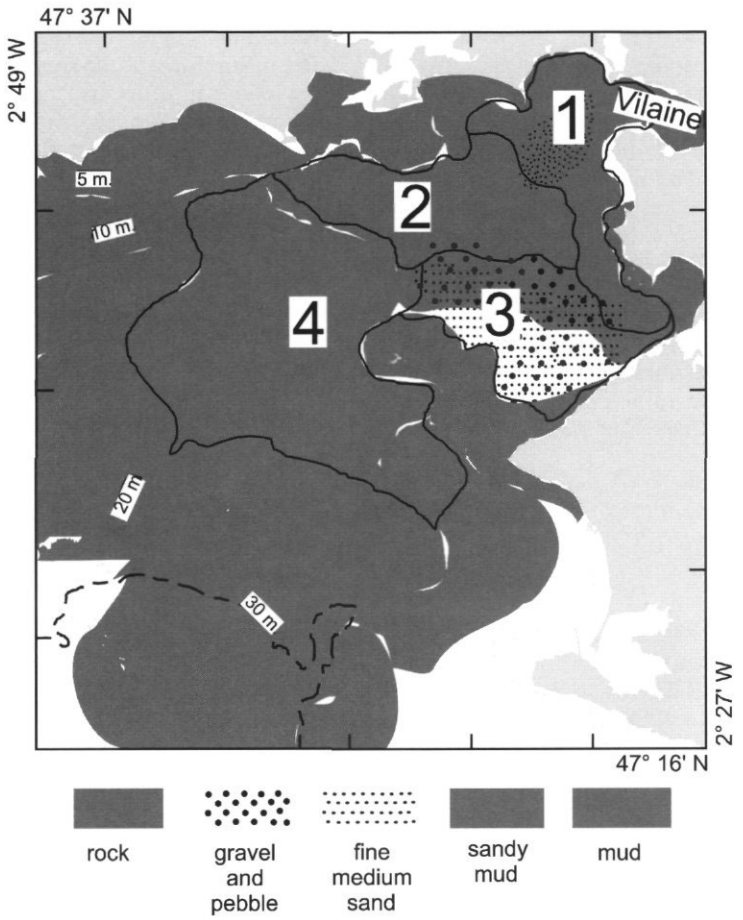


Figure 2. Map of the Vilaine Bay study site showing sampling strata 1 to 4, sediment types (Pinot and Vaney, 1972), and 5, 10, 20, and 30 m isobaths.

and the relationship between climate change and sole stock evolution in the Bay of Biscay.

Materials and methods

Beam trawl surveys in Vilaine Bay

Fourteen surveys were conducted in the autumn in Vilaine Bay from 1981 to 1997 (IFREMER, RV "Gwen Drez" and "Roselys"; Table 1). This season was chosen because it coincides with the distribution of juvenile flatfish during the growth period and is the most appropriate for the study of nursery grounds (Dorel *et al.*, 1991). The sampling scheme involved four strata of homogeneous depth and sediment (Figure 2). The beam trawl opening was 2.9 m wide and 0.50 m high, and the net had 20×10^{-3} m stretched mesh in the codend. The trawl had no tickler chain ahead of the foot rope. Operating conditions were checked and standardized from the first survey. Hauls were performed only in daylight at neap tides, at 2.5 knots for 20 min. On average, each haul covered 4500 m^2.

Table 1. Beam trawl surveys carried out in the Vilaine Bay (the strata are shown on Figure 2).

Period		No. of hauls				
		Stratum 1	Stratum 2	Stratum 3	Stratum 4	Total
1981	23–25 Nov	6	7	6	6	25
1982	20–23 Oct	9	9	7	5	30
1983	3–10 Nov	8	11	10	16	45
1984	30 Oct–3 Nov	9	10	9	8	36
1985	20–27 Sep	6	7	15	8	36
1986	18–27 Sep	8	17	11	11	47
1987	4–13 Sep	18	26	18	10	72
1988	20–23 Sep	12	13	14	10	49
1989	19–22 Sep	12	12	9	13	46
1990	15–18 Sep	12	14	10	15	51
1992	14–18 Sep	12	15	12	16	55
1993	4–7 Sep	10	15	11	15	51
1996	16–20 Sep	6	10	8	14	38
1997	11–18 Sep	9	10	9	20	48

Abundance of juvenile sole in Vilaine Bay

All sole were counted and measured. The age groups were determined from age-length keys established after otolith reading. As sampling to catch very small (0-group) individuals living in shallow intertidal areas is likely to be inaccurate (Riley *et al.*, 1981; Rogers and Millner, 1996), our study was based only on the catch rates of 1-group juvenile flatfish. Dorel *et al.* (1991) and Hanson (1996) have shown that these 1-group fish live in deeper water than 0-groups, where fishing surveys are easier to perform and provide more consistent results.

For each stratum, estimated density was multiplied by area, and the total population was estimated as the sum of these four strata (Pennington and Grosslein, 1977).

Abundance of juvenile sole in the Bay of Biscay

Data for the abundance index of juvenile sole in the Bay of Biscay were obtained from the RESSGASC survey trawl series (IFREMER, RV "Gwen Drez") conducted from 1987 to 1999 in the French part of the continental shelf. These data were also used as an abundance index by the ICES Southern Shelf Demersal Working Group for the ICES Division VIIIa/b sole stock (ICES, 2001). As the RESSGASC survey was not sufficiently coastal to provide an abundance index for estuarine nursery grounds, juvenile abundance was estimated from the spring RESSGASC survey for the 2-group of juvenile sole. According to Dorel *et al.* (1991), 2-group individuals in winter–spring are the youngest juvenile sole living in the open sea, i.e. where the RESSGASC survey provides a reliable abundance index. The use of these data rather than the Virtual Population Analysis output (ICES, 2001) for the abundance of 1-year-old sole avoids any bias due to the analytical technique applied to estimate population size. Moreover, G. Biais (pers. comm.) has noted that the assessment of juvenile sole given by Virtual Population Analysis is not sufficiently reliable because of a considerable bias in bycatch estimates.

Relationship between juvenile abundance and river flow

The monthly flows of the Vilaine, Loire, Charente, Gironde, and Adour, the five main rivers in the Bay of Biscay (Figure 1) were obtained from the national hydrologic databank of the French Ministry of the Environment.

A preliminary typology of the interannual and seasonal variations of the Vilaine river flow was used to select the period most likely to affect recruitment success.

The mean flows of the five main rivers were taken into account in order to study the impact of freshwater inputs on sole recruitment strength at the Bay of Biscay stock scale. To ensure the uniformity of the approach, these flows were considered during the same period as that determined from the Vilaine river typology. Two different indices based on these river flows were used. First, the flows of all five rivers were summed; second, an index of river flow anomaly into the Bay of Biscay was built to combine the five rivers without taking their respective mean flows into account:

- the flow anomaly was calculated for each of the five rivers [Equation (1)]

$$\mathrm{cr(RF)}_{y,r} = \frac{\mathrm{RF}_{y,r} - \overline{\mathrm{RF}^{1985\text{–}1997}}_{r}}{\sigma^{1985\text{–}1997}(\mathrm{RF}_{r})} \qquad (1)$$

  with $\mathrm{RF}_{y,r}$: flow of the river "r" for the year "y", $\overline{\mathrm{RF}^{1985\text{–}1997}}_{r}$: average of $\mathrm{RF}_{y,r}$ from 1985 to 1997, $\sigma^{1985\text{–}1997}(\mathrm{RF}_{r})$: standard error of $\mathrm{RF}_{y,r}$ from 1985 to 1997, $\mathrm{cr(RF)}_{y,r}$: centered reduced value of $\mathrm{RF}_{y,r}$.
- these river flow anomalies were summed [Equation (2)]

$$A_{y} = \sum_{r}^{5\,\text{rivers}} \mathrm{cr(RF)}_{y,r} \qquad (2)$$

  with A_y: River flow anomaly in the Bay of Biscay for year "y".

The influence of river flow on recruitment was first studied on a nursery scale in Vilaine Bay and then on a stock scale in the Bay of Biscay. As susceptibility to habitat is high for the youngest juvenile sole, then decreases with age (Koutsikopoulos *et al.*, 1989b), the relationship with river flow was assumed to influence the young of the year sole. Accordingly, abundance was compared for the 1-group in Vilaine Bay nursery grounds and the 2-group in the Bay of Biscay in terms of the river flow index for their year of birth. Thus, in the analysis below, abundance is expressed for the year of birth (the year "n-1" for the Vilaine Bay 1-group and the year "n-2" for the Bay of Biscay 2-group). The relationship between the river flow index (explanatory variables) and juvenile abundance (response variables) was studied using simple linear regression analysis. The application conditions of linear regression were previously verified without contra-indication.

Results

Typology of Vilaine river flows

The mean monthly flows of the Vilaine river showed large variations, with values of 15 $m^3\ s^{-1}$ in summer

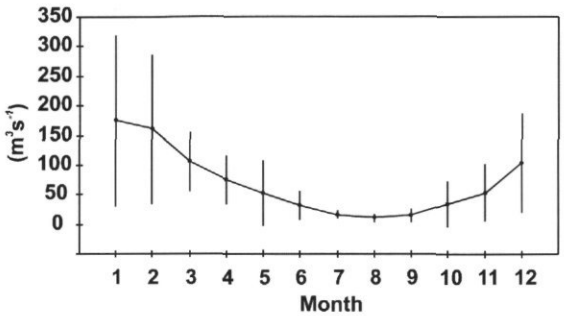


Figure 3. Mean values and standard deviations for monthly Vilaine river flows from 1980 to 1997.

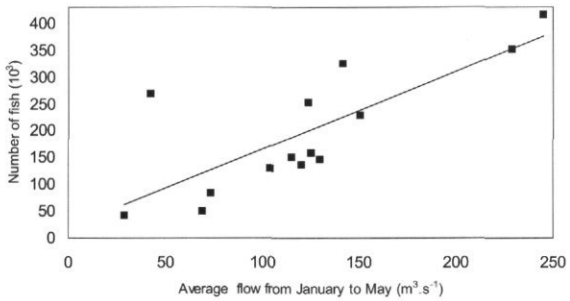


Figure 4. Linear regression between winter–spring flows from 1980 to 1996 and 1-group sole abundance during the next year in Vilaine Bay.

and around 130 $m^3 s^{-1}$ in winter (Figure 3). The highest monthly flows reached 300 to 400 $m^3 s^{-1}$ in January and February. A transition occurred between May and June from a potentially strong and highly variable river flow (winter conditions) to a steady, low summer flow.

Two considerations were taken into account in studying the relationship between river flow and the density of young of the year sole:

- A period of rising flow should have a greater influence than a low-water period.
- The fluvial discharge likely to influence sole recruitment enters the estuary before or at the beginning of the benthic life of young of the year sole, when the role played by habitat is maximal.

Thus, the recruitment of sole was compared with river flow between January and May. The previous part of the flood period (October to December) was considered to be too early, in terms of the settlement period (April to June, Marchand, 1991; Amara *et al.*, 2000) to influence recruitment strength, and subsequent months were within the low-water period when freshwater input into Vilaine Bay is very limited.

Relationship between river flow and young sole density in Vilaine Bay

The number of 1-group juvenile sole in Vilaine Bay differed by one order of magnitude between 1981 and 1997 without any temporal trend.

Linear regression analysis showed a significant relation (Figure 4, $\rho = 0.77$, $\alpha = 0.01$) between winter–spring flow (January to May) in the year n and 1-group densities measured in the following year. These results indicate that fluvial discharges during the first 5 months of the year (the period of larval immigration into the estuarine nursery area) had a positive influence on the number of juvenile sole in the Bay of Vilaine nursery ground.

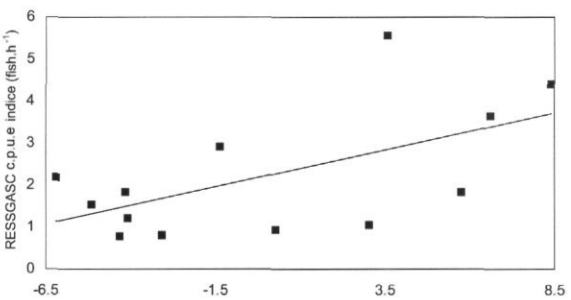


Figure 5. Linear regression between the winter–spring flow anomaly from 1985 to 1997 and sole density measured at age 2 in spring during the year "n + 2" in the Bay of Biscay.

Relationship between freshwater input and young sole density in the Bay of Biscay

Interannual variability in the density of 2-group sole in the Bay of Biscay ranged between factors 1 and 7; no temporal trend could be observed at this stock scale.

To ensure uniformity with the analysis for Vilaine Bay, the January-to-May flows of the five main rivers were taken into account for freshwater inputs into the Bay of Biscay. The sum of these flows and the sum of the river flow anomalies (cf. Materials and Methods) were used separately as explanatory variables.

Linear regression analyses showed a significant relation ($\rho = 0.57$, $\alpha < 0.05$ for the sum of the river flow, and $\rho = 0.58$ and $\alpha < 0.05$ for the river flows anomalies; Figure 5) between these indices in the year "n" and 2-group densities measured in the spring of the year "n + 2" on a survey led at the Bay of Biscay stock scale. Nevertheless', the correlation was lower than that obtained for Vilaine Bay.

Discussion

Influence of river flow on recruitment

As estuarine areas are more productive than other parts of the coast, they serve as nursery grounds for the sole and the relationship between recruitment level and the area of estuarine nursery grounds has been demonstrated in comparisons of different systems (Rijnsdorp *et al.*, 1992). The relationship between river flow and recruitment strength obtained both for Vilaine Bay on a nursery ground and for the Bay of Biscay at the stock scale, confirms this estuarine dependence of juvenile sole. According to Boehlert and Mundy (1988), interannual variations of winter–spring river flows can affect the coastal habitat, and hence recruitment strength directly and indirectly:

1) A direct effect concerns the offshore range of the low salinity plume. Migration of sole larvae from offshore spawning grounds to coastal nursery grounds is essentially driven by diffusion in the Bay of Biscay (Koutsikopoulos *et al.*, 1991; Ramzi *et al.*, 2000). In the region subject to Loire and Vilaine river flows, as far as 30 to 40 km from the estuaries, the water layer near the bottom moves towards the coast in conjunction with offshore surface movements (Lazure and Salomon, 1991), facilitating the transport of transforming larvae towards the nursery area. This mechanism favours the immigration of young stages and tends to maximize the number of 0-group fish in the nursery. Moreover, the conditions of haline stratification are probably determinant for sole settlement, as vertical migration is modified (Marchand, 1991), and low salinity facilitates the attraction and metamorphosis of larvae (Koutsikopoulos *et al.*, 1989b).

2) An indirect effect relates to the hydrological characteristics of the bay and thus to the quality of the invertebrate benthic community that constitutes the food supply for young fish (Howell *et al.*, 1999). For the Vilaine and Loire estuaries, Marchand and Masson (1989) and Marchand (1993) have shown the impact of salinity and turbidity on the settling of benthic communities (dominated by young stages of polychaetes and bivalves) preyed upon by euryhaline fishes. Moreover, Costa and Bruxelas (1989) and Rogers (1992) have determined that young sole prefer habitats offering a homogeneous substrate with the highest densities of polychaetes and bivalves. The settling and development of a community tolerant to low salinity provides suitable food for young sole, which can rely on this supply until at least the second autumn of their life (Dorel *et al.*, 1991).

Thus, the fluvial regime determines in part the type of habitat existing in the estuaries, thereby affecting the survival and growth of young sole and, hence, the recruitment (Gibson, 1994). Nevertheless, in addition to the positive relation between river flow and young sole density, complementary factors need to be stressed.

First, human pressure, and hence anthropogenic disturbance, is especially high in these estuarine areas and their watersheds. If juveniles are confined within peri-estuarine habitats, there is a risk of hypoxic conditions, particularly in summer (Phelan *et al.*, 2000; Ferber, 2001). Nutrient excess or pollution loading (Meng *et al.*, 2000) could restrict the growth of juvenile fish in estuarine nursery grounds. An anoxic crisis in Vilaine Bay in July 1982 (Rossignol-Strick, 1985) led to the death of various organisms and delayed growth of 0-group sole (Koutsikopoulos *et al.*, 1989b).

Secondly, even though variability in sole density can be partly explained by the impact of river flow, determining recruitment cannot be limited to this factor alone. A number of factors defining the habitat, both quantitatively and qualitatively, have a combined effect on recruitment variability (Gibson, 1994; van der Veer *et al.*, 2000; Pihl *et al.*, 2000). No single factor can account for the total variability in recruitment strength. Environmental or anthropogenic factors, independent of the hydrological regime, i.e. density-dependent processes relative to food supply and predation (Nash and Geffen, 2000), diseases and spawning dynamics (Nash *et al.*, 2000), bycatches by shrimp trawlers, etc., affect juvenile abundance. These additional factors allow us to understand why the correlation obtained at the stock scale is lower than that observed at the nursery scale: stock size, cohort by cohort, results from the contributions of the different nursery grounds (van der Veer *et al.*, 2000) and temporal variation in recruitment is governed by factors operating on several (local to population) spatial scales (Pihl *et al.*, 2000). Thus, variations in recruitment strength on a stock scale are smoothed and cannot be as responsive to changes in freshwater inputs as on a nursery scale.

The essential result is that strong river flows in winter and spring have a dominant effect on the nursery habitat for a sustained period, and thus on recruitment strength. However, the interplay of other environmental variations tends to damp down this effect.

General interest for determinism of flatfish recruitment

As larval settlement in the Bay of Biscay shows low interannual variability (Koutsikopoulos and Lacroix, 1992) and recruitment strength on a nursery scale is variable, it would seem that river flow is the main factor governing the abundance of young sole in the Bay of Biscay. As for plaice in the Irish

Sea (Nash and Geffen, 2000), year-class strength seems to be determined during the nursery ground phase for Bay of Biscay sole.

A pool of factors, including hydrodynamics during pelagic larval life (Symonds and Rogers, 1995; Nielsen *et al.*, 1998; Chant *et al.*, 2000), density-dependent effects on food supply and predation (Nash and Geffen, 2000; Cowan *et al.*, 2000), and freshwater inputs in estuarine nursery grounds (present study), can influence flatfish recruitment strength (Pihl *et al.*, 2000; Schmitt and Holbrook, 2000; van der Veer *et al.*, 2000). The balance between these different factors differs according to area. Flatfish populations can exhibit different strategies, and the mechanisms determining year-class strength are not the same everywhere (van der Veer *et al.*, 2000).

Sole recruitment variability in the Bay of Biscay during recent decades

If the variability of sole recruitment depends on fluvial discharge, the lack of trend in river run-off regimes during past decades in the Bay of Biscay (Planque *et al.*, 2003) prevents any forecast on the evolution of sole stock with regard to climate changes. In accord with this conclusion it is not possible to show any trend in sole recruitment level, neither in the Vilaine Bay nursery ground nor at the Bay of Biscay stock scale. The lack of trend in sole recruitment has already been demonstrated by Dorel and Désaunay (1991) in Vilaine Bay and the VPA analysis of the Bay of Biscay stock (ICES, 2001) led to the same conclusion.

Acknowledgements

We are grateful to Anne Marie Jégou and Nicole Faury (IFREMER) for river flow data and to André Battaglia, Gérard Biais, and Jacques Labastie for data on the Bay of Biscay sole stock. We also thank the anonymous reviewers for their fruitful suggestions. This article is dedicated to the memory of our friends Jean-Louis Durand and Jocelyne Marchand.

References

Amara, R., Lagardère, F., Désaunay, Y., and Marchand, J. 2000. Metamorphosis and estuarine colonisation in the common sole, *Solea solea* (L.): implications for recruitment regulation. Oceanologica Acta, 23: 469–483.

Boehlert, G. W., and Mundy, B. C. 1988. Roles of behavioral and physical factors in larval and juvenile fish recruitment to estuarine nursery areas. *In* Workshop on Larval Fish and Shellfish Transport, Ocean Springs MD, USA. American Fisheries Society, Bethesda, MD, USA, 3: 51–67.

Chant, R. J., Curran, M. C., Able, K.W., and Glenn, S. M. 2000. Delivery of winter flounder (*Pseudopleuronectes americanus*) larvae to settlement habitats in coves near tidal inlets. Estuarine Coastal and Shelf Science, 51: 529–541.

Costa, M. J., and Bruxelas, A. 1989. The structure of fish communities in the Tagus estuary, Portugal, and its role as a nursery for commercial fish species. *In* Topics in Marine Biology. Proceedings of the 22nd European Marine Biology Symposium. Scientia Marina, 53: 561–566.

Cowan, J. H., Rose, K. A., and de Vries, D. R. 2000. Is density-dependent growth in young of the year fishes a question of critical weight? Reviews in Fish Biology and Fisheries, 10: 61–89.

Dorel, D., and Désaunay, Y. 1991. Variation of recruitment in flatfishes on a nursery ground of the Northern Bay of Biscay, from 1981 to 1990. ICES CM/G: 74. 9 pp.

Dorel, D., and Désaunay, Y. 1991. Comparison of three *Solea solea* (L.) nursery grounds of the Bay of Biscay: distribution, density and abundance of 0-group and 1-group. ICES CM 1991/G: 75.

Dorel, D., Koutsikopoulos, C., Désaunay, Y., and Marchand, J. 1991. Seasonal distribution of young sole (*Solea solea* L.) in the nursery ground of the Bay of Vilaine (Northern Bay of Biscay). Netherlands Journal of Sea Research, 27: 297–306.

Ferber, D. 2001. Keeping the stygian waters at bay. Science, 291: 968–973.

Gibson, R. N. 1994. Impact of habitat quality and quantity on the recruitment of juvenile flatfishes. Netherlands Journal of Sea Research, 32: 191–206.

Guérault, D., Dorel, D., and Désaunay, Y. 1996. Cartographie des nourriceries littorales de poissons du Golfe de Gascogne. Report for the Ministry of Agriculture, Fishing and Food Supply, IFREMER, Nantes, France 95–11–01–02. 150 pp.

Hanson, J. M. 1996. Seasonal distribution of juvenile Atlantic cod in the southern Gulf of St Lawrence. Journal of Fish Biology, 46: 1138-1152.

ICES. 2001. Report of the Working Group on the Assessment of Southern Shelf Demersal Stocks. ICES CM 2001/Assess: 4. 800 pp.

Howell, P. T., Molnar, D. R., and Harris, R. B. 1999. Juvenile winter flounder distribution by habitat type. Estuaries, 22: 1090–1095.

Koutsikopoulos, C., Désaunay, Y., Dorel, D., and Marchand, J. 1989a. The role of coastal areas in the life history of sole (*Solea solea* L.) in the Bay of Biscay. *In* Topics in Marine Biology. Ed. by J. Ros. Proceedings of the 22nd European Marine Biology Symposium, Barcelona, Spain, 53: 567–575.

Koutsikopoulos, C., Karakiri, M., Désaunay, Y., and Dorel, D. 1989b. Response of juvenile sole (*Solea solea* L.) to environmental changes investigated by otolith microstructure analysis. ICES Marine Science Symposia, 191: 281–286.

Koutsikopoulos, C., Fortier, L., and Gagné, J. A. 1991. Cross-well dispersion of dover sole (*Solea solea* (L.)) eggs and larvae in Biscay Bay and recruitment to inshore nurseries. Journal of Plankton Research, 13: 923–945.

Koutsikopoulos, C., and Lacroix, N. 1992. Distribution and abundance of sole (*Solea solea* L.) eggs and larvae in the Bay of Biscay between 1986 and 1989. Netherlands Journal of Sea Research, 29: 81–91.

Koutsikopoulos, C., Dorel, D., Désaunay, Y., Le Cann, B., and Forest A. 1995. Interactions entre processus physiques et comportement individuel, conséquences sur l'organisation et le fonctionnement du stock de sole *Solea solea* (L.) du Golfe de Gascogne. *In* ORSTOM, Paris, France (Ed.),

Premier Forum d'Halieumétrique. Colloques et Séminaires, 49–74.

Lagardère, F. 1982. Environnement péri-estuarien et biologie des Soleidae dans le golfe de Gascogne (zone sud) à travers l'étude du céteau *Dicologoglossa cuneata* (Moreau, 1881), (Thesis). University of Aix-Marseille II, France. 303 pp.

Lazure, P., and Salomon, J.-C. 1991. Coupled 2-D and 3-D modelling of coastal hydrodynamics. Oceanologica Acta, 14: 173–180.

Lenanton, R. C. J., and Potter, I. C. 1987. Contribution of estuaries to commercial fisheries in temperate Western Australia and the concept of estuarine dependence. Estuaries, 10: 28–35.

Marchand, J. 1991. Influence of environmental conditions on the settlement, the distribution and the growth of the 0-group sole (*Solea solea*) in a macrotidal estuary. Netherlands Journal of Sea Research, 27: 307–316.

Marchand, J. 1993. The influence of seasonal salinity and turbidity maximum variations on the nursery function of the Loire estuary (France). Netherlands Journal of Aquatic Ecology, 27: 427–436.

Marchand, J., and Masson, G. 1989. Process of estuarine colonization by 0-group sole (*Solea solea*): hydrological conditions, behaviour and feeding activity in the Vilaine estuary. ICES Marine Science Symposia, 191: 287–295.

Meng, L., Gray, C., Talpin, B., and Kupcha, E. 2000. Using winter flounder growth rates to assess habitat quality in Rhode Island coastal lagoons. Marine Ecology Progress Series, 201: 287–299.

Miller, J. M., Reed, J. P., and Pietrafesa, L. J. 1984. Patterns, mechanisms and approaches to the study of migrations of estuarine dependent fish larvae and juveniles. *In* Mechanisms of Migration in Fishes, pp. 209–225. Ed. by J. D. McCleave *et al.* Plenum Press, New York.

Nash, R. D. M., and Geffen, A. J. 2000. The influence of nursery ground processes in the determination of year-class strength in juvenile plaice *Pleuronectes platessa* L. in Port Erin Bay, Irish Sea. Journal of Sea Research, 44: 101–110.

Nash, R. D. M., Witthames, P. R., Pawson, M., and Alesworth, E. 2000. Regional variability in the dynamics of reproduction and growth of Irish Sea plaice, *Pleuronectes platessa* L. Journal of Sea Research, 44: 55–64.

Nielsen, E., Bagge, O., and MacKenzie, B. R. 1998. Wind-induced transport of plaice (*Pleuronectes platessa*): early life history stages in the Skagerrak–Kattegat. Journal of Sea Research, 39: 11–28.

Pennington, M. R., and Grosslein, M. D. 1977. Accuracy of abundance indices based on stratified random trawl surveys. ICNAF (International Commission for North Atlantic Fisheries) Research Document, 78/VI/77: 1–41.

Phelan, B. A., Goldberg, R., Bejda, A. J., Pereira, J., Hagan, S., Clark, P., Studholme, A. L., Calabrese, A., and Able, K. W. 2000. Estuarine and habitat-related differences in growth rates of young of the year winter flounder (*Pseudopleuronectes americanus*) and tautog (*Tautoga onitis*) in three northeastern US estuaries. Journal of Experimental Marine Biology and Ecology, 247: 1–28.

Pihl, L., Modin, J., and Wennhage, H. 2000. Spatial distribution patterns of newly settled plaice (*Pleuronectes platessa* L.) along the Swedish Skagerrak archipelago. Journal of Sea Research, 44: 65–80.

Pinot, J. P., and Vaney, J. R. 1972. Carte sédimentologique sous-marine des côtes de France au 1/100000. National Geographical Institute, France.

Planque, B., Gohin, F., Jégou, A. M., Lazure, P., Petitgas P., and Puillat, I. 2003. Large-scale hydrodynamics variability in the Bay of Biscay. ICES Marine Science Symposia, 219: 61–70. (This volume.)

Ramzi, A., Arino, O., Koutsikopoulos, C., Boussouar, A., and Lazure, P. 2001. Modelling and numerical simulations of larval migration of the sole (*Solea solea* (L.)) of the Bay of Biscay. Part 1: Modelling. Oceanologica Acta, 24: 101–112.

Rijnsdorp, A. D., van Beek, F. A., Flatman, S., Millner, R. M., Riley, J. D., Giret, M., and De Clerck, R. 1992. Recruitment of sole, *Solea solea* (L.), stocks in the Northeast Atlantic. Netherlands Journal of Sea Research, 29: 173–192.

Riley, J. D., Symonds, D. J., and Woolner, L. 1981. On the factors influencing the distribution of 0-group demersal fish in coastal waters. Rapports et Procès-Verbaux des Réunions du Conseil International pour l'Exploration de la Mer, 178: 223–238.

Rogers, S. I. 1992. Environmental factors affecting the distribution of sole (*Solea solea* L.) within a nursery area. Netherlands Journal of Sea Research, 29: 153–161.

Rogers, S. I., and Millner, R. S. 1996. Factors affecting the annual abundance and regional distribution of English inshore demersal fish populations: 1973 to 1995. ICES Journal of Marine Science, 53: 1094–1112.

Romana, L. A. 1998. Le potentiel de recherche français sur les estuaires. *In* Les estuaires français, évolution naturelle et artificielle, Paris, France, 26–27 November 1997. Actes de Colloque 22, pp. 320–328. IFREMER eds, Nantes, France.

Rossignol-Strick, M. 1985. A marine anoxic event on the Brittany coast, July 1982. Journal of Coastal Research, 1: 11–20.

Schmitt, R. J., and Holbrook, S. J. 2000. Habitat-limited recruitment of coral reef damselfish. Ecology, 81: 3479–3494.

Symonds, D. J., and Rogers, S. 1995. The influence of spawning and nursery grounds on the distribution of sole *Solea solea* (L.) in the Irish Sea, Bristol Channel adjacent areas. Journal of Experimental Marine Biology and Ecology, 190: 243–261.

Thiel, R., Nellen, W., Sepulveda, A., Oesmann, S., Tebbe, K., and Drenkelfort, T. 1997. Spatial gradients of food consumption and production of dominant fish species in the Elbe estuary, Germany. ICES CM/S: 04. 23 pp.

Van der Veer, H. W., Berghahn, R., Miller, J. M., and Rijnsdorp A. D. 2000. Recruitment in flatfish, with special emphasis on North Atlantic species: progress made by the flatfish symposia. ICES Journal of Marine Science, 57: 202–215.

ICES Marine Science Symposia, 219: 249–260. 2003

Variability of groundfish communities of the Cantabrian Sea during the 1990s

Francisco Sánchez and Alberto Serrano

Sánchez, F., and Serrano, A. 2003. Variability of groundfish communities of the Cantabrian Sea during the 1990s. – ICES Marine Science Symposia, 219: 249–260.

Changes in the structure of fish communities of the Cantabrian Sea Shelf are analysed using information from bottom-trawl surveys carried out every autumn during the period 1990–1999. The trend of ecological indices (species richness and diversity) has been less stable in the shallowest strata during the decade. The effect of environmental variables on the fish communities is explained by interset correlation of canonical axis of canonical correspondence analysis (CCA) with the abiotic variables considered (depth, near-bottom temperature, near-bottom salinity, longitude, and geographic stratum) to determine the assemblages of fishes each year. Interannual variations in the structure of the communities are analysed using multitable methods. In contrast to adjacent areas, the narrowest surface of the Cantabrian Sea Shelf produces strong environmental gradients over a short distance. Depth is the most influential and stable factor determining the assemblages observed. The coastal, outer shelf, and shelf-break communities are the strongest sources of variation, both intra-annual and interannual. Using time-series of indices of the main hydrographic driving agents, Navidad current, and upwelling, we try to discover the causes of the instability of spatial structure of assemblages not explained by the abiotic variables considered in the analyses.

Keywords: canonical analysis, Cantabrian Sea, decadal changes, fish communities, multitable methods, Navidad current, upwelling.

F. Sánchez and A. Serrano: Instituto Español de Oceanografía, PO Box 240, ES-39080 Santander, Spain. Correspondence to F. Sánchez [tel: +34 942 291060; fax: +34 942 275072; e-mail: f.sanchez@st.ieo.es]

Introduction

In terms of biogeography, the Cantabrian Sea area is the subtropical/boreal transition zone of the Eastern Atlantic. Typical temperate water species from the south cohabit along with others of northern origin and, consequently, high biodiversity indices exist in relation to adjacent areas (Olaso, 1990; Sánchez, 1993; OSPAR, 2000). In addition, the topographical complexity and the wide range of substrates on its narrow continental shelf give rise to many different types of habitat. This diversity is reflected in the biological richness of the region, which includes a wide range of species, many of which are of commercial interest. Fisheries, in which approximately 200 000 t of fish per year are landed, have an enormous effect on the structure and dynamics of the Cantabrian Sea ecosystem (Sánchez and Olaso, 2001, 2002).

Study of the temporal development of marine ecosystems through the analysis of historical time-series from surveys has usually centred on the study of descriptive indices (richness, diversity, dominance, etc.) and on describing the structure of communities, through multivariate analyses, for one particular year. It has become evident in many studies that ecological indices show very poor descriptive effectiveness in this kind of work. Although a decline in richness and diversity with fishing effort has been described (Jennings and Reynolds, 2000), increases in diversity at low levels of fishing intensity (ICES, 2000) and even as a response to heavy exploitation (Bianchi *et al.*, 2000) have also been reported. Consequently, it is necessary to extend the information supplied by these indices by providing overall explanations on the changes in the environment.

The Atlantic influence in the western area of the Cantabrian Sea is considered to diminish towards the interior of the Bay of Biscay. More recently, two main seasonal hydrographic driving agents that establish the local oceanography of the Cantabrian Sea have been described: the winter Navidad current and the spring–summer upwelling. In winter, the Navidad appears as an eastward-flowing shelf-break

current that transports warm and saline waters along the continental shelf (Frouin *et al.*, 1990; Pingree and Le Cann, 1990). This current is a prolongation of Poleward Current coming from the Portuguese Shelf and partially aided by southwesterly winds. This flow is the main energy input in the Cantabrian Sea during wintertime (Gil and Sánchez, 2001). In spring–summer, westward winds force surface waters offshore by the Ekman effect, and these are replaced by subsurface cold waters, leading to seasonal upwelling and consequently high primary production events (Botas *et al.*, 1990). The intensity and frequency of both phenomena are highly variable, leading to very different non-macroscale and non-permanent oceanographic scenarios along the Cantabrian Sea Shelf every year. Nevertheless, it is normally accepted that abundance and distribution patterns of groundfish reflect mainly depth and bottom characteristics. More recently, it has been shown that some demersal fish species in the study area also depend upon the physical dynamics and mesoscale water mass patterns (Sánchez and Gil, 2000; Sánchez *et al.*, 2001).

One problem facing the study of the impact of fisheries on ecosystems by means of the analysis of historical series from surveys is in discerning between the natural causes of variation and anthropogenic impacts (Rogers *et al.*, 1999; Bianchi *et al.*, 2000; Frid and Clark, 2000; Jennings and Reynolds, 2000; Rice, 2000). To this end, it is necessary to carefully determine the sources of spatial and temporal variation, and explain as far as possible the changes occurring each year with respect to the stable part of the series by means of environmental and biological information. In this article we analyse the structure and composition of demersal fish communities living over the continental shelf of the Cantabrian Sea and the influence certain environmental variables have on them. Similarly, an attempt is made to explain the changes observed during the 1990–1999 decade in relation to the different environmental scenarios present in the area.

Material and methods

The data of species abundance and distribution come from a series of bottom-trawl surveys carried out every autumn from 1990 to 1999 using standardized methodology (ICES, 1997). The survey area was stratified according to depth and geographical criteria and a stratified random sampling scheme was adopted (Figure 1A). In addition, extra hauls at less than 70 m and deeper than 500 m were accomplished during each survey. The first geographical sector (S1) of the historical series of surveys, situated to the south of Cape Finisterre, was not used in this study because of its different biogeographical characteristics. The number of hauls per stratum was proportional to the trawlable surface, and the sampling unit was made up of 30-min hauls at a speed of 3.0 knots using the baca 44/60 otter trawl gear (Sánchez, 1993; Sánchez *et al.*, 1995; ICES, 1997). The hydrographic characteristics were determined by Seabird CTD probe. Sampling stations were distributed throughout the area of study during the bottom-trawl survey, covering the continental shelf, slope, and adjacent oceanic areas (Figure 1B) according to mesoscale structure resolution criteria (Sánchez and Gil, 2000).

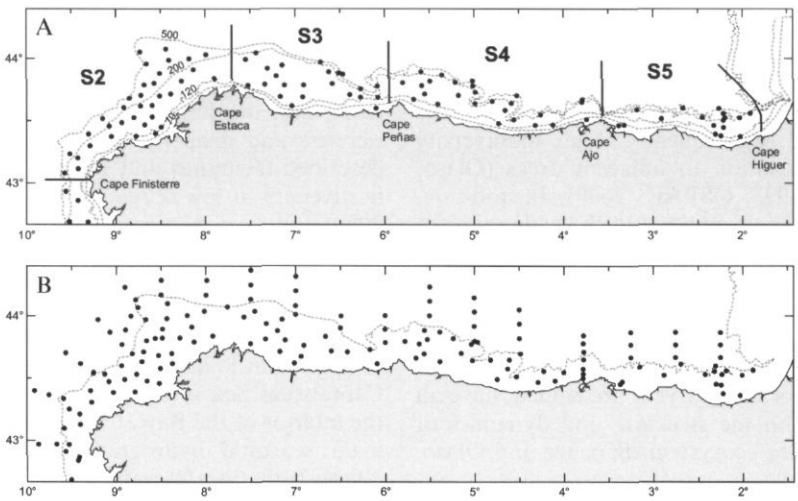


Figure 1. Study area: (A) Bottom-trawl survey stratification and hauls location during the 1998 survey; (B) hydrographic stations during the 1998 survey.

The total number of fish species caught over the trawlable area of the continental shelf, following the methodology previously described, was 152 Sánchez *et al.*, 2002). For each year, the value of the mean richness indices (number of species by haul), biomass indices (weight in g by haul), and the mean Shannon-Wiener diversity index (Shannon and Weaver, 1963) were obtained.

For the multivariate analysis and based on previous studies (Sánchez, 1993, 1997), a group of only 46 species was selected (Table 1), rejecting pelagic species which were poorly represented in samples using the bottom trawl. In this way, rare or occasional species (i.e. those present in less than 5% of hauls) were eliminated with the aim of reducing the percentage of zeros in the matrices. In this group of 46 species, 6 were analysed by age classes (according to the age-length keys obtained in the surveys), due to age-related changes in their behaviour and habitat.

The explanation of temporal variability due to the effect of environmental variables on communities was carried out using canonical correspondence analysis (CCA) (Ter Braak, 1987, 1988; Ter Braak and Verdonschot, 1995). The statistical significance of the direct methods of ordination was obtained by the Monte Carlo test (Verdonschot and Ter Braak, 1994). From the CCA of each survey a biplot between species and environmental variables was obtained which represents the influence of these variables on the axes of the analysis, quantified in correlations with the factorial axes (Ter Braak, 1990).

The abiotic variables used in the analysis were depth, near-bottom temperature, near-bottom salinity, Western longitude (Atlantic influence), and geographical sector (Figure 1A). The inclusion of the geographical sectors as variable is due to its different geomorphologic characteristic (large shelf in S2 and S3, deeper canyons and rocky bottoms in S4 and very narrow shelf and muddy bottoms in S5). It is noted that depth changes involve subsequent changes in several environmental factors such as pressure, light, temperature, etc. The canonical analysis was only carried out for the period 1993–1999, since hydrographic measurements began on the bottom-trawl surveys in 1993.

For the multivariate analysis of interannual variability of the historical series, a multitable system was used, following the procedure described in Chessel and Gaertner (1997) and Gaertner *et al.* (1998). This system performs the analysis of K-tables with the logic of correspondence analysis (CA), and was carried out by means of the STATIS routine of the program ADE-4 (Thioulousse *et al.*, 1997). The use of these analyses is not widespread in articles on marine ecology, although in the few articles that exist its usefulness in analysing time or spatial series is proven (Gaertner *et al.*, 1998; Blanc, 2000; Ghertsos *et al.*, 2001). The biomass matrices of 51 species were transformed by $\log(1+x)$ to minimize the dominant effect of exceptional catches.

In the STATIS multitable method, a CA was performed as the first step in calculating the matrix of scalar products between species for each survey, with the aim of standardizing the dimensions of

Table 1. List of 46 species of fishes (51, including age classes) considered in the multivariate analysis.

Code	Species	Code	Species
AMA	*Antonogadus macrophthalmus*	LCR	*Lampanyctus crocodilus*
ASP	*Argentina sphyraena*	LEQ	*Lepidion eques*
ALA	*Arnoglossus laterna*	MLA	*Malacocephalus laevis*
BPR	*Bathysolea profundicola*	MME0	*Merluccius merluccius* 0-group
BLU	*Buglossidium luteum*	MME1	*Merluccius merluccius* 1-group
CLY	*Callionymus lyra*	MME2	*Merluccius merluccius* 2-plus group
CMA	*Callionymus maculatus*	MVA	*Microchirus variegatus*
CAP	*Capros aper*	MPO	*Micromesistius poutassou*
CEP	*Cepola macrophthalma*	MSU	*Mullus surmuletus*
CCU	*Chelidonichtys cuculus*	NBO	*Notacanthus bonapartei*
CGU	*Chelidonichtys gurnardus*	PAC	*Pagellus acarne*
CLU	*Chelidonichtys lucerna*	PBO	*Pagellus bogaraveo*
COB	*Chelidonichtys obscura*	PER	*Pagellus erythrinus*
CMO	*Chimaera monstrosa*	PBL	*Phycis blennoides*
CCO	*Conger conger*	RCL	*Raja clavata*
DCA	*Deania calceus*	RMO	*Raja montagui*
ESP	*Etmopterus spinax*	SCA1	*Scyliorhinus canicula* 1-group
GAR	*Gadiculus argenteus*	SCA2	*Scyliorhinus canicula* 2-plus group
GME	*Galeus melastomus*	SLA	*Solea lascaris*
HDA	*Helicolenus dactylopterus*	SVU	*Solea vulgaris*
LBO0	*Lepidorhombus boscii* 0-group	TDR	*Trachinus draco*
LWH0	*Lepidorhombus whiffiagonis* 0-group	TSC	*Trachyrhynchus scabrus*
LBU0	*Lophius budegassa* 0-group	TLU	*Trisopterus luscus*
LBU1	*Lophius budegassa* 1-plus group	TMI	*Trisopterus minutus*
LPI0	*Lophius piscatorius* 0-group	ZFA	*Zeus faber*
LPI1	*Lophius piscatorius* 1-plus group		

the tables for the calculation of a matrix of scalar products between the tables of the surveys. After the diagonalization of this matrix, 10 coefficients of the first eigenvector of each survey were used to weight the 10 matrices of scalar products between species and build a table of maximum inertia, called a compromise table. Surveys with common structures contribute to this table to a greater extent. The multivariate analysis through CA of the compromise table defines axes and coefficients which describe the stable part of the surveys. The projection of the analyses separated from the 10 matrices of surveys on the compromise analysis shows interannual variations and the trajectories of temporal variation of species with respect to the stable structure (Chessel and Gaertner, 1997; Gaertner *et al.*, 1998).

Lastly, and in order to make a comparison with the descriptors of variability observed in the decade, we used the indices of Navidad current and upwelling described in R. Sánchez R *et al.* (2003) as a measure of the influence of this main hydrographic event each year. Upwelling strength has been estimated calculating the percentage of shelf planar (PA) area occupied by (negative) temperature anomalies (TA-) at 50 m depth with respect to the 1993–2000 mean. The relative Navidad strength has been evaluated with January salinities at 80 m, from a time-series of oceanographic recordings at a fixed station at the central shelf of the Cantabrian Sea (43°34.5′N–3°47.0′W).

Results

The analysis of the evolution of mean values of species richness by haul (Figure 2A) showed a relatively stable pattern in the different strata. In general terms a decrease in richness was seen with depth. In the coastal stratum, two periods were observed: the first (1990–1994) was characterized by a fall in richness. After 1994, the richness index rose progressively from 17 species to about 25 (Figure 2A). The 121–200 and 201–500 strata (middle shelf and outer shelf) presented greater interannual stability.

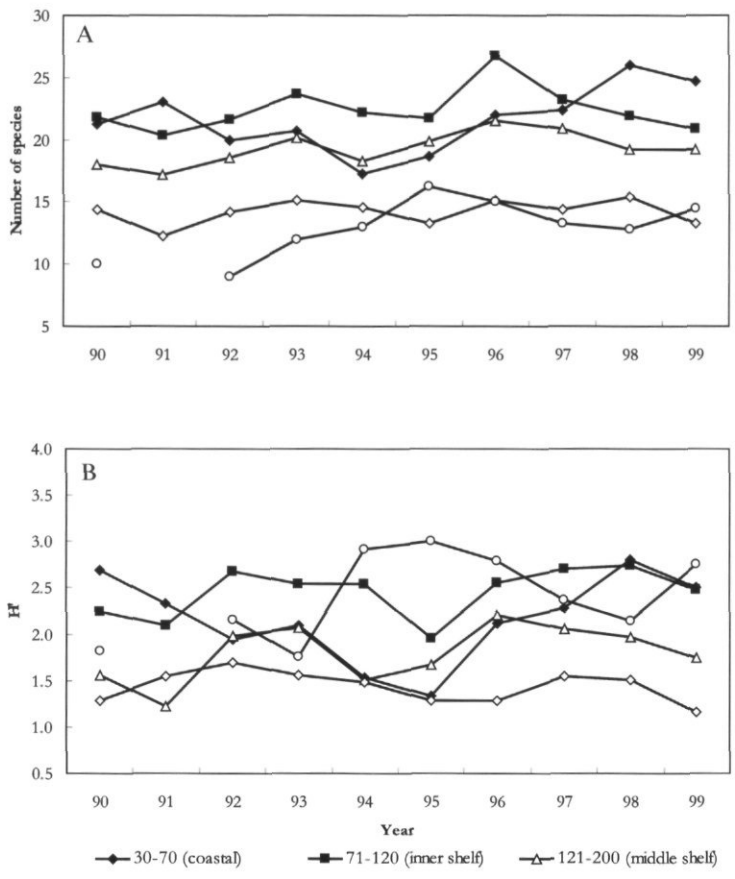


Figure 2. Mean values of indices by year for depth strata: (A) richness (number of species of fishes); (B) Shannon-Wiener diversity index of fish abundance in terms of number (H').

Regarding the diversity in number, as with richness, in the coastal stratum a decrease in values was observed from 1990 to 1995, followed by an increase to 1999. Although diversity was generally more variable than richness, the middle shelf and outer shelf strata were again the most stable, and show the lowest values in the time-series. The fall in diversity in the middle shelf strata in 1991 is noteworthy, although it is mainly due to a significant increase in blue whiting (*Micromesistius poutassou*) biomass. In general terms, the diversity increases towards the extreme strata (shallowest and deepest).

Effect of environmental variables on the structure of communities over the 1993–1999 period

The previous canonical analyses, by means of DCCA, showed a unimodal response model of species against environmental variables; for this reason a CCA was chosen. The analysis for each year separately showed a constant structure of communities throughout the series, as can be seen in the examples of 1993 and 1998 in Figure 3. In each year, species groupings were determined, similar to the bathymetric groups described by Sánchez (1993) using principal component analysis (PCA), and were distributed on the biplot with a pronounced Guttman effect (Figure 3). The Guttman effect arises when the main two environmental factors are autocorrelated (Greenacre, 1984); in this case, depth and temperature. The most discriminatory were the coastal group and the deepest strata groups (outer shelf and shelf break), situated at the extremes of the environmental gradients analysed. On the other hand, in the middle segments of these gradients, the inner shelf and middle shelf groups displayed reduced dispersion, with a position closer to the centroid of the biplot. This centroid is occupied by ubiquitous species of a wide optimal environmental range.

As shown in Figure 4, the formation of the CCA axes according to the environmental variables is fairly constant throughout the decade. In all years the most discriminatory variable is depth, with an interset correlation higher than 0.90 with the first axis (Table 2), correlation that increases slightly throughout the decade. Axis 2 is correlated mainly with salinity and, to a lesser extent, with longitude. The variable longitude, i.e. the Atlantic factor, is much less discriminatory in the years 1994 and 1995, but is of greater importance in 1997 (Table 2). The westernmost sector (S2) is more discriminatory, and so more distinct, in the period 1996–1999 than in previous years, where sectors discriminate with similar weight. However, it is difficult to obtain clear conclusions of assemblages' spatial zonation from the ordination of the different geographical sectors. The radial pattern is not constant, probably due to the interaction of salinity–temperature pattern of each sector with other abiotic variables, which were not taken into consideration.

Temperature contributes similarly to both axes, opposite to depth, salinity, and longitude. This depth–salinity–temperature–longitude relationship pattern obtained from CCA reflects the characteristic hydrological dynamics of the Cantabrian Sea and their influence on the main groundfish assemblages (Figure 3). The set of these four abiotic variables explains 21.4% of the variance of species data and 72.9% of the variance of species-environment relationship (mean values for the decade; Table 2).

Stability of communities' structure over the 1990–1999 decade

A CA was performed among the 10 surveys and a very high value of intraperiod inertia (inertia is the multivariate measure of the amount of variation in a data set) was found (97.5%) against interperiod inertia (2.5%). The differences between surveys were considered significant ($p < 0.05$) according to a permutation test. The multitable analysis shows a balanced contribution of surveys to the compromise analysis (Table 3). The best fits to the compromise table are found in 1990 and from 1994, 1996 being the survey which deviated the least ($\cos^2 = 0.68$; Table 3). In contrast, the fit of the 1991 survey to the compromise is the lowest ($\cos^2 = 0.28$) in addition to being the survey which contributes least to the analysis (weight = 0.28).

Figure 5 shows the structure of fish communities in the compromise analysis, i.e. the stable part of the 10 surveys used in the analysis. There is a great pattern of spatial reproducibility throughout the decade, since the representation of the compromise analysis (represented as an empty circle in Figure 5) faithfully reproduces the structure described by the canonical analysis from each year (Figure 3). A clear Guttman effect can also be observed, with two branches which separate the species into two well-differentiated groups of little more than 10 species, and a transition group very close to the origin, of less discriminatory species. This discrimination is a product of a first bathymetric factor, leading to the identification of axis 1 with depth. In this representation the 5 bathymetric groups already described can be distinguished, as in the canonical analysis.

The group of species situated in the negative quadrant of both axes corresponds to coastal species, where the most discriminatory ones are *Solea lascaris* and *Pagellus erythrinus*, along with a small group of species, all of them preferentially coastal (*Pagellus bogaraveo, Buglossidium luteum, Trachinus*

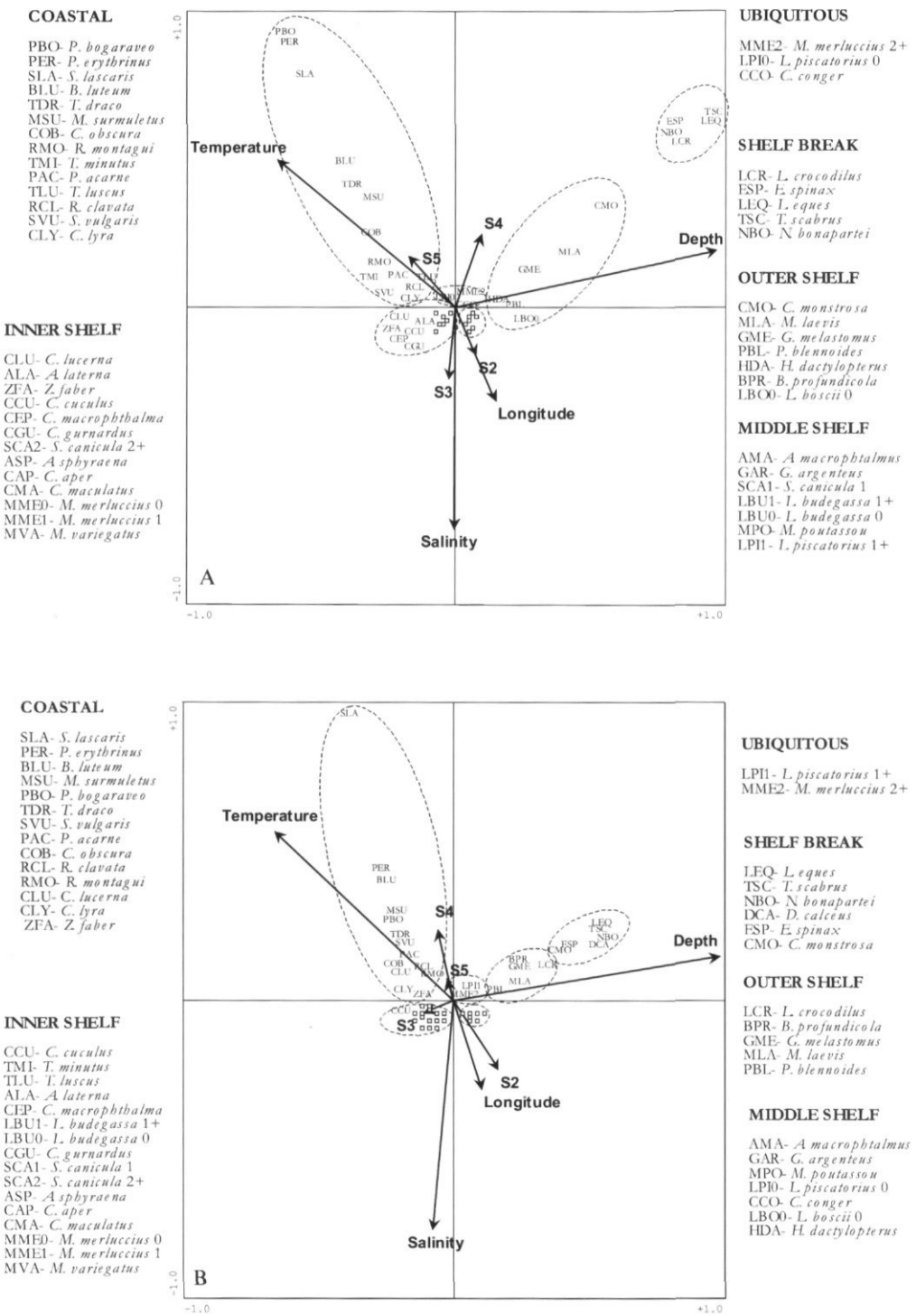


Figure 3. CCA biplot of species vs. environmental variables. (A) 1993 survey; (B) 1998 survey.

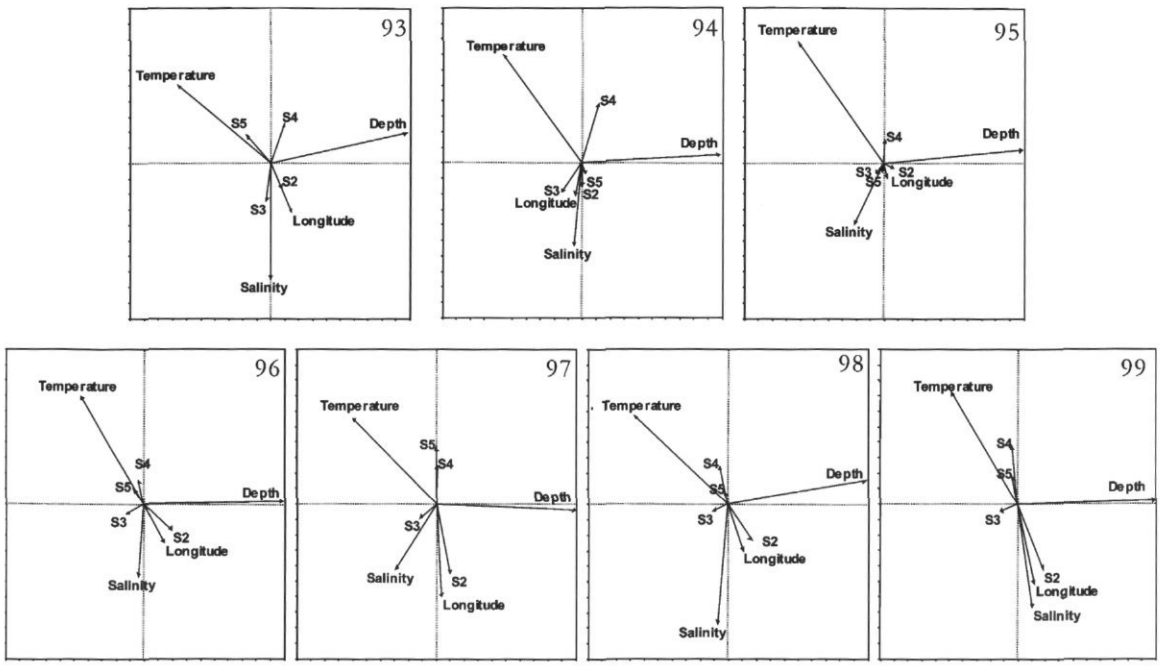


Figure 4. Correlation of environmental variables on the first two canonical axis of CCA for the surveys 1993–1999.

Table 2. Interset correlations by year between environmental variables and the first and second canonical axis. Eigenvalues and percentage of variance of species data and of species-environment relation explained by the CCA plane.

		1993	1994	1995	1996	1997	1998	1999
Axis 1	Depth	0.902	0.925	0.944	0.964	0.966	0.952	0.971
	Temperature	–0.619	–0.526	–0.585	–0.437	–0.578	–0.642	–0.475
	Salinity	–0.004	–0.054	–0.203	–0.038	–0.281	–0.073	0.100
	Longitude	0.140	–0.049	0.022	0.138	0.038	0.102	0.117
	Sector 2	0.072	0.000	0.063	0.195	0.098	0.160	0.179
	Sector 3	–0.027	–0.135	–0.059	–0.123	–0.116	–0.103	0.126
	Sector 4	0.092	0.111	0.004	–0.037	0.007	–0.059	–0.042
	Sector 5	–0.163	0.021	–0.014	–0.067	–0.003	–0.019	–0.035
Axis 2	Depth	0.145	0.031	0.065	0.016	–0.028	0.120	0.018
	Temperature	0.374	0.429	0.597	0.504	0.386	0.460	0.546
	Salinity	–0.561	–0.330	–0.302	–0.338	–0.292	–0.628	–0.505
	Longitude	–0.239	–0.127	–0.072	–0.183	–0.417	–0.245	–0.391
	Sector 2	–0.124	–0.089	–0.029	–0.120	–0.310	–0.191	–0.319
	Sector 3	–0.184	–0.117	–0.051	–0.047	–0.064	–0.037	–0.037
	Sector 4	0.187	0.235	0.114	0.112	0.168	0.193	0.281
	Sector 5	0.132	–0.041	–0.043	0.068	0.253	0.060	0.130
Eigenvalues Axis 1		0.309	0.350	0.436	0.442	0.408	0.434	0.484
Eigenvalues Axis 2		0.180	0.103	0.188	0.180	0.122	0.211	0.190
% Var species data		19.3	17.7	23.7	24.3	20.0	22.4	22.1
% Var spp.–environment relation		67.1	70.5	72.3	76.6	74.0	74.4	75.1

draco, Mullus surmuletus). Near the centroid are the species of transition in the bathymetric gradient, characteristic of the continental shelf, with very poor discrimination. Two groups can be distinguished, one of inner shelf species which show more affinity for the shallowest waters (*S. canicula, M. merluccius* classes 0 and 1, *L. whiffiagonis* class 0, *L. budegassa* class 1 plus, *L. piscatorius* class 0) and another of middle shelf species (*Micromesistius poutassou, L. budegassa* class 0, *Conger conger, L. boscii* class 0, *Helicolenus dactylopterus, Gadiculus argenteus*). The top predators of the demersal and benthic domains, respectively, *M. merluccius* (class 2 plus) and *L. piscatorius* (class 1 plus) do not belong to any group, and are situated closer to the centroid, indicating their wide optimal environmental range,

Table 3. Number of stations for survey, contribution of each survey in the compromise (weight), and fit of each survey to the compromise (cos^2).

Survey	Stations	Weight	Cos^2
1990	103	0.33	0.48
1991	88	0.28	0.28
1992	97	0.30	0.44
1993	92	0.29	0.44
1994	100	0.33	0.58
1995	101	0.32	0.58
1996	100	0.33	0.68
1997	104	0.32	0.46
1998	101	0.33	0.53
1999	105	0.31	0.45

which increases their number of available preys (Sánchez, 1993).

The other branch, situated in the positive x-axis quadrant, contains the deepwater species. This group can be split into two according to a bathymetric criterion. The cluster of outer shelf species groups together *Chimaera monstrosa, Bathysolea profundicola, Galeus melastomus, Phycis blennoides*, and *Malacocephalus laevis*. The other group corresponds to the shelf-break community and is made up of species such as *Notacanthus bonapartei, Trachyrhynchus scabrus, Lepidion eques, Deania calceus, Etmopterus spinax*, and *Lampanyctus crocodilus*.

Figure 5 also shows the interannual variations (represented as empty squares) from the stable structure. The largest interannual deviations are found in the coastal and shelf-break communities. The continental shelf (inner and middle shelf) communities are those that have the lowest range of variation. In particular, the ubiquitous species *M. merluccius* (class 2 plus) and *L. piscatorius* (class 1 plus) present the lowest values of interannual variability.

Finally, Figure 6 shows the relationship of the descriptive parameters of multivariate, canonical, and multitable analyses, and the external indices used to describe the main hydrographic driving agents. In the period with biological–physical data (1993–1999), three different hydrographic scenarios were observed: (A) strong *Navidad* current and weak upwelling index (years 1993, 1998, and 1999); (B) moderate *Navidad* current and high upwelling index (years 1994 and 1997), and (C) weak *Navidad* current and high upwelling index (years 1995 and 1996). The dynamics that originate these three types of scenarios in the area and their occurrence are described in Gil and Sánchez (2001). It can be seen that the years with the maximum percentage of variance explained by the abiotic variables considered in the CCA analysis correspond with scenario type C (24%). Low percentages of variance explained correspond with scenario type B (18–20%). Also, years with maximun values of upwelling indices (1994 to 1997) coincide with those of least discrimination in salinity and longitude (except 1997). A relationship also seems to exist between the variance explained by the environmental variables in the canonical analysis and the fit of each year to the stable part in the multitable analysis, since the years that contribute most to the stable part (Table 3) are those which are best explained by the set of environmental variables used.

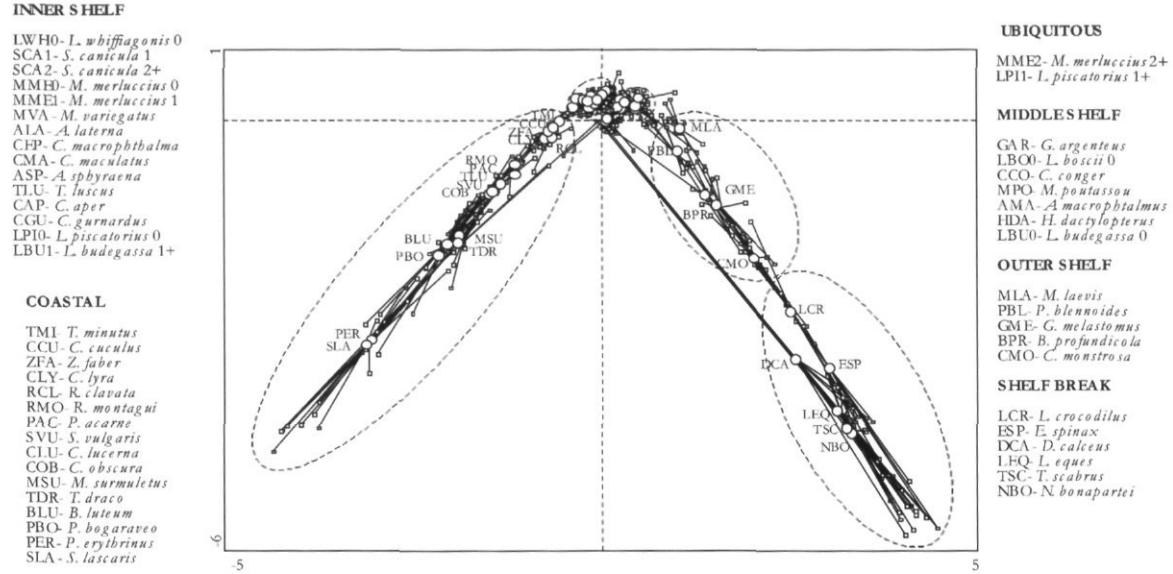


Figure 5. Stable structure of species projected on the first factorial plane of compromise in the decade of 1990s and variations inter-surveys of the species around the stable structure. Position in the compromise (O); position in each survey (□).

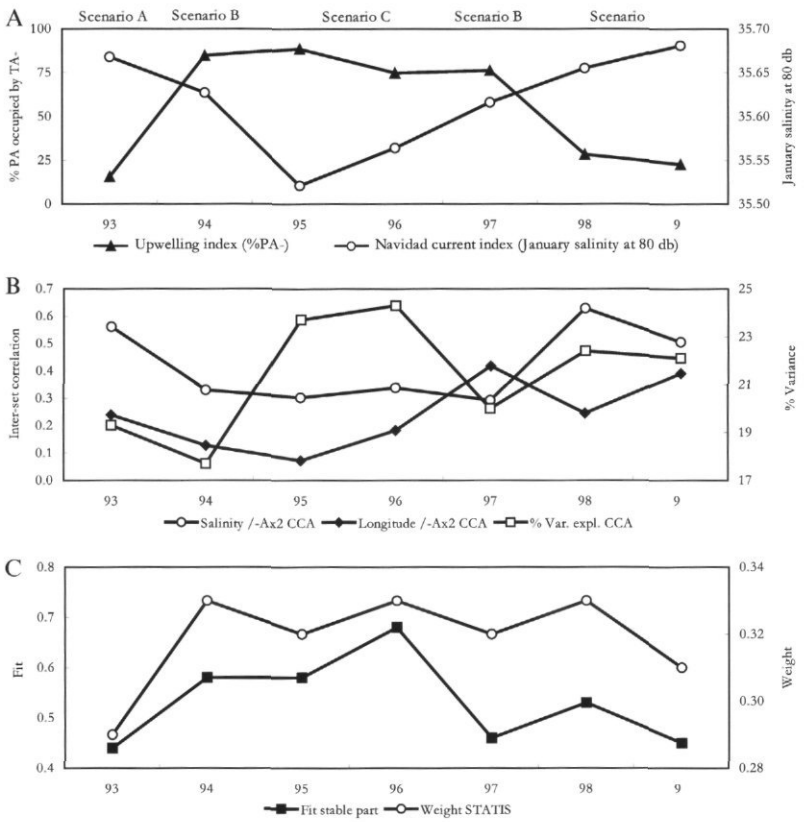


Figure 6. Values during the 1993–1999 period of (A) main hydrographic driving agents indices and scenarios, (B) correlation between environmental variables and canonical axis of CCA, and variance of species data explained by this first CCA plane, (C) fit of each survey with the stable part (compromise) and weight of this surveys in the multitable analysis.

Discussion

The sources of variation existing in the results may differ in spatial variability, which has been revealed to be mainly bathymetric, and temporal variability, which is partly related to the evolution of the main hydrographic driving agents described in the area.

The bathymetric differences show a progressive decrease in mean fish species richness with depth, as described in the Cantabrian Sea by Sánchez (1993) and in adjacent areas by Fariña *et al.* (1997a). This pattern is reasonably stable in the decade. The decline in the number of species with depth is probably brought about by the higher productivity of the coastal waters, in contrast to the inverse phenomena appearing in invertebrates (Olaso, 1990; Fariña *et al.*, 1997b), which prefer deeper water and muddy substrates because of their predominantly detritivorous feeding habits. Interannual variations of diversity can be explained only in part by the action of the main hydrographic events which govern the area, because this index is strongly affected by the values of dominance of migratory gregarious species with a wide range of distribution area (i.e. blue whiting, horse mackerel, and silvery pout (*Gadiculus argenteus*)). The period of years with strong upwelling indices corresponds to the lowest diversity of the coastal community. This may be caused by the direct effect of the increase in primary production in the coastal area, and consequently on the levels of biomass of some planktophagous fish (with high reproductive rates and fast growth) and particularly schools of juveniles of horse mackerel. The spatial structure shows how variability is mainly detected in the coastal, outer shelf and shelf break strata, that is, at the extremes of the environmental gradients, while the central continental shelf strata are more stable. This difference in stability is visible in all the analyses performed: in the ecological indices (especially for the coastal stratum), in the canonical analyses by survey, in the representation of the stable part of the decade and in the trajectories followed by species around this stable structure. The central strata of the continental shelf are those that have suffered greater pressure from the trawl fleet for decades, and consequently a greater degree of simplification of communities must be expected

(Sánchez, 1993). At the same time, the geomorphology of the ground is more homogeneous, minimizing the ecotonal effect.

Overlying the temporal variability, there is a reproducible spatial structure throughout the decade, in which some unvarying bathymetric groups can be found. It can therefore be said that fish communities remained relatively stable throughout the period studied, with a high degree of reproducibility of the bathymetric spatial pattern. This defined bathymetric structure has been described in previous studies carried out in the area (Sánchez, 1993, 1997; Fariña *et al.*, 1997a) and in other nearby areas (Zendrera, 1990; Lauroz, 1993; Gaertner *et al.*, 1998; Souissi *et al.*, 2001). The smaller depth discrimination on the demersal fish assemblages obtained by Fariña *et al.* (1997a) in the area near Galicia is due to the lack of sampling on the coastal and shelf-break strata during the study period (1980–1991). Our results identify the most extreme strata of the Cantabrian sea shelf (coastal and shelf break) as the main source of variability in the decade. In the Gulf of Lions area, Gaertner *et al.* (1998) derived similar results through a multitable analysis, finding the greatest trajectories of species for each year in the extreme strata (coastal region and continental slope) with respect to the representation of the stable part of the period 1983–1992. A possible explanation for this larger variability in the Cantabrian Sea (usually considered as a nursery area) is a greater influence over the coastal communities of recruitment to the bottom of abundant species in the area, which are driven by yearly hydrographic scenarios (Sánchez and Gil, 2000; Sánchez *et al.*, 2001; Gil and Sánchez, 2001). The subsequent ontogenetic migratory behaviour towards deeper zones, described for some species (Fariña and Abaunza, 1991; Sánchez, 1993), increases this variability. On the other hand, the shelf-break communities may be influenced by the environmental variability on the eastward slope current, which has a strong impact in the distribution and dispersion of the early stages of fish in the area (Reid, 2001). Also, the vertical motion of the water, produced by the associated eddies, enhanced the production processes of subsurface layers (Piontkovsky *et al.*, 1995) over the shelf break. This fact determines the reproductive behaviour of many demersal species that migrate to these shelf-break areas with larger productivity and transport mechanisms facilitating larval survivorship (i.e. hake, red sea-bream).

On the other hand, the Navidad current seems to determine haline-longitudinal variability. Years with strong current indices (1993, 1998, and 1999) of hydrographic scenario type A create haline gradients which are translated into greater discrimination of the salinity factor in the CCA analysis, and because of its entrance from the west, of the longitudinal factor. A moderate Navidad current is required to prevent larvae and pre-recruits of demersal fish being transported off the progressively narrow shelf of the Cantabrian Sea. Scenario type B is an optimal situation that occurs after the adequate development of an upwelling front over the shelf area and surrounded by its associated mesoscale structures. This energetic scenario is responsible for high hake recruitment in the period considered (Sánchez and Gil, 2000; Sánchez *et al.*, 2001; Sánchez *et al.*, 2002), and probably also has similar consequences for many other demersal species. The mesoscale dynamics have a strong impact on biological variability and patchiness (Mann and Lazier, 1991) and are probably the cause of the low variance value explained in our CCA analysis for the years 1994 and 1997.

Finally, our results show that the hydrographic scenario type C is the one that is better explained by the set of environmental variables used in the CCA analysis, and makes up the most stable structure of groundfish assemblages throughout the decade. This scenario (i.e. 1995 and 1996) is characterized by the considerable width of the cold coastal fringe and by the anticyclonic eddies located further away from the shelf area (Sánchez and Gil, 2000; Gil and Sánchez, 2001). The lack of mesoscale activity over the shelf probably produces a more homogeneous situation over the bottom, with less disturbance of the stable structure of the communities, increasing the discriminant value of depth, near-bottom temperature, near bottom salinity, and the other abiotic variables considered.

The aim of the present article is not to draw conclusions relating to the evolution of ecological structures ascribed to the fishing pressure, which has been applied to the area, but to establish this evolution and explain it through the environmental information available. In this sense, the combined analysis of individual surveys with a multitable analysis, which separates the stable part from the interannual variations, seems useful for the interpretation of historical series. Later, with more information on the changes in fishing fleet strategies, distribution of effort in the area, identification of vulnerable species (Rogers *et al.*, 1999; Jennings and Reynolds, 2000), and with experiments on fishing exclusion areas (Hoffmann and Dolmer, 2000; Sumaila *et al.*, 2000), the effect of fishing on groundfish communities in the Cantabrian Sea may be determined.

Acknowledgements

This study was made possible thanks to the invaluable work of all the participants in the North of Spain bottom-trawl surveys and the crew(s) of the RV "Cornide de Saavedra". The work was partially supported by the Marcelino Botín Foundation.

References

Bianchi, G., Gislason, H., Graham, K., Hill, L., Jin, X., Koranteng, K., Manickchand-Heileman, S., Payá, I., Sainsbury, K., Sánchez, F., and Zwanenburg, K. 2000. Impact of fishing on size composition and diversity of demersal fish communities. ICES Journal of Marine Science, 57: 558–571.

Blanc, L. 2000. Données spatio-temporelles en écologie et analyses multitableux: examen d'une relation. These Université Claude-Bernard-Lyon I. 266 pp.

Botas, J. A., Fernández, E., Bode A., and Anadón, R. 1990. A persistent upwelling off the Central Cantabrian Coast (Bay of Biscay). Estuarine, Coastal and Shelf Science, 30: 185–199.

Chessel, D., and Gaertner, J. C. 1997. Analyses des correspondances et K-tableaux. Documentation ADE-4. Université Lyon I. Thema 59. 24 pp.

Fariña, A. C., and Abaunza P. 1991. Contribución al estudio de los juveniles de merluza entre Cabo Villano y Cabo Prior mediante prospecciones pesqueras. Bol. Inst. Esp. Oceanogr., 7, 155–163.

Fariña, A. C., Freire, J., and Gonzalez-Gurriaran, E. 1997a. Demersal fish assemblages in the Galician continental shelf and upper slope (NW Spain): spatial structure and long-term changes. Estuarine, Coastal and Shelf Science, 44: 435–454.

Fariña, A. C., Freire, J., and Gonzalez-Gurriaran, E. 1997b. Estructura espacial y cambios a largo plazo de las comunidades megabentónicas de la plataforma continental y talud superior de Galicia (noroeste de España): análisis comparativo de peces y crustáceos decápodos. Publ. Esp. Inst. Esp. Oceanogr., 23: 53–70.

Frid, C. L. J., and Clark, R. A. 2000. Long-term changes in North Sea benthos: discerning the role of fisheries. *In* Effects of Fishing on Non-Target Species and Habitats. Biological, Conservation and Socio-economic Issues, pp. 198–216. Ed. by Kaiser and de Groot. Blackwell Science, Oxford.

Frouin, R., Fiúza, A. F. G., Ambar, I., and Boyd, T. J. 1990. Observations of a Poleward Surface Current off the coasts of Portugal and Spain during winter. Journal of Geophysical Research, 5 (C1): 679–691.

Gaertner, J. C., Chessel, D., and Bertrand, J. 1998. Stability of spatial structures of demersal assemblages: a multitable approach. Aquatic Living Resources, 11: 75–85.

Ghertsos, K., Luczak, C., and Dauvin, J. C. 2001. Identification of global and local components of spatial structure of marine benthic communities: example from the Bay of Seine (Eastern English Channel). Journal of Sea Research, 45: 63–77.

Gil, J., and Sánchez, R. 2001. The importance of the main external driving agents in the Bay of Biscay hydrographic changes. *In* Oceanographie du golfe de Gascogne. VII° Colloq. Int., Biarritz, 4–6 avril 2000. Ed. Ifremer, Actes Colloq., 31: 43–48.

Greenacre, M. 1984. Theory and Applications of Correspondence Analysis. London: Academic Press.

Hoffmann, E., and Dolmer, P. 2000. Effect of closed areas on distribution of fish and epibenthos. ICES Journal of Marine Science, 57: 1310–1314.

ICES. 1997. Report of the International Bottom Trawl Survey Working Group. ICES CM 1997/H: 6. 50 pp.

ICES. 2000. Report of the Working Group on Ecosystems Effects of Fishing Activities. ICES CM 2000/ACME:2/ ACFM+E. 93 pp.

Jennings, S., and Reynolds, J. D. 2000. Impacts of fishing on diversity: from pattern to process. *In* Effects of Fishing on Non-Target Species and Habitats. Biological, Conservation and Socio-economic Issues, pp. 235250. Ed. by Kaiser and de Groot. Blackwell Science, Oxford.

Jongman, R. H. G., Ter Braak, C. J. F. and Van Tongeren, O. F. R. 1987. Data analysis in community and landscape ecology. Pudoc Wageningen. 286 pp.

Labropoulou, M., and Papaconstantinou, C. 2000. Community structure of deep-sea demersal fish in the North Aegean Sea (northeastern Mediterranean). Hydrobiologia, 440: 281–296.

Lauroz, K. 1993. Description et cartographie des associations d'especes vagiles (poissons et invertebres) dans le golfe de Gascogne et sur le plateau celtique. Memoire. Univ. d'Aix Marseille II.

Leps, J., and Smilauer, P. 1999. Multivariate analysis of ecological data. Faculty of Biological Sciences, University of South Bohemia, Weské Budéjovice. 110 pp.

Manly, B. F. J. 1991. Randomization and Monte Carlo Methods in Biology. Chapman and Hall, London. 281 pp.

Mann, K. H., and Lazier, J. R. N. 1991. Dynamics of marine ecosystems: biological-physical interactions in the oceans. Blackwell Scientific Publications, Boston.

Olaso, I. 1990. Distribución y abundancia del megabentos invertebrado en fondos de la plataforma cantábrica. Publ. Esp. Inst. Esp. Oceanogr., 5. 128 pp.

OSPAR. 2000. Quality Status Report 2000. Region IV: Bay of Biscay and Iberian Coast. OSPAR Commission, London. 134 + xiii pp.

Pingree, R. D., and Le Cann, B. 1990. Structure, strength and seasonality of the slope currents in the Bay of Biscay region. J. Mar. Biol. Ass. U.K., 70: 857–885.

Piontkovsky, S. A., Willians, R., Peterson, W., and Kosnirev, V. K. 1995. Relationship between mesozooplankton and energy of eddy fields. Mar. Ecol. Progr. Ser., 128: 35–41.

Reid, D. G. 2001. SEFOS – shelf edge fisheries and oceanography studies: an overview. Fisheries Research, 50: 1–15.

Rice, J. C. 2000. Evaluating fishery impacts using metrics of community structure. ICES Journal of Marine Science, 57: 682–688.

Rogers, S. I., Maxwell, D., Rijnsdorp, A. D., Damm, U., and Vanhee, W. 1999. Fishing effects in northeast Atlantic shelf seas: patterns in fishing effort, diversity and community structure. IV. Can comparisons of species diversity be used to assess human impacts on demersal fish faunas? Fisheries Research, 40: 135–152.

Romesburg, H. C. 1985. Exploring, confirming and randomization tests. Computers and Geosciences, 11: 19–37.

Sánchez, F. 1993. Las comunidades de peces de la plataforma del Cantábrico. Publ. Esp. Inst. Esp. Oceanogr., 13. 137 pp.

Sánchez, F. 1997. Study of homogeneity of depth strata in the Northern Spanish bottom trawl surveys. *In* IBTS WG Report. ICES CM 1997/H: 6. 50 pp.

Sánchez, F., Blanco, M., and Gancedo, R. 2002. Atlas de los peces demersales y de los invertebrados de interés comercial de Galicia y el Cantábrico. Otoño 1997–1999. Publ. Esp. Inst. Esp. Oceanogr. (In press.)

Sánchez, F., de la Gándara, F., and Gancedo, R. 1995. Atlas de los peces demersales de Galicia y el Cantábrico. Otoño 1991–1993. Publ. Esp. Inst. Esp. de Oceanogr., 20. 99 pp.

Sánchez, F., and Gil, J. 2000. Hydrographic mesoscale structures and Poleward Current as a determinant of hake (*Merluccius merluccius*) recruitment in southern Bay of Biscay. ICES Journal of Marine Science, 57: 152–170.

Sánchez, F., Gil, J., Sánchez, R., Mahe, J. C., and Moguedet, Ph. 2001. Links between demersal species distribution pattern and hydrographic structures in the Bay of Biscay and Celtic Sea. *In* Oceanographie du golfe de Gascogne. VII°

Colloq. Int., Biarritz, 4–6 avril 2000. Ed. IFREMER, Actes Colloq., 31: 173–180.

Sánchez, F., and Olaso, I. 2001. Cantabrian Sea ecosystem model and fishery resources management. *In* Oceanographie du golfe de Gascogne. VII° Colloq. Int., Biarritz, 4–6 avril 2000. Ed. IFREMER, Actes Colloq., 31: 187–194.

Sánchez, F., and Olaso, I. 2002. Effects of fisheries on the Cantabrian Sea shelf ecosystem. Ecological Modelling. (In press.)

Sánchez, R., Sánchez, F., and Gil, J. 2003. The optimal environmental window that controls hake (*Merluccius merluccius*) recruitment in the Cantabrian Sea. ICES Marine Science Symposia, 219: 415–417. (This volume.)

Shannon, C. E., and Weaver, W. 1963. The Mathematical Theory of Communication, pp. 117–127. Urbana University Press, Illinois, USA.

Sumaila, U. R., Guénette, S., Alder, J., and Chuenpagdee, R. 2000. Addressing ecosystem effects of fishing using marine protected areas. ICES Journal of Marine Science, 57: 752–760.

Ter Braak, C. J. F. 1987. The analysis of vegetation-environment relationships by canonical correspondence analysis. Vegetatio, 69: 69–77.

Ter Braak, C. J. F. 1988. Partial canonical correspondence analysis. *In* Classification Methods and Related Methods of Data Analysis, pp. 551–558. Ed. by H. H. Bock. North Holland, Amsterdam.

Ter Braak, C. J. F. 1990. Interpreting canonical correlation analysis through biplots of structure correlations and weights. Psychometrika, 55: 519–531.

Ter Braak, C. J. F., and Prentice, I. C. 1988. A theory of gradient analysis. Advances in Ecological Research, 18: 271–314.

Ter Braak, C. J. F., and Verdonschot, P. F. M. 1995. Canonical correspondence analysis and related multivariate methods in aquatic ecology. Aquatic Sciences, 57. 3 pp.

Thiolouse, J., Chessel, D., Doledec, S., and Olivier, J. M. 1997. ADE-4: a mulivariate analysis and graphical display software. Statistic and Computing, 7: 75–83.

Van Wijngaarden, R. P. A., Van Den Brink, P. J., Oude Voshaar, J. H., and Leeuwangh, P. 1995. Ordination techniques for analysing response of biological communities in toxic stress in experimental ecosystems. Ecotoxicology, 4: 61–77.

Verdonschot, P. F. M., and Ter Braak, C. J. F. 1994. An experimental manipulation of oligochaete communities in mesocosms treated with chlorophytos or nutrient additions: multivariate analyses with Monte Carlo permutation tests. Hydrobiologia, 278: 251–266.

Zendrera, N. 1990. Typologie du golfe de Gascogne a partir de l'analyse des associations faunistiques. Oceanologie Biologique: Ecosystems marins. Option parametrisation et modelisation. Univ. Pierre et Marie Curie (Paris VI).

ICES Marine Science Symposia, 219: 261–270. 2003.

Changes in fish distribution in the eastern North Atlantic: Are we seeing a coherent response to changing temperature?

K. Brander, G. Blom, M. F. Borges, K. Erzini, G. Henderson, B. R. MacKenzie, H. Mendes, J. Ribeiro, A. M. P. Santos, and R. Toresen

Brander, K., Blom, G., Borges, M. F., Erzini, K., Henderson, G., MacKenzie, B. R., Mendes, H., Ribeiro, J., Santos, A. M. P., and Toresen, R. 2003. Changes in fish distribution in the eastern North Atlantic: Are we seeing a coherent response to changing temperature? – ICES Marine Science Symposia, 219: 261–270.

The temperature of the upper 300 m of the North Atlantic increased by about 0.57°C between 1984 and 1999, but this underlying trend was overlain with substantial geographic and interannual variability. Northward shifts occurred in the distribution of many commercial and non-commercial fish species in the NE Atlantic during the 1990s. New records were established for a number of Mediterranean and NW African species on the south coast of Portugal. Red mullet (*Mullus surmuletus*) and bass (*Dicentrarchus labrax*) extended their ranges northward to western Norway and catches of the former increased throughout the 1990s in the North Sea. Abundance or relative abundance of warm-water commercial species of gadoids and flatfish generally increased during the 1990s, but like the warming trend the changes in distribution and abundance were by no means uniform and there was considerable interannual variability. There were also examples of southward shifts for some species, which can be related to local hydrographic conditions, such as upwelling. Information on distribution and abundance of Greenland cod (*Gadus morhua* L.) and Norwegian spring-spawning herring (*Clupea harengus*) during a previous warming period in the late 1920s and 1930s is also presented and compared with changes in the 1990s.

Keywords: climate change, fish distribution, Northeast Atlantic, temperature.

K. Brander: ICES, Palaegade 2–4, DK-1261 Copenhagen K, Denmark [e-mail: keith@ices.dk]. G. Blom: Department of Fisheries and Marine Biology, University of Bergen, High Technology Centre, N-5020 Bergen, Norway. M. F. Borges, H. Mendes, and A. M. P. Santos: Fisheries and Sea Research Institute, Avenida de Brasilia 1449-006, Lisboa, Portugal. K. Erzini and J. Ribeiro: CCMAR, Universidade do Algarve, 8000 Faro, Portugal. G. Henderson: FRS Marine Laboratory Aberdeen, PO Box 101, Victoria Road, Aberdeen AB11 9DB, Scotland. B. R. MacKenzie: Danish Institute for Fisheries Research, Department of Marine Ecology and Aquaculture, Kavalergården 6, DK-2920 Charlottenlund, Denmark. R. Toresen: Institute of Marine Research, PO Box 1870, N-5024 Bergen, Norway.

Introduction

Given the recent concern over global warming, it is not surprising that information about changes in distribution of fish have appeared in both popular (Brown, 2000) and scientific (Quero *et al.*, 1998; Stebbing *et al.*, 2002) sources over the past few years, and have been related to increased sea temperatures. We present evidence of changes in fish distribution from many parts of the Northeast Atlantic (Figure 1) during the 1990s and relate this to observed temperature variability. In order to avoid bias we made a particular effort to find information on distribution changes which appeared to contradict the "global warming" scenario.

Although the main aim of the article is to look at evidence of changes in distribution, some information on changes in abundance is also included. The distribution of a species is determined by the geographic area it occupies and also by its relative abundance within that geographic area. For example, an increase in abundance near the northern end of its range and/or a decrease in abundance near the southern end can be regarded as a northward shift in distribution, even if the overall range remains the same.



Figure 1. ICES Fishing Areas and place names referred to in the text.

Changes in distribution have many causes, but thermal effects are pervasive and reasonably well known (e.g. Welch *et al.*, 1998). We know the thermal responses and limits for many fish species (Alderdice and Forester, 1971; Magnuson and Destasio, 1997) and it is therefore possible to consider whether observed distribution changes are commensurate with the observed scale of temperature change. Changes in temperature permit extension of geographic range in some areas and limit distribution in others. Changes in temperature may also indicate changes in the movement and distribution of water masses, which transport species to new areas (Holliday and Reid, 2001).

An analysis of distribution change, restricted mainly to thermal effects, is inevitably incomplete, but there are nevertheless scientific and practical justifications for doing so. Temperature affects the rates of physiological, metabolic, and behavioural processes (Brett, 1979; Wood and McDonald, 1997) and hence the population dynamics of the species via growth (Brander, 1995), recruitment (O'Brien *et al.*, 2000), and mortality. We have better information about temperature fields than any other environmental variable affecting fish, which does not mean that we have adequate temperature information in all cases, but it is much better than for any other variable.

Given the large scale in time and space which is covered here and the limited amount of matching ambient environmental information, the analysis is mainly qualitative. Our aim is to compare observations of changes in fish distribution and abundance with changes in temperature, and to evaluate whether the response is coherent in the sense of following a common principle.

Materials and methods

Climate indicators

Although a large amount of data on sea temperature exists, no consistent, comprehensive, standardized source of information was available at the time of writing. Information about temperature variability in the eastern North Atlantic has been taken from two principal sources: sea temperature data are from the Annual ICES Ocean Climate Status Summary 2000/2001 (ICES, 2002); air temperature data are from the IPCC Data Distribution Centre, (http://ipcc-ddc.cru.uea.ac.uk/), which provides visualizations of annual mean air temperature anomalies (relative to the mean for 1961–1990).

The ICES Ocean Climate Status Summary has begun to bring together time series representing particular sea areas, but they are not presented in a standard way and most cover only a limited period of time. It is therefore difficult to obtain the necessary background information on the temperature variability over all the areas and time periods reviewed here. In order to gain a more comprehensive overview, air temperature data are included for all areas, because they are available in a standard format back to 1900. This allows comparisons between different areas over long time periods. The degree of similarity between trends in sea and air temperature can be judged by comparing them for areas for which time series of both are plotted in Figure 2.

The temperature of the upper 300 m of the North Atlantic rose by about 0.57°C between 1984 and 1998 (Figure 3). The increase was not geographically uniform, with some areas showing quite different trends; therefore a coherent response, in the sense of fish distribution behaving uniformly throughout the NE Atlantic, cannot be expected.

Mean bottom temperature data used to compare different areas are taken from Brander (1995) and from the ICES oceanographic database.

Fish population indicators

Information on fish distribution and abundance comes from catches by commercial fishing vessels

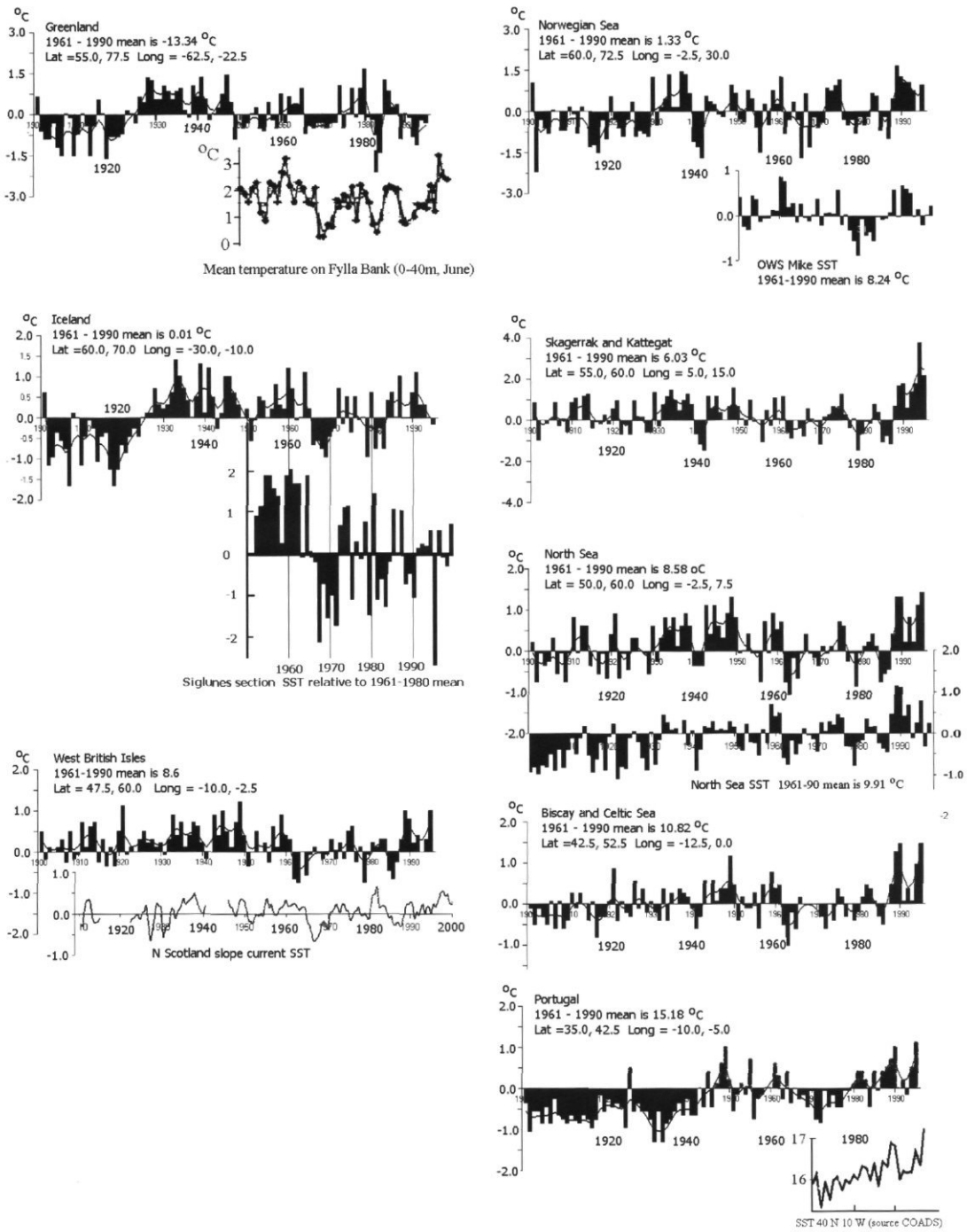


Figure 2. Mean annual air temperature and sea surface temperature (SST) anomalies for the main areas of the NE Atlantic. Air temperature data (1900–1995) are from the IPPC Data Distribution Centre, from which information concerning the mean 1961–1990 climatology and the anomaly time series can be obtained. SST data and anomalies are from the ICES Ocean Climate Status Summary (ICES, 2002).

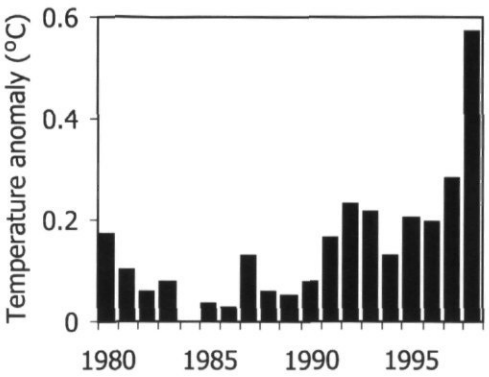


Figure 3. Volume mean temperature anomaly for the North Atlantic 0–300 m. 1984 is set to 0°C. Replotted from Levitus *et al.* (2000).

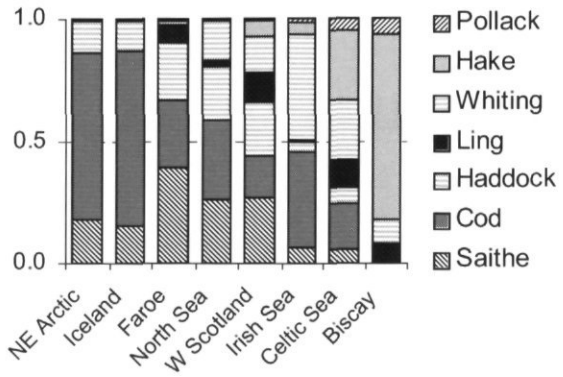


Figure 4. Proportions of seven principal gadoid species in the fishing areas of the NE Atlantic, 1973–1998.

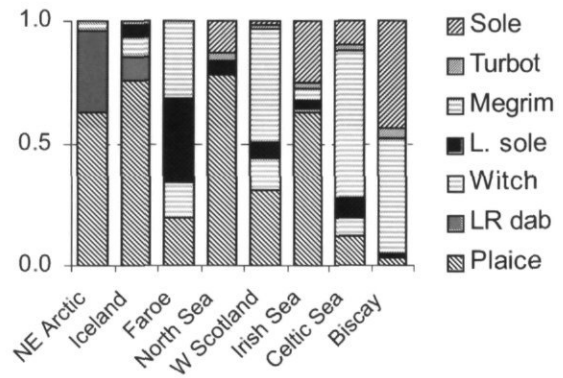


Figure 5. Proportions of the seven principal flatfish species in the fishing areas of the NE Atlantic, 1973–1998.

(catch statistics reported to ICES and available from the ICES STATLANT database http://www.ices.dk/fish/statlant.htm), research sampling and records of unusual species from a variety of sources. All of these sources have shortcomings which limit the strength and detail of interpretations drawn from them, but consistent patterns can nevertheless be derived.

Catch statistics are used here to show the varying proportion of seven principal gadoid and seven flatfish species in the areas NE Arctic, Iceland, Faroe, North Sea, West of Scotland, Irish Sea, Celtic Sea, and Biscay (Figure 1). The proportion of each gadoid species in relation to the total catch of all seven gadoids (for the period 1973–1998) is shown in Figure 4, and Figure 5 shows the same pattern for the flatfish. Since all of these species are marketed commercially and are in many cases caught in the same fisheries, the catches are a reasonable representation of their relative abundance in the different areas. Thus the absence of hake from the catches in the NE Arctic, Iceland, and Faeroe, or of saithe from the Bay of Biscay, is because they do not occur there.

Further relevant details about the nature and source of particular catch records are provided in the sections on each area below.

Results

Climate indicators

As previously mentioned, the mean temperature anomaly for the upper 300 m of the North Atlantic increased by about 0.57°C between 1984 and 1998 (Figure 3). Atlantic water along the NW European shelf edge has been warming since 1987 at a rate of 0.5°C/decade (ICES Ocean Climate Status Summary 2000/2001). The long-term trends in sea surface temperature (SST) are similar to those in air temperature for this area (Figure 2).

The pattern of temperature change on the European continental shelf from 43°N to 60°N and from 15°E to 12°W (areas marked Skagerrak and Kattegat, North Sea, West of British Isles, and Biscay and Celtic Sea in Figure 2) can be characterized as a period of positive air temperature anomalies from 1930 to 1961 (apart from a 3-year cold period from 1940 to 1942), then 2 years of rapid cooling. During the period 1964 to 1986 the temperature fluctuated about the mean, and from 1987 rose quickly to high positive anomalies.

The period of warming of the North Atlantic from 1918 to 1933 was much more marked at Greenland, Iceland, Faroe, and the Norwegian Sea than it was further south. The former three areas maintained positive air temperature anomalies until 1950 and the main cooling period was from 1963 to 1970 (Figure 2).

Fish population indicators

Ria Formosa and the south coast of Portugal

The Ria Formosa is a 55-km-long lagoon in the Algarve (southern Portugal), with a surface area of approximately 16 300 hectares. The fish fauna has been well studied, particularly by Monteiro (1989) and Monteiro *et al.* (1987, 1990). They sampled 8 stations (three replicates each) monthly over a 7-year period (1980 to 1986) using a 50-m-long, 3.5-m-high beach seine with a 14 mm mesh size. Sixty-seven species were reported and their annual patterns of abundance and migration described.

Since September 2000, sampling with beach seines has been carried out on a monthly basis in the Ria Formosa in order to evaluate changes in species composition and relative abundance. In the 9 months to May 2001, 85 fish species have been recorded in the beach seine, of which 52 were reported by Monteiro (1989). For species that were not common to the two studies, information on geographic distribution was obtained from Whitehead *et al.* (1984, 1986) and their occurrence or disappearance between the earlier period and the present was evaluated.

The increase was largely due to species not previously recorded in Portuguese waters and in particular to species whose distribution was previously limited to the Mediterranean and/or NW Africa (Whitehead *et al.*, 1984): *Parablennius incognitus* (Blenniidae), *Michrochirus boscanon* (Soleidae), *Pomadasys incisus* (Haemulidae), *Symphodus ocellatus* (Labridae), and *Bothus podas* (Bothidae). Other largely Mediterranean or NW African species, such as *Spicara flexuosa* and *Spicara maena* (Whitehead *et al.*, 1984), were found in the Ria recently, but not in 1980–1986. A few northerly species, such as the gobies *Gobius couchi* and *Pomatoschistus pictus* have apparently increased their range to the south.

Of the northerly species recorded by Monteiro (1989) but not found in 2000–2001, Portugal and/or NW Africa and the Mediterranean were the southern limits according to Whitehead *et al.* (1984). Examples are *Hyperoplus lanceolatus* (Ammodytidae), not recorded from the Mediterranean or NW Africa, *Alosa fallax* (Clupeidae), previously recorded as far south as Morocco, and *Trisopterus luscus* (Gadidae), reported from the Mediterranean and Morocco. Since the ongoing study has not completed a full annual cycle, it is possible that the species reported by Monteiro (1989), but not found recently, could be summer visitors, which may appear in catches in June–August.

The increase in diversity shown from just 9 months of data is remarkable and indicates that important changes have taken place. Given the proximity to the Mediterranean and NW Africa and the fact that the south of Portugal is a transition zone, heavily influenced in terms of oceanography by the Mediterranean in particular, these findings are not surprising.

In addition to the research trawl survey of the fish community of the Ria Formosa, information and specimens from local fishermen, who occasionally bring rare or new species to the University, also provide evidence that warm water species have been extending their range to southern Portugal. In recent years for example, a lesser African threadfin (*Galeoides decadactylus*), found between the Canary Islands and Angola (Whitehead *et al.*, 1984), was caught in a gillnet in the Algarve. Two specimens of the Atlantic lizardfish (*Synodus saurus*), primarily insular in the eastern Atlantic and Mediterranean, were also brought in by gillnet fishermen. Further evidence of a warming trend is the increasing abundance of large pelagics such as the white marlin (*Tetrapturus albidus*) and the blue marlin (*Makaira nigricans*) in the summer months. These are species generally not found in waters less than 20°C. Over the past few years they have been so abundant in Algarve coastal waters that sport fishing tournaments are now common from July to September.

West coast of Portugal

There is evidence of both northward and southward shifts in fish distribution on the west coast of Portugal. Portuguese catch statistics, estimated back to 1896 by Mendes (2001) and published here for the first time, indicate that the sardine (*Sardina pilchardus*) population has shifted southward since the late 1970s (Figure 6). The shift was also observed in egg distributions (Stratoudakis *et al.*, 2002) and is associated with increased northerly winds during the spawning season (Santos *et al.*, 2001; Borges *et al.*, 2002), which result in increased upwelling.

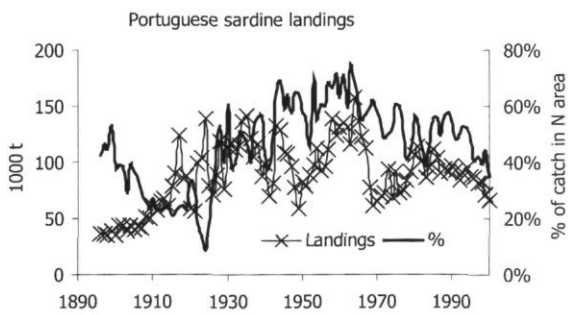


Figure 6. Landings of sardines in Portugal and landings from the northern area as a percentage of total landings.

The migratory snipefish (*Macrorhamphosus* sp.), a non-commercial species associated with warm and saline water, extended its distribution northwards during the late 1990s. Research surveys in 1979 showed that the distribution did not extend north of Lisbon (Afonso dos Santos and Moura, 1980). In September 1991, extensive schools of juvenile snipefish were found migrating from southwest of the Ormond Seamount towards the Algarve and Gulf of Cadiz and then north along the shelf edge as far as the latitude of Lisbon (Dias *et al.*, 1996). In the late 1990s, this species was observed in the trawl surveys at the extreme north of the Portuguese coast (41–42°N) and probably continuing further north along the shelf edge (Borges, 1998).

European shelf edge

A variety of tropical species have extended their ranges northward along the European continental slope since the early 1960s (Quero *et al.*, 1998). A particularly striking example is the Sailfin dory (*Zenopsis conchifer*), of which 36 have been taken since it was first recorded in European waters in 1966 at 38°N off the coast of Portugal. By the early 1990s it had been found north of 55°N. The depth range of capture is 100–500 m.

Distribution and abundance of the principal gadoid and flatfish species

The relative abundance of the principal gadoid and flatfish species taken in commercial fisheries in the eastern North Atlantic varies depending on the characteristic temperature regime of the area. Cod is the principal gadoid, along with saithe and haddock in cold areas, whereas in warm areas the principal gadoid is hake, with whiting and pollock (Figure 4). For the smaller flatfish (i.e. excluding halibut and Greenland halibut) the cold-adapted species are plaice and long rough dab, while the warm-adapted species are sole and megrim (Figure 5).

The differences in species composition between areas can be expressed as a ratio of catches of warm to cold adapted species. A pair of gadoid species (pollock and saithe) and a pair of flatfish species (sole and plaice) were chosen for the analysis. They are frequently caught by the same fishing gear in areas where their distributions overlap, and may therefore be expected to undergo similar changes in fishing mortality with time. For both of these species pairs, the ratio increases from zero at the Faroes (i.e. no catch of pollock or sole) to nearly 1 in Biscay (Figure 7). The distributions are clearly related to other factors in addition to temperature (e.g. depth, distance from coast), but there is no evidence that they are related to latitude.

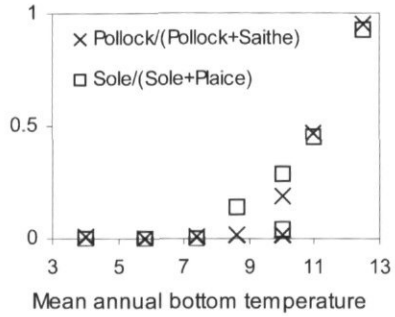


Figure 7. Proportions of "southern" vs. "northern" species in the fishing areas of the NE Atlantic. (a) Pollock vs. saithe, (b) sole vs. plaice. Mean annual bottom temperatures are Iceland 5.8°C, Faeroe 7.4°C, North Sea 8.6°C, West of Scotland 10°C, Irish Sea 10°C, Celtic Sea 11°C, Biscay 12.5°C (Brander, 1995).

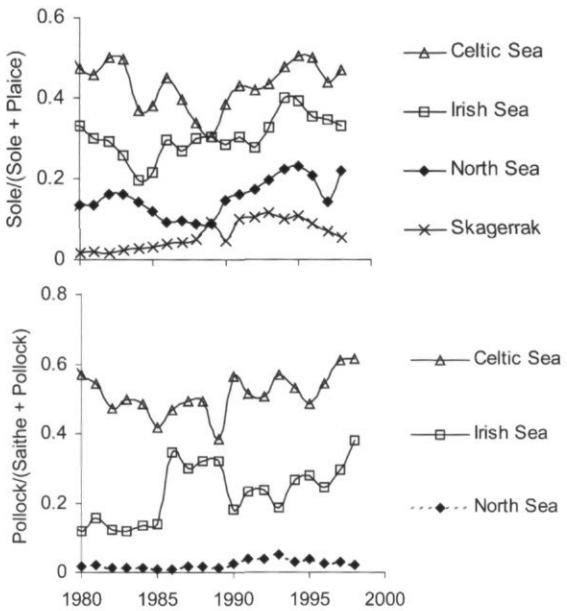


Figure 8. Temporal changes in the proportions of "southern" vs. "northern" species in the fishing areas of the NE Atlantic.

The catch ratio of warm to cold-adapted species also changes with time. Temporal trends in the ratios for areas with bottom temperatures, which lie between those of Faroes and Biscay, are shown in Figure 8. There is a general increase in the proportion of the "southern" species during the 1990s in most cases.

In the Celtic Sea the proportion of both "southern" species (pollock and sole) decreased from the late 1970s until 1989, before increasing again. In the Irish Sea there has been an underlying rise since 1973, but with substantial fluctuations. The West of

Scotland has much lower proportions of the "southerly" species and shows an increase in the proportion of sole, but not of pollock. The North Sea also shows an increase in sole relative to plaice, but pollock is always at a very low level.

Red mullet (Mullus surmuletus) *and bass* (Dicentrarchus labrax)

The ranges and fishery for these two species have been the subject of numerous articles in the popular and angling press (e.g. Brown, 2000). They are valuable, easily recognized species which have extended their ranges northwards and increased in abundance around the British Isles. The trend in commercial catches of red mullet in the English Channel and Central North Sea over the period since 1980 is particularly striking (Figure 9).

Records of catches of red mullet and bass in Scottish waters between 1984 and 2000 do not show a trend, but are not based on standard sampling (Figure 10). However, the International Young Fish Survey carried out by RV "Scotia" in February each year and covering a series of standard stations in the NW North Sea caught 1, 5, and 0 red mullet, respectively, in 1995–1997, and 98, 28, and 46, respectively, in 1998–2000 (Figure 9).

Red mullet and bass have recently been caught in western Norway for the first time as follows:

- Red mullet – several catches (at least 3 since 1993) in Hordaland county (ca. 60°N, 5°E)
- Sea bass – caught in Førdefjord, western Norway (61.5°N, 5.1°E) on 4 November 2000
- Other exotic fishes caught in Norwegian waters in September/October 2000 include:
- Swordfish (*Xiphias gladius*) caught in Sognefjorden, western Norway (61°N, 5°E)
- Sunfish (*Mola mola*) caught in Drammensfjorden, eastern Norway (59.7°N, 10.3°E)

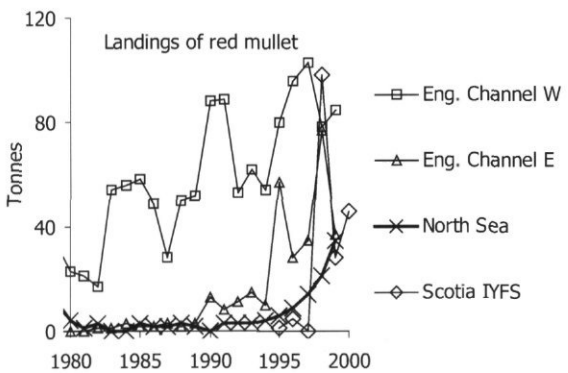


Figure 9. Annual landings of red mullet by Denmark, Ireland, The Netherlands, and UK. RV "Scotia" International Young Fish Survey (IYFS) catches are number of fish.

Sole in the Kattegat–Skagerrak (ICES Division IIIA)

Sole have been landed in the Kattegat–Skagerrak area throughout the period for which we have catch records, but landings increased from 200 to 500 t per year during the period 1952–1985 to 1000–1400 t per year during the period 1990–1995 (Fig. 11; ICES, 2001). Landings have fallen to ca. 700 t per year since the early 1990s but are still approximately double the long-term level during the 1950s–1970s. Most (ca. 70–80%) of the sole caught in the region are captured in the Kattegat.

Sole are captured in a multispecies fishery which targets cod, plaice, and Norway lobster. Effort information is available only since the 1980s. Danish gillnet and trawler fleets in the Kattegat capture >90% of all sole in the fishery and represent the major trends in effort for the entire stock. Effort has been relatively stable, but catch per unit effort indices do not take differences in vessel power, net size, net soak time, etc., into account and cannot fully

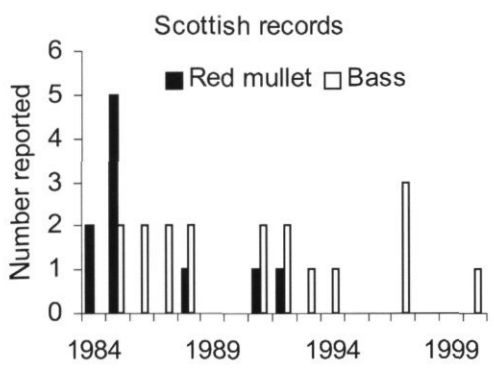


Figure 10. Numbers of bass and red mullet reported landed in Scotland.

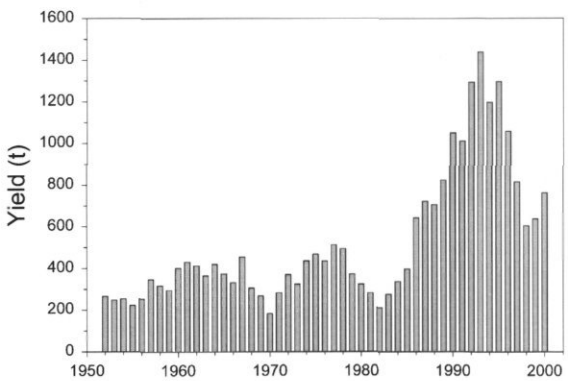


Figure 11. Annual landings of sole in the Kattegat–Skagerrak (ICES Division IIIA).

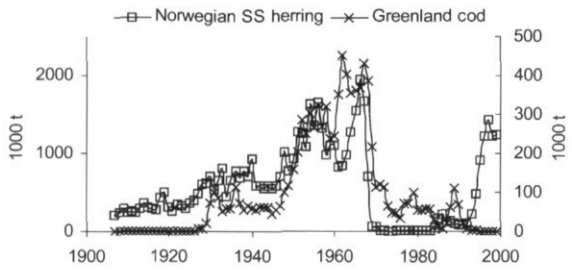


Figure 12. Annual landings of Norwegian spring-spawning herring and Greenland cod.

explain either the fluctuations in landings or fishing mortality rates during the same time period (ICES, 2001).

The environmental factors that might affect recruitment to the stock or other aspects of stock biology are poorly known (ICES, 2001). The stock is located near the edge of its geographical range (Muus and Nielsen, 1999) and therefore may be susceptible to environmental effects (Leggett and Frank, 1997; Myers, 1998; Brander, 2000). The distribution of the stock in the Baltic is limited by low salinity; sole are rare in the Belt Sea (ICES Subdivision 22) and absent in the western and eastern Baltic Sea (ICES Subdivisions 24–32; Muus and Nielsen 1999). Although good quality information on ambient temperature and other environmental factors is not available, the correspondence with the trends in air temperature and SST in the adjacent North Sea over the same period is striking (Figure 2).

Big northern stocks and the warming period of the 1920s and 1930s

The time series of catches of cod at Greenland and of Norwegian spring-spawning herring (Toresen and Østvedt, 2000) over the past century are remarkably similar (Figure 12). At their peak the catches from these stocks were so large that they constituted a significant proportion of the global pelagic and demersal catches, and in both cases the stock biomass increased and decreased by over three orders of magnitude.

The rising catch and biomass during the 1920s and 1930s was due to the warming that took place at Iceland and Greenland at this time (Figure 2) and which resulted in a poleward extension of the range of many species of fish, benthos, marine mammals, and also terrestrial fauna (Jensen, 1939).

The decline in both stocks in the late 1960s occurred during a major cooling episode, when the Polar Front moved south in the Greenland Sea and herring no longer migrated around the north coast of Iceland. Temperature on the Siglunes section north of Iceland declined by 4°C between 1964 and 1967 (Figure 2). However, both stocks were being heavily fished at the time and their collapse was probably due to a combination of lower temperature and overfishing.

The history of two stocks has been very different since the early 1970s. The Norwegian spring spawning herring recovered from a spawning biomass of less than 3000 t in 1972 to around 12 million t in 1997. It has resumed its summer feeding migration in the Norwegian Sea (Toresen and Østvedt, 2000), but does not penetrate into the area north of Iceland as it did prior to 1965. The temperature north of Iceland has not returned to the values found prior to 1965 (Figure 2).

The biomass of cod at Greenland remains low and the catch declined from 68 000 t in 1990 to less than 1000 t in 1999. Evidence from past recruitment indicates that temperatures above 1.5°C are necessary to produce big year classes (Brander, 2000); therefore it is not surprising that the stock has failed to recover. The temperature increased at West Greenland throughout the 1990s, but only exceeded 1.5°C at Fylla Bank in June in 1996, 1998, and 1999. Since cod in this area take 6 or 7 years to reach maturity, any rebuilding of the stock is likely to be slow.

Discussion

The absence of comprehensive, standard, up-to-date information on sea temperature and other hydrographic information for the NE Atlantic makes the task of explaining changes in fish distribution during the 1990s and relating it to earlier periods of the 20th century more difficult. Information on sea and air temperature is presented here (Figure 2) in an attempt to show the long-term background of temperature change, for all parts of the NE Atlantic, but a more complete and systematic treatment is needed. The ICES Ocean Climate Status Summary (ICES, 2002) has made a start on putting together such information, but to date this is fragmentary; the records are based on small numbers of stations or sections and often represent only a fraction of the depth range and seasonal cycle. The duration of the records is variable and they are not presented in a standard format.

Air and sea temperatures over most of the NE Atlantic have risen by at least 0.4°C in the decade since the late 1980s. In the northwestern part of the area, at Greenland and Iceland, the 1990s began with sea temperatures which were below the long-term average, and although temperatures rose during the decade they did not reach the levels

which occurred during the warm period from the mid-1920s to 1960. The eastern parts of the North Atlantic, from the Norwegian Sea down to Portugal, were warmer during the 1990s than during previous decades of the 20th century, but the middle years of the decade were relatively cool in most areas.

Northward shifts occurred in the distribution of many commercial and non-commercial fish species during the 1990s from southern Portugal to northern Norway. The abundance of commercial gadoid and flatfish species that occur in warmer waters (e.g. pollock and sole) increased relative to colder water species (e.g. saithe and plaice) in areas where their distribution overlaps. The absolute abundance of sole doubled during the 1990s in the Skagerrak and Kattegat, which is at the cold end of its range. A few examples of southward shifts, such as the sardine distribution off Portugal, which appear to contradict the overall pattern can be related to specific local hydrographic features. The scale and geography of the northward changes in fish distribution recorded here are similar to those shown for calanoid copepods during the period from 1960–1967 to 1992–1997 (Beaugrand *et al.*, 2002).

Trends in landings and biomass of Norwegian spring-spawning herring and of cod at Greenland have followed a similar pattern since the early 20th century, with both showing very substantial increases during the late 1920s and 1930s, declining in the late 1960s, but only the herring stock recovering during the 1990s. Both of these stocks are at the lower end of their temperature range and both extended their range northward during the warm period from the mid-1920s to the early 1960s. They did not reoccupy these northern limits during the 1990s. In the case of cod around Greenland this could be because low temperatures during most of the decade restricted both spawning and range extension. Also, the stock is at an extremely low level and could take many years to recover, providing it does not suffer excessive mortality due to the existing shrimp fisheries. The Norwegian spring-spawning herring stock did recover during the 1990s but has not reoccupied its previous feeding areas north of Iceland, probably because of the low temperatures and low plankton production which persist north of the polar front.

Acknowledgements

KB was funded by the US National Science Foundation Grant OCE-0075263, the UK Ministry of Agriculture Fisheries and Food Project MF0424, the Norwegian Research Council Project 13744/120, the Canadian Department of Fisheries and Oceans, and the Icelandic Ministry of Fisheries. He was also supported by the International Council for the Exploration of the Sea.

References

Afonso dos Santos, G., and Moura, O. 1980. Abundância e distribuição do trombeteiro (*Macroramphosus scolopax*) na costa portuguesa em Novembro de 1978 e Maio, Agosto e Novembro de 1979. IPIMAR Report (unpublished).

Alderdice, D. F., and Forester, C. R. 1971. Effects of salinity, temperature and dissolved oxygen on early development of the Pacific cod (*Gadus macrocephalus*). Journal of the Fishery Research Board of Canada, 28: 883–902.

Beaugrand, G., Reid, P. C., Ibañez, F., Lindley, J. A., and Edwards, M. 2002. Reorganization of North Atlantic marine copepod biodiversity and climate. Science, 296: 1692–1694.

Borges, L. 1998. Biologia, Distribuição e Comportamento do apara-lápis (*Macroramphosus* spp.) na costa Continental Portuguesa. Master dissertation, Instituto de Ciências Biomédicas de Abel Salazar, Porto.

Borges, M. F., Santos, A. M. P., Crato, N., Mendes, H., and Mota, B. 2002. Sardine regime shifts off Portugal: a time series analysis of catches and wind conditions. Scientia Marina. (In press.)

Brander, K. 1995. The effect of temperature on growth of Atlantic cod (*Gadus morhua* L.). ICES Journal of Marine Science, 52: 1–10.

Brander, K. 2000. Effects of environmental variability on growth and recruitment in cod (*Gadus morhua*) using a comparative approach. Oceanologica Acta, 23: 485–496.

Brett, J. R. 1979. Environmental factors and growth. *In* Fish Physiology, vol. VIII, pp. 599–675. Academic Press, London.

Brown, A. 2000. Mediterranean fish colonise North Sea. The Observer. 17 September.

Dias, C. A., Marques V., Soares 1996. Condições oceanográficas e distribuição de juvenis de trombeteiro (*Macroramphosus scolopax*) ao largo da costa de Portugal em Setembro de 1991. IPIMAR Technical Report (unpublished).

Holliday, N. P., and Reid, P. C. 2001. Is there a connection between high transport of water through the Rockall Trough and ecological changes in the North Sea? ICES Journal of Marine Science, 58: 270–274.

ICES. 2001. Report of the Baltic Fisheries Assessment Working Group. ICES CM 2001/ACFM: 18.

ICES. 2002. The Annual ICES Ocean Climate Status Summary 2000/2001. Ed. by W. Turrell and N. P. Holliday. ICES Cooperative Research Report, No. 245. 19 pp

Jensen, A. S. 1939 Concerning a change of climate during recent decades in the Arctic and SubArctic regions, from Greenland in the west to Eurasia in the east, and contemporary biological and geophysical changes. Det Kgl. Danske Videnskabernes Selskab. Biologiske Medd. XIV, 8: 75 pp.

Leggett, W. C., and Frank, K. T. 1997. A comparative analysis of recruitment variability in North Atlantic flatfishes: testing the species range hypothesis. Journal of Sea Research, 37: 281–299.

Levitus, S., Antonov, J. I., Boyer, T. P., and Stephens, C. 2000. Warming of the World Ocean. Science, 287: 2225–2229.

Magnuson, J. J., and Destasio, B. T. 1997. Thermal niche of fishes and global warming. Society of Experimental Biology Seminar Series 61: Global Warming: Implications for freshwater and marine fish, pp. 377–408. Ed. by C. M. Wood and D. G. McDonald. Cambridge University Press, Cambridge.

Mendes, H. 2001. Relatório de Actividades no âmbito do Projecto PO-SPACC (PRAXIS/P/CTE/1128/1998). IPIMAR Technical Report (unpublished).

Monteiro, C., Lasserre, G., and Lam Hoai, T. 1990. Organisation spatiale des communautés ichtyologiques de la lagune Ria Formosa (Portugal). Oceanol. Acta 13: 79–96.

Monteiro, C. 1989. La faune ichtyologique de la Ria Formosa; organisation spatio-temporelle. Thèse Doctorat, Université de Montpellier, France. 219 pp.

Monteiro, C., Lam Hoai, T., and Lasserre, G. 1987. Distribution chronologique des poissons dans deux stations de la lagune Ria Formosa (Portugal). Oceanologica Acta, 10: 359–371.

Muus, B. J., and Nielsen, J. G. 1999. Sea fish. First: 1–340 Hedehusene, Denmark, Scandinavian Fishing Year Book.

Myers, R. A. 1998. When do environment-recruitment correlations work? Review Fish Biol. Fisheries, 8: 285–305.

O'Brien, C. M., Fox, C. J., Planque, B., and Casey, J. 2000. Climate variability and North Sea cod. Nature, 404: 142.

Quero, J.-C., Du Buit, M-H., and Vayne, J.-J. 1998 Les observations de poissons tropicaux et le rechauffement des eaux dans l'Atlantique europeen. Oceanologica Acta, 21: 345–351.

Santos, A. M. P., Borges, M. F., and Groom, S. 2001. Sardine and horse mackerel recruitment and upwelling off Portugal. ICES Journal Marine Science, 58: 589–596.

Stratoudakis, Y., Bernal, M., Borchers, D., and Borges, M. F. 2002. Spatio-temporal changes in the distribution of sardine eggs and larvae off Portugal. Fisheries Oceanography. (In press.)

Stebbing, A. R. D., Turk, S. M. T., Wheeler, A., and Clarke, K. R. 2002. Immigration of southern fish species to south-west England linked to warming of the North Atlantic (1960–2001) Journal of the Marine Biological Association, U.K., 82: 177–180.

Toresen, R., and Østvedt, O. J. 2000. Variation in abundance of Norwegian spring-spawning herring (*Clupea harengus*, Clupeidae) throughout the 20th century and the influence of climatic fluctuations. Fish and Fisheries, 1: 231–256.

Welch, D. W., Ishida, Y., and Nagasawa, K. 1998. Thermal limits and ocean migrations of sockeye salmon (*Oncoryhynchus nerka*): long-term consequences of global warming. Canadian Journal of Fisheries and Aquatic Science, 55: 937–948.

Whitehead, P. J. P., Bauchot, M.-L., Hureau, J.-C., Nielsen, J., and Tortonese, E. 1984, 1986. Fishes of the North-eastern Atlantic and the Mediterranean. Unesco, vols. I, II and III. 1473 pp.

Wood, C. M., and McDonald, D. G. (Eds.) 1997. Society of Experimental Biology Seminar Series 61: Global Warming: Implications for Freshwater and Marine Fish. Cambridge University Press, Cambridge. 425 pp.

ICES Marine Science Symposia, 219: 271–282. 2003

Growth and expansion of haddock (*Melanogrammus aeglefinus* L.) stocks to the west of the British Isles in the 1990s

M. Dickey-Collas, M. J. Armstrong, R. A. Officer, P. J. Wright, J. Brown, M. R. Dunn, and E. F. Young

Dickey-Collas, M., Armstrong, M. J., Officer, R. A., Wright, P. J., Brown, J., Dunn, M. R., and Young, E. F. 2003. Growth and expansion of haddock (*Melanogrammus aeglefinus* L.) stocks to the west of the British Isles in the 1990s. – ICES Marine Science Symposia, 219: 271–282.

A marked expansion of haddock (*Melanogrammus aeglefinus*) distribution and abundance to the west of the British Isles in the 1990s is described using fisheries landings and research survey data. The expansion appeared to begin at approximately the same time (1994–1995) across the region and led to the establishment of new fisheries on haddock in the Irish and Celtic Seas. Fish in different sea areas showed different characteristics of length at age, maturity, and recruitment patterns. Haddock in the Irish Sea were much larger (60 cm at age 5) than those west of Scotland (40 cm at age 5). Fifty percent of the females were mature at 27 cm in the Irish and Celtic Seas and at 22 cm to the west of Scotland. It is shown that these characteristics allow populations at the southern extreme of the species range in Europe to respond rapidly to more favourable conditions. Such conditions could have occurred over a large region allowing substantial growth of existing populations. Alternatively, introductions of ichthyoplankton by advection, or the spread of juveniles from densely populated areas, could take place to create a large self-sustaining introduced population in areas such as the Irish Sea. However, any mixing appears to have been limited as recruitment patterns differed among areas. Owing to the synchrony of the expansion in the different areas, it is concluded that some condition, or combination of conditions, changed to enable haddock to exploit resources in all the areas to the west of the British Isles in the late 1990s.

Keywords: Celtic Sea, expansion, groundfish surveys, haddock, Irish Sea, Malin Shelf.

M. Dickey-Collas and M. J. Armstrong: Agricultural and Environmental Sciences Division, Department of Agriculture and Rural Development, Newforge Lane, Belfast BT95PX, Northern Ireland [e-mail: mark.dickey-collas@dardni.gov.uk]. R. A. Officer: Marine Institute, Snugboro Road, Abbotstown, Dublin 15, Republic of Ireland. P. J. Wright: Fisheries Research Services, PO Box 101, Victoria Road, Aberdeen, AB9 8DB, Scotland. J. Brown, E. F. Young, and M. R. Dunn: The Centre for Environment, Fisheries and Aquaculture Science, Pakefield Road, Lowestoft, Suffolk, NR33 0HT, England. Correspondence to M. Dickey-Collas.

Introduction

Haddock (*Melanogrammus aeglefinus*) stocks exhibit large interannual variations in recruitment between years (Fogarty *et al.*, 2001), the magnitude of which differs geographically (Bradford and Cabana, 1997; Ottersen and Loeng, 2000). In contrast, their geographic distribution on the northwest shelf of Europe is considered fairly stable (Jamieson and Birley, 1989; Cushing, 1995), with populations in the North Sea, off the northwest coast of Scotland, and at Rockall (Figure 1A). However, during the mid-1990s, catches of haddock began to increase at the southern edge of their range (Figure 1B) and an apparent expansion of the distribution of haddock occurred.

Haddock is caught as a targeted fishery and as bycatch in most waters of the British Isles. In the 1980s, 98% of the catch came from the North Sea, west Scotland, and Rockall, but by the mid-1990s the proportion of the catch from the southwest waters (Irish Sea, Celtic Sea, and west of Ireland) had increased from 2% to 10%. While this proportional increase was partly due to reduced catches in northern waters (Figure 1B) it was also as a result of increased abundance of haddock to the south,

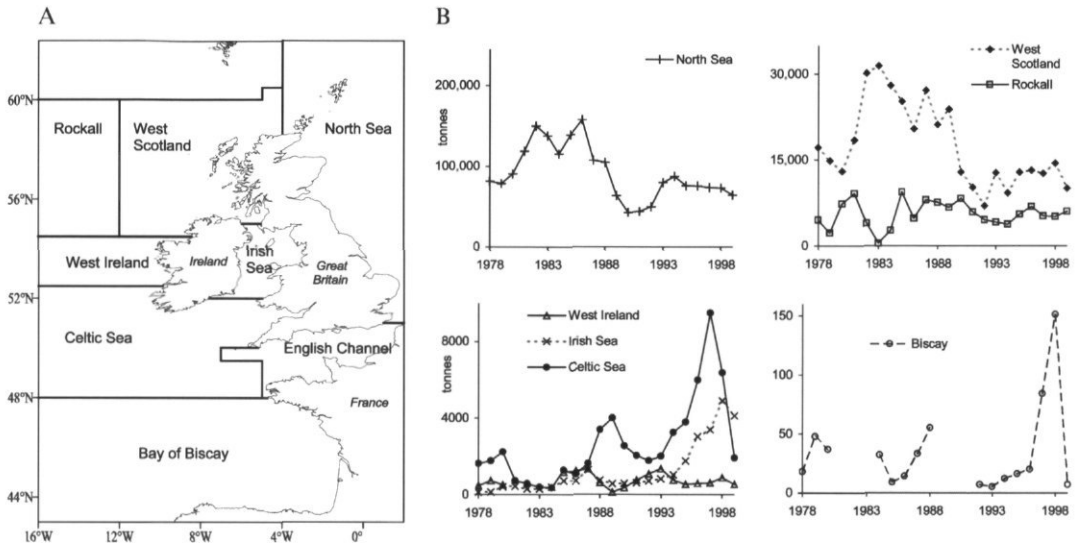


Figure 1. Official international landings of haddock from waters around the British Isles from 1978 to 1999. A. Geographic areas to which landings are attributed. B. Annual landings (tonnes) from each area, Irish Sea landings from 1995 to 1999 include adjustments for misreporting (ICES, 2001). Note different y-axis scales.

where new targeted fisheries for haddock were established. This article reviews the expansion of the haddock stocks to the west of the British Isles in the 1990s and describes geographic differences in some of the life history characteristics of the fish. It combines fisheries data with research survey results from four national fisheries institutes and considers possible mechanisms for the southerly expansion in light of the ecology and biology of haddock.

Materials and methods

Geographic expansion over time

Data from mixed-species bottom-trawl fisheries have the potential to give good spatial and temporal resolution of abundance of demersal fish such as haddock. Reported landings of haddock by rectangle and year were obtained from log-sheet data kept by four national fishery institutes: the Centre for Environment, Fisheries, and Aquaculture Science (CEFAS) in England, the Marine Institute (MI) in the Republic of Ireland, the Fisheries Research Services (FRS) in Scotland, and the Department of Agriculture and Rural Development (DARD) in Northern Ireland. However, due to misreporting of catches in some areas with restrictive quotas in the 1990s (ICES, 1997), reported landings figures alone could give a distorted picture of the distribution and abundance of haddock. An alternative index based only on frequency of occurrence was obtained for each year and ICES rectangle as:

$$P_{had} = N_{had} / N_{total}$$

where N_{had} is the number of otter trawl landings in which haddock were recorded and N_{total} is the total number of otter trawl landings made by the fleet. Rectangle / year combinations with $N_{total} < 3$ were discarded from the data set. In the early stages of population growth, the frequency of occurrence of landings with haddock will be expected to increase, as the population becomes more widespread on the traditional fishing grounds. Further population growth may lead to targeting of haddock and could result in the majority of landings containing some haddock.

The annual mean index, calculated over rectangles, was used as an indicator of abundance over the whole area investigated, while its coefficient of variation was used as an index of the spread or homogeneity of haddock across the region.

Spawning and nursery areas

All four institutes carry out annual research surveys of demersal fish that cover the distribution of haddock to the west of the British Isles (Table 1). It was not possible to standardize catch rates between the four institutes because of the differing selectivities of their vessels and gears. The mean catch rates of haddock per 1-h tow, at age 1 and at all older age classes combined (2+), were determined for each ICES rectangle. The distribution of 2+ fish in March was considered to indicate potential spawning grounds, assuming similar spawning dates

Table 1. Research surveys on demersal gadoids carried out in the 1990s to the west of the British Isles.

Institute	Area	Month	Time-series	No. of ICES rectangles	Gear
Centre for Environment, Fisheries and Aquaculture Science (CEFAS)	Celtic Sea	March	1991–2001	44 (64 stations)	Portuguese high headline trawl
Department of Agriculture and Rural Development (DARD)	Irish Sea	March and October	1992–2001	12 (44 stations)	Rockhopper trawl
Fisheries Research Services (FRS)	West Scotland Irish Sea	March March	1990–2001 1996–2001	38 10	GOV rock-hopper trawl
Marine Institute (MI)	West Scotland and West Ireland	October	1993–2000	34	Otter trawl

in spring in all regions (see maturity section below), while the distribution of age-1 fish indicated settlement and nursery areas. In some areas the spawning time of haddock can vary by up to 3 months between years (Page and Frank, 1989), but there is no evidence for this in haddock to the west of the British Isles. The west of Ireland surveys took place in October, so the abundance of 2+ fish could not be used to indicate spawning areas as haddock spawn in the spring; however, the abundance of 0-group fish was used to suggest nursery areas.

Characteristics of the stocks

Regional differences in mean length at age were inferred from samples taken by the MI port-sampling scheme. These were the only data readily available that covered the whole of the area of study with continuity of sampling schemes, age-readers, and fleet characteristics. Although the length composition will be affected by the selection and discarding patterns of the fisheries in different areas, it was assumed that mean lengths in fully selected age classes would provide a robust indicator of regional differences in growth. An otolith-exchange scheme carried out in 2000 (DARD, unpublished data) showed a high level of agreement in age allocation for haddock between age readers in MI, FRS, and DARD.

Comparative maturity-at-length ogives of haddock were obtained from the March surveys of CEFAS, DARD, and FRS (Table 1). Trawl catches were sampled using a length-stratified scheme. Maturity stages were distinguished using macroscopic appearance of the gonads (Bowers, 1954). Owing to the timing of the surveys near the peak of spawning, errors in identifying mature fish were considered to be potentially small. The maturity-at-length data were not corrected for length-stratified sampling in calculating maturity at age. This will lead to overestimation of the proportion of mature fish in younger age classes if there is a length-dependence of maturity within age classes, and the age-based results given here must be considered as indicative only.

Time series of recruitment strength, derived where possible using extended survivors analysis (XSA; Shepherd, 1999; ICES, 2000) were compared. For the west of Ireland stock the mean abundance of age-1 fish from the October MI surveys was used as a proxy for recruitment. Each time series was standardized to its mean and expressed as year class. Longer-term changes in the variability of recruitment to the west of Scotland stock were investigated calculating the geometric mean of recruitment by decade. The establishment of year-class strength was investigated for the Irish Sea stock by comparing indices of abundance of pelagic 0-group fish from Methot Isaacs-Kidd frame net (5-mm mesh; Dickey-Collas *et al.*, 1997) in May and June with post-settlement indices from groundfish surveys.

Results

Geographic expansion over time

The distribution of landings from Scottish vessels (west of 4°W) changed little from the early to the late 1990s (Figure 2), although more fish were caught to the northwest of Scotland and in the south of the region in the second period. In contrast, the frequency of occurrence of landings containing haddock increased dramatically because of the growth of the stocks from the mid-1990s onwards (Figure 3). The Celtic Sea generally has larger landings of haddock than the Irish Sea (Figure 1), but even here there was a marked increase from 1996 onwards. By 1997, 41% of catches of the non-Scottish fleets in the total area contained haddock (Table 2) and its presence had become almost ubiquitous in 1996 to 1998 (shown by reduced coefficient of variation; Table 2). There is some evidence for a decline in haddock distribution in 2000 (Figure 3, Table 2). The present methods do not clarify whether the apparent increase at Rockall is due to greater abundance of the fish, or to a change in the fishing practices (Figure 3).

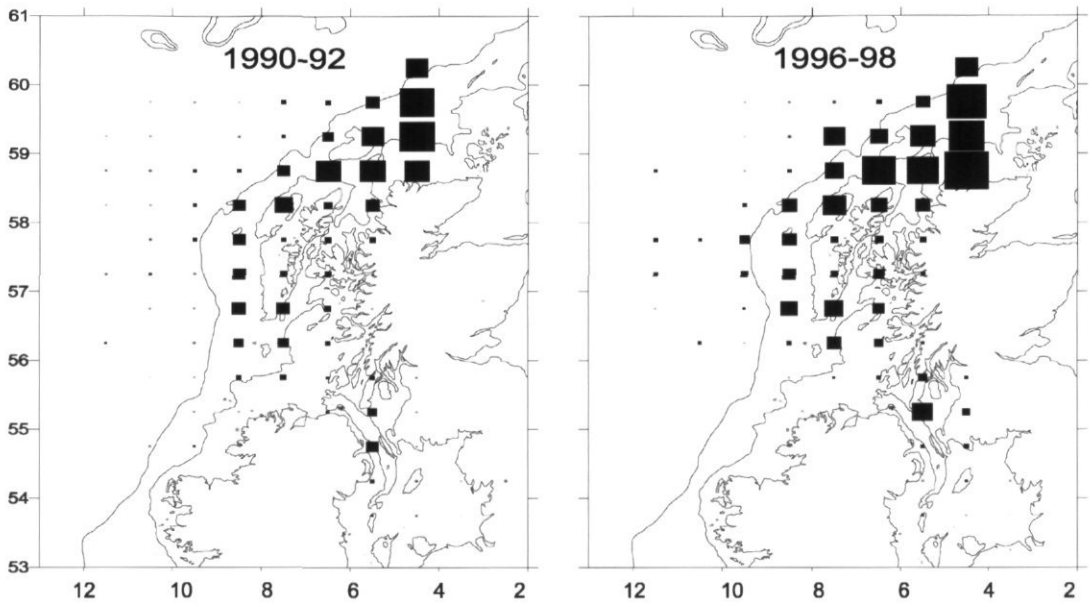


Figure 2. Mean annual landings of haddock by the Scottish fleets by ICES rectangle from west of 4°W, from two 3-year periods (1990 to 1992 and 1996 to 1998). Black rectangles represent square root transformed values, largest rectangle = 4000 t.

Spawning and nursery areas

In the early 1990s, relatively high catch rates of 2+ haddock off northwest Scotland in March indicated that the bulk of spawning may have been in this area. The pattern was similar in 1996–1998, although high catch rates were recorded over a wider area including the extreme western boundary of the surveys (Figure 4). More dramatic changes were observed in the Celtic and Irish Seas (Figure 4). By the late 1990s, high catch rates of 2+ haddock were more widespread in the inshore areas off southern Ireland and in the western Irish Sea. A feature of the Irish Sea surveys has been a consistent concentration of juvenile and adult haddock in the western region, and only a relatively small build-up of the stock in the eastern region. The nursery grounds are closely associated with the spawning grounds inferred from distribution of 2+ fish in March (Figure 4).

Characteristics of the stocks

The mean length of haddock appeared to increase in an anticlockwise cline around Ireland (Figure 5), varying at 5 years old from 40 cm at Rockall and west of Scotland to 50 cm off the west of Ireland and 60 cm in the Irish Sea. At age 4, the Irish Sea fish tended to be 50% longer than those from the west of Scotland. The ranking of lengths of fish by area is fairly stable as the fish age (Figure 5).

Maturity varies in these stocks with both age and length. In the Irish and Celtic Seas the length at which 50% of the females were mature (L_{50}) was approximately 27 cm (1992–2001). Celtic Sea males had a lower L_{50} due to larger 1-year-olds being classified as mature. The L_{50} for west of Scotland haddock from 1995–2000 was approximately 20–22 cm in both sexes. The majority of 2-year-olds in all three areas were mature.

As is well known, the recruitment of haddock stocks is highly variable (Figure 6). There does not appear to be a consistent pattern, in terms of relative recruiting year-class strength, in the stocks to the west of the British Isles (Figure 6A). Recruitment to a majority of stocks was above average in 1994 and below average in 1993, 1995, 1997, and 1998. Comparing recruitment strengths in the "non-converged" recent period of an XSA is prone to errors, so the precision of the estimates later than 1996 should be considered poor. The pattern of recruitment in the large west of Scotland stock changed in the 1990s. Prior to that it was characterized by intermittent very strong year classes followed by a few years of below average recruitment (Figure 6B). Recruitment in the early 1990s was less variable around the geometric mean and there were no major troughs until 1998.

Comparison between MIK-net indices of pelagic juvenile abundance and subsequent groundfish survey indices in the Irish Sea in the 1990s suggest that year-class strength is determined in the first 2 months after spawning. There are strong significant

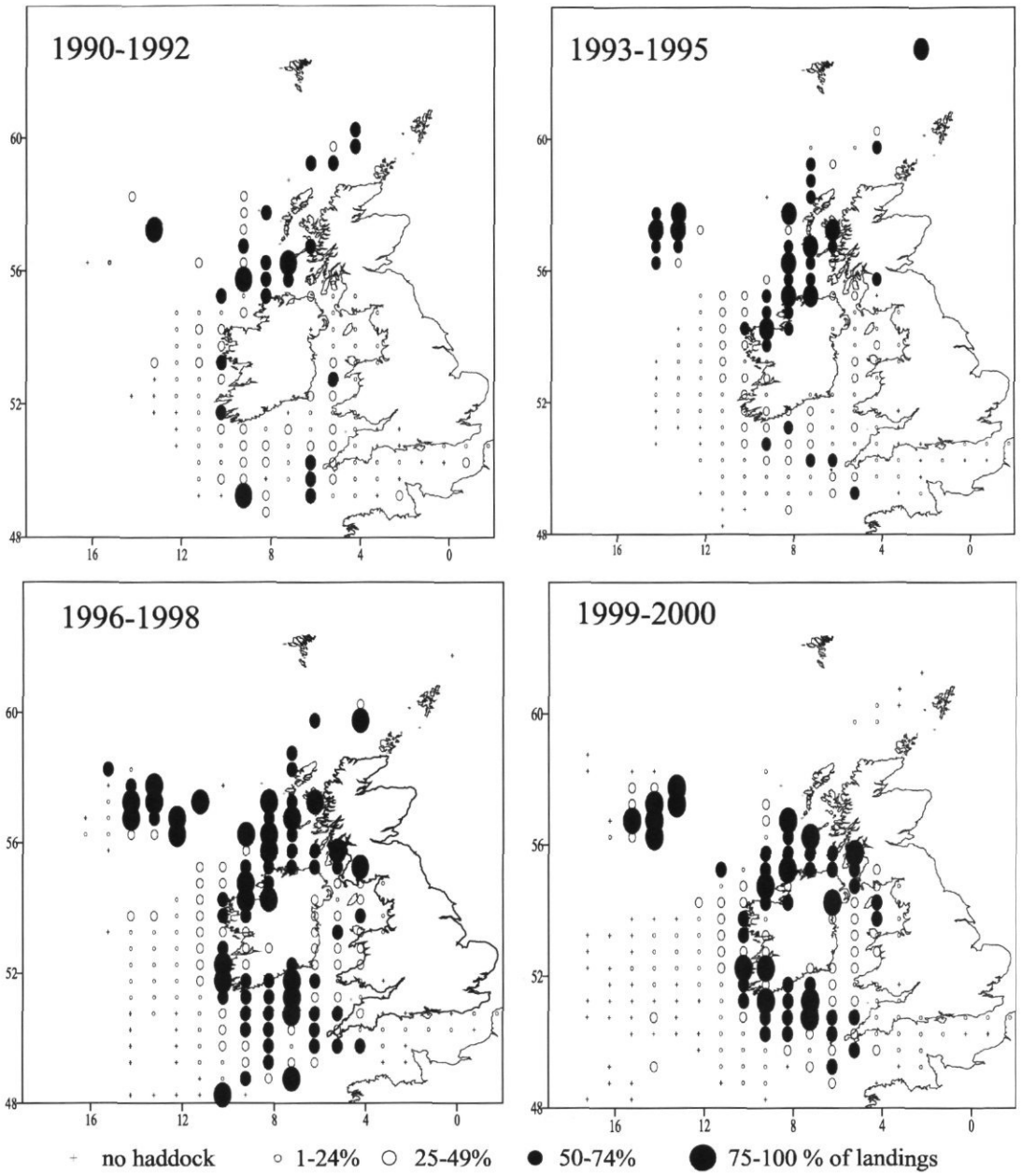


Figure 3. Proportion of otter or light trawl landings by ICES rectangle that contained haddock (means of 3 years) by the Irish, Northern Irish, English, and Welsh fleets.

correlations between the abundance of 2-month-old haddock (sampled in June) and both the abundance of 1-year-olds in the following March (DARD demersal fish survey, $r = 0.92$, $p < 0.005$, $n = 8$) and the number of recruits estimated by XSA ($r = 0.91$, $p < 0.005$, $n = 7$). There was no significant auto-correlation in the time-series. The time-series was too short to determine residuals from a Ricker curve.

Discussion

Overview

Whether by considering reported tonnes landed or the frequency of occurrence of landings with haddock, it is clear that the distribution of post-recruit haddock expanded considerably in the 1990s. This article does not propose that this is a new or a

Table 2. The mean proportion of landings containing haddock by year, from the English and Welsh, Northern Irish and Irish trawler fleets in western waters. Mean proportion is used as a proxy for abundance while coefficient of variation of the mean (CV) is used as a proxy for homogeneity. N = number of ICES rectangles in which more than three catches were made that year. Total numbers of landings are those that comprise n.

Year	Mean proportion	CV	n	Total no landings
1989	0.36	0.94	84	53 960
1990	0.29	1.18	86	58 540
1991	0.22	1.15	107	61 690
1992	0.21	1.03	131	64 880
1993	0.21	1.22	135	63 830
1994	0.24	1.15	139	50 920
1995	0.30	0.95	165	76 670
1996	0.36	0.81	170	68 780
1997	0.41	0.80	165	74 820
1998	0.39	0.82	175	74 050
1999	0.32	0.97	173	66 850
2000	0.29	1.01	192	61 300

unique event. Anecdotal information and comments suggest that the last expansion of haddock to the west of the British Isles was in the late 1960s and early 1970s (ICES, 2000) and prior to that in the early 1950s. Unfortunately the time-series of catches and surveys do not extend back to these periods, precluding comparison with the gadoid outburst in the North Sea (Jones and Hislop, 1978).

Haddock is at the southern extreme of its European range in the Celtic Sea and Bay of Biscay and, strangely, in the 1990s the increased catches have coincided with an increase in the water temperature in the Irish Sea (DARD unpublished data). The much higher stock density and persistence of haddock in the colder waters off the west coast of Scotland and in the northern North Sea suggest that these regions are generally more favourable for haddock than the Irish Sea and off the south and west coasts of Ireland. "Favourable" in this context could reflect the potential for spawning and the retention and survival of eggs, larvae, and pre-recruits, and the carrying capacity of the habitat for post-recruits. Periodic expansions of the more southerly populations could indicate more favourable conditions for spawning and survival to recruitment in small extant local populations, and/or a geographic expansion of the larger more northerly stocks. The latter could result from movements of post-recruit fish or drift of eggs, larvae, or pelagic post-larvae. Geographic expansion of stocks at high abundance is a well-known phenomenon, particularly in pelagic fish (Lasker and MacCall, 1983). MacCall's "basin model" predicts that fish stocks will expand into areas normally less favourable for spawning when conditions in the intrinsically more favourable areas decline due to density-dependent reductions in survival. This model could also apply

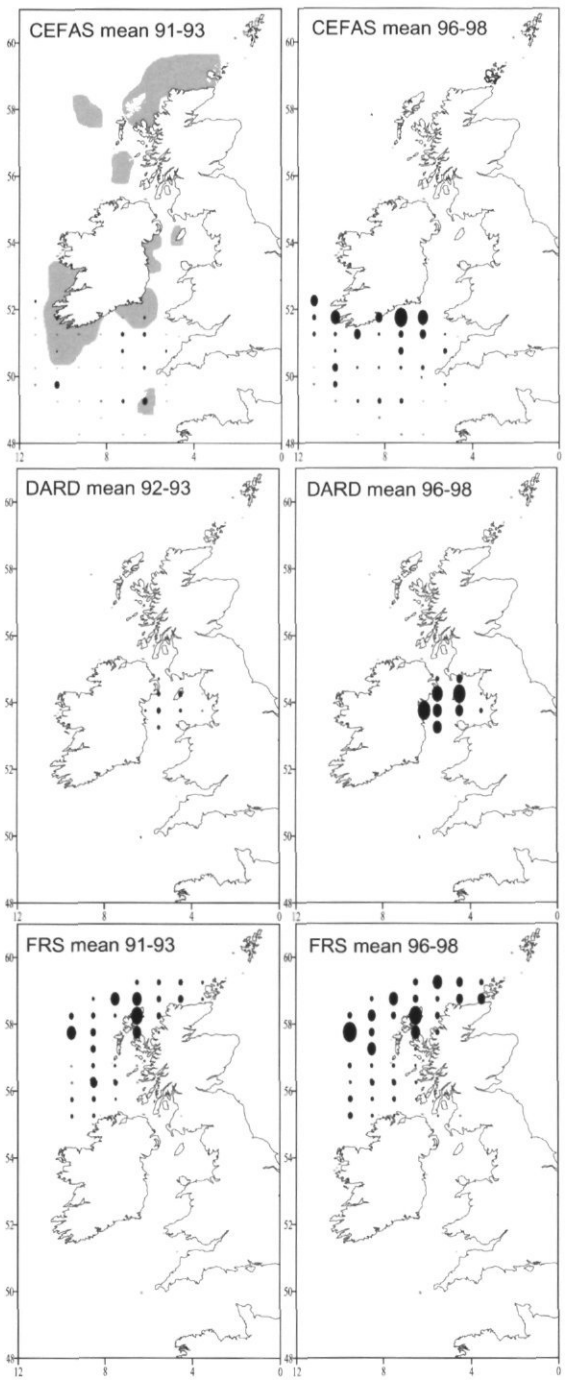


Figure 4. Distribution of spawning haddock to the west of the British Isles, determined from relative catch of 2+ fish on research surveys in spring. The surveys from the different institutes are not inter-calibrated, but the scales between the two time periods for each institute are the same. FRS catches in the Irish Sea in the late 1990s are not included as no comparative catches in 1991–1993 were taken. Grey shading indicates nursery areas, as determined by the presence of 1-year-old fish in the surveys, and include 0-group catches from the Marine Institute October surveys to the west of Ireland.

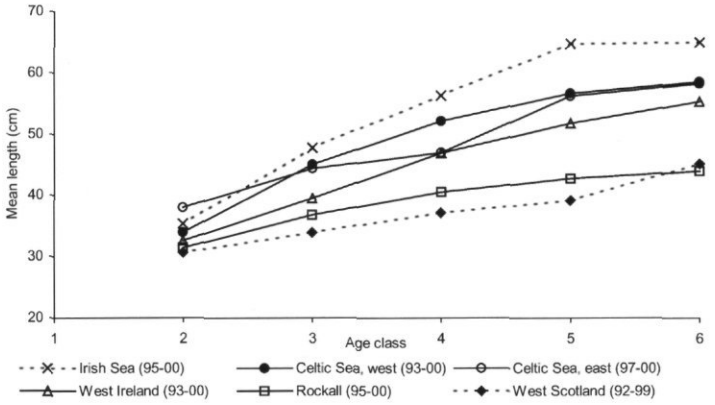


Figure 5. Mean length-at-age of haddock landed in Ireland during the 1990s from different sea areas to the west of the British Isles. Fish from the Celtic Sea are split into west ICES area VIIj and east ICES area VIIg. Figures in parentheses denote years of sampling.

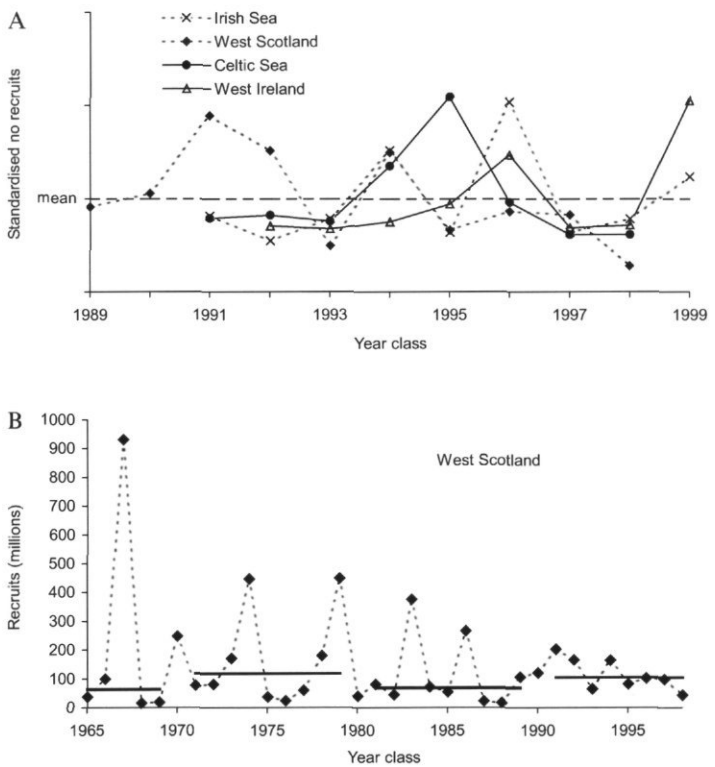


Figure 6. Time-series of haddock recruitment. A. Strength of recruitment relative to the mean in four sea areas, data from SPA analysis (ICES, 2001). West Ireland recruitment inferred from Irish survey data. B. Recruitment by year class to haddock stock in West Scotland 1965 to 1998, ICES area VIa. Solid horizontal bar denotes geometric mean recruitment for each decade.

to temporary colonization events following spill-over of the main populations if colonizing fish remain in the habitat while feeding conditions are adequate and are able to sustain the population through local spawning and larval retention. It would be expected that environmental conditions at an organism's distributional limit would be more variable with respect to the organism's tolerance range, and hence result in fluctuations in abundance (Southward *et al.*, 1988).

Temporal patterns

The spatial expansion of haddock was not just due to higher abundances at local pockets or favourite fishing sites. Their spread increased and their abundance became more homogeneous in many areas of the Irish Sea and Celtic Sea (Figure 3, Table 2). The expansion occurred in the Celtic Sea before the Irish Sea (Figure 1B), with an apparent 1-year lag in catches of haddock between the regions. Research survey results did not show a "creep" south each year and the expansion appears to have begun in approximately 1994 to 1995, at the same time as the above-average year class in 1994 (Figure 6A).

Spawning and nursery areas

The location of spawning sites has apparently remained unaltered as the stock has expanded. The same sites were used by haddock in 1991 to 1993 and 1996 to 1998 but by more fish (Figure 4). Data on egg production or abundance to confirm these spawning sites are limited. The few ichthyoplankton studies that have mapped the abundance of late-stage haddock eggs or larvae do not contradict the spawning sites inferred from aggregations of mature fish in March (Saville, 1959; Heath *et al.*, 1994; Fox *et al.*, 1997). The late-stage eggs and larvae of haddock are quite often coincident with stratified waters (Lough and Bolz, 1989; Page *et al.*, 1989). Haddock larvae are frequently found to be in better condition in stratified water compared to those in mixed water columns (Buckley and Lough, 1987; Frank and McRuer, 1989). Haddock either spawn in retentive areas prone to stratification (Page *et al.*, 1999), or in areas where eggs and larvae will be advected into stratified water (Campana *et al.*, 1989a; Gallego *et al.*, 1999). Heath and Gallego (1998) commented on the processes affecting the spawning sites to the west of Scotland and suggested that much of the west of Scotland production is advected into the North Sea. The inferred spawning sites in both the western Irish Sea and eastern Celtic Sea are in areas that become thermally stratified in late spring. In the western Irish Sea the resulting gyre circulation is generally accepted as retentive (Dickey-Collas *et al.*, 1997; Horsburgh *et al.*, 2000). In the central Celtic Sea circulation is weak following stratification, while in the vicinity (~40 km) of the Irish coast a strong density-driven circulation advects water westward and northward parallel to the coast (Brown *et al.*, submitted), corresponding with the spread of the nursery area to the west of Ireland (Figure 4). It is concluded that suitable conditions for spawning and for retention of eggs and larvae occur in the areas that have experienced substantial growth of haddock populations in the 1990s. These regions also support self-sustaining populations of other important gadoids, particularly cod and whiting.

Conditions for growth and maturation

The differences in mean length-at-age of landed haddock in each region (Figure 5) are consistent across age classes and are unlikely to be a result of different selection characteristics of the fisheries. Marshall and Frank (1999), following individual year classes, found that once a group of juvenile fish was considered large, its relative bigger size continued through its adult life. Hence, conditions for growth during the early years of life are the most critical. Temperature is known to be a dominant factor influencing growth of fish (Brander, 1995). Mean annual surface temperatures in the Celtic Sea are 1°C and 2°C warmer than in the Irish Sea and west of Scotland Shelf, respectively. Length-at-age in the Irish Sea appears greater than in the Celtic Sea despite the slightly cooler conditions. However, the bottom temperature may not show the same regional difference as the surface temperature. Density dependent effects on growth, shown by Marshall and Frank (1999) for Scotian Shelf haddock, have not yet been examined for Irish Sea or Celtic Sea haddock.

The difference in maturity by length between areas is largely driven by the difference in length-at-age 2. As most haddock in the Irish and Celtic Seas are mature by age 2, and they tend to be bigger, hence their length at 50% maturity (L_{50}) is larger. Since 1995, most haddock from the west of Scotland also appear to mature by age 2. The L_{50} within a stock can vary over time (Waiwood and Buzeta, 1989) and has been linked to density-dependent processes. The L_{50} for haddock to the west of the British Isles found by this study is much smaller than for stocks in the Northwest Atlantic (Waiwood and Buzeta, 1989) or the North Sea in the 1970s (Hislop and Shanks, 1981).

Recruitment variations

Spawning and nursery areas for haddock were found in all the regions around Ireland investigated in the present study, as well as to the west of Scotland. Haddock to the west of the British Isles show a pattern common in haddock stocks, namely intermittent strong year classes between smaller but less variable year classes (Fogarty *et al.*, 2001). The time-series of recent recruitment were poorly correlated between stocks, as has been found in other regions (Campana *et al.*, 1989b). However, the

comparisons between stocks may not be valid, as the expanding stocks (Irish and Celtic Sea) are, by nature, on the ascending slope of the stock-recruitment curve, while established stocks (west of Scotland) are more prone to density-dependent controls of recruitment (Marshall and Frank, 1995, 1999). Recruitment strength in the Irish Sea, like some other stocks (Campana *et al.*, 1989b), appears to be established by the pelagic post-larval stage, as surveys of 2-month-old pelagic juvenile haddock are significantly correlated with recruitment. However, because of the short time-series and proximity to the origin of any stock-recruitment relationship, it is difficult to quantify the effects of stock size or the environment.

Larval advection

It is possible that the expansion of the stock in the Irish Sea might have resulted from, or at least been aided by, an advection of young larvae from established spawning areas to the north and south of the Irish Sea. The dynamics of the continental shelf waters of the British Isles in winter and spring are strongly controlled by wind forcing (Davies and Jones, 1992; Brown and Gmitrowicz, 1995). A three-dimensional non-orthogonal curvilinear hydrodynamic model (Young *et al.*, 2001) was employed to investigate whether wind-induced events could be responsible for a 'pulse' of young larvae into the Irish Sea. There were two good year classes in 1994 and 1995 in the Celtic Sea. During early February 1994 an intense atmospheric low pressure was centred over western Ireland, causing the strongest flushing of the Irish Sea for a decade (Knight and Howarth, 1999). Approximately 25–30% of the volume of the Irish Sea passed northward through the North Channel in February, one-third of this volume was associated with the 3-day intense low. In addition, at the beginning of April there was a 2-week period of anomalous high southward flow into the Irish Sea through the North Channel. Model simulations (Figure 7A) predict a mean inflow greater than two times the long-term mean outflow. The timing of haddock spawning to the south of Ireland is unclear, but particle trajectories during February simulated by the model (assuming particles were near the surface) (Lough and Potter, 1993) (Figure 7B) indicate advection in excess of 200 km from the apparent spawning site off southeastern Ireland. As year-class strength of haddock in the Irish Sea is determined before settlement, and recruitment patterns are different from the Celtic Sea, mixing between the areas may be an uncommon event.

Although there are no major spawning areas near the northern end of the North Channel, significant southward fluxes of water into the Irish Sea occasionally take place. In April (day 60 in Figure 7A) particles may conceivably have been advected from the Malin Shelf to the southern end of the North Channel (Figure 7C), where spring discharges of riverine water and subsequent summer stratification cause southward flow along the Irish coast and retention within the western Irish Sea (e.g.

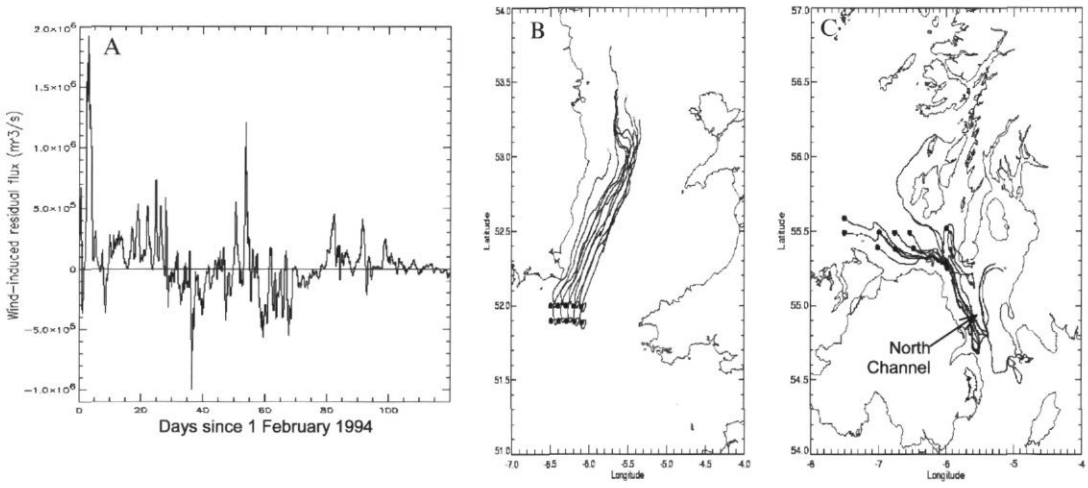


Figure 7. Wind-induced fluxes and transport events into the Irish Sea in 1994, from a three-dimensional, curvilinear, wind and tidally-driven hydrodynamic model (Young *et al.*, 2001). A. Wind-induced fluxes in the North Channel in spring 1994. Positive values are fluxes to the north, negative to the south. B. Wind-induced particle trajectories in February 1994 from the Celtic Sea, particles released (dark circles) and tracked for 31 days at 10 m depth. C. Wind-induced particle trajectories in April 1994 from north of Ireland, particles released (dark circles) and tracked for 30 days at the depth mean.

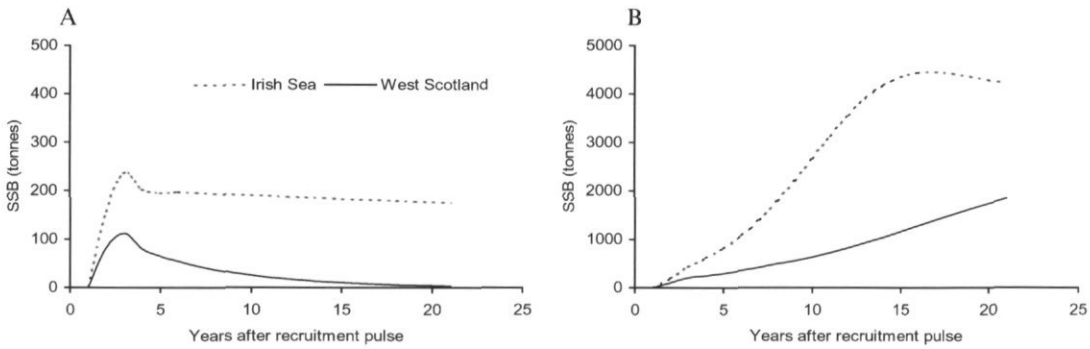


Figure 8. Simulation of effect of a recruitment pulse of haddock on colonization (local spawning-stock biomass), using life history traits from West Scotland (solid line) and Irish Sea (dotted line) under two scenarios: (A) at recent estimates of fishing mortality in West Scotland, (B) zero fishing mortality. Note different y-axis scales.

Dickey-Collas *et al.*, 1997; Horsburgh *et al.*, 2000). Although not conclusive, it is feasible that during 1994 comparatively rare sustained transport events coincided with periods of spawning or early larval development and were responsible for introductions of haddock eggs or young larvae from neighbouring areas.

Population growth

The different biological characteristics in the regions studied will affect the population dynamics of the stocks. A combination of fast growth and early maturity at the southern limit of the species' range will represent optimum life-history traits for stocks in areas with more unpredictable environmental conditions for larval survival and potentially higher mortality of adults. The effect of the differing characteristics on the population dynamics following a recruitment pulse was simulated using a simple population model. The mean weights-at-age and maturity ogives for west of Scotland and Irish Sea haddock were taken from ICES (2000) and the present study. It was assumed that spawning-stock biomass in an area was initially zero or very close to zero, and that a self-sustaining population with no interchange with surrounding areas would develop following the initial recruitment input. The same Ricker stock-recruitment relationship was applied to each simulated stock, and the initial recruitment pulse was the maximum recruitment. Natural mortality was assumed to be 0.2 $year^{-1}$ for all ages (ICES, 2000). Rates of stock growth were examined for zero fishing mortality and for a fishing mortality similar to the current estimates for west of Scotland (0.2 for age 1, 0.4 for age 2, and 0.6 for ages 3 and over). The simulations were run for 21 years after the initial recruitment pulse. The simulation results suggest that fish in the Irish Sea can increase their biomass more rapidly than those with west of Scotland characteristics (Figure 8). At higher fishing mortalities, the Irish Sea fish persisted for longer (Figure 8A). These differences were due to the higher weights-at-age and the slightly higher proportion mature at age 2 in the Irish Sea fish.

Conclusions

We have shown that the existing small indigenous populations have the potential to respond rapidly to more favourable conditions. To the same extent, a one off introduction may have taken place (as ichthyoplankton or juveniles) which created a large self-sustaining introduced population in areas such as the Irish Sea. It is possible that DNA microsatellite work could be used to test some of these hypotheses (Lage *et al.*, 2001), although it may be difficult to detect differences in transitory populations. As the expansion occurred at approximately the same time across the southern regions and resulted in a fairly homogeneous spread of haddock, with different recruitment patterns across the south of Ireland (Figure 3), it is more likely that some condition, or combination of conditions, changed to enable haddock to exploit resources in all these areas. It would be easy to speculate further about the possible ecological changes that may have caused the expansion of haddock populations (e.g. more stable water column, reduction in cod, or changes in plankton structure), but data are not available at present to rigorously test any hypotheses.

Acknowledgements

The crews and officers of the respective research vessels are thanked for their help and assistance.

The comments and ideas of Ivan Heaney and Bob Dickson are gratefully acknowledged. The work of Andrew Newton at FRS is acknowledged. CEFAS staff were funded by the Department of the Environment Food and Rural Affairs, using understanding gained under projects AE1012, AE1203, and AE1214. FRS work was carried out within the funding of SEERAD project MF0462.

References

Bowers, A. B. 1954. Breeding and growth of whiting (*Gadus merlangus* L.) in Isle of Man waters. Journal of the Marine Biological Association UK, 33: 97–122.

Bradford, M. J., and Cabana, G. 1997. Interannual variability in stage-specific survival rates and the causes of recruitment variation. *In* Early Life History and Recruitment in Fish Populations, pp. 469–493. Ed. by R. C. Chambers and E. A. Trippel. Chapman and Hall, London.

Brander, K. M. 1995. The effect of temperature on growth of Atlantic cod (*Gadus morhua*). ICES Journal of Marine Science, 52: 1–10.

Brown, J., Carillo, L., Fernand, L., Horsburgh, K. J., Hill, A. E., and Young, E. F. 2002. Observations of the physical structure and seasonal jet-like circulation of the Celtic Sea and St. George's Channel of the Irish Sea. Continental Shelf Research (submitted).

Brown, J., and Gmitrowicz, E. M. 1995. Observations of the transverse structure and dynamics of the low frequency flow through the North Channel of the Irish Sea. Continental Shelf Research, 15: 1133–1156.

Buckley, L. J., and Lough, R. G. 1987. Recent growth, biochemical composition and prey field of larval haddock (*Melanogrammus aeglefinus*) and Atlantic cod (*Gadus morhua*) on Georges Bank. Canadian Journal of Fisheries and Aquatic Science, 44: 14–25.

Campana, S. E., Smith, S. J., and Hurley, P. C. F. 1989a. A drift-retention dichotomy for larval haddock (*Melanogrammus aeglefinus*) spawned on Browns Bank. Canadian Journal of Fisheries and Aquatic Science, 46 (Suppl 1): 93–102.

Campana, S. E., Frank, K. T., Hurley, P. C. F., Koeller, P. A., Page, F. H., and Smith, P. C. 1989b. Survival and abundance of young Atlantic cod (*Gadus morhua*) and haddock (*Melanogrammus aeglefinus*) as indicators of year-class strength. Canadian Journal of Fisheries and Aquatic Science, 46 (Suppl 1): 171–182.

Cushing, D. 1995. Population production and regulation in the sea: a fisheries perspective. Cambridge University Press, Cambridge. 354 pp.

Davies, A. M., and Jones, J. E. 1992. A three-dimensional wind-driven circulation model of the Celtic and Irish Seas. Continental Shelf Research, 12: 159–188.

Dickey-Collas, M., Brown, J., Fernand, L., Hill, E. D., Horsburgh, K. J., and Garvine, R. W. 1997. Does the western Irish Sea gyre influence the distribution of pelagic juvenile fish? Journal of Fish Biology, 51 (Suppl A): 206–229.

Fogarty, M. J., Myers, R. A., and Bowen, K. G. 2001. Recruitment of cod and haddock in the North Atlantic: a comparative analysis. ICES Journal of Marine Science, 58: 952–961.

Fox, C. J., Dickey-Collas, M., and Winpenny, A. J. 1997. Spring plankton surveys of the Irish Sea in 1995: the distribution of fish eggs and larvae. CEFAS Science Series Technical Report, 104. 106 pp.

Frank, K. T., and McRuer, J. K. 1989. Nutritional status of filed collected haddock (*Melanogrammus aeglefinus*) larvae from southwestern Nova Scotia: an assessment based on morphometric and vertical distribution data. Canadian Journal of Fisheries and Aquatic Science, 46 (Suppl 1): 125–133.

Gallego, A., Heath, M. R., Basford, D. J., and Mackenzie, B. R. 1999. Variability in growth rates of larval haddock in the northern North Sea. Fisheries Oceanography, 8: 77–92.

Heath, M. R., and Gallego, A. 1998. Bio-physical modelling of the early life stages of haddock *Melanogrammus aeglefinus*, in the North Sea. Fisheries Oceanography, 7: 110–125.

Heath, M. R., Rankine, P., and Cargill, L. 1994. Distribution of cod and haddock eggs in the North Sea in 1992 in relation to oceanographic features and compared with distributions in 1952–1957 (Abstract). ICES Marine Science Symposia, 198: 438–439.

Hislop, J. R. G., and Shanks, A. M. 1981. Recent investigations on the reproductive biology of the haddock, *Melanogrammus aeglefinus*, of the northern North Sea and the effects on fecundity of infection with the copepod parasite *Lernaeocera branchialis*. Journal du Conseil International pour l'Exploration de la Mer, 39: 244–251.

Horsburgh, K. J., Hill, A. E., Brown, J., Fernand, L., Garvine, R. W., and Angelico, M. M. P. 2000. Seasonal evolution of the cold pool gyre in the western Irish Sea. Progress in Oceanography, 46: 1–58.

ICES. 1997. Report of the Working Group on the Assessment of Northern Shelf Demersal Stocks. ICES CM 1997/Assess: 2. 443 pp.

ICES. 2000. Report of the Working Group on the Assessment of Northern Shelf Demersal Stocks. ICES CM 2000/ACFM: 1. 471 pp.

ICES. 2001. Report of the ICES Advisory Committee on the Fisheries Management 2000. ICES Cooperative Research Report, No. 242. 911 pp.

Jamieson, A., and Birley, A. J. 1989. The distribution of transferrin alles in haddock stocks. Journal du Conseil International pour l'Exploration de la Mer, 45: 248–262.

Jones, R., and Hislop, J. R. G. 1978. Changes in North Sea haddock and whiting. Rapports et Procès-Verbaux des Réunions du Conseil International pour l'Exploration de la Mer, 172: 58–71.

Knight, P. J., and Howarth, M. J. 1999. The flow through the North Channel of the Irish Sea. Continental Shelf Research, 19: 693–716.

Lage, C., Purcell, M., Fogarty, M., and Kornfield, I. 2001. Microsatellite evaluation of haddock (*Melanogrammus aeglefinus*) stocks in the northwest Atlantic Ocean. Canadian Journal of Fisheries and Aquatic Science, 58: 982–990.

Lasker, R., and MacCall, A. 1983. New ideas on the fluctuations of the Clupeoid stocks off California. Proceedings of the Joint Oceanographic Assembly 1982 General Symposia, pp. 110–120. Canadian National Committee on Oceanic Research, Ottawa, Ontario.

Lough, R. G., and Bolz, G. R. 1989. The movement of cod and haddock larvae onto the shoals of Georges Bank. Journal of Fish Biology, 35 (Suppl A): 71–79.

Lough, R. G., and Potter, D. C. 1993. Vertical distribution patterns and diel migrations of larvael and juvenile haddock *Melanogrammus aeglefinus* and Atlantic cod *Gadus morhua* on Georges Bank. Fishery Bulletin, 91: 281–303.

Marshall, C. T., and Frank, K. T. 1995. Density-dependent habitat selection by juvenile haddock (*Melanogrammus aeglefinus*) on the southwestern Scotian Shelf. Canadian Journal of Fisheries and Aquatic Science, 52: 1007–1017.

Marshall, C. T., and Frank, K. T. 1999. Implications of density-dependent juvenile growth for compensatory recruitment regulation of haddock. Canadian Journal of Fisheries and Aquatic Science, 56: 356–363.

Ottersen, G., and Loeng, H. 2000. Covariability in early growth and year-class strength of Barents Sea cod, haddock, and herring: the environmental link. ICES Journal of Marine Science, 57: 339–348.

Page, F. H., and Frank, K. T. 1989. Spawning time and egg stage duration in northwest Atlantic haddock (*Melanogrammus aeglefinus*) stocks with emphasis on Georges and Browns Bank. Canadian Journal of Fisheries and Aquatic Science, 46 (Suppl 1): 68–81.

Page, F. H., Frank, K. T., and Thompson, K. R. 1989. Stage dependent vertical distribution of haddock (*Melanogrammus aeglefinus*) eggs in a stratified water column: observations and model. Canadian Journal of Fisheries and Aquatic Science, 46 (Suppl 1): 55–67.

Page, F. H., Sinclair, M., Naimie, C. E., Loder, J. W., Losier, R. J., Berrien, P. L., and Lough, R. G. 1999. Cod and haddock spawning on Georges Bank in relation to water residence times. Fisheries Oceanography, 8: 212–226.

Saville, A. 1959. The planktonic stages of the haddock in Scottish waters. Marine Research, 3: 3–23.

Shepherd, J. G. 1999. Extended survivors analysis: an improved method for the analysis of catch-at-age data and abundance indices. ICES Journal of Marine Science, 56: 584–591.

Southward, A. J., Boalch, G. T., and Maddock, L. 1988. Fluctuations in the herring and pilchard fisheries of Devon and Cornwall linked to change in climate since the 16th century. Journal of the Marine Biological Association UK, 68: 423–445.

Waiwood, K. G., and Buzeta, M. I. 1989. Reproductive biology of southwest Scotian shelf haddock (*Melanogrammus aeglefinus*). Canadian Journal of Fisheries and Aquatic Science, 46 (Suppl 1): 153–170.

Young, E. F., Brown, J., and Aldridge, J. N. 2001. Application of a large area curvilinear model to the study of the wind-forced dynamics of flows through the North Channel of the Irish Sea. Continental Shelf Research, 21: 1403–1434.

ICES Marine Science Symposia, 219: 283–293. 2003

Interannual variability in the physical environment: zooplankton, capelin (*Mallotus villosus*), and Northeast Arctic cod (*Gadus morhua*) in the Barents Sea

V. K. Ozhigin, S. S. Drobysheva, N. G. Ushakov, N. A. Yaragina, O. V. Titov, and A. L. Karsakov

Ozhigin, V. K., Drobysheva, S. S., Ushakov, N. G., Yaragina, N. A., Titov, O. V., and Karsakov, A. L. 2003. Interannual variability in the physical environment: zooplankton, capelin (*Mallotus villosus*), and Northeast Arctic cod (*Gadus morhua*) in the Barents Sea. – ICES Marine Science Symposia, 219: 283–293.

This article describes the variability in the Barents Sea environment (from time series of air and water temperature, salinity, ice coverage, oxygen and phosphate content) and its biota (abundance and biomass of plankton, capelin, and cod). With an emphasis on the 1990s, comparisons are made with earlier years and decades. Strong relationships are found between most of the environmental indices, indicating a common source of variability. Few links are found between the environmental and biological variables, the exception being between oxygen levels in the near bottom layers and cod recruitment as measured at age 3.

Keywords: Barents Sea, climate, fish, plankton, variability.

V. K. Ozhigin, S. S. Drobysheva, N. G. Ushakov, N. A. Yaragina, O. V. Titov, and A. L. Karsakov: Knipovich Polar Research Institute of Marine Fisheries and Oceanography (PINRO), 6, Knipovich Str., Murmansk, 183763, Russia [tel:/fax: +47 789 10 518; e-mail: inter@pinro.murmansk.ru].

Introduction

The first detailed description of the hydrographic conditions of the Barents Sea was presented in a monograph by Knipovich (1906) based on the results of the Fisheries Research Expedition started in 1898. In 1900, during the expedition, the first oceanographic investigations were performed along the Kola Section (Figure 1). Knipovich assumed that the variability of temperature in the southern part of the Barents Sea was caused mainly by variations in the properties of the Atlantic waters brought by the eastward-flowing North Cape Current. He was one of the first to draw attention to the major effect of environmental variability on the marine biota. He believed that the fish resources and their environment were closely intertwined and should be studied simultaneously. Knipovich (1938) continued to develop the idea of a comprehensive study of seas and oceans in another monograph, in which he analysed and summarized the results of national and foreign investigations in hydrography, marine biology, and ichthyology of the Barents Sea and other seas.

Izhevskii (1961, 1964), who attempted to connect the variations in the sea environment and biota, believed that the Norwegian, Greenland, and Barents Seas, as well as a large part of the North Atlantic influenced by the Gulf Stream, were characterized by common dynamics involving air–sea interactions, and that these determined biological productivity in the area. He underlined the importance of regular observations along the Kola Section for studies of interrelations between environment and marine organisms and for the prediction of commercial fish stocks.

Regular and comprehensive oceanographic investigations in the Barents Sea were initiated in the 1950s, when attempts were already underway studying plankton variability and identifying its causes. By the 1960s, Russian plankton specialists had developed two main hypotheses. According to Kamshilov (1961), the variability in the timing and intensity of plankton development is determined by the inter-species relationships. Galkin (1963), however, believed the plankton variability was a response to changes in water temperature.

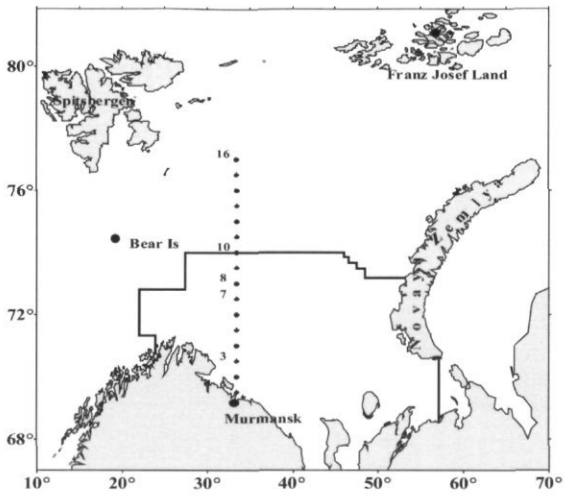


Figure 1. The Barents Sea. Small dots denote the Kola Section, numbers denote station number. Large dots give the position of meteorological stations used in the article. Solid lines show the area over which euphausiid abundance was averaged.

Knowledge of the variability of environment and its influence on the plankton and commercial fish species of the Barents Sea continued to accumulate and was summarized in papers presented at three joint Norwegian–Russian symposia held in Leningrad in 1983 (Ponomarenko, 1984; Randa, 1984; Saetersdal and Loeng, 1984), in Bergen in 1984 (Ozhigin and Luka, 1985), and in Murmansk in 1986 (Boytsov and Drobysheva, 1987; Ellertsen *et al.*, 1987; Skjoldal *et al.*, 1987; Ushakov and Ozhigin, 1987). In more recent years, the influence of oceanographic conditions on fish stocks has been considered in a number of publications (Loeng, 1989; Loeng *et al.*, 1995; Ottersen and Loeng, 2000; Ottersen *et al.*, 1994; Ottersen *et al.*, 1998; Ozhigin *et al.*, 1996; Ozhigin *et al.*, 1999). In addition, results of investigations carried out in the 1950 through the 1990s allowed a more detailed analysis of the interannual variability of the plankton community and its relationship with the environment (Degtyareva, 1979; Nesterova, 1990; Drobysheva, 1994). Long-term variations in hydrochemical variables of the Barents Sea have been analysed and described by Titov (1999, 2001a, b).

This article describes the interannual variability of the environment, zooplankton, capelin, and cod in the Barents Sea in the past 15–50 years, with a special focus on the 1990s. Time-series of temperature, salinity, oxygen, phosphate, biomass of mesozooplankton at the Kola Section, and macrozooplankton in the southern part of the Sea, as well as indices of abundance and biomass of capelin and cod, are presented and analysed. We also examine the relationships between these time-series as a means towards revealing the possible causes of their variability.

Material and methods

Variations in temperature, salinity, and other oceanographic parameters along the Kola Section (Figure 1) have a 100-year history. However, regular observations were only initiated in the early 1950s. In recent decades, the section has been occupied 10–12 times a year. For the calculation of vertically averaged temperature, salinity, and other parameters, the section is divided into three parts: (1) stations 1–3 (69°30'–70°30'N) – coastal waters with low salinity; (2) stations 3–7 (70°30'–72°30'N) – the Murman Current; and (3) stations 8–10 (73°00'–74°00'N) – the Atlantic waters.

Variations in sea temperature in the 0–200 m layer at stations 3–7 closely correlate with temperature in the southern and northern parts of the section ($r > 0.9$). In addition, they were closely correlated with temperatures in other standard sections in the southern Barents Sea (Tereshchenko, 1997). Therefore temperatures at stations 3–7 of the Kola Section represent conditions in the entire southern Barents Sea and can be considered as an index of marine climate in the region.

Hydrochemical observations along the Kola Section have been carried out more than 200 times since the first occupation, 45 of those in 1990–1999. Chemical analysis of water samples was done onboard the vessel. Oxygen content in water samples was determined by the Winkler method and phosphate content by the Deniges-Atkins' method as modified by PINRO (Anon., 1980). Continuous time-series of mean monthly and mean annual anomalies of hydrochemical parameters at stations 3–7 were calculated using the method described by Titov (1999, 2001a), analogous to that used for temperature and salinity. In this article, we restrict our analysis to oxygen saturation and phosphate concentration in the bottom 10-m layer.

Air temperatures over the Barents Sea were taken from stations on Bear Island, in Murmansk, and on Franz Josef Land (Figure 1), as submitted by the Murmansk Area Department for Hydrometeorology and Environmental Monitoring (MADHEM). Data on ice coverage (percentage of area covered by ice) were also obtained from MADHEM. As a climatic index of large-scale atmospheric circulation over the North Atlantic, the winter (December/March) NAO index (Hurrell, 1995) was used.

Sampling of mesoplankton in May/June has been conducted annually since 1959. Samples were collected in depth layers over the entire water column using a Juday net (gauze no. 38, diameter of the entrance hole 37 cm), along 8 standard sections in the southern Barents Sea (south of 74°30'N). After 1992, sampling was essentially limited to the Kola Section. Long-term observations showed that data from this section generally reflect the dynamics of plankton development in the southwestern part of the sea. We therefore assume that the data from the

Kola Section can be used as an indicator of interannual variations in the biomass of mesozooplankton. For the present study, data on the biomass of *Calanus finmarchicus* in the 0–50 m layer between stations 3 and 7 were used.

Sampling of macroplankton in the Barents Sea began in 1952 and nowadays is carried out in October–December over the entire area, except in the northeast. The most complete and regular coverage has been in southern parts of the Sea. The macroplankton are sampled during a trawl-acoustic survey for demersal fish. The plankton net (gauze no. 140, diameter of the entrance hole 50 cm) is fastened on the headline of the trawl and takes samples in the bottom 10-m layer where plankton are most densely concentrated. Laboratory processing includes the full biological analysis of organisms. The abundance of macroplankton was assessed in mg m^{-3}. Catch per 1 h of a net filtering 1000 m^3 of water at the speed of 2.5–3 knots (individuals/1000 m^3) was taken as the abundance index. In this article, we analyse the time-series of mean euphausiid abundance in the southern Barents Sea (see Figure 1 for area boundaries).

Catch statistics for cod and capelin, data on the year-class abundance and recruitment to the

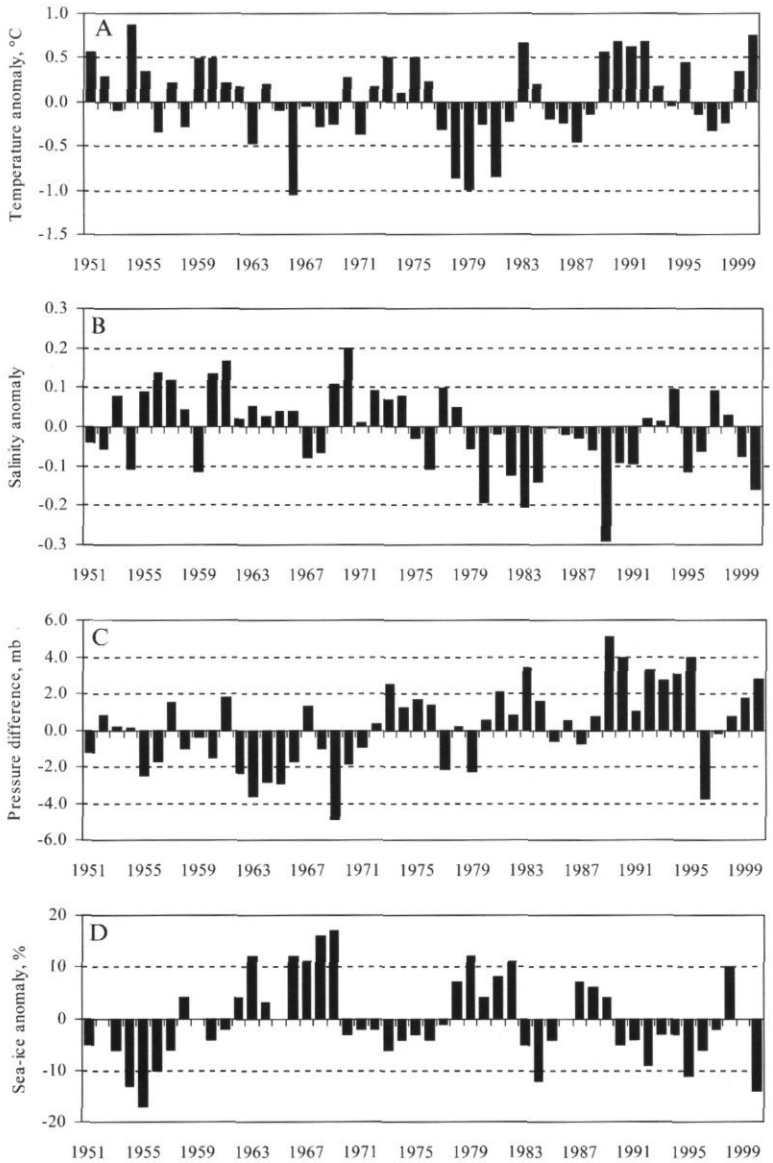


Figure 2. Anomalies: (A) the Murman Current temperature (70°30'–72°30'N, 33°30'E); (B) coastal water salinity (69°30'–70°30'N, 33°30'E); (C) winter NAO index; (D) ice coverage of the Barents Sea.

commercial stock, on the stock status and seasonal migrations were obtained by PINRO and from reports by the ICES Arctic Fisheries and Northern Pelagic and Blue Whiting Working Groups (ICES, 1999, 2000, 2001a).

Results

Figure 2 presents annual anomalies of temperature and salinity on the Kola Section, the NAO index, and the Barents Sea ice coverage. Temperatures in the 0–200-m layer in the Murman Current were well above or close to the long-term mean in 1990–1995, as well as in 1989. The highest positive anomalies (0.5–0.7°C) were observed in 1989–1992. A slight cooling in 1996–1998 was followed by a considerable temperature increase in the late 1990s. Prior to the 1990s, annual temperature anomalies on the Kola Section varied by approximately ±1°C. In the 1950s, they were predominantly warm, while in the 1960s they tended to be below the long-term normal. The most intense cooling that persisted the longest occurred in 1977–1982.

Over the 50-year time series, variations in salinity at stations 1–3 and 3–7 were not correlated with temperature fluctuations in the Murman Current (Table 1). However, in the late 1980s and during the 1990s, increases in the temperature of the Murman Current were often accompanied by decreases in coastal water salinity and vice versa (Figure 2B). Interannual variations in salinity of Atlantic water (stations 8–10) were not so marked as in the coastal waters, but they were more closely related to temperature fluctuations in the Murman Current (Table 1).

Variations of NAO index (Figure 2C) show large interannual variability, which is similar to the temperature fluctuations in the Murman Current. There is a weak but statistically significant relationship between them. A similar relationship is observed between the NAO and air temperatures at the Murmansk station (Table 1).

Ice coverage of the Barents Sea was also subjected to large interannual variations (Figure 2D). The period 1990–1997 was the longest when the ice coverage was far below the long-term mean. Fluctuations in ice coverage significantly correlate with water temperature variations along the Kola Section, as well as with air temperature fluctuations over Bear Island and Franz Josef Land (Table 1).

Mean annual anomalies of air temperature on Bear Island, in Murmansk, and on Franz Josef Land are shown in Figure 3. Despite the great distance between stations, temperature variations there show similar trends. In the 1990s, air temperatures were predominantly warmer-than-normal, with the highest anomalies at the beginning of the decade. Air temperature fluctuations at these stations are also correlated with water temperature fluctuations in the Murman Current (Table 1).

Table 1. Coefficients of correlation between environmental and fish population parameters (r), number of observations (n), and significance (p).

Parameters	r	n	p
Sea temperature, Kola Section, Stations 3–7: Salinity, Kola Section, Stations 3–7	0.02	50	—
Sea temperature, Kola Section, Stations 3–7: Salinity, Kola section, Stations 1–3	−0.27	50	—
Sea temperature, Kola Section, Stations 3–7: Salinity, Kola Section, Stations 8–10	0.53	50	<0.01
Winter NAO index: Sea temperature, Kola Section, Stations 3–7	0.45	50	<0.01
Winter NAO index: Air temperature, Murmansk	0.47	50	<0.01
Ice coverage: Sea temperature, Kola Section, Stations 3–7	−0.65	50	<0.01
Ice coverage: Air temperature, Bear Island	−0.57	50	<0.01
Ice coverage: Air temperature, Franz Josef Land	−0.71	50	<0.01
Air temperature, Bear Island: Sea temperature, Kola Section, Stations 3–7	0.49	50	<0.01
Air temperature, Murmansk: Sea temperature, Kola Section, Stations 3–7	0.60	50	<0.01
Air temperature Franz Josef Land: Sea temperature, Kola Section, Stations 3–7	0.48	50	<0.01
Oxygen: Sea temperature, Kola Section, Stations 3–7	0.46	40	<0.01
Oxygen: Ice coverage	−0.54	40	<0.01
Oxygen: Cod recruitment at age 3 year	0.49	40	<0.01
Oxygen: Logarithm of cod recruitment at age 3 years	0.56	40	<0.01

The range of variations of oxygen saturation in the bottom 10-m layer of the Kola Section in the 1990s was the same as in previous decades (Figure 4A). Lower than normal oxygen saturation was observed at the beginning and end of the decade, as well as in 1994–1995. The decadal mean oxygen saturation was 92.3%, close to the long-term mean (92.7%). Oxygen saturation in the bottom layer correlates with water temperature at stations 3–7 with the time-lag of 1 year and with ice coverage. There is also a significant correlation between oxygen saturation and the log of the abundance of cod year classes at age 3, with a time-lag of 1 year (Figure 4B, Table 1).

Phosphate concentrations in the bottom layer at the Kola Section exhibit large low-frequency variability with generally below normal values from the early 1960s to the mid-1970s, followed by 10 years of predominantly positive anomalies (Figure 4D). Phosphate in the 1990s did not vary much between years, with an average content of 0.82 μM, just slightly lower than the long-term mean (0.84 μM).

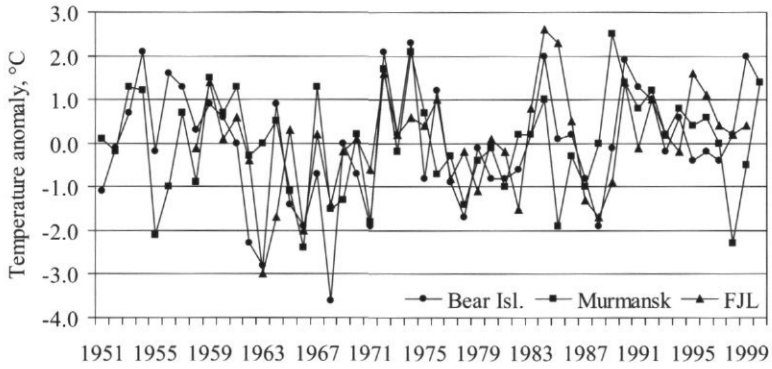


Figure 3. Mean annual anomalies of air temperature at Bear Island, Murmansk, and Franz Jozef Land (FJL).

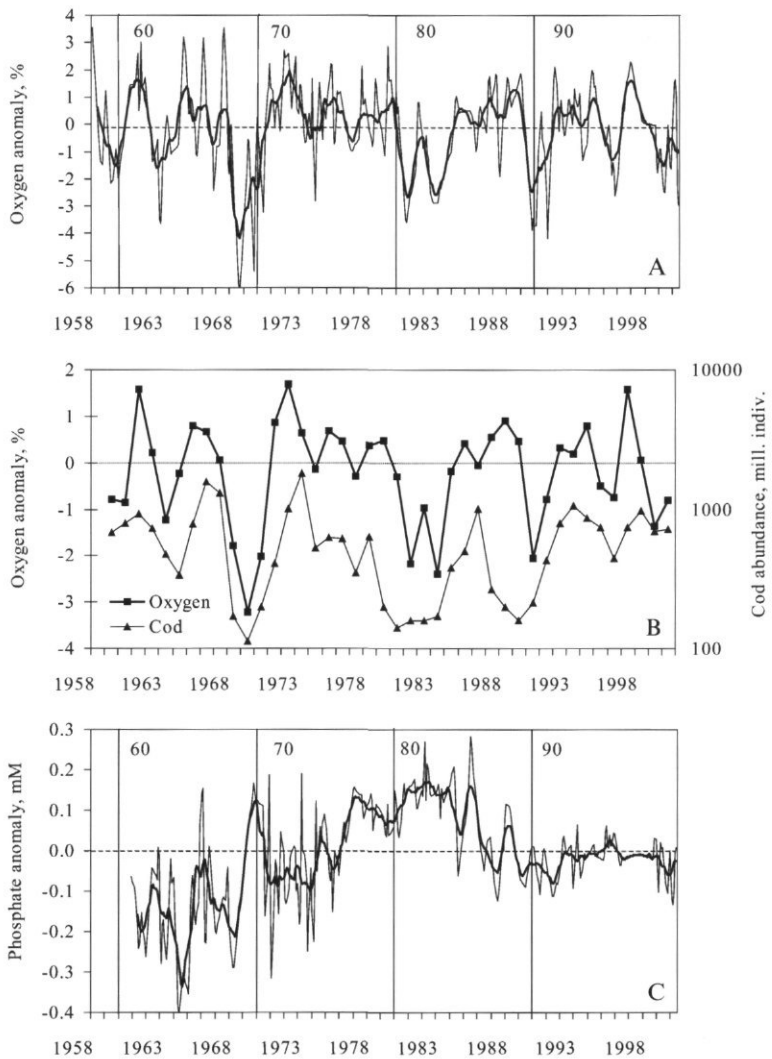


Figure 4. (A) Mean monthly (thin lines) and 12-month (thick lines) running means of anomalies of oxygen saturation in the bottom layer of the Kola Section. (B) Oxygen saturation anomalies in the bottom layer of the Kola Section averaged for the 12 months preceding the appearance of cod year classes and logarithm of abundance of these year classes at age 3 years. (C) Mean monthly (thin lines) and 12-month (thick lines) running means of anomalies of phosphate concentration in the bottom layer of the Kola Section.

Long periods of high variability in mesozooplankton (*Calanus finmarchicus*) biomass (the 1960s and 1980s) alternated with periods with relatively low variability (the 1970s and 1990s) (Figure 5A). A low but relatively stable biomass of *C. finmarchicus* (ca. 100–150 mg m^{-3}) was observed in the 1990s.

The abundance of euphausiids in the southern Barents Sea was also subject to large interannual fluctuations (Figure 5B), with the mean decadal values increasing from 200 individuals/1000 m^3 in the 1950–1960s to 400–500 individuals/1000 m^3 in the 1980–1990s. Periods of high euphausiid abundance were observed at 10- to 12-year intervals. In 1992–1993, the abundance of euphausiids did not exceed 50 individuals/1000 m^3, which is close to the minimum over the entire period of observations. After that, the abundance increased rapidly up to 1118 individuals/1000 m^3 in 1998. At the end of the decade, abundances had declined to near the long-term average. An inverse relationship between euphausiid abundance and capelin biomass has been observed during the past 15 years (Figure 5C).

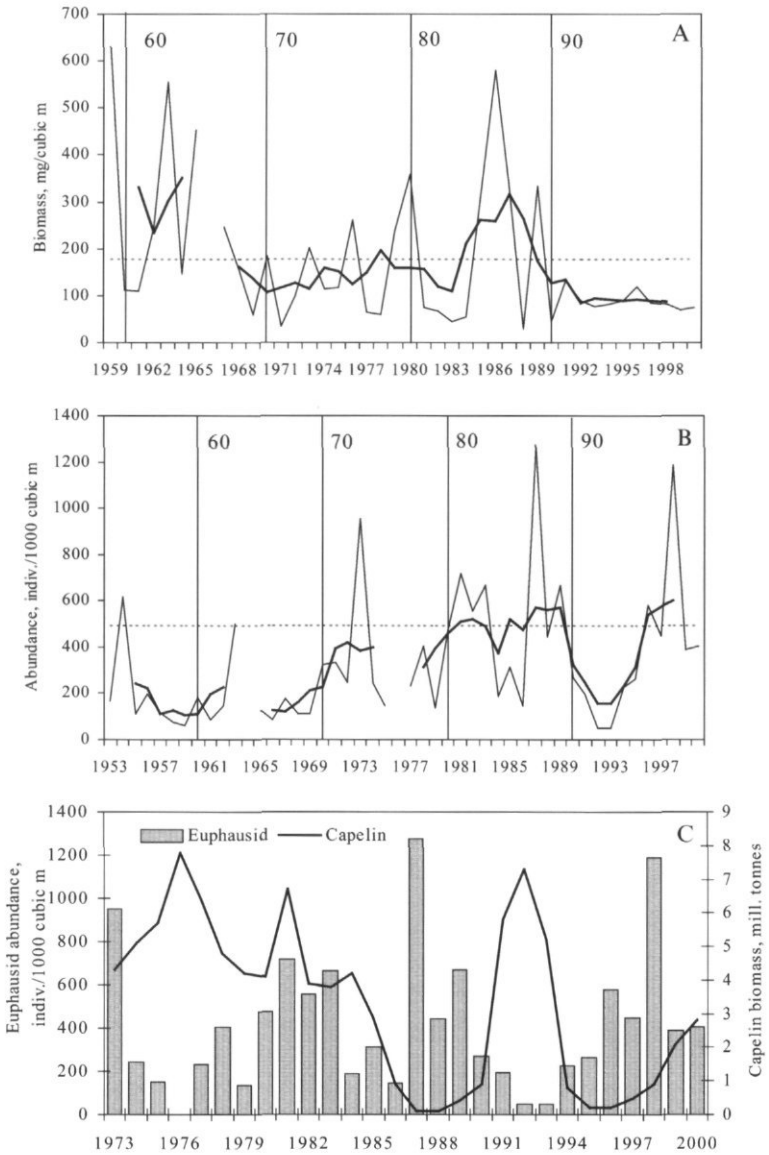


Figure 5. (A) Biomass of *Calanus finmarchicus* in the 0–50 m layer at stations 3–7 of the Kola Section in June (thin line) and 5-year running mean (thick line). (B) Euphausiid abundance in the southern Barents Sea in October–December (thin line) and 5-year running mean (thick line). (C) Euphausiid abundance and capelin biomass.

In the early 1980s, capelin biomass declined from 6715 to 2964 thousand tonnes, with an annual catch of 1400–2300 thousand tonnes (ICES 1999, 2000; Figure 6A). However, in the mid to late 1980s the capelin stock was drastically low. In the autumn of 1986, a ban on the capelin fishery was imposed that lasted until 1990. Data from trawl-acoustic assessment surveys of pelagic fish (ICES 1999, 2000) suggest that 1989 was one of the largest year classes on record. Subsequent year classes, especially those of 1992–1996, were very poor, but abundant year classes appeared again in 1997–1999.

The increase in the capelin stock in 1990–1992 (Figure 6A) allowed resumption of the fishery. A cautious fishery helped to conserve the spawning stock, such that by the beginning of the spawning season in 1991 and 1992 it was respectively 1582 and 996 thousand tonnes, which was well above the advised 500 thousand tonnes. The growth of cod and haddock stocks in the same period caused a considerable increase in the natural mortality of capelin, however. Owing to a gradual dying-out of the abundant 1989 year class, the capelin stock was again in a state of depression, resulting in a fishery ban from autumn 1993 to 1998.

In the mid-1990s, the natural mortality of capelin decreased considerably, but restoration of the capelin stock was slow. Only after the occurrence of the strong year classes of 1997 and 1998 (from a small spawning stock, but under favourable conditions of young fish survival) did the total biomass of the stock reach 2.0 million tonnes in 1998 and 2.8 million tonnes in 1999. The spawning stock as of 1 January 1998, 1999, and 2000 was estimated at 245, 712, and 1333 thousand tonnes, respectively. The capelin fishery was resumed owing to the growth of the spawning stock.

In 1989–1992, feeding capelin migrated further north and northeast (Figure 8). In 1996–1998, the areas of capelin distribution shrank and shifted to the southwest.

In 1990, the biomass of the commercial cod stock (individuals of age 3 and older) was estimated at 1 million tonnes, close to the 1989 minimum of 0.89 million tonnes (Figure 6B). It quickly bounced back, reaching its maximum (2.3 million tonnes) in 1993. By 2000, the commercial stock biomass declined to 1.04 million tonnes, and well below the long-term mean (2.03 million tonnes). The spawning stock varied from 873 thousand tonnes in 1992 to 223 thousand tonnes in 2000. In 1991–1997 the spawning stock was above the long-term mean of 373 thousand tonnes (ICES, 2001b).

The abundance of cod year classes in the 1990s was quite high. That period produced 1 strong (1990), 8 average, and only 2 weak (1999, 2000) year classes (Figure 6B). By comparison, in the preceding decade a large number of poor year classes occurred (8 out of 10).

Variations in growth rates of cod from different year classes were large in the late 1980s and the first half of the 1990s. In the late 1980s, the length and weight of most cod from different age groups were below the long-term mean (Figure 7). Growth rate increased in the early 1990s, reaching the maximum in 1992–1994, after which the length and weight decreased again.

Fisheries statistics and data from Russian trawl-acoustic surveys of demersal fish carried out in October–December both show that during the warming in the early 1990s feeding cod migrated

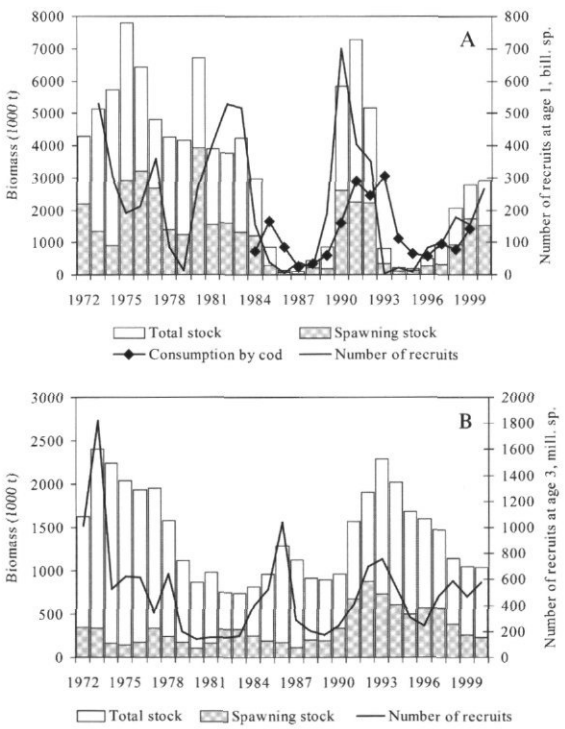


Figure 6. (A) Capelin total stock, spawning stock, consumption by cod, and number of recruits at age 1+. (B) Total and spawning stock of cod and the abundance of recruits at age 3.

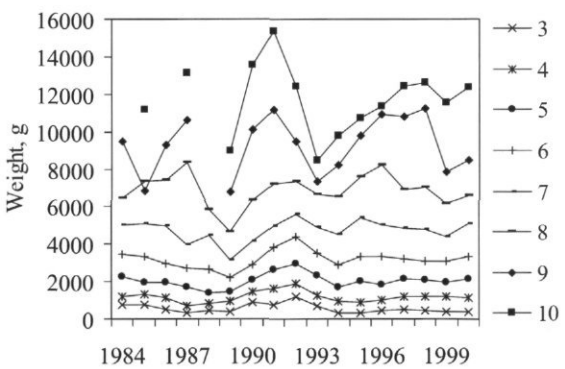


Figure 7. Weight of cod at ages from 3 to 10 years.

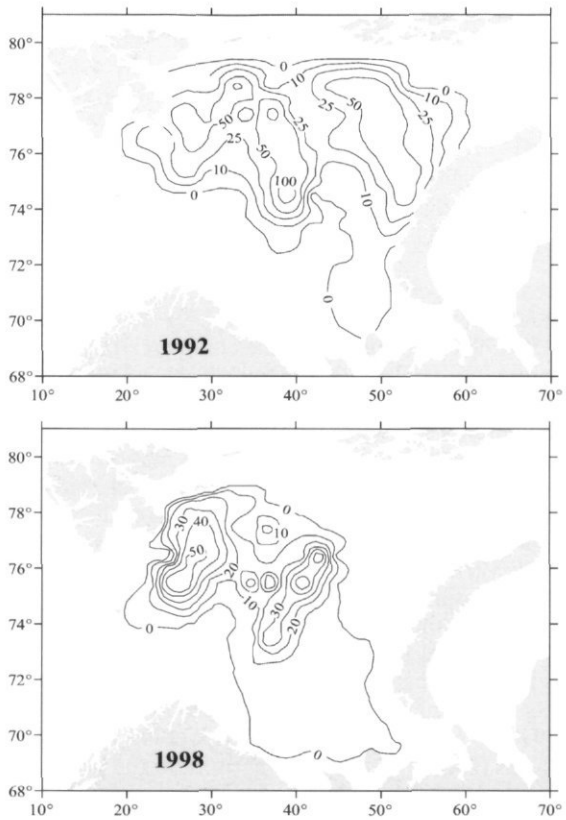


Figure 8. Distribution of capelin in September during warm (1992) and cold (1998) years (in tonnes mile^2).

further to the north and east than in the cold period of 1996–1998.

Discussion

The results from our study confirm that large-scale atmosphere--ocean interactions in the Barents Sea and in the North Atlantic are interrelated (Table 1).

The variations in air temperature at the Murmansk station and sea temperatures in the Kola Section are related to NAO index variations (Table 1). In the periods of positive NAO index, the air and ocean temperatures increase, and decrease in years of low NAO. However, the relationships of the NAO index with both air and water temperature in the Barents Sea area, while significant, are not high. The NAO index accounts for about 20% of the temperature variability in both air and water, suggesting that local processes of air–sea interaction play a greater role in the variations of water and air temperature in the Barents Sea, as proposed by Ådlandsvik and Loeng (1991).

Ice coverage is weakly correlated with NAO, but correlates more strongly with water temperatures in the Kola Section and air temperature in the west and northeast of the Barents Sea (Table 1). The correlation between ice coverage and air temperature was highest at the station on Franz Josef Land, suggesting that the influence of atmospheric processes in the Arctic on ice coverage variations is greater than that due to heat advection by currents.

Variations of temperature and salinity at stations 3–7 on the Kola Section are not interrelated (Table 1), which is probably due to shifts in the haline front between stations 4 and 6 separating coastal waters from the salt Atlantic waters. Out-of-phase variations in the coastal water salinity and the Murman Current temperature in the late 1980s and during the 1990s suggest that at this time temperature in the southern Barents Sea was considerably influenced by the Norwegian Coastal Current.

The relationship between the hydrochemical parameters and climatic fluctuations is difficult to interpret, and is probably determined indirectly by the stratification and chemical composition of inflowing Atlantic waters (Titov, 2001a, b). The recruitment and biomass of commercial stocks are related to the variations in hydrochemical parameters of the Barents Sea (Titov, 1999, 2001a, b). The relationship between long-term variations of cod recruitment and oxygen saturation in the bottom layer of the Barents Sea (Figure 4B) is similar to that for the Baltic Sea. However, the Barents Sea is characterized by a time-lag of 1 year in the variations of oxygen saturation and cod abundance. The nature of this relationship is not yet clear and requires further investigation.

The impact of temperature on *Calanus* biomass is inconclusive, with no significant correlation between these time-series. A general coincidence of interannual biomass fluctuations and water temperature was observed only in the periods of low and relatively stable biomass and was absent when biomass fluctuated significantly. The influence of temperature on the interannual fluctuations of plankton biomass coincided with the sudden decline in predation. Plankton biomass notably increased in the 1960s, when the abundance of young cod decreased, and in the 1980s, when the capelin stock declined. In the 1970s, when predation was high (capelin stock of ca. 5–7 million tonnes) and *Calanus* biomass was low, the interannual variations of plankton biomass generally corresponded to temperature fluctuations. The reasons for the low and relatively stable biomass of *Calanus* at the Kola Section in the 1990s are still unclear.

Comparing interannual variations in euphausiid and capelin abundance and water temperature indicates domination of the biotic factor, which was especially pronounced in the late 1980s and during 1990s. Capelin stock and euphausiid abundance were inversely interrelated at that time (Figure 5C). In the years of low capelin stock (1987–1989 and 1994–1998), the abundance of euphausiids increased

greatly, while when capelin biomass was high (1991–1993) plankton abundance declined significantly. This relationship was not observed in the 1970s. The effect of temperature fluctuations consists mostly in the "re-distribution" of the euphausiid stock between western and eastern areas of the sea. In the west, the warm-water species, *Meganictyphanes norvegica*, prevails, while in the east the cold-water species, *Thysanoessa raschii*, dominates (Drobysheva, 1979).

The increase of capelin in the early 1990s was caused by the extremely favourable temperature conditions in 1989–1991 and low natural mortality. These ensured the successful spawning of capelin, good survival of young fish, the appearance of the very strong year class of 1989, and high growth rate. All these factors led to the increase of capelin stock up to 5.1–7.2 million tonnes in 1990–1992.

Our study shows no clear relationship between capelin abundance and oceanographic conditions in the Barents Sea. Strong and average year classes appeared more often during the comparatively cold period (the 1970s), and less abundant year classes during the warm period (the 1990s) (Figure 6A). However, the most abundant year class (1989) appeared in the period of warming. The reduced predation pressure (natural mortality was minimal for the whole period from 1973) favoured survival of the exceptionally strong year class of 1989.

Migration patterns of feeding capelin in the 1990s (Figure 8) were similar to those described by Ozhigin and Luka (1985). Due to the warmer temperatures and the good state of the stock at the beginning of the decade, the distribution of capelin extended farther to the north and northeast. The cooling in 1996–1998 resulted in a shift of the main autumn feeding grounds back towards the west and southwest.

Cod migrations showed similar trends. However, interannual variations in the distribution of cod were less pronounced than those of capelin. Cod inhabits warmer waters than capelin and is mainly distributed in the coastal and Atlantic water, rarely making massive migrations across the polar front.

A number of hypotheses have been proposed to explain the mechanisms defining the strength of cod year classes (Hjort, 1914, 1926; Melle and Ellertsen, 1984; Ponomarenko, 1984; Sinclair and Tremblay, 1984). These hypotheses consider mortality at early life stages, feeding conditions in the "critical period" of life, predation by herring, ctenophores and jellyfish, the presence of eggs and larvae in the areas with favourable survival conditions, etc. Izhevskii (1961, 1964) suggested that the Barents Sea temperature undergoes cyclical variations with periods of 4–5, 8–10, and 18–20 years, with the strongest year classes of cod corresponding to the time of the coincidence of maxima of these cycles, and the weakest ones with the coincidence of their minima. Ozhigin *et al.* (1999) showed that the approach of Izhevskii can be used to forecast recruitment. For example, the strong year class of 1990 and average of 1991 appeared at the coincidence of maxima of 4–5 and 8–10 year cycles. However, sometimes this approach does not explain year-class strength, which might be related to variations in both amplitude and periodicity of the fluctuations. The calculations based on the Izhevskii's approach led to the conclusion that poor year classes would appear in 1996 and strong ones in 2000–2001. However, poor year classes appeared in 1999–2000, while that of 1996 was average.

Saetersdal and Loeng (1984) suggested that strong year classes appear when a cold period shifts to a warm one and the temperatures reach the maximum. Consistent with this, the strong year class of 1990 appeared after the transition from the cold year of 1988 to the warm year of 1989.

Loeng (1989) noted that poor year classes of cod constituted approximately 66% of the total number of year classes in 1902–1987. Average year classes made up 21% and strong ones only 13%. In 1990–2000, 73% of 11 year classes were average and 18% were poor; the proportion of strong year classes was close to the long-term mean (9%). High abundance was obviously related to the spawning-stock biomass, which was above the long-term mean in 7 years out of 11 (Figure 7B). This supports the suggestion of Ponomarenko (1996) that the appearance of many poor year classes in the 1980s was related to the low abundance of eggs caused by the decline of the spawning stock and the disruption of its structure.

Considerable variations in the growth rate of cod are mostly caused by large fluctuations in the abundance of prey, primarily capelin (Jørgensen, 1972; Nilssen *et al.*, 1994; Ozhigin *et al.*, 1995). In the 1990s, capelin stock underwent large fluctuations, increasing to 5–7 million tonnes in 1991–1993 with a subsequent decrease to 200–900 thousand tonnes in 1994–1998 (Figure 6A). The growth rate of cod (Figure 7) generally reflected the dynamics of capelin stock with a certain lag of minima and maxima. The growth rate was the highest in 1992–1994, with a following decline to the average level related to the change to other prey (young cod, shrimp, euphausiids, Themisto, polar cod), which could not fully compensate for the lack of capelin.

Concluding remarks

Our results support the notions of Izhevskii (1961, 1964) that the Barents Sea can be considered an integrated system with common trends in the variability of the oceanographic and atmospheric processes, which in turn determine the fluctuations in sea productivity. However, most of the statistically

significant relationships are those between environmental time series. Though the environmental and biological parameters are interrelated, these relationships become uncertain already at the trophic levels of zooplankton and capelin. Variations in fish stock parameters are caused by a great number of biological factors, including trophic relationships, which cannot be fully assessed. In addition, the interactions in the marine ecosystem are largely destabilized by multispecies fisheries, which removes different portions of individuals at different trophic levels.

Acknowledgements

We thank Dr. K. Drinkwater and two anonymous reviewers for their valuable advice and comments. We also thank V. Tereshchenko for useful discussions and V. Nesterova for the data on zooplankton.

References

Ådlandsvik, B., and Loeng, H. 1991. A study of the climatic system in the Barents Sea. Proceedings of the Pro Mare Symposium on Polar Marine Ecology, Trondheim, 12–16 May 1990. Polar Research, 10: 45–49.

Anon. 1980. Instructions and Directions. PINRO Press, Murmansk. 246 pp. (In Russian.)

Boytsov, V. D., and Drobysheva, S. S. 1987. Effect of hydrometeorological factors on the regularity of the long-term variations in euphausiid (Crustacea, Euphausiacea) abundance in the southern Barents Sea. *In* The Effect of Oceanographic Conditions on Distribution and Population Dynamics of Commercial Fish Stocks in the Barents Sea, pp. 91–100, Ed. by H. Loeng. Proceedings of the Third Soviet–Norwegian Symposium, Murmansk, 26–28 May 1986. Institute of Marine Research. Bergen.

Degtyareva, A. A. 1979. Regularities of zooplankton quantitative development in the Barents Sea. Trudy PINRO, 43: 22–53. (In Russian.)

Drobysheva, S. S. 1979. Development of euphausiid aggregations in the Barents Sea. Trudy PINRO, 43: 54–76. (In Russian.)

Drobysheva, S. S. 1994. The Barents Sea Euphausiids and their Role in Fisheries Productivity. PINRO Press, Murmansk. 139 pp. (In Russian.)

Ellertsen, B., Fossum, P., Solemdal, P., Sundby, S., and Tilseth S. 1987. The effect of biological and physical factors on the survival of Arcto-Norwegian cod and the influence on recruitment variability. *In* The Effect of Oceanographic Conditions on Distribution and Population Dynamics of Commercial Fish Stocks in the Barents Sea, pp. 101–126. Ed. by H. Loeng. Proceedings of the Third Soviet–Norwegian Symposium, Murmansk, 26–28 May 1986. Institute of Marine Research. Bergen.

Galkin, Y. I. 1963. Sea temperature and zooplankton productivity in the southern Barents Sea. Okeanologiya, 3: 324–330. (In Russian.)

Hjort, J. 1914. Fluctuations in the great fisheries of northern Europe viewed in the light of biological research. Rapports et Procès-Verbaux des Réunions du Conseil International pour l'Exploration de la Mer, 20: 1–228.

Hjort, J. 1926. Fluctuations of the year-classes of important food fishes. Journal du Conseil International pour l' Exploration de la Mer, 1: 1–38.

Hurrell, J. W. 1995. Decadal trends in the North Atlantic Oscillation: regional temperatures and precipitation. Science, 169: 676–679.

ICES. 1999. Report of the Northern Pelagic and Blue Whiting Fisheries Working Group. ICES CM 1999/ACFM: 18. 238 pp.

ICES. 2000. Report of the Northern Pelagic and Blue Whiting Fisheries Working Group. ICES CM 2000/ACFM: 16. 170 pp.

ICES. 2001a. Report of the Arctic Fisheries Working Group. ICES CM 2001/ACFM: 02. 340 pp.

ICES. 2001b. Report of the Arctic Fisheries Working Group. ICES CM 2001/ACFM: 19. 380 pp.

Izhevskii, G. K. 1961. Oceanological principles as related to the fishery productivity of the seas. Moscow: Pishcepromizdat. [Transl. 1964: Israel Progr. Sci. Transl., Jerusalem]. 186 pp.

Izhevskii, G. K. 1964. Forecasting of oceanological conditions and the reproduction of commercial fish. Moscow. [Transl. 1966: Israel Progr. Sci. Transl., Jerusalem]. 95 pp.

Jørgensen, T. 1992. Long-term changes in growth of North-east Arctic cod (*Gadus morhua*) and some environmental influences. ICES Journal of Marine Science, 49: 263–277.

Kamshilov, M. M. 1961. The importance of mutual relationships between organisms in evolution. Academy of Science Press, Moscow–Leningrad. 136 pp. (In Russian.)

Knipovich, N. M. 1906. Hydrography Fundamentals of the European Arctic Ocean. St. Petersburg. 42. 1510 pp. (In Russian.)

Knipovich, N. M. 1938. Hydrography of Seas and Brackish Waters (in Application to the Fishery). Moscow–Leningrad. 513 pp. (In Russian.)

Loeng, H. 1989. The influence of temperature on some fish population parameters in the Barents Sea. Journal of Northwest Atlantic Fishery Science, 9: 103–113.

Loeng, H., Bjørke, H., and Ottersen, G. 1995. Larval fish growth in the Barents Sea. *In* Climate Change and Northern Fish Populations, pp. 691–698, Ed. by R. J. Beamish. Canadian Special Publications of Fisheries and Aquatic Sciences, 121.

Melle, W., and Ellertsen, B. 1984. Predation on cod eggs and larvae; potential predators in the spawning ground of the Northeast Arctic cod. Report of the ICES Working Group on Larval Fish Ecology, Hirtshals, Denmark, 25–27 June 1984. ICES CM 1984/L: 37. 78 pp.

Nesterova, V. N. 1990. Plankton Biomass at the Drift Routes of Cod Larvae: Reference Material. PINRO Press, Murmansk. 64 pp. (In Russian.)

Nilssen, E. M., Pedersen, T., Hopkins, C. C. E., Thyholdt, K., and Pope, J. G. 1994. Recruitment variability and growth of Northeast Arctic cod: influence of physical environment, demography, and predator–prey energetics. ICES Marine Science Symposia, 198: 449–470.

Ottersen, G., and Loeng, H. 2000. Covariability in early growth and year-class strength of Barents Sea cod, haddock, and herring: the environmental link. ICES Journal of Marine Science, 57: 339–348.

Ottersen, G., Loeng, H., and Raknes, A. 1994. Influence of temperature variability on recruitment of cod in the Barents Sea. ICES Marine Science Symposia, 198: 471–481.

Ottersen, G., Michalsen, K., and Nakken, O. 1998. Ambient temperature and distribution of north-east Arctic cod. ICES Journal of Marine Science, 55: 67–85.

Ozhigin, V. K., and Luka, G. I. 1985. Some peculiarities of capelin migrations depending on thermal conditions in the

Barents Sea. *In* The Barens Sea Capelin, pp. 135–147. Ed. by H. Gjosaeter. Proceedings of the Soviet–Norwegian Symposium, Bergen, 14–19 August 1984. Institute of Marine Research, Bergen.

Ozhigin, V. K., Tretyak, V. L., Yaragina, N. A., and Ivshin, V. A. 1995. Growth of Arcto-Norwegian cod in dependence on environmental conditions and feeding. ICES CM 1995/P: 10. 22 pp.

Ozhigin, V. K., Tretyak, V. L., Yaragina, N. A., and Ivshin, V. A. 1999. Oceanographic Conditions of the Barents Sea and their Influence on the Survival and Development of Young Northeast Arctic Cod. PINRO Press, Murmansk. 88 pp. (In Russian.)

Ozhigin, V. K., Yaragina, N. A., Tretyak, V. L., and Ivshin, V. A. 1996. Growth of Arcto-Norwegian Cod. PINRO Press, Murmansk. 60 pp. (In Russian.)

Ponomarenko, I. Y. 1984. Survival of bottom-dwelling young cod in the Barents Sea and the factors determining it. *In* Reproduction and Recruitment of Arctic Cod, pp. 213–229. Ed. by O. R. Godoe and S. Tilseth. Proceedings of the Soviet–Norwegian Symposium, Leningrad, 26–30 September 1983. Institute of Marine Research, Bergen.

Ponomarenko, I. Y. 1996. The development of year-classes and role of environment. Abundance dynamics. *In* The Barents Sea Cod (Biological and Fisheries Outline), pp. 157–199. PINRO Press, Murmansk. (In Russian.)

Randa, K. 1984. Abundance and distribution of 0-group Arcto-Norwegian cod and haddock 1965–1982. *In* Reproduction and Recruitment of Arctic Cod, pp. 192–212. Ed. by O. R. Godø and S. Tilseth. Proceedings of the Soviet–Norwegian Symposium, Leningrad, 26–30 September 1983. Institute of Marine Research, Bergen.

Saetersdal, G., and Loeng, H. 1984. Ecological adaptation of reproduction in Arctic cod. *In* Reproduction and Recruitment of Arctic Cod, pp. 13–35. Ed. by O. R. Godø and S. Tilseth. Proceedings of the Soviet–Norwegian Symposium, Leningrad, 26–30 September 1983. Institute of Marine Research, Bergen.

Sinclair, M., and Tremblay, M. J. 1984. Timing of spawning of Atlantic herring (*Clupea harengus harengus*) populations and the match/mismatch theory. Canadian Journal of Fisheries and Aquatic Sciences, 41: 1055–1065.

Skjoldal, H.-R., Hassel, A., Rey, F., and Loeng, H. 1987. Spring phytoplankton and zooplankton reproduction in the central Barents Sea in the period 1979–1984. *In* The Effect of Oceanographic Conditions on Distribution and Population Dynamics of Commercial Fish Stocks in the Barents Sea, pp. 59–89. Ed. by H. Loeng. Proceedings of the Third Soviet–Norwegian Symposium, Murmansk, 26–28 May 1986. Institute of Marine Research, Bergen.

Tereshchenko, V. V. 1997. Seasonal and year-to-year variation in temperature and salinity of the main currents along the Kola section in the Barents Sea. PINRO Press, Murmansk. 71 pp. (In Russian.)

Titov, O. V. 1999. Long-term cyclic succession of the Barents Sea ecosystem and prognostication of recruitment of commercial fish population. ICES CM 1999/O: 01. 20 pp.

Titov, O. V. 2001a. Long-term variations of hydrochemical parameters along the Kola Section as indicators of variability in the Barents Sea ecosystem. Okeanologiya, 41: 518–526. (In Russian.)

Titov, O. V. 2001b. If the natural eutrophication of the Barents Sea is possible? ICES CM 2001/S: 11. 19 pp.

Ushakov, N. G., and Ozhigin, V. K. 1987. The abundance of year classes of the Barents Sea capelin and peculiarities of the distribution of the young in relation to hydrographic conditions. *In* The Effect of Oceanographic Conditions on Distribution and Population Dynamics of Commercial Fish Stocks in the Barents Sea, pp. 159–167. Ed. by H. Loeng. Proceedings of the Third Soviet–Norwegian Symposium, Murmansk, 26–28 May 1986. Institute of Marine Research, Bergen.

ICES Marine Science Symposia, 219: 294–306. 2003

Fish stock development in the Central Baltic Sea (1974–1999) in relation to variability in the environment

Friedrich W. Köster, Christian Möllmann, Stefan Neuenfeldt, Morten Vinther, Michael A. St. John, Jonna Tomkiewicz, Rüdiger Voss, Hans-Harald Hinrichsen, Brian MacKenzie, Gerd Kraus, and Dietrich Schnack

Köster, F. W., Möllmann, C., Neuenfeldt, S., Vinther, M., St. John, M. A., Tomkiewicz, J., Voss, R., Hinrichsen H.-H., MacKenzie, B., Kraus, G., and Schnack, D. 2003. Fish stock development in the Central Baltic Sea (1974–1999) in relation to variability in the environment. – ICES Marine Science Symposia, 219: 294–306.

Cod, sprat, and herring are the commercially most important fish species in the Central Baltic Sea. In the present study, dynamics of stock abundance and biomass of these species were reconstructed using Multispecies Virtual Population Analysis. The cod stock declined from an historic high during the early 1980s to its lowest level on record at the beginning of the 1990s, showing no sign of recovery afterwards. The sprat stock size increased to a historic high level concurrently, while herring abundance was slightly reduced. However, a substantial reduction in herring weight at age resulted in a continuous decline of the total biomass from the early 1980s. A review of recruitment processes influenced by the variable physical environment was performed for cod and sprat, i.e. the species most intensively studied and showing the largest variability in stock sizes. The most important processes are (i) egg production in dependence of ambient hydrographic conditions and food availability, (ii) egg developmental success in relation to oxygen concentration and temperature at depths of incubation, (iii) egg predation by clupeids dependent on predator–prey overlap, (iv) larval development in relation to hydrographic processes and food availability, and (v) predation on juveniles. All the above processes negatively affected the cod population, while the sprat stock benefited from them, despite a developing industrial fishery, resulting in a regime shift from a cod to a sprat dominated system in the Central Baltic.

Keywords: Baltic Sea, environmental variability, fish stock development, regime shift, reproductive success, species interaction.

F. W. Köster[1], C. Möllmann, R. Voss, H.-H. Hinrichsen, G. Kraus, and D. Schnack: Institute of Marine Sciences, Duesternbrooker Weg 20, D-24105 Kiel, Germany [tel: +49 431 600 4557; fax: +49 600 1515; e-mail: fkoester@ifm.uni-kiel.de; cmoellmann@ifm.uni-kiel.de; rvoss@ifm.uni-kiel.de; gkraus@ifm.uni-kiel.de; hhinrichsen@ifm.uni-kiel.de; dschnack@ifm.uni-kiel.de]. S. Neuenfeldt, M. Vinther, and J. Tomkiewicz[2]: Danish Institute for Fisheries Research, Charlottenlund Castle, DK-2920 Charlottenlund, Denmark [tel: +45 3396 3460; fax: +45 3396 3349; e-mail: stn@dfu.min.dk; mv@dfu.min.dk; jt@dfu.min.dk]. M. A. St. John: Institute of Hydrobiology and Fisheries Science, Hamburg University, Olbersweg 24, D-22767 Hamburg, Germany [tel: +49 40 42838 6600; fax: +49 40 42838 6618; e-mail: michael.st.john@uni-hamburg.de]. [1]Present address: Danish Institute for Fisheries Research, Charlottenlund Castle, DK-2920 Charlottenlund, Denmark [tel: +45 3396 3350; fax: +45 3396 3333; e-mail: fwk@dfu.min.dk]. [2]Present address: Institute of Marine Sciences; Duesternbrooker Weg 20, D-24105 Kiel, Germany [tel: +49 431 600 4569; fax: +49 600 1515; e-mail: jtomkiewicz@ifm.uni-kiel]

Introduction

The Baltic Sea is characterized by large horizontal and vertical hydrographic gradients which have significant influence on the spatial distribution and regional community structure of the fish species as well as their zooplankton and benthic prey (Arndt, 1989). As is typical for estuaries, marine and freshwater organisms are found in a regional succession with species-specific ranges of distribution. Depending on their preferences and tolerances for salinity, oxygen, and temperature, most species in the Baltic

approach the limits of their general distribution. Hence, they show an increased vulnerability and stock size variability related to changes in the environment which potentially affect the fishery.

The fish community in the open sea areas of the Baltic can be characterized by three dominant species, i.e. cod (*Gadus morhua callarias* L.), sprat (*Sprattus sprattus* L.), and herring (*Clupea harengus menbras* L.), sustaining more than 95% of the commercial catch (Sparholt, 1994). Throughout the past two decades, the cod stock declined from an historic high (early 1980s) to its lowest level on record (beginning of the 1990s), hardly recovering afterwards (ICES, 2001a). This stock development was caused by a combination of recruitment failure and high fishing intensity (Bagge *et al.*, 1994). The decline of this top predator in the system resulted in a release in predation pressure on sprat (Sparholt, 1994), and in combination with high reproductive success and relatively low fishing mortalities caused a pronounced increase in sprat stock size (Parmanne *et al.*, 1994; Köster *et al.*, 2001a). Both cod and sprat aggregate in deep Baltic basins to spawn, and historically their spawning times overlap (Bagge *et al.*, 1994; Parmanne *et al.*, 1994). Nevertheless, their reproductive success appears to be out of phase and largely independent of their spawning stock size, suggesting that environmental processes significantly affect recruitment success (e.g. Köster *et al.*, 2002). The population development of the other abundant clupeid species in the Baltic, herring, seems to be more stable and independent of the cod stock, because only juvenile herring are preyed upon intensively by cod (Parmanne *et al.*, 1994).

In the present study, we reconstructed the stock abundance and biomass of cod, sprat, and herring in the Central Baltic Sea using Multispecies Virtual Population Analysis (MSVPA). Further, we reviewed recruitment processes, especially those possibly influenced by the variable physical environment. In this review, we concentrated on cod and sprat as both species show high contrast in stock development and detailed information on processes affecting their reproductive success has accumulated throughout the 1990s.

Although not all processes are completely understood and quantified yet, they explain most recent cod and sprat stock trends. Based on this information, we describe how these processes resulted in a regime shift from a cod to a sprat-dominated system in the Central Baltic.

As fisheries also have a pronounced impact on the population dynamics of both species, information on the development of the fishing intensity is given. However, the present study does not intend to give a comprehensive overview of interrelationships between hydrographic conditions, fisheries actions, and ultimately stock dynamics, although this is a potentially rewarding research area.

Material and methods

The MSVPA incorporates cod as the top predator in the system and cod, sprat, and herring as prey (Sparholt, 1994). This allows quantification of predation on juveniles and the determination of pre-recruit abundance not available from standard assessment (ICES, 2001a; Köster *et al.*, 2001a).

The stock units utilized in the present MSVPA for the Central Baltic are: cod and herring in ICES Subdivisions 25–29 and 32 and sprat in Subdivisions 25–32 (Figure 1). As the sprat population in Subdivisions 30 and 31 is extremely low (ICES, 1999a), the MSVPA derived stock estimates refer in principal also to Subdivisions 25–29 and 32.

In the present analysis, the stocks are composed of age groups 0 to 7+ for cod, 0 to 9+ for herring, and 0 to 7 for sprat, with the + indicating the oldest category included – age 7 and older for cod and age 9 and older for herring. Quarterly catch-at-age in numbers and weight-at-age in the catch were revised by ICES (1999a) for the years 1977–1997 and updated for the period 1976 and 1998–2000 by ICES (2001a). Weight-at-age in the catch was assumed to be equal to the weight-at-age in the stock, exceptions being age groups 0 to 2 for cod. Here, because of size selection by commercial gears, period-specific (before 1989 and after 1990) average weights derived from trawl surveys and compiled by ICES (1999a) were applied.

To identify the spawning component of the cod stock, existing maturity estimates were employed as averages over the periods 1980–1984 (applied also before 1980), 1985–1989, and 1990–1994, year-specific data for 1995–1997 for combined sexes as presented in ICES (1999a), updated with data for 1998 and 1999 according to ICES (1999b and 2000). For 2000 an average over the years 1997–1999 was utilized. Maturity ogives of sprat and herring were used as given in ICES (1996), being constant over time and areas.

Quarterly relative diet compositions and individual food rations are based on cod stomach content data covering the period 1977–1993 according to Subdivision (ICES, 1997a). The Subdivision-specific data were averaged applying relative distribution patterns obtained from trawl surveys as spatial weights (ICES, 1997a) kept constant for 1996–2000. The quarterly consumption rates were revised based on re-calculated ambient temperatures (ICES, 2001b) according to the procedure outlined by ICES (1999a). The consumption model in use corresponds to the model applied in the North Sea (ICES, 1997b), based on a general model of gastric evacuation, considering actual environmental temperatures and predator weights as additional variables (Temming and Herrmann, 2002). As stomach content data are available for most of the quarters

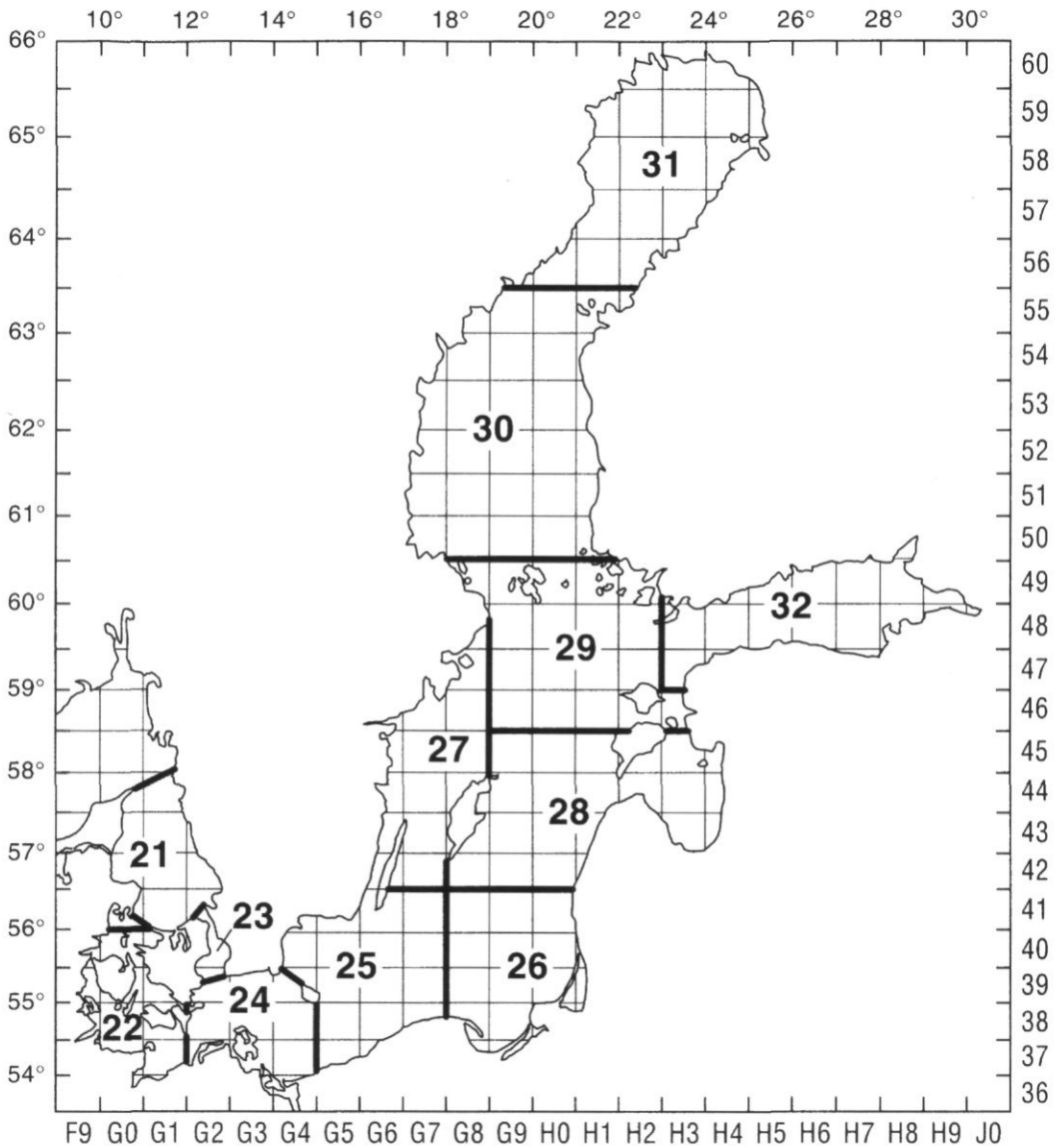


Figure 1. Study area of the Baltic with ICES Subdivisions (numbers).

and years covered by the present MSVPA, consumption rates were computed for every predator age group, quarter, and year. Missing quarters/years, i.e. also the years 1976–1977 and 1994–2000 were predicted by a multiple linear regression model with Subdivision, year, and predator weight as independent variables (ICES, 1999a).

The residual natural mortality rate was assumed to be 0.2 per year for all three species, equally distributed over quarters, corresponding to standard MSVPA runs in the Baltic (Sparholt, 1991). Suitability coefficients of prey species age groups as food of specific predator age groups (Sparre, 1991) were estimated according to the standard suitability sub-model implemented in the Baltic MSVPA, with the biomass of other food set constant over time, corresponding to earlier MSVPA runs (ICES, 1997a).

The tuning of the MSVPAs was performed with the new 4M-programme routine iteratively running XSAs (Extended Survivor Analysis) and MSVPAs (Vinther, 2001). Abundance indices utilized for tuning originated from the international bottom trawl survey directed to cod, performed annually in February/March (Sparholt and Tomkiewicz, 2000) and the international hydroacoustic survey directed to herring and sprat, conducted in September/October (ICES, 2001a). XSA settings were identical to those used in the standard assessment (ICES, 2001a). Fishing mortalities in the terminal year for

the 0-groups and for 1-group cod were not estimated in the XSA tuning, and values were tuned to reach abundances close to the average values estimated in period 1995 to 1999.

Results

Stock abundance

The stock abundance of cod in the Central Baltic is characterized by a pronounced increase from 1976 to 1980, remaining high until 1983, afterwards steadily declining to its lowest level on record in 1991, and since then has been close to the historic minimum (Figure 2). The estimated stock size of sprat shows a reverse trend, with a decline from 1975 to 1980, low levels until 1988, followed by a pronounced increase to the highest stock size on record in 1996 and a decline in most recent years. In contrast, the herring stock appears to be fairly stable, with deviations of less than 25% around the long-term mean and a slight downward trend in most recent years.

Spawning stock biomass

Spawning stock biomass (SSB) of cod and sprat follow similar time trends as the abundance; however, some deviations are apparent (Figures 3A, B). Cod SSB remained longer on a high level until 1985 and recovered to a certain degree after the minimum in early 1990s, which is barely noticeable from abundance estimates. Sprat SSB declined by 26% from 1997 to 1999 (Figure 3B), while abundance showed a more pronounced decline by nearly 40%. In contrast, SSB of herring declined by around 50% from the early 1980s (Figure 3C), a trend which is far less pronounced in stock abundance.

Recruitment

Examining the effect of the spawning stock on recruitment revealed a high reproductive success in cod at intermediate SSB values in the 1970s and declining reproductive success at historically high spawning stocks from 1981 to 1985 (Figure 3A). Sprat recruitment showed a positive development from the mid-1980s to the mid-1990s, with high fluctuations in most recent years, virtually independent of the SSB (Figure 3B). For herring, an overall trend of declining recruitment with declining SSB is indicated, however, with considerable inter-annual variability (Figure 3C).

Weight-at-age

Concurrent with the decline in stock size of cod, there was an increase in weight-at-age 3 and older

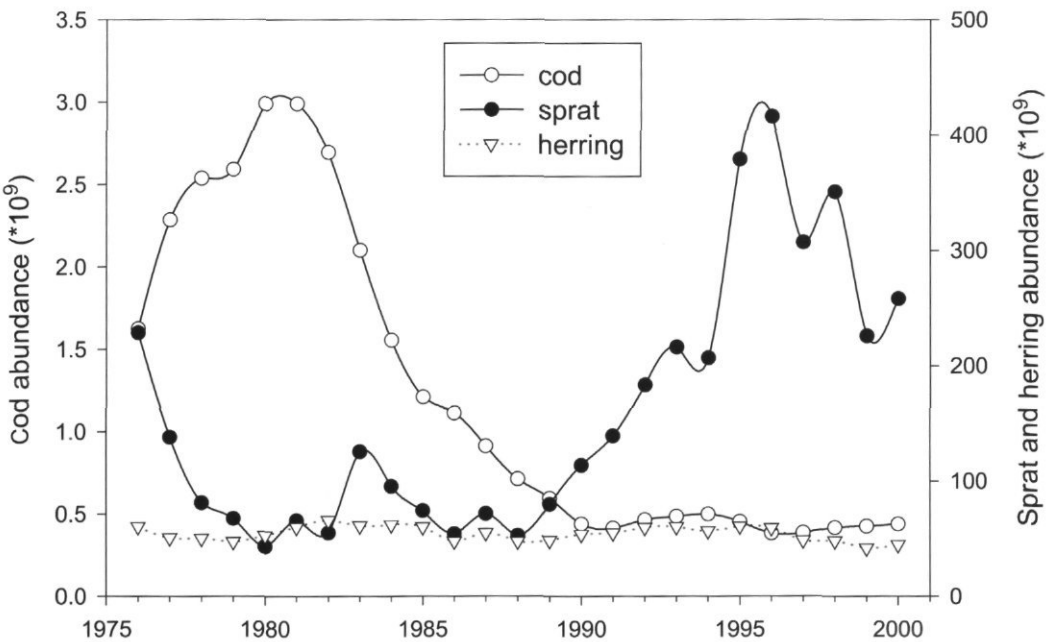


Figure 2. Population sizes of cod, sprat, and herring (age group 1 and older, beginning of the year) in the Central Baltic.

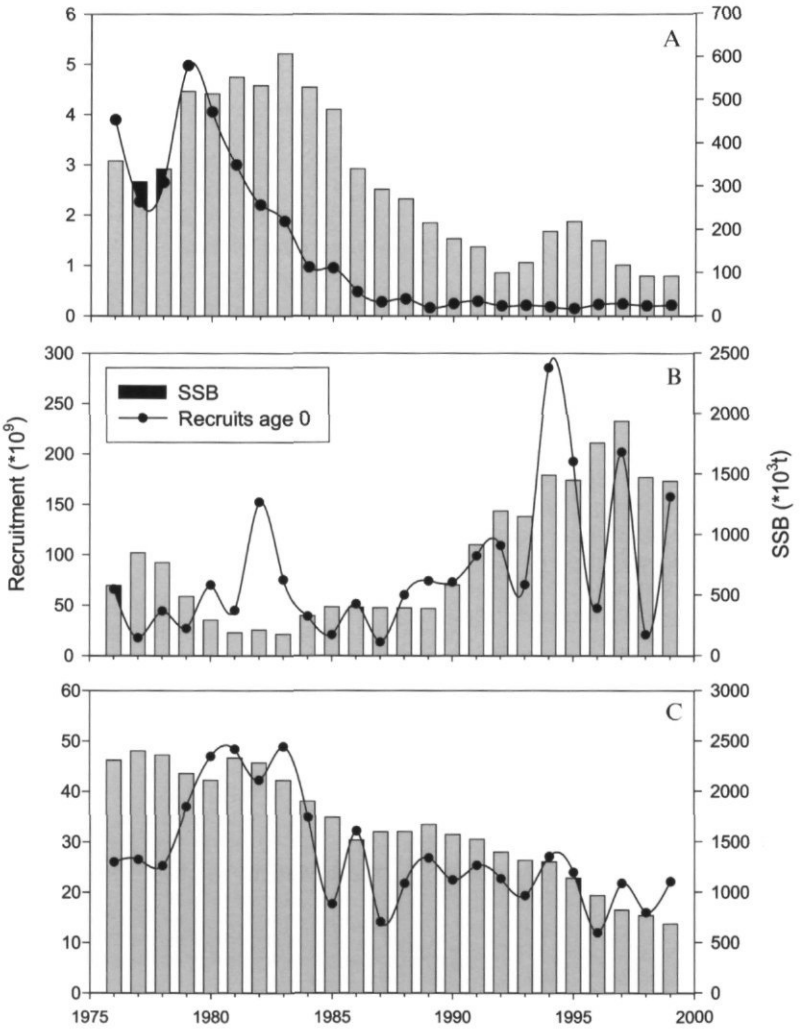


Figure 3. Spawning stock biomass (SSB) (2nd quarter) and recruitment (age group 0) of cod (A), sprat (B), and herring (C) in the Central Baltic.

(Figure 4A). Average weight-at-age of sprat showed a substantial decline from 1990 to 1997 and a reverse trend in most recent years (Figure 4B) also concurrent with the opposite trend in stock abundance. Independent of stock size, the weight-at-age of herring declined from 1983 to 1996 by more than 50% (Figure 4C).

Predation mortality

A pronounced time trend in the estimated mortality of cod through cannibalism is apparent (Figure 5A), with increasing predation mortalities until 1983 and a decline until 1991, being stable and low afterwards. Age-specific differences in predation mortality are obvious, with cannibalism rates on 0-group being considerably higher (instantaneous mortality due to predation reaching maximum values >1.0) than on 1-group cod (maximum 0.61), especially when considering that the mortality rates on 0-group refer only to a half-year period. Predation on 2-group cod was in general low, i.e. less than 50% of the applied residual mortality of 0.2. 0-group sprat do not suffer from high predation pressure, while age-group 1 (maximum around 1.1) and also, to a lesser degree, adult sprat do (maximum 0.51). Intense predation pressure on sprat occurred in 1979–1983, with a subsequent decrease until 1991 driven by the decline in predator population size (Figure 5B). The time trend in predation mortality of herring is similar to that of sprat; however, the absolute values are lower for age-group 1 (in maximum 0.66) and especially for adult herring (in maximum 0.17), while 0-group mortality rates are similar in both species (Figure 5C).

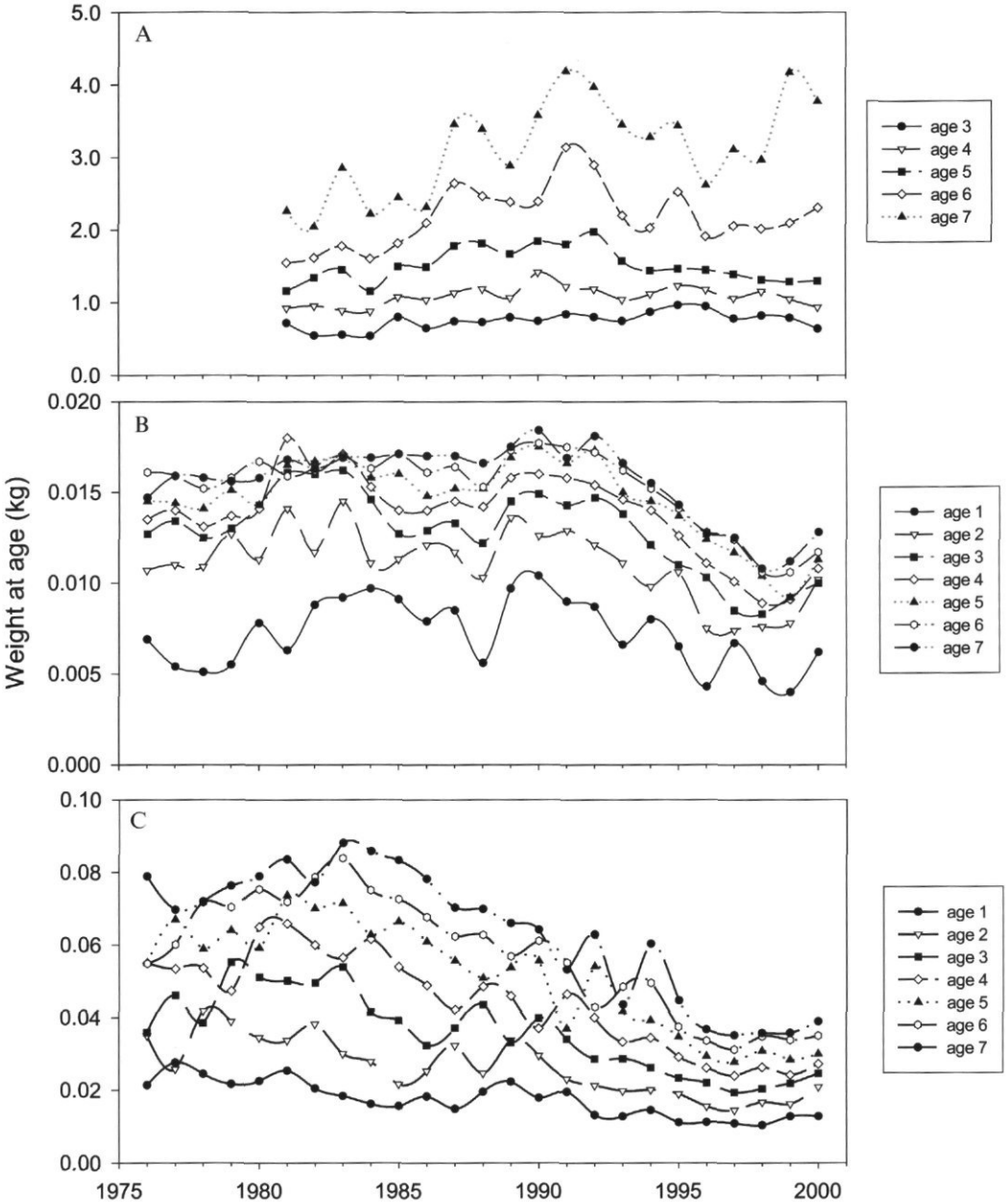


Figure 4. Average weight-at-age (beginning of the year) of cod (A), sprat (B), and herring (C) in the Central Baltic.

Fishing mortality

The average fishing mortality of cod age groups 4–7 increased from 0.4 in 1979 to 1.4 in 1991 and decreased sharply to the lowest level on record in the following two years (Figure 6A). This reduction is caused by rigid enforcement of management measures, i.e. a TAC reduction for the entire Baltic from 171×10^3 t in 1991 to 100×10^3 t in 1992 and 40×10^3 t in 1993. Afterwards, a pronounced increase in fishing mortalities to the original high level is indicated due to increasing fishing effort (ICES, 1998) at declining stock size. The fishing mortality of sprat and herring were substantially lower throughout the entire time period, i.e. ranging from 0.09 to 0.48 with an increasing trend since the early 1990s.

The corresponding yield to biomass ratios followed in general the development of the fishing mortality, with a less steep decline for cod at the beginning of the 1990s (Figure 6B). On average, 41% of the cod biomass available at the beginning of the year was removed by the fishery, ranging between 22% in 1978 and 64% in 1991. In sprat and

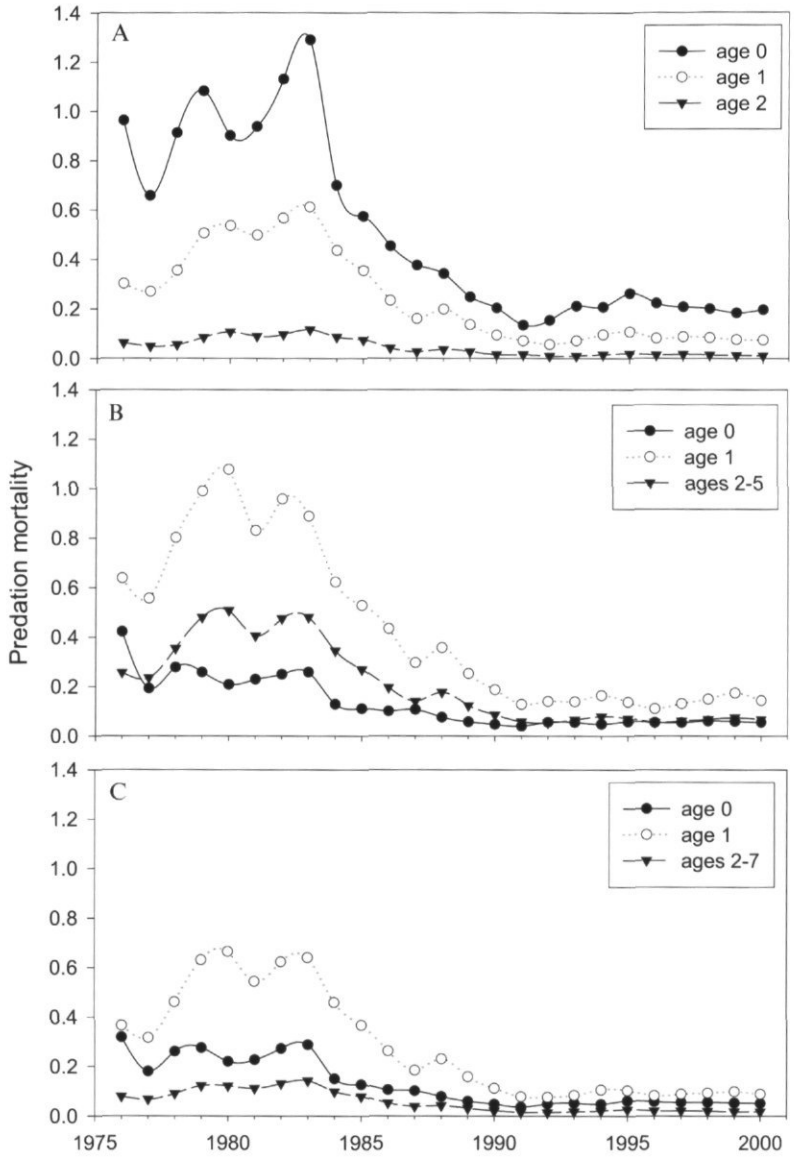


Figure 5. Annual predation mortality rates of cod age group 0, 1, and 2 (A), sprat age group 0, 1, and 2–5 (B), herring 0, 1, and 2–7 (C) in the Central Baltic. Note predation mortality of 0-group refers to 3rd and 4th quarters.

herring the corresponding removals are on average 11% and 16%, respectively, with higher variability in sprat.

Discussion

Validation of stock trends

Stock development trends derived by the multispecies and the standard stock assessment (ICES, 2001a) are similar, with the MSVPA additionally covering younger age groups (i.e. age group 0 and for cod also age group 1). Revision of the quarterly consumption rates of cod did not change this feature. The reconstructed stock abundances are furthermore in accordance with trawl and hydroacoustic surveys utilized for tuning of the MSVPA (Vinther, 2001). Deviations between time trends in stock abundance and spawning stock biomass can be explained in all three species by changes in weight-at-age, and in cod additionally by an earlier maturation in the 1990s compared to the 1980s (Tomkiewicz *et al.*, 1997).

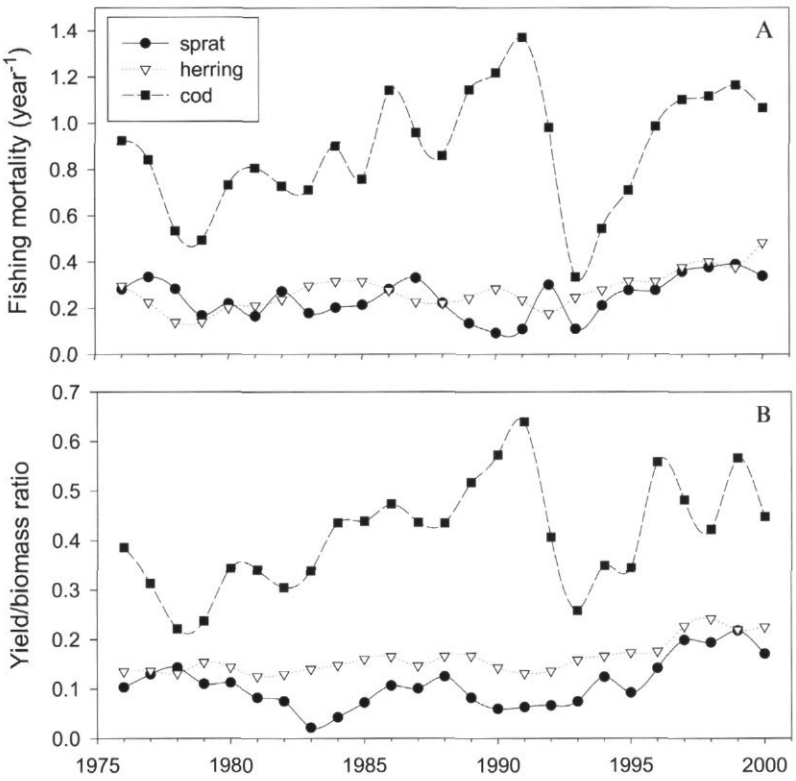


Figure 6. Annual average fishing mortality rates of sprat and herring age groups 3–5 and cod age groups 4–7 (A) and yield per biomass ratio of the three species in the Central Baltic (B).

Egg production

Timing and duration of spawning is potentially an important source of variability in the reproductive success of Baltic fish stocks owing to seasonal changes in: (i) environmental parameters (MacKenzie *et al.*, 1996), (ii) spatial overlap of early life stages with predators (Köster and Möllmann, 2000a), and (iii) transport of larvae into areas with sufficient food supply (Hinrichsen *et al.*, 2001 and 2002a). Duration of the spawning activity of the cod stock depends on its size structure and sex composition; however, the timing of peak spawning is hardly affected by these factors (Tomkiewicz and Köster, 1999). Consequently, the observed shift in the main spawning time of cod from May/June to July/August at the beginning of the 1990s is likely to be caused by other processes as well (Wieland *et al.*, 2000). Potential candidates include removal of early spawners by the fishery, which is mainly directed to pre-spawning and early spawning concentrations (ICES, 1999b) and a coupling to ambient temperature (Wieland *et al.*, 2000).

Age-specific sex ratios and maturity ogives of cod derived from the International Baltic Trawl Survey (Tomkiewicz *et al.*, 1997; STORE, 2001) showed: (i) a dominance of females with increasing age, (ii) that males generally mature at a younger age than females, (iii) that the age at which sexual maturation occurs increases with distance from the Kattegat and the Danish Straits, as the transition area between the North Sea and the Baltic, and (iv) that maturity-at-age shows significant variability between different time periods. Thus, the quantity of the egg production of Baltic cod depends on the age structure of the stock, as well as the location and time period. Variability in maturation appears to be coupled to growth rates, reflected in decreasing age at sexual maturity concurrent with increasing weight-at-age (STORE, 2001).

An analysis of individual Baltic cod fecundity revealed that the relative fecundity, i.e. the total number of developing oocytes per unit of body weight, is independent of body size (Kraus *et al.*, 2000). Relative fecundity varied significantly between years, but not between spawning areas nor between different months within one spawning season (Kraus *et al.*, 2000). On an individual level, a weak impact of the nutritional status of the female on the relative fecundity was detected, while on a population level a clear dependence on food availability has been shown (Kraus *et al.*, 2002). Inclusion of temperature improved the relationship further, but overall had a limited influence on

relative fecundity. In conclusion, an increase in weight-at-age, a decline in size/age of attaining maturity and an increasing individual fecundity with decreasing stock size and increasing prey availability has had a compensating effect on the total egg production by the stock.

In Baltic cod a significant relationship exists between the potential egg production by the spawning stock and the realized egg production as determined from egg surveys (Köster *et al.*, 2002). Apart from problems in parametrization of each of the input data series, remaining variability may be related to (i) atresia, i.e. resorption of oocytes before spawning, due to unfavourable environmental conditions during spawning, as demonstrated for Atlantic cod (Kjesbu *et al.*, 1991), (ii) variable fertilization success in relation to salinity changes (Westin and Nissling, 1991), and (iii) differences in egg mortality already in the first developmental stage.

A number of investigations on different species, including cod, suggest that egg and larval viability is positively related to egg size (see Trippel *et al.* (1997) for review), and that egg size varies according to female age/size and condition as well as spawning experience. For Baltic cod, significant positive relationships between (i) egg size and female size, (ii) egg size and larval size/growth, (iii) egg size and survival during the yolk sac stage, and (iv) egg size and egg buoyancy, have been established (Nissling *et al.*, 1998; Vallin and Nissling, 2000). This implies higher egg and larval survival for offspring originating from large females, especially as larger and more buoyant eggs have a higher chance of avoiding oxygen-depleted bottom water layers. Consequently, the reduction in the share of older females in the spawning stock from the mid-1980s to the early 1990s (Wieland *et al.*, 2000), caused by heavy fishing pressure, has had a negative effect on the reproductive success of the Central Baltic cod stock (Vallin and Nissling, 2000).

The temporal pattern of sprat spawning with peak spawning in May has remained relatively stable throughout the 1990s (STORE, 2001). Consequently, in the 1990s sprat spawned significantly earlier than cod, thus encountering different environmental conditions and reducing the temporal overlap with their predator in spawning areas. This may explain deviations in reproductive success of both species.

Available data on sexual maturity-at-age indicate significant interannual variability in proportions of sprat being sexually mature at age 1, which was earlier related to winter temperature (Elwertowski, 1960). Furthermore, the relative batch fecundity shows a significant intra- and interannual variability (Alekseeva *et al.*, 1997; STORE, 2001). An existing significant relationship between SSB and realized egg production can be improved by incorporating temperature in the intermediate water in May and growth anomaly through the preceding three-quarters of the year as a measure of the nutritional status of the adults (Köster *et al.*, 2002). Low winter temperature, reflected in low intermediate water temperature in May, may be responsible for changes in the nutritional condition and growth of sprat (e.g. Elwertowski, 1960) and by this reducing the individual egg production or may as well directly affect batch fecundity and numbers of batches spawned (Petrowa, 1960).

The decline in apparent growth rate of sprat appears to be related to a reduced food availability of calanoid copepods per individual sprat, mainly caused by a reduction in abundance of the largest copepod species *Pseudocalanus elongatus* (Möllmann *et al.*, 2003) and a concurrent increase in stock size of sprat. This limitation in food availability may have caused a decrease in individual egg production and potentially an increased age of attaining sexual maturation. However, given the high interannual variability in recruitment success in the second half of the 1990s, other variability generating processes appear to be of higher importance for the reproductive success.

Egg developmental success

In the Baltic, fish early life stage survival is known to be highly influenced by hydrographic conditions in the spawning areas (e.g. Bagge *et al.*, 1994; Grauman and Yula, 1989; Plikshs *et al.*, 1993; Parmanne *et al.*, 1994, Wieland *et al.*, 1994). The observation that live cod eggs are only encountered in water layers with oxygen concentrations >2 ml l^{-1} and temperatures >1.5°C, and that a salinity of 11 is necessary for successful fertilization, led to the definition of the so-called reproductive volume (RV), i.e. the water volume sustaining cod egg development (Plikshs *et al.*, 1993). Processes affecting the RV are: (i) the magnitude of inflows of saline oxygenated water from the western Baltic (MacKenzie *et al.*, 2000), (ii) temperature regimes in the western Baltic during winter, which affect the oxygen solubility prior to advection (Hinrichsen *et al.*, 2002b), (iii) river run-off (Hinrichsen *et al.*, 2002b) and (iv) oxygen consumption by biological processes (Hansson and Rudstam, 1990). Resolving the potential egg production by cod spatially showed that in some years a substantial fraction of the total annual egg production has been unsuccessful (in terms of recruit production), because eggs were exposed to extremely low oxygen concentrations in eastern spawning areas (Köster *et al.*, 2001b). This mismatch in egg production and suitable environmental conditions for egg development explains the drastic decline in reproductive success of cod from 1981 to 1985 despite high egg production.

Due to differences in egg specific gravity, egg development of cod and sprat occurs at different depths. Whereas cod eggs are neutrally buoyant at salinities of 12–17 (Nissling *et al.*, 1994), the range for sprat eggs is 7–13 (Grauman, 1965), i.e. the majority of sprat eggs occur shallower than cod. This implies that sprat egg survival is less affected by poor oxygen conditions than the survival of cod eggs. As sprat eggs occur at depths where the water temperature is affected by winter cooling (Wieland and Zuzarte, 1991), egg and larval development may be influenced by extreme water temperatures. In fact, weak year classes of Baltic sprat have been associated with severe winters accompanied by low water temperatures during peak spawning (e.g. Kalejs and Ojaveer, 1989; Grauman and Yula, 1989). A significant impact of temperature on egg developmental success has been found in the North Sea (Thompson *et al.*, 1981) and confirmed for the Baltic (Nissling, 2002), with temperatures below 4°C significantly reducing egg survival. As these temperatures occur regularly in the intermediate water layer, an effect on egg survival especially after severe winters is expected. In this respect, the absence of severe winters since 1986/1987 indicates favourable thermal conditions for sprat egg survival and most likely contributes to the generally high recruitment.

Egg predation

Substantial predation on cod eggs by clupeids has been described for the major spawning area of the Baltic cod stock, i.e. the Bornholm Basin. Egg predation is most intense at the beginning of the cod spawning season, with sprat being the major predator (Köster and Möllmann, 2000a). At this time spring spawning herring concentrate in their coastal spawning areas and do not contribute to the predation-induced egg mortality of cod. Sprat spawn in the Bornholm Basin from March to July, thus concentrating in cod spawning areas at times of high cod egg abundance. After cessation of spawning, the part of the sprat population leaves, resulting in a reduced predation pressure on cod eggs. With the return of the herring from the coastal areas to their feeding grounds in the Bornholm Basin, the predation on cod eggs by herring increases to considerable levels (Köster and Möllmann, 2000a).

The shift of cod peak spawning time from spring to summer (Wieland *et al.*, 2000) resulted in a decreasing predation pressure on cod eggs by sprat because of a reduced temporal overlap between predator and prey. Additionally, a decline in individual sprat predation on cod eggs was observed from 1993 to 1996, despite relatively high cod egg abundance in the plankton. This is partly explainable by a reduced vertical overlap between predator and prey. Owing to the increased salinity after the 1993 major Baltic inflow (Matthäus and Lass, 1995), cod eggs were floating in shallower water layers, while clupeids occurred deeper, because of enhanced oxygen concentration in the bottom water (Köster and Möllmann, 2000a) Thus, predation pressure on cod eggs appears to be higher in stagnation periods, characterized by the absence of inflows of oxygenated saline water from western neighbouring Baltic basins.

Egg cannibalism was found to be an important source of sprat egg mortality in the Bornholm Basin (Köster and Möllmann, 2000b), but appears to be less important in the more eastern areas. This has been explained by a more limited vertical overlap between predator and prey in these areas (STORE, 2001).

Larval development

Behaviour studies demonstrated that cod larvae exposed to oxygen concentration below 2 ml l^{-1} for 2 days were mostly inactive or moribund (Nissling, 1994) and that egg incubation at oxygen saturations of 40% or lower impacts on larval activity as well (Rohlf, 1999). Furthermore, Rohlf revealed that vertical migration into upper water layers does not start before day 4 after hatching. Hence, a significant impact on larval survival of the environment within and below the halocline can be expected. In an attempt to explain the variability of late cod egg production and larval abundance in the Bornholm Basin, Köster *et al.* (2001b) tested various environmental variables, i.e. the oxygen concentration in and below the halocline, temperature in the intermediate water, and wind-driven transport, for their explanatory power. However, these authors were unable to explain the major part of the variability in larval abundance. This led to the conclusion that either other factors influence the survival until the larval stage, or the variability in larval abundance (integrated over all developmental stages) is too high for a major impact of the tested factors to be detected.

For sprat, an impact of the temperature in the intermediate water on larval survival has been described by Köster *et al.* (2002). An increased larval abundance at above average spring temperatures has been explained earlier by the positive effect of higher temperature on the dynamics of the copepod *Temora longicornis*, which is the main prey species of sprat larvae (Grauman and Yula, 1989; Kalejs and Ojaveer, 1989). Consequently, warm winters since the late 1980s favoured sprat egg production and survival, as well as larval growth and survival.

The effect of food availability on growth and survival of cod larvae has been investigated using a coupled hydro/trophodynamic individual-based

model (IBM) (Hinrichsen *et al.*, 2002a). Model results suggest the necessity of co-occurrence of peak prey and larval abundances as well as favourable oceanographic conditions for high survival rates. The strong decline of the *Pseudocalanus elongatus* stock during the past two decades as a result of low salinities (Möllmann *et al.*, 2000) meant that early cod larvae changed from a non-food limited to a food limited state. If *P. elongatus* nauplii are present in the model, high survival rates occurred during spring and early summer, whereas omitting *P. elongatus* resulted in high mortality rates and only late hatched larvae survived (Hinrichsen *et al.*, 2002a). Thus, low *P. elongatus* availability may have contributed to the reduced recruitment of cod since the late 1980s.

Also, sprat larvae may face food limitations; however, they usually drift out of the spawning areas more rapidly than cod larvae due to their residing in shallower depths (e.g. Wieland and Zuzarte, 1991). Thus, rapid drift to coastal water areas with higher abundance of *Acartia* spp. and *Temora longicornis* nauplii being their preferred food items (Voss and Köster, 2002) appears to be the normal case.

Predation on juveniles

Juvenile cod suffer from cannibalism (Sparholt, 1994; Neuenfeldt and Köster, 2000). As in other cod stocks, the intensity of cannibalism is related to predator abundance, but also to the juvenile concentrations, which depend upon the habitat volume occupied and the overall abundance of cod (Anderson and Gregory, 2000). Apart from medium- to long-term distribution changes, interannual variability in cannibalism may be influenced by changing hydrographic conditions as well (Uzars and Plikshs, 2000). For example, low oxygen concentration in the deep Baltic basins may force the adults into shallower slope areas and low temperature in shallow waters may force juveniles into deeper water, by this increasing the spatial overlap between predator and prey and hence cannibalism. This suggests that the process is most pronounced in stagnation periods, especially after cold winters.

Predation on 0-group sprat by cod occurs regularly, although predation mortality rates from MSVPA are significantly lower than for 1-group sprat. The intensity of the predation is most likely modulated also by hydrographic conditions and by species-specific preferences and tolerance levels to hydrographic variables, resulting in variable potential predator/prey encounter volumes (Neuenfeldt, 2002).

Regime shift from a cod-dominated to a sprat-dominated system

As seen from the results of the MSVPA, the upper trophic levels of the Central Baltic changed during the past 20 years from a cod- to a sprat-dominated system (Figure 7). The decline of the cod stock was caused by a continued high fishing pressure and a concurrent recruitment failure, which according to our review was mainly driven by: (i) anoxic conditions in deep water layers of spawning sites causing high egg mortalities, (ii) high egg predation by clupeid predators, (iii) reduced larval survival due to the decrease in abundance of the main food

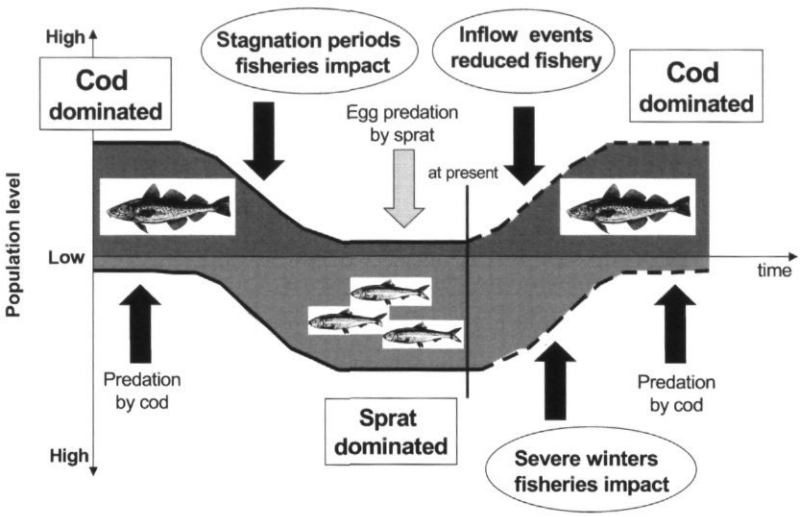


Figure 7. Schematic presentation of processes stabilizing a cod-dominated or sprat-dominated system in the Central Baltic. Note the vertical line represents the situation in the 2nd half of the 1990s with the regime shift taking place in late 1980s and early 1990s.

item *P. elongatus*, and (iv) high juvenile cannibalism at high stock density. The intensity and significance of all these processes are in one way or the other steered by the hydrographic conditions, which in the 1990s were characterized by low salinity due to a lack of inflow of highly saline water from the North Sea, Skagerrak, and Kattegat, as well as increased river run-off, but also by warmer thermal conditions. An increasing fishing pressure accelerated the decline of the cod stock, with current exploitation levels being still on a very high level. The decline of the cod stock released sprat from predation pressure, which in combination with high reproductive success, due to in general favourable temperature conditions enhancing egg and larval survival, resulted in exceptionally high sprat stock sizes in the 1990s. Indications for compensatory processes in growth, maturation, and individual egg production exist for both species; however, they appear to have limited impact on their stock dynamics.

As a result of these processes, the dominance of one or either predator may stabilize a cod-dominated or a sprat-dominated system. Destabilization of the sprat-dominated system may be caused either by unfavourable hydrographic conditions for reproduction, e.g. low water temperatures in spring following severe winters and subsequent recruitment failures of sprat, or high mortalities caused by the fishery, with concurrent low fishing pressure on cod and the presence of inflow events into the deep Baltic basins.

Acknowledgements

All participants of the Baltic STORE project have contributed their experience and knowledge to the present review and this is gratefully acknowledged. We thank Drs. Eero Aro and Ken Drinkwater for their valuable comments and improvements to the manuscript. The present study was carried out with financial support from the Commission of the European Communities, Agriculture and Fisheries (FAIR) specific RTD programme: CT98-3959 "STORE" as a contribution to CT97-3805 "SAP". It does not necessarily reflect the view of the Commission and in no way anticipates the Commission's future policy in this area.

References

Alekseeva, E. I., Baranova, M. M., Dmitrieva, M. A., and Ryazantseva, E. F. 1997. Ovaries maturation, batch eggs forming, batch fecundity and distribution during sex cycle of Baltic sprat *Sprattus sprattus* Balticus. ICES CM 1997/U: 02.

Anderson, J. T., and Gregory, R. S. 2000. Factors regulating survival of northern cod (NAFO 2J3KL) during their first 3 years of life. ICES Journal of Marine Science, 57: 349–359.

Arndt, E. A. 1989. Ecological, physiological, and historical aspects of brackish water fauna distribution. *In* Reproduction, Genetics and Distribution of Marine Organisms, pp. 327–338. Ed. by S. Ryland and A. Tyler. Olsen & Olsen, Fredensborg.

Bagge, O., Thurow, F., Steffensen, E., and Bay, J. 1994. The Baltic cod. Dana, 10: 1–28.

Elwertowski, J. 1960. Biologische Grundlagen der Sprottenfischerei in der westlichen und mittleren Ostsee. Fischerei Forschung, 3: 1–19.

Grauman, G. B. 1965: Some data on the reproduction of sprat in the southern part of the Baltic Sea in the period 1958–1964. ICES CM 1965/Baltic-Belt Seas Committee Paper No. 121.

Grauman, G. B., and Yula, E. 1989. The importance of abiotic and biotic factors in early ontogenesis of cod and sprat. Rapports et Procès-Verbaux des Réunions du Conseil International pour l'Exploration de la Mer, 190: 207–210.

Hansson, S., and Rudstam, L. G. 1990. Eutrophication and Baltic fish communities. Ambio, 19: 123–125.

Hinrichsen, H.-H., St. John, M. A., Aro, E., Grønkjær, P., and Voss, R. 2001. Testing the larval drift hypothesis in the Baltic Sea: retention versus dispersion caused by wind driven circulation. ICES Journal of Marine Science, 58: 973–984.

Hinrichsen, H. H., Möllmann, C., Voss, R., Köster, F. W., and Kornilovs, G. 2002a. Bio-physical modelling of larval Baltic cod (*Gadus morhua*) survival and growth. Canadian Journal of Fisheries and Aquatic Sciences, 59: 1958–1973.

Hinrichsen, H. H., St. John, M. A., Lehmann, A., MacKenzie, B. R., and Köster, F. W. 2002b. Resolving the impact of physical forcing variations on the eastern Baltic cod spawning environment. Journal of Marine Systems, 32: 281–294.

ICES. 1996. Report of the Working Group on Multispecies Assessments of Baltic Fish. ICES CM 1996/Assess: 2.

ICES. 1997a. Report of the Study Group on Multispecies Model Implementation in the Baltic. ICES CM 1997/J: 2.

ICES. 1997b. Report of the Multispecies Working Group. ICES CM 1997/Assess: 16.

ICES. 1998. Report of the Baltic Fisheries Assessment Working Group. ICES CM 1998/ACFM: 16.

ICES. 1999a. Report of the Study Group on Multispecies Model Implementation in the Baltic. ICES CM 1999/H: 5.

ICES. 1999b. Report of the Baltic Fisheries Assessment Working Group. ICES CM 1999/ACFM: 15.

ICES. 2000. Report of the Baltic Fisheries Assessment Working Group. ICES CM 2000/ACFM: 14.

ICES. 2001a. Report of the Baltic Fisheries Assessment Working Group. ICES CM 2001/ACFM: 18.

ICES. 2001b. Report of the Study Group on Multispecies Prediction in the Baltic. ICES CM 2001/H: 4.

Kalejs, M., and Ojaveer, E. 1989. Long-term fluctuations in environmental conditions and fish stocks in the Baltic. Rapports et Procès-Verbaux des Réunions du Conseil International pour l'Exploration de la Mer, 190: 153–158.

Kjesbu, O. S., Klungsoyr, J., Kryvi, H., Witthames, P. R., and Greer Walker, M. 1991. Fecundity, atresia and egg size of captive Atlantic cod (*Gadus morhua*) in relation to proximate body composition. Canadian Journal of Fisheries and Aquatic Sciences, 48: 2333–2343.

Köster, F. W., and Möllmann, C. 2000a. Trophodynamic control by clupeid predators on recruitment success in Baltic cod? ICES Journal of Marine Science, 57: 310–323.

Köster, F. W., and Möllmann, C. 2000b. Egg cannibalism in Baltic sprat *Sprattus sprattus*. Marine Ecology Progress Series, 196: 269–277.

Köster, F. W., Möllmann, C., St. John, M. A., Neuenfeldt, S., Plikshs, M., and Voss, R. 2001a. Developing Baltic cod recruitment models. I: Resolving spatial and temporal

dynamics of spawning stock and recruitment. Canadian Journal of Fisheries and Aquatic Sciences, 58: 1516–1533.

Köster, F. W., Hinrichsen, H.-H., St. John, M. A., Schnack, D., MacKenzie, B. R., Tomkiewicz, J., and Plikshs, M. 2001b. Developing Baltic cod recruitment models. II: Incorporation of environmental variability and species interaction. Canadian Journal of Fisheries and Aquatic Sciences, 58: 1535–1557.

Köster, F. W., Hinrichsen, H.-H., Schnack, D., St. John, M. A., MacKenzie, B. R., Tomkiewicz, J., Möllmann, C., Kraus, G., Plikshs, M., Makarchouk, A., and Aro, E. 2002. Recruitment of Baltic cod and sprat stocks: identification of critical life stages and incorporation of environmental variability into stock-recruitment relationships. Scientia Marina, 67 (Suppl 1): 129–154.

Kraus, G., Müller, A., Trella, K., and Köster, F. W. 2000. Fecundity of Baltic cod: temporal and spatial variation. Journal of Fish Biology, 56: 1327–1341.

Kraus, N., Tomkiewicz, J., and Köster, F. W. 2002. Egg production of Baltic cod in relation to variable sex ratio, maturity and fecundity. Canadian Journal of Fisheries and Aquatic Sciences, 59: 1908–1920.

MacKenzie, B. R., St. John, M. A., and Wieland, K. 1996. Eastern Baltic cod: perspectives from existing data on processes affecting growth and survival of eggs and larvae. Marine Ecology Progress Series, 134: 265–281.

MacKenzie, B. R., Hinrichsen, H.-H., Plikshs, M., Wieland, K., and Zezera, A. S. 2000: Quantifying environmental heterogeneity: estimating the size of habitat for successful cod egg development in the Baltic Sea. Marine Ecology Progress Series, 193: 143–156.

Matthäus, W., and Lass, H. U. 1995. The recent salt inflow into the Baltic Sea. Journal of Physical Oceanography, 25: 280–286.

Möllmann, C., Kornilovs, G., and Sidrevics, L. 2000. Long-term dynamics of main mesozooplankton species in the Central Baltic Sea. Journal of Plankton Research, 22: 2015–2038.

Möllmann, C., Kornilovs, K., Sidrevics, L., and Köster, F. W. 2003. Interannual variability in population biology of calanoid copepods in the Central Baltic Sea. ICES Marine Science Symposia, 219: 220–230. (This volume.)

Neuenfeldt, S. 2002. The influence of distributional overlap of predator (cod, *Gadus morhua*) and prey (herring, *Clupea harengus*) in the Bornholm basin of the Baltic Sea. Fisheries Oceanography, 11: 11–17.

Neuenfeldt, S., and Köster, F. W. 2000. Trophodynamic control on recruitment success: the influence of cannibalism. ICES Journal of Marine Science, 57: 300–309.

Nissling, A. 1994. Survival of eggs and yolk-sac larvae of Baltic cod (*Gadus morhua* L.) at low oxygen levels in different salinites. ICES Marine Science Symposia, 198: 626–631.

Nissling, A. 2002. Effects of temperature on egg and larval survival of cod (*Gadus morhua*) and sprat (*Sprattus sprattus*) in the Baltic Sea: implications for stock development. Hydrobiologica. (In press.)

Nissling, A., Kryvi, H., and Vallin, L. 1994. Variation of egg buoyancy of Baltic cod *Gadus morhua* and its implications for egg survival in prevailing conditions in the Baltic Sea. Marine Ecology Progress Series, 110: 67–74.

Nissling, A., Larsson, R., Vallin, L., and Frohlund, K. 1998. Assessment of egg and larval viability in cod, *Gadus morhua*: methods and results from an experimental study. Fisheries Research, 38: 169–186.

Parmanne, R., Rechlin, O., and Sjöstrand, B. 1994. Status and future of herring and sprat stocks in the Baltic Sea. Dana 10: 29–59.

Petrowa, E. G. 1960. On the fecundity and the maturation of the Baltic sprat. Trudy Vsesojuznyj naucno issledovatelskij. Institut Morskogo Rybnogo Xozjajstva i Okeanografii, 42: 99–108.

Plikshs, M., Kalejs, M., and Grauman, G. 1993. The influence of environmental conditions and spawning stock size on the year-class strength of the eastern Baltic cod. ICES CM 1993/J: 22.

Rohlf, N. 1999. Aktivität und Vertikalwanderung der Larven des Ostseedorsches (*Gadus morhua callarias*) während der Dottersackphase. Berichte aus dem Institut für Meereskunde, Nr. 312. 52 pp.

Sparholt, H. 1991. Multispecies assessment of Baltic fish stocks. ICES Marine Science Symposia, 193: 64–79.

Sparholt, H. 1994. Fish species interactions in the Baltic Sea. Dana, 10: 131–162.

Sparholt, H., and Tomkiewicz, J. 2000. A robust method to compile trawl survey data applied in assessment of Central Baltic cod. Archives of Fisheries and Marine Research, 48: 125–151.

Sparre, P. 1991. Introduction to multispecies virtual population analysis. ICES Marine Science Symposia, 193: 12–21.

STORE. 2001. Environmental and fisheries influences on fish stock recruitment in the Baltic Sea. EU-Project FAIR CT98 3959, Consolidated Progress Report, Part I. 336 pp.

Temming, A., and Herrmann, J.-P. 2002. Gastric evacuation in cod. Prey specific evacuation rates for use in North Sea, Baltic Sea and Barents Sea multi-species models. Fisheries Research, 63: 21–41.

Thompson, B. M., Milligan, S. P., and Nichols, J. H. 1981. The development rates of sprat (*Sprattus sprattus* L.) eggs over a range of temperatures. ICES CM 1981/H: 15.

Tomkiewicz, J., and Köster, F. W. 1999. Maturation processes and spawning time of cod in the Bornholm Basin of the Baltic Sea: preliminary results. ICES CM 1999/Y: 25.

Tomkiewicz, J., Eriksson, M., Baranova, T., Feldman, V., and Müller, H. 1997. Maturity ogives and sex ratios for Baltic cod: establishment of a database and time series. ICES CM 1997/CC: 20.

Trippel, E., Kjesbu, O. S., and Solemdal. P. 1997. Effects of adult age and size structure on reproductive output in marine fishes. *In* Early Life History and Recruitment in Fish Populations, pp. 29–62. Ed. by C. R. Chambers and E. A. Trippel. Chapman and Hall, London.

Uzars, D., and Plikshs, M. 2000. Cod (*Gadus morhua callarias* L.) cannibalism in the Central Baltic: interannual variability and influence of recruitment abundance and distribution. ICES Journal of Marine Science, 57: 324–329.

Vallin, L., and Nissling, A. 2000. Maternal effects on egg size and egg buoyancy of Baltic cod, *Gadus morhua*. Implications for stock structure effects on recruitment. Fisheries Research, 49: 21–37.

Vinther, M. 2001. *Ad hoc* multispecies VPA tuning applied for the Baltic and North Sea fish stocks. ICES Journal of Marine Science, 58: 311–320.

Voss, R., Köster, F. W., and Dickmann, M. 2003. Comparing the feeding habits of co-occurring sprat and cod larvae in the Bornholm Basin, Baltic Sea. Fisheries Research, 63: 97–111.

Westin, L., and Nissling, A. 1991. Effects of salinity on spermatozoa motility, percentage of fertilized eggs and egg development of Baltic cod *Gadus morhua*, and implications for cod stock fluctuations in the Baltic. Marine Biology, 108: 5–9.

Wieland, K., and Zuzarte, F. 1991. Vertical distribution of cod and sprat eggs and larvae in the Bornholm Basin (Baltic Sea) 1987–1990. ICES CM 1991/J: 37.

Wieland, K., Waller, U., and Schnack, D. 1994. Development of Baltic cod eggs at different levels of temperature and oxygen content. Dana, 10: 163–177.

Wieland, K., Jarre-Teichmann, A., and Horbowa. K. 2000. Changes in the timing of spawning of Baltic cod: possible causes and implications for recruitment. ICES Journal of Marine Science, 57: 452–464.

B. Posters Presented at the Symposium

ICES Marine Science Symposia, 219: 309–310. 2003

The ICES Annual Ocean Climate Status Summary: 2000/2001

W. R. Turrell and N. P. Holliday

Turrell, W. R. and Holliday, N. P. 2003. The ICES Annual Ocean Climate Status Summary: 2000/2001. – ICES Marine Science Symposia, 219: 309–310.

Each year the ICES Working Group on Oceanic Hydrography generates a summary of oceanic conditions in a series of regions around the North Atlantic. The time-series are reviewed in the context of atmospheric conditions represented by the North Atlantic Oscillation. The summary for the 2000 period is presented and the reader alerted to the location of the report and the data upon which it is based.

Keywords: interannual variability, NAO, North Atlantic, ocean climate.

N. P. Holliday: Southampton Oceanography Centre, European Way, Southampton, SO14 3ZH, UK [tel: +44 (0) 23 8059 6206; fax: +44 (0) 23 8059 6204; e-mail: nph@soc.soton.ac.uk]. W. R. Turrell: Marine Laboratory Aberdeen, PO Box 101, Victoria Road, Aberdeen, AB11 9DB, Scotland, UK [tel: +44 (0) 1224 295429; fax: +44 (0) 1224 295511; e-mail: turrellb@marlab.ac.uk]

Since the North Atlantic Oscillation (NAO) is known to control or modify three of the main parameters that drive the circulation in the ocean area covered by this climate summary (i.e. wind speed, air/sea heat exchange, and evaporation/precipitation), a knowledge of its past and present behaviour forms an essential context for the interpretation of observed ocean climate changes in 2000. The NAO index is defined by the difference in sea level pressure between the Iceland low-pressure system and the Azores high-pressure system. The NAO alternates between a "high index" pattern, characterized by strong mid-latitude westerly winds, and a "low index" pattern in which the westerly winds over the Atlantic are weakened. High index years are associated with warming in the southern North Atlantic and Northwest European Shelf seas, and cooling in the Labrador and Nordic Seas. Low index years generally show the reverse.

The 1960s were generally low-index years, while the 1990s were high index years. There was a major exception to this pattern occurring between the winters of 1995 and 1996, when the index flipped from being one of its most positive values to its most negative value this century. The index then rose from this extreme low and the recovery continued through to 2000 when it had a positive NAO index.

Although the simple index returned to positive values during the winters of 1999 and 2000, the actual pattern of the NAO over the ICES area did not recover to a "normal" distribution expected during high NAO years, but was rather displaced towards the east or northeast. This subtle change had the largest impact in the Northwest Atlantic, where instead of strong northwesterly airflow promoting cooling there, as it did in the early 1980s and 1990s, the northwesterly airflow was mainly confined to the east of Greenland, while the Labrador Sea was occupied by light or anomalous southerly winds.

An overview of the oceanic conditions in the areas covered by the summary (Figure 1) is given below.

Area 1: West Greenland lies within the area which normally experiences cool conditions when the NAO index is positive. However, throughout the 1990s the surface temperatures off West Greenland have been increasing following a drop at the end of the 1980s and a record low in 1991. The warm waters were due to increasingly mild atmospheric conditions and a relatively high inflow of Irminger Water.

Area 2: The Northwest Atlantic generally showed increasing temperature and salinities during the 1990s, followed by slight decreases in 2000. Off eastern Newfoundland the depth-averaged ocean temperature ranged from a record low during 1991 (high NAO index in preceding winter), a near record high in 1996 (following the reversal in the NAO index), and above the long-term (1961–1990) average in 1999 and 2000. Summer salinities, which were below normal during most of the early 1990s, returned to near normal values during 2000.

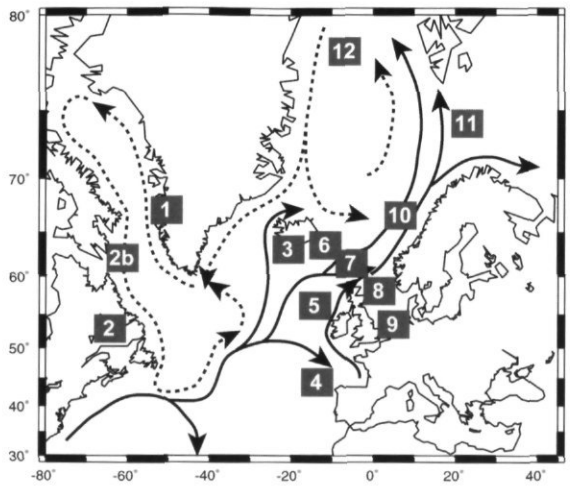


Figure 1. Schematic of North Atlantic upper layer circulation showing location of the time-series covered by the ICES Annual Ocean Climate Status Summary. Warm saline water represented by solid black lines, cold fresh water by dashed lines.

Area 2b: Cold winters and strong winds during the high NAO-index conditions of the first half of the 1990s gave rise to the formation of a notably dense, deep Labrador Sea water mass. Since then, relatively warm winters have produced only shallow convection. The convection that took place in the 1999–2000 winter dominated the layer between 200 m and 1000 m. This water mass penetrated 300 m deeper on average than during the previous winter. The upper 1000 m was up to 0.3°C cooler and 0.02 fresher in 2000 than in 1999. The associated density increase of the upper kilometre of the Labrador Sea was accompanied by a 5-cm lowering in sea level, according to TOPEX/POSEIDON altimeter measurements.

Area 3: In Icelandic waters, 2000 revealed relatively high temperatures and salinities similar to 1997–1999 and following the very cold years of 1995 and 1996. Temperatures in 2000 were cooler than 1999, however. The salinity in the warm water from the south was higher than has been observed over recent decades, conditions that have been evident since 1997.

Area 4: The annual mean air temperature over the southern Bay of Biscay during 2000 was similar to the two preceding years, slightly over the average, but below the high values detected in 1994, 1995, and 1997. Surface waters were slightly cooler and fresher than in the previous years mainly due to the cool winter and the reduction of salinity from 1999 following a high salinity period with a maximum in 1995–1996.

Area 5: Early 2000 saw a peak in the temperature of surface waters in the Rockall Trough caused by an influx of unusually warm water into the region. The temperature was more than 0.5°C above the long-term mean (since 1975), with most of the warming having taken place from 1995 to 2000. By the spring of 2000, the temperature had dropped somewhat, although it remained above the long-term mean. Through the 1990s, the mean salinity increased from a low in 1991 to a peak in 1998, followed by a slight decrease in 1999 and 2000.

Area 7: On the Northwest European Shelf, the surface Atlantic Water has been warming at a rate of 0.5°C per decade. In 1998, both temperature and salinity peaked and have since been declining.

Areas 8 and 9: Temperature and salinity were high in the North Sea at the start of the 1990s, decreased to lows in 1995/1996, and rose again in the second half of the decade. The year 2000 was the 6th warmest since 1971 in the North Sea in terms of annual mean sea surface temperature. There was evidence of a large input of freshwater from the Baltic into the Kattegat and Skaggerak in 2000.

Area 10: Temperature and salinity have been increasing in the southern and central Norwegian Sea since 1996 following a sharp decrease in both. In 2000, the warming continued at the southern section while cooling occurred at the central section. In the northern Norwegian Sea the temperature and salinity since 1996 have been close to the long-term average, though with a decreasing trend since 1990.

Area 11: After a period with high temperatures and salinities in the first half of the 1990s, the values in the Barents Sea dropped to slightly below the long-term average over the whole area in 1996 and 1997. Since then the salinity rose to a peak in 1998 and returned to average conditions in 2000. However, the temperature has risen since 1997 to more than 0.5°C above the long-term mean by 2000.

Area 12: Conditions in the Greenland Sea were fairly stable throughout the 1990s, with the exception of a sharp decrease in salinity and temperature in 1997. In 2000, a larger than normal inflow of Atlantic Water resulted in the warmest and highest saline conditions of the decade.

The full report and the time-series data may be found at http://www.ices.dk/status/clim0001/.

ICES Marine Science Symposia, 219: 311–314. 2003

Climatic variations in the North Atlantic and the North Pacific in the 1990s: a comparative study

Andrei S. Krovnin and George P. Moury

Krovnin, A. S., and Moury, G. P. 2003. Climatic variations in the North Atlantic and the North Pacific in the 1990s: a comparative study. – ICES Marine Science Symposia, 219: 311–314.

The study is based on the results of the analysis of spatial and temporal features of winter sea surface temperature anomaly (SSTA) variations in the North Atlantic and the North Pacific during the past four decades. Several large-scale regions with coherent SSTA fluctuations within each region were defined in both oceans. SSTA variations in these regions are strongly related to the well-known atmospheric teleconnection patterns in the Northern Hemisphere. Four distinct decadal climatic regimes were identified in the North Atlantic during the period 1957–2000. The last regime, established in 1989, continued through the 1990s. In the North Pacific, the climatic regime established in the second half of the 1970s continued until 1998–1999. The 1990–1999 decade was the warmest in both oceans compared with the previous three decades. Climatic variations in the North Atlantic during the past 40 years were characterized by the second, interdecadal, mode of variability associated with a gradual northeastward warming of surface waters. In the North Pacific this mode was not so clear, though some signs of the northeastward spreading of warming were noted in the 1980s and 1990s.

Keywords: decadal changes, interdecadal changes, sea surface temperature anomaly (SSTA).

A. S. Krovnin and G. P. Moury: Russian Federal Research Institute of Fisheries and Oceanography (VNIRO), 17 Verkhnyaya Krasnoselskaya, Moscow 107140, Russia [tel: +7 095 264 8401; fax: +7 095 264 9187; e-mail: akrovnin@vniro.ru; moury @vniro.ru]

Introduction

During the past decade, globally averaged air surface temperatures have been higher than in any decade since the mid-18th century (Jones *et al.*, 1999). However, there are significant regional differences in the extent and timing of warming. The main objective of this study was to compare the development of large-scale processes in the atmosphere and ocean in the North Atlantic and the North Pacific against a background of global warming.

Data

Data covering the period 1960 to 2000 were provided by the NOAA-CIRES Climate Diagnostics Center. They included mean winter (Dec–Feb) sea level pressure, geopotential heights on the 500 hPa surface, Northern Hemisphere teleconnection indices, and mean winter (Jan–Apr) Northern Hemisphere reconstructed Reynolds sea surface temperatures (SSTs). We used mean winter (Jan–Apr) SSTs at grid points of 5° latitude by 5° longitude in the North Atlantic and the North Pacific for the period 1957–2001, obtained from the Russian Hydrometeorological Center, to partition both the oceans into several large-scale subdomains with coherent SST anomaly fluctuations in each subdomain on the basis of the hierarchical clustering method known as Ward's method (Ward, 1963).

Results

Decadal variations

In each ocean we defined several large-scale subdomains with coherent SST anomaly (SSTA)

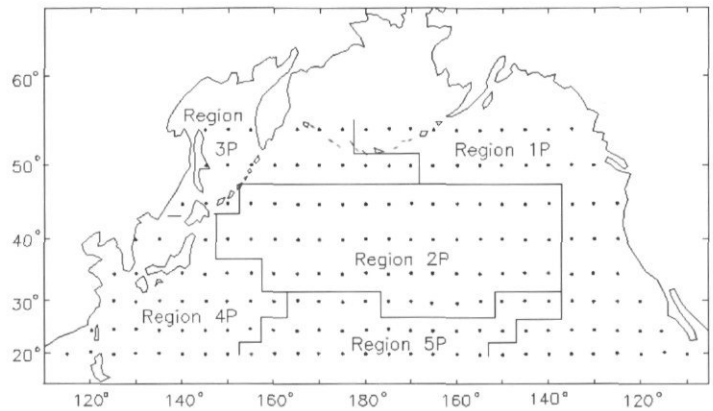


Figure 1. Results of cluster analysis for the SST anomaly field in the North Atlantic and the North Pacific. Dots show the position of the 5° latitude by 5° longitude grid for the SST data set.

Table 1. Loadings on the first 3 principal components from a principal component analysis of the 38 physical time-series in the Northern Hemisphere. The loadings are correlation coefficients between each time-series and each PC score (asterisks correspond to $|r| > 0.45$).

Physical time-series	PC1	PC2	PC3
	19.8%	17.1%	9.2%
Western Atlantic teleconnection pattern (TP) index (500 hPa surface)	−0.67*	0.27	0.24
Eastern Atlantic TP index (500 hPa surface; Wallace and Gutzler, 1981)	−0.11	−0.03	−0.38
Eastern Atlantic TP index (500 hPa surface, Barnston and Livezey, 1987)	0.43	0.38	0.30
Eastern Atlantic-Jet TP index (500 hPa surface)	0.34	0.20	0.13
Western Pacific TP index (500 hPa surface)	0.31	0.41	0.46*
Eastern Pacific TP index (500 hPa surface)	0.00	−0.29	0.49*
North Pacific (NP) TP index (500 hPa surface)	0.17	0.05	−0.11
Pacific/North American TP index (500 hPa surface)	0.05	0.69*	−0.26
East Atlantic/West Russia TP index (500 hPa surface)	0.35	0.15	−0.36
Scandinavian TP index (500 hPa surface)	−0.23	0.06	0.22
Tropical/ Northern Hemisphere TP index (500 hPa surface)	0.07	−0.53*	−0.24
Polar/Eurasia TP index (500 hPa surface)	0.48*	0.09	−0.41
Pacific Transition TP index (500 hPa surface)	−0.02	−0.05	0.51*
Subtropical Zonal TP index (500 hPa surface)	0.02	0.04	0.34
Asia Summer TP index (500 hPa surface)	0.25	0.31	0.23
Winter (Dec–Mar) NAO index	0.90*	0.02	−0.12
Winter (Nov–Mar) North Pacific SLP index	0.02	−0.75*	0.18
Pacific Decadal Oscillation index	0.00	0.82*	−0.11
Sea level pressure (SLP) (Reykjavik)	−0.87*	0.14	−0.10
SLP (Gibraltar)	0.77*	0.06	−0.02
SLP (Darwin)	0.25	0.78*	0.02
SLP (Tahiti)	0.11	−0.76*	0.09
Southern Oscillation index (SOI)	−0.08	−0.86*	0.04
Arctic Oscillation index	0.86*	−0.18	−0.17
Azores High longitude	0.35	0.18	0.04
Aleutian Low longitude	0.04	0.75*	−0.12
Area-averaged mean winter SSTA in Region 1A	0.65*	−0.09	0.46*
Area-averaged mean winter SSTA in Region 2A	0.72*	−0.04	−0.02
Area-averaged mean winter SSTA in Region 3A	−0.52*	−0.03	0.48*
Area-averaged mean winter SSTA in Region 4A	−0.43*	0.48*	0.41
Area-averaged mean winter SSTA in Region 5A	0.30	0.42	0.53*
Area-averaged mean winter SSTA in Region 6A	0.26	−0.07	−0.18
Area-averaged mean winter SSTA in Region 1P	0.05	0.71*	−0.24
Area-averaged mean winter SSTA in Region 2P	0.30	−0.65*	0.10
Area-averaged mean winter SSTA in Region 3P	0.34	0.10	−0.47*
Area-averaged mean winter SSTA in Region 4P	0.48*	0.22	0.60*
Area-averaged mean winter SSTA in Region 5P	0.53*	−0.09	0.49*
Winter Tw anomalies (0–200 m) at Kola Section	0.61*	−0.07	−0.09

fluctuations. The results of cluster analysis for the North Atlantic and their discussion are given in the article by Krovnin and Moury (2003). The results of partitioning of the North Pacific are shown in Figure 1. The spatial structure of the SSTA fluctuations in the North Pacific is characterized by two independent patterns, one occurring in the eastern (region 1P) and central (region 2P) Pacific, and the second in its northwestern (region 3P) and southwestern (region 4P) parts. The changes in SSTA between regions 1P and 2P, as well as between regions 3P and 4P, are out of phase.

As in the North Atlantic, the SSTA variations in regions defined in the North Pacific are strongly related to the well-known teleconnection patterns at the 500 hPa surface in the Northern Hemisphere first described by Wallace and Gutzler (1981). The SSTA variations in the central (region 1P) and eastern (region 2P) North Pacific appear to be associated with the Pacific/North American (PNA) pattern, while those in two western regions seem associated with the Western Pacific (WP) pattern (maps not shown).

We used principal component analysis (PCA) to define the most important patterns of common variability in the 38 physical time-series in the North Atlantic and the North Pacific. They included time-series of indices of teleconnection patterns both in the sea level pressure (SLP) field (e.g. NAO index, North Pacific pressure index) and in the middle troposphere (at the 500 hPa surface, e.g., index of Eastern Atlantic teleconnection pattern), time-series of SLP at fixed points and area-averaged SSTA for regions defined in both the oceans. The first principal component (PC1) is associated with the NAO, and its time-series shows 4 distinct regimes between 1957 and 2000: 1957–1971; 1972–1976, 1977–1988, and 1989 through 2000, with the most abrupt transition in 1989 (Table 1; Figure 2a). PC2 is associated with the Southern Oscillation and Pacific Decadal Oscillation (PDO) pattern (Mantua *et al.*, 1997) and shows the rather prominent shift in 1977 with the predominance of negative values in the pre-1977 period and positive values since 1977. PC3 is related to the WP pattern. Its time-series shows the prominent shift from the predominant positive to negative values in the mid-1970s and the reverse shift in 1998.

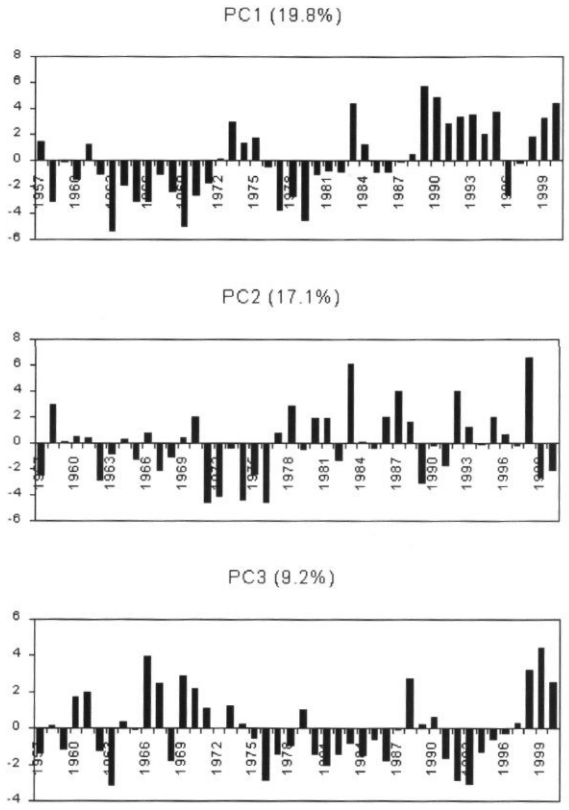


Figure 2. The first 3 principal component scores from a principal component analysis of the 38 physical time-series in the North Atlantic and the North Pacific. The scores are normalized time-series.

Interdecadal variations

Figure 3 (left panel) shows SLP changes between two consecutive decades over the North Pacific–North Atlantic sector. It demonstrates an intensification and eastward shift of low- and high-pressure anomaly cells south of 50°N and general strengthening of zonal flow over the North Atlantic north of 50°N from the 1970s to 1990s. Figure 3 (right panel) shows a gradual northeastward spreading of warming in the North Atlantic in accordance with the shift of the high pressure anomaly cell, but north of 50°N SST changes were not correspondent to changes in local winds. In the North Pacific, SST changes in the 1970s–1980s were, in general, consistent with the changes in atmospheric circulation. At the same time, the signs of the northeastward propagating warming appeared in the 1980s and in the 1990s the warming was observed over most of the North Pacific.

Conclusion

Using data for 1890–1940, Bjerknes (1964) concluded that the long warming trend during the first quarter of the last century in the North Atlantic was linked to a basin-scale interaction in which the Gulf Stream and the North Atlantic Current responded to the intensifying circulation in the subtropical

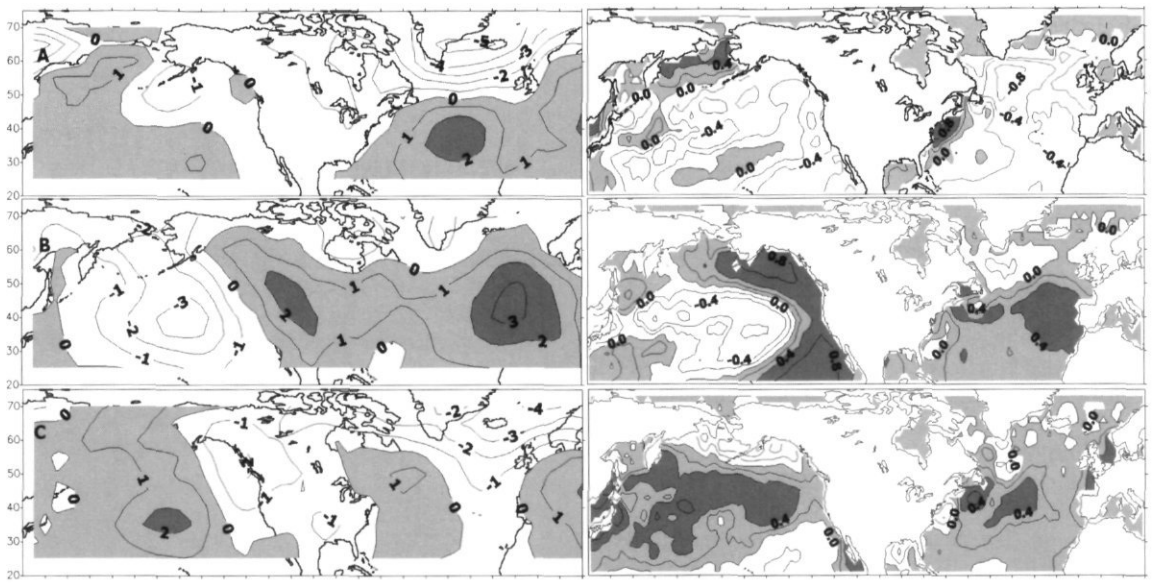


Figure 3. Difference maps for SLP (left panel) and SST (right panel) anomalies in the North Pacific–North Atlantic Region between: 1970–1979 and 1960–1969, 1980–1989 and 1970–1979, and 1990–1999 and 1980–1989. Positive values are shaded.

anticyclone. The interdecadal changes in the North Atlantic characterized by the warming trend during the 1970s–1990s resembled in many aspects the warming of the 1920s–1930s described by Bjerknes. In particular, there were inconsistent changes in SSTA and local winds north of 50°N. In the North Pacific the heat exchange at the sea surface contributes to SSTA changes on an interdecadal time scale to a larger extent than in the North Atlantic. Thus, unlike the North Atlantic, the effect of oceanic circulation in the North Pacific on the interdecadal SSTA changes is seen only in the periods of general lessening of atmospheric circulation.

Acknowledgements

We thank NOAA-CIRES Climate Diagnostics Center, Boulder, Colorado, for data available at their website at http://www.cdc.noaa.gov.

References

Barnston, A. G., and Livezey, R. E. 1987. Classification, seasonality and peristence of low-frequency atmospheric circulation patterns. Monthly Weather Review, 115: 1083–1126.

Bjerknes, J. 1964. Atlantic air-sea interaction. Advances in Geophysics, 10: 1–82.

Jones, P. D., New, M., Parker, D. E., Martin, S., and Rigor, I. G. 1999. Surface air temperature and its changes over the past 150 years. Reviews of Geophysics, 37: 173–199.

Krovnin, A. S., and Moury, G. P. 2003. The 1990s in the context of climatic changes in the North Atlantic region during the past 40 years. ICES Marine Science Symposia, 219: 315–318. (This volume.)

Mantua, N. J., Hare, S. R., Zhang, Y., Wallace, J. M., and Fransis, R. C. 1997. A Pacific interdecadal climate oscillation with impacts on salmon production. Bulletin of the American Meteorological Society, 78: 1069–1079.

Wallace, J. M., and Gutzler, D. S. 1981. Teleconnections in the geopotential height field during the Northern Hemisphere winter. Monthly Weather Review, 109: 784–812.

Ward, J. H. Jr. 1963 Hierarchical grouping to optimize an objective function. Journal of American Statistical Association, 58: 236–244.

ICES Marine Science Symposia, 219: 315–318. 2003

The 1990s in the context of climatic changes in the North Atlantic region during the past 40 years

Andrei S. Krovnin and George P. Moury

Krovnin, A. S., and Moury, G. P. 2003. The 1990s in the context of climatic changes in the North Atlantic region during the past 40 years. – ICES Marine Science Symposia, 219: 315–318.

The wintertime surface climate variations in the North Atlantic during the past 40 years were characterized by two modes of variability. The first mode is associated with decadal variations in atmospheric circulation and sea surface temperature (SST). The spatial structure of decadal SST anomaly (SSTA) variations is characterized by the existence of six large-scale regions with coherent SSTA fluctuations within each region. Four distinct decadal climatic regimes were identified during the 1957–2000 period: 1957–1971, 1972–1976, 1977–1988, and 1989–2000. The 1990–1999 decade was very warm in the North Atlantic. The second mode of variability in the North Atlantic during the past 40 years was associated with a gradual northeastward warming of surface waters, which is possibly driven by changes in the large-scale oceanic circulation.

Keywords: decadal variations, interdecadal changes, North Atlantic, sea surface temperature anomaly.

A. S. Krovnin and G. P. Moury: Russian Federal Research Institute of Fisheries and Oceanography (VNIRO), 17 Verkhnyaya Krasnoselskaya, Moscow 107140, Russia [tel: +7 095 264 8401; fax: +7 095 264 9187; e-mail: akrovnin@vniro.ru; moury@vniro.ru]

Introduction

During the past decade, globally averaged surface temperatures have been higher than in any decade since the mid-18th century, and the seven warmest years of the global record have all occurred since 1990 (Jones *et al.*, 1999). However, significant regional differences in the extent and timing of warming exist. The main objective of this article is to consider the development of large-scale processes in the atmosphere and ocean in the North Atlantic region against a background of global warming.

Data

We used mean winter (Dec–Feb) values of sea-level pressure, geopotential heights on the 500 hPa surface, surface air temperature, indices of the North Atlantic teleconnection patterns, mean winter (Jan–Apr) reconstructed Reynolds SSTs in the Northern hemisphere for the 1960–2000 period provided by the NOAA-CIRES Climate Diagnostics Center. Additionally, mean winter (Jan–Apr) SSTs at grid points of 5° latitude by 5° longitude in the North Atlantic for the period 1957–2001, obtained from the Russian Hydrometeorological Center, were also used to partition the North Atlantic into several large-scale subdomains with coherent SST anomaly fluctuations in each subdomain based on the hierarchical clustering method known as Ward's method (Ward, 1963).

Results

1. Decadal variations

Results of cluster analysis show that the North Atlantic can be divided into six major regions with respect to the similarity in the SST anomaly (SSTA) variations (Figure 1). The SSTA fluctuation in the northeastern (1A) and southwestern (2A) regions are opposite to those in the northwestern (3A) and southeastern (4A) regions (maps not shown).

The SSTA variations in the defined regions are strongly related to the well-known teleconnection patterns in the northern hemisphere. Thus, SSTA

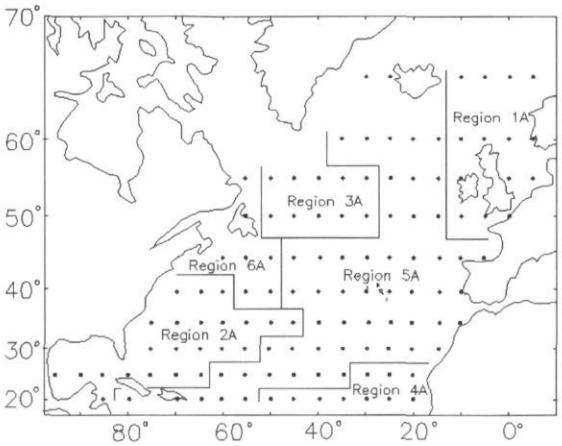


Figure 1. Results of cluster analysis for the SST anomaly field in the North Atlantic. Dots show the position of the 5° latitude by 5° longitude grid for the SST data set.

fluctuations in regions 1–3 may be forced by the Eastern Atlantic (Barnston and Livezey, 1987) and the Western Atlantic patterns (Wallace and Gutzler, 1981) (correspondent maps not shown). The SSTA changes in Region 4 are associated with both the Eastern Atlantic and Pacific/North American (PNA) patterns. Moreover, the SSTA fluctuations in the central North Atlantic appear to be connected with the PNA pattern, while there is no significant relationship with the North Atlantic teleconnection patterns.

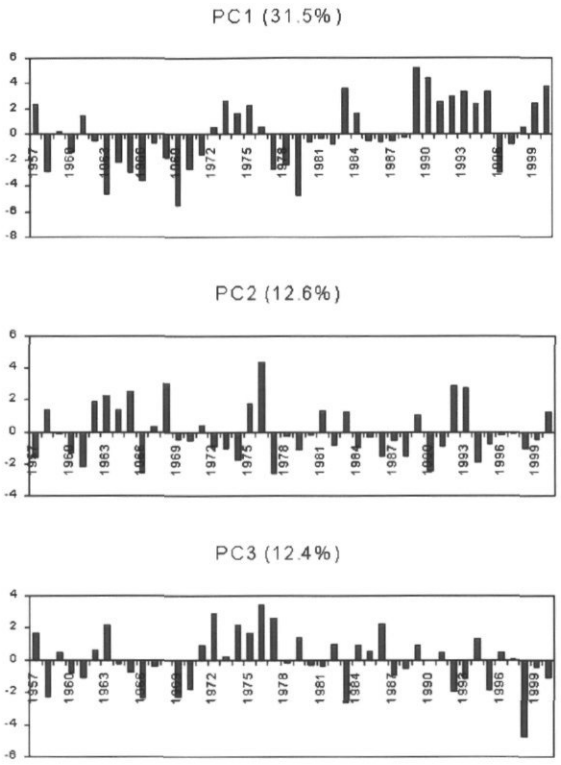


Figure 2. The first three principal component scores from a principal component analysis of the 22 physical time-series in the North Atlantic. The scores are normalized time-series.

Table 1. Loadings on the first three principal components (PC) from a principal component analysis of the 21 physical time-series in the North Atlantic. The loadings are correlation coefficients between each time-series and each PC score. (Asterisks indicate $|r| > 0.45$).

Physical time-series	PC1	PC2	PC3
	31.5%	12.6%	12.4%
Western Atlantic (WA) pattern	−0.72*	0.27	−0.43
Eastern Atlantic (EA) pattern (WG)[1]	−0.10	0.92*	−0.01
Eastern Atlantic (EA) pattern (BL)[2]	0.38	−0.70*	−0.34
East Atlantic Jet pattern (EA-Jet)	0.29	−0.25	−0.30
East Atlantic/West Russia pattern (EA/WR)	0.35	0.44	−0.05
Scandinavian pattern (SCA)	−0.23	−0.63*	0.08
Tropical/Northern Hemisphere pattern (TNH)	0.16	−0.17	0.72*
Polar/Eurasian pattern (POL)	0.48*	0.43	−0.05
Winter NAO index	0.92*	−0.03	−0.04
SLP (Reykjavik)	−0.88*	0.16	0.07
SLP (Gibraltar)	0.79*	0.15	−0.27
Southern Oscillation Index (SOI)	0.00	0.03	0.63*
Arctic Oscillation Index	0.86*	0.31	0.03
Azores High Longitude	0.32	0.10	−0.38
SSTA (Jan–Apr) in Region 1	0.60*	−0.18	−0.28
SSTA (Jan–Apr) in Region 2	0.72*	−0.27	0.16
SSTA (Jan–Apr) in Region 3	−0.58*	0.17	−0.35
SSTA (Jan–Apr) in Region 4	−0.54*	−0.13	−0.62*
SSTA (Jan–Apr) in Region 5	0.18	−0.12	−0.74*
SSTA (Jan–Apr) in Region 6	0.30	0.35	−0.05
Winter T_w anomalies (0–200 m) at Kola Section	0.62*	0.22	−0.12

[1] WG = Wallace and Gutzler (1981). [2] BL = Barnston and Livezey (1987).

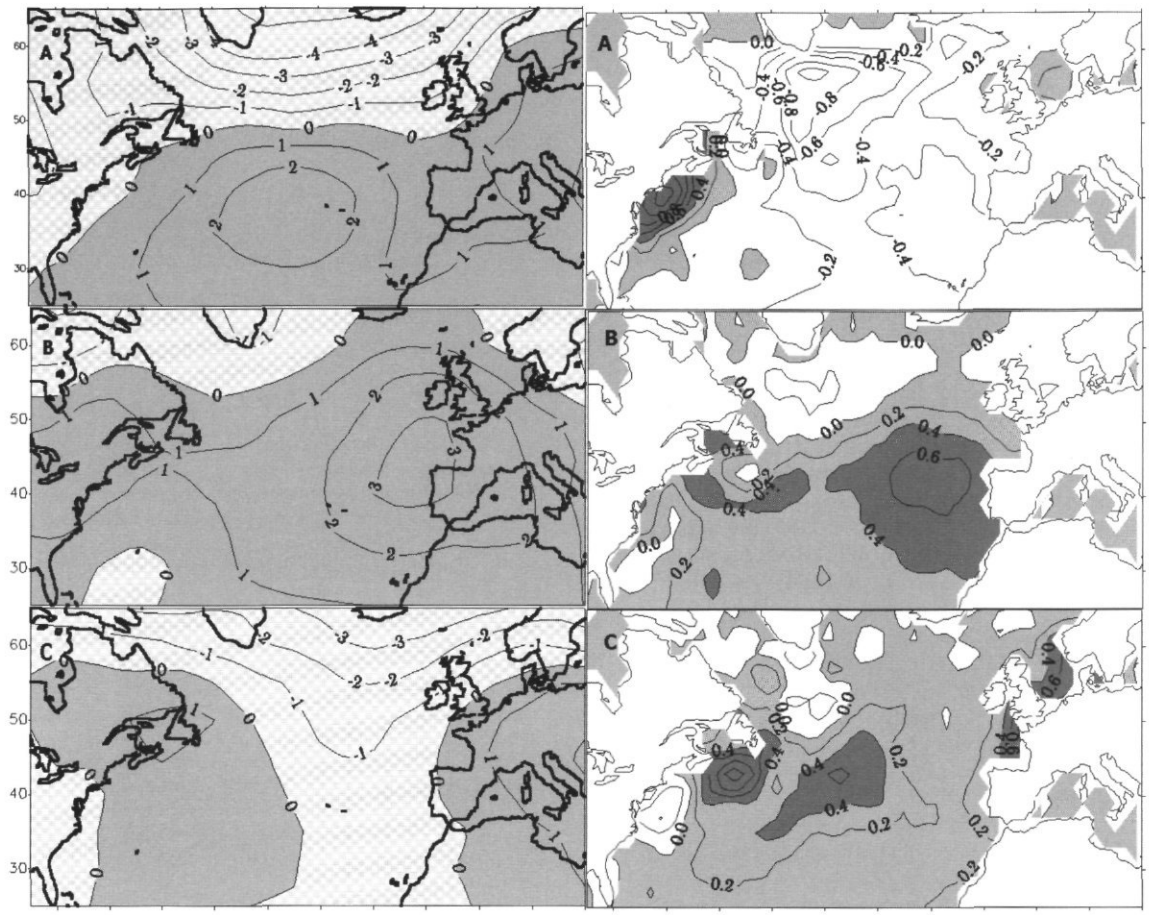


Figure 3. Difference maps for SLP (left panel) and SST (right panel) change in the North Atlantic between 1970–1979 and 1960–1969, 1980–1989 and 1970–1979, and 1990–1999 and 1980–1989. Positive values are shaded.

We used principal component analysis (PCA) to define objectively the most important patterns of common variability in the 21 physical time-series in the North Atlantic. The time-series of the first principal component (PC1), associated with the North Atlantic Oscillation, shows four distinct regimes between 1957 and 2000: 1957–1971, 1972–1976, 1977–1988, and 1989 through 2000, with the most abrupt transition in 1989 (Table 1; Figure 2). The second PC, related to the Eastern Atlantic teleconnection patterns shows the prominent shift in 1969 with the predominance of positive values in the pre-1969 period and negative values since 1969. PC3 is related to the Tropical-Northern Hemisphere (TNH) teleconnection pattern, which in turn is associated with the Southern Oscillation (Barnston and Livezey, 1987). Note the high inverse correlation of SSTA variations in the central and southeastern parts of the ocean (Regions 4–5) with PC3.

2. Interdecadal variations

Figure 3 (left panel) shows SLP changes between two consecutive decades (i.e. 1970–1979 minus 1960–1969, etc.) over the North Atlantic region. There was a general increase in SLP, a clear eastward shift of a high pressure anomaly cell south of 50°N and a gradual decrease in SLP to the north of this latitude from the 1970s to the 1990s. This indicated the strengthening of zonal atmospheric flow north of 50°N. Figure 4 (right panel) demonstrates a gradual northeastward warming of the North Atlantic in accordance with the interdecadal shift of the high pressure anomaly cell.

Discussion

Using data for 1890–1940, Bjerknes (1964) provided evidence that interannual fluctuations in SST are

governed by wind-induced changes in latent and sensible heat fluxes at the sea surface. Deser and Blackmon (1993) showed that the surface climate over the North Atlantic exhibited coherent decadal variations that resembled the fluctuations on an interannual time scale. However, as it was concluded by Bjerknes that the long warming trend in the first quarter of the last century was linked to a basin-scale interaction in which the Gulf Stream and the North Atlantic Current responded to the intensifying circulation in the subtropical anticyclone. A similar idea was used to explain the cooling trend in the North Atlantic that occurred during the 1950s and 1960s (Greatbach *et al.*, 1991; Kushnir, 1992). The warming trend in the North Atlantic during the 1970s–1990s resembles in many aspects the warming of the 1920s–1930s described by Bjerknes. In particular, SST changes in the Northeast Atlantic in the 1980s and southwest of Newfoundland in the 1990s did not correspond to the changes in local winds. Thus, the observed warming trend is possibly driven by changes in the large-scale oceanic circulation.

Thus, changes in the winter surface climate of the North Atlantic during the past 40 years have been characterized by two modes of variability. The first mode was associated with decadal variations in the atmospheric circulation and resulting SST changes. The second mode of variability in the North Atlantic during the past 40 years was associated with a gradual northeastward warming of surface waters, possibly driven by changes in the large-scale oceanic circulation.

Acknowledgements

We thank NOAA-CIRES Climate Diagnostics Center, Boulder, Colorado, for making their data available at website http://www.cdc.noaa.gov.

References

Barnston, A. G., and Livezey, R. E. 1987. Classification, seasonality and persistence of low-frequency atmospheric circulation patterns. Monthly Weather Review, 115: 1083–1126.

Bjerknes, J. 1964. Atlantic air-sea interaction. Advances in Geophysics, 10: 1–82.

Deser, C., and Blackmon, M. L. 1993. Surface climate variations over the North Atlantic Ocean during winter: 1900–1989. Journal of Climate, 6: 1743–1753.

Greatbatch, R. J., Fanning, A. F., and Goulding, A. D. 1991. A diagnosis of interpentadal circulation changes in the North Atlantic. Journal of Geophysical Research, 96, C12: 22,009–22,023.

Jones, P. D., New, M., Parker, D. E., Martin, S., and Rigor, I. G. 1999. Surface air temperature and its changes over the past 150 years. Reviews of Geophysics, 37: 173–199.

Kushnir, Y. 1992. Interdecadal variations in the North Atlantic sea surface temperature and associated atmospheric conditions. Journal of Climate, 7: 141–157.

Wallace, J. M., and Gutzler, D. S. 1981. Teleconnections in the geopotential height field during the Northern Hemisphere winter. Monthly Weather Review, 109: 784–812.

Ward, J. H. Jr. 1963 Hierarchical grouping to optimize an objective function. Journal of American Statistical Association, 58: 236–244.

ICES Marine Science Symposia, 219: 319–325. 2003

Temporal switching between sources of the Denmark Strait overflow water

Bert Rudels, Patrick Eriksson, Erik Buch, Gereon Budéus, Eberhard Fahrbach, Svend-Aage Malmberg, Jens Meincke, and Pentti Mälkki

Rudels, B., Eriksson, P., Buch, E., Budéus, G., Fahrbach, E., Malmberg, S.-A., Meincke, J., and Mälkki, P. 2003. Temporal switching between sources of the Denmark Strait overflow water. – ICES Marine Science Symposia, 219: 319–325.

The Denmark Strait overflow water derives from several distinct sources. Arctic Intermediate Water from the Iceland Sea, Atlantic Water of the West Spitsbergen Current recirculating in the Fram Strait, and Arctic Atlantic Water returning from the different circulation loops in the Arctic Ocean all take part in the overflow. Denser water masses, such as the upper Polar Deep Water and the Canadian Basin Deep Water from the Arctic Ocean and Arctic Intermediate Water from the Greenland Sea, are occasionally present at the sill and could contribute the deepest part of the overflow plume. A comparison between hydrographic observations made during the Greenland Sea Project in the late 1980s and early 1990s and during the European Sub Polar Ocean Programme (ESOP) and Variability of Exchanges in the Northern Seas (VEINS) programmes in the late 1990s shows that the Greenland Sea Arctic Intermediate Water has largely replaced the Arctic Ocean deep waters. In the less dense fraction of the overflow the Recirculating Atlantic Water and Arctic Atlantic Water carried by the East Greenland Current have become more prominent than the Iceland Sea Arctic Intermediate Water. If the Denmark Strait overflow were to switch between different sources, it would lead to changes in the characteristics of the overflow water that add to the variations caused by the variability of the source waters.

Keywords: Denmark Strait, East Greenland Current, overflow water, water masses.

Bert Rudels, Patrick Eriksson and Pentti Mälkki: Finnish Institute of Marine Research, Helsinki, Finland; Erik Buch, Danish Meteorological Institute, Copenhagen, Denmark; Gereon Budéus and Eberhard Fahrbach: Alfred-Wegener-Institut für Polar und Meeresforschung, Bremerhaven, Germany; Svend-Aage Malmberg: Marine Research Institute, Reykjavik, Iceland; Jens Meincke: Institut für Meereskunde der Universität Hamburg, Hamburg, Germany.

Introduction

The northernmost part of the North Atlantic – the Arctic Mediterranean Sea – is the end and the beginning of the global thermohaline circulation. The strong heat loss, the excess precipitation, and the large run-off all contribute to the water mass transformations in the Arctic Mediterranean. Northward flowing Atlantic Water that crosses the Greenland–Scotland Ridge becomes transformed, partly into low salinity surface water, but mainly into cold, dense intermediate and deep waters that return as "overflow waters" to the deep North Atlantic (Worthington, 1970). The most important sites and processes for dense water formation are the seasonal cooling of the Atlantic Water in the Norwegian Sea, the cooling and brine rejection occurring in the Barents Sea and on the shelves of the Arctic Ocean, and the winter convection in the Greenland and Iceland Seas.

Cooled Atlantic Water flows in the West Spitsbergen Current to Fram Strait, where one part recirculates and forms the Recirculating Atlantic Water, the rest entering the Arctic Ocean and becoming the Arctic Atlantic Water. Dense waters from the Barents Sea and from the Arctic shelves drain into the deep Arctic Ocean forming the Arctic Ocean intermediate and deep water masses that eventually exit through the Fram Strait and, along with the Arctic Atlantic Water returning from its loops in the different basins, forms the East Greenland Current. In Fram Strait these waters are joined by

the Recirculating Atlantic Water and continue southward along the Greenland slope. On its route, the East Greenland Current interacts with the waters of the Greenland Sea. Some deep waters, the Eurasian Basin Deep Water and part of the Canadian Basin Deep Water enter the Greenland Sea (Aagaard *et al.*, 1985) and Arctic Intermediate Water is incorporated into the East Greenland Current, which continues across the Jan Mayen Fracture Zone into the Iceland Sea. The dense water formed in the Iceland Sea, the Iceland Sea Arctic Intermediate Water, does not join the East Greenland Current but instead flows directly towards the Denmark Strait, constituting a separate source of overflow water (Swift *et al.*, 1980).

Waters too dense to cross the Jan Mayen Fracture Zone and the sill in Denmark Strait eventually reach the Norwegian Sea and pass through the Faeroe–Shetland Channel to the North Atlantic. The Denmark Strait Overflow Water and the Faeroe–Shetland Overflow Water supply the North Atlantic Deep Water and feed the Deep Western Boundary Current and thus the lower limb of the global thermohaline circulation. The Denmark Strait overflow has a closer connection with the different sources than the Faeroe–Shetland overflow, which mainly drains the pool of dense water in the Norwegian Sea, and reflects more strongly the interplay between and the variability of the different sources.

Observations

The present discussion is based on hydrographic observations gathered by several institutions over the past 15 years: AWI, Bremerhaven; Finnish Institute of Marine Research, Helsinki; Institut für Meereskunde, Hamburg; Marine Research Institute, Reykjavik; Norwegian Polar Research Institute, Tromsø; Royal Danish Administration of Navigation and Hydrography, Copenhagen as part of different international projects: European Sub Polar Ocean Programme (ESOP); Greenland Sea Project (GSP); Marginal Ice Zone Experiment (MIZEX); World Ocean Circulation Experiment (Nordic WOCE); Variability of Exchanges in the Northern Seas (VEINS). Only a few representative stations are shown and their positions are indicated in Figure 1.

Fram Strait

During the past 10–15 years the water mass characteristics in Fram Strait have changed considerably. Rudels *et al.* (2000) compared sections from 1984 and 1997 and found that the deeper layers had become warmer and more saline, indicating a stronger presence of Arctic Ocean deep waters. In 1984 the warm, saline Atlantic layer located between 100 and 600 m, comprising the northward flowing and the recirculating part of the West Spitsbergen Current, reached across the entire strait from Svalbard to the Greenland continental slope. In 1997 the recirculation was less extensive, leaving a corridor, about 1/5th of the total width of the Strait, east of the Greenland slope and allowing an almost free passage for the Arctic Atlantic Water exiting the Arctic Ocean. This suggests that the recirculation in the Fram Strait has weakened and that a larger part of the West Spitsbergen Current enters the Arctic Ocean.

Central Greenland Sea

Figure 2 shows θ-S curves and potential temperature and salinity profiles from the centre (75°N, 2°W) and the western part (75°N, 7°W) of the Greenland Sea gyre taken in 1988, 1993, and 1998. After convection deeper than 2500 m in 1988 the convection depth diminished, and the penetration of the Arctic Ocean deep waters, no longer stirred into the Greenland Sea Deep Water by the local convection, from the rim towards the centre of the gyre became visible. First the deep salinity maximum deriving from the Eurasian Basin Deep Water grew in prominence and then the intermediate temperature maximum of the Canadian Basin Deep Water appeared. The latter has more or less become the deep boundary for the local convection, and the convection in the Greenland Sea presently produces Arctic Intermediate Water spreading out above the temperature maximum rather than deep water. The salinity and temperature of the deeper layers have gradually increased, while the temperature maximum is displaced downwards (Budéus *et al.*, 1998). The confinement of the convection to above the temperature maximum could be instrumental in pushing the maximum downwards.

The Iceland Sea

The Jan Mayen Fracture Zone prevents the densest water of the East Greenland Current from entering the Iceland Sea. The characteristics of the waters that cross the ridge do not display large along-slope variations between the Greenland Sea and the Iceland Sea as compared to the annual variability. The warm Recirculating Atlantic Water–Arctic Atlantic Water core as well as the thermocline above the core retained their properties since Fram Strait. The characteristics of the thermocline correspond to

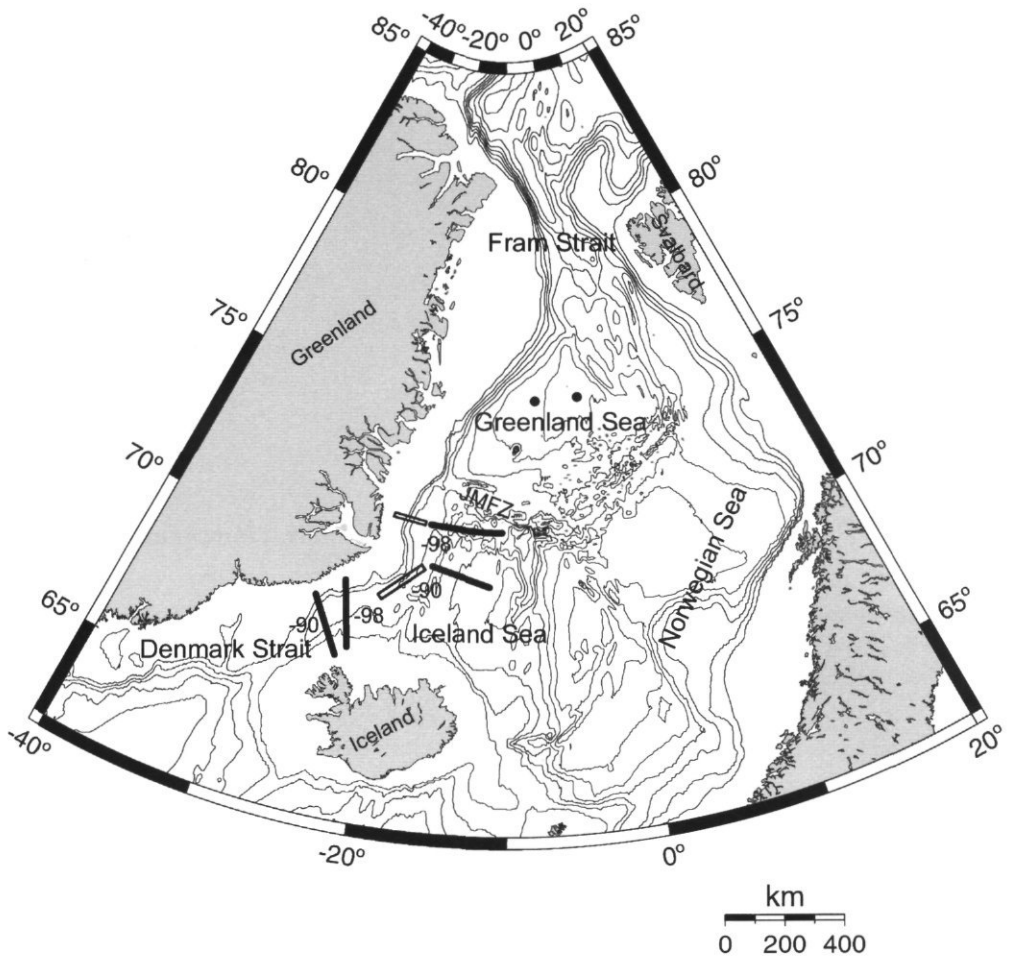
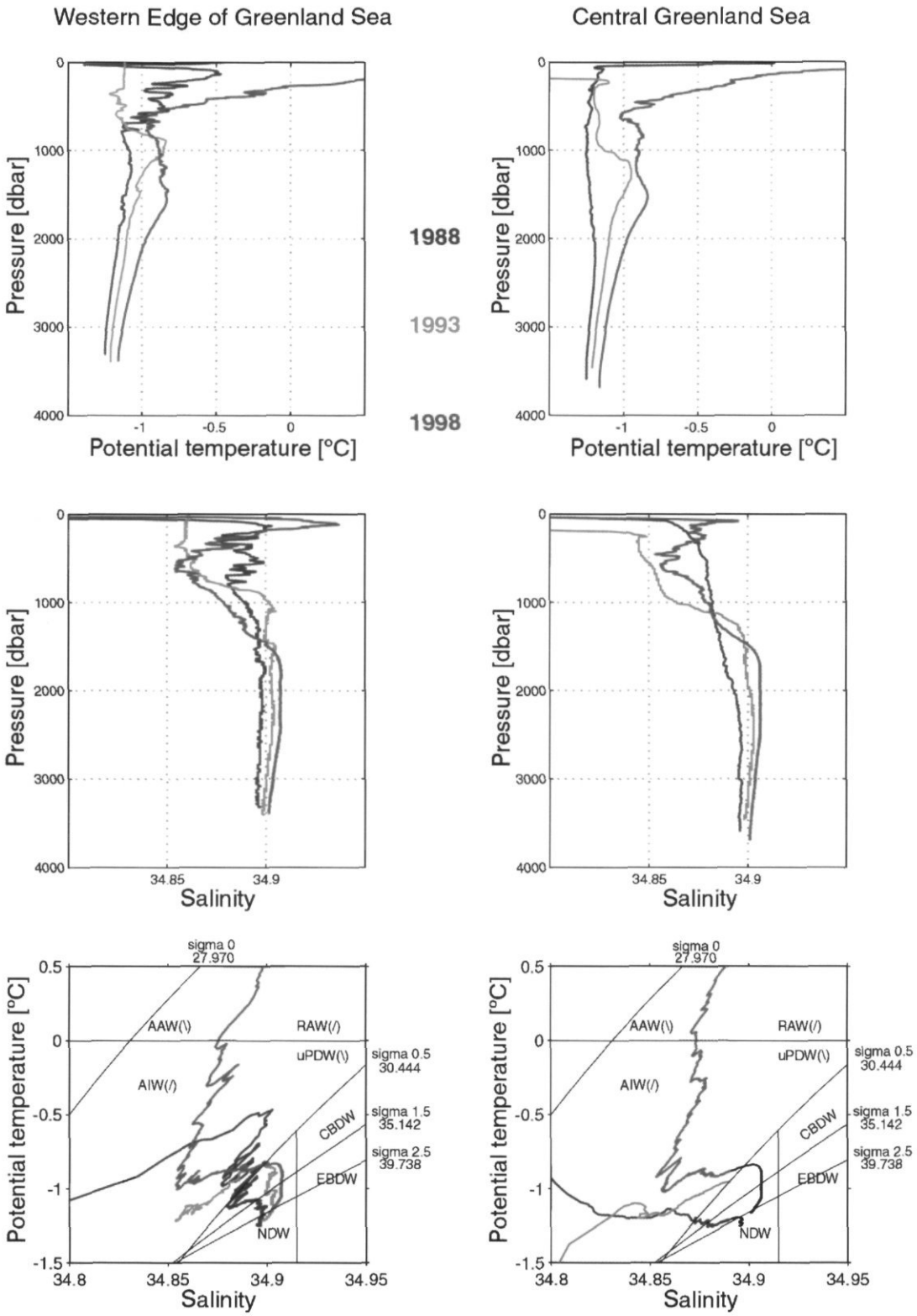


Figure 1. Map of the Nordic Seas. The positions of the Greenland Sea stations are shown as dots, and the bars indicate the positions of the sections from 1990 and 1998 in the Iceland Sea and northern Denmark Strait. The filled bars correspond to the blue stations, the open bars to the red stations in Figure 3. JMFZ (Jan Mayen Fracture Zone).

those of the Polar Intermediate Water (Malmberg, 1972), and the Arctic Ocean is therefore a probable source for the Polar Intermediate Water.

The central Iceland Sea appeared disconnected from the western area dominated by the East Greenland Current and the year to year variations of the Iceland Sea Arctic Intermediate Water, comprising an upper temperature minimum and a lower temperature maximum (Swift and Aagaard, 1981; Carmack, 1990), did not follow the advected changes in the East Greenland Current. Figure 3 compares the waters of the East Greenland Current and in the central Iceland Sea just south of the Jan Mayen Ridge in 1990 and 1998. The upper Iceland Sea Arctic Intermediate Water temperature minimum was almost removed by summer heating in 1990 but in 1998 its temperature was close to freezing. The salinity was around 34.6, which is considerably more saline than the 34.2–34.4 that characterize the knee between the halocline and the thermocline in the East Greenland Current and supports the notion that the temperature minimum is formed locally in the Iceland Sea. The temperature maximum also varied from year to year but it was always cooler and less saline than the warm, saline Arctic Atlantic Water–Recirculating Atlantic Water core in the East Greenland Current.

The salinity in the deeper layer has decreased between early and late 1990s (Figure 3). This is caused by a change in the water masses crossing the Jan Mayen Fracture Zone. During the stronger convection in the 1980s the convecting waters were denser and the less dense Canadian Basin Deep Water was forced across the ridge into the Iceland Sea. In the late 1990s the less saline, and now the less dense, Arctic Intermediate Water rather than the Canadian Basin Deep Water crossed the Jan Mayen Ridge into the Iceland Sea.


Western Edge of Greenland Sea
Central Greenland Sea
1988
1993
1998
Pressure [dbar]
Potential temperature [°C]
Salinity
Potential temperature [°C]
sigma 0
27.970
AAW(\)
RAW(/)
uPDW(\)
AIW(/)
CBDW
EBDW
NDW
sigma 0.5
30.444
sigma 1.5
35.142
sigma 2.5
39.738

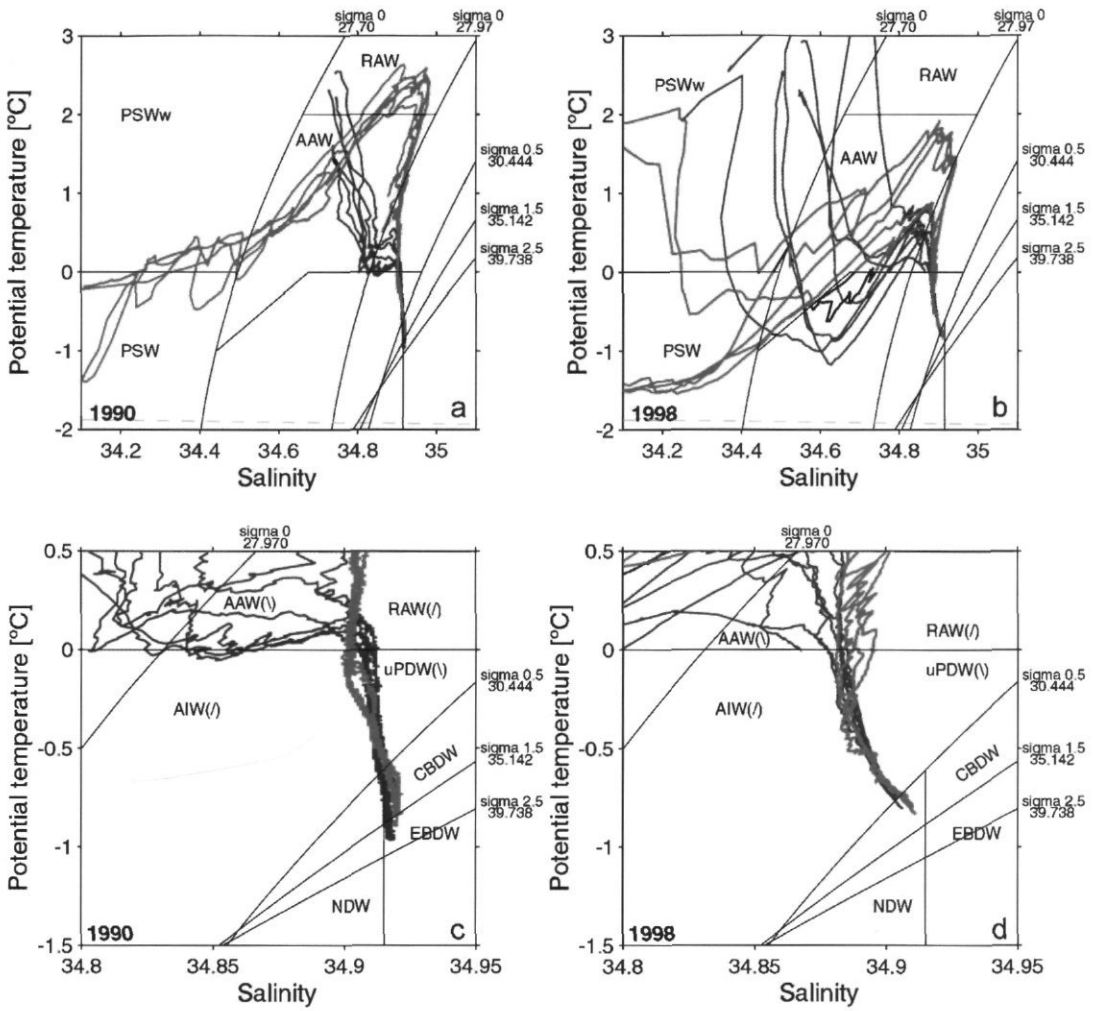


Figure 3. θ-S diagrams (full scale and blow-up) from stations in the East Greenland Current (red lines) and in the central Iceland Sea (blue lines) just south of the Jan Mayen Fracture Zone taken in 1990 and in 1998.

Denmark Strait

On sections between Greenland and Iceland just north of Denmark Strait (Figure 4) the upper layer was dominated by low salinity polar water and no temperature minimum that could have originated in the Iceland Sea was observed. The temperature of the temperature maximum was generally between that of the East Greenland Current and the Iceland Sea temperature maxima, which suggests mixing between the two sources. The temperature was higher in 1998 than in 1990, implying an increased fraction of Recirculating Atlantic Water–Arctic Atlantic Water in the Denmark Strait overflow. The trend of decreasing salinity in the deeper layers noticed further north in the Iceland Sea was also seen in Denmark Strait.

Figure 2. Profiles of potential temperature, salinity, and Q-S diagrams (blow-up) from stations in the centre (75°N, 2°W) and at the western rim (75°N, 7°W) of the Greenland Sea gyre taken in 1988 (blue lines), 1993 (green lines), and 1998 (red lines). The water mass classification indicated on this (and on other Q-S diagrams below) is aimed for Fram Strait (see Rudels *et al.*, 1999b). PSW (Polar Surface Water), PSWw (Polar Surface Water warm) (ice melt on top of Atlantic Water from the south), RAW (Recirculating Atlantic Water), AAW (Arctic Atlantic Water), uPDW (upper Polar Deep Water), CBDW (Canadian Basin Deep Water), EBDW (Eurasian Basin Deep Water), NDW (Nordic Deep Water, comprising both Greenland Sea Deep Water (GSDW) and Norwegian Sea Deep Water (NSDW)). (/) and (\) indicate the most prominent slope of the water mass in regions where the characteristics of two water masses overlap. The water mass boundaries are shown as orientation, although the classification does not apply outside Fram Strait.

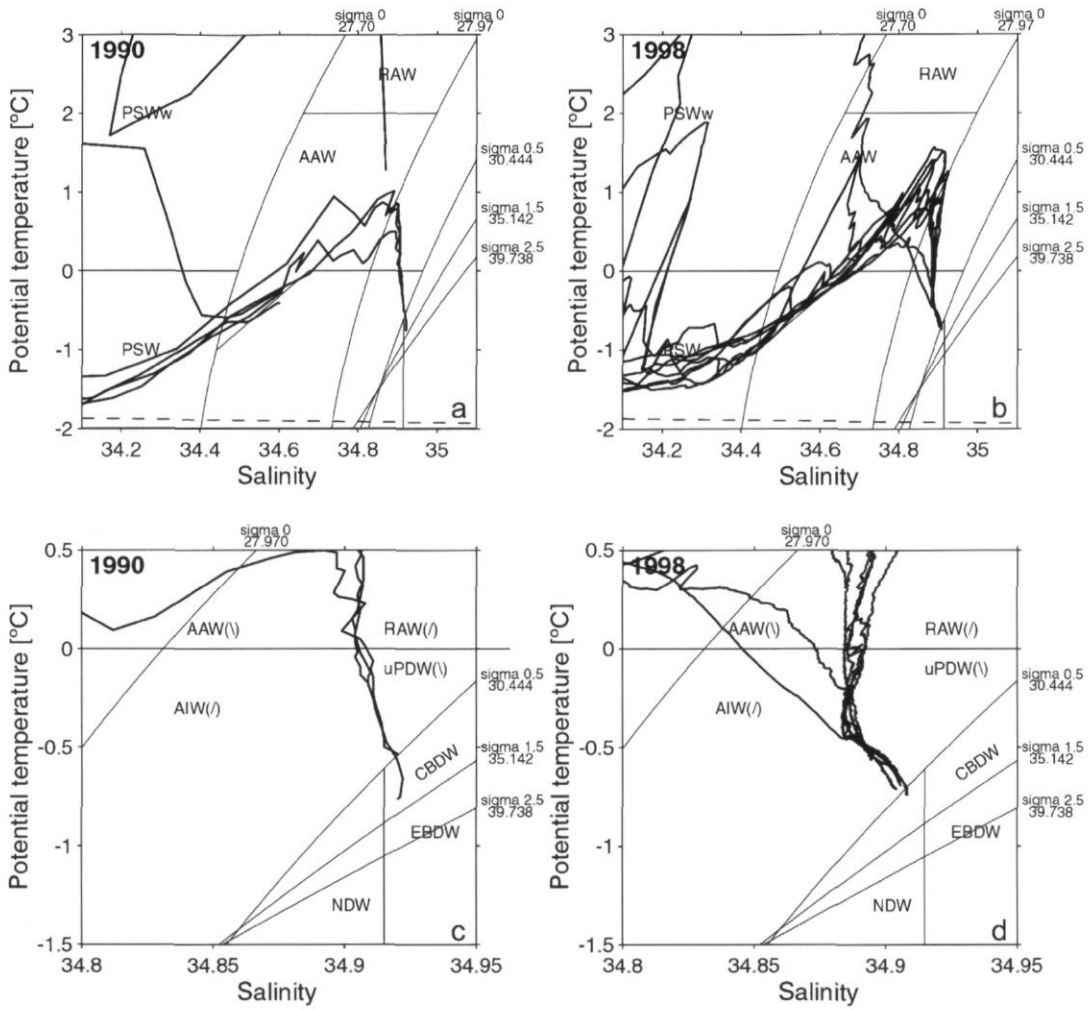


Figure 4. θ-S diagrams (full scale and blow-up) from stations in northern Denmark Strait taken in 1990 and in 1998.

Sections taken at the sill displayed yearly changes but even stronger variability over a week are present (Ross, 1984; Rudels *et al.*, 1999a). A possible cause of these rapid changes could be the encounter between the East Greenland Current and the Irminger Current from the south. The two currents contend for space in the central part of the Denmark Strait and a strong presence of Irminger Current water will obstruct the passage of the East Greenland Current. The overflow shifts westward onto the Greenland shelf, and the southward passage of denser overflow waters could temporarily become obstructed.

Summary

The variability of the Denmark Strait overflow is manifested on several time scales from a few days to more than 10 years. The contest between the Irminger Current and the East Greenland Current will affect the overflow in periods of a week and this variability is likely caused by local weather conditions. The characteristics of the intermediate water of the Iceland Sea change from year to year due to variations in the wintertime heat loss. Changes in the wind fields over periods of months to years are likely to create conditions favouring either a flow of Iceland Sea waters or East Greenland Current waters to the Denmark Strait. Variability on still longer time scales is seen in the Greenland Sea, where a change from convective deep water renewal to a period of mainly Arctic Intermediate Water production occurred in less than 10 years. During this period the deep Greenland Sea has become transformed into a passive "bay" more or less dominated by the Arctic Ocean deep waters. The shallower convection, on the other hand, creates an almost direct communication between the

Greenland Sea, the East Greenland Current and Denmark Strait. In 1998 the Greenland Sea produced water for the Denmark Strait overflow rather than for the Faeroe–Shetland overflow, which was the case in the deep convecting situation. The prominence of the Recirculating Atlantic Water in Fram Strait has decreased during the same period as the weakening of the Greenland Sea convection, indicating less recirculation and larger exchanges between the Nordic Seas and the Arctic Ocean in this density range. Changes with still longer periods are expected for the intermediate and deep waters of the Arctic Ocean, where variations in the water mass characteristics occur over 10–100 years.

The state of the convection in the Greenland Sea could be one key to the 5–10 years variability. A strong Greenland Sea convection creates a denser central dome in the Greenland Sea that intensifies the cyclonic circulation. This could, in addition to keeping the Arctic Ocean deep waters above the convecting water and closer to the rim, also force the Atlantic Water of the West Spitsbergen Current to recirculate in Fram Strait rather than enter the Arctic Ocean (Rudels *et al.*, 2000). The inflow to the Arctic Ocean would then comprise denser, deeper lying water masses formed by convection in the Greenland Sea. The stronger recirculation restricts the outflow of Arctic Atlantic Water and the Recirculating Atlantic Water would dominate in the East Greenland Current and in the Denmark Strait overflow. Weaker convection slackens the doming (Meincke *et al.*, 1997) and the recirculation in Fram Strait would diminish, causing more Arctic Atlantic Water and less Recirculating Atlantic Water to enter the East Greenland Current. Such a shift in the flow pattern would change the overflow characteristics from the fairly saline flow reported by Dickson and Brown (1994) for the 1980s, to the less saline overflow observed in the 1990s (Dickson *et al.*, 1998). The climatic conditions behind these changes in convection activity in the Greenland Sea are, of course, not answered by speculation like this, but must be found by a complete study of the different components of the climate system.

References

Aagaard, K., Swift, J. H., and Carmack, E. C. 1985. Thermohaline circulation in the Arctic Mediterranean Seas. Journal of Geophysical Research, 90: 4833–4846.

Budéus, G., Schneider, W., and Krause, G. 1998. Winter convective events and bottom water warming in the Greenland Sea. Journal of Geophysical Research, 103: 18513–18527.

Carmack, E. C. 1990. Large-scale physical oceanography of Polar Oceans. *In* Polar Oceanography, Part A, pp. 171–212. Ed. by W. O. Smith Jr. Academic Press, San Diego, California. 406 pp.

Dickson, R. R., and Brown, J. 1994. The production of North Atlantic Deep Water: sources, rates and pathways. Journal of Geophysical Research, 99: 12319–12341.

Dickson, R. R., Osborn, T. J., Hurrell, J. W., Meincke, J., Blindheim, J., Ådlandsvik, B., Vinje, T., Alekseev, G., and Maslowski, W. 1998. The Arctic Ocean response to the North Atlantic Oscillation. Journal of Climate, 13: 2671–2696.

Malmberg, S.-A. 1972. Intermediate Polar Water in the Denmark Strait: "overflow" August 1971. ICES CM 1972/C: 6. 6 pp.

Meincke, J., Rudels, B., and Friedrich, H. 1997. The Arctic Ocean–Nordic Seas Thermohaline System. ICES Journal of Marine Sciences, 54: 283–299.

Ross, G. K. 1984. Temperature—salinity characteristics of the "overflow" water in Denmark Strait during "Overflow 1973". Rapports et Procès-Verbaux des Réunions du Conseil International pour l'Exploration de la Mer, 185: 111–119.

Rudels, B., Eriksson, P., Grönvall, H., Hietala, R., and Launiainen, J. 1999a. Hydrographic observations in Denmark Strait in Fall 1997, and their implications for the entrainment into the overflow plume. Geophysical Research Letters, 26: 1325–1328.

Rudels, B., Friedrich, H. J., and Quadfasel, D. 1999b. The Arctic Circumpolar Boundary Current. Deep-Sea Research Part II, 46: 1023–1062.

Rudels, B., Meyer, R., Fahrbach, E., Ivanov, V. V., Østerhus, S., Quadfasel, D., Schauer, U., Tverberg, V., and Woodgate, R. A. 2000. Water mass distribution in Fram Strait and over the Yermak Plateau in summer 1997. Annales Geophysicae, 18: 687–705.

Swift, J. H., and Aagaard, K. 1981. Seasonal transitions and water mass formation in the Icelandic and Greenland Seas. Deep-Sea Research, 28: 1107–1129.

Swift, J. H., Aagaard, K., and Malmberg, S.-Aa. 1980. The contribution of the Denmark Strait overflow to the deep North Atlantic. Deep-Sea Research, 27: 29–42.

Worthington, L. V. 1970. The Norwegian Sea as a Mediterranean basin. Deep-Sea Research, 17: 77–84.

ICES Marine Science Symposia, 219: 326–328. 2003

Flow of Atlantic Water west of Iceland and onto the north Icelandic Shelf

Steingrímur Jónsson and Jóhannes Briem

Jónsson, S., and Briem, J. 2003. Flow of Atlantic Water west of Iceland and onto the north Icelandic Shelf. – ICES Marine Science Symposia, 219: 326–328.

The Marine Research Institute in Iceland has been monitoring the inflow of Atlantic Water onto the north Icelandic Shelf using Aanderaa current meters on one mooring since 1985. In August 1999 three moorings were deployed along the Hornbanki section and recovered a year later, and these data are used along with CTD data from the section to estimate the flow of Atlantic Water to the north Icelandic Shelf. The mean transport during this period was found to be 0.95 Sv. This is lower than a previous estimate using a single mooring from the Kogur section. No clear seasonal variations were found in the transport. Interannual variations were studied using data from the single mooring at the Hornbanki section for the period 1994–2000. There are no significant variations in the velocity, but the temperature shows interannual variability. The year 1995 stands out with extremely low temperatures and during that year an anomalously small amount of Atlantic Water was found over the north Icelandic Shelf. This may show that current measurements alone do not indicate the flow of Atlantic Water, and measurements of the water properties are needed to distinguish what kind of water is flowing along the Shelf.

Keywords: Atlantic Water, currents, Iceland, Iceland Sea, Irminger Current.

S. Jónsson: Marine Research Institute and University of Akureyri, Glerárgata 36, PO Box 224, 602 Akureyri, Iceland; J. Briem: Marine Research Institute, Skúlagata 4, PO Box 1390, 121 Reykjavík, Iceland [tel: +354 4630948; fax: +354 4630998; e-mail: steing@unak.is]. Correspondence to S. Jónsson.

Introduction

Along the west coast of Iceland there is a flow of Atlantic Water (AW) with the Irminger Current. Most of this water circulates across the Irminger Sea, but a small branch continues over the Icelandic Shelf into the north Icelandic Shelf area. Because of its importance for the ecosystem there, the Marine Research Institute in Iceland has been monitoring this flow since 1985 using Aanderaa current meters on one mooring.

Data

The mooring was situated on the Kogur section from 1985 to 1994, after which it was moved to the Hornbanki section (Figure 1). In this article, only measurements from the Hornbanki section are discussed; the measurements from the Kogur section have been described by Kristmannsson (1998). In September 1999 the measurements were extended to three moorings, H1 shallowest, H2, and H3 deepest, with a total of 5 instruments that were recovered in September 2000 (Figure 2). During that period the Hornbanki section was covered five times using CTD.

Results

As an example, Figure 2 shows the distribution of salinity on the Hornbanki section in November 1999. The extent of AW is variable in the sections. There is usually a core of AW with salinity above 35. Its position and extent are variable, however. The AW does not seem to reach deeper than 200 m. Below this depth, colder and less saline water from the Iceland Sea is present. It could be argued that the fresher water seen close to shore is really AW that has been slightly diluted by freshwater run-off from Iceland. Determining the outer boundary of the flow of AW is difficult with the present data set. However, when the CTD measurements have extended beyond the five stations, AW has not been found at the sixth station.

Monthly means of the east–west component of the velocity have been calculated. The current is highly barotropic at both stations H2 and H3, which is in agreement with the findings of Kristmannsson

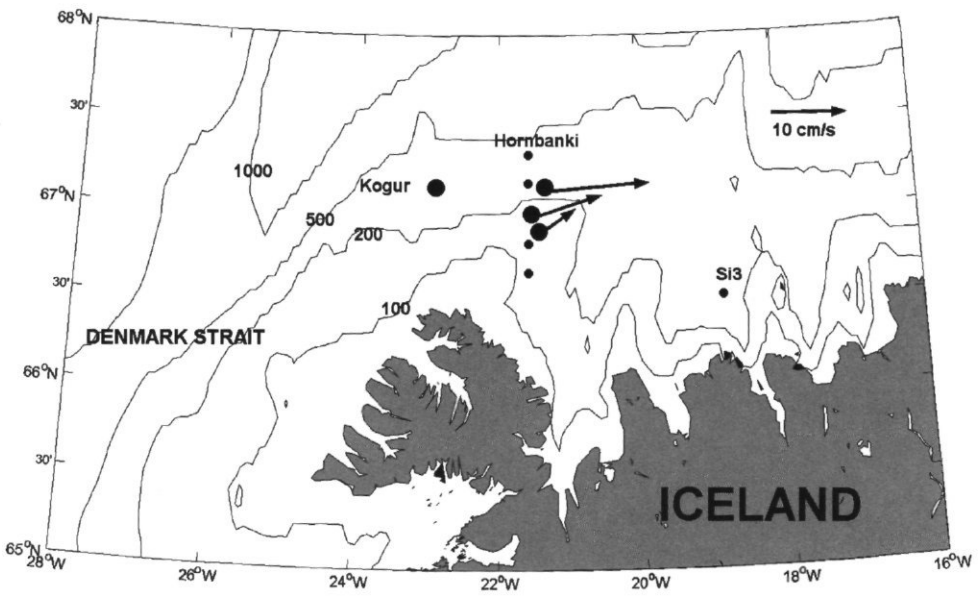


Figure 1. Map of the area. The large dots denote current meter positions and the small denote CTD stations. Depth contours are 100, 200, 500, and 1000 m. Also shown are the average currents at 80 m depth at Hornbanki during 1999–2000.

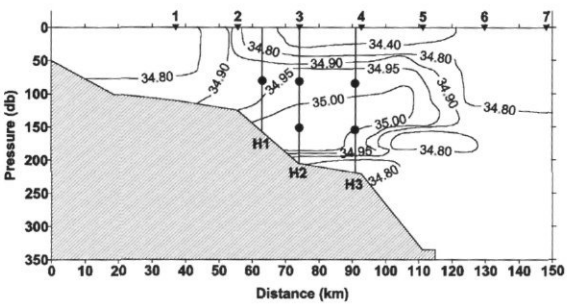


Figure 2. Salinity on the Hornbanki section in November 1999. The positions of the current meters are shown as dots. The hydrographic stations are marked at the top.

(1998) at the Kogur station. The horizontal structure of the currents is more complicated, and while the correlations between the monthly means of all the current meters are always positive, in some cases they are quite small, especially between H1 and H3, although the spatial separation between these moorings is 28 km. Almost without exception, the monthly means increase with distance from the shore. This is especially evident during spring and summer when large values are observed at the outermost mooring, H3.

There is considerable short-term variability in the records that is not picked up at all by the CTD sections. For example, the temperature at all current meters fell by almost 3°C from the time the CTD section was taken in mid-November 1999 until the end of that month. Thus the water mass properties were probably very much changed during that time.

The transport of AW through the section can be estimated using the CTD sections and the currents. The current seems to be largely depth independent and it is therefore assumed that at 80 m depth it is representative of the current from the surface down to 115 m. The current at 150 m is used below that, down to 200 m, below which there does not seem to be AW. It has been assumed that the velocity decreases linearly from the innermost mooring to 0 cm s^{-1} at 66°20′N, which is where the section plot in Figure 2 starts. South of that point, there are very shallow areas towards the shore. Determining the outer boundary of the current is not obvious and it is assumed that the current terminates midway between hydrographic stations 4 and 5. Each current meter is assigned an area of the section and the velocity perpendicular to the section is multiplied by the area, thus obtaining a transport. The results for the monthly values of the transports are shown in Figure 3. The average transport during the whole period is 0.95 Sv. Extending the transport estimate to station 5 will make the average 1.20 Sv.

The estimates presented here are lower than the 1.5 Sv estimated by Kristmannsson (1998) for the Kogur section for the period 1985–1990. During that period there was also less AW present on the north Icelandic Shelf than in 1999–2000. Kristmannsson had only one mooring and might therefore easily have overestimated the current, since it is evident from the data presented here that the current is not horizontally homogeneous.

Current measurements have been made almost continuously at H2 since September 1994. The

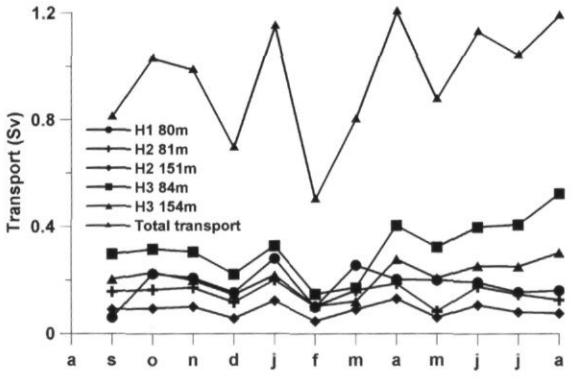


Figure 3. Monthly values of the transport. The average transport during the period September 1999 to August 2000 is 0.95 Sv. Also shown is the contribution from each of the current meters.

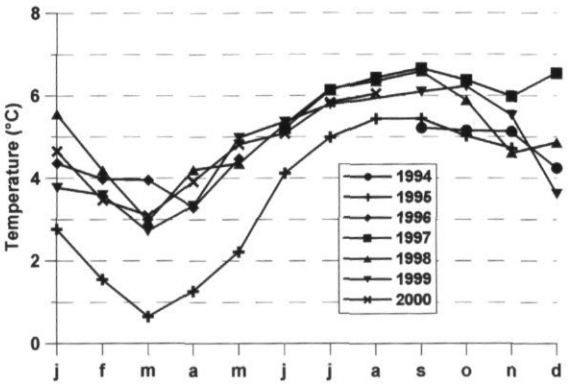


Figure 5. Monthly means of temperature from the current meter at H2 at ca. 80 m depth for different years. All available data have been used.

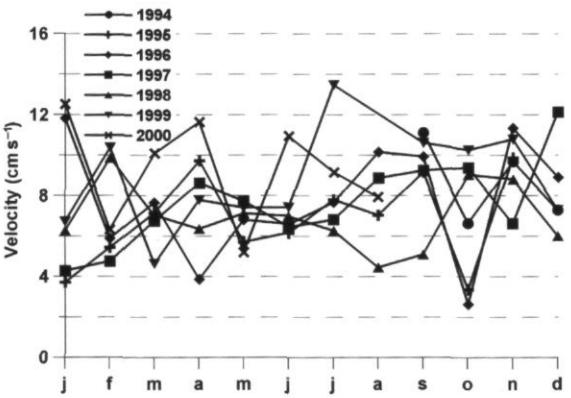


Figure 4. Monthly means of E–W component of velocity from the current meter at H2 at ca. 80 m depth for different years. All available data have been used.

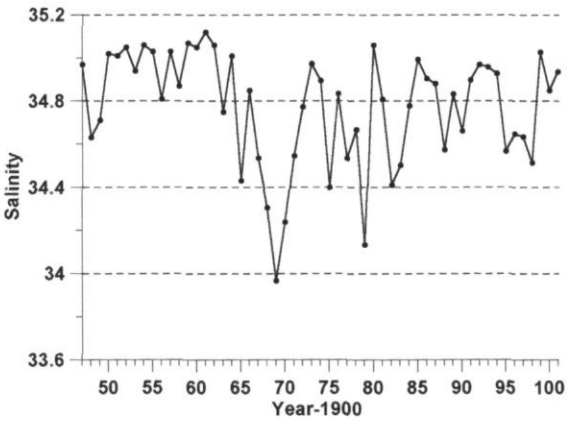


Figure 6. Salinity at 50 m depth at Siglunes (Si3 in Figure 1) in May/June since 1947.

current at nominally 80 m depth can be used to study the interannual variability of the flow of water along the Shelf. The monthly means of the east–west component of the velocity is shown in Figure 4. It shows very little seasonal and interannual variability. A look at the temperature reveals a different story (Figure 5). There is a clear seasonal signal, usually with a minimum in March and a maximum in September. Interannual variability is also present in the temperature records, since the temperature during 1995 was much lower than average for most of the year, especially in winter and spring. It was also observed on CTD cruises that little AW was observed over the north Icelandic Shelf at that time. However, no simultaneous decrease in the current was observed. This may indicate that current measurements alone do not indicate the flow of AW and measurements of the water properties are needed to distinguish the kind of water that is flowing along the shelf. Since 1996, favorable conditions with strong flow of AW have prevailed off the north coast and thus the current measurements can be assumed to measure the flow of AW during that period.

To put the results shown here in a longer term climate context the salinity measured at 50 m depth in May/June from 1947–2001 at Si3 in Figure 1 is shown in Figure 6. This illustrates the period until 1965 when warm and saline AW was dominating the north Icelandic Shelf area. During the years 1965–1971 Polar Water and drift ice were frequently observed in the area. The past few years have been characterized by the presence of AW with high temperature and salinity almost equalling that of the period before 1965.

Reference

Kristmannsson, S. S. 1998. Flow of Atlantic Water into the northern Icelandic shelf area, 1985–1989. ICES Cooperative Research Report 225, 124–135.

ICES Marine Science Symposia, 219: 329–332. 2003

Winter mixed layer nutrients in the Irminger and Iceland Seas, 1990–2000

Jón Ólafsson

Ólafsson, J. 2003. Winter mixed layer nutrients in the Irminger and Iceland Seas, 1990–2000. – ICES Marine Science Symposia, 219: 329–332.

The winter mixed layer depth was variable in the Irminger and Iceland Seas in the period 1990–2000, but reached much deeper in the Irminger Sea as a halocline limits vertical convection in the Iceland Sea. The ranges of the related variations in salinity, density, and nutrient concentrations were similar in both regions. The nutrient variations were proportionately greater in the Iceland Sea. Statistical relationships between mixed layer depth and surface water properties were stronger for the Iceland Sea, but interannual variations in advection had more effects in the Irminger Sea.

Keywords: Iceland Sea, Irminger Sea, mixed layer, nutrients, winter.

Jón Ólafsson: University of Iceland and Marine Research Institute, Skúlagata 4, PO Box 1390, IS 121 Reykjavik, Iceland.

Introduction

The Irminger and Iceland Seas undergo strong seasonal variations. Relatively warm and saline Atlantic Water prevails west of Iceland in the Irminger Sea, but northeast of Iceland in the Iceland Sea Arctic Water usually predominates but some Polar Water influence in the surface layers is common (Malmberg and Kristmannsson, 1992).

Convective mixing is induced in both regions in winter by winds and heat loss to the atmosphere. The nutrient concentrations in the surface layer that result from the winter vertical mixing processes may vary interannually. The nutrients from vertical mixing and those carried by eddy diffusion into the euphotic zone have strong influence on the regional scope for new production and uptake of CO_2 from the atmosphere (Dugdale and Goering, 1967). Advective processes may also affect the supply of new nutrients and horizontal and vertical Ekman transfers can supply nutrients for new production in the North Atlantic (Williams and Follows, 1998).

Using data from February 1991 it has previously been shown that the preformed nutrient concentrations in the Irminger Sea are significantly higher than those of the central Iceland Sea (Stefánsson and Ólafsson, 1991). The objective of the present investigation was to examine the interannual variations in the winter-time nutrient concentrations and their relation to surface layer properties and the depth of the mixed layer.

Materials

Data on water column properties in winter are from a station at 1000-m depth (64°20′N 28°00′W) west of Iceland in the Irminger Sea and from a station NE of Iceland at 1850-m depth in the central Iceland Sea (at 68°00′N 12°20′W).

Generally the stations have been worked in February, but occasionally in January (Irminger Sea 1994) or early March. Because meteorological conditions prevented occupation of the Irminger Sea station in 1993 and the Iceland Sea station in 1998, data from adjacent stations, 20–30 nmi distant, are used.

The mixed layer depth (MLD) was evaluated from CTD data as the shallowest maximum in $d\sigma\theta/dz$. The surface layer nutrient concentrations and oxygen saturation were calculated as the mean of all observations in the 0- to 50-m depth interval.

Results and discussion

The conditions in the Irminger and Iceland Seas differ substantially in winter (Figure 1). The Iceland Sea surface is about 6°C colder than the Irminger Sea and the salinity about 0.3 lower.

In the Irminger Sea the winter MLD ranged from 263 m in 1994 to 765 m in 1995 (Figure 2). The 1994 early January observation was most likely obtained

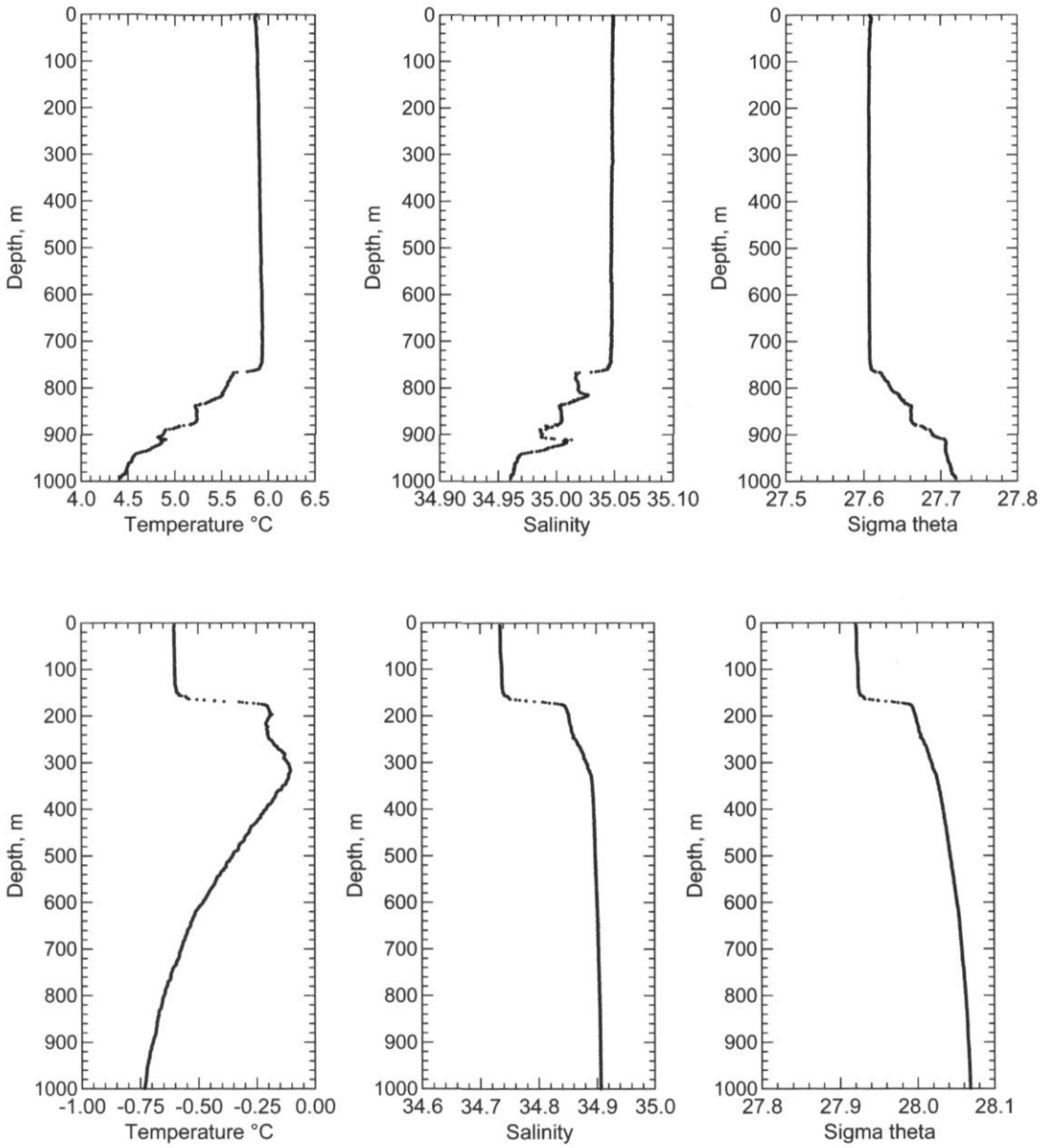


Figure 1. Vertical profiles from February 1995. The upper three frames show temperature, salinity, and density in the Irminger Sea and the lower profiles the same properties in the Iceland Sea. The bottom depth is just over 1000 m in the Irminger Sea, but for the Iceland Sea the bottom depth is 1850 m; only the uppermost 1000 shown here.

before winter conditions fully developed. In the Iceland Sea, the MLD was always less than in the Irminger Sea. It ranged from 82 m in 1997 to 210 m in 1993. The reason for these different regional characteristics is evident from late summer data (J. Ólafsson, pers. comm.). Then salinity and temperature contributed almost equally to the stratification of the uppermost 100 m in the Iceland Sea. However, in the Irminger Sea, the contribution of temperature to the stratification is overwhelming (about 85%) and a halocline offers little resistance to convective mixing caused by surface heat loss.

The dissolved oxygen saturation ranged from 94 to 100% in both locations, indicating active air-sea gas fluxes. The oxygen saturation was frequently marginally higher in the Iceland Sea than in the Irminger Sea.

It is evident that apart from the MLD in the Irminger and Iceland Seas the ranges over which the variations of surface layer properties extend were

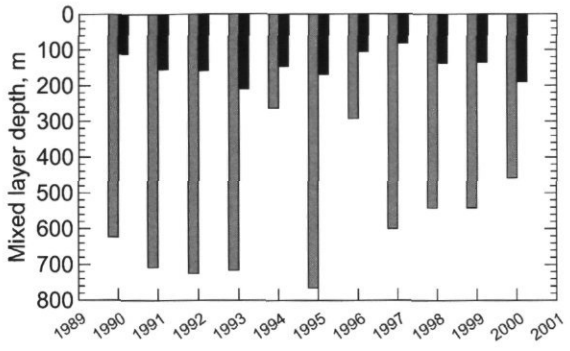


Figure 2. Mixed layer depths in winter in the Irminger Sea (grey) and in the Iceland Sea (dark grey) 1990–2000.

similar in both ocean regions (Figure 3). The winter nutrient concentrations in the Irminger Sea were around 30% higher than in the Iceland Sea. Therefore, the potential impact of the interannual nutrient concentration variations on new production will be proportionately greater in the Iceland Sea.

Statistical linear regressions between the MLD and the surface water properties reveal significant positive relationships, except for nitrate in the Irminger Sea (Figure 3). The slopes of the regression lines are higher for the Iceland Sea than for the Irminger Sea and the correlation coefficients explain greater proportions of the variations in the Iceland Sea. For the Iceland Sea r^2 is 0.62, 0.75, 0.68, and 0.65 for salinity, sigma-t, phosphate and nitrate,

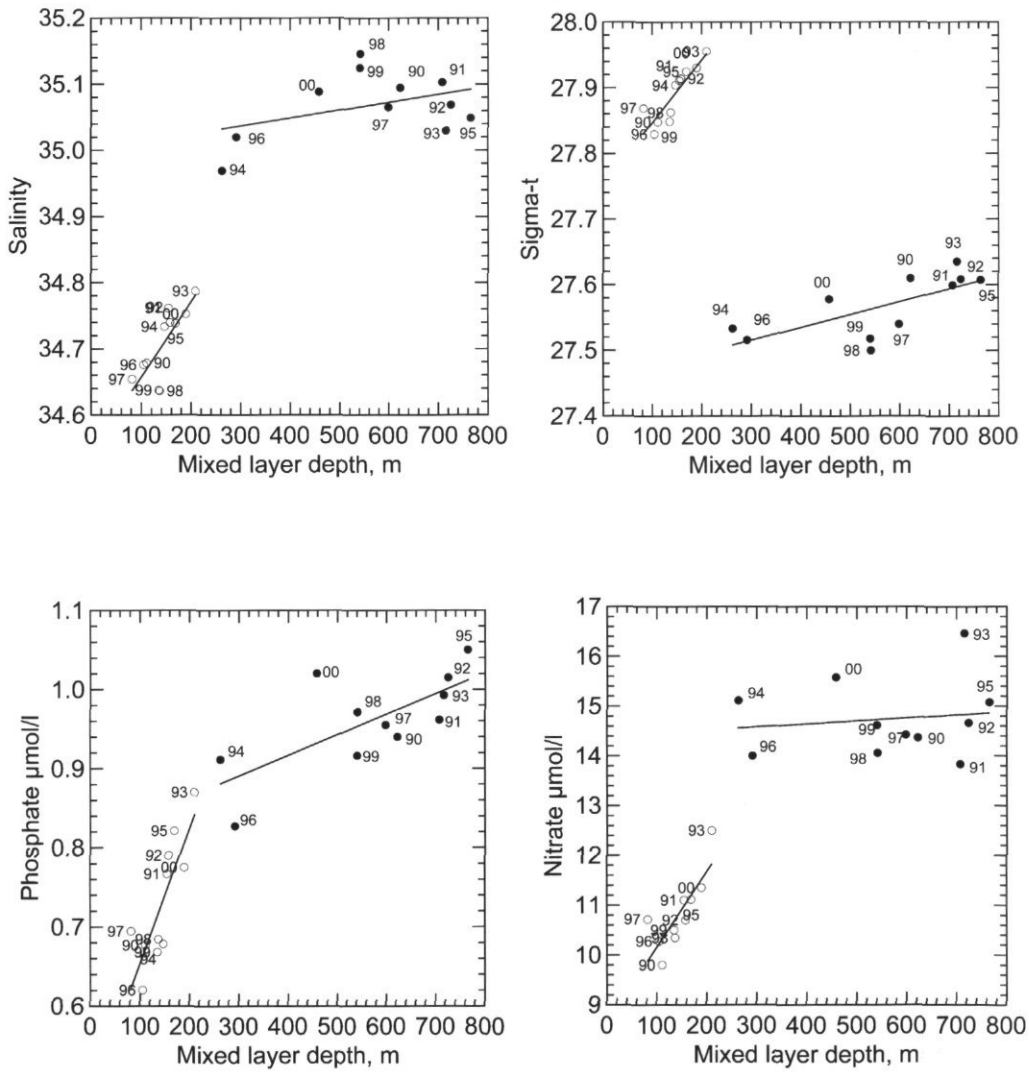


Figure 3. The relationships of surface layer properties to the mixed layer depth in winter. Iceland Sea: open circles and Irminger Sea: filled circles. Numbered symbols indicate years.

respectively, but for the Irminger Sea r^2 is 0.16, 0.50, 0.52, and 0.02, respectively, for the same properties.

For the Iceland Sea this suggests that over the period examined here, convective mixing has essentially reached into subsurface water of relatively constant composition. In the Irminger Sea, however, where mixing extends to far greater depth, there were significant variations in the subsurface water over this period. Thus, in the early years of the period, up to 1996, the region was influenced by Labrador Sea Water which had spread rapidly from its region of formation (Bersch *et al.*, 1999). In the latter part of the period more direct influence from the North Atlantic Current resulted in higher salinity and temperature in the Irminger Sea (Malmberg and Valdimarsson, 2002). The effects of these hydrographic changes are quite evident in the years 1997, 1998, and 1999, particularly in the relations between the MLD, salinity, and density (Figure 3).

Conclusions

The Irminger Sea and the Iceland Sea are distinctively different regions in terms of winter-time properties. The MLD is much greater in the Irminger Sea, where the salinity and nutrient concentrations are higher. These winter-time properties do, however, exhibit significant interannual variations, which potentially may affect the new production in spring and summer. The interannual nutrient variations are similar in magnitude in both regions. As the nutrient concentration levels in winter are lower in the Iceland Sea, the variations are proportionately larger there and therefore likely to have greater impact on new production than in the Irminger Sea.

Acknowledgements

This is a contribution from the Nordic Council of Ministers Project: Carbon Cycle and Convection in the Nordic Seas and the EC Project: MAST III ESOP 2.

References

Bersch, B., Meincke, J., and Sy, A. 1999. Interannual thermohaline changes in the northern North Atlantic 1991–1996. Deep-Sea Research II, 46: 55–75.

Dugdale, R. C., and Goering, J. J. 1967. Uptake of new and regenerated forms of nitrogen in primary productivity. Limnology and Oceanography, 12: 196–206.

Malmberg, S. A., and Kristmannsson, S. S. 1992. Hydrographic conditions in Icelandic waters, 1980–1989. ICES Marine Science Symposia, 195: 76–92.

Malmberg, S. A., and Valdimarsson, H. 2003. Hydrographic conditions in Icelandic Waters, 1990–1999. ICES Marine Science Symposia, 219: 50–60. (This volume.)

Stefánsson, U., and Ólafsson, J. 1991. Nutrients and fertility of Icelandic waters. Rit Fiskideildar, 12: 1–56.

Williams, R. G., and Follows, M. J. 1998. The Ekman transfer of nutrients and maintenance of new production over the North Atlantic. Deep-Sea Research I, 45: 461–489.

ICES Marine Science Symposia, 219: 333–336. 2003

Mesoscale, interannual, and seasonal hydrological variability over the French continental shelf of the Bay of Biscay during the 1990s

I. Puillat, P. Lazure, A. M. Jégou, B. Planque, and L. Lampert

Puillat, I., Lazure, P., Jégou, A. M., Planque, B., and Lampert, L. 2003. Mesoscale, interannual, and seasonal hydrological variability over the French continental shelf of the Bay of Biscay during the 1990s. – ICES Marine Science Symposia, 219: 333–336.

Hydrological processes on the French continental shelf of the Bay of Biscay are strongly influenced by the high freshwater run-offs from the Loire and Gironde rivers, which are expected to result in high variability of salinity distribution. However, this variability is poorly understood owing to the lack of field salinity data. Although some mesoscale structures have been recognized, most have rarely been studied specifically. Similarly, specific studies of the interannual and seasonal haline variability have not yet been carried out. Here, we analyse unpublished hydrological data collected during the 1990s. We describe several mesoscale structures: southern Brittany upwellings, lower salinity lenses (originating from river plume), and the so-called cold pool. The extent of the interannual and seasonal variability of the low salinity ($S < 35$) surface water is also described, and it is shown how wind and river run-off influence variability (mesoscale, interannual, and seasonal).

Keywords: Bay of Biscay, cold pool, continental shelf, hydrology, low salinity lens, seasonal variability, upwelling.

I. Puillat [e-mail: ipuillat@lseet.univ-tln.fr], P. Lazure [e-mail: plazure@ifremer.fr], A. M. Jégou [e-mail: amjegou@ifremer.fr]: IFREMER/DEL/AO, BP70, F-29280 Plouzane, France; B. Planque [e-mail: bplanque@ifremer.fr]: IFREMER/Laboratoire d'Ecologie Halieutique, BP 21105, F-44311 Nantes Cedex 03, France. L. Lampert [e-mail: lampert@shom.fr]: SHOM/CMO/RE, 13, rue du Chatellier, BP 30316, F-29603 Brest Cedex, France. Correspondence to P. Lazure.

Introduction and method

The salinity distribution over the French continental shelf is strongly influenced by the discharge from the Loire and Gironde rivers (~900 $m^3 s^{-1}$), as well as by wind-induced circulation. In addition to mesoscale variability (horizontal scale: 10–100 km; time scale: days to months), it is assumed that the salinity distribution varies seasonally and interannually in response to seasonal and interannual variability in river discharge and wind conditions. Nevertheless, salinity records have been scarce and some mesoscale structures that have been reviewed in the past (e.g. Koutsikopoulos and le Cann, 1996) have not yet been investigated specifically.

Here we analyse previously unpublished *in situ* hydrological data collected during the past decade over the Bay of Biscay French continental shelf. We investigate three main mesoscale physical phenomena: upwellings, lower salinity water lenses, and the cold pool. The cold pool is constituted by a water mass isolated on the bottom between the ~50 and ~120 m isobaths with temperatures varying between 11 and 12°C from spring to autumn (Vincent and Kurc, 1969; Vincent, 1973). We study the interannual haline variability by comparing the spreading of the surface low salinity water ($S < 35$) on monthly haline maps from selected years and we relate the extent of this water to meteorological forcings (river run-off and wind). Finally, the seasonal haline variability is assessed by comparing an average spring situation (mean salinity from March to May) to an average autumn situation (mean salinity from September to October).

Results

Mesoscale structures

Past studies have revealed upwellings along the coast of Landes and Vendée (south of 47°N). Here, using *in situ* temperature measurements, we provide the first evidence for upwelling off southern Brittany (Figure 1). We also show an example of a lower

salinity lens (L, Figure 2), a structure frequently observed in this area. The spatio-temporal properties of this structure are: vertical length: ~surface–40 m; horizontal length: ~50–100 km; duration: ~1 week at least. Those two types of structure have been linked to north–northwesterly winds (over several days) which push the low salinity surface coastal waters offshore (Ekman drift), generating a coastal upwelling where saltier water is advected from the bottom to the surface layer in the coastal area (Figure 2).

Bottom temperature measurements reveal the extent of the cold pool (CP in Figures 3 and 4). There is significant interannual variability in the

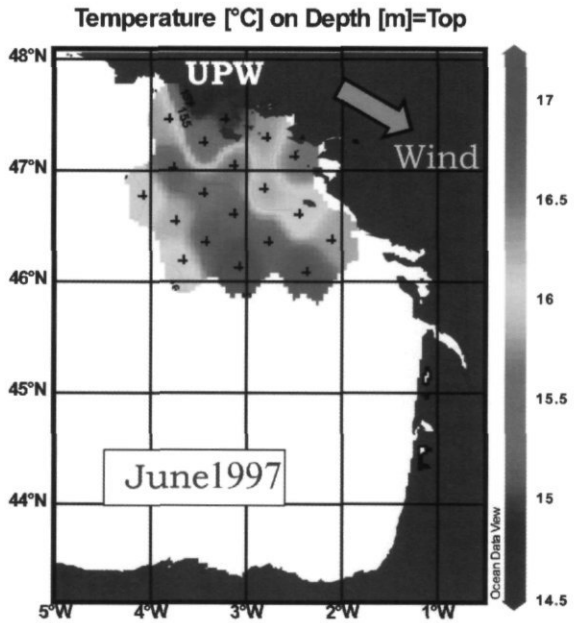


Figure 1. Surface temperature map calculated from Modycot 97-1 data (June 1997, from SHOM/CMO, France). UPW = southern Brittany upwelling. Windspeed: 8–12 m s^{-1}.

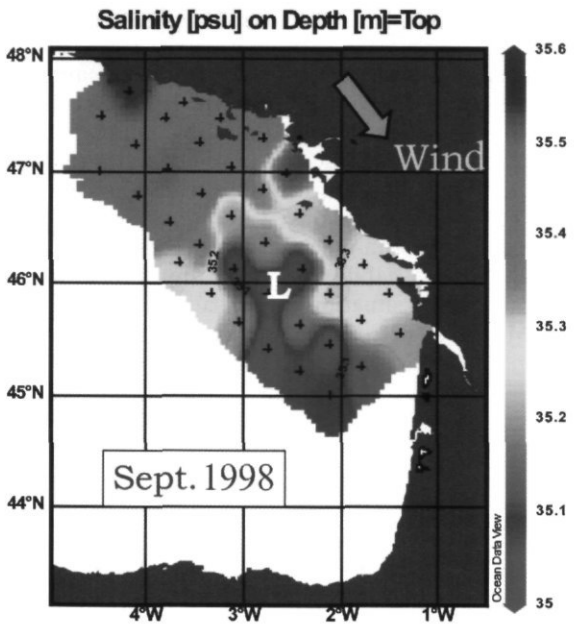


Figure 2. Surface salinity maps calculated from Modycot 98-4 data (September 1998, from SHOM/CMO, France). L = low salinity lens. Windspeed 8–12 m s^{-1}.

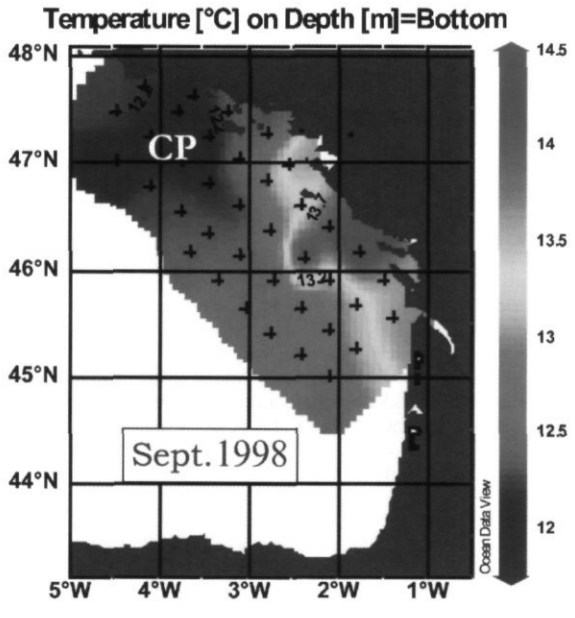


Figure 3. Bottom temperature map calculated from Modycot 98-4 cruise (September 1998, from SHOM/CMO, France). CP = Cold Pool (T < 12.2°C).

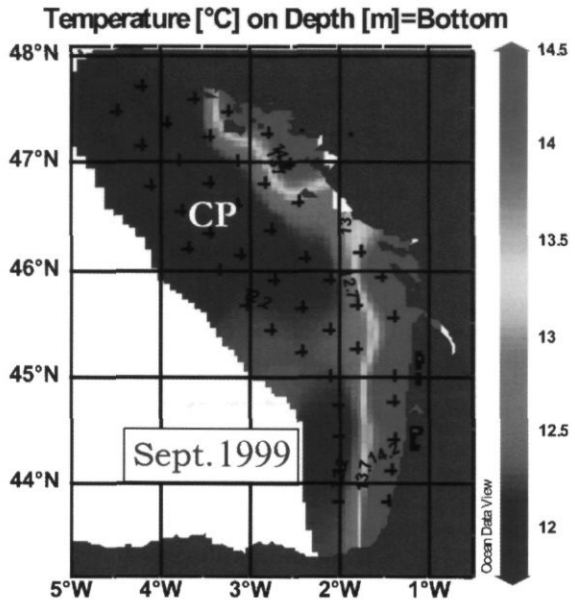


Figure 4. Bottom temperature map calculated from Modycot 99-3 cruise (September 1999, from SHOM/CMO, France). CP = cold pool (T < 12.2°C).

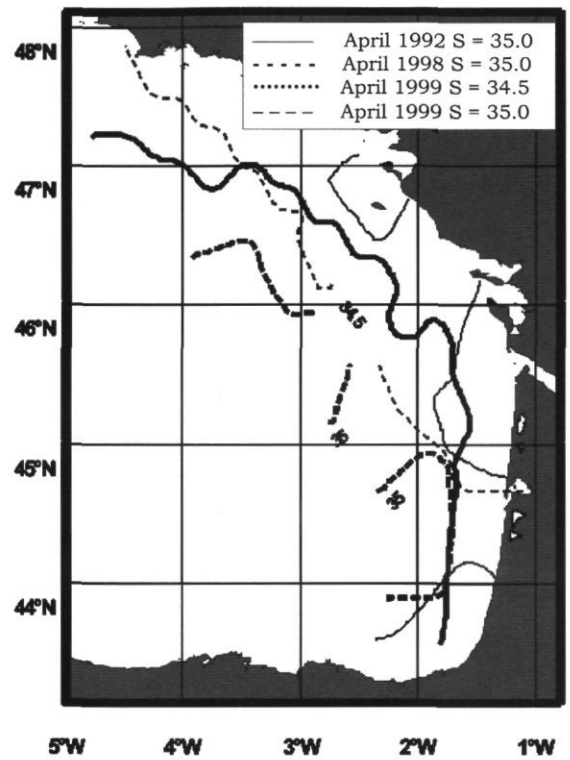


Figure 5. Interannual variability of the low salinity (S < 35) water extent in the surface layer in April 1992, 1998, and 1999.

extent of the cold pool between September 1998 and September 1999. We assume that in September 1998 wind-induced mixing down to the bottom reduced thermal stratification and hence eroded the cold pool.

Interannual variability in surface salinity

We show that the spreading of low salinity surface water (S < 35) varies strongly between years (Figure 5) depending on the winds and river run-off (Figure 6). These two forcings can act on different time

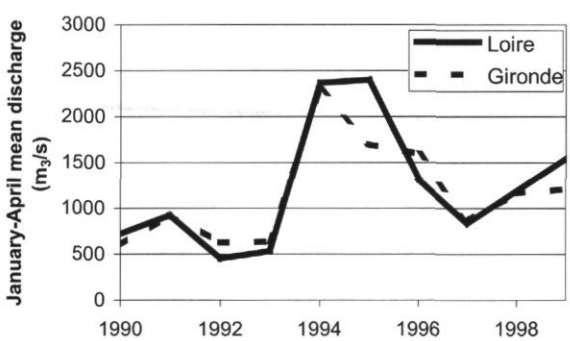


Figure 6. January to April mean discharge of the Loire and Gironde rivers between 1990 and 1999.

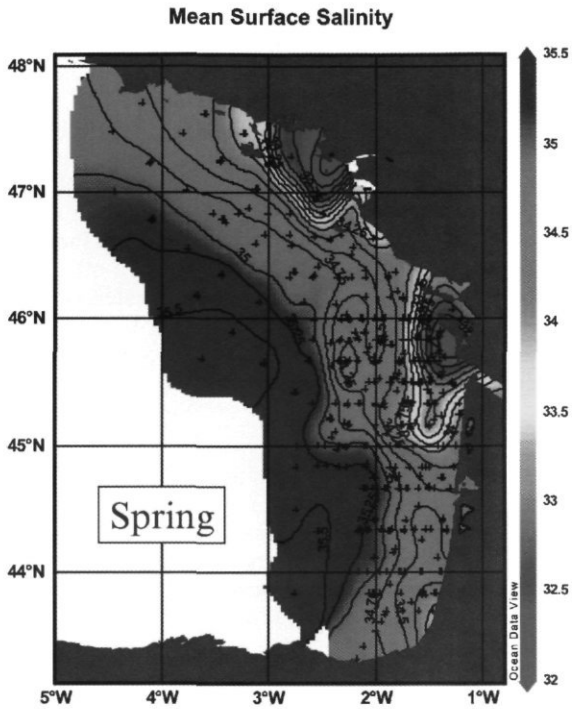


Figure 7. Spring (March–May) mean surface salinity map. Data from April 1992, March–May 1994 and 1998, April 1999, March 2000.

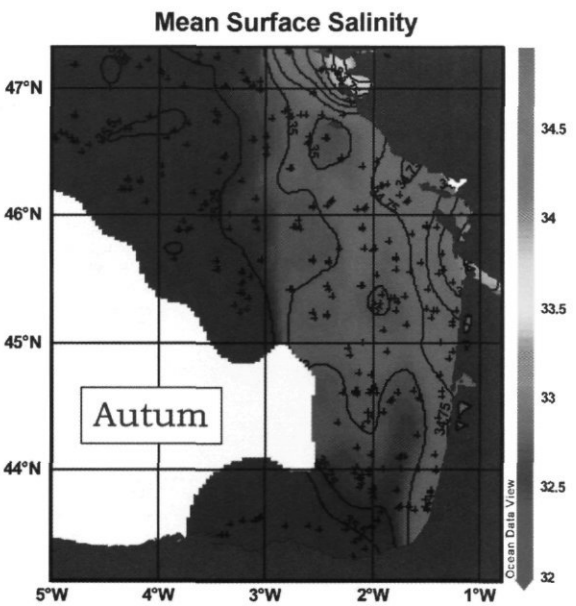


Figure 8. Autumn (September–November) mean surface salinity map. Data from September–October 1992 and 1994, September 1998 and 1999.

scales: from a few days for winds to a few months for river run-off. In April 1992, the low salinity water located closest to the coast corresponds to the lowest river discharge recorded over the 1990s (Figure 6: 500–700 $m^3 s^{-1}$ in January–April 1992). In April 1998, the spread of low salinity water is intermediate between that in 1992 and 1999 and corresponds to intermediate river run-off. In April 1999, low salinity water spreads furthest offshore in response to the synergy of high river run-off (1200 and 1600 $m^3 s^{-1}$) and strong northwesterly wind (15 m s^{-1}) during the first weeks of April. In the vertical dimension (not shown), this low salinity water extends in a ~20–40 m layer from the surface.

Seasonal variability in surface salinity

Average seasonal salinity maps have been constructed by combining 4–6 years of data (Figures 7, 8). Although the interannual variability may have distorted these seasonal patterns, there are clear differences between spring and autumn. In spring, the low salinity water ($S < 35$) borders the entire French coast (Figure 7) in a band 50–100 km wide. Minimal average salinities of 32–34 are encountered in the vicinity of the Loire and Gironde estuaries. In autumn this band is less marked (Figure 8): it has disappeared in southern Brittany and it is half the width south of 44°30′N. All over the shelf, salinity is greater than 34.

Conclusion

This study reveals the strong hydrological variability encountered over the French continental shelf of the Bay of Biscay. We show that wind events and/or river run-off drive the generation of surface mesoscale structures. In addition, they are responsible for the distribution of the surface salinity and contribute to its interannual variability. These forcings act on a time scale of a few days to ~6 months. Our results suggest that mesoscale and interannual variability can be equal to or greater than seasonal variability.

Acknowledgements

We thank CMO (Brest), Ecohal/IFREMER (Nantes), and SISMER for allowing us to use the hydrological data presented here, but also the Remote Sensing Data Analysis Service (RSDAS, Plymouth, UK, http://www.npm.ac.uk/rsdas/) for infrared images and R. Schlitzer for the free soft Ocean Data View (http://www.awi bremerhaven.de/GEO/ODV/2002). For the river run-off data set we thank the DIREN centers: service du bassin Loire-Bretagne, the autonomous port of Bordeaux, the Ministère de l'Environnement: banque nationale de données pour l'hydrométrie et l'hydrologie.

References

Koutsikopoulos, C., and Le Cann, B. 1996. Physical processes and hydrological structures related to the Bay of Biscay anchovy. Sciencia Marina, 60 (2 Suppl), 9–19.

Vincent, A., and Kurc, G. 1969. Hydrologie, variations saisonnières de la situation thermique du Golfe de Gascogne en 1967. Revue des Travaux de l'Institut scientifique des Pêches maritimes, 33: 79–96.

Vincent, A. 1973. Les variations de la situation thermique dans le Golfe de Gascogne en 1969 et 1979. Revue des Travaux de l'Institut scientifique des Pêches maritimes, 37: 5–18.

ICES Marine Science Symposia, 219: 337–339. 2003

Aspects concerning the occurrence of summer upwelling along the southern Bay of Biscay during 1993–2000

Julio Gil and Ricardo Sánchez

Gil. J., and Sánchez, R. 2003. Aspects concerning the occurrence of summer upwelling along the southern Bay of Biscay during 1993–2000. – ICES Marine Science Symposia, 219: 337–339.

The occurrence of coastal upwelling along the southern Bay of Biscay in response to easterly winds shows clear seasonal variability, with peak development centred during the spring and summer. The historical series (1993–2000) of autumn temperatures has allowed identification of different patterns of upwelling. One of the main conclusions deals with the non-permanent character of the upwelling fringe along the Galicia–Cantabrian coast. This feature is related to the magnitude, time-span and synoptic occurrence of the winds. The occurrence of westerly winds pushes warm waters onto the coastal regions and leads to a reversal of the current pattern over the continental shelf. This may affect the survival of fish recruits *via* reduced primary production and its subsequent affect on zooplankton.

Keywords: Bay of Biscay, hake recruitment, upwelling.

J. Gil and R. Sánchez: Instituto Español de Oceanografía, PO Box 240, E-39080, Santander, Spain [tel: +34 94227 5033; fax: +34 94227 5072; e-mail: julio.gil@st.ieo.es, rleal@ualg.pt]. Correspondence to J. Gil.

Introduction

Meridional displacements of the Azores High govern meteorological conditions offshore of the Iberian Peninsula. In summer, the Azores High drifts towards the north and the trade winds blow from the northeast along the Cantabrian and Galician coast. A conspicuous upwelling appears along with an equatorward surface flow. On the contrary, the weakening or southward migration of the Azores High leaves the western Iberian Peninsula under the influence of westerly winds. The upper layer circulation pattern is characterized by a poleward surface flow with absence of coastal upwelling.

In the Cantabrian Sea during summer the water mass distributions over the shelf and adjacent areas depend on the strength of the upwelling. If upwelling is strong and persistent, there is a coastal band of cold, upwelled water over the shelf area, an intermediate zone of warm-core anticyclonic mesoscale eddies, and cool waters along the outer slope. On the other hand, if summer upwelling is weak or the wind regime is westerly, the picture is different, with warm water over the shelf and relatively cool water off the shelf break (Sánchez and Gil, 1999). In this article the changes in the upwelling strength off northern Spain during the 1990s are examined.

Data and methods

Data come from the Spanish autumn bottom-trawl surveys between 1993 and 2000. Sampling stations were distributed throughout the continental shelf, slope, and adjacent oceanic area to resolve mesoscale features. The wind data come from a Seawatch buoy anchored at 43°44′N, 6°10′W (http//www.puertos.es/clima.html). To show the variability in upwelling strength, the temperature field at 50 m was chosen. At this level, the horizontal temperature gradients are maximum and the temperature front between the onshore-upwelled waters and warm offshore waters is clearly defined.

Results and discussion

The early autumn distribution of water masses along the Cantabrian Sea depends to a great extent on the wind regime prevalent in July and August. Unfortunately, buoy wind measurements are available only from 1997 onwards. The wind time-series shows that in July–August 1997, the u-component of wind (east–west) was persistently negative (towards the west), clearly under the influence of the easterly trade winds. On the contrary, in 1998, the

zonal wind was predominantly westerly from the middle of July to the end of August. As a result, two different oceanographic situations were observed in the two years. In 1998 (Figure 1B) coastal upwelling was weak. There was general intrusion of warm water over most of the Cantabrian Sea shelf area. A radically different situation occurred in 1997 (Figure 2B), when a strip of warm water (over 16°C) separated the coastal band of cold upwelled water from the cool offshore oceanic water.

Three different hydrographic patterns were observed between the years 1993 and 2000. The first one corresponds to a distribution of water masses similar to 1998 and was also observed in 1993, 1999, and 2000 (Figures 1A–D). The upper homogeneous layer was deep and temperatures at 50 m were relatively high. An intense pycnocline between 50 m and 100 m was ubiquitous (not shown). The second pattern was similar to 1997 and also observed in 1994 (Figures 2A, B) when a conspicuous temperature front separated the coastal band of cold upwelled water from the offshore warm waters. The narrowness of the coastal upwelling permitted a succession of anticyclonic warm cores eddies to develop over offshore areas but relatively close to the shelf. Finally, in 1995 and 1996 (Figures 3A, B) the width of the cold coastal band was considerable, yet it did not appear as a continuous feature along the shelf area. The non-continuous nature of the upwelling may reflect wind reversals.

The establishment of any of these hydrographic patterns brings about important, ecological consequences. When upwelling is absent along the shelf area, the intense thermocline that separates the waters at 50 m (~17°C) from those at 100 m (~12°C) limits the vertical diffusion of nutrients onto the euphotic layer. In contrast, when upwelling takes

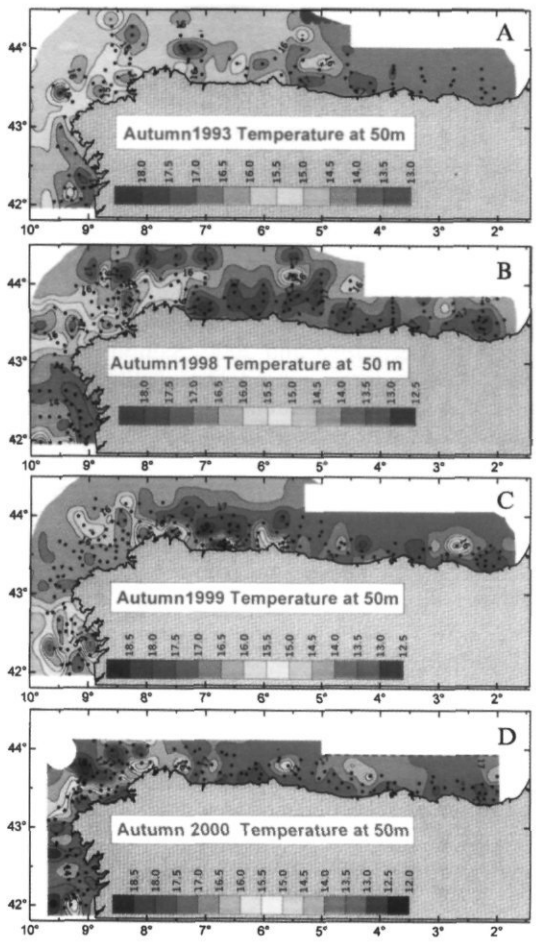


Figure 1. Temperature at 50 m (A) 1993, (B) 1998, (C) 1999, and (D) 2000.

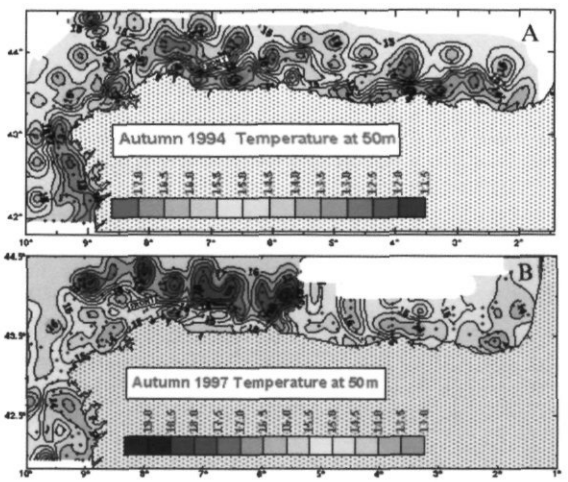


Figure 2. Temperature at 50 m (A) 1994, and (B) 1997.

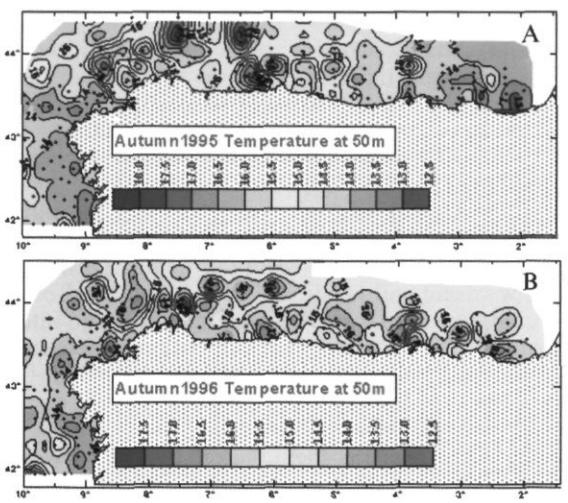


Figure 3. Temperature at 50 m (A) 1995, and (B) 1996.

place, the vertical temperature gradients are minimized and the vertical diffusion is enhanced.

The importance of the generation of mesoscale activity is also important, as shown by Gil (1995) and Gil *et al.* (2002). The presence of mesoscale structures (cyclonic and anticyclonic rings, meandering fronts, filaments) has been observed to enhance nutrification and to affect zooplankton and ichthyoplankton distributions. In the low upwelling strength years, the mesoscale activity is generally scarce, with nearly homogeneous horizontal temperature fields (see the 1993 temperature distribution). Conversely, in years when the upwelling is well developed (1994), there are strong horizontal temperature gradients and conspicuous mesoscale ring activity.

Relationships between recruitment of demersal fishes (such as European hake) and upwelling have been studied elsewhere (Sánchez and Gil, 1999; Sánchez *et al.*, 2002). It is proposed that the lack of mesoscale generation in years under upwelling unfavourable winds may affect the survival of fish recruits *via* reduced primary production and its subsequent effect on zooplankton and ichthyoplankton.

References

Gil, J. 1995. Inestabilidades, fenómenos de mesoescala y movimiento vertical a lo largo del borde sur del Golfo de Vizcaya. Boletín del Instituto Español de Oceanografía, 11: 141–159. (In Spanish.)

Gil, J., Valdés, L., Moral, M., Sánmchez, R., and Garcia-Soto, C. 2002. Mesoscale variability in a high-resolution grid in the Cantabrian sea (southern Bay of Biscay), May 1995. Deep-Sea I. (In press).

Sánchez, F., and J. Gil. 1999. Hydrographic mesoscale structures and Poleward Current as a determinant of hake (*Merluccius merluccius*) recruitment in southern Bay of Biscay. ICES Journal of Marine Science, 57: 152–170.

Sánchez, R., Sánchez, F., and Gil, J. 2003. The optimal environmental window that controls hake (*Merluccius merluccius*) recruitment in the Cantabrian Sea. ICES Marine Science Symposia, 219: 415–417. (This volume.)

ICES Marine Science Symposia, 219: 340–342. 2003

Temperature and salinity fluctuations along the Basque Coast (southeastern Bay of Biscay), from 1986 to 2000, related to climatic factors

Victoriano Valencia, Ángel Borja, Almudena Fontán, Fiz F. Pérez, and Aida F. Ríos

Valencia, V., Borja, Á., Fontán, A., Pérez, F. F., and Ríos, A. F. 2003. Temperature and salinity fluctuations along the Basque Coast (southeastern Bay of Biscay), from 1986 to 2000, related to climatic factors. – ICES Journal of Marine Science, 219: 340–342.

Time-series of oceanographic and meteorological data collected off the Basque coast, SE Bay of Biscay, show tendencies concurring with the anomaly patterns described for the NE Atlantic area as a whole during the late 1980s and 1990s. Temperature and salinity maxima were reached in the early 1990s after a period of dry and relatively warm winters related to the dominance of south and westerly winds. In the SE corner of the Bay of Biscay, this atmospheric regime increases the occurrence of Eastern North Atlantic Central Water (ENACW) over the continental shelf. Other maxima were recorded during the second half of the 1990s, but the correspondence between the increase of temperature and salinity and the occurrence of ENACW type waters is lower than in the previous period of observation. It would appear that the same climatic regime that favours the intrusion of the ENACW into the SE Bay of Biscay is also associated with warm and dry weather conditions that maintain the temperature-salinity characteristics of the Atlantic Central Waters in this area.

Keywords: Bay of Biscay, climate, decadal changes, Eastern North Atlantic Central Water, temperature-salinity.

V. Valencia, A. Borja, and A. Fontán: Fundación AZTI, Herrera Kaia Portualdea, z/g. 20110 Pasaia (Gipuzkoa) Spain [tel: +34 943 004800; fax: +34 943 004801 e-mail: vvalencia@pas.azti.es; aborja@pas.azti.es; afontan@pas.azti.es]. F. F. Pérez and A. F. Ríos: Instituto de Investigación Mariñas (CSIC) C/ Eduardo Cabello, 6. 36208 Vigo, Spain [e-mail: fiz@iim.csic.es; aida@iim.csic.es]. Correspondence to V. Valencia.

Introduction

Oceanographic data collected at 43°30′N 2°W over the continental shelf of the SE Bay of Biscay (Figure 1) show a significant coupling with the meteorological data collected in the same region of the NE Atlantic Ocean (Valencia, 1993; Valencia *et al.*, 1996). The monthly time-series of temperature and salinity (from surface to 100 m water depth) for the shelf waters of the Basque coast from 1986 to 2000 show tendencies that concur with the general anomaly patterns described for the NE Atlantic Ocean during the late 1980s and 1990s. The simultaneous increase in temperature and salinity of the surface waters from the mid-1980s until 1992 has been reported by several authors, both from coastal monitoring and from oceanic cruises, all around the intergyre zone of the NE Atlantic (e.g. Dauvin *et al.*, 1991; Ellett and Turrell, 1992; Valencia, 1993, Pingree, 1994). This anomaly pattern has been related to local climatic variables (air temperature, precipitation minus evaporation balance, river run-off), as well as to external driving factors such as the atmospheric circulation represented by the North Atlantic Oscillation index (Pérez *et al.*, 1995; Valencia *et al.*, 1996; Pérez *et al.*, 2000). For other periods, dissimilar tendencies have also been reported, e.g. Lavín *et al.* (1998) describe the increase in temperature and the strong decrease of salinity during the period 1991–1995.

Results and discussion

The Basque coast has some distinctive climatic, geographic, and morphodynamic characteristics and

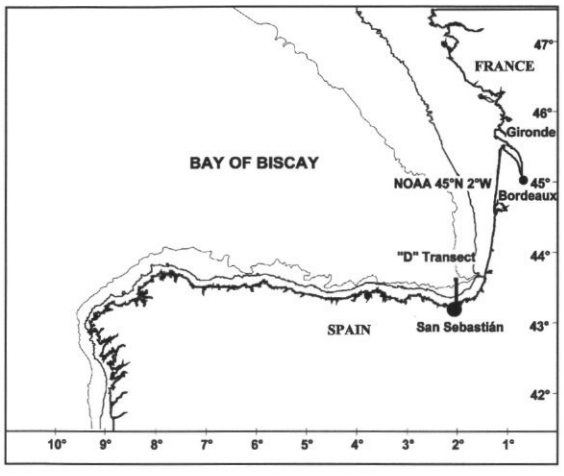


Figure 1. Study area. The southeastern Bay of Biscay and the Basque coast. Meteorological data and SST daily data are from INM and from the Aquarium of San Sebastián. Gironde river flow data are from Bordeaux. The vectorial wind data are from NOAA (45°N 2°W). *In situ* hydrographic data are from D transect of AZTI starting from San Sebastián.

is a convergence area. Calculations of the Ekman transport along the Spanish (east to west) and French (north to south) coasts indicate the dominance of onshore transport. Results based on vectorial wind data obtained from NOAA for 45°N 2°W give an average yearly value of 125 $m^3 s^{-1} km^{-1}$ for the total Ekman downwelling in the area (Valencia *et al.*, 1996). The concavity of the SE corner of the Bay of Biscay produces a continental influence in this region and hence the shelf waters of this area are colder in winter and warmer and less saline in summer than the waters of the areas located westward at equivalent latitudes. Hence, Eastern North Atlantic Central Water (ENACW) entering the SE Bay of Biscay is modified and frequently loses its characteristic T–S relationships, not only in the layer above the seasonal thermocline but also in the whole water column over the continental shelf out to the 120-m isobath (Valencia, 1993).

Nevertheless, against a background of variability within the coastal waters, data series of temperature and salinity for the coastal area and the adjacent continental shelf reflect the general tendencies described for the NE Atlantic. Changes in trends of temperature, salinity, residence time, and the proportion of the water column occupied by ENACW-type waters have been observed throughout the 1986–2000 period.

The observed changes may have been the result of a change in the magnitude of inflow of ENACW to the SE Bay of Biscay, or a change in the characteristics of that water mass (e.g. Pollard and Pu, 1985; Dickson *et al.*, 1988). A combination of climatic parameters affecting the T–S signature of the water masses (the in situ modification hypothesis) and those determining the circulation of the water masses (the advective hypothesis) may be considered for the assessment of the cause and effect of the observed anomaly patterns.

As a first approximation, the air temperature may be considered representative of the main thermal atmosphere–ocean interchanges. The precipitation minus evaporation balance and the river run-off may be considered as the main variables related to changes observed in salinity. The eastward and northward transport of water can be related to upwelling and downwelling, respectively, along the Basque and French coasts.

Monthly averages of the atmospheric temperature at San Sebastián correlate significantly with the monthly average sea surface temperature ($r^2 = 0.90$; $\alpha < 0.0001$; d.f. = 178). Even if the autocorrelation between data sets of time-series is taken into account (lag 1 residual autocorrelation = 0.30) the relationship between air temperature and SST remains statistically significant ($\alpha < 0.01$).

Figure 2 shows the accumulated anomalies of quarterly average flow of the Gironde River, the precipitation in San Sebastián, and the average salinity (100 m water depth) of the shelf waters along the Basque coast. The form of the curve of the accumulated river flow anomalies is similar to other variables related to the thermal and saline balance within the shelf waters (e.g. hours of sunshine, relative humidity, evaporation, precipitation minus evaporation balance), especially in the timing of extreme values.

On the other hand, almost all the points within the hydrographic series associated with changes in the tendency of the T–S characteristics of the waters in the SE Bay of Biscay, and the occurrence of ENACW

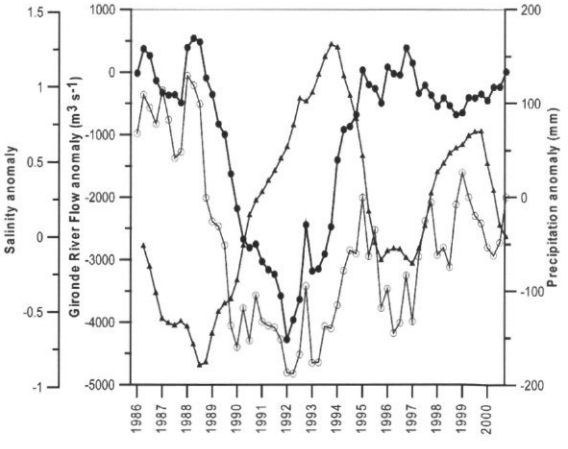


Figure 2. Accumulated anomalies (quarterly) of the Gironde River flow (solid dots), precipitation in San Sebastián (dots) and salinity in 100 m water column off the Basque coast (triangles).

in the area, are related to events of intensification or moderation of the eastward and poleward transports. The intensification of these transports is related to the dominance of southerly and westerly winds that provide simultaneously warm and dry weather in the area.

It would appear that the same climatic regime favouring the intrusion of ENACW into the SE Bay of Biscay is also associated with the warm and dry conditions that maintain the T–S characteristics of the Atlantic Central Waters in this area. The anomaly patterns and the relationships between the variables considered show similar tendencies to those observed in other areas of the intergyre zone of the NE Atlantic (Pérez *et al.*, 2000). Hence, the series of climatic and hydrographic data for the Basque coast reflect the general tendencies described for the NE Atlantic as a teleconnected response related to general indices of environmental forcing such as the NAO.

Acknowledgements

The meteorological data are from the Observatory of San Sebastián (Instituto Nacional de Meteorología). SST daily data are from the Aquarium of San Sebastián (Sociedad Oceanográfica de Gipuzkoa). Gironde river flow data are from the Harbour Authority of Bordeaux. The calculation of Upwelling Index is made from vectorial data furnished by NOAA. The Basque Government (Department of Agriculture and Fisheries) financed the project "VARIACIONES", which includes acquisition of the *in situ* data and review of the external time-series.

References

Dickson, R. R., Meincke, J., Malmberg, S., and Lee, A. J. 1988. The "Great Salinity Anomaly" in the Northern North Atlantic 1968–1982. Progress in Oceanography, 14: 103–151.

Dauvin, J. C., Joncourt, M., and Birrien, J. L. 1991. Température et salinité de l'eau de mer au large de Rosscoff de 1998 à 1990. Cahiers de Biologie Marine, 32: 545–550.

Ellett, D. J., and Turrell, W. R. 1992. Increased salinity levels in the NE Atlantic. ICES CM 1992/C: 20.

Lavín, A., Valdés, L., Gil, J., and Moral, M. 1998. Seasonal and inter-annual variability in properties of surface water off Santander, Bay of Biscay, 1991–1995. Oceanologica Acta, 21: 179–190.

Pérez, F. F., Pollard, R. T., Read, J. F., Valencia, V., Cabanas J. M., and Ríos, A. F. 2000. Climatological coupling of the thermohaline decadal changes in Central Water of the Eastern North Atlantic. Scientia Marina, 64: 347–353.

Pérez, F. F., Ríos, A. F., King, B. A., and Pollard, R. T. 1995. Decadal changes of the θ–S relationship of the Eastern North Atlantic Central Water. Deep-Sea Research I, 42: 1849–1864.

Pingree, R. D. 1994. Winter warming in the southern Bay of Biscay and Lagrangian eddy kinematics from a deep-drogued Argos Buoy. Journal of the Marine Biological Association of the United Kingdom, 74: 107–128.

Pollard, R. T., and Pu, S. 1985. Structure and circulation of the upper Atlantic Ocean north-east of the Azores. Progress in Oceanography, 14: 443–462.

Valencia, V. 1993. Estudio de la variación temporal de la hidrografía y el plancton en la zona nerítica frente a San Sebastián entre 1988 y 1990. Informes Técnicos del Departamento de Agricultura y Pesca del Gobierno Vasco, 52. 105 pp.

Valencia, V., Borja, A., and Franco, J. 1996. Estudio de las variaciones de parámetros oceanográficos y meteorológicos de interés para las pesquerías del Golfo de Vizcaya. Informes Técnicos del Departamento de Agricultura y Pesca del Gobierno Vasco, 75. 232 pp.

ICES Marine Science Symposia, 219: 343–345. 2003

Seasonal cycle and interannual variability of the heat content on a hydrographic section off Santander (southern Bay of Biscay), 1991–2000

César G.-Pola and Alicia Lavín

G.-Pola, C., and Lavín A. 2003. Seasonal cycle and interannual variability of the heat content on a hydrographic section off Santander (southern Bay of Biscay), 1991–2000. – ICES Marine Science Symposia, 219: 343–345.

A standard hydrographical section in the southwestern Bay of Biscay northward from Santander (3°47′W, 43°30′/43°54′N) was sampled monthly from 1991 by the "Instituto Español de Oceanografía". Changes were observed in the heat content and temperature at the surface in the East North Atlantic Central Water (ENACW) and also at the Mediterranean Water (MW) layers. At the surface, in addition to the typical seasonal cycle that shows rapid warming in the spring and slower cooling in the autumn, there was also a suggestion of a warming trend, but it was not statistically significant. Local and occasional sources of variability, such as coastal upwelling, were also detected. Significant warming trends were found for the shallower ENACW, where water mass characteristic changes occurred along the temperature–salinity diagram (around 0.03 to 0.06°C yr^{-1}), and also for the Mediterranean influenced water mass, where its evolution takes place along the isopycnal surface (around 0.02°C yr^{-1}).

Keywords: Bay of Biscay, heat content, seasonal cycle, warming trend.

C. G.-Pola and A. Lavín: Instituto Español de Oceanografía, C.O. de Gijón, c/Camino del Arbeyal, Apdo 55, CP: 33212, Gijón, Spain [tel: +34 985 308672; fax: +34 985 326277; e-mail: cesar.pola@gi.ieo.es; alicia.lavin@st.ieo.es]

Introduction

A standard section northward from Santander (43°30′N 3°47′W, 43°54′N 3°47′W) has been sampled monthly since 1991 from the RV "José Rioja" of the "Instituto Español de Oceanografía". The data were collected at 7 stations, for the first period only for upper waters and from 1993 up to 1000 m depth (or to the maximum depth in the shallower stations) using a CTD profiler (see Figure 1).

Below the surface waters of the Bay of Biscay, there is a broad layer of East North Atlantic Central Water (ENACW). Its deeper part is influenced by Mediterranean Water (MW) which, after leaving the Gibraltar Strait, spreads off into the Atlantic Basin and finds its buoyancy equilibrium at this position. Below that there is a layer of East North Atlantic Deep Water formed in the Denmark Strait and Labrador Sea (OSPAR Commission, 2000).

Methods

The statistical fitting of the data from the mixing layer, where a seasonal cycle is present, was performed using annual and semi-annual harmonic terms in addition to a linear trend. Statistical significance was determined using the inverse of the statistical F cumulative distribution function, and the confidence region calculated for the six fitting parameters (independent and linear terms and amplitudes for sinusoidal and co-sinusoidal for both annual and semi-annual terms) following Jenkins and Watts (2000). Such fitting makes the confidence region an M-dimensional ellipse and, as the functions used for the fitting are not orthogonal, we could not take the confidence intervals as the ellipse semi-axes directly, so they were calculated following Chelton (1983). In regions without a seasonal cycle we have performed a simple linear fitting using the same methodology.

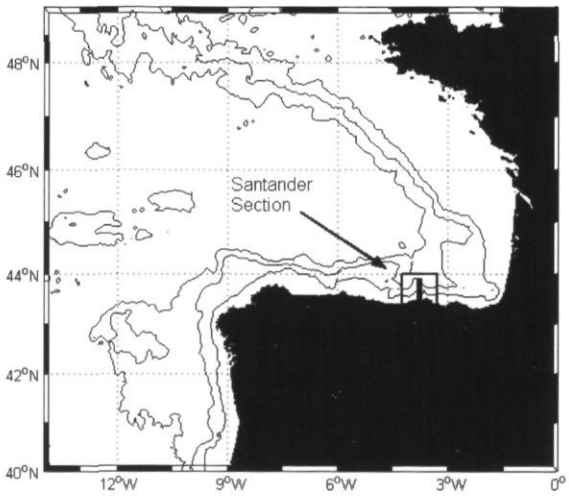


Figure 1. Chart showing location of the hydrographic section northward of Santander.

Upper water layer variability

The surface water layer depends on a seasonal cycle of solar radiation, but is also highly influenced by surface currents, wind regimes, river run-off (mainly in the Eastern part of the Bay of Biscay), and coastal upwelling events (Lavín *et al.*, 1998).

Upper layer water temperature does not follow a sinusoidal seasonal cycle but experiences a rapid warming period in late spring while the autumn cooling process is usually less abrupt, so the semi-annual term is needed to achieve a correct fitting. Our data set reveals a positive warming trend for upper water at all stations (around 0.06°C yr^{-1} for external stations and less at shelf stations where coastal variability is higher), but at none of the stations was the trend statically significant at the 95% level. This is similar to the warming trend found by Koutsicopoulos *et al.* (1998) in the Southern Bay of Biscay, derived from SST images (0.06°C yr^{-1}) from 1973 to 1993, and is also in accord with the winter warming trend shown by Pingree (1994) in the slope region in the same area. On the other hand there is a clear reduction in trends when comparing with previous analysis of the data for a shorter period (Lavín *et al.*, 1998).

Central water evolution in the 1990s

Heat content stored in the water column was calculated for 100 m layers from the limit of the seasonal cycle (200 m) down to 1000 m and fit with a linear trend line. At station 8 (the more oceanic and best sampled deep station), there was increasing heat content through the 1990s in all layers. The increases in the 200 to 500 m layers and also the 700 to 900 m layers (from 100 to 300 kJ m^{-3} yr^{-1}) were significantly different from zero.

From the heat content, we calculated the average rate of increase in temperature for each depth layer assuming standard (35, 10, 0) seawater (Figure 2). They ranged from 0.02°C yr^{-1} to 0.06°C yr^{-1} in such regions with statistical significance, with the largest increase in the shallowest (200–300 m) layer and almost no trend in the 600–700 m layer. Unfortunately, the lack of data at deeper depths prevents us from determining whether there were significant trends in other water masses.

For the shallower part of the ENACW there was an increase of warmer water quantity. This change occurred along the T–S relationship defined by the historic water mass characteristics. As reported by Pérez *et al.* (2000), analysing the $\sigma_\theta = 27.1$ kg m^{-3} (corresponding to around our 200 to 300 m depth branch) ENACW of the eastern North Atlantic responds quickly to climatological forcing and hence these variations are highly correlated with the NAO index; an especially warm decade at the North Atlantic could have caused the observed trends for this water mass at the southern Bay of Biscay.

In the case of the deeper layer (Mediterranean influenced seawater) the T–S was in fact transformed, showing a clear displacement towards warmer and salty regions. Changes were along constant, locally defined, density surfaces (Pingree, 1972).

This surprising behaviour may be explained by an increase in outflow of MW at Gibraltar, a stronger northward transport of MW, a variation in the characteristics of the MW – or the Atlantic waters that mixed with it – in the mixing rate between these water masses, or perhaps a combination of all of these possibilities. In fact the warming and the increasing salinity of the Mediterranean intermediate and deep layers have been reported (Rohling and Bryden, 1992). Variations in Mediterranean water

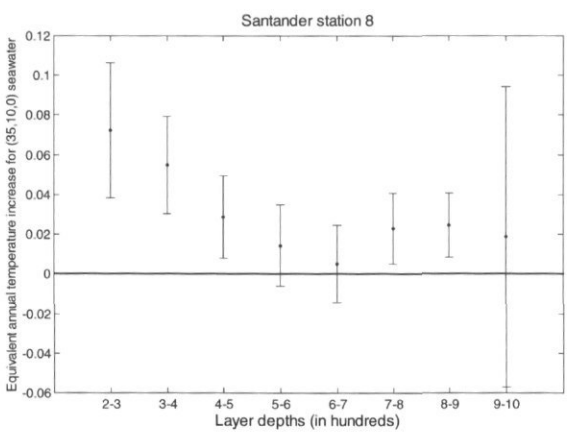


Figure 2. Estimated annual increase in temperature by 100 m layers derived from the linear fit of the heat content. Vertical lines indicate the 95% confidence limits.

mass in the Eastern North Atlantic have not yet been reported, perhaps because the intense diapycnal mixing which occurs during spreading, and the lack of homogenization of the branch until it reaches the southern Bay of Biscay renders analysis, such as the one performed by Rohling and Bryden (1992), difficult, since it involved compiling data from several stations from different cruises over a wide area.

Acknowledgements

We thank Luis Valdés, coordinator of the IEO time-series programme, Ignacio Reguera and the crew of the RV "José Rioja". We also thank Manuel Vargas for his help with the statistics.

References

Chelton, D. B. 1983. Effects of sampling errors in statistical estimation. Deep-Sea Research, 30: 1083–1103.

Jenkins, G. M., and Watts, D. G. 2000. Spectral Analysis and its Applications. Emerson Adams Pr Inc, pp. 132–139.

Koutsikopoulos, C., Beillois, P., Leroy, C., and Taillefer, F. 1998. Temporal trends and spatial structures of the sea surface temperature in the Bay of Biscay. Oceanologica Acta, 21: 335–344.

Lavín, A., Valdes, L., Gil, J., and Moral, M. 1998. Seasonal and inter-annual variability in properties of surface water off Santander, Bay of Biscay, 1991–1995. Oceanologica Acta, 21: 179–190.

OSPAR. 2000. OSPAR Commission Quality Status Report 2000. Region IV, Bay of Biscay and Iberian Coast. Chapter II, pp. 14–16.

Pérez , F. F., Pollard, R. T., Read, J. F., Valencia, V., Cabanas, J. M., and Ríos, A. F. 2000. Climatological coupling of the thermohaline decadal changes in Central Water of the Eastern North Atlantic. Scientia Marina, 64: 347–353.

Pingree, R. D. 1972. Mixing in the deep stratified ocean. Deep-Sea Research, 19: 549–561.

Pingree, R. D. 1994 . Winter warming in the southern Bay of Biscay and Lagrangian eddy kinematics from a deep-drogued Argos buoy. Journal of the Marine Biological Association, 74: 107–128.

Rohling, E. J., and Bryden, H. L. 1992. Man-induced salinity and temperature increases in Western Mediterranean Deep Water. Journal of Geophysical Research. C. Oceans, 97 C7: 11191–11198.

ICES Marine Science Symposia, 219: 346–348. 2003

Changes in subarctic and subtropical water masses in the upper layer of the northern North Atlantic during the 1990s

Jens Meincke, Manfred Bersch, Klaus-Peter Koltermann, and Alexander Sy

Meincke, J., Bersch, M., Koltermann, K.-P., and Sy, A., 2003. Changes in subarctic and subtropical water masses in the upper layer of the northern North Atlantic during the 1990s. – ICES Marine Science Symposia: 219: 346–348.

Multiple occupations of transatlantic hydrographic sections at 58°N and 46°N between 1991 and 1999 reveal a significant redistribution of subarctic and subtropical water masses north of 40°N, following a sharp drop from extremely high to extremely low values of the North Atlantic Oscillation index in 1996 and its slow recovery towards the end of the decade. This led to significant shifts of the Subarctic Front, indicating a contraction and re-expansion of the Subpolar Gyre.

Keywords: interannual changes, North Atlantic Oscillation, Northern North Atlantic Ocean, Subpolar Gyre.

J. Meincke and M. Bersch: Institute of Oceanography, University of Hamburg, Troplowitzstr. 7, D-22529 Hamburg, Germany [tel: +49 40 42838 5985; fax: +49 40 42838 4644; e-mail: meincke@ifm.uni-hamburg.de, bersch@ifm.uni-hamburg.de]. K.-P. Koltermann and A. Sy: Federal Maritime Agency, Postfach 30 12 20, D-20305 Hamburg, Germany [tel: +49 40 3190 3540, fax: +49 40 3190 5035, e-mail: koltermann@bsh.d400.de, alexander.sy@bsh.d400.de]

As a component of the World Ocean Circulation Experiment (WOCE), trans-Atlantic sections WOCE A1E and WOCE A2 were repeated 7 and 5 times, respectively, in the period 1991–1999 (see Figure 1). Here we report on changes in the distribution of cold, low saline subarctic waters and warm, saline subtropical waters in the upper layers of the Northern North Atlantic. They are separated by the Subarctic Front (SAF), which is related to the coldest branch of the North Atlantic Current (Sy *et al.*, 1992). The period under review is a most unusual one in the climatic history of the North Atlantic, one in which the North Atlantic Oscillation (NAO) index evolved to extreme positive values until 1995. Following a sharp drop to extreme negative values in 1996 the index slowly recovered to positive values at the end of the decade (Dickson and Meincke, 2003). Since the NAO index is related to the regime of the westerlies over the North Atlantic, changes have to be expected in the North Atlantic gyre circulation.

After the dramatic drop of the NAO index in winter 1996 a westward shift of the SAF was observed in the Iceland Basin which led to a higher salinity of the upper 600 m along A1E between the Reykjanes Ridge and the Porcupine Bank (Figure 2). The salinity increase in the order of 0.1 is the equivalent of a net evaporation rate of 4.7 mm day^{-1} over 1 year (Bersch, 2001), which is about 5 times the estimated change of the freshwater flux at the sea surface between NAO high and low phases (Hurrell, 1995). The temperature increase of the upper 600 m amounted to about 0.8°C; the density increase was about 0.05 kg m^{-3}.

The westward shift of the SAF was the result of a reduced eastward spreading of cold, low saline, and dense Subarctic Surface and Subarctic Intermediate waters (θ<7°C, S<35.0) from the Labrador Sea and an increased northward spreading of warm, saline, and less dense Subpolar Mode Water from the subtropics. These changes suggest a westward contraction of the subpolar gyre. Observations by Pollard *et al.* (1999) indicate that in October/November 1996 the 35.0 isohaline of the SAF, which was found in the Iceland Basin on A1E until 1995, had shifted to 30°W near the Charlie-Gibbs Fracture Zone, about 350 km westward of A1E. Observations along A1E in 1999 show that with increasing NAO index the low saline subarctic water masses begin to re-occupy the Iceland Basin and the region off the Rockall Plateau and the Rockall Trough (Figure 2) indicating an eastward shift of the SAF and a re-expansion of the subpolar gyre (Bersch, 2001).

Along A2 (Figure 3), similar temporal behaviour was observed east of the Mid-Atlantic Ridge in the West European Basin, where salinity increases are evidence of a northward expansion of the subtropical gyre in 1996–1997. At the western end of A2, in the Newfoundland Basin, Figure 3 shows

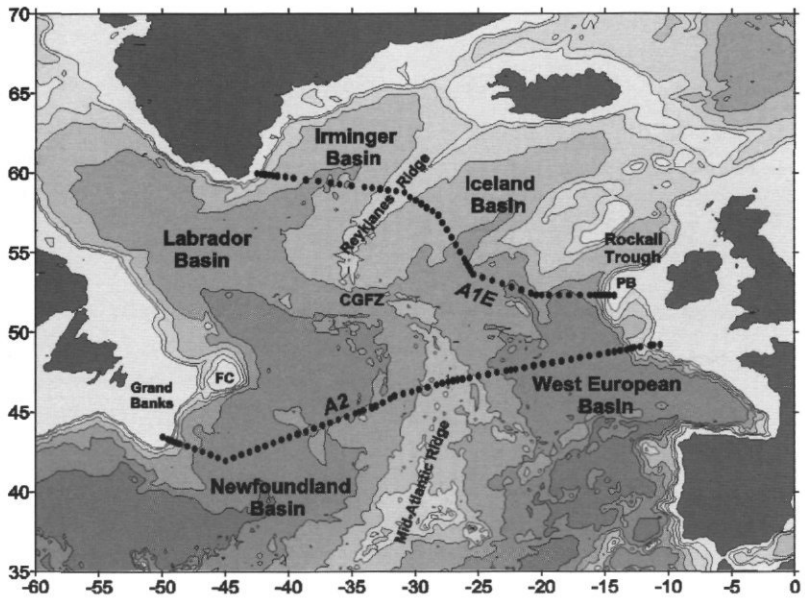


Figure 1. Location of WOCE hydrographic sections A1E and A2 and bottom topography in the northern North Atlantic. CGFZ = Charlie-Gibbs Fracture Zone, PB = Porcupine Bank, FC = Flemish Cap.

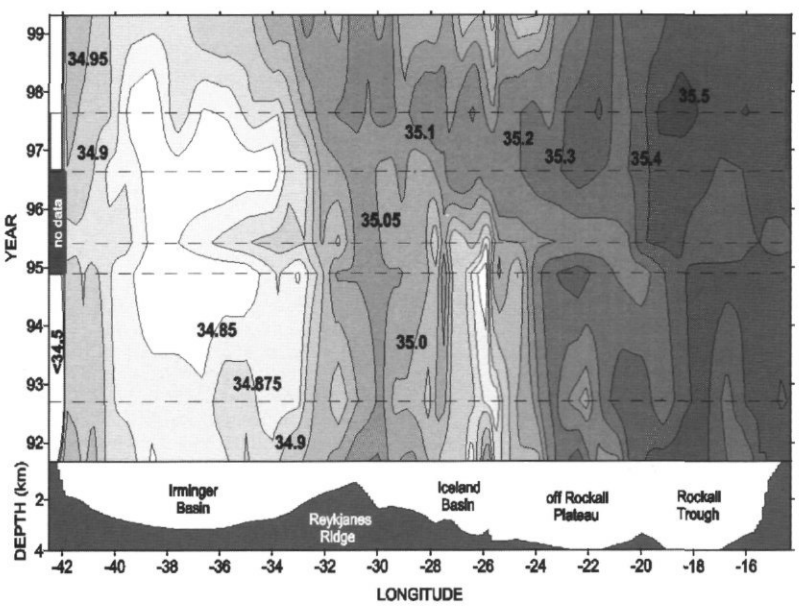


Figure 2. Temporal changes in the mean salinity of the upper 600 m along section A1E, recorded 7 times between September 1991 and May 1999. The beginning of each year is indicated on the vertical axis. The lower panel shows the bottom topography along the section (extended from Bersch *et al.*, 1999).

evidence of an eastward shift of the SAF in the period 1996 to 1998 and was found at 45°W in 1997, about 200 km farther east than in 1993. A corresponding southward shift of the north wall of the Gulf Stream at 70°W in 1996 and 1997 was observed by Rossby and Gottlieb (1998).

The redistribution of subarctic and subtropical water masses north of 40°N, associated with the pronounced weakening of the westerlies in 1996 and 1997, resulted in an increase of the mean salinity of the upper layer in the eastern basins and a decrease in the Newfoundland Basin especially west of 45°W

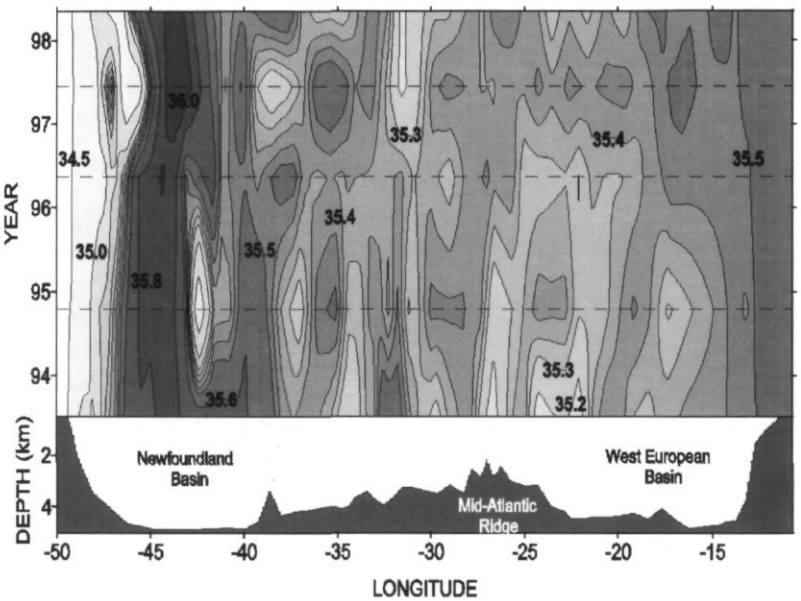


Figure 3. Temporal changes in the mean salinity of the upper 1000 m along section A2, recorded 5 times between July 1993 and May 1998. The beginning of each year is indicated on the vertical axis. The lower panel shows the bottom topography along the section (after Bersch, 2001).

above the continental slope. A reduced eastward spreading of subarctic waters with the North Atlantic Current and an intensified southward spreading of subarctic waters with the Labrador Current were suggested, while the northward spreading of subtropical waters was intensified in the northeastern North Atlantic. This led to the corresponding shifts of the SAF in the different regions and thus a change of the shape of the subpolar gyre.

References

Bersch, M. 2001. NAO-induced changes of the upper-layer circulation in the northern North Atlantic Ocean. Journal Geophysical Research (submitted).

Bersch, M., Meincke, J., Sy, A. 1999. Interannual thermohaline changes in the northern North Atlantic 1991–1996. Deep-Sea Research II, 46: 55–75.

Dickson, R. R., and Meincke, J. 2003. The NAO and the ocean's response in the 1990s. ICES Marine Science Symposia, 219: 15–24. (This volume).

Hurrell, J. W. 1995. Decadal trends in the North Atlantic Oscillation: Regional temperatures and precipitation. Science, 269: 676–679.

Pollard, R., Read, J., Holliday, P., and Leach H. 1999. Circulation and mode waters of the North Atlantic subpolar gyre in 1996. International WOCE Newsletter, 37: 21–27.

Rossby, T., and Gottlieb, E. 1998. The Oleander Project: Monitoring the variability of the Gulf Stream and adjacent waters between New Jersey and Bermuda, Bulletin American Meteorological Society, 79: 5–18.

Sy, A., Schauer, U., and Meincke, J. 1992. The North Atlantic Current and its associated hydrographic structure above and eastwards of the Mid-Atlantic-Ridge. Deep-Sea Research, 39: 825–853.

ICES Marine Science Symposia, 219: 349–351. 2003

XBT-Transects along 60°N, Greenland–Scotland, 1989–1999

M. Stein

Stein, M. 2003. XBT-Transects along 60°N, Greenland–Scotland, 1989–1999. – ICES Marine Science Symposia, 219: 349–351.

During the annual autumn cruises of RV "Walther Herwig" (II and III) to East and West Greenland, the vertical distribution of temperature down to 800-m depth was measured using XBTs. The data presented in the article are transects that cross the North Atlantic Ocean at about 60°N from Cape Farewell to the Pentland Firth, taken between 1989 and 1999. Interannual variations in the water column are discussed. At depths of 400 m in the Irminger Sea Proper (60°N, 37°W) as well as south off Iceland in the North Atlantic Current (60°N, 20°W), temperatures range from 3.4°C to 5.5°C, and from 7.4°C to 8.9°C, respectively, with 1996 being the warmest year at both sites.

Keywords: Irminger Sea, North Atlantic Current, redfish, temperature.

M. Stein: Institut für Seefischerei, Palmaille 9, D-22767 Hamburg, Germany.

Introduction

The structure of the upper ocean thermal field of the North Atlantic along 60°N between Cape Farewell and the British Isles is significantly influenced by the Mid-Atlantic Ridge (Figure 1). Doming of the isotherms to the west of the ridge (Figure 2) shows the Irminger Sea thermal properties: a deep reaching, nearly homogenous water mass below the upper thermocline. The upper 1000 m of the water column east of the ridge comprises the waters of the North Atlantic Current, structured during the preceding summer. Distribution of fish in the North Atlantic, e.g. the pelagic species redfish (*Sebastes mentella*) in the Irminger Sea, seems to depend on water mass fluctuations. To estimate thermal variations at least on an annual scale, XBT-measurements were performed by RV "Walther Herwig" (II and III) on her eastbound transects crossing the North Atlantic Ocean during autumn.

Material and methods

After leaving Cape Farewell (the south tip of Greenland) XBT probes were launched every 3 h until reaching the continental shelf off Scotland. A vertical temperature profile was therefore obtained about every 30 nmi. Data analysis was done in the German Hydrographic Office (now the Federal Maritime and Hydrographic Agency of Germany) using the technique described by Sy and Ulrich (1994). Plotting of vertical sections (Figures 2, 3) was done using Ocean Data View Software (Schlitzer, 2001). To estimate the temporal variation of temperature during 1989–1999, two test points were taken from the data set: at 60°N, 37°W (Irminger Sea), and 60°N, 20°W (south of Iceland). The approximate locations are indicated in Figure 1. A polynome trend line was applied to the data points of the time-series to analyse thermal changes over the decade of the 1990s (Figures 4, 5).

Results and discussion

The 4°C isotherm with a dome-like shape dominates the Irminger Sea portion of the transect during 1989 from a depth of 200 m downwards (Figure 2). It indicates upwelling in the centre of the cyclonic gyre which is topographically steered by the Mid-Atlantic Ridge. Ten years later, the water mass structure in the centre of the Irminger Sea gyre has changed (Figure 3), and the < 4°C water dominates the water column only below 400-m depth with the top layer temperatures being > 6°C. The boundary between the less stratified Irminger Sea and the warm waters of the North Atlantic Current reveal temperatures well above 9°C during November 1989, and they exceed 10°C during November 1999. Inspection of thermal variation between 1989 and 1999 at two points of the transect (37°W, 20°W) shows considerable changes during the decade of the 1990s. At 400-m depth, temperatures range from 3.4°C to 5.5°C at 37°W, and from 7.4°C to 8.9°C at

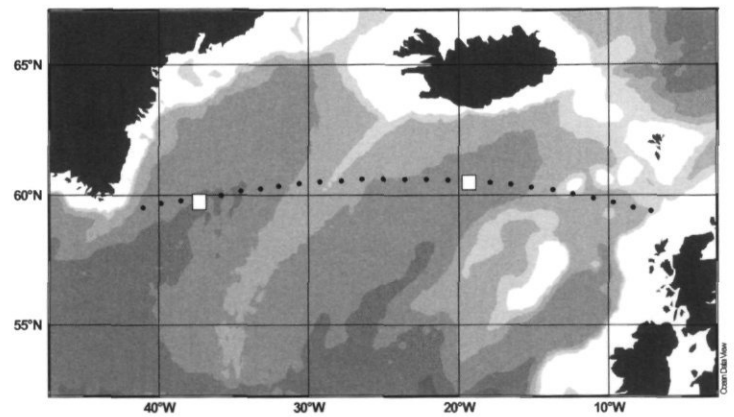


Figure 1. Location of XBT stations on Eastbound Transects; rectangles 37°W, 20°W.

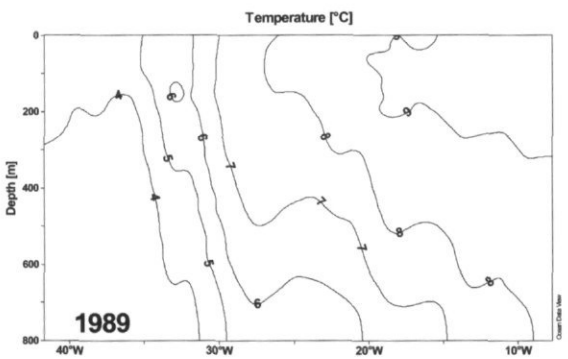


Figure 2. Vertical distribution of temperature (°C) along Eastbound Transect (Figure 1) during 1989.

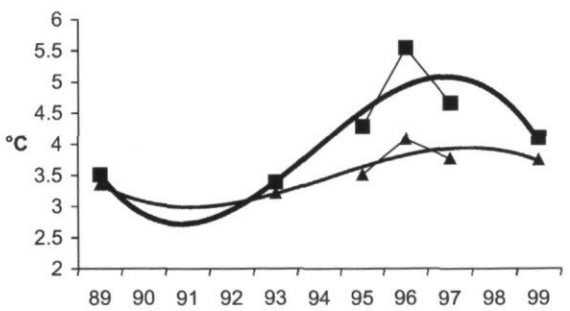


Figure 4. Variation of temperature in the Irminger Sea proper (60°N, 37°W) at 400-m and 600-m depths.

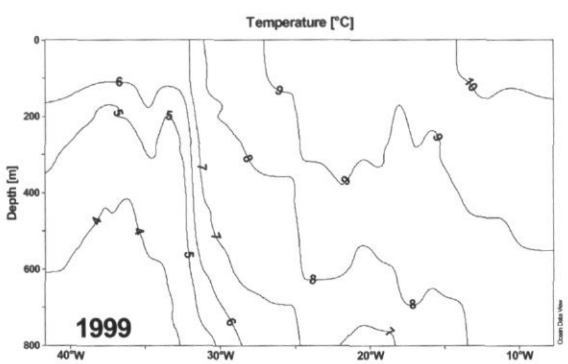


Figure 3. Vertical distribution of temperature (°C) along Eastbound Transect (Figure 1) during 1999.

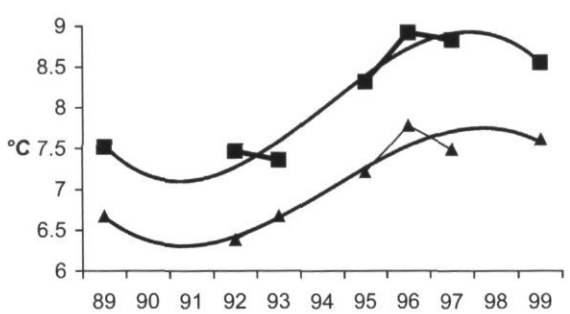


Figure 5. Variation of temperature south off Iceland (60°N, 20°W) at 400-m and 600-m depths.

20°W, with 1996 being the warmest year at both sites. At 600-m depth the observed changes in the Irminger Sea are rather small, ranging from 3.2°C to 4.1°C. South of Iceland, temperatures at 600-m depth range from 6.4°C to 7.8°C (Figure 5).

The data suggest that coldest conditions were encountered during the early 1990s, both in the depths of the Irminger Sea (Figure 4) and to the south of Iceland (Figure 5).

Conclusions

The data indicate that in the main distribution area of oceanic redfish (*Sebastes mentella*), in the Irminger Sea, thermal conditions varied considerably during the decade of the 1990s. Within the depth range around 400 m thermal changes were detected which amount to more than 2°K. Whether the warm conditions as experienced during 1996 have initiated the westward movement of the oceanic redfish stock remains speculative.

Acknowledgements

Thanks to my colleagues Sy and Ulrich in the Federal Maritime and Hydrographic Agency of Germany for analysing the XBT data. I also thank the technicians and scientists of the Federal Research Centre for Fisheries, Hamburg, who did the XBT measurements at sea during long nights and rough sea conditions from 1989 to 1999.

References

Schlitzer, R. 2001. Ocean Data View. http://www.awi-bremerhaven.de/GEO/ODV.

Sy, A., and Ulrich, J. 1994. North Atlantic Ship-of-Opportunity XBT Programme 1990: Data Report, WOCE-NORD. Berichte des BSH, No. 1. 134 pp.

ICES Marine Science Symposia, 219: 352–355. 2003

Climate of UK waters at the millennium: status and trends

Graham Alcock, Ben Moate, and Lesley Rickards

Alcock, G., Moate, B., and Rickards, L. 2003. Climate of UK waters at the millennium: status and trends. – ICES Marine Science Symposium, 219: 352–355.

The UK Inter-Agency Committee on Marine Science and Technology (IACMST) has produced a report and website summarizing the present status and trends of marine physical parameters and plankton in UK waters. Parameters included are sea surface temperature, salinity, sea level, waves, plankton, and the weather. Some of these may be indicative of climate change. The report puts recent conditions into the context of longer-term trends and wider factors, for example the North Atlantic Oscillation (NAO), which is a significant factor in the variation of marine parameters in UK waters.

Keywords: chlorophyll, climate, NAO, nutrients, plankton, salinity, sea level, sea temperature, UK waters, waves, weather.

G. Alcock, B. Moate, and L. Rickards: British Oceanographic Data Centre, Bidston Observatory, Prenton, Merseyside, CH43 7RA, UK [tel: +44 151 653 8633; fax: +44 151 652 3950; e-mail: grahama@onetel.net.uk; bdm@bodc.ac.uk; ljr@bodc.ac.uk]. Correspondence to L. Rickards.

The effective and sustainable management of the UK's marine environment needs the comprehensive collection and use of marine data in order to assess its present state, identify changes, and meet future forecasting needs. As a first step towards this, data provided by a number organizations have been used to produce a document (Alcock and Rickards, 2001) for the UK Inter-Agency Committee on Marine Science and Technology (IACMST). This describes the present (1999/2000) status and trends of weather, climate, sea temperature, salinity, sea level, waves, and plankton in UK territorial waters. Some data from adjacent areas are included to provide a regional and global context. There are also some representative data sets of chlorophyll and nutrients. It is intended that this will be the first of a series of ocean climate status and trends reports for UK waters.

This poster presentation summarizes the aims of the report and its conclusions; the latter illustrated by sample time-series plots of temperature (Figure 1) and plankton (Figure 2). The general aim of the document is to demonstrate the value of longterm marine measurements in aiding the effective management of the UK's marine environment, thus encouraging their commencement, their continuation, or their restoration. More specific aims are to:

1) stimulate further scientific study of the parameters and their interactions
2) increase public awareness of the present status and trends in UK waters
3) enhance marine data inventories
4) provide reference measurements for the validation of, and assimilation into, operational marine forecasting models (EuroGOOS, 1996)
5) enhance the use of marine indicators of climate change (Hulme and Jenkins, 1998; DETR, 1999), whether due to natural variability or as a result of human activity, and
6) provide input to a wider study on Environmental Indicators and the State of the Seas by the UK's Marine Pollution Monitoring Management Group.

The main conclusions of the report are:

1) Sea surface temperatures at most sites show a warming trend during the 20th century, but with lower values in 1999 and 2000 compared to 1998.
2) Salinity (both surface and bottom) records show considerable interannual variation, but do not indicate any overall long-term trend in recent decades. Generally, salinities in 1999 and 2000 were lower than in 1998.
3) Mean sea level, relative to the land, rose by about 1.5 mm per year in the 20th century, but is now rising on average less fast than over a base period of 1921–1990. Trends in extreme sea levels match those of mean sea level closely, but there are no significant long-term trends in surge levels.
4) Although there is large spatial and temporal variability in wave height, there is evidence of an increase between the 1960s and 1990s.

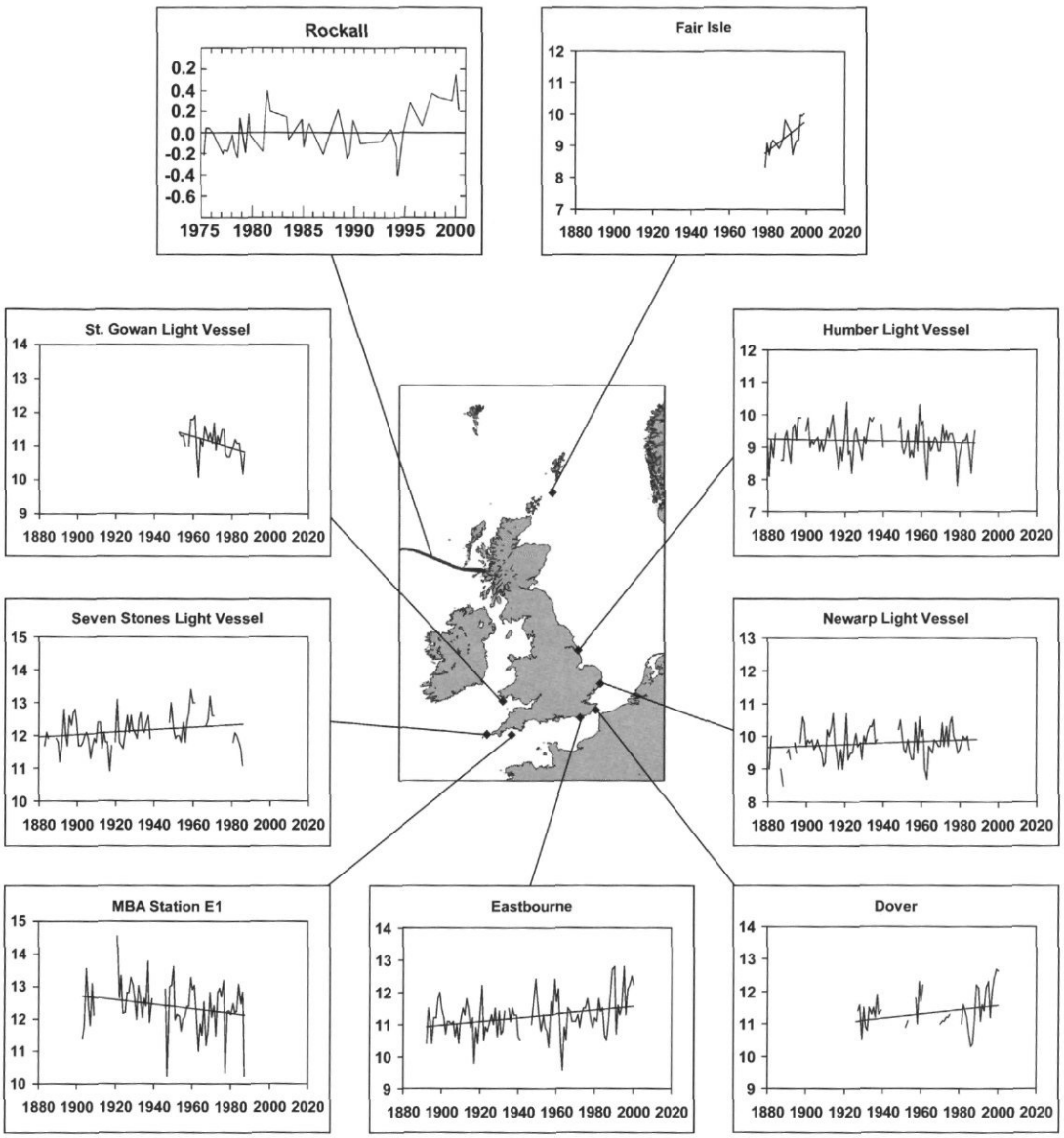


Figure 1. Annual SST °C (with trend line) at sites around the UK. Note: Rockall shows anomalies from de-seasonalized averages over the upper 800 m with no trend line.

5) The abundance of the zooplankton *Calanus finmarchicus* has declined in the North Sea and the NW Approaches since the 1960s. Elsewhere, numbers are relatively low and show considerable interannual variability, making it difficult to infer any trends.
6) The abundance of phytoplankton shows an upward trend since the 1960s, except in the Irish Sea.
7) Any trends in nutrients, metals, or biological parameters are difficult to infer from existing measurements, because of short sampling duration or interannual variability in the longer records.
8) There is potential to monitor the status and trends of chlorophyll from the operational SeaWiFS instrument.
9) Changes in the North Atlantic Oscillation, and hence the strength of the westerly airflow, are a significant factor in the variation of marine parameters in UK waters.
10) Contemporary data for some parameters are not available because measurements have never been made or have been discontinued.

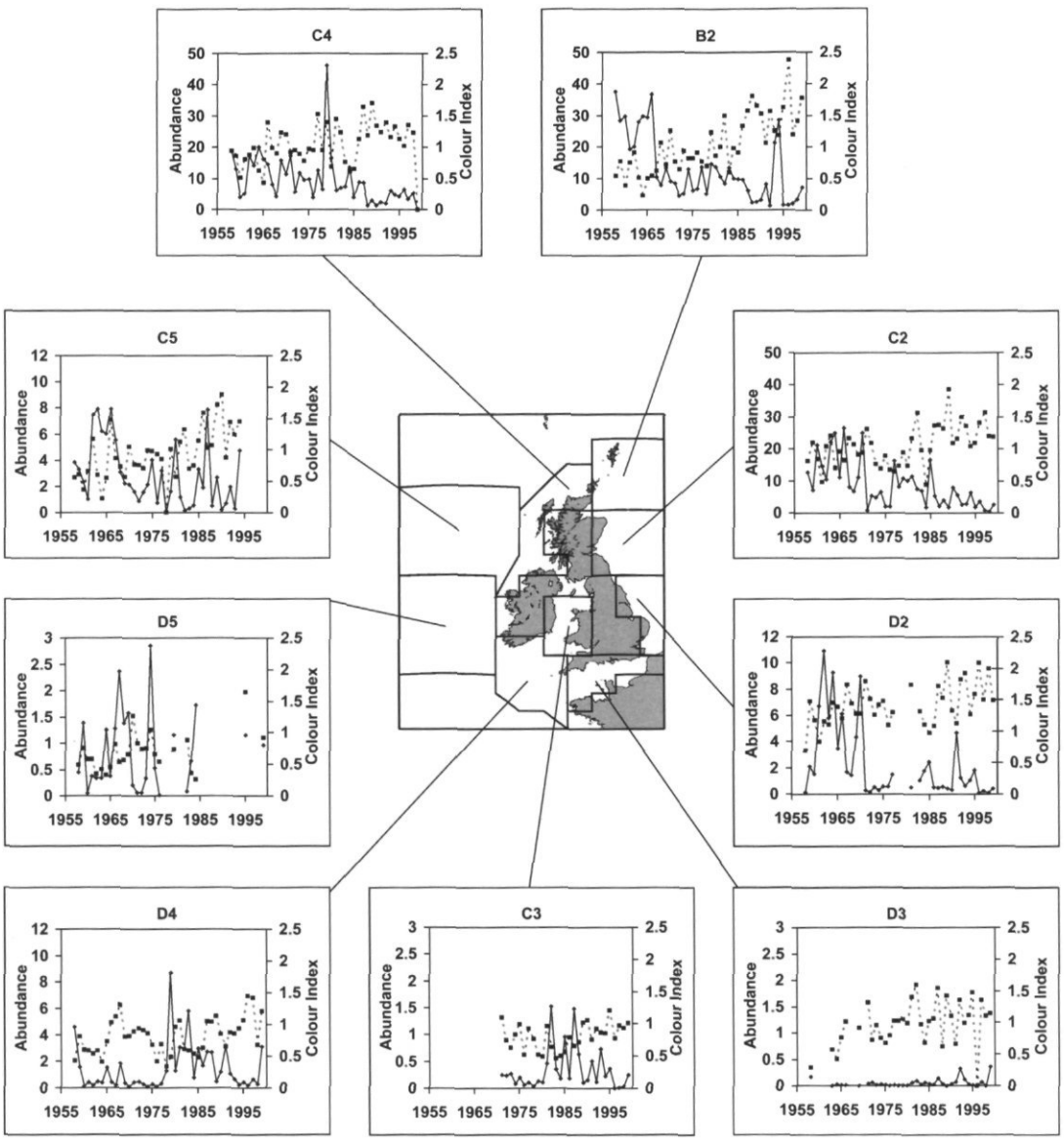


Figure 2. Annual abundance of zooplankton and phytoplankton from the CPR. Dotted lines with squares = colour index, solid line with diamonds = abundance of *Calanus finmarchicus*. Note changes of scale in zooplankton abundance.

11) Much better use can be made of existing data, especially if processing methods are standardized and data dissemination improved, including the timely provision of data to users and national, regional, and international data banks.
12) The existing observation programmes provide a sound basis for a comprehensive observation, processing, and analysis programme for UK waters. This is needed to assess the present state and trends of the UK's marine environment, as a necessary part of its effective management.

A web version of the document is available (www.oceannet.org/UKclimate-status), etogether with links to other sites containing marine data and information.

References

Alcock, G., and Rickards, L. 2001. Climate of UK waters at the millennium: status and trends. IACMST Information Document No. 9. 48 pp.

DETR (Department of Transport, Environment and the Regions), 1999. Indicators of Climate Change in the UK. Compiled and edited by M. G. R. Cannell, J. P. Palutikov, and T. H. Sparks. Produced by the Climatic Research Unit (University of East Anglia) and the Centre for Ecology and Hydrology.

EuroGOOS. 1996. The strategy for EuroGOOS: 1996–2006 Contained on the EuroGOOS website at: www.eurogoos.org

Hulme, M., and Jenkins, G. J. 1998. Climate change scenarios for the UK: scientific report. UKCIP Technical Report No. 1, Climate Research Unit, Norwich. 80 pp.

Norris, S. W. 2001. Near surface sea temperatures in coastal waters in the North Sea, English Channel and Irish Sea, Vol. II. CEFAS Scientific Series Data Report No. 40.

Sir Alister Hardy Foundation for Ocean Science (SAHFOS) 2001. Website at: www.npm.ac.uk/sahfos

WASA (Waves and Storms in the Northeast Atlantic) Group, 1998. Changing waves and storms in the northeast Atlantic. Bulletin of the American Meteorological Society, 79: 741–760.

Woodworth, P. L., Tsimplis, M. N., Flather, R. A., and Shennen, I. 1999 A review of the trends observed in British Isles mean sea level data measured by tide gauges. Geophysical Journal International, 136: 651–670.

ICES Marine Science Symposia, 219: 356–358. 2003

Frontal climatology based on advanced very high resolution radiometer sea surface temperatures in the eastern North Sea

Anne E. Lucas and W. Paul Budgell

Lucas, A. E., and Budgell, W. P. 2003. Frontal climatology based on advanced very high resolution radiometer sea surface temperatures in the eastern North Sea. – ICES Marine Science Symposia, 219: 356–358.

In an attempt to map the distribution of fronts within the North Sea, a two-pass filtering technique is used to identify temperature gradients on NOAA-AVHRR SST data. Even with 8-day, 9-km resolution, seasonal trends in frontal regimes can be identified.

Keywords: AVHRR, fronts, GIS, SST.

A. E. Lucas: Department of Geography, University of Bergen, Breiviksveien 40, NO-5045 Bergen, Norway [tel: +47 55 959659; fax: +47 55 959393; e-mail: anne.lucas@geog.uib.no]; W. P. Budgell: Institute of Marine Research, PO Box 1870, Nordnes, NO-5817 Bergen, Norway [tel: +47 55 238628; fax: +47 55 238584; e-mail: paul.budgell@imr.no]. Correspondence to A. E. Lucas.

Introduction

The remote sensing component of the EU LIFECO project (available at http://www.lifeco.dk) involves mapping and characterizing frontal conditions in the North Sea and Skagerrak from advanced very high resolution radiometer (AVHRR) sea surface temperature (SST) imagery. The mapped frontal distributions are to be used as a basis for the interpretation of biomass and fisheries recruitment data. This article describes the methodology used to identify areas prone to frontal activity as defined by steep temperature gradients.

Materials

SST data have been obtained from the Physical Oceanography Distributed Active Archive (PODAAC, available at http://podaac.jpl.nasa.gov) and processed through a suite of spatial tools, including Matlab 6.1, ENVI/IDL 3.4, and MFWorks 2.6. The daytime satellite passes are processed as 8-day 9-km composites from the original GAC imagery (with a nominal 4-km spatial resolution) for the period 1990–1999 and subsetted to cover the area shown in Figure 1. For each 8-day period, missing data (or cloud contaminated pixels) are removed from the analysis. Data are scaled to yield SST values from −3°C to 30°C (PODAAC, 1999).

Methods

The present analysis investigates long-term large-scale patterns as captured by the 8-day averages for the 10-year time-series. Interannual variability will be dealt with elsewhere.

Frontal areas are identified using a GIS-based two-pass filter method. In the first stage, a low-pass filter with a 3×3 kernel is used to reduce high frequency noise through spatial averaging. In the second pass, a standard 3×3 Sobel filter based on the gradient discontinuity identifies edges and is sensitive to changes in both the horizontal and vertical directions (Jensen, 1986).

Prior to running the filter procedure, each data set was interpolated landwards using an inverse distance algorithm. This allowed the filter procedure to relax smoothly at the shoreline, effectively eliminating edge detection at the land/water boundary. At the same time, the few remaining cloud-covered pixels were also filled.

Results

The 46 resultant maps were overlain with bathymetric data. A temporal analysis of the data indicates that there are three areas of interest; the area associated with the shelf break around southern Norway, Dogger Bank and the inflow through the English Channel. These are indicated on Figure 1. In each

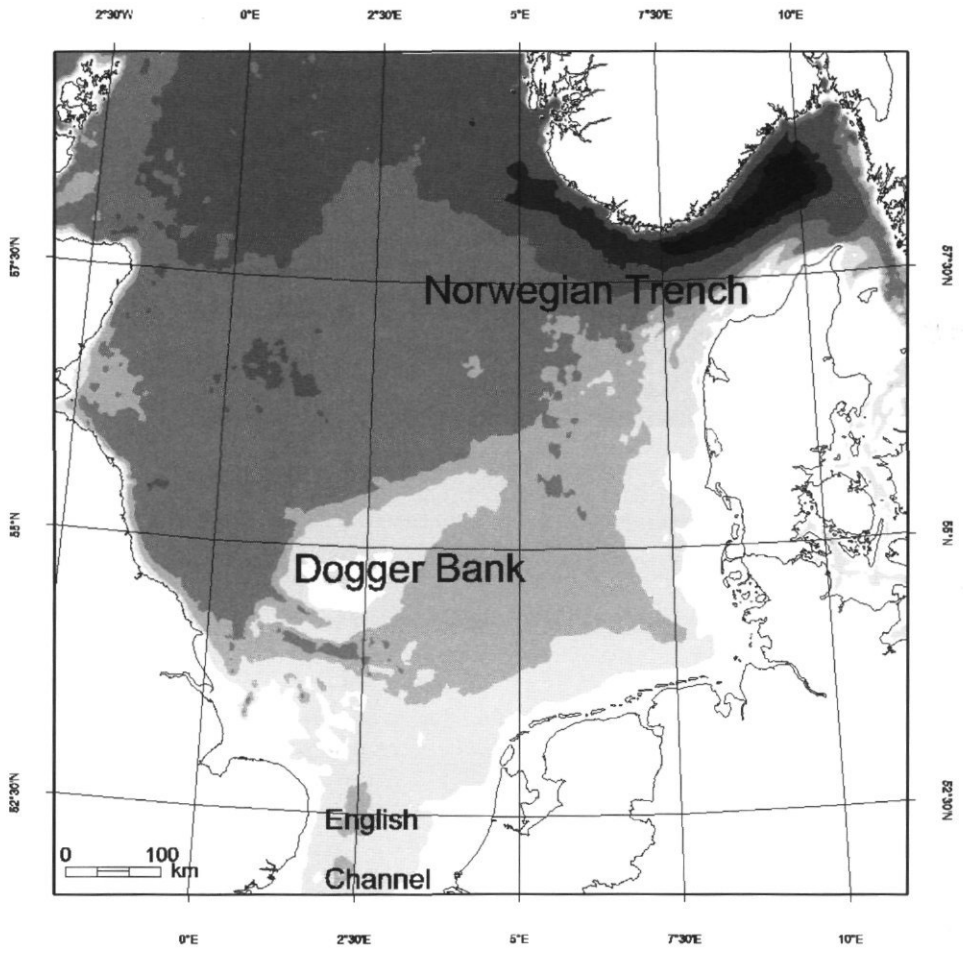


Figure 1. Location map with bathymetry. Deepest (darkest) areas exceed 600 m. Dogger Bank has an average depth of 29 m.

case, the frontal regime exhibited strong temperature gradients and high variability throughout the seasonal cycle.

At the shelf break, temperature gradients are strongest during the winter months (periods 1–16, 43–46), producing a nearly continuous zone of frontal activity. By mid-May the temperature gradients have weakened and the appearance through the summer is a more confused (or complex) state.

The inflow through the English Channel varies from a bifurcated state during the winter to stronger temperature gradients on the north side by period 10. During the spring and summer, the pattern reverses, such that there is a broad zone of intense temperature gradients on the south side of the channel.

The area around Dogger Bank shows the most complex regime. Frontal activity is most intense on the south slope during the winter. By early spring the northeast slope shows most activity, after which there is a period of calm. The fronts return late May on the south and southwest slope. A number of these features are illustrated in the frontal distribution map from period 6, shown in Figure 2.

Discussion

Even at this spatial and temporal scale, patterns emerge. The seasonal development of frontal regimes is repeated consistently over the decadal analysis period. The distribution of fronts through time and space is more complex than had been anticipated, based on the frontal distribution shown in Becker (1981). Future analysis will investigate the interannual variability of the distribution and intensity of frontal activity.

SST values inferred from AVHRR may be representative of only the upper few millimeters of the water column; surface effects can mask the horizontal structure of temperature through the upper layer (Cracknell, 1999). Furthermore, thermal fronts are not necessarily dynamical fronts; density will not

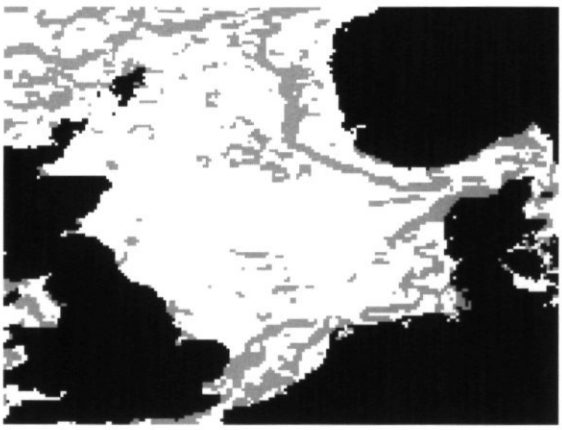


Figure 2. Sample output from period 6. Areas of high frontal activity are shown in grey. Other water areas have been masked out and appear white. Land areas are black.

vary across the front if salinity variations compensate for the temperature gradient. For these reasons, it is wise to supplement the SST analysis with other data sources.

References

Becker, G. A. 1981. Bieträge zur hydrographie und wärmebilanz der Nordsee. Deutsche Hydrographische Zeitschrift, 34: 167–202.

Cracknell, A. P. 1999. The Advanced Very High Resolution Radiometer. Taylor and Francis, London.

Jensen, J. R. 1986. Introductory digital image processing: a remote sensing perspective. Prentice-Hall, Englewood Cliffs, NJ.

PODAAC 1999. AVHRR Oceans Pathfinder Sea Surface Temperature Data Sets. Available from: http://podaac. jpl. nasa.gov:2031/DATASET_DOCS/avhrr_pathfinder_sst. html [Document Revision Date 27 April 1999].

ICES Marine Science Symposia, 219: 359–361. 2003

One-hundred-and-forty years of daily observations in a tidal inlet (Marsdiep)

Hendrik M. van Aken

van Aken, H. M. 2003. One-hundred-and-forty years of daily observations in a tidal inlet (Marsdiep). – ICES Marine Science Symposia, 219: 359–361.

From 1861 to 1962 daily observations of temperature and salinity were carried out in the Marsdiep tidal inlet near Den Helder. Since 1947 similar measurements have been made in the Marsdiep on the coast of the island of Texel. Monthly mean differences for temperature and salinity were determined from the overlapping years. With these differences the Den Helder series could be extended to a homogeneous series from 1861 until 2001. The seasonal and annual mean salinities and temperatures are presented. The years 1999 and 2000 were the two warmest since 1861, and 1996 was among the five coldest years. The mean annual temperatures reflect the West European climatic variability and are highly correlated with the annual mean air temperature in Den Helder. Ice winters with monthly mean temperatures below 0°C occur generally in winters with a low NAO index. The salinity shows a persistent decreasing tendency related to increased river discharge since the beginning of the observations.

Keywords: salinity, temperature, time-series, Wadden Sea.

H. M. van Aken: Royal Netherlands Institute for Sea Research, PO Box 59, 1790AB, Den Burg/Texel, The Netherlands [tel: +31 222 369416; fax: +31 222 319674; e-mail: aken@nioz.nl]

The Marsdiep is a tidal inlet between Den Helder and the island of Texel in the northwestern part of The Netherlands (Figure 1). It connects the western basin of the Wadden Sea with the North Sea. Up until 1932 the large brackish Zuiderzee was connected directly with the Wadden Sea. In that year an enclosure dyke was built, and the former Zuiderzee became the freshwater lake IJsselmeer. The Dutch Wadden Sea forms an extensive estuarine environment, characterized by high productivity, high energy fluxes, and strong hydrographic variability. It is a nursery for several commercial fish species, and a feeding ground for a number of seabirds and waders. In the western basin of the Wadden Sea the main exchange with the North Sea takes place through the Marsdiep. The main source of freshwater in the western basin is the River Rhine and its branch, the Ijssel, via the outlet sluices in the enclosure dyke. Additional Rhine Water enters the Marsdiep via the Dutch coastal waters between Hoek van Holland and Den Helder.

Halfway through the 19th century, scientific interest in fisheries emerged in The Netherlands, when it was decided to monitor hydrographic parameters at a series of coastal stations. One of these stations was situated on the Den Helder sea dyke along the Marsdiep and has resulted in a 140-year time-series of daily hydrographic observations carried out successively by different institutes.

From 1861 to 1962, daily observations of temperature and salinity were carried out on the Den Helder side of the Marsdiep. Water samples were taken with a bucket at 08:00. The temperature was determined with a calibrated seawater thermometer. For determination of the salinity areometer measurements, chemical titration and conductivity measurements were used successively. Since 1947, similar measurements have been made in the Marsdiep on the coast of the Island of Texel, allowing determination of a monthly mean offset to relate observations on both sides of the inlet. Until 1981 the data set was quality controlled and described by van der Hoeven (1982). In 1982, NIOZ took over responsibility for the Marsdiep series. Since March 2000 temperature and salinity have been measured continuously by means of electronic sensors.

Annual mean values are given in Figure 2. The water temperature in the Marsdiep is determined by the fast response of the air–sea interaction in the shallow Wadden Sea and the slower response in the

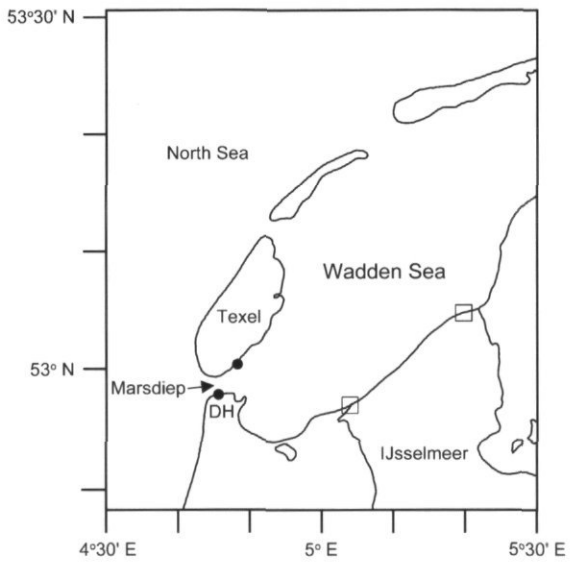


Figure 1. Map of the western Wadden Sea. The observation points in Den Helder (DH) and Texel are marked with black dots. The positions of the outlet sluices in the enclosure dyke between Wadden Sea and IJsselmeer are indicated with squares.

deeper North Sea. The typical thermal response time of the Wadden Sea is less than 2 weeks (J. Ettema, pers. comm.). The annual mean temperature correlates well with the annual mean air temperature in Den Helder. The five warmest years were 1999, 2000, 1868, 1989, and 1863, the five coldest 1888, 1963, 1879, 1909, and 1996. The mean annual salinity has a significant correlation of –0.72 with time. This decreasing trend is related to the long-term increasing trend in the discharge of the river IJssel and the outlet sluices in the enclosure dyke. This is due to a changing hydrological management of the Dutch waters, since such a trend is absent in the discharge of the River Rhine as it enters The Netherlands. Since the enclosure of the Zuiderzee, the interannual variability has increased, probably because of the decreased buffer capacity of the Wadden Sea following the enclosure.

On average, the lowest temperatures are observed in December to March and the lowest salinities from January to April. Since 1947, ice winters, with at least one monthly mean temperature near Texel below zero, occurred in 1947, 1954, 1956, 1963, 1979, 1986, 1996, and 1997, characterized by a

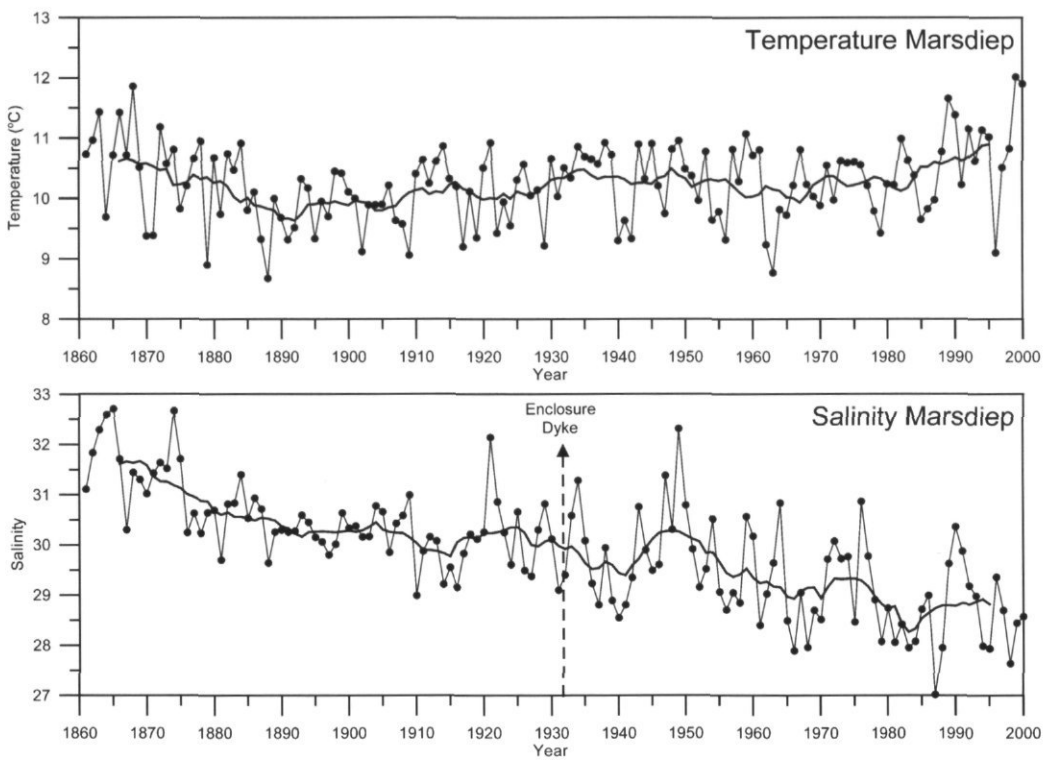


Figure 2. Plot of the annual mean sea surface temperature and salinity in the Marsdiep tidal inlet from 1861 to 2000 (dotted line). The 10 years running mean is shown with a thick line.

North Atlantic Oscillation index of –0.54 ± 0.32. In comparison, the winter NAO index for the period 1947 to 2000 was +0.36 ± 0.14. Of 30 months with a mean salinity below 25.0 only 4 were not found in the period January to April.

The Marsdiep time-series is the last surviving of a number of time-series in Dutch coastal waters, started in the 19th or early 20th century. Other series have been terminated because of budget cuts, and because responsible institutes lost interest in maintaining the series. The temperature–salinity time-series from the Marsdiep is used regularly for biological and environmental research in the western Wadden Sea. NIOZ intends to maintain this series in the future as one of a number of environmental time-series in the western Wadden Sea.

Acknowledgements

This publication is dedicated to the memory of the late Henk Beumkes, who took care of the Marsdiep observations for tens of years. The monthly mean data are freely available on request for scientific research (aken@nioz.nl, see also http://www.nioz.nl/en/deps/fys/niozteso/enhtml/master.html). This is NIOZ contribution 3626.

Reference

van der Hoeven, P. C. T. 1982. Observations of surface water temperature and salinity. State Office of Fishery Research (RIVO): 1860–1981, KNMI Scientific Report W.R. 82–2. 118 pp.

ICES Marine Science Symposia, 219: 362–364. 2003

Long-term variations of the hydrography around Sweden

Lars S. Andersson and Karin M. Borenäs

Andersson, L. S., and Borenäs, K. B. 2003. Long-term variations of the hydrography around Sweden. – ICES Marine Science Symposia, 219: 362–364.

Time-series of salinity and temperature from the waters around Sweden have been constructed for the period 1960–2000. These show indications of long-term variations, especially for the surface salinity in the Baltic Proper.

Keywords: Baltic, hydrographic time-series, Kattegat, Skagerrak.

L. Andersson and K. Borenäs: SMHI, Nya Varvet 31, SE-426 71 Västra Frölunda, Sweden [tel: +46 11 4958000; fax: +46 31 751 8980; e-mail: karin.borenas@smhi.se; lars.s.andresson@smhi.se]. Correspondence to K. M. Borenäs.

Introduction

The seas around Sweden (see Figure 1) are characterized by large salinity variations. In the Skagerrak, water masses from different parts of the North Sea are present. The salinity is high, around 35, except along the Swedish and Norwegian coasts, where the outflow from the Baltic is transported out into the North Sea.

The Kattegat is a transition area between the Baltic and the Skagerrak. Here the water is strongly stratified with a permanent halocline at a depth of approximately 15 m. The deep water mainly consists of Skagerrak Water, while the surface layer is a mixture of deep water and water from the Baltic.

The upper part of the Baltic Proper is rather homogeneous down to about 80 m. The deep water, which enters through the Belts and the Sound, can be stagnant in the inner basins for long periods. In the relatively shallow area south of Sweden smaller inflows pass relatively quickly and the conditions in the deep water are variable. The salinity in the Gulf of Bothnia varies from about 6 in the south down to 2 in the north. This area is ice covered during winter.

The data

The map in Figure 1 displays the position of the stations used in the study with the respective depth in parentheses. Time-series of temperature and salinity, in the form of 5-year running means, have been constructed for the period 1960–2000. The results are based on summer measurements (Jun–Aug) for the Baltic and spring measurements (Mar–May) for Kattegat and Skagerrak. The reason for this choice is that these seasons had the best data coverage for the period in question. Since the analysis of the time-series is at an initial stage, only preliminary results are available at the moment.

Some preliminary conclusions

In the 1990s the surface salinity has in general increased in Kattegat/Skagerrak, while the values in the deep water do not indicate any trend. The temperature variations in the Kattegat/Skagerrak deep water show large similarities (see Figure 2). After peak values in the early 1990s the temperature decreased until 1995, since when it has been increasing.

In the Baltic Proper, as well as in the Gulf of Bothnia, the surface salinity reached minimum values in the late 1960s and 1990s, as demonstrated in Figure 3. This pattern is coupled to the freshwater discharge (cf. Winsor *et al.*, 2001), and its time scale is much longer than those associated with NAO.

At stations BY5 and BY15 the salinity in the deep water has increased from a minimum around 1990 while the temperature is fairly constant.



Figure 1. Map showing the waters around Sweden and the position of the hydrographic stations. The station depths are given in parentheses.

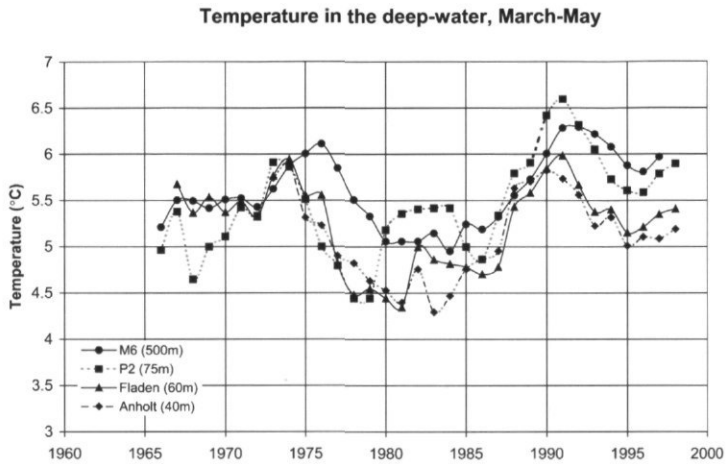


Figure 2. Time-series (5-year running means) of the deepwater temperature in Kattegat and Skagerrak based on spring measurements.

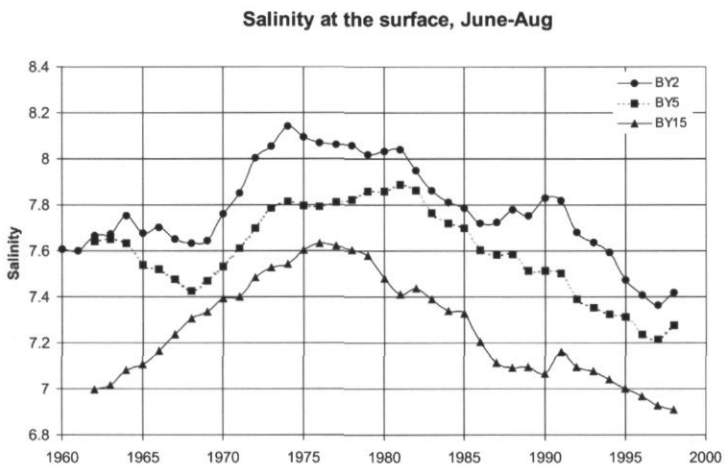


Figure 3. Time-series (5-year running means) of the surface salinity in the Baltic based on summer measurements.

Reference

Winsor, P., Rodhe, J., and Omstedt, A. 2001. Baltic Sea ocean climate: an analysis of 100 years of hydrographic data with focus on the freshwater budget. Climate Research, 18: 5–15.

ICES Marine Science Symposia, 219: 365–366. 2003

The North Atlantic Oscillation and sea level variations in the Baltic Sea

Kimmo K. Kahma, Hanna Boman, Milla M. Johansson, and Jouko Launiainen

Kahma, K. K., Boman, H., Johansson, M. M., and Launiainen, J. 2003. The North Atlantic Oscillation and sea level variations in the Baltic Sea. – ICES Marine Science Symposia, 219: 365–366.

The long-term trend in the mean sea level of the Baltic Sea is dominated by the rise in global sea level and, in the northern part of the area, by land uplift. Long-term variations around this general trend are strongly correlated with the long-term changes of the North Atlantic Oscillation index (NAO). The short-term, intra-annual variations also show long-term changes. During the high NAO index of recent decades the sea level in the Gulf of Finland has no longer decreased with the land uplift. This, together with the observed increase in the probability of extremely high sea levels, has resulted in more pronounced erosion of the coastal areas than before.

Keywords: Baltic Sea, mean sea level, NAO.

K. K. Kahma, H. Boman, M. M. Johansson, and J. Launiainen: Finnish Institute of Marine Research, PO Box 33, FIN-00931 Helsinki, Finland [tel: +358 9 613 941; fax: +358 9 613 944 94; e-mail: Kimmo.Kahma@fimr.fi]. Correspondence to K. K. Kahma.

Besides the rise in global sea level and land uplift, the water balance plays an important role in the mean sea level of the Baltic Sea. The amount of water in the Baltic Sea varies by some 370 km^3 on a time scale of a few weeks, which corresponds to a change of about 1 m in the sea level. Short-term variations on a scale of days are mainly related to windstress and differences in air pressure, but on a scale of months the water balance of the Baltic Sea is important. The variability is dominated by the exchange of water through the Danish Straits, and because the Baltic Sea is nearly enclosed long-term variations in the water balance do not average out on the annual scale, nor even on a 15-year time scale. The annual mean sea level may deviate by as much as 10 cm from the long-term average.

It is clear that the water balance should somehow be correlated with meteorological factors. Correlations have been reported with air temperature (Lisitzin, 1958) and river run-off of the Vuoksi (Launiainen *et al.*, 1987). In Vermeer *et al.* (1988) it was shown, however, that high river run-off cannot be the reason for a high sea level. If that were the case, the river run-off would be high earlier or at the same time as the increased water level, but in fact the high mean sea level precedes a high river run-off by about half a year. This clearly points toward a common external cause – the cyclonic weather disturbances passing over Finland and releasing rain and snow, and at the same time pushing water from the North Sea into the Baltic Sea.

Attempts to explain the water balance in the Baltic Sea by local winds or pressure distributions have been unsatisfactory. When the area was extended to include the North Atlantic, a correlation between water levels and air pressure patterns was observed by Heyen *et al.* (1994, 1996).

The dominant component of the air pressure patterns that influence the Baltic Sea water balance seems to be well described by the North Atlantic Oscillation (NAO) (Kahma, 1999; Johansson *et al.*, 2001). The NAO index is defined as the normalized pressure difference between Gibraltar and Iceland, and is a measure of the strength of the westerly flow.

The NAO index varies most during the winter and the best correlation seems to be between the long-term mean sea level and the mean of winter-time NAO. Figure 1 shows the 15-year running mean of winter-time NAO index (Jones *et al.*, 1997) and the residual water level at Hanko. The correlation coefficient for these long-term changes is 0.8. At the annual level the correlation coefficient is only 0.6, but the correlation is statistically more significant owin to more degrees of freedom.

The same high correlation between the winter NAO index and the residual variations in the sea level is evident in all the tide gauges along the Finnish coast (Johansson *et al.*, 2001). Using the regression equation between NAO and the residual long-term variations of the sea level at Hanko, a hindcast for the mean sea level can be made.

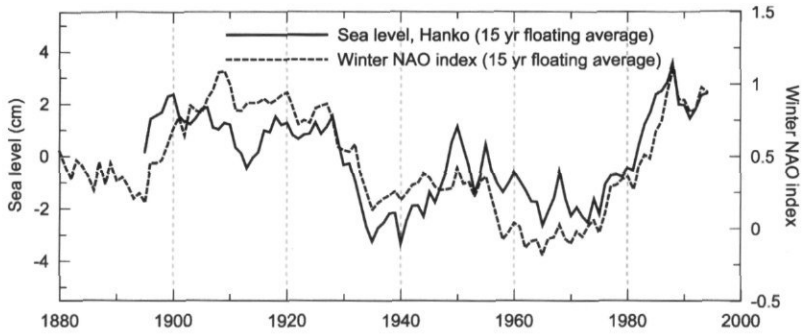


Figure 1. When the linear trend of land uplift and global sea level rise has been removed from the sea level data from Hanko, the residual shows a marked correlation with the winter-time North Atlantic Oscillation index.

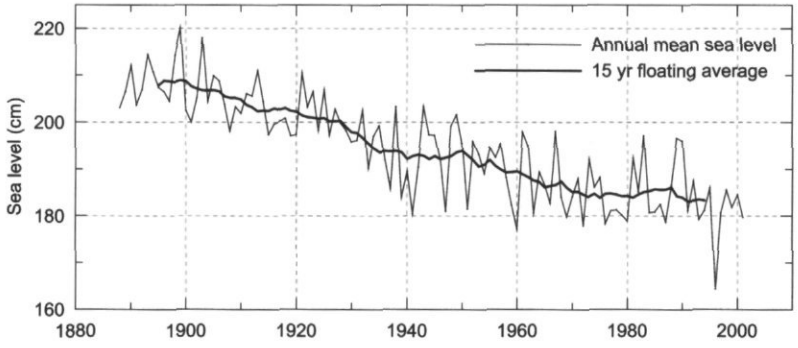


Figure 2. The mean sea level in the mouth of the Gulf of Finland (Hanko).

As Figure 2 shows, the apparent steady long-term trend from the beginning of the 20th century changed in 1970. This situation continued in the 1990s. In the Southern Baltic Sea this has meant a rise in the mean sea level of about 3 mm year^{-1}. In the Gulf of Finland, land and sea are both rising at approximately the same speed, which means that the shoreline has become steady after centuries of slow shifting. While this is the most conspicuous feature of the 1990s in the mean sea level of the Baltic Sea, the properties of short-term variations have changed, too. The probability distribution of sea levels has widened and the probability of extremely high sea levels has increased. The annual maximum when referenced to the annual mean sea level has increased from 1888 to 2000, whereas the minima have remained the same. This has led to increased erosion of vulnerable shores, except in the Gulf of Bothnia. For example, Kont (2000) has reported that in Estonia there has been erosion of sandy beaches almost everywhere in recent decades, and in some places the sea is advancing again.

References

Heyen, H., Zorita, E., and von Storch, H. 1994. Statistical downscaling of monthly mean North Atlantic air-pressure to sea level anomalies in the Baltic Sea. MPI Report, 150.

Heyen, H., Zorita, E., and von Storch, H. 1996. Statistical downscaling of monthly mean North Atlantic air-pressure to sea level anomalies in the Baltic Sea. Tellus, 48A: 312–323.

Johansson, M., Boman, H., Kahma, K. K., and Launiainen, J. 2001. Trends in sea level variability in the Baltic Sea. Boreal Environment Research, 6: 159–179.

Jones, P. D., Jonsson, T., and Wheeler, D. 1997. Extension to the North Atlantic Oscillation using early instrumental pressure observations from Gibraltar and South-West Iceland. International Journal of Climatology, 17: 1433–1450.

Kahma, K. 1999. Atlantin ilmapaine vaikuttaa Itämereen. Merentutkimuslaitos, Vuosikertomus 1999. (In Finnish with English summary.)

Kont, A. 2000: Implications of Accelerated Sea-Level Rise (ASLR) for Estonia. *In* Proceedings of SURVAS Expert Workshop on: "European Vulnerability & Adaptation to Impacts of Accelerated Sea-Level Rise (ASLR)", pp. 106–108. Ed. by A. C. de la Vega-Leinert, R. J. Nicholls, and R. S. J. Tol. Hamburg, Germany.

Launiainen, J., Matthäus, W., Fonselius, S., and Francke, E. 1987. Baltic Sea Environment Proceedings 17B: Chapter 1, Hydrography. Helsinki, 1987.

Lisitzin, E. 1958. Der Wasserstand in der Ostsee als Indikator der Strenge des Winters. Geophysica, 5: 162–175.

Vermeer, M., Kakkuri, J., Mälkki, P., Boman, H., Kahma, K. K., and Leppäranta, M. 1988. Land uplift and sea level variability spectrum using fully measured monthly means of tide gauge readings. Finnish Marine Research, 256: 3–75.

ICES Marine Science Symposia, 219: 367–370. 2003

Variability of the surface circulation of the Nordic Seas during the 1990s

Philip K. Jakobsen, Mads H. Nielsen, Detlef Quadfasel, and Torben Schmith

Jakobsen, P. K., Nielsen, M. H., Quadfasel, D., and Schmith, T. 2003. Variability of the surface circulation of the Nordic Seas during the 1990s. – ICES Marine Science Symposia, 219: 367–370.

The surface circulation of the Nordic Seas and its variability during the 1990s is investigated using current data obtained from satellite-tracked drifters. We find a seasonal intensification of the circulation during winter and during the first half of the 1990s, both due to the enhanced atmospheric momentum forcing.

Keywords: drifters, mean circulation, Nordic Seas, variability.

P. K. Jakobsen: Danish Meteorological Institute, Lyngbyvej 100, DK-2100 Copenhagen Ø, Denmark [tel: +45 39157 204; fax: +45 3927 0684; e-mail: pkj@dmi.dk]. M. H. Nielsen: Greenland Institute for Natural Resources, Nuuk, Greenland. Presently at Danish Meteorological Institute, Lyngbyvej 100, DK-2100 Copenhagen Ø, Denmark [tel: +45 3915 7207; e-mail: mhn@dmi.dk]; D. Quadfasel: Department of Geophysics, Niels Bohr Institute, University of Copenhagen, Juliane Maries Vej 30, DK-2100, Copenhagen Ø, Denmark [+45 3532 0609; e-mail: dq@gfy.ku.dk]; T. Schmith: Danish Meteorological Institute, Lyngbyvej 100, DK-2100 Copenhagen Ø, Denmark [tel: +45 3915 7444; e-mail: ts@dmi.dk]. Correspondence to P. K. Jakobsen.

Introduction

The near surface circulation of the Nordic Seas is cyclonic, with two meridional boundary currents on either side, the northward flowing Norwegian Current and the southward East Greenland Current. This general pattern has been known for a long time (Pettersson, 1900; Helland-Hansen and Nansen, 1909) and is based on ship drift observations and geostrophic estimates. As more data became available in the course of time, details were added to this picture. While Pettersson (1900) showed just one large-scale cyclonic circulation regime, Poulain *et al.* (1996) find four cyclonic gyres embedded between the boundary currents, tightly locked to the local bottom topography. In this article we study the near surface circulation of the Nordic Seas and the region south of the Greenland–Scotland Ridge using current data obtained with satellite tracked drifters during the 1990s. In addition to the mean flow we discuss the variability of the circulation on seasonal and interannual time scales.

Data and methods

Within the area between 58°N–80°N and 30°W –30°E more than 50 000 buoy days of position data were obtained from 266 surface drifters drogued at 15 m depth. These drifters were deployed within several international programmes during the 1990s, such as the World Ocean Circulation Experiment. The data distribution in time and space is not uniform. During the first half of the decade the majority of the data were obtained north of the Greenland–Scotland Ridge, while during the second half drifters were mainly released south of the ridge. This limits the quality of our results, in particular with respect to the discussion of interannual variability. Only drogued data are considered here. In a first step the position data were interpolated to 6-h time intervals and velocities calculated. Then tidal and inertial waves were removed from the calculated velocity time-series of the individual drifters using a low-pass filter with a cut-off period of 2 days. Finally we separated the meso-scale variability from the time-series by filtering with a cut-off of 18 days (Jakobsen, 2000).

Information about the circulation can be obtained directly from the Lagrangian data, as in Figure 1. However, for the discussion of variability we transformed the data into "pseudo-Eulerian" averages (vectors in Figure 2) – a technique discussed by Garraffo *et al.* (2001) for example. This enables the calculation of differences between seasons and years.

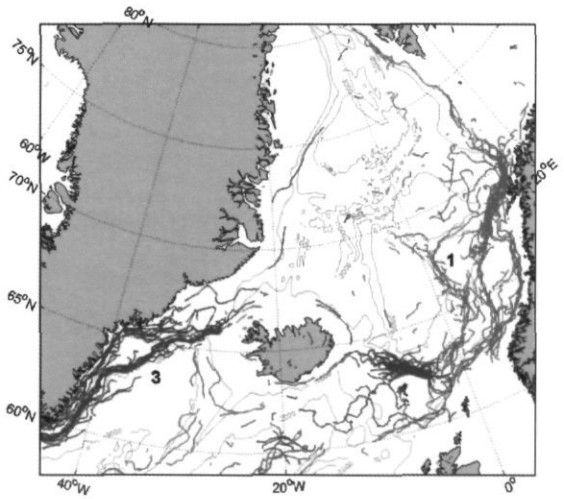


Figure 1. Trajectories of the satellite tracked drifters when the mean flow exceeded 25 cm s^{-1}. Red lines indicate northward and blue lines southward movement. Numbers refer to the circulation features discussed in the text. Black lines indicate the 1000, 2000, and 3000 isobaths.

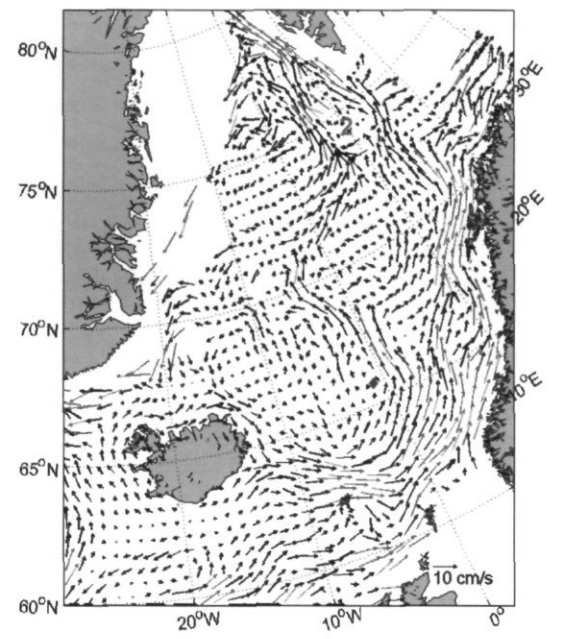


Figure 2. Pseudo-Eulerian description of the mean flow. The length of the vector scales with the velocity, but vectors in excess of 15 cm s^{-1} are held fixed and marked red. Numbers refer to the circulation features discussed in the text. The marking at 1°W, 65°45′N represents the minimal westward extend of Atlantic Water found by Blindheim *et al.* (2000).

Mean circulation

Since about half of our data are identical to those used in Poulain *et al.* (1996) we describe the mean circulation only briefly. The numbers refer to those indicated in Figures 1 and 2.

(1) There are three branches of the eastern boundary current system. The coastal current and the two branches of the Norwegian Current, one on continental slope and one spreading further offshore towards the Greenland Basin. (2) These two outer branches continue into the West Spitsbergen Current, following the shelf edge and the Arctic Front Jet east of the Greenland Sea Basin. (3) Two branches of the East Greenland Current system are seen in the Denmark Strait, a near coastal one over the shelf and one on the slope originating from the eastern side of the Denmark Strait. Further south at 65°N the two branches diverge, indicating topographic steering.

Blindheim *et al.* (2000) found that the westward extent of water with salinity above 35, measured on a 65°45′N transect, shifted between 0° and 7°W with changing NAO conditions. This led Blindheim *et al.* (2001) to state that a strong western branch of the Norwegian Atlantic Current is absent during high North Atlantic Oscillation Index conditions. We cannot confirm this finding, as our drifter data do show such a branch, even though the 1990s are characterized by the highest NAO Index conditions of the century. To show that our western branch is most likely carrying water of Atlantic origin rather than recirculated water, we show the minimal westward extent of the 35 isohaline measured in the study of Blindheim *et al.* (2000) in Figure 2.

Seasonal variability

To examine the seasonal variability we subtracted the mean Eulerian summer flow (May to October) from the mean winter flow (November to April) (Figure 3). Over most of the Nordic Seas and the North Atlantic the difference is positive, indicating a winter intensification of the circulation. This holds in particular for the strong eastern boundary currents and jets associated with topographic features. The winter increase of the flow is in the order 5 cm s^{-1}, which corresponds to about 20% of the mean flow, but in some areas, such as close to the Norwegian continental slope, it may be up to 15 cm s^{-1} stronger. Such seasonal variability has also been observed in long-term measurements with moored instruments, for example in the Norwegian Current near 63°N (Orvik *et al.*, 1999) and in the east Greenland Current near 75°N (Woodgate *et al.*, 1999). It can be related to the strengthening of the wind forcing during winter (not shown), although its amplitude is much weaker than a direct Sverdrup response to the forcing would suggest. This is likely

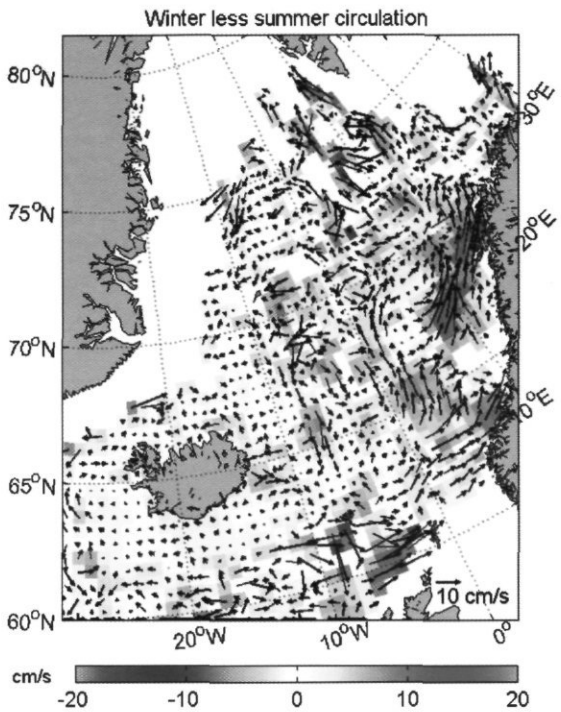


Figure 3. Seasonal variability of the surface circulation, depicted as difference vectors between the winter mean (Nov–Apr) and the summer mean (May–Oct) circulation. Colours indicate the difference in rms values.

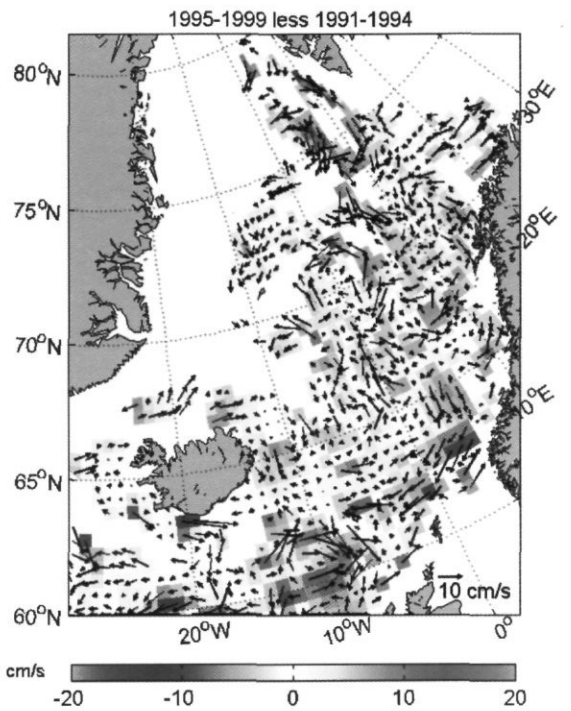


Figure 4. Interannual variability of the surface circulation, depicted as difference vectors between the 1995–1999 mean and the 1991–1994 mean circulation. Colours indicate the difference in rms values.

due to the influence of the bottom topography, which upsets a simple Sverdrup balance. In addition, the relatively stronger baroclinic forcing during summer keeps up the circulation during this period of weak wind forcing.

Interannual variability

The distribution of the drifter data in time allows a comparison of the mean circulation during the two periods 1991–1994 and 1995–1999 (Figure 4). The distribution of the differences is rather scattered in the regions of weak mean currents, but is clearer in the Atlantic inflow regime. The west Norwegian and West Spitsbergen currents are about 5 cm s^{-1} stronger during the first period, which is comparable to the seasonal variability.

For the eastern boundary currents, the weakening towards the second half of the decade can be related to the wind forcing. The windstress curl over the eastern Nordic seas during 1996–1997 was less than half of the mean during the rest of the 1990s (Figure 5). Our drifter data do not allow separation of these 2 years, but the low values could explain the weaker Atlantic flow during 1995–1999.

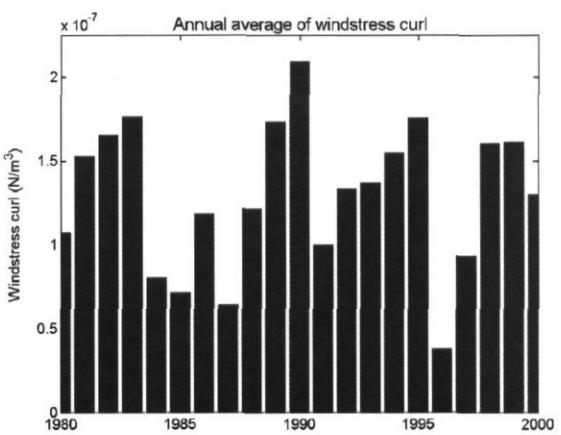


Figure 5. Interannual variability of the windstress curl over the area 10°W–10°E, 60°N–75°N. Shown are yearly averages in N m^{-3} derived from the NCEP/NCAR data set (Kalnay *et al.*, 1996) during the period 1980–2000.

Conclusions

The analysis of 9 years of drifter data from the Nordic seas shows substantial variability of the

circulation, in particular within the Atlantic regime. The variability on seasonal and interannual time scales is related to, and at least partly driven by, the wind forcing in the region. The wind-driven circulation in the Nordic Seas is generally thought to redistribute water masses, while the exchanges with the North Atlantic are thermohaline driven (Hansen and Østerhus, 2000). However, the latter is dependent on the redistribution of water (Dickson *et al.*, 1996). Since the Atlantic Water provides the heat for a mild northern Europe, and the salt for maintaining deep convection and the thermohaline overturning circulation, this aspect should also be considered in climate studies in addition to the usual buoyancy forcing.

Acknowledgements

We thank Dr. Jürgen Sellschopp at SACLANTC and Tracey Dougherty-Poupore at MEDS for making drifter data available. Financial support for the study came from the EU project ESOP, the Danish Research Academy and the project "OceanKlima" sponsored by the Nordic Council of Ministers.

References

Blindheim, J., Borovkov, V., Hansen, B., Malmberg, S.-A., Turrell, W., and Østerhus, S. 2000. Upper layer cooling and freshening in the Norwegian Sea in relation to atmospheric forcing. Deep-Sea Research I, 47: 655–680.

Blindheim, J., Toresen, R., and Loeng, H. 2001. Fremtidige klimatiske endringer og betydningen for fiskeressursene. Havets miljø, 73–78.

Dickson, R., Lazier, J., Meincke, J., Rhines, P., and Swift, J. 1996. Long-term coordinated changes in the convective activity of the North Atlantic. Progress in Oceanography 39: 241–295.

Garraffo, Z. D., Griffa, A., Mariano, A. J., and Chassignet, E. P. 2001. Lagrangian data in a high-resolution numerical simulation of the North Atlantic II. On the Pseudo-Eulerian averaging of Lagrangian data. Journal of Marine Systems, 29: 177–200.

Hansen, B., and Østerhus, S. 2000. North Atlantic–Norwegian Sea exchanges. Progress in Oceanography, 45: 109–208.

Helland-Hansen, B., and Nansen, F. 1909. The Norwegian Sea. Its physical oceanography based upon the Norwegian Researches 1900–1904. Report on Norwegian Fishery and Marine Investigation, 2: 1–390.

Jakobsen, P. K. 2000. Meso-scale eddies in the Nordic Seas. Master's Thesis. Roskilde Universitetscenter. 130 pp.

Kalnay, E., Kanamitsu, M., Kistler, R., Collins, W., Deaven, D., Gandin, L., Iredell, M., Saha, S., White, G., Woollen, J., Zhu, Y., Chelliah, M., Ebisuzaki, W., Higgins, W., Janowiak, J., Mo, K. C., Ropelewski, C., Wang, J., Leetmaa, A., Reynolds, R., Jenne, R. and Joseph, D. 1996: The NMC/NCAR 40-year reanalysis project. Bulletin of the American Meteorological Society, 77: 437–471.

Orvik, K. A., Skagseth, Ø., and Mork, M. 1999. Atlantic inflow to the Nordic Seas in the Svinøy section. International WOCE Newsletter, 37: 18–20.

Pettersson, O. 1900. Die Wasserzirkulation im Nordatlantischen Ozean. Petermanns Geographischen Mitteilungen Heft III and IV, 1–15.

Poulain, P.-M., Warn-Varnas, A., and Niiler, P. P. 1996. Near-surface circulation of the Nordic Seas as measured by Lagrangian drifters. Journal of Geophysical Research (Oceans), 101: 18237–18258.

Woodgate, R. A., Fahrbach, E., and Rohardt, G. 1999. Structure and transport of the East Greenland Current from moored current meters. Journal of Geophysical Research (Oceans), 104: 18059–18072.

ICES Marine Science Symposia, 219: 371–374. 2003

Variability at Ocean Weather Station M in the Norwegian Sea

Jan Even Øie Nilsen

Nilsen, J. E. Ø. 2003. Variability at Ocean Weather Station M in the Norwegian Sea. – ICES Marine Science Symposia, 219: 371–374.

Time-series of temperature and salinity from Ocean Weather Station M are analysed for periodic cycles of interannual to decadal scale. Time evolutions of the spectra show various spectral peaks at all depths, but none of these cycles show persistence throughout the 50 years. In addition, isopycnal surfaces and temperature and salinity values on these surfaces are estimated and studied in terms of the relative influence of horizontal advection and vertical movement on the observed changes of water properties.

Keywords: isopycnal levels, Norwegian Sea, variability, wavelet analysis.

J. E. Ø. Nilsen: Geophysical Institute, Allégt. 70, NO-5007 Bergen, Norway [tel: +47 55588697; fax: +47 55589883; e-mail: even@gfi.uib.no]

Introduction

The Ocean Weather Station Mike (OWSM) at 66°N 2°E (Gammelsrød *et al.*, 1992) is situated over the 2000 m isobath on the steep slope from the Vøring Plateau to the deep Norwegian Basin. It monitors the deep Norwegian Sea as well as the topographically locked subsurface front between Arctic Waters and inflowing Atlantic Water (Smart, 1984). This study aims to uncover some of the time dependencies of spectral properties in the time-series from OWSM, as well as investigating the possibility of separating vertical or cross-isopycnal motion from advection.

Data and methods

The oceanic data sampling at OWSM is done around standard depths. The program has been running since 1948 and consists of daily casts down to 1000 m and weekly down into the deep, resulting in the approximately 10 000 profiles of salinity and temperature which were used in this study. The data have been interpolated to standard depths by weighted parabolic interpolation (Reiniger and Ross, 1968) and to chosen isopycnal (σ_t) surfaces by logarithmic interpolation (Fofonoff, 1962). Average profiles are shown in Figure 1. Monthly mean values were calculated from months containing more than one profile. The depths of the chosen isopycnal levels were found by linear interpolation on dense depth interpolated σ_t profiles (Figure 2).

Wavelet transforms of the monthly data have been found using a Morlet mother wavelet (Torrence and Compo, 1997). Wavelet transformation is a method of time-frequency localization of oscillations in non-stationary records. It is similar to windowed Fourier transformation, but gives better temporal resolution due to the use of basis functions that are localized in time and of length according to their frequency (Graps, 1995). Before this spectral analysis, gaps in the time-series were filled by a local variance- and trend-conserving method using information from the data neighbouring the gaps.

Long-term trends

At all standard depths there is a weak negative overall trend in salinity. This trend is stronger in the intermediate waters (400–1200 m), where there is a pronounced salinity maximum in the early 1970s preceding a clear linear decrease into a fresher than mean 1990s (Figure 3B). In deep waters the salinity breaks off from the trend with an increase since 1997. This late 1990s salinity increase is also seen in the shallower waters (25–300 m; Figure 3A). There is a similarity between the trends on standard depths and those on corresponding isopycnal surfaces (Figures 3C, D). The trends on isopycnal surfaces below 400 m follow the changes in isopycnal depths (Figure 2), i.e. the freshening since the 1970s is accompanied by a deepening of isopycnal surfaces.

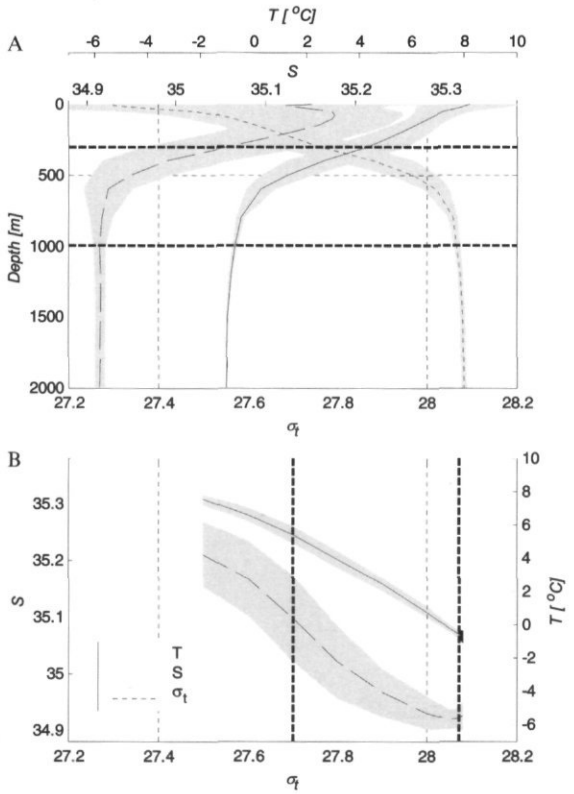


Figure 1. Average profiles from OWSM in depth (A) and sigma coordinates (B). Shaded regions illustrate standard deviation. As can be seen, these are in the pycnocline and the intermediate/deep waters, respectively.

There are no significant temperature trends on standard depths of the upper 400 m (Figure 3E). Between 400 m and 800 m there is a very weak overall cooling trend, with a stronger cooling during the 1990s, accompanying the freshening at the same depths. Deeper than 1000 m, the overall trend is dominated by a strong warming since 1980 (Figure 3F) making the 1990s significantly warmer than average (Østerhus and Gammelsrød, 1999). As salinity and temperature are closely allied on the same isopycnal surface, their time-series are nearly identical and temperature trends are the same as the salinity trends described above. Thus the abyssal warming is not present on the isopycnal surfaces, and there is a cooling trend on the shallow isopycnal surfaces.

Interannual variability

Prior to 1975 there was a pronounced 10-year period oscillation in the halocline (Figure 3G). There is also a biennial periodicity in the early part of the series that weakens and seems to increase its period, possibly towards a persistent 5-year oscillation during 1980–1995. On the corresponding isopycnal surface, this oscillation is more pronounced and shifted towards longer periods (Figure 3I). More significant in this series is a decadal oscillation in the 1960s, changing toward a ca. 20-year period in 1980–2000,

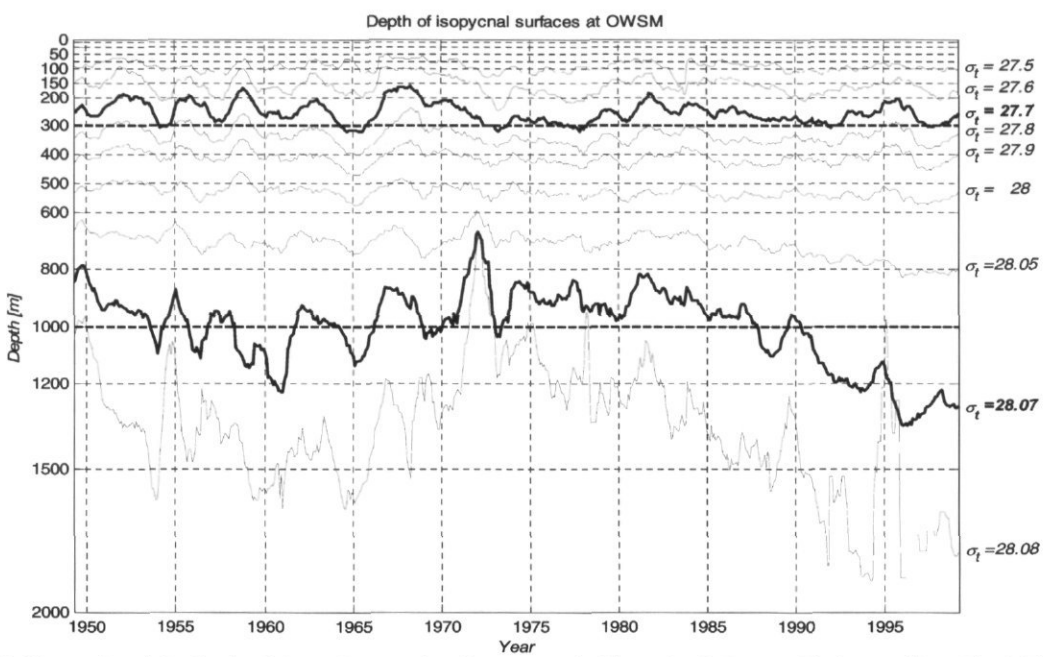


Figure 2. Time-series of the depth of chosen isopycnal surfaces, smoothed by a simple 1-year wide boxcar filter. The thick lines represent the depths and isopycnal levels analysed in Figure 3.

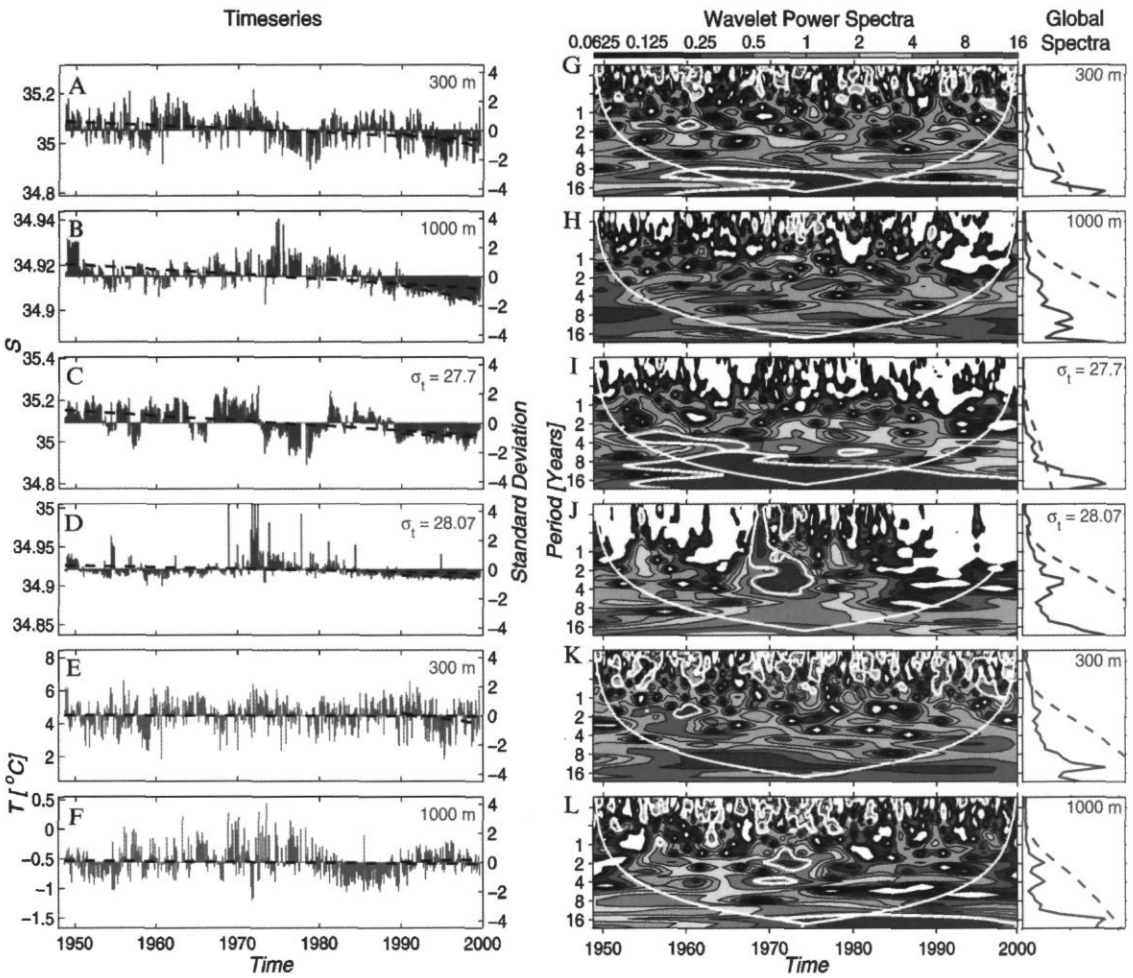


Figure 3. Time-series of monthly salinity at two chosen standard depths (A, B) and at their corresponding isopycnal surfaces (C, D), and time-series of monthly temperature at same depths (E, F). Since salinity and temperature are closely allied on the same isopycnal surface, isopycnal series of temperature is also represented by (C, D). Dashed lines represent linear trends. Panels G-L show Wavelet Power Spectra of variance normalized by $1/\sigma^2$. White curves give "Cones-of-Influence" outside which edge effects affect the result. White contours enclose regions of greater than 95% confidence for a red noise process with a lag1 coefficient of 0.72. The global wavelet spectrum is similar to a "regular" (Fourier) spectrum for the whole time-series, and here plotted together with the mean red noise spectrum (dashed line).

possibly affected by edge effects in the wavelet transform but evident in the time series (Figure 3). In the deep waters, there are no persistent salinity oscillations present at constant depths, but sporadic energy is found at periods around 2.5, 4, and 8 years (Figure 3H). Deep isopycnal surfaces ($\sigma_t = 28.07$) are dominated by a strong localized (possibly spurious) effect of the narrow maximum in the early 1970s (Figure 3J).

In temperature, as in salinity, there is a biennial oscillation around 1960, but with a more transient character. Temperature series of the intermediate waters are dominated by a single 20-year oscillation (best seen in Figure 3F), but studies of time-series from all levels render this a result of a warm anomaly from above in the late 1970s and the 1990s abyssal warming from below. There are also transient 2 and 4-year cycles at 1000 m (Figure 3I) localized around the warm anomaly around 1975.

Discussion

Although the changes in water properties at constant depths cannot be related to those on nearby isopycnal surfaces, they can be attributed to water movement perpendicular to isopycnals (usually

vertical movement). If on the other hand changes occur concurrently on isopycnal surfaces and constant depths, one can suspect they are also seeing the effects of isopycnal (horizontal) water motion. Most trends and interannual variability show similarities between properties on isopycnal surfaces and at constant depth, indicating that these changes are advected into the area. High frequency variability, on the other hand, is markedly more pronounced at constant depths, and must be attributed to oscillation of the isopycnals (Figure 3A, C).

With the water structures in the pycnocline at OWSM (Figure 1), changes in depth of isopycnal levels caused by vertical motion should be in phase with both salinity and temperature variations. The overall freshening since 1970 as well as most of the interannual variability of salinity are in opposite phase with the depth of the isopycnal surfaces (Figure 2), indicating that changing isopycnal depths do not determine the changes in salinity. Temperature, on the other hand, seems to be in phase with isopycnal depth, and not strongly related to its counterpart on the isopycnal surface (Figures 2 and 3E, F), which is not surprising since changes in surface temperature have the strongest influence on the mixed layer depth.

Summary and conclusions

Trends and interannual variability are in most cases coherent at constant depths and on isopycnal surfaces, and thus results of (isopycnal) advection into the area. High frequency variability can be attributed to oscillation of the isopycnal surfaces, and thus separated from the advection by this method. The Wavelet analysis of interannual variability shows no clear or persistent periodicity throughout the series, but there is evidence of transient oscillations often in a bimodal structure with variability in both 2–5 year and 10–20 year bands.

Acknowledgements

Svein Østerhus is thanked for helping with preparation of the data. Wavelet software was provided by C. Torrence and G. Compo, and is available at URL: http://paos.colorado.edu/research/wavelets/

References

Blindheim, J. 1990. Arctic Intermediate Water in the Norwegian Sea. Deep-Sea Research, 37: 1475–1489.

Fofonoff, N. 1962. Machine computations of mass transport in the North Pacific Ocean. Journal of Fisheries Research Board Canada, 19: 1121–1141.

Gammelsrød, T., Østerhus, S., and Godøy, Ø. 1992. Decadal variations of ocean climate in the Norwegian Sea observed at Ocean Station "Mike" (66°N 2°E). *In* Hydrobiological Variability in the ICES Area, 1980–1989. ICES Marine Science Symposia, 195: 68–75.

Graps, A. 1995. An introduction to wavelets. IEEE Computational Science and Engineering, 2: 50–61.

Østerhus, S., and Gammelsrød, T. 1999. The abyss of the Nordic Seas is warming. Journal of Climate, 12: 3297–3304.

Reiniger, R., and Ross, C. 1968. A method of interpolation with application to oceanographic data. Deep-Sea Research, 15: 185–193.

Smart, J. H. 1984. Spatial variability of major frontal systems in the North Atlantic–Norwegian Sea Area: 1980–1981. Journal of Physical Oceanography, 14: 185–192.

Torrence, C., and Compo, G. P. 1997. A practical guide to wavelets. Bulletin of the American Meteorological Society, 79: 61–78.

ICES Marine Science Symposia, 219: 375–377. 2003

Formation of intermediate water in the Greenland Sea during the 1990s

Johannes Karstensen, Peter Schlosser, Johann Blindheim, John Bullister, and Douglas Wallace

Karstensen, J., Schlosser, P., Blindheim, J., Bullister, J., and Wallace, D. 2003. Formation of intermediate water in the Greenland Sea during the 1990s. – ICES Marine Science Symposia, 219: 375–377.

The transformation rates of upper water into intermediate water (500 to 1600 m) of the central Greenland Sea are deduced from annual changes in CFC tracer inventories between 1991 and 2000. Transformation was found to be intermittent in time, mainly taking place in the winters of 1994/1995 and 1999/2000. Formation rates are of the order of 0.2 to 0.9 Sv ($1\ Sv = 10^6\ m^3\ s^{-1}$), equivalent to a 10-year average of up to 0.2 Sv. Associated changes in heat content of the intermediate layer are consistent with a winter-time heat loss of 20 W m^{-2} over 1 month (75 W m^{-2} over 1 week) at the sea surface.

Keywords: Greenland Sea, heat flux, variability, water mass formation.

J. Karstensen and P. Schlosser: Lamont-Doherty Earth Observatory of Columbia University, 61 Rt 9W, Palisades, NY, 10964, USA [tel: +1 845 3658707; fax: +1 845 3658176; e-mail: jkarsten@ldeo.columbia.edu; peters@ldeo.columbia.edu]; J. Blindheim: IMR, PO Box 1870, NO-5024 Bergen, Norway [tel: +47 5 238569; fax: +47 5 238531; e-mail: johan.blindheim@imr.no]; J. Bullister: PMEL/NOAA, 7600 Sand Point Way, N.E. Seattle, WA, 98115, USA [tel: +1 206 5266741; fax: +1 206 5266744; e-mail: johnb@pmel.noaa.gov]; D. Wallace: IfM, Düsternbrooker Weg 20, D-24105 Kiel, Germany. [tel: +49 431 6004200; fax: +49 431 6004202; e-mail: dwallace@ifm.uni-kiel.de]. Correspondence to J. Karstensen.

Introduction

The Greenland Sea is a prominent site for water mass transformation. Its wind-driven cyclonic circulation causes a doming of the isopycnals towards the gyre center that promotes convection due to winter-time buoyancy loss. Convection to intermediate depth (of the order of 1500 m) was observed frequently from the late 1980s, whereas deeper convection was never directly observed. The convection to intermediate depth forms Greenland Sea Arctic Intermediate Water (GSAIW) (Swift and Aagaard, 1981; Blindheim, 1990). Here we explore formation rates of GSAIW for the time interval 1991 to 2000 combining hydrographic and transient tracer data along a 75°N section crossing the Greenland Sea gyre.

Characteristics and formation of GSAIW

The convection process is the first step in the process of ventilating the ocean's interior. The intensity of atmospheric heat loss is the major driver in the process, whereas salt fluxes play a role at least in triggering convection of surface water (Rudels, 1990). Variable surface forcing leads to variable transformation of upper waters in terms of transformed volume and tracer characteristics.

The temporal evolution of temperature and CFC 11 (Figure 1) show a deep penetration of tracers during the winters of 1994/95 and 1999/2000 as a consequence of convection and subsequent transport into the interior. In particular, these convection events changed the CFC inventories substantially (Figure 2).

Formation rates were calculated as the amount of mixed-layer water needed to produce the observed change in CFC inventory. As the ocean does not lose CFCs through its surface (in contrast to for example heat) and atmospheric time histories are quasi-constant over the period considered in this study (Walker *et al.*, 2000), inventories can be assumed either to increase or remain quasi-constant, as upper waters have only weak lateral gradients. Thus, our strategy was to calculate the height of a

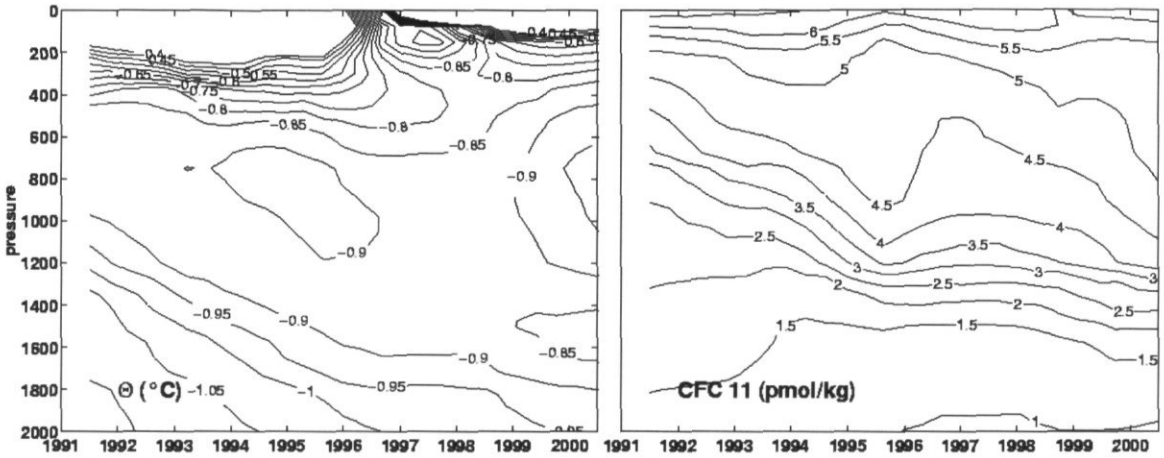


Figure 1. Temporal evolution of potential temperature (°C; left) and CFC 11 (pmol kg^{-1}; right) between November 1991 and May 2001. Note the convective events in winter 1994/1995 and 1999/2000 bringing cold water with high CFC 11 signals to intermediate depths. Contours are produced assuming that the tracer signal is imprinted in March of each year of observation.

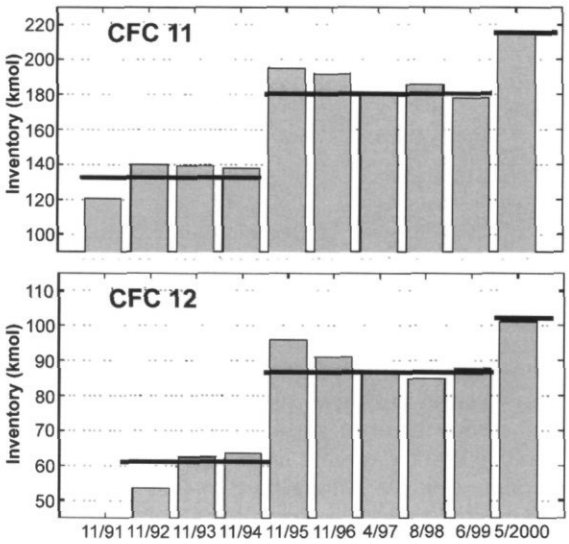


Figure 2. Change in CFC 11 and CFC 12 inventories (1×10^3 mol) considering an area of 4.5×10^{10} m^2 and a depth range from 500 to 1600 m. Note the inventory change between 1994/95 and 1999/2000.

column of upper waters required to yield the observed increases in the CFC inventory over time. We assumed that the Atlantic Water layer plays a role in the convection process and analyzed the changes in inventories in the water column that reaches from below the core of this layer (500 m depth) to a depth of 1600 m, where no increase in CFC was observed during the 1991 to 2000 time interval (Figure 1).

For CFC 11 we found an increase in the inventory of about 30 to 40 kmol in both winters with corresponding values for CFC 12 between 20 and 30 kmol (Figure 2). This translates into replacement of a water layer of 100 to 200 m depth, corresponding to volumes between 4.5 and 9×10^{12} m^3, respectively (radius of gyre 1.2×10^5 m). These numbers assume that the CFCs are completely confined in the gyre after convection and only "older waters" are removed from the gyre by the addition of recently ventilated, high CFC waters. However, considering a 50% entrainment of "older water" with a pre-convective CFC inventory, water equivalent to a column of about 300 m thickness has to be exchanged to yield the observed increase in CFC inventories.

Export of newly formed water

The related export of water from the convective site (subduction) is most likely caused by isopycnal eddy transfer, as shown by Khatiwala and Visbeck (2000) for the Labrador Sea. They found a relaxation time of the density field in the order of 7 months. Using this value we obtain a transport between 0.3 and 0.6 Sv for both winters, which increases to 0.9 Sv using a 50% entrainment. The annual average transport is in the order of 0.1 to 0.2 Sv, because only two major convection events occurred during the 10 years for which data were analyzed. The average numbers compare well with the findings of Rhein (1996) averaging over the 1980s and early 1990s.

Although a salinification of the intermediate layer is observed over the 10 years, interannual salinity changes do not appear to be significant. In contrast, temperature is affected in a sense that the convection interrupts the general warming trend in the

layer (0.02 K yr^{-1}) by holding the average temperature at a constant level between successive winters. Surface heat fluxes calculated from this value yield reasonable values of about 20 W m^{-2} if averaged over 1 month or 75 W m^{-2} if averaged over 1 week.

Conclusions

The transformation of surface water into intermediate water in the Greenland Sea during the 1990s was found to be intermittent in time (two main events) and associated with an average transport of about 0.2 Sv. Frequently, the North Atlantic Oscillation (NAO) index is used as indicator for the atmospheric forcing and thus convection activity. A positive (negative) index is related to weak (strong) convection activity in the Greenland Sea. Since the mid-1970s, a generally positive NAO index (with a few exceptions) prevailed and the highest values were observed in the 1990s. Thus, if this correlation holds, low GSAIW formation rates are not surprising. As the GSAIW spreads into the Nordic Seas, lower formation rates may have consequences for the ventilation of the deeper waters in this region. However, the present data set is not sufficiently dense to provide hard evidence for such a conclusion.

Acknowledgements

We thank the crew of the RV "Johann Hjort" as well as all the cruise participants for helping to collect the data over the years. The study was supported by the National Oceanographic and Atmospheric Administration through grant NA86GP0375.

References

Blindheim, J. 1990. Arctic Intermediate Water in the Norwegian Sea. Deep-Sea Research, 37: 1475–1489.

Khatiwala, S., and Visbeck, M. 2000. An estimate of the eddy-induced circulation in the Labrador Sea. Geophysical Research Letters, 27: 2277–2280.

Rhein, M. 1996. Convection in the Greenland Sea, 1982–1993. Journal of Geophysical Research, 101: 18183–18192.

Rudels, B. 1990. Haline convection in the Greenland Sea. Deep-Sea Research, 37: 1491–1511.

Swift, J. H., and Aagaard, K. 1981. Seasonal transitions and water mass formation in the Iceland and Greenland Sea. Deep-Sea Research, 28: 1107–1129.

Walker, S. J., Weiss, R. F., and Salameh, P. K. 2000. Reconstructed histories of the annual mean atmospheric mole fractions for the halocarbons CFC-11, CFC-12, CFC-113 and carbon tetrachloride. Journal of Geophysical Research, 105: 14285–14296.

ICES Marine Science Symposia, 219: 378–381. 2003

Direct measurements of heat and mass transports through Fram Strait

Eberhard Fahrbach, Gerd Rohardt, Ursula Schauer, Jens Meincke, Svein Østerhus, and Jennifer Verduin

Fahrbach, E., Rohardt, G., Schauer, U., Meincke, J., Østerhus, S., and Verduin, J. 2003. Direct measurements of heat and mass transports through Fram Strait. – ICES Marine Science Symposia, 219: 378–381.

To determine volume and heat transports through Fram Strait, an array of current meter moorings was maintained in the Strait between 1997 and 2001, with annual redeployments. The transports obtained by averaging the monthly means from the first 2 years were 9.5 Sv to the north and 11.1 Sv to the south ($1Sv = 10^6 m^3 s^{-1}$). The net transport over the 2 years was 4.2 Sv to the south, taking into account that there is some recirculation from the eastern to the western side of the transect which has a meridional offset of 10 nmi. The northward transport consists of about 50% of Atlantic Water, of which about 65% recirculates north of the transect. The northward heat flow, 85% of which is by Atlantic Water, is 16TW (1997/1998) and 41TW (1998/1999).

Keywords: Arctic Ocean, Atlantic Water, Fram Strait, measurements, transports.

E. Fahrbach, G. Rohardt, U. Schauer, J. Verduin: Alfred-Wegener-Institut für Polar- und Meeresforsch., Postfach 12 01 61, 27515 Bremerhaven, Germany [e-mail: efahrbach @awi-bremerhaven.de; grohardt@awi-bremerhaven.de; uschauer@awi-remerhaven.de; VerJnnfr@aol.com]. J. Meincke: Institut für Meereskunde, Universität Hamburg, Troplowitzstr. 7, 22529 Hamburg, Germany [e-mail: meincke@meer.ifm.uni-hamburg.de]. S. Østerhus: Bjerknes Center, Geophysical Institute and Norwegian Polar Institute, Allegaten 70, NO-5007 Bergen, Norway [e-mail: Svein.Osterhus@gfi.uib.no]. Correspondence to E. Fahrbach.

Introduction

Exchanges between the North Atlantic and the Arctic Ocean result in the most dramatic water mass conversions in the world ocean: warm and saline Atlantic waters flowing through the Nordic Seas into the Arctic Ocean are separated by cooling and freezing into shallow fresh waters (and ice) and saline deep waters. The outflow from the Nordic Seas to the south provides the initial driving of the global thermohaline circulation cell; the one to the north is of major impact to the large-scale circulation of the Arctic Ocean. Measuring these fluxes is a major requirement to quantify the turnover rates within the large circulation cells of the Arctic and the Atlantic Oceans and a basic condition for understanding the role of these ocean areas in climate variability on interannual and decadal scales.

Data

With the aim of assessing the accuracy of the transport estimates which can be obtained by direct measurements, 14 current meter moorings were deployed in Fram Strait from September 1997 until August 2001, with replacements in September of 1998, 1999, and 2000 (Figures 1, 2). The recovery of the present array is planned for 2002 after a 2-year deployment period. From 1999 to 2000 the 3 central moorings (F7, F8, and F9) were omitted. The moored instruments covered the water column from 10 m above the seabed to approximately 60 m below the surface. Three moorings in the East Greenland Current were equipped with upward-looking Doppler Current Meters reaching to the sea surface. In the horizontal the measurements extend from 6°51′W (the eastern Greenland shelf break) to 8°40′E (the western shelf break off Spitsbergen), on a line along 78°50′N on the eastern part and along 79°N on the western part of the transect. The flow field through the Strait was compiled by interpolation based on the records of 40 current meters for the first year and 45 for the second. The temperature and salinity distributions were obtained with significantly higher spatial resolution by CTD measurements during the cruises.

Results

Monthly volume transports were calculated from the velocity field interpolated over the cross-section

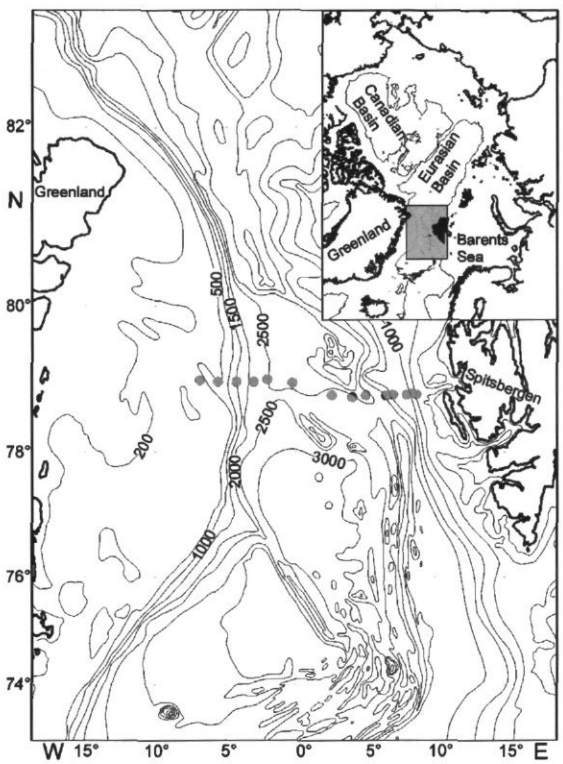


Figure 1. Map of Fram Strait with the positions of moorings deployed during VEINS and until 2001.

of Fram Strait. Because of the superimposed eddy field, 1 month is the shortest period for sufficient averaging to reduce aliasing by eddies and still to resolve the seasonal variation (Fahrbach *et al.*, 2001). The transports obtained by averaging the monthly means from the 2 years were 9.5 Sv to the north and 11.1 Sv to the south (1 Sv = 10^6 m^3 s^{-1}). However, it has to be taken into account that the eastern and western parts of the section are meridionally shifted by 10 nmi (Figure 1). The average recirculation across this 10-nmi-wide section is 2.6 Sv to the west on. Taking into account this recirculation, the net transport over the 2 years is 4.2 Sv to the south (Fahrbach *et al.* 2001). The monthly transports reveal an intensive seasonal variation with large northward transports in winter and weaker ones in summer. This is reflected in the net transport time-series with southward transports in May/June and northward ones in February and April. Strong semi-annual fluctuations are superimposed. The results of transport calculations depend strongly on the applied schemes, which take into account the non-linear character of transports with a variable regional extent. Uncertainties due to different interpolation schemes and the way gaps caused by failing instruments are closed in the time-series are in the range of 1 to 2 Sv. This uncertainty affects the estimates given below in the range of 20%.

Forty-five percent (1997/1998) and 55% (1998/1999) of the northward transport across the transect consists of Atlantic Water defined by water with a temperature above 1°C. From the Atlantic Water 80% (1997/1998) and 50% (1998/1999) recirculates. The northward heat flow of Atlantic Water (rather temperature flow relative to –0.1°C due to the

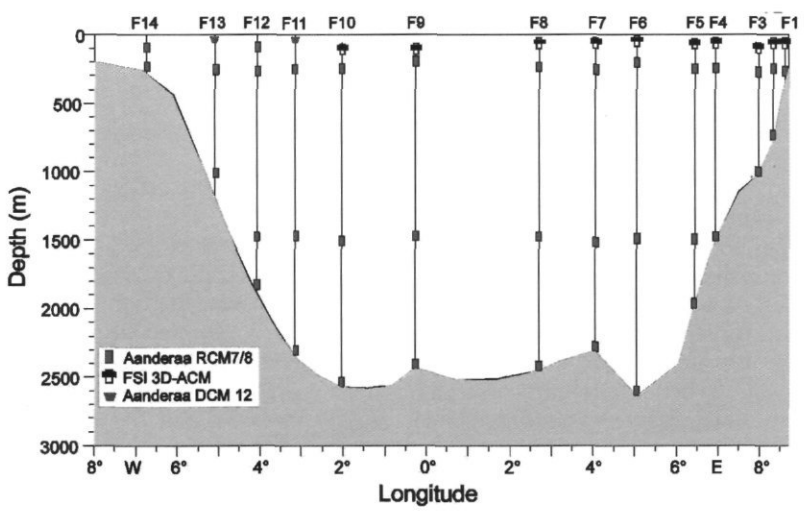


Figure 2. Vertical transect across Fram Strait with the moored instruments deployed from September 1997 to September 1999.

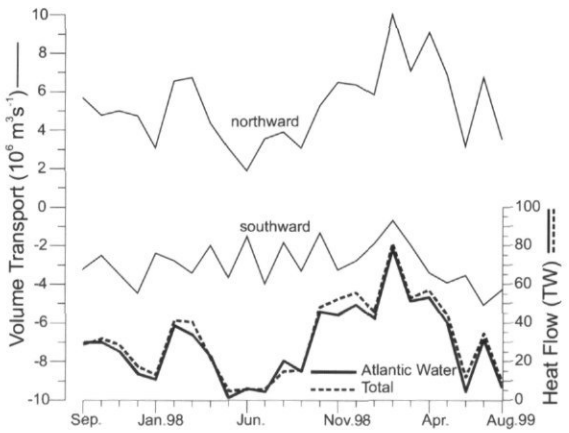


Figure 3. Monthly averages of volume transports through Fram Strait by Atlantic Water (temperature above 1°C) and of associated temperature transports (relative to –0.1°C) determined from the data of the moored instruments as an indicator of the heat transport.

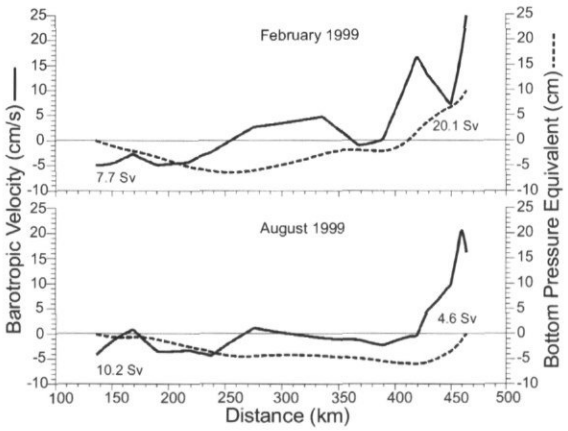


Figure 4. Monthly averages of the barotropic velocities (solid line) along the transect across Fram Strait determined from the moored instruments for February (top) and August 1999 (bottom) and the associated northward (left) and southward (right) volume transports given as numbers (1Sv = 10^6 m^3 s^{-1}). The dashed line indicates the equivalent bottom pressure profile, which is derived from the barotropic currents relative to the western end of the transect and expressed in sea-level elevation (cm) under the assumption of geostrophic equilibrium.

unbalanced volume flow) across the complete section results as 16TW (1997/1998) and 41TW (1998/1999) (Figure 3). In both years, 85% of the heat transport is caused by the flow of Atlantic Water. The reference temperature of –0.1°C was selected in agreement with Aagaard and Greisman (1975) and Simonsen and Haugan (1996) to obtain results which can be compared with earlier work. The obtained range of heat transports suggests an interannual variation of 50%. During both years the transport was within the range of previous estimates (e.g. Simonsen and Haugan, 1996). The transport has its maximum in winter and varies by about 50% within the annual cycle. The variance is mainly due to volume transport variability and only to a minor extent to temperature fluctuation. The time-series is still not long enough to address decadal time-scales. However, it gives a hint on the effort which is needed to eliminate seasonal and interannual variations before longer time-scales can be assessed properly.

It is planned to continue the measurements to obtain a reliable estimate of the interannual variability of the transports and the effect on the Arctic Ocean. Different possibilities will be examined to reduce the number of instruments and moorings. Since the currents are highly barotropic, measurements with bottom pressure recorders, after careful calibration, might allow better estimates of transport variations. Bottom pressure variations related to transport variations can be expected under the assumption of a geostrophically balanced barotropic current. Their seasonal range is derived from current meter records by calculating the horizontal profile of bottom pressure relative to western end of the transect for two seasons (Figure 4). It is in the range to be measured by available pressure recorders, which were deployed in the meantime. Omitting moorings in the recirculation area in the centre of the Strait does not seem promising, since 30% of the volume transport will then not be captured. Correlation of transport time-series with monthly mean zonal current velocities at selected locations seems promising. However, results based on 2-year long time-series cannot simply be transferred onto longer periods, since the present time-series are dominated by the annual cycle. Consequently a longer evaluation period is needed.

Acknowledgements

We are grateful to Matthias Monsees, Ekkehard Schütt, and Andreas Wisotzki, who participated in the work at sea, the data-processing, and provided drawings. We appreciate the valuable contribution of Rebecca A. Woodgate to advance the project during her stay in Bremerhaven and the later analysis by intensive and fruitful discussions. A significant part of the work occurred under the European Union MAST III Programme VEINS (Variability of Exchanges in the Northern Seas) Contract number MAS3-CT96-0070.

References

Aagaard, K., and Greisman, P. 1975. Toward new mass and heat budgets for the Arctic Ocean. Journal of Geophysical Research, 80: 3821–3827.

Fahrbach, E., Meincke, J., Østerhus, S., Rohardt, G., Schauer, U., Tverberg. V., and Verduin, J. 2001. Direct measurements of volume transports through Fram Strait. Polar Research, 29: 217–224.

Simonsen, K., and Haugan, P. M. 1996. Heat budgets of the Arctic Mediterranean and sea surface heat flux parameterisations for the Nordic Seas. Journal of Geophysical Research 101, C3: 6553–6576.

ICES Marine Science Symposia, 219: 382–383. 2003

Interannual variability in hydrobiological variables in the coast of A Coruña (NW Spain) from 1991 to 1999

Nicolás González, Antonio Bode, Manuel Varela, and Rosario Carballo

González, N., Bode, A., Varela, M., and Carballo, R. 2003. Interannual variability in hydrobiological variables in the coast of A Coruña (NW Spain) from 1991 to 1999. – ICES Marine Science Symposia, 219: 382–383.

Results of monthly sampling at a 70-m-deep shelf station off A Coruña (NW Spain) from 1991 to 1999 illustrate the relationships between changes in biological productivity, seasonal upwelling, and interannual changes in the composition of Eastern North Atlantic Central Waters (ENACW). During most of the 1990s the North Atlantic Oscillation (NAO) index was positive, resulting in warm and wet weather off NW Spain. It also produced a subsurface poleward current, which transported ENACW of high salinity and low nutrient content. In contrast, negative NAO index values in 1995 and 1996 coincided with the return of low-salinity, nutrient-rich ENACW.

Key words: North Atlantic Central Water, North Atlantic Oscillation, nutrients, productivity, upwelling.

N. Gonzalez [e-mail: nicolas.gonzalez@co.ieo.es], A. Bode, M. Varela, and R. Carballo: Instituto Español de Oceanografía, Centro Oceanográfico de A Coruña. Apdo 130, E-15080, A Coruña, Spain. Correspondence to Nicolás González.

Introduction

Biological productivity in the Galician Shelf (NW Spain) strongly depends on the seasonal upwelling of nutrient-rich Eastern North Atlantic Central Waters (ENACW) driven by northeasterly winds from spring to autumn (Blanton *et al.*, 1987). The intensity and duration of the upwelling period is known to vary between years but there is limited information on other sources of variability, such as the nutrient load of the upwelled waters. Here we report results from monthly sampling from 1991 to 1999 at a 70-m-deep shelf station off A Coruña. Water properties were measured with a CTD and dissolved nutrients and chlorophyll concentrations were analysed from water samples collected with bottle casts (Casas *et al.*, 1997). An upwelling index was calculated following Blanton *et al.* (1987). Variability in large-scale atmospheric processes in the study area was taken to be reflected in the North Atlantic Oscillation index (NAO), as calculated by Hurrell (1995). Our objective is to illustrate interannual differences in the physical and chemical properties of the upwelling waters and of concurrent changes in biological production.

Interannual variability in upwelling waters

Episodic upwelling events, indicated by relatively cold, high-chlorophyll surface water and nutrientrich subsurface water, were clearly identified in all years of the study. Temperature at 70-m depth and the upwelling index follow similar patterns (Figure 1). However, the characteristics of the upwelled water were fairly variable (Figure 2). For instance, in 1992 and 1993 upwelling during the spring was characterized by water of high salinity (>35.8 psu) and low nutrients (5 μM NO_3). This type of ENACW was associated with persistent southwesterly winds, which also leads to a subsurface poleward current along the western Iberian Peninsula (Fiuza *et al.*, 1998). Low-salinity, nutrient-rich (12 μM NO_3) ENACW returned in 1995 and 1996 when the spring chlorophyll concentrations remained high and even increased during the summer (i.e. August 1995). Such conditions usually accompany northerly winds (Dickson *et al.*, 1988). Also, the unusual persistence of harmful algal blooms in 1995 suggests that these nutrient-rich ENACW might favour blooms of toxic phytoplankton species.

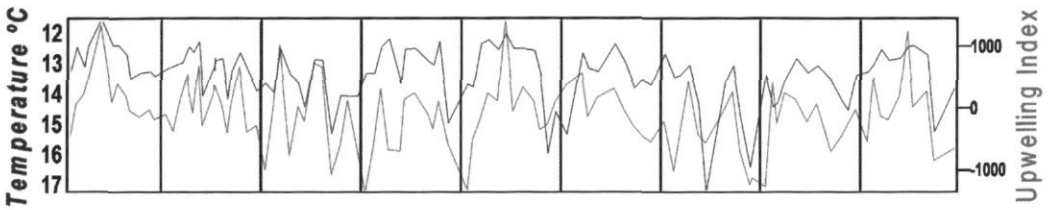


Figure 1. Upwelling Index ($m^2 s^{-1} \times 1000$) and the 70-m depth temperature (°C) during the sampling period.

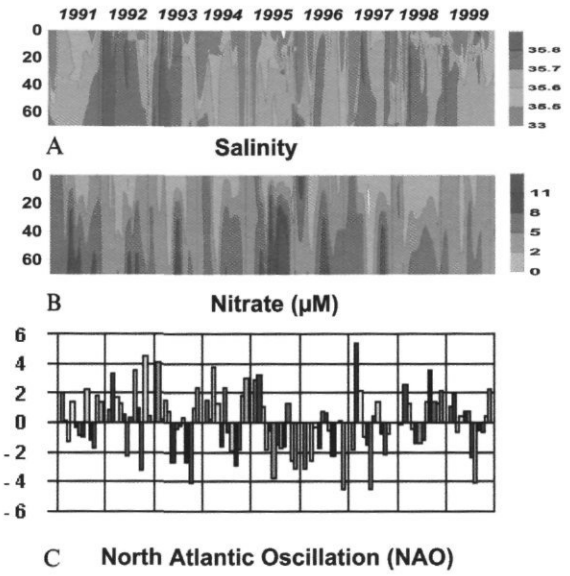


Figure 2. Decadal distribution of: (a) Nitrates (µg-at. N l^{-1}), (b) salinity, and (c) North Atlantic Oscillation Index.

Interannual climatic variability

Positive NAO values are associated with more frequently southwesterly winds that bring warm and wet weather off northwestern Spain and produce a warm, high salinity poleward current. Negative NAO values lead to more northerly winds that result in cold, dry air and an equatorward current carrying cooler, lower salinity water. Values of NAO from 1990 to 1999 exhibited considerable variability with a tendency to be positive over most of this period. As a consequence, episodic upwelling events were often associated with the high salinity ENACW and only between 1995 and 1996 when there was persistent upwelling associated with negative NAO values was low-salinity ENACW observed, consistent with Dickson *et al.* (1988). We postulate that the origin of the ENACW, which upwells near the coast, influences biological production in the study area through differences in nutrient inputs, along with variable water stability gradients induced by differences in salinity between water layers in the upper water-column.

References

Blanton, J. O., Tenore, K. R., Castillejo, F., Atkinson, L. P., Schwing, F. B., and Lavin, A. 1987. The relationship of upwelling to mussel production in the rias on the western coast of Spain. Journal of Marine Research, 45: 497–511.

Casas, B., Varela, M., Canle, M., González, N., and Bode, A. 1997. Seasonal variations of nutrients, seston and phytoplankton, and upwelling intensity off La Coruña (NW Spain). Estuarine and Coastal Shelf Science, 44: 767–778.

Dickson, R. R., Kelly, P. M., Colebrook, J. M., and Cushing, D. H. 1988. North winds and production in the eastern North Atlantic. Journal of Plankton Research, 10: 151–169.

Fiúza, A. F. G., Hamann, M., Ambar, I., Diaz del Rio, G., González, N., and Cabanas, J. M. 1998. Water masses and their circulation off western Iberia during May 1993. Deep-Sea Research, 45: 1127–1160.

Hurrell, J. W. 1995. Decadal trends in the North Atlantic Oscillation: regional temperatures and precipitation. Science, 269: 676–679

ICES Marine Science Symposia, 219: 384–386. 2003

Inter- and intra-annual variations in the stratification, timing, and intensity of phytoplankton blooms in the Central North Sea in the 1990s

Morten Holtegaard Nielsen and Michael St. John

Nielsen, M. H., and St. John, M. 2003. Inter- and intra-annual variations in the stratification, timing, and intensity of phytoplankton blooms in the Central North Sea in the 1990s. – ICES Marine Science Symposia, 219: 384–386.

A model for thermal stratification has been coupled with a biochemical model including one nutrient (dissolved inorganic nitrogen) and one type of phytoplankton (diatoms). The coupled model has been applied to the central North Sea for the period 1990–2000. The results show considerable variations within and between years as a function of differences in meteorological forcing. In terms of total primary production, outstanding years of the 1990s are 1991, 1998, and 1999. Most prominently, 1991 has both a high peak in net primary production and a spring bloom of long duration.

Keywords: ecosystem modeling, North Sea, phytoplankton blooms, stratification.

M. H. Nielsen: Danish Institute for Fisheries Research, Department of Marine and Coastal Ecology, Charlottenlund, Denmark. Present address: Woods Hole Oceanographic Institution, Department of Physical Oceanography, Mail Stop #21, 360 Woods Hole Road, Woods Hole, MA 02543, USA [tel: (+1) 508 289 2916; fax: (+1) 508 457 2181; e-mail: mnielsen@whoi.edu. M. St. John: University of Hamburg, Institute of Hydrobiology and Fisheries Science, Hamburg, Germany.

Introduction

The spatial and temporal dynamics of the North Sea ecosystem are dependent upon vertical mixing processes which modify the availability of light and limiting nutrients for phytoplankton production. In order to examine the effects of inter and intra-annual variations in stratification on ecosystem dynamics in the 1990s we coupled a model for thermal stratification and a biochemical model with variables for limiting nutrients and phytoplankton biomass. The coupled model was then used to study the historic conditions in the central North Sea (roughly at 56.5°N 2°E – see the map in St. John *et al.*, 2003), where the influence of frontal (i.e. horizontal) processes can be neglected.

Materials and methods

The model for thermal stratification (thoroughly described in Nielsen and St. John, 2001) is a potential energy model based on the energy equation for turbulence (Bo Pedersen, 1986). It is driven by heat input from the atmosphere and input of mixing energy from tidal current and wind. The boundary data are obtained from meteorological observations from the Ekofisk oil platform located near the study area. Examples of the boundary data can be found in Nielsen and St. John (2001).

The biochemical model is as presented by Sharples and Tett (1994) and is based on dissolved inorganic nitrogen (DIN) as the limiting nutrient and utilizes the rates of uptake and growth typical for diatoms as the modelled phytoplankton. The biological model is driven by the availability of light and nutrients as calculated from the stratification model.

Results

Figure 1 shows the model output for 1997 (the boundary data for this year can be found in St. John *et al.*, 2003), a year that is characterized by a rapid build-up of stratification starting on 25 April and leading to a high chlorophyll peak in the surface layer of almost 20 mg m^{-3}. A mixing event, due to cold and dry air around 5 May, accounts for entrainment of nutrient-rich bottom layer water into the euphotic zone causing a bloom that persists for a

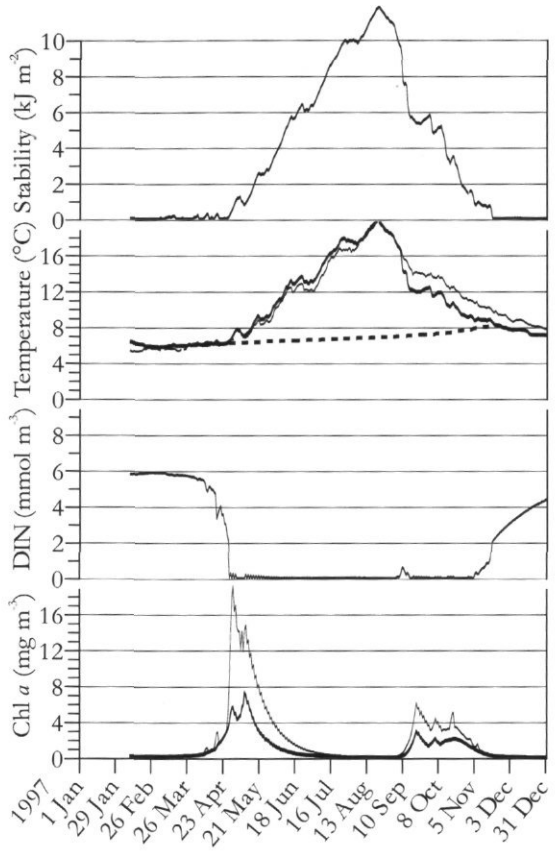


Figure 1. Model output for 1997. Top: stability of the water column. Second from top: upper layer temperature (thick, solid line), lower layer temperature (thick, dashed line), observed sea surface temperature (thin, solid line). Third from top: upper layer DIN. Bottom: upper layer chlorophyll concentration (thin, solid line), depth-mean chlorophyll concentration (thick line).

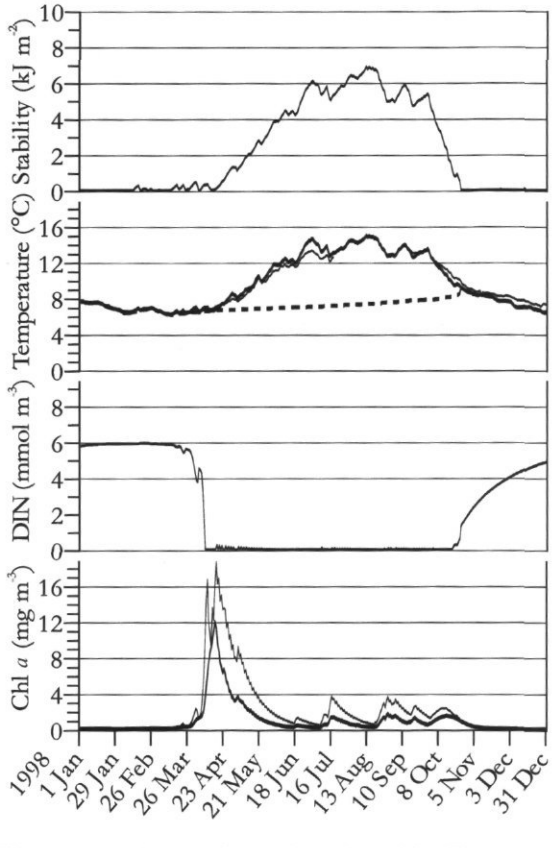


Figure 2. Model output for 1998. See legend for Figure 1.

couple of weeks. However, owing to the strong stability of the water column the depth-mean chlorophyll concentration amounts to only 7 mg m^{-3}. The fall bloom commences in the middle of August owing to two strong wind events and is fed by more entrainment due to wind as well as cooling.

Figure 2 shows the model output for 1998, a year characterized by a month-long period beginning on 20 March, during which stability exists but is weak. This allows for both the building up of the phytoplankton biomass as well as a continuous input of nutrients, thereby leading to a very high depth-mean chlorophyll concentration. This year is also characterized by a strong wind event in July, causing a small midsummer bloom, and a relatively calm fall leading to a prolonged and not so intense fall bloom.

Figure 3 shows the calculated depth-integrated chlorophyll concentration for 1991 and 1997, two contrasting years of the 1990s, compared with the

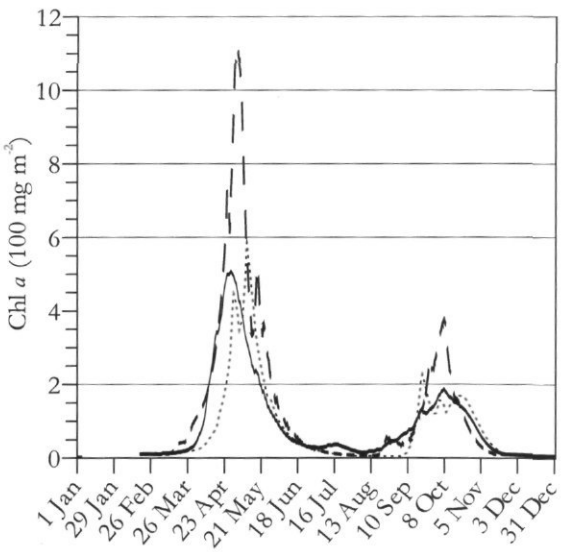


Figure 3. Calculated depth-integrated chlorophyll for 1991 (dashed line), 1997 (dotted line), and as daily mean from 1990 to 2000 (thick, solid line).

mean situation in the 1990s. Other outstanding years of the 1990s in terms of high productivity are 1998 and 1999.

Conclusions

Timing, intensity, and duration of phytoplankton blooms are important aspects that can influence the transfer of biomass to higher trophic levels of the food chain. Resolution of inter and intra-annual variations in phytoplankton blooms, a necessity for resolving the effects of climate variability on ecosystem dynamics, requires consideration of the temporal variation of heat input and mixing by wind and tide as well as the build-up of biomass. Following our coupled modelling approach we have identified years of highly variable climatic forcing during the spring period which are associated with high total primary production, prominent examples being 1991, 1998, and 1999.

In particular we find 1991 to be the outstanding year in the 1990s, having both a high peak in net primary production as well as a spring bloom of long duration. Future research in the EU funded LIFECO programme will examine the variations in higher trophic level dynamics resulting from variation in North Sea mixing processes.

Acknowledgements

We thank the Norwegian Meteorological Institute for providing meteorological observations from the Ekofisk oil platform and ICES for providing oceanographic observations from its Hydrographic Database. This study was carried out as part of the EU-funded LIFECO Project.

References

Bo Pedersen, F. 1986. Environmental Hydraulics: Stratified Flows. Springer-Verlag, Berlin.

Nielsen, M. H., and St. John, M. 2001. Modelling thermal stratification in the North Sea: application of a 2-D potential energy model. Estuarine, Coastal and Shelf Science, 53: 607–617.

Sharples, J., and Tett, P. 1994. Modelling the effect of physical variability on the midwater chlorophyll maximum. Journal of Marine Research, 52: 219–238.

St. John, M., Budgell, P., Nielsen, M. H., and Lucas, A. 2003. Resolving variations in the timing and intensity of the Spring Bloom in the Central North Sea during the 90's: a comparison of remote sensing and a 2-D modelling approach. ICES Marine Science Symposia, 219: 190–198. (This volume.)

ICES Marine Science Symposia, 219: 387–389. 2003

Increased phytoplankton production in the Gullmar Fjord, Sweden, 1985–1999

Odd Lindahl, Andrea Belgrano, and Björn A. Malmgren

Lindahl, O., Belgrano, A., and Malmgren, B. A. 2003. Increased phytoplankton production in the Gullmar Fjord, Sweden, 1985–1999. – ICES Marine Science Symposia, 219: 387–389.

We analyse a 15-year time-series comprising 280 single *in situ* measurements. Using the ^{14}C-incorporation technique, the study was carried out at a station in the mouth area of the Gullmar Fjord on the western coast of Sweden. Primary production estimates show a general increase between 1985 and 1999 of approximately 2.7 gC m^{-2} $year^{-1}$, representing approximately 1.1% of the total annual production. The possible causes behind this and some of the resulting ecological effects are discussed.

Keywords: Gullmar Fjord, North Atlantic Oscillation (NAO), primary production, Skagerrak, time-series.

O. Lindahl: The Royal Swedish Academy of Sciences, Kristineberg Marine Research Station, SE-450 34 Fiskebäckskil, Sweden [tel: +46 523 18512; fax: +46 523 18502; e-mail: odd.Lindahl@kmf.gu.se]. A. Belgrano: University of New Mexico, Department of Biology, Albuquerque, USA. B. A. Malmgren: Göteborg University, Department of Marine Geology, Gothenburg, Sweden. Correspondence to O. Lindahl.

Introduction

The pelagic ecosystem of the Gullmar Fjord and adjacent waters on the west coast of Sweden has been studied since the late 1970s, principally in relation to oceanographic variability in the Skagerrak and the possible influence of climatic forcing on this area (Lindahl and Hernroth, 1983; Andersson and Rydberg, 1993; Heilmann *et al.*, 1994; Lindahl *et al.*, 1998; Belgrano *et al.*, 1999). The hydrographic features of the waters along the Swedish west coast are strongly influenced by low salinity Baltic water, which causes stratification in the Kattegat and coastal waters of the Skagerrak.

Phytoplankton productivity has been measured at the mouth of the Gullmar Fjord since 1985. While elevated values of primary production are observed during spring (March–April), the highest contribution to annual production occurs during May–September (Lindahl, 1995).

In this article we examine whether the primary productivity increased during the period 1985–1999.

Materials and methods

Primary productivity was measured *in situ* by the ^{14}C-incorporation technique at 10 depths (0, 1, 2, 3, 4, 6, 8, 10, 15, and 20 m), following the recommendations of the Baltic Marine Biologists (Baltic Marine Biologists (BMB), 1976). A total of 280 sets of measurements were taken between 1985 and 1999 with the annual number varying between 12 and 24. There was an increase in sampling frequency during the summer half of the year. Dark-bottle incubations were performed at 0 and 20 m. The incubations were carried out during a 4-h period around noon and the results were transformed into daily production by the light factor method (BMB, 1976). The annual production of each year was calculated using linear interpolation between measurements.

Linear regression analysis was employed to determine the presence of a trend in the moving averages of the monthly mean productivity time-series as well as of the annual production time-series. Use of the slope of the linear regression line to test for trends requires that the residual observations (the difference between observed values and values predicted by the regression function) are random, normally distributed, and uncorrelated. We applied a runs test to analyse for randomness, the W and normalized W statistics devised by Royston (1982) to test for normality (this method is in turn based on the Shapiro-Wilk non-parametric procedure), and the Durbin-Watson test to test for correlation between consecutive residuals. In case these assumptions are

not fulfilled, the non-parametric Kendall τ test has to be used instead (Kendall, 1948; Kendall and Ord, 1990). This test considers the time-series as a whole rather than just the differences between neighbouring values (Legendre and Legendre, 1998).

Results

The monthly mean productivity (Fig. 1), calculated from measured 1-day productivity values, showed no significant trend. However, using 12-month moving averages of the monthly mean productivity, the presence of a significant trend ($\tau = 0.250$, $p = 0.1\%$) was found, suggesting that the monthly mean productivity had increased during the period 1985–1999 (the residuals were not normal and were correlated, so we had to re-utilize the Kendall test).

Furthermore, the 3-year moving average of the annual production was also tested for a trend using linear regression analysis (here the residuals are random, normal and uncorrelated). The slope of the regression line was found to be 4.02 and significant at the 2% level for 11 degrees of freedom.

The mean annual increase in production during 1985–1999 was estimated by taking the difference between the mean production of the first 5 years of the time-series ($P_{m.\ 1985\text{–}1989} = 224$ gC m^{-2}) and the last 5 years ($P_{m.\ 1995\text{–}1999} = 265$ gC m^{-2}). This difference of 41 gC m^{-2} corresponds to an increase of 2.7 gC m^{-2} year^{-1}, which is 1.1% of the annual mean production of the whole time-series ($P_{m.\ 1985\text{–}1999} = 248$ gC m^{-2}). This increase in annual production corresponds approximately to the production of two summer days each year, or the production of one summer month during the whole period.

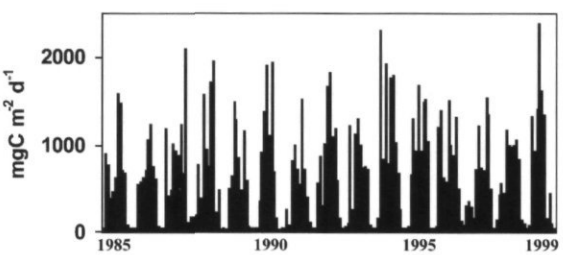


Figure 1. Monthly means of 1-day measured primary productivity 1985–1999.

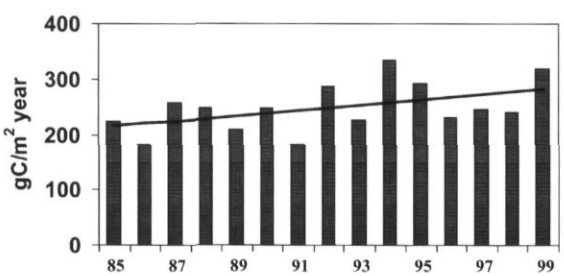


Figure 2. Calculated annual primary production 1985–1999. Line shows trend indicating an annual increase of 1.1%, corresponding to an increase of 2.7 gC m^{-2} year^{-1}.

Discussion

Several studies have examined the effect of weather/climatic forcing on physical–chemical processes in relation to primary productivity of the Gullmar Fjord. Their results suggest the presence of an indirect link between the North Atlantic Oscillation index (NAO), the supply of nutrients to the Kattegat, wind direction, and primary production (Lindahl *et al.*, 1998; Belgrano *et al.*, 1999). Statistical models suggest that with no lag winds play an important role through mixing and the subsequent availability of nutrients to the euphotic zone. Winds and the NAO index were important to primary production at lags of 1 month (Belgrano *et al.*, 2001). Another study carried out just outside the mouth area of the Gullmar Fjord showed that deep water nitrogen concentration was the most important factor determining chlorophyll concentrations of the surface water, but the exact transport mechanism is unknown (Hagberg, 2002).

Although phosphate supply to the Kattegat/Skagerrak area has decreased, nitrate supply has been unchanged or decreased since 1985 (Forum Skagerrak, 2001). These results indicate that the nutrient supply did not cause the observed increase in primary production. A hypothesis to be tested in the future is whether the availability of deep-water nutrients has changed over time as a result of the climate forcing caused by the strong positive NAO index during the late 1980s and especially during the 1990s (http://www.cgd.ucar.edu/cas/papers/science 1995/Fig1_update.html). Long-term changes in macroalgal vegetation of the inner parts of the Gullmar Fjord (Eriksson *et al.*, 2002) have been shown to be related to the effects of large-scale climate variability (NAO) linking Baltic Sea and Kattegat water transport and nutrients dynamics. A plausible mechanism for the observed changes in primary production may be related to an increase in the entrainment of deep water as a result of changes in the intensity of the coastal (Baltic) current due to the forcing associated with the NAO.

An analysis of the relationship between primary phytoplankton production and sedimentation of particulate material from the boreal coastal zone of the North Atlantic, including the Gullmar Fjord (Lindahl, 1988), has been compiled by Wassman (1990). A regression analysis indicated that the

sedimentation (= export production, P_E) was positively and non-linearly correlated with total production P_T ($P_E = 0.049 P_T^{1.41}$, $r^2 = 0.94$). Using this relationship, it is estimated that the sedimentation (P_E) in the Gullmar Fjord may have increased from approximately 120 gC m^{-2} $year^{-1}$ in the mid-1980s to almost 150 gC m^{-2} $year^{-1}$ by the end of the century (more or less out of range of the relationship). This would correspond to an increase in the organic load to the deep part of Gullmar Fjord below the photic zone of about 20%. A decrease in oxygen concentration in the deep water of the Gullmar Fjord was observed during the last decades of the 1900s (Forum Skagerrak, 2001) and an increased sedimentation may be one of the main causes.

Ultimately our results suggest that the seasonal growth of phytoplankton has been extended during a positive phase of the NAO and warmer sea surface temperature conditions observed from the late 1980s on the Swedish west coast (Belgrano *et al.*, 1999). A similar pattern has been observed in the Continuous Plankton Record data, indicating a particularly steep increase in the phytoplankton biomass in the North Sea during the high NAO years from the late 1980s (Reid *et al.*, 1998).

References

Andersson, L., and Rydberg, L. 1993. Exchange of water and nutrients between the Skagerrak and Kattegat. Estuarine and Coastal Shelf Science, 36: 159–181.

Baltic Marine Biologists. 1976. Recommendations on methods for marine biological studies in the Baltic Sea. BMB Publication No. 1. 98 pp.

Belgrano, A., Lindahl, O., and Hernroth, B. 1999. North Atlantic Oscillation, primary productivity and toxic phytoplankton in the Gullmar Fjord, Sweden (1985–1996). Proceedings of the Royal Society London B, 266: 425–430.

Belgrano, A., Malmgren, B., and Lindahl, O. 2001. Application of artificial neural networks (ANN) to primary production time-series data. Journal of Plankton Research, 23: 651–658.

Eriksson, B. K., Johansson, G., and Snoeijs, P. 2002. Long-term changes in the macroalgal vegetation of the inner Gullmar Fjord, Swedish Skagerrak coast. Journal of Phycology, 38: 284–296.

Forum Skagerrak. 2001. The Skagerrak – environmental state and monitoring prospects. ISBN 91-89507-04-5. (Available at the Swedish Meteorological and Hydrological Institute (SMHI)).

Hagberg, J. 2002. Climatic effects on the community dynamics of the benthic fauna in the Skagerrak. Doctoral thesis, Faculty of Science, Göteborg University, Sweden. 30 pp.

Heilmann, J. P., Richardson, K., and Ærtebjerg, G. 1994. Annual distribution and activity of phytoplankton in the Skagerrak–Kattegat frontal region. Marine Ecology Progress Series, 112: 213–223.

Kendall, M. G. 1948. Rank Correlation Methods. Charles Griffin & Co., London. 160 pp.

Kendall, M. G., and Ord, J. K. 1990. Time Series, 3rd edn. Edward Arnold, Sevenoaks, Kent. 296 pp.

Legendre, P., and Legendre, L. 1998. Numerical Ecology, 2nd edn. Elsevier, Amsterdam. 853 pp.

Lindahl, O. 1988. Sedimentation and oxygen consumption below sill level in the Gullmar fjord, Sweden. *In* Sediment Trap Studies in the Nordic Countries 1, pp. 149–158. Ed. by P. Wassman and A.-S. Heiskanen. Tvärminne Zoological Station, Finland. 207 pp.

Lindahl, O. 1995. Long-term studies of primary phytoplankton production in the Gullmar fjord, Sweden. *In* Ecology of Fjords and Coastal Waters, pp. 105–112. Ed. by H. R. Skjoldal, C. Hopkins, K. E. Erikstad, and H. P. Leinaas. Elsevier Science Publishers B.V. 623 pp.

Lindahl, O., and Hernroth, L. 1983. Phyto-zooplankton community in coastal waters of Western Sweden: an ecosystem off balance? Marine Ecology Progress Series, 10: 119–126.

Lindahl, O., Belgrano, A., Davidsson, L., and Hernroth, B. 1998. Primary production, climatic oscillations, and physico-chemical processes: the Gullmar Fjord time-series data set (1985–1996). ICES Journal of Marine Science, 55: 723–729.

Reid, P. C., Edwards, M., Hunt, H. G., and Warner, A. J. 1998. Phytoplankton change in the North Atlantic. Nature, 391: 546.

Royston, J. P. 1982. Algorithm AS181: the *W* test for normality. Applied Statistics, 31: 176–180.

Wassman, P. 1990. Relationship between primary and export production in the boreal, coastal zone of the North Atlantic. Limnology and Oceanography, 35: 464–471.

ICES Marine Science Symposia, 219: 390–392. 2003

Interannual correlation between hemispheric climate and northern Norwegian wintering stocks of two *Calanus* spp.

Stig Skreslet and Angel Borja

Skreslet, S., and Borja, A. 2003. Interannual correlation between hemispheric climate and northern Norwegian wintering stocks of two *Calanus* spp. – ICES Marine Science Symposia, 219: 390–392.

Calanus finmarchicus and *Calanus hyperboreus* were sampled by five replicate Juday net tows from bottom to surface in February and October 1983–2000 in two deep fjord basins with different sill depths. *C. finmarchicus* was an order more abundant than *C. hyperboreus* in both fjords. Seasonal stock changes probably expressed the difference between rates of mortality and immigration. The interannual variability in abundance was about an order of magnitude. Only *C. finmarchicus* was positively correlated with North Atlantic Oscillation, in opposite phase with its abundance in the North Sea, possibly due to changing winds that generated latitudinal shifts in the *C. finmarchicus* base population of the Northeast Atlantic. However, latitudinal shifts in westerly storm tracks possibly also forced vernal river flow from Norway to regulate the neritic plankton productivity and growth in the population of *C. finmarchicus*. Positive correlation between Arctic Oscillation and both species may be due to forcing of advected recruitment. Arctic Oscillation possibly also regulated population size in *C. hyperboreus*.

Keywords: Arctic Oscillation, *Calanus finmarchicus*, *Calanus hyperboreus*, ecology, immigration, mortality, North Atlantic Oscillation.

S. Skreslet: Faculty of Fisheries and Natural Sciences, Bodø College, N-8049 Bodø, Norway (tel: +47 7551 7496; fax: +47 7551 7484; e-mail: stig.skreslet@hibo.no). A. Borja: Department of Oceanography, AZTI, 20110 Pasaia, Spain. Correspondence to S. Skreslet.

Introduction

Calanus finmarchicus and *Calanus hyperboreus* form wintering stocks in Norwegian coastal waters (Figure 1). This study tests the hypothesis that their stock sizes reflect effects of climate on their population systems.

Material and methods

Saltfjord and Mistfjord (Figure 1) were selected for sampling. They are 382 and 297 m deep, and separated from the Vestfjord by 220 and 34 m deep sills, respectively. At one station in each fjord, twice each year in 1983–2000, five replicate vertical tows from about 10 m above the bottom to the surface were made using a 180 μm 0.1 m^2 Juday net. *Calanus helgolandicus* and *Calanus glacialis* were not distinguished from *C. finmarchicus* and *C. hyperboreus*, respectively, but represent little contamination of our abundance estimates (Skreslet et al., 2000; K. Olsen pers. comm.).

We correlated abundance estimates from stereomicroscopic counts with indices of North Atlantic Oscillation (NOA) (Lamb and Peppler, 1987) and Arctic Oscillation (AO) (Thompson and Wallace, 1998) obtained from http://www.cgd.ucar.edu/jhurrel/nao.html and http://jisao.washington.edu/data/annularmodes/Data/ ao_index.html. Though there was no autocorrelation, we corrected the degrees of freedom according to Quenouille (1952).

Results

Differences in abundance between replicates of both species were within an order of magnitude, while the interannual variability exceeded an order of magnitude (Figure 2). *C. finmarchicus* was more abundant than *C. hyperboreus* in both fjords. Their abundance usually declined from October to February. *C. finmarchicus* was usually more abundant in Saltfjord than Mistfjord, and *C. hyperboreus* the opposite. All significant correlations of abundance with either NAO or AO were positive (Table 1). *C. hyperboreus*

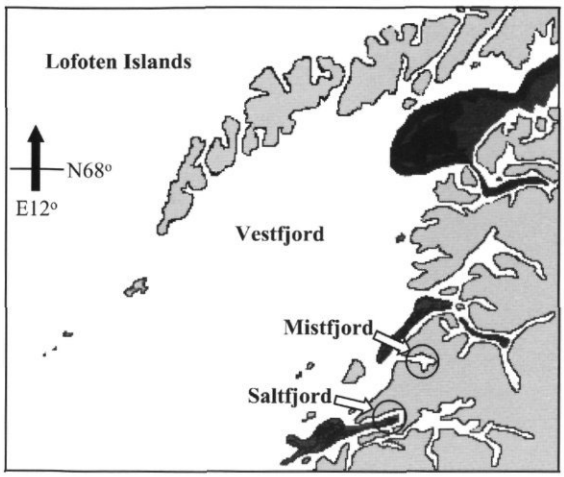


Figure 1. The Vestfjord area, north Norway (68°N 14°E). The 200 m depth contour is indicated. Dark: Wintering habitats of *Calanus finmarchicus* and *C. hyperboreus*, and spawning habitats of *C. hyperboreus*. Hatched: Main spawning of *C. finmarchicus* and post-spawning of *C. hyperboreus* in April. Sea surface isotherms for 3, 3.5, and 5°C in Mar–Apr 1922 (after Sømme, 1934). Arrows: sampling stations 1983–2000.

was significantly correlated only with AO. *C. finmarchicus* was significantly correlated with both, but its Mistfjord abundances in October and February were inconsistent, being correlated with AO in different years. In both fjords, the October abundance of *C. finmarchicus* was correlated with NAO averaged over March–July of the same year. Its February abundance in Mistfjord was correlated with the same average. In Saltfjord, the October abundance of both species was correlated with the average AO of July–September. In Mistfjord, the abundance of *C. hyperboreus* in both October and the next February was correlated with the same annual average of AO.

Discussion

Shelf water advects *C. finmarchicus* into the Saltfjord during September–October (Skreslet *et al.*, 2000). The accumulated stock is part of a larger population system in the Nordic Seas (Heath *et al.*, 2000). That may also be the case with *C. hyperboreus.*

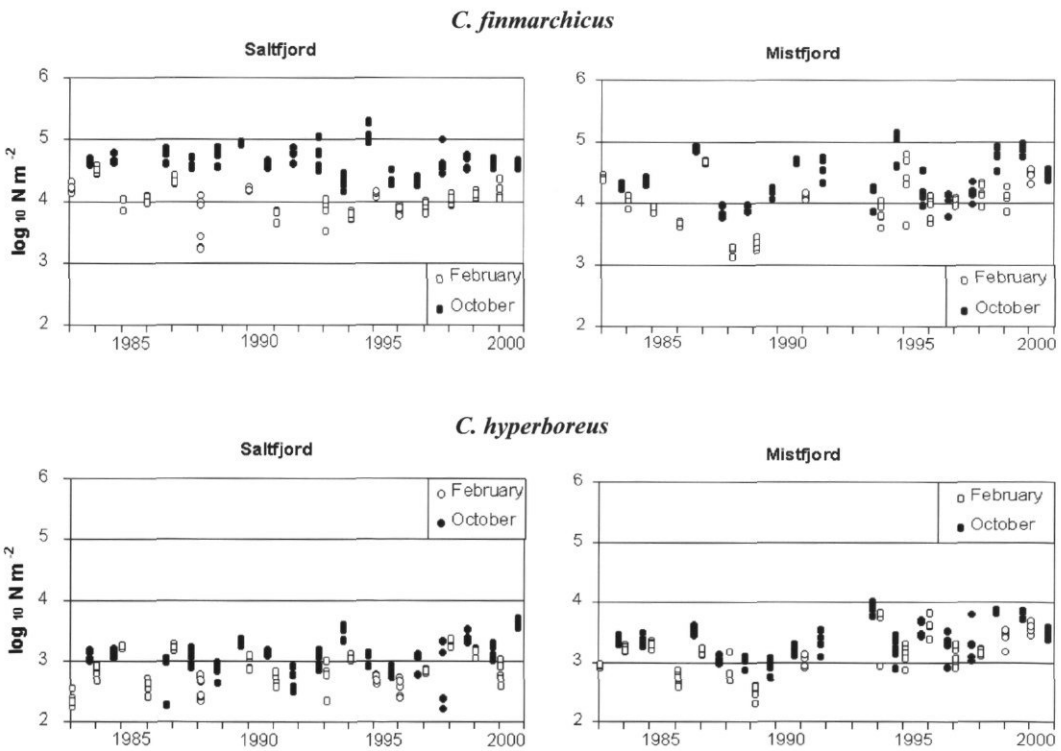


Figure 2. Abundance of *Calanus finmarchicus* and *C. hyperboreus* per square meter sea surface in five intended replicate samples.

Table 1. Significance levels (p) of correlation (r) between the abundances of two *Calanus* spp. in October and February, and the best average North Atlantic Oscillation and Arctic Oscillation indices of different seasons or the whole year. The lag indicates whether the abundance refers to an average index of the same (0) or the previous (−1) year. NS = No significant correlations with any season or year.

Species/site	Abundance month	NAO				AO			
		Season	Lag	r	p	Season	Lag	r	p
C. finmarchicus									
Saltfjord	Oct	Mar–Jul	0	0.717	0.01	Jul–Sep	0	0.587	0.05
	Feb	–	–	–	NS	–	–	–	NS
Mistfjord	Oct	Mar–Jul	0	0.738	0.01	Jul–Sep	−1	0.833	0.01
	Feb	Mar–Jul	−1	0.723	0.01	Oct–Dec	−1	0.586	0.05
C. hyperboreus									NS
Saltfjord	Oct	–	–	–	NS	Jul–Sep	0	0.832	0.01
	Feb	–	–	–	NS	–	–	–	NS
Mistfjord	Oct	–	–	–	NS	Year	0	0.687	0.01
	Feb	–	–	–	NS	Year	−1	0.602	0.05

In both fjords, both species had a patchy distribution that may have been caused by predation or predator avoidance. The winter season change in abundance was probably a function of both import and mortality rates.

Positive correlation between NAO and abundance of *C. finmarchicus* in both fjords contrasts with negative correlation in the North Sea (Fromentin and Planque, 1996), probably due to a common process. Positive NAO forces westerly winds to advect seawater northwards along the Norwegian shelf (Dickson *et al.*, 2000), and may shift the copepod's base population towards the north. During negative NAO, northerly winds develop over the Northeast Atlantic and may favour accumulation of *C. finmarchicus* in the North Sea. In Scandinavia, positive NAO also increases the winter precipitation (Dickson *et al.*, 2000) and accumulation of snow that causes meltwater discharge in early summer. Thus, the observed correlation with March–July NAO is in accordance with a model where vernal river flow generates proportional production in plankton communities along the coast of Norway (Skreslet, 1997).

It is possible that AO exerted independent influence on both *Calanus* spp., preferably by effects on processes that advected them into their wintering habitats. In *C. hyperboreus* the absence of any correlation with NAO may indicate that its population system was weakly affected by Atlantic forcing, while its correlation with annual AO in Mistfjord suggests Arctic forcing on the population level.

Acknowledgements

We thank M. Krogstad, R. Nicolaisen, K. Olsen, and other technical staff for their support. The Norwegian Research Council for Science and the Humanities, grant no. 457.91/008, and the European Commission, contract no. EVK3-CT-1999-00012, supported financially.

References

Dickson, R. R., Osborn, T. J., Hurrell, J. W. *et al.* 2000. The Arctic Ocean response to the North Atlantic Oscillation. Journal of Climate, 13: 2671–2696.

Fromentin, J. M., and Planque, B. 1996. *Calanus* and environment in the eastern North Atlantic. II. Influence of the North Atlantic Oscillation on *C. finmarchicus* and *C. helgolandicus*. Marine Ecology Progress Series, 134: 111–118.

Heath, M. R., Astthorsson, O. S., Dunn, J. *et al.* 2000. Comparative analysis of *Calanus finmarchicus* demography at locations around the Northeast Atlantic. ICES Journal of Marine Science, 57: 1562–1580.

Lamb, P. J., and Peppler, R. A. 1987. North Atlantic Oscillation: concept and an application. Bulletin of the American Meteorological Society, 68: 1218–1225.

Quenouille, M. H. 1952. Associated Measurements. Butterworths, London. 241 pp.

Skreslet, S. 1997. A conceptual model of the trophodynamical response to river discharge in a large marine ecosystem. Journal of Marine Systems, 12: 187–198.

Skreslet, S., Olsen, K., Mohus, Å., and Tande, K. 2000. Stage specific habitats of *Calanus finmarchicus* and *Calanus helgolandicus* in a stratified north Norwegian fjord. ICES Journal of Marine Science, 57: 1656–1663.

Sømme, J. D. 1934. Animal plankton of the Norwegian coast waters and the open sea. 1. Production of *Calanus finmarchicus* (Gunner) and *Calanus hyperboreus* (Krøyer) in the Lofoten area. Fiskeridirektoratets Skrifter, Serie Havundersøkelser, 4: 1–163.

Thompson, D. W. J., and Wallace, J. M. 1998. The Arctic Oscillation signature in wintertime geopotential height and temperature fields. Geophysical Research Letters, 25: 1297–1300.

ICES Marine Science Symposia, 219: 393–395. 2003

Influence of mixed-layer depth variations on primary production

Henning Wehde

Wehde, H. 2003. Influence of mixed-layer depth variations on primary production. – ICES Marine Science Symposia, 219: 393–395.

The influence of mixed-layer depth variations on primary production in the open ocean was investigated by field observations and numerical process studies. Cruises were conducted in late winter 1999 to investigate the relationship between oceanic convection and phytoplankton development in the North Atlantic/Nordic Seas. The phytoplankton concentration was closely related to the depth of the convectively mixed layer. By using a coupled convection-primary production model, the oceanic convection was found to influence the contact duration and return frequency of a plankton cell within the euphotic zone.

Keywords: field observations, numerical process studies, oceanic convection, primary production.

H. Wehde: Institut für Meereskunde, Universität Hamburg, Troplowitzstrasse 7, D-22529 Hamburg, Germany [tel: +49 (0)40 42838 2988; fax: +49 (0)40 5605724; e-mail: wehde@dkrz.de].

Introduction

The development of phytoplankton has been the subject of intensive studies, mostly focused on the spring bloom and summer conditions. Investigations of their evolution in winter are rare. An exception was Dale *et al.* (1999), who presented a summary of the seasonal development of phytoplankton at Ocean Weather Ship M. To date, there is no convincing explanation for the availability of phytoplankton in the open ocean water column in winter.

The aim of this study is the extrapolation of the recently published findings about "Phyto-Convection" (Backhaus *et al.*, 1999) from the shallow polar seas to the open ocean. The hypothesis is that due to the orbital motions caused by convection the plankton cells are dispersed within the convectively mixed part of the water column. The simultaneously existing upward and downward motion cause a repeated return of the plankton cells to the euphotic zone (EZ), thereby enabling the plankton to grow prior to the establishment of a seasonal thermocline. A schematic view of the annual evolution of the convectively mixed layer (CML) and the plankton dispersion within the water column is shown in Figure 1. To test the hypothesis, i.e. to prove whether increased phytoplankton concentrations can be found in the CML, field observations were undertaken. Furthermore, a coupled convection-primary production model was used to study the effect of varying heat loss and windspeed on the contact duration and return frequency of plankton to the EZ. To my knowledge, such numerical studies have not been carried out previously.

Field observations

Cruises with RV "Valdivia" (Cruise V176-V179, February–May 1999) were conducted to investigate the relationship between oceanic convection and phytoplankton development. A total of 201 CTD Stations were taken.

Results from a quasimeridional transect from 57°N to 75°N are shown to illustrate the increased phytoplankton biomass within the CML (Figure 2). The penetration depth of oceanic convection varied considerably from station to station along the transect. In the Icelandic Basin, the penetration depth varied from 300 m in the south to about 800 m in the north, i.e. to the south of the Iceland–Faroe Ridge (~63°N). North of the Ridge, i.e. in the Icelandic and Norwegian Seas, a meridional gradient in convection depth was not observed, and the depth was generally confined to depths less than 300 m.

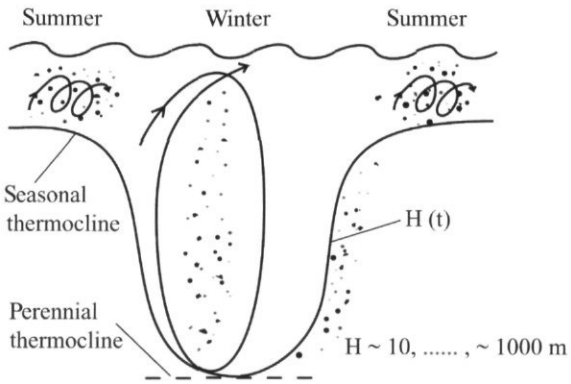


Figure 1. Schematic diagram of the annual evolution of the convectively mixed layer (CML). The dots represent plankton cells that drifted within the convective motion (J. Backhaus, pers. comm.).

Results from the field experiments support the validity of the Phyto-Convection hypothesis as elevated chlorophyll *a* concentrations were found within the CML (Figure 2). Below the perennial thermocline, i.e. the penetration depth of the CML, chlorophyll *a* concentrations were always insignificant and a sharp decline in chlorophyll tended to occur at the thermocline. The phytoplankton concentrations generally were higher with shallower CMLs. Nevertheless, the integrated biomass within the water column was not influenced by the CML thickness.

Numerical process studies

Numerical process studies were carried out to investigate the potential influence of the CML thickness on the return frequency of phytoplankton to the EZ and the duration of the contact of the phytoplankton with the EZ. Their aim was to obtain quantitative estimates of contact duration of tracers with the EZ. The studies were conducted for a stratified open ocean and an unstratified shelf water column to highlight the similarity of a homogeneous water column and a CML of similar depth. Furthermore, the modification to the frequency and duration of contacts of plankton with the EZ under variable wind and thermal forcing was investigated.

A non-hydrostatic convection model was coupled to a Lagrangian primary production model. The physical model is based on the non-linear primitive equations. The 2.5-D model uses an isotropic grid size with a resolution of 5 m. Phytoplankton are introduced as Lagrangian tracers. For each tracer a simple model predicts changes to the phytoplankton stock due to gross primary production, respiration, mortality, and grazing. A detailed description of the coupled model is given in Wehde (2001) and Wehde and Backhaus (2000).

A sharp density gradient (open ocean) and a homogeneous water column (shelf) are used as initial conditions. The tracers are homogeneously distributed within the CML/water column. All process studies cover a period of 10 days. The studies show a strong dependence of mean contact duration of the

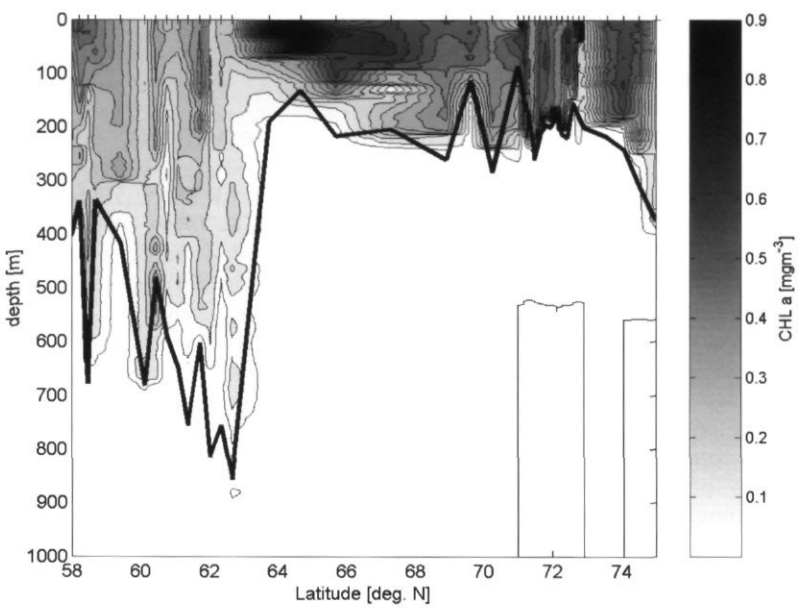


Figure 2. Chlorophyll *a* concentrations (mg m^{-3}) and mixed-layer depth (m) (solid line) along the quasimeridional transect (57°N–75°N).

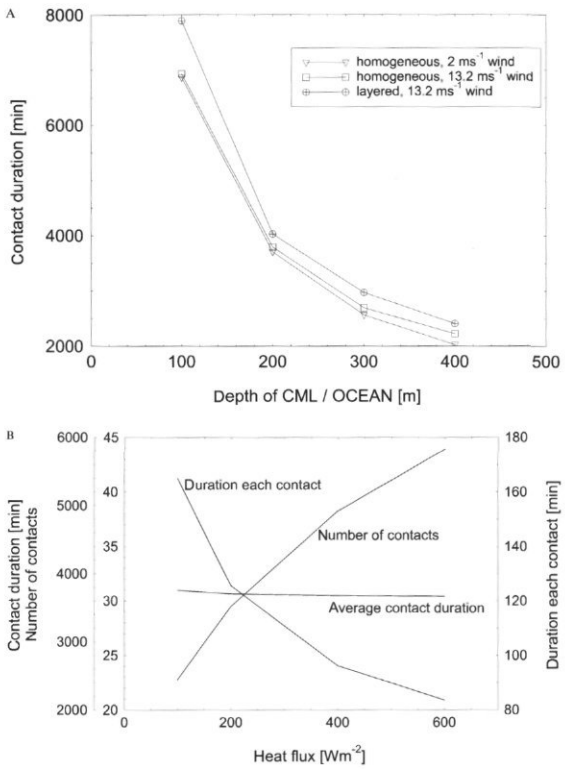


Figure 3. Average contact duration of cells with the euphotic zone (EZ) depending on varied physical environment/forcing. A. Variation of the depth of the convectively mixed layer (CML) or the ocean bottom in the case of a homogenous water column over the shelf under different wind forcing. B. Influence of heat flux on the number of contacts and the duration of a single contact of a cell with the euphotic zone.

tracer with the EZ on the depth of the CML or the total depth in the case of the homogeneous shelf (Figure 3A). The density gradient in the open ocean plays the same role as the bottom on a shelf. There is no significant change in the average contact duration of a tracer with the EZ under variable wind velocities (Figure 3A) or heat fluxes (not shown) for the simulation period. Nevertheless, for longer simulations the effect of CML deepening caused by increased heat losses led to a decrease of contact duration. Focusing on the single contacts instead of the mean contact duration increased convective activity caused by increased heat flux shows an immediate influence on the duration of each contact. The decrease of contact duration is compensated by the increased frequency of the return to the EZ (Figure 3B) so that the average contact duration during the simulation period is not influenced. For higher latitudes, the higher frequency of returns to the EZ may be important, i.e. due to frequent returns to the EZ, the chance of reaching the EZ during daytime, and thus to receive light necessary for production, increases.

Acknowledgements

Components were used for this investigation model which were developed with support from the European Union (DG-XII, MAST II and III), within ESOP I and ESOPII and the ongoing CONVECTION Project (MAS2-CT93-0057, MAS3-CT95-0015). The ship time was provided by the German federal state City of Hamburg. I greatly acknowledge Else Nøst-Hegseth, Corinna Schrum, and Jan Backhaus for many fruitful discussions and encouragement. I acknowledge the fruitful comments of Ken Drinkwater and two anonymous reviewers.

References

Backhaus, J. O., Wehde, H., Nøst Hegseth, E., and Kämpf, J. 1999. "Phyto Convection": On the role of oceanic convection in primary production. Marine Ecology Progress Series, 189: 77–92.

Dale, T., Rey, F., and Heimdal, B. R. 1999. Seasonal development of phytoplankton at a high latitude oceanic site. Sarsia, 84: 419–435.

Wehde, H., and Backhaus, J. O. 2000. The fate of passive Lagrangian tracers in oceanic convective conditions: on the influence of oceanic convection in primary production. Nonlinear Analysis, Real World Applications, 1: 3–21.

Wehde, H. 2001. Phytokonvektion im offenen Ozean – Feldexperiment und numerische Prozessstudien –. Berichte aus dem Zentrum für Meeres und Klimaforschung, Reihe B, Band 38, 144 pp. (In German.)

ICES Marine Science Symposia, 219: 396–399. 2003

Environmental indicators and the predictability of commercial fish stocks

Miles A. Sundermeyer, Brian J. Rothschild, and Allan R. Robinson

Sundermeyer, M. A., Rothschild, B. J., and Robinson, A. R. 2003. Environmental indicators and the predictability of commercial fish stocks. – ICES Marine Science Symposia, 219: 396–399.

Commercial landings data for Atlantic cod (*Gadus morhua*) and haddock (*Melanogrammus aeglefinus*) were examined along with historical conductivity, temperature, and depth (CTD) data to demonstrate an approach for assessing seasonal, annual, and interannual relationships between fish stocks and their environment, and to develop predictive models for the distributions of stocks over Georges Bank. A spatially explicit analytical/numerical model was used to demonstrate the predictive capability of such relationships. Results show that bottom temperature alone accounts for up to 40% of the spatial variance within the smoothed monthly catch distributions. Less than 20% is explained by bottom sediment type and bottom depth. The same model accounts for a much smaller percentage of the observed catch variance in individual years.

Keywords: cod, environmental indicators, Georges Bank, haddock, numerical model.

M. A. Sundermeyer and B. J. Rothschild: School for Marine Science and Technology, University of Massachusetts Dartmouth, 706 S. Rodney French Blvd., New Bedford, MA 02744, USA [tel: + 1 508 999 8892; fax: + 1 508 910 6371; e-mail: msundermeyer@umassd.edu; brothschild@umassd.edu]. A. R. Robinson: Division of Engineering and Applied Sciences, Harvard University, Cambridge, MA 02138, USA [tel: + 1 617 495 2819; e-mail: robinson@pacific.harvard.edu]. Correspondence to M. A. Sundermeyer.

Introduction

Several studies have related environmental variables to fish distributions and abundances in the Northwest Atlantic (Smith *et al.*, 1991; Mountain and Murawski, 1992; O'Brien and Rago, 1996). Others have examined how such relationships can be used to predict distributions and abundances of commercial fish stocks over a variety of time and space scales (Bertignac *et al.*, 1998; Stefánsson and Pálsson, 1997). The present study is an analysis of environmental indicators of commercial fish stocks in the Northwest Atlantic, specifically, Georges Bank. We build on previous results in two ways. First, we use commercial landings data to extend results of previous regional studies based on seasonal bottom trawl surveys. Second, we use a spatially explicit analytical/numerical model to test the predictive skill of empirically based correlations.

Materials and methods

Historical data sets

Cod and haddock commercial landings data for 1982–1992 were obtained from the US National Marine Fisheries Service. The data included the landed weight and total fishing time per fishing subtrip, from which we compute catch per unit fishing effort (c.p.u.e.). Historical CTD data were obtained from a variety of sources including the National Oceanographic Data Center; the Atlantic Fisheries Adjustment Program; the Marine Resources Monitoring, Assessment and Prediction Program; the Global Ocean Ecosystems program; and numerous smaller field programs. Bottom sediment grain size over Georges Bank was obtained from published data by Twichell *et al.* (1987; republished from Schlee, 1973).

A spatially explicit numerical model

An analytical/numerical model was used to demonstrate the predictive capability of empirically derived correlations. The model represents the concentration of fish by a continuous tracer, and uses an advection/diffusion parameterization to describe tactic searching behavior of fish towards preferred environmental variables (e.g. Grunbaum, 1999).

The model solves the advection/diffusion:

$$\partial C/\partial t - \partial/\partial x(f_x C) - \partial/\partial y(f_y C) = \kappa\, \partial^2 C/\partial x^2 + \kappa\, \partial^2 C/\partial y^2, \quad (1)$$

where C represents the fish concentration,

$$f_x(x,y,t) = S\, \partial/\partial x(\theta^2/2), \quad (2)$$

$$f_y(x,y,t) = S\, \partial/\partial y(\theta^2/2), \quad (3)$$

$$\theta^2 = (T - T_c)^2, \quad (4)$$

T represents bottom temperature, T_c is the preferred temperature, and κ is an effective horizontal diffusivity.

Advection terms in (1) represent fish's swimming tendency towards a preferred value of bottom temperature, or any variable for which they have an affinity. Here f_x and f_y can be thought of as fish swimming velocities such that the further the fish are from their preferred temperature, the faster they swim towards it, and the larger the temperature gradient, the faster they swim. The scalar parameter, S, sets the overall strength of this affinity; a larger S implies a greater swimming speed. The horizontal diffusion term in (1) can be thought of as a parameterization of random searching behavior, and of the tendency of the fish to avoid aggregating to arbitrarily high concentrations at any given location.

Equations (1)–(4) formally represent the vertically integrated abundance of cod or haddock, i.e. number of fish per unit area; or, alternatively, the number of individuals per unit volume near the bottom. While the precise relationship between c.p.u.e. and abundance is a widely debated topic, for the purpose of the present study we assume that c.p.u.e. is proportional to abundance, and use c.p.u.e. as a proxy for fish abundance (to within a constant of proportionality) both in (1)–(4) and in our discussion.

Results

Empirical correlations

Mean bottom temperatures and weighted mean catch temperatures over Georges Bank were computed by month by multiplying the temperature at each catch location by the natural log (ln) of c.p.u.e. for that location. Results show a seasonal cycle in mean bottom temperature and weighted mean catch temperature, as well as a tendency for ln(c.p.u.e.)-weighted temperature to be consistently less than mean bottom temperature for large bottom temperature (Figure 1A). To assess variations in

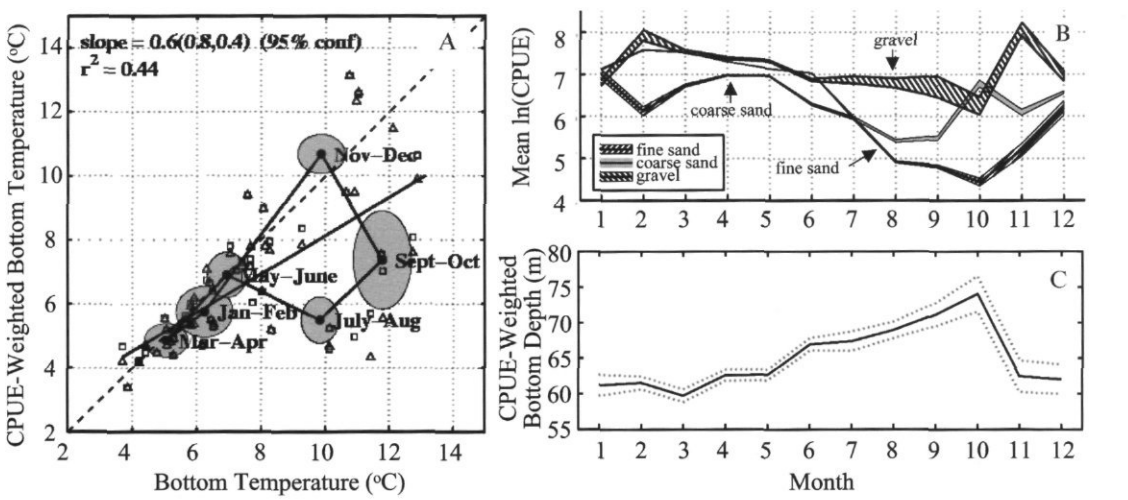


Figure 1. (A) Cod (squares) and haddock (triangles) ln(c.p.u.e.)-weighted bottom temperature versus mean bottom temperature, and bi-monthly average values of the same for cod (shaded ellipses). Regression statistics for a straight line fit through the cod data are cited in the figure. Time-series of (B) monthly averaged cod ln(c.p.u.e.) over each sediment type and (C) cod ln(c.p.u.e.)-weighted bottom depth over Georges Bank from 1982–1992. Error estimates for the curves in panels (B) and (C) are shown by shading and dashed lines, respectively.

c.p.u.e. over different sediment types, we further computed the average ln(c.p.u.e.) over each of three sediment grain size classes as defined by Twitchell *et al.* (1987): 1/16–1/4 mm (fine sand), ¼–1 mm (medium-to-coarse sand), and > 1 mm (gravel). Time-series of monthly averaged ln(c.p.u.e.) over Georges Bank showed that for all three sediment classes, cod and haddock follow an annual cycle of higher values in winter/spring and lower values in summer/fall. Furthermore, throughout the year both species tend to yield significantly higher c.p.u.e. over coarse sand and gravel compared to fine sand (Figure 1B). Finally, we computed ln(c.p.u.e.)-weighted monthly average depth. This showed a tendency by both species towards shallower waters during winter/spring and deeper waters in summer/fall.

Numerical model results

A spatially explicit model was used to evaluate the predictive skill of these correlations. For each month (1)–(4) were integrated until a steady state was reached. Per equation (1), this is equivalent to the assumption that fish are in equilibrium with their preferred environment. Integration was repeated for each environmental variable by replacing T and T_c in (4) by their appropriate counterparts, and for all three environmental variables combined by adding respective terms of the form (2)–(3) to (1). Integration was on a 3 km × 3 km grid spanning Georges Bank.

Comparison between model predictions and observed monthly c.p.u.e. indicates that temperature alone accounts for between 0%–40% and 0%–15% of the total variance in the observed monthly ln (c.p.u.e.) fields of cod and haddock, respectively. Sediment type and bottom depth account for between 0%–15% and 0%–20% of the variance, respectively. The three environmental variables combined account for approximately the same or slightly greater variance than any one individually (Figure 2A, B).

To assess model performance on interannual time-scales, the procedure was repeated for monthly distributions of the full 11-year time-series. Rather than using monthly mean spatial distributions of bottom temperature, each month's temperature was adjusted by an amount equal to the mean temperature anomaly of that month of that year. This time, the percentage variance accounted for by the model in either species ranged from less than zero (the model over-predicted the observed variance) to as much as 60% (Figure 2C, D). (Note that the percent variance explained is computed as the [(observed variance) – (variance of the (predicted – observed fields))]/(observed variance). Hence the percentage variance explained is negative if the variance of the predicted–observed fields exceeds the observed variance.)

Discussion

In the context of the models (1)–(4), bottom temperature can account for up to 40% of the spatial variance in the observed monthly ln(c.p.u.e.) fields of either cod or haddock over Georges Bank. Bottom sediment type and bottom depth account for up to 15% of the observed variance in either species. This suggests that bottom temperature, bottom sediment type, and bottom depth are all significant

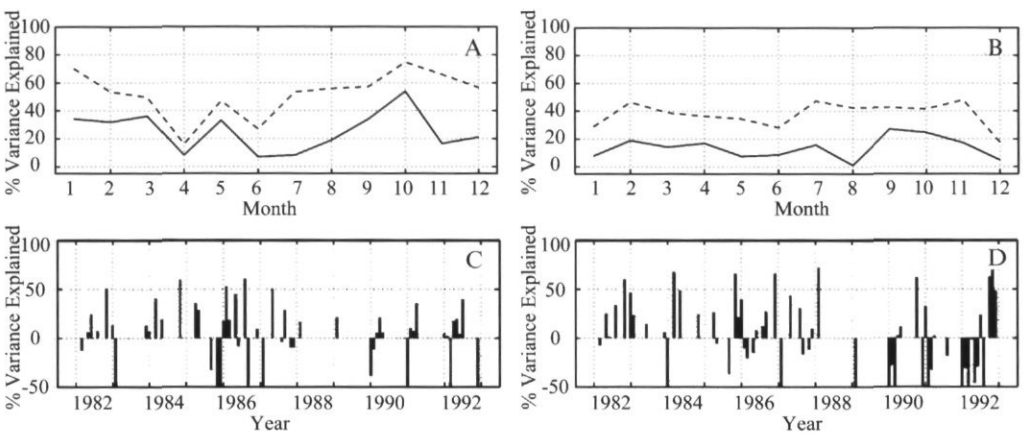


Figure 2. Monthly time-series of percentage variance accounted for in (A) cod and (B) haddock distributions over Georges Bank by (1)–(4) using bottom temperature, sediment type, and bottom depth combined (solid) and optimal interpolation of the data (dashed); percentage variance accounted for in 11-year time-series of (C) cod and (D) haddock by bottom temperature, sediment type and depth combined.

indicators for distributions of cod and haddock on Georges Bank. That bottom temperature preference accounts for more of the observed variance than do bottom type and bottom depth may indicate that temperature has a greater effect on the distributions of these species over the Bank. However, variations in the variance accounted for by each of these variables also suggest that the dominance of temperature as an indicator may vary seasonally.

Acknowledgments

Funded by the National Aeronautics and Space Administration grant number NAG13-48. The cooperation of the US National Marine Fisheries Service is gratefully acknowledged. Initial processing of landings data at SMAST was by Eric Grist. We thank Dr. Lyon Lanerolle for insightful discussions.

References

Bertignac, M., Lehodey, P., and Hampton, J. 1998. A spatial population dynamics simulation model for tropical tunas using a habitat index based on environmental parameters. Fisheries Oceanography, 7 (314): 326–334.

Grunbaum, D. 1999. Advection–diffusion equations for generalized tactic searching behavior. Journal of Mathematical Biology, 38: 169–194.

Mountain, D. G., and Murawski, S. A. 1992. Variation in the distribution of fish stocks on the northeast continental shelf in relation to their environment, 1980–1989. ICES Marine Science Symposia, 195: 424–432.

O'Brien, L., and Rago, P. 1996. An application of the generalized additive model to groundfish survey data with Atlantic cod off the Northeast coast of the United States as an example. NAFO Scientific Council Studies, 28: 79–95.

Schlee, J. S. 1973. Atlantic continental shelf and slope of the United States: sediment texture of the northeastern part. US Geological Survey Professional Paper, 529L. 64 pp.

Smith, S. J., Perry, R. I., and Fanning, L. P. 1991. Relationships between water mass characteristics and estimates of fish population abundance from trawl surveys. Environmental Monitoring and Assessment, 17: 227–245.

Stefánsson, G., and Pálsson, O. K. 1997. A framework for multi-species modeling of Boreal systems. Working Paper to NAMMCO SC, Tromso, SC/5/ME12.

Twichell, D. C., Butman, B., and Lewis, R. S. 1987. Shallow structure, surficial geology, and the processes currently shaping the Bank. *In* Georges Bank. Ed. by R. H. Backus. MIT Press, Cambridge, MA. 539 pp.

ICES Marine Science Symposia, 219: 400–402. 2003

Influence of oceanographic parameters on recruitment of megrim (*Lepidorhombus whiffiagonis*) and four-spot megrim (*L. boscii*) on the Northern Spanish continental shelf (ICES Division VIIIc)

Ricardo Sánchez, Francisco Sánchez, Jorge Landa and Ángel Fernández

Sánchez, R., Sánchez, F., Landa, J., and Fernández, Á. 2003. Influence of oceanographic parameters on recruitment of megrim (*Lepidorhombus whiffiagonis*) and four-spot megrim (*L. boscii*) on the Northern Spanish continental shelf (ICES Division VIIIc). – ICES Marine Science Symposia, 219: 400–402.

Over the past decade, recruitment processes of the two species of *Lepidorhombus* that overlap in the southern Bay of Biscay seem to respond to similar patterns. This appears to be partially explained by density independent factors. Before summer, egg and larval drift by the currents over the continental shelf play a key role. After summer, the upwelling strength seems to influence survival of juveniles through food availability.

Keywords: Cantabrian Sea, *Lepidorhombus*, optimal environmental window, recruitment.

R. Sánchez: Instituto Español de Oceanografía (IEO), PO Box 240, ES-39080 Santander, Spain [tel: +34 942 291060; fax: +34 942 275072; e-mail: rleal@ualg.pt]. F. Sánchez, J. Landa, and Á. Fernández: Instituto Español de Oceanografía (IEO), PO Box 240. ES-39080 Santander, Spain. Correspondence to R. Sánchez.

Introduction

Spawning of megrim and four-spot megrim occurs in the Cantabrian Sea during March (BIOSDEF, 1998). Recruits appear geographically distributed along the shelf break, preferentially east of 7°W (Sánchez *et al.*, 1998). These species are bathymetrically segregated, but the recruitment process seems to respond to similar forcing, since recruitment indices have experienced similar year-to-year variations over the past decade. Two seasonal driving agents dominate the local oceanography: the winter Poleward Current (PC) and the spring–autumn upwelling (Sánchez and Gil, 2000). In this article, relationships between recruitment of both species of megrim and environmental variables are explored.

Data and methods

Data are derived from Spanish autumn bottom-trawl surveys during 1993–2000. Normalized indices of megrim and four-spotted megrim recruitment have been estimated following the procedures of Sánchez *et al.* (1998). These are based on displaced age-1 class abundance indices, since the age-0 year class is poorly sampled by the gear. Upwelling strength in early autumn was evaluated calculating the percentage of shelf planar area (%PA) occupied by negative temperature anomalies at 50 m. The anomalies are temperature differences between the individual surveys and the 1993–2000 mean. Winter and spring conditions were evaluated by the salinity in January at 100 m and temperature in April at 10 m, from a time-series of oceanographic recordings at a fixed station on the shelf in the central Cantabrian Sea.

Results and discussion

Recruitment indices for both species of megrim were strongly correlated ($r = 0.95$) and responded similarly to abiotic factors. Recruitment indices were associated with April temperatures by a non-linear, parabolic relationship (Figure 1A). Moderate temperatures coincided with best megrim recruitment. Such a relationship was also observed between recruitment indices and January subsurface salinities. These define an optimal environmental window (OEW) of winter (subsurface) salinities and spring

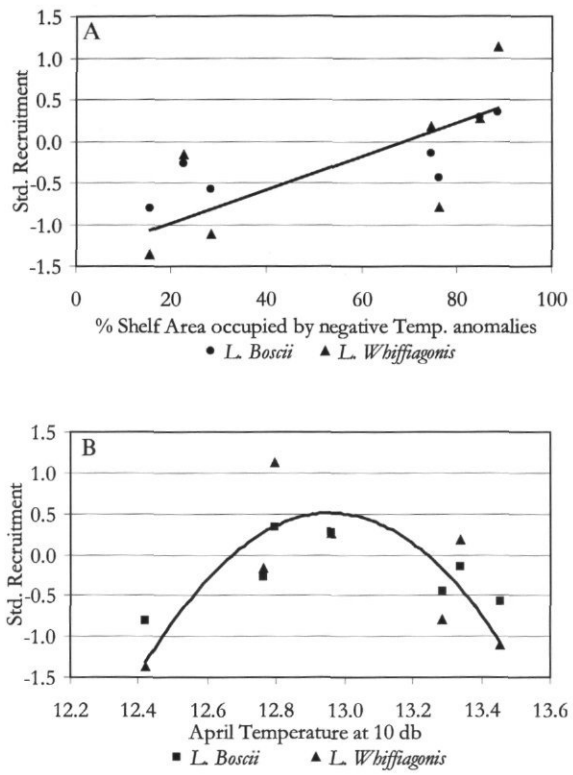


Figure 1. Scatter plots of megrim recruitment versus: (a) April temperature at 10 m at the shelf in the Central Cantabrian Sea and (b) shelf area occupied by negative temperature anomalies at 50 m with respect to the 1993–2000 mean (representative of the summer–autumn upwelling area)

(surface) temperatures for megrim recruitment in the Cantabrian Sea (Figure 2).

The main warm and saline input into the Bay of Biscay in the winter at the time of megrim spawning is introduced by the Iberian Poleward Current (IPC) (Pingree and Le Cann, 1990). The link between winter subsurface salinity and megrim recruitment is thought to occur through the IPC with the non-seasonal subsurface salinity signal considered a proxy for the residual poleward transport. Thus, moderate IPC development is hypothesized to set up adequate winter transport of ichthyoplankton towards nursery grounds along the eastern Cantabrian Sea. Excessive transport would bring about loss of eggs and larvae from the shelf habitat.

April surface temperatures may be considered as an estimator of upwelling intensity at the time of megrim recruitment. Recruitment of pelagic species has also been found to have an OEW for upwelling intensity in Ekman-type upwellings (Cury and Roy, 1989). Upwelling could exert the control of the megrim biological response by 'bottom-up' processes controlling the survival of larvae at low upwelling rates (enrichment hypothesis). Excessive upwelling, on the other hand, could lead to offshore advection of larvae from the shelf.

Recruitment indices and percentage of PA (autumn upwelling) were positively correlated ($r = 0.71$) (Figure 1B). It is inferred that 'bottom-up' processes control the survival of recruits after settlement. This response is different from that for hake recruitment, which shows an OEW with respect to autumn upwelling (Sánchez *et al.*, 2003).

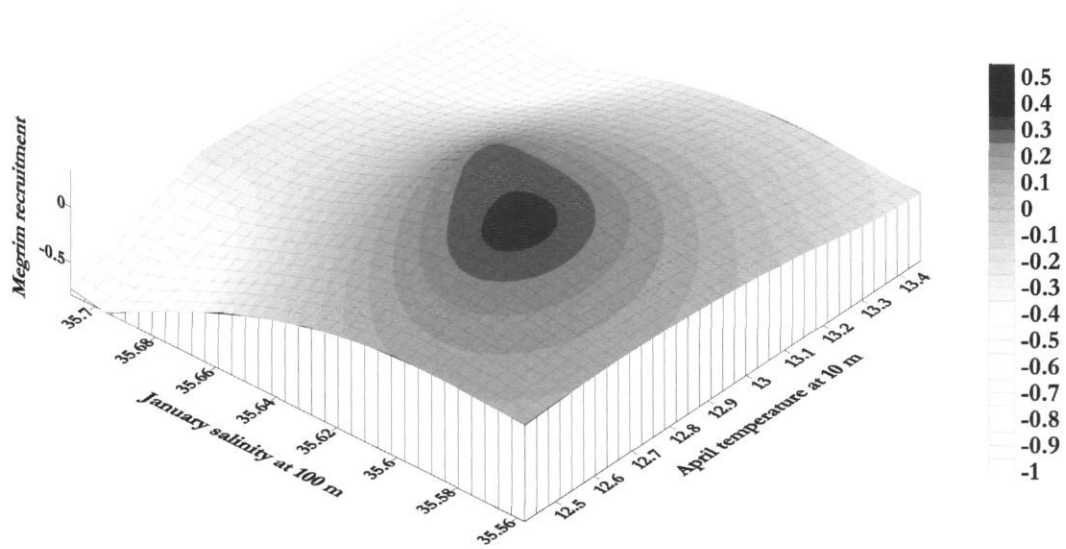


Figure 2. Surface plot of normalized megrim recruitment versus January salinity at 100 m and April temperature at 10 m in the central Cantabrian Sea.

Acknowledgements

Thanks to the crew(s) of the RV "Cornide de Saavedra" and "José Rioja", J. Gil, and the Project "Studies on Time Series of Oceanographic Data", managed by the IEO (L. Valdés, A. Lavín, and C. González).

References

BIOSDEF. 1998. Biological studies of demersal fish. Final Report (UE DG XIV Project 95/038).

Cury, P., and Roy, C. 1989. Optimal environmental window and pelagic fish recruitment success in upwelling areas. Canadian Journal of Fisheries and Aquatic Sciences, 46: 670–680.

Pingree, R. D., and Le Cann, B. 1990. Structure, strength and seasonality of the slope currents in the Bay of Biscay Region. Journal of the Marine Biological Association, UK, 70: 857–885.

Sánchez, F., and Gil, J. 2000. Hydrographic mesoscale structures and Poleward Current as a determinant of hake (*Merluccius merluccius*) recruitment in southern Bay of Biscay. ICES Journal of Marine Science, 57: 152–170.

Sánchez, F., Pérez, N., and Landa, J. 1998. Distribution of megrim (*Lepidorhombus boscii* and *L. whiffiagonis*) on the northern Spanish shelf. ICES Journal of Marine Science, 55: 494–514.

Sánchez, F., and Gil, J., 2000. Hydrographic mesoscale structures and Poleward Current as a determinant of hake (*Merluccius merluccius*) recruitment in southern Bay of Biscay. ICES Journal of Marine Science, 57: 152–170.

Sánchez, R., Sánchez, F., and Gil, J. 2003. The optimal environmental window that controls hake (*Merluccius merluccius*) recruitment in the Cantabrian Sea. ICES Marine Science Symposia, 219: 415–417.

ICES Marine Science Symposia, 219: 403–407. 2003

Environmental variability in the Atlantic and Iberian waters and its influence on horse mackerel recruitment

A. Lavín, X. Moreno-Ventas, P. Abaunza, and J. M. Cabanas

Lavín, A., Moreno-Ventas, X., Abaunza, P., and Cabanas, J. M. 2003. Environmental variability in the Atlantic and Iberian waters and its influence on horse mackerel recruitment. – ICES Marine Science Symposia, 219: 403–407.

Time-series (1967–1997) of environmental variables such as air and sea surface temperature (SST), precipitation, wind, Ekman transport, and mean sea level, as well as time-series (1985–1997) of recruitment of horse mackerel, were studied in Atlantic Iberian waters. All time-series were analysed for autocorrelation. The results indicate a statistically significant relationship between the North Atlantic Oscillation and air temperature in Santander. In western Iberia, winter Ekman transport is significantly correlated with the annual Gulf Stream position and sea level with the winter Gulf Stream position. Horse mackerel recruitment is negatively correlated with the annual and spring values of air temperature in the Cantabrian Sea and SST and air temperature in western Iberia. Correlation between recruitment and upwelling index is significant in spring and summer. Recruitment is also negatively correlated with the annual and winter Ekman transport. After multicolinearity analysis, a multivariate regression model of non-correlated variables (air temperature in Vigo and upwelling index) from April to September has been applied and explains 81.63% of the variance.

Keywords: Atlantic Iberian waters, environmental conditions, factor analysis, horse mackerel recruitment, regression model.

A. Lavín: Instituto Español de Oceanografía, Apdo 240 39080 Santander, Spain [tel: +34 942 291060; fax: +34 942 275072; e-mail: alicia.lavin@st.ieo.es; morenox@unican.es; pablo.abaunza@st.ieo.es; jmanuel.cabanas@vi.ieo.es]. Correspondence to A. Lavín.

Introduction

Time-series (1967–1997) of some environmental variables, such as air and sea surface temperature (SST), precipitation, wind, and mean sea level in the north (Santander) and in western Iberian (Vigo), Ekman transport off Vigo, as well as time-series (1985–1997) of the recruitment of horse mackerel, an important commercial fish, were studied in Atlantic Iberian waters. The aim of this work was to determine the relationship between the variability observed during recent decades, and establish whether the North Atlantic Oscillation (NAO) index (Hurrell, 1995) or the position of the Gulf Stream (GULF index; Taylor, 1996) is a good proxy for the climate regime over this area of the North Atlantic. Our study also describes the environmental conditions observed during the past decades and their influence on the horse mackerel population of ICES Divisions VIIIc and IXa (Figure 1).

Methods

From monthly values, the quarterly and annual means were obtained for all environmental variables given in Table 1. In the case of Ekman transport during the upwelling season, (April–September), the upwelling index (Ekman transport) value was also used (Lavín *et al.*, 1991, 2000). The study of the relationship between variables was made using the Pearson correlation coefficient. Significance levels were $p < 0.05$, and all the variables were normalized by removing resting the average and dividing by the standard deviation. Prior to analysis, each series was first-differenced to reduce autocorrelation and hence increase statistical reliability of the results (Thompson and Page, 1989). In the multiple regression analysis, variables were first searched for multicolinearity. The methodology used to find the best sequence of variables in the regression equation was the sequential inclusion or elimination

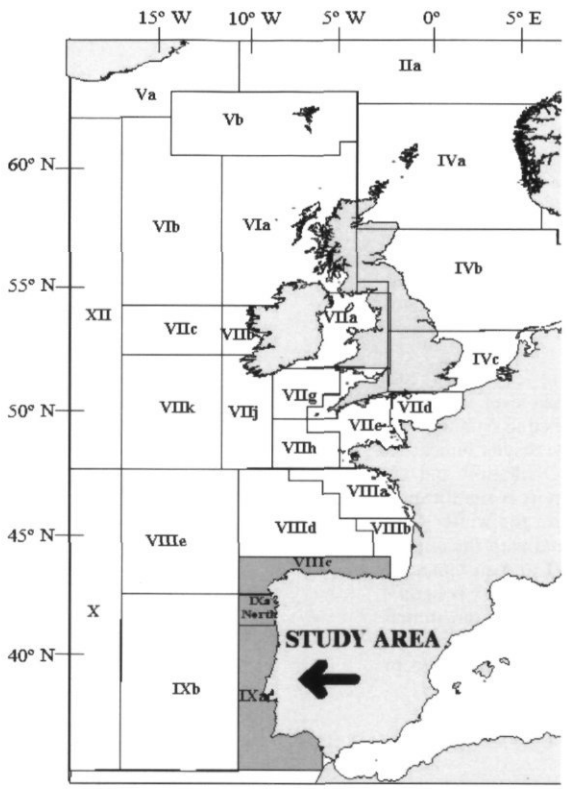


Figure 1. Area of study and location of local measurements.

of independent variables as a function of the degree of significance to the regression as a whole (forward stepwise). The estimates from the historical series of the recruitment of the southern stock of horse mackerel come from the application of the Extended Survivor Analysis (XSA) method (ICES, 2001).

Results and discussion

Results indicate a statistically significant relationship between the NAO and air temperature in Santander, and with air temperature in Vigo but at a lower significance (Table 2A). Winter Ekman transport at Vigo is significantly correlated with the annual Gulf Stream position, while sea level is correlated with winter Gulf Stream position. Although significant, the correlation between NAO index and temperature decreases southwards from the region of the North Sea. Jones (2003) suggests that 40°N is the latitude of transition from positive to negative correlation. Rodwell *et al.* (1999) suggest that a small area covering the Bay of Biscay exhibits significant correlation with the NAO. Although the present study suggests significant correlations, values are too low to permit prediction using our results.

Table 1. Environmental variables used in this work. Location and data originsource (INM stands for Instituto Nacional de Meteorologia, COADS for Comprehensive Ocean Atmosphere Data Set and IEO for Instituto Español de Oceanografía).

Environmental variables	Location	Data source
Air temperature	Santander (43.5°N, 3.8°W)	INM
Rainfall	Santander (43.5°N, 3.8°W)	INM
Sea surface temperature (SST)	Off Santander (45°N, 4°W)	COAD
East component, wind (U)	Off Santander (45°N, 4°W)	COADS
North component, wind (V)	Off Santander (45°N, 4°W)	COAD
Scalar windspeed (W)	Off Santander (45°N, 4°W)	COADS
Turbulence (W^3)	Off Santander (45°N, 4°W)	COADS
Sea level	Santander (43.5°N, 3.8°W)	IEO
Air temperature	Off Vigo (43°N, 11°N)	COADS
Sea surface temperature (SST)	Off Vigo (43°N, 11°N)	COADS
East component, wind (U)	Off Vigo (43°N, 11°N)	COADS
North component, wind (V)	Off Vigo (43°N, 11°N)	COADS
Scalar windspeed (W)	Off Vigo (43°N, 11°N)	COADS
Turbulence (W^3)	Off Vigo (43°N, 11°N)	COADS
Sea level	Vigo (42.2°N, 8.7°N)	IEO
Ekman transport	Off Vigo (43°N, 11°N)	Lavín *et al.*, 1991, 2000

Table 2. Correlations of environmental variables with the annual (GULF annual) and the December–March Gulf Stream value ($GULF_{DEFM}$) and North Atlantic Oscillation index (A) and horse mackerel recruitment (B). (Correlations in bold are significant at $p < 0.05$).

A	GULF annual	$GULF_{DEFM}$	NAO
Air temperature Santander	0.34	0.17	**0.63**
Air temperature off Vigo	0.32	0.06	0.57
Sea level Vigo	−0.27	**−0.60**	−0.46
Winter Ekman transport	**−0.61**	−0.18	−0.36
Autumn air temperature Santander	0.28	−0.08	**0.64**
Autumn air temperature off Vigo	0.41	0.06	0.54

B	Recruitment
Air temperature Santander	**−0.74**
SST off Vigo	**−0.80**
Air temperature off Vigo	**−0.73**
Annual Ekman transport	**−0.87**
Upwelling Index (Apr–Sep)	**0.69**
Winter Ekman transport	**−0.71**
Spring air temperature Santander	**−0.87**
Spring ir temperature off Vigo	**−0.82**

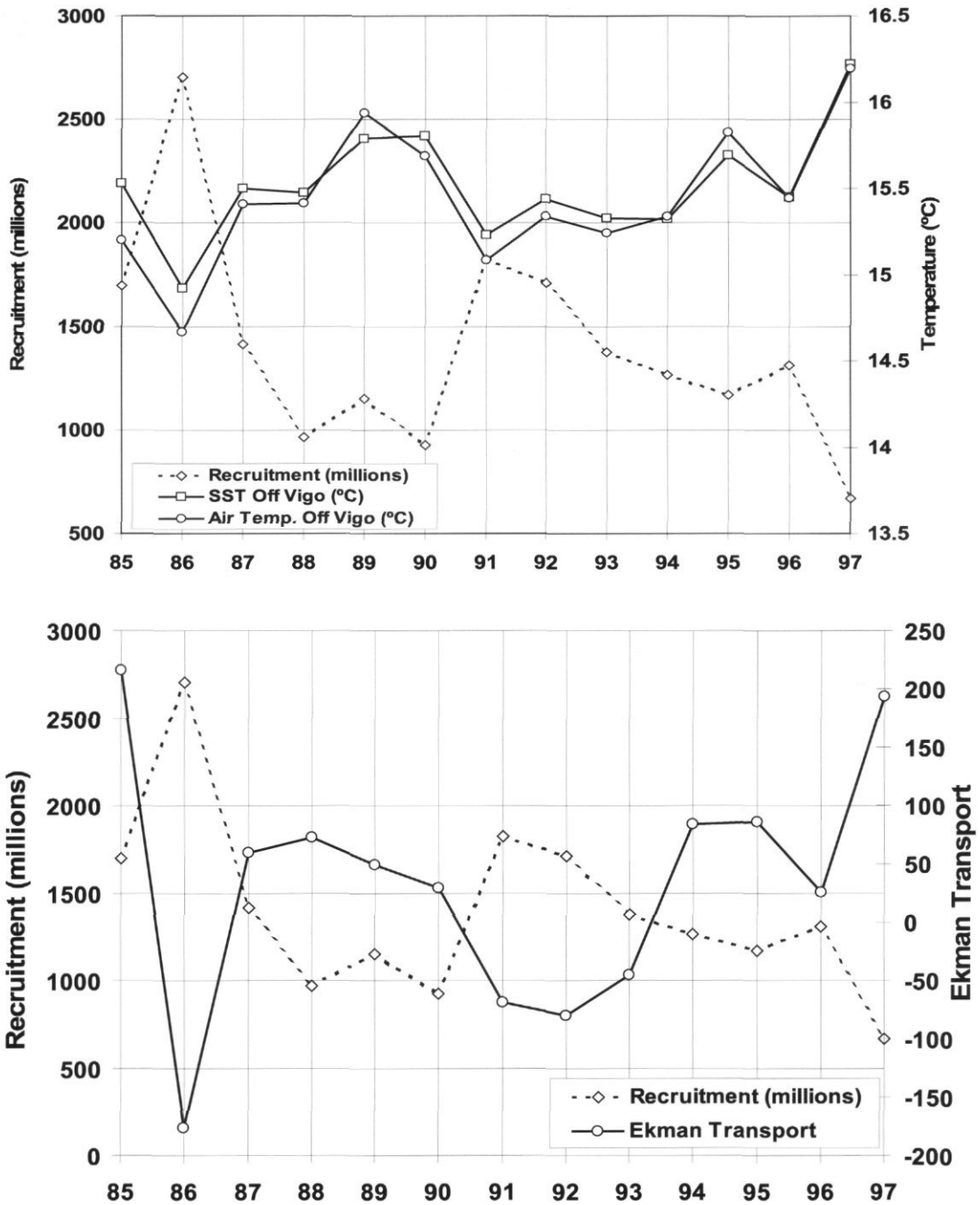


Figure 2. Time-series of ICES Divisions VIIIc and IXa horse mackerel recruitment: (A) SST and air temperature off Vigo and (B) annual Ekman transport at 43°N, 11°W.

Table 3. Statistics of the regression analysis. R: multiple correlation coefficient; R^2: coefficient of multiple determination; Adjusted $R^2 := 1 - [(\text{Residual SS/d.f.})/(\text{Total SS/d.f.})]$; SS: error sum of squares; d.f.: number of degrees of freedom; F: F test; B: unstandardized coefficients; BETA: standardized coefficient; t-value and resulting p-level value are used to test the hypothesis that the intercept is equal to 0. S.d. Error: standard error.
Regression Summary for Dependent Variable: RECRUITMENT
$R = 0.9203$, $R^2 = 0.847$ Adjusted $R^2 = 0.8164$
$F(2,10) = 27.674$ $p < 0.00008$ s.d. Error of estimate: 2199×10^2

	BETA	Std. error of BETA	B	Std. error of B	t(10)	p-level
Intercept			12387808.8	1727936.22	7.1691	3.0351E-05
Air temperature off. Vigo	0.8299	0.1237	770445.642	114878.438	6.7066	5.3207E-05
Upwelling index. (Apr–Sep)	0.3775	0.1237	1806.473	592.115	3.0509	0.0122

Horse mackerel recruitment is negatively correlated with annual air temperature in the Cantabrian Sea and SST and air temperature in Western Iberia (Figure 2A), and also with the spring air temperature values (Table 2B). Correlation between recruitment and upwelling index is significant in spring and summer. Recruitment is also negatively correlated with the annual and winter Ekman transport (Figure 2B).

The considerable and sustained changes in the magnitude of recruitment from year to year are due to two factors: changes in egg production and changes in survival (Cushing, 1995). Horse mackerel is a serial spawner with an extended spawning period, which in Iberian waters covers approximately the first 8 months of the year (Arruda, 1984; Sola *et al.*, 1990). In general, the relationship between water temperature and the spawning of marine animals is widely recorded. The eggs of horse mackerel are pelagic and temperature is one of the fundamental factors influencing their development and viability (Pipe and Walker, 1987). Temperature is also related with other changes in physical factors on the climatic scene, such as wind strength and upwelling processes that finally have influence on recruitment. The growth of fish larvae is nearly always food limited (Blaxter, 1988). Upwelling processes are connected with high primary productions, and therefore also with the availability of food for horse mackerel larvae.

Owing to the large variability explained by the abiotic components, multiple regression analysis has been applied. The regression takes four variables: air temperature in Vigo, upwelling index during the upwelling period (spring and summer), air temperature in Santander, and Offshore Ekman transport in autumn. Variables were searched for multicolinearity and then only two of these variables were considered in the regression model: air temperature in Vigo and upwelling index in spring and summer. The regression explains 81% of the variability. Table 3 gives the statistics.

Conclusions

Temperature and the spring–summer upwelling index explain the large variability in the environmental parameters, and are also significantly correlated with horse mackerel recruitment. Low values of upwelling index and high temperatures are related to poor recruitments (1997). High values of upwelling index and low temperatures are associated with good recruitment, as in 1986 and 1991. Recruitment is negatively correlated with Ekman transport in autumn and winter (1990, 1995, and 1997). The multivariate regression model proposed explains 81% of the variance in the recruitment time-series.

The fit of the multivariate regression model proposed to explain horse mackerel recruitment variability is surprisingly good. This model includes temperature and upwelling related variables and provides a very useful tool for estimating recent recruitment strength and predicting that ofthis for the near future.

Acknowledgements

We thank the CMZCA del INM and COADS for the data-series on meteorological and oceanographic variables; J. Hurrell and B. Dickson for the NAO index; A. Taylor for Gulf index; M. J. García from the IEO for the sea-level time-series; and J. Carranza for his help.

References

Arruda, L. M. 1984. Sexual maturation and growth of *Trachurus trachurus* (L.) along the Portuguese coast. Investigacion Pesquera, 48: 419–430.

Blaxter, J. H. S. 1988. Pattern and variety in development. *In* Fish Physiology XIa, pp. 1–58. Ed. by W. S. Hoar and D. Randall. Academic Press, Chichester and New York.

Cushing, D. 1995. Population Production and Regulation in the Sea: a Fisheries Perspective. Cambridge University Press, Cambridge. 354 pp.

Hurrell, J. J. 1995. Decadal trends in the North Atlantic Oscillation: regional temperatures and precipitation. Science, 269: 676–679.

ICES. 2001. Report of the Working Group on the Assessment of Mackerel, Horse Mackerel, Sardine and Anchovy. ICES CM 2001/ACFM: 6. 251 pp.

Jones, P. D. 2003. The decade of the 1990s over the Atlantic in comparison to longer instrumental and paleoclimatic records. ICES Marine Science Symposia, 219: 25–31. (This volume.)

Lavín, A., Díaz del Río, G., Cabanas, J. M., and Casas, G. 1991. Afloramiento en el noroeste de la península Ibérica. Índices de afloramiento para el punto 43°N 11°W. Periodo 1966–1989. Informes Técnicos del Instituto Español de Oceanografía, 91. 40 pp.

Lavín, A., Díaz del Río, G., Cabanas, J. M., and Casas, G. 2000. Afloramiento en el noroeste de la península Ibérica. Índices de afloramiento para el punto 43°N 11°W. Periodo 1990–1999. Datos y resúmenes Instituto Español de Oceanografía, 15. 25 pp.

Pipe, R. K., and Walker, P. 1987. The effect of temperature on development and hatching of scad, *Trachurus trachurus* L., eggs. Journal of Fish Biology, 31: 675–682.

Rodwell, M. J., Rodwell, D. P., and Folland, C. K. 1999. Oceanic forcing of the wintertime North Atlantic Oscillation and European climate. Nature, 398: 320–323.

Solá, A., Motos, L., Franco, C., and Lago de Lanzos, A. 1990. Seasonal occurrence of pelagic fish eggs and larvae in the Cantabrian Sea (VIIIc) and Galicia (IXa) from 1987 to 1989. ICES CM 1990/H: 25.

Taylor, A. H. 1996. North–South shifts of the Gulf Stream: Ocean–atmosphere interactions in the North Atlantic. International Journal of Climatology. 16, 559–583.

Thompson, K. R., and Page, F. H. 1989. Detecting synchrony of recruitment using short, autocorrelated time series. Canadian Journal of Fisheries and Aquatic Sciences, 46: 1831–1838.

ICES Marine Science Symposia, 219: 408–410. 2003

Annual variations in the prey of demersal fish in the Cantabrian Sea and their implications for food web dynamics

F. Velasco, I. Olaso, and F. Sánchez

Velasco, F., Olaso, I., and Sánchez, F. 2003. Annual variations in the prey of demersal fish in the Cantabrian Sea and their implications for food web dynamics. – ICES Marine Science Symposia, 219: 408–410.

Using data from 72 372 stomach contents of 24 demersal fish species from the Cantabrian Sea, decadal variability of trophic levels (TLs) of each of the predators was studied. No clear trends were observed throughout the decade of the 1990s, but a relationship between TL variability and upwelling index was observed. TL variability suggests that it may not be as conservative an attribute of marine species as previously thought.

Keywords: Bay of Biscay, Cantabrian Sea, decadal variability, demersal predators, food web, trophic level, upwelling index.

F. Velasco, I. Olaso, and F. Sánchez: Instituto Español de Oceanografía (IEO). PO Box 240, ES-39080 Santander, Spain [e-mail: francisco.velasco@st.ieo.es]. Correspondence to F. Velasco.

Introduction

Marine trophic level (TL) is a numerical representation of an organism's place in the marine food web. There is some evidence that average TLs in the world's fisheries have been declining at a rate of 0.1 per decade (Pauly *et al.*, 1998). One effect of the overall biomass depletion in marine ecosystems is that sealife is now relatively more concentrated in the lower TL. The aim of this study is to investigate possible changes in the TL of the most abundant demersal fish species in the Cantabrian Sea (southern part of the Bay of Biscay, North Spanish coast) during the past decade.

Material and methods

TL was calculated by predator species, length, and year using the equation given by Christensen *et al.* (2000) that estimates TL as the average TL of the preys plus 1, weighted by the share of each prey in the predator diet. Prey were grouped into 28 categories and initial estimates of TL were obtained from the trophodynamic model for the Cantabrian Sea by Sánchez and Olaso (2001). The diet composition of the fish comes from the analysis of 72 372 stomachs carried out from autumn bottom-trawl surveys between 1990 and 2000 in the Cantabrian Sea following the methodology described in Olaso *et al.* (1998). To study TL evolution throughout the decade, it was estimated by species, length, and year and compared with the decadal average by species and length range. Predators were grouped by their feeding preferences into planktonic, megabenthos, and ichthyophagous predators. Within each of these groups the number of species with a TL larger/smaller than the average ± confidence limit (95%) was studied. Upwelling index (only available for the Cantabrian Sea from 1993 to 2000 from Sánchez *et al.*, 2003) was evaluated as the percentage of shelf planar area occupied by (negative) temperature anomalies at 50 m depth with respect to the 1993–2000 mean.

Results, discussion, and conclusions

Our results show no clear trend throughout the 1990s in the TLs of any of the species examined. Nevertheless, comparing TL decadal evolution with upwelling indices in the area from 1993 to 2000, there are clear associations between years with high upwelling indices and years in which many predators of all ecological niches increase their TL

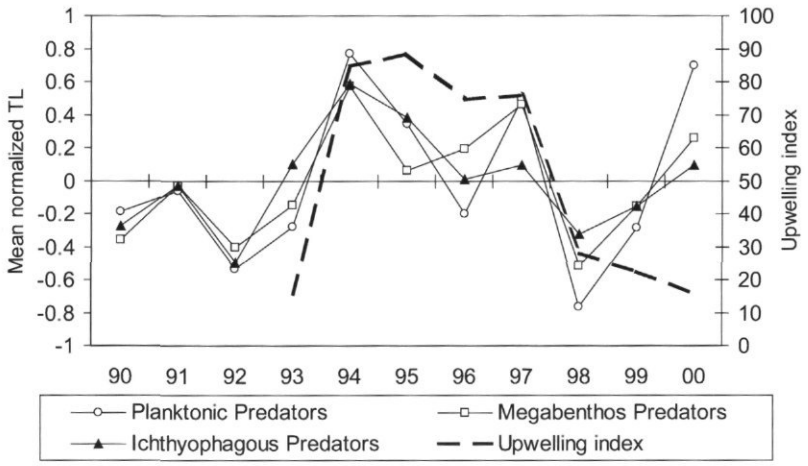


Figure 1. Annual average of normalized decadal (1990–2000) distribution of trophic level (TL) per predator ecological group and upwelling index from 1993 to 2000.

(Figure 1). The percentage of predators with TL higher than the decadal average plus confidence limit was largest in the years 1994–1997 (Figures 2A–C). In addition, TL deviations from the average were larger in those years than in others (Figure 1). On the other hand, years with weak upwelling, i.e. 1993 and 1998, led to a general decrease in predator TL (Figures 1, 2). This association between upwelling indices and predator TLs does not hold up in 2000, when, despite the low upwelling indices, TL figures were similar to those of former years with higher upwelling indices (P.C.I. Pearson correlation indices between TL deviations from the average and upwelling index in 1993–2000 for each predator

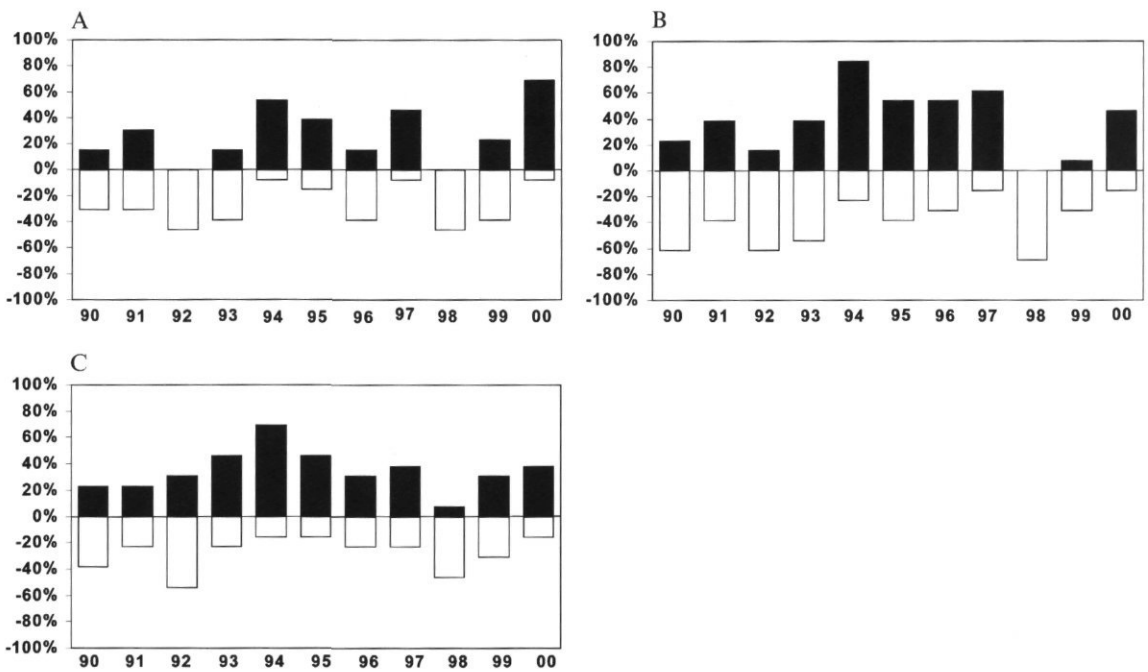


Figure 2. Annual percentage of predator species with trophic level (TL) out of TL decadal average confidence limits. (a) Planktonic predators, (b) megabenthos predators, (c) ichthyophagous predators. In black and positive: percentage of predator species with TL higher than decadal average plus confidence limit, empty squares and negative: percentage of predator species with TL smaller than decadal average minus confidence limit.

guild are: planktonic 0.45; megabenthic 0.61, and ichthyophagous 0.63). If we do not consider the anomalous year 2000, correlation indices are much higher (P.C.I. planktonic 0.79; megabenthic 0.78, and ichthyophagous 0.70), and associations are more marked in planktonic predators than in those feeding mainly on megabenthos and even less so in ichthyophagous predators.

An unsolved question is why higher upwellings, and therefore higher abundances of plankton, lead to an increase in TL. Possible explanations to be investigated should be included in the "Bottom-Up" control mechanisms; that is to say due to the effect of variations in the abundance of groups with low TL on predators' prey selection behaviour, and may be different for different ecological groups.

Variability in TL and the changes observed from year to year suggest that TL may not be as conservative an attribute of marine species as has previously been thought.

References

Christensen, V., Walters, C. J., and Pauly, D. 2000. Ecopath with Ecosim: a User's Guide, October 2000 Edition. Fisheries Centre, University of British Columbia, Vancouver, Canada and ICLARM, Penang, Malaysia. 130 pp.

Olaso, I., Velasco, F., and Pérez, N. 1998. Importance of blue whiting (*Micromesistius poutassou*) discarded in the diet of lesser-spotted dogfish (*Scyliorhinus canicula*) in the Cantabrian Sea. ICES Journal of Marine Science, 55: 331–341.

Pauly, D., Christensen, V., Dalsgaars, J., Froese, R., and Torres, F. 1998. Fishing down marine food webs. Science, 279: 860–863.

Sánchez, F., and Olaso, I. 2001. Cantabrian Sea ecosystem model and fisheries resources management. *In* Océanographie du golfe de Gascogne. VII^{C} Colloq. Int., Biarritz, 4–6 avril 2000. Éd. Ifremer, Actes Colloq., 31: 187–194.

Sánchez, R., Sánchez, F., and Gil, J. 2003. The optimal environmental window that controls hake (*Merluccius merluccius*) recruitment in the Cantabrian Sea. ICES Marine Science Symposia, 219: 415–417.

ICES Marine Science Symposia, 219: 411–414. 2003

Variability in the demersal fish assemblages of the Bay of Biscay during the 1990s

Jean-Charles Poulard, Fabian Blanchard, Jean Boucher, and Sami Souissi

Poulard, J.-C., Blanchard, F., Boucher, J., and Souissi, S. 2003. Variability in the demersal fish assemblages of the Bay of Biscay during the 1990s. – ICES Marine Science Symposia, 219: 411–414.

Data were collected during autumn groundfish surveys carried out on the eastern continental shelf of the Bay of Biscay from 1987 to 2000. The spatial organization of the demersal fish assemblages is examined using multitable factorial analysis. It shows the species assemblages are organized according to three major spatial structuring factors. Two are orientated mainly along a bathymetric gradient, while the third is linked to a large muddy bottom area near 100 m depth. These features fit well with the 11 surveys analysed. Of the 49 species considered in this study, 11 exhibited limited temporal variations in their abundance and spatial distributions. The variability of mesoscale hydrodynamic features has no measurable effect on the scale of species assemblages, but large-scale hydroclimatic changes seem to affect those species that are at the limit of their distribution range in the Bay of Biscay.

Keywords: Bay of Biscay, demersal fish assemblage, multitable factorial analysis.

Jean-Charles Poulard: IFREMER, Laboratoire d'Ecologie Halieutique, Rue de l'Ile d'Yeu, BP 21105, F-44311 Nantes Cedex 3, France [tel: +33 2 40 37 41 08, fax: +33 2 40 37 40 75, e-mail: Jean.Charles.Poulard@ifremer.fr]; Fabian Blanchard and Jean Boucher: IFREMER, Ressources Halieutiques, BP 70, F-29280 Plouzané Cedex, France; Sami Souissi: Université des Sciences et Technologies de Lille 1, CNRS-UPRES A 8013 ELICO, Station Marine, BP 80, F-62930 Wimereuz, France. Correspondence to Jean-Charles Poulard.

Introduction

The spatial pattern of groundfish distribution is influenced by the physical, environmental, and habitat characteristics. In the case of shelf and upper-slope demersal assemblages, depth is often the main gradient along which faunal changes occur.

Data collected during annual autumn surveys are used to analyse the spatial organization of species assemblages on the eastern continental shelf of the Bay of Biscay in the period 1987–2000. The study of the multispecies spatial structures over time requires the combined analysis of different tables of species density sampled at different stations. This is done using multitable factorial analysis.

Available data

Data were collected during the 11 groundfish surveys carried out by IFREMER since 1987 in the Bay of Biscay from October to December (ICES, 1997). The survey area is between 48°30′N and 43°30′N. The sampling scheme is stratified according to latitude and depth. A 36/47 GOV trawl is used with a 20-mm mesh codend liner. Haul duration is 30 min at a towing speed of 4 knots. Fishing is mainly restricted to daylight hours.

Three changes occurred in the sampling procedure beginning in 1997: (a) a stratified random scheme replaced the fixed station sampling strategy used since 1987; (b) the number of hauls made per survey decreased from about 120 to 80; and (c) operations were carried out from a different research vessel.

The data obtained from 1163 hauls were analysed. A total of 209 fish species were caught but only 49 demersal fish species, present on average in at least 5% of the tows, were included in the analysis. The numbers per tow were log-transformed before conducting the analysis to minimize the dominant effect of exceptional catches.

Data analysis

The analysis methods used are described in Gaertner *et al.* (1998). The table of the total number of individuals per survey and per species (matrix with 11 surveys and 49 species) was used as input in a between-class correspondence analysis (CoA) to test the existence of a survey effect in the overall species composition. The significance of between-survey differences was checked by means of a permutation test.

The CoA version (Gaertner *et al.*, 1998) of the STATIS multitable method (Lavit, 1988) was then used to describe the stable part and the variable part of the spatial structuring of the assemblages. The first stage of the STATIS method consists of calculating a distance matrix between species for each survey. This allows comparison between surveys by calculation of a distance matrix between surveys. The 11 elements of the first eigenvector of the diagonalized between-survey distance matrix are then used to weight the 11 species distance matrices to construct a mean table of maximum inertia (compromise table). The analysis (correspondence analysis) of the compromise table defines axes and components, which express the stable part of the spatial structures. In addition, the projection of the 11 matrices into the compromise space allows a plot of the species trajectories. These represent the temporal variations of each species with respect to the common structure and identify the relative location of the sampling stations.

Results

The inter-survey CoA demonstrates the occurrence of weak but significant temporal variations ($p<0.05$) in overall species composition between the surveys at the scale of the Bay of Biscay.

Table 1. STATIS analysis: contribution of each survey to the construction of the compromise table (weight) and fit of each survey to the compromise (Cos^2).

Survey	No. of sampled stations	Weight	Cos^2
1987	127	0.30	0.61
1988	132	0.32	0.75
1989	139	0.30	0.66
1990	135	0.31	0.71
1992	105	0.30	0.63
1994	101	0.30	0.66
1995	112	0.31	0.77
1997	89	0.31	0.74
1998	74	0.29	0.63
1999	70	0.29	0.65
2000	79	0.29	0.61

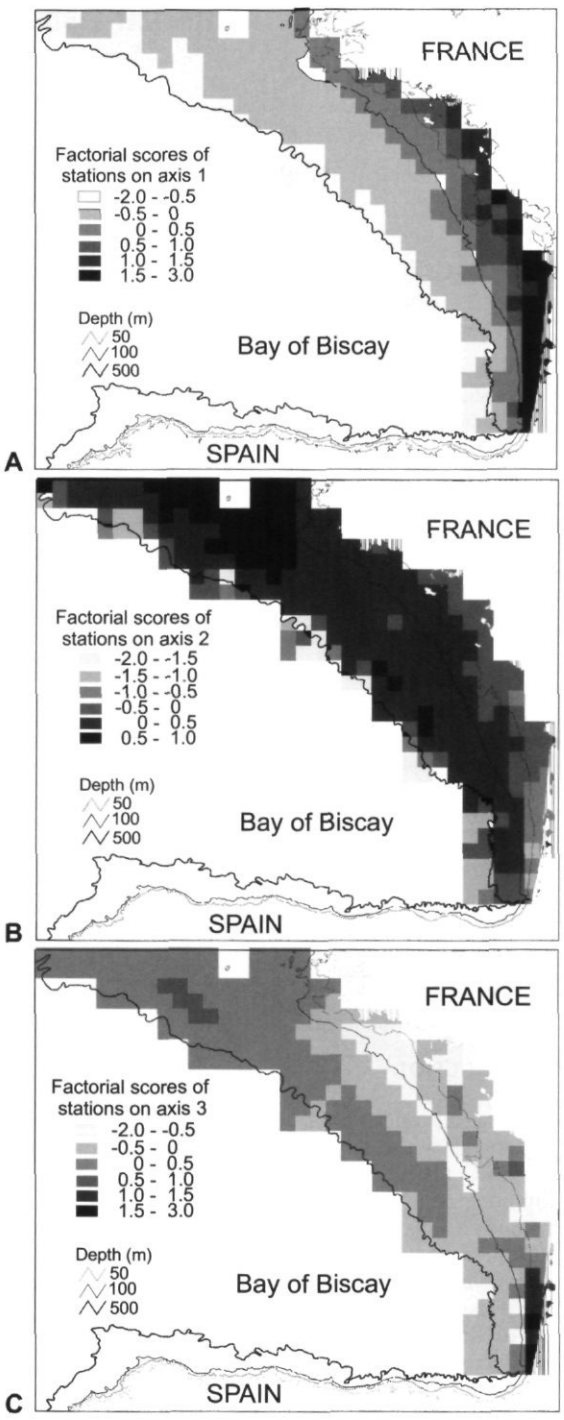


Figure 1. Map of the stable structure of the demersal fish assemblages and of the factorial scores of the sampling stations on the first three axes (A to C) of the correspondence analysis of the STATIS compromise table.

Table 2. Main indicator species defining the first three components of the stable structure of the spatial organization of the assemblages from the STATIS compromise table analysis.

Axis	Species	Coordinate sign
1	*Spondyliosoma cantharus*	+
	Mullus surmuletus	+
	Trachinus draco	+
	Argentina silus	–
	Gadiculus argenteus	–
	Capros aper	–
2	*Trisopterus minutus*	+
	Capros aper	+
	Aspitrigla cuculus	+
	Galeus melastomus	–
	Argentina silus	–
	Chimaera monstrosa	–
3	*Trachinus draco*	+
	Boops boops	+
	Liza ramada	+
	Merlangius merlangus	–
	Pomatoschistus minutus	–
	Lesueuriogobius friesii	–

The STATIS results (Table 1) show that the contribution of the different surveys to the construction of the compromise table is well balanced. The fit of each survey to the compromise table is relatively constant and does not exhibit temporal trends.

The first three axes of the correspondence analysis of the compromise table explain more than one-third of the inertia of the stable part of the spatial structuring of the assemblages. They represent the main spatial organizational directions of the species assemblages. Axis 1 (Figure 1A) shows that the depth gradient is the main structuring factor over the survey area. In the shallower part of the continental shelf (less than 100 m) a weak latitude gradient also exists. The indicator species of gradient extreme values are listed in Table 2. On axis 2 (Figure 1B), positive scores demarcate the central part of the continental shelf. High positive scores in the northern part of the shelf are associated with *Aspitrigla cuculus* and *Capros aper*. High negative scores on axis 3 (Figure 1C) are closely related to the spatial distribution of *Lesueuriogobius friesii* and encompass the muddy bottoms, which occur between 60 and 120 m depth.

Eleven species mainly contributed to the inter-survey variations (Figure 2). Their positions with respect to the gradients and in relation to other species show, however, that variations were confined to species natural ranges. Five species were widely distributed over the outer part of the continental shelf, while the spatial distributions of the six other species were restricted to shallower waters. Changes in abundance or spatial distribution patterns were identified. They were temporary for some species and exhibited time trends for others.

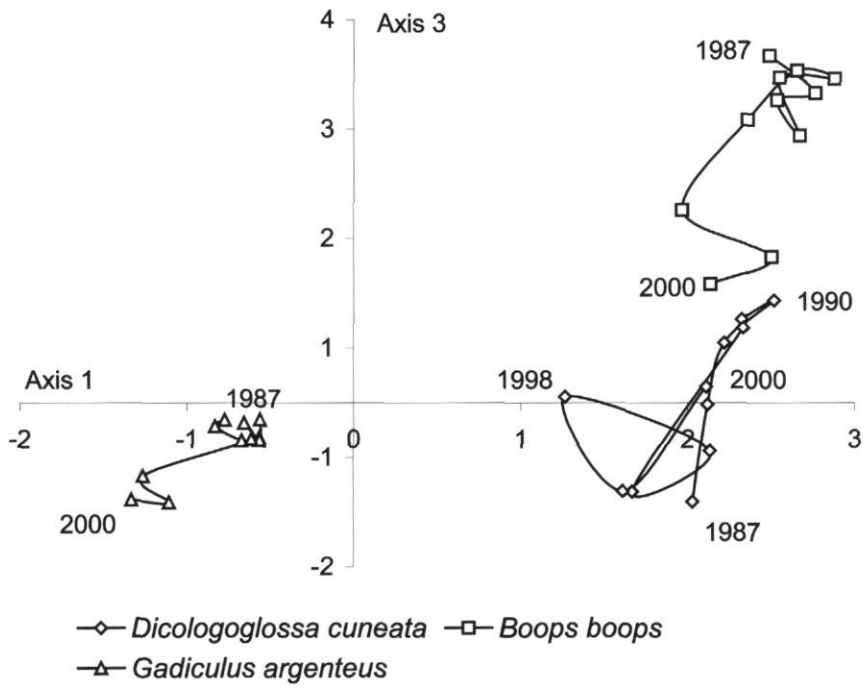


Figure 2. Details of the projection of the trajectories over time of some of the 11 characteristic species on the factorial plane 1–3 of the STATIS compromise.

Synthesis and conclusion

The demersal fish species assemblages on the Bay of Biscay eastern continental shelf are spatially organized according to depth, latitude, and substrate type represented by the large muddy bottom area near the 100 m depth contour. A common structure is identified over the 11 autumns sampled in the period 1987–2000. Small inter-survey variations are shown. They are linked to changes occurring in the abundance or the spatial distribution patterns over time of 11 species.

The relative stability of the demersal fish communities throughout the study period contrasts with the strong variability of some mesoscale hydrodynamic features (upwellings, lower salinity water lenses, and cold pool) encountered on the French continental shelf of the Bay of Biscay (Puillat *et al.*, 2003). These changes seem not to have measurable effects at the scale of the demersal fish species assemblages because they were too short in duration, not intense enough, too small spatially, or some combination of these.

On the other hand, large-scale hydroclimatic changes, as indicated by increases in sea surface temperature (Planque *et al.*, 2003), seem to affect species that are at their limit of distribution range in the Bay of Biscay. *Dicologglossa cuneata* and *Boops boops*, two shallow-water species having their northern distribution limit in the Bay of Biscay, show increasing abundance trends and increases in theirareas of distribution over the study period in response to the observed warming.

References

Gaertner, J.-C., Chessel, D., and Bertrand, J. 1998. Stability of spatial structures of demersal assemblages: a multitable approach. Aquatic Living Resources, 11: 75–85.

ICES. 1997. Report of the International Bottom Trawl Survey Working Group. CM 1997/H: 6, 50 pp.

Lavit, C. 1988. Analyse conjointe de tableaux quantitatifs. Masson, Paris. 251 pp.

Planque, B., Beillois, P., Jégou, A. M., Petitgas, P., and Puillat, I. 2003. Large-scale hydroclimatic variability in the Bay of Biscay. The 1990s in the context of interdecadal changes. ICES Marine Science Symposia, 219: 61–70. (This volume.)

Puillat, I., Lazure, P., Jégou, A. M., and Planque, B. 2003. Mesoscale, interannual, and seasonal hydrological variability over the French continental shelf of the Bay of Biscay during the 1990s. ICES Marine Science Symposia, 219: 333–336. (This volume.)

ICES Marine Science Symposia, 219: 415–417. 2003

The optimal environmental window that controls hake (*Merluccius merluccius*) recruitment in the Cantabrian Sea

Ricardo Sánchez, Francisco Sánchez, and Julio Gil

Sánchez, R., Sánchez, F., and Gil, J. 2003. The optimal environmental window that controls hake (*Merluccius merluccius*) recruitment in the Cantabrian Sea. – ICES Marine Science Symposia, 219: 415–417.

Biological-physical variability in the Cantabrian Sea is examined from data collected between 1993 and 2000. High hake recruitment occurs during years of high but not maximum upwelling in autumn and intermediate subsurface salinities in winter. These results define an optimal environmental window for successful hake recruitment. The variability in the subsurface salinities is believed to be related to the strength of the winter Poleward Current, which in turn is considered to influence hake recruitment through its effect on aggregation and dispersion of pre-recruits. Recruitment is also hypothesized to be negatively affected through insufficient food resources at low upwelling levels and through offshore transport at extremely high levels.

Keywords: Bay of Biscay, hake recruitment, optimal environmental window, Poleward Current, upwelling.

R. Sánchez: Instituto Español de Oceanografía (IEO), PO Box 240, ES-39080 Santander, Spain [tel: +34 942 291060; fax: +34 942 275072; e-mail: rleal@ualg.pt]; F. Sánchez and J. Gil: Instituto Español de Oceanografía (IEO), PO Box 240, ES-39080 Santander, Spain. Correspondence to R. Sánchez.

Introduction

In the Cantabrian Sea, the geographical distribution of hake recruits is generally constrained to 25–30 km^2 patches in areas near the main capes, but with year-to-year variability of aggregation densities. Much of the recruitment variability may be attributed to density-independent factors. Two seasonal driving agents set the local oceanography: the spring–summer upwelling and the winter Poleward Current (PC) (Sánchez and Gil, 2000). In this article, the relationship between recruitment and these two environmental features is explored.

Data and methods

Fisheries and environmental data come from the autumn bottom-trawl surveys carried out by the Instituto Español de Oceanografía (IEO) in the period 1993–2000. Hake recruitment has been estimated following standard procedures as described in Sánchez and Gil (2000). Upwelling strength was evaluated by calculating the percentage of planar shelf area (%PA) at 50 m depth occupied by negative temperature anomalies. Higher percentage PA indicates stronger upwelling. The anomalies are defined as differences between the survey temperatures and the 1993–2000 mean values. Winter oceanographic conditions are evaluated from January salinities at 80 m recorded at a fixed station on the slope in the central Cantabrian Sea.

Results and discussion

High hake recruitment occurs during years of strong upwelling (80%PA) but declines rapidly with increased upwelling (> 80%PA; Figure 1A). It can be seen that moderate winter salinities are required for hake to recruit successfully (Figure 1B). Thus, hake recruitment indices are associated with autumn temperatures and winter salinities by a non-linear, dome-shaped relationship (Figure 2). This defines an optimal environmental window (OEW) for hake recruitment in the Cantabrian Sea.

The warm and saline input into the Bay of Biscay during the winter is introduced by the Iberian Poleward Current or IPC (Pingree and Le Cann, 1990). The variability in the subsurface salinity is considered an estimator of the strength of the residual poleward transport by the IPC with higher transport producing higher salinities and lower transport,

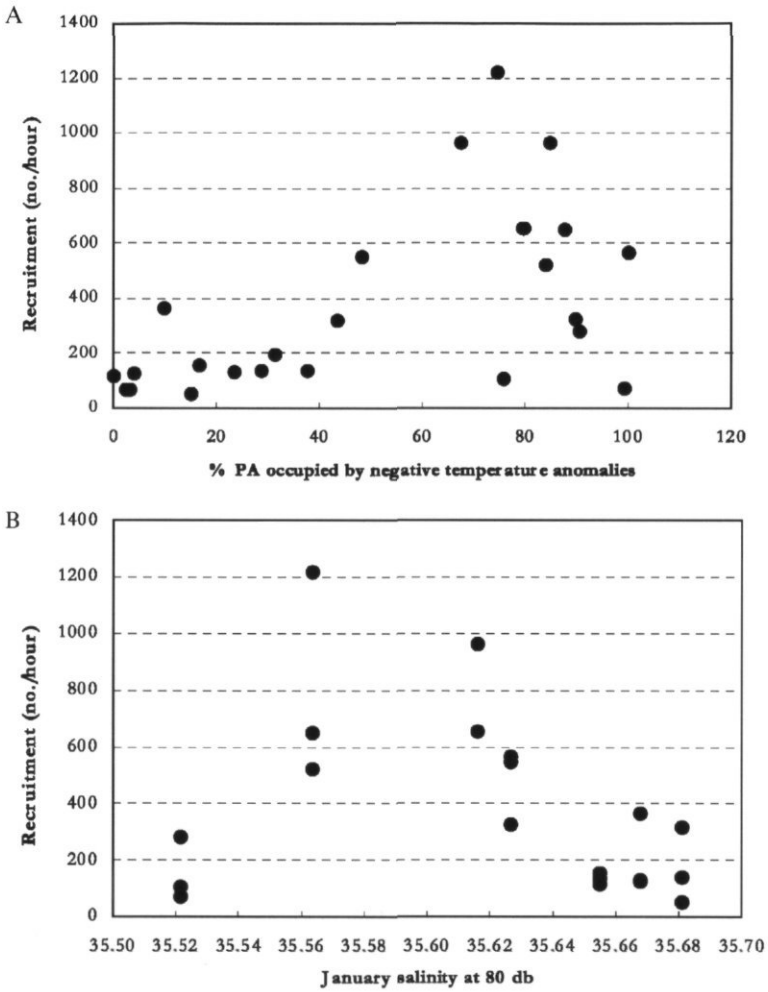


Figure 1. Scatter plot of hake recruitment (numbers hour^{-1}) versus (a) planar shelf area (PA) occupied by negative temperature anomalies at 50 m with respect to the 1993–2000 mean (representative of the summer–autumn upwelling area), and (b) January salinity at 80 m at the central Cantabrian Sea fixed station (representative of the relative strength of the Poleward Current).

lower salinities. The link between winter subsurface salinity and hake recruitment is thought to be through the IPC. This shelf edge flow is believed to play a key role in transporting hake eggs from their winter spawning areas and also in their subsequent larval development (Sánchez and Gil, 2000). In addition to the large-scale transport of hake eggs and larvae, mesoscale eddies pinched off the main current bring about large offshore advections of neritic material (Fernández *et al*, in press). This is thought to be a key density-independent factor negatively affecting recruitment of fish species spawning during the wintertime.

The Cantabrian Sea experiences seasonal upwelling and an associated upwelling front. The front separates freshly upwelled cold, high salinity and nutrient-rich water from warmer, nutrient-depleted oceanic waters. An alongshore equatorward jet plus associated eddy activity develop along the front (e.g. Smith, 1995). Negative temperature anomalies appear along the inner shelf during periods of stronger than normal upwelling. Absence of upwelling brings about the reversal of the current pattern plus the weakening of mesoscale eddy activity (Sánchez and Gil, 2000). We propose the following hypotheses to account for the relationship between hake recruitment and upwelling as indicated by the %PA. The control of hake recruitment by the upwelling could be exerted first by establishing an appropriate aggregation pattern of hake larvae. 'Bottom-up' processes associated with food availability could reduce the survival of larvae at low upwelling rates

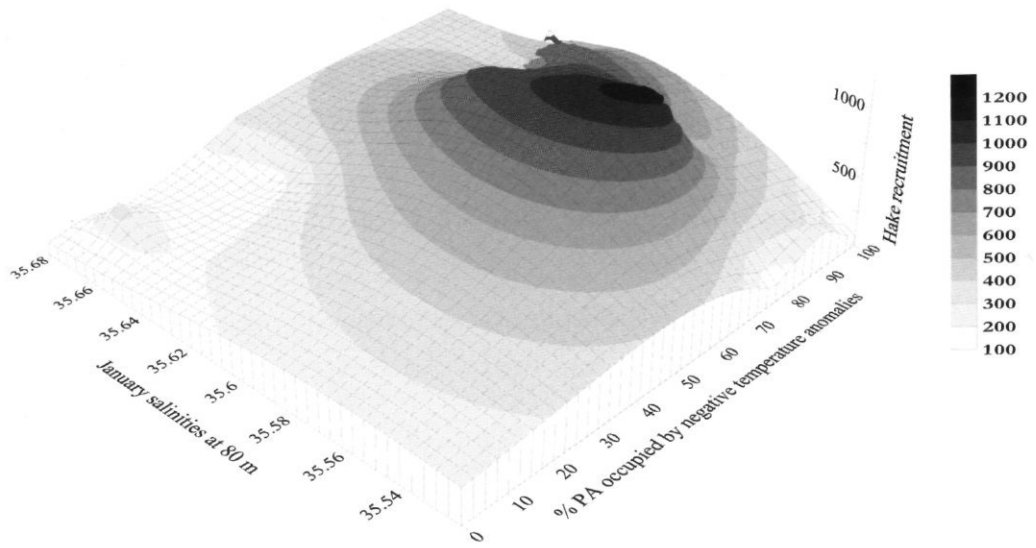


Figure 2. Surface plot of hake recruitment (in numbers hour^{-1}) versus January salinity at 80 m (Poleward Current index) and the %PA (autumn upwelling index). Note the dome-shaped peak in recruitment that defines the optimal environmental window.

(enrichment hypothesis). Extreme upwelling suggests the possibility of excessive offshore transport and loss of hake larvae from the coastal habitat. The optimal situation requires adequate development of a moderately upwelled fringe over the shelf, as previously noted by Sánchez and Gil (2000).

Finally, it is interesting to note that the OEW for upwelling we observed for hake recruitment is similar to that for recruitment of several pelagic species found by Cury and Roy (1989).

Acknowledgements

Thanks to the crews of the RV "Cornide de Saavedra" and RV "José Rioja", the personnel of the C. O. Santander (IEO) and the Project "Studies on time series of oceanographic data", managed by the IEO (especially to L. Valdés, A. Lavín, and C. González).

References

Cury, P., and Roy, C. 1989. Optimal environmental window and pelagic fish recruitment success in upwelling areas. Canadian Journal of Fisheries and Aquatic Sciences, 46: 670–680.

Fernández, E., Álvarez, F., Anadon, R., *et al.* 2002. An overview of the physical, chemical and ecological properties of a Slope Water Oceanic anticyclonic eDDY (SWODDY) in the Southern Bay of Biscay. Deep-Sea Research. (In press.)

Pingree, R. D., and Le Cann, B. 1990. Structure, strength and seasonality of the slope currents in the Bay of Biscay region. Journal of the Marine Biological Association of the United Kingdom, 70: 857–885

Sánchez, F., and Gil, J. 2000. Hydrographic mesoscale structures and Poleward Current as a determinant of hake (*Merluccius merluccius*) recruitment in southern Bay of Biscay. ICES Journal of Marine Science, 57: 152–170.

Smith, R. L. 1995. The physical processes of coastal ocean upwelling systems. *In* Upwelling in the Ocean: Modern Processes and Ancient Records, pp. 39–64. Ed. by C. P. Summerhayes, K. C. Emeis, M. V. Angel, R. L. Smith, and B. Zeithzchel. John Wiley and Sons Ltd. 422 pp.

ICES Marine Science Symposia, 219: 418–420. 2003

Effect of recruitment, individual weights, fishing effort, and fluctuating longline catchability on the catch of Faroe Plateau cod (*Gadus morhua* L.) in the period 1989–1999

Petur Steingrund, Lise Helen Ofstad, and Dagunn Hilda Olsen

Steingrund, P., Ofstad, L. H., and Olsen, D. H. 2003. Effect of recruitment, individual weights, fishing effort, and fluctuating longline catchability on the catch of Faroe Plateau cod (*Gadus morhua* L.) in the period 1989–1999. – ICES Marine Science Symposia, 219: 418–420.

The catch of Faroe Plateau cod fluctuated more in the 1990s than during almost any time in the previous 90 years, and one main aim of this study was to investigate whether the behaviour of cod was anomalous (e.g. large-scale migrations) during these years. It was found that the behaviour of cod was normal in the 1990s (except possibly in 1996) and that variations in recruitment, individual fish weights, fishing effort, and catchability (catch per unit effort divided by stock abundance) were the most important factors that determined the catch of cod. The fluctuating catchability especially applied to longlines where a negative relationship between catchability and individual growth rate of cod was found, indicating that cod preferred longline baits when the abundance of natural food organisms, was scarce. The study also shows that cod production was highly correlated with primary production. This indicates that primary production was the driving force behind recruitment and individual growth and hence the collapse of the cod stock in 1991 as well as its rapid recovery in 1995.

Keywords: catchability, cod production, *Gadus morhua*, growth, individual weights, primary production, recruitment.

Petur Steingrund, Lise Helen Ofstad, and Dagunn Hilda Olsen: Faroese Fisheries Laboratory, Nóatún 1, PO Box 3051, FO-110 Tórshavn, Faroe Islands [tel: +298 31 50 92; fax: +298 31 82 64; email: peturs@frs.fo]

The catch of the Faroe Plateau cod has normally fluctuated between 20 and 40 thousand tonnes (Jákupsstovu and Reinert, 1994). During the period 1991–1994, however, catches were less than 10 thousand tonnes (ICES, 2001). The stock recovered rapidly thereafter (23 and 40 thousand tonnes landed in 1995 and 1996, respectively), and this study investigates the possible causes behind these large fluctuations.

An index of primary production was taken from Gaard *et al.* (2002). Fisheries data on fish weights, recruitment, and fishing mortality were taken from ICES (2001). Age disaggregated catch per unit effort for pair trawlers and longliners (taking the majority of the cod catches) was provided by the Faroese Fisheries Laboratory, Faroe Islands.

When illustrating why the annual catch of cod in a particular year was lower or higher than the average level, four scenarios were performed using different input values for recruitment, fish weights (W), and fishing mortalities (F). The resulting catch in each scenario was calculated and the change in catch between scenarios was taken as a measure of the factor that was changed. In Scenario 1, the input values were held on a constant (average) level, and gave, of course, a constant catch using the formula $W_t N_t(1-\exp(-M-F))(F/(M+F))$, and summing for all ages. The stock numbers were calculated according to $N_{t+1} = N_t \exp(-M-F)$, starting with the number of recruits. In Scenarios 2–4, the recruitment, fish weights, and fishing mortalities, respectively, were changed to the values obtained in the assessment in ICES (2001). The effect of fishing mortality (EF = Catch in Scenario 4 – Catch in Scenario 3) was split into four components.

1) The effect of fluctuating catchability of longlines (Q). First, adjusted longline catchabilities were calculated that corresponded to average fish growth: adjusted catchability = observed catchability – slope × (average growth – observed growth), where the slope was obtained from a simple linear regression of catchability at age versus growth. The effect on catch was calculated as individual weights × observed catch in numbers

for longliners × (adjusted catchability – observed catchability) / observed catchability, and summed for all ages.

2) The effect of unexplained catchability for longliners (UL). In the regression between longline catchability and growth, the difference between observed and predicted values was taken as a measure of unexplained error of catchabilities (probably indicating cod migrations). The catch corresponding to this error was calculated as individual weights × observed catch in numbers for longliners × (predicted catchability – observed catchability) / observed catchability, and summed for all ages.
3) The effect of unexplained catchability for pair trawlers (UP). Since there was no correlation between pair trawler catchabilities and growth, the regression lines had a slope of zero. The catch corresponding to the error was calculated as individual weights × observed catch in numbers for pair trawlers × (predicted catchability – observed catchability) / observed catchability, and summed for all ages.
4) The effect of fishing effort, which was quantified by EF – (Q + UL + UP).

Cod production, resulting from the primary production in year t, was defined as weight increase of the cod population (Pitcher and Hart, 1982): $P_t = N_{t+1} \times (W_{t+1} - W_t)$, where $W_{t+1} - W_t$ denotes the individual weight increase from summer in year t to the next year. N_{t+1} (stock population numbers at 1 January) was used as a proxy for the average number of cod in the time period. The contributions from the ages 2–6 were summed to give the total cod production.

The results show that the low catch at the beginning of the 1990s was caused by a combination of recruitment failure, low individual weights, and low fishing effort (Figure 1). The rapid increase in catch was caused by good recruitment combined with increased growth and fishing effort. In 1996 a substantial part of the catch was caused by high unexplained catchabilities, probably indicating anomalous cod behaviour that particular year. Poor growth in 1997 gave a high catchability with longlines, whereas the opposite occurred in 1995. Figure 1 should be interpreted in a qualitative way, since the results to some extent depended on the way of calculation, e.g. the sequence of the four scenarios, and which longline sets or pair trawler hauls were selected for the c.p.u.e. calculations.

Recruitment and individual weights often covaried (good recruitment and large weights the same year; Figure 1), corresponding to periods of low and high cod production, respectively. Cod production was highly correlated with primary production (Figure 2), suggesting a direct relationship between primary production, production of food organisms, and cod production. The species composition of food organisms may vary considerably from year to year (unpublished data), making an opportunistic

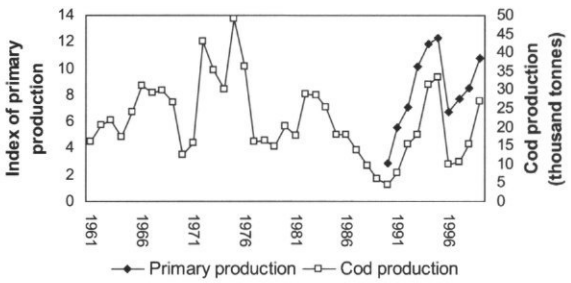


Figure 2. Index of potential new primary production on the Faroe Shelf and corresponding production of 2 to 6-year-old Faroe Plateau cod.

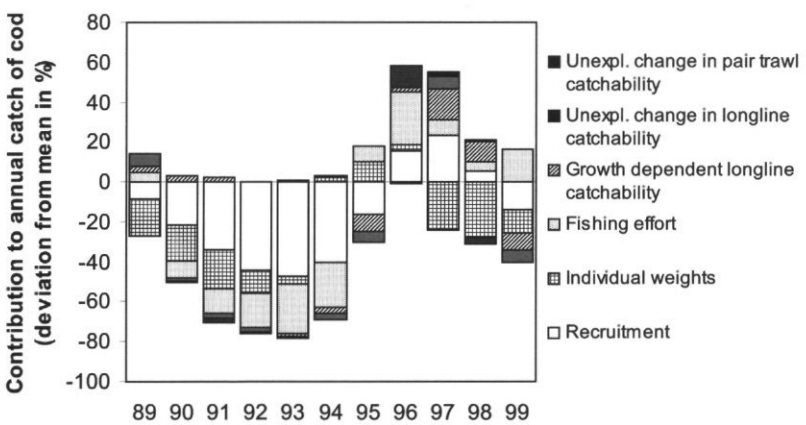


Figure 1. Illustration of the importance of recruitment, individual fish weights, fishing effort, and catchabilities on annual catch of Faroe Plateau cod (deviation from mean).

feeding behaviour necessary in order to capture the energy flow. Also the competition from other fish species, e.g. saithe and haddock, may be limited, since the diet is quite different (unpublished data).

Since the total cod production (production of recruiting cod and older cod) is fixed by the primary production, the recruitment is constrained to certain limits, as the recruiting cod and the older cod are competing for limited food resources. Even if the maximum possible recruitment in a given year is rather well defined (recruiting cod contributing 100% to the total cod production), the actual recruitment is hard to predict, since this depends on early life history of recruiting cod and the outcome of the competition with older cod. Thus both stochastic processes in early life, e.g. match-mismatch (Cushing, 1990), and deterministic processes (e.g. density-dependent mortality) seem to determine recruitment, as found for different cod populations in southern Norway (Fromentin *et al.*, 2001).

Acknowledgements

We thank Dr. Eilif Gaard for providing us with the data on primary production. We also greatly appreciate the comments from two anonymous referees on an earlier version of the manuscript.

References

Cushing, D. H. 1990. Plankton production and year class strength in fish populations: an update of the match/mismatch hypothesis. Advances in Marine Biology, 26: 249–293.

Fromentin, J.-M., Myers, R. A., Bjørnstad, O. N., Stenseth, N. C., Gjøsæter, J., and Christie, H. 2001. Effects of density-dependent and stochastic processes on the regulation of cod populations. Ecology, 82: 567–579.

Gaard, E., Hansen, B., Olsen, B., and Reinert, J. 2002. Ecological features and recent trends in the physical environment, plankton, fish stocks and seabirds in the Faroe shelf ecosystem. *In* Large Marine Ecosystems of the North Atlantic: Changing States and Sustainability, pp. 245–265. Ed. by K. Sherman and H. R. Skjoldal. Elsevier, Amsterdam.

ICES. 2001. Report of the North-Western Working Group. ICES CM 2001/ACFM: 20. 417 pp.

ICES. 2002. Report of the North-Western Working Group. ICES CM 2002/ACFM: 20. 405 pp.

Jákupsstovu, S. H., and Reinert, J. 1994. Fluctuations in the Faroe Plateau cod stock. ICES Marine Science Symposia, 198: 194–211.

Pitcher, T. J., and Hart, P. J. B. 1982. Fisheries Eecology. Croom Helm. 414 pp.

ICES Marine Science Symposia, 219: 421–425. 2003

Hydrobiological variability on the northwest European continental shelf during the 1990s and its relation to changes in fish stocks

S. L. Hughes, W. R. Turrell, and A. Newton

Hughes, S. L., Turrell, W. R., and Newton, A. 2003. Hydrobiological variability on the northwest European continental shelf during the 1990s and its relation to changes in fish stocks. – ICES Marine Science Symposia, 219: 421–425.

Multidisciplinary survey data have been obtained from the first quarter ICES International Bottom Trawl Surveys from 1986 to 1999. The data include estimates of the number of young demersal fish by ICES Square (based on numbers caught per hour of research vessel fishing), along with near-bed temperature, salinity, and water depth. The database forms a near-synoptic picture of the winter distribution of young fish in the North Sea, particularly in relation to hydrographic conditions. Two species have been selected for examination, cod and haddock. Their average distribution over the observation period with respect to temperature indicated that the young haddock had a more restricted temperature range, centred on approximately 8°C and were not found in waters with a temperature of less than 5°C. Young cod were found in a wider range of temperatures, from less than 1°C to 9°C, but with a maximum at approximately 6°C. This is partly explained by their different geographical distributions, with young haddock confined to the deeper northern North Sea, and young cod to the shallower southern areas. The data have also been used to examine the interannual variability of both temperature and young fish numbers. The influence of the Atlantic inflow is clear when looking at data from the northern North Sea, as interannual variability of temperature was less than in the shallower southern areas. In the south, temperatures were closely associated with the variability of the North Atlantic Oscillation index (NAO). The 1990s was a decade of warming in the North Sea. However, 1996 was a particularly cold year, which may have influenced the large catch of young cod in the following winter.

Keywords: climate change, cod, haddock, NAO, North Sea.

S. L. Hughes, W. R. Turrell, and A. Newton: FRS Marine Laboratory, PO Box 101, Aberdeen AB11 9DB, Scotland [tel: +44 1224 29 5429; fax: +44 1224 29 5511; e-mail: hughess@marlab.ac.uk]. Correspondence to S. L. Hughes.

Introduction

The multidisciplinary data from the ICES International Bottom Trawl Surveys (IBTS) undertaken in January/February each year 1986 to 1999 (IBTS, Quarter1) form a near-synoptic picture of the winter distribution of young fish in the North Sea, particularly in relation to the hydrographic conditions (Turrell, 2000). Heesen and Daan (1994) have undertaken an analysis of the IBTS dataset in relation to cod distribution for the period 1977–1991. The data presented here extend this analysis through the decade of the 1990s.

Two species, cod and haddock, were selected for initial examination from the IBTS dataset. The spatial distribution and relationship with near-bed temperature of these two species have been examined. The data have also been used to examine interannual variability of temperature and numbers of young fish caught.

Data

The annual IBTS Quarter 1 survey is usually undertaken in February, for the purpose of stock assessment. Standardized trawl hauls and plankton net tows are taken in each ICES box along with near-bed and near-surface temperature, salinity, and nutrient measurements. At some sites, including the fishing grounds marked in Figure 1, winter temperatures are available from 1970 to 1999. For this

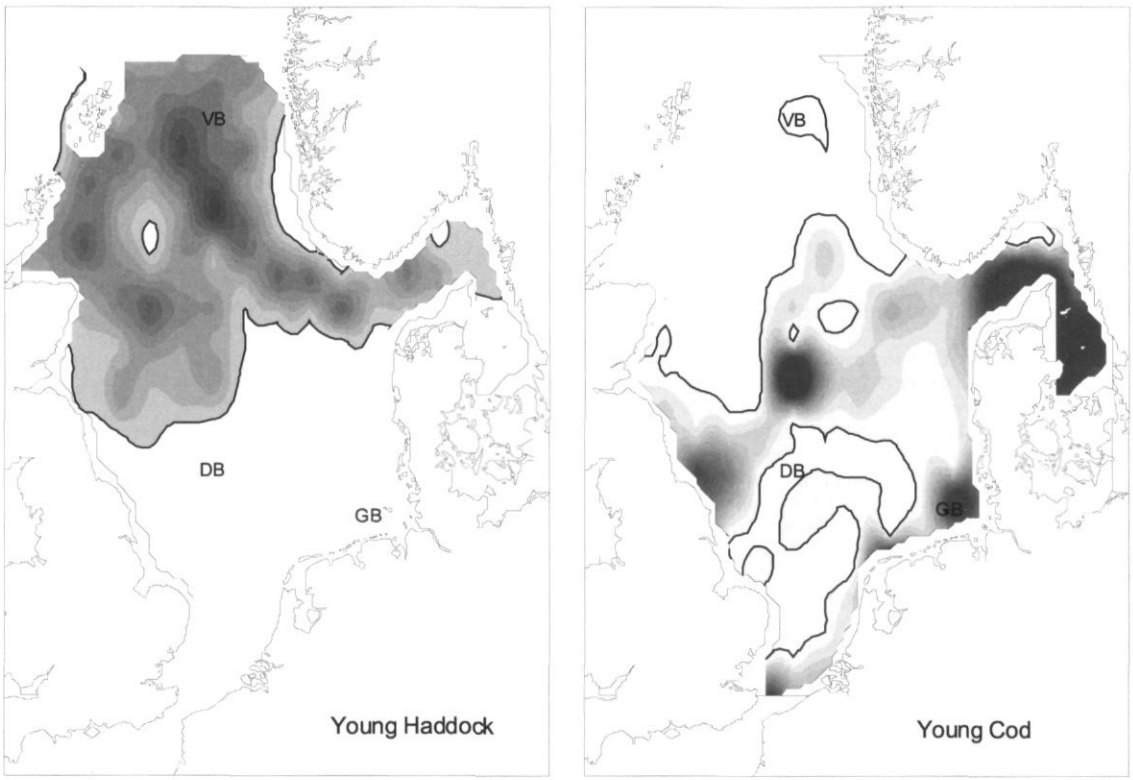


Figure 1. The average winter distribution of young cod and haddock in the North Sea, 1986–1999. The shaded areas indicate where young fish of each species were caught. The intensity of shading indicates the number of young fish caught; a darker shade indicates a higher catch. The location of the following fishing grounds are marked on the map: VB – The Viking Bank, DG – The Dogger Bank, and GB – German Bight.

study, corresponding catch data were only available from 1986 to 1999. A variety of methods have been employed during the multi-national surveys, but have basically employed fish sampling using standardized demersal trawls, and hydrographic sampling using reversing water bottles and, more recently, CTDs. In this study, the numbers of year 1 cod and haddock are investigated. The winter North Atlantic Oscillation index (NAO) has been obtained from http://www.cgd.ucar.edu/~jhurrell/nao.html (Hurrell, 1995).

Results

The waters of the northern North Sea are modified by inflowing Atlantic Water and so, in winter, are warmer and less variable than the waters of the southern North Sea. Winter near-bed temperatures from three North Sea fishing grounds (Viking Bank-VB, Dogger Bank-DG, and German Bight-GB) are shown in Figure 2. In the deep northern fishing grounds of the Viking Bank, winter near-bed temperatures only fell below 6°C on one occasion between 1970 and 1999. In the shallower southern grounds of the German Bight, the winter near-bed temperatures during the same period were rarely higher than 6°C. During the study period, the winters of 1989, 1990, and 1991 were warmer for the whole of the North Sea, for these years the winter temperatures in the German Bight were between 6.2 and 6.5°C. The winters of 1986, 1987, and 1996 were particularly cold. The winter of 1996 stood out as the coldest of the study period; during this year winter temperatures in the German Bight reached –0.2°C. During the winter months the waters of the North Sea are generally well mixed and so the near-bed temperature is indicative of temperature throughout the water column.

The period 1976–1999 has been identified by the Intergovernmental Panel on Climate Change (IPCC) as one of warming for the whole of the Northern Hemisphere. To identify the trends in the winter near-bed temperature of the North Sea over

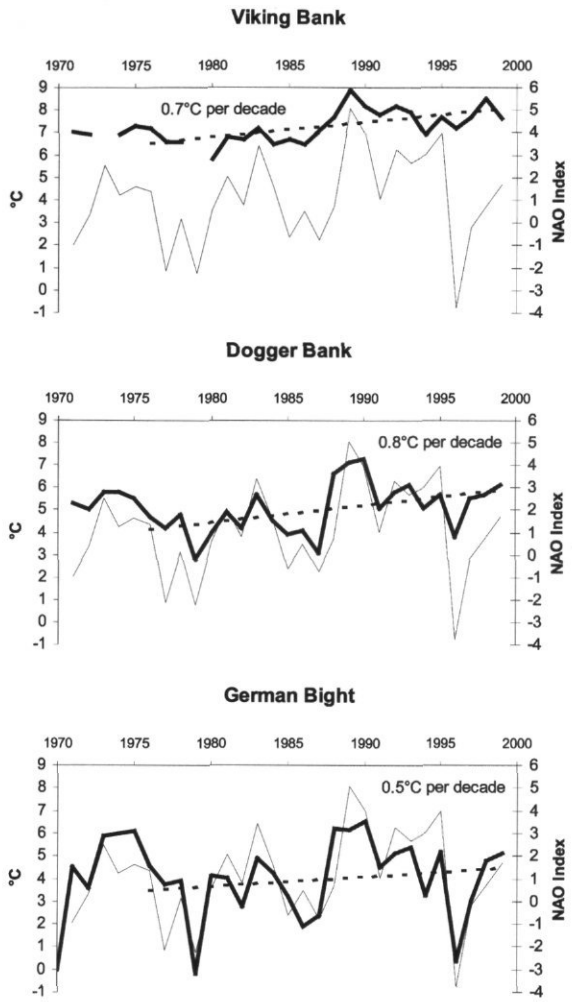


Figure 2. Winter near-bed temperatures at selected North Sea fishing grounds (VB, DB, GB); the locations of these fishing grounds are marked in Figure 1. The figure also shows the changes in the North Atlantic Oscillation (NAO) during this period. The dotted line on each graph is the linear trend of temperature for the period 1980 to 1999. Left axis (thick line) is winter near-bed temperature (°C); right axis (fine line) is the NAO winter index.

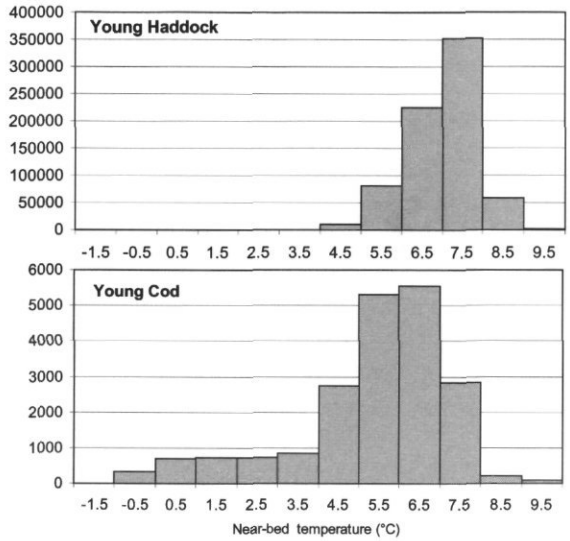


Figure 3. The relationship between catches of young cod and haddock in the North Sea and the near-bed temperature at which they were caught. The catch numbers refer to the total number of young fish caught per hour of fishing during the Quarter 1 International Bottom Trawl Surveys 1986 to 1999.

this period (1976 to 1999), a linear fit was applied to the data (Figure 2). These data show warming of between 0.5°C and 0.8°C per decade at all sites, a warming trend that has been observed at sites throughout the North Sea (Turrell, 2000). The interannual variability of temperatures of the North Sea is known to be well correlated with that of the winter NAO index, with warmer winter temperatures associated with positive NAO index values (Becker and Pauly, 1996).

The spatial distribution of catches of young cod and haddock showed a marked difference between the species. Young haddock were found mainly in the deeper northern North Sea, whereas young cod were found in the southern North Sea (Figure 1). Over the study period, catches of young cod were concentrated at particular sites such as the German Bight, and to the north of the Dogger Bank. In contrast, young haddock appear to have been more evenly distributed.

The difference between the distribution of the two species is also evident when comparing the frequency of catches to the near-bed temperature. Over the period of study (1986 to 1999), young haddock were only caught in waters warmer than 4°C, with the highest catches occurring in waters close to 7°C, whereas young cod were caught in waters with a much larger temperature range, the highest catch occurred in water between 5°C and 7°C (Figure 3). Heesen and Daan (1994) present the frequency of catch data by year compared to the temperatures 'available' to the fish in that year. Figures 4 and 5 illustrate this relationship for cod and haddock between 1986 and 1999.

Catches of both cod and haddock were low during the cold winter of 1996. However, it is interesting to note that in 1997 there was a marked increase in the catch of 1-year-old cod (these fish would have spawned during the colder winter of 1996). If lagged by 1 year, the annual catches of young cod since 1986 show some correlation with

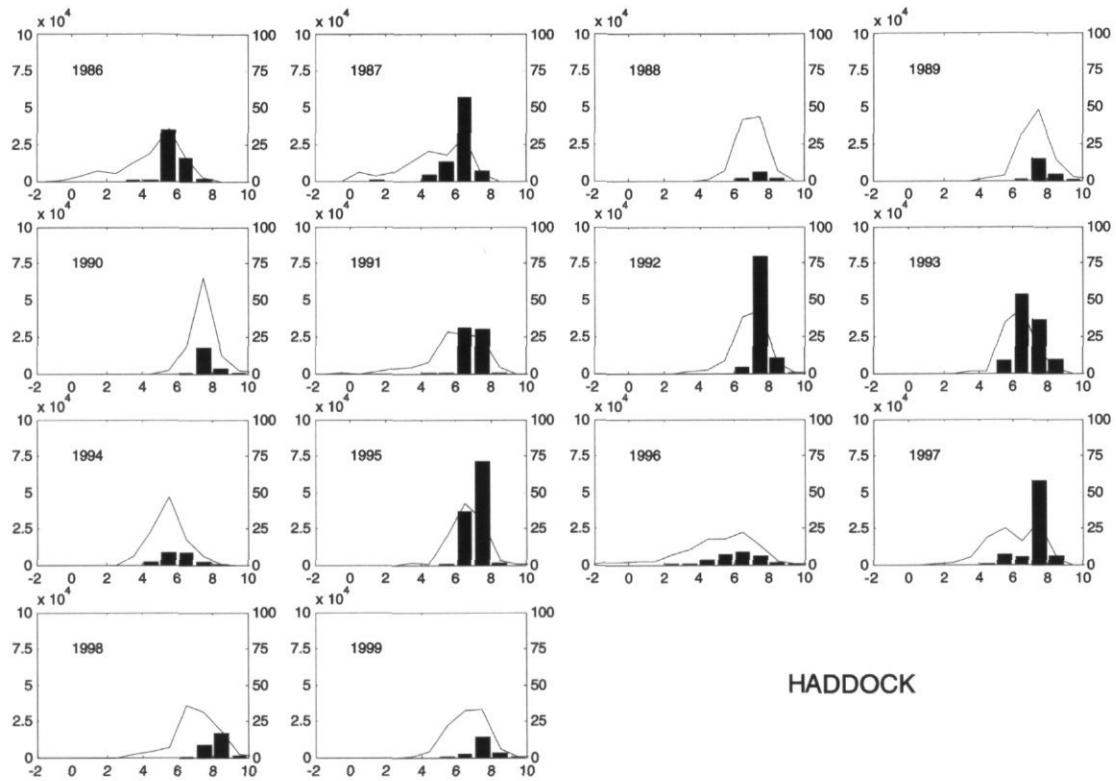


Figure 4. The numbers of young haddock caught by temperature at which they were caught for each year 1986–1999. Catch data are numbers of young fish caught in each 1°C temperature band (left axis). The grey line (right axis) represents the percentage of the total survey area characterized by each temperature band.

winter near-bed temperatures on the Dogger Bank (Figure 6).

Discussion

The cod spawning-stock biomass in the North Sea is estimated to have been below the ICES precautionary level since 1984 (ICES, 2001). The decade of the 1990s was a period of warming for the North Sea, with warming trends of between 0.5 and 0.8°C per decade. Heesen and Dann (1994) analysed the relationship between cod distribution and temperature in the North Sea using IBTS data from 1977 to 1991. They looked at the temperature of water in which young cod were caught and dismissed the possibility that juvenile cod had a specific preference to lower or higher temperatures or that the distribution of cod in the North Sea was significantly affected by a gradual increase in temperature. However, they did acknowledge that there is a possibility that temperature would have an effect on the larval and early 0-group phase.

It is possible that climatic factors such as temperature have been more important during the 1990s, while cod stocks have been low. This may be reflected in the relationship between catches of year-1 cod and the NAO in the previous year, which is representative of the conditions they encountered while in their early stages (Figure 6). However, a longer time-series of data would be needed to quantitatively examine a correlation between these parameters.

There are many biological and physical factors determining the survival of young fish and these have not been investigated here. The variation of water temperature and catches of young cod and haddock throughout the 1990s have been presented, and the suggested correlation between winter temperatures and catches of young cod is worthy of further investigation. An ability to predict winter temperatures in the North Sea may prove to be a useful tool for fisheries management.

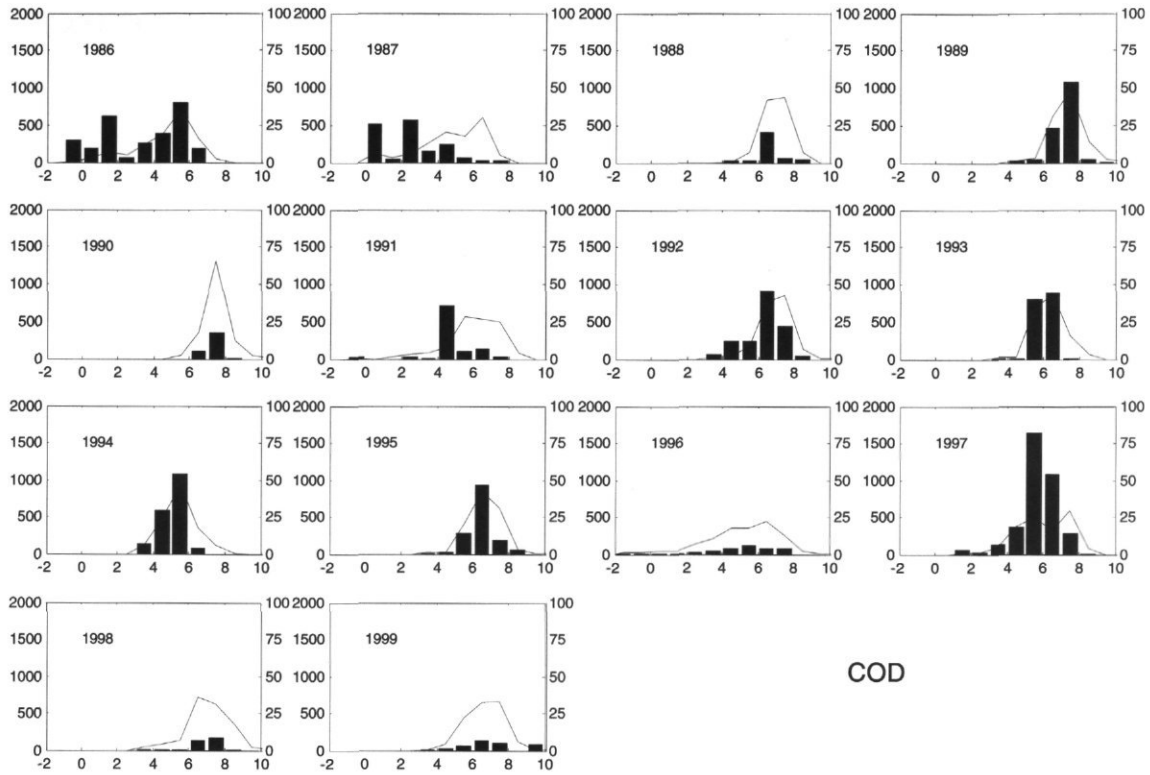


Figure 5. The numbers of young cod caught by temperature at which they were caught for each year 1986–1999. Catch data are numbers of young fish caught in each 1°C temperature band (left axis). The grey line (right axis) represents the percentage of the total survey area characterized by each temperature band.

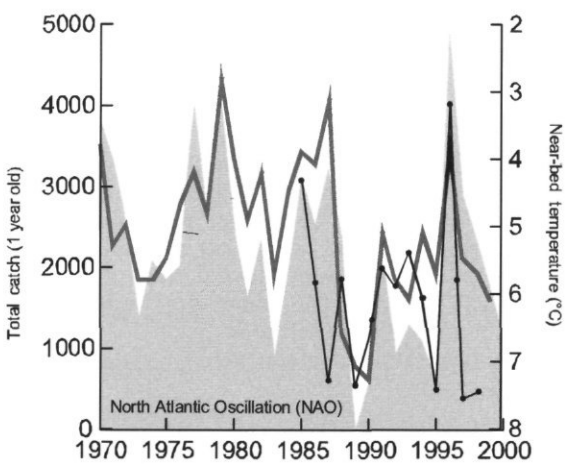


Figure 6. The total number of young cod caught during the Quarter 1 International Bottom Trawl Surveys 1986 to 1999 (fine black line with dots). For comparison, the winter near-bed temperature at Dogger bank (grey line) and the winter NAO index (shaded light grey) are plotted on an inverse axis. Catch data have been lagged by 1 year (i.e. 1986 catch plotted as 1985).

References

Becker, G., and Pauly, M. 1996. Sea surface temperature changes in the North Sea and their causes. ICES Journal of Marine Science, 53: 887–898.

Heesen, H. J. L., and Daan, N. 1994. Cod distribution and temperature in the North Sea. ICES Marine Science Symposia, 198: 244–253.

Hurrell, J. W. 1995: Decadal trends in the North Atlantic Oscillation. Regional Temperatures and Precipitation Science, 269: 676–679.

ICES. 2001. Advisory Committee of Fishery Management (ACFM) Report. Cod in Sub-area IV (North Sea), Division VIId (Eastern English Channel) and Division IIIa (Skagerrak).

Turrell, W. R. 2000. Scottish Ocean Climate Status Report 1999. Fisheries Research Services Report No. 06/00. (http://www.marlab.ac.uk/PDF/Oceanclimate99.pdf).

ICES Marine Science Symposia, 219: 426–429. 2003

Development of ecological indicators for the Dutch section of the North Sea

Saa H. Kabuta and Elizabeth M. Hartgers

Kabuta, S. H., and Hartgers, E. M. 2003. Development of ecological indicators for the Dutch section of the North Sea. – ICES Marine Science Symposia, 219: 426–429.

Sustainable use of marine waters has a high priority as part of international and national agendas. The quality of marine ecosystems reflects both the level of human pressures and natural environmental processes. Knowledge is key to making efficient policy recommendations regarding ecosystem management. In the past decade, the development of indicators has played an important role in enabling policy-makers to understand ecosystem changes while helping them make concrete recommendations towards improvement of their marine environments. Such indicators should describe the quality of the ecosystem, have strong scientific basis, and have the advantage of simplicity. This article presents the steps taken to develop ecological indicators for The Netherlands section of the North Sea. Among the current set of indicators used in The Netherlands, two are presented to illustrate how they are used in ecosystem management.

Keywords: ecological indicator, ecosystem approach, ecosystem management, GONZ, SOVON.

S. H. Kabuta: National Institute for Coastal and Marine Management (RIKZ), PO Box 20907, 2500 EX The Hague, The Netherlands [tel:+31 70 311 4324; fax: +31 70 311 4321; e-mail: s.h.kabuta@rikz.rws.minvenw.nl]. E. M. Hartgers: Regional Directorate for Water Management, North Holland, PO Box 3119, 2001 DC Haarlem, The Netherlands [tel: +31 23 530 1301; fax: +31 23 530 1302; e-mail: hartgers@DNH.rws.minvenw.nl]. Correspondence to S. H. Kabuta.

Introduction

The Netherlands has implemented various projects to improve the level of knowledge of the ecosystem of The Netherlands section of the North Sea (Kabuta and Duijts, 2000). The GONZ project (GONZ is the Dutch acronym for indicator development for the North Sea) was designed to use monitoring data in the development of ecological indicators to evaluate the level of human impact on the quality of the ecosystem. Ecological indicators are used to measure ecosystem integrity and may incorporate multi-dimensional information. Those developed in the GONZ project are based on biological components of the ecosystem including information on species, groups of species, and communities. Associated with these components are various organizational levels and functional elements of the ecosystem that include productivity, predation, and reproduction.

The development of indicators in the GONZ project started by integrating the relevant ecological components of the National policies for Water Management and Nature Conservation in The Netherlands (Duel *et al.*, 1997). Two main policy themes were selected: the conservation of biodiversity and the sustainable use of the ecosystem. Ecosystem indicators were identified for each of these two themes (Table 1). Biodiversity covers diversity of species, community, and habitat, while sustainability is linked to various uses of the ecosystem (e.g. fishing, shipping, sand extraction) as well as ecological processes (e.g. production and predation among ecological groups). The indicators were selected based on the following criteria:

- representative of a functional response of the ecosystem
- easy and inexpensive to monitor or be based on modelling results
- relevant to existing policy recommendations
- sensitive to the changes in the ecosystem
- sensitive to specific human activities
- availability of long-term time-series.

The final list of indicators was screened by a committee of scientists, policy-makers, stakeholders and managers (Duel *et al.*, 1997). Information about changes in the ecosystem were obtained using long-term data on the indicators (Kabuta and

Table 1. The current set of ecosystem indicators.

Parameters/ecological groups	Zoo and phytoplankton	Macrozoobenthos	Marine fishes	Sea mammals	Coast and sea birds
Species diversity	No. of species (SW)	No. of species (SW)	No. of species (SW)		
Population density		Density / m^2	Density per species	No. / km^2	Breeding population
Community structure	Ratio flagellates/ diatoms	r/k strategy	Length / weight per species		
Primary production	Production level C gr cm^2 / year				
Secondary production (grazers)	Copepod density	Biomass benthos g / m^2			
Tertiary (somatic) production			Biomass commercial landings per species	Individual biomass	
Food web					
Top predator density			Population size and distribution	Population size and distribution	Population size and distribution
Size of food storage		Prey organism spisula (m^2)	Prey organism (herring)		
Trophic structure		Types of feeders (IT index)			Types of feeders

SW = Shannon-Wiener index; empty boxes indicate no ecosystem indicator yet selected.

Duijts, 2000). In the remainder of the article we discuss two ecosystem indicators.

Example 1. Changes in breeding populations of the sandwich tern *(Sterna sandvicensis)* as an indicator for coastal and marine habitat conservation. – Policy recommendations for habitat conservation in The Netherlands stress the need for nature conservation regions in both marine and coastal areas. The increase in breeding populations of birds in these areas form one of the elements for assessing the success of this policy.

The sandwich tern is a coastal seabird often found foraging (up to depths of 20 m) in the Dutch Coastal Zone and estuaries (Delta and Wadden Sea) (Stone *et al.*, 1995). Their food comprises mainly small fish such as sprat, young herring, and sandeel. The breeding population is affected by water quality and the accessibility of food. The tern lives in large groups on the beach during the breeding season and at sea when not breeding. At all times of the year, the tern shows a high sensitivity to various forms of human influences, including recreational activities, toxic substances, and fisheries. The size of the population is strongly associated with the richness and availability of nesting grounds (Stone *et al.*, 1995).

Data on sandwich tern populations are collected primarily through an annual monitoring programme conducted by the National Institute for Coastal and Marine Management (RIKZ). Additional data are collected by various voluntary study groups specializing in nature conservation in The Netherlands. The data on breeding birds are managed by SOVON. The breeding success of the sandwich tern is determined annually in a number of colonies in the Delta estuary and in the Wadden Sea.

Following a minimum in 1991, the number of breeding pairs of sandwich terns in the Delta increased (Figure 1). This trend is directly related to management policies. In 1991, high intensity of recreational activities in the Delta area disrupted the breeding population of terns, causing them to migrate in huge numbers to the nearby coast of Zeebrugge, Belgium (Meininger *et al.*, 1999). As a direct result of policies to severely limit human encroachment on the breeding birds, there was a major decrease in recreational activity in 1993 and a large number of the breeding sandwich terns returned to the Delta region.

Example 2. Changes in the structure of macrozoobenthos infaunal communities in the North Sea as an indicator of disturbances on the seabed. – Fishing and sand extraction in the North Sea affect benthos fauna communities in various ways. These communities are often removed from their habitats, buried under organic matter, or killed directly. Demersal fisheries activities are also considered

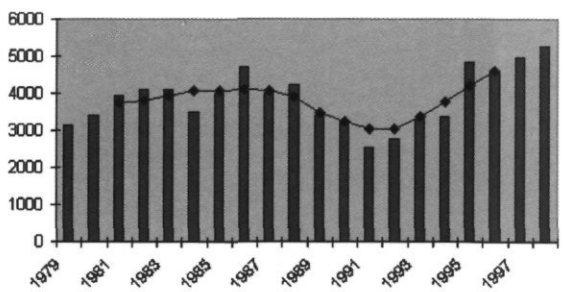


Figure 1. Changes in the breeding population of the sandwich tern.

responsible for major changes in both the functional and the organizational structures of the local benthos communities.

From the point of view of sustainability in The Netherlands North Sea, management actions are being directed towards reducing the negative effects of human activities, such as fisheries, on the ecosystem. Monitoring data have long been used to calculate diversity indices as a measure of the quality of the benthos communities. These indices, in principle, describe the level of species richness in the various parts of the Dutch section of the North Sea (Holtmann, 1997). Besides these diversity indices, few other indices are used to describe the impact of human activities on benthos communities in the North Sea. One exception is the Infaunal Trophic (IT) index (Word, 1979).

Word (1979) characterized the coastal waters of South California using the IT index, which selects a number of species within a given area based on their frequency of occurrence and dominance (>40%) in the samples collected during monitoring. Omnivorous, predatory, and herbivorous species are excluded. The selected species are divided on the basis of their feeding strategies. Group 1 consists of organisms that feed by capturing suspended particles drifting into their mucous traps or filter systems. These "suspension feeders" tend to dominate areas where sediment levels of BOD are relatively low. Group 2 comprises "interface feeders" with most of the male organisms feeding on suspended particulate matter while the females feed on surface detritus. Group 3 species feed on detritus on the seabed and are called "surface deposit feeders". They dominate where BOD levels are slightly increased due to anthropogenic activities. Group 4 feed on detritus found under the surface of the seabed. Significant amounts of mud pass through the guts of these "subsurface feeders". The values of the IT index for Groups 1 through 4 are between 100 and 75, 74 and 49, 48 and 25, and 24 and 0, respectively.

The IT index is measured by using the selected number of species belonging to each of the four groups. The index is calculated by using the formula:

$$\text{IT index} = 100 - (100 \times (0n_1 + 1n_2 + 2n_3 + 3n_4))/3n_1 + n_2 + n_3 + n_4$$

where n_1, n_2, n_3, and n_4 are the numbers of individuals in Groups 1, 2, 3, and 4, respectively. The value of the IT index lies between 0 and 100. The closer the number is to 100, the less disturbed the seabed, and suspension feeders dominate. When the index is closer to 0, the seabed is relatively highly disturbed and subsurface feeders dominate.

The IT indices for The Netherlands section of the North Sea between 1991 and 1998 show the highest index, indicative of less seabed disturbance, to the north of the oyster grounds (Figure 2). In the offshore regions of the North Sea, lower indices were observed, although they were slightly higher in 1994 and 1995, indicating less seabed disturbances in those years. The indices in the coastal region lie between 30 and 60, indicative of continuous disturbance during the study period.

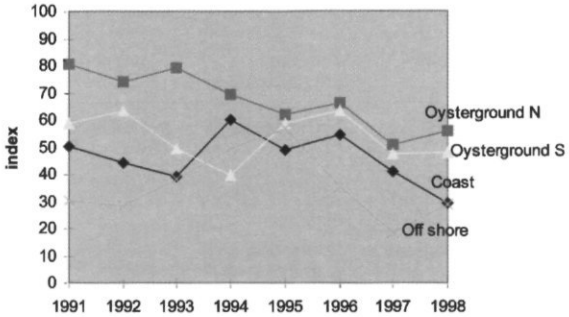


Figure 2. The time-series of the Infaunal Trophic (IT) index for four regions of The Netherlands section of the North Sea.

Conclusions

A suite of indicators is presently being used to evaluate nature policy objectives for The Netherlands section of the North Sea. The techniques learned within the GONZ project have served as input to the development of ecological quality objectives (ECOQO) for the North Sea. The development of ecological indicators is far from complete. Future work includes the development of scientifically sound and politically acceptable reference values for the indicators. Further efforts should be geared towards integrating different sets of indicators (socio-economics, governance, physical and morphological) and to link the indicators with specific human activities.

Acknowledgements

We gratefully acknowledge the support of our RIKZ colleagues and those individuals and institutions that participated in the development of the ecological indicators for The Netherlands section of the North Sea.

References

Duel, H., Heessen, H., Jak, R., Lanters, R., Leopold, M., and Marchand M. 1997. GONZ Indicator development for the North Sea, assessment system for the water and nature policy for the North Sea. WL, Delft, The Netherlands.

Holtmann, S. E. 1999. GONZ III Graadmeter Ontwikkeling Noordzee. Infaunal Trophic Index (ITI) and Structure macrobehthos gemeenschap (verhouding r-en k-strategen) op 25 astations van het NCP (1991–1998). NIOZ rapport. (In Dutch.)

Kabuta, S. H., and Duijts, H. 2000. Indicators for the North Sea, the end report of GONZ III. RIKZ report, RIKZ/2000/022.

Meininger, P. L., Berrevoets, C. M., Flamant, R., and Hoogendoorn, W. 1999. Migration and wintering of Mediterranean gulls *Larus melanocephalus* ringed in the Netherlands and Belgium: a progress report. *In* Proceedings of the 1st International Mediterranean Gull Meeting at Le Portel, Pas-de-Calais, France, 4–7 September 1998: Econum Merville. Ed. by P. Raevel, W. Hoogendoorn, P. L. Meininger, and R. Flamant.

Meininger, P. L., Berrevoets, C. M., and Strucker, R. C. W. 1999. Kustbroedvogels in het Deltagebied: een terugblik op twentig jaar monitoring (1979–1998). Rijksinstituut voor Kust en Zee, Rapport RIKZ-99.025. Middelburg, The Netherlands. (In Dutch.)

Stone, C. J., Webb, A., Barton, C., Ratacliff, N., Reed, T. C., Tasker, M.L., Camphuysen, C. J., and Peinkowski, M. W. 1995. An atlas of sea bird distribution in the north-west European waters. JNCC Petersborough.

Word, J. Q. 1979. The Infaunal Trophic Index. *In* Southern Californian Coastal Water Research Project, Annual Report 1978, pp. 19–39. California.

ICES Marine Science Symposia, 219: 430–432. 2003

Eutrophication and herring reproduction success in the northern Baltic Sea

Lauri Urho, Jakob Kjellman, and Tea Pelkonen

Urho, L., Kjellman, J., and Pelkonen, T. 2003. Eutrophication and herring reproduction success in the northern Baltic Sea. – ICES Marine Science Symposia, 219: 430–432.

We analysed a 14-year (1982–1995) data set of age-0 herring taken with a littoral beach seine during June–August in three adjacent bays off Helsinki in the Gulf of Finland in the Baltic Sea. In all three bays, the abundance of littoral age-0 herring was lower with higher primary production (270–3800 mg C m^{-3} d^{-1}). Age-0 herring catches also showed a significant negative correlation with turbidity. Eutrophication level explained 40% of the 0+ herring catches.

Keywords: clupeiforms, juvenile, nutrient load, reproduction.

L. Urho: Finnish Game and Fisheries Research Institute, PO Box 6, FIN-00721 Helsinki, Finland [tel: +348 205 751 258; fax: +358 205 751 201; e-mail: lauri.urho@rktl.fi]; J. Kjellman: Department of Limnology and Environmental Protection, University of Helsinki, PO Box 27, FIN-00014 Helsinki, Finland; T. Pelkonen: Finnish Game and Fisheries Research Institute, Quark Fisheries Research Station, Korsholmanpuistikko 16, FIN-65100 Vaasa, Finland. Correspondence to L. Urho.

Introduction

Nutrient levels in Baltic Sea Water vary greatly within a year; in general, however, they are highest in nearshore areas. In some coastal areas, nutrient levels peaked in the 1970s and 1980s, although relatively high discharges of nutrients continue to enter the Baltic Sea through land drainage and river run-off. These coastal areas serve as excellent sites for studying the response of fish reproduction to eutrophication. The larval profit theory of fish production states that not only the extent of larval and nursery areas but also the conditions prevailing in them determine overall survival and hence population size (Urho, 2002). In this artile, we examine whether a relationship exists between water quality parameters and 0+ herring abundance.

In the Archipelago Sea, a known area of eutrophication, Kääriä *et al.* (1988) observed that herring catches in 1973–1986 increased in the outer areas of the sea and decreased in the areas nearer to shore. Correspondingly, in the Helsinki region, Anttila (1973) reported that herring had started spawning farther offshore. In the 1980s, Urho and Hildén (1990) found that herring larvae hatching outside the shallow bay areas shifted inshore annually to take advantage of warmer waters in areas where waste water treatment had already started to improve the quality of the water. As an indication of this local remedy, Lappalainen and Pesonen (2000) caught herring, even at spawning time, when conducting test fishing in an inshore bay (Laajalahti) off Helsinki in 1997. We use a 14-year (1982–1995) continuous data set on age-0 herring abundance in three adjacent inner bays off Helsinki, each with a slightly different eutrophic status, to study changes in the reproductive success of herring at different eutrophication levels. We hypothesized that age-0 catches could be linked to primary production capacity.

Materials and methods

To study the effects of wastewater effluent, annual sampling of the nearshore abundances of 0+ fish was started in three bays off Helsinki in 1982. The bays, Laajalahti, Vanhankaupunginlahti and Vartiokylänlahti, in the Gulf of Finland, are shallow (mean depth 1.4–2.4 m) and brackish (salinity < 6‰). Of the three, Laajalahti is the largest, 5.3 km^2, and artiokylänlahti the smallest, 3.3 km^2. Better sewage treatment has gradually improved the water quality of the most eutrophic bays (Table 1) (Pellikka and Viljamaa, 1998).

Table 1. Summer phytoplankton primary production capacity (mgC $m^{-3} d^{-1}$) and turbidity (FTU) for three bays (Laa = Laajalahti, Van = Vanhankaupunginlahti, and (Var = Vartiokylänlahti) off Helsinki, in the Baltic Sea.

Year/ Bay	Primary production			Turbidity		
	Laa	Van	Var	Laa	Van	Var
1982	1700	3800	590	7.6	26.1	4.25
1983	1800	3800	560	5.45	10.7	5.15
1984		2100			17.5	
1985	1800		570	7.25		2.7
1986	1400	1600		12.1	21	
1987	780		270	7.6		4.35
1988	1200	1350	500	9.55	22	4.25
1989	1000	1700	520	14.5	12.5	4.6
1990	970	1200	460	12	12.5	6.8
1991		1400			12	
1992		730	450		9	6.4
1993	680	740		9.1	18	
1994		720			7.5	
1995	580	890		11	7	

The aim of this study was to relate age-0 herring catches to the eutrophication level. The majority of the fish samples were taken in July, but also some in June (first sample 10 June) and August (last sample 24 August). In all three bays, the fish monitoring was carried out with similar beach seines: arms 9–10.5 m long, depth 2.5 m, and mesh size 5 mm in the arms and 1 mm in the codend. The age-0 fish were sampled and analysed as catch per haul (c.p.u.e.) by pulling the seine by hand towards the beach or an anchored boat (4–5 m in length) with 20 m ropes. The intention was to haul 10 stations in one day in each bay, 3–4 times per summer. The same stations were used every year. Mean daily ln-transformed catches (c.p.u.e.+1) were used to calculate mean annual catches. These age-0 herring catches were related to the annual summer phytoplankton primary production capacity and turbidity (Pellikka and Viljamaa, 1998) of each bay (Table 1).

Results

Herring larvae appeared in all three bays every year from 1982 to 1995. Catches of age-0 herring decreased with increasing primary production (270–3800 mg C m^{-3} d^{-1}) in all three bays. Furthermore, the age-0 herring catches were significantly negatively correlated with turbidity, and turbidity positively correlated with primary production (Table 2). However, there was no significant partial correlation ($r = -0.08$, $p > 0.10$, $n = 30$) between turbidity and age-0 herring catch when the effect of primary production was considered for both herring catches and turbidity. Because turbidity was not partially correlated with herring catch, we did not include turbidity in any of our later analyses.

Table 2. Correlation coefficient (r_p) and corresponding Bonferroni corrected probabilities in parentheses among age-0 herring catch, primary production capacity (PP), and turbidity (FTU) for three bays off Helsinki, 1982–1995 (n = 30).

	ln(catch + 1)	ln(PP)
ln(PP)	−0.62 (0.00)	
ln(FTU)	−0.44 (0.04)	0.63 (0.00)

Primary production and bay as covariates account for the bulk of the variability in the herring age-0 catches in the shallow nearshore areas (GLM. full model, $r^2 = 0.43$, $p < 0.01$, $n = 30$). The crossed variable, bay * ln(primary production) and bay, did not contribute significantly to the function. Primary production alone accounted for 38% of the age-0 herring catches (Figure 1) but indicated that the mean catch in Vartiokylänlahti in 1990 was an outlier. Excluding this outlier did not change the results, however. Primary production was still the only significant factor affecting herring 0+ catches ($r^2 = 0.369$, $p < 0.01$, $n = 29$).

Discussion

Aneer (1985) was probably the first to consider the possibility that increased nutrient levels might pose a problem for the early stages of herring. In a review

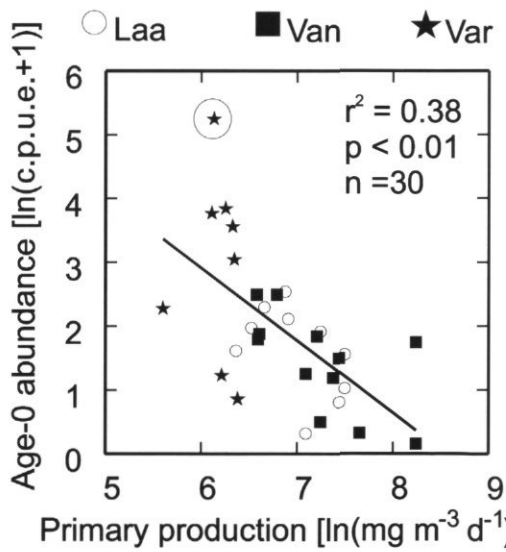


Figure 1. Relationship between reproductive success, as littoral catches of age-0 herring, and phytoplankton primary production capacity in three bays (Laa = Laajalahti, Van = Vanhankaupunginlahti, and Var = Vartiokylänlahti) off Helsinki, the Baltic Sea, 1982–1995. The regression outlier is encircled.

article on the effects of eutrophication on fish stocks in the Baltic, however, Hansson and Rudstam (1990) concluded that young herring were more numerous in the eutrophic Himmerfjärden than in a nearby reference area in the northern Baltic proper. This is well in line with the finding of Boehlert and Morgan (1985) that slight turbidity increases the feeding success of herring larvae.

The negative relationship we found between eutrophication and age-0 herring abundance does not necessarily conflict with the positive relationships reported by Hansson and Rudstam (1990) and Boehlert and Morgan (1985). It may be a question of eutrophication level. Boehlert and Morgan (1985) found that slight turbidity enhances feeding success. With an increase in turbidity, however, the success starts to diminish. We recorded the lowest age-0 herring catches when the phosphorus content exceeded 20 or even 50 mg PO_4-P dm^{-3}. The water phosphate level during the growth season in the immerfjärden area (http://www.ecology.su.se/dbhfj/h5start.htm) seems to correspond to the lower values of the Helsinki area. Thus, it could be that Hansson and Rudstam (1990) recorded the rising left limb, and we the declining right limb, of the bell-shaped eutrophication – reproductive success function.

References

Aneer, G. 1985. Some speculations about the Baltic herring (*Clupea harengus membras*) in connection with the eutrophication of the Baltic Sea. Canadian Journal of Fisheries and Aquatic Sciences, 42: 83–90.

Anttila, R. 1973. Effects of sewage on the fish fauna in the Helsinki area. Oikos, Supplement, 15: 226–229.

Boehlert, G. W., and Morgan, J. B. 1985. Turbidity enhances feeding abilities of larval Pacific herring, *Clupea harengus pallasi*. Hydrobiologia, 123: 161–170.

Hansson, S., and Rudstam, L. G. 1990. Eutrophication and the Baltic fish communities. Ambio, 19: 123–125.

Kääriä, J., Eklund, J., Hallikainen, S., Kääriä, R., Rajasilta, M., Ranta-aho, K., and Soikkeli, M. 1988. Effects of coastal eutrophication on the spawning grounds of the Baltic herring in the SW Archipelago of Finland. Kieler Meeresforsh Sonderh, 6: 348–356.

Lappalainen, A., and Pesonen, L. 2000. Changes in fish community structure after cession of waste water discharge in a coastal bay area west of Helsinki, northern Baltic Sea. Archive for Fisheries Marine Research, 48: 226–241.

Pellikka, K., and Viljamaa, H. 1998. Eläinplankton Helsingin merialueella 1969–1996. Helsingin kaupungin ympäristökeskuksen julkaisuja 12. (In Finnish.)

Urho, L. 2002. The importance of larvae and nursery areas for fish production. Ph.D. thesis, University of Helsinki, Finland. 118 pp + appendix.

Urho, L., and Hildén, M. 1990. Distribution patterns of Baltic herring larvae, *Clupea harengus* L., in the coastal waters off Helsinki, Finland. Journal of Plankton Research, 12: 41–54.

ICES Marine Science Symposia, 219: 433–436. 2003

Principal developments in the structure and dynamics of main fish stocks in the northeastern Baltic in the 1990s within the context of environmental changes

Tiit Raid, Ahto Järvik, Olavi Kaljuste, Ain Lankov, and Tenno Drevs

Raid, T., Järvik, A., Kaljuste, O., Lankov, A., and Drevs, T. 2003. Principal developments in the structure and dynamics of main fish stocks in the northeastern Baltic in the 1990s within the context of environmental changes. – ICES Marine Science Symposia, 219: 433–436.

The mean weight-at-age of herring and sprat has shown a decreasing trend, following a decrease in the marine component of the zooplankton during an extended period of absence of large inflows to the Baltic Sea. Simultaneously, the open-sea herring stocks have decreased in abundance, while some gulf stocks of herring and sprat stock have increased. The changes observed have had an effect not only on relationships within the ecosystem, but also on the assessment and exploitation of fish stocks in the Baltic Sea.

Keywords: cod, herring, mean weight, salinity, sprat, zooplankton.

T. Raid, A. Järvik, O. Kaljuste, A. Lankov and T. Drevs: Estonian Marine Institute, 18B Viljandi Rd., Tallinn 11216, Estonia [tel: + 372 628 1603; fax: +372 628 1563; e-mail: raid@sea.ee; ahto@ness.sea.ee; olavik@sea.ee; ainparnu@hotmail.com; haugas@ness.sea.ee]

Introduction

As a result of a prolonged period (1977–1993) without major inflows from the North Sea, the salinity of the northeastern Baltic Sea decreased significantly in the 1980s to early 1990s. At the same time the mean water temperature increased in the early 1990s because of the series of mild winters. The aim of the present study was to elucidate possible links between these environmental factors and copepod abundance, and the recent trends in fish stocks.

Material and methods

The available time-series of stock size and mean weight-at-age of herring and sprat in recent decades were scrutinized against temperature and salinity as well as abundance of zooplankton. The studies were focused on the northeastern Baltic, particularly on the Gulf of Finland and the Gulf of Riga. The following parameters were analysed:

- Surface temperature and salinity at 0–60 m in the Gulf of Finland,
- Abundance of copepods, *Limnocalanus grimldii* and *Pseudocalanus elongatus* in the Gulf of Finland and the Gulf of Riga,
- Mean annual consumption rate of herring in the Gulf of Finland.
- Mean weight-at-age of herring in the Gulf of Riga and in the Gulf of Finland.
- Mean weight-at-age of sprat in the Gulf of Finland.
- Abundance of herring in the Gulf of Riga.
- Abundance of sprat in the Baltic.

Results and discussion

The species composition of the catches of the major commercial fishes in the Baltic has changed significantly in the 1990s, while the total catch has remained steady or slightly increased. Cod and herring were dominant in the 1980s but both started to decline rapidly in the second half of the 1980s, while sprat catches increased. In the 1990s, sprat was the major contributor to total catch, while the share of cod fell to below 20% (ICES, 2001). The changes in

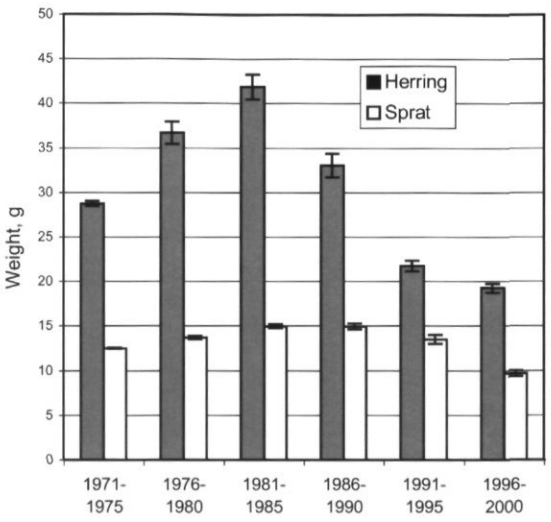


Figure 1. Mean weight of herring and sprat in age groups 3–6 in the Gulf of Finland in 1971–2000 by periods.

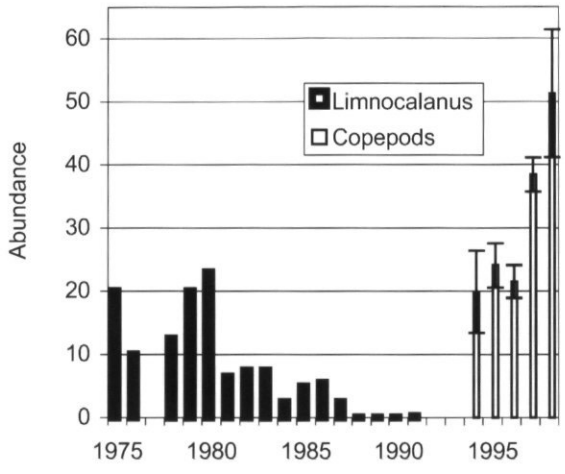


Figure 2. Mean abundance of *Limnocalanus grimaldii* from 1975–1992, (10 ind m^{-3}; Sidrevics *et al.*, 1993) and copepods in 1994–1998 (ind m^{-3}; Ojaveer *et al.*, 1999) in the Gulf of Riga.

abundance indices essentially followed the trends in catch composition with cod abundance decreasing by a factor of 5, while sprat increased six-fold by the 1990s. Herring stocks in the Baltic Proper have also decreased, while some local herring stocks in gulfs, e.g. the Gulf of Riga, have gained in abundance in the 1990s (ICES, 2001).

The changes in abundance have been accompanied by decreasing mean weight-at-age for herring since the mid-1980s and for sprat since the early 1990s (Figure 1). Since the second half of 1990s, the mean weight of herring has stabilized in the northeastern Baltic.

Decreases in mean weight-at-age of herring brought about decreases in its market value and also complicated the perception of biomass estimates.

Simultaneously to the changes mentioned above, the mean salinity of the euphotic layer decreased almost four times, both in the Baltic Proper and in gulfs of the northeastern Baltic by the early 1990s (HELCOM, 1997). In addition, the amount of heat accumulated in the sea increased significantly due to mild winters (Toompuu, 1998).

The results of observations show temporal coincidence of trends in salinity and the abundance of traditional food items of herring such as copepods *Limnocalanus grimaldii* and *Pseudocalanus elongatus* (Sidrevics *et al.*, 1993, Ojaveer *et al.*, 1998) (Figure 2), expressed as a strong positive correlation. At the same time, the abundance of those copepods is negatively correlated with temperature (Table 1). These facts suggest that environmental changes of the late 1980s and early 1990s had a negative effect on feeding conditions for herring. This is supported by the observed decrease of mean consumption rate of herring and the increase in the percentage of the total number of individuals without food in their stomachs (Figure 3, Table 1).

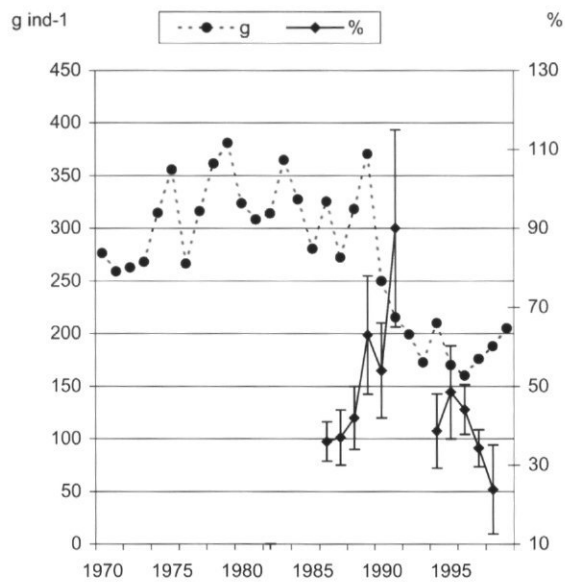


Figure 3. Estimated mean annual ration (g ind^{-1}) of herring in the Gulf of Finland and mean percent of herring with empty stomachs in the northeastern Baltic in 1980–1990s.

Table 1. Estimated correlations between different Baltic fish stock parameters, zooplankton, temperature and salinity in 1980s and 1990s. Significant correlations (not adjusted for autocorrelation) are in bold.

Category	Temperature.Fin	Salinity.Fin	Copepods.Fin	Pseudocalanus.Fin	Limnocalanus.Riga	Copepods.Riga	Her.Consumption	Weight.Her.Fin	Weight.Her.Riga	Weight.Sprat.Fin	Numbers Her.Riga	Numbers Sprat.22–32
Temperature.Fin	1.000											
Salinity.Fin	–0.336	1.000										
Copepods.Fin	–0.296	0.412	1.000									
Pseudocalanus.Fin	**–0.613**	**0.803**	0.574	1.000								
Limnocalanus.Riga	–0.485	**0.756**	**0.727**	**0.777**	1.000							
Copepods.Riga	0.050	0.090	**0.774**	0.095	0.519	1.000						
Her.Consumption (g/ind)	0.184	0.472	0.379	0.353	0.489	–0.184	1.000					
Weight.Her.Fin	–0.124	**0.606**	**0.508**	**0.649**	0.481	–0.290	**0.866**	1.000				
Weight.Her.Riga	–0.118	**0.588**	0.321	**0.639**	0.435	–0.294	**0.787**	**0.908**	1.000			
Weight.Sprat.Fin	–0.009	0.034	0.167	–0.347	–0.368	–0.484	0.690	**0.733**	0.616	1.000		
Numbers.Her.Riga	–0.009	–0.621	–0.429	–0.677	–0.588	0.177	–0.934	–0.945	–0.893	–0.709	1.000	
Numbers.Sprat.22–32	–0.081	–0.416	–0.207	–0.720	–0.428	0.361	–0.802	–0.809	–0.747	–0.764	**0.866**	1.000

Her- Herring
Fin- Gulf of Finland
Riga- Gulf of Riga
22–32- Subdivisions 22–32

The increased abundance of copepods, after a slight increase in salinity resulting from the moderate inflow of 1993, seems to have had a positive effect on herring feeding in the second half of the 1990s, despite low abundances of both *Limnocalanus* and *Pseudocalanus*. Grazing on copepods has probably been the main reason for the increased consumption rate and the decrease in the number of starving herring after 1995, as well as for the stabilized mean weight (Figures 2, 3). Also, the list of herring prey has been supplemented by new items, such as the locally abundant non-indigenous cladoceran *Cercopagis pengoi,* which appeared in the herring diet in the late 1990s (Ojaveer, *et al.*, 1999).

The mean weight-at-age of sprat seems to be driven by the same factors as in herring, i.e. copepod abundance (Table 1). However, a high negative correlation between the mean weight-at-age and stock size of both herring and sprat implies that the latter cannot be ruled out as a factor influencing the mean weight (Table 1).

The recent changes in the prey of herring, which overlaps that of sprat, has probably increased food competition between these pelagic species, particularly during the present high abundance of sprat.

References

HELCOM, 1997. Third periodic Assessment of the State of the Marine Environment of the Baltic Sea, 1989–1993. Background document, Baltic Sea Environment, Proceedings 64, HELCOM, Helsinki. 252 pp.

ICES. 2001. Report of the Baltic Fisheries Assessment Working Group. ICES CM 2001/ACFM: 18. 546 pp.

Ojaveer, E., Lumberg, A., and Ojaveer, H. 1998. Highlights of zooplankton dynamics in Estonian waters (Baltic Sea). ICES Journal of Marine Science, 55: 748–755.

Ojaveer, H., Lankov, A., Eero, M., Kotta, J., Kotta, I., and Lumberg, A. 1999. Changes in ecosystem of the Gulf of Riga from the 1970s to the 1990s. ICES Journal of Marine Science, 56 Supplement: 33–40.

Sidrevics, L., Line, R., Berzinsh, V., and Kornilovs, G. 1993. Long-term changes in zooplankton abundance in the Gulf of Riga. ICES CM 1993/L: 15. 14 pp.

Toompuu, A. 1998. Estimating the climatic variability of total amounts of heat and salt in the Baltic Sea. *In* Climate Change Studies in the Baltic Sea, pp. 65–84. Ed. by T. Kallaste and P. Kuldna. SEI, Tallinn. 200 pp.

ICES Marine Science Symposia, 219: 437–439. 2003

Baltic Sea benthos in the 1990s: a comparison of the distribution of oxygen deficiency and macrozoobenthos communities

Ari O. Laine and Susanne Unverzagt

Laine, A. O., and Unverzagt, S. 2003. Baltic Sea benthos in the 1990s: a comparison of the distribution of oxygen deficiency and macrozoobenthos communities. – ICES Marine Science Symposia, 219: 437–439.

Semi-permanent oxygen deficiency characterizes large areas of the Central Baltic Sea. In this study, changes in the depth and area of hypoxia and anoxia and consequent variability in macrozoobenthos are described for the 1990s. The early 1990s are characterized by the end of a long stagnation period with relatively restricted but severe anoxia in the very deep areas. The inflow events in 1993–1994 caused a temporary improvement but led quickly to stronger stratification and consequent expansion of the area suffering oxygen depletion. Consequently, the state of the macrofauna communities had deteriorated by the end of the 1990s compared with the beginning of the decade. Different communities (abundance, species composition) were found between areas with different oxygen states, indicating the ecological importance of oxygen conditions in the deep Baltic.

Keywords: anoxia, Baltic Sea, hypoxia, macrozoobenthos, oxygen deficiency.

Ari O. Laine: Finnish Institute of Marine Research, PO Box 33, FIN-00931 Helsinki, Finland [e-mail: ari.laine@fimr.fi; Susanne Unverzagt: University of Greifswald, Geographical Institute, Jahnstr. 16, D-17489 Greifswald, Germany [e-mail: unverzgt@uni-greifswald.de]

Introduction

Owing to the permanent salinity stratification and restricted water exchange, deep-water oxygen deficiency prevails in large areas of the Baltic Sea; an exception is the Gulf of Bothnia (e.g. Fonselius, 1981; Matthäus, 1995). This strongly affects the distribution of benthic animal communities. The hypoxic areas (dissolved oxygen concentration < 2 ml l^{-1}) occasionally cover up to 77 000 km^2, corresponding to 36% of the Baltic Proper and western Gulf of Finland area. Toxic hydrogen sulphide is formed in areas of anoxia (no oxygen), covering up to 14 000 km^2 of bottom (Unverzagt, 2001). However, the extent and severity of oxygen depletion varies strongly between years, depending on the climate-related hydrography (Hänninen *et al.*, 1999; Zorita and Laine, 2000). Along the depth-related oxygen gradient, different stages of macrozoobenthic communities are found and long-term deterioration or recolonization can be observed depending on the change of oxygen conditions (e.g. Rumohr *et al.*, 1996; Laine *et al.*, 1997). The 1990s were characterized by major changes in the hydrography, due to the end of a long stagnation period caused by high salinity, deep-water inflows in 1993–1994 (see discussion). In this study we describe the extent and succession of areas suffering hypoxia and anoxia on the basis of long-term oxygen data since 1969 and their effect on the macrofauna from data collected during the 1990s.

Material and methods

Data on dissolved oxygen and hydrogen sulphide concentrations originate from monitoring programmes carried out by Baltic research institutes (see Unverzagt, 2001). The depths of the upper limits of both the hypoxic area and the anoxic area with hydrogen sulphide formation were calculated. These we call the border depths. First, a logistic function was found to describe the changes in the oxygen concentrations with increasing depth at all measurement points. The parameters of this function and the location of the two border depths were determined by a linear-weighted regression at each sampling station. To estimate the location of the border depths between the sampled points, geostatistical methods (Kriging and Indicator Kriging; Journal, 1989) were used.

Thus, information from all points was involved in the estimation of depths in which the border surfaces are situated at non-easured points. For a detailed description of the methodology, see Unverzagt (2001).

The macrozoobenthos material consists of long-term monitoring data collected by the Finnish Institute of Marine Research (see Laine *et al.*, 1997). The samples were taken annually, in May–June, with a Van Veen grab (ca. 3 replicate samples per sampling occasion, 1-mm sieve) at fixed stations, representing soft bottom habitats deeper than 50 m. The zoobenthos data were correlated to oxygen data collected during the corresponding season, April–June.

Results

The depth of the 2 ml l^{-1} oxygen concentration shows an increasing long-term trend, reversing after a maximum of 115 m in 1993–1994 (Figure 1). The upper limit of the anoxic layer is more variable but shows a corresponding change at the same time. In 1994–1996, anoxia was almost absent, followed in later years by a decreasing border depth. In 1999, anoxia reached shallower areas with a mean depth of only 112 m.

The area (Figure 2) of oxygen deficiency shows a similar pattern, a long-term decline in the extent of the hypoxia (resulting in a minimum of 14 900 km^2 in 1993) but relatively large areas affected by anoxia and hydrogen sulphide in the early 1990s. Since 1994–1995 an expansion of the hypoxic area and volume has taken place again.

In Figure 3 the extent of the areas suffering hypoxia and anoxia and the distribution of macrofauna (total abundance) is shown for selected years, describing different hydrographical phases. The years 1991 and 1993 represent the conditions at the end of the long stagnation period, when hypoxia and anoxia were restricted to the deep basins in the central and northern parts. As a consequence of the effective inflows of the North Sea waters, anoxia and hydrogen sulphide disappeared in 1994. Since 1995 the conditions started to deteriorate, and hydrogen sulphide was formed again. In 1999 hypoxia was very widespread, covering all of the deeper basins.

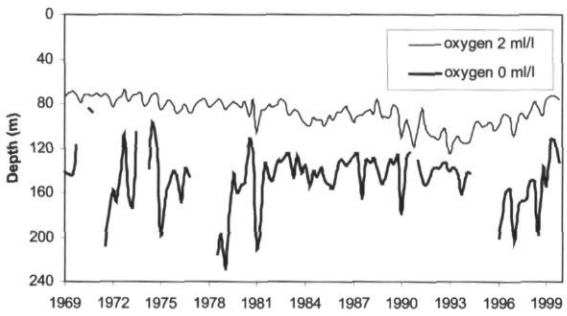


Figure 1. Changes in the depth (upper limit of occurrence) of hypoxia (dissolved oxygen concentration 2 ml l^{-1}) and anoxia (no oxygen, hydrogen sulphide present) in 1969–1999.

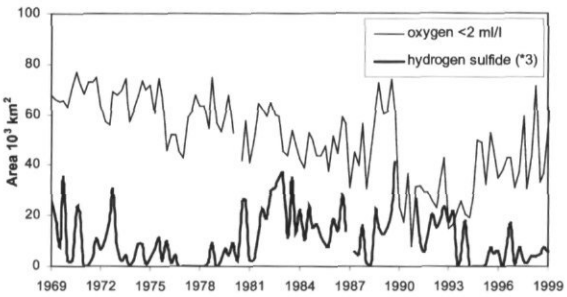


Figure 2. Changes in the area of hypoxia and anoxia in 1969–1999. Note that the area of anoxia has been multiplied by three to fit the scales.

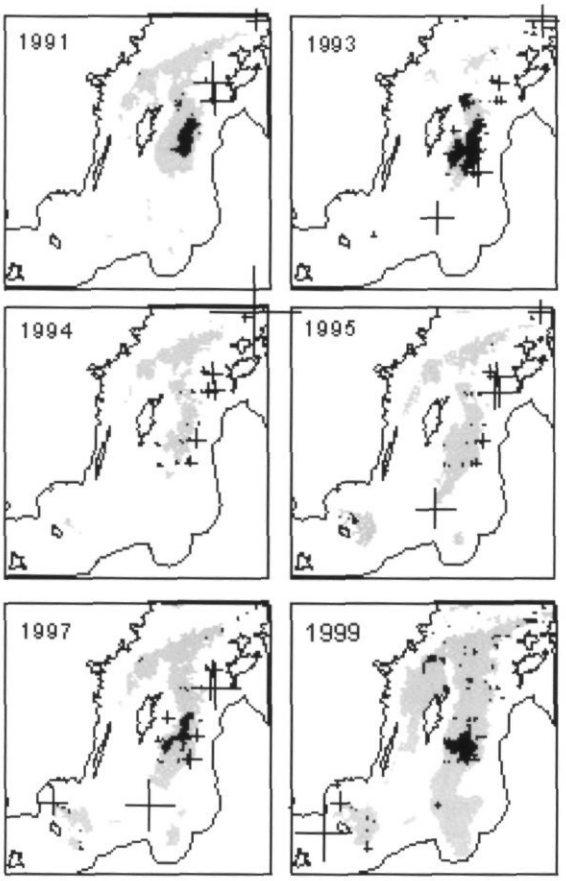


Figure 3. The maps give examples of the distribution of hypoxia (dissolved oxygen concentration < 2 ml l^{-1}, grey areas) and anoxia (no oxygen, hydrogen sulphide present, black areas) in different years of the 1990s. The scaled cross hairs indicate the variability of macrozoobenthos (symbol size related to total abundance) at the monitoring sites.

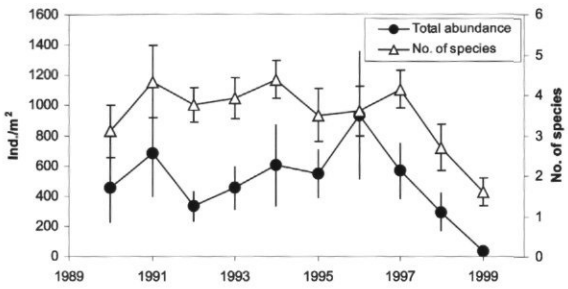


Figure 4. Changes of macrozoobenthos total abundance and species number (mean ± S.E.) in the 70–100 m depth zone in the central and northern parts of the study area in 1990–1999.

The oxygen conditions are clearly reflected in the distribution of macrofauna. A significant difference ($p < 0.001$, Kruskal-Wallis ANOVA) between areas of anoxia, hypoxia and higher oxygen concentrations was found for total abundance (on average 7.2, 67.5, 480.6 ind. m^{-2}, respectively) and number of species (0.2, 1.0, 3.4, respectively). In central and northern parts of the study area, 4 of the 12 recorded macrofauna species clearly dominated the community (amphipod *Pontoporeia femorata* ≫ bivalve *Macoma baltica* > amphipod *Monoporeia affinis* > polychaete *Harmothoe sarsi*) when oxygen concentration was > 2 ml l^{-1}. In areas of hypoxia, three of nine species were dominant (*P. femorata* ≫ *H. sarsi* > *M. baltica*) and in anoxic areas only *H. sarsi* was recorded and in low numbers. The total abundance and species number in the 70–100 m depth zone showed no clear change at the beginning of the 1990s but since 1996–1997 a decline in both variables is obvious (Figure 4), due to the deterioration in oxygen conditions.

Discussion

In the deep basins of the Baltic Sea, the 1990s were first characterized by a small hypoxic area but relatively large anoxic area as a consequence of the preceding long stagnation period from 1977 to 1993. This was accompanied by a decline in salinity, a lowering of the halocline and an accumulation of hydrogen sulphide (Matthäus, 1995; Samuelsson, 1996). Deep-water inflows in 1993–1994 (Matthäus and Lass, 1995) caused only a temporary improvement in the oxygen conditions of the deep areas but also led to a strengthening of the stratification due to the deep-water salinity increase. This soon resulted in an expansion of the area of the bottom with oxygen deficiency and a decline in the macrobenthic communities. Oxygen deficiency is the most important single factor structuring the macrobenthic communities in the deep subhalocline areas and extensive changes in hydrography determine the state of the macrozoobenthos in large areas of the central Baltic basins (Laine *et al.*, 1997).

References

Fonselius, S. H. 1981. Oxygen and hydrogen sulphide conditions in the Baltic Sea. Marine Pollution Bulletin, 12: 187–194.

Hänninen, J., Vuorinen, I., and Hjelt, P. 1999. Climatic factors in the Atlantic control the oceanographic and ecological changes in the Baltic Sea. Limnology and Oceanography, 45: 703–710.

Journal, A. G. 1989. Fundamentals of geostatistics in five lessons. Short Course in Geology 8. 40 pp.

Laine, A. O., Sandler, H., Andersin, A.-B., and Stigzelius, J. 1997. Long-term changes of macrozoobenthos in the Eastern Gotland Basin and the Gulf of Finland (Baltic Sea) in relation to the hydrographical regime. Journal of Sea Research, 38: 135–159.

Matthäus, W. 1995. Natural variability and human impacts reflected in long-term changes in the Baltic deep water conditions: a brief review. Deutsche Hydrographische Zeitschrift, 47: 47–65.

Matthäus, W., and Lass, H. U. 1995. The recent inflow into the Baltic Sea. Journal of Physical Oceanography, 25: 280–286.

Rumohr, H., Bonsdorff, E., and Pearson, T. 1996. Zoobenthic succession in Baltic sedimentary habitats. Archive for Fisheries and Marine Research, 44: 19–214.

Samuelsson, M. 1996. Interannual salinity variations in the Baltic Sea during the period 1954–1990. Continental Shelf Research, 16: 1463–1477.

Unverzagt, S. 2001. Räumliche und zeitliche Veränderungen der Gebiete mit Sauerstoffmangel und Schwefelwasserstoff im Tiefenwasser der Ostsee. Greifswalder Geographische Arbeiten 19. 123 pp.

Zorita, E., and Laine, A. 2000. Dependence of salinity and oxygen concentration in the Baltic Sea on the large-scale atmospheric circulation. Climate Research, 14: 25–41.

ICES Marine Science Symposia, 219: 440–442. 2003

Impact of the environmental changes in the northeastern Baltic on the Estonian fishery in the 1990s

Ahto Järvik and Tiit Raid

Järvik, A., and Raid, T. 2003. Impact of the environmental changes in the northeastern Baltic on the Estonian fishery in the 1990s. – ICES Marine Science Symposia, 219: 440–442.

The duration of ice-coverage is one of the key environmental factors directly affecting the northeastern Baltic fisheries. The 1990s can be characterized as years of relatively warm winters and reduced ice-coverage. As a result, the open sea trawl fishery became possible year round, except in the most eastern part of the Gulf of Finland and close to the coast. The increased possibilities for the winter trawl fishery encouraged Estonian fishermen to employ bigger open sea trawlers. At the same time, substantial declines in demersal fish stocks occurred, in part due to environmental processes. This included reduced inflow of saline water from the North Sea that resulted in reduced salinity and oxygen levels in the northeastern Baltic and contributed to the collapse of bottom trawling for cod and flounder. These resulted in significant changes in the exploitation pattern on the main fish stocks of herring, sprat, cod, and flounder with important socio-economical implications for Estonia.

Keywords: fleet changes, ice cover, northeastern Baltic, salinity, trawl fishery.

Ahto Järvik and Tiit Raid: Estonian Marine Institute, 18B Viljandi Rd. Tallinn 11216, Estonia [tel: +372 6529714; fax: +372 6281563; e-mail: ahto@ness.sea.ee and raid@sea.ee]. Correspondence to Ahto Järvik.

Introduction

The temporal and spatial distribution of the Estonian offshore fishery in winter is directly and strongly dependent on sea-ice coverage in the northeastern Baltic. Besides making fishing impossible in those areas covered by ice, even inside adjacent ice-free areas, small fishing vessels are not allowed for safety reasons. Another important environmental factor that indirectly impacts the Baltic fishery through effects on the distribution and abundance of fish is salinity, the variability of which is driven by the inflow of saline water from the North Sea and freshwater run-off. The main aim of the present study is to determine the impacts of sea ice and salinity on the Estonian offshore fishery in the Baltic, and discuss its socio-economical consequences.

Environmental changes

On the basis of maximum extent of ice cover, the winters in the Baltic Sea area are classified as: extremely mild, ice cover 52 000–81 000 km^2; mild, 81 001–139 000 km^2; average, 139 001–279 000 km^2; severe, 279 001–383 000 km^2; and extremely severe, 383 001–420 000 km^2 (Seinä and Palosuo, 1995). In the 1990s, the winters of 1994 and 1996 can be classified as average, with the Gulf of Finland, the Gulf of Riga and the northeastern Baltic Proper mostly covered by ice during January to March. All other winters of the 1990s can be characterized as mild or extremely mild with full ice cover only in the eastern part of the Gulf of Finland for 1–3 months (Trinkuinaite, 2000).

During the prolonged period of absence of deep inflows from the North Sea in 1977–1993, the salinity and oxygen conditions in the northeastern Baltic declined substantially (HELCOM, 2001). A moderate inflow in 1993 did not cause a substantial increase of salinity in the northeastern Baltic and, furthermore, large volumes of freshwater run-off observed in 1998 had additional negative effects on salinity conditions (HELCOM, 2001). While oxygen levels near bottom initially increased after the inflow of 1993, they quickly declined and continued to decrease through the remainder of the 1990s (HELCOM, 2001).

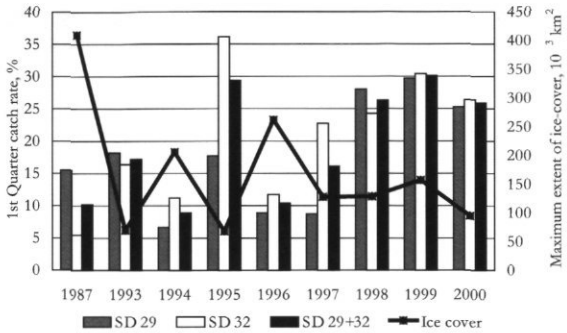


Figure 1. Share of first quarter in annual catches of herring in 1987 and 1993–2000 in Subdivisions 29 and 32 and maximum extent of the ice cover of the Baltic Sea (Seinä *et al.*, 2001; Seinä & Palosuo, 1996).

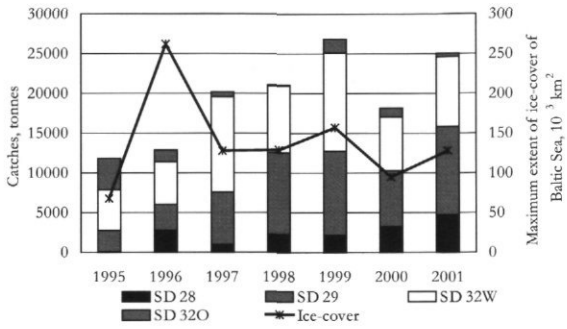


Figure 2. Total catch of herring and sprat in Estonian pelagic trawl fishery in January–February 1995–2001 and maximum extent of ice cover of the Baltic Sea (Seinä *et al.*, 2001, Seinä & Palosuo, 1996, Vainio, pers. comm.).

Effects on fish and fish catches

The virtual absence of permanent ice cover in most of the northeastern Baltic in the 1990s resulted in the presence of a winter trawl fishery. This is opposite to the 1980s, when heavy ice conditions severely restricted winter fishing and when the percentage of the annual catch taken during the first quarter of the year was very low (Figure 1). Not surprisingly, a negative correlation ($R^2 = 0.66$) was found between the percentage of the annual catch of herring in Subdivisions 29 and 32 taken during the first quarter of the year and the maximum extent of ice cover. For Subdivision 32 this negative correlation proved to be even higher ($R^2 = 0.77$).

The low oxygen and salinity conditions mentioned above resulted in a decrease in cod abundance. At the same time, however, there was a gradual increase in the abundance of flounder (Drevs, 1999). The stocks of pelagic species, such as herring and sprat, fluctuated but did not undergo drastic changes in the northeastern Baltic (Anon., 2000).

Consequences for the fishery

The bottom trawl fishery for cod, and hence also for flounder, which is primarily a bycatch of the cod fishery, decreased substantially in the northeastern Baltic in the 1990s, and even collapsed in the Gulf of Finland. This situation occurred at a time of decreasing opportunities for the Estonian fishing fleet in the southern areas of the eastern Baltic Sea. Under these conditions, the Estonian trawl fleet switched to catching the national quotas for herring and sprat.

The increased possibility for trawl fishing virtually all year around due to eased ice conditions in winter during the 1990s (Figure 2) resulted in the requirement for more powerful trawlers. They began to fish with larger gear and were equipped with more efficient facilities, thus allowing them to operate in bad weather and to extend the length of their fishing trips.

Before the use of these larger boats, the previously existing trawl fleet was already fully capable of taking the Estonian quotas for herring and sprat.

Table 1. Information on the Estonian Baltic Sea fishing fleet in the 1990s: the number of fishing vessels including those that are idle, the annual Gross Registered Tonnage, the total power of the engines in kilowatts and the average engine power per vessel in kilowatts.

Year	No. of fishing vessels (including idle vessels)	Annual GRT	Total power of engines, KW	Average engine power per vessel, KW
1993	184	13,096	29,025	157.7
1994	208	13,978	31,463	151.3
1995	219	14,015	32,417	148.1
1996	218	13,773	32,895	150.9
1997	225	15,450	36,937	164.2
1998	216	15,414	38,063	176.2
1999	201	13,896	35,005	174.2
2000	189	13,059	33,283	176.1

With the larger boats, the actual overcapacity of the Estonian trawl fleet was estimated to be more than 50% (Raid and Järvik, 2001). Therefore, the medium-size fleet, earlier based in the eastern part of the Estonian coast adjacent to the Gulf of Finland, was partly relocated to the areas close to the Baltic Proper and others were forced to sit idle. The total number of Estonian trawlers working to full capacity noticeably diminished during the latter years of the 1990s.

The decline in demersal fish abundance and the increase in the winter fishery resulted in substantial changes in the structure of the Estonian fishing fleet, and ultimately led to a remarkable reduction in the number of offshore fishermen in Estonia (Table 1). In some coastal areas, particularly in Eastern Estonia, the decline in the number of fishermen and the reduced catches have caused serious social problems at the regional level, since the fishery has been one of the main fields of employment in this area.

Acknowledgements

We thank our colleague at the Estonian Marine Institute, Dr. Tarmo Kõuts, for consultations on ice conditions and the anonymous reviewers of the manuscript for their helpful comments.

References

Anon. 2000. Report of the Baltic Fisheries Assessment Working Group. ICES, 10–19 April. 512 pp.

Drevs, T. 1999. Population dynamics of flounder *(Platichthys flesus)* in Estonian waters. Proceedings of the Estonia Academy of Sciences (Biology-Ecology), 48: 310–320.

HELCOM. 2001. Environment of the Baltic Sea Area 1994–1998. 28 pp.

Raid, T., and Järvik, A. 2001. Baltic herring fisheries management in Estonia: a biological, technical, and socio-economic approach. *In* Herring, Expectations for a New Millennium. Ed. by F. Funk, J. Blackburn, D. Hay, A. J. Paul, R. Stephenson, R. Toresen, and D. Witherell. Alaska Sea Grant AK-SG-01-04, Fairbanks, pp. 703–720.

Seinä, A., Grönvall, H., Kalliosaari, S., and Vainio, J. 2001. Ice seasons 1996–2000 in Finnish sea areas. MERI – Report Series of the Finnish Institute of Marine Research, 43: 3–98.

Seinä, A., and Palosuo, E. 1996. The classification of the maximum annual extent of ice cover in the Baltic Sea 1720–1995. MERI – Report Series of the Finnish Institute of Marine Research, 27: 79–91.

Trinkuinaite, R. 2000. Climate Change. *In* 2nd Baltic State of the Environment Report, pp. 29–38. Riga, Latvia.

ICES Marine Science Symposia, 219: 443–446. 2003

Hydrographic conditions in the Norwegian Sea in the 1990s and their influence on plankton status and Atlanto-Scandian herring migrations

Evgeniy Sentyabov, Vladimir Borovkov, Nina Plekhanova, and Alexander Krysov

Sentyabov E, Borovkov V, Plekhanova N, Krysov A. 2003. Hydrographic conditions in the Norwegian Sea in the 1990s and their influence on plankton status and Atlanto-Scandian herring migrations. – ICES Marine Science Symposia, 219: 443–446.

On the basis of data from annual summertime oceanographic surveys, conducted by PINRO in the Norwegian Sea, considerable variations in the maritime climate of this region during the 1990s have been identified. The early and later parts of the 1990s were characterized by significant increases of water temperature of the Norwegian Current comparable to that in the early 1960s and mid-1970s. In the mid-1990s, transgression of cold water from the East Icelandic Current into the central part of the Norwegian Sea was accompanied by an abnormal decline of sea water temperature similar in magnitude to that observed at the end of the 1960s and early 1980s. Alternation of variation of water temperature anomalies in the Norwegian Sea during the 1990s took place against a considerable increase of water temperature in the Northeast Atlantic. The observed variations of climate influenced substantially the status of zooplankton (*Calanus finmarchicus*) and migration pattern of Atlanto-Scandian herring.

Keywords: Atlanto-Scandian herring, *Calanus finmarchicus*, distribution, hydrographic conditions, Norwegian Sea, zooplankton.

E. Sentyabov, V. Borovkov, N. Plekhanova, and A. Krysov: Polar Research Institute of Marine Fisheries and Oceanography (PINRO), 6, Knipovich Street, 183763, Murmansk, Russia [tel: +7 81 5247 3424; fax:+47 7891 0518; e-mail: sentyab@pinro.murmansk.ru borisber@pinro.murmansk.ru].

Introduction

Against a background of long-term change in the thermal condition of the Norwegian Sea during the second half of the 20th century, the 1990s were characterized by significant negative and positive anomalies of water temperature. The peculiarity of the period described consists of the alternation of considerable warming and cooling periods over relatively short time intervals.

The goal of this article is to reveal possible reasons for these abrupt changes in the Norwegian Sea heat content in the 1990s, and to show the influence these variations had on the development and distribution of the arcto-boreal copepod *Calanus finmarchicus (Gunnerus)*, on the zooplankton biomass as a whole during the summer period, as well as on the change of Atlanto-Scandian herring migrations.

Material and methods

Hydrographic and plankton observations were obtained during summer cruises conducted by PINRO to the Norwegian Sea in 1990–1999 (Figure 1). In addition, the article deals with the results of previous PINRO hydrographic investigations and uses data from the ICES Northern Pelagic and Blue Whiting Fisheries Working Group (Anon., 1995, 1999). Mean values of water temperature were calculated and compared with the 1951–1990 average in the upper 200 m layer in standard sections crossing the Norwegian and East Icelandic Currents and in mixed waters at the boundaries (Alexeev and Istoshin, 1956, 1960).

The status of *C. finmarchicus* was determined in the upper 50 m layer by its stage composition during the summer period of 1990–1999, by its abundance distribution (both total and at every age stage), as

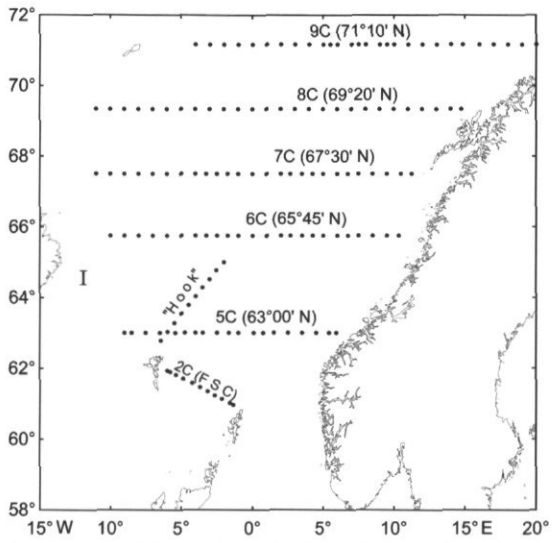


Figure 1. Position of standard section stations in the Norwegian Sea.

well as by the variation of zooplankton biomass in 1980–1999. The dynamics of plankton biomass was traced both in the Atlantic Water and in the mixed waters of the Norwegian Sea (averaged in sections along 65°45′N and 67°30′N).

Results and discussion

The special feature of hydrographic conditions in the Norwegian Sea in the 1990s was the abrupt transition within the Atlantic waters from warming in 1990–1991 to cooling in 1995–1997, followed by the significant increase in temperature in 1998–1999 (Figure 2A). 1990–1991 and 1998–1999 were characterized as warm years; 1993, 1995, and 1997 as cold years; 1992, 1994, and 1996 as intermediate years.

In the early 1990s, warming was noticed throughout the area of the Norwegian Sea, suggesting that warm water inflow from the Northeast Atlantic was

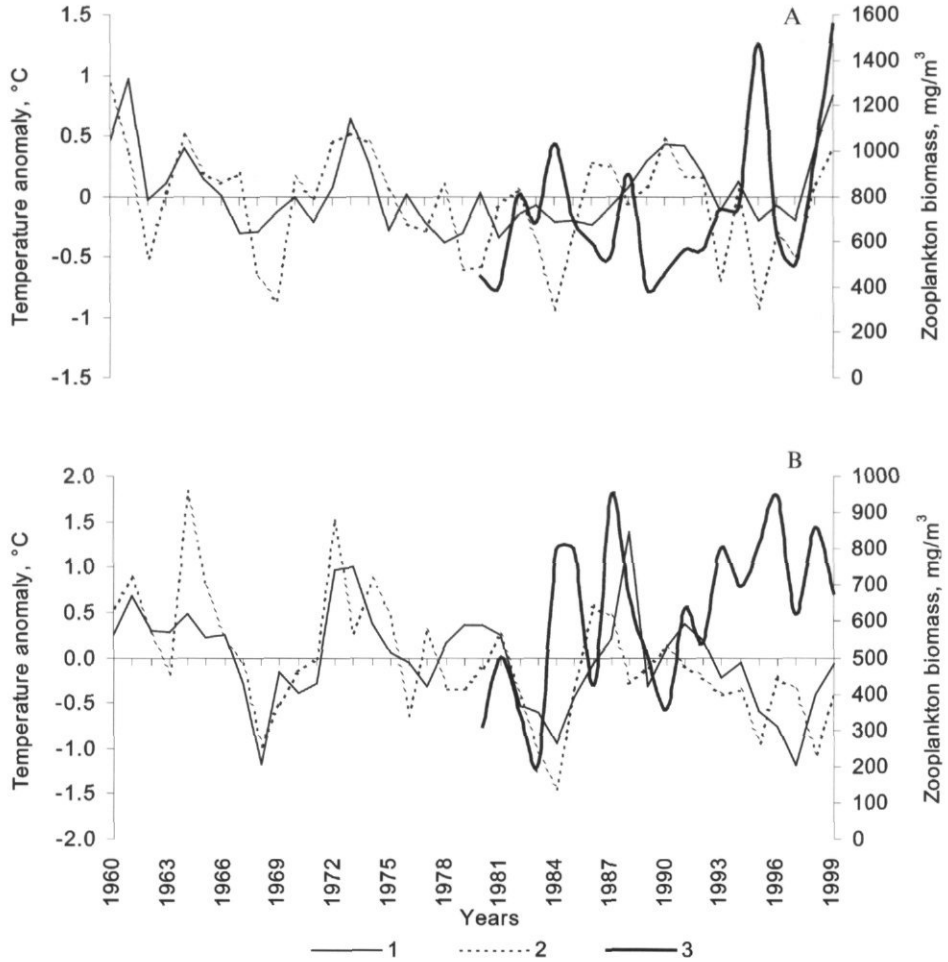


Figure 2. Time-series of temperature anomalies of Norwegian Current water (A) and mixed waters (B), averaged in the depth 0–200 m, obtained from the sections along 67°30′N (1) and 65°45′N (2) in the Norwegian Sea in June 1960–1999 and zooplankton biomass in 0–50 layer in the central part of the Norwegian Sea in June 1980–1999 (3).

strengthened by southwesterly winds. In the late 1990s, warming was only registered in the waters of the Norwegian Current. This regional warming may have been caused by the propagation of low pressure systems over the west and central areas of the Norwegian Sea during 1998 and the first half of 1999, resulting in a prevalence of more southerly winds against a background of continued warming in the Northeast Atlantic as a whole.

Cooling in the first and second halves of the 1990s resulted from strengthening in the East-Icelandic Current and the increase in the volume of Subarctic waters in the central part of the Norwegian Sea (mixed waters, Figure 2B). However, in the first half of the 1990s, cooling was caused by the weakening of the westerly air mass transport and the strengthening of the northerly one, and in the second half by the expansion of the Icelandic depression to the south, the recurrent increase of southeasterly winds, and the decrease in the southerly transport of the resident air masses.

These changes had a considerable influence on the food plankton (*C. finmarchicus*) and the character of Atlanto-Scandian herring migrations. During the periods of warming in 1990 and 1998–1999, the mass spawning of *C. finmarchicus* took place earlier in the year compared to the cold years of 1993, 1995, and 1997. This resulted in significant concentrations of juveniles in the central Norwegian Sea in June, especially during 1998–1999. Additionally, the enhancement of the polar frontal zone in the southern and central Norwegian Sea during 1998–1999 resulted in the slow growth of juveniles and low abundance of *C. finmarchicus*, within the elder age groups from the summer year class, in the central areas, and more limited areas of dense concentrations of *C. finmarchicus* as compared to previous years (Figure 3). In the cold years of 1993, 1995, and 1997 in the southern and central Norwegian Sea, late spawning of *C. finmarchicus* was observed, resulting in pre-spawning and spawning individuals being most prevalent in June. This resulted in a high plankton biomass over a

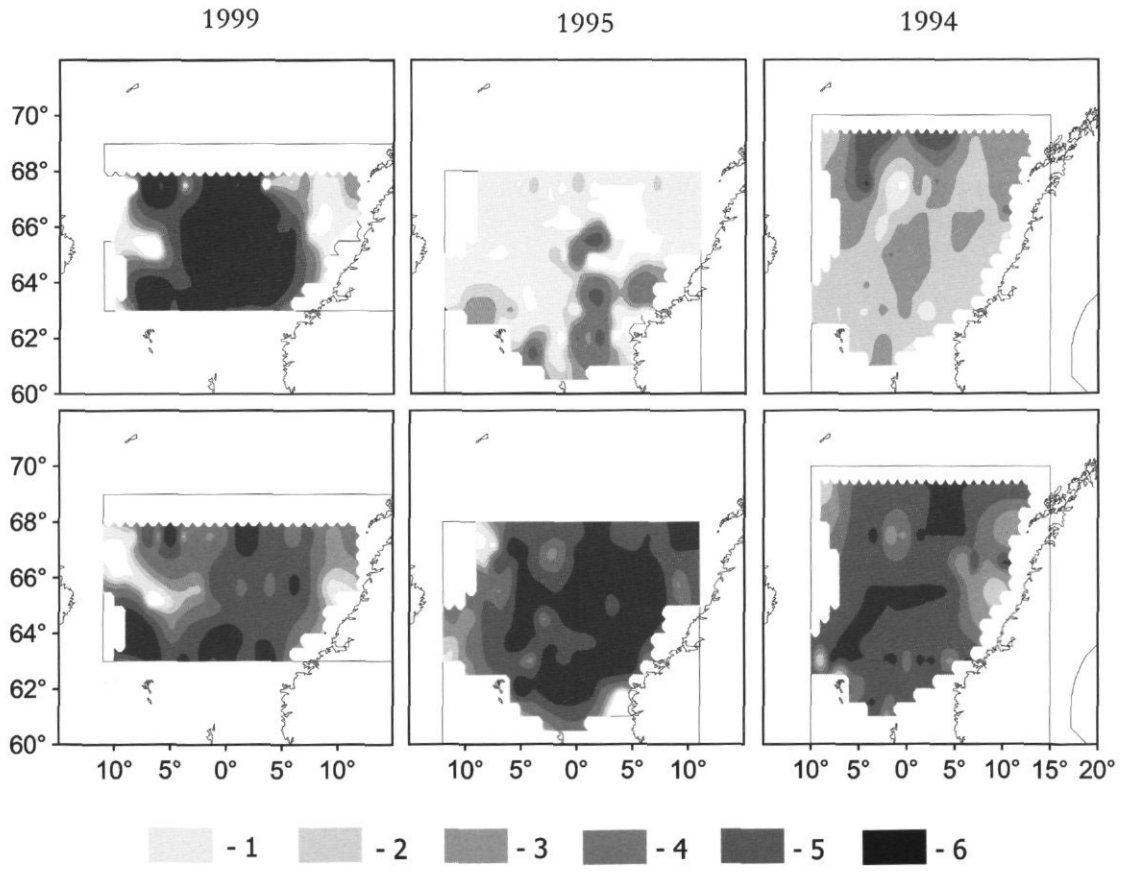


Figure 3. Abundance distribution of *Calanus finmarchicus* (top – copepodites of young CI-CIII; bottom – old ages CIV-CV) in the upper 50 m layer in June of warm 1999, cold 1995, and intermediate 1994. 1: 1–50, 2: 51–100, 3: 101–200, 4: 201–500, 5: 501–1000, 6: more 1000 individuals/m^3.

wide area of the Norwegian Sea. In June, *C. finmarchicus* juveniles were recorded only in small regions of the Norwegian Sea. Dense aggregations of *C. finmarchicus* (CIV-CV) from summer year classes occurred in the south and in the east. In the central area, the aggregations were represented by individuals of over-wintering *C. finmarchicus* (CIV-CV). In 1992, 1994, and 1996, which were intermediate in terms of the hydrographic conditions, with weakly defined warm temperatures in the east and cold temperatures in the west, the shift of dense concentrations of all ages of *C. finmarchicus* towards the central Norwegian Sea was observed.

While comparing variations of zooplankton biomass and temperature anomalies in the Atlantic and mixed waters of the central Norwegian Sea during1980–1999, we note a negative relationship between zooplankton biomass and water temperature (Figure 2). A positive relationship is only noticed during abrupt changes of temperature (e.g. in 1980–1981 and 1998–1999). Zooplankton biomass is likely to be conditioned by many abiotic, as well as biotic factors.

Lowered heat content in the west and central areas, noticed since the middle of the 1990s, favoured the pronounced eastern orientation of herring summer migrations and, possibly, led to the shift of the herring over-wintering areas compared to the 1960s, when they were mainly located east of Iceland and in Norwegian fjords.

Thus, the most significant feature of hydrographic conditions in the Norwegian Sea during the 1990s was the abrupt transition within the Atlantic waters from warming during 1990–1991 to cooling during 1995–1997, followed by significant warming again during 1998–1999. In the Atlantic and mixed waters of the central Norwegian Sea during the 1990s, except for 1998–1999, we noted a negative relationship between zooplankton biomass and water temperature. Considerable reduction of heat content in the south and central Norwegian Sea areas during the decade may have conditioned the more easterly distribution of herring feeding and over-wintering migrations compared to the 1960s.

References

Alexeev, A. P., and Istoshin, B. V. 1956. Scheme of the constant currents of the Norwegian and Greenland Seas. Trudy PINRO, No. 9: 62–68. (In Russian.)

Alexeev, A. P., and Istoshin, B. V. 1960. Some results of oceanographic investigations in the Norwegian and Greenland Seas. *In* The Soviet Fishery Investigations in the Seas of the European North, No. 8: 23–37. (In Russian.)

Anon. 1995. Report on surveys of the distribution and migrations of the Norwegian spring spawning herring and the environment of the Norwegian Sea and adjacent waters in spring and summer of 1995. Reykjavik, 11–13 September 1995. MRI, Reykjavik, Iceland.

Anon. 1999. Report on surveys of the distribution, abundance and migrations of the Norwegian spring-spawning herring, other pelagic fish and the environment of the Norwegian Sea and adjacent waters in late winter, spring and summer of 1999. ICES CM 1999/D: 3. 16 pp.

ICES Marine Science Symposia, 219: 447–449. 2003

Status of food zooplankton in the feeding period of capelin from the central latitudinal zone of the Barents Sea in cold and warm years

E. L. Orlova, V. D. Boitsov, M. Yu. Antsiferov, V. N. Nesterova, and N. G. Ushakov

Orlova, E. L., Boitsov, V. D., Antsiferov, M. Yu., Nesterova, V. N., and Ushakov, N. G. 2003. Status of food zooplankton in the feeding period of capelin from the central latitudinal zone of the Barents Sea in cold and warm years. – ICES Marine Science Symposia, 219: 447–449.

The impact of environmental conditions on the period of development and formation of plankton biomass in August during the cold and warmer-than-usual years is discussed. Predation is shown to dominate over abiotic effects in influencing the distribution of copepods during the years of high capelin abundance.

Keywords: Barents Sea, *Calanus*, copepod, biomass, plankton, temperature.

E. L. Orlova, V. D. Boitsov, V. N. Nesterova, and N. G. Ushakov: Polar Research Institute of Marine Fisheries and Oceanography (PINRO), 6 Knipovich Street, 183763 Murmansk, Russia [tel: +7 815 247 3424; fax: +47 789 10518; e-mail: inter@pinro.murmansk.ru]. Correspondence to E. L. Orlova.

Introduction

Feeding conditions of the Barents Sea capelin change due to the effects of sea temperature, food supply, their own abundance, their migration pattern, and competition for food. This study was aimed at estimating capelin food supply considering the abundance of their population and zooplankton status in the feeding areas.

Material and methods

Data for 1987, 1989, and 1992 were obtained during PINRO's research cruises undertaken in the central Barents Sea (Figure 1). Plankton were collected with a Juday net (37 cm diameter of opening, gauze No. 38) in the layers 0–50, 50–100 m, and from 100 m to the bottom. In total, 425 samples were processed. The plankton biomass was weighed and expressed in weight per m^3; the biomass of some species was calculated by their amount in 1 m^3 and standard weights.

Results and discussion

The analysis of hydrographic conditions in the covered years showed their essential differences. In August of the cold year of 1987, water masses with negative temperature (61% of the total volume of waters) predominated. The 0–50 m layer contained freshened Arctic waters, with the Barents Sea salt waters below them.

In August 1989, the Atlantic waters were characterized by greater heat supply, but lowered salinity. In the northeast of the latitudinal zone, the Arctic waters prevailed. In the zone of their contact with Atlantic waters, the horizontal Gradients of density were raised, indicating intensification of the currents. In the west of the area surveyed, the hydrographic conditions developed as in the warm years, and in the east, as in the moderate cold ones.

1992 was the warmest among the years analysed. The waters in the upper 50 m layer were characterized by high temperature and salinity, and the dynamics of warm and cold currents was, probably, weakened.

In those years, in the 0–50 m layer, the predominance of *C. finmarchicus* in the plankton community structure was widespread (Table 1). The relative number of cold water species increased with depth and copepod vertical distribution was different. *C. finmarchicus* descent in August was mainly caused by maturation, while the majority of cold water species (primarily old copepodites) occurred there continuously. *M. longa* formed dense concentrations at all the development stages, often making up 60–90% of the total abundance.

In the years reviewed, plankton biomass varied significantly in the different parts of the central zone (Figure 2). Their raised values (500 and more) were

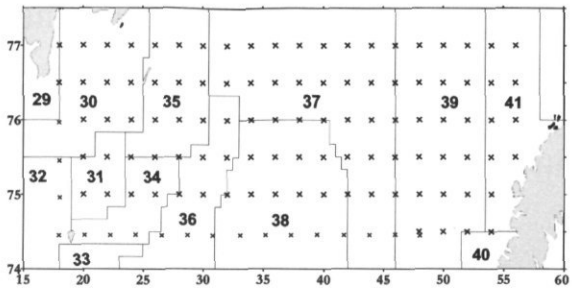


Figure 1. Fishing areas and position of stations in the latitudinal area surveyed in the central Barents Sea. *Oceanographic and plankton stations: 29 – the West Spitsbergen; 30 – the South Cape Deep; 31 – the Spitsbergen Bank; 32 – the Western slope of Bear Island Bank; 33 – the Southern slope of Bear Island Bank; 34 – the Eastern slope of Bear Island Bank; 35 – the Hopen Island area; 36 – the Western Deep; 37 – the Persey Elevation; 38 – the Central Elevation; 39 – the Novaya Zemlya Sallows; 40 – the Sukhoy Nos area; 41 – the Admiralteistvo Islands area.

Table 1. Relative abundance *Calanus finmarchicus* and *Calanus glacialis* in the 0–50 m layer in fishing areas of the central Barents Sea in 1987, 1989, and 1992 (in %).

Copepod species	Areas								
	30	31	34	35	36	37	38	39	41
					1987				
C. finmarchicus	98	70	99	98	–	96	91	93	74
C. glacialis	2	30	1	2	–	3	2	3	22
					1989				
C. finmarchicus	74	47	77	64	62	76	84	79	82
C. glacialis	24	52	16	27	37	18	11	13	15
					1992				
C. finmarchicus	–	–	–	94	87	58	68	68	64
C. glacialis	–	–	–	0	11	7	0	2	16

Fishing areas in accordance with numeration and their location are given Figure 1.

registered at separate stations in August. Mean values in the 0–50 m layer (on conversion to a station) were essentially different, amounting to 156 mg m^{-3} (1987), 269 mg m^{-3} (1989), and 177 mg m^{-3} (1992).

Forming biomass, to a great extent, depended on specific and age composition of copepods, the rates of their growth and maturation. In cold 1987, in the majority of central and eastern areas, where the mean temperature in the 0–50 m layer did not exceed 1°C, 80–90% of plankton (not counting small species) were represented by nauplii and small copepodites (I–II stages). Only in some areas was the prevalence noticed of *C. finmarchicus* copepodites at Stages III and IV–VI (Nos. 31, 34, 38) and *C. glacialis* (No. 31), which also remained in the 50–100 m layer.

In 1989, despite continuing spawning of copepods in the north and northeast (Nos. 37, 39, 41), accompanied by the high abundance of nauplii and young copepodites (to 600–2000 ind./m^3 or 70–90%), together with them, in all the areas, the essential numbers of old copepodites, primarily *C. finmarchicus* and *C. glacialis*, occurred. Their largest number (250–600 ind. m^{-3}) was registered in some western areas (Nos. 30, 34, 35). In the 50–100 m layer it was somewhat lower.

In August of the warm year of 1992, in the central and eastern latitudinal zone, nauplii and young copepodites, as well as old copepodites of *C. finmarchicus* and *C. glacialis*, were less abundant (with maximal values of 300–400 ind. m^{-3}), excluding the eastern areas, where the aggregations of the latter reached 400–500 ind. m^{-3}. They were also predominant in the 50–100 m layer. In the west, the surveys for plankton were stopped because of low concentrations of plankton. We have considered plankton distribution in the warm years more minutely in another article (Orlova *et al.*, 2000a).

As a result, the contribution of every species to the total biomass was dissimilar (Table 2). In most cases, in 1987 and 1989, the raised *C. finmarchicus* biomass was recorded to 100-m depths in the areas affected by the Atlantic waters. In warm 1992, their biomass also increased in the area of the Admiralteistvo Peninsula (Table 2), located in the zone of cold current effect. In some areas, the high biomass due to the presence of *C. finmarchicus* was also observed in the near-bottom layers (to 50–90 mg m^{-3} in 1987, 40–45 mg m^{-3} in 1989, 20 mg m^{-3} in 1992).

In a number of cases, high biomass of *C. glacialis* was also recorded in the same areas (mainly in the 50–100 m layer), but its values were maximum (90–130 mg m^{-3}) in the areas where the Arctic Water masses predominated (Table 2), as well as in the near-bottom layers.

C. hyperboreus played a smaller part in forming biomass. In 1987, in the western parts, their values were under 5 mg m^{-3}, in the central and western ones, 20–30 mg m^{-3} in all the layers. In 1989, the biomass of that species was the same, but distributed more evenly all over the area. Although more abundant, the biomass of *Metridia* was not high, because of the great number of younger copepodites. In the lower layers, the maximal values did not exceed 20–30 mg m^{-3}.

As early as August, alongside the old copepodites (main food supply of adult fish), a high abundance of *Calanoida* nauplii remained in the plankton. On the one hand, they are the main food component of capelin juveniles and other fishes, and on the other hand they characterize food potential in separate areas. We (Orlova *et al.*, 2002b) noticed the high correlation between the abundance of nauplii in

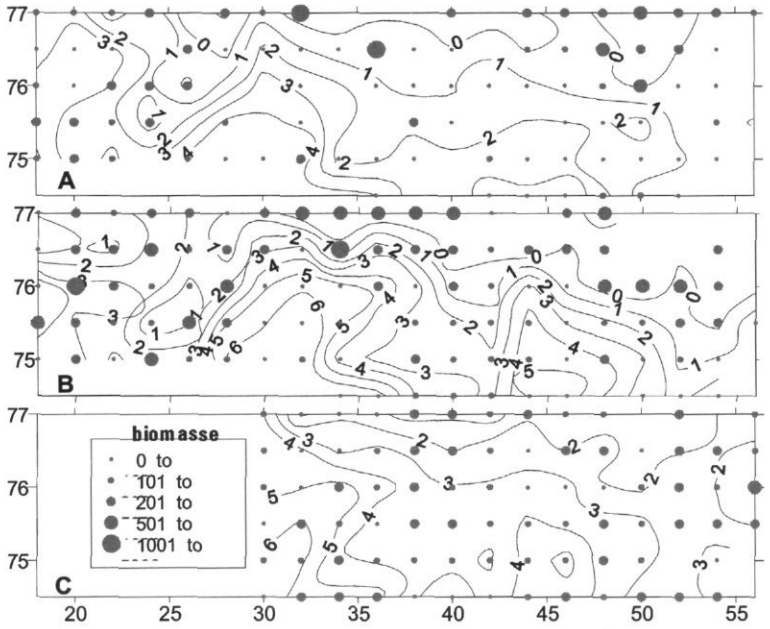


Figure 2. Distribution of plankton biomass (mg m^{-3}) and mean water temperature (°C) in the 0–50 m layer in August in 1987 (A), 1989 (B), and 1992 (C).

Table 2. Mean biomass of *Calanus finmarchicus* and *Calanus glacialis* in the 0–50 m and 50–100 m layers in fishing areas of the central Barents Sea in 1987, 1989, and 1992 (mg m^{-3}).

Copepod species	Depth, (m)	Areas								
		30	31	34	35	36	37	38	39	41
					1987					
C. finmarchicus	0–50	36	36	64	31	–	17	36	15	11
C. glacialis	50–100	50	–	68	1	–	9	41	22	11
C. finmarchicus	0–50	10	89	8	16	–	11	9	20	20
C. glacialis	50–100	49	–	27	1	–	16	15	28	2
					1989					
C. finmarchicus	0–50	84	5	180	90	16	36	24	61	8
C. glacialis	50–100	43	–	25	40	–	24	24	20	–
C. finmarchicus	0–50	54	16	80	132	29	55	21	33	12
C. glacialis	50–100	80	–	19	74	–	25	49	37	–
					1992					
C. finmarchicus	0–50	–	–	–	16	10	22	14	88	108
C. glacialis	50–100	–	–	–	–	23	15	2	21	35
C. finmarchicus	0–50	–	–	–	0	5	19	0	20	186
C. glacialis	50–100	–	–	–	–	0	18	0	15	48

Fishing areas in accordance with numeration and their location are given Figure 1.

July, capelin consumption, and index of fullness in August ($r = 0.86 - 0.92$).

The abundant, widely distributed eurythermal species *Pseudocalanus elongatus* also certainly played a role as a food supply for small capelin. Its abundance was close to and even greater than that of *C. finmarchicus*, especially in 1992. Owing to that species, the biomass reached great values at certain times (10–50 mg m^{-3} in 1987 and 20–100 mg m^{-3} in 1992).

Quite a close relationship between zooplankton biomass in the 0–50 m layer and some oceanographic factors was revealed for 1987 and 1989. Raised biomass occurred most often in waters with decreased temperature and salinity (correlation coefficient $r = -0.60 - 0.65$). In these parts of the latitudinal zone, the density gradient was more within the limits of the pycnocline and its upper border was located closer to the surface than in warmer and saltier waters. For 1992, the relationship between zooplankton biomass and environmental parameters was absent. In this year, capelin predation obviously had a great influence on the distribution of food organisms.

References

Orlova, E. L., Boitsov, V. D., Nesterova, V. N., and Ushakov, N. G. 2002a. Structure and distribution copepod plankton: the basic component of capelin feeding field in the central part of the Barents Sea in moderate and warm years. Problems of fisheries, 3, N 1(9): 36–52.

Orlova, E. L., Boitsov, V. D., Nesterova, V. N., Ushakov, N. G., and Antsiferov, M. Yu. 2002b. Peculiarities of capelin feeding migration in the area of Bear Island and the Spitsbergen in the 80s and 90s. The complex investigation of the Spitsbergen nature. Apatity: Publ. Ksc Ras 175–182.

ICES Marine Science Symposia, 219: 450–453. 2003

Feeding and food consumption of the most abundant fishes of the Barents Sea in the 1990s

Andrey V. Dolgov

Dolgov, A. V. 2003. Feeding and food consumption of the most abundant fishes of the Barents Sea in the 1990s. – ICES Marine Science Symposia, 219: 450–453.

Data from the Russian–Norwegian database were used to study food composition of the most abundant Barents Sea fishes (cod, haddock, Greenland halibut, long rough dab, and thorny skate) in the 1990s. Total food consumption by these species is estimated and the impact of these predators on the stock status of commercial species is considered.

Keywords: Barents Sea, cod, feeding, food consumption, Greenland halibut, haddock, long rough dab, thorny skate.

A. V. Dolgov: Polar Research Institute of Marine Fisheries and Oceanography (PINRO), 6 Knipovich Street, 183763 Murmansk, Russia [tel: + 7 8152 472469; fax: +47 789 10518; e-mail: matlab@pinro.murmansk.ru]. Correspondence to A. V. Dolgov

Introduction

In the 1980s, a stomach sampling programme run by the Institute of Marine Research (Bergen, Norway) and PINRO (Murmansk, Russia) began in the Barents Sea. Feeding was analysed primarily for two species, cod (*Gadus morhua*) and haddock (*Melanogrammus aeglefinus*). Since the mid-1990s, stomach samples have been collected for several other species, including Greenland halibut (*Reinhardtius hippoglossoides*), long rough dab (*Hippoglossoides platessoides*), thorny skate (*Raja radiata*), and one or two other species.

Materials and methods

The data were taken from the Russian–Norwegian database on fish (107 178 cod stomachs, 1990–2000; 3533 haddock stomachs, 1990–1991) (Mehl and Yaragina, 1992), as well as from PINRO sources (9666 haddock stomachs, 1993–1999; 8110 Greenland halibut stomachs, 1990–2000; 5659 long rough dab stomachs, 1990–2000; 1692 thorny skate stomachs, 1994–2000). Stomachs of fish from all observed length classes were analysed.

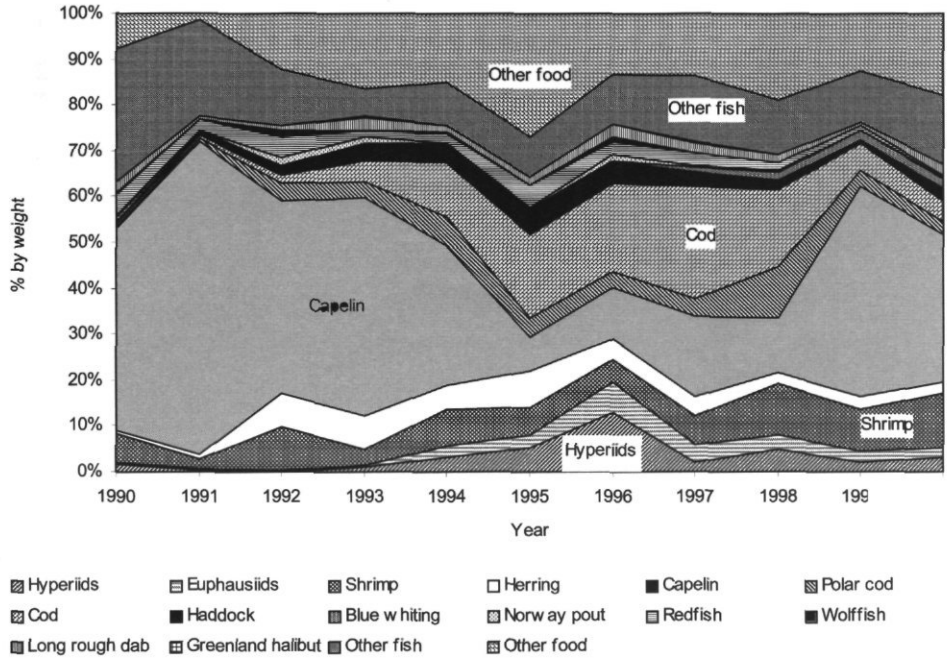
Consumption by all species was estimated for the entire sea on a quarterly basis using data on food composition, daily food consumption, mean weight of stomach contents, and mean weight of separate food items (from feeding data), as well as data on mean weight and mean abundance of each age/length group of predator (from the research surveys).

Results and discussion

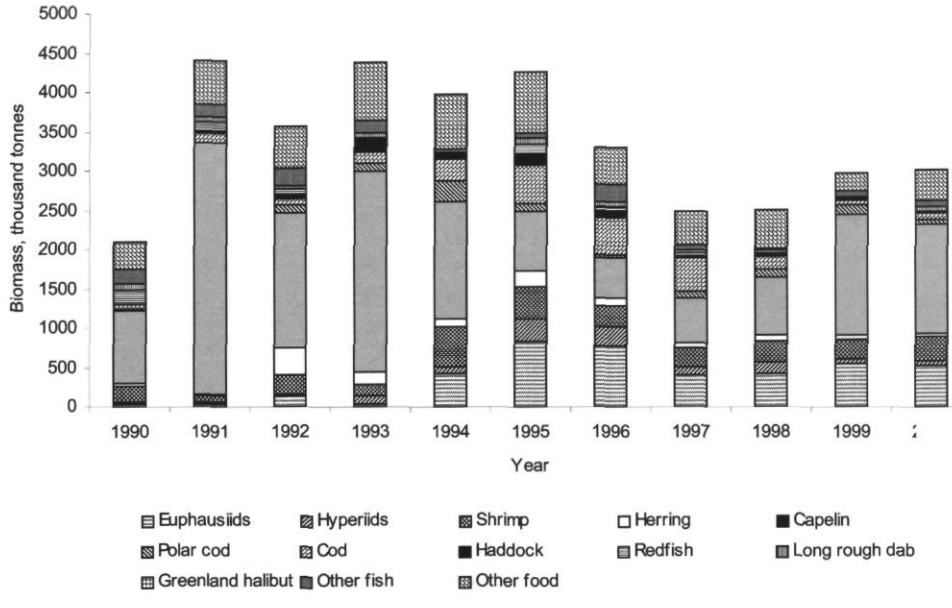
In the 1990s notable changes were observed, both in the food supply of the Barents Sea fishes and in fish feeding. The capelin (*Mallotus villosus*) stock, after a restoration in 1990–1993, declined again in 1994–1995 down to 500 000 t (ICES, 2001a). At the same time a number of strong year classes of herring (*Clupea harengus*) (1992–1995) and cod (1990–1993) appeared in the Barents Sea (ICES, 2001a, b), which led to changes in the food composition of a number of fishes.

The mean annual portion of juvenile cod in the diet of adult cod increased sharply after 1993 and in the period up to 1999 ranged from 4–7% to 20–24%. Prior to 1993 they did not exceed 3% of the diet (Figure 1A). Since 1991, haddock have fed upon young cod, but the mean annual value only contributed 0.2–1% of the total biomass (Figure 2A). In the 1980s, however, haddock virtually did not feed on this species. At the same time herring began to play a more important role in the diet of cod and haddock, making up 7–8% and 3–7% by mass, respectively, as compared to 0.1–3% in 1984–1991.

Foraging conditions for some species may have deteriorated over the 1990s and could have led to the increased consumption of low-value or non-traditional food items. In the 1990s, long rough dab, thorny skate, and Greenland halibut consumed more fisheries waste on the fishing grounds, with an annual mean of up to 50–70% by stomach content weight, whereas in the 1980s the role of fisheries waste was much lower (Berestovsky, 1989, 1996).



A



B

Figure 1. Percentage (A) and total food consumption (B) by weight for Atlantic cod in the Barents Sea.

Comparison of the total biomass of food consumed by different predators in 1990–2000 shows that the largest amount of food is consumed by cod and harp seal (up to 34%) and by minke whale (18%). The analysis of consumption of commercial species by fishes and marine mammals (Nilssen *et al.*, 2000; Folkow *et al.*, 2000) indicates that the consumption of most prey by cod is comparable to

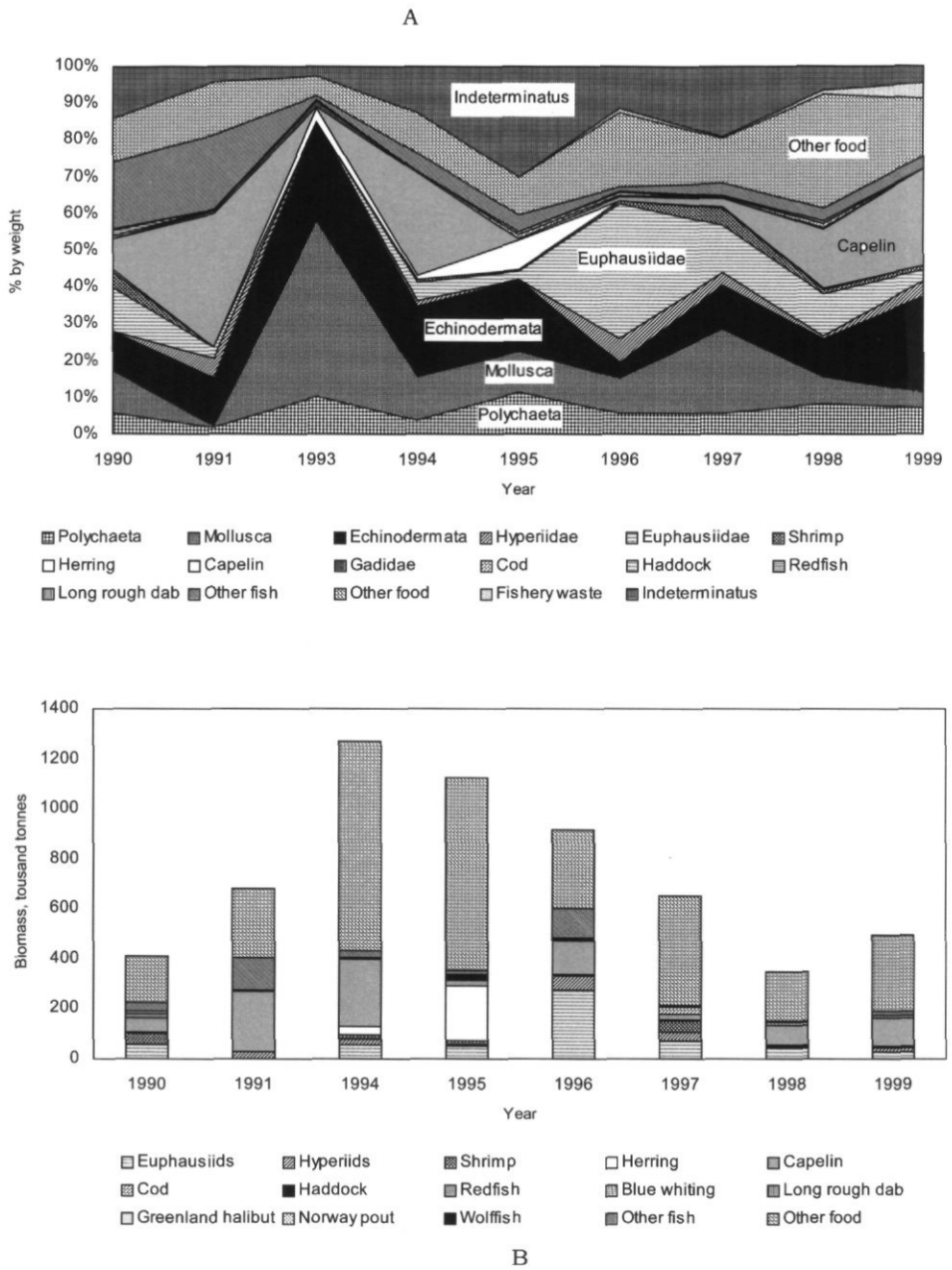


Figure 2. Percentage (A) and total food consumption (B) by weight for haddock in the Barents Sea.

that by all other predators. The exceptions are herring, young cod, and haddock, which are to a greater degree consumed by minke whale.

Conclusion

Based on the amount of biomass of commercial species consumed, cod has the greatest impact on the Barents Sea ecosystem. This applies to both the variety of species eaten and the high abundance of cod. The other most important predators that can affect the dynamics of commercial marine species are Greenland halibut, long rough dab, and thorny skate. Haddock predation is less important because of the rather reduced role of commercial species in its diet.

Acknowledgements

I thank two anonymous referees for making helpful comments on the manuscript.

References

Berestovsky, E. G. 1989. Feeding of skates *Raja radiata* Donovan and *Raja fyllae* Lutken (Rajidae) in the Barents and Norwegian Seas. Journal of Ichthyology, 29(6): 994–1002. (In Russian.)

Berestovsky, E. G. 1996. Feeding of long rough dab in the Barents and Norwegian Seas. Abstract of Ph.D. thesis. Moscow, 23 pp. (In Russian.)

Dolgov, A. V. 1999. Feeding and trophic relations of the Barents Sea cod in the 1980–90s. Abstract of Ph.D. thesis. Murmansk, 24 pp. (In Russian.)

Folkow, L. P., Haug, T., Nilssen, K. T., and Nordøy, E. S. 2000. Estimated food consumption of minke whale *Balaenoptera acutirostrata* in Northeast Atlantic waters in 1992–1995. NAMMCO Science Publication 2: 65–80.

ICES. 2001a. Report of the Northern Pelagic and Blue Whiting Fisheries Working Group. ICES CM 2001/ACFM: 17.

ICES. 2001b. Report of Arctic Fisheries Working Group. ICES CM 2001/ACFM: 19.

Mehl, S., and Yaragina, N. A. 1992. Methods and results in the joint PINRO-IMR stomach sampling program. *In* Interrelations Between Fish Populations in the Barents Sea. Ed. by B. Bogstad and S. Tjelmeland. Proceedings of the Fifth PINRO-IMR Symposium, Murmansk, 12–16 August 1991, pp. 5–16.

Nilssen, K. T., Pedersen, O.-P., Folkow, L. P., and Haug, T. 2000. Food consumption estimates of Barents Sea harp seals. NAMMCO Science Publication, 2: 9–27.

ICES Marine Science Symposia

Actes du Symposium

This series, known until 1991 as *Rapports et Procès-Verbaux des Réunions*, contains the scientific papers and proceedings of symposia or other special meetings held under the auspices of the International Council for the Exploration of the Sea. Volumes in this series have been published since 1903 and many of them are still available. Since 1995 most of these volumes have been included in the series *ICES Journal of Marine Science*. A list of titles with current prices may be obtained from the Secretariat of the Council.

The latest volumes are as follows:

Volume 218:	Acoustics in Fisheries and Aquatic Ecology. Part 1. (Montpellier, 2002). ICES Journal of Marine Science, vol. 60, no. 3. 2003. DKK 550.00
Volume 217:	Seventh International Conference on Artificial Reefs and Related Aquatic Habitats. (San Remo, 1999). ICES Journal of Marine Science, vol. 59 Supplement. 2002. DKK 600.00
Volume 216:	Capelin—What Are They Good For? Biology. Management, and the Ecological Role of Capelin. (Reykjavík, 2001). ICES Journal of Marine Science, vol. 59, no. 5. 2002. DKK 550.00
Volume 215:	100 Years of Science under ICES. (Helsinki, 2000). 2002. DKK 700.00
Volume 214:	Recruitment Dynamics of Exploited Marine Populations: Physical–Biological Interactions. Part 2. (Baltimore, Maryland, 1997). ICES Journal of Marine Science, vol. 58, no. 5. 2001. DKK 360.00
Volume 213:	Environmental Effects of Mariculture. (St Andrews, New Brunswick, 1999). ICES Journal of Marine Science, vol. 58, no. 2. 2001. DKK 340.00
Volume 212:	Population Dynamics of *Calanus* in the North Atlantic. (Tromsø, 1999). ICES Journal of Marine Science, vol. 57, no. 6. 2000. DKK 700.00
Volume 211:	Marine Benthos Dynamics: Environmental and Fisheries Impacts. (Crete, 1998). ICES Journal of Marine Science, vol. 57, no. 5. 2000. DKK 500.00
Volume 210:	Ecosystem Effects of Fishing. (Montpellier, 1999). ICES Journal of Marine Science, vol. 57, no. 3. 2000. DKK 640.00
Volume 209:	Recruitment Dynamics of Exploited Marine Populations: Physical–Biological Interactions. Part 1. (Baltimore, Maryland, 1997). ICES Journal of Marine Science, vol. 57, no. 2. 2000. DKK 550.00

These publications may be ordered from: ICES Secretariat, Palægade 2–4, DK-1261 Copenhagen K, Denmark. Fax: +45 33 93 42 15, e-mail: info@ices.dk. An invoice including the cost of postage and handling will be sent. Publications are usually dispatched within one week of receipt of payment. Further information about this series, including ordering and payment, may be found at: www.ices.dk/products/symposiareports.asp.